MATLAB/SIMULINK MODULES FOR MODELING AND SIMULATION OF POWER ELECTRONIC CONVERTERS AND ELECTRIC DRIVES

A thesis submitted in fulfilment of the requirements for the degree of

MASTER OF ENGINEERING (BY RESEARCH)

to the Graduate School of

The University of Technology, Sydney

by

NARAYANASWAMY. P.R. IYER B.Sc.(Engg), M.Sc.(Engg)

2006

Dedicated to

the Loving memory of my parents

Late Prof. P.K. Ramanatha Iyer and Late Smt. P.N. Kavery Ammal

Certificate of Authorship/Originality

I certify that the work presented in this thesis has not previously been submitted for a degree nor has it been submitted as part of requirements for a degree except as fully acknowledged within the text.

I also certify that this thesis has been written by me. Any help that I have received in my research work and the preparation of the thesis itself has been acknowledged. In addition, I certify that all information sources and literature used are indicated in the thesis.

Production Note:
Signature removed prior to publication.

(P.R. NARAYANASWAMY)

ACKNOWLEDGEMENTS

The author is grateful to Dr. Venkat Ramaswamy, Senior Lecturer , Faculty of Engineering, for introducing and encouraging me to take up this research project presented in this thesis. I am also sincerely thankful to him for his valuable supervision, help and support throughout the course of this project work.

The author wishes to express his sincere gratitude and appreciation to Dr. Jianguo zhu, Professor, Faculty of Engineering, for his supervision and support during the course of this project work.

The author wishes to thank Dr. Peter Watterson, Dr. Quang Ha, Mr. Rob Jarman, Dr. Ben Rodanski and Dr. Johnson Agbinya all of the Faculty of Engineering for their constructive criticism and valuable suggestions for improvement of my project work.

The author wishes to thank all the technical staff in the laboratories of the Center for Electrical Machines and Power Electronics (CEMPE) for their help and support in doing the experimental work. In particular, the author wishes to thank Mr. Bill Holliday, Faculty of Engineering, for providing literature on Lybotec Inverter, Mr. Russel Nicholson and Mr. Shan for their help in the laboratory of the CEMPE.

The author also wishes to thank Mr. Hai Wei Lu, Research candidate, Faculty of Engineering, for his help in the experimental work on Permanent Magnet Synchronous Motor Drive in the laboratory of the CEMPE.

The author wishes to thank Ms. Rosie Hamilton, Ms. Sharmaine Gewohn, former Research Administrators and Ms. Wenshan Guo, Research Administrative Assistant, Faculty of Engineering for their valuable help in the conduct of this project work.

The author is grateful to University Graduate School for providing me the Research Training Scheme (RTS) to support my candidature.

Lastly I wish to thank my wife Mythili, son Ramnath and daughter Rekha for their patience and understanding throughout the course of this project work.

LIST OF SYMBOLS

The following are some of the predominant symbols used. The other symbols are explained within the text in the appropriate places.

C - Capacitor in Farads
D - Damping constant
CF - Filter Capacitor in Farads
E - E.M.F. Source
f, fsw - Frequency in Hertz
I, i - Current
J - Moment of Inertia in kg.m^2.
L, L1 - Inductance in Henries
Lm - Mutual Inductance in Henries
P - Number of Poles
R - Resistance in Ohms
SF - Switch Function
SF_BAR - Inverse Switch Function
T - Switching Period
Tem - Electromagnetic torque in Nw-M
Tmech - Mechanical Load Torque
V, v - Voltage
α - Firing angle
ω - Angular frequency in rad per sec
ω_C - Angular frequency of the arbitrary reference frame in rad per sec
ω_S - Angular frequency of the Stationary or Stator reference frame in rad per sec.
ω_r - Angular frequency of the rotor reference frame in rad per sec.
φ - Phase advance angle
θ - Angle the reference frame makes with the stator abc axis.
λ - Flux linkage

ψ - Flux Linkage per second

λm - Rotor Magnet Constant in volt.sec per elec.rad.

ωre - Rotor speed in electrical radians per second

ωrm - Rotor speed in Mechanical radians per second

Suffix:

d - Direct axis

q - Quadrature axis

e - Electrical

m - Mechanical

re - Rotor electrical

c - Arbitrary

s - Stationary or Stator

r - Rotor

a,b,c - Three phase ac A, B, C

r,y,b - Three Phase ac R, Y, B

n -Neutral

L, l - Line

dc - DC Link

ACRONYMS

BJT - Bipolar Junction transistor

CCM - Continuous Conduction Mode

CS - Clipped Sinusoid

DCM - Discontinuous Conduction Mode

DCTLI - Diode Clamped Three Level Inverter

FCTLI - Flying Capacitor Three Level Inverter

FWDBR – Full Wave Diode Bridge Rectifier

FWCBR – Full Wave Controlled Bridge Rectifier

GTO - Gate Turn off Thyristor

HI - Harmonic Injection

IGBT - Insulated gate Bipolar Transistor

MOSFET - Metal Oxide Semiconductor Field Effect Transistor

IM - Induction Motor

OP.AMP. – Operational Amplifier

PMSM - Permanent Magnet Synchronous Motor

PWM - Pulse Width Modulation.

SCR - Silicon Controlled Rectifier

SMPS – Switched Mode Power Supply

THI - Third Harmonic Injection

ABSTRACT

Modelling and simulation of power electronic converters and electric drives play a vital role in the academic curriculum and also in the industry. A number of modelling and simulation tools are used to study the performance of power electronic converters and electric drives. For the analysis and simulation of three phase electric drives, the three (abc) axis to two (dq) axis transformation is used [1]. The results in the dq axis is transformed to abc axis by suitable inverse transformation.

Over the past, several analog, hybrid and digital computers were used for simulation of converter fed electric drives [2, 13, 29, 30, 33, 34, 35]. In the recent years, a number of software packages have been developed to study the performance of power electronic converters and converter fed electric drives [3 - 9].

SIMULINK developed by **Mathworks Inc., USA.** is one of the softwares used for power electronic converters and electric drive simulation [3, 4, 11]. This software is used for modelling the power electronic converters and electric drives discussed in this thesis.

This thesis describes the interactive modelling of power electronic converters such as ac to dc, dc to ac, dc to dc and ac to ac and ac drives such as the three phase IM and Six Step Inverter fed PMSM, using the software SIMULINK. **Unless specified otherwise, the term "model" in this thesis refers to SIMULINK model.** Interactive Library Building Blocks are developed using SIMULINK for the above power electronic converters. These library models are then used to develop PWM converters. The models for well known PWM techniques such as Sine, HI, THI are presented. The interactive model for a totally new PWM technique known as Clipped Sinusoid PWM (CSPWM) is presented in this thesis. Where possible the results are compared with literature references, by theoretically derived formula and also by Electronic Circuit Simulation software..

Abstract

Interactive Circuit Model of a Digital Gate Drive for a Three Phase 180 Degree mode two level inverter using four line to one line multiplexer is presented and the results compared with well known literatures on power electronics and also by experimental verification.

Interactive system Models for three phase ac Line fed IM drive in all reference frames using dq0 voltage – current and flux linkage equations in state space are presented and simulation results compared with the literature references. This is followed by various system models for three phase Pulse Width Modulated Inverter fed IM drive.

Interactive system models for Six Step Continuous and Discontinuous current mode inverter fed PMSM drives are presented and the results are compared experimentally, by theoretically derived formula and also with the literature references.

Interactive system models for Buck Converter Switched Mode Power Supply (SMPS) are given and the results compared with the literature references and also by electronic circuit simulation.

Interactive system models for Three phase DCTLI and FCTLI are presented and the result compared with literature references and also by theoretical derivations.

Harmonic analysis of six step continuous current mode two level inverter and three phase three level inverter are presented in APPENDIX A. Experimental data and MATLAB programs to calculate the parameters of the six step Lybotec inverter fed PMSM drive in the laboratories of CEMPE are presented in APPENDIX B. The block diagram schematic of the six step Lybotec Inverter in the laboratories of CEMPE is provided in APPENDIX C. Some data sheets for selected integrated circuits are provided in APPENDIX D. Comparison of the model performance of Power Electronic Converters and Electric Drives presented in this thesis made with the Electronic Circuit Simulation Software PSIM, MICROCAP8 and the SimPowerSystems Block set of SIMULINK is presented in APPENDIX E. The list of publications from this thesis is given in APPENDIX F..

TABLE OF CONTENTS

CHAPTER 1

INTRODUCTION

1.1 Background

The performance of power electronic converters and converter fed electric drives can be studied using mathematical equations which describe the behaviour of the particular converter and the drive fed by this converter. For example the voltage, current, flux linkage and electromagnetic torque relationship can be expressed in terms of machine parameters such as resistance and inductance of stator and rotor, number of poles, frequency, speed etc. The simplest mathematical model of the three phase IM is its equivalent circuit, obtained by no load and locked rotor test. It is possible to predict the performance of the three phase IM, for various loads using this equivalent circuit, even without conducting the actual load test in the laboratory. Similarly in the case of PMSM, the various mathematical equations describing the behaviour of this machine can be used to study the performance of this machine by developing a suitable system model. Similarly the power electronic converter supplying power to these electric drives can be developed either as a system model which duplicates the performance of this converter or as a circuit model using the actual power electronic component.

To enable mathematical modelling of three phase AC machines, R.H. Park proposed the three axis, abc to two axis, dq0 transformation, known as generalised machine model [1]. This transformation enables the three phase parameters such as voltages, currents and flux linkages to be evaluated in the dq0 axis and transfer them back to abc axis. Such a simple abc to dq0 transformation matrix is given in equation 1:

$$\begin{bmatrix} f_q \\ f_d \\ f_0 \end{bmatrix} = \frac{2}{3} * \begin{bmatrix} \cos(\theta) & \cos(\theta - \frac{2.\pi}{3}) & \cos(\theta + \frac{2.\pi}{3}) \\ \sin(\theta) & \sin(\theta - \frac{2.\pi}{3}) & \sin(\theta + \frac{2.\pi}{3}) \\ \frac{1}{2} & \frac{1}{2} & \frac{1}{2} \end{bmatrix} * \begin{bmatrix} f_a \\ f_b \\ f_c \end{bmatrix} \qquad (1.1)$$

The inverse transformation matrix to transfer from dq0 axis to abc axis is in equation 2.

$$\begin{bmatrix} f_a \\ f_b \\ f_c \end{bmatrix} = \begin{bmatrix} \cos\theta & \sin\theta & 1 \\ \cos(\theta - \frac{2.\pi}{3}) & \sin(\theta - \frac{2.\pi}{3}) & 1 \\ \cos(\theta + \frac{2.\pi}{3}) & \sin(\theta + \frac{2.\pi}{3}) & 1 \end{bmatrix} * \begin{bmatrix} f_q \\ f_d \\ f_0 \end{bmatrix} \qquad (1.2)$$

In equations 1.1 and 1.2, the term f represents either a voltage, current or flux linkage. θ is the angle between q axis and reference phase A shown in Fig. 1.1.

Using the above abc to dq0 transformation, all types of three phase ac machine analysis can be brought under one roof. Over the past decade several computer programs have been developed based on above transformations to predict the performance of these converter fed three phase ac machines [2, 13, 29, 30, 33, 34, 35]. A number of softwares have been developed recently in the past one decade to study the performance of power electronic converters and converter fed electric drives. Some of them are SIMULINK[3, 4], PSIM[5], CASPOC[6] and SIMPLORER[7], PSPICE[8] and MICROCAP[9].

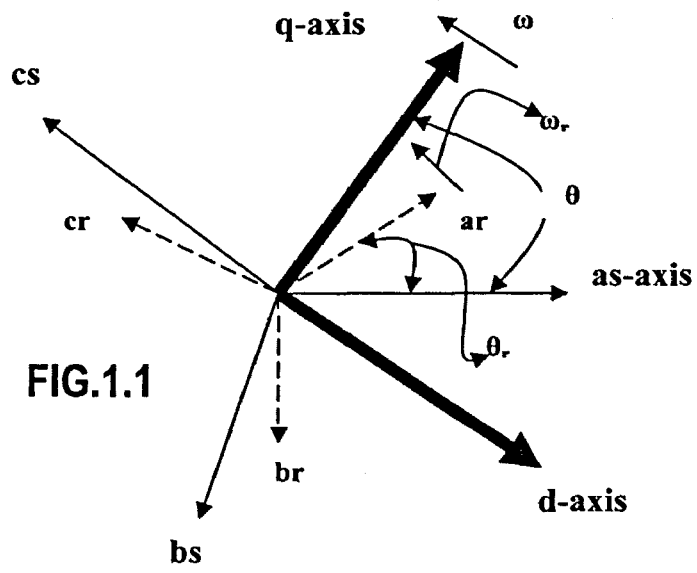

FIG.1.1

1.2 Scope of this Project

This project aims in developing library building blocks of system models for various power electronic converters. The various library models of converters developed are ac to dc, dc to ac, dc to dc and ac to ac. The three phase ac drive models developed are that for three phase IM and Six Step Inverter fed PMSM. Open loop and closed loop system models for line fed and Pulse Width Modulated inverter fed three phase IM drive have been developed. System models for six step continuous and discontinuous conduction mode inverter fed PMSM drive have also been developed. The performance obtained

by simulation of the model with that by experiment is compared for the case of the Lybotec six step inverter fed PMSM drive in the CEMPE laboratory. In all other cases the performance of the model is compared either with the literature reference or with theoretically derived formula along with the literature reference and also by Electronic Circuit Simulation software. The models developed in this thesis are system models which solves the equations describing the behaviour of the system, whether algebraic or differential. A relatively new concept known as "Switching Function Concept" is used to simulate the behaviour of the Power Electronic Converters [45, 46, 54, 55, 61]. Although the three Phase IM and PMSM built in Models are available in the SimPowerSystems blockset of SIMULINK, these built in models are NOT used here. Original machine models based on their characteristic equations in the dq0-axis reference frame are developed using the various blocks in the SIMULINK block set. At this stage it will be appropriate mention the difference between the system model and that obtained by Electronic Circuit simulation software. While system model solves the characteristic equation describing the behaviour of the system, electronic circuit simulators use the passive and active semiconductor component parameters, such as for example, switch ON and OFF resistance, voltage and current gain values, parasitic or stray capacitances between junctions, junction potentials, inherent inductive reactance and so on arranged as a sub-circuit (also called the equivalent circuit of the semiconductor component or the device) to solve a given power electronic converter or a machine model.

1.3 Why Use SIMULINK ?

SIMULINK has the following advantages compared to other software packages:

- Can be used to study the models of electric drives with fixed or time varying loads.
- The performance of developed models of electric drives can be easily verified with built in electric drives model in the SimPowerSystems block set.
- The Harmonic analysis of Power Electronic Devices driving AC machines can be easily made with Powergui in SimPowerSystems block set.

- Many non-linear phenomenon such as Pulse Width Modulation techniques can be easily verified.
- Many Power electronic circuits can be studied by modelling techniques and can be verified by semiconductor components in the SimPowerSystems block set i.e. it is possible to develop either system models based on the characteristic equations describing the behaviour of the system or electronic circuit models utilising the equivalent circuit parameters of the semiconductor component.
- Facility to study analog and digital gate drives used in Power Electronic Circuits.
- Facility to save data in workspace, which can be later brought to MATLAB window for further mathematical processing, editing graphics etc.
- Facility to develop interactive models with user dialog boxes for power electronics and drive systems with which any given power electronic converter and drive can be tested by entering the parameters in the dialog boxes without actually going into each block of the model to enter the data. This saves time for the user and finds applications in virtual power electronics and drives laboratory. This is one of the unique features in SIMULINK.

1.4 Significance of Modelling

The significance of the term modelling is summarised below:

- Modelling a physical system refers to the analysis and synthesis to arrive at a suitable mathematical description encompassing the dynamic characteristics of the system in terms of its parameters [11]
- Models are used to predict the performance of the given system [11].
- Model prediction permits engineers to think of its potential applications, practical implementation and to develop various control strategies [11].
- Reduces time involved or shortens the overall design process [17, 58].
- Saves time and money as compared to procuring, installing and testing the system in the laboratory, especially when the system is too bulky [11].
- Simulation refers to performing experiments on the model [11].

- Computer simulation plays a vital role in the R & D of power electronic devices for its high manoeuvrability, low cost and ability to speed up system implementation [53].

1.5 Simulation tools

Essential tools formerly and presently used for simulation of electrical system are:

1. Network Analyser
2. Analog and Hybrid computers
3. Digital computers.

1.6 Thesis novelty

The thesis work mainly concentrates on modelling selected power electronic converters and three phase IM and PMSM drives using SIMULINK. This project novelties are given below:

1) The three phase CSPWM technique is a NEW discovery and such a PWM technique hitherto does not appear in the literature references (paper 2 in APPENDIX F).

2) Interactive Models as developed in my project work for three phase DCTLI and FCTLI are not available in the literature references.

3) Interactive Model for three phase IM in all reference frames (stationary, synchronous and arbitrary) with provision to select the frame in a single model schematic is not available in the literature references (Paper 7 in APPENDIX F). .

4) Interactive Model for three phase inverter in the discontinuous current mode with switching angle advancing facility suitable for analysing PMSM drives are not reported in the literature references (paper 4, 5, 6 and 8 in APPENDIX F).

5) Interactive Models for dc to dc converters developed in my project work, particularly for the boost and buck-boost converter are not available in the literature references.

6) Interactive Models for three phase thyristor ac to ac converters (ac controllers) are not at all available in the literature references.

7) Interactive Model for buck converter SMPS especially feedback control part is new and different from that existing in the literature references (paper 3 in APPENDIX E).

8) Interactive Model for single phase ac to dc converter using diodes developed in my project work is much different from that existing in the literature references.

9) Interactive Model for single phase ac to dc converter using SCRs developed in my project work is not available in the literature references.

10) Interactive Models for three phase I.M. using dq0-axis flux linkage equations and also the flux linkage per second equations in state space are totally new and makes use of the advanced features of SIMULINK. Such models hitherto are not available in the literature references (Paper 7 in APPENDIX F).

1.7 Thesis outline

This thesis mainly concentrates on modelling power electronic converters and converter fed three phase IM and PMSM drives. Interactive Library models for power electronic converters have been developed. The parameters for PMSM drive is obtained by experiment in the laboratories of the CEMPE.

Chapter 1 provides the Introduction. Chapter 2 provides the literature review. The literature review for ac to dc, dc to ac, dc to dc and ac to ac converters and their modelling aspects are provided. This is followed by the literature review for pulse width modulated inverters, SMPS, Multilevel inverters. Literature review for modelling

of three phase ac line fed IM is provided, followed by that for PWM inverter fed IM drive. Literature review for hybrid/digital computer modelling of PMSM drives fed by six step continuous and discontinuous current mode inverter is then presented. Chapter 3 to 6 provides building interactive library models for ac to dc, dc to ac, dc to dc and ac to ac converters respectively. In the library models for these power electronic converters, it is the aim to test and simulate any given power electronic converter by entering the parameters of the converter in the appropriate boxes and / or 'pop-up' menus, without altering the inner details of the model. This easy to use library model is suitable for virtual power electronic laboratory applications. Chapter 7 provides interactive models for three phase ac line fed Induction Motor Drive. Chapter 8 gives an account of the interactive models for six step continuous and discontinuous current mode inverter fed PMSM drive. Chapter 9 provides interactive circuit model for a digital gate drive for a three phase 180 degree mode inverter using four line to one line multiplexer. Chapter 10 provides the interactive system model for a buck converter SMPS. Interactive models for three phase SINE, HI, THI and CS PWM inverter fed I.M. Drive are discussed in Chapter 11. Interactive models for three phase DCTLI and FCTLI are given in Chapter 12. The conclusions drawn from this thesis work is presented in Chapter 13. All these models provided from Chapter 7 to Chapter 12 are interactive in the sense the user can enter the data in the appropriate boxes / pop-up-menus provided without altering the inner details of the model. These models find applications in virtual power electronics laboratory. Appendix A provides the Harmonic Analysis of Line to Line voltage of Three Phase 180 degree mode inverter and also for the three phase three level inverter using MATLAB. Appendix B provides the MATLAB program for calculating the Lybotec six step inverter fed PMSM parameters from experimental data. Appendix C gives the block diagram layout of Lybotec Six Step Inverter. Appendix D gives the data sheet for selected digital Integrated Circuits. Appendix E provides the comparison of the model performance of Power Electronic Converters and Electric Drives discussed in this thesis with the Electronic Circuit Simulation softwares PSIM, MICROCAP and also with the SimPowerSystem Block set of SIMULINK. The publications arising from this thesis work is given under Appendix F. The literature referred to are given under the list of references.

CHAPTER 2

REVIEW OF LITERATURE

2.1 Introduction

This project mainly concentrates on the interactive modelling of power electronic converters and three phase ac drives. SIMULINK has been used for modelling for reasons mentioned in the introduction. The purpose of developing models is given in section 1.4. Of the various power electronic converters and electric drives, the selected models of AC to DC, DC to AC, DC to DC and AC to AC Converters are developed. In the modelling of three phase ac drives, models of IM and PMSM are developed. In particular the models of single phase diode and SCR bridge rectifiers and three phase diode bridge rectifiers were developed under the ac to dc converter modelling. The models of three phase 180 degree mode and 120 degree mode inverters have been developed under the category dc to ac converter modelling. Under the dc to dc to converter modelling, models of buck, boost and buck-boost converters have been developed. In ac to ac converter modelling, model of back to back connected thyristors in series with the three phase ac lines connected to star connected resistive load and model of back to back connected thyristors in series with resistive load connected in delta to a three phase ac lines are developed. Models of three phase SINE, HI, THI and CS PWM inverters have also been developed. Circuit model for digital gate drive for a three phase 180 degree mode inverter using four line to one line multiplexer is also presented. In addition models for buck converter SMPS and multilevel inverters are developed. Under multi level inverter category, models of three phase DCTLI and FCTLI are developed.

In three phase ac drive modelling, models for ac line fed three phase IM followed by three phase SINE, HI, THI, and CS pulse width modulated inverter fed IM drive have been developed. In addition models of six step continuous current mode and discontinuous current mode inverter fed PMSM drive with sinusoidal back e.m.f. have

also been developed. The data for PMSM drive model is obtained by experiment on the Lybotec six step inverter fed PMSM in the laboratories of CEMPE.

Many literatures have been referred for the above model development. The detailed review of these literature is given below:

2.2 AC to DC Converter

In the section on ac to dc converter modelling, single phase and three phase full wave diode bridge rectifiers and single phase SCR bridge rectifiers are discussed [14-18, 54, 61]. Reference 54 provides system modelling of single phase and three phase diode bridge rectifiers using the concept of switching functions. Switch functions for the upper and lower arm diodes are defined and are used to develop the model considering other system parameters such as resistance and inductance of the source and the load, filter capacitor etc. In reference 61, detailed system modelling of three phase diode bridge rectifiers using separate Heavyside functions for arm voltages and phase voltages are developed. The abc axis voltages of the three arms are transformed to αβ axis and the modelling equations are developed for a given source resistance and inductance. Separate models are developed for purely resistive load and RL load. The results in αβ axis is then transformed to abc axis.

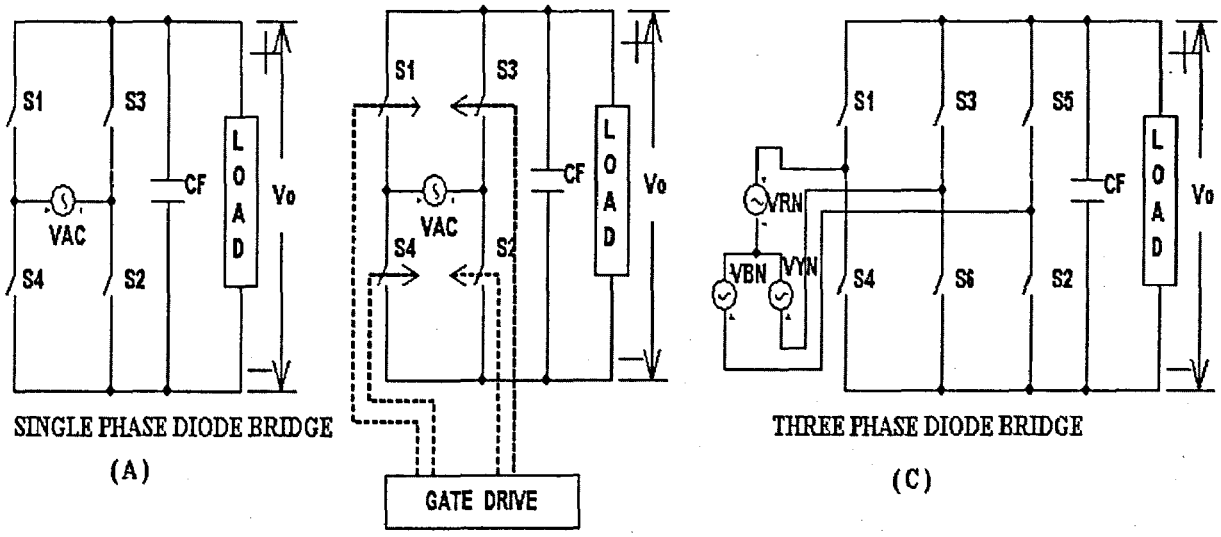

FIG. 2.1

This thesis provides system modelling of single phase FWDBR, FWCBR and three phase FWDBR, the general schematic of which is shown in Fig.2.1(A), (B) and (C). User interface is provided where data relating to the particular ac to dc converter can be entered. The models can be copied to various future applications as data entered by the user can be changed without changing the inner details of the model.

2.3 DC to AC Converter

In dc to ac converter modelling mainly system models for three phase inverter is discussed [14 – 18, 45 – 46]. Reference 45 and 46 provides modelling of three phase 180 degree mode inverter, triangle carrier and sine PWM technique using the concept of switching functions. Further models for the ac to dc boost rectifier, hysteresis current controller are given. Further a modelling technique to separate the free wheeling diode current and switch current are given.

FIG. 2.2

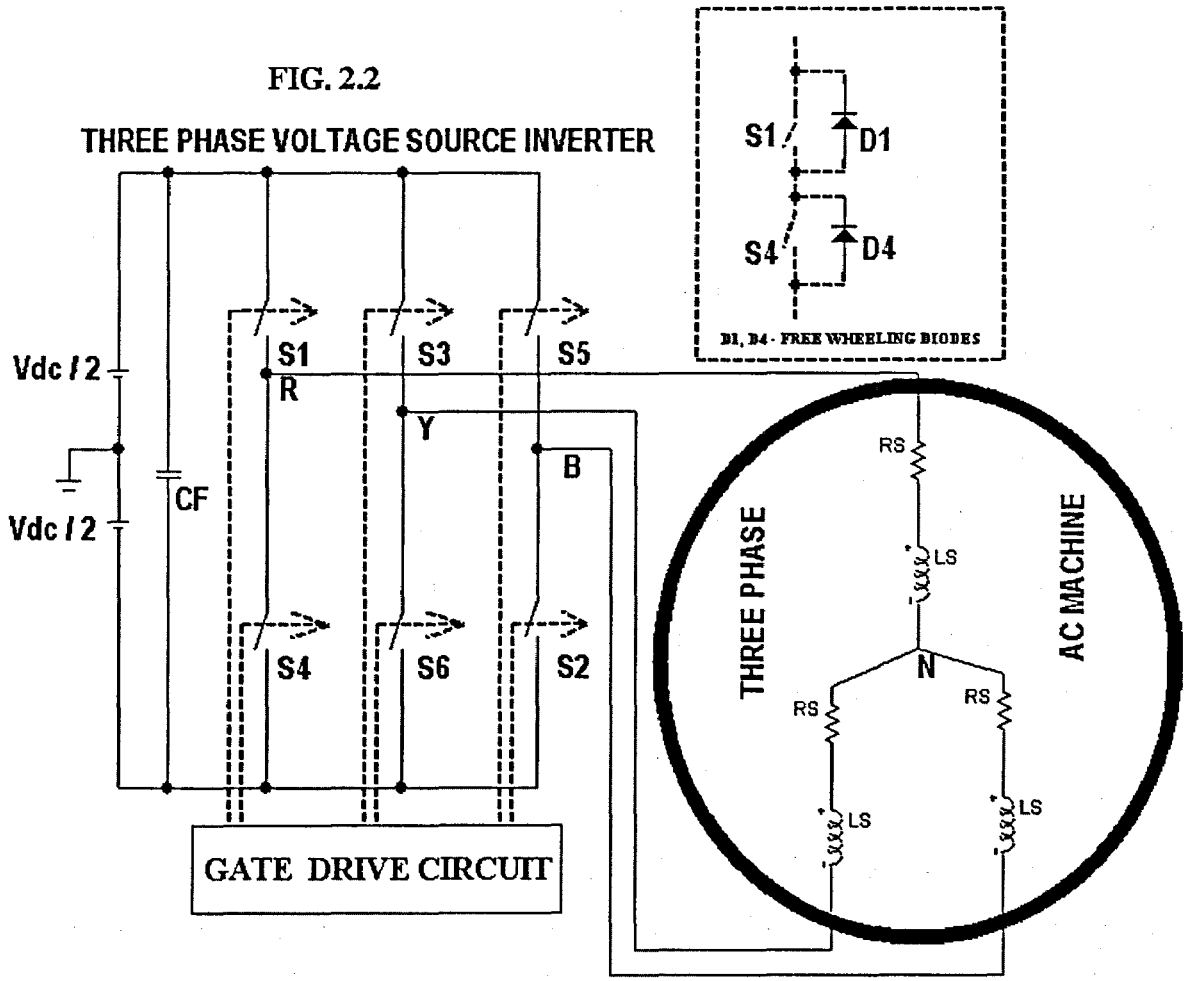

This thesis provides system modelling of three phase 180 degree and 120 degree mode inverter, a general schematic of which is shown in Fig.2.2. User interface is provided where data relating to the particular dc to ac converter can be entered. The models can be copied to various future applications as data entered by the user can be changed without changing the inner details of the model.

2.4 DC to DC Converter

In the section on dc to dc converter modelling, mainly system models for buck, boost and buck-boost converters are discussed [14 -18, 54 – 57]. Reference 54 provides a detailed system modelling of Buck converter considering discontinuous conduction mode using switching functions. Separate switch functions are defined for the switch and diode. References 55 and 56 provide system modelling of quasi resonant converters. They have two inductors and two capacitors in their circuits and fall in the category of fourth order converters. Model for step down quasi resonant converter with feedback controller is also given. Reference 57 provides a non-linear model of the buck converter. In this, modelling is done separately for the fully controlled generator, output filter and the compensation circuit. Fully controlled generator comprises of the switch, diode, gate drive and PWM modulator. The unit delay block from discrete block set is used to generate the square pulse $(-1)^{k.}$, where k = 1,2,3,4 etc....., with sample time Ts set to switching period. Two variable transport delay from continuous block set is used, one to shift the square pulse by arbitrary delay and the other to shift the same square pulse by an arbitrary delay plus the pulse width of the switching pulse. These two resulting signals are exclusively ORed using EXOR gate and this output is multiplied by supply voltage Vdc to get the PWM output across diode of the buck converter. The output filter is realised by using state space approach using inductor current and voltage across capacitor as output and PWM voltage across diode as input. The compensation circuit is realised using op.amp, resistor and capacitor models. Bode plots for control to output transfer function is given.

This thesis provides system models for buck, boost and buck-boost converter using switching function concept, the general schematic of which is shown in Fig.2.3. User interface is provided where data relating to the particular dc to dc converter can be

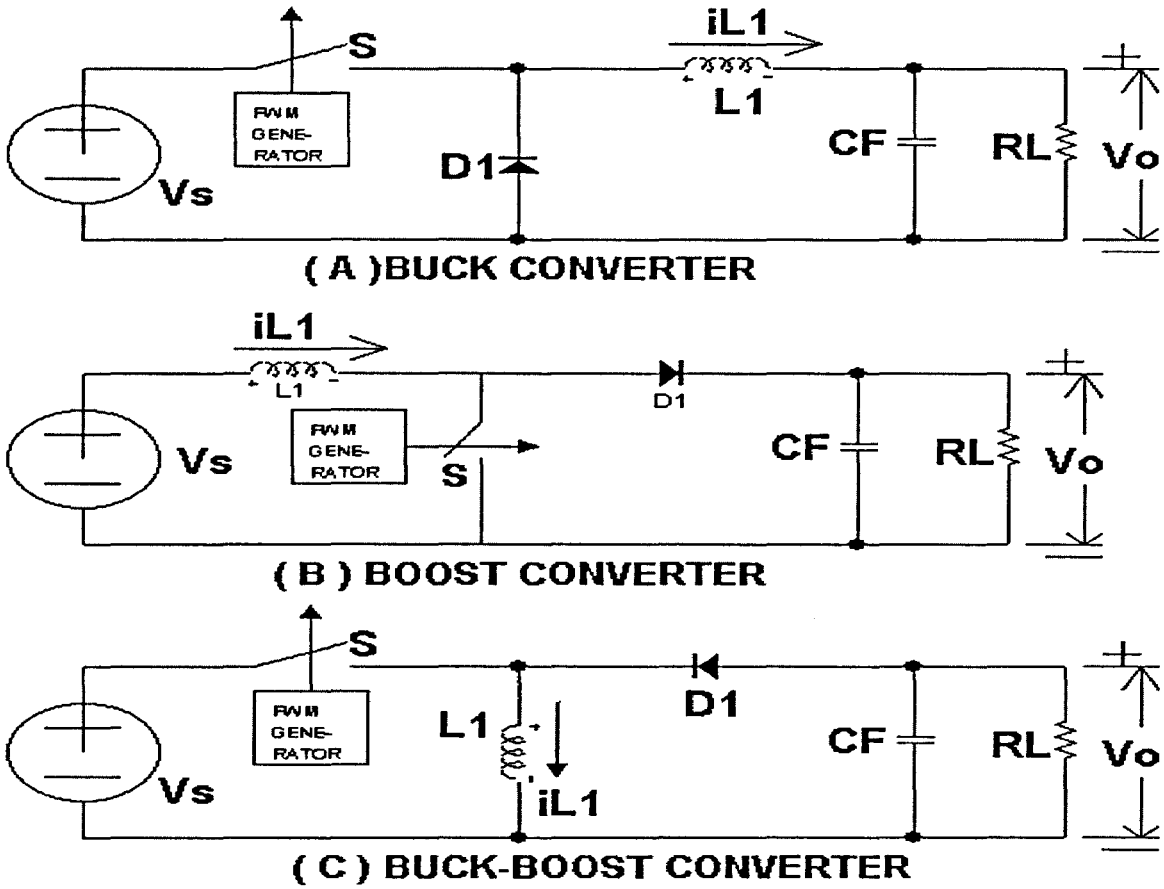

FIG. 2.3

entered. The models can be copied to various future applications as data entered by the user can be changed without changing the inner details of the model.

2.5 AC to AC Converter

In the section on models for AC to AC Converters, mainly system models for thyristor three phase ac controllers are discussed [14 – 17]. Not much of models for ac to ac converter is given in the literature references.

This thesis provides new and original system models for back to back connected thyristors in series with the three phase ac lines connected to star connected resistive load and also for the back to back connected thyristors in series with resistive load connected in delta to a three phase ac line, the schematic of which is shown in Fig.2.4. Switching function concept is used in developing these models. User interface is provided where data relating to the particular ac to ac converter can be entered. The

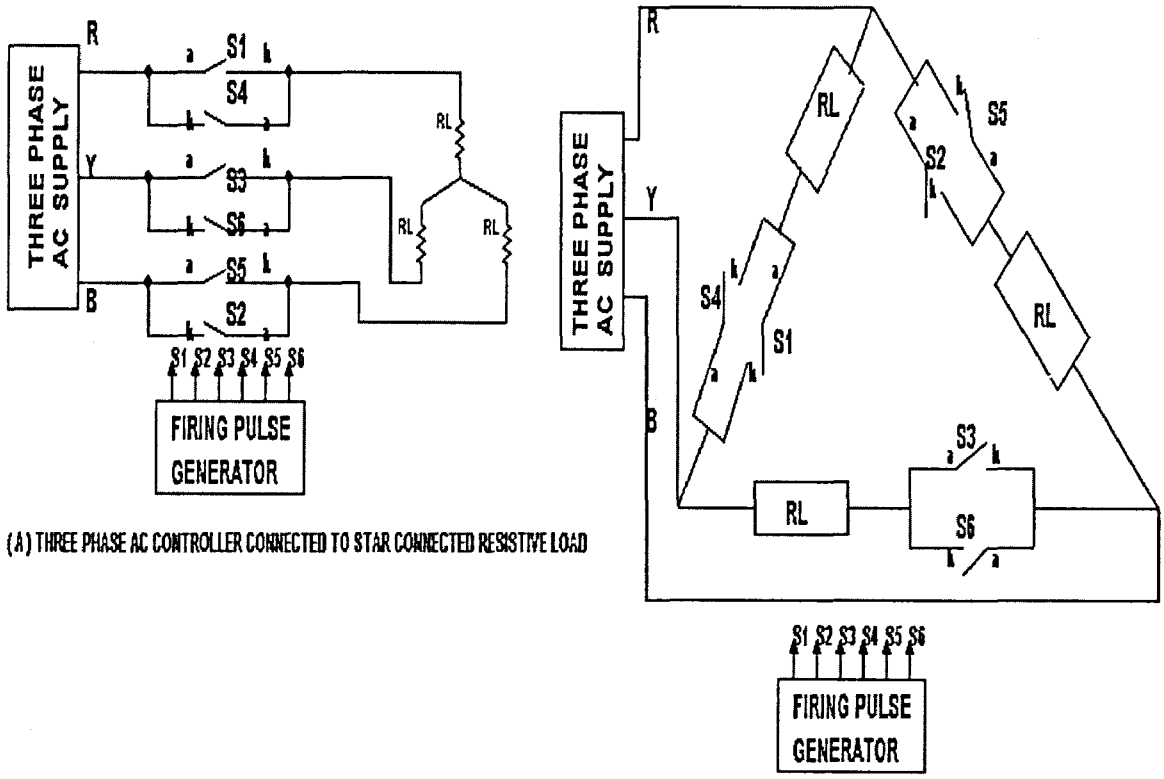

(A) THREE PHASE AC CONTROLLER CONNECTED TO STAR CONNECTED RESISTIVE LOAD

(B) THREE PHASE AC CONTROLLER IN SERIES WITH DELTA CONNECTED RESISTIVE LOAD

FIG. 2.4

models can be copied to various future applications as data entered by the user can be changed without changing the inner details of the model.

2.6 Pulse Width Modulated Inverters

A number of pulse width modulation technique is available for the voltage control of inverters. Some of them are SINE, HI, THI, TRAPEZOIDAL and DELTA. The SINE PWM is the fundamental technique [14 – 18, 47 – 48]. The HI and THI were proposed for obtaining higher output line to line voltage with reduced distortion compared to SINE PWM [14, 49 – 50]. TRAPEZOIDAL modulation is also used for higher output line to line voltage compared to SINE PWM [51 – 52]. DELTA modulation also known as hysteresis modulation produces output voltage equal to the dc link voltage of the inverter. The DELTA modulation can control the ratio of voltage to frequency which is a desirable feature for ac motor control [14].

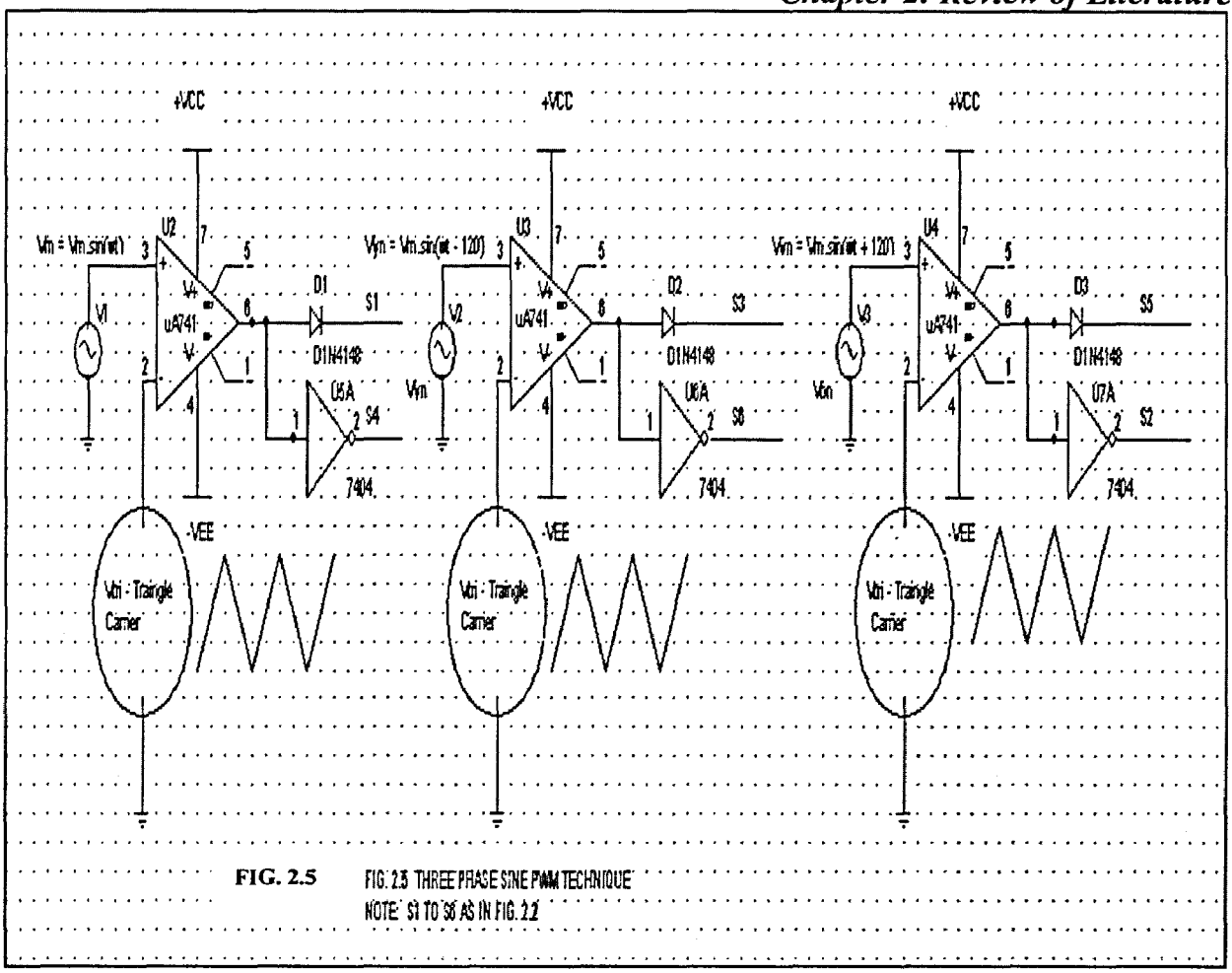

FIG. 2.5 FIG. 2.5 THREE PHASE SINE PWM TECHNIQUE
NOTE: S1 TO S6 AS IN FIG. 2.2

This thesis provides interactive model for three phase SINE PWM inverter using the concept of switching functions [45 – 46]. This principle of three phase SINE PWM is illustrated in Fig.2.5. The principle of HI, THI and CS are the same as for SINE PWM, except that the three phase SINE modulating signals in Fig.2.5 are replaced by corresponding three phase HI, THI and CS modulating signal. Interactive models for HI and THI presented in this thesis are totally new and original. The interactive model for a totally new Pulse Width Modulation technique known as Clipped Sinusoid (CS) PWM is presented in this thesis.

2.7 Digital Gate Drives for Three Phase Inverters

The gate drive for three phase inverters are normally using analog op.amp ICs used as zero crossing comparators for each of the three phases. The gate drive can be 180 degree mode or 120 degree mode. Three phase 180 degree mode inverter is used for IM drives, while both 180 and 120 degree mode inverter are used for PMSM drives. The MC8 simulated drive pattern for a three phase 180 and 120 degree mode inverter are

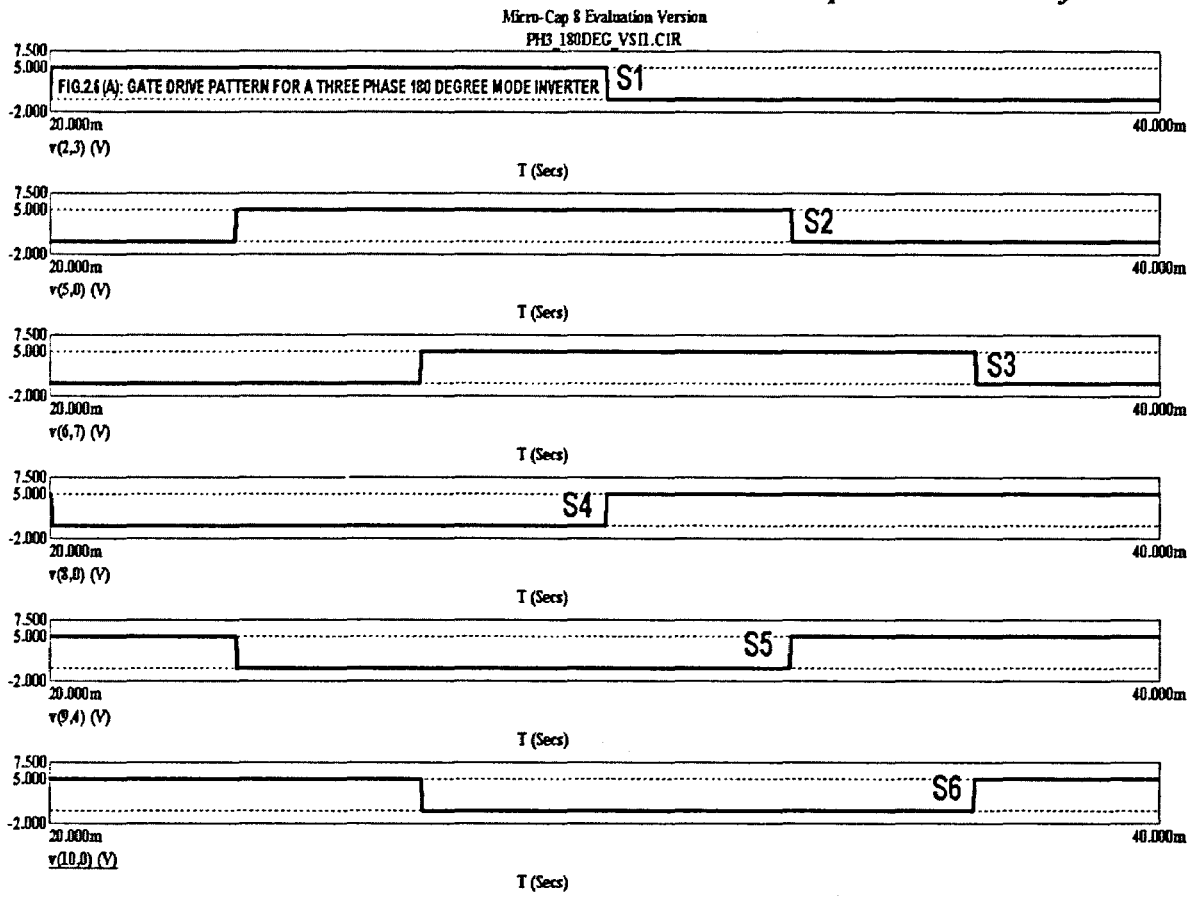
Micro-Cap 8 Evaluation Version
PH3_180DEG_VSI1.CIR
FIG.2.6 (A): GATE DRIVE PATTERN FOR A THREE PHASE 180 DEGREE MODE INVERTER
S1
S2
S3
S4
S5
S6
7.500
5.000
-2.000
20.000m
40.000m
v(2,3) (V)
v(5,0) (V)
v(6,7) (V)
v(8,0) (V)
v(9,4) (V)
v(10,0) (V)
T (Secs)

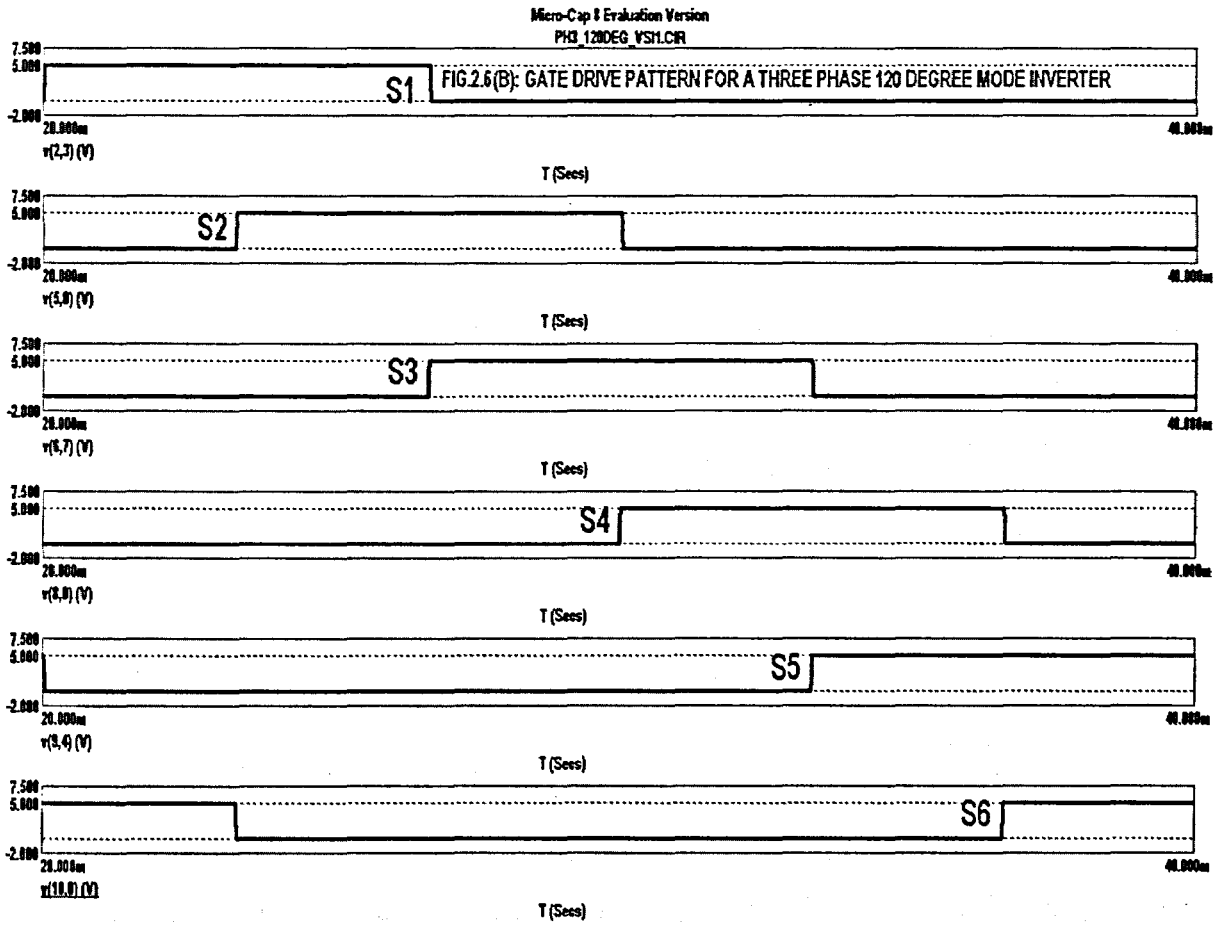
Micro-Cap 8 Evaluation Version
PH3_120DEG_VSI1.CIR
FIG.2.6(B): GATE DRIVE PATTERN FOR A THREE PHASE 120 DEGREE MODE INVERTER
S1
S2
S3
S4
S5
S6
7.500
5.000
-2.000
v(2,3) (V)
v(5,0) (V)
v(6,7) (V)
v(8,0) (V)
v(9,4) (V)
v(10,0) (V)
T (Secs)

shown in Fig.2.6(A) and (B) respectively. Microprocessors / microcontrollers, DSPs and EPROM are also used as gate drives [14 – 18]. A conventional gate drive for a three phase 180 degree mode inverter using op.amps is shown in Fig.2.7 (A).

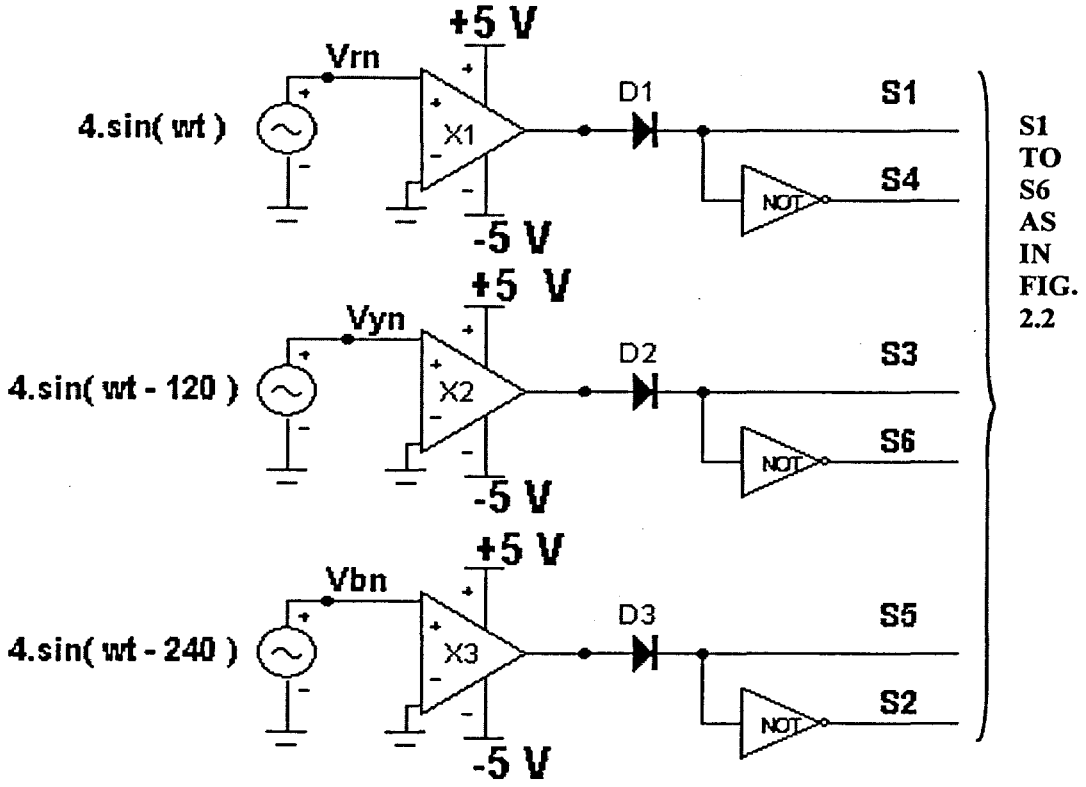

FIG.2.7(A)

THREE PHASE 180 DEGREE MODE INVERTER GATE DRIVE

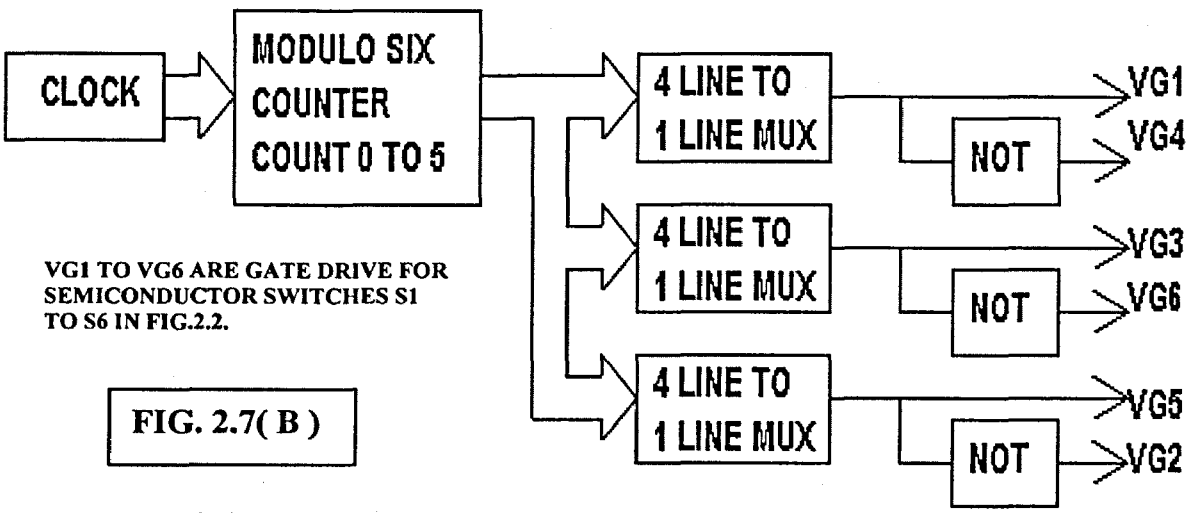

FIG.2.7(B)

GENERAL DIGITAL GATE DRIVE FOR THREE PHASE VSI

This thesis provides the interactive circuit model of a digital gate drive for a three phase 180 degree mode inverter using four line to one line multiplexer, the general schematic

of which is shown in Fig.2.7(B). Experimental waveform of the switching function is also given.

2.8 Switched Mode Power Supplies

SMPS using buck converter are used to obtain nearly constant output dc voltage irrespective of variation in the input dc voltage [14 – 18]. PSPICE model for SMPS using Quasi Resonant Converter available in the literature reference [56]. A system model of SMPS is provided in the literature reference [57].

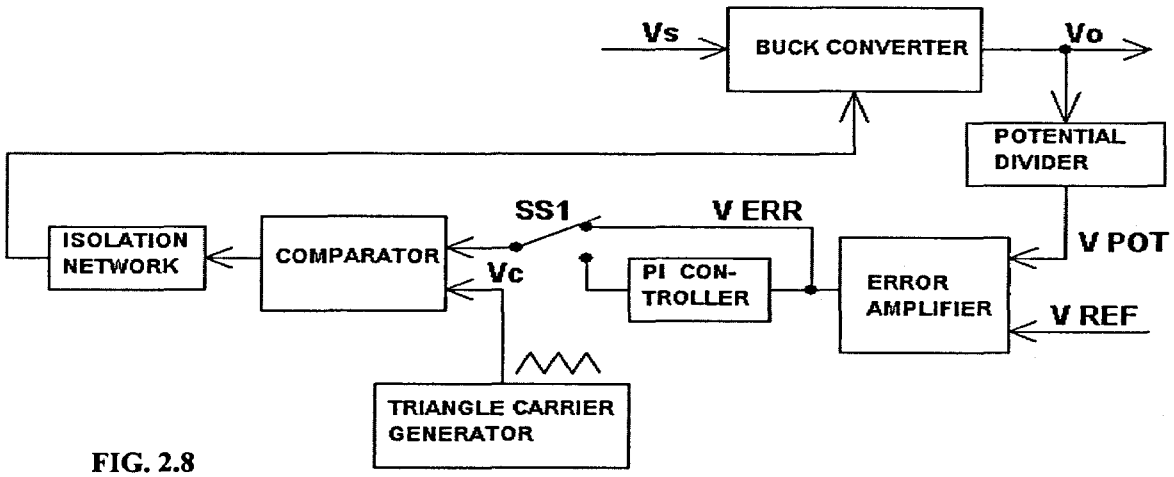

FIG. 2.8
GENERAL MODEL OF THE BUCK CONVERTER SMPS

This thesis provides a new interactive system model for a buck converter SMPS suitable for power electronics laboratory applications, a schematic of which is shown in Fig.2.8. Switching function concept is used in developing this model [54 – 56].

2.9 Multilevel Inverters

Multilevel inverters have drawn the attention of the power industry, as they have features for reactive power compensation. Increasing the inverter voltage levels without the need for higher rating for individual device/component increases the power rating. Multilevel inverters produce higher output voltage with low harmonics without the need for step up transformers or series connected synchronised switching device. As the number of levels of the inverter increases, the harmonic content of the output voltage is reduced significantly [14, 66 - 71]. The two topology for multilevel inverters are Diode Clamped and the Flying capacitor topology. Circuit model for three phase

DCTLI is provided in the literature [53]. In this the three phase DCTLI is developed using GTOs from Universal Bridge in the SimPowerSystems block set. MATLAB program is used for the controller. A survey of various multi level inverter topologies are presented in the literature references, defining the relation connecting the number of levels for the line to ground and line to line voltages [67 – 69]. A derivation for the time duration required for the zero voltage level to reduce the T.H.D. of line to line voltage from 31.08 % to 16.86 % is reported in the literature reference [70].

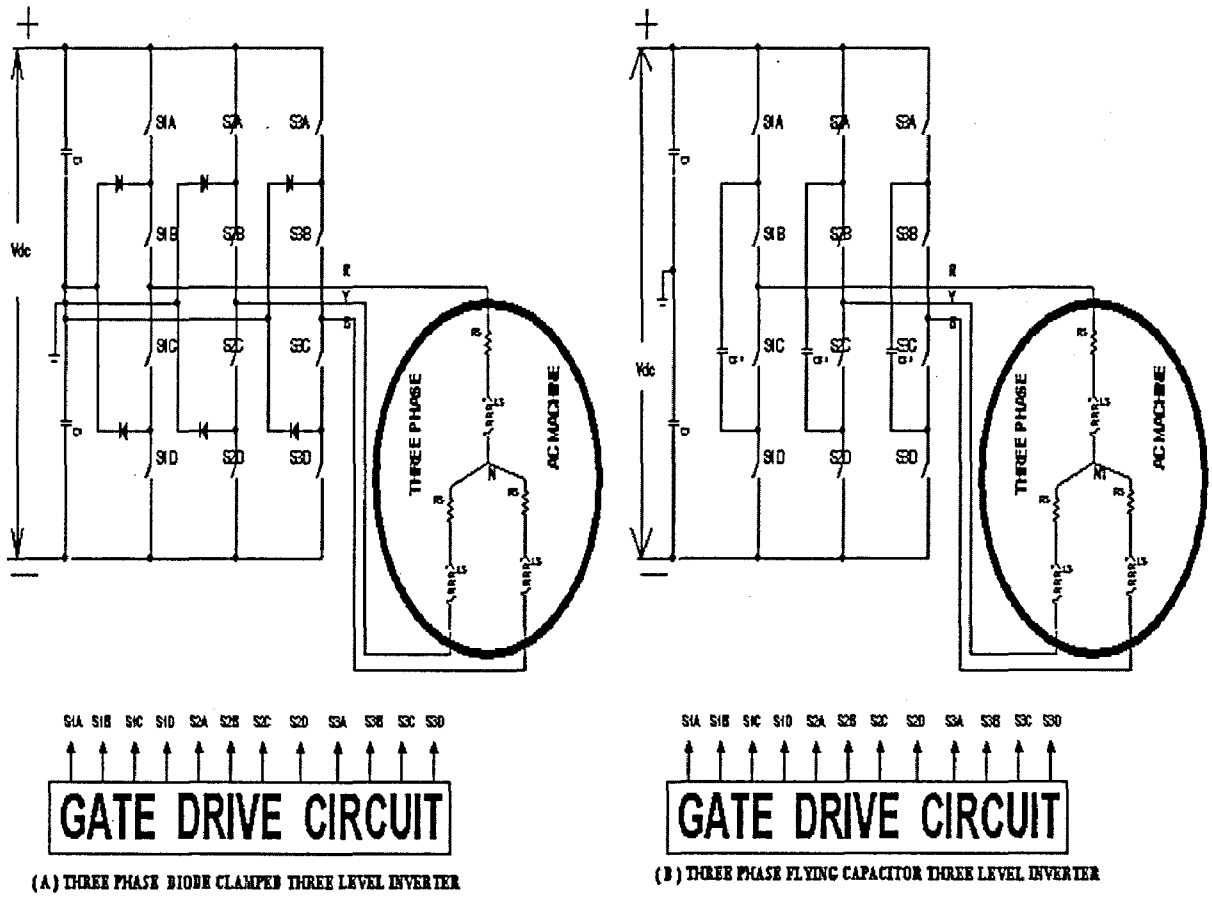

(A) THREE PHASE DIODE CLAMPED THREE LEVEL INVERTER

(B) THREE PHASE FLYING CAPACITOR THREE LEVEL INVERTER

FIG. 2.9

This thesis provides new and original interactive system models for Three Phase DCTLI and FCTLI, a circuit schematic of which is shown in Fig.2.9.

2.10 Induction Motor Drive

Reference 11 and 24 provides models for three phase ac line fed IM using flux linkage equations and also using the dq0 equivalent circuit in the stationary reference frame. Reference 11 provides models for three phase continuous current mode inverter fed IM

drive, models for open loop volts/hertz control and Field oriented control. Reference 24 provides models for open loop volts/hertz control and indirect vector control of three phase IM drives. Reference 25 and 26 provide modelling of three phase IM using dq-axis voltage - current equations in synchronous frame of reference. Power semiconductor switches in the three phase VSI are modelled using dynamic node technique in which each switch is a binary resistance of HIGH value in the OFF state and LOW value in the ON state. Reference 27 provides model for three phase ac line fed IM drive using dq0-axis current equations. The model takes voltage or current as input and gives speed and electromagnetic torque as output. Internal resistance of the power source is considered. The torque expression and dq-axis flux linkage expressions in terms of dq-axis currents are used for modelling torque of the motor. Reference 28 provides the modelling of three phase ac line start IM using dq0-axis voltage – current equations in stationary reference frame. The dqo-axis voltage – current equations in stationary frame in terms of machine parameters is brought to the state space form and then the model is implemented. Simulation results for two cable resistances of the power supply are provided.

This thesis provides interactive models for three phase ac line fed IM in the open loop using dq0 voltage – current equations and also using dq0 flux linkage equations in state space, both cases in all reference frames. This is followed by models for three phase SINE, HI, THI and CS PWM inverter fed IM drive.

2.11 Permanent Magnet Synchronous Motor Drives

PMSM drives are inverter driven. Inverter switching is by rotor position sensing [19 - 21]. Models for three phase PMSM drive which have a sinusoidal back emf is only presented. Digital computer models for six step continuous and discontinuous conduction mode inverter fed PMSM drives are available in the literature [29 – 39, 41 – 44]. Reference 29 provides digital computer model for six step continuous current mode inverter fed PMSM drive in the rotor reference frame. Sinusoidal back emf for the PMSM is assumed. The phase or switching angle of the inverter voltage can be varied relative to the rotor position. Expression for phase advance angle for maximum torque of PMSM is derived. Advancing the phase of the stator voltage advances the

phase of the fundamental component of the stator current relative to phase voltage. Steady state harmonic current and torque calculation is also given. It is shown that the average steady state torque is maximised by phase advancing the stator phase voltage relative to the rotor position. Reference 30 and 31 provides modelling of a vector controlled six step inverter fed PMSM drive with hysteresis current control. Both simulated waveform using the digital computer and experimental waveforms are given. Reference 32 provides the modelling of six step inverter fed PMSM using state space approach to determine the initial conditions. The modelling equations of the PMSM in dq-axis rotor frame is first expressed in state space form **x_dot = A.x + B.u** and solved in time domain to obtain the initial conditions of PMSM rotor. Then Runga-Kutta method is used to solve the governing differential equations of the PMSM in MATLAB. Improved accuracy is possible as initial conditions of the PMSM is considered. In reference 33, Electronically Commutated Motor (ECM) also known BLDCM is modelled using digital computer. Sinusoidal flux distribution is assumed and the modelling solution is carried out for both six step 180 degree mode and 120 degree mode inverter fed ECM with switching angle advancing facility. The flow chart for executing the modelling equations of ECM using DEC VAX 11/780 digital computer is also given. Simulation results are given for varying switching angle advance. In reference 34 the digital computer modelling of the six step 120 degree mode inverter fed brushless dc motor is presented. Sinusoidal back emf is assumed. Six distinct equal switching intervals (SI - I to VI) are defined, starting from ($-30 - \varphi$) to ($330 - \varphi$), where φ is the firing angle or switching angle advance in radians. This value of φ can be varied by appropriate switching of the inverter. The stator current in phase b for the switching interval SI-II is plotted by simulation for various rotor speed. In reference 35, additionally the abc axis voltages when phase b current is zero i.e. for SI - II is transformed to dq-axis voltages in rotor frame. This dq-axis voltage is then integrated over the SI – II range which is ($30 - \varphi$) to ($90 - \varphi$) and then divided by $\pi/3$ to get the average value of dq-axis voltages. These average values of dq-axis voltages are then substituted in the machine model in rotor frame and the average model is developed using various gain blocks. In reference 36 to 39, the model of a three phase inverter fed BLDCM with sinusoidal flux distribution is developed along an arbitrary axis called γ-δ axis. The sensorless method uses the difference between detected actual state variable and the estimated state variable calculated using the motor model in the controller. The

results using DSP controller are given which confirms the validity of the proposed method. References 40 to 43 discuss modelling of six step 120 degree mode inverter fed PMBLDCM with TRAPEZOIDAL back emf. The stator current waveform is rectangular. The mutual inductance between stator and rotor is non-sinusoidal. The analysis is done in the abc axis. In reference 43, in addition PID controller is used and the simulation is developed using MATLAB M file. Reference 44 gives the modelling of six step inverter fed PMSM drive with sinusoidal back emf in the closed loop with PID controller under transient load torque disturbance. Simulation results using SIMULINK are given.

In this thesis the modelling of six step continuous and discontinuous conduction mode inverter fed PMSM drive in the open loop for various switching advance angle are given. The parameters for modelling are obtained by experiment on six step Lybotec inverter fed PMSM drive in the CEMPE laboratory.

CHAPTER 3

LIBRARY MODELS FOR AC TO DC CONVERTERS

3.1 Introduction

In this chapter, building library modules for ac to dc converters also known as rectifiers are presented. Rectifier circuits use either diodes or thyristors (SCRs). Modern rectifiers use BJTs, MOSFETs, IGBTs and GTOs. Here library system models for single phase FWDBR, FWCBR using SCRs and Three Phase FWDBR are developed. Switching function concept is used in developing these models. These library modules have pop-up-menu or dialog box where the required data relating to the ac to dc converter is entered by the user. These system models use Simulink blocks which solves the governing equations relating to the relevant ac to dc converter. No semiconductor circuit component is used in the model.

3.2 Single Phase Full Wave Diode Bridge Rectifier

The single phase FWDBR circuit schematic is shown in Fig.3.1 [14 – 18]. The resistive load or RLE load selection using SS1 is shown for convenience only. During the positive half cycle of VS, diodes D1 and D2 conduct from 0 to π and during the negative half cycle diodes D3 and D4 conduct from π to 2π The essential derivations of the output voltage are given below for purely resistive load [14].

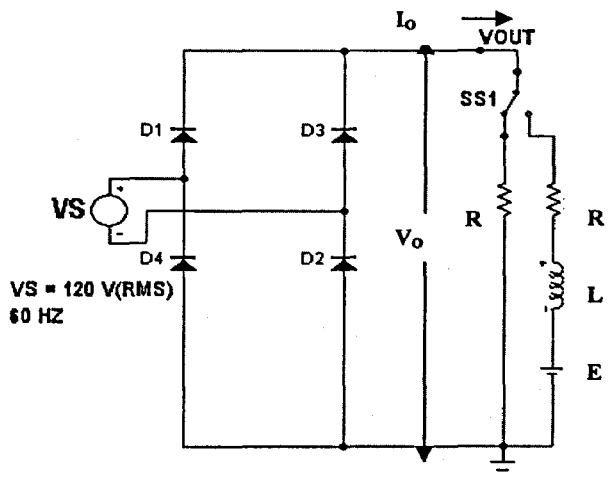

FIG.1: SINGLE PHASE DIODE BRIDGE RECTIFIER

$$V_{O\_avg} = \frac{1}{\pi}.\int_{0}^{\pi} V_m .\sin(\omega t).d(\omega t) = \frac{2V_m}{\pi} \qquad (3.1)$$

$$I_{O\_avg} = \frac{V_{dc}}{R} \qquad (3.2)$$

$$V_{O\_rms} = \left[\frac{1}{\pi}\int_{0}^{\pi}\left[V_m^2 .\sin^2(\omega t).d(\omega t)\right]\right] = \frac{V_m}{\sqrt{2}} \qquad (3.3)$$

$$I_{O\_rms} = \frac{V_{rms}}{R} \qquad (3.4)$$

The output voltage derivations are done below for RLE load [14].

$$L\frac{di_O}{dt} + R.i_O + E = \sqrt{2}.V_m \sin(\omega t) \qquad (3.5)$$

The solution gives the following

$$i_O = \frac{\sqrt{2}V_m}{Z}.\left[\sin(\omega t-\theta)+\frac{2}{1-e^{-(R.\pi)/(L.\omega)}}.\sin(\theta).e^{-(R.t/L)}\right]-\frac{E}{R} \qquad (3.6)$$

for $0 \le (\omega t-\theta) \le \pi$ *and* $i_O \ge 0$

3.2.1 Library Model for Single Phase FWDBR with Purely Resistive or with RLE Load

The system model for the single phase FWDBR is shown in Fig.3.2. The purely resistive or RLE load selection is combined in one model. The various dialog boxes are shown in Fig.3.3, where user can enter the appropriate data required. One model can be used for different system parameters. In Fig.3.2, the selector switch can be double clicked to select either purely resistive load or RLE load option. The value of the Line to neutral RMS voltage, frequency, the value of RLE loads used and/or that of purely resistive load used are entered in the appropriate dialog boxes in Fig.3.3. These values are tabulated in TABLE 3.1 [14].

TABLE 3.1

SL.NO.	PARAMETER	VALUE
1	Line to Neutral RMS Voltage	120 Volts
2	Supply Frequency	60 Hz
3	RLE Load	2.5 Ohms, 6.5e-3 H, 10 Volts
4	Purely Resistive Load	25 Ohms

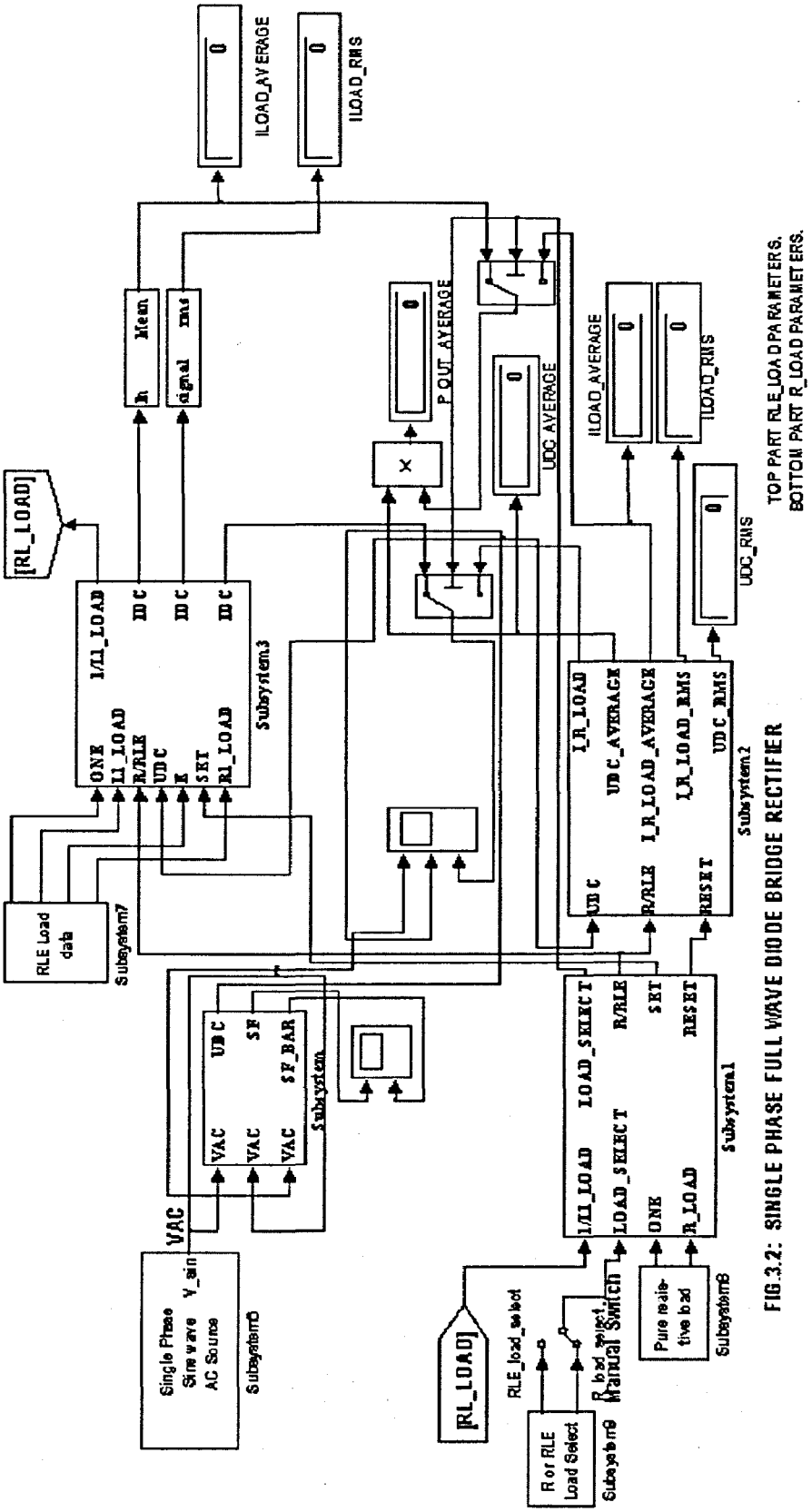

FIG.3.2: SINGLE PHASE FULL WAVE DIODE BRIDGE RECTIFIER

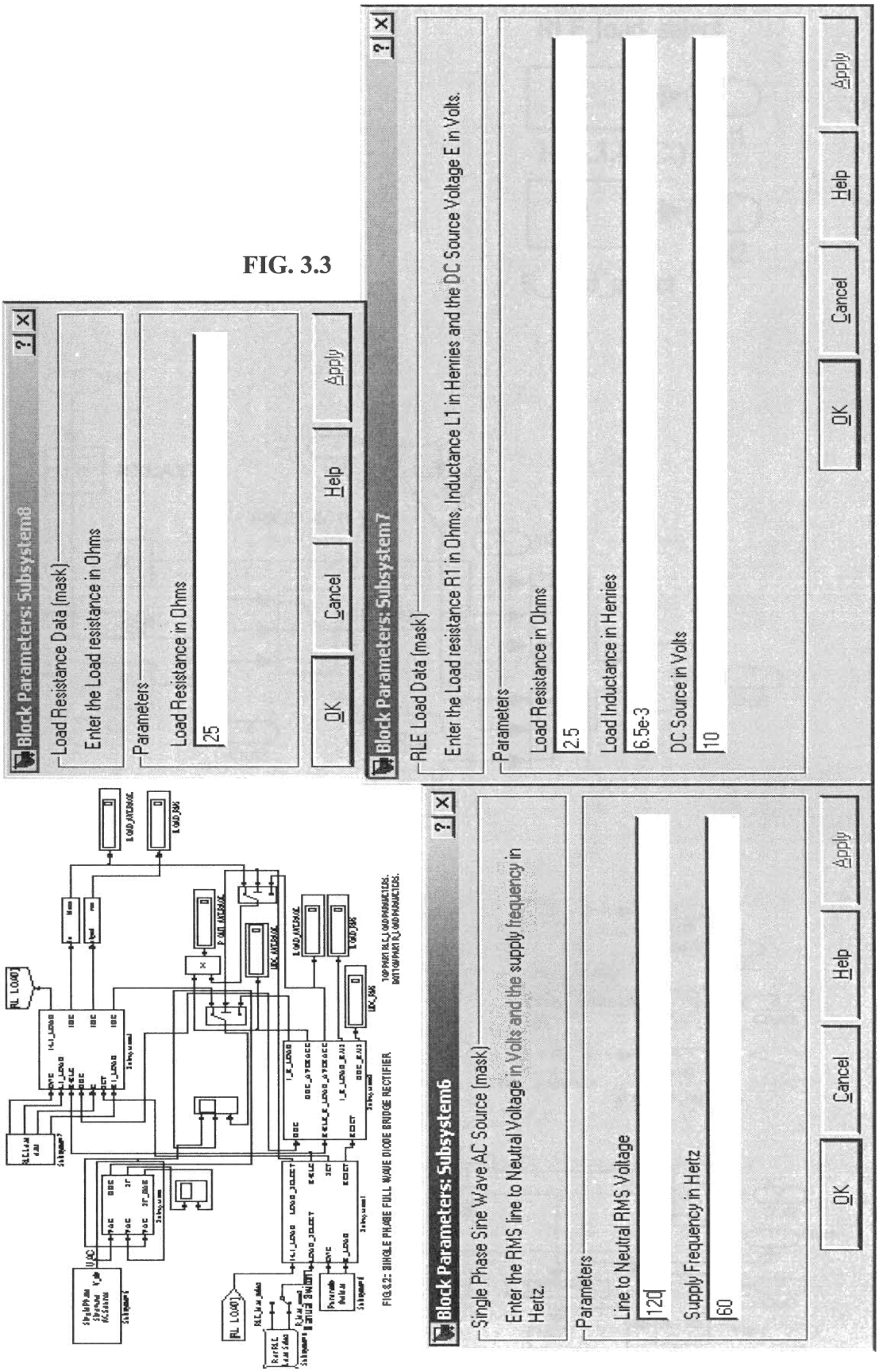
Block Parameters: Subsystem8
Load Resistance Data (mask)
Enter the Load resistance in Ohms
Parameters
Load Resistance in Ohms
25
OK
Cancel
Help
Apply
Block Parameters: Subsystem7
RLE Load Data (mask)
Enter the Load resistance R1 in Ohms, Inductance L1 in Henries and the DC Source Voltage E in Volts.
Parameters
Load Resistance in Ohms
2.5
Load Inductance in Henries
6.5e-3
DC Source in Volts
10
OK
Cancel
Help
Apply
Block Parameters: Subsystem6
Single Phase Sine Wave AC Source (mask)
Enter the RMS line to Neutral Voltage in Volts and the supply frequency in Hertz.
Parameters
Line to Neutral RMS Voltage
120
Supply Frequency in Hertz
60
OK
Cancel
Help
Apply

FIG. 3.3

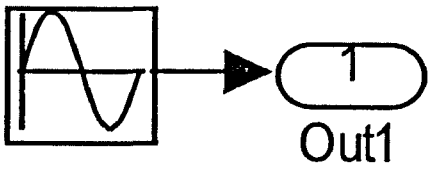

FIG.3.4(A)

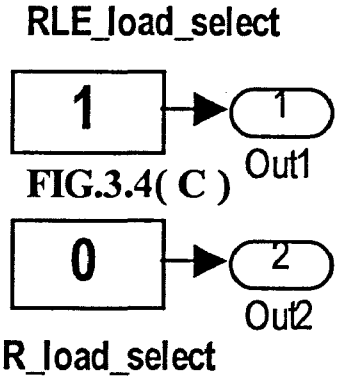

FIG.3.4(C)

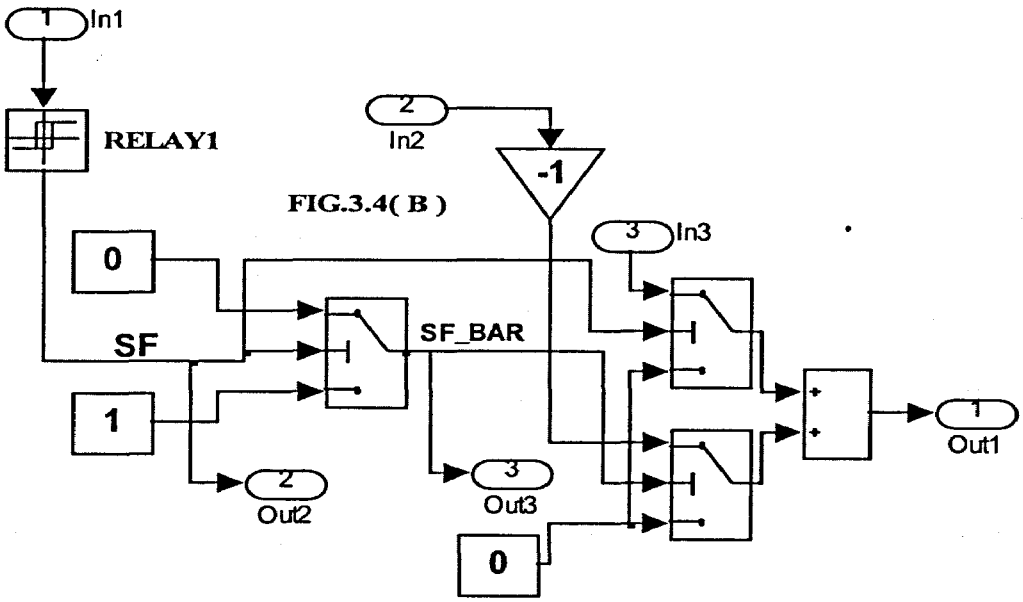

FIG.3.4(B)

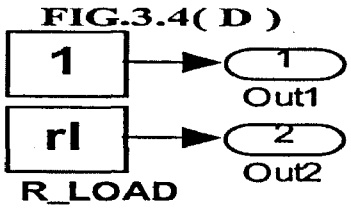

FIG.3.4(D)

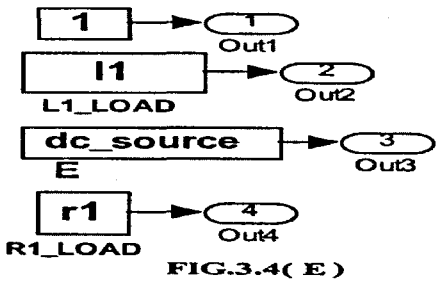

FIG.3.4(E)

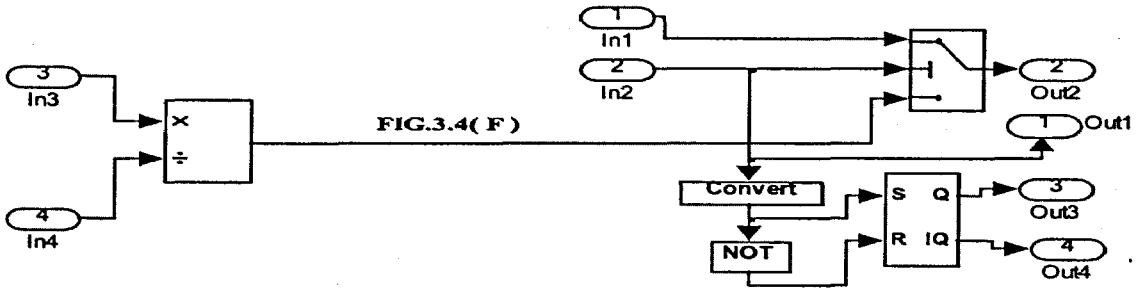

FIG.3.4(F)

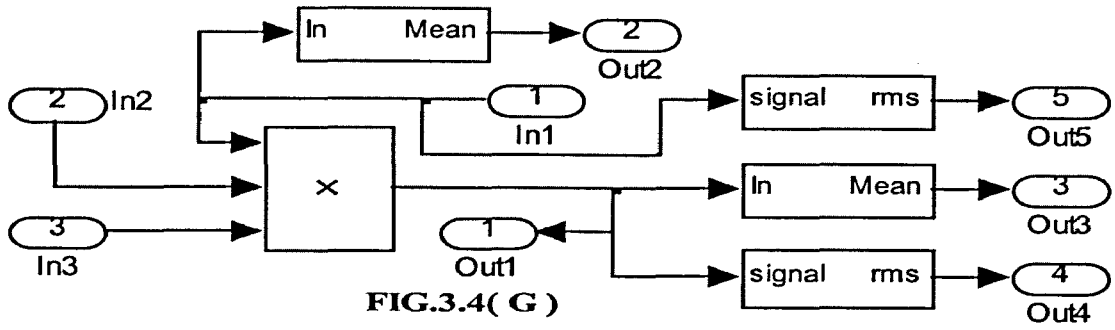

FIG.3.4(G)

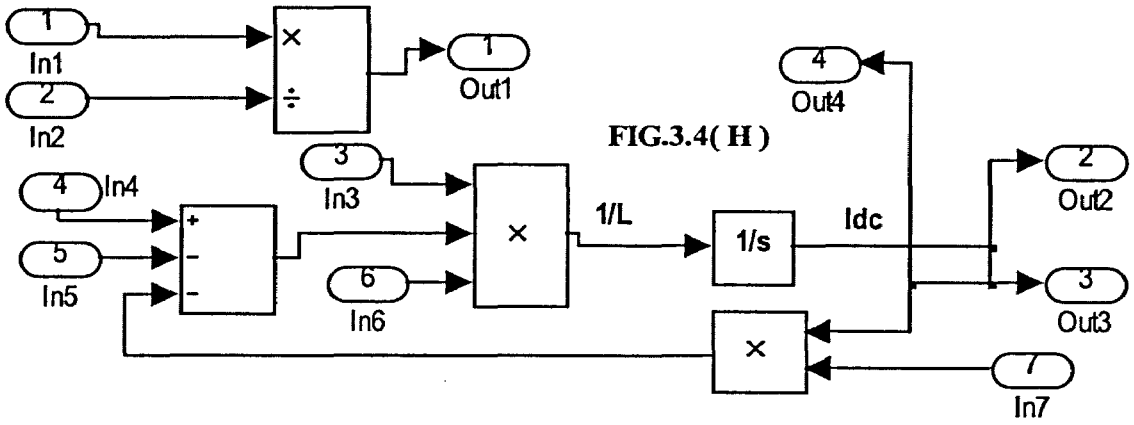

FIG.3.4(H)

The various subsystem of the above model are shown in Fig.3.4(A) to (H). These are briefed below.

The single phase sine wave ac source in Fig.3.4(A) is from sources block set in the Simulink block. The dialog box for this is shown in Fig.3.3. The line to neutral RMS voltage in volts and the frequency in Hertz are entered in this dialog box. This line to neutral RMS voltage and frequency are internally multiplied by 1.414 and 2π respectively. This sine wave output is given to relay1 in Fig.3.4(B). The output of relay1 is the switch function SF. The inverse switch function SF_BAR is generated using a switch from signal routing block set. SF and SF_BAR are defined below:

$$SF = \begin{cases} 1 & for \quad 0 \le \omega t \le \pi \\ 0 & for \quad \pi \le \omega t \le 2\pi \end{cases} \qquad (3.7)$$

$$SF\_BAR = \begin{cases} 0 & for \quad 0 \le \omega t \le \pi \\ 1 & for \quad \pi \le \omega t \le 2\pi \end{cases} \qquad (3.8)$$

The switch generating SF_BAR has 0 and 1 as its first (u(1)) input and third (u(3)) input respectively, while the second (u(2)) input is SF. This switch threshold is 0.5. This switch output is u(1) when input u(2) is greater than or equal to threshold value, else output is u(3). SF and SF_BAR are given to the input u(2) of the top and bottom switch respectively in Fig.3.4(B). The u(1) input to top switch is the ac supply voltage while that for the bottom switch is negative of this supply voltage. The u(3) input to top and bottom switches are both zero. The threshold values for top and bottom switches are both 0.5. This top and bottom switches operate in the same way as the switch generating SF_BAR. The output of the top and bottom switches are added using the sum block. The output of this sum block is the rectified dc output voltage Udc.

Referring to Fig.3.4(B), the output voltage of the sum block Udc can be expressed as follows:

$$\left.\begin{aligned} U_{dc} &= \left[\left(SF.Vs + SF\_BAR.\left(-V_S\right)\right)\right] \\ &= V_S \quad for \quad 0 \le \omega t \le \pi \\ &= -V_S \quad for \quad \pi \le \omega t \le 2\pi \end{aligned}\right| \quad (3.9)$$

In equation 3.9, Vs is the sine wave input.

The type of load select module shown in Fig.3.4(C) has two constants 1 and 0 as input to the SPDT switch. Double clicking the SPDT switch in Fig.3.2, selects either the purely resistive load or the RLE load.

Fig.3.4(D) and (E) corresponds to the dialog box for Load resistance data and the RLE Load Data respectively, shown in Fig.3.3.

If SPDT switch is thrown to 0, then purely resistive load R_LOAD is selected. Referring to Fig.3.4(D), (F) and (G), it is seen that the value of Udc/(R_LOAD) is calculated. The set-reset latch enables the bottom display in Fig.3.2. The RMS value of load voltage Udc, the mean and RMS value of load current are displayed.

If SPDT switch is thrown to 1, then RLE load is selected. Referring to Fig.3.4(E), (F) and (H), it is seen that the value of load current Idc is calculated using the equation

3.2.5. The set-reset latch enables the top display in Fig.3.2. The RMS and average value of load voltage Udc, the mean and RMS value of load current and the average power output are displayed.

3.2.2 Simulation Results

The simulation of the model for single phase FWDBR using ode15s(Stiff/NDF) solver for data given in TABLE 3.1, for purely resistive load and RLE load were conducted. The simulation results for purely resistive load is shown in Fig.3.5(A) to (C) and that for RLE load is shown in Fig.3.6(A) to (C).. The meter reading observed are tabulated in TABLE 3.2 for both cases.

TABLE 3.2

Sl.No.	Type of Load	Udc(RMS) Volts	Udc(AVG) Volts	I_load(RMS) Amps	I_load(AVG) Amps	P_out Watts
1	R only	120	108	4.799	4.321	466.8
2	RLE	120	108	40.3	39.21	4235

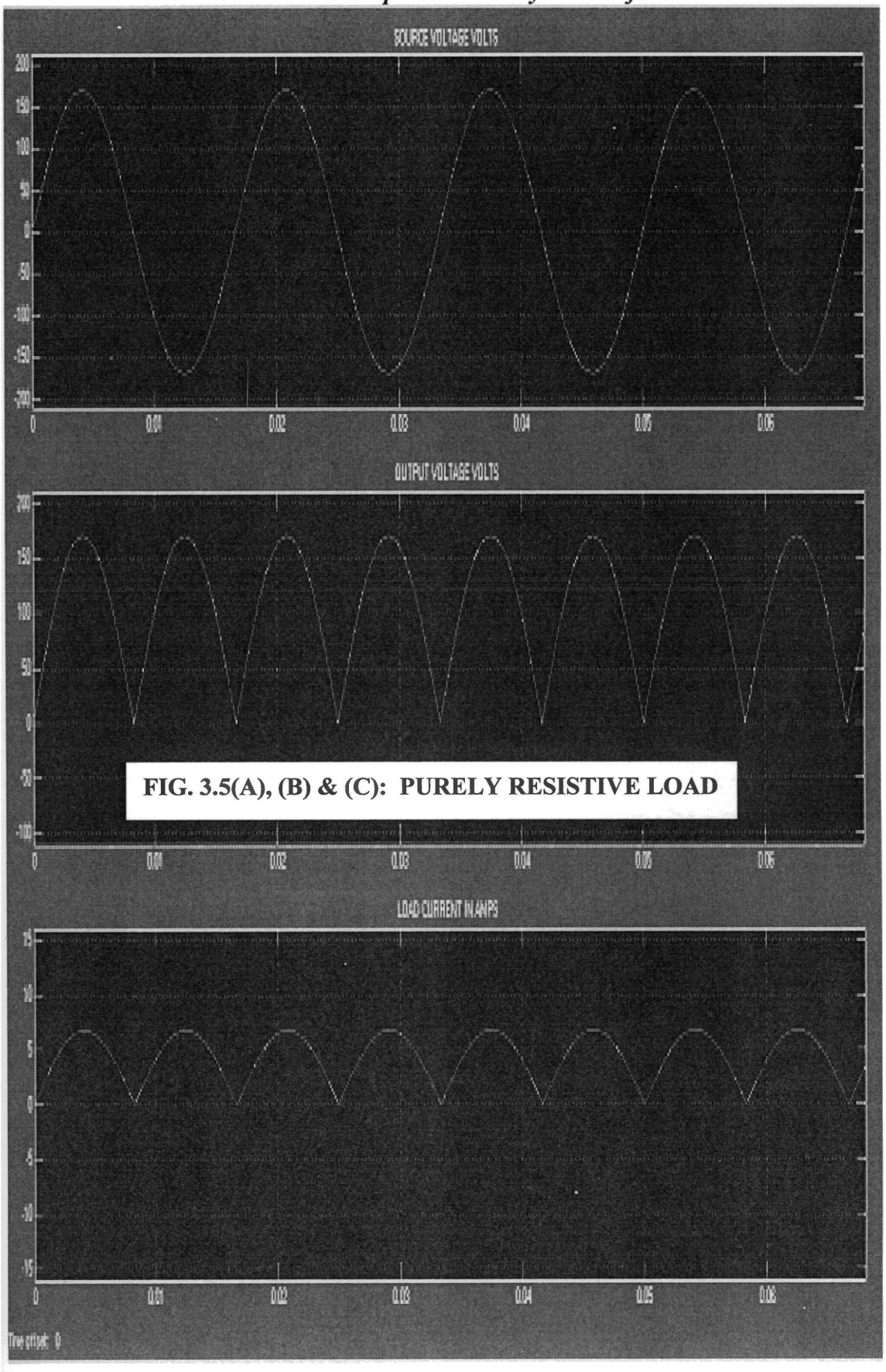

FIG. 3.5(A), (B) & (C): PURELY RESISTIVE LOAD

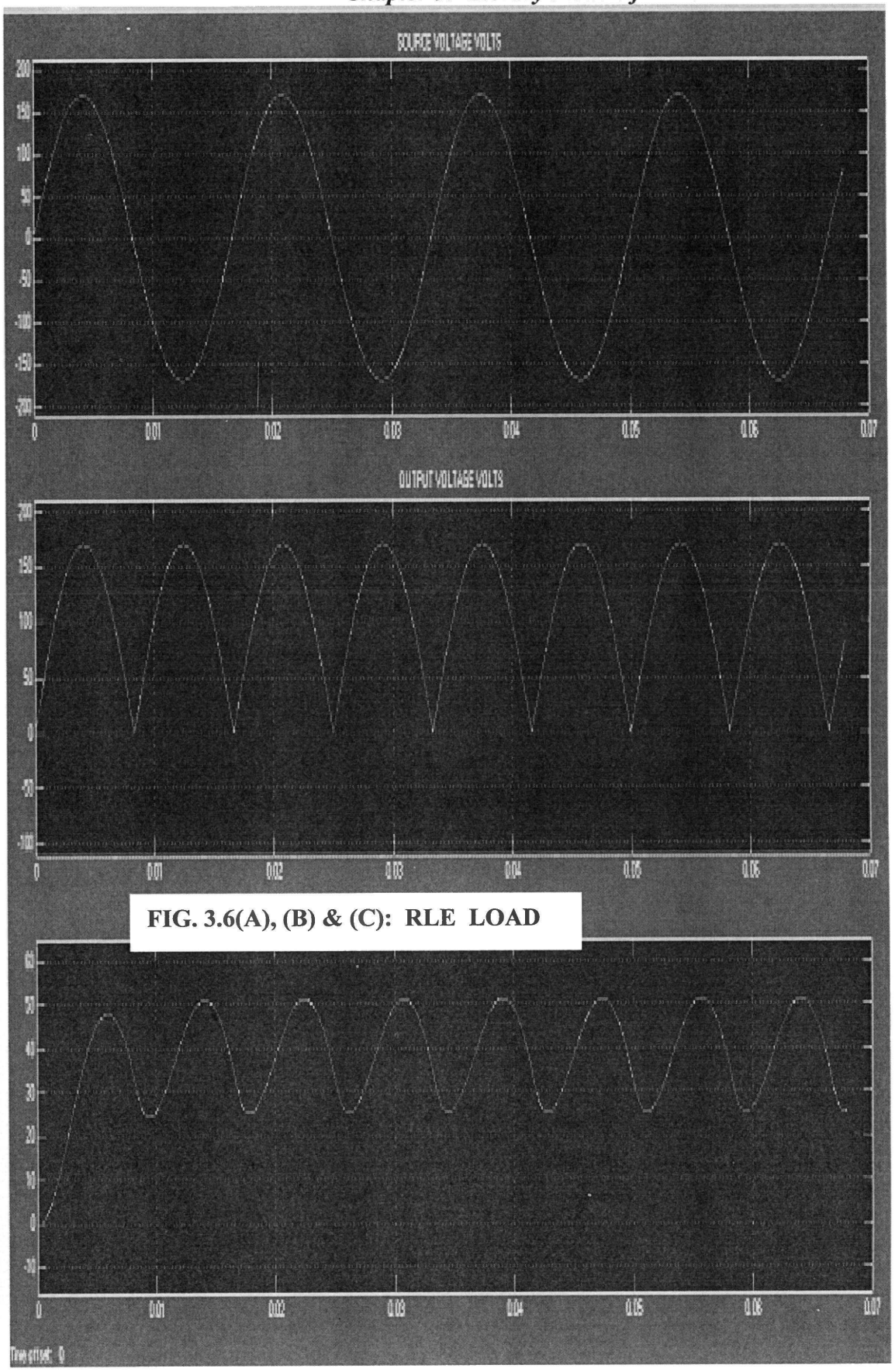

FIG. 3.6(A), (B) & (C): RLE LOAD

3.3 Single Phase Full Wave SCR Bridge

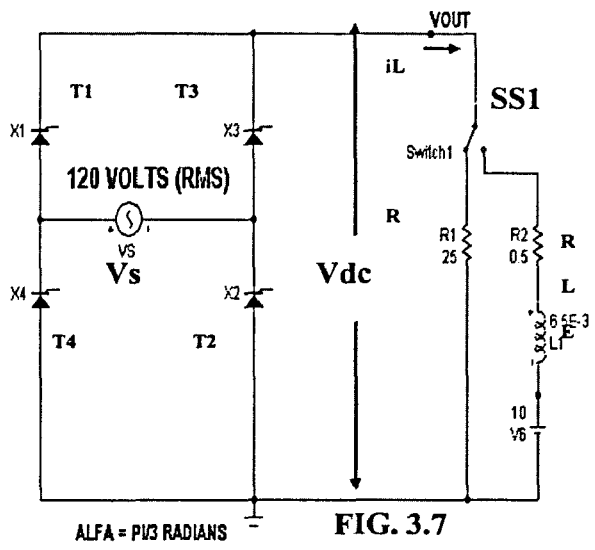

FIG. 3.7

: SINGLE PHASE FULL WAVE SCR BRIDGE RECTIFIER

The single phase full wave SCR bridge rectifier is also known as single phase full wave controlled bridge rectifier, represented as FWCBR [14 – 18]. This is shown in Fig.3.7. Assuming pure resistive load, during the positive half cycle of VS, thyristors T1 and T2 are fired at an angle α and conduct from α to π. During the negative half cycle of VS, thyristors T3 and T4 are fired at angle (π +α) and conduct from (π +α) to 2π. Thus by varying the firing angle α, the average voltage across the load can be varied. The library system model for this FWCBR is developed combining the purely resistive load and RLE load in one model. For RLE load, continuous load current conduction is assumed. In this case with RLE load, thyristors T1 and T2 conduct from α to (π +α) when fired at an angle α during the positive half cycle of VS and thyristors T3 and T4 conduct from (π +α) to (2π +α), when fired at an angle (π +α) during the negative half cycle of VS. This model can be used for continuous conduction mode only with RLE load.

The essential derivation for output voltage and load current is done below for purely resistive load.

$$V_{dc} = \frac{1}{\pi}.\left[\int_{\alpha}^{\pi} V_m .\sin(\omega t).d(\omega t)\right] = \frac{V_m}{\pi}.[1 + \cos(\alpha)] \qquad (3.10)$$

$$V_{rms} = \sqrt{\frac{1}{\pi}.\left[\int_{\alpha}^{\pi} V_m^2 .\sin^2 \omega t.d(\omega t)\right]} = \frac{V_m}{\sqrt{2}} * \left|\sqrt{1 - \frac{\alpha}{\pi} + \frac{\sin 2\alpha}{2\pi}}\right| \qquad (3.11)$$

$$Average \quad Input \quad power \quad P_{in} = \frac{1}{\pi R}.\left[\int_{\alpha}^{\pi} \left(V_m .\sin(\omega t)\right)^2 .d(\omega t)\right] \qquad (3.12)$$

$$= \frac{V_m^2}{2R}.\left[\left(1 - \frac{\alpha}{\pi}\right) + \frac{\sin 2\alpha}{2\pi}\right] \qquad (3.13)$$

The essential derivation for output voltage and load current is done below for RLE load.

$$V_{dc} = \frac{1}{\pi}.\left[\int_{\alpha}^{\pi+\alpha} V_m .\sin(\omega t).d(\omega t)\right] = \frac{2V_m}{\pi}.\cos(\alpha) \qquad (3.14)$$

$$V_{rms} = \sqrt{\frac{1}{\pi}.\left[\int_{\alpha}^{\pi+\alpha} V_m^2 .\sin^2(\omega t).d(\omega t)\right]} = \frac{V_m}{\sqrt{2}} \qquad (3.15)$$

$$L\frac{di_L}{dt} + Ri_L + E = \sqrt{2}.V_m.\sin(\omega t) \quad \text{for} \quad i_L \geq 0 \quad (3.16)$$

The solution is

$$i_L = \frac{\sqrt{2}V_m}{Z}.\sin(\omega t - \theta) - \frac{E}{R} + \left[I_{LO} + \frac{E}{R} - \frac{\sqrt{2}V_m}{Z}.\sin(\alpha - \theta)\right].e^{(R/L).(\alpha/\omega - t)} \qquad (3.17)$$

where $I_{LO} = I_{L1}$ *is given by*

$$I_{LO} = I_{L1} = \frac{\sqrt{2}V_m - \sin(\alpha - \theta) - \sin(\alpha - \theta).e^{-(R/L).(\pi/\omega}}{Z..\ (1 - e^{-(R/L).(\pi/\omega)}\ )} - \frac{E}{R} \quad \text{for} \quad I_{LO} \geq 0 \qquad (3.18)$$

3.3.1 Library Model for Single Phase FWCBR with Purely Resistive or with RLE Load

The system model for the single phase FWCBR is shown in Fig.3.8. The purely resistive or RLE load selection is combined in one model. The various dialog boxes are shown in Fig.3.9, where user can enter the appropriate data required. One model can be used for different system parameters. In Fig.3.8, the selector switch can be double clicked to select either purely resistive load or RLE load option. The value of the Line to neutral RMS voltage, frequency, the value of RLE loads used and/or that of purely resistive load used are entered in the appropriate dialog boxes in Fig.3.9. These values are tabulated in TABLE 3.3 [14]. The various subsystem of the above model are shown in Fig.3.10(A) to (I). These are briefed below.

The blocks in Fig.3.10(A) along with the mux and Fcn block in Fig.3.10(B) generates the single phase sine wave ac input V_S. The dialog box for this is shown in Fig.3.9. The line to neutral RMS voltage in volts, the frequency in Hertz and the firing angle α are entered in this dialog box. This line to neutral RMS voltage and frequency

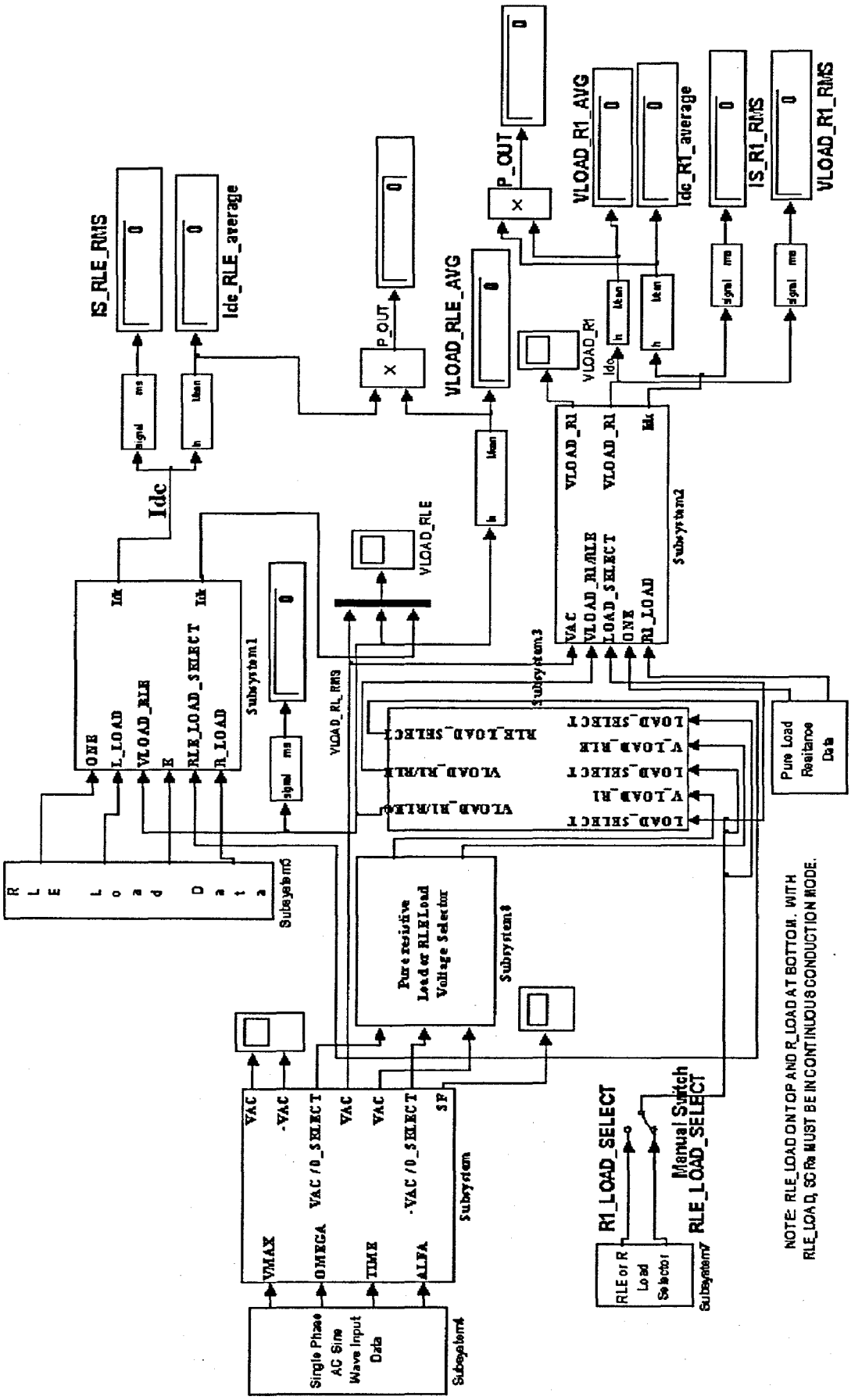

FIG.3.8: SINGLE PHASE FULL WAVE SCR BRIDGE RECTIFIER

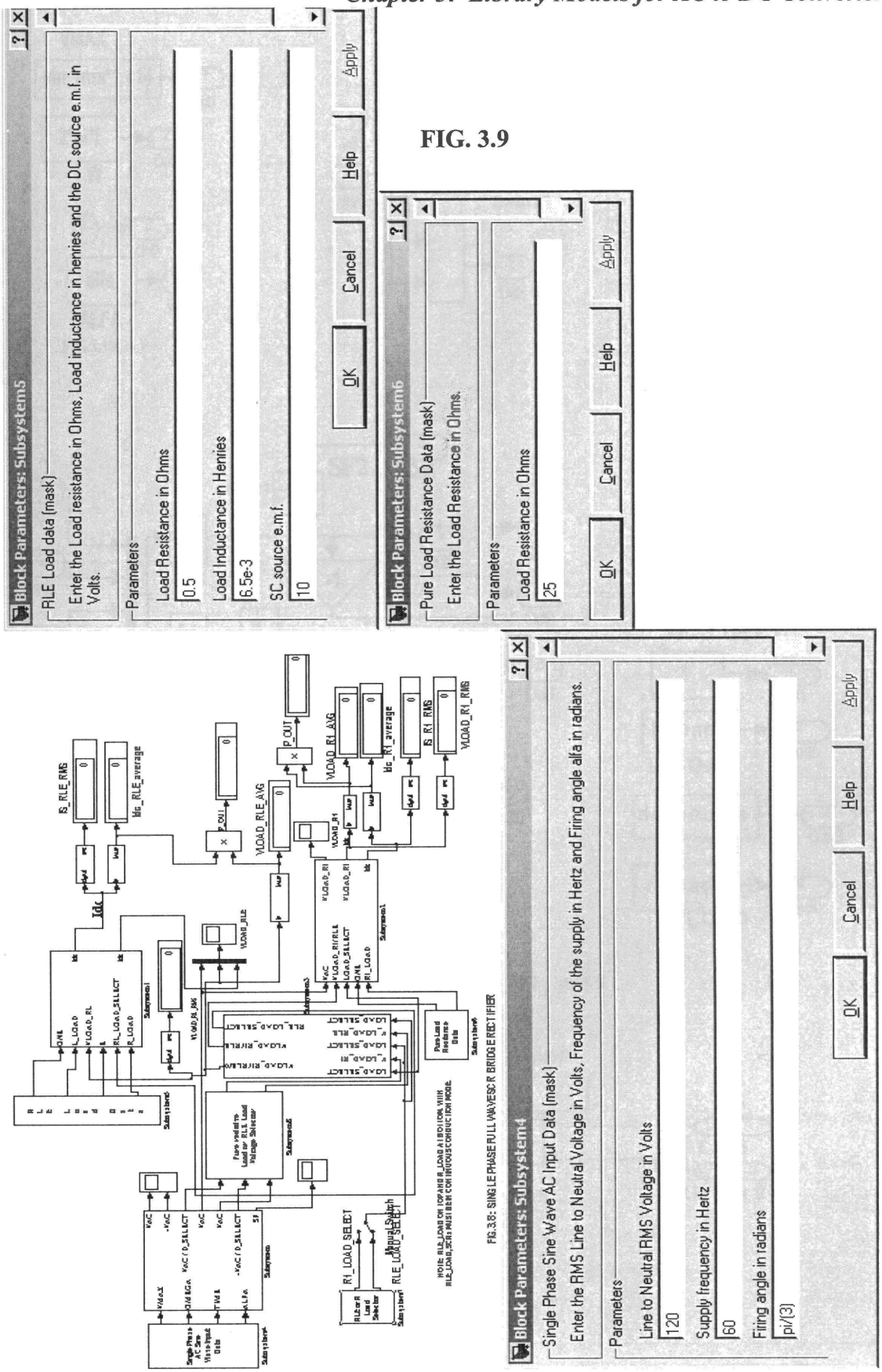
Block Parameters: Subsystem5
RLE Load data (mask)
Enter the Load resistance in Ohms, Load inductance in henries and the DC source e.m.f. in Volts.
Parameters
Load Resistance in Ohms
0.5
Load Inductance in Henries
6.5e-3
SC source e.m.f.
10
OK
Cancel
Help
Apply
Block Parameters: Subsystem6
Pure Load Resistance Data (mask)
Enter the Load Resistance in Ohms.
Parameters
Load Resistance in Ohms
25
OK
Cancel
Help
Apply
Block Parameters: Subsystem4
Single Phase Sine Wave AC Input Data (mask)
Enter the RMS Line to Neutral Voltage in Volts, Frequency of the supply in Hertz and Firing angle alfa in radians.
Parameters
Line to Neutral RMS Voltage in Volts
120
Supply frequency in Hertz
60
Firing angle in radians
pi/[3]
OK
Cancel
Help
Apply

FIG. 3.9

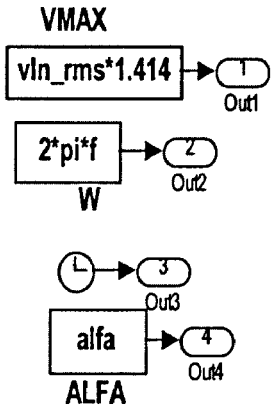

FIG.3.10(A)

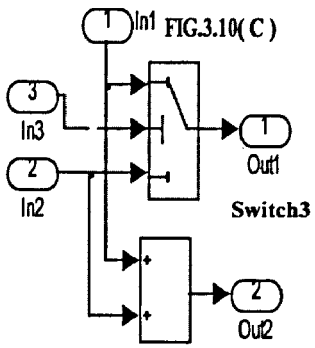

FIG.3.10(C)

FIG.3.10(D)

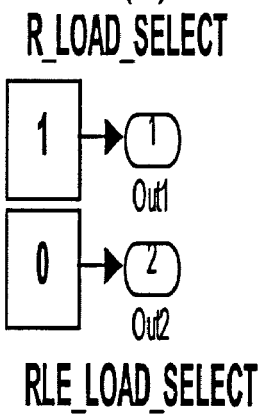

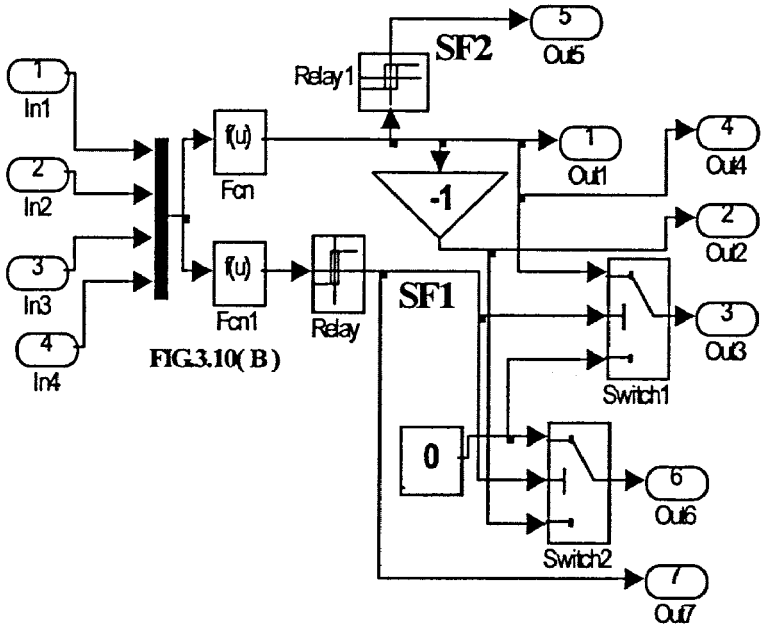

FIG.3.10(B)

FIG.3.10(E)

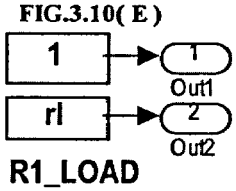

FIG.3.10(F)

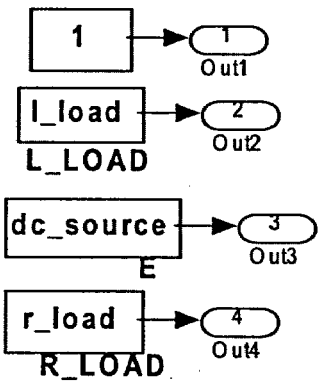

FIG .3.10(G)

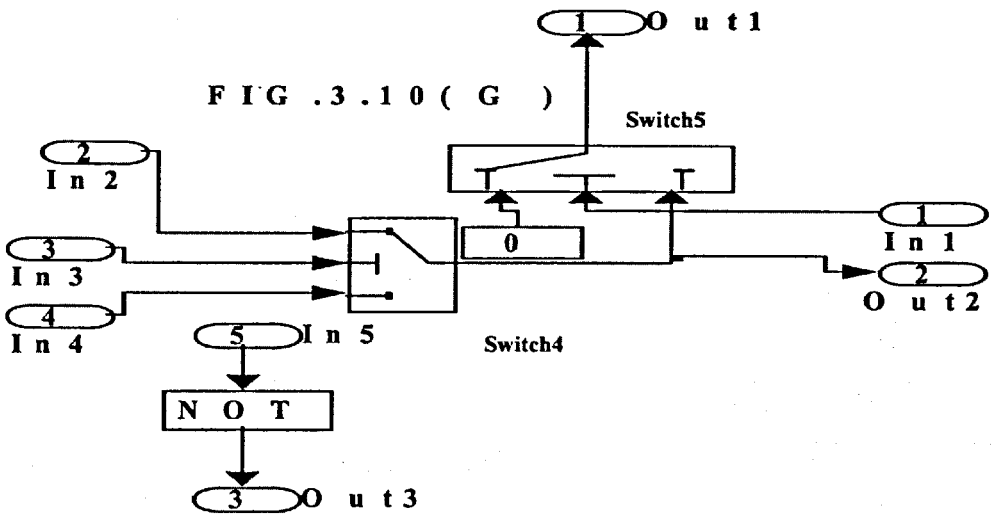

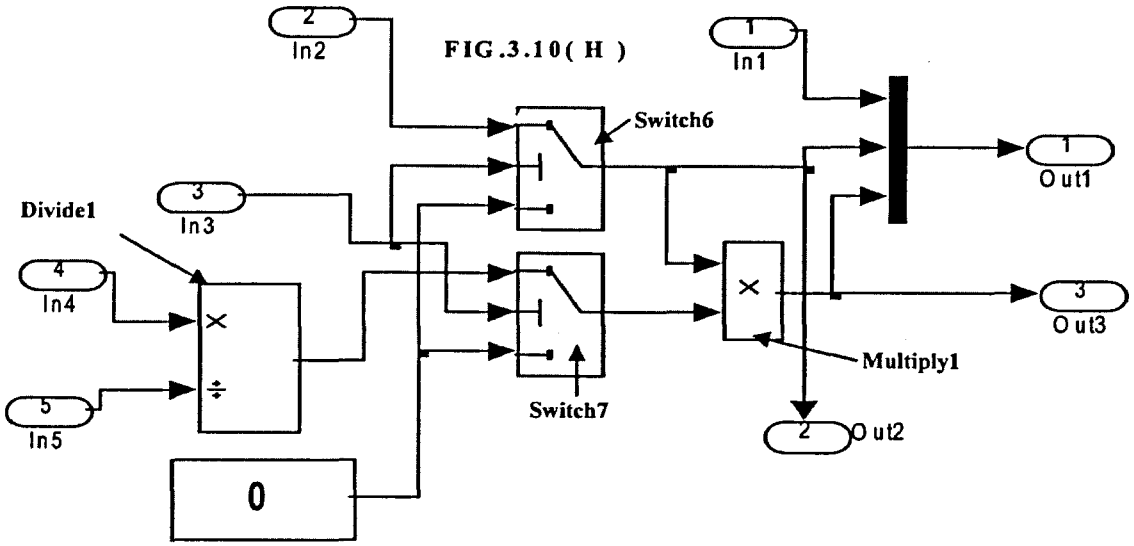

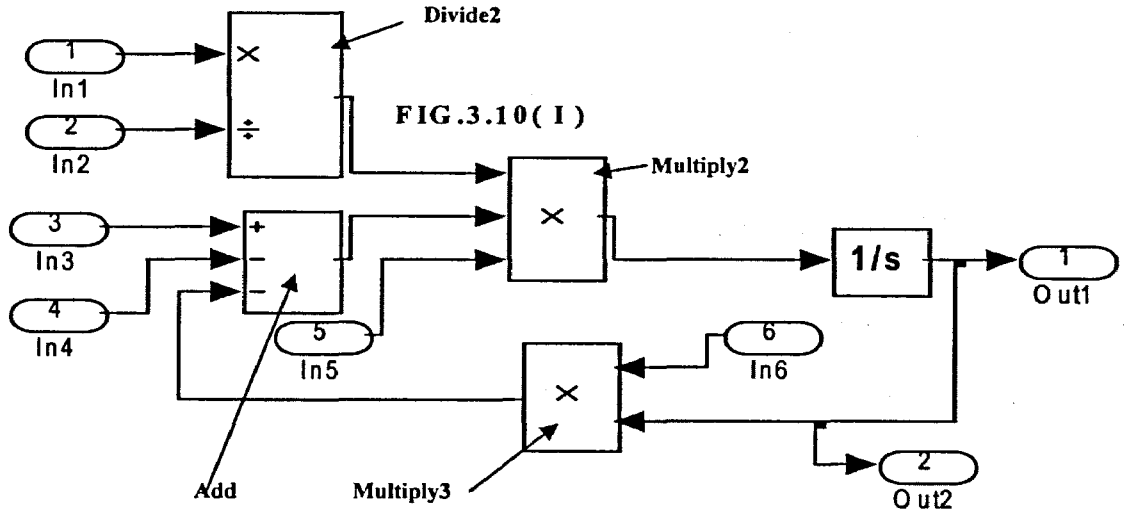

TABLE 3.3

SL.NO.	PARAMETER	VALUE
1	Line to Neutral RMS Voltage	120 Volts
2	Supply Frequency	60 Hz
3	RLE Load	0.5 Ohms, 6.5e-3 H, 10 Volts
4	Purely Resistive Load	25 Ohms
5	Firing angle α	$\pi / 3$ radians

are internally multiplied by 1.414 and 2π respectively. Another Fcn1 block in Fig.3.10(B) generates the delayed sine wave lagging by firing angle α with respect to the input sine wave. The delayed or lagging sine wave is given to relay which generates switch function SF1. This sine wave input voltage is given to relay1 which generates another switch function SF2. The switch function SF1 and SF2 are defined below:

$$SF1 = \begin{cases} 1 \quad for \quad \alpha \leq \omega t \leq (\pi+\alpha) \\ 0 \quad for \quad (\pi+\alpha) \leq \omega t \leq (2\pi+\alpha) \end{cases} \quad (3.19)$$

$$SF2 = \begin{cases} 1 \quad for \quad 0 \leq \omega t \leq \pi \\ 0 \quad for \quad \pi \leq \omega t \leq 2\pi \end{cases} \quad (3.20)$$

The switch1 and 2 has a threshold value of 0.5. The switches operate in the same way as explained in section 3.2.1. Referring to the mode of connection of Switch1 and Switch2 in Fig.3.10(B), the respective output of Switch1 and 2 can be mathematically expressed as follows:

$$Output \quad of \quad Switch1 \quad Out3 = SF1.V_S \quad (3.21)$$

$$Output \quad of \quad Switch2 \quad Out6 = (1 - SF1).(-V_S) \quad (3.22)$$

Switch1 and 2 output are given to u(1) and u(3) and SF2 is given to u(2) in of switch3, in Fig.3.10(C). The threshold for switch3 is 0.5 and operate as explained in section 3.2.1. The output of Switch3 can be expressed mathematically as follows:

$$Output \quad of \quad Switch3 \quad Out1 = SF2\left(SF1.V_S\right)+\left(1-SF2\right).\left(1-SF1\right).\left(-V_S\right) \quad (3.23)$$

The output of Switch3 can be expressed as follows from equations 3.19., 3.20 and 3.23 as follows::

$$Output \quad of \quad Switch3 \quad Out1 = \begin{cases} V_S \quad for \quad \alpha \leq \omega t \leq \pi \\ -V_S \quad for \quad (\pi+\alpha) \leq \omega t \leq 2\pi \end{cases} \quad (3.24)$$

The equation 3.24 represent the output voltage of single phase FWCBR with purely resistive load.

In Fig.3.10(C), the output of the adder or Sum block can be expressed as follows:

$$Output \quad Sum \quad Block \quad = \quad V_S \quad for \quad \alpha \leq \omega t \leq (\pi + \alpha)$$

$$-V_S \quad for \quad (\pi + \alpha) \leq \omega t \leq (2\pi + \alpha) \qquad (3.25)$$

Equation 3.25 represents the output voltage the single phase FWCBR with either RL or RLE load in the **continuous conduction mode.**

The type of load select module shown in Fig.3.10(D) has two constants 1 and 0 as input to the SPDT switch. Double clicking the SPDT switch in Fig.3.8, selects either the purely resistive load or the RLE load.

Fig.3.10(E) and (F) corresponds to the dialog box for Load resistance data and the RLE Load Data respectively, shown in Fig.3.9.

If SPDT switch is thrown to 1, then purely resistive load is selected. Referring to Fig.3.10(E), (G) and (H), it is seen that the load voltage Vdc across purely resistive load appears at the output of Switch4 and switch6, while the value 1/(R1_LOAD) appears at the output of switch7. The multiplier in Fig.3.10(H) calculates the value of load current through the purely resistive load. Switch4, 5, 6 and 7 have a threshold value of 0.5 and operate in the same principle explained above.

RLE load is selected by throwing SPDT to 0. Referring to Fig.3.10(F), (G) and (I), it is seen that Switch4 and Switch5 output Load voltage across RLE load. The Divide2 block calculates 1/(L). The Add block along with Multiply2, Multiply3, Divide2 and integrator block solves equation 3.3.7 to find the load current through the RLE load. Using the NOT gate in Fig.3.10(G) connected to SPDT switch, the upper indicating

meters are enabled for the RLE load and the lower indicating meters are enabled for the purely resistive load.

3.3.2 Simulation Results

The simulation of the single phase FWCBR model was done using ode15s(stiff/NDF) solver, for the data given in TABLE 3.3 , for purely resistive and RLE load. The simulation results for purely resistive load is shown in Fig.3.11(A) to (C) and that for RLE load is shown in Fig.3.12(A) to (C).. The meter reading observed are tabulated in TABLE 3.4 for both cases.

TABLE 3.4: FIRING ANGLE $\alpha = \pi / 3$ RADIANS

Sl.No.	Type of Load	Vdc(RMS) Volts	Vdc(AVG) Volts	I_load(RMS) Amps	I_load(AVG) Amps	P_out Watts
1	R only	107.5	81.07	4.301	3.243	262.9
2	RLE	119.9	54.11	89.86	87.77	4749

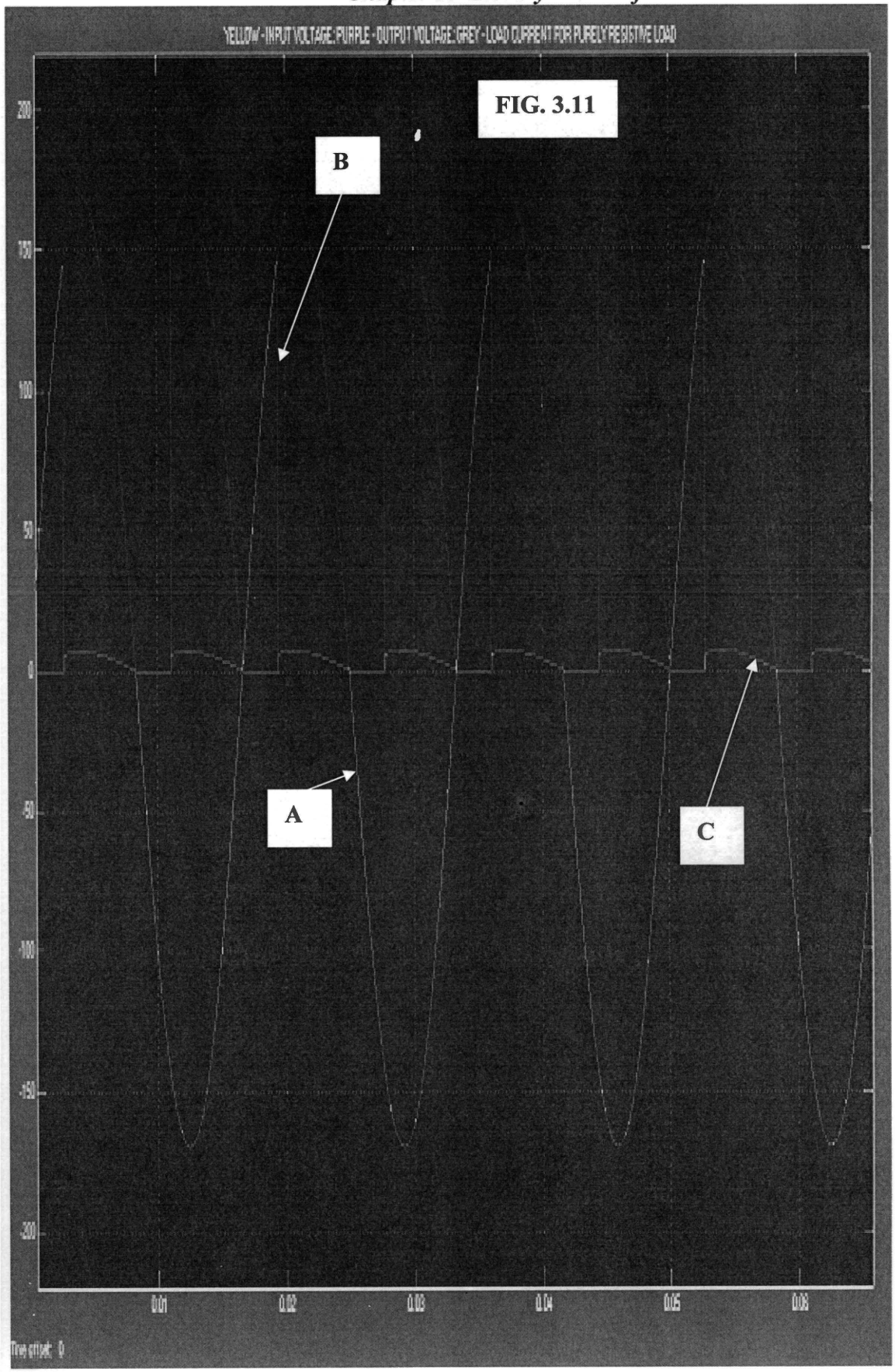
YELLOW - INPUT VOLTAGE : PURPLE - OUTPUT VOLTAGE : GREY - LOAD CURRENT FOR PURELY RESISTIVE LOAD
FIG. 3.11
B
A
C

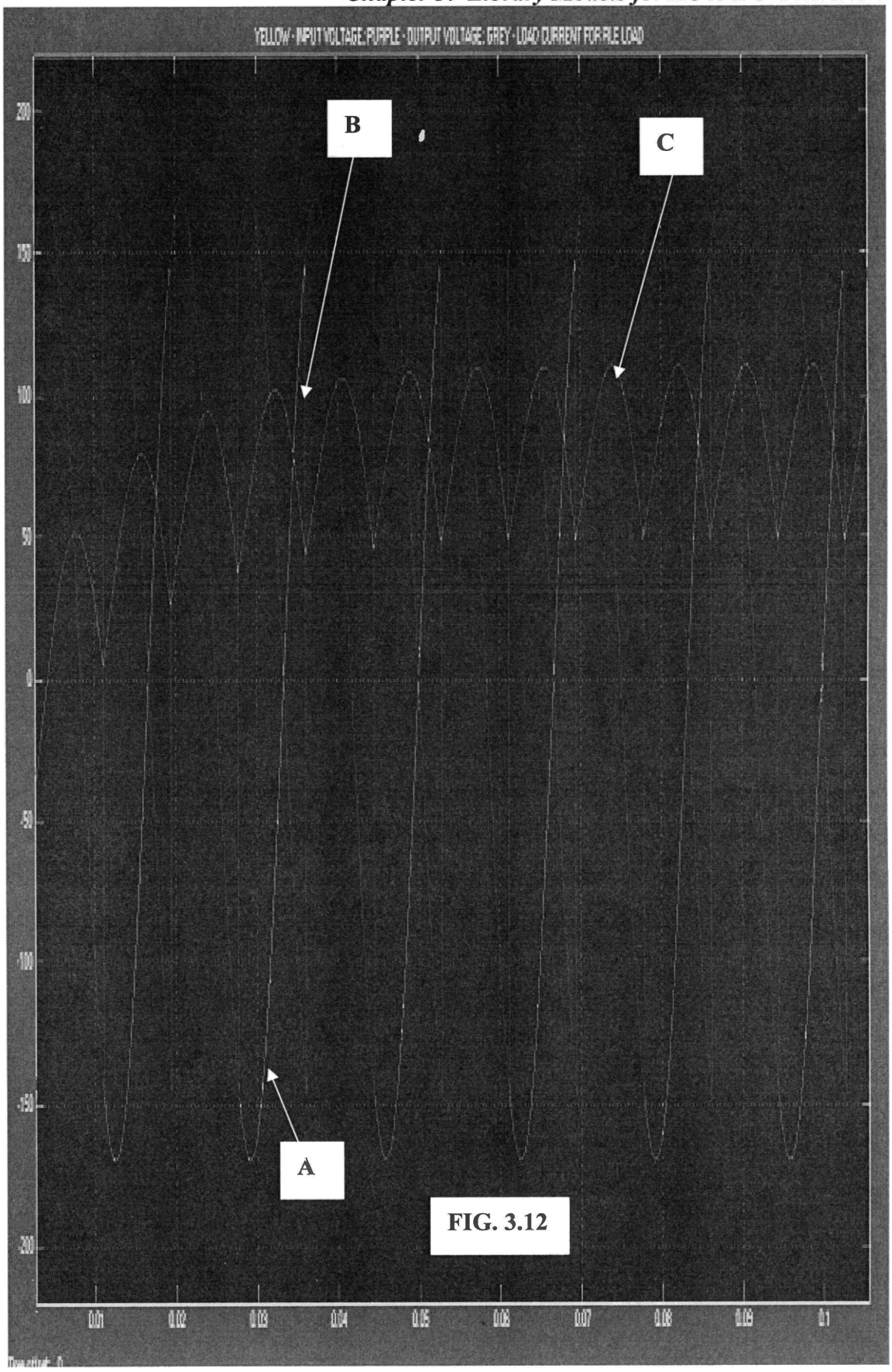
YELLOW - INPUT VOLTAGE; PURPLE - OUTPUT VOLTAGE; GREY - LOAD CURRENT FOR RLE LOAD
B
C
A

FIG. 3.12

3.4 Three Phase Full Wave Diode Bridge Rectifier

The three phase FWDBR schematic is shown in Fig.3.13. It is used for high power app-

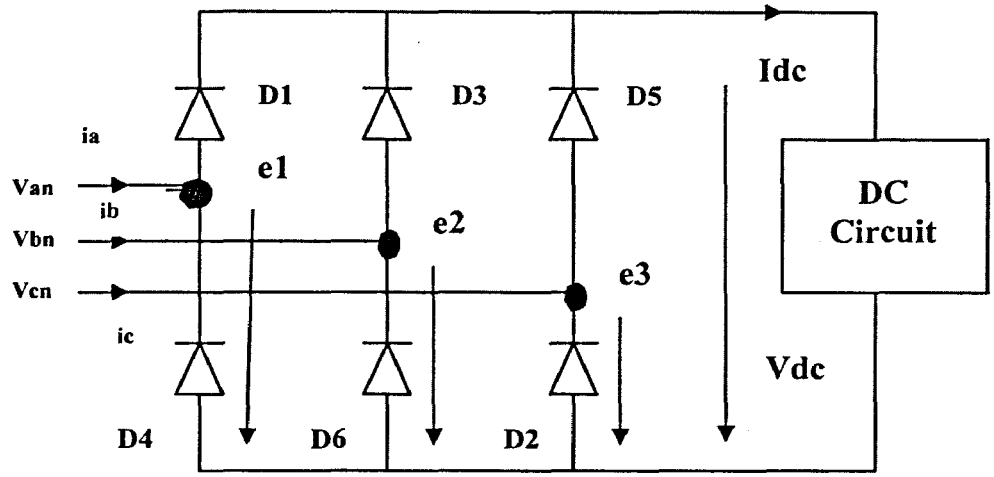

FIG. 3.13: THREE PHASE FWDBR

lications. The diodes are numbered in conduction sequences and each diode conduct for 120 degrees. The conduction sequence for diodes are: D1 – D2, D3 – D2, D3 – D4, D5 – D4, D5 – D6, D1 – D6, D1 – D2 and so on, giving six pulses of ripples at the output voltage. The pair of diodes which are connected between that pair of lines having the highest amount of instantaneous line to line voltage will conduct [14 – 18].

The essential derivation for purely resistive load is done below [14]:.

$$\left.\begin{aligned} V_{an} &= V_m \sin(\omega t) \\ V_{bn} &= V_m \sin(\omega t - 120) \\ V_{cn} &= V_m \sin(\omega t - 240) \end{aligned}\right\} \qquad (3.26)$$

$$\left.\begin{aligned} V_{ab} &= \sqrt{3}\, V_m \sin(\omega t + 30) \\ V_{bc} &= \sqrt{3}\, V_m \sin(\omega t - 90) \\ V_{ca} &= \sqrt{3}\, V_m \sin(\omega t - 210) \end{aligned}\right| \qquad (3.27)$$

The average output voltage Vdc is derived below:

$$V_{dc} = \frac{6}{\pi}.\int_{\pi/6}^{\pi/2} V_m .\sin(\omega t).d(\omega t) = \frac{6}{\pi}.\int_{0}^{\pi/6} \sqrt{3}.V_m .\cos(\omega t).d(\omega t)$$

$$= \frac{3\sqrt{3}.V_m}{\pi} = 1.654.V_m \qquad (3.28)$$

The RMS output voltage Vrms is derived below:

$$V_{rms} = \sqrt{\frac{6}{\pi}.\int_{\pi/6}^{\pi/2} V_m^2 .\sin^2(\omega t).d(\omega t).} = \sqrt{\frac{6}{\pi}.\int_{0}^{\pi/6} 3V_m^2 .\cos^2(\omega t).d(\omega t).}$$

$$= \sqrt{\left(\frac{3}{2} + \frac{9.\sqrt{3}}{4\pi}\right)} * V_m = 1.6554.V_m \qquad (3.29)$$

If the load resistance is purely resistive, the peak or maximum current through the diode is $I_m = \sqrt{3}.V_m / R$, where R is the load resistance. The RMS value of the diode current is derived below:

$$I_r = \sqrt{\left[\frac{4}{2\pi}.\int_{0}^{\pi/6} I_m^2 .\cos^2(\omega t).d(\omega t)\right]}$$

$$= 0.5518.I_m \qquad (3.30)$$

The RMS value of the supply current or line current is derived below:

$$I_S = \sqrt{\left[\frac{8}{2\pi}.\int_{0}^{\pi/6} I_m^2 .\cos^2(\omega t).d(\omega t)\right]}$$

$$= 0.7804.I_m \qquad (3.31)$$

where in equation 3.4.5 and 3.4.6, I_m is the peak value of the three phase line current.

If Ls is the source inductance in each of the three phases and f is the supply frequency, then average reduction in output voltage due to source or commutating inductances is given as follows:

$$V_X = 6 . f . L_S . I_{dc} \quad (3.32)$$

where Idc is the load current.

3.4.1 Library Model for Three Phase FWDBR with Purely Resistive Load

Before describing the subsystems in detail, the development of the system model for three phase FWDBR is explained below.

Fig.3.14: Definition of the gk function (k = 1,2,3,...)

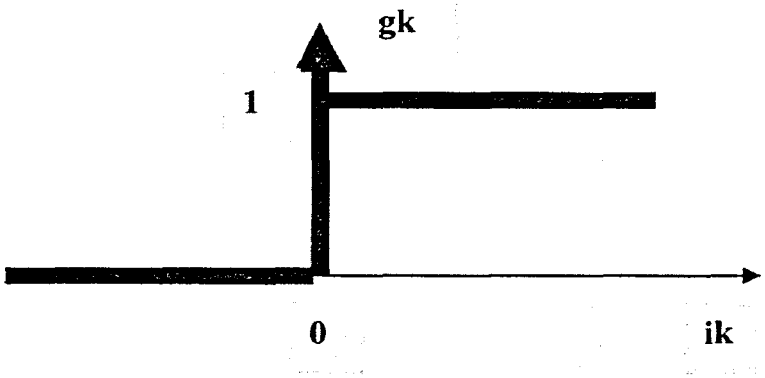

The system model for three phase FWDBR is developed based on reference 61. Heaviside function gk for k = 1,2,3 ... is defined in Fig.3.14. This Heaviside function determines whether the diode is conducting or in the blocking state [61]. In Fig.3.13, let e1, e2 and e3 are the arm voltages and u1, u2 and u3 are the phase voltages. The relation connecting them are given below:

$e1 = g1*Vdc$ .... (333) $\quad u1 = f1*Vdc$ .... (3.36)
$e2 = g2*Vdc$ .... (3.34) $\quad u2 = f2*Vdc$ .... (3.37)
$e3 = g3*Vdc$ .... (3.35) $\quad u3 = f3*Vdc$ .... (3.38)

where functions f1, f2 and f3 are defined below:

$$f_1 = \frac{2g1 - g2 - g3}{3} \quad (3.39)$$

$$f2 = \frac{2g2 - g3 - g1}{3} \quad (3.40)$$

$$f3 = \frac{2g3 - g1 - g2}{3} \quad (3.41)$$

The dc current is given below:

$$I_{dc} = g1.i1 + g2.i2 + g3.i3 \quad (3.42)$$

If R_f and L_f are the resistance and inductance of each phase of the ac mains, then e1, e2 and e3 are related as follows:

$$e1 = R_f . i_a + L_f . \frac{di_a}{dt} + u1 \qquad (3.43)$$

$$e2 = R_f . i_b + L_f . \frac{di_b}{dt} + u2 \qquad (3.44)$$

$$e3 = R_f . i_c + L_f . \frac{di_c}{dt} + u3 \qquad (3.45)$$

To simplify modelling and procedure, abc to dq and dq to abc transformation is defined as given below:

$$\begin{bmatrix} x1 \\ x2 \\ x3 \end{bmatrix} = \begin{bmatrix} \cos\theta & \sin\theta \\ \cos(\theta - 2\pi/3) & \sin(\theta - 2\pi/3) \\ \cos(\theta + 2\pi/3) & \sin(\theta + 2\pi/3) \end{bmatrix} * \begin{bmatrix} xd \\ xq \end{bmatrix} \qquad (3.46)$$

$$\begin{bmatrix} xd \\ xq \end{bmatrix} = \frac{2}{3} \begin{bmatrix} \cos\theta & \cos(\theta - 2\pi/3) & \cos(\theta + 2\pi/3) \\ \sin\theta & \sin(\theta - 2\pi/3) & \sin(\theta + 2\pi/3) \end{bmatrix} * \begin{bmatrix} x1 \\ x2 \\ x3 \end{bmatrix} \qquad (3.47)$$

In equation 3.46 and 3.47, *x* can be a voltage, current or Heavyside function..
The dq axis voltages and load current Idc are defined below:

$$I_{dc} = gd.id + gq.iq \qquad (3.48)$$

$$v_d = Rf.id + Lf.\frac{did}{dt} + ud \qquad (3.49)$$

$$v_q = Rf.iq + Lf.\frac{diq}{dt} + uq \qquad (3.50)$$

The equations from 3.33 to 3.50 are used to develop the system model for the three phase FWDBR.

The system model for the three phase FWDBR is shown in Fig.3.15. The various user dialog box are shown in Fig.3.16. The dialog box for discrete virtual PLL is from SimPowerSystems block set. The user can enter the required data in the appropriate dialog box. This model is suitable only for purely resistive load. The various subsystems are shown in Fig.3.17(A) to (I) which are described below.

Fig.3.17(A) correspond to the dialog box in Fig.3.15, where the line to neutral RMS voltage in volts and frequency in Hertz are entered. Fig.3.17(B) generates three phase AC using the three input mux and the three Fcn blocks. The abc to dq0 block shown in Fig.3.17(C) is from SimPowerSystems block set which transforms abc axis voltages to dq0 axis voltages. The discrete virtual PLL block shown in Fig.3.17(D), generating frequency f, $2*\pi*f*t$ and sine and cosine of $2*\pi*f*t$ is also from SimPowerSystems block set. Fig.3.17(E) solves the equation for dq axis line currents given by equations 3.4.1.17 and 3.4.1.18. In Fig.3.17(E), rs and ls represents the ac line resistance and inductance in each phase, corresponding to Rf and Lf in equations 3.4.1.17 and 3.4.1.18. Fig.3.17(E) opens up dialog box for source resistance and inductance which is shown in Fig.3.16. Fig.3.17(F) transforms the dq axis line currents back to abc axis line currents. Fig.3.17(G) has the abc axis line currents as inputs and generates Heavyside function g1, g2 and g3 for the three phase as defined in Fig.3.14 and then using g1, g2 and g3, the functions fa, fb and fc are generated as defined by equations 3.4.1.7 to 3.4.1.9 where f1, f2 and f3 correspond to fa, fb and fc. Fig.3.17(H) opens the dialog box for Load resistance and Filter data, which is shown in Fig.3.16. In Fig.3.17(H), Load current Idc is calculated using equation 3.4.1.16 using Id and Iq as inputs. This value of Idc is used to calculate Idc*R to calculate the load voltage Vdc without filter, where R is the load resistance. With capacitor filter CF in parallel to the load resistance, Vdc is calculated by calculating the capacitor filter current Ic as follows:

$$\left.\begin{aligned} I_C &= I_{dc} - (V_{dc} / R) \\ V_{dc} &= \int I_C \, .dt \end{aligned}\right| \qquad (3.51)$$

Equation 3.51 is solved using the module in Fig.3.17(H). Further Fig.3.17(H) is used to find ud and uq corresponding to phase voltages u1, u2 and u3. Fig.3.17(I) is used to find the three line to line voltages and its inverted value.

The value of the RMS line to neutral voltage in volts, frequency in Hertz, source resistance in Ohms and inductance in Henries, Load resistance in Ohms and filter capacitor in farads are entered in the appropriate dialog box in Fig.3.16. These values are shown Table 3.4 [61].

3.4.2 Simulation Results

The simulation of the three phase FWDBR was carried out using ode1(Euler) Fixed-step solver for purely resistive load first by excluding the filter capacitor from the circuit and then by including the filter capacitor, for the data shown in Table 3.4 [61]. The simulation results of input voltage, output voltage, average load current excluding the filter capacitor from the circuit is shown in Fig.3.18(A) to (C). The simulation results for the above including the filter capacitor is shown in Fig.3.19(A) to (C). The values of the average load voltage, average load current observed for both cases by simulation are recorded in Table 3.5. The average and RMS value of load voltage by calculation using equations 3.28. and 3.29 yields 514.5 and 515 volts respectively. The reduction in the output voltage due to source inductance of 1 milli Henries was calculated using equation 3.32. and the net value of the output voltage is found to be 507.9 volts. The average load current calculated using the formula comes to 22.37 amps. The respective values recorded in Table 3.5 by simulation closely agrees with the theoretically calculated values [61].

TABLE 3.4

SL.NO	*PARAMETERS*	*VALUE*
1	**Line to Neutral RMS Voltage**	**220 Volts**
2	**Supply Frequency**	**50 Hz**
3	**Source resistance**	**0 Ohms**
4	**Source Inductance**	**1e-3 Henries**
5	**Load Resistance**	**23 Ohms**
6	**Filter capacitance**	**0.0011 Farads**

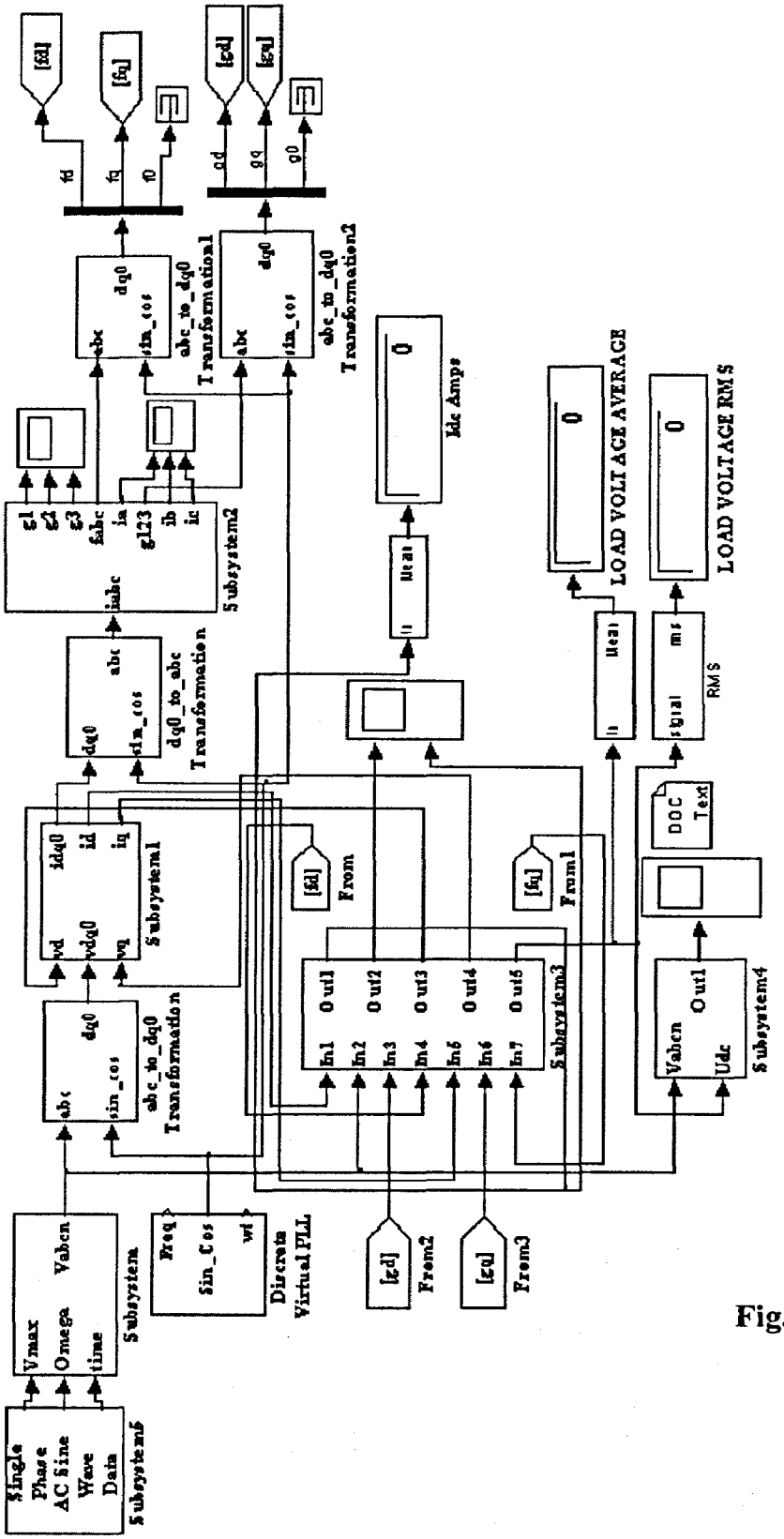

Fig. 3.15 3.14: THREE PHASE FULL WAVE BRIDGE RECTIFIER

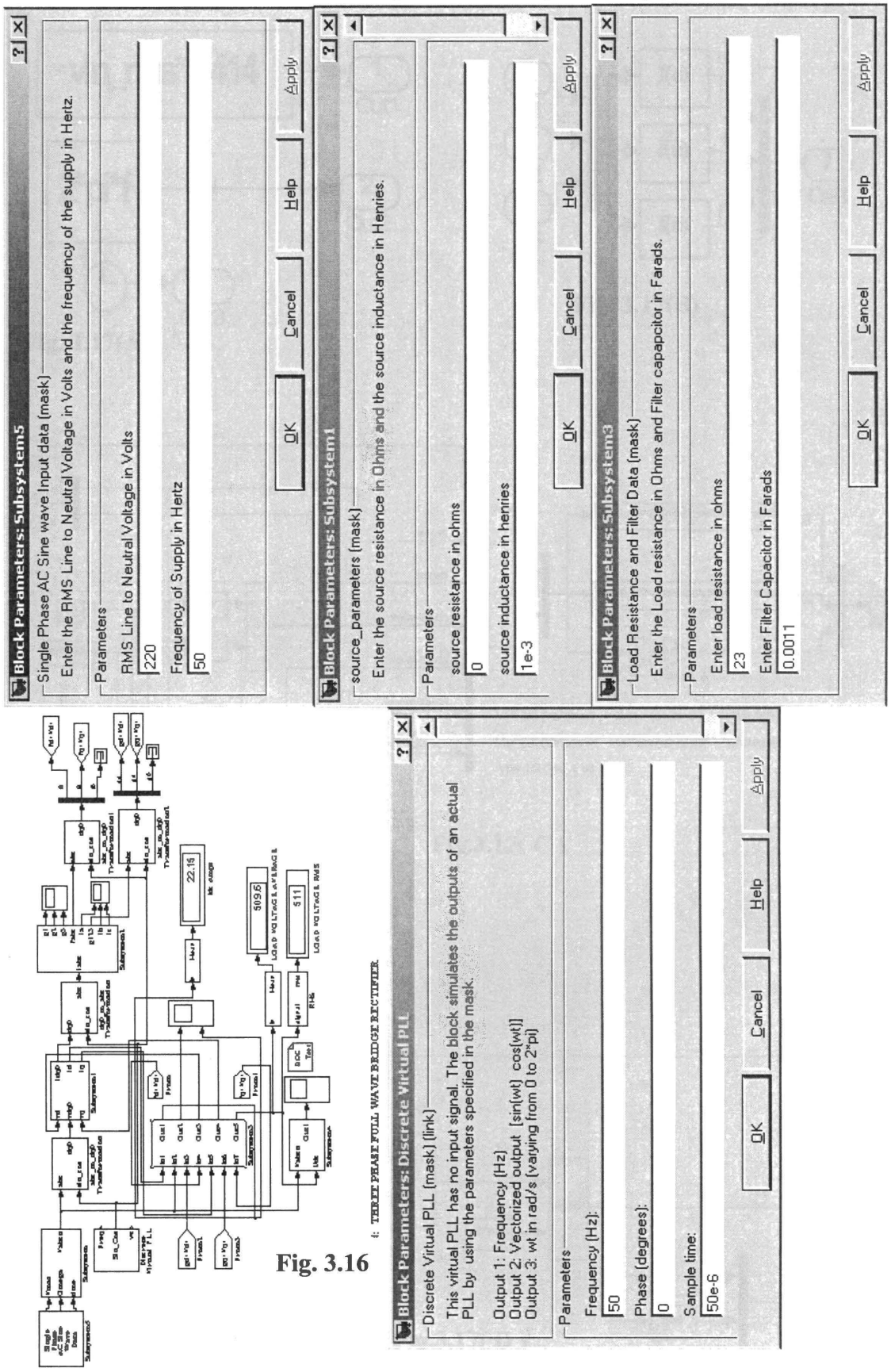
Block Parameters: Subsystem5
Single Phase AC Sine wave Input data (mask)
Enter the RMS Line to Neutral Voltage in Volts and the frequency of the supply in Hertz.
Parameters
RMS Line to Neutral Voltage in Volts
220
Frequency of Supply in Hertz
50
OK
Cancel
Help
Apply
Block Parameters: Subsystem1
source_parameters (mask)
Enter the source resistance in Ohms and the source inductance in Henries.
Parameters
source resistance in ohms
0
source inductance in henries
1e-3
OK
Cancel
Help
Apply
Block Parameters: Subsystem3
Load Resistance and Filter Data (mask)
Enter the Load resistance in Ohms and Filter capapcitor in Farads.
Parameters
Enter load resistance in ohms
23
Enter Filter Capacitor in Farads
0.0011
OK
Cancel
Help
Apply
Block Parameters: Discrete Virtual PLL
Discrete Virtual PLL (mask) (link)
This virtual PLL has no input signal. The block simulates the outputs of an actual PLL by using the parameters specified in the mask.
Output 1: Frequency (Hz)
Output 2: Vectorized output [sin(wt) cos(wt)]
Output 3: wt in rad/s (varying from 0 to 2*pi)
Parameters
Frequency (Hz):
50
Phase (degrees):
0
Sample time:
50e-6
OK
Cancel
Help
Apply
22.15
509.6
511
LOAD VOLTAGE AVERAGE
LOAD VOLTAGE RMS

Fig. 3.16

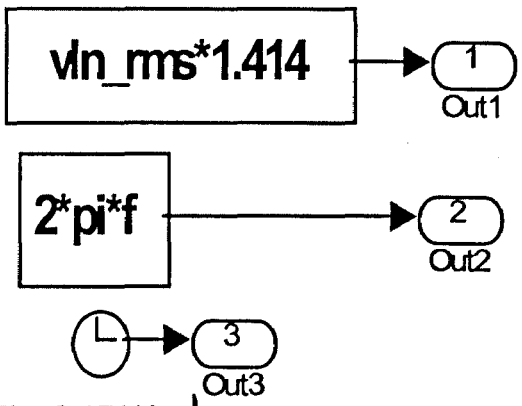

Fig. 3.17(A)

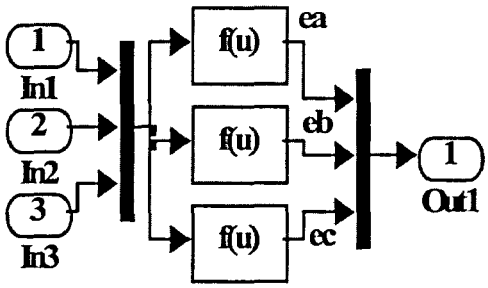

Fig. 3.17(B)

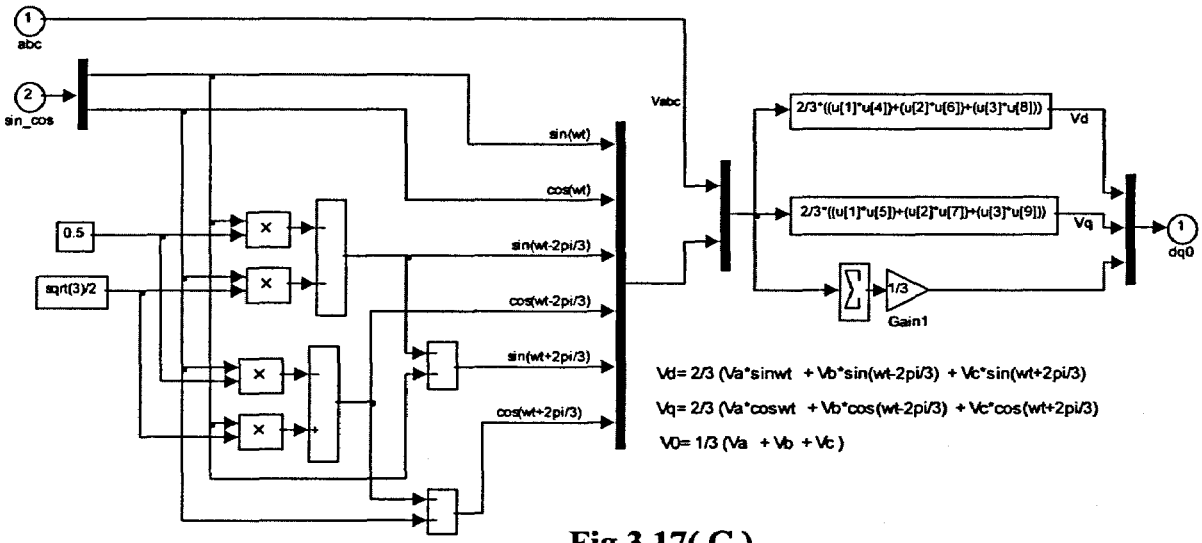

Fig.3.17(C)

Discrete Virtual PLL

Pierre Giroux, Gilbert Sybille
Power System Simulation Laboratory
IREQ, Hydro-Quebec

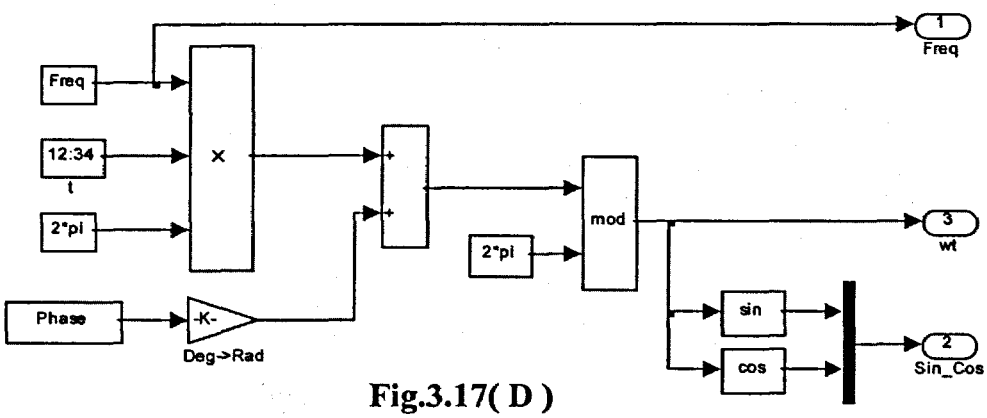

Fig.3.17(D)

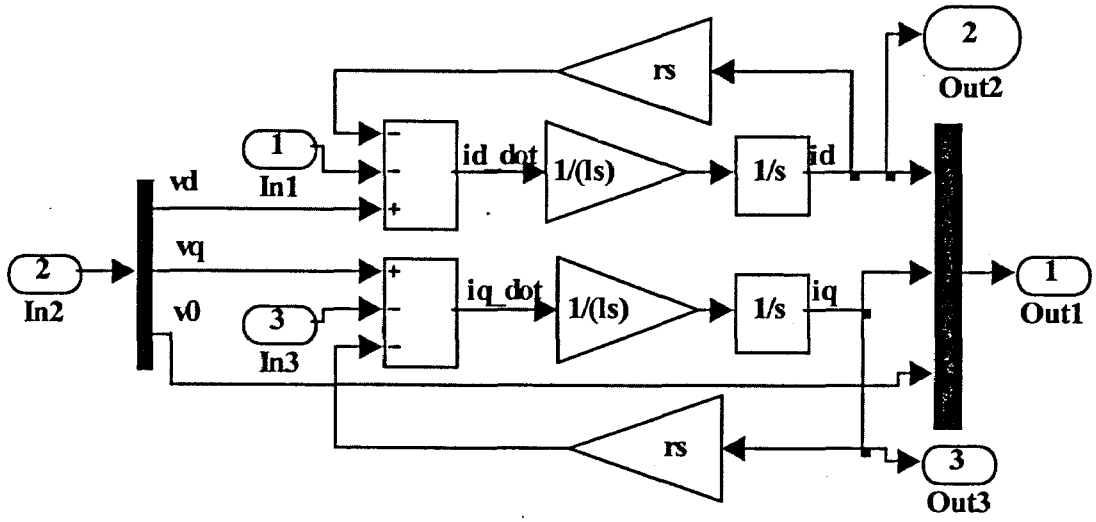

Fig.3.17(E)

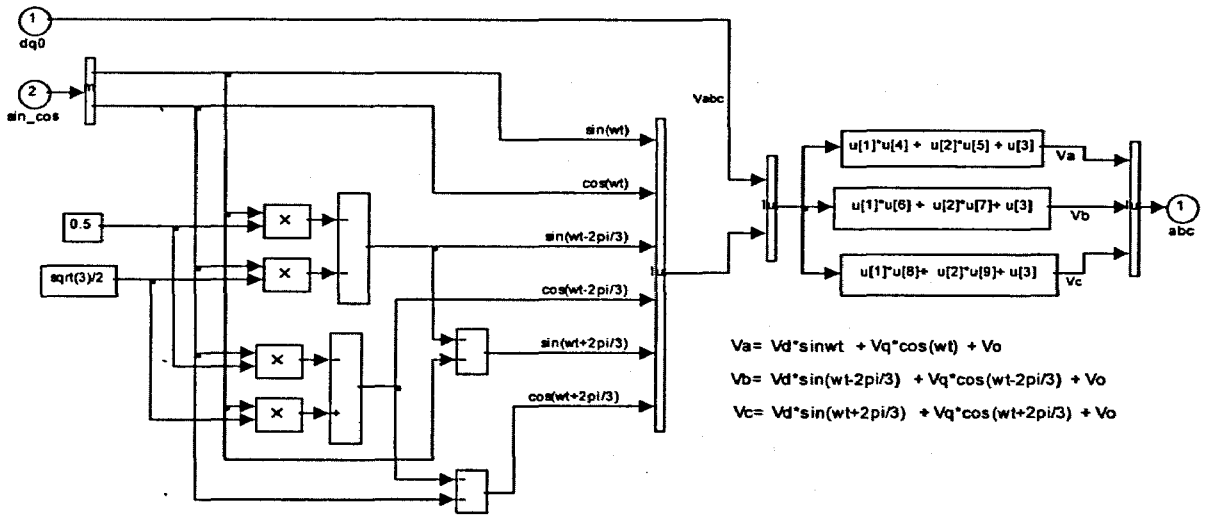

Fig.3.17(F)

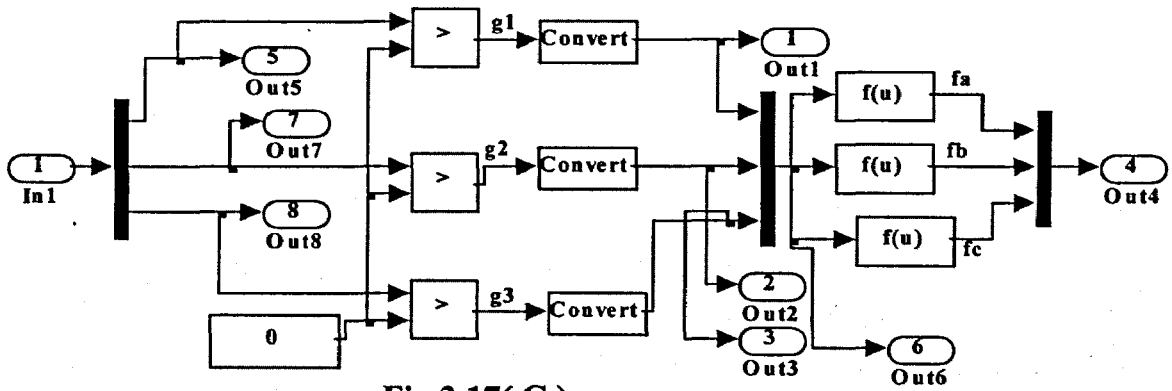

Fig.3.17(G)

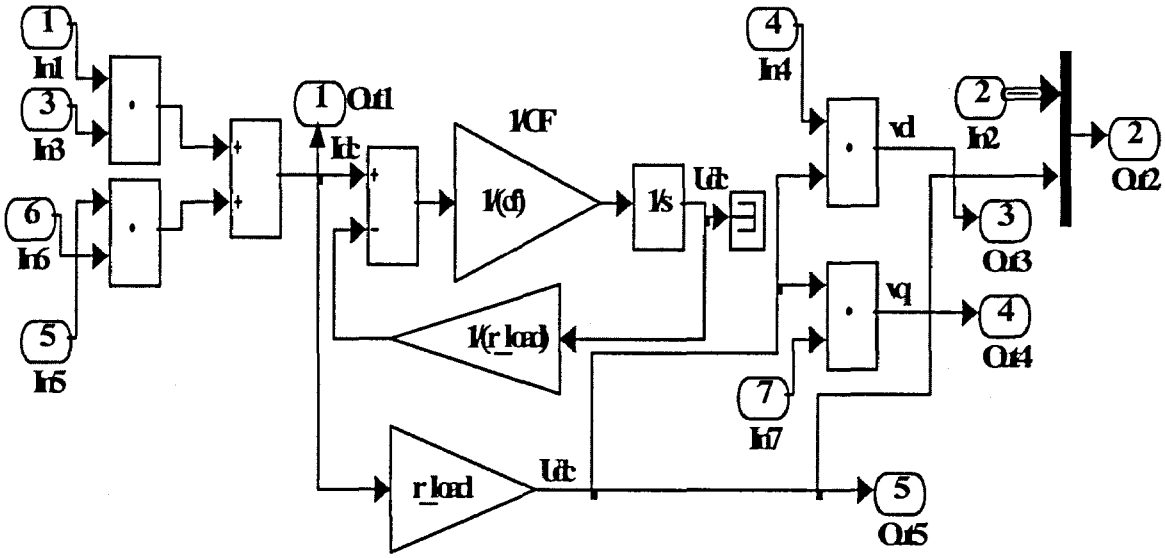

Fig.3.17(H)

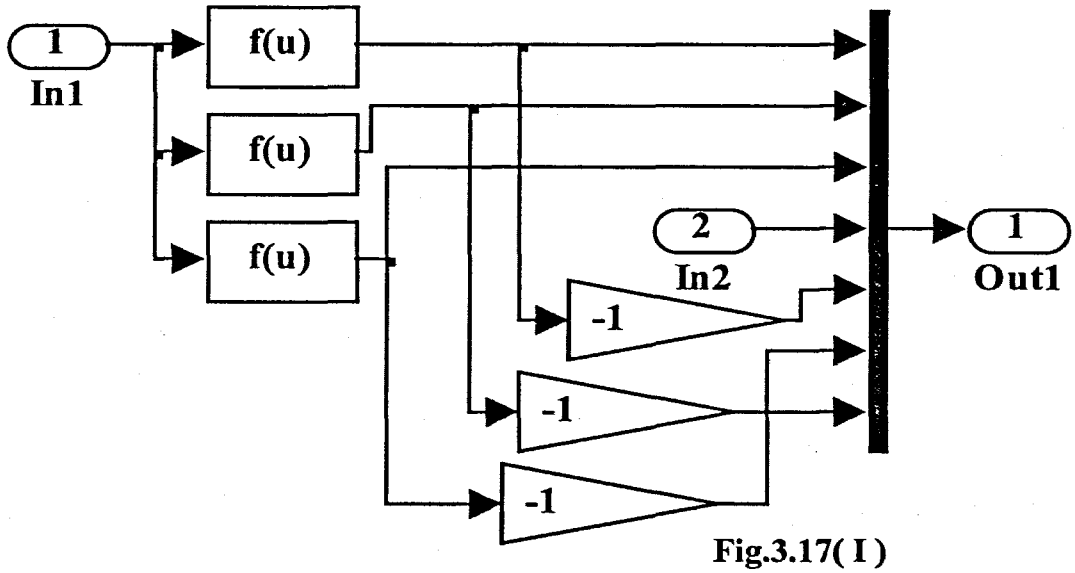

Fig.3.17(I)

TABLE 3.5

Sl.No.	*RMS Load Voltage(Volts)*	*Average Load Voltage(Volts)*	*Average Load Current(Amps)*	*Remarks*
1	511	509.6	22.15	NO Filter Capacitor
2	508	508	21.68	With Filter capacitor of 0.0011 Farads

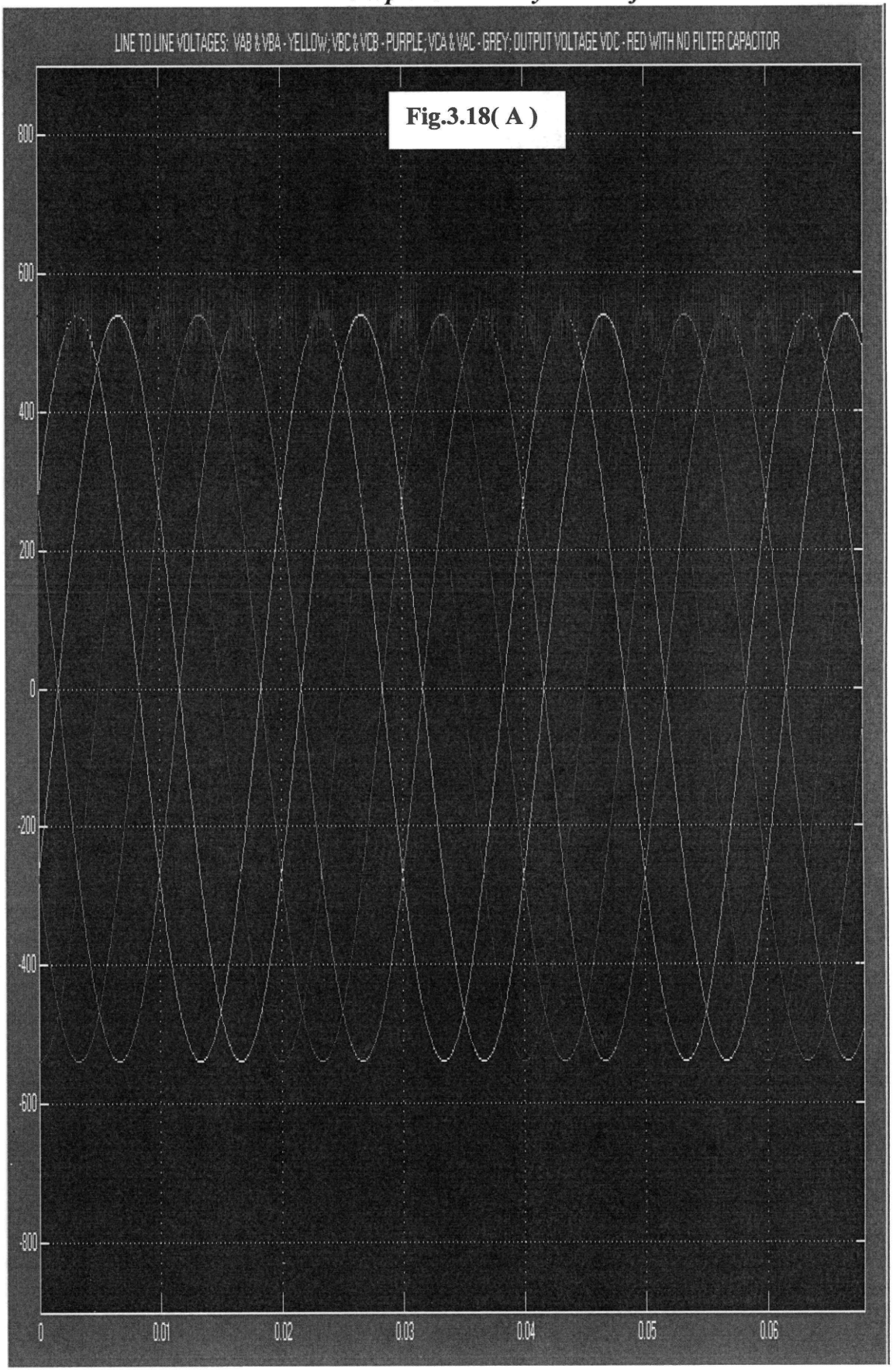
LINE TO LINE VOLTAGES: VAB & VBA - YELLOW; VBC & VCB - PURPLE; VCA & VAC - GREY; OUTPUT VOLTAGE VDC - RED WITH NO FILTER CAPACITOR
800
600
400
200
0
-200
-400
-600
-800
0
0.01
0.02
0.03
0.04
0.05
0.06

Fig.3.18(A)

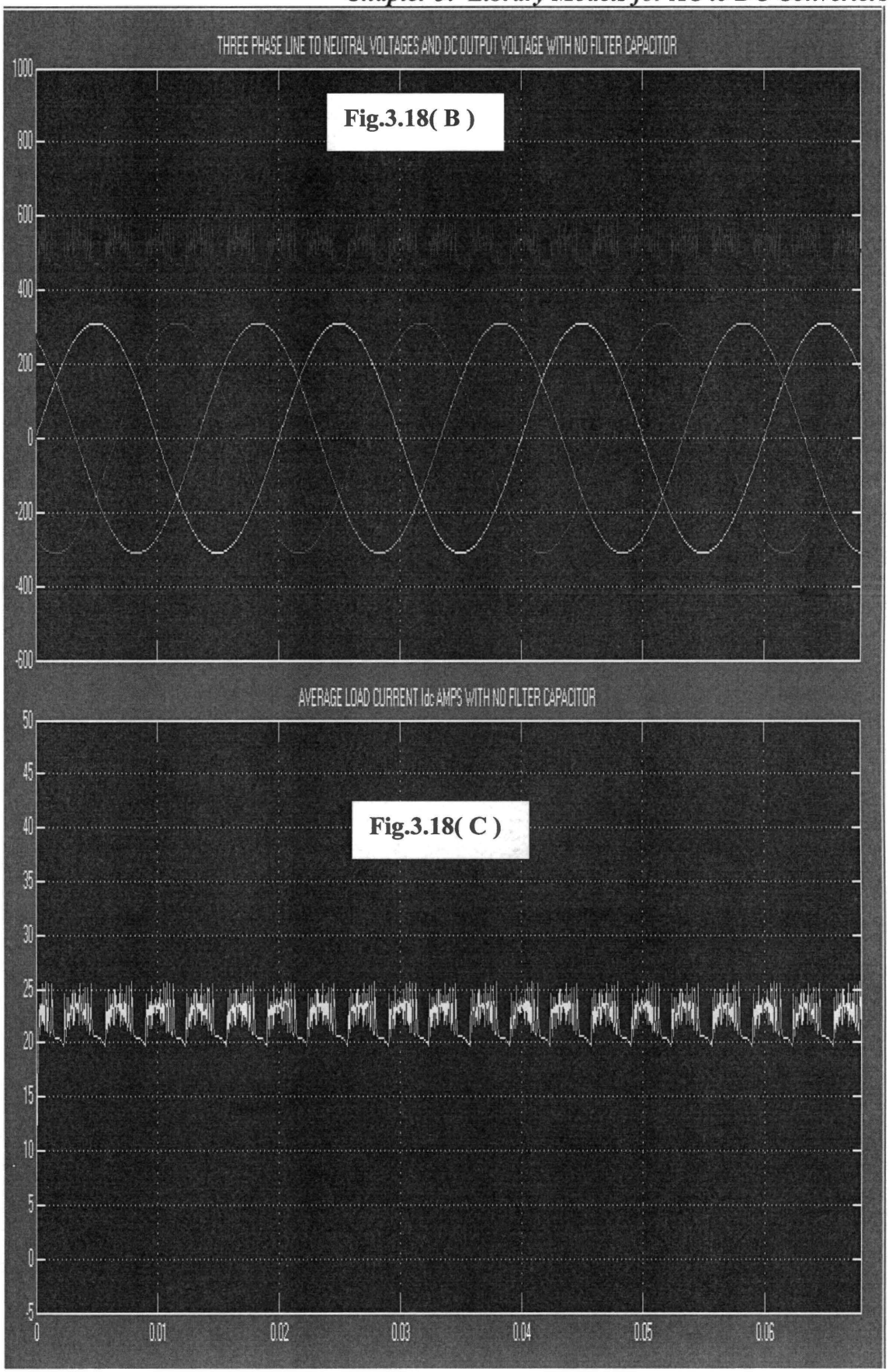

Fig.3.18(B)

Fig.3.18(C)

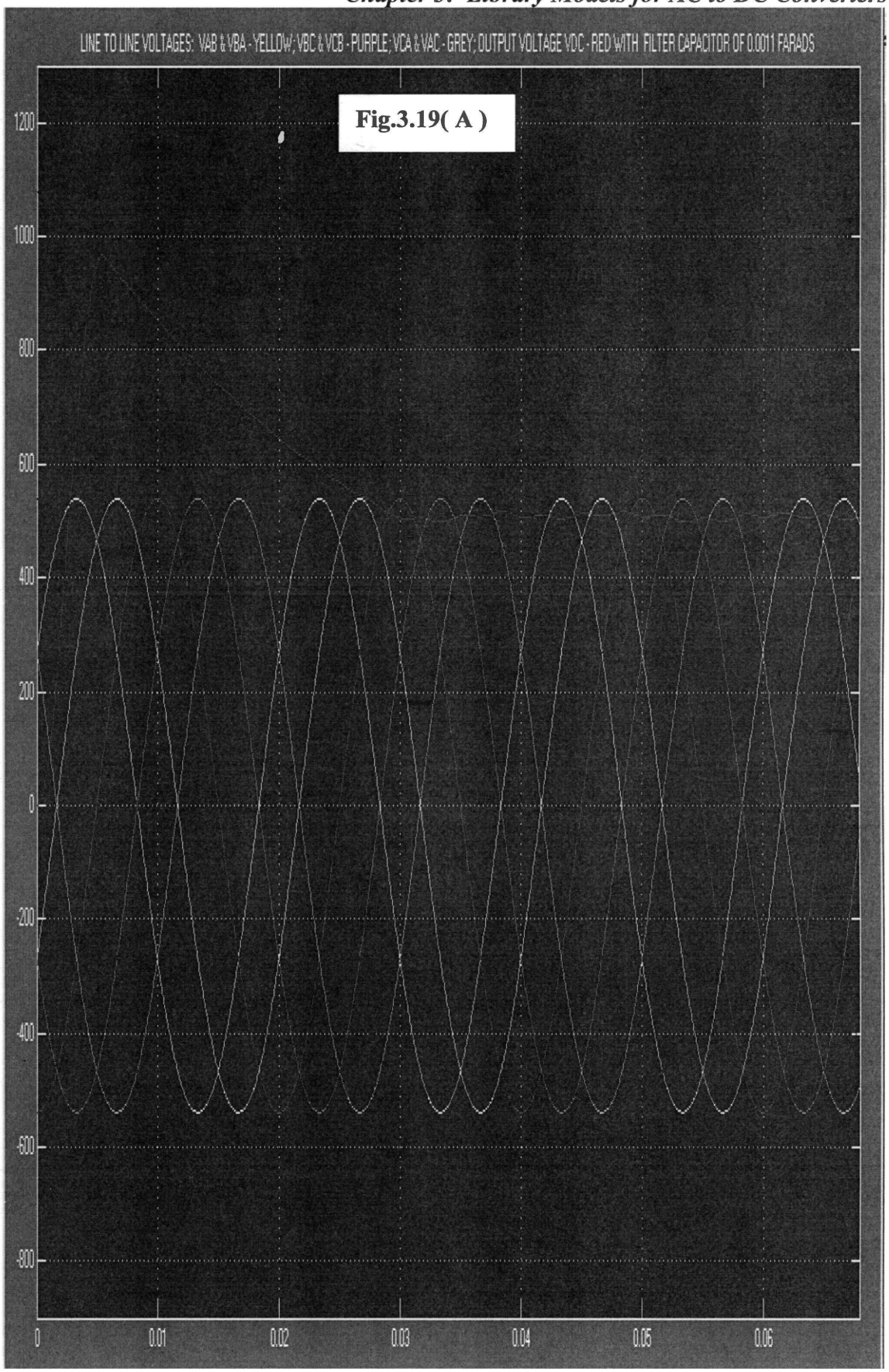
LINE TO LINE VOLTAGES: VAB & VBA - YELLOW; VBC & VCB - PURPLE; VCA & VAC - GREY; OUTPUT VOLTAGE VDC - RED WITH FILTER CAPACITOR OF 0.0011 FARADS
1200
1000
800
600
400
200
0
-200
-400
-600
-800
0
0.01
0.02
0.03
0.04
0.05
0.06

Fig.3.19(A)

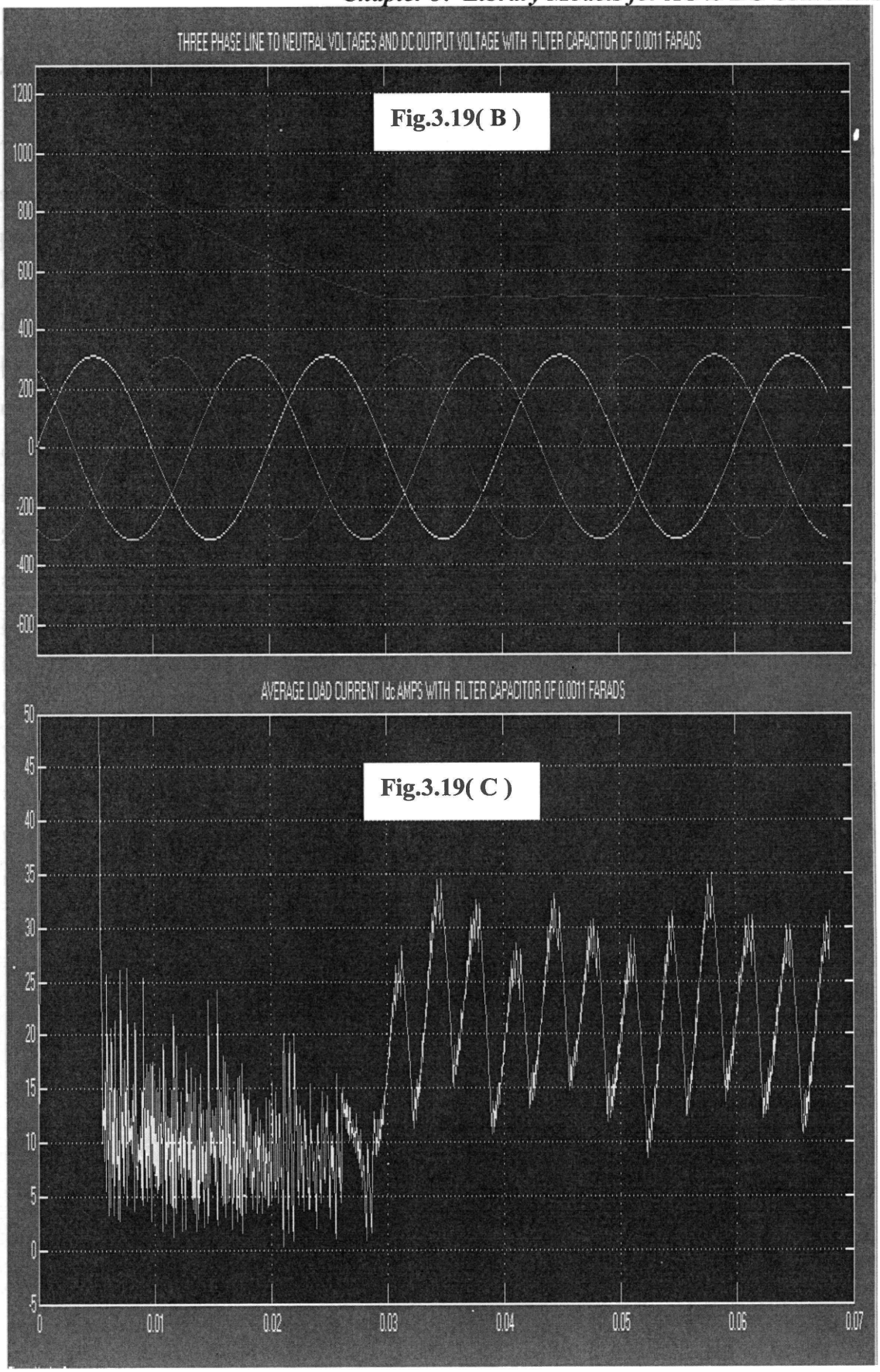

Fig.3.19(B)

Fig.3.19(C)

3.5 Conclusions

The library module for the single phase FWDBR based on the equations describing the system is presented. User dialog box can be used to modify data depending on the problem in hand. One model is suitable for either a purely resistive load or the RLE load. The type of load is easily selected using selector switch. Simulation results in Fig.3.5 and 3.6 and the values in TABLE 3.2 well agree with the literature reference [14]. The library module for the single phase FWCBR based on the equations describing the system is presented. User dialog box can be used to modify data depending on the problem in hand. One model is suitable for either a purely resistive load or the RLE load. The type of load is easily selected using selector switch. Simulation results in Fig.3.11 and 3.12 and the calculated values in TABLE 3.3 well agree with the literature reference [14]. A novel method of system modelling three phase FWDBR using Heaviside function is presented. The method is closely similar to the one discussed in reference 61, except that here abc to dq and dq to abc transformation are used instead of abc to αβ and αβ to abc transformation. The recorded values of average and RMS load voltage and load current by simulation closely well agree with the corresponding values calculated using the formula. Appendix E provides the simulation of the single phase FWDBR, FWCBR and three phase FWDBR for selected values, using PSIM7.0 demo version. .

CHAPTER 4

LIBRARY MODELS FOR DC TO AC CONVERTERS

4.1 Introduction

In this chapter, building library modules for dc to ac converters also known as inverters are presented. Inverter circuits use SCRs, BJTs, MOSFETs, IGBTs and GTOs. SCR inverters require auxiliary thyristors for forced commutation and their modelling is not discussed here. Here library system models for three phase 180 degree mode and 120 degree mode inverters using semiconductor switches such as BJTs, MOSFETs, IGBTs and GTOs are presented. These modes are also known as continuous conduction and discontinuous conduction modes. Switching function concept is used in developing these models. These library modules have pop-up-menu or dialog box where the required data relating to the dc to ac converter is entered by the user. These system models use Simulink blocks which solves the governing equations relating to the relevant ac to dc converter. No semiconductor circuit component is used in the model.

4.2 Three Phase 180 Degree Mode Inverter

Three Phase Inverter topology is shown in Fig.4.1, where each switch Q1 to Q6 can be semiconductor component such as BJTs, MOSFETs, IGBTs or GTOs. Vdc is the DC link voltage. The 180 degree gate drive pattern is used to drive the switch which is shown in Fig.2.6(A) [14 – 18]. The PSPICE simulation of the three phase 180 degree mode 50 Hz inverter is shown in Fig.4.2(A) to (F). Fig.4.2(A) to (F) are respectively Three phase line to ground voltages, line to line voltages, Line to line voltage and its RMS value, Harmonic spectrum of line to line voltage, Line to Neutral voltages, Line to Neutral voltage and its RMS value, Harmonic spectrum of line to neutral voltage.

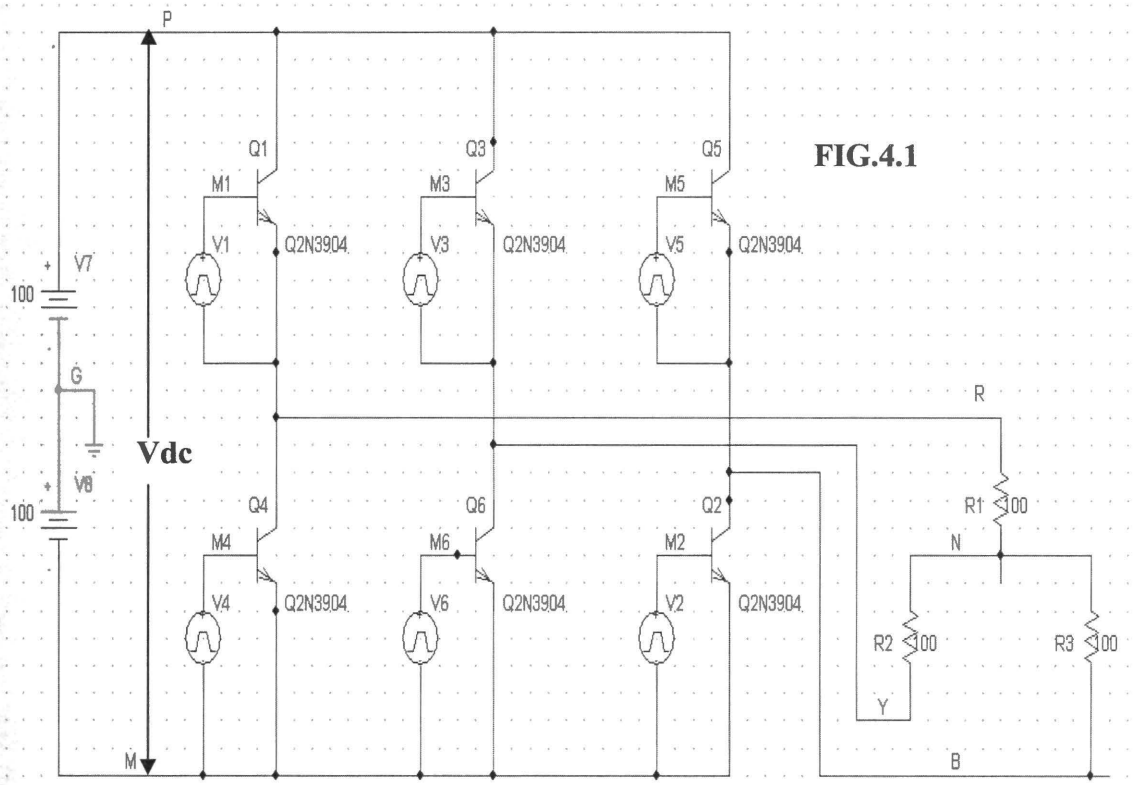

FIG.4.1

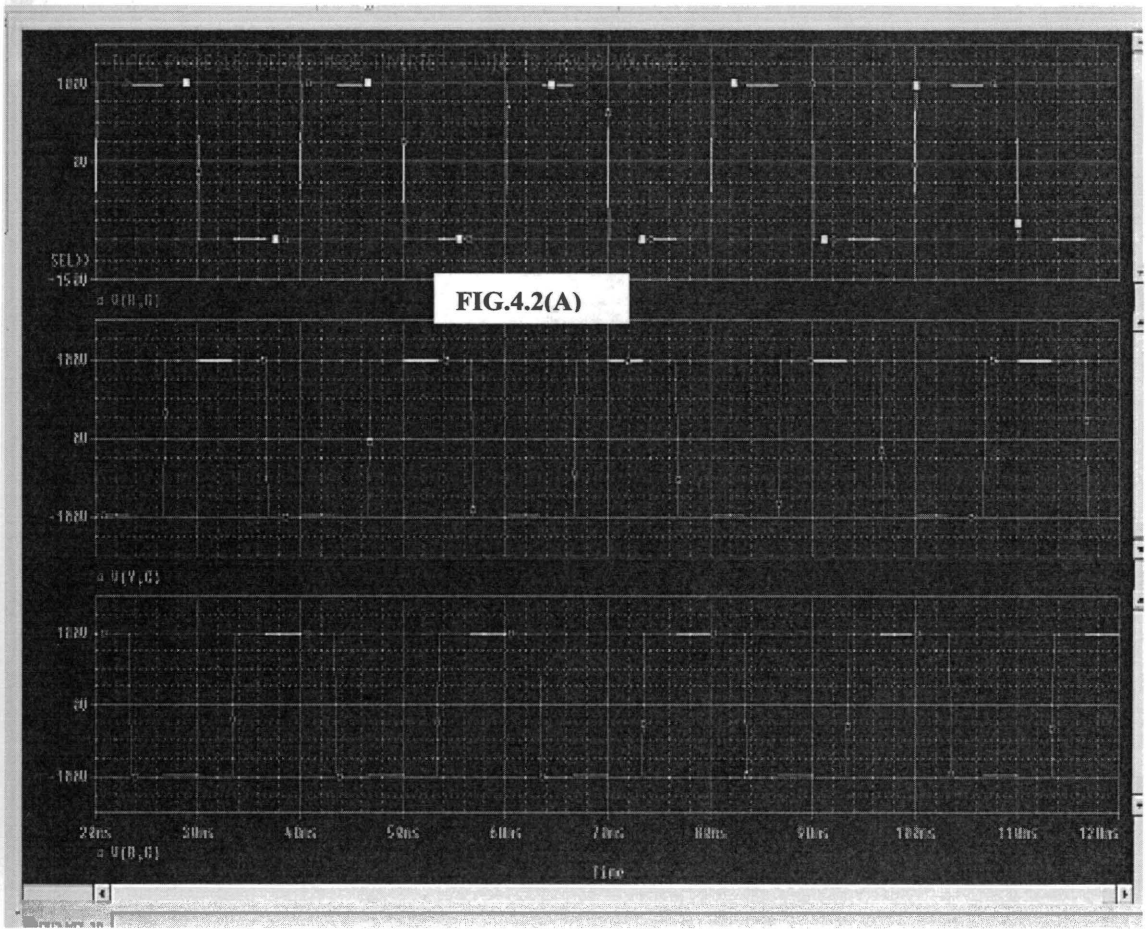

FIG.4.2(A)

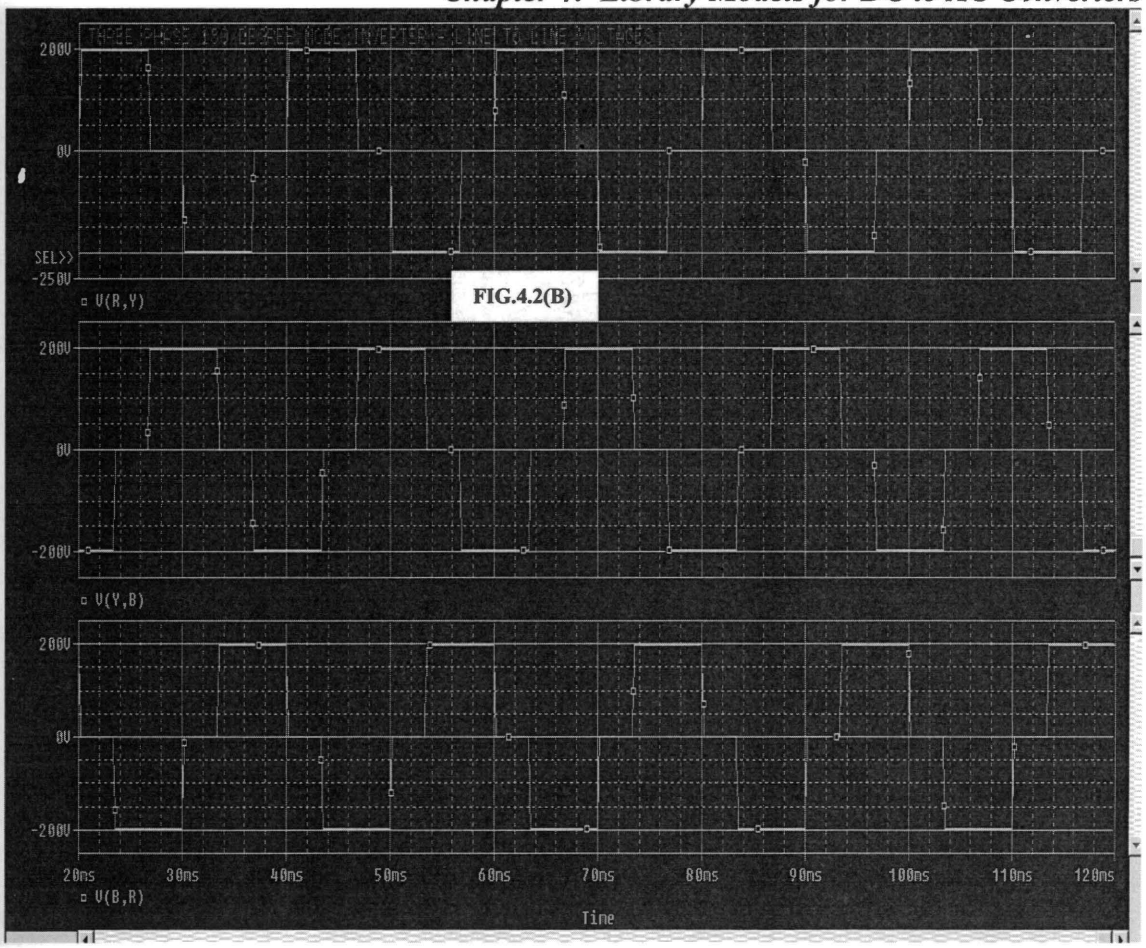

FIG.4.2(B)

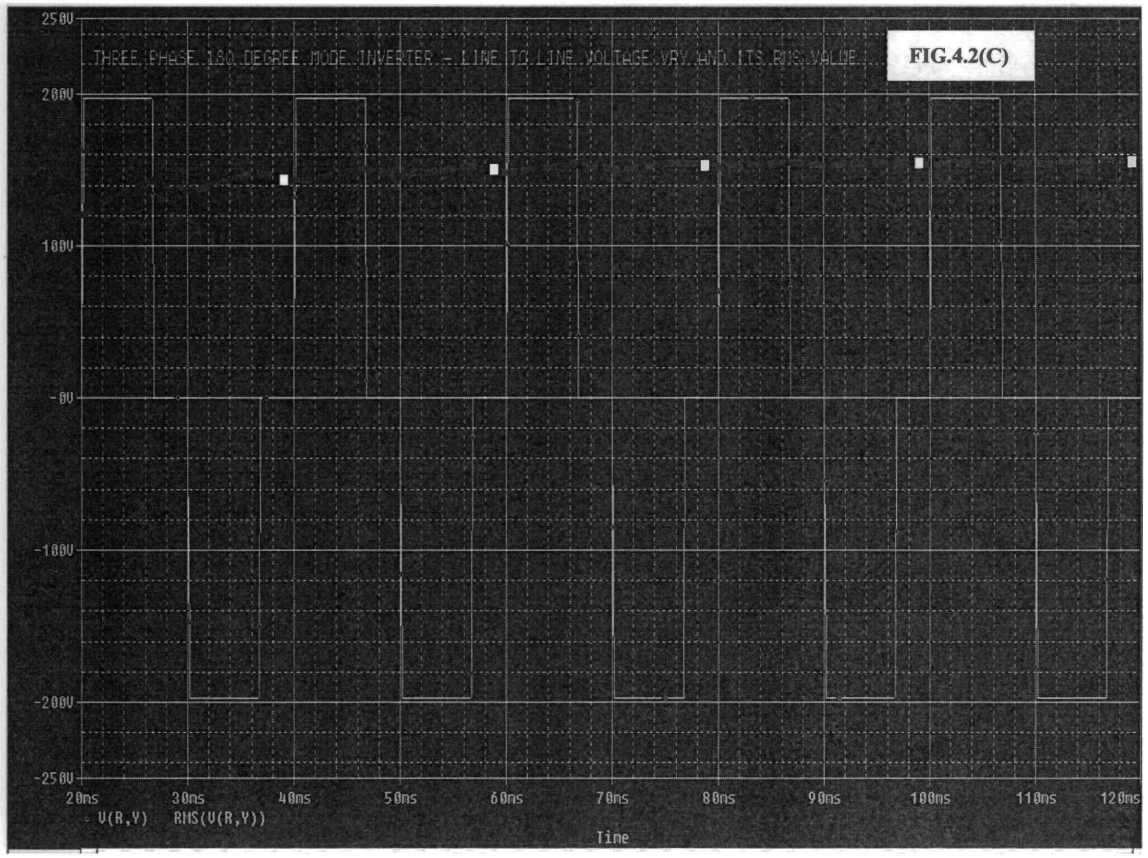

FIG.4.2(C)

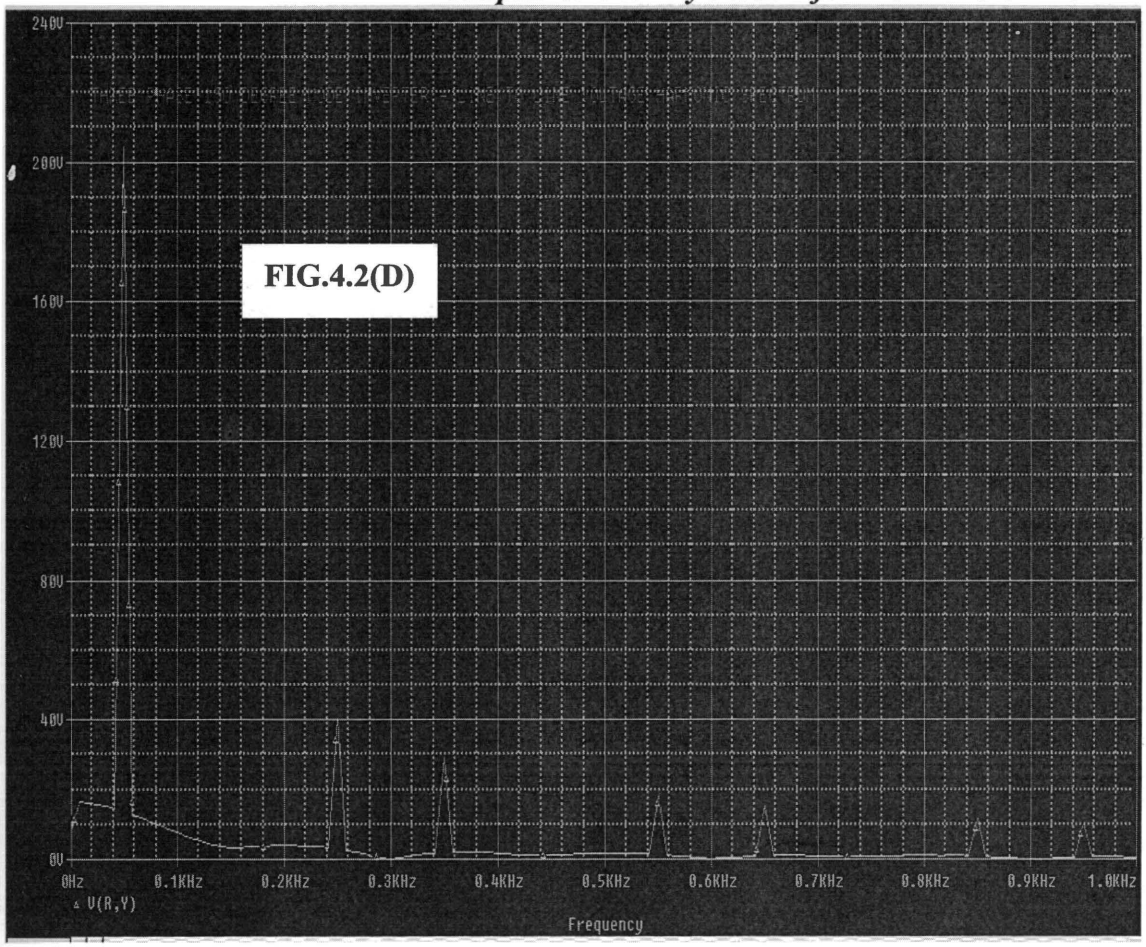

FIG.4.2(D)

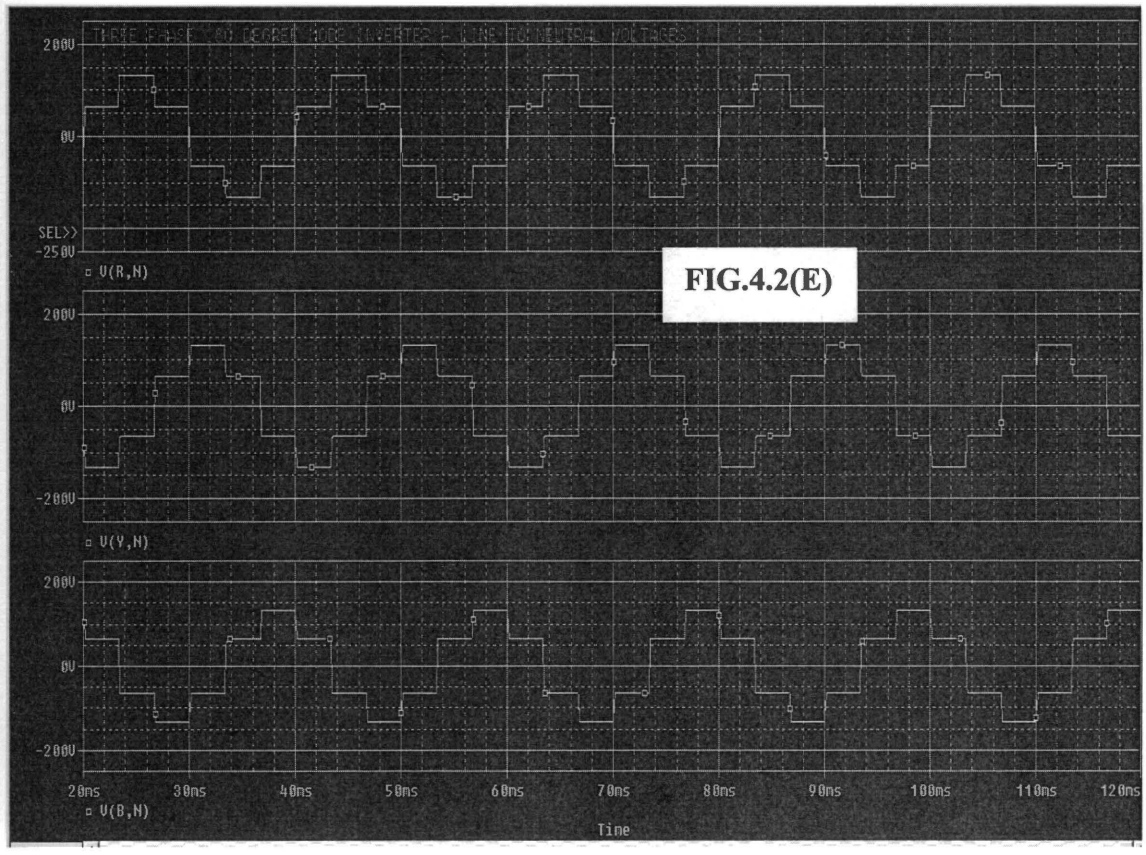

FIG.4.2(E)

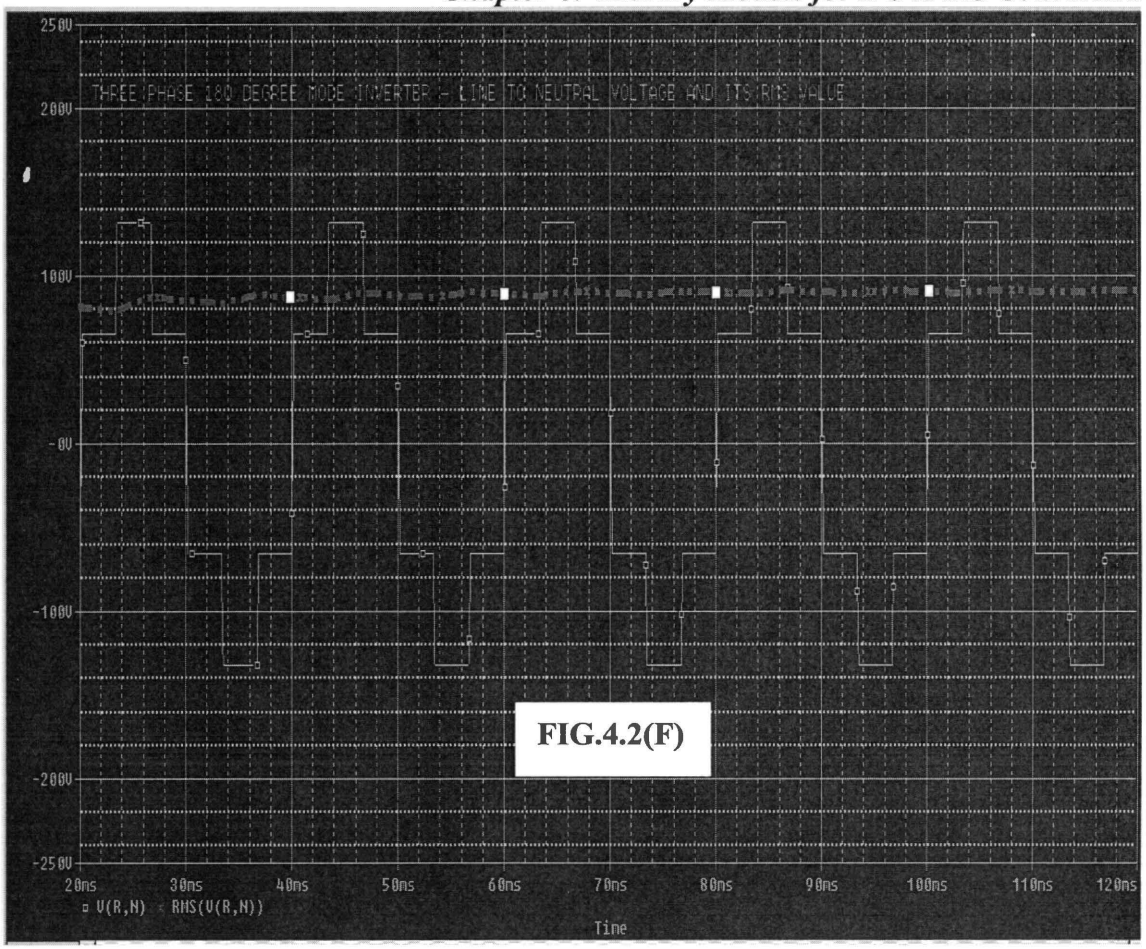

FIG.4.2(F)

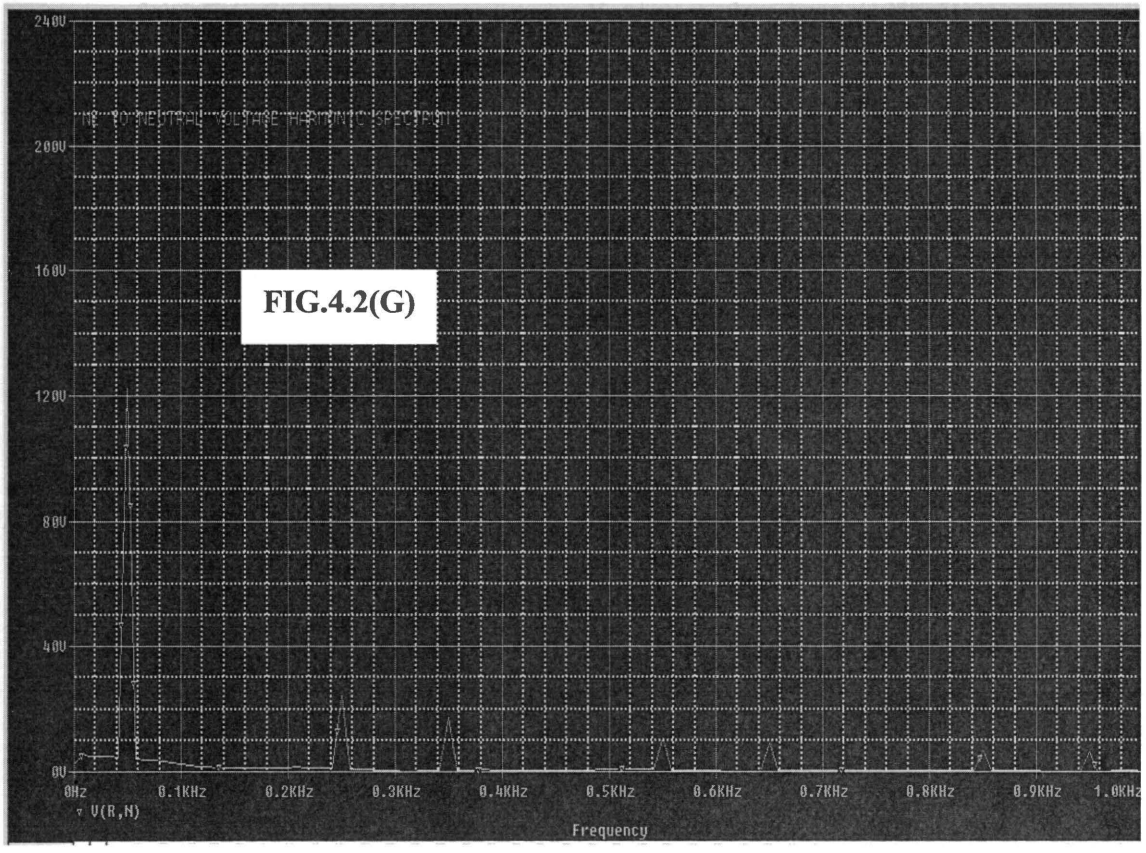

FIG.4.2(G)

4.2.1 Analysis of Line to Line Voltage

The analysis of line to line voltage of three phase 180 degree mode inverter is done in this section. The line to line voltage Vry is shown in Fig.4.2(C). The theoretical derivation of Line to Line voltage waveform is shown in section 4.2.2. Shifting the axis of Fig.4.2(C) by π/6 makes the function odd i.e. f(-t) = -f(+t). The even harmonics are zero. The Fourier coefficient bn can be defined as follows:

$$b_n = \frac{4}{\pi} * \left[\int_{\pi/6}^{\pi/2} -V_{dc} .\sin(n.\omega t).d(\omega t) \right]$$

$$= \frac{4.V_{dc}}{n\pi} . \left[\cos \frac{n\pi}{6} \right] \quad for \quad n = 1,3,5,7... \qquad (4.1)$$

The line to line voltage Vry can be expressed by Fourier series as follows:

$$V_{ry} = \sum_{n=1,3,5,7....}^{\infty} \frac{4.V_{dc}}{n\pi} . \left(\cos \frac{n\pi}{6} \right) .\sin \left(n\omega t + \frac{n\pi}{6} \right) \qquad (4.2)$$

The RMS value of Vry is given below:

$$V_{ry(rms)} = \sqrt{\left[\frac{1}{\pi} . \int_{0}^{2\pi/3} V_{dc}^{2} .d(\omega t) \right]}$$

$$= \sqrt{\frac{2}{3}} . V_{dc} \quad = \quad 0.8165 . V_{dc} \qquad (4.3)$$

The RMS value of the fundamental component of Vry is given below:

$$V_{ry1(rms)} = \frac{4.V_{dc} .\cos \left(\frac{\pi}{6} \right)}{\sqrt{2} .\pi} \quad = \frac{\sqrt{6}}{\pi} . V_{dc} \qquad (4.4)$$

The RMS value of line to line voltage for a dc link voltage of 200 Volts shown in Fig.4.2(C) and the peak value of the fundamental component of Vry shown in Fig.4.2(D) well agree with the equations 4.3 and 4.4.

4.2.2 Analysis of Line to Neutral Voltage

In the following section, the r.m.s. value and fft of line to neutral voltage of a six step 180 degree mode inverter is derived.

For clarity the line to neutral voltage of a three phase 180 degree mode inverter is derived by simulation using PSPICE, shown in Fig.4.1. Resistive star connected load is used for convenience only, as inductive load may give rise to voltage spikes in the waveform. The simulated Line to neutral voltage is shown in fig.4.2(F). The dotted line in fig.4.2(F) indicates its r.m.s. value computed by PSPICE. A three phase 50 Hz waveform is generated. The waveform can be theoretically derived as follows:

By taking the ground g as the midpoint of the two dc voltage sources, the line to ground voltage Vrg, Vyg and Vbg can be easily derived for three phase 180 degree mode gate drive, by observation of Fig.4.1. This waveform is described below:

$$V_{rg} = +\frac{V_{dc}}{2} \quad for \quad 0 \le \omega t \le \pi$$

$$= -\frac{V_{dc}}{2} \quad for \quad \pi \le \omega t \le 2\pi \quad .....(4.5)$$

$$V_{yg} = +\frac{V_{dc}}{2} \quad for \quad 2\pi/3 \le \omega t \le 5\pi/3$$

$$= -\frac{V_{dc}}{2} \quad for \quad 0 \le \omega t \le 2\pi/3 \quad and$$

$$for \quad 5\pi/3 \le \omega t \le 2\pi \quad .....(4.6)$$

$$V_{bg} = +\frac{V_{dc}}{2} \quad for \quad 0 \le \omega t \le \pi/3 \quad and$$

$$for \quad 4\pi/3 \le \omega t \le 2\pi$$

$$= -\frac{V_{dc}}{2} \quad for \quad \pi/3 \le \omega t \le 4\pi/3 \quad .....(4.7)$$

Equations 4.5 to 4.7 well confirm the simulated waveform for three phase Line to ground voltage shown in Fig.4.2(A).

Then we have the following line to line voltage values:

$$V_{ry} = V_{rg} - V_{yg} \quad .....(4.8)$$

$$V_{yb} = V_{yg} - V_{bg} \quad .....(4.9)$$

$$V_{br} = V_{bg} - V_{rg} \quad .....(4.10)$$

From equations 4.8 to 4.10, it is possible to derive the three phase line to neutral voltages of star connected load, using the following relation:

$$\begin{bmatrix} V_{rn} \\ V_{yn} \\ V_{bn} \end{bmatrix} = \frac{1}{3} \cdot \begin{bmatrix} 1 & 0 & -1 \\ -1 & 1 & 0 \\ 0 & -1 & 1 \end{bmatrix} * \begin{bmatrix} V_{ry} \\ V_{yb} \\ V_{br} \end{bmatrix} \qquad (4.11)$$

Such a theoretically derived waveform well agrees with the one shown in fig.4.2(E) and (F).

The waveform derived by using equations 4.5 to 4.11, gives the following coordinates for Vrn:

(0, +Vdc/3), (pi/3, +Vdc/3), (pi/3, +2Vdc/3), (2pi/3, +2Vdc/3), (2pi/3, +Vdc/3), (pi, +Vdc/3), (pi, -Vdc/3), (4pi/3, -Vdc/3), (4pi/3, -2Vdc/3), (5pi/3, -2Vdc/3), (5pi/3, -Vdc/3), (2pi, -Vdc/3), (2pi, +Vdc/3) and so on. These coordinates well agree with Fig.4.2(F). Referring to Fig.4.2(F) and noting the coordinates given above, we have the following equation for RMS value of line to neutral voltage.

$$V^2_{rn(rms)} = \left[\frac{1}{\pi} * \left\{ \frac{V^2_{dc}}{9} * \int_0^{\pi/3} d(\omega t) + \frac{4V^2_{dc}}{9} * \int_{\pi/3}^{2\pi/3} d(\omega t) + \frac{V^2_{dc}}{9} * \int_{2\pi/3}^{\pi} d(\omega t) \right\} \right] \qquad (4.12)$$

Simplification of equation 4.12 yields the following:

$$V_{rn(rms)} = \frac{\sqrt{2}\,.\,V_{dc}}{3} \quad ...(4.13)$$

The Fourier transform of Line to Neutral voltage Vrn is derived below:

Referring to Fig.4.2(F), the axis of symmetry is the origin where f(-t) = -f(+t) and the function is odd. Thus Fourier coefficient bn is given by

$$b_n = \frac{2}{\pi} * \left[\int_0^{\pi/3} \frac{V_{dc}}{3}.\sin(n\omega t).d(\omega t) + \int_{\pi/3}^{2\pi/3} \frac{2V_{dc}}{3}.\sin(n\omega t).d(\omega t) + \int_{2\pi/3}^{\pi} \frac{V_{dc}}{3}.\sin(n\omega t).d(\omega t) \right] \quad (4.14)$$

$$i.e. \quad b_n = \frac{2V_{dc}}{3\pi n} * \cos\left(\frac{n\pi}{3}\right) - \frac{2V_{dc}}{3\pi n} * \cos\left(\frac{2n\pi}{3}\right) + \frac{2V_{dc}}{3\pi n} * \left[1 - \cos(n\pi)\right] \quad (4.15)$$

Substituting n = 1, 2, 3 etc, we have the following general expression for the fft of line to neutral voltage

$$V_{rn} == \frac{2V_{dc}}{\pi} * \left[\sin(\omega t) + \frac{1}{5}.\sin(5\omega t) + \frac{1}{7}.\sin(7\omega t) + ... \right] ...(4.16)$$

The RMS value of the fundamental component of Vrn is given below:

$$V_{rn1(rms)} = = \frac{\sqrt{2}\,.\,V_{dc}}{\pi} \quad (4.17)$$

For a DC link voltage of 200 volts, the RMS value given by equation 4.13 and the peak fundamental component of Vrn given by equation 4.16 well agree with the simulation results shown in Fig.4.2(F) and (G).

4.2.3 Total Harmonic Distortion

The output voltage of the three phase inverter contains harmonics and hence the waveform is distorted. Total Harmonic Distortion is a measure of the closeness between a distorted waveform and its fundamental component. Thus THD is the ratio

of the RMS value of the distorted waveform and the RMS value of its fundamental component. The THD of the voltage waveform is defined below:

$$THD = \sqrt{\left(\frac{V_{S,RMS}}{V_{S1,RMS}}\right)^2 - 1} \qquad (4.18)$$

The same definition for THD given by equation 4.2.1.18 holds good for currents as well.

Using equations 4.3, 4.4, 4.13, 4.17 and 4.18, the THD of Line to line and Line to neutral voltages are calculated below:

$$THD \quad of \quad V_{LL} = \sqrt{\left(\frac{2.V_{dc}^2/3}{6.V_{dc}^2/\pi^2}\right) - 1} = 30.9\% \qquad (4.19)$$

$$THD \quad of \quad V_{LN} = \sqrt{\left(\frac{2.V_{dc}^2/9}{2.V_{dc}^2/\pi^2}\right) - 1} = 30.9\% \qquad (4.20)$$

4.2.4 Model for Three Phase 180 Degree Mode Inverter

The model of the three phase 180 degree mode inverter is shown in Fig.4.3. The various dialog box where user can enter data is given in Fig.4.4. The dialog box mainly correspond to entering the frequency of switching the inverter and its DC link voltage. The phase advance is entered zero for operation with IM and appropriate value for use with PMSM. For PMSM, the frequency of switching the inverter is derived from the rotor speed. The details of the various subsystems of Fig.4.3 are shown in Fig.4.5(A) to (D). The function of the various subsystems are explained below:

Fig.4.5(A) is the subsystem for the three phase 180 degree mode inverter gate drive parameters. The corresponding dialog box is shown in Fig.4.4. **The frequency entered is 60 Hz** and phase advance is zero. This frequency is internally multiplied by

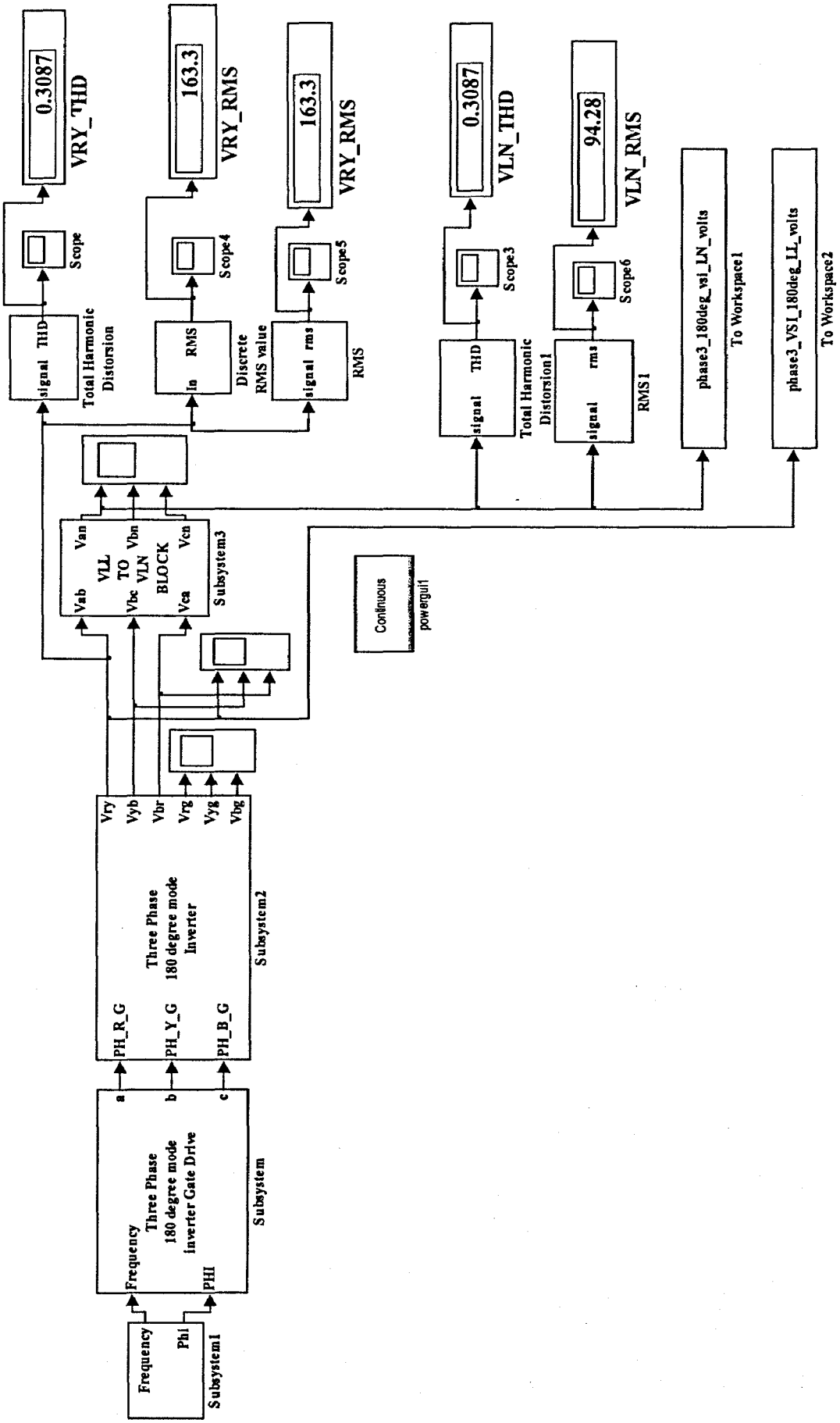

FIG.4.3 MODEL OF A THREE PHASE 180 DEGREE MODE INVERTER

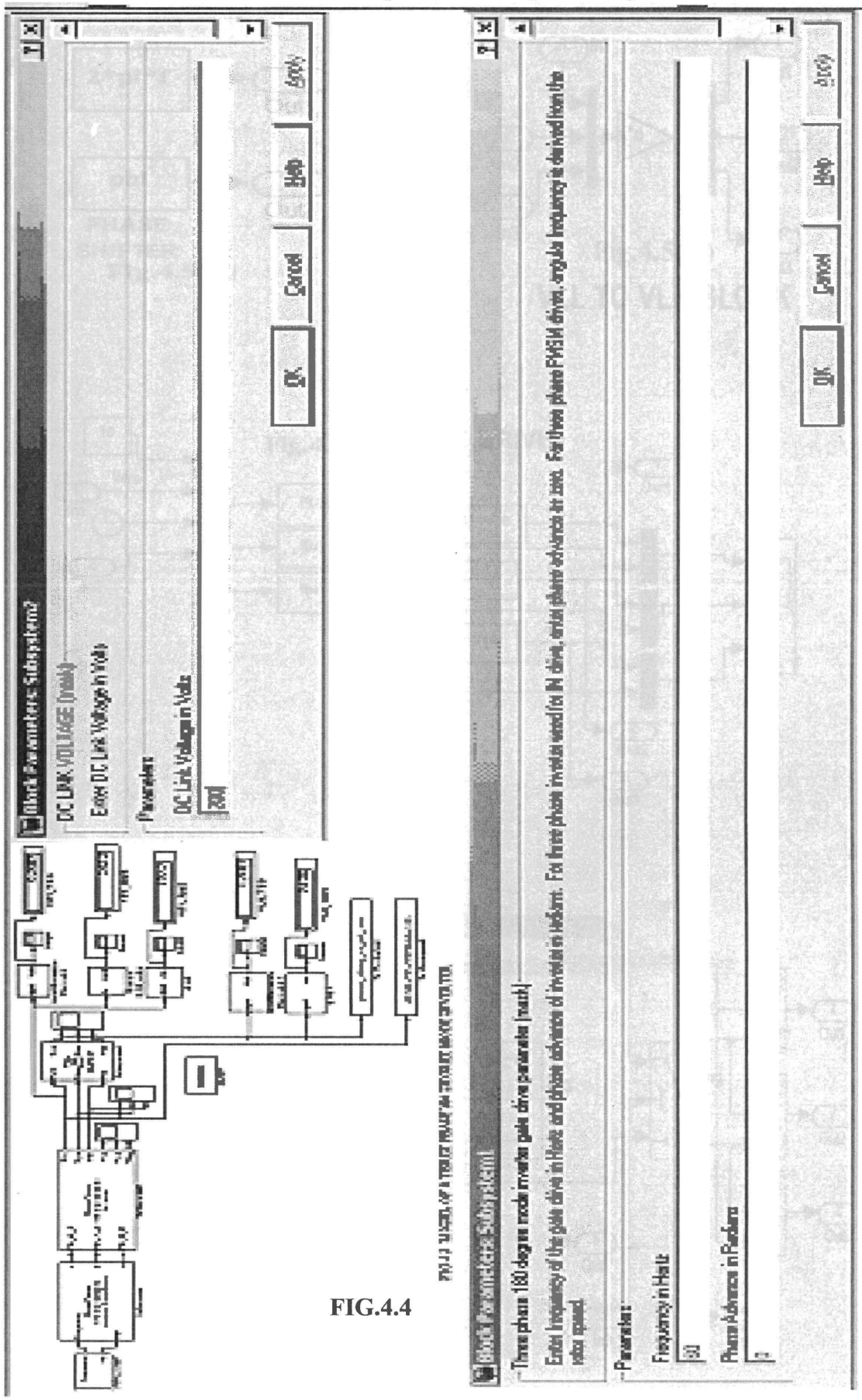
Block Parameters: Subsystem2
DC LINK VOLTAGE (mdl)
Enter DC Link Voltage in Volts
Parameters
DC Link Voltage in Volts
250
OK
Cancel
Help
Apply
Block Parameters: Subsystem1
Three phase 180 degree mode inverter gate drive parameters (mask)
Enter frequency of the gate drive in Hertz and phase advance of inverter in Radians. For three phase inverter used for IM drive, enter phase advance as zero. For three phase PMSM drive, angular frequency is derived from the rotor speed.
Parameters
Frequency in Hertz
50
Phase Advance in Radians
0
OK
Cancel
Help
Apply

FIG.4.4

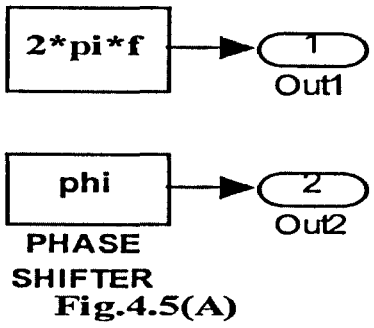

Fig.4.5(A)

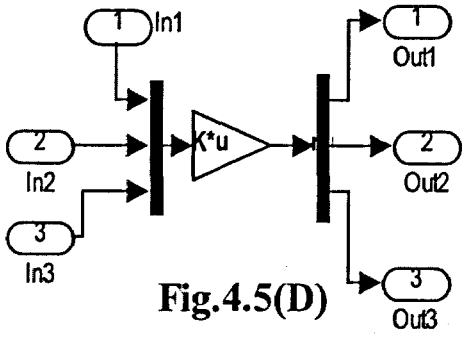

Fig.4.5(D)
VLL TO VLN BLOCK

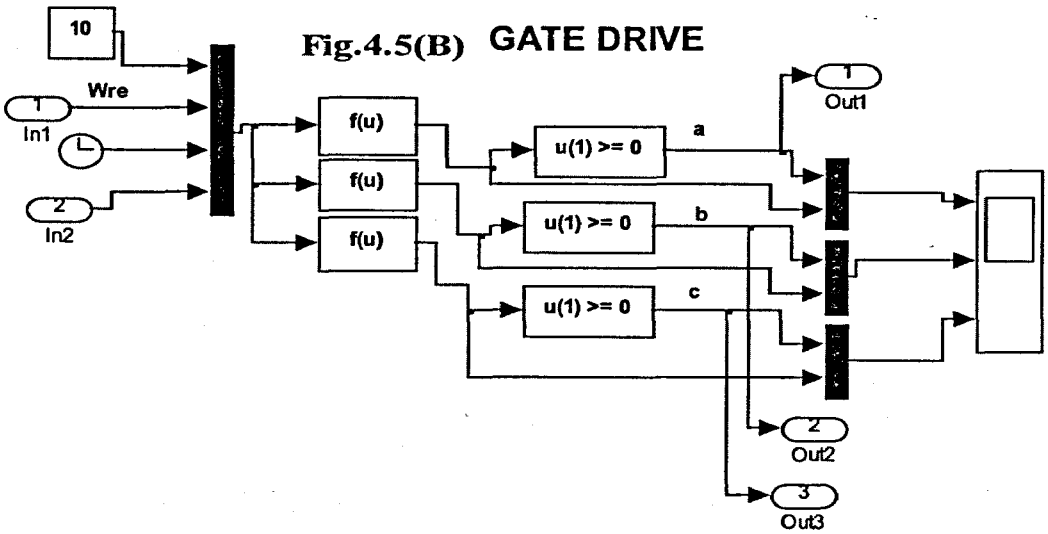

Fig.4.5(B) GATE DRIVE

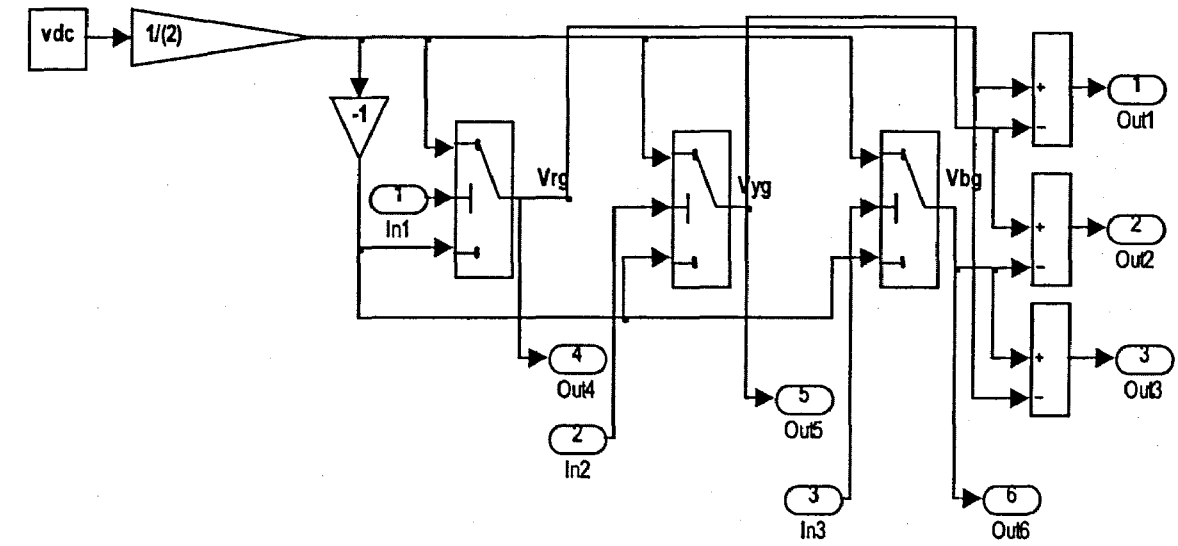

Fig.4.5(C) SIX STEP INVERTER

2π to get the angular frequency to generate the sine wave and the gate drive for inverter..

The outputs of Fig.4.5(A) is given to the four input mux in Fig.4.5(B). In Fig.4.5(B), the three Fcn blocks connected to four input mux generates three phase sine wave at the above entered frequency with phase advance added. The three phase sine wave output is connected to three Fcn blocks which compare the respective input u(1) with zero, generate logic 1 if u(1) is greater than or equal to zero, else output logic 0. The output of the three Fcn blocks are the switch functions a, b and c.

The a, b and c output of the three Fcn blocks in Fig.4.5(B) are given to u(2) of input of the three threshold switches in Fig.4.5(C). The u(1) and u(3) input to these three threshold switches are +Vdc/2 and –Vdc/2 respectively. When the u(2) input to these three switches is greater than or equal to the threshold value of 0.5, the output of these switches are +Vdc/2, else the outputs are –Vdc/2. Thus the three switches generate the three phase line to ground voltages Vrg, Vyg and Vbg respectively. These line to ground voltages are subtracted in pairs using subtract block to generate the three phase line to line voltages Vry, Vyb and Vbr respectively. Fig.4.5(C) opens up the dialog box shown in Fig.4.4.for DC Link voltage. **The DC link voltage entered is 200 Volts.**

The three phase line to line voltages Vry, Vyb and Vbr are respectively applied to the three input mux shown in Fig.4.5(D). The matrix gain block in Fig.4.5(D) multiplies Vry, Vyb and Vbr by the matrix defined in equation 4.2.1.11 to get the line to neutral voltages Vrn, Vyn and Vbn at the output of the demux block.

The THD and RMS values of line to line and line to neutral voltages are measured using appropriate measurement blocks from SimPowerSystems Block set. The powergui from SimpowerSystems block set is used to display the harmonic spectrum of the line to neutral and line to line voltages.

4.2.5 Simulation Results

The simulation of the three phase 180 degree mode inverter model was conducted using

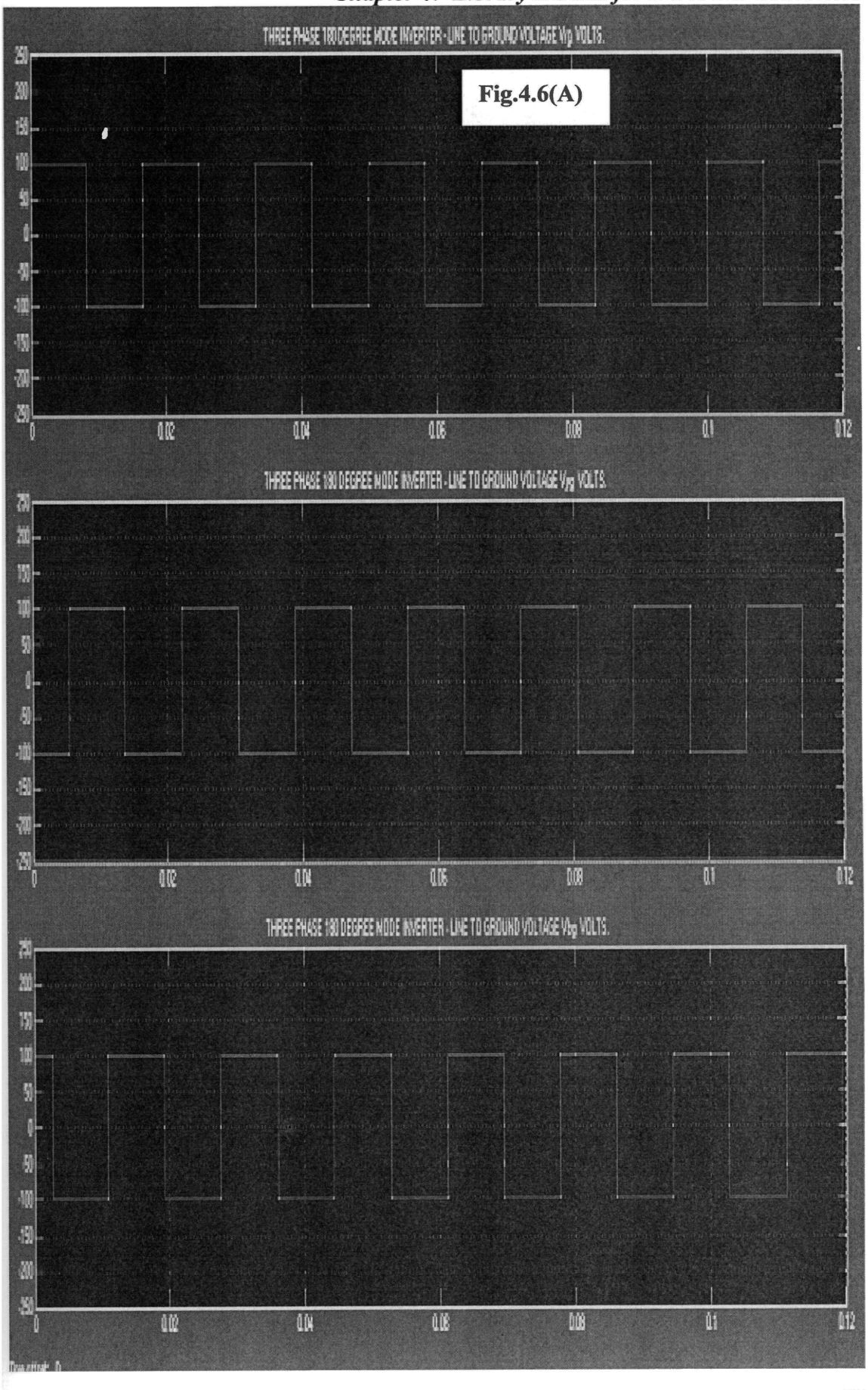
THREE PHASE 180 DEGREE MODE INVERTER - LINE TO GROUND VOLTAGE Vrg VOLTS.
THREE PHASE 180 DEGREE MODE INVERTER - LINE TO GROUND VOLTAGE Vyg VOLTS.
THREE PHASE 180 DEGREE MODE INVERTER - LINE TO GROUND VOLTAGE Vbg VOLTS.
0
0.02
0.04
0.06
0.08
0.1
0.12

Fig.4.6(A)

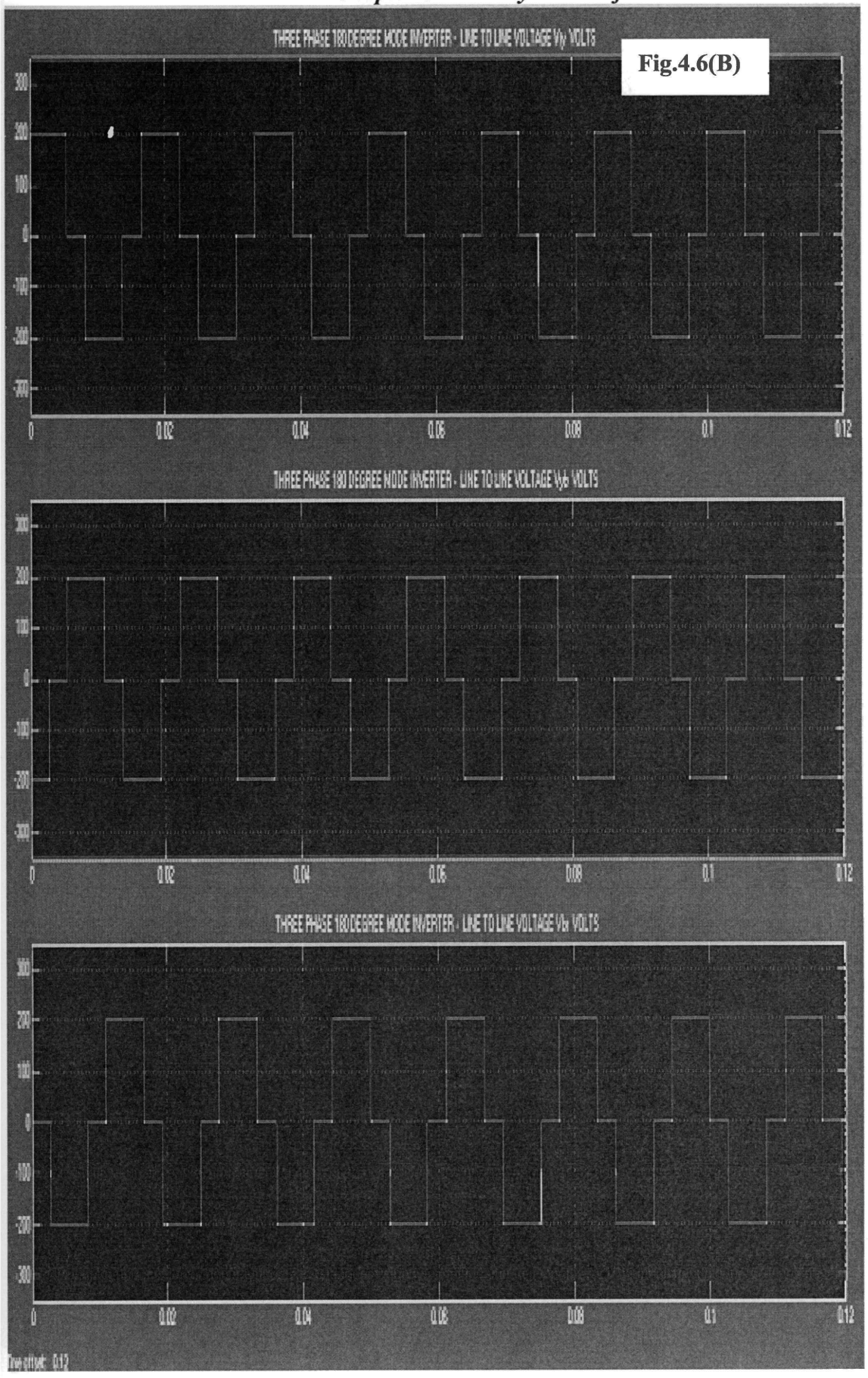
THREE PHASE 180 DEGREE MODE INVERTER - LINE TO LINE VOLTAGE Vy VOLTS
THREE PHASE 180 DEGREE MODE INVERTER - LINE TO LINE VOLTAGE Vb VOLTS
THREE PHASE 180 DEGREE MODE INVERTER - LINE TO LINE VOLTAGE Vb VOLTS
0
0.02
0.04
0.06
0.08
0.1
0.12

Fig.4.6(B)

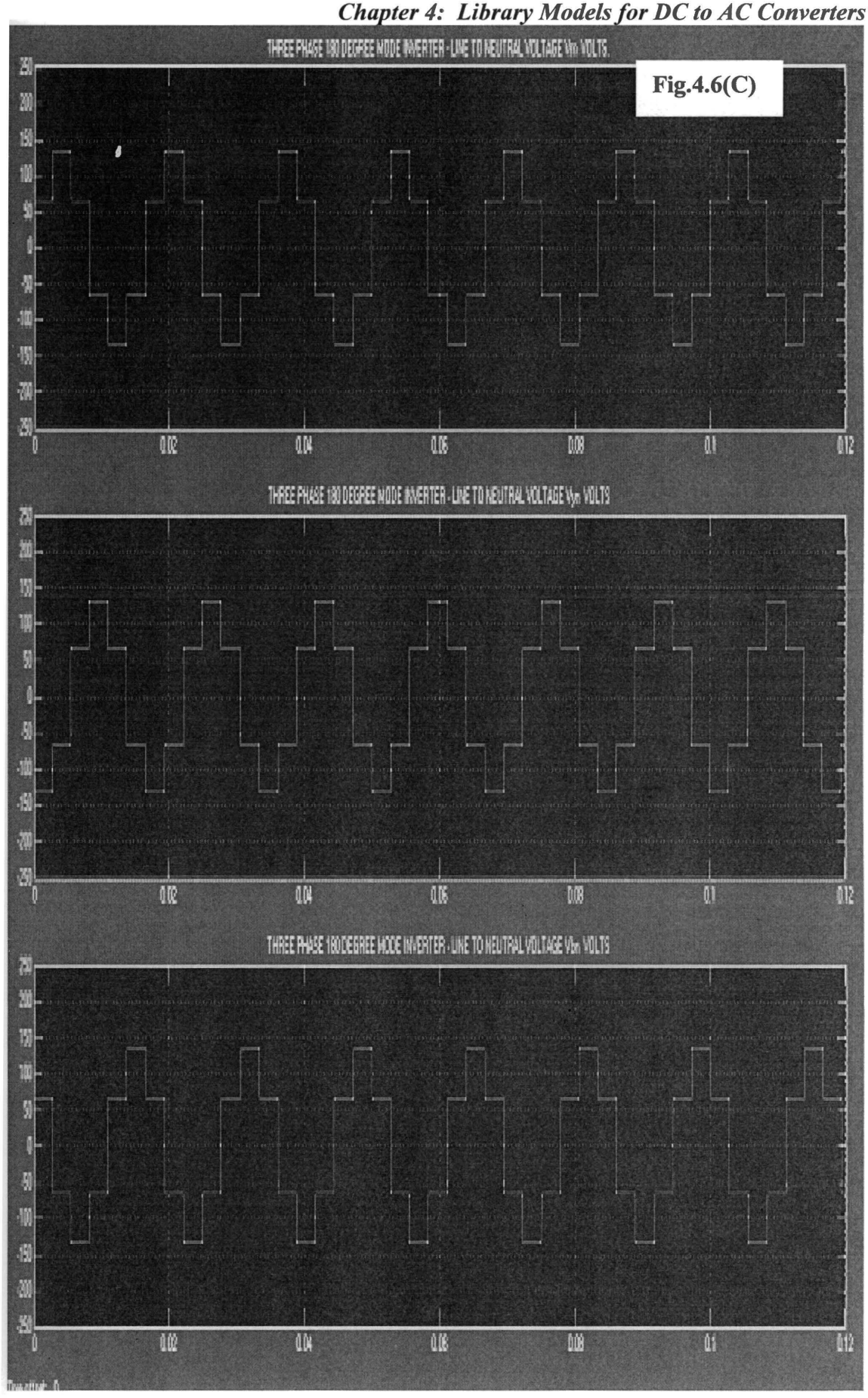
THREE PHASE 180 DEGREE MODE INVERTER - LINE TO NEUTRAL VOLTAGE Van VOLTS.
THREE PHASE 180 DEGREE MODE INVERTER - LINE TO NEUTRAL VOLTAGE Vbn VOLTS
THREE PHASE 180 DEGREE MODE INVERTER - LINE TO NEUTRAL VOLTAGE Vcn VOLTS

Fig.4.6(C)

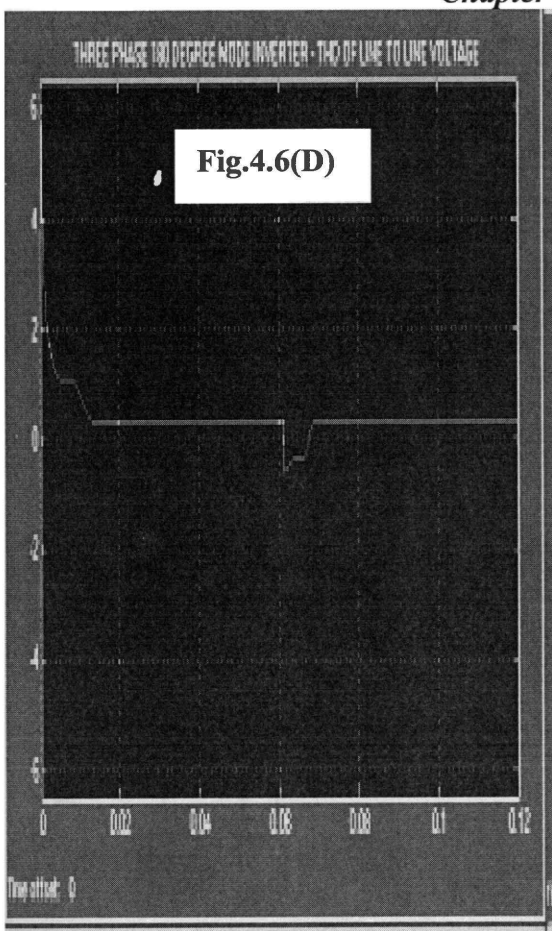
THREE PHASE 180 DEGREE MODE INVERTER - THD OF LINE TO LINE VOLTAGE
Fig.4.6(D)

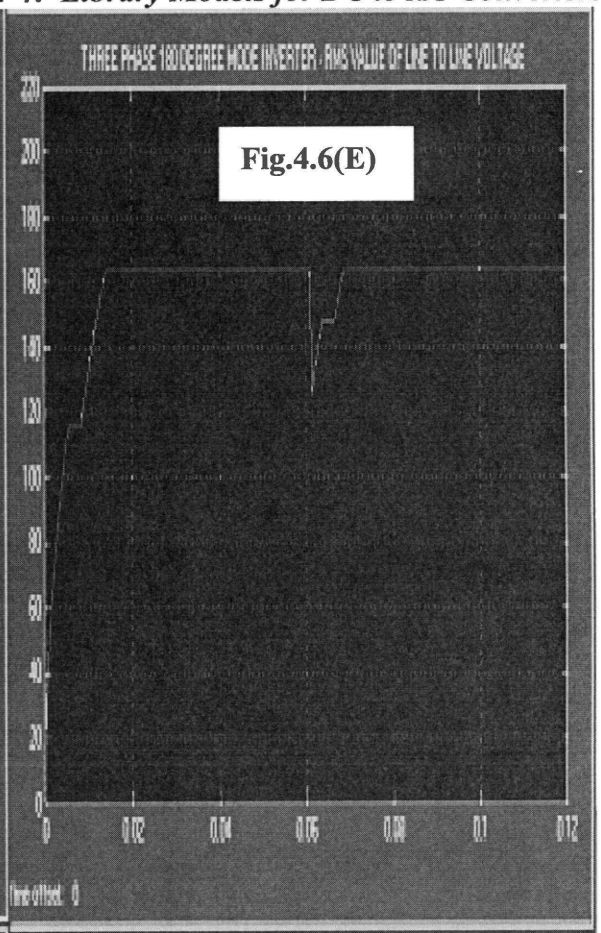
THREE PHASE 180DEGREE MODE INVERTER - RMS VALUE OF LINE TO LINE VOLTAGE
Fig.4.6(E)

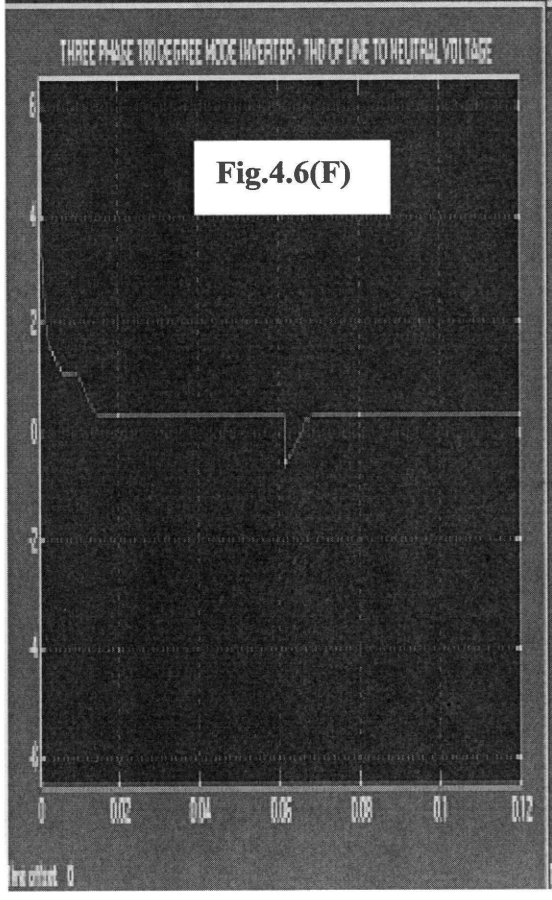
THREE PHASE 180DEGREE MODE INVERTER - THD OF LINE TO NEUTRAL VOLTAGE
Fig.4.6(F)

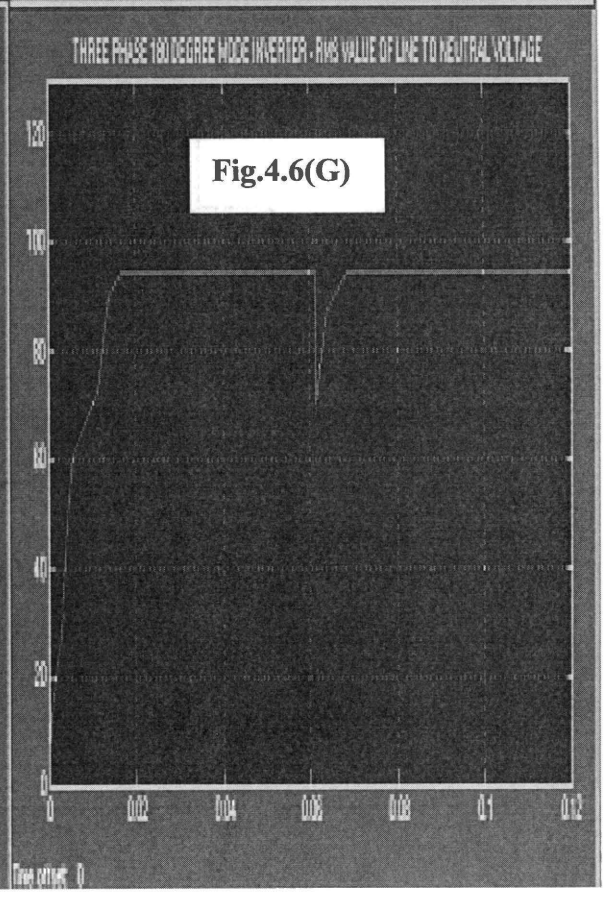
THREE PHASE 180 DEGREE MODE INVERTER - RMS VALUE OF LINE TO NEUTRAL VOLTAGE
Fig.4.6(G)

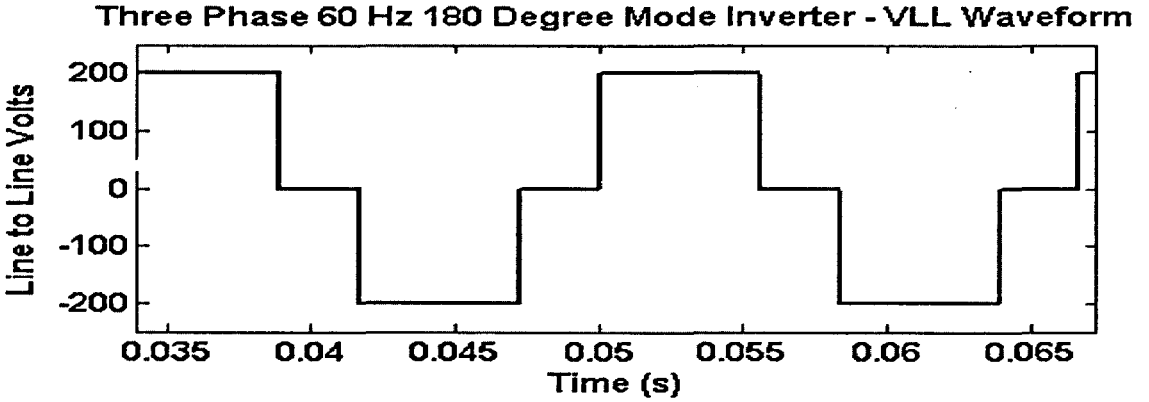

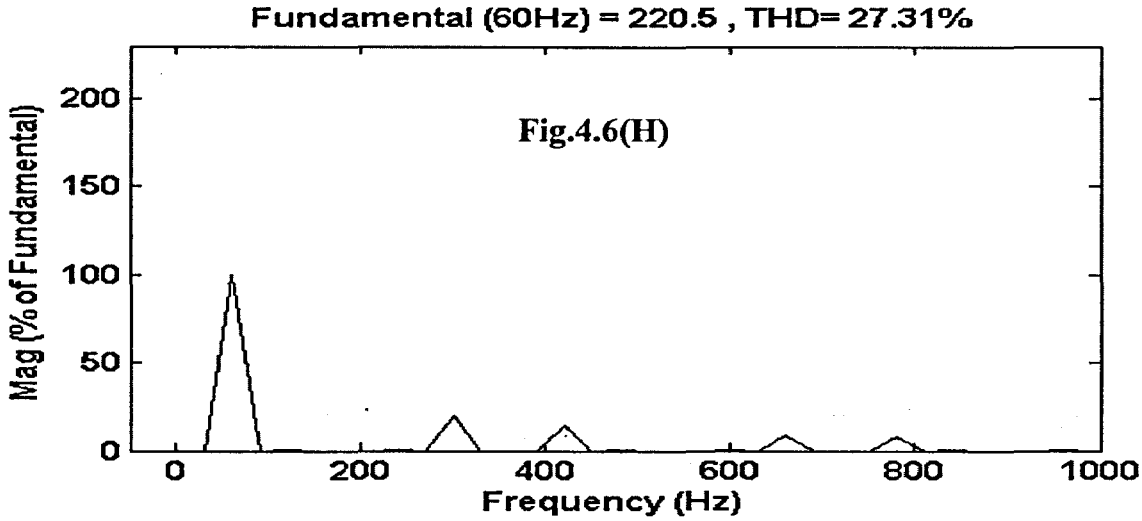

Fig.4.6(H)

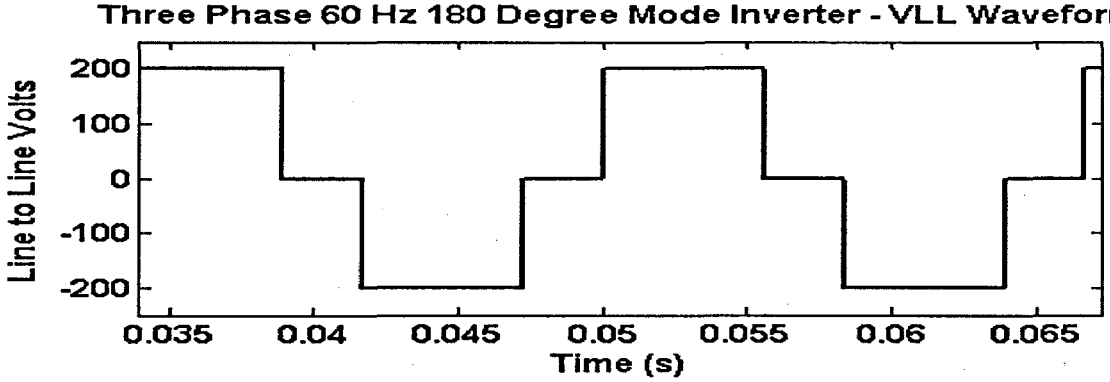

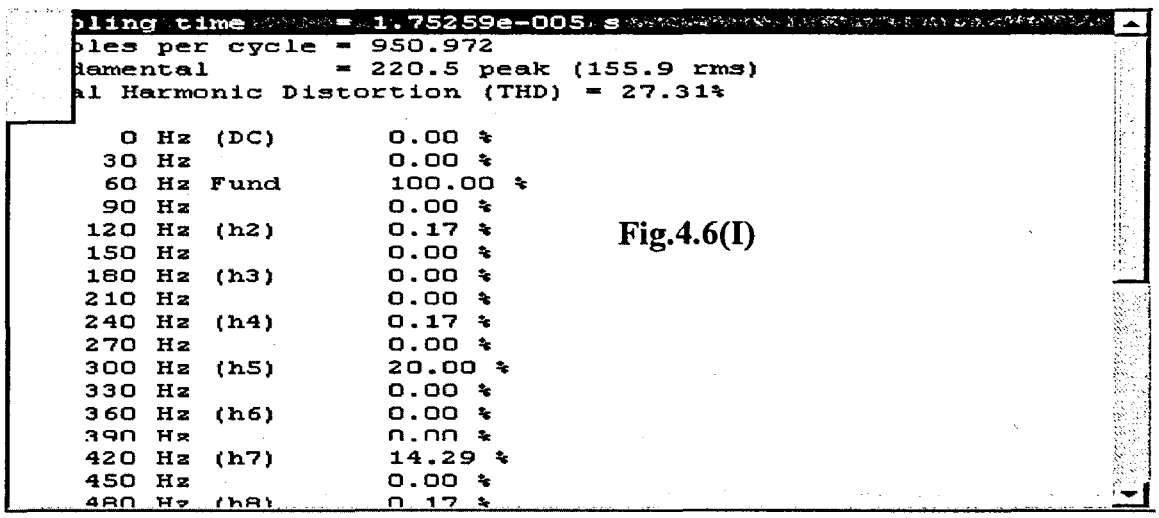

```
pling time          = 1.75259e-005 s
ples per cycle = 950.972
damental           = 220.5 peak (155.9 rms)
al Harmonic Distortion (THD) = 27.31%

  0 Hz (DC)        0.00 %
 30 Hz             0.00 %
 60 Hz Fund       100.00 %
 90 Hz             0.00 %
120 Hz (h2)       0.17 %
150 Hz             0.00 %
180 Hz (h3)       0.00 %
210 Hz             0.00 %
240 Hz (h4)       0.17 %
270 Hz             0.00 %
300 Hz (h5)      20.00 %
330 Hz             0.00 %
360 Hz (h6)       0.00 %
390 Hz             0.00 %
420 Hz (h7)      14.29 %
450 Hz             0.00 %
480 Hz (h8)       0.17 %
```

Fig.4.6(I)

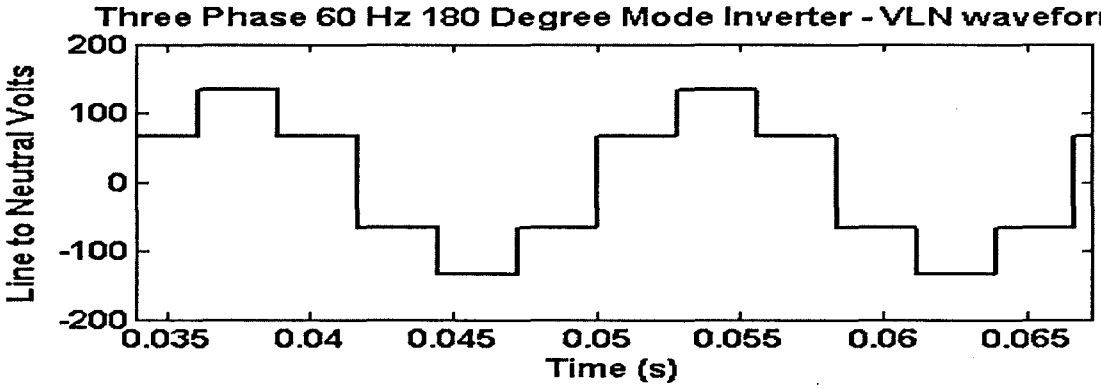

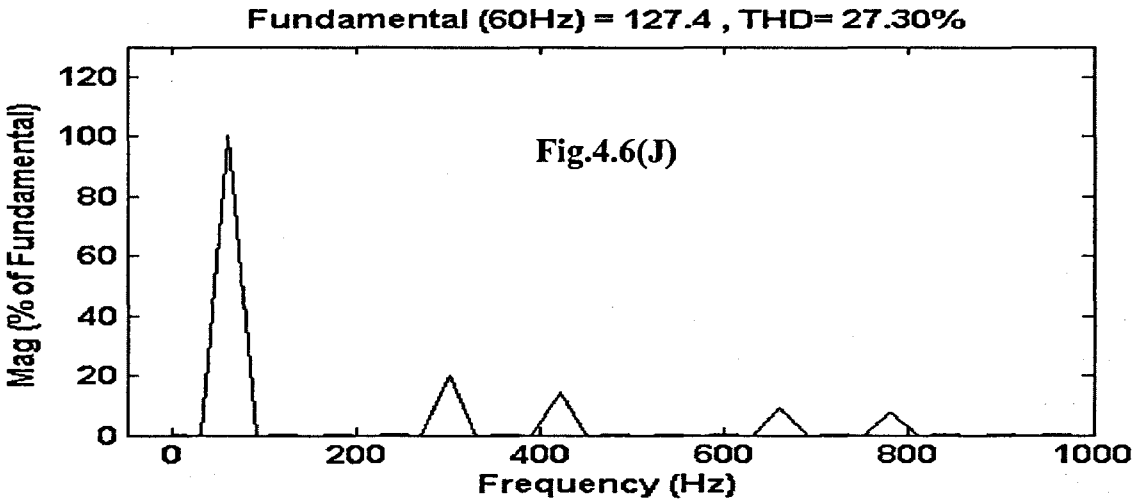

Fig.4.6(J)

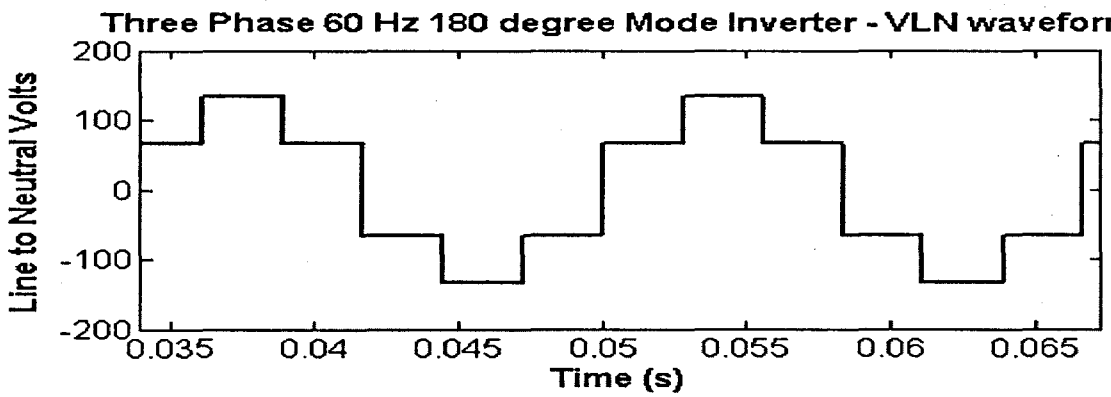

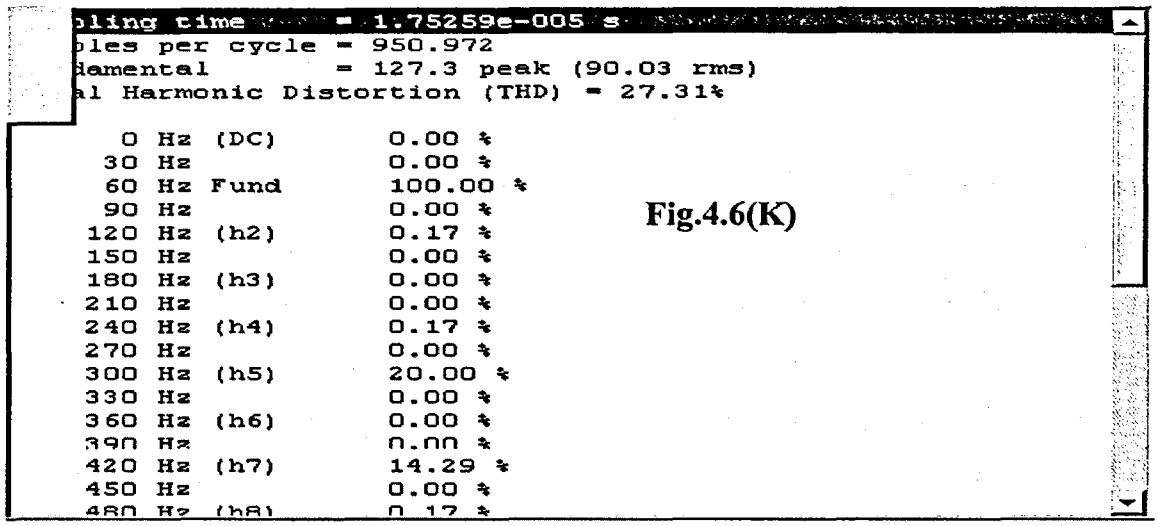

Fig.4.6(K)

ode15s(stiff/NDF) solver. The three phase line to ground voltages, Line to Line voltages and the Line to Neutral voltages are shown in Fig.4.6(A) to (C) respectively. The THD and RMS values of line to line voltage is shown in Fig.4.6(D), (E) and that corresponding to Line to Neutral voltages are shown in Fig.4.6(F) and (G) respectively. The harmonic spectrum of line to line voltage is shown in Fig.4.6(H), (I) and that corresponding to Line to Neutral voltages are shown in Fig.4.6(J) and (K) respectively. The results observed for THD and RMS values of line to line voltages and that corresponding to Line to Neutral voltages are displayed in the meter in Fig.4.3. These simulation results displayed in Fig.4.3.are also tabulated in Table 4.1. The theoreticaly

TABLE 4.1: Three Phase 180 degree Mode Inverter – simulation results

Sl.No.	Frequency Hz	DC Link Voltage – Volts	% THD of VLL	RMS VLL Volts	% THD of VLN	RMS VLN Volts
1	60	200	30.87	163.3	30.87	94.28

TABLE 4.2: Three Phase 180 degree Mode Inverter – calculated values

Sl.No.	Frequency Hz	DC Link Voltage – Volts	% THD of VLL	RMS VLL Volts	% THD of VLN	RMS VLN Volts
1	60	200	30.9	163.28	30.9	94.27

calculated values for THD and RMS values of line to line and line to neutral voltages using equations 4.3, 4.4, 4.13 and 4.17 are tabulated in TABLE 4.2 [14].

4.3 Three Phase 120 Degree Mode Inverter

The three phase inverter shown in Fig.4.1. can also be driven by 120 degree gate drive. This gate drive pattern is shown in Fig.2.6(B) [14 – 17]. The PSPICE simulation of the three phase 120 degree mode 50 Hz inverter is shown in Fig.4.7(A) to (F). Fig.4.7(A) to (F) are respectively three phase line to ground voltages, line to line voltages, Line to line voltage and its RMS value, Harmonic spectrum of line to line voltage, Line to Neutral voltages, Line to Neutral voltage and its RMS value, Harmonic spectrum of line to neutral voltage.

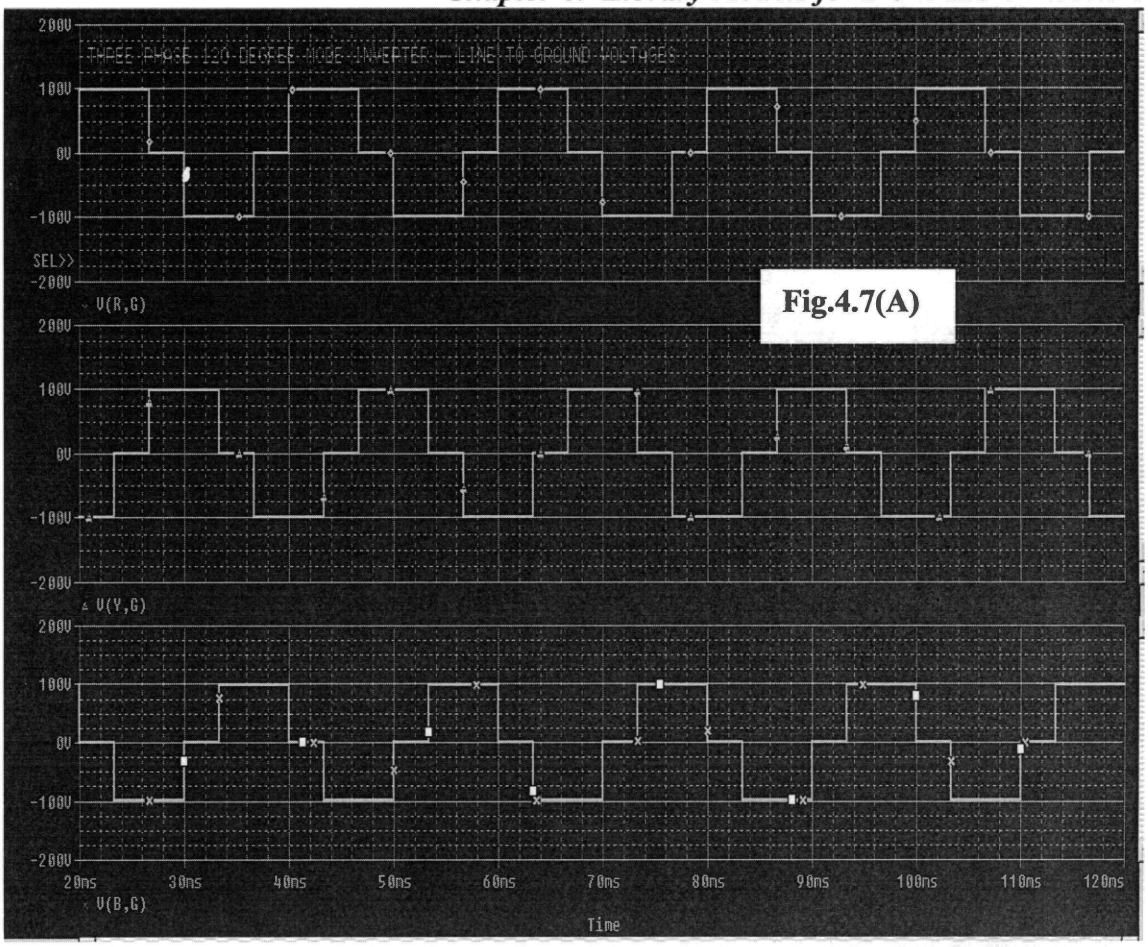

Fig.4.7(A)

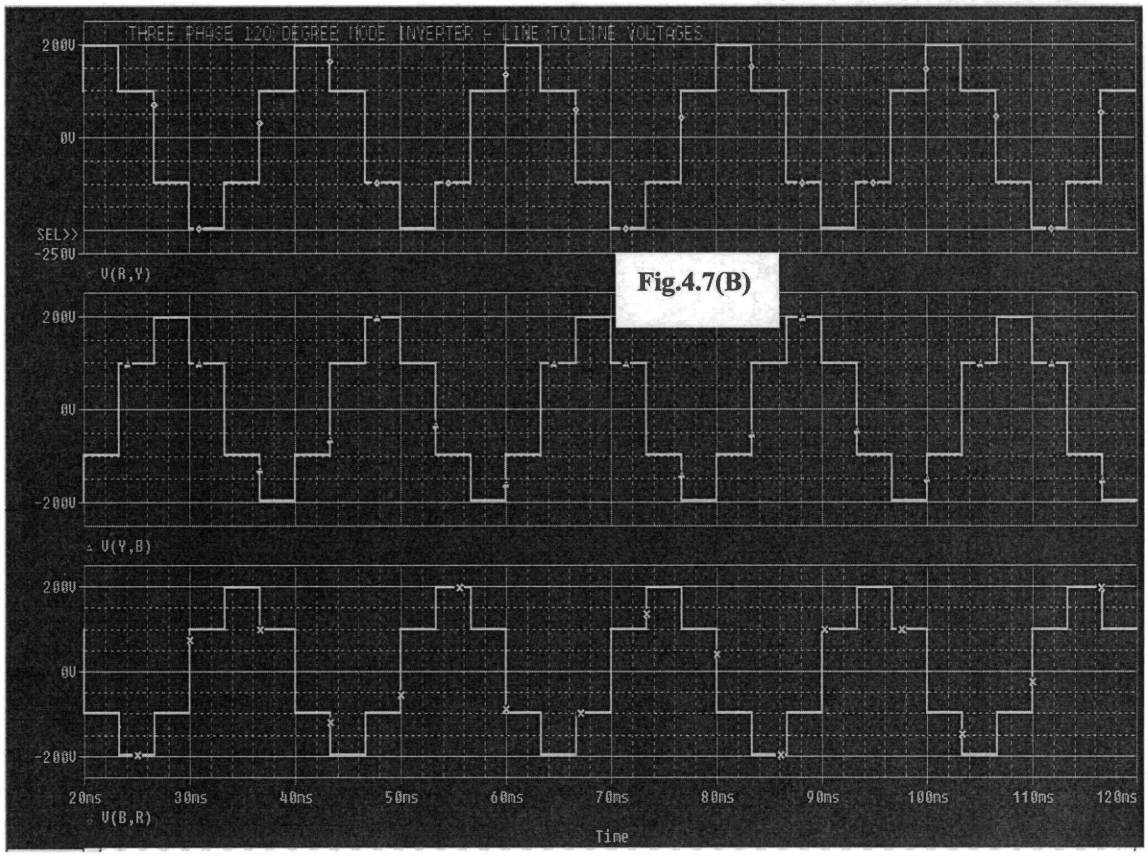

Fig.4.7(B)

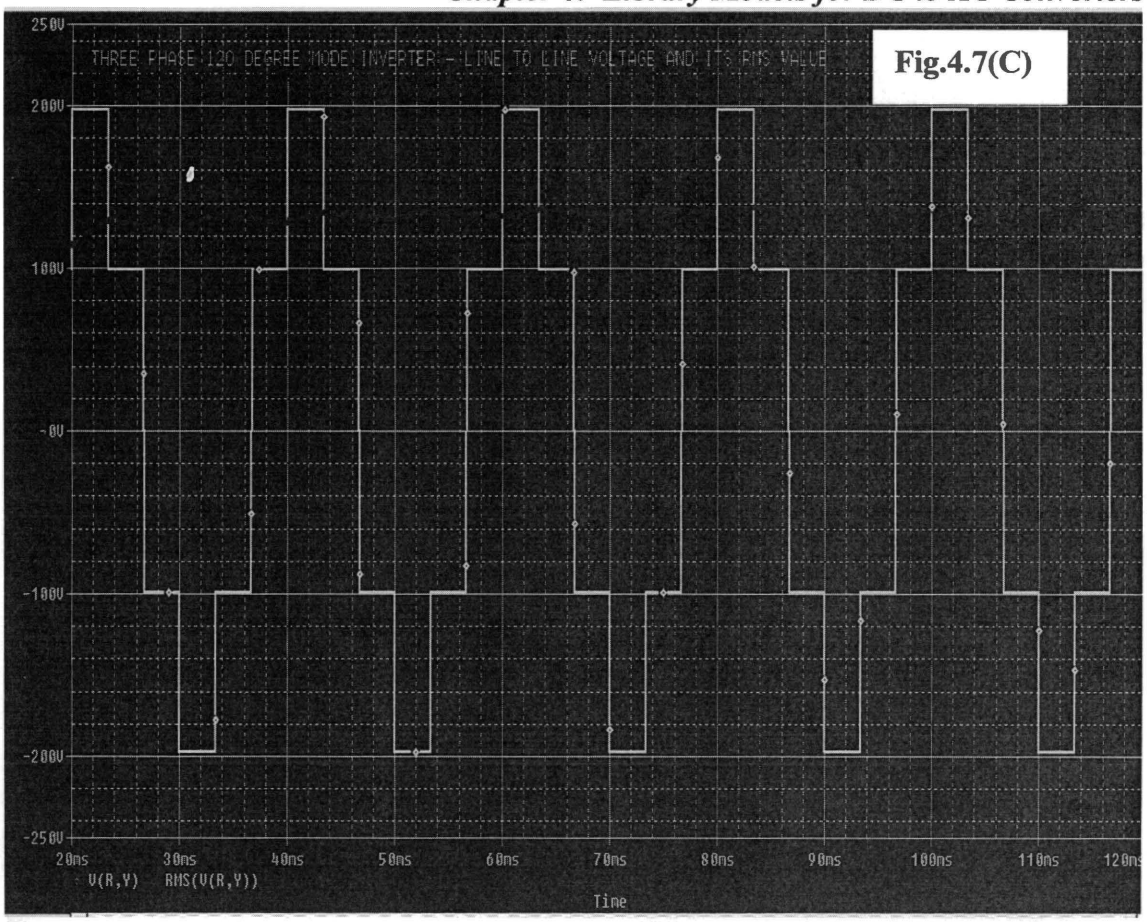

Fig.4.7(C)

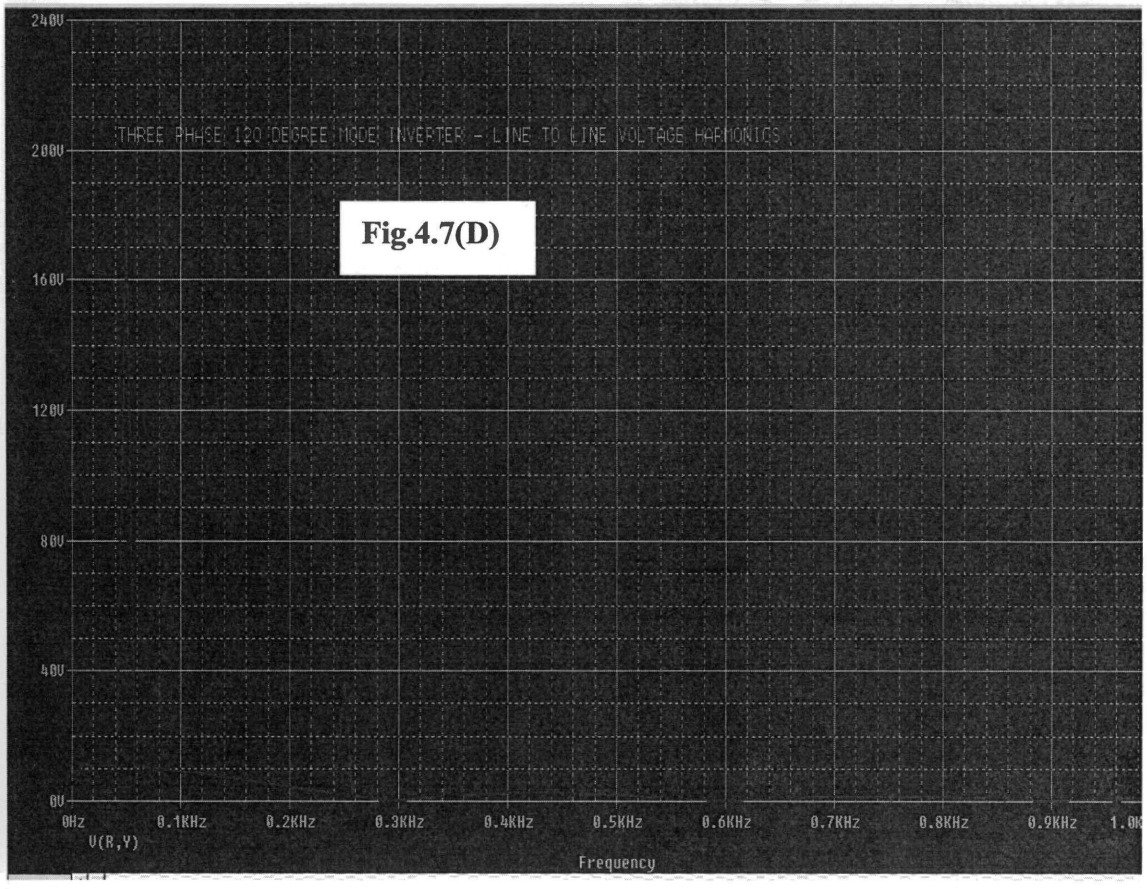

Fig.4.7(D)

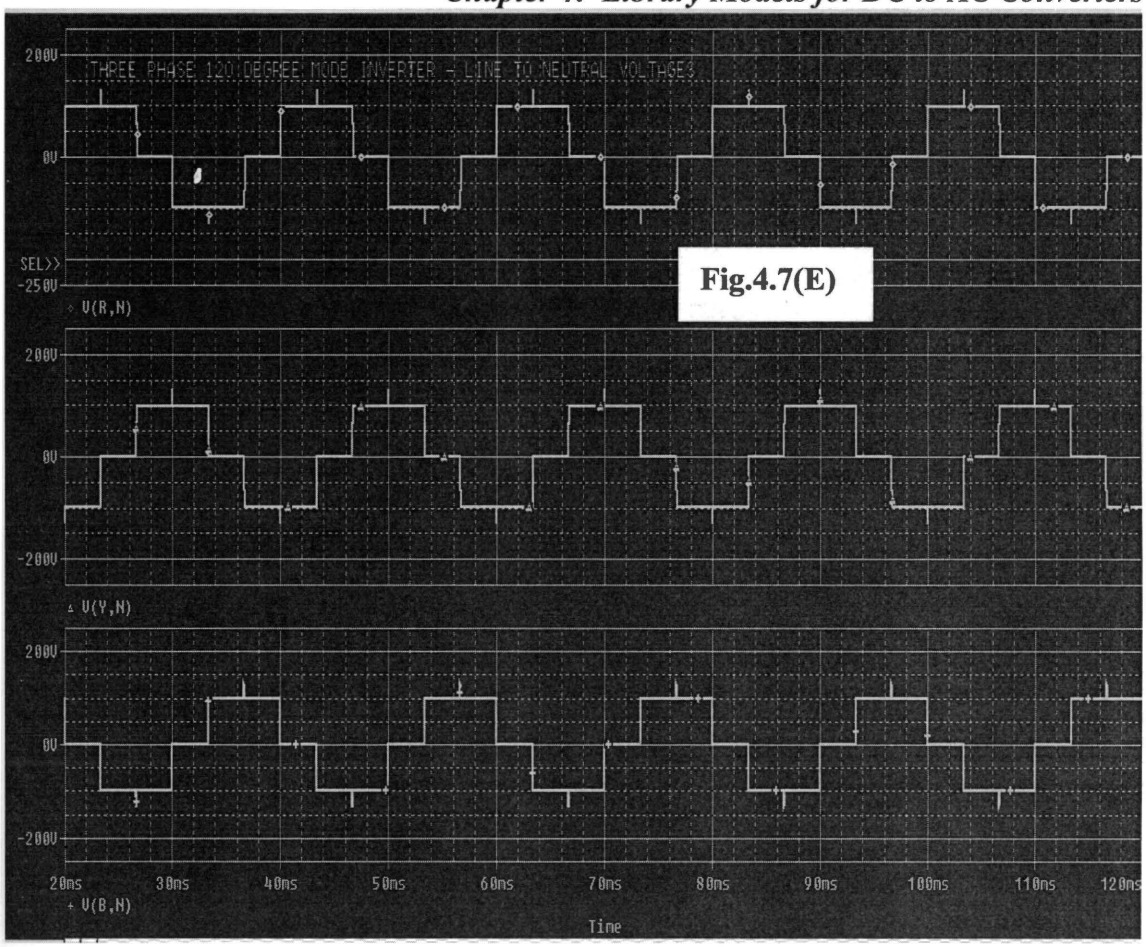

Fig.4.7(E)

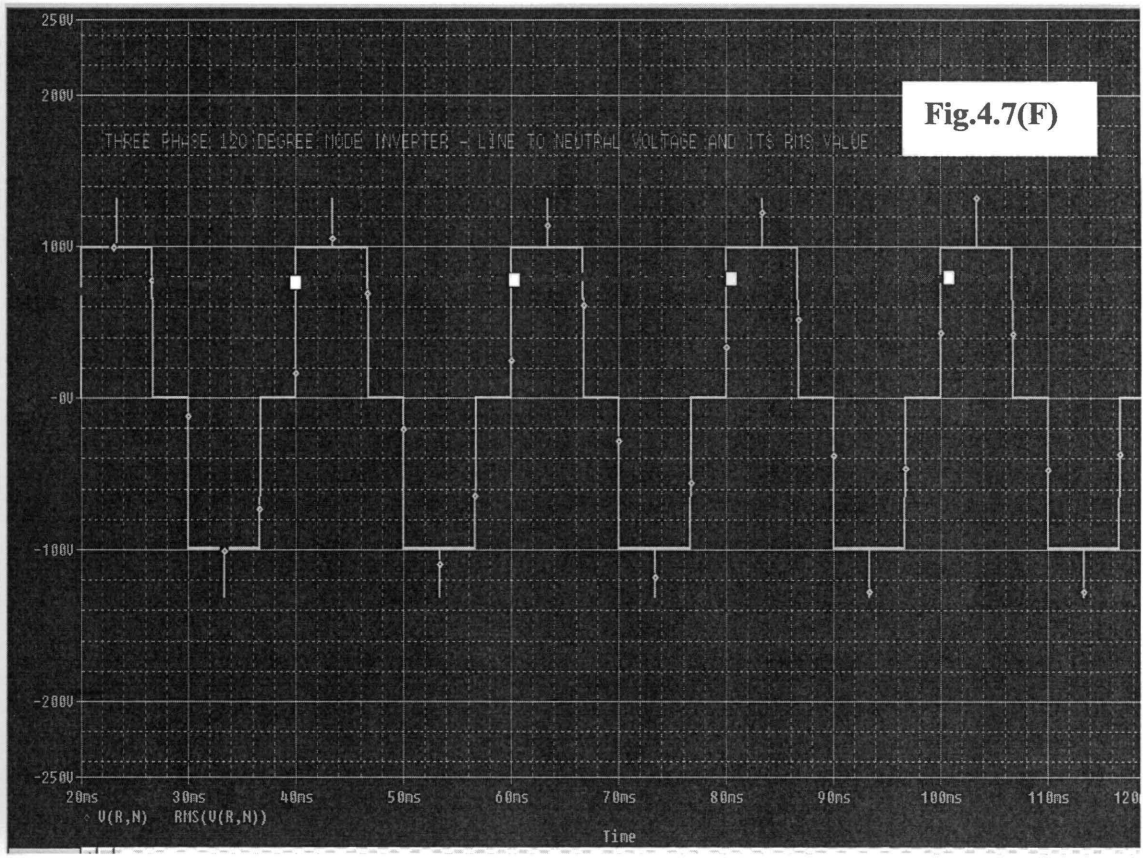

Fig.4.7(F)

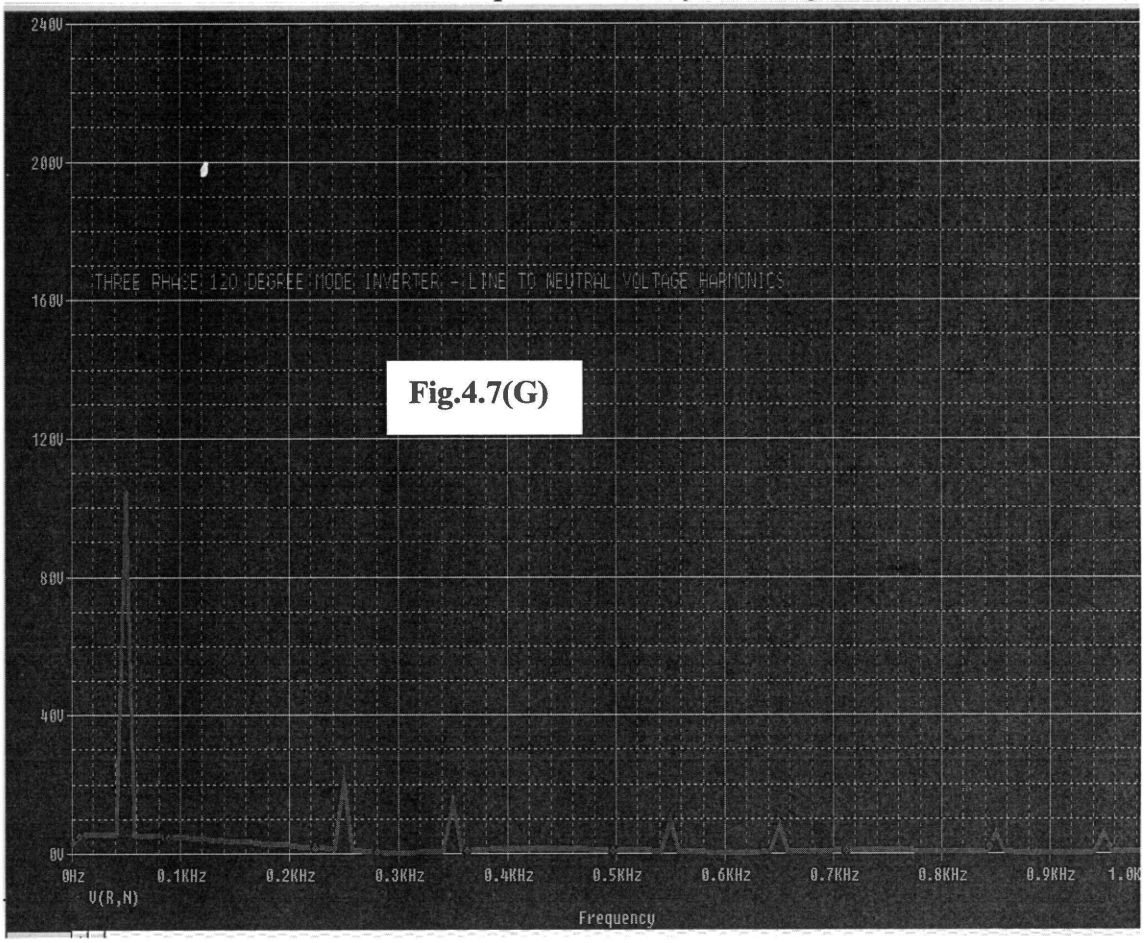

Fig.4.7(G)

4.3.1 Analysis of Line to Line Voltage

The analysis of line to line voltage of three phase 120 degree mode inverter is done in this section. The line to line voltage Vry is shown in Fig.4.7(C). The theoretical derivation of Line to Line voltage waveform is shown in section 4.3.2. Shifting the axis of Fig.4.7(C) by π/3 makes the function odd i.e. f(-t) = -f(+t). The even harmonics are zero. The Fourier coefficient bn can be defined as follows:

$$b_n = \frac{4}{\pi}.\left[\int_0^{\pi/3} \frac{V_{dc}}{2}.\sin(n\omega t).d(\omega t) + \int_{\pi/3}^{\pi/2} V_{dc}.\sin(n\omega t).d(\omega t)\right]$$

$$= \sum_{n=1,3,5,7....}^{\infty} \frac{2.V_{dc}}{\pi n} * \left(1 + \cos\frac{n\pi}{3}\right) \qquad (4.21)$$

The line to line voltage Vry can be expressed by Fourier series as follows:

$$V_{ry} = = \sum_{n=1,3,5,7....}^{\infty} \frac{2.V_{dc}}{\pi.n} * \left(1 + \cos\frac{n\pi}{3}\right) * \sin\left(n\omega t + \frac{n\pi}{3}\right) \quad (4.22)$$

The RMS value of Vry is given below:

$$V_{ry(rms)} = \sqrt{\frac{1}{\pi} * \left[\int_0^{\pi/3} V_{dc}^2 .d(\omega t) + \int_{\pi/3}^{2\pi/3} \frac{V_{dc}^2}{4} .d(\omega t) + \int_{2\pi/3}^{\pi} \frac{V_{dc}^2}{4} .d(\omega t)\right]}$$

$$= \frac{V_{dc}}{\sqrt{2}} \quad (4.23)$$

The RMS value of the fundamental component of Vry from equation 4.3.1.2 is given below

$$V_{ry1(rms)} = \frac{3}{\sqrt{2}} \cdot \left(\frac{V_{dc}}{\pi}\right) \quad (4.24)$$

The RMS value of line to line voltage for a dc link voltage of 200 Volts shown in Fig.4.7(C) and the peak value of the fundamental component of Vry shown in Fig.4.7(D) well agree with the equations 4.3.1.3 and 4.3.1.4.

4.3.2 Analysis of Line to Neutral Voltage

In the following section, the r.m.s. value and fft of line to neutral voltage of a six step 120 degree mode inverter is derived.

For clarity the line to neutral voltage of a three phase 120 degree mode inverter is derived by simulation using PSPICE, shown in Fig.4.1. Resistive star connected load is used for convenience only, as inductive load may give rise to voltage spikes in the waveform. The simulated Line to neutral voltage is shown in fig.4.7(F). The dotted line in fig.4.7(F) indicates its r.m.s. value computed by PSPICE. A three phase 50 Hz waveform is generated. The waveform can be theoretically derived as follows:

By taking the ground g as the midpoint of the two dc voltage sources, the line to ground voltage Vrg, Vyg and Vbg can be easily derived for three phase 120 degree mode gate drive, by observation of Fig.4.1. This waveform is described below:

Vrg = +Vdc/2 for $0 \leq wt \leq 2pi/3$
= 0 for $2pi/3 \leq wt \leq pi$
= -Vdc/2 for $pi \leq wt \leq 5pi/3$
= 0 for $5pi/3 \leq wt \leq 2pi$ .....(4.25)

Vyg = +Vdc/2 for $2pi/3 \leq wt \leq 4pi/3$
= 0 for $4pi/3 \leq wt \leq 5pi/3$
= -Vdc/2 for $5pi/3 \leq wt \leq 2pi$ and
for $0 \leq wt \leq pi/3$
= 0 for $pi/3 \leq wt \leq 2pi/3$ ..... (4.26)

Vbg = +Vdc/2 for $4pi/3 \leq wt \leq 2pi$
= 0 for $0 \leq wt \leq pi/3$
= -Vdc/2 for $pi/3 \leq wt \leq pi$
= 0 for $pi \leq wt \leq 4pi/3$ .....(4.27)

From equations 1, 2 and 3 the line voltages can be expressed as follows:

Vry = Vrg - Vyg .....(4.28)

Vyb = Vyg - Vbg ..... (4.29)

Vbr = Vbg - Vrg ..... (4.30)

The line to neutral voltages Vrn, Vyn and Vbn can be derived as follows:

$$\begin{bmatrix} V_{rn} \\ V_{yn} \\ V_{bn} \end{bmatrix} = \frac{1}{3} \cdot \begin{bmatrix} 1 & 0 & -1 \\ -1 & 1 & 0 \\ 0 & -1 & 1 \end{bmatrix} * \begin{bmatrix} V_{ry} \\ V_{yb} \\ V_{br} \end{bmatrix} \quad ...(4.31)$$

The waveform derived using equation 4.3.1.11 looks much the same way as shown in V(R,N) in fig.4.7(F).

The waveform derived by using equations 4.25 to 4.31, gives the following coordinates for Vrn:

(0, 0), (0, +Vdc/2), (2pi/3, +Vdc/2), (2pi/3, 0), (pi, 0), (pi, -Vdc/2), (5pi/3, -Vdc/2), (5pi/3, 0), (2.pi, 0), (2.pi, +Vdc/2) and so on.

Referring to Fig.4.7(F) and noting the coordinates given above, we have the following equation for RMS value of line to neutral voltage.

$$V_{rn(rms)} = \sqrt{\left[\frac{1}{\pi}.\left(\int_{0}^{2\pi/3}\left(\frac{V_{dc}^{2}}{4}\right).d(\omega t)\right)\right]} = \frac{V_{dc}}{\sqrt{6}} \quad ...(4.32)$$

The Fourier transform of Line to Neutral voltage Vrn is derived below:

Referring to Fig.4.7(F), shifting the axis of symmetry by π/6 from the origin where f(-t) = -f(+t) and the function is odd. The even harmonics are zero. Thus Fourier coefficient bn is given by

$$b_n = \frac{2}{\pi} * \left[\int_{\pi/6}^{(\pi-\frac{\pi}{6})} \frac{V_{dc}}{2}.\sin(n\omega t).d(\omega t)\right]$$

$$= \frac{2.V_{dc}}{n.\pi}.\cos\left(\frac{n.\pi}{6}\right) \quad for \quad n = 1,3,5,7... \quad (4.33)$$

The line to neutral voltage Vrn can be expressed by Fourier series as follows:

$$V_{rn} = \sum_{n=1,3,5,7,...}^{\infty} \frac{2.V_{dc}}{n.\pi}.\cos\left(\frac{n.\pi}{6}\right).\sin\left(n\omega t + \frac{n.\pi}{6}\right) \quad (4.34)$$

The RMS value of the fundamental component of Vrn from equation 4.3.1.14 is given below

$$V_{rn1(rms)} = \sqrt{\frac{3}{2}} \cdot \left(\frac{V_{dc}}{\pi} \right) \qquad (4.35)$$

The RMS value of line to neutral voltage for a dc link voltage of 200 Volts shown in Fig.4.7(F) and the peak value of the fundamental component of Vrn shown in Fig.4.7(G) well agree with the equations 4.32 and 4.34.

4.3.3 Total Harmonic Distortion

The THD of the voltage wave form is defined by equation 4.18 in section 4.2.3.

Using equations 4.23, 4.24, 4.32, 4.35, the THD of Line to line and Line to neutral voltages are calculated below:

$$THD \quad of \quad V_{LL} = \sqrt{\left(\frac{V_{dc}^2/2}{9.V_{dc}^2/2.\pi^2} \right) - 1} = 30.9\% \qquad (4.36)$$

$$THD \quad of \quad V_{LN} = \sqrt{\left(\frac{V_{dc}^2/6}{3.V_{dc}^2/2.\pi^2} \right) - 1} = 30.9\% \qquad (4.37)$$

4.3.4 First Model for Three Phase 120 Degree Mode Inverter

The first model of the three phase 120 degree mode inverter is shown in Fig.4.8. The various dialog box where user can enter data is given in Fig.4.9. The dialog box mainly correspond to entering the frequency of switching the inverter and its DC link voltage. The phase advance is entered zero for operation with IM and appropriate value for use with PMSM. For PMSM, the frequency of switching the inverter is derived from the

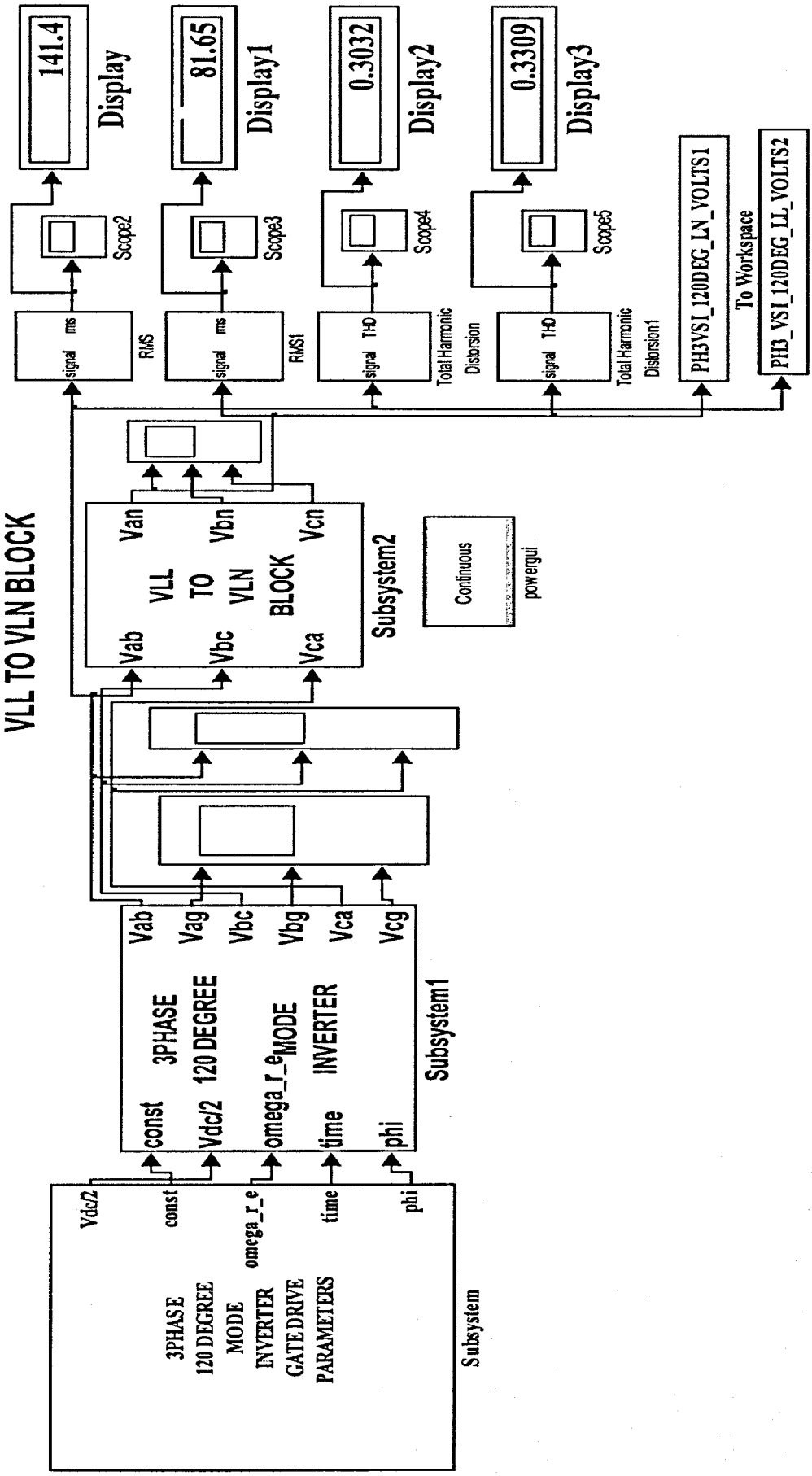

FIG.4.8: THREE PHASE 120 DEGREE MODE GATE DRIVE CUM INVERTER

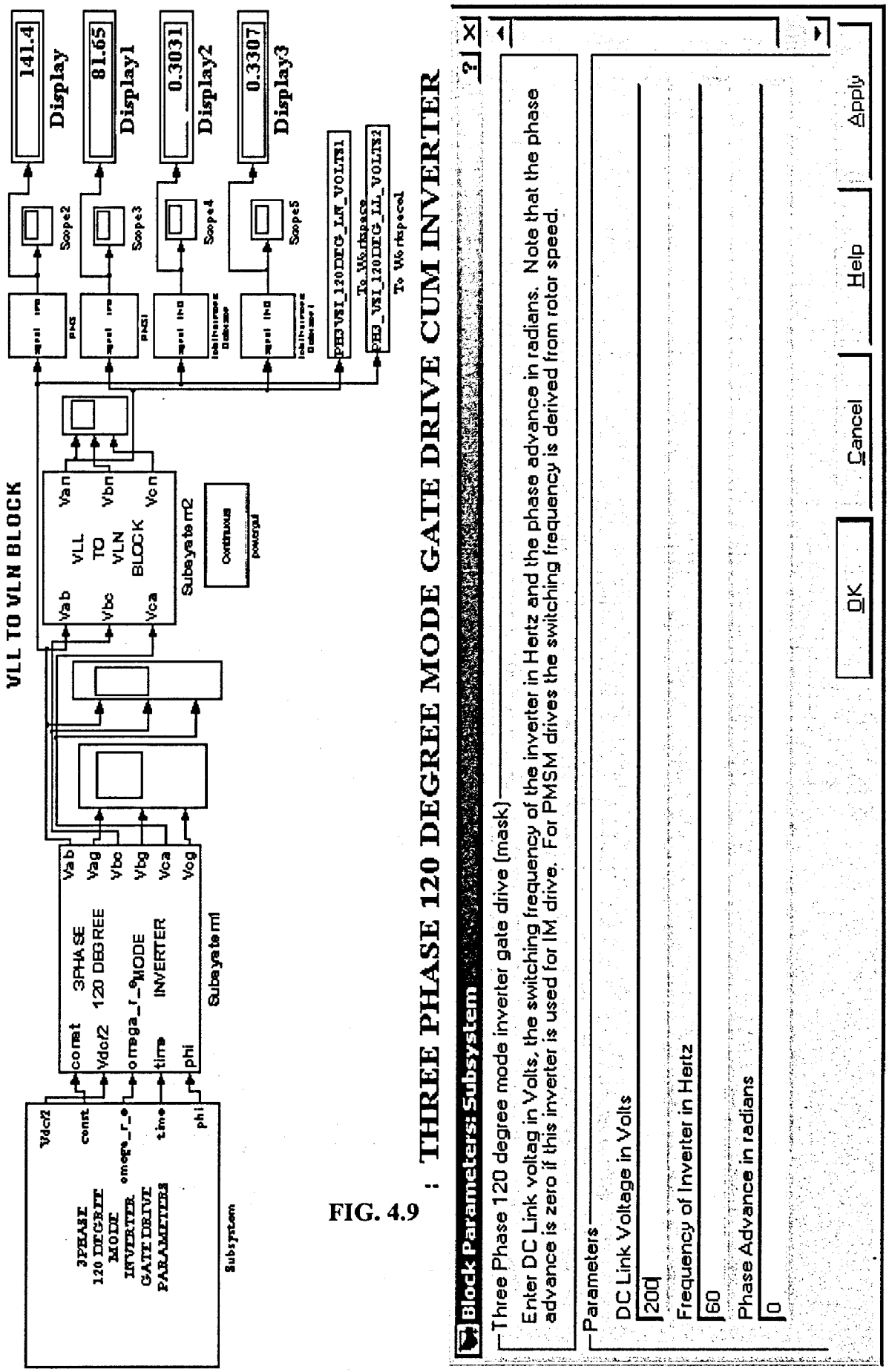
VLL TO VLN BLOCK
Display
Display1
Display2
Display3
141.4
81.65
0.3031
0.3307
Scope2
Scope3
Scope4
Scope5
Subsystem
Subsystem1
Subsystem2
3PHASE 120 DEGREE MODE INVERTER GATE DRIVE PARAMETERS
3PHASE 120 DEGREE MODE INVERTER
VLL TO VLN BLOCK
To Workspace
To Workspace1
To Workspace2
: THREE PHASE 120 DEGREE MODE GATE DRIVE CUM INVERTER
Block Parameters: Subsystem
Three Phase 120 degree mode inverter gate drive (mask)
Enter DC Link voltag in Volts, the switching frequency of the inverter in Hertz and the phase advance in radians. Note that the phase advance is zero if this inverter is used for IM drive. For PMSM drives the switching frequency is derived from rotor speed.
Parameters
DC Link Voltage in Volts
200
Frequency of Inverter in Hertz
60
Phase Advance in radians
0
OK
Cancel
Help
Apply

FIG. 4.9

Fig.4.10(A)

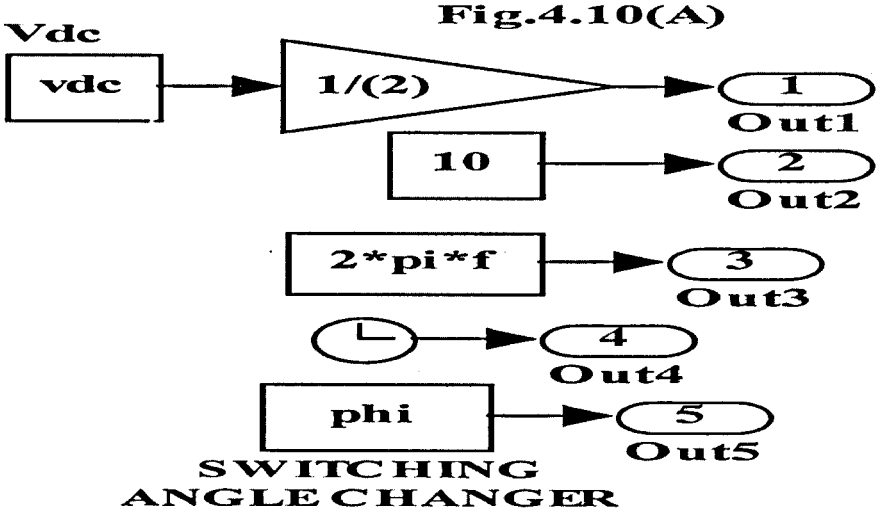

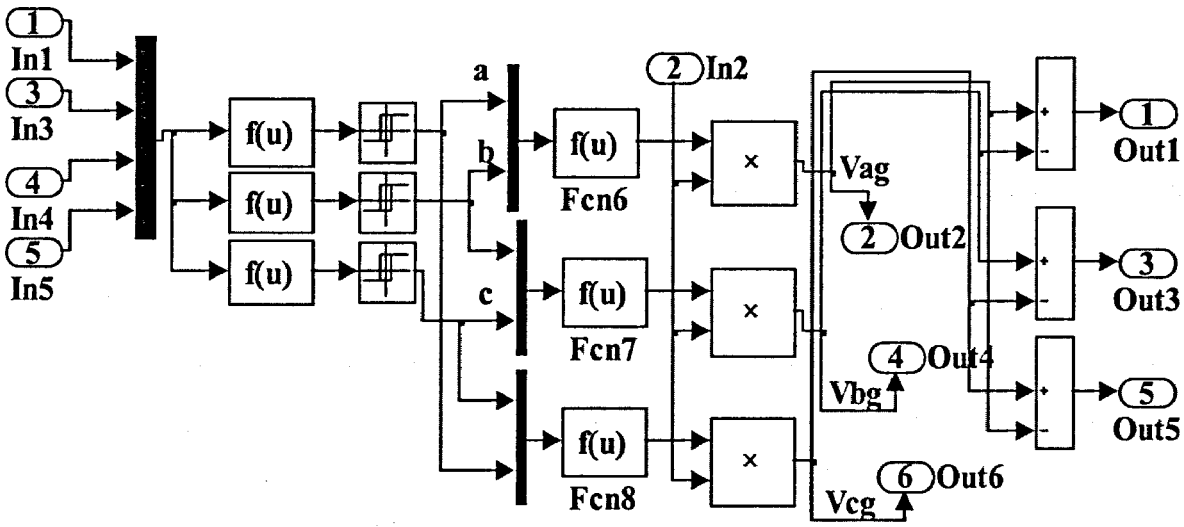

Fig.4.10(B)

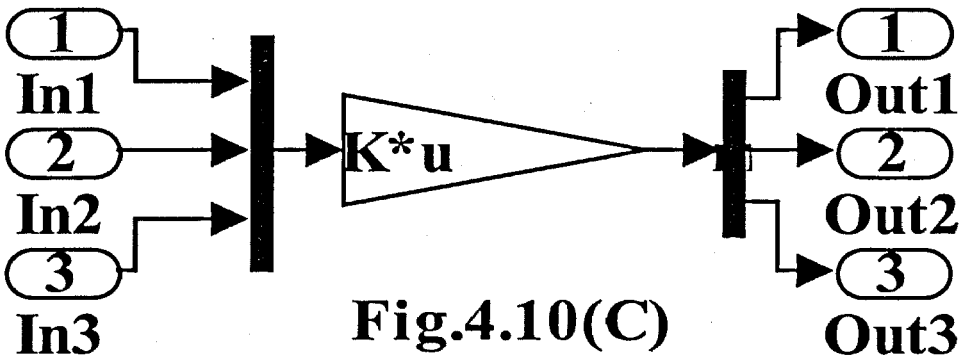

Fig.4.10(C)

rotor speed. The details of the various subsystems of Fig.4.8 are shown in Fig.4.10(A) to (C). The function of the various subsystems are explained below:

Clicking the subsystem corresponding to Fig.4.10(A), opens up the dialog box for Three Phase 120 Degree Mode Inverter gate Drive shown in Fig.4.9. The DC Link voltage and frequency of switching the inverter are entered in the appropriate box. The phase advance is entered zero in the appropriate box. The frequency is internally multiplied by 2π to get the angular switching frequency ω_{re} of the inverter in radians per second.

The three phase 120 degree mode gate drive cum inverter block is shown in Fig.4.10(B). The four input to the mux are the arbitrary constant, angular frequency ω_{re}, time and switching angle advance. The three phase sine wave AC with angular frequency ω_{re} with phase advance added is generated using three Fcn blocks. Each of the three phase AC output are then compared in a Schmitt trigger relay comparator used as zero crossing comparators, with output logic 1 when the input crosses zero and goes positive and logic 0 when the input crosses zero and goes negative. The a, b, c output of the three relays are given to three Fcn blocks. The three Fcn blocks Fcn6, Fcn7 and Fcn8 subtracts the two inputs to their respective mux. The resulting output of these three Fcn blocks are then multiplied by Vdc/2 using multiplier blocks to generate line to ground voltages Vag, Vbg and Vcg of the three phase 120 degree mode inverter. The three subtract blocks are used to generate the three phase line to line voltages, Vab, Vbc and Vca.

The three line to line voltages Vab, Vbc and Vca are given as input to the mux in Fig.4.10(C). The three demux outputs are the line to neutral voltages Van, Vbn and Vcn respectively. The matrix gain block in Fig.4.10(C) multiplies the three line to line voltage inputs by a matrix K defined in equation 4.31 to get the three line to neutral voltages.

4.3.5 Simulation Results for First Model

The simulation of the three phase 120 degree mode inverter was carried out using

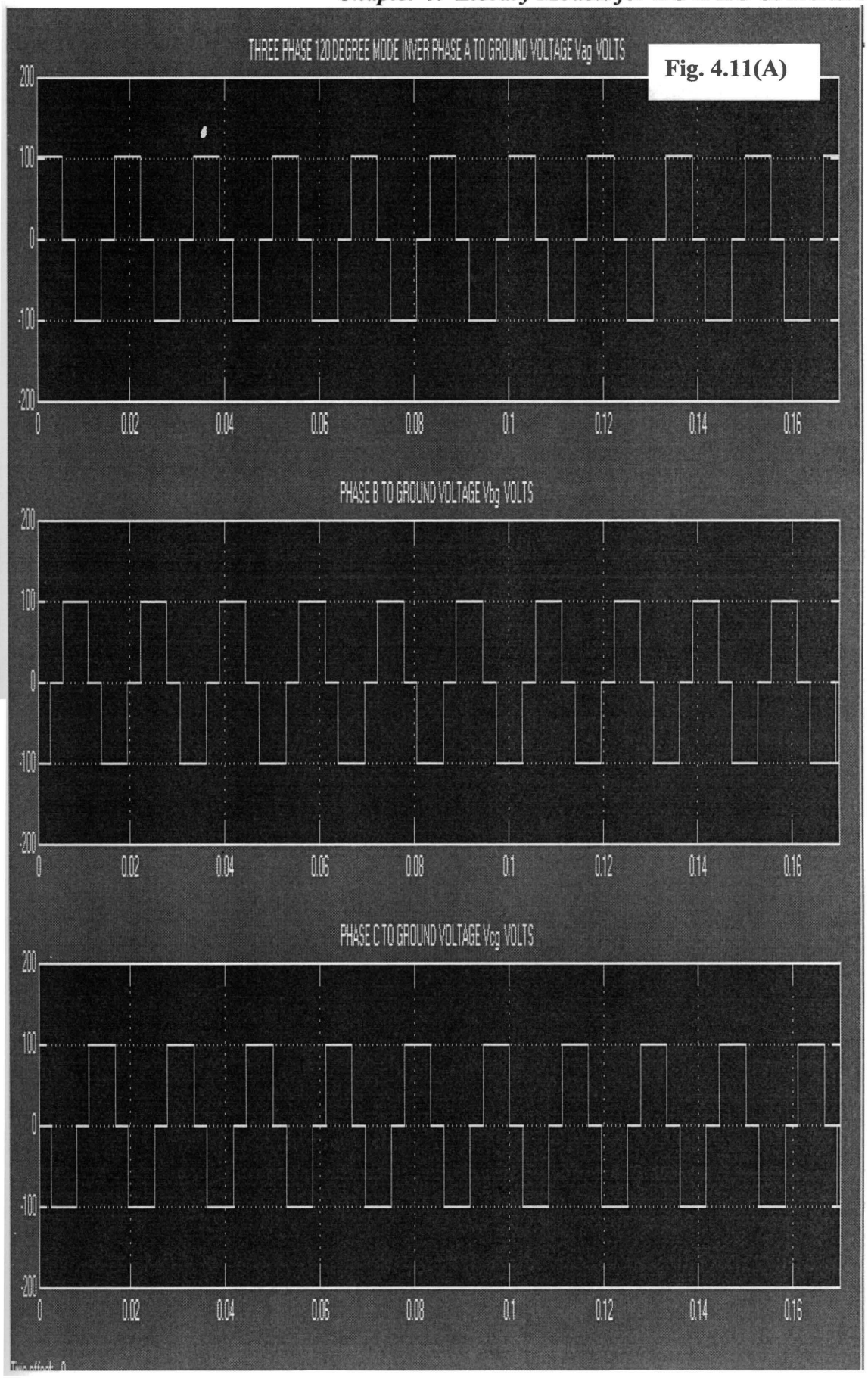
THREE PHASE 120 DEGREE MODE INVER PHASE A TO GROUND VOLTAGE Vag VOLTS
200
100
0
-100
-200
0
0.02
0.04
0.06
0.08
0.1
0.12
0.14
0.16
PHASE B TO GROUND VOLTAGE Vbg VOLTS
200
100
0
-100
-200
0
0.02
0.04
0.06
0.08
0.1
0.12
0.14
0.16
PHASE C TO GROUND VOLTAGE Vcg VOLTS
200
100
0
-100
-200
0
0.02
0.04
0.06
0.08
0.1
0.12
0.14
0.16

Fig. 4.11(A)

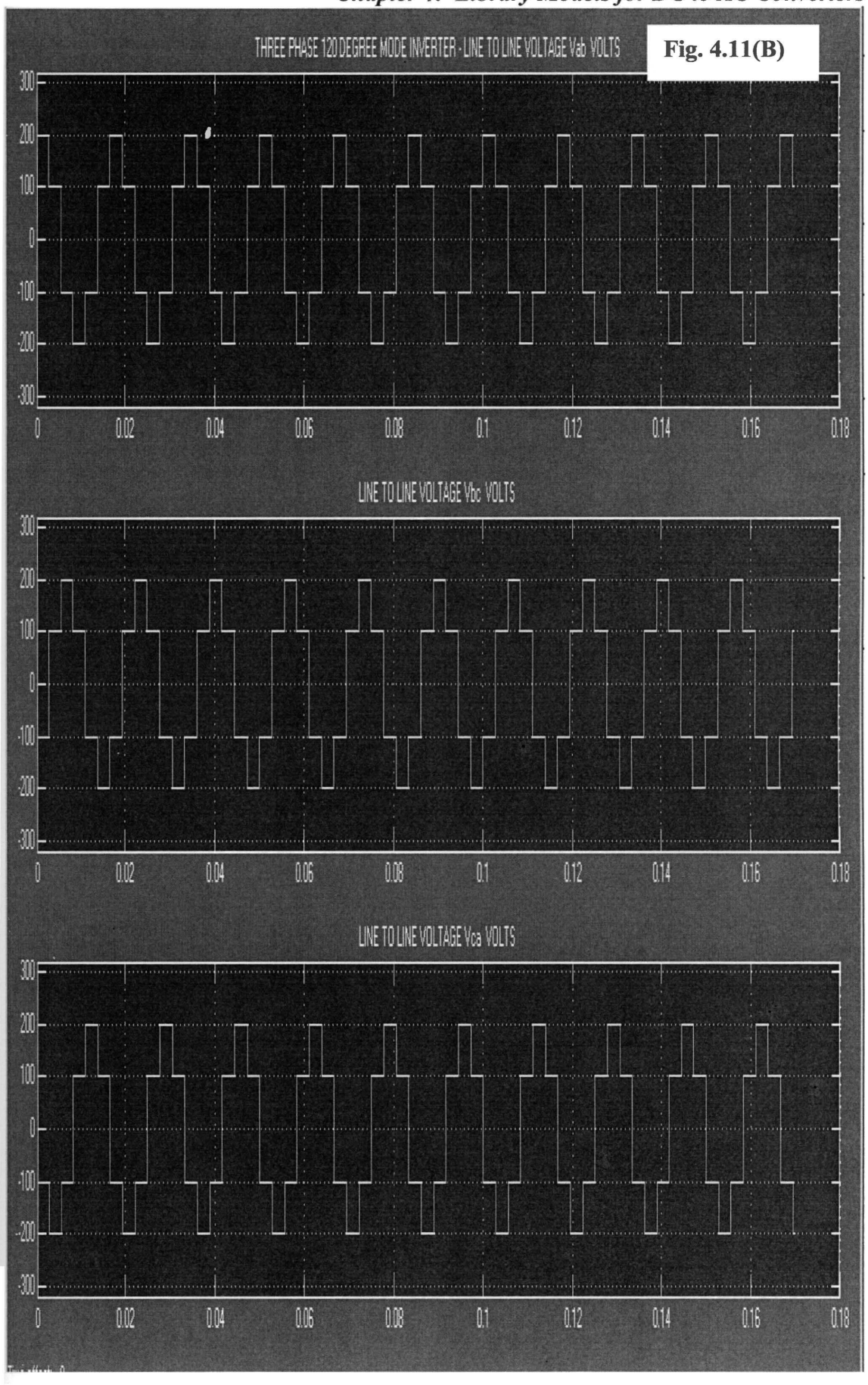
THREE PHASE 120 DEGREE MODE INVERTER - LINE TO LINE VOLTAGE Vab VOLTS
300
200
100
0
-100
-200
-300
0
0.02
0.04
0.06
0.08
0.1
0.12
0.14
0.16
0.18
LINE TO LINE VOLTAGE Vbc VOLTS
300
200
100
0
-100
-200
-300
0
0.02
0.04
0.06
0.08
0.1
0.12
0.14
0.16
0.18
LINE TO LINE VOLTAGE Vca VOLTS
300
200
100
0
-100
-200
-300
0
0.02
0.04
0.06
0.08
0.1
0.12
0.14
0.16
0.18

Fig. 4.11(B)

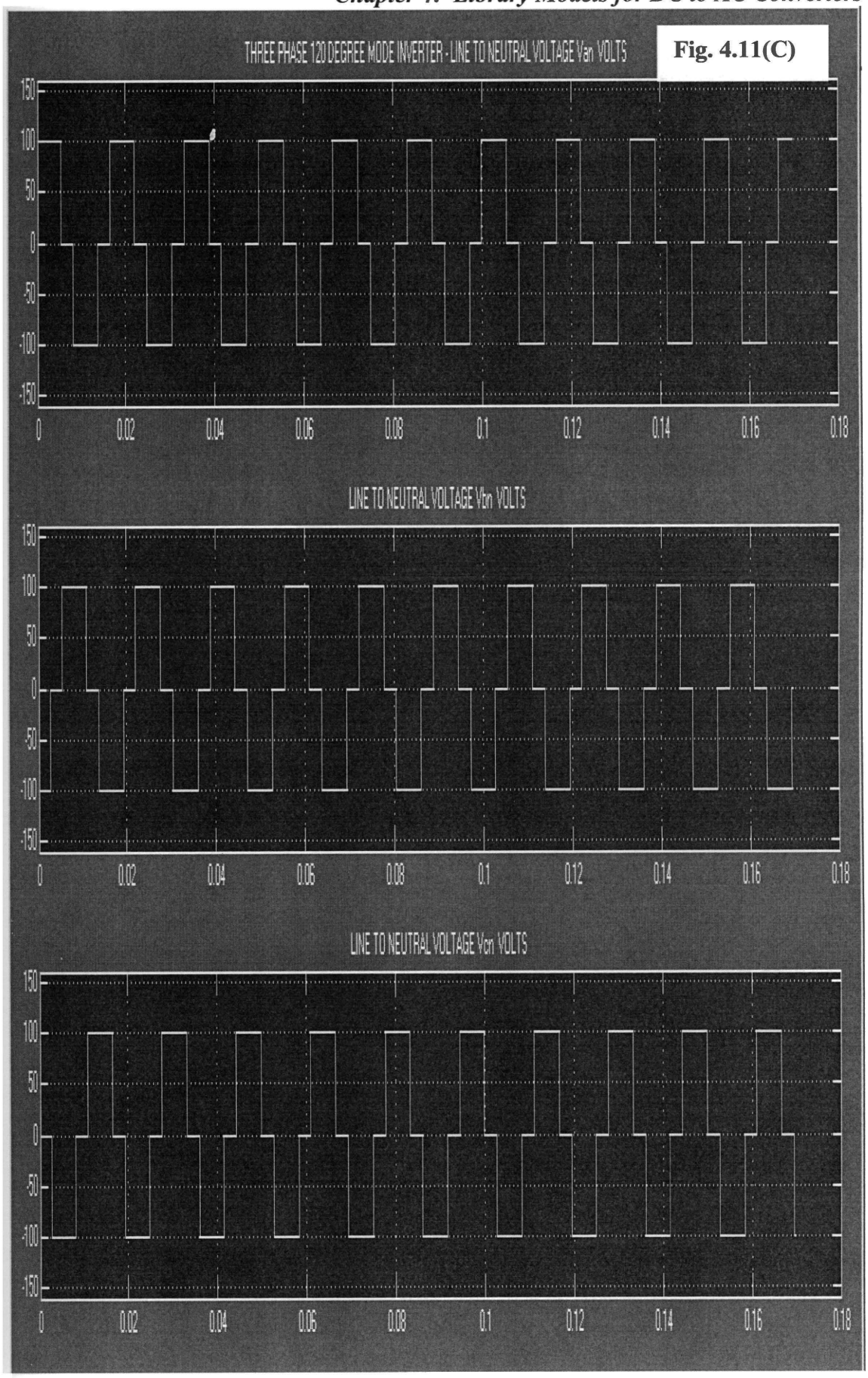
THREE PHASE 120 DEGREE MODE INVERTER - LINE TO NEUTRAL VOLTAGE Van VOLTS
150
100
50
0
-50
-100
-150
0
0.02
0.04
0.06
0.08
0.1
0.12
0.14
0.16
0.18
LINE TO NEUTRAL VOLTAGE Vbn VOLTS
150
100
50
0
-50
-100
-150
0
0.02
0.04
0.06
0.08
0.1
0.12
0.14
0.16
0.18
LINE TO NEUTRAL VOLTAGE Vcn VOLTS
150
100
50
0
-50
-100
-150
0
0.02
0.04
0.06
0.08
0.1
0.12
0.14
0.16
0.18

Fig. 4.11(C)

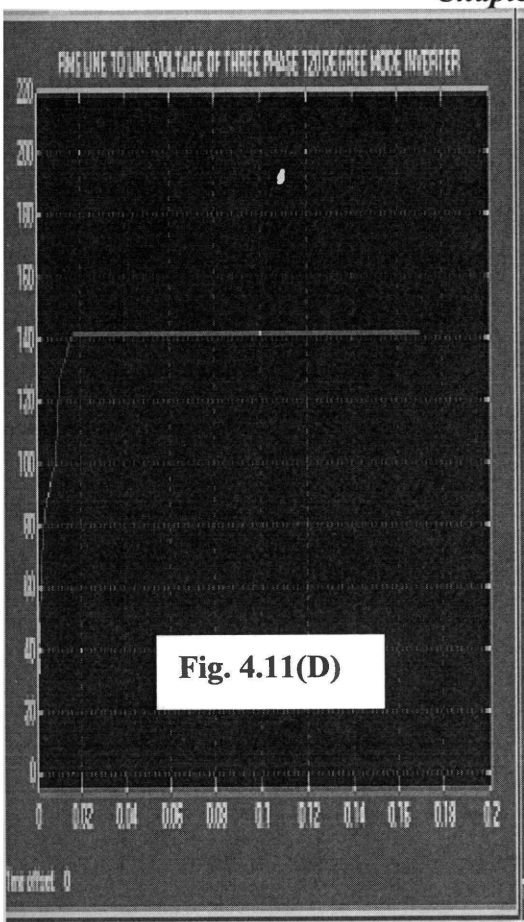

Fig. 4.11(D)

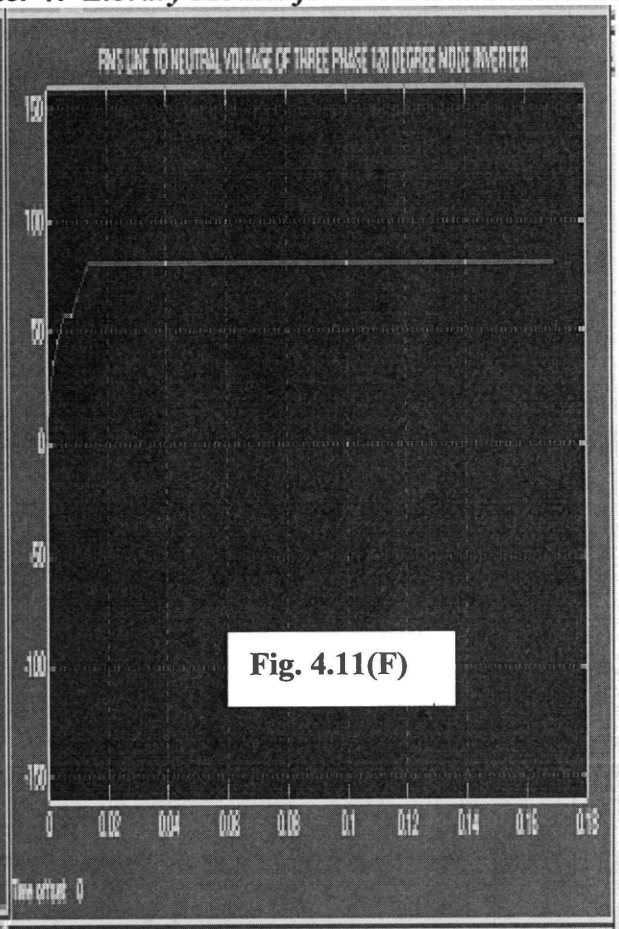

Fig. 4.11(F)

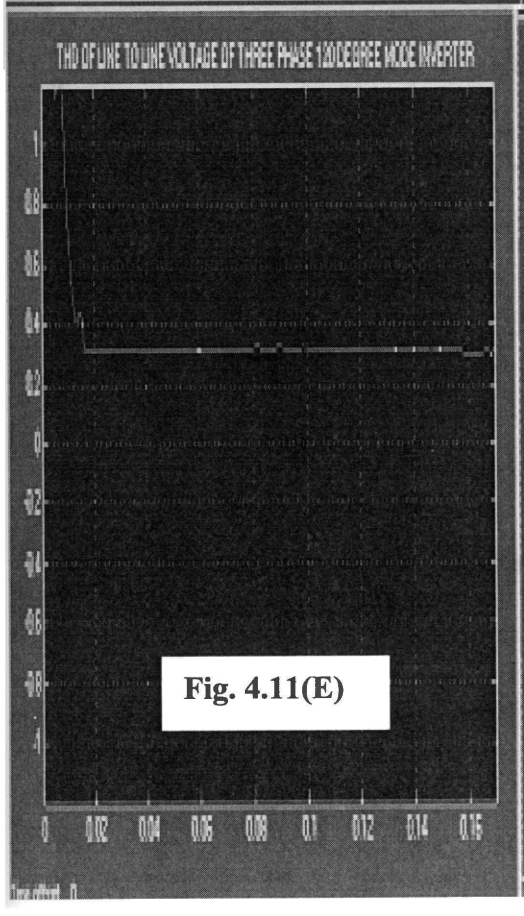

Fig. 4.11(E)

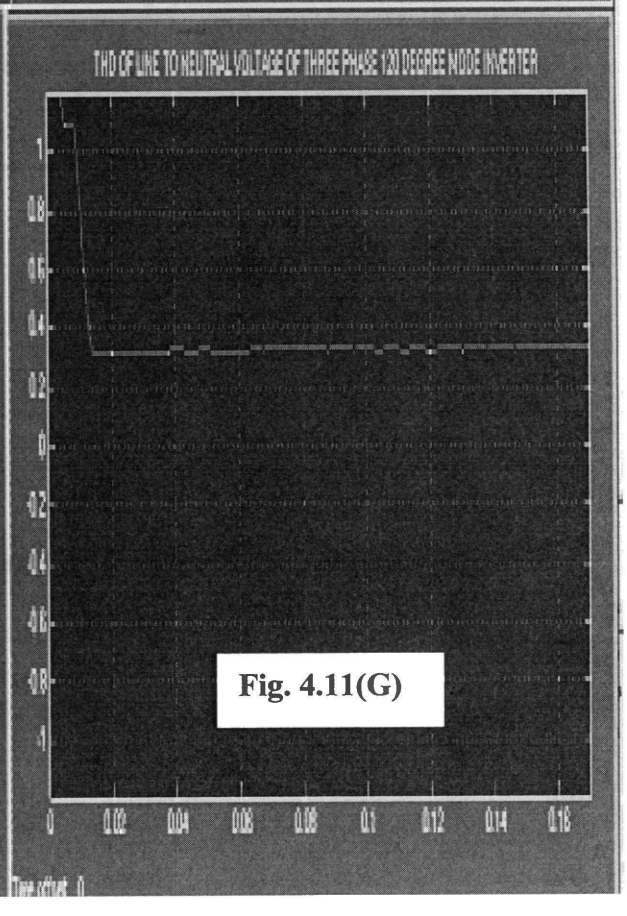

Fig. 4.11(G)

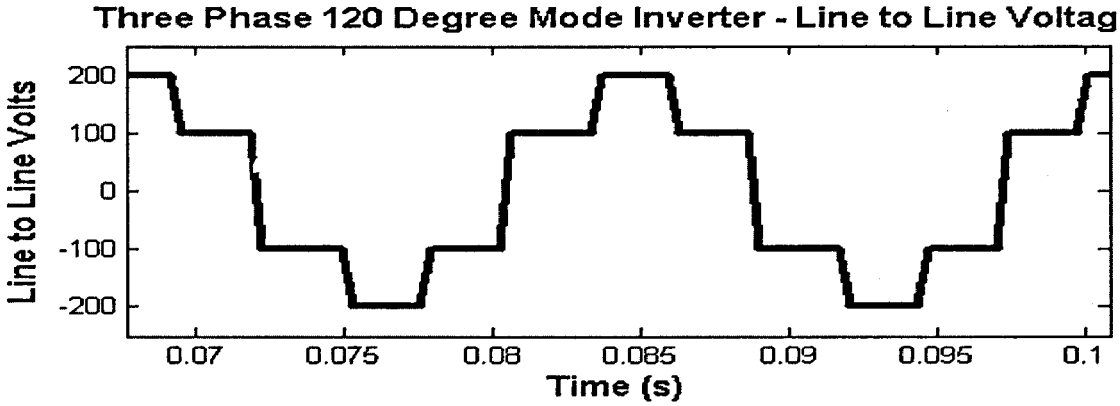

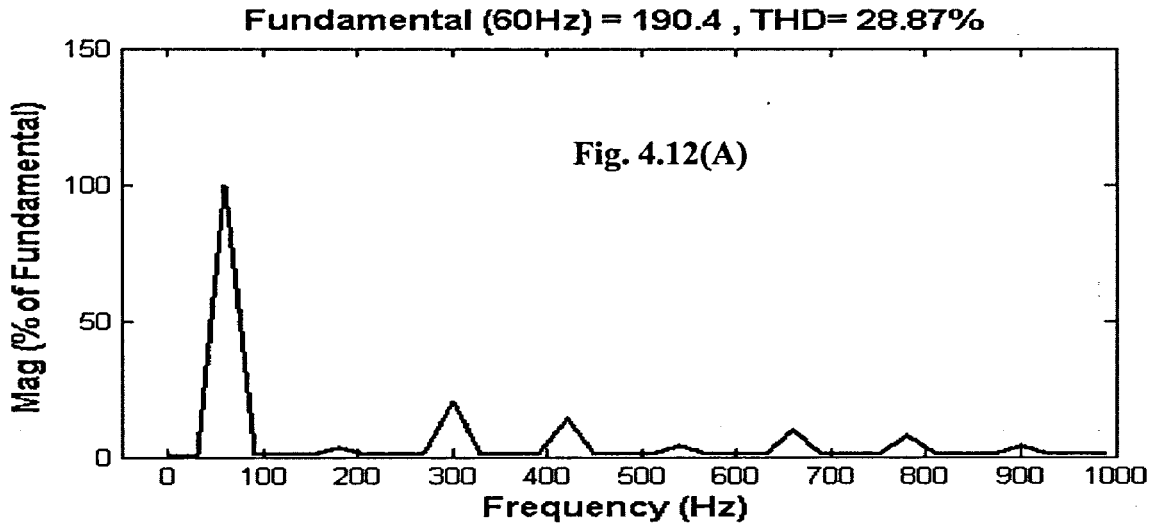

Fig. 4.12(A)

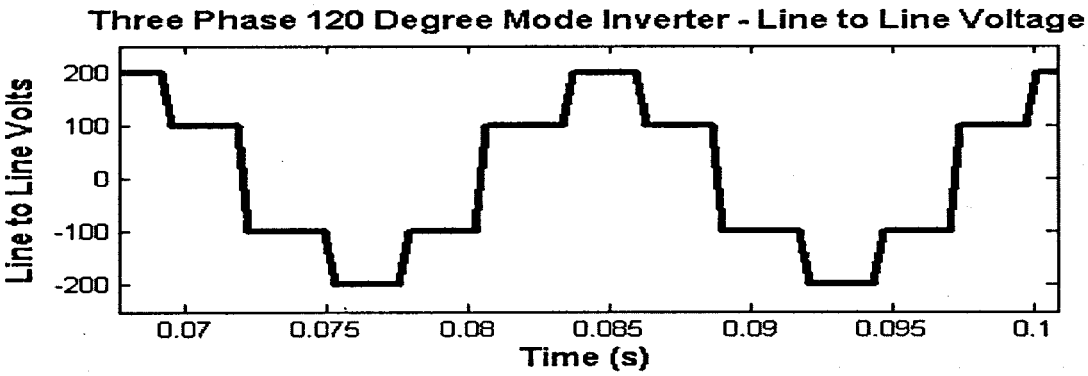


```
ling time      = 0.000380313 s
les per cycle = 43.8235
amental        = 190.4 peak (134.6 rms)
l Harmonic Distortion (THD) = 28.87%

  0 Hz (DC)       0.60 %
 30 Hz            1.19 %
 60 Hz Fund     100.00 %
 90 Hz            1.19 %
120 Hz (h2)       1.19 %
150 Hz            1.19 %
180 Hz (h3)       3.61 %
210 Hz            1.19 %
240 Hz (h4)       1.19 %
270 Hz            1.19 %
300 Hz (h5)      20.49 %
330 Hz            1.19 %
360 Hz (h6)       1.19 %
390 Hz            1.19 %
420 Hz (h7)      14.19 %
450 Hz            1.19 %
480 Hz (h8)       1.19 %
510 Hz            1.19 %
540 Hz (h9)       3.80 %
```

Fig. 4.12(B)

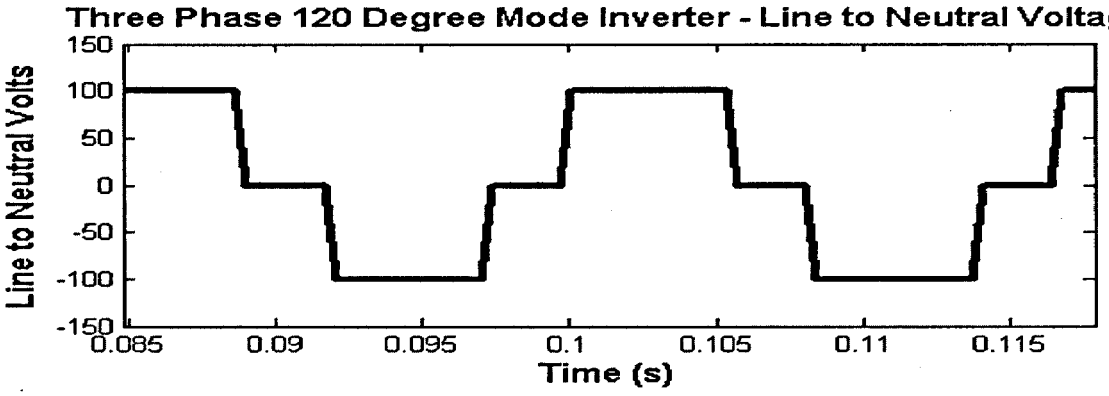

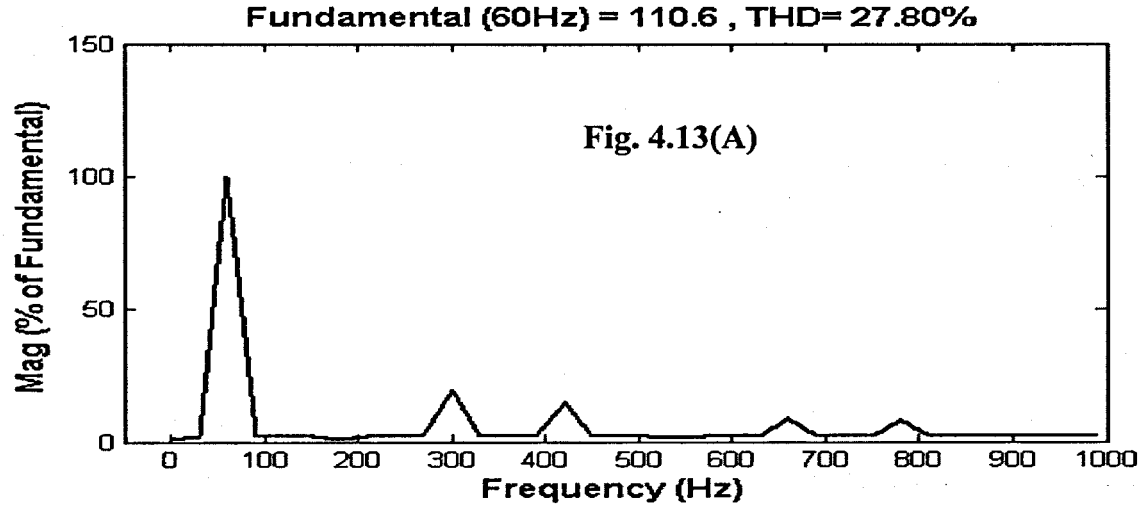

Fig. 4.13(A)

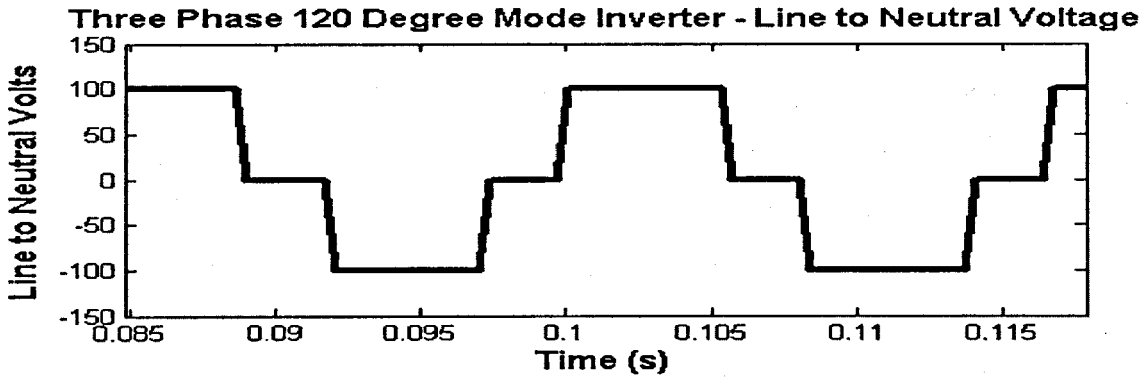

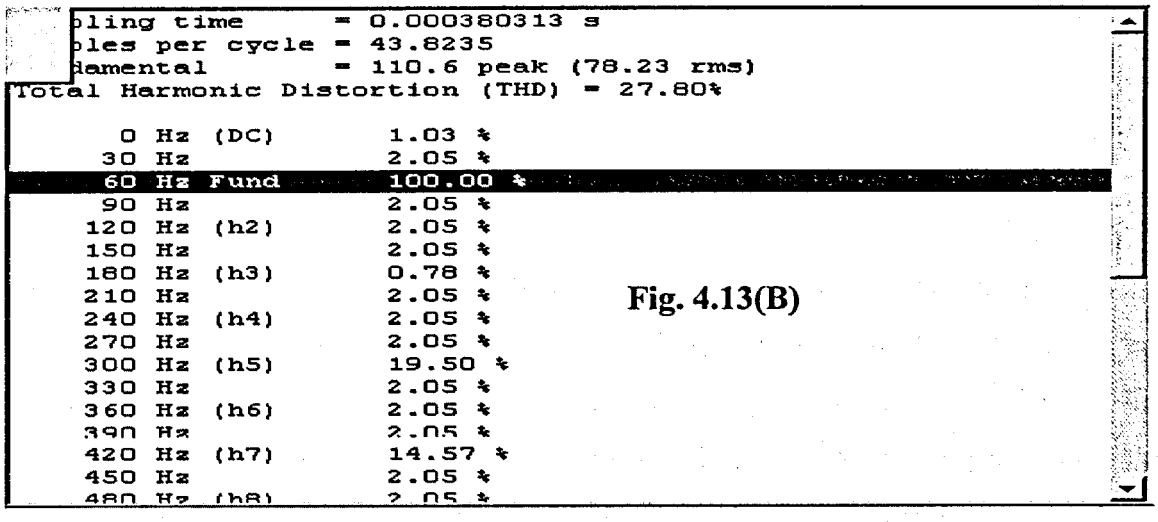

```
bling time      = 0.000380313 s
bles per cycle  = 43.8235
damental        = 110.6 peak (78.23 rms)
Total Harmonic Distortion (THD) = 27.80%

     0 Hz (DC)        1.03 %
    30 Hz             2.05 %
    60 Hz Fund      100.00 %
    90 Hz             2.05 %
   120 Hz (h2)        2.05 %
   150 Hz             2.05 %
   180 Hz (h3)        0.78 %
   210 Hz             2.05 %
   240 Hz (h4)        2.05 %
   270 Hz             2.05 %
   300 Hz (h5)       19.50 %
   330 Hz             2.05 %
   360 Hz (h6)        2.05 %
   390 Hz             2.05 %
   420 Hz (h7)       14.57 %
   450 Hz             2.05 %
   480 Hz (h8)        2.05 %
```

Fig. 4.13(B)

TABLE 4.3: Three Phase 120 degree Mode Inverter – simulation results for First Model

Sl.No.	Frequency Hz	DC Link Voltage – Volts	% THD of VLL	RMS VLL Volts	% THD of VLN	RMS VLN Volts
1	60	200	30.31	141.4	33.07	81.65

TABLE 4.4: Three Phase 120 degree Mode Inverter – calculated values

Sl.No.	Frequency Hz	DC Link Voltage – Volts	% THD of VLL	RMS VLL Volts	% THD of VLN	RMS VLN Volts
1	60	200	30.9	141.44	30.9	81.66

ode15s(stiff/NDF) solver. The **DC Link voltage and frequency entered were 200 volts and 60 Hz** respectively. The three phase line to ground voltages, Line to Line voltages and the Line to Neutral voltages are shown in Fig.4.11(A) to (C) respectively. The RMS and THD values of line to line voltage are shown in Fig.4.11(D), (E) and that corresponding to Line to Neutral voltages are shown in Fig.4.11(F) and (G) respectively. The harmonic spectrum of line to line voltage is shown in Fig.4.12(A), (B) and that corresponding to Line to Neutral voltages are shown in Fig.4.13(A) and (B) respectively. The results observed for THD and RMS values of line to line voltages and that corresponding to Line to Neutral voltages are displayed in the meter in Fig.4.8. These simulation results displayed in Fig.4.8.are also tabulated in TABLE 4.3. The theoretically calculated values for THD and RMS values of line to line and line to neutral voltages using equations 4.23, 4.32, 4.36 and 4.37 are tabulated in TABLE 4.4 [14].

4.3.6 Second Model for Three Phase 120 Degree Mode Inverter

The second model of the three phase 120 degree mode inverter is shown in Fig.4.14.. The various dialog box where user can enter data is given in Fig.4.15. The dialog box mainly correspond to entering the frequency of switching the inverter and its DC link voltage. The phase advance is entered zero for operation with IM and appropriate value for use with PMSM. For PMSM, the frequency of switching the inverter is derived

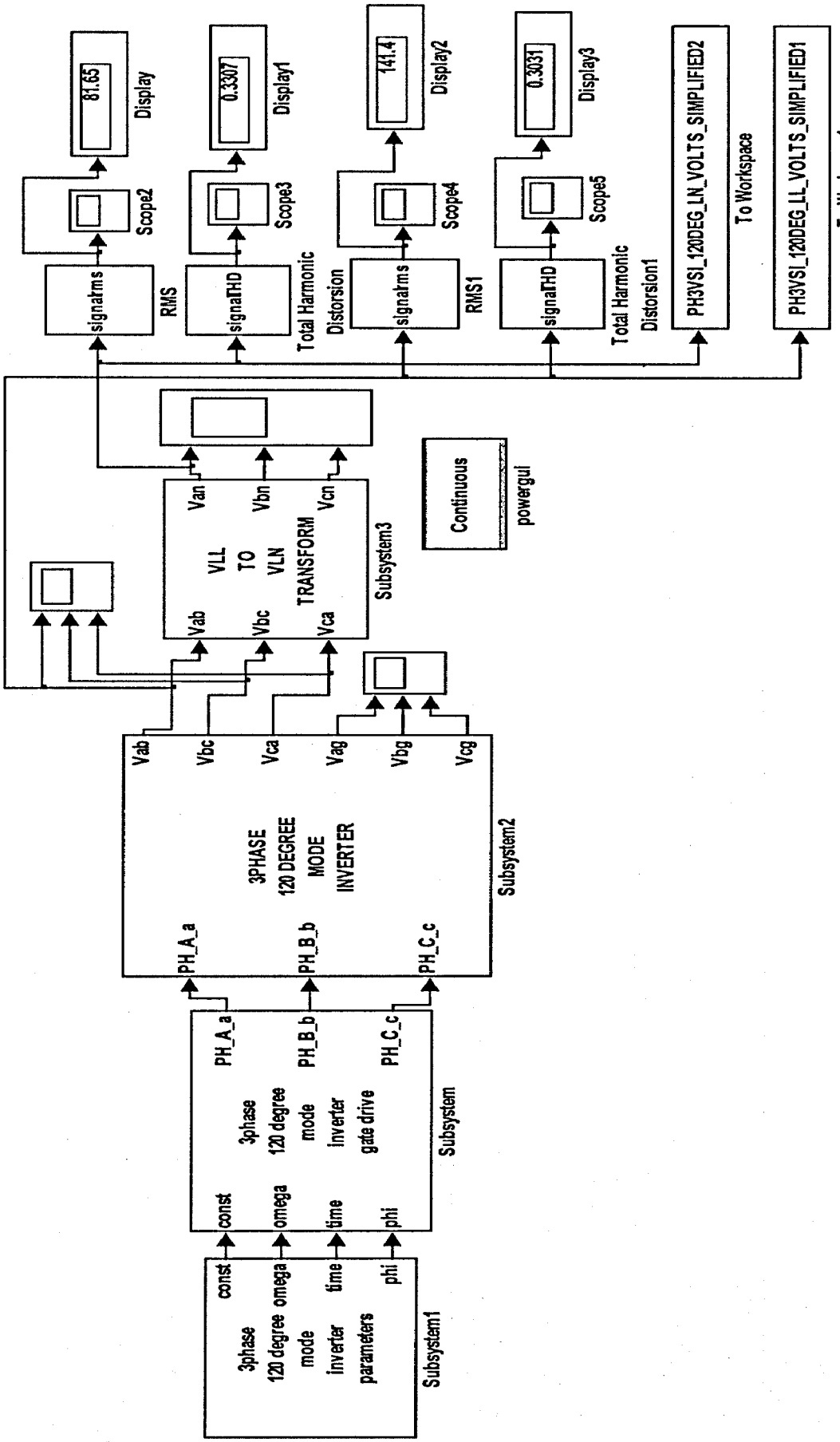

FIG.4.14 THREE PHASE 120 DEGREE MODE INVERTER - SECOND MODEL

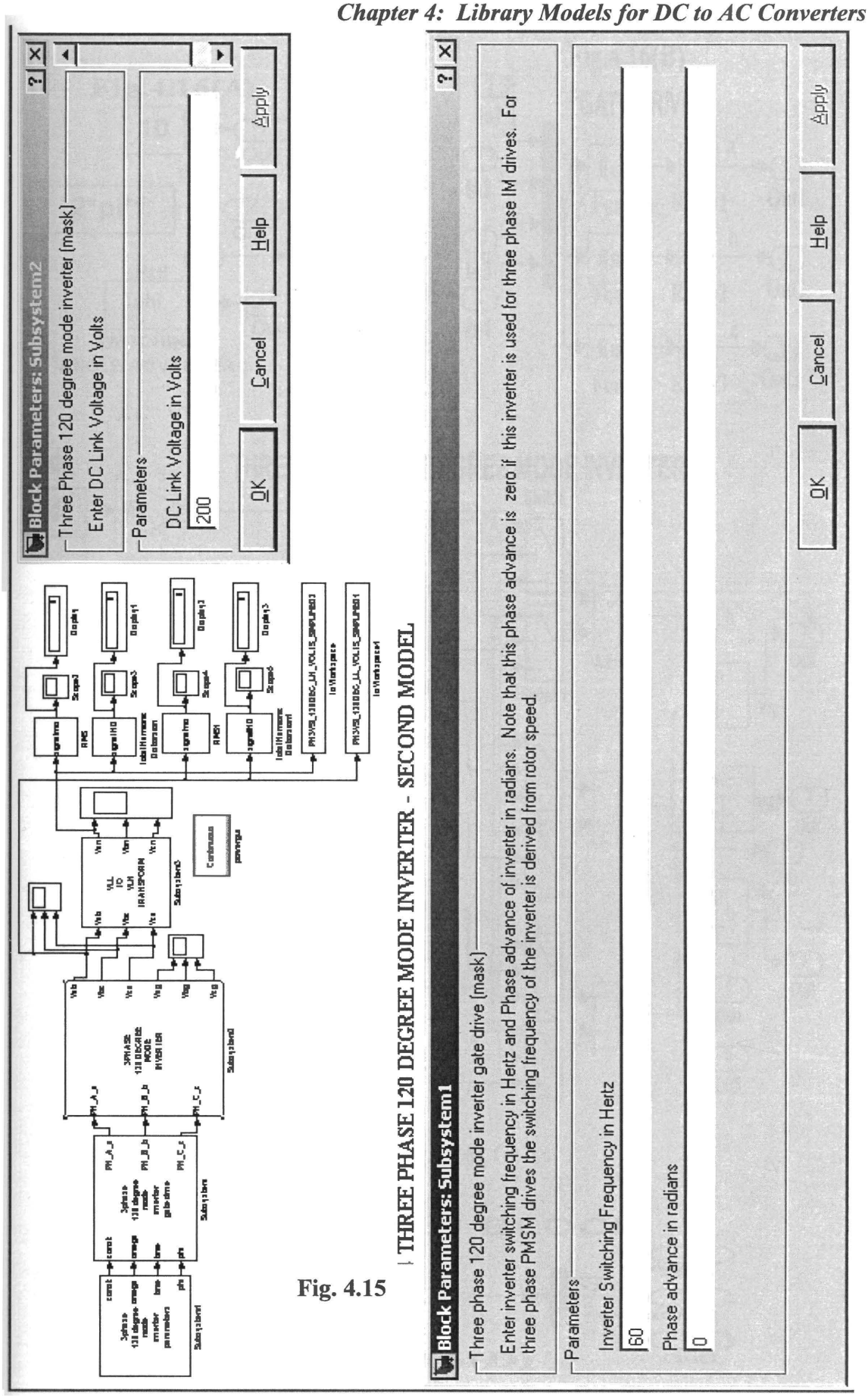
THREE PHASE 120 DEGREE MODE INVERTER - SECOND MODEL
Block Parameters: Subsystem2
Three Phase 120 degree mode inverter (mask)
Enter DC Link Voltage in Volts
Parameters
DC Link Voltage in Volts
200
OK
Cancel
Help
Apply
Block Parameters: Subsystem1
Three phase 120 degree mode inverter gate drive (mask)
Enter inverter switching frequency in Hertz and Phase advance of inverter in radians. Note that this phase advance is zero if this inverter is used for three phase IM drives. For three phase PMSM drives the switching frequency of the inverter is derived from rotor speed.
Parameters
Inverter Switching Frequency in Hertz
60
Phase advance in radians
0
OK
Cancel
Help
Apply

Fig. 4.15

Fig.4.16(A)

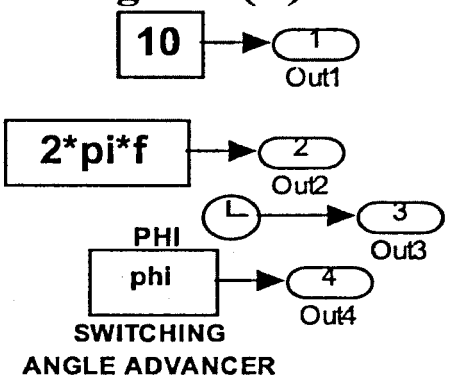

Fig.4.16(B)

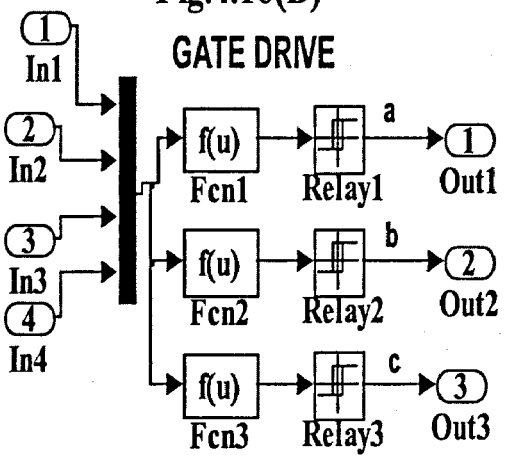

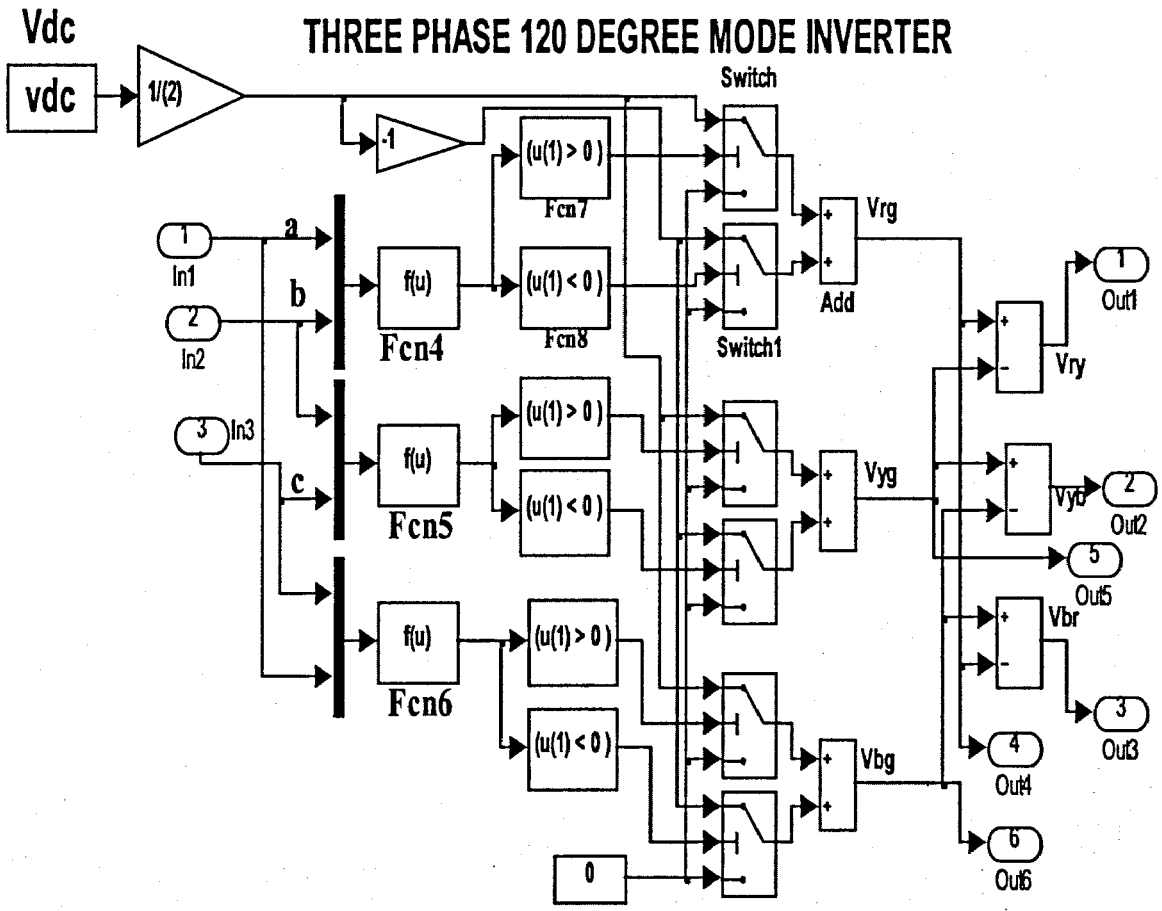

Fig. 4.16 (C)

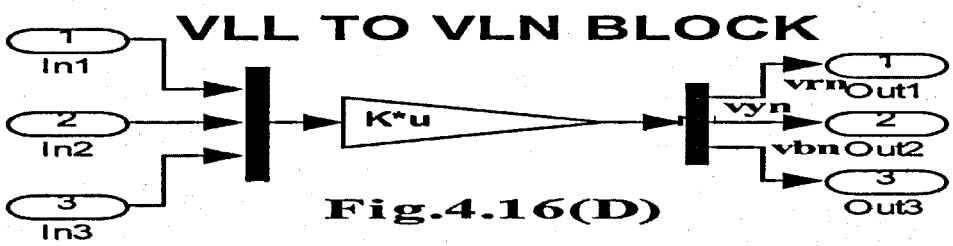

Fig.4.16(D)

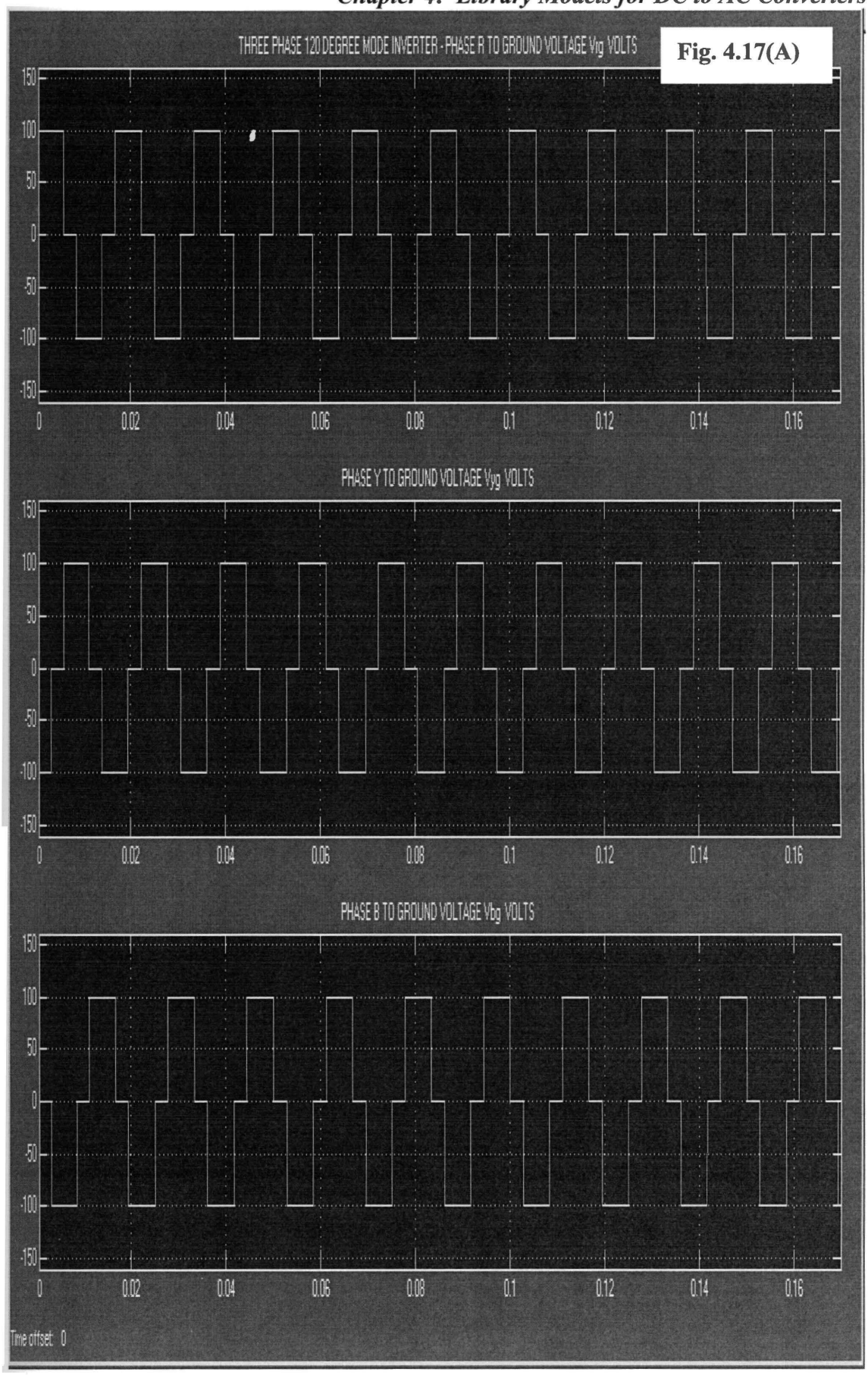
THREE PHASE 120 DEGREE MODE INVERTER - PHASE R TO GROUND VOLTAGE Vrg VOLTS
150
100
50
0
-50
-100
-150
0
0.02
0.04
0.06
0.08
0.1
0.12
0.14
0.16
PHASE Y TO GROUND VOLTAGE Vyg VOLTS
150
100
50
0
-50
-100
-150
0
0.02
0.04
0.06
0.08
0.1
0.12
0.14
0.16
PHASE B TO GROUND VOLTAGE Vbg VOLTS
150
100
50
0
-50
-100
-150
0
0.02
0.04
0.06
0.08
0.1
0.12
0.14
0.16
Time offset: 0

Fig. 4.17(A)

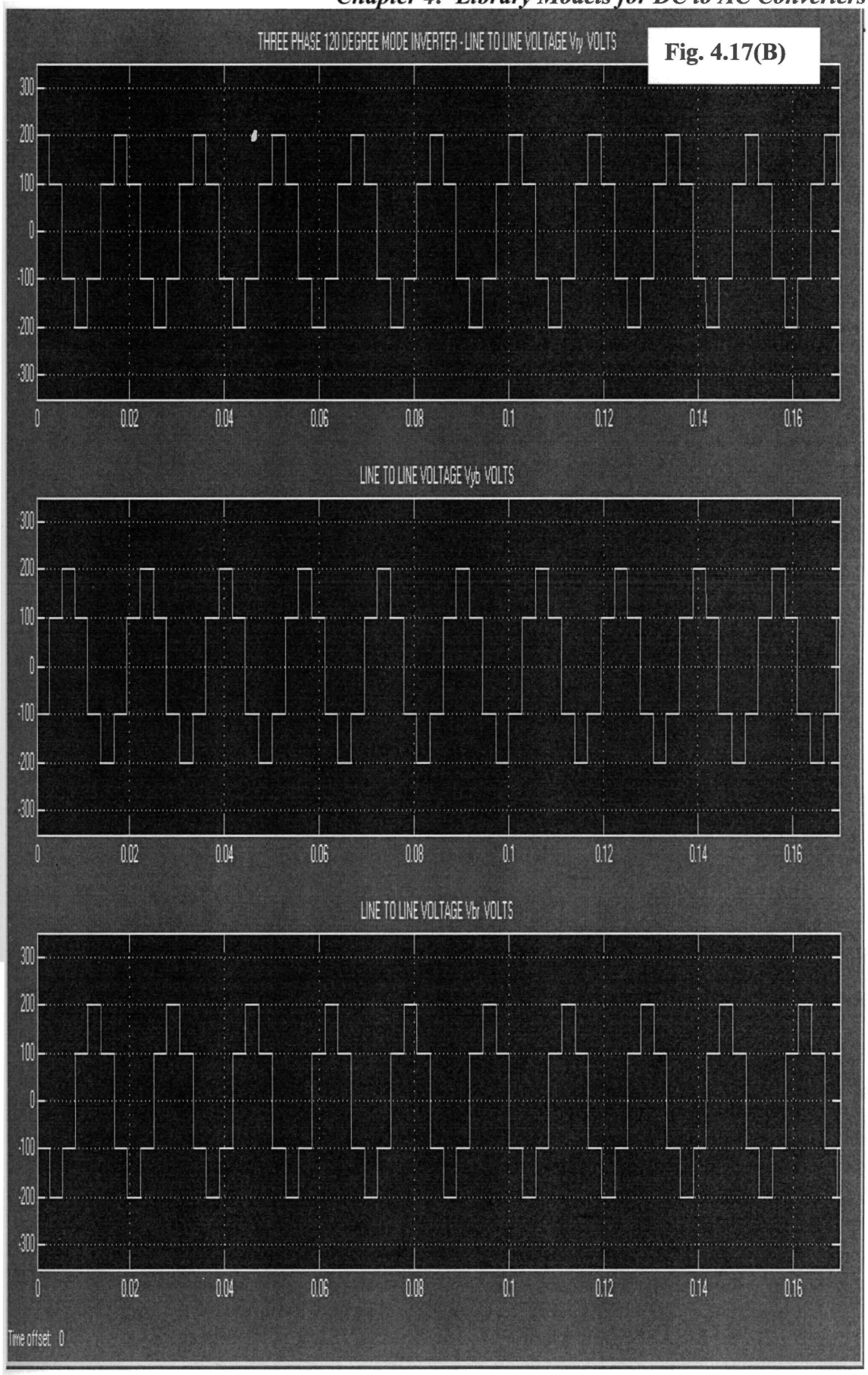
THREE PHASE 120 DEGREE MODE INVERTER - LINE TO LINE VOLTAGE Vry VOLTS
300
200
100
0
-100
-200
-300
0
0.02
0.04
0.06
0.08
0.1
0.12
0.14
0.16
LINE TO LINE VOLTAGE Vyb VOLTS
300
200
100
0
-100
-200
-300
0
0.02
0.04
0.06
0.08
0.1
0.12
0.14
0.16
LINE TO LINE VOLTAGE Vbr VOLTS
300
200
100
0
-100
-200
-300
0
0.02
0.04
0.06
0.08
0.1
0.12
0.14
0.16
Time offset: 0

Fig. 4.17(B)

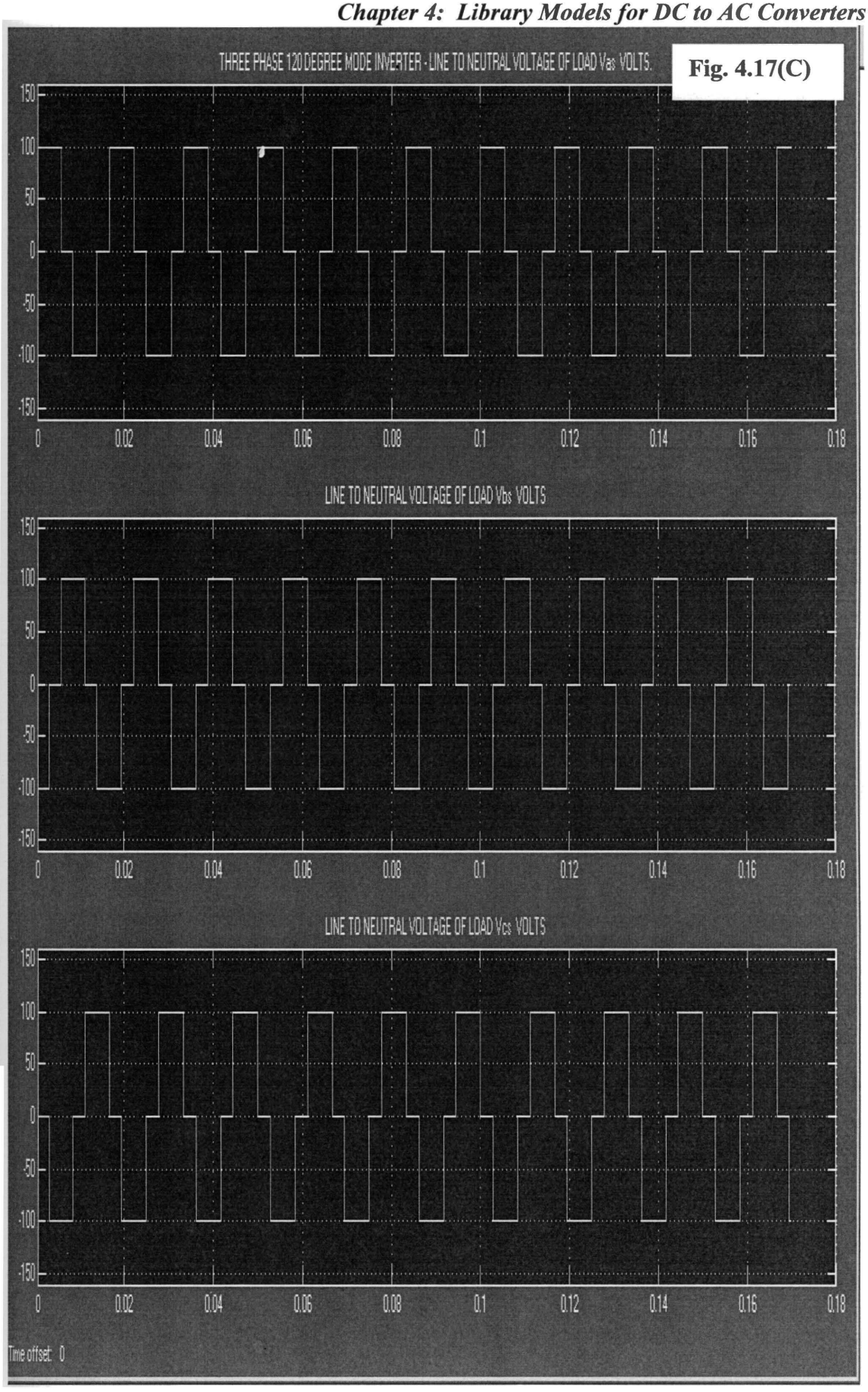
THREE PHASE 120 DEGREE MODE INVERTER - LINE TO NEUTRAL VOLTAGE OF LOAD Vas VOLTS.
150
100
50
0
-50
-100
-150
0
0.02
0.04
0.06
0.08
0.1
0.12
0.14
0.16
0.18
LINE TO NEUTRAL VOLTAGE OF LOAD Vbs VOLTS
LINE TO NEUTRAL VOLTAGE OF LOAD Vcs VOLTS
Time offset: 0

Fig. 4.17(C)

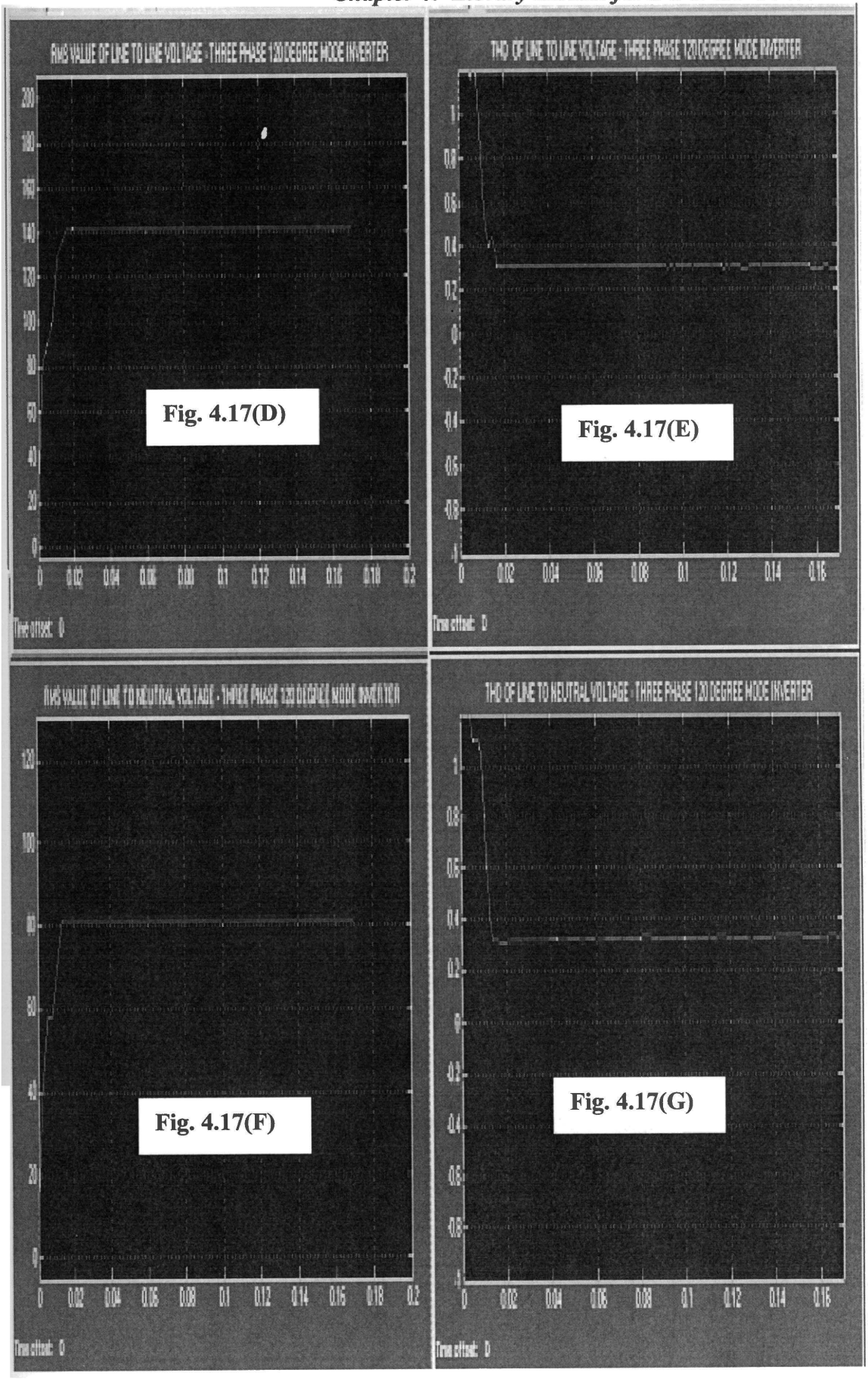
RMS VALUE OF LINE TO LINE VOLTAGE : THREE PHASE 120 DEGREE MODE INVERTER
Fig. 4.17(D)
THD OF LINE TO LINE VOLTAGE : THREE PHASE 120 DEGREE MODE INVERTER
Fig. 4.17(E)
RMS VALUE OF LINE TO NEUTRAL VOLTAGE : THREE PHASE 120 DEGREE MODE INVERTER
Fig. 4.17(F)
THD OF LINE TO NEUTRAL VOLTAGE : THREE PHASE 120 DEGREE MODE INVERTER
Fig. 4.17(G)

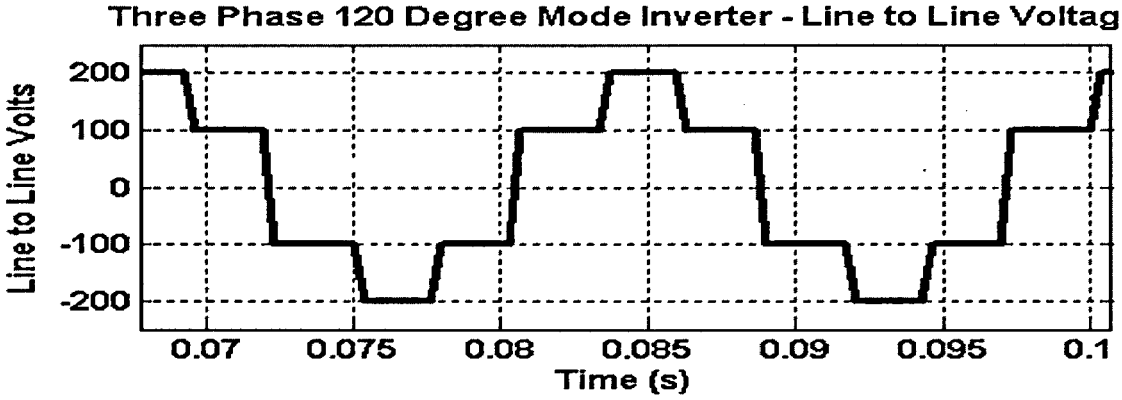

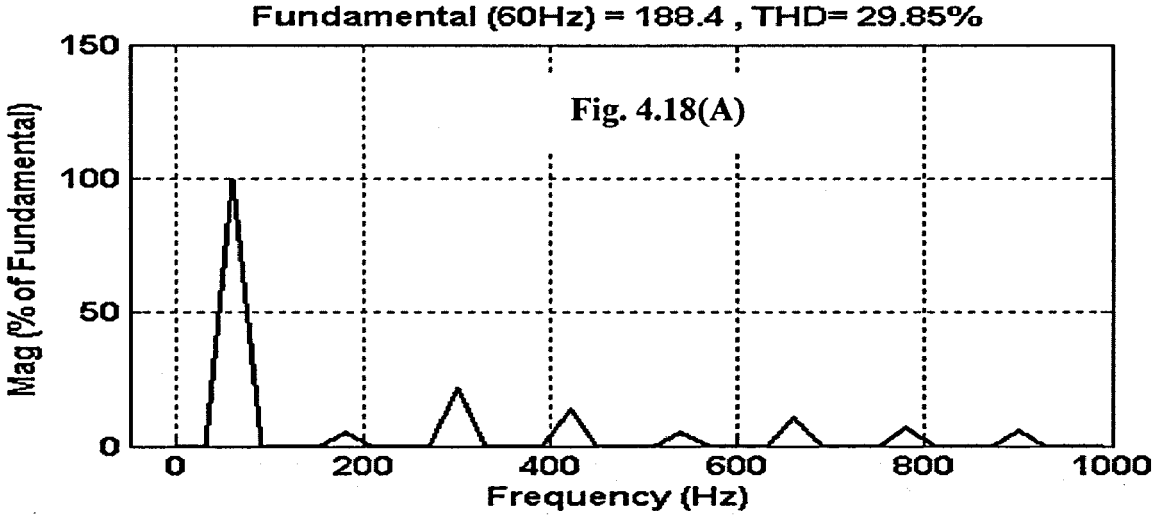

Fig. 4.18(A)

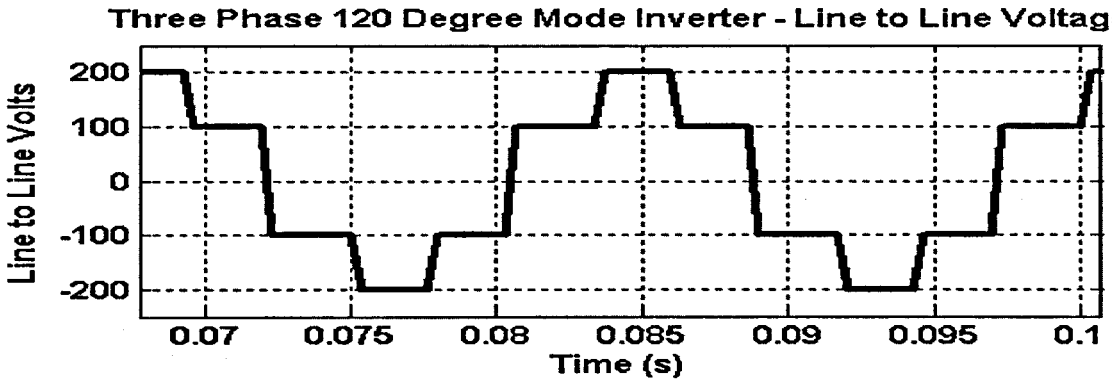


```
bling time      = 0.000378619 s
bles per cycle = 44.0196
damental       = 188.4 peak (133.2 rms)
al Harmonic Distortion (THD) = 29.85%

  0 Hz (DC)        0.00 %
 30 Hz             0.00 %
 60 Hz Fund      100.00 %
 90 Hz             0.00 %
120 Hz (h2)        0.00 %
150 Hz             0.00 %
180 Hz (h3)        4.85 %
210 Hz             0.00 %
240 Hz (h4)        0.00 %
270 Hz             0.00 %
300 Hz (h5)       21.75 %
330 Hz             0.00 %
360 Hz (h6)        0.00 %
390 Hz             0.00 %
420 Hz (h7)       13.26 %
450 Hz             0.00 %
480 Hz (h8)        0.00 %
```

Fig. 4.18(B)

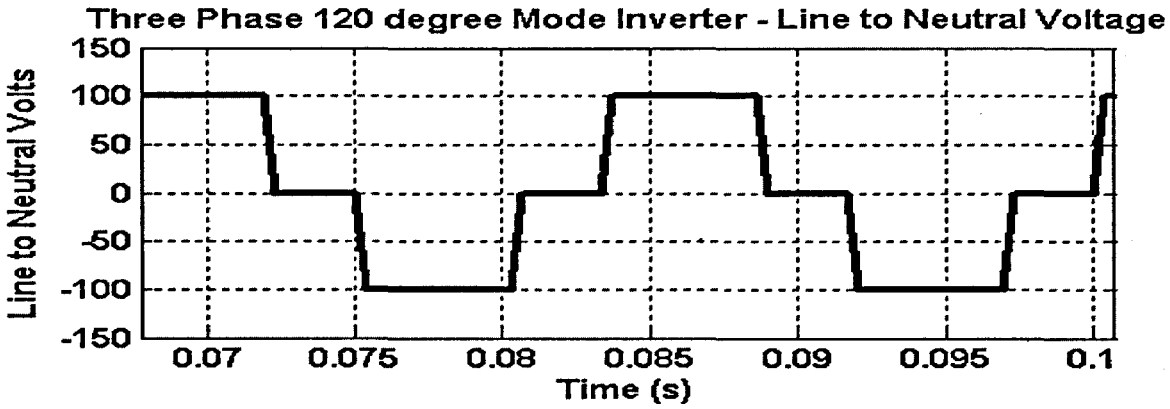

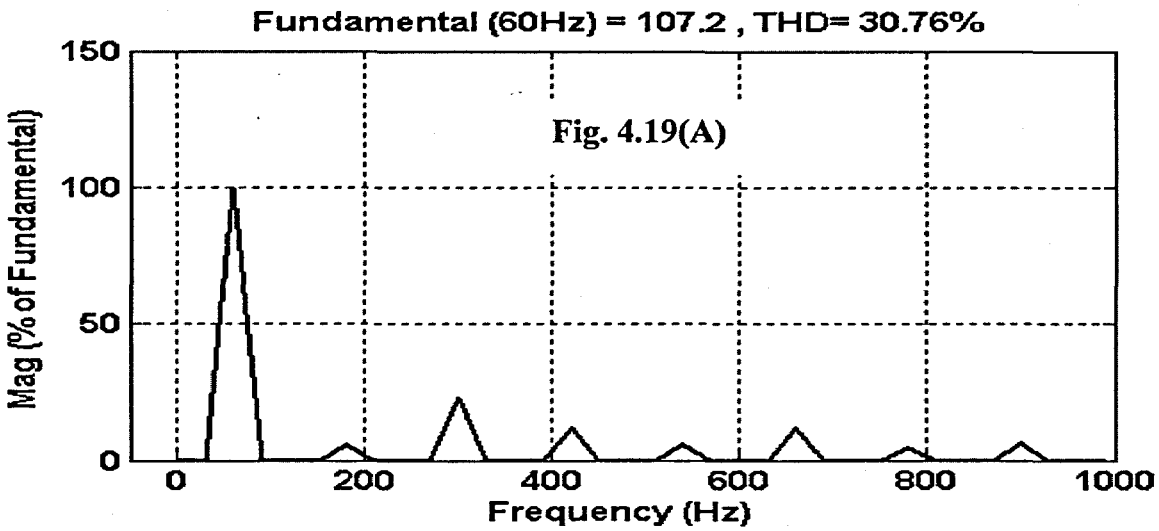

Fig. 4.19(A)

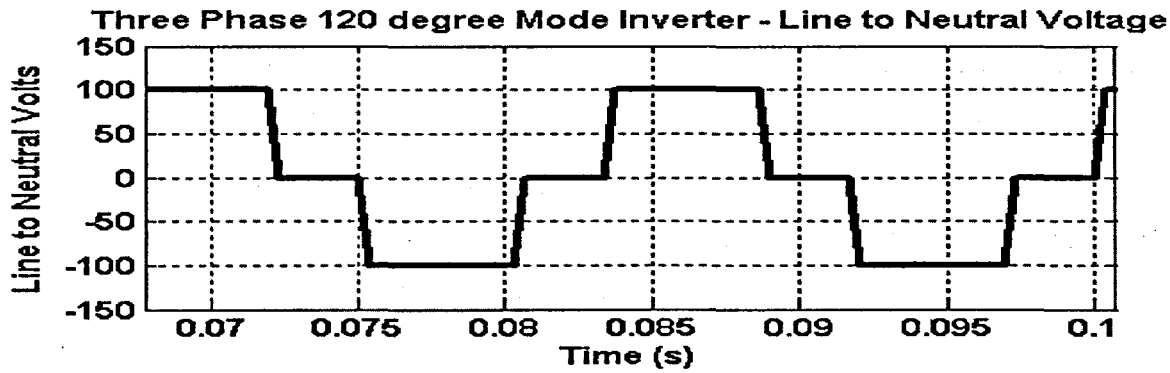

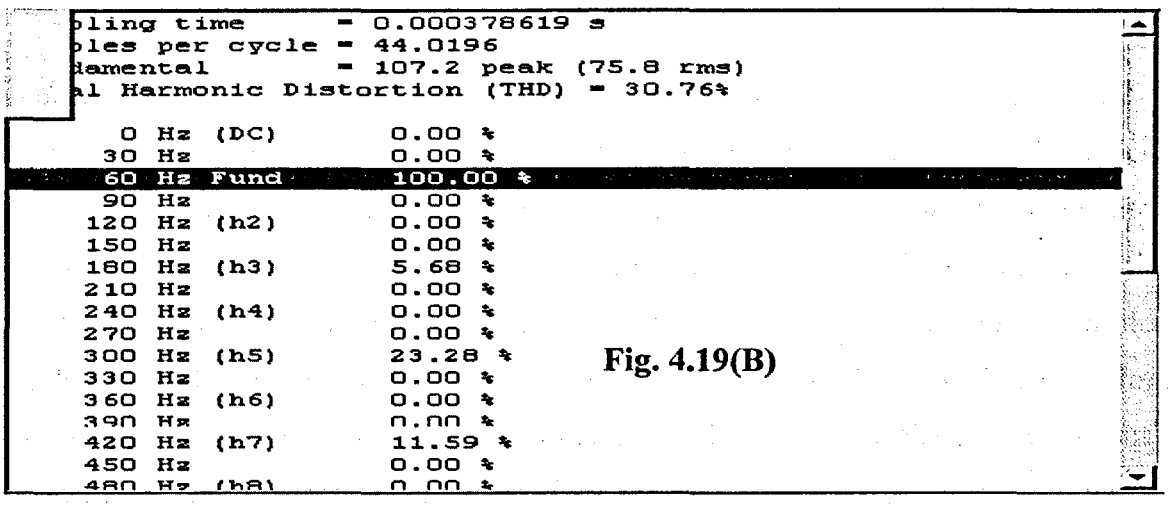

Fig. 4.19(B)

TABLE 4.5: Three Phase 120 degree Mode Inverter – simulation results for second model

Sl.No.	Frequency Hz	DC Link Voltage – Volts	% THD of VLL	RMS VLL Volts	% THD of VLN	RMS VLN Volts
1	60	200	30.31	141.4	33.07	81.65

from the rotor speed. The details of the various subsystems of Fig.4.14 are shown in Fig.4.16(A) to (D). The function of the various subsystems are explained below:

Fig.4.16(A) corresponds to the dialog box with the name Three Phase 120 Degree Mode Inverter Gate Drive shown in Fig.4.15. The value of 60 is entered in the dialog box corresponding to inverter switching frequency and zero corresponding to phase advance. This frequency is internally multiplied by 2π to get the angular switching frequency of the inverter.

The three phase 120 degree mode inverter gate drive block is shown in Fig.4.16(B). The four input to the mux are the arbitrary constant, angular switching frequency, time and the switching angle advance. The three phase sine wave AC with angular frequency corresponding to frequency entered, with phase advance added is generated using the Fcn1, Fcn2 and Fcn3 blocks. Each of the three phase AC output are then compared in a Schmitt trigger relay comparators, relay1, 2 and 3 used as zero crossing comparators. The output of relay1, 2 and 3 goes to logic 1 when the respective input crosses zero and goes positive and their output goes to logic 0 when their respective input crosses zero and goes negative.

The inverter block is shown in Fig.4.16(C). The a, b, c output of relay1, 2 and 3 are given in pairs to three Fcn blocks using three two input mux. The three Fcn blocks Fcn4, 5 and 6 subtract the two inputs to their respective mux. Each of the three subtract blocks are given to a pair of zero comparison blocks. The Fcn7 block output logic 1 when the input u(1) is greater than zero, else output logic 0. Similarly the Fcn8 block output logic 1 when the input u(1) is less than zero, else output logic 0. The same logic holds good for zero comparison block pairs connected to Fcn5 and Fcn6. The output of Fcn7 and Fcn8 are given to u(2) input of switch and switch1 respectively. The u(1)

input for switch and switch1 are respectively +Vdc/2 and –Vdc/2 and the u(3) inputs to both switches are zeros. Both the switch and switch1 output u(1) when u(2) is greater than or equal to 0.5, else their output is u(3). The output of switch and switch1 are connected to add block. The same principle holds good for the switch pairs corresponding to Fcn5 and Fcn6 blocks. Thus each of the add blocks generate the line to ground voltages, Vrg, Vyg and Vbg respectively. The three phase line to ground voltages are subtracted in pairs using the subtract block to generate the three phase line to line voltages Vry, Vyb and Vbr.

The line to line to line to neutral transformation block is shown in Fig.4.16(D). The three line to line voltages Vry, Vyb and Vbr are given to a matrix gain block using a three input mux. The gain matrix K of the matrix gain block is defined by equation 4.31. The three phase line to neutral voltages Vrn, Vyn and Vbn are obtained at the output of the demux block.

Apart from the above RMS and THD blocks from SimPowerSystems block set is used to measure the RMS value and THD of line to line and line to ground voltages. Scopes are used to display the three phase line to ground, line to line and line to neutral voltages. Powergui from SimPowerSystems block set is used for harmonic analysis of line to line and line to neutral voltages.

4.3.7 Simulation Results for Second Model

The simulation of the second model of the three phase 120 degree mode inverter was carried out using ode15s(stiff/NDF) solver. The **DC Link voltage and frequency entered were 200 volts and 60 Hz** respectively. The three phase line to ground voltages, Line to Line voltages and the Line to Neutral voltages are shown in Fig.4.17(A) to (C) respectively. The RMS and THD values of line to line voltage are shown in Fig.4.17(D), (E) and that corresponding to Line to Neutral voltages are shown in Fig.4.17(F) and (G) respectively. The harmonic spectrum of line to line voltage is shown in Fig.4.18(A), (B) and that corresponding to Line to Neutral voltages are shown in Fig.4.19(A) and (B) respectively. The results observed for THD and RMS values of line to line voltages and that corresponding to Line to Neutral voltages are displayed in

the meter in Fig.4.14. These simulation results displayed in Fig.4.14.are also tabulated in TABLE 4.5. The theoretically calculated values for THD and RMS values of line to line and line to neutral voltages using equations 4.23, 4.32, 4.36 and 4.37 are tabulated in TABLE 4.4 [14].

4.4 Conclusions

The simulation results in Table 4.3 for the first model reveals that the RMS values of line to line and line to neutral voltages are close to the theoretically calculated values using the formula given in Table 4.4. The simulation result of THD of the line to line voltage differs by around 0.6 % and that of line to neutral voltage differs by around 2.1 % compared to the theoretically calculated value. Examination of the harmonic spectrum of line to line voltage of first model in Fig.4.12(A) and (B) reveals that the fifth and seventh harmonic contributions are 20.49 % and 14.19 % respectively, where as their theoretical values are 20 % and 14.28 %.. Examination of the harmonic spectrum of line to neutral voltage of first model in Fig.4.13(A) and (B) reveals that the fifth and seventh harmonic contributions are 19.5 % and 14.57 % respectively, where as their theoretical values are 20 % and 14.28 %.. The discrepancy in both cases are negligibly small. The simulation results in Table 4.5 for the second model reveals that the RMS values of line to line and line to neutral voltages are close to the theoretically calculated values using the formula given in Table 4.4. The simulation result of THD of the line to line voltage differs by around 0.6 % and that of line to neutral voltage differs by around 2.1 % compared to the theoretically calculated value. Examination of the harmonic spectrum of line to line voltage of second model in Fig.4.18(A) and (B) reveals that the fifth and seventh harmonic contributions are 21.75 % and 13.26 % respectively, where as their theoretical values are 20 % and 14.28 %.. Examination of the harmonic spectrum of line to neutral voltage of second model in Fig.4.19(A) and (B) reveals that the fifth and seventh harmonic contributions are 23.28 % and 11.59 % respectively, where as their theoretical values are 20 % and 14.28 %. The discrepancy for line to neutral voltage harmonics is slightly larger for the second model. Appendix E provides simulation of the above three phase inverters using the demo version of Electronic Circuit Simulation software PSIM 7.0

CHAPTER 5

LIBRARY MODELS FOR DC TO DC CONVERTERS

5.1 Introduction

DC to DC converters are used for transforming the dc input voltage to dc output voltage. There are three fundamental topologies for dc to dc converters such as Buck, Boost and Buck-Boost converter. These are second order converters and have a semiconductor switch, diode, one inductor, one capacitor and one load resistor. Advanced converters known as fourth order converts use two inductors and two capacitors apart from the semiconductor switch, diode and load resistor. Fourth order converters can be built by cascading any two second order topologies. Additionally Cuk, Sepic and Zeta converters fall under the category of fourth order converters. Buck converters find applications in Switched Mode Power Supplies and so also is the case with Buck-Boost converters. Boost converters are used for power factor improvement of ac-dc-ac converters used for ac drives.

This chapter mainly deals with the system modelling of fundamental topologies of second order converters such as Buck, Boost and Buck-Boost. Switching Function concept is used for modelling these converters. The developed models are valid as long as the inductor current is continuous.

5.2 Buck Converter Analysis

The Buck converter topology using BJT switch is shown in Fig.5.1 [14-18]. In fact the switch can be any one of MOSFET, IGBT or GTO. The switch is driven by an external PWM drive whose period is T and duty cycle is D. Figs.5.2(A) and (B) shows the

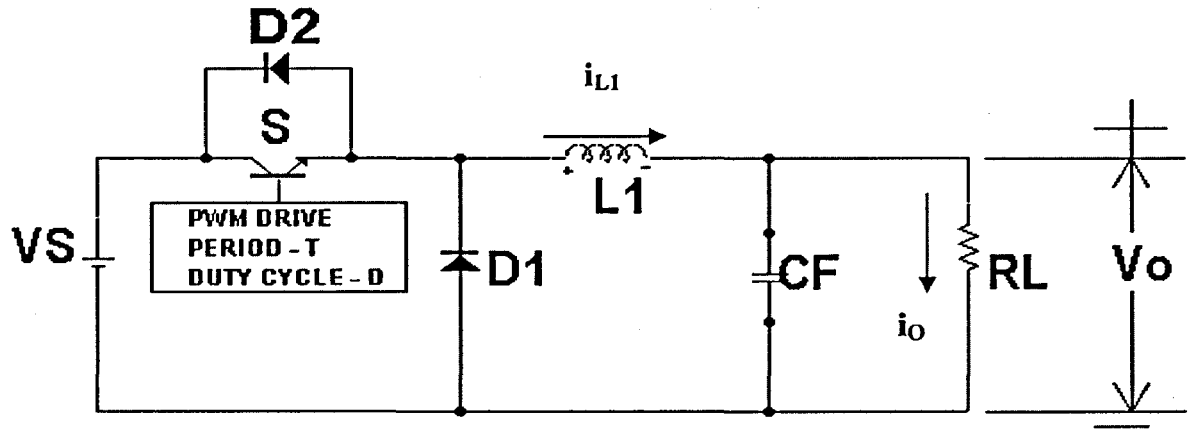

FIG.5.1

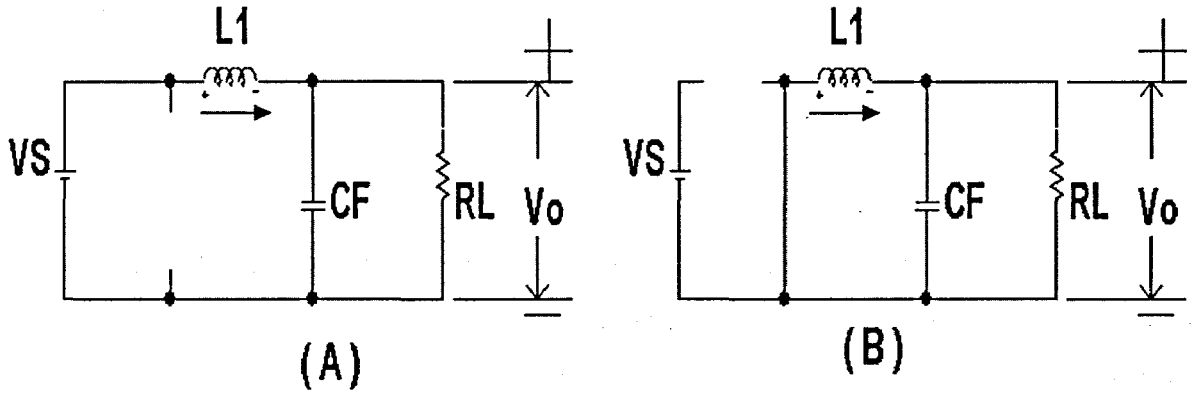

FIG.5.2

equivalent circuit of Fig.5.1 when the switch is ON from 0 to DT seconds and OFF from DT to T seconds respectively. This analysis assumes CCM, i.e the inductor curr - ent is continuous or always greater than zero. Noting that the change in inductor current during the ON time and OFF time are equal or the average inductor current over one switching cycle is zero, the following equation can be derived.

$$\frac{(V_S - V_O).D.T}{L_1} + \frac{(-V_O).(1-D).T}{L_1} = 0 \qquad (5.1)$$

$$\frac{V_O}{V_S} = D \qquad (5.2)$$

During the switch ON time, inductor current grows linearly and reaches a maximum value I_{L1max} and during the switch OFF period, the inductor current decays and reaches a minimum value I_{L1min}. The maximum and minimum inductor current are given below:

$$I_{L1max} = D.V_S\left(\frac{1}{R_L} + \frac{(1-D).T}{2L_1}\right)$$

$$I_{L1min} = D.V_S\left(\frac{1}{R_L} - \frac{(1-D).T}{2L_1}\right) \qquad (5.3)$$

The critical inductance L_{1crit} required to maintain CCM is obtained by equating I_{L1min} to zero. This gives the following value for L_{1crit}.

$$L_{1crit} = \left(\frac{1 - D}{2}\right).T.R_L \qquad (5.4)$$

The ratio of ripple voltage to output voltage is given below:

$$\frac{\Delta V_{CF}}{V_O} = \frac{(1 - D)}{8.L_1.(CF).f_{SW}^2} \qquad (5.5)$$

where $f_{SW} = (1/T)$ is the switching frequency in Hertz, L_1 is the inductor in Henries and CF is the filter capacitor in Farads.

5.2.1 Model for Buck Converter

Models for Buck converter are available in the literature references [54 – 57]. Switching function concept is used to model the Buck converter [54 – 56]. The library model of the Buck converter is shown in Fig.5.3. The various dialog boxes are shown in Fig.5.4. The various subsystems of the model are shown in Fig.5.5(A) to (D). The development of the modelling equations for Buck converter is explained below:

Referring to Fig.5.2, the following equations can be derived.

$$\frac{di_{L1}}{dt} = \frac{(V_S - V_O)}{L_1} \quad for\ 0<=t<=D.T \qquad (5.6)$$

$$\frac{di_{L1}}{dt} = \frac{(-V_O)}{L_1} \quad for\ D.T<=t<=T \qquad (5.7)$$

Now for the switch S, switching function SF is defined as follows:

$$SF = 1 \quad for \quad 0 \le t \le D.T$$
$$= 0 \quad for \quad D.T \le t \le T \qquad ...(5.8)$$

Using equation 5.8 in equations 5.6 and 5.7, we have the following:

$$\frac{di_{L1}}{dt} = \frac{(SF * V_S - V_O)}{L_1} \qquad (5.9)$$

$$V_O = \frac{i_{L1} * R_L}{\left(R_L . CF.s + 1\right)} \qquad (5.10)$$

The various subsystems are explained below:

Fig.5.5(A) shows the Pulse Generator Block from Sources block set and the corresponding dialog box marked Switch Function Generator is shown in Fig.5.4. In this dialog box, the switching period in seconds and the Pulse Width in percentage of period are entered. Fig.5.5(B) corresponds to the dialog box marked Buck Converter Data in Fig.5.4. In this dialog box, the dc input voltage in Volts and the inductor value in Henries are entered. In Fig.5.5(C), the four inputs SF, VS, Vo and L1 are given as input to the MUX. The Fcn block connected to this mux solves equation 5.9 and the integrator block output gives the inductor current. The inductor current output is given to the Transfer Fcn block in Fig.5.5(D). The dialog box named Resistive Load and Capacitive Filter in Fig.5.4 corresponds to Fig.5.5(D). The resistive load in Ohms and the capacitor filter in farads are entered in this dialog box. The transfer Fcn block in Fig.5.5(D) gives the output voltage Vo across the load. This output voltage Vo is multiplied by the gain block (1/rl) to get the current through the load resistor.

5.2.2 Simulation Results

The data relating to the Buck Converter is shown in TABLE 5.1 [14-16]. The simulation results of the Buck Converter are shown in Fig.5.6(A) to (D). The output voltage is also

TABLE 5.1 – Buck Converter Data

Sl.No.	Input Voltage Vs Volts	Switching Period T Seconds	Duty Cycle D	Inductor L1 Henries	Filter Capacitor CF Farads	Load Resistor RL Ohms
1	48	25e-6	0.6	97.5e-6	100e-6	10

displayed in Fig.5.3. The simulation results are displayed in Table 5..2 and the calculated values in Table 5.3.

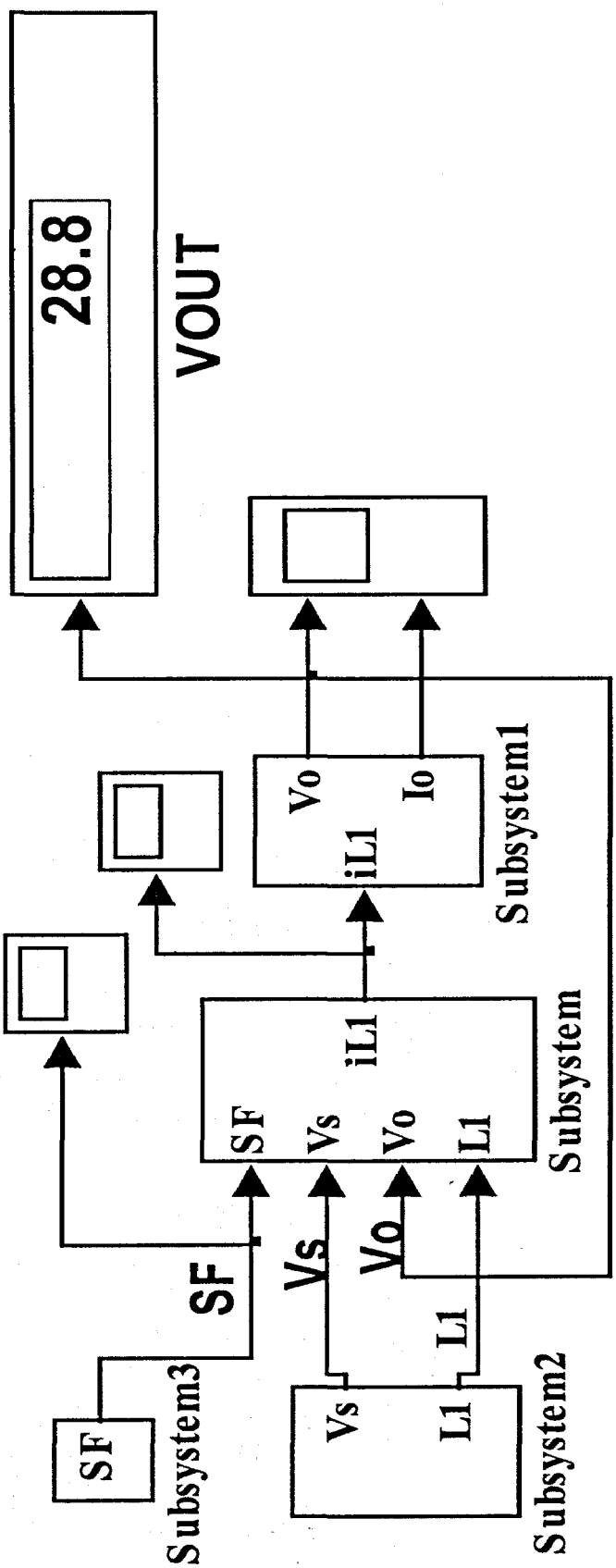

FIG.5.3: BUCK CONVERTOR

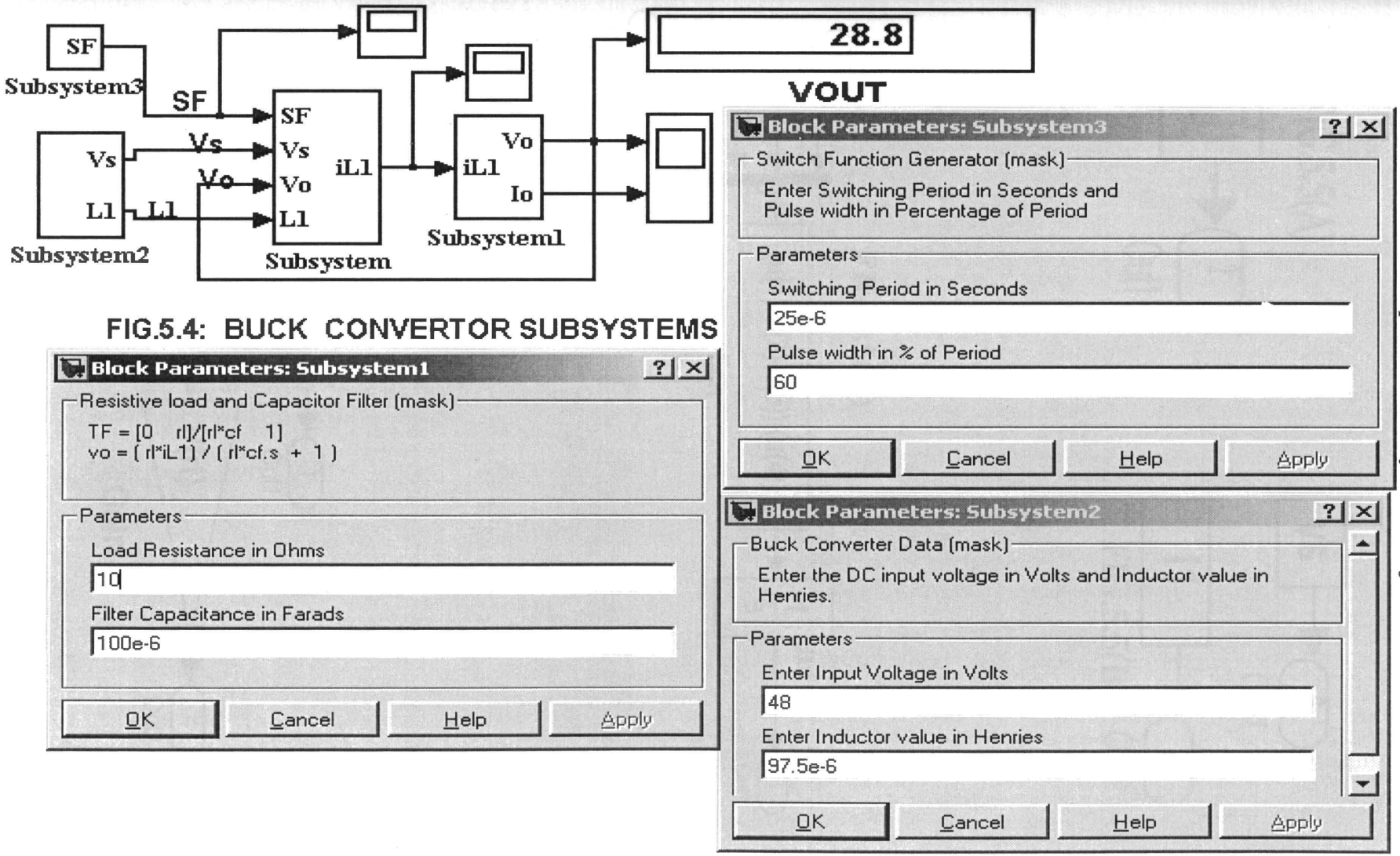

FIG.5.4: BUCK CONVERTOR SUBSYSTEMS

FIG.5.5(A)

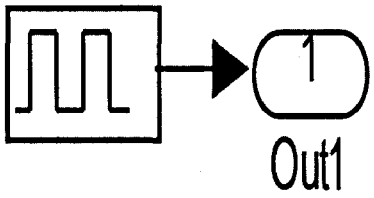

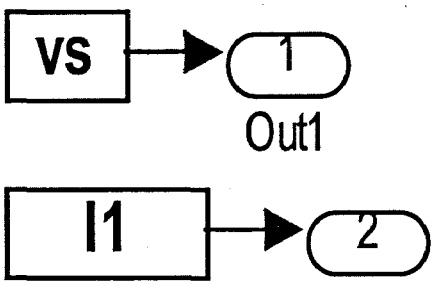

FIG.5.5(B)

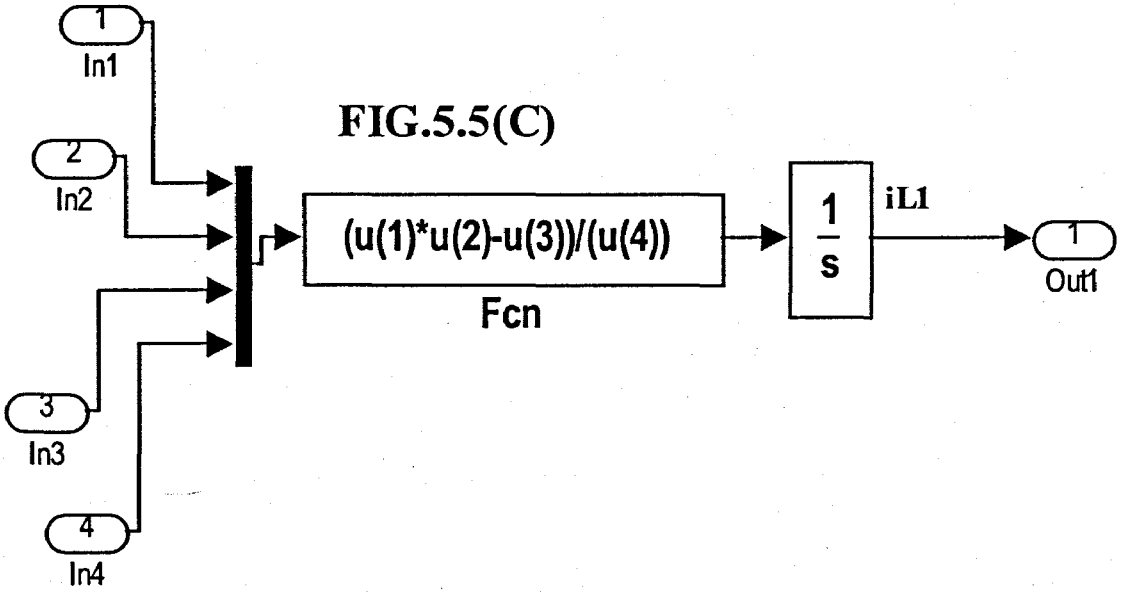

FIG.5.5(C)

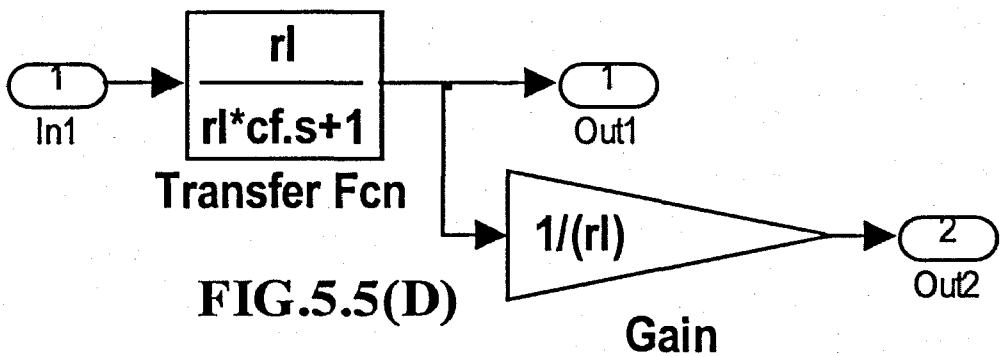

FIG.5.5(D)

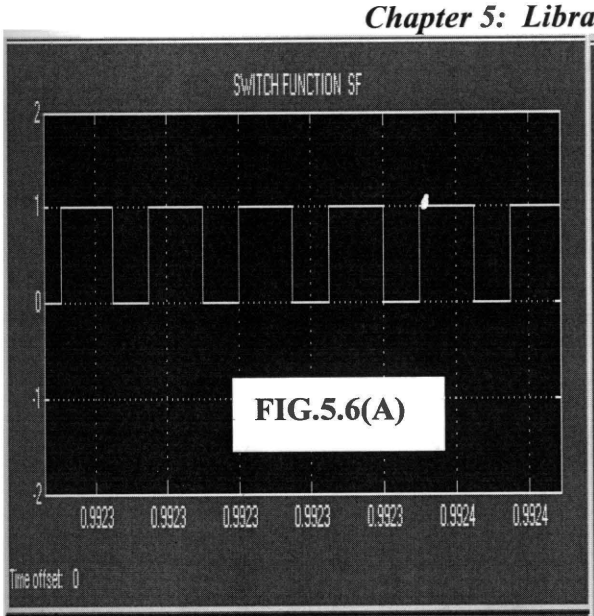

FIG.5.6(A)

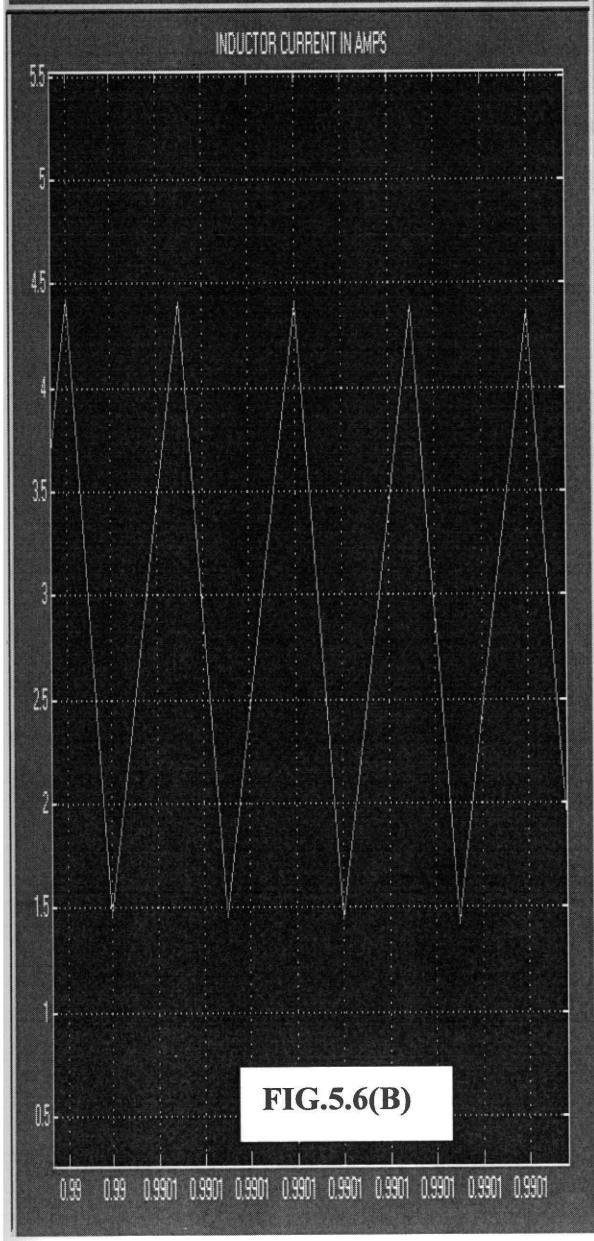

FIG.5.6(B)

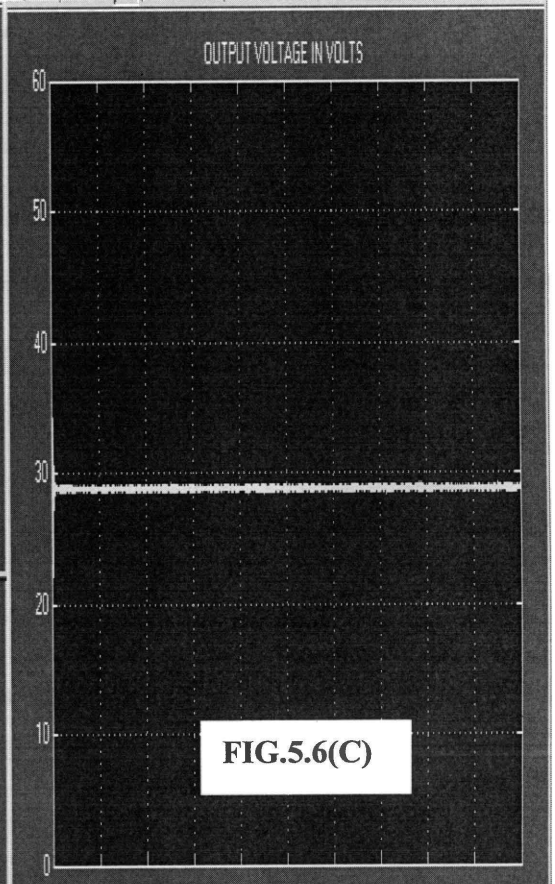

FIG.5.6(C)

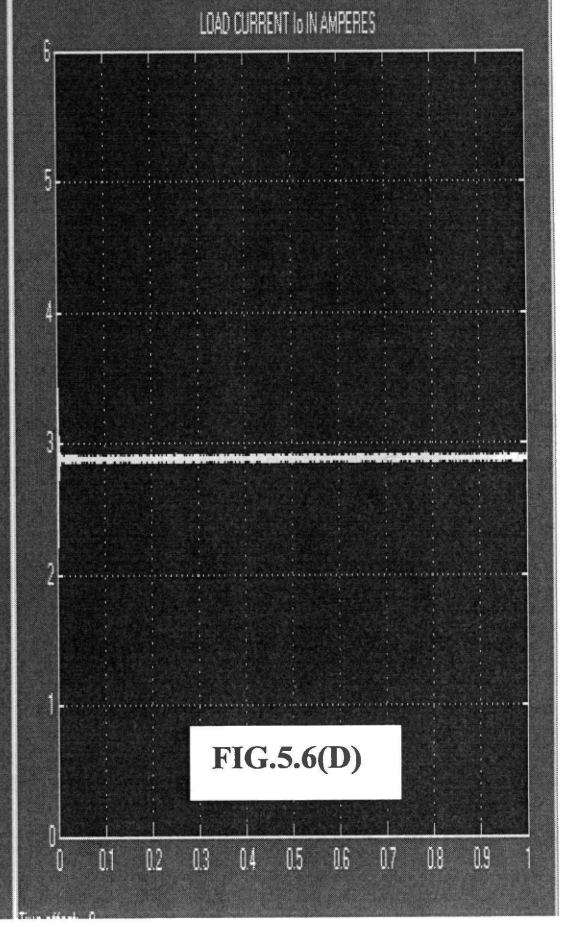

FIG.5.6(D)

TABLE 5.2 – SIMULATION RESULTS

Sl.No.	Output Voltage Vo Volts	Minimum Inductor Current Amps	Maximum Inductor Current Amps	Load Current Amps
1	28.8	1.5	4.4	2.9

TABLE 5.3 – CALCULATED VALUES

Sl.No.	Output Voltage Vo Volts	Minimum Inductor Current Amps	Maximum Inductor Current Amps	Load Current Amps
1	28.8	1.403	4.357	2.88

The oscilloscope waveform of switch function, inductor current, output voltage and load current are plotted in Fig.5.6(A) to (D) respectively.

5.3 Boost Converter Analysis

The Boost converter topology using MOSFET switch is shown in Fig.5.7 [14-18]. In fact the switch can be any one of BJT, IGBT or GTO. The switch is driven by an external PWM drive whose period is T and duty cycle is D. Fig.5.8(A) and (B) shows the equivalent circuit of Fig.5.7 when the switch is ON from 0 to DT seconds and OFF from DT to T seconds respectively. This analysis assumes CCM, i.e the inductor curr - ent is continuous or always greater than zero. Noting that the change in inductor current during the ON time and OFF time are equal or the average inductor current over one switching cycle is zero, the following equation can be derived.

$$\left(\frac{V_S}{L_1}\right).DT+\left(\frac{V_S-V_O}{L_1}\right).(1-D).T \quad =0 \quad (5.11)$$

$$\frac{V_O}{V_S} = \frac{1}{(1-D)} \quad (5.12)$$

During the switch ON time, inductor current grows linearly and reaches a maximum value I_{L1max} and during the switch OFF period, the inductor current decays and reaches a minimum value I_{L1min}. Neglecting switching losses, input and output power are equal.

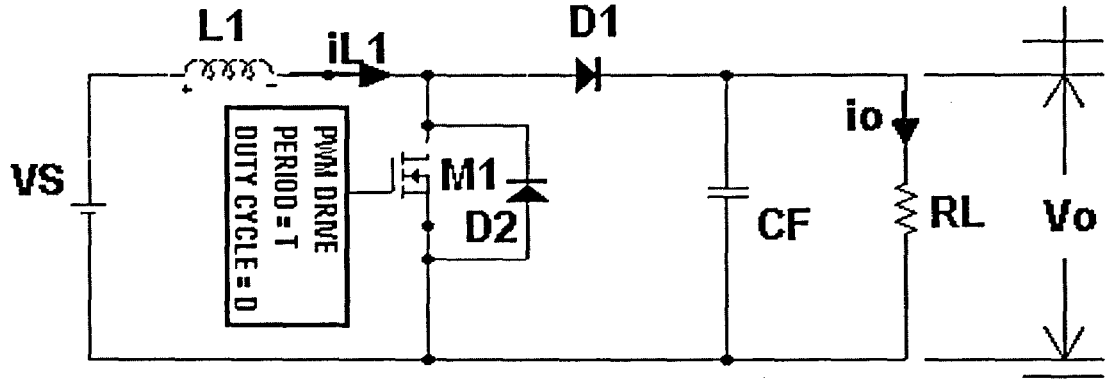

FIG.5.7

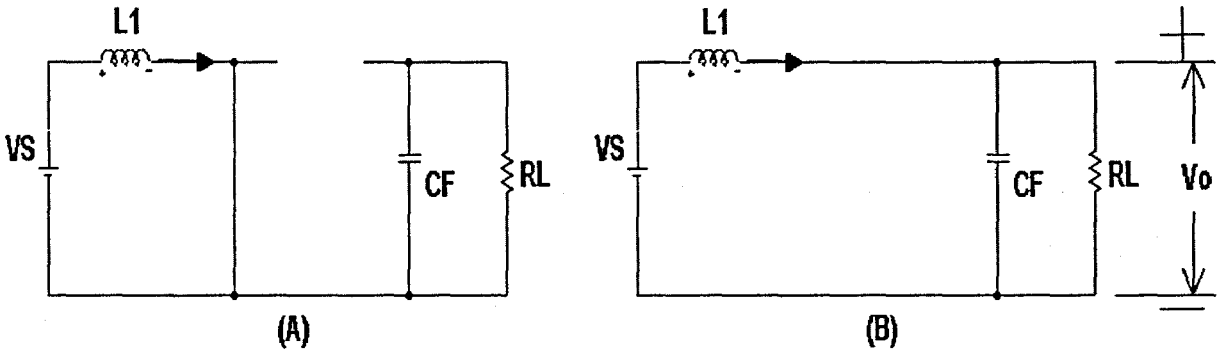

FIG.5.8

The inductor current is derived below:

$$V_S \cdot I_{L1} = \frac{V_O^2}{R_L} \qquad (5.13)$$

Using equation 5.12 and 5.13, inductor current I_{L1} is given below:

$$I_{L1} = \left[\frac{V_S}{(1-D)^2 \cdot R_L} \right] \qquad (5.14)$$

The maximum and minimum inductor current are derived below:

$$I_{L1max} = \left[\frac{V_S}{(1-D)^2 \cdot R_L} + \frac{V_S \cdot D.T}{2.L_1} \right] \qquad (5.15)$$

$$I_{L1min} = \left[\frac{V_S}{(1-D)^2 \cdot R_L} - \frac{V_S \cdot D.T}{2.L_1} \right] \qquad (5.16)$$

The critical inductance L_{1crit} required to maintain CCM is obtained by equating I_{L1min} to zero. This gives the following value for L_{1crit}.

$$L_{1crit} = \frac{R_L.T}{2}.(1-D)^2.D \qquad (5.17)$$

The ratio of ripple voltage to output voltage is given below:

$$\frac{\Delta V_O}{V_O} = \frac{D.T}{R_L.(CF)} \qquad (5.18)$$

5.3.1 Model for Boost Converter

Models for Buck, Quasi Resonant and Flyback converters are available in the literature [54 – 57]. PSPICE Models for dc to dc converters are reported in the literature [14, 17]. This section provides a method for the system modelling of the Boost converter. The Boost Converter model is shown in Fig.5.9. The various dialog boxes are shown in Fig.5.10. The subsystems of Boost converter model are shown in Fig.5.11(A) to (C). The development of the model is explained below:

Referring to Fig.5.8, the following equations can be derived.

$$\frac{di_{L1}}{dt} = \frac{V_S}{L_1} \qquad for\ 0<=t<=D.T \qquad (5.19)$$

$$\frac{di_{L1}}{dt} = \frac{(V_S - V_O)}{L_1} \qquad for\ D.T<=t<=T \qquad (5.20)$$

Now define the Switching Function SF and Inverse Switching Function SF_BAR as follows:

$$SF = 1 \quad for \quad 0 \le t \le D.T$$
$$= 0 \quad for \quad D.T \le t \le T \qquad ...(5.21)$$
$$SF\_BAR = 0 \quad for \quad 0 \le t \le D.T$$
$$= 1 \quad for \quad D.T \le t \le T \qquad (5.22)$$

Equations 5.19 and 5.20 can be written as follows using equations 5.21 and 5.22:

$$\frac{di_{L1}}{dt} = \frac{(SF + SF\_BAR).V_S - (SF\_BAR).V_O}{L_1} \qquad (5.23)$$

Integrating equation 5.23, the inductor current i_{L1} is obtained. Referring to Fig.5.8, it is seen that only the inductor current during switch OFF period contributes to the load voltage. The inductor current during switch ON flows through the short circuit caused by the switch. Therefor the load voltage Vo can be expressed as follows:

$$V_O = \frac{(SF\_BAR).i_{L1}.R_L}{(R_L.CF.s + 1)} \qquad (5.24)$$

The various subsystems are explained below:

Fig.5.11(A) shows the Pulse Generator Block from Sources block set and the corresponding dialog box marked Switch Function Generator is shown in Fig.5.10. In this dialog box, the switching period in seconds and the Pulse Width in percentage of period are entered. Fig.5.11(B) corresponds to the dialog box marked Boost Converter Data in Fig.5.10. In this dialog box, the dc input voltage in Volts and the inductor value L1 in Henries are entered. Fig.5.11(C) shows the Boost converter model. The switch function SF is the u(2) input of the threshold switch, while u(1) and u(3) inputs are logic 0 and 1 respectively. Threshold value for the switch is 0.5. When u(2) is HIGH or logic 1, the output SF_BAR is logic 0 and viceversa. The five input MUX in Fig.5.11(D) has the inputs VS, SF, SF_BAR, Vo, and L1 from u(1) to u(5) respectively. The Fcn block in Fig.5.11(C) solves the equation 5.23 and the integrator block outputs the inductor current i_{L1}. Fig.5.11(D) corresponds to the dialog box Resistive load and Filter in Fig.5.10. The inductor current i_{L1} is given as u(1) input to the threshold switch in Fig.5.11(D). The u(2) and u(3) inputs to this switch are SF_BAR and zero respectively. The inductor current output of this threshold switch corresponds to the case when the semiconductor switch of the Boost converter is turned OFF. This inductor current during switch OFF multiplied by the transfer function (rl) / (rl*cf.s + 1) gives the output voltage Vo. The output voltage Vo is multiplied by the gain block by the factor 1 /(rl) to get the load current Io through the load resistor.

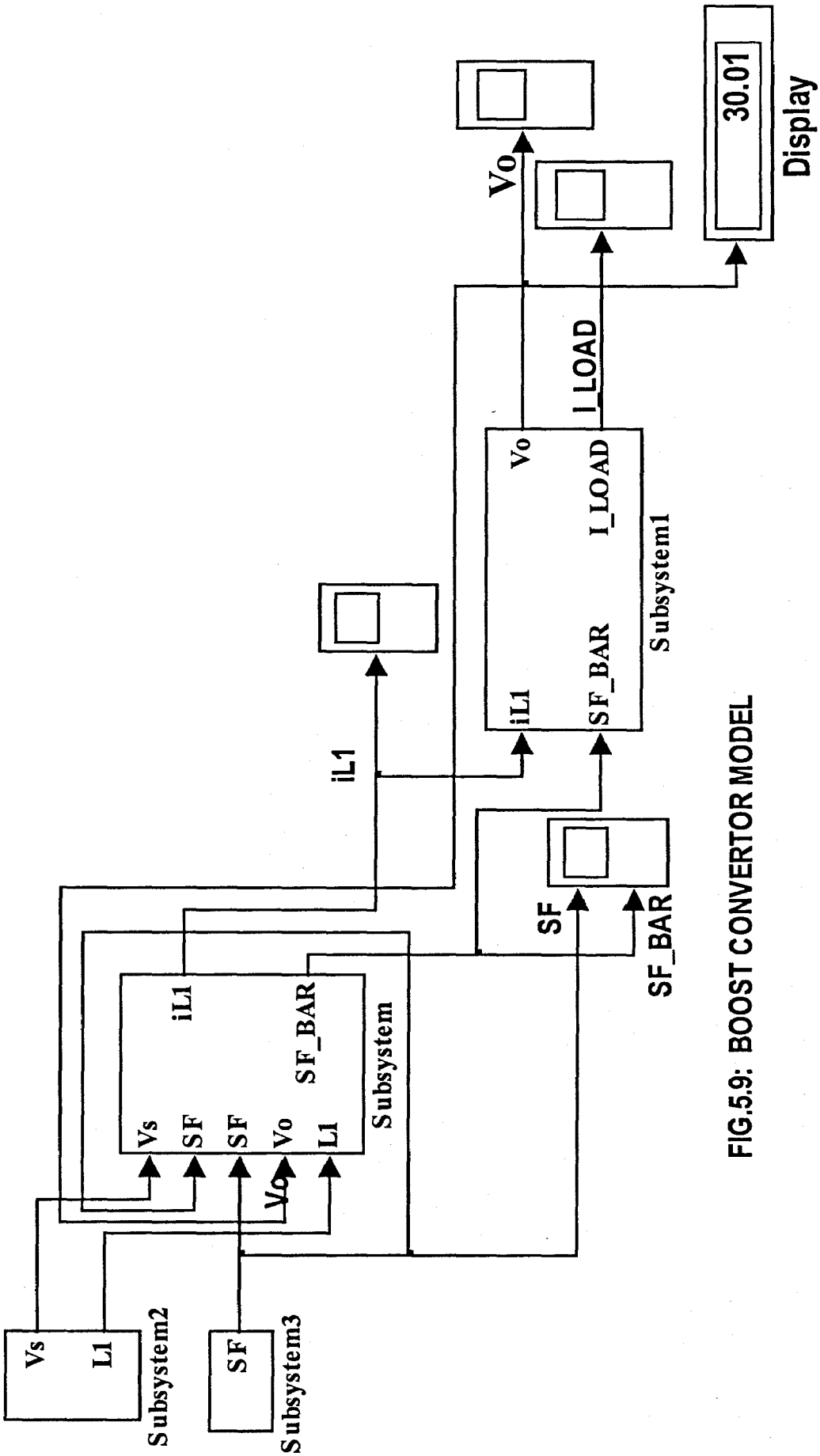

FIG.5.9: BOOST CONVERTOR MODEL

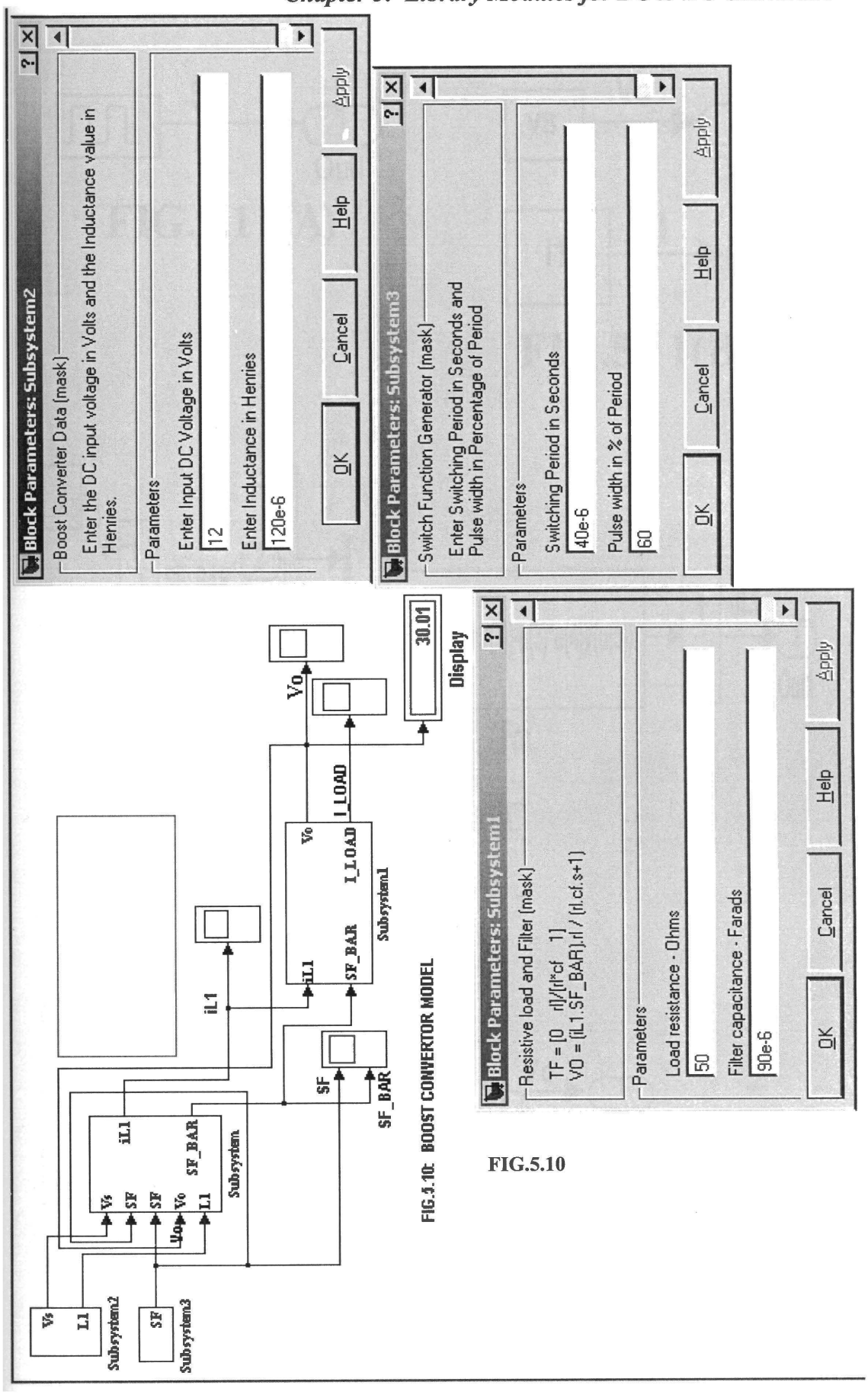

FIG.5.10: BOOST CONVERTOR MODEL

FIG.5.10

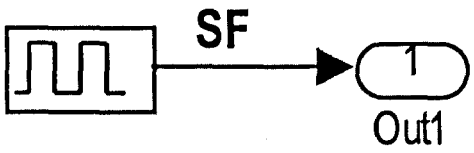

FIG.5.11(A)

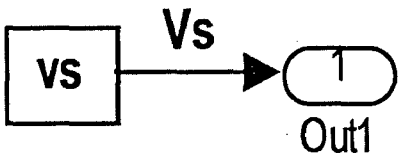

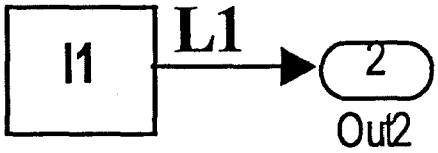

FIG.5.11(B)

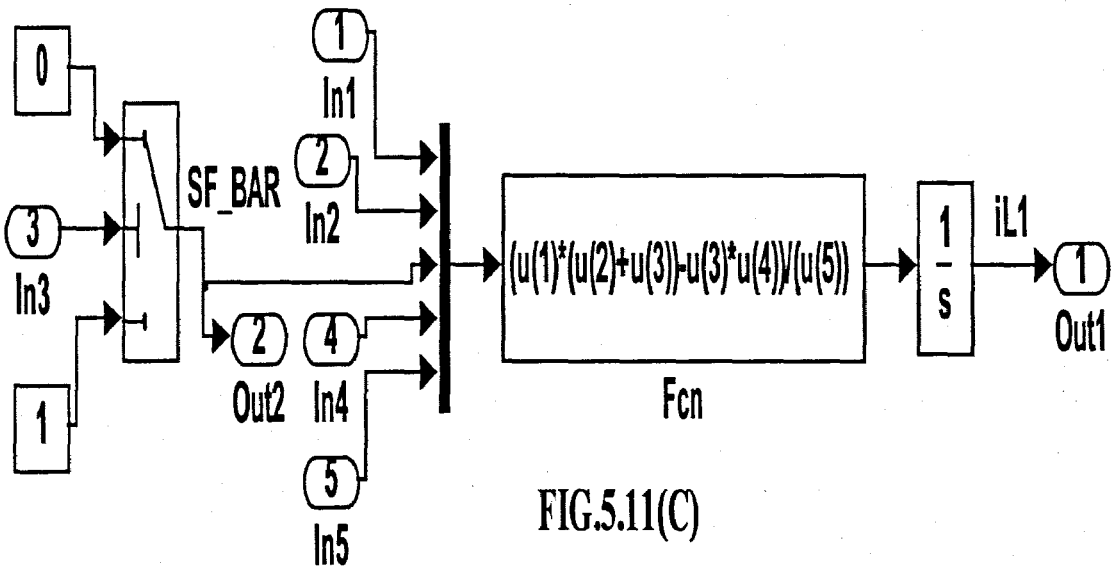

FIG.5.11(C)

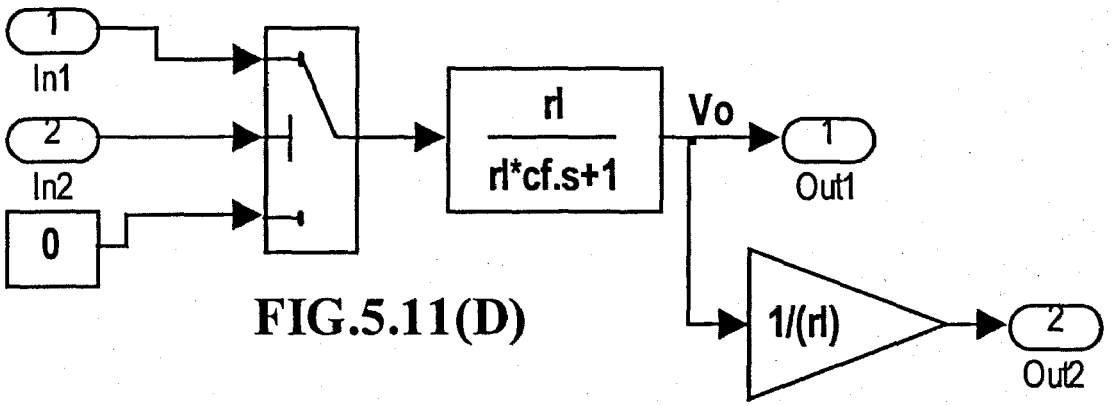

FIG.5.11(D)

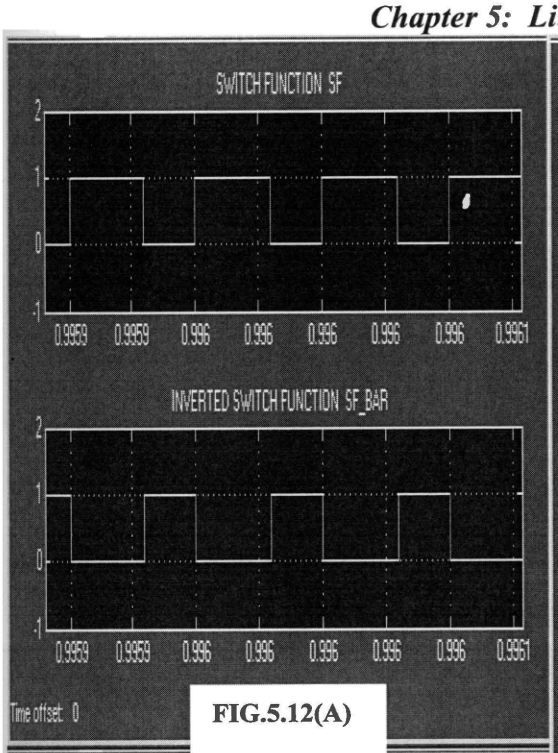

FIG.5.12(A)

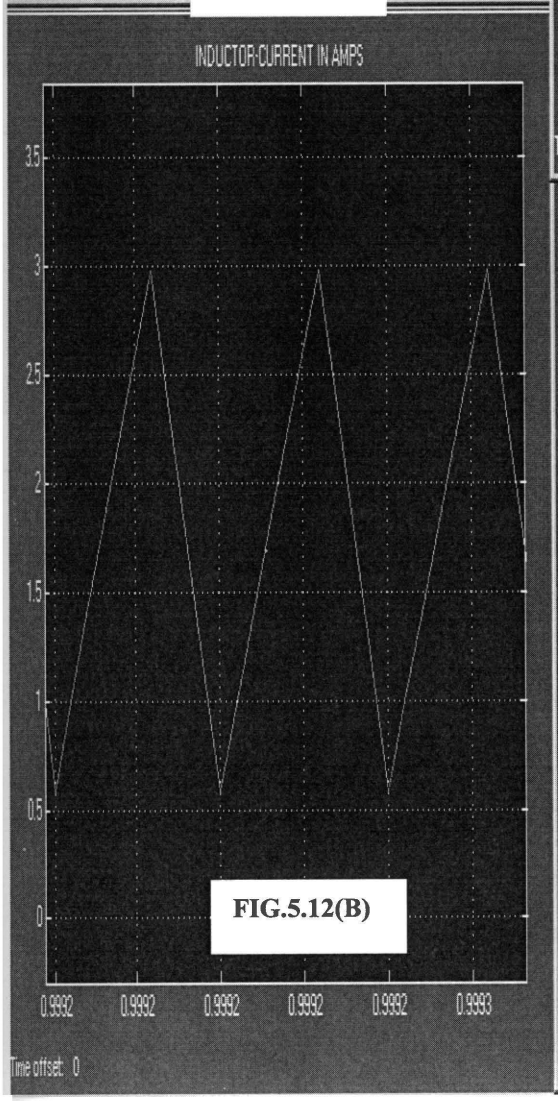

FIG.5.12(B)

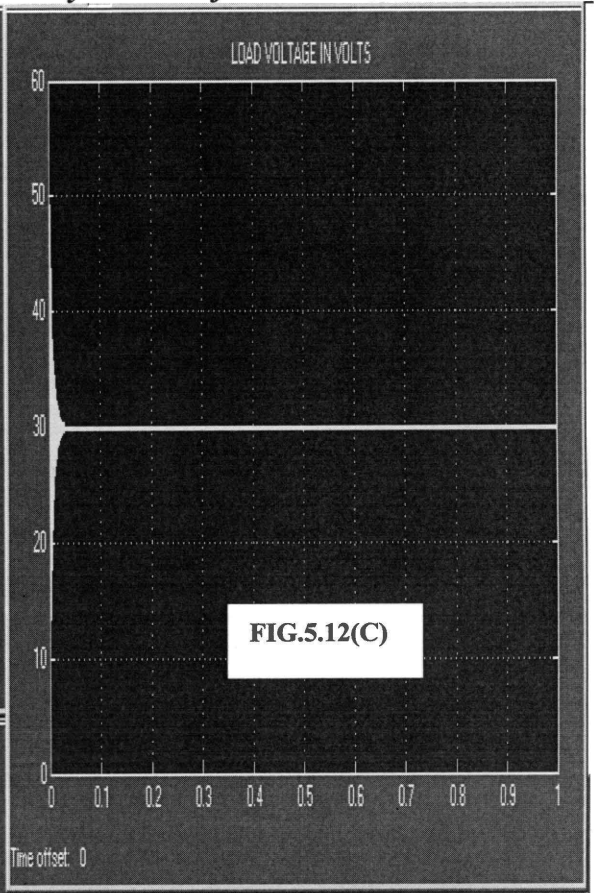

FIG.5.12(C)

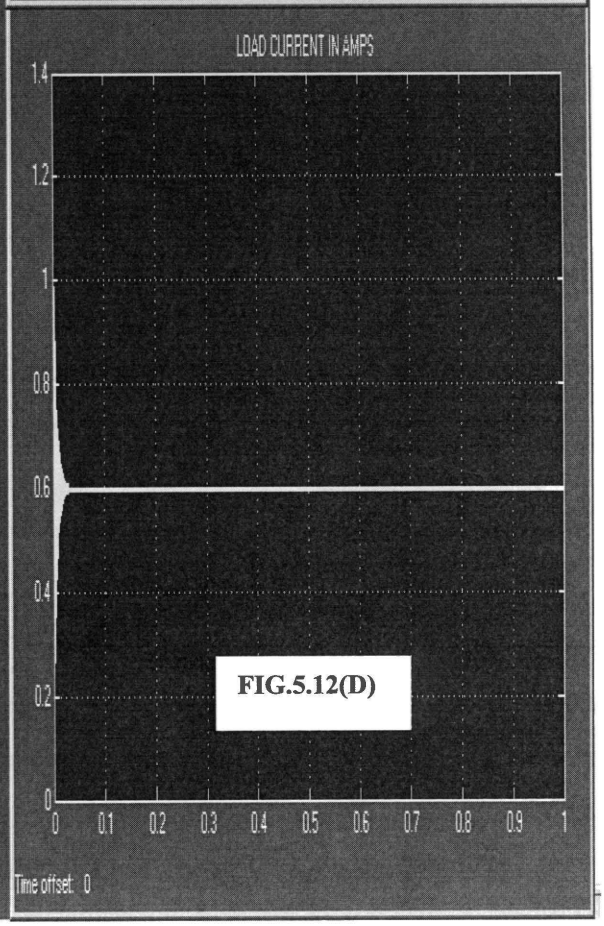

FIG.5.12(D)

5.3.2 Simulation Results

The data relating to the Boost Converter is shown in TABLE 4 [14-16]. The simulation results of the Boost Converter are shown in Fig.5.12(A) to (D). The output

TABLE 5.4 – Boost Converter Data

Sl.No.	Input Voltage Vs Volts	Switching Period T Seconds	Duty Cycle D	Inductor L1 Henries	Filter Capacitor CF Farads	Load Resistor RL Ohms
1	12	40e-6	0.6	120e-6	90e-6	50

voltage is displayed in Fig.5.9.. The simulation results are displayed in Table 5 and the calculated values in Table 6.

TABLE 5.5 – SIMULATION RESULTS

Sl.No.	Output Voltage Vo Volts	Minimum Inductor Current Amps	Maximum Inductor Current Amps	Load Current Amps
1	30.01	0.5	3.0	0.6

TABLE 5.6 – CALCULATED VALUES

Sl.No.	Output Voltage Vo Volts	Minimum Inductor Current Amps	Maximum Inductor Current Amps	Load Current Amps
1	30	0.3	2.7	0.6

The oscilloscope waveform of switch function and inverted switch function, inductor current, output voltage and load current are plotted in Fig.5.12(A) to (D) respectively.

5.4 Buck-Boost Converter Analysis

The Boost converter topology using IGBT switch is shown in Fig.5.13 [14-17]. In fact the switch can be any one of BJT, MOSFET or GTO. The switch is driven by an external PWM drive whose period is T and duty cycle is D. Fig.5.14(A) and (B) shows the equivalent circuit of Fig.5.13 when the switch is ON from 0 to DT seconds and OFF from DT to T seconds respectively. This analysis assumes CCM, i.e the inductor curr -

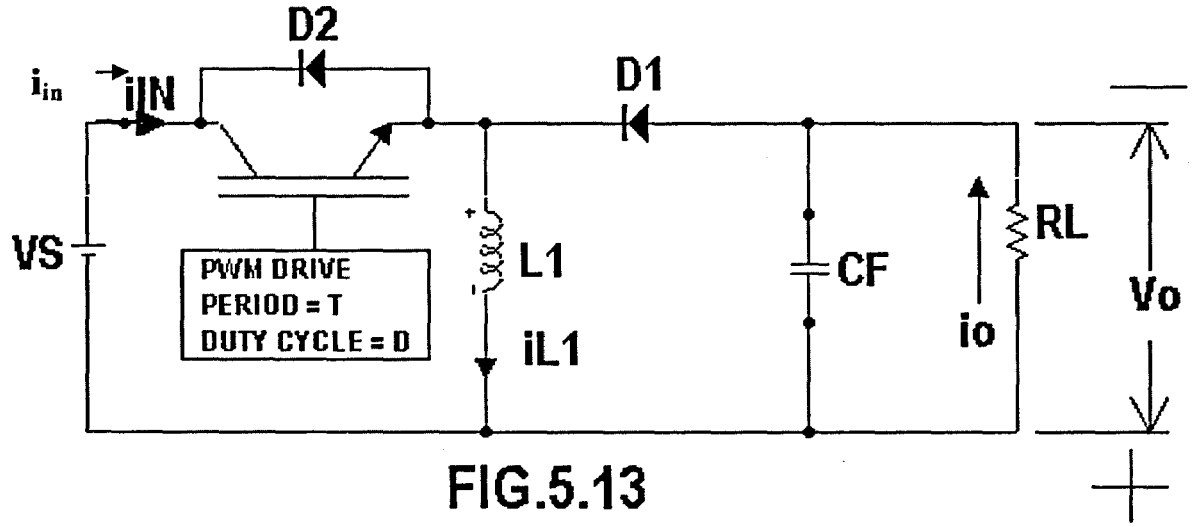

FIG.5.13

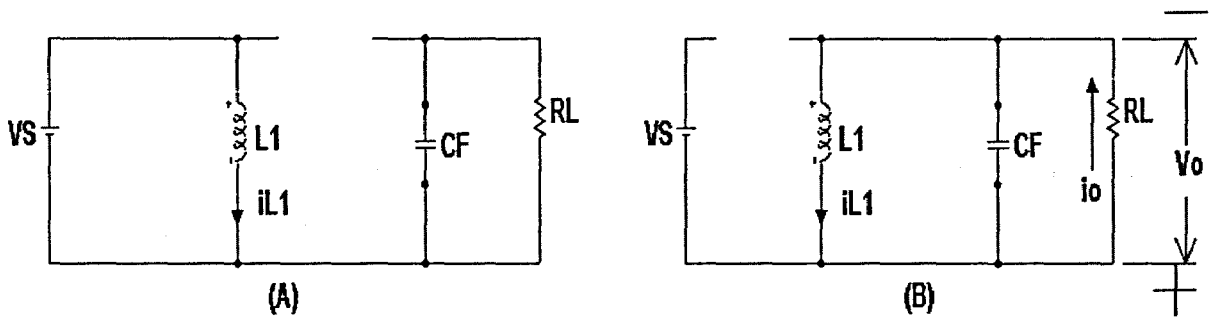

FIG.5.14

ent is continuous or always greater than zero. Noting that the change in inductor current during the ON time and OFF time are equal or the average inductor current over one switching cycle is zero, the following equations can be derived.

$$\left(\frac{V_S}{L_1}\right).D.T+\left(\frac{-V_O}{L_1}\right).(1-D).T \quad = 0 \qquad (5.25)$$

$$\frac{V_O}{V_S} = \frac{D}{(1-D)} \qquad (5.26)$$

The polarity of Vo is negative at the top terminal and positive at the bottom terminal. Let i_{in} be the current supplied by the source. Neglecting losses, the input and output power are equal, giving the following equation.

$$V_S \cdot I_{in} = \frac{V_O^2}{R_L} \qquad (5.27)$$

Referring to Fig.5.14(A) and (B), noting that $I_{in} = D.I_{L1}$ and using equations 5.26 and 5.27, the following equations can be derived.

$$I_{L1} = \frac{V_O^2}{V_S.D.R_L} \qquad (5.28)$$

$$i.e. \quad I_{L1} = \frac{V_S.D}{(1-D)^2.R_L} \qquad (5.29)$$

$$\Delta I_{L1} = \frac{V_S.D.T}{L_1} \qquad (5.30)$$

Using equations 5.26, 5.29 and 5.30, the maximum and minimum inductor current can be expressed as follows:

$$I_{L1max} = \left[\frac{V_S.D}{(1-D)^2.R_L} + \frac{V_S.D.T}{2.L_1}\right] \qquad (5.31)$$

$$I_{L1min} = \left[\frac{V_S.D}{(1-D)^2.R_L} - \frac{V_S.D.T}{2.L_1}\right] \qquad (5.32)$$

The critical inductance L_{1crit} required to maintain CCM is obtained by equating I_{L1min} to zero. This gives the following value for L_{1crit}.

$$L_{1crit} = \frac{R_L.T}{2}.(1-D)^2 \qquad (5.33)$$

The ratio of ripple voltage to output voltage is given below:

$$\frac{\Delta V_O}{V_O} = \frac{D.T}{R_L.(CF)} \qquad (5.34)$$

5.4.1 Model for Buck-Boost Converter

Models for Buck, Quasi Resonant and Flyback converters are available in the literature [54 – 57]. PSPICE Models for dc to dc converters are reported in the literature [14, 17]. This section provides a method for the system modelling of the Buck-Boost converter. The Buck-Boost Converter model is shown in Fig.5.15. The various dialog boxes are shown in Fig.5.16. The subsystems of Buck-Boost converter model are shown in Fig.5.17(A) to (C). The development of the model is explained below:

Referring to Fig.5.14, the following equations can be derived.

$$\frac{di_{L1}}{dt} = \frac{V_S}{L_1} \quad for\ 0<=t<=D.T \quad (5.35)$$

$$\frac{di_{L1}}{dt} = \frac{(-V_O)}{L_1} \quad for\ D.T<=t<=T \quad (5.36)$$

Now define the Switching Function SF and Inverse Switching Function SF_BAR as follows:

$$SF = 1 \quad for \quad 0 \le t \le D.T$$

$$= 0 \quad for \quad D.T \le t \le T \quad ...(5.37)$$

$$SF\_BAR = 0 \quad for \quad 0 \le t \le D.T$$

$$= 1 \quad for \quad D.T \le t \le T \quad (5.38)$$

Equations 5.35 and 5.36 can be written as follows using equations 5.37 and 5.38:

$$\frac{di_{L1}}{dt} = \frac{(SF).V_S - (SF\_BAR).V_O}{L_1} \quad (5.39)$$

Integrating equation 5.39, the inductor current i_{L1} is obtained. Referring to Fig.5.14, it is seen that only the inductor current during switch OFF period contributes to the load voltage. The inductor current during switch ON flows through the short circuit caused by the switch. Therefor the load voltage Vo can be expressed as follows:

$$V_O = \frac{-(SF\_BAR).i_{L1}.R_L}{(R_L.CF.s + 1)} \qquad (5.40)$$

The various subsystems are explained below:

Fig.5.17(A) shows the Pulse Generator Block from Sources block set and the corresponding dialog box marked Switch Function Generator is shown in Fig.5.16. In this dialog box, the switching period in seconds and the Pulse Width in percentage of period are entered. Fig.5.17(B) corresponds to generation of SF_BAR. The switch function SF is the u(2) input of the threshold switch, while u(1) and u(3) inputs are logic 0 and 1 respectively. Threshold value for the switch is 0.5. When u(2) is HIGH or logic 1, the output SF_BAR is logic 0 and viceversa. Fig.5.17(C) shows the Buck-Boost converter model data and the corresponding dialog box Buck-Boost converter data is shown in Fig.5.16. In this dialog box, the input DC voltage in Volts and the inductance value in Henries are entered. Fig.5.17(D) shows the Buck-Boost converter model. The five input MUX in Fig.5.17(D) has the inputs SF, VS, SF_BAR, Vo, and L1 from u(1) to u(5) respectively. The Fcn block in Fig.5.17(D) solves the equation 5.39 and the integrator block outputs the inductor current i_{L1}. Fig.5.17(E) corresponds to the dialog box Resistive load and Capacitor Filter in Fig.5.16. The inductor current i_{L1} is given as u(1) input to the threshold switch in Fig.5.17(E). The u(2) and u(3) inputs to this switch are SF_BAR and zero respectively. The inductor current output of this threshold switch corresponds to the case when the semiconductor switch of the Buck-Boost converter is turned OFF. This inductor current during switch OFF multiplied by the transfer function (rl) / (rl*cf.s + 1) gives the output voltage Vo. The output voltage Vo is multiplied by the gain block by the factor 1 /(rl) to get the load current Io through the load resistor.

5.4.2 Simulation Results

The data relating to the Buck-Boost Converter is shown in TABLE 5.7 [14-16]. The output voltage is displayed in Fig.5.15.. The simulation results are displayed in Table 5.8 and the calculated values in Table 5.9.

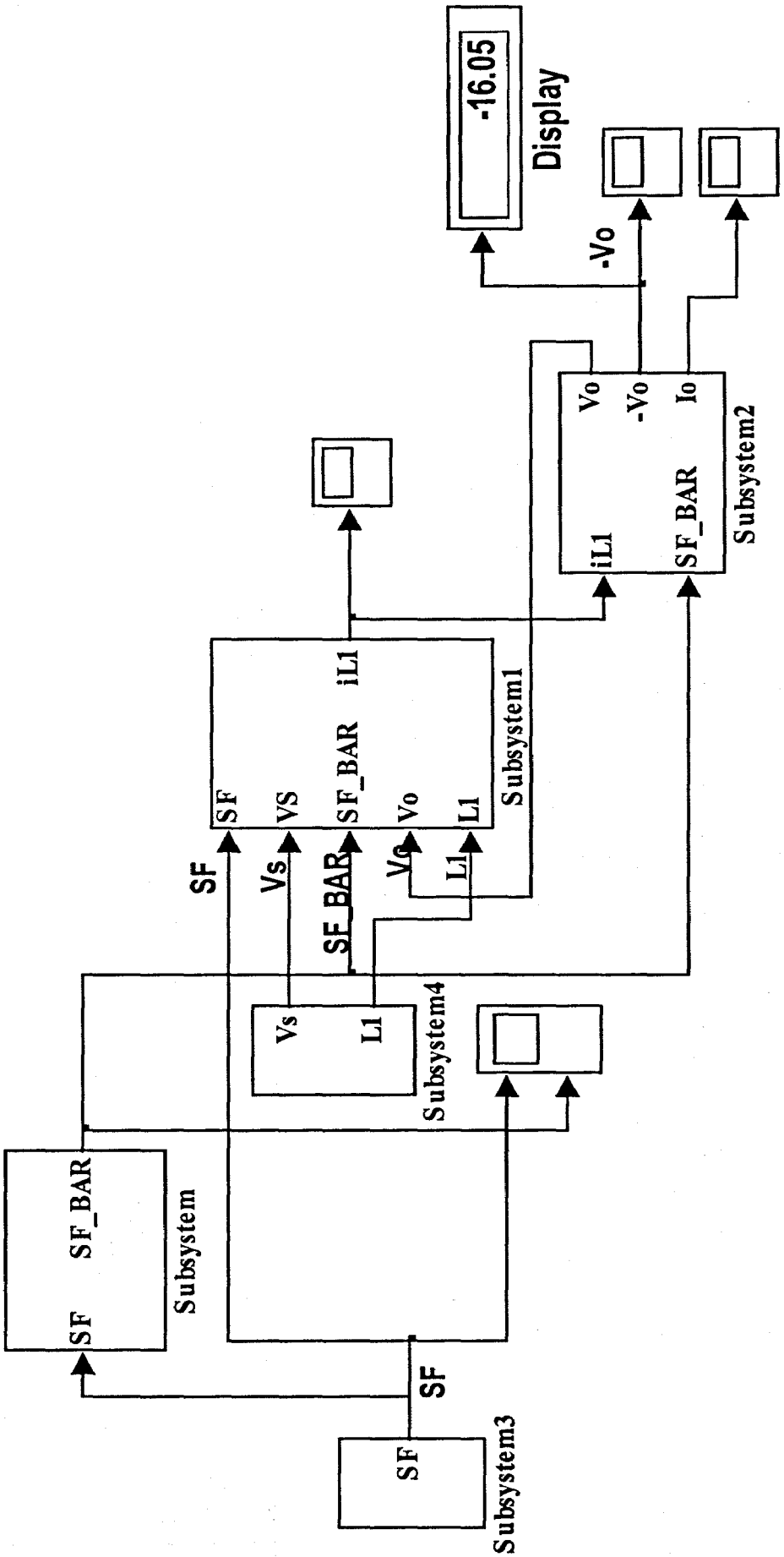

FIG.5.15: BUCK-BOOST CONVERTOR

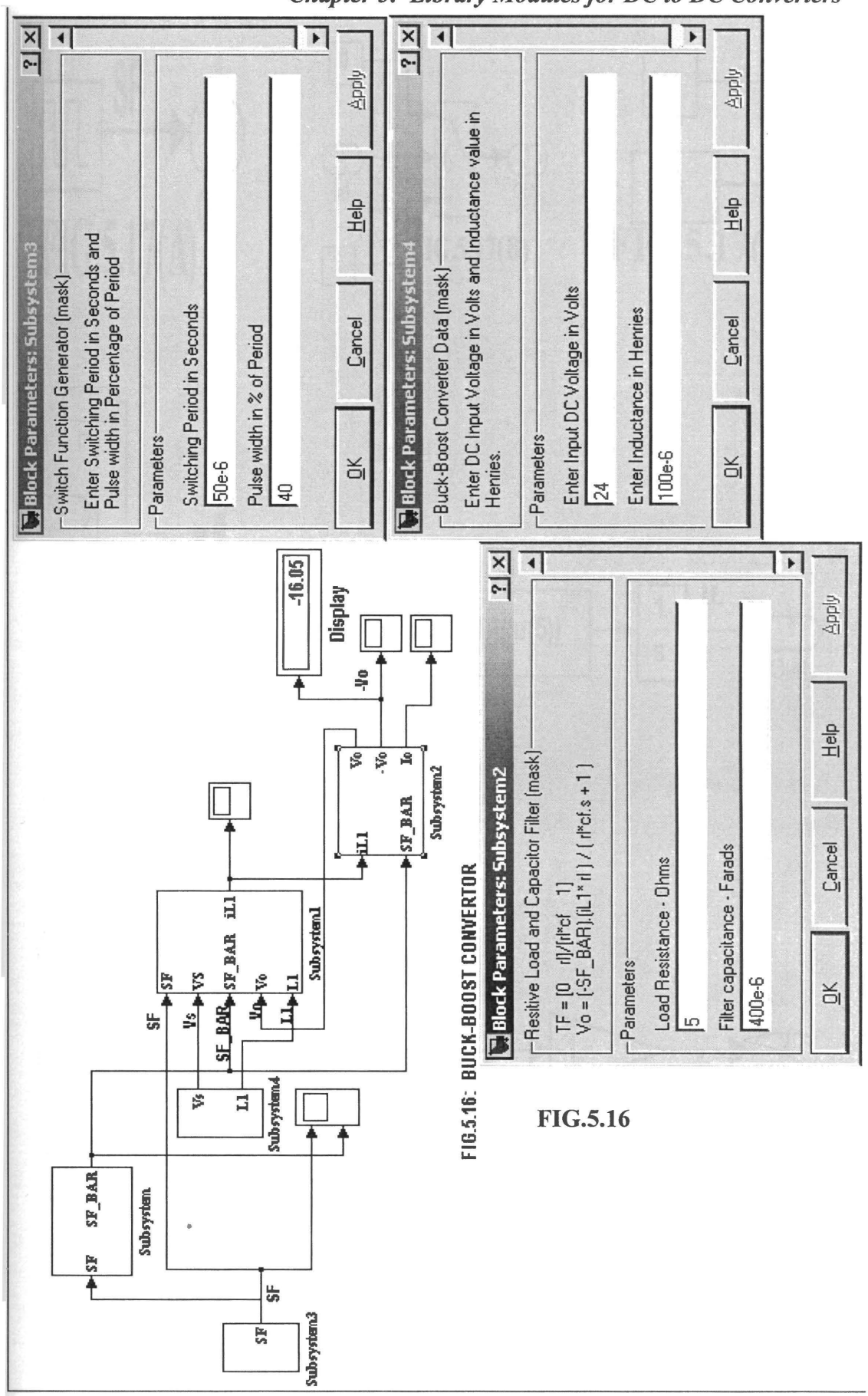

FIG.5.16: BUCK-BOOST CONVERTOR

FIG.5.16

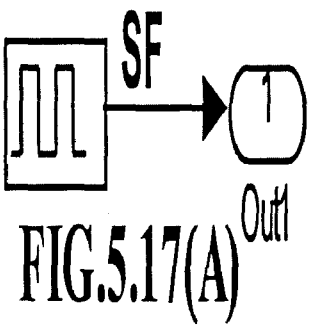

FIG.5.17(A)

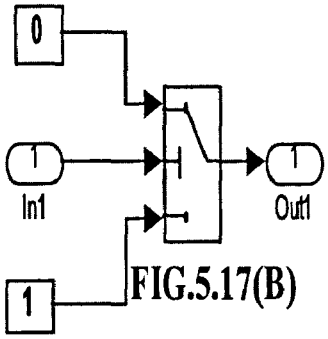

FIG.5.17(B)

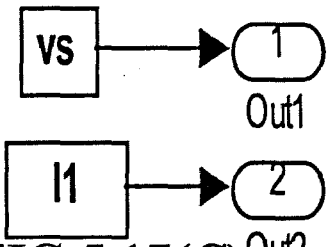

FIG.5.17(C)

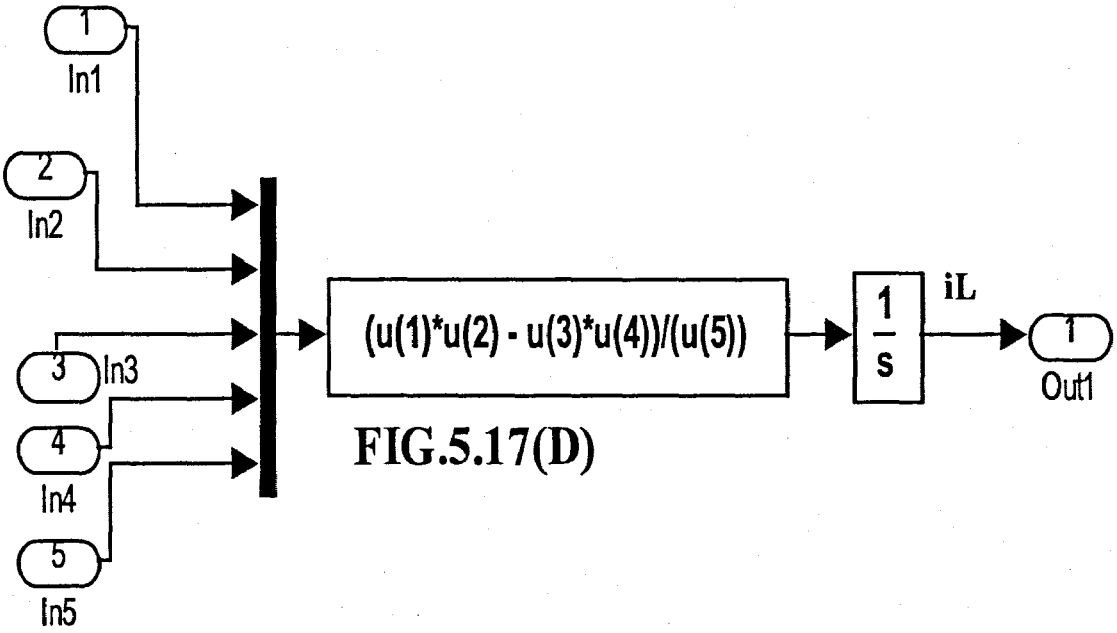

FIG.5.17(D)

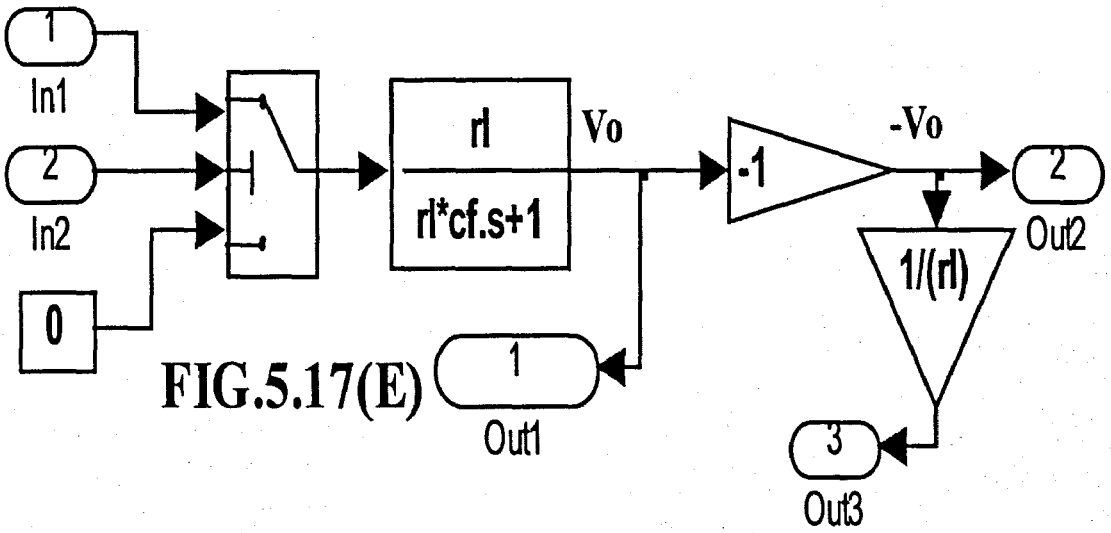

FIG.5.17(E)

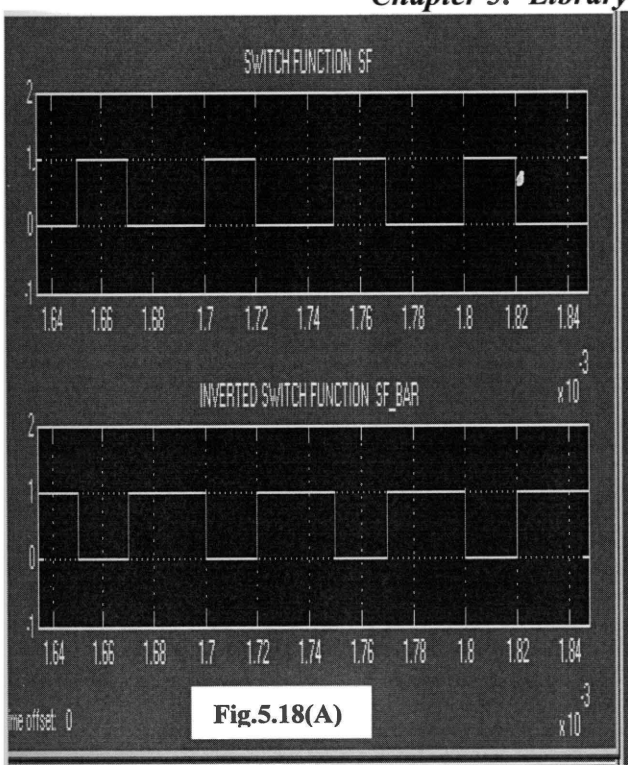

Fig.5.18(A)

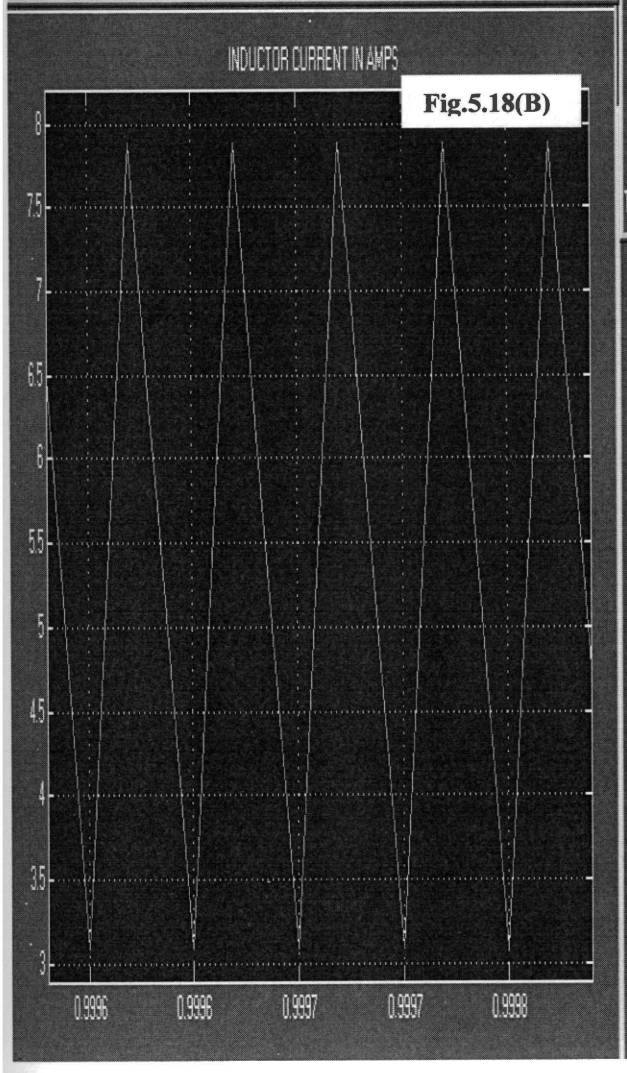

Fig.5.18(B)

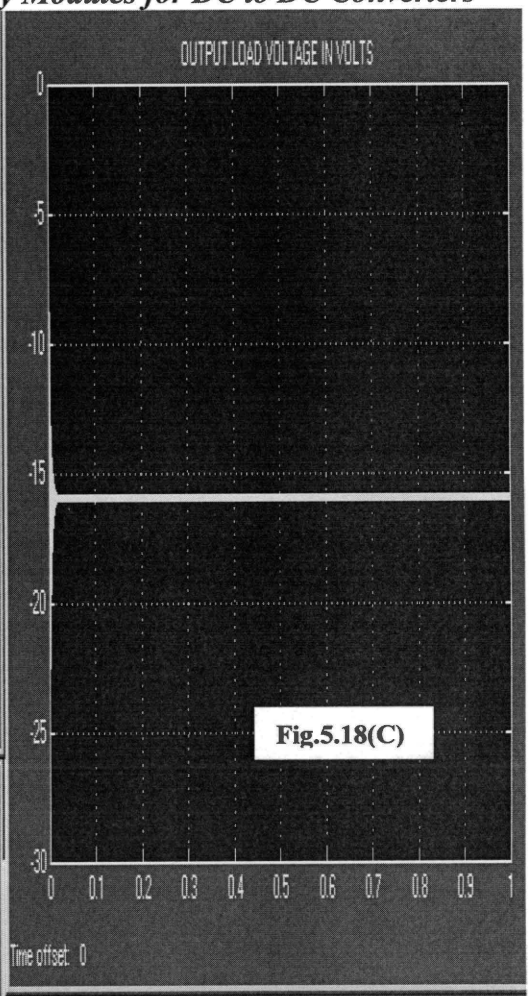

Fig.5.18(C)

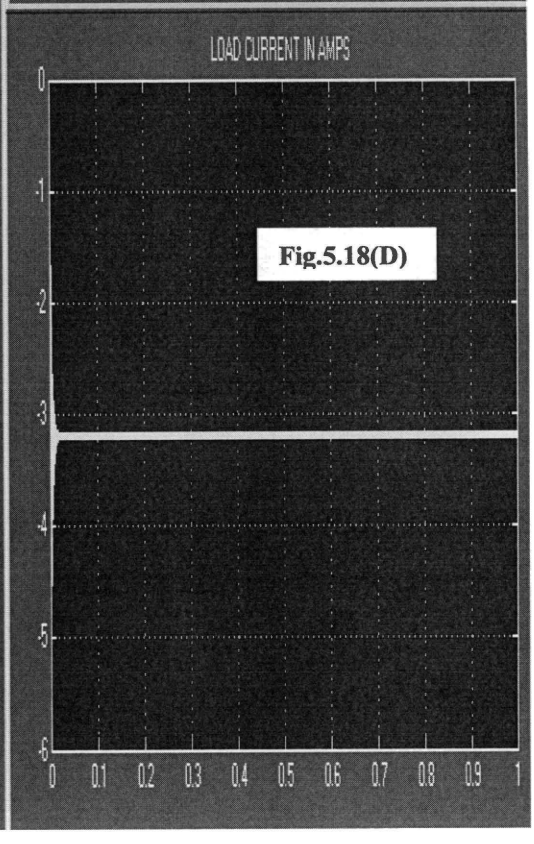

Fig.5.18(D)

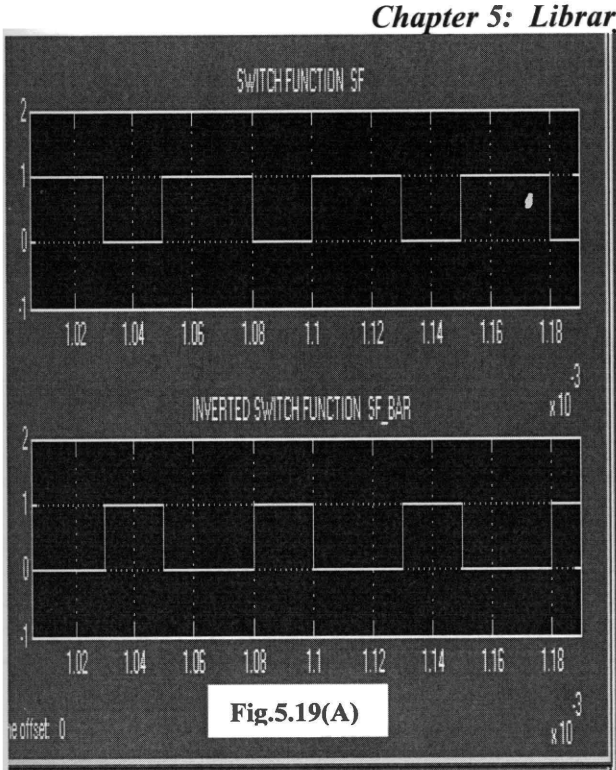

Fig.5.19(A)

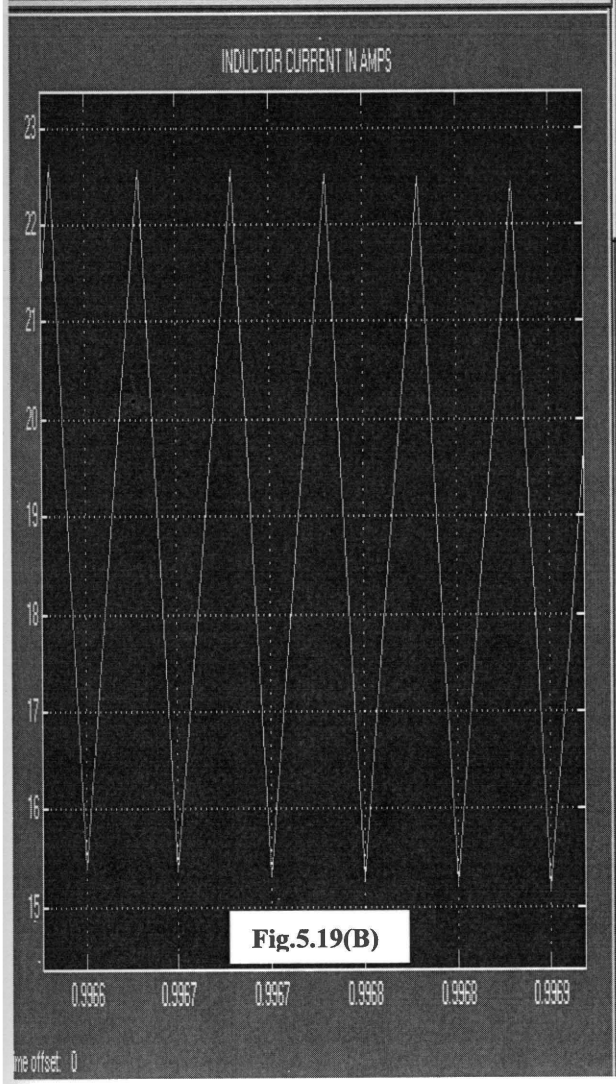

Fig.5.19(B)

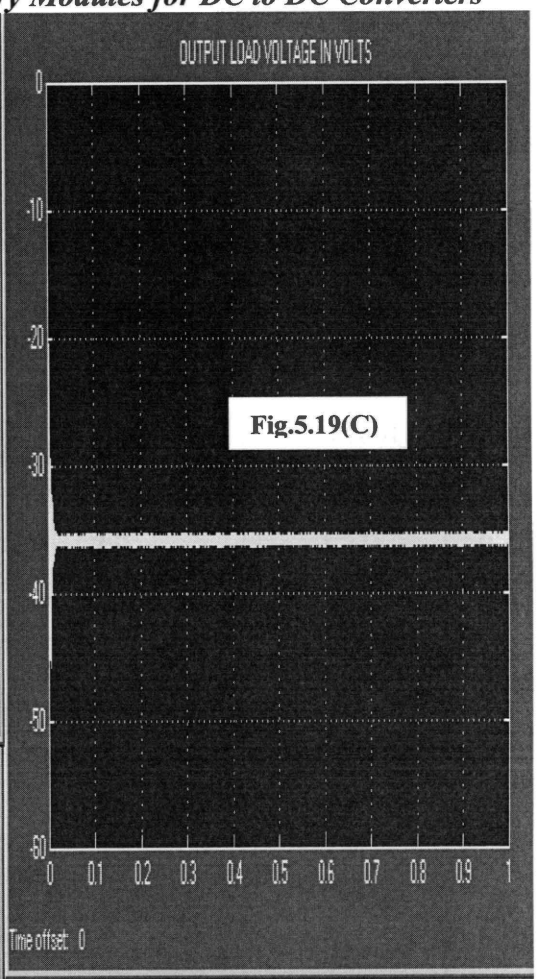

Fig.5.19(C)

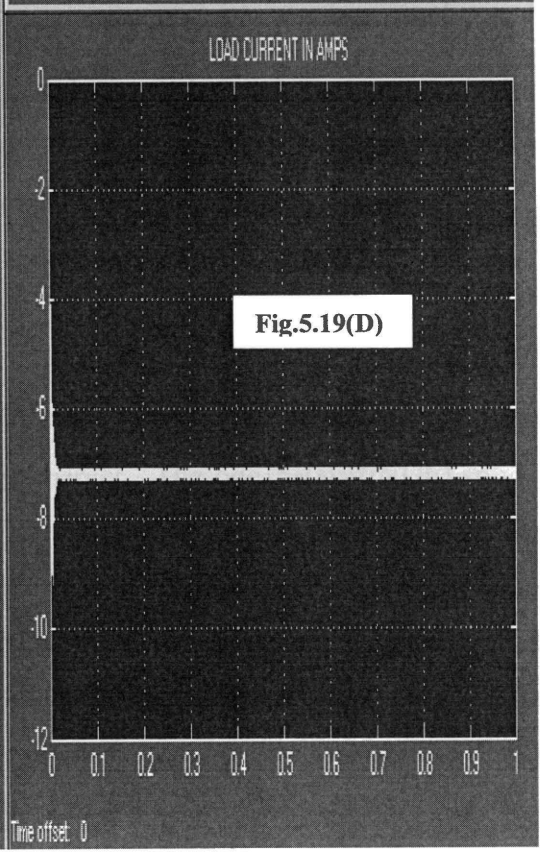

Fig.5.19(D)

TABLE 5.7 – Buck-Boost Converter Data

Sl.No.	Input Voltage Vs Volts	Switching Period T Seconds	Duty Cycle D	Inductor L1 Henries	Filter Capacitor CF Farads	Load Resistor RL Ohms
1	24	50e-6	0.4	100e-6	400e-6	5
2	24	50e-6	0.6	100e-6	400e-6	5

TABLE 5. 8 – SIMULATION RESULTS

Sl.No.	Output Voltage Vo Volts	Minimum Inductor Current Amps	Maximum Inductor Current Amps	Load Current Amps	Duty Cycle
1	-16.05	3.1	7.9	3.21	0.4
2	-36.29	15.5	22.5	7.26	0.6

TABLE 5.9 – CALCULATED VALUES

Sl.No.	Output Voltage Vo Volts	Minimum Inductor Current Amps	Maximum Inductor Current Amps	Load Current Amps	Duty Cycle
1	-16	2.933	7.733	3.2	0.4
2	-36	14.4	21.6	7.2	0.6

The oscilloscope waveform of switch function and inverted switch function, inductor current, output voltage and load current are plotted in Fig.5.18(A) to (D) respectively for 0.4 duty cycle and in Fig.5.19(A) to (D) respectively for 0.6 duty cycle.

5.5 Conclusions

The system model development for Buck, Boost and Buck-Boost converter using the switching Function concept is presented in this chapter. The ode15s(stiff/NDF) solver was used for simulation of the three models. The simulation and the theoretical results using the formula are separately tabulated. In the case of Boost converter, the minimum inductor current deviates a little higher than the calculated value using formula. In all other cases the simulation results and the theoretical results calculated using the formula almost well agree. The simulation of the above dc to dc converters using the demo version of PSIM 7.0 software is given in Appendix E.----------

CHAPTER 6

LIBRARY MODELS FOR AC TO AC CONVERTERS

6.1 Introduction

The ac to ac converters used to vary the rms value of the load at a constant frequency are known as ac voltage controllers or ac regulators. The voltage control is accomplished by phase control or on-off control. A single phase ac controller uses a pair of SCRs connected back to back or antiparallel between the supply and the load. Several configurations for three phase ac controller are available employing three single phase ac controllers. This chapter describes the system modelling of two predominant three phase ac controller configurations namely three phase ac controller with back to back SCRs in series with the ac lines with star connected resistive load with isolated neutral and three phase ac controllers in series with delta connected resistive load connected to the lines.

6.2 Analysis of A Fully Controlled Three Phase Three Wire AC Voltage Controller With Star Connected Resistive Load and Isolated Neutral

The three phase three wire AC voltage controller with back to back SCRs and star connected resistive load with isolated neutral is shown in Fig.6.1 [14, 16]. By varying the firing angle α, the rms voltage across the load can be varied. The firing sequence is T1, T2, T3, T4, T5 and T6. This is derived below:

$$\left.\begin{aligned} v_{AN} &= \sqrt{2}.V_S.\sin(\omega.t) \\ v_{BN} &= \sqrt{2}.V_S.\sin\left(\omega.t - \frac{2\pi}{3}\right) \\ v_{CN} &= \sqrt{2}.V_S.\sin\left(\omega.t + \frac{2\pi}{3}\right) \end{aligned}\right| \qquad (6.1)$$

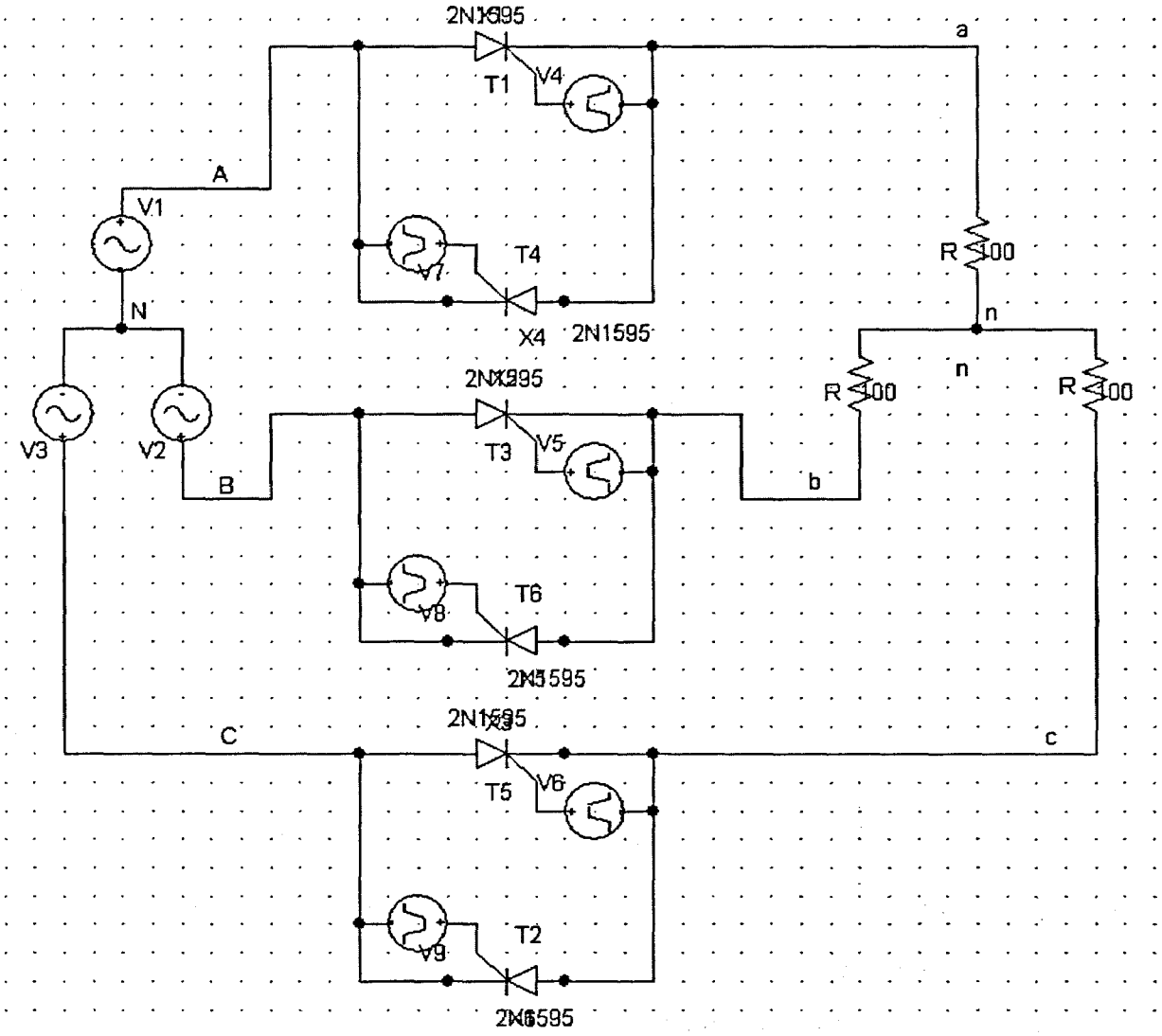

FIG.6.1: THREE PHASE AC BACK TO BACK CONNECTED THYRISTOR CONTROLLER

In equation 6.1, v_{AN}, v_{BN} and v_{CN} are the three phase instantaneous line to neutral input voltages. The three phase instantaneous line to line input voltages are given below:

$$\left.\begin{aligned} v_{AB} &= \sqrt{6}.V_S.\sin\left(\omega.t + \frac{\pi}{6}\right) \\ v_{BC} &= \sqrt{6}.V_S.\sin\left(\omega.t - \frac{\pi}{2}\right) \\ v_{CA} &= \sqrt{6}.V_S.\sin\left(\omega.t - \frac{7\pi}{6}\right) \end{aligned}\right\} \qquad (6.2)$$

The rms line to neutral voltage across the star connected resistive load for various range of firing angle α are given below [14]:

$$For \quad 0 \le \alpha < 60^{O}$$

$$V_{O} = V_{or(rms)} = \sqrt{6}.V_{S}\sqrt{\left[\frac{1}{6} - \frac{\alpha}{4\pi} + \frac{\sin 2\alpha}{8\pi}\right]} \qquad (6.3)$$

$$For \quad 60^{O} \le \alpha < 90^{O}$$

$$V_{O} = V_{or(rms)} = \sqrt{6}.V_{S}\sqrt{\left[\frac{1}{12} + \frac{3\sin 2\alpha}{16\pi} + \frac{\sqrt{3}.\cos 2\alpha}{16\pi}\right]} \qquad (6.4)$$

$$For \quad 90^{O} \le \alpha \le 150^{O}$$

$$V_{O} = V_{or(rms)} = \sqrt{6}.V_{S}\sqrt{\left[\frac{5}{24} - \frac{\alpha}{4\pi} + \frac{\sin 2\alpha}{16\pi} + \frac{\sqrt{3}\cos 2\alpha}{16\pi}\right]} \qquad (6.5)$$

For $0 \le \alpha < 60^{O}$, immediately before firing of T1, two thyristors conduct. When T1 is fired, three thyristors conduct. When the thyristor current reverses, the particular thyristor turns OFF. For $60^{O} \le \alpha < 90^{O}$, only two thyristors conduct at any time. For $90^{O} \le \alpha < 150^{O}$, although two thyristors conduct any time, there are periods when NO thyristors are ON. The output voltage becomes zero for α of 150 degrees.

6.2.1 Modelling of A Fully Controlled Three Phase Three Wire AC Voltage Controller With Star Connected Resistive Load and Isolated Neutral

This section describes the modelling of the three phase AC controller shown in Fig.6.1. The model for a firing angle α of $\pi/6$ radians is shown in Fig.6.2. The various dialog boxes are shown in Fig.6.3 and the various subsystems in Fig.6.4(A) to (D). The various subsystems are explained below:

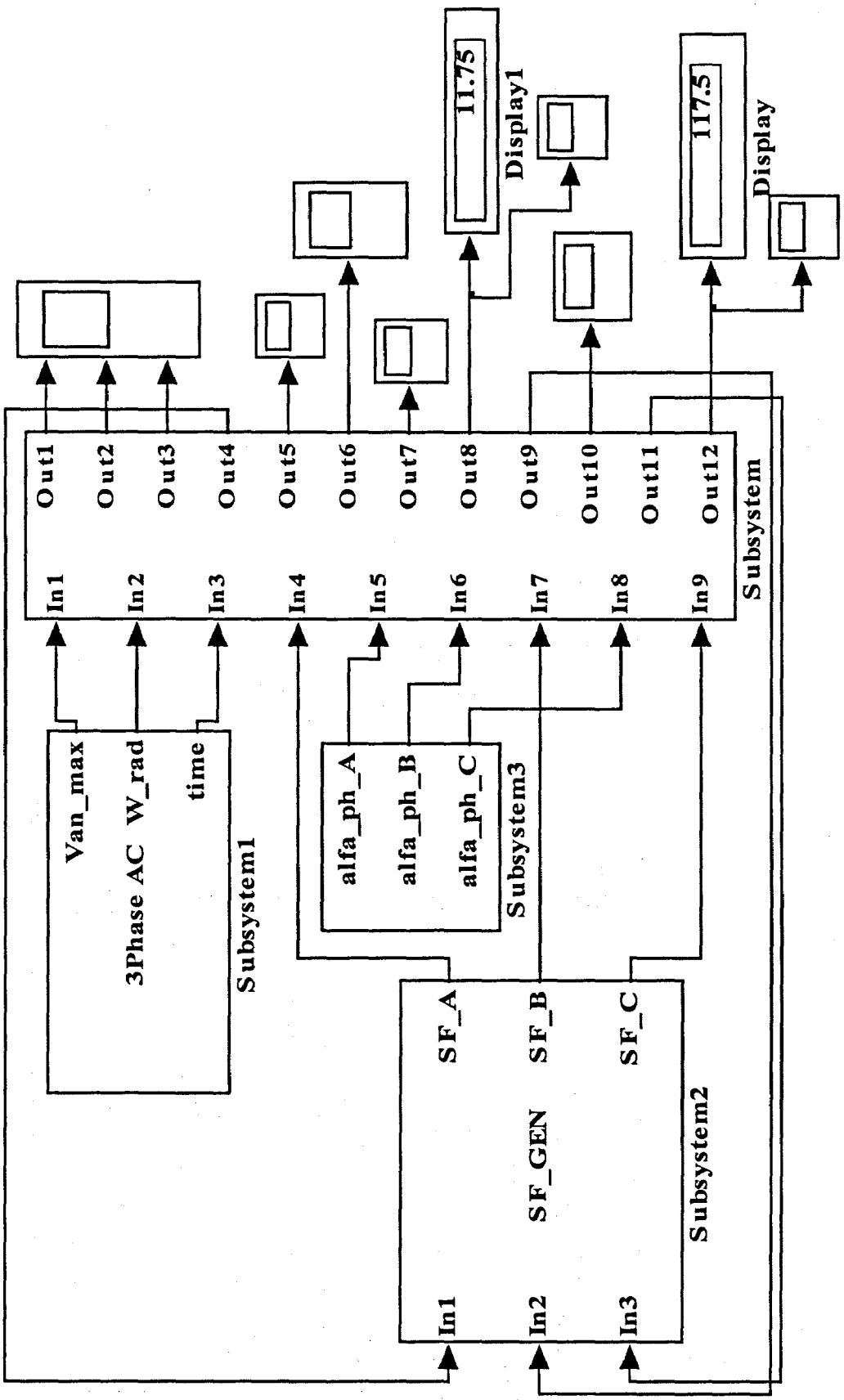

FIG.6.2: MODEL OF THREE PHASE FULLY CONTROLLED SCR CONTROLLER WITH STAR CONNECTED RESISTIVE LOAD AND ISOLATED NEUTRAL FOR ALFA = 30 DEGREES

FIG.6.3: MODEL OF THREE PHASE FULLY CONTROLLED SCR CONTROLLER WITH STAR CONNECTED RESISTIVE LOAD AND ISOLATED NEUTRAL FOR ALFA = 30 DEGREES
Block Parameters: Subsystem1
Three Phase AC Data (mask)
Enter RMS Line to Neutral Voltage in Volts and Frequency In Hertz
Parameters
RMS Line to Neutral Voltage in Volts
120
Frequency in Hertz
60
OK
Cancel
Help
Apply
Block Parameters: Subsystem3
Firing Angle (mask)
Enter Firing Angle alfa in radians from 0 to 5pi / 6.
Parameters
Firing angle in radians
pi/(6)
OK
Cancel
Help
Apply
Block Parameters: Subsystem
Load Resistance Data (mask)
Enter the Load Resistance in Ohms per Phase.
Parameters
Enter the per Phase Load Resistance in Ohms
10
OK
Cancel
Help
Apply
Van_max
3 Phase AC W_rad
time
Subsystem1
alfa_ph_A
alfa_ph_B
alfa_ph_C
Subsystem3
SF_A
SF_B
SF_C
SF_GEN
Subsystem2
In1
In2
In3
In4
In5
In6
In7
In8
In9
Out1
Out2
Out3
Out4
Out5
Out6
Out7
Out8
Out9
Out10
Out11
Out12
Subsystem
11.75
Display1
117.5
Display

FIG.6.4(A)

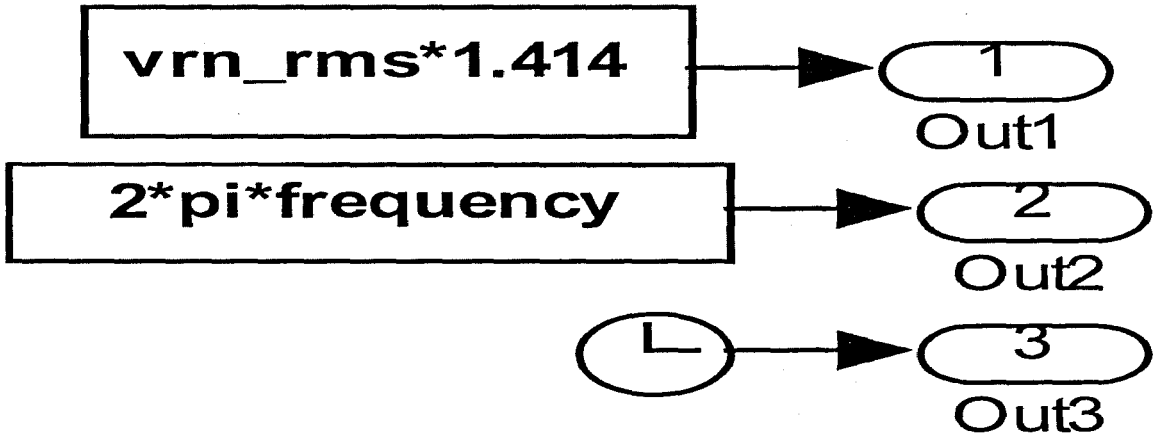

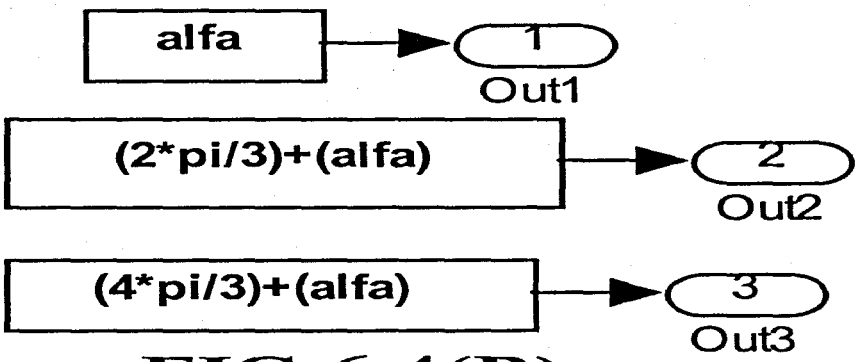

FIG.6.4(B)

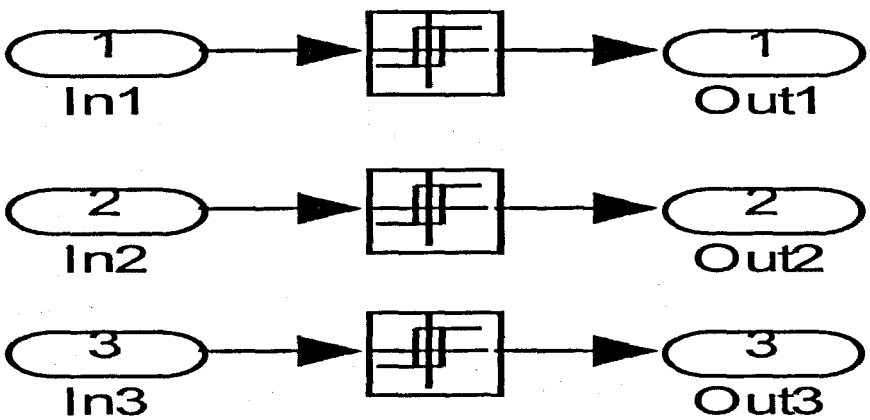

FIG.6.4(C)

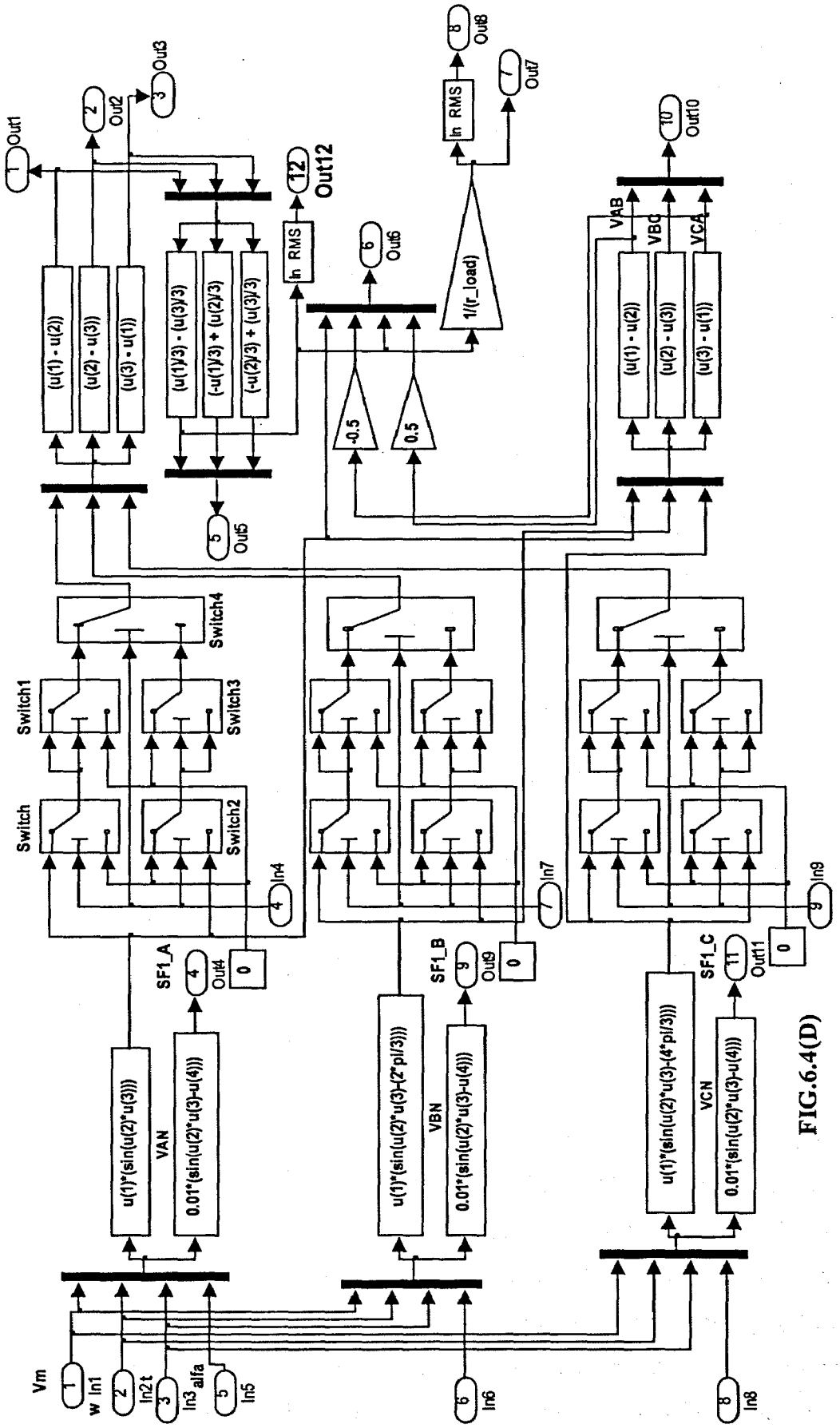
Out1
Out2
Out3
Out4
Out5
Out6
Out7
Out8
Out9
Out10
Out11
Out12
In RMS
In RMS
1/(r_load)
-0.5
0.5
VAB
VBC
VCA
(u(1) - u(2))
(u(2) - u(3))
(u(3) - u(1))
(u(1)/3) - (u(3)/3)
(-u(1)/3) + (u(2)/3)
(-u(2)/3) + (u(3)/3)
Switch
Switch1
Switch2
Switch3
Switch4
In4
In7
In9
SF1_A
SF1_B
SF1_C
VAN
VBN
VCN
u(1)*(sin(u(2)*u(3)))
0.01*(sin(u(2)*u(3)-u(4)))
u(1)*(sin(u(2)*u(3)-(2*pi/3)))
0.01*(sin(u(2)*u(3)-u(4)))
u(1)*(sin(u(2)*u(3)-(4*pi/3)))
0.01*(sin(u(2)*u(3)-u(4)))
Vm
w In1
In2 t
In3 alfa
In5
In6
In8

FIG.6.4(D)

Fig.6.4(A) corresponds to the dialog box Three Phase AC Data in Fig.6.3. In this dialog box, the rms line to neutral voltage in Volts and the frequency in Hertz are entered. The peak voltage Vm and angular frequency ω are internally calculated. Fig.6.4(B) corresponds to the dialog box Firing Angle in Fig.6.3. The firing angle α in radians is entered in this dialog box. Fig.6.4(B) has three constant blocks which generates α, [(2π/3) + α], [(4π/3) + α] for the three phases. Fig.6.4(C) generates the switch function SF for the three phases. The Switch Function corresponds to the Firing Pulses for the back to back connected thyristors in the three phases. These Switch Functions SF_A, SF_B and SF_C in Fig.6.4(C) are defined below:

$$\left.\begin{aligned} SF\_A &= +1 \quad for \quad \alpha \le \omega t \le (\pi + \alpha) \\ &= -1 \quad for \quad (\pi + \alpha) \le \omega t \le (2\pi + \alpha) \\ SF\_B &= +1 \quad for \quad \left(\frac{2\pi}{3} + \alpha\right) \le \omega t \le \left(\frac{5\pi}{3} + \alpha\right) \\ &= -1 \quad for \quad \left(\frac{5\pi}{3} + \alpha\right) \le \omega t \le \left(\frac{8\pi}{3} + \alpha\right) \\ SF\_C &= +1 \quad for \quad \left(\frac{4\pi}{3} + \alpha\right) \le \omega t \le \left(\frac{7\pi}{3} + \alpha\right) \\ &= -1 \quad for \quad \left(\frac{7\pi}{3} + \alpha\right) \le \omega t \le \left(\frac{10\pi}{3} + \alpha\right) \end{aligned}\right\} \qquad (6.6)$$

The dialog box Load Resistance Data in Fig.6.3 corresponds to Fig.6.4(D). The load resistance value in Ohms per phase is entered in this dialog box. Fig.6.4(D) corresponds to the model of the back to back connected thyristors in the three phases and the star connected resistive load. The development of this model in Fig.6.4(D) is given below:

Referring to the top most four input MUX corresponding to Phase A, the inputs u(1) to u(4) are respectively peak line to neutral voltage Vm ($\sqrt{2}$.Vs), supply angular frequency ω, time t and firing angle α. The Fcn block at the top marked VAN generates v_{AN} given by equation 6.1. while the bottom Fcn block generates an attenuated value of v_{AN} lagging by the firing angle α. The two Fcn blocks corresponding to Phase B and C respectively generates v_{BN} given by equation 6.1 and attenuated v_{BN} lagging by [(2.π /3) + α], v_{CN} given by equation 6.1 and attenuated v_{CN} lagging by [(4.π /3) + α]. The bottom MUX output of each phase marked SF1_A, SF1_B and SF1_C in Fig.6.4(D) are

given as input In1, In2 and In3 to the three Relays in Fig.6.4(C). All these three Relays output 1, when the respective input crosses zero and goes positive and output -1, when the respective input crosses zero and goes negative.

Considering Phase A for clarity, SF1_A is given as u(2) input to threshold switches marked Switch and switch2 in Fig.6.4(D). The VAN output of Fcn block is given as u(1) input to Switch and u(3) input to Switch2. Zero is given to u(3) input of Switch and u(1) input to Switch2. The output of Switch is given to u(1) and u(2) input of Switch1 and its u(3) input is zero. The Switch2 output is given to u(2) and u(3) input of Switch3 and its u(1) input is zero. The output of Switch 1 and Switch3 are given as u(1) and u(3) input to Switch4 and its u(2) input is SF_A. The Switch, Switch1, Switch2, Switch3 and Switch4 all have a threshold value of zero and all these switches output corresponds to u(1) when u(2) is greater than or equal to zero, else all these switch output corresponds to u(3) input. The threshold switches corresponding to Phase B and Phase C operate in the same principle as for Phase A.

Referring to threshold switches in Phase A shown in Fig.6.4(D) and noting the definition of SF_A in equation 6.6, the output of various threshold switches can be explained as follows:

The 'Switch' and Switch2 has the following output given by equation 6.7 and 6.8 respectively.

$$Switch \quad output = +Vm\sin(\omega t) \quad for \quad \alpha \le \omega t \le (\pi + \alpha)$$
$$= 0 \quad for \ other \ time \ intervals \qquad (6.7)$$

$$Switch2 \quad output = -Vm\sin(\omega t) \quad for \quad (\pi + \alpha) \le \omega t \le (2\pi + \alpha)$$
$$= 0 \quad for \ other \ time \ intervals \qquad (6.8)$$

Switch1 and Switch3 has the following output given by equations 6.9 and 6.10 respectively:

$$\begin{aligned} Switch1 \quad output &= +Vm\sin(\omega t) \quad for \quad \alpha \le \omega t \le \pi \\ &= 0 \quad for \ other \ time \ intervals \end{aligned} \qquad (6.9)$$

$$\begin{aligned} Switch3 \quad output &= -Vm\sin(\omega t) \quad for \quad (\pi+\alpha) \le \omega t \le 2\pi \\ &= 0 \quad for \ other \ time \ intervals \end{aligned} \qquad (6.10)$$

Switch4 has the following output given by equation 6.11 below:

$$\begin{aligned} Switch4 \quad output &= +Vm\sin(\omega t) \quad for \quad \alpha \le \omega t \le \pi \\ &= -Vm\sin(\omega t) \quad for \quad (\pi+\alpha) \le \omega t \le 2\pi \\ &= 0 \quad for \ other \ time \ intervals \end{aligned} \qquad (6.11)$$

The Switch4 output of Phase A and the corresponding Switch output of Phase B and Phase C are connected to a three input MUX as shown in Fig.6.4(D). The three Fcn blocks calculate the three phase line to line voltage across the star connected resistive load using the following formula:

$$\begin{bmatrix} v_{L1L2} \\ v_{L2L3} \\ v_{L3L1} \end{bmatrix} = \begin{bmatrix} 1 & -1 & 0 \\ 0 & 1 & -1 \\ -1 & 0 & 1 \end{bmatrix} * \begin{bmatrix} v_{L1N} \\ v_{L2N} \\ v_{L3N} \end{bmatrix} = \begin{bmatrix} u(1)-u(2) \\ u(2)-u(3) \\ u(3)-u(1) \end{bmatrix} \qquad (6.12)$$

In equations 6.12, L1, L2, L3 and N corresponds to the terminals as marked in Fig.6.1. In Fig.6.4(D) out1, out2 and out3 corresponds to these line to line voltages across the star connected load. These three voltages are given to another set of three input MUX as shown in Fig.6.4(D). The three Fcn blocks connected to this MUX calculates the line to neutral voltages across the star connected resistive load using the following formula:

$$\begin{bmatrix} v_{L1n} \\ v_{L2n} \\ v_{L3n} \end{bmatrix} = \begin{bmatrix} \frac{1}{3} & 0 & \frac{-1}{3} \\ \frac{-1}{3} & \frac{1}{3} & 0 \\ 0 & \frac{-1}{3} & \frac{1}{3} \end{bmatrix} * \begin{bmatrix} v_{L1L2} \\ v_{L2L3} \\ v_{L3L1} \end{bmatrix} = \begin{bmatrix} \frac{u(1)}{3} - \frac{u(3)}{3} \\ \frac{-u(1)}{3} + \frac{u(2)}{3} \\ \frac{-u(2)}{3} + \frac{u(3)}{3} \end{bmatrix} \qquad (6.13)$$

In equation 6.13, n is the load neutral point as shown in Fig.6.1. The line to neutral voltage v_{L1n} is multiplied by 1/(r_load) to get the load current through each of the resistors.

6.2.2 Simulation Results

The simulation of the Fully Controlled three phase AC controller with star connected load and with the neutral isolated was carried out using ode15s(stiff/NDF) solver, for various firing angle α of π /6, π /4, π /3, π /2 and 2.π /3. The data used for this controller is given in Table 6.1 [14]. The simulation results for firing angle α of π /6, π /4, π /3, π /2 and 2.π /3 are shown from Fig.6.5 to Fig.6.19. The names of the various waveforms are given at the top of each simulation result. The results of RMS line to neutral voltage across the load and load current for a firing angle α of π /6 are displayed in Fig.6.2. The simulation results for various firing angle α are tabulated in Table 6.2. The RMS line to neutral voltage across resistive load calculated by using equation 6.3 to 6.5 and also the RMS load current by calculation are given in Table 6.3.

TABLE 6.1 – Data for Three Phase Controller with Star connected Resistive Load

Sl.No.	Line to Neutral Voltage in Volts	Frequency Hertz	Firing Angle α radians	Per Phase Load Resistance in Ohms
1	120	60	π / 6	10
2	120	60	π / 4	10
3	120	60	π / 3	10
4	120	60	π / 2	10
5	120	60	2 π / 3	10

TABLE 6.2 – Simulation Results for Three Phase Controller with Star connected Resistive Load

Sl.No.	Line to Neutral Voltage in Volts	Frequency Hertz	Firing Angle α radians	Per Phase Load Resistance in Ohms	RMS Line to Neutral Load Voltage in Volts	RMS Load Current in Amps
1	120	60	π / 6	10	117.7	11.77
2	120	60	π / 4	10	112.4	11.24
3	120	60	π / 3	10	103.2	10.32
4	120	60	π / 2	10	74.84	7.484
5	120	60	2 π / 3	10	43.18	4.318

TABLE 6.3 –Calculated Values for Three Phase Controller with Star connected Resistive Load

Sl.No.	Line to Neutral Voltage in Volts	Frequency Hertz	Firing Angle α radians	Per Phase Load Resistance in Ohms	RMS Line to Neutral Load Voltage in Volts	RMS Load Current in Amps
1	120	60	π / 6	10	117.38	11.738
2	120	60	π / 4	10	111.53	11.153
3	120	60	π / 3	10	100.88	10.088
4	120	60	π / 2	10	64.97	6.497
5	120	60	2 π / 3	10	35.22	2.511

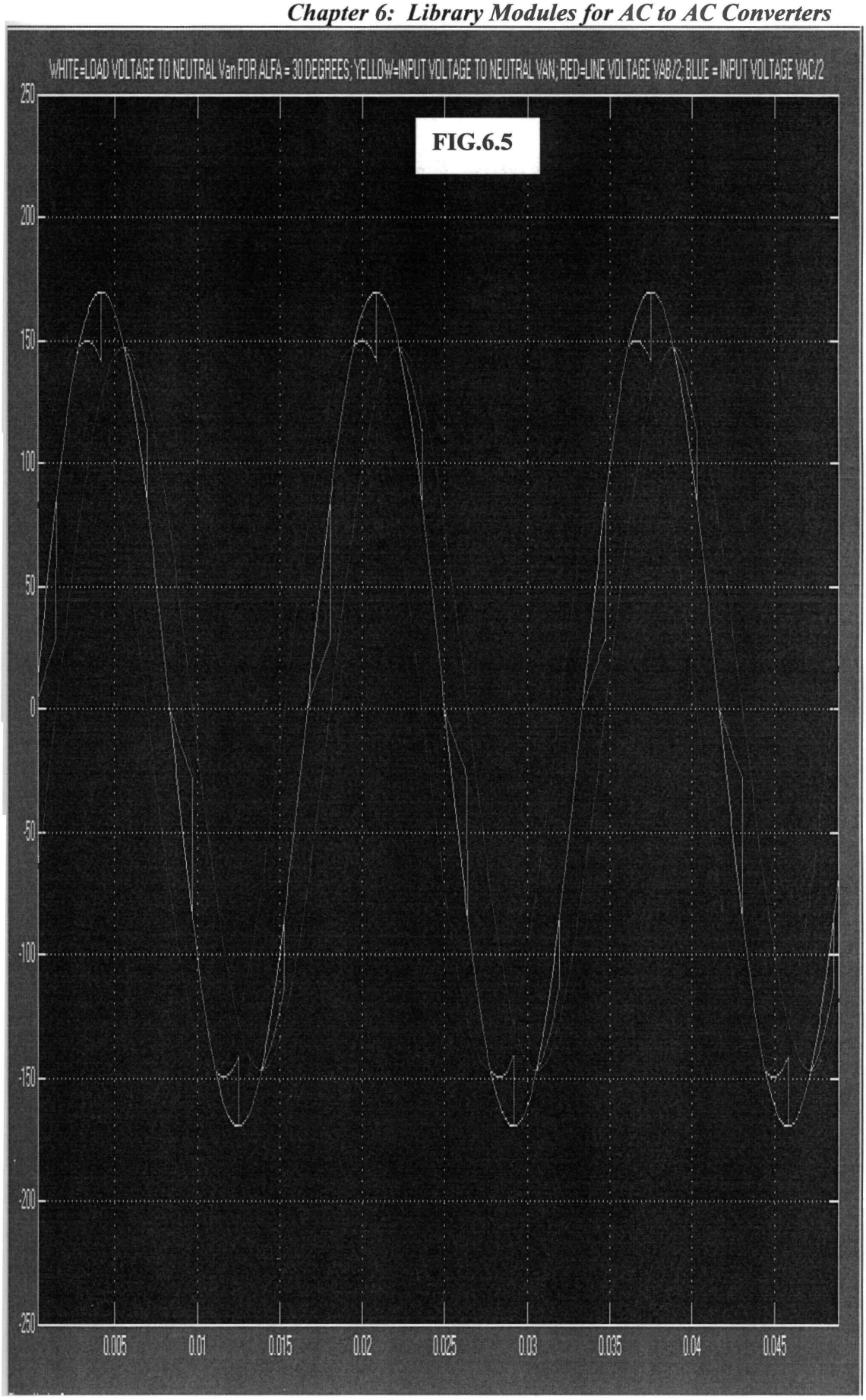
WHITE=LOAD VOLTAGE TO NEUTRAL Van FOR ALFA = 30 DEGREES; YELLOW=INPUT VOLTAGE TO NEUTRAL VAN; RED=LINE VOLTAGE VAB/2; BLUE = INPUT VOLTAGE VAC/2
250
200
150
100
50
0
-50
-100
-150
-200
-250
0.005
0.01
0.015
0.02
0.025
0.03
0.035
0.04
0.045

FIG.6.5

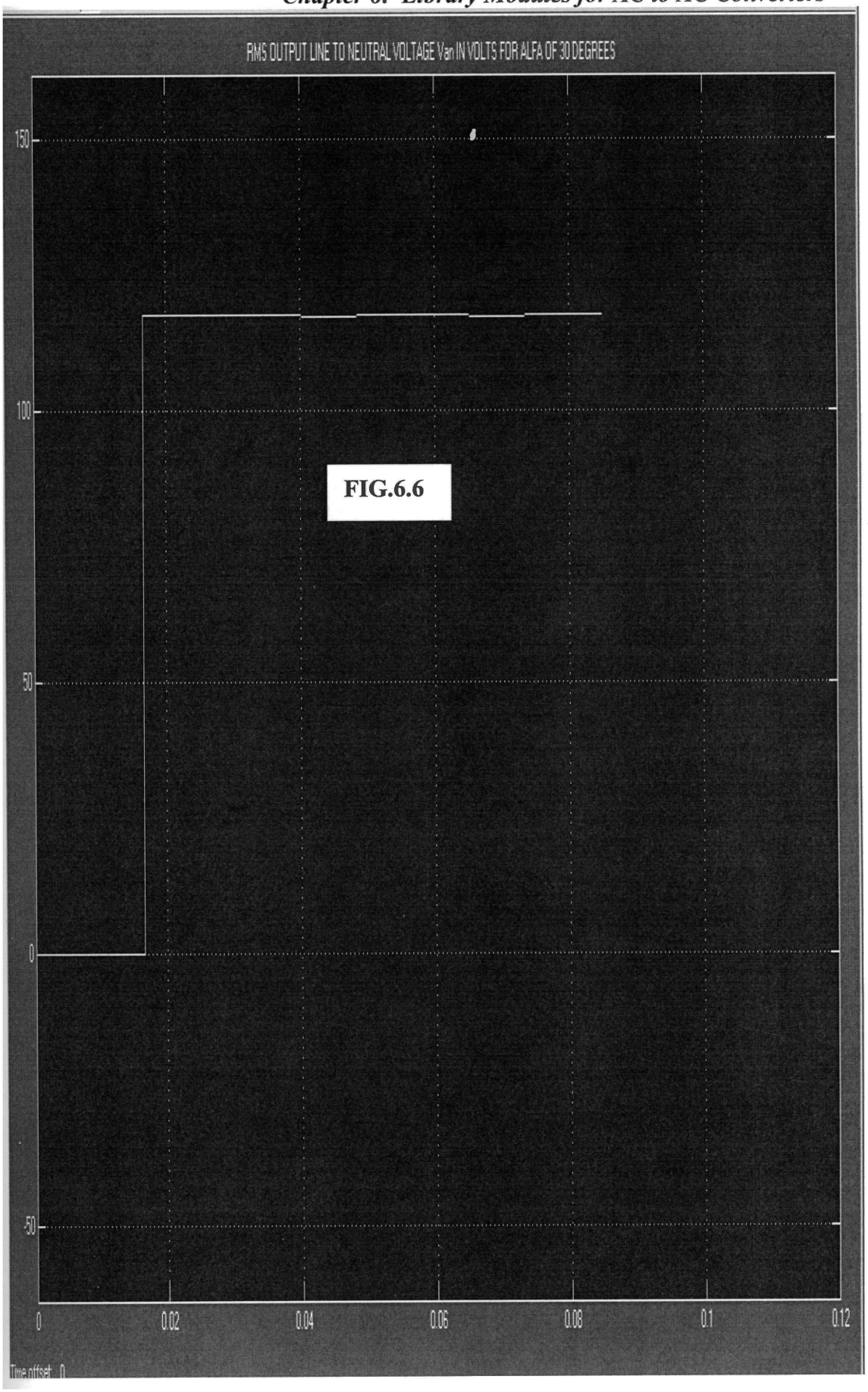
RMS OUTPUT LINE TO NEUTRAL VOLTAGE Van IN VOLTS FOR ALFA OF 30 DEGREES
150
100
50
0
-50
0
0.02
0.04
0.06
0.08
0.1
0.12
Time offset: 0

FIG.6.6

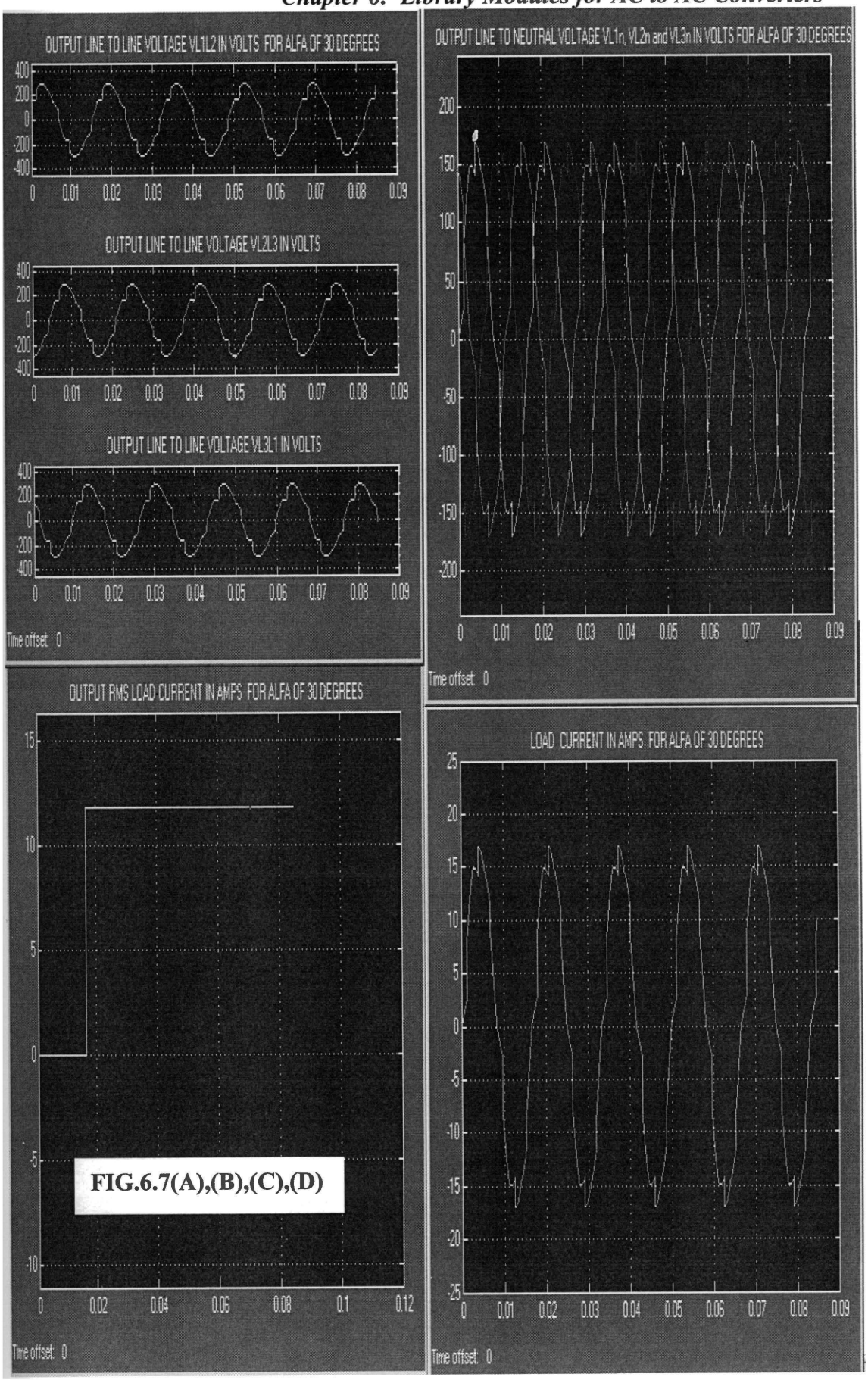
OUTPUT LINE TO LINE VOLTAGE VL1L2 IN VOLTS FOR ALFA OF 30 DEGREES
OUTPUT LINE TO LINE VOLTAGE VL2L3 IN VOLTS
OUTPUT LINE TO LINE VOLTAGE VL3L1 IN VOLTS
Time offset: 0
OUTPUT LINE TO NEUTRAL VOLTAGE VL1n, VL2n and VL3n IN VOLTS FOR ALFA OF 30 DEGREES
Time offset: 0
OUTPUT RMS LOAD CURRENT IN AMPS FOR ALFA OF 30 DEGREES
Time offset: 0
LOAD CURRENT IN AMPS FOR ALFA OF 30 DEGREES
Time offset: 0

FIG.6.7(A),(B),(C),(D)

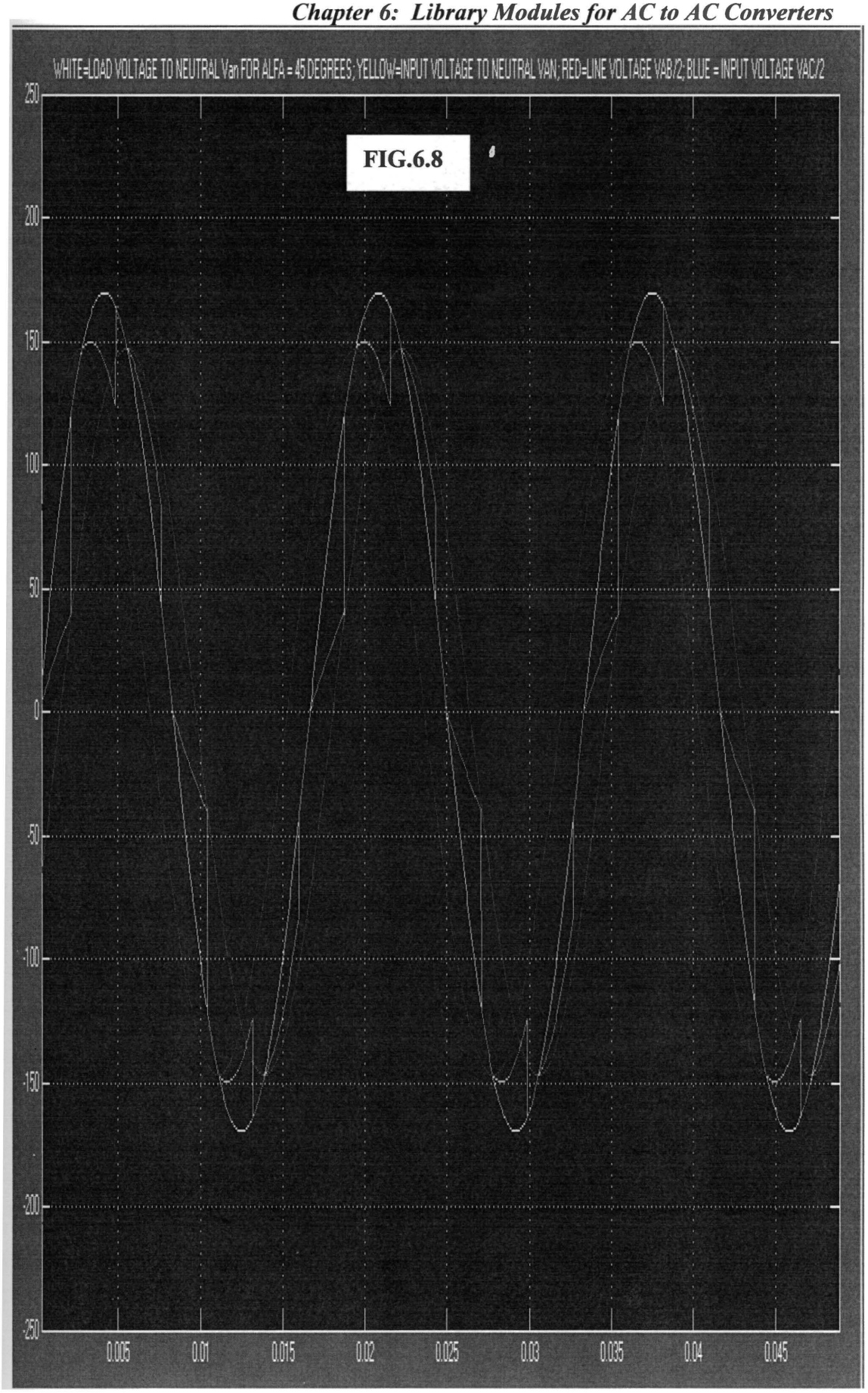
WHITE=LOAD VOLTAGE TO NEUTRAL Van FOR ALFA = 45 DEGREES; YELLOW=INPUT VOLTAGE TO NEUTRAL VAN; RED=LINE VOLTAGE VAB/2; BLUE = INPUT VOLTAGE VAC/2
250
200
150
100
50
0
-50
-100
-150
-200
-250
0.005
0.01
0.015
0.02
0.025
0.03
0.035
0.04
0.045

FIG.6.8

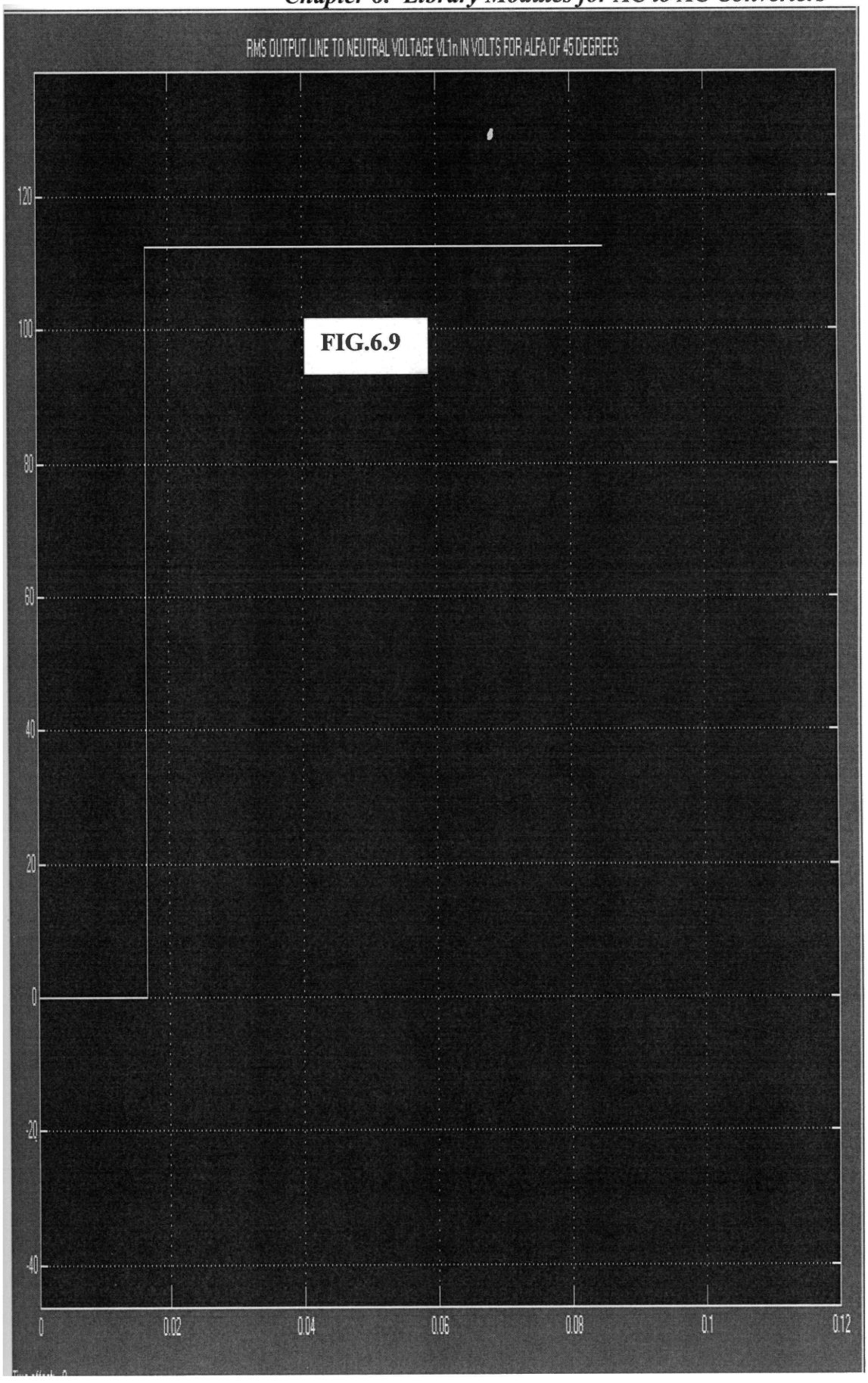
RMS OUTPUT LINE TO NEUTRAL VOLTAGE VL1n IN VOLTS FOR ALFA OF 45 DEGREES
120
100
80
60
40
20
0
-20
-40
0
0.02
0.04
0.06
0.08
0.1
0.12

FIG.6.9

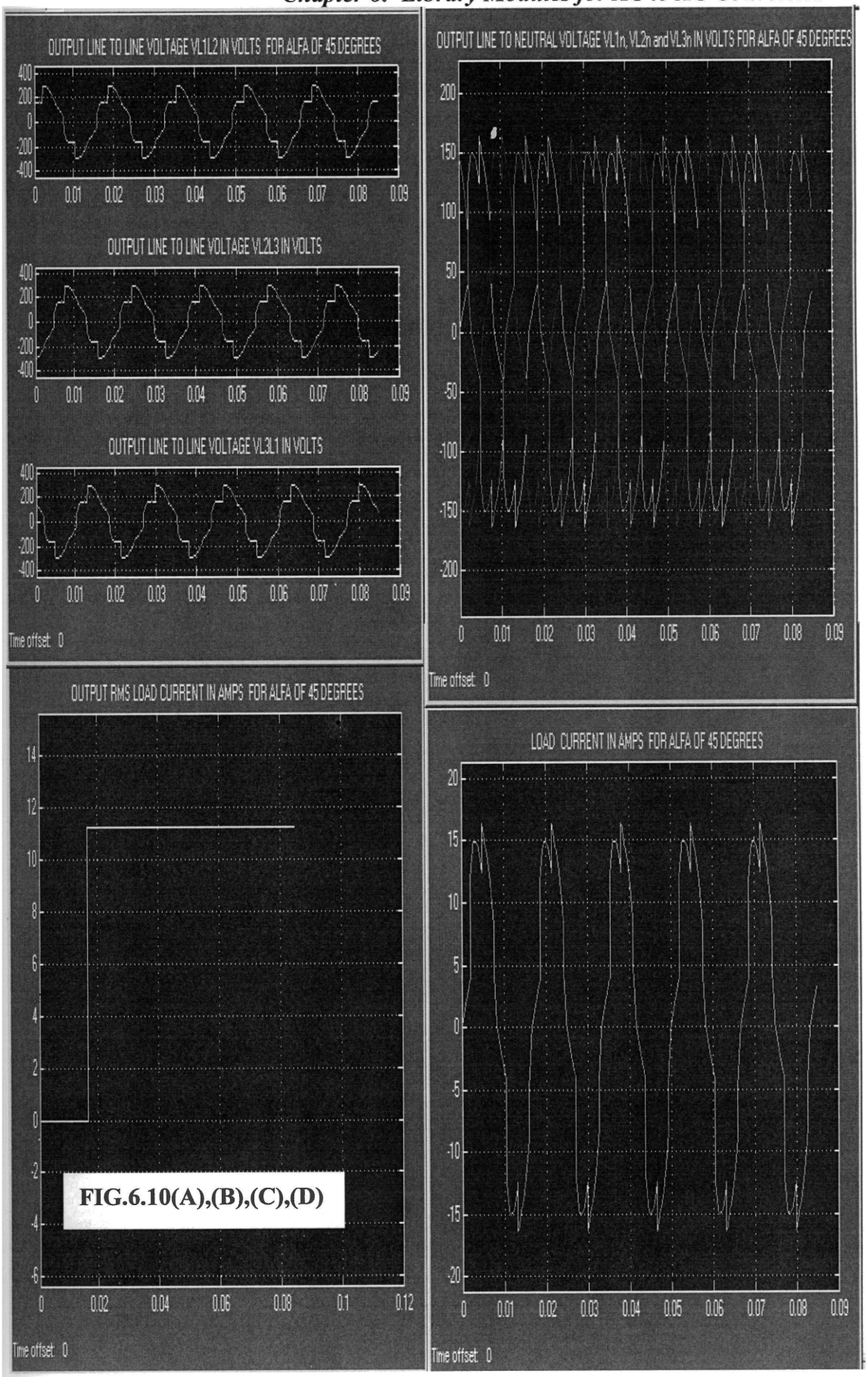
OUTPUT LINE TO LINE VOLTAGE VL1L2 IN VOLTS FOR ALFA OF 45 DEGREES
OUTPUT LINE TO LINE VOLTAGE VL2L3 IN VOLTS
OUTPUT LINE TO LINE VOLTAGE VL3L1 IN VOLTS
Time offset: 0
OUTPUT LINE TO NEUTRAL VOLTAGE VL1n, VL2n and VL3n IN VOLTS FOR ALFA OF 45 DEGREES
Time offset: 0
OUTPUT RMS LOAD CURRENT IN AMPS FOR ALFA OF 45 DEGREES
Time offset: 0
LOAD CURRENT IN AMPS FOR ALFA OF 45 DEGREES
Time offset: 0

FIG.6.10(A),(B),(C),(D)

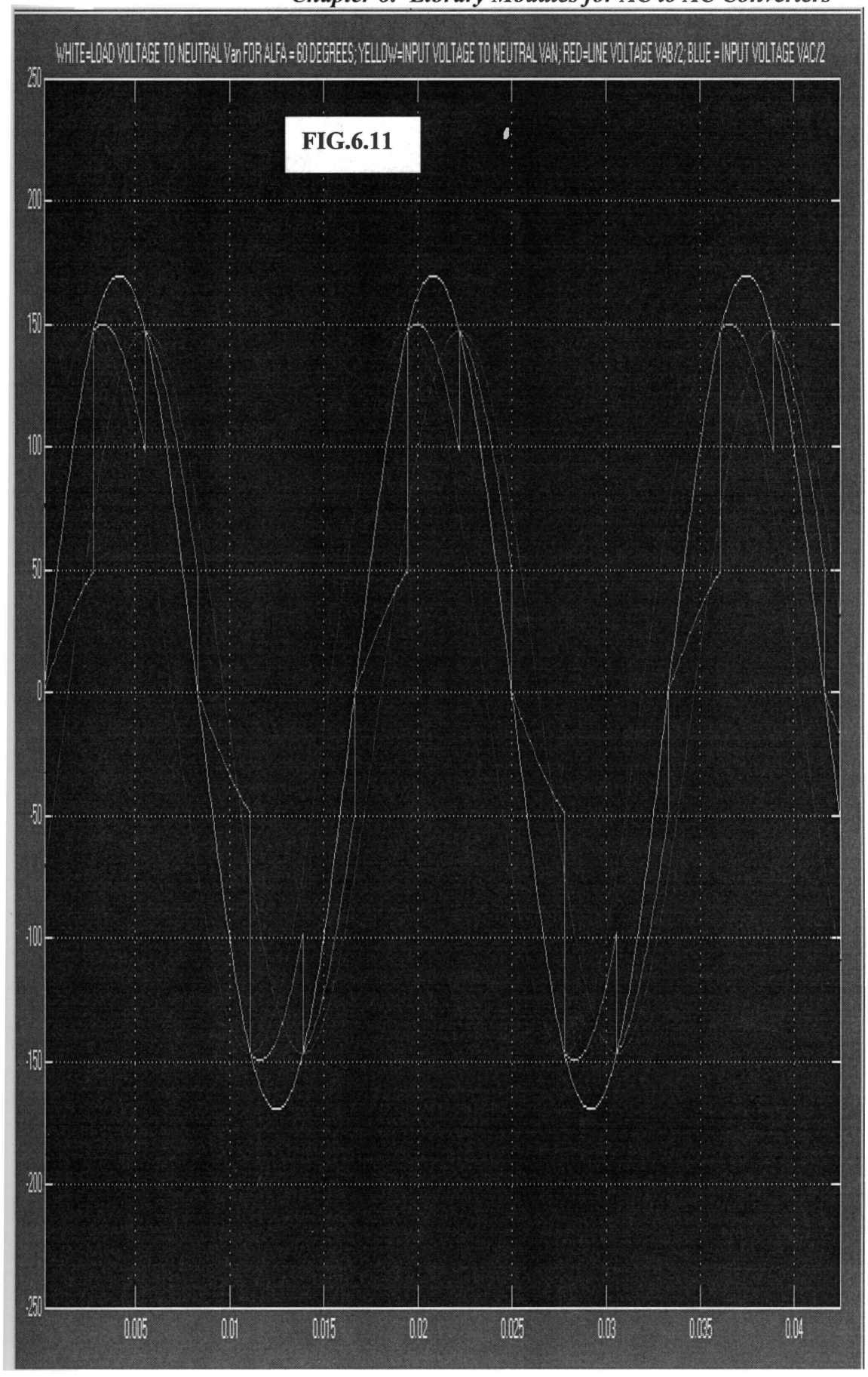
WHITE=LOAD VOLTAGE TO NEUTRAL Van FOR ALFA = 60 DEGREES; YELLOW=INPUT VOLTAGE TO NEUTRAL VAN; RED=LINE VOLTAGE VAB/2; BLUE = INPUT VOLTAGE VAC/2
250
200
150
100
50
0
-50
-100
-150
-200
-250
0.005
0.01
0.015
0.02
0.025
0.03
0.035
0.04

FIG.6.11

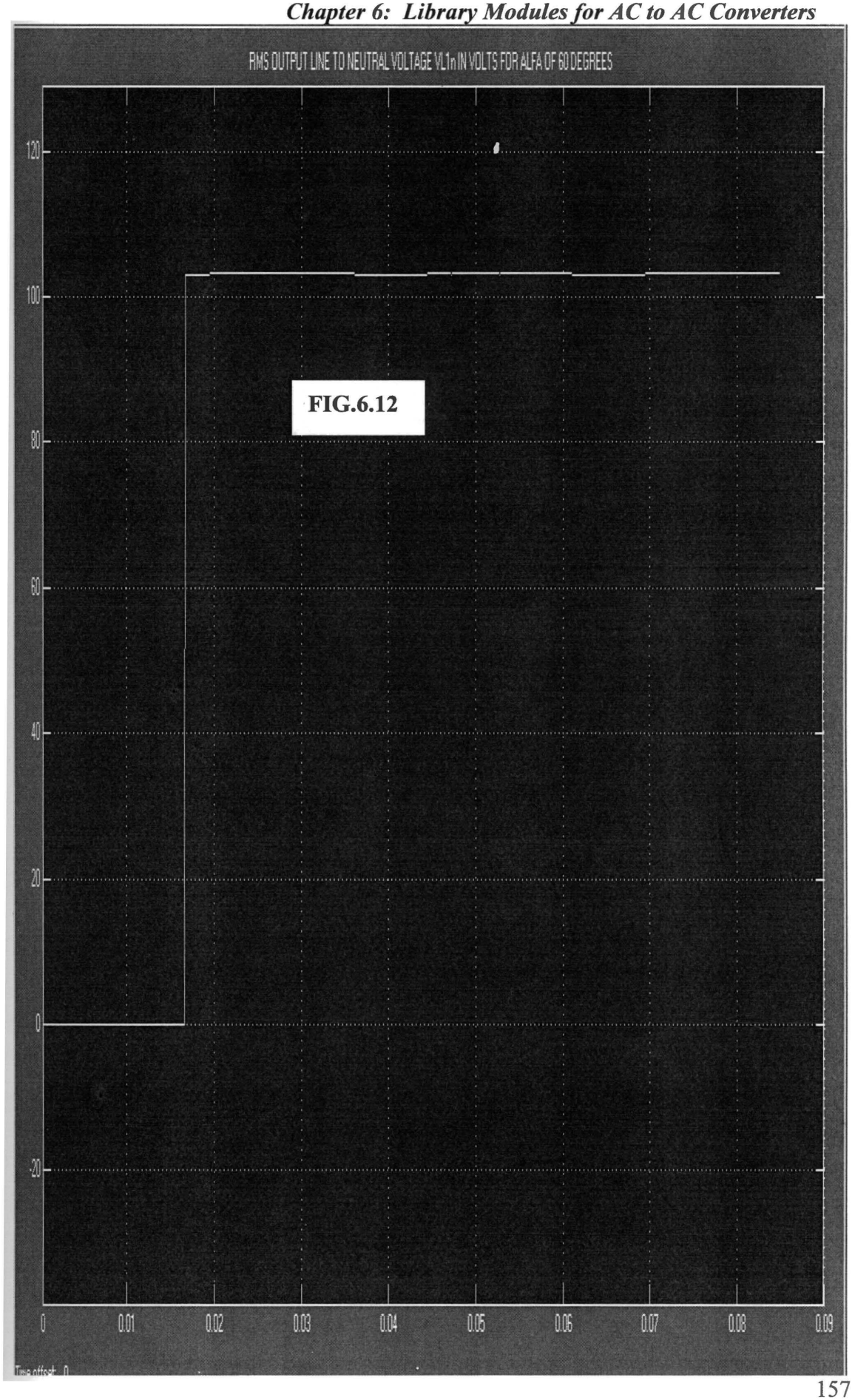
RMS OUTPUT LINE TO NEUTRAL VOLTAGE VL1n IN VOLTS FOR ALFA OF 60 DEGREES
120
100
80
60
40
20
0
-20
0
0.01
0.02
0.03
0.04
0.05
0.06
0.07
0.08
0.09
Time offset: 0

FIG.6.12

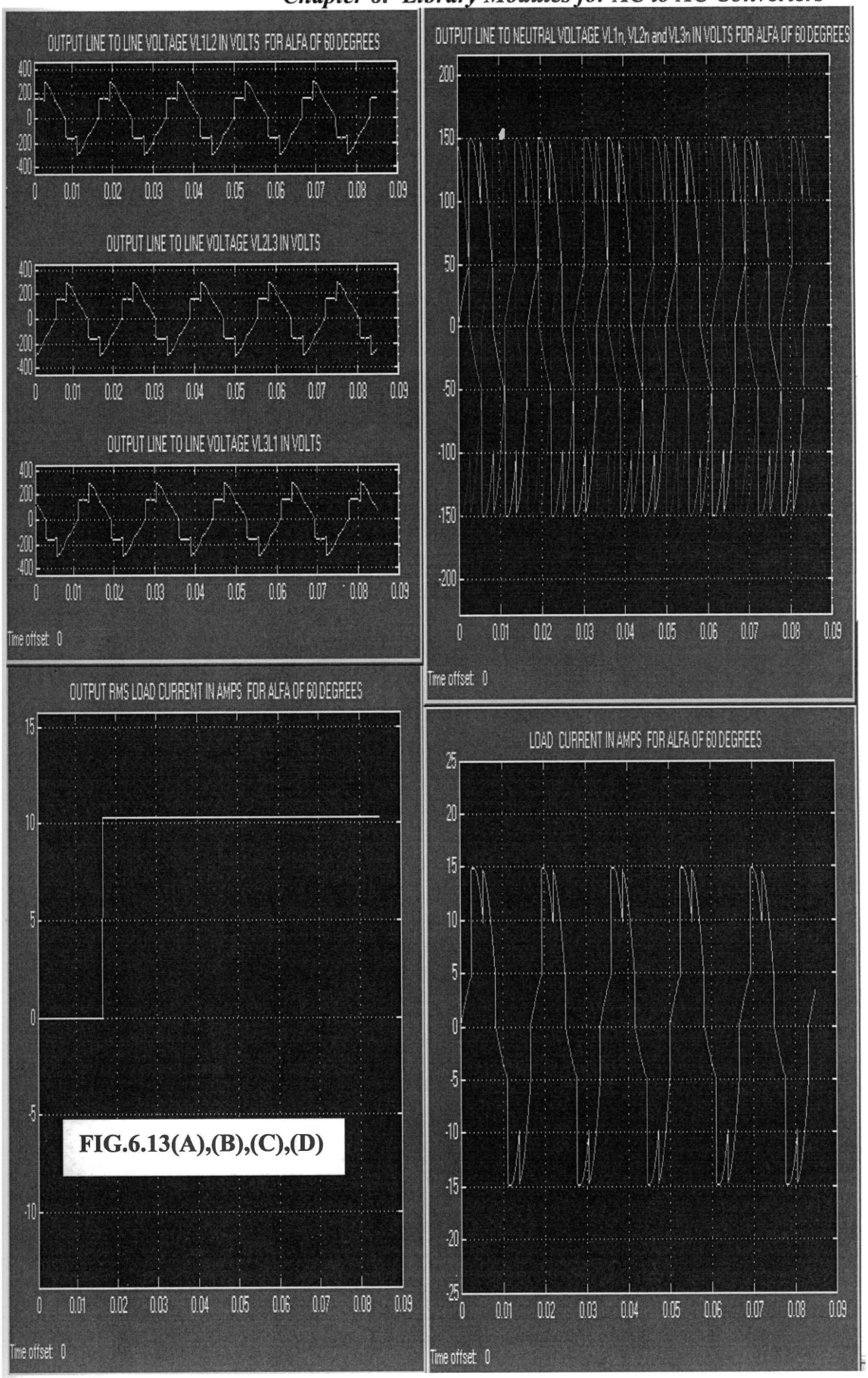
OUTPUT LINE TO LINE VOLTAGE VL1L2 IN VOLTS FOR ALFA OF 60 DEGREES
OUTPUT LINE TO LINE VOLTAGE VL2L3 IN VOLTS
OUTPUT LINE TO LINE VOLTAGE VL3L1 IN VOLTS
Time offset: 0
OUTPUT LINE TO NEUTRAL VOLTAGE VL1n, VL2n and VL3n IN VOLTS FOR ALFA OF 60 DEGREES
Time offset: 0
OUTPUT RMS LOAD CURRENT IN AMPS FOR ALFA OF 60 DEGREES
Time offset: 0
LOAD CURRENT IN AMPS FOR ALFA OF 60 DEGREES
Time offset: 0

FIG.6.13(A),(B),(C),(D)

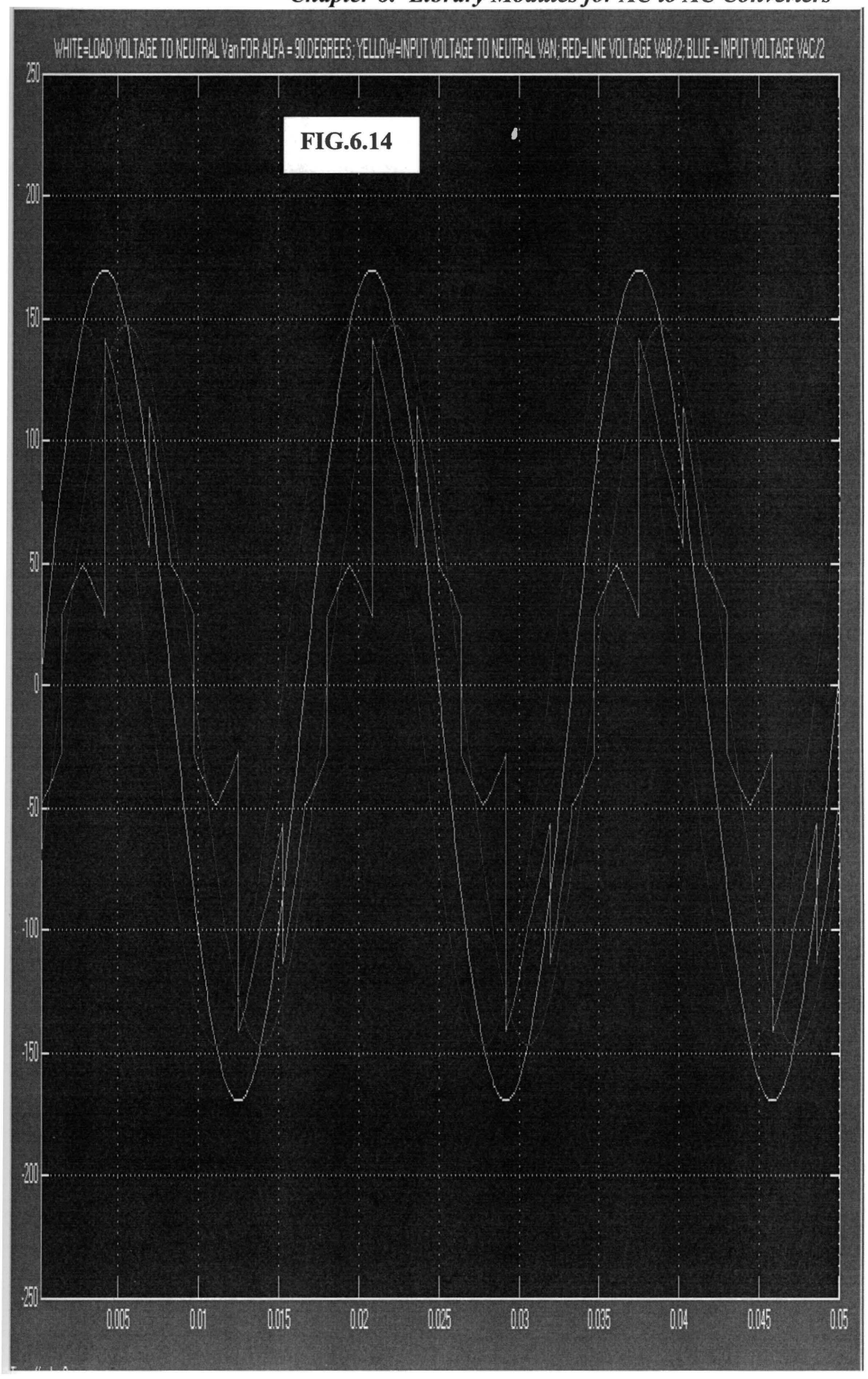
WHITE=LOAD VOLTAGE TO NEUTRAL Van FOR ALFA = 90 DEGREES; YELLOW=INPUT VOLTAGE TO NEUTRAL VAN; RED=LINE VOLTAGE VAB/2; BLUE = INPUT VOLTAGE VAC/2
250
200
150
100
50
0
-50
-100
-150
-200
-250
0.005
0.01
0.015
0.02
0.025
0.03
0.035
0.04
0.045
0.05

FIG.6.14

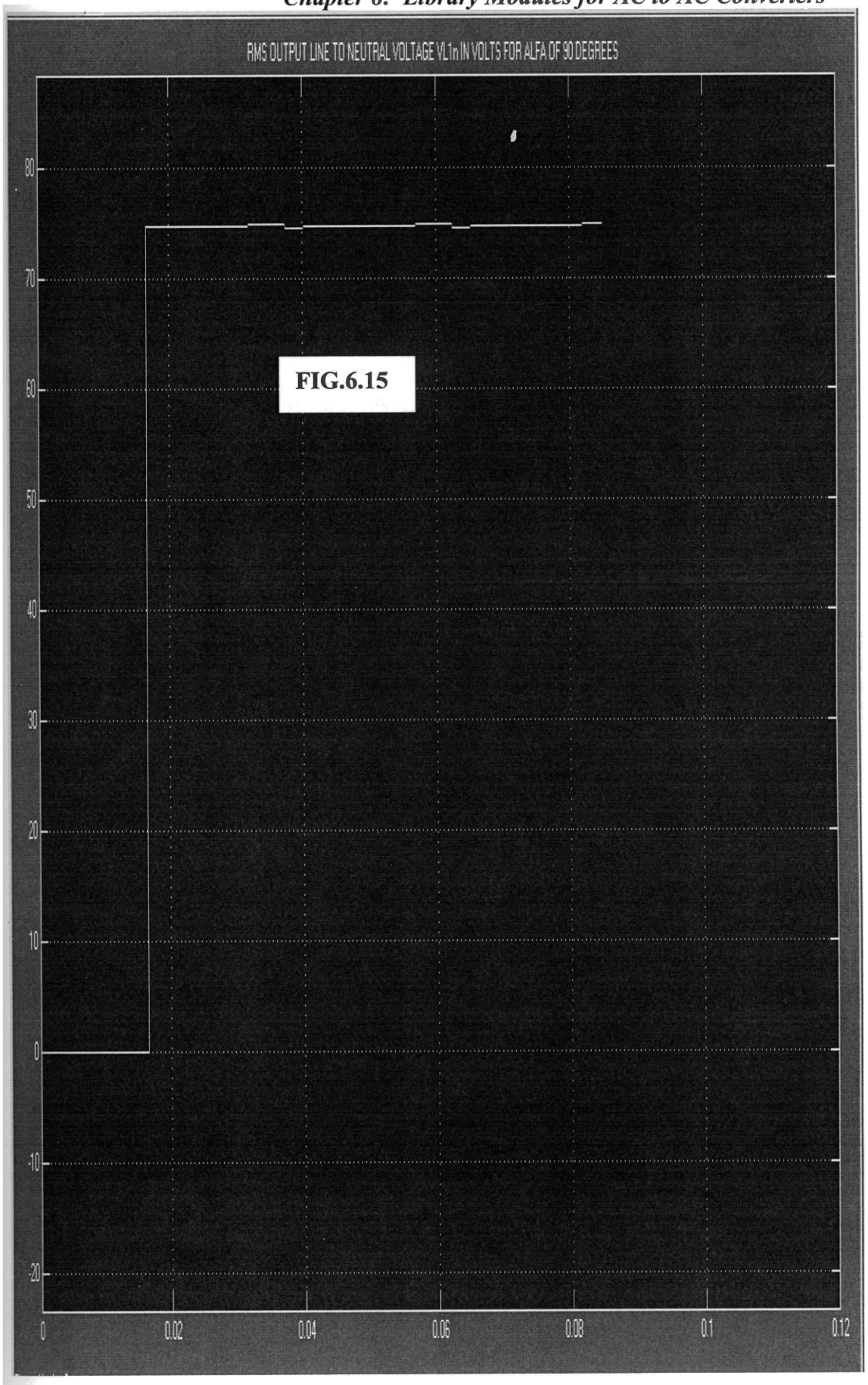
RMS OUTPUT LINE TO NEUTRAL VOLTAGE VL1n IN VOLTS FOR ALFA OF 90 DEGREES
80
70
60
50
40
30
20
10
0
-10
-20
0
0.02
0.04
0.06
0.08
0.1
0.12

FIG.6.15

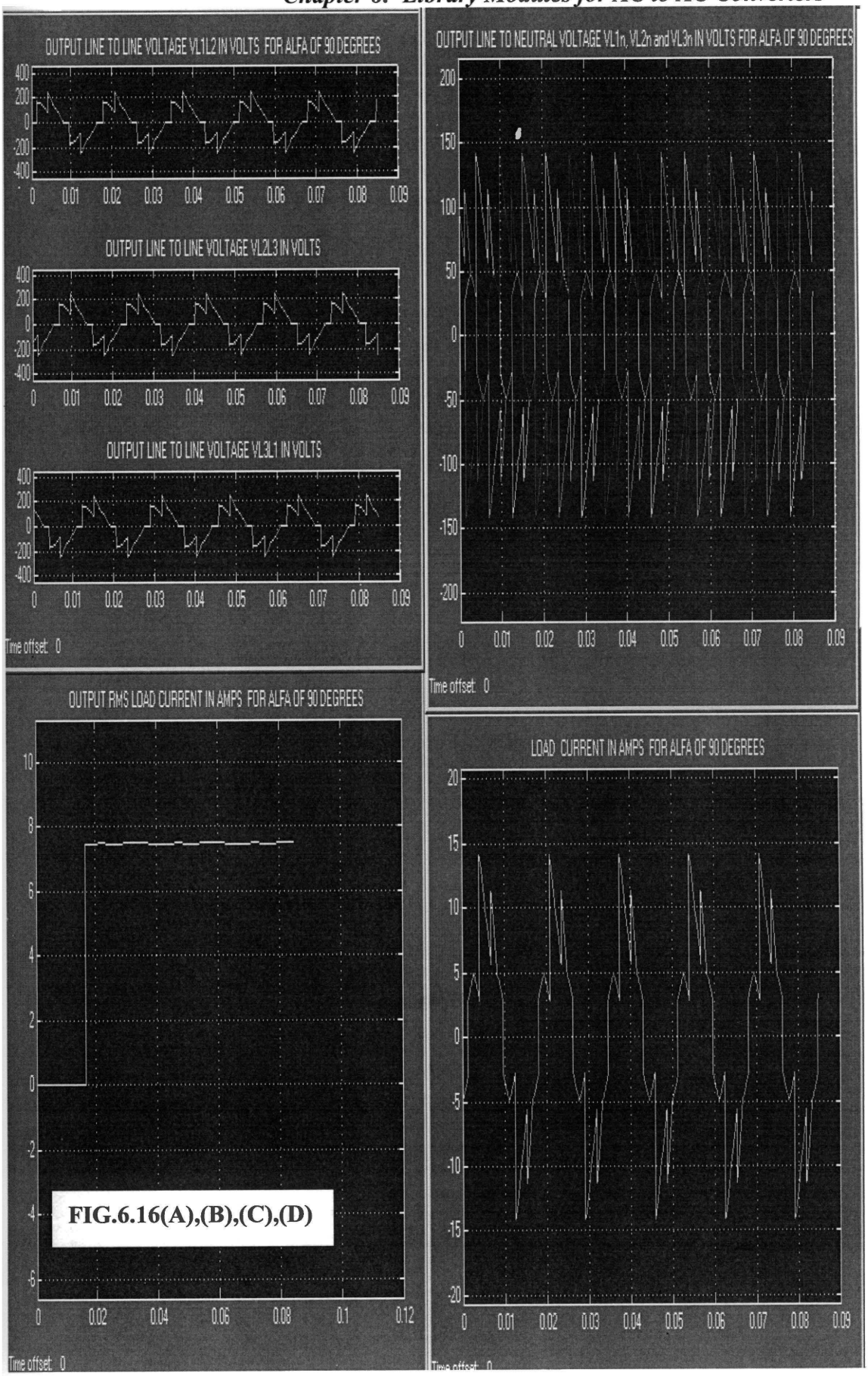
OUTPUT LINE TO LINE VOLTAGE VL1L2 IN VOLTS FOR ALFA OF 90 DEGREES
OUTPUT LINE TO LINE VOLTAGE VL2L3 IN VOLTS
OUTPUT LINE TO LINE VOLTAGE VL3L1 IN VOLTS
Time offset: 0
OUTPUT LINE TO NEUTRAL VOLTAGE VL1n, VL2n and VL3n IN VOLTS FOR ALFA OF 90 DEGREES
Time offset: 0
OUTPUT RMS LOAD CURRENT IN AMPS FOR ALFA OF 90 DEGREES
Time offset: 0
LOAD CURRENT IN AMPS FOR ALFA OF 90 DEGREES

FIG.6.16(A),(B),(C),(D)

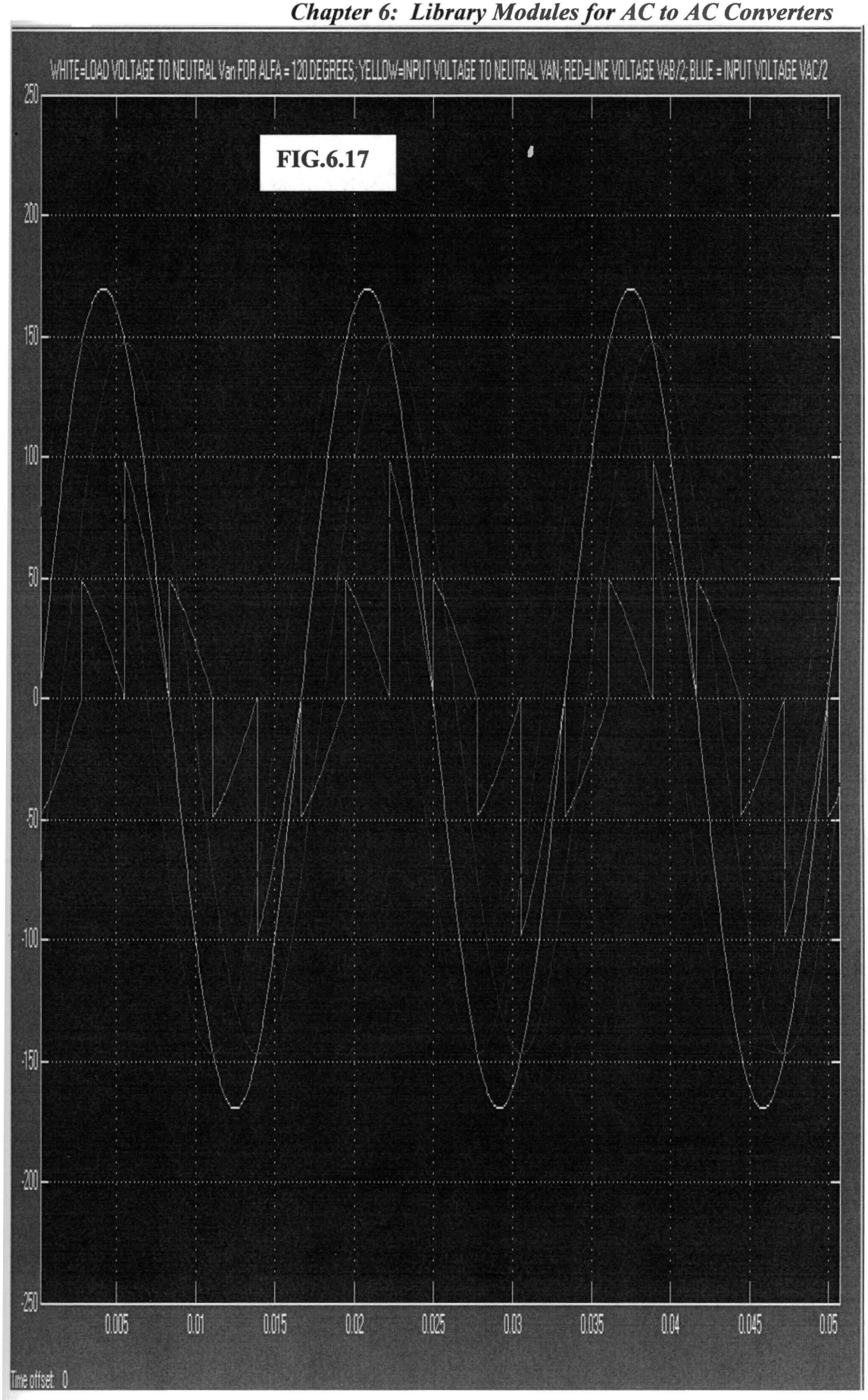
WHITE=LOAD VOLTAGE TO NEUTRAL Van FOR ALFA = 120 DEGREES; YELLOW=INPUT VOLTAGE TO NEUTRAL VAN; RED=LINE VOLTAGE VAB/2; BLUE = INPUT VOLTAGE VAC/2
250
200
150
100
50
0
-50
-100
-150
-200
-250
0.005
0.01
0.015
0.02
0.025
0.03
0.035
0.04
0.045
0.05
Time offset: 0

FIG.6.17

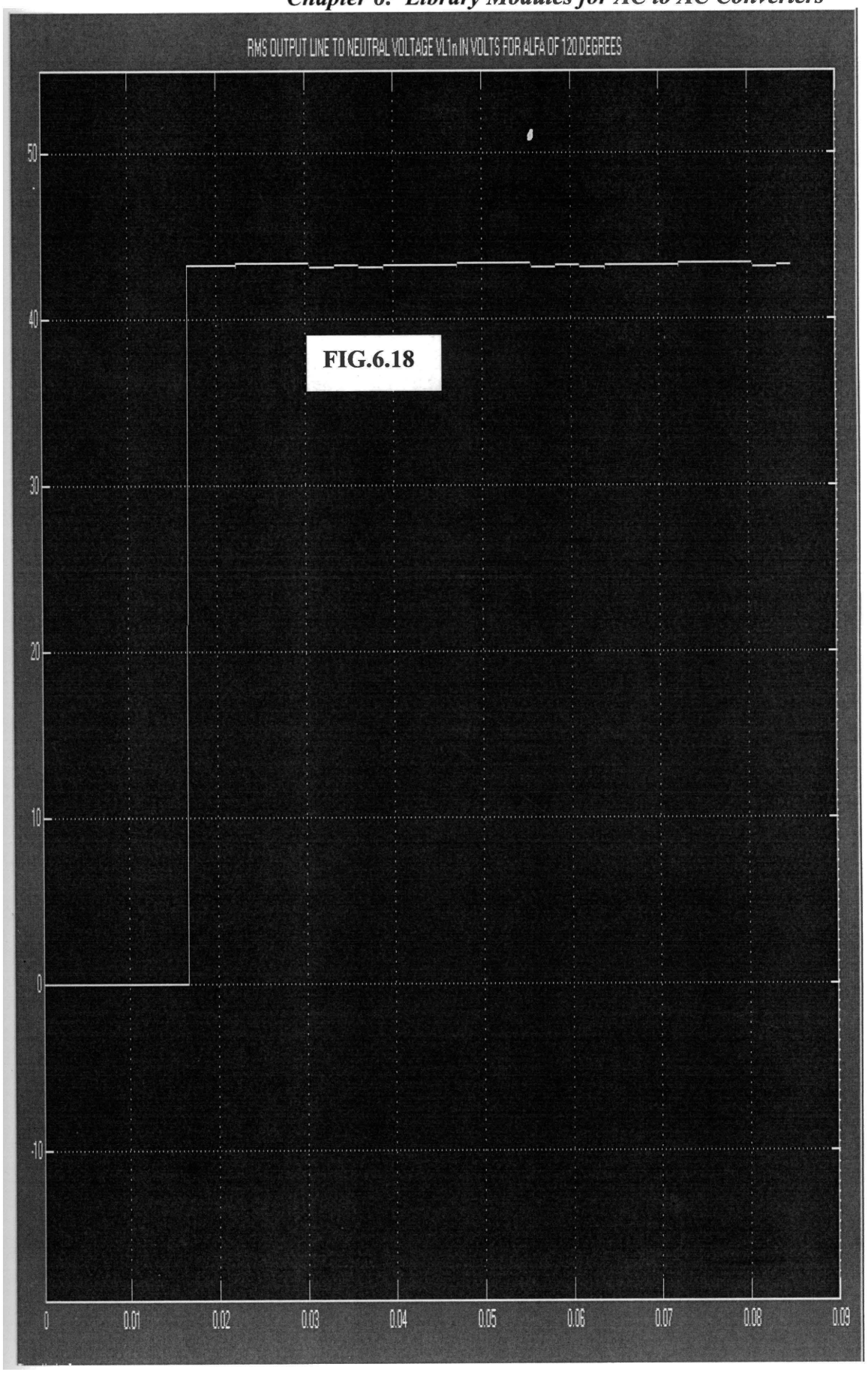
RMS OUTPUT LINE TO NEUTRAL VOLTAGE VL1n IN VOLTS FOR ALFA OF 120 DEGREES
50
40
30
20
10
0
-10
0
0.01
0.02
0.03
0.04
0.05
0.06
0.07
0.08
0.09

FIG.6.18

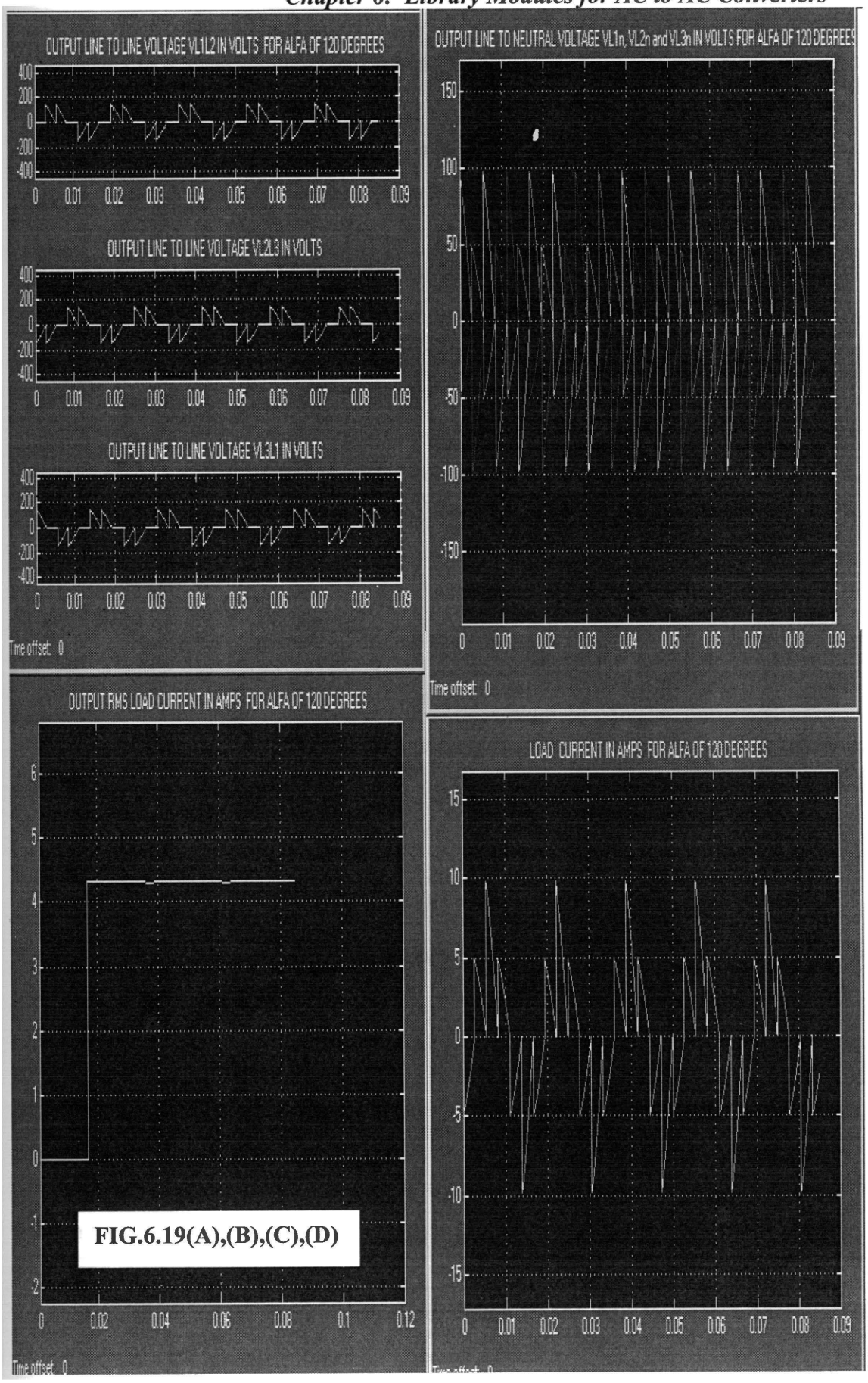
OUTPUT LINE TO LINE VOLTAGE VL1L2 IN VOLTS FOR ALFA OF 120 DEGREES
OUTPUT LINE TO LINE VOLTAGE VL2L3 IN VOLTS
OUTPUT LINE TO LINE VOLTAGE VL3L1 IN VOLTS
Time offset: 0
OUTPUT LINE TO NEUTRAL VOLTAGE VL1n, VL2n and VL3n IN VOLTS FOR ALFA OF 120 DEGREES
Time offset: 0
OUTPUT RMS LOAD CURRENT IN AMPS FOR ALFA OF 120 DEGREES
Time offset: 0
LOAD CURRENT IN AMPS FOR ALFA OF 120 DEGREES

FIG.6.19(A),(B),(C),(D)

in Fig.6.2. The values obtained by simulation and that by theoretical calculations using equations 6.3 to 6.5 are tabulated in Table 6.2 and Table 6.3 respectively.

6.3 Analysis of A Fully Controlled Three Phase AC Voltage Controller in Series with Resistive Load Connected in Delta

The three phase three wire AC voltage controller with back to back SCRs in series with resistive load connected in delta is shown in Fig.6.20 [14, 16]. By varying the firing angle α, the rms current through the load can be varied. The firing sequence is T1, T2, T3, T4, T5 and T6. This is derived below:

$$\left.\begin{aligned} v_{AB} &= \sqrt{2}.V_S.\sin(\omega.t) \\ v_{BC} &= \sqrt{2}.V_S.\sin\left(\omega.t - \frac{2\pi}{3}\right) \\ v_{CA} &= \sqrt{2}.V_S.\sin\left(\omega.t + \frac{2\pi}{3}\right) \end{aligned}\right| \qquad (6.14)$$

In equation 6.14, v_{AB}, v_{BC}, v_{CA} are the instantaneous line to line voltages. As the load resistance is in series with the back to back connected SCRs forming a delta configuration , the RMS phase Voltage Vo can be derived as follows, for any firing angle α.

$$V_O = \sqrt{\left[\frac{1}{\pi}\int_{\alpha}^{\pi} 2.V_S^2.\sin^2(\omega t).d(\omega t)\right]}$$

$$= V_S.\sqrt{\left[1 - \frac{\alpha}{\pi} + \frac{\sin(2\alpha)}{2\pi}\right]} \qquad (6.15)$$

The range of firing angle is $0 \le \alpha \le \pi$. In Fig.6.20, i_{ab}, i_{bc} and i_{ca} are the phase currents through the load. Also $i_a = i_{ab} - i_{ca}$, $i_b = i_{bc} - i_{ab}$ and $i_c = i_{ca} - i_{bc}$ are the line currents.

6.3.1 Modelling of A Fully Controlled Three Phase AC Voltage Controller in Series with Resistive Load Connected in Delta

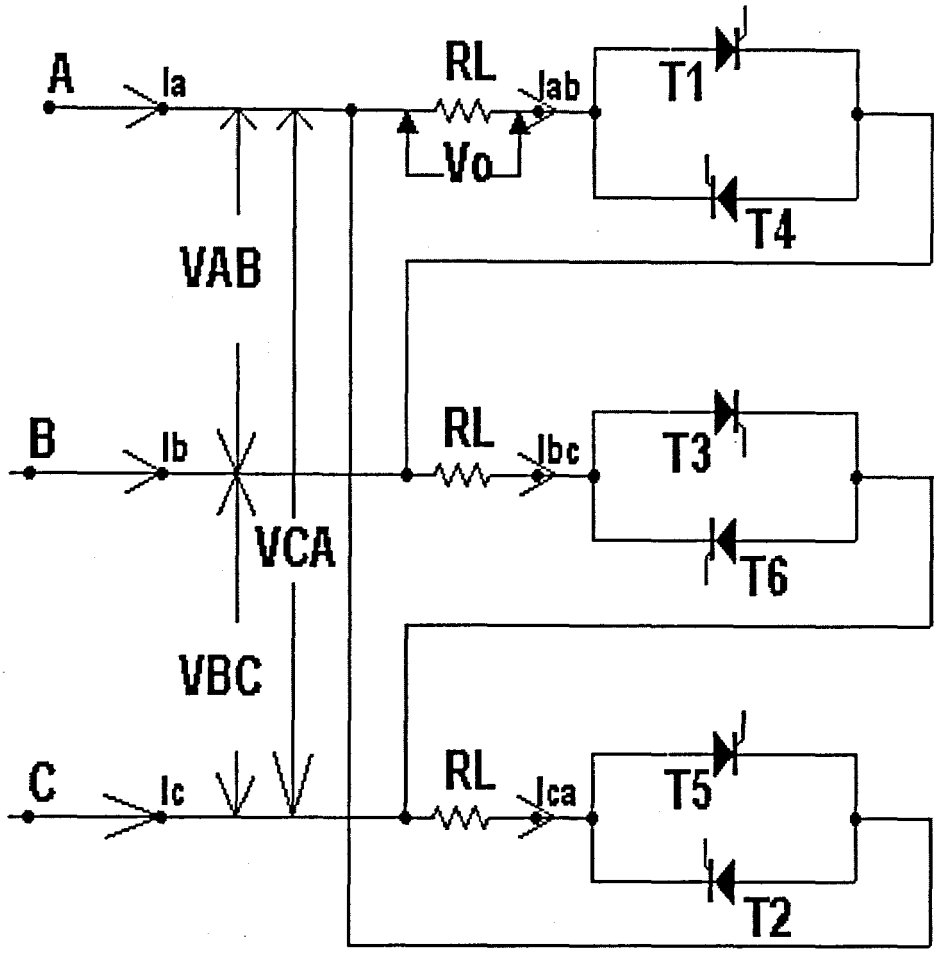

FIG.6.20: DELTA CONNECTED THREE PHASE AC THYRISTOR CONTROLLER

This section describes the modelling of the three phase delta connected AC controller shown in Fig.6.20. The model for a firing angle α of 2π /3 radians is shown in Fig.6.21. The various dialog boxes are shown in Fig.6.22 and the various subsystems in Fig.6.23(A) to (D). The various subsystems are explained below:

Fig.6.23(A) corresponds to the dialog box Three Phase AC Supply Data in Fig.6.22. In this dialog box, the rms line to line voltage in Volts and the frequency in Hertz are entered. The peak voltage Vm and angular frequency ω are internally calculated. Fig.6.23(B) corresponds to the dialog box Firing Pulse Generator in Fig.6.22. The firing angle α in radians is entered in this dialog box. Fig.6.23(B) has three constant blocks which generates α, [(2π/3) + α], [(4π/3) + α] for the three phases. Fig.6.23(C) generates the switch function SF for the three phases. The Switch Function corresponds

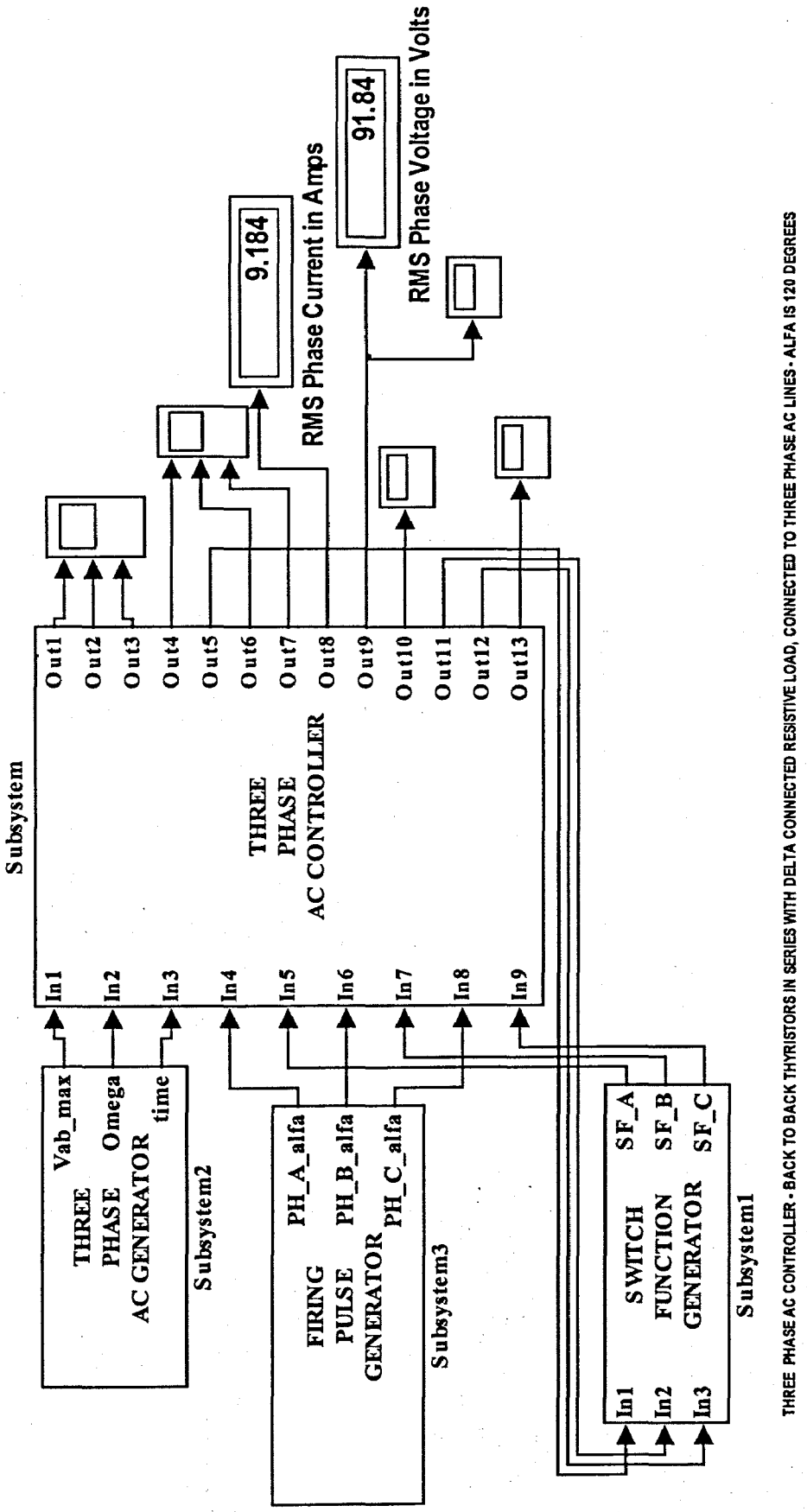
Subsystem
THREE PHASE AC CONTROLLER
In1
In2
In3
In4
In5
In6
In7
In8
In9
Out1
Out2
Out3
Out4
Out5
Out6
Out7
Out8
Out9
Out10
Out11
Out12
Out13
9.184
RMS Phase Current in Amps
91.84
RMS Phase Voltage in Volts
THREE PHASE AC GENERATOR
Vab_max
Omega
time
Subsystem2
FIRING PULSE GENERATOR
PH_A_alfa
PH_B_alfa
PH_C_alfa
Subsystem3
SWITCH FUNCTION GENERATOR
SF_A
SF_B
SF_C
In1
In2
In3
Subsystem1
THREE PHASE AC CONTROLLER - BACK TO BACK THYRISTORS IN SERIES WITH DELTA CONNECTED RESISTIVE LOAD, CONNECTED TO THREE PHASE AC LINES - ALFA IS 120 DEGREES

FIG. 6.21

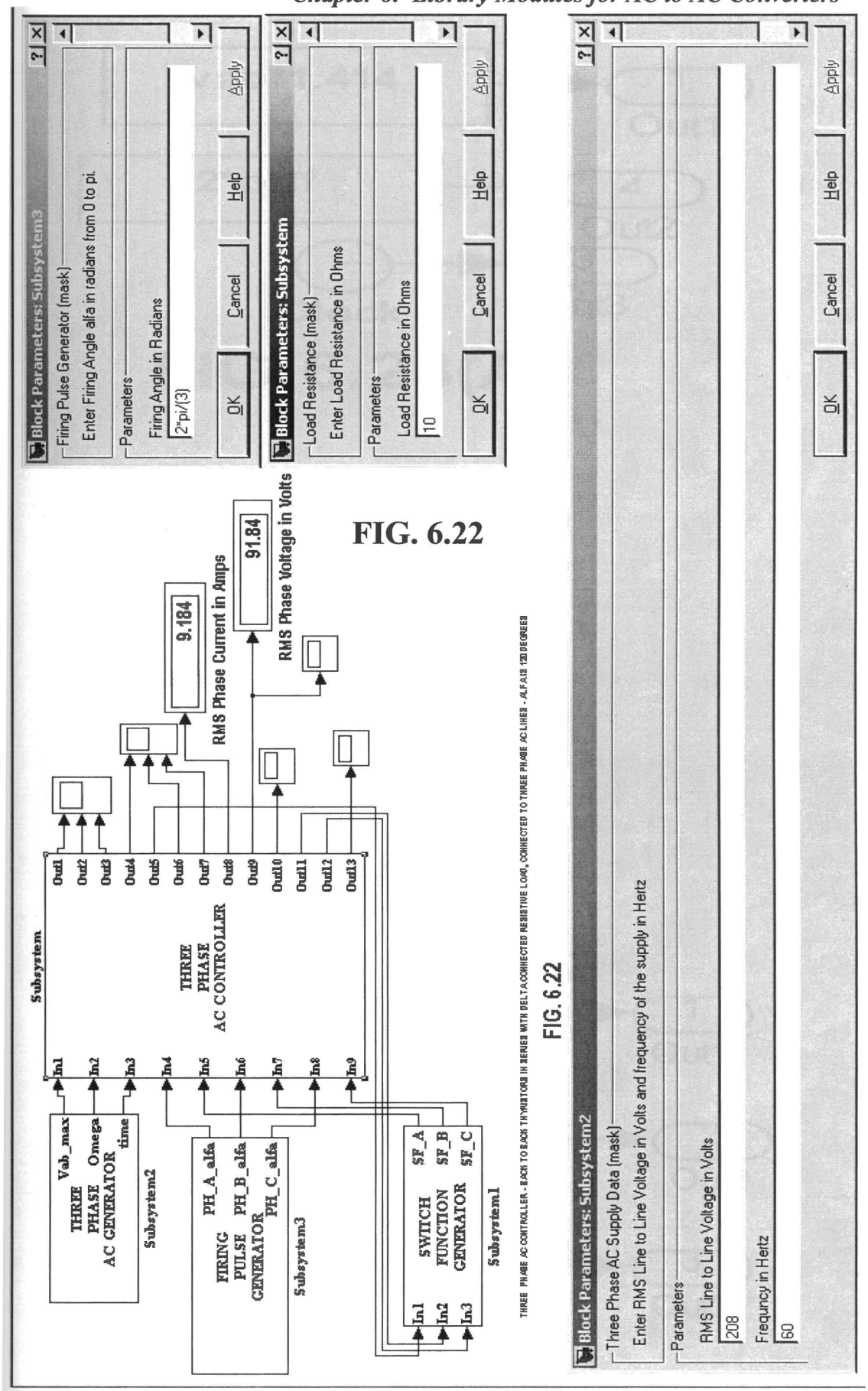

FIG. 6.22

FIG. 6.22

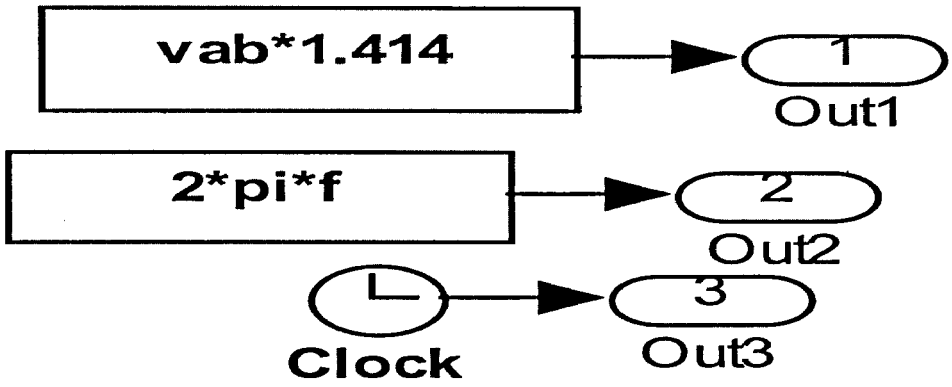

FIG.6.23(A)

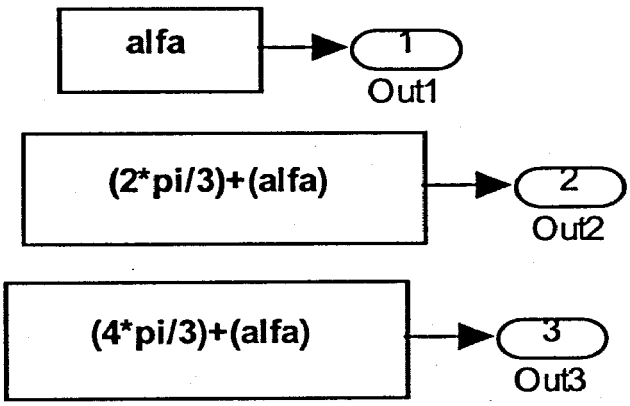

FIG.6.23(B)

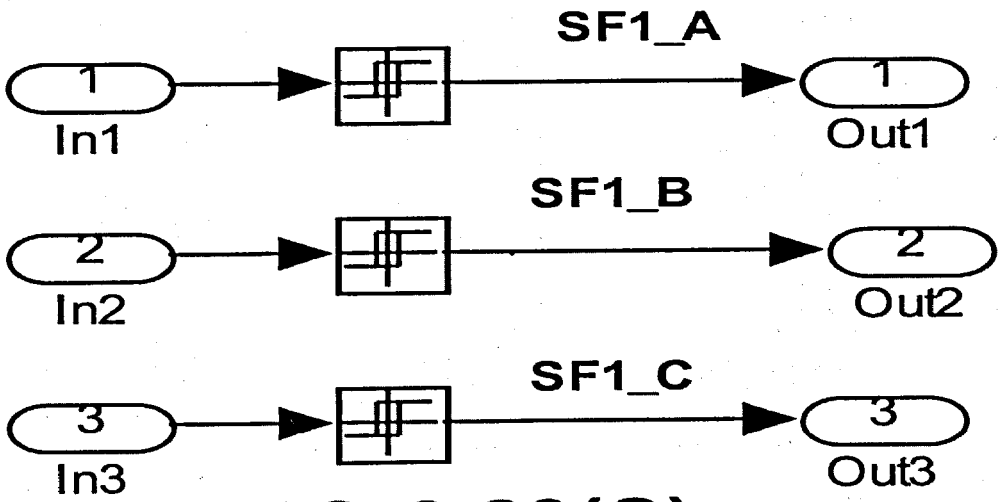

FIG.6.23(C)

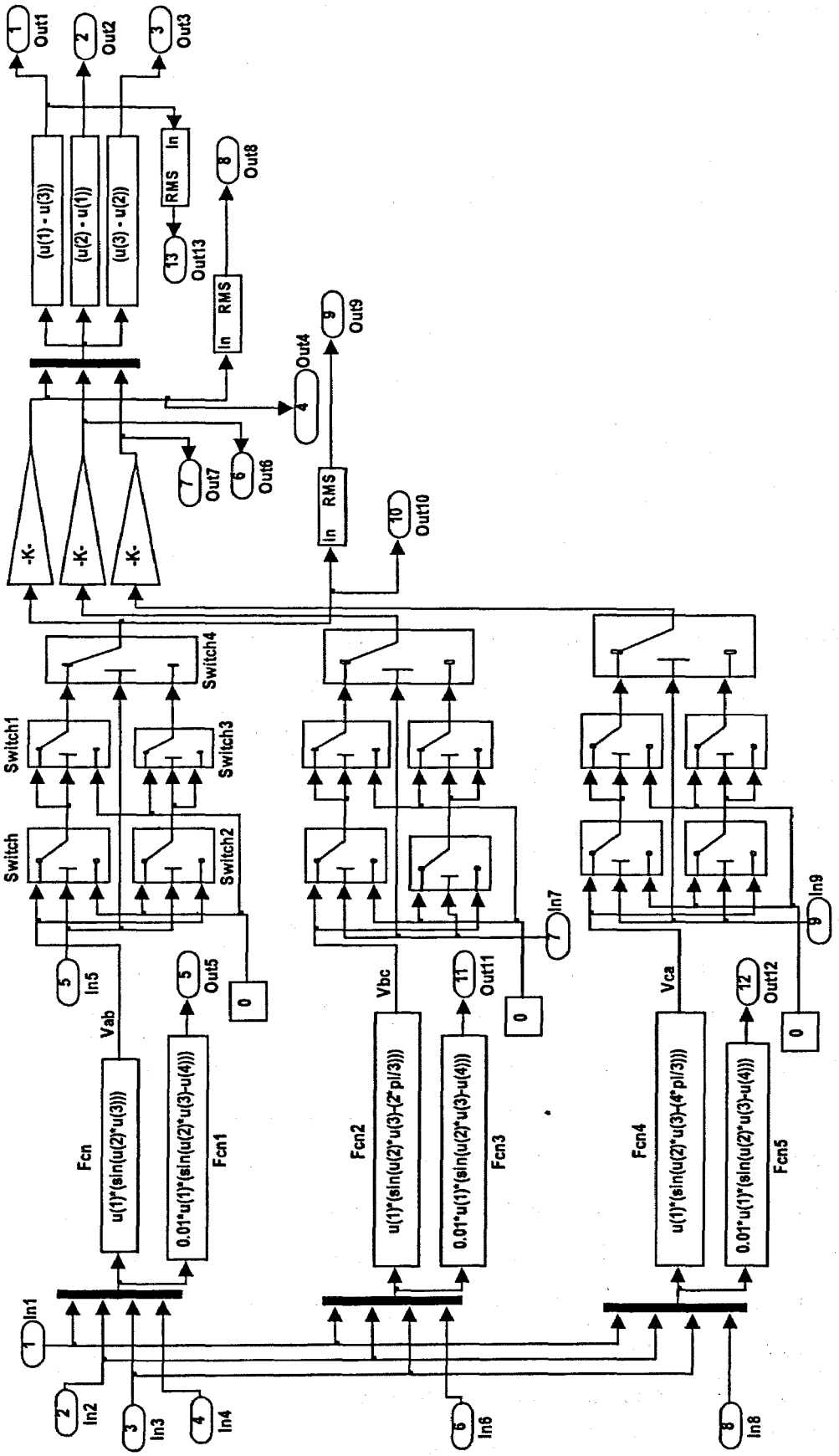
Out1
Out2
Out3
(u(1) - u(3))
(u(2) - u(1))
(u(3) - u(2))
RMS
In
Out13
Out8
RMS
In
Out4
Out9
Out7
Out6
-K-
-K-
-K-
RMS
In
Out10
Switch4
Switch1
Switch3
Switch
Switch2
In5
Out5
Vab
Fcn
u(1)*(sin(u(2)*u(3)))
Fcn1
0.01*u(1)*(sin(u(2)*u(3)-u(4)))
In7
Vbc
Out11
Fcn2
u(1)*(sin(u(2)*u(3)-(2*pi/3)))
Fcn3
0.01*u(1)*(sin(u(2)*u(3)-u(4)))
In9
Vca
Out12
Fcn4
u(1)*(sin(u(2)*u(3)-(4*pi/3)))
Fcn5
0.01*u(1)*(sin(u(2)*u(3)-u(4)))
In1
In2
In3
In4
In6
In8

FIG.6.23(D)

to the Firing Pulses for the back to back connected thyristors in the three phases. These Switch Functions SF_A, SF_B and SF_C in Fig.6.23(C) are defined below:

$$\left.\begin{aligned} SF\_A &= +1 \quad for \quad \alpha \le \omega t \le (\pi + \alpha) \\ &= -1 \quad for \quad (\pi + \alpha) \le \omega t \le (2\pi + \alpha) \\ SF\_B &= +1 \quad for \quad \left(\frac{2\pi}{3} + \alpha\right) \le \omega t \le \left(\frac{5\pi}{3} + \alpha\right) \\ &= -1 \quad for \quad \left(\frac{5\pi}{3} + \alpha\right) \le \omega t \le \left(\frac{8\pi}{3} + \alpha\right) \\ SF\_C &= +1 \quad for \quad \left(\frac{4\pi}{3} + \alpha\right) \le \omega t \le \left(\frac{7\pi}{3} + \alpha\right) \\ &= -1 \quad for \quad \left(\frac{7\pi}{3} + \alpha\right) \le \omega t \le \left(\frac{10\pi}{3} + \alpha\right) \end{aligned}\right\} \qquad (6.16)$$

The dialog box Load Resistance in Fig.6.22 corresponds to Fig.6.23(D). The load resistance value in Ohms per phase is entered in this dialog box. Fig.6.23(D) corresponds to the model of the back to back connected thyristors in the three phases and the star connected resistive load. The development of this model in Fig.6.23(D) is given below:

Referring to the top most four input MUX corresponding to Phase A, the inputs u(1) to u(4) are respectively peak line to line voltage Vm ($\sqrt{2}$.Vs), supply angular frequency ω, time t and firing angle α. The Fcn block at the top marked Fcn generates v_{AB} given by equation 6.14. while the bottom Fcn1 block generates attenuated v_{AB} lagging by the firing angle α. The two Fcn blocks corresponding to Phase B and C respectively generates v_{BC} given by equation 6.1 and attenuated v_{BC} lagging by [(2.π /3) + α], v_{CA} given by equation 6.1 and attenuated v_{CA} lagging by [(4.π /3) + α]. The bottom Function block output i.e. output of Fcn1, Fcn3 and Fcn5 of each phase marked in Fig.6.23(D) are given as input In1, In2 and In3 to the three Relays in Fig.6.23(C). All these three Relays output 1, when the respective input crosses zero and goes positive and output -1, when the respective input crosses zero and goes negative.

Considering Phase A for clarity, SF1_A is given as u(2) input to threshold switches marked Switch and switch2 in Fig.6.23(D). The output of Fcn block is given as u(1) input to Switch and u(3) input to Switch2. Zero is given to u(3) input of Switch and u(1) input to Switch2. The output of Switch is given to u(1) and u(2) input of Switch1 and its u(3) input is zero. The Switch2 output is given to u(2) and u(3) input of Switch3 and its u(1) input is zero. The output of Switch 1 and Switch3 are given as u(1) and u(3) input to Switch4 and its u(2) input is SF_A. The Switch, Switch1, Switch2, Switch3 and Switch4 all have a threshold value of zero and all these switches output corresponds to u(1) when u(2) is greater than or equal to zero, else all these switches output corresponds to u(3) input. The threshold switches corresponding to Phase B and Phase C operate in the same principle as for Phase A.

Referring to threshold switches in Phase A shown in Fig.6.23(D) and noting the definition of SF_A in equation 6.16, the output of various threshold switches can be explained as follows:

The 'Switch' and Switch2 has the following output given by equation 6.17 and 6.18 respectively.

$$\begin{aligned} Switch \quad output &= +Vm\sin(\omega t) \quad for \quad \alpha \le \omega t \le (\pi+\alpha) \\ &= 0 \quad for\ other\ time\ intervals \end{aligned} \tag{6.17}$$

$$\begin{aligned} Switch2 \quad output &= -Vm\sin(\omega t) \quad for \quad (\pi+\alpha) \le \omega t \le (2\pi+\alpha) \\ &= 0 \quad for\ other\ time\ intervals \end{aligned} \tag{6.18}$$

Switch1 and Switch3 has the following output given by equations 6.19 and 6.20 respectively:

$$\begin{aligned} Switch1 \quad output &= +Vm\sin(\omega t) \quad for \quad \alpha \le \omega t \le \pi \\ &= 0 \quad for\ other\ time\ intervals \end{aligned} \tag{6.19}$$

$$\begin{aligned} Switch3 \quad output &= -Vm\sin(\omega t) \quad for \quad (\pi+\alpha) \le \omega t \le 2\pi \\ &= 0 \quad for\ other\ time\ intervals \end{aligned} \tag{6.20}$$

Switch4 has the following output given by equation 6.21 below:

$$\begin{aligned} Switch4 \quad output &= +Vmsin(\omega t) \quad for \quad \alpha \leq \omega t \leq \pi \\ &= -Vmsin(\omega t) \quad for \quad (\pi+\alpha) \leq \omega t \leq 2\pi \\ &= 0 \quad for \ other \ time \ intervals \end{aligned} \qquad (6.21)$$

The Switch4 output in Fig.6.23(D) corresponds to the Phase Voltage Vo across the load resistor. This Vo is multiplied by 1/(r_load) using gain multiplier blocks to obtain the phase currents i_{ab}, i_{bc} and i_{ca} through the load resistor. These respective phase currents are given to a three input MUX. The three Fcn blocks performing [u(1) –u(3)], [u(2) – u(1)] and [u(3) – u(2)] output the line currents i_a, i_b and i_c.

6.3.2 Simulation Results

The simulation of the Fully Controlled three phase AC controller in series with delta connected resistive load was carried out using ode15s(stiff/NDF) solver, for various firing angle α of π /6, π /4, π /3, π /2, 2.π /3 and π . The data used for this controller are given in Table 6.4 [14]. The simulation results for firing angle α of π /6, π /4, π /3, π /2, 2.π /3 and π are shown from Fig.6.24 to Fig..6.29. The names of the various waveforms are given at the top of each simulation result. The results of RMS line to line voltage across the load and load current for a firing angle α of 2π /3 is displayed in Fig.6.21.

TABLE 6.4 – Data for Three Phase AC Controller with Delta connected Resistive Load

Sl.No.	RMS Line to Line Supply Voltage in Volts	Frequency Hertz	Firing Angle α radians	Per Phase Load Resistance in Ohms
1	208	60	π / 6	10
2	208	60	π / 4	10
3	208	60	π / 3	10
4	208	60	π / 2	10
5	208	60	2 π / 3	10
6	208	60	π	10

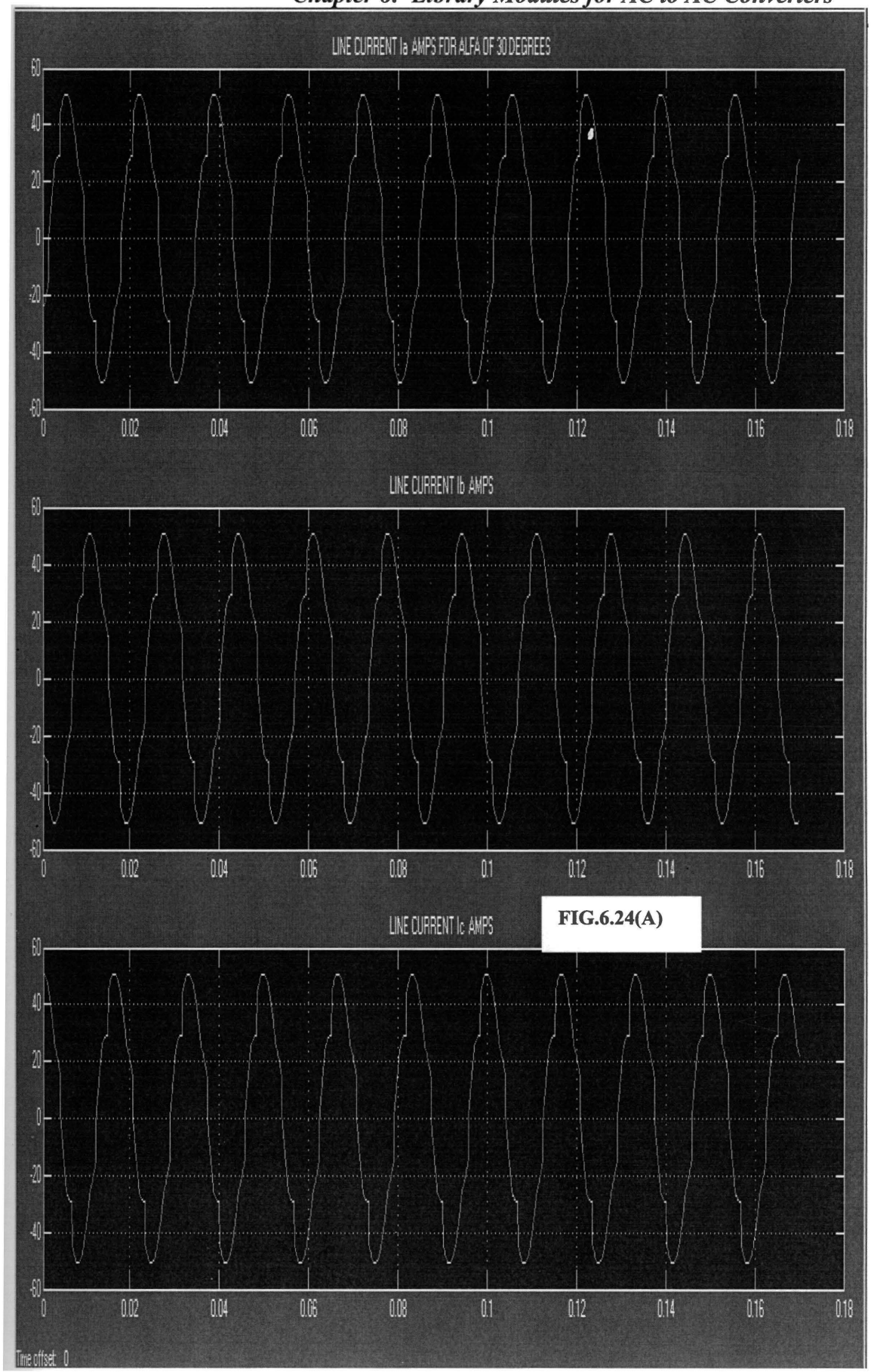
LINE CURRENT Ia AMPS FOR ALFA OF 30 DEGREES
60
40
20
0
-20
-40
-60
0
0.02
0.04
0.06
0.08
0.1
0.12
0.14
0.16
0.18
LINE CURRENT Ib AMPS
LINE CURRENT Ic AMPS
Time offset: 0

FIG.6.24(A)

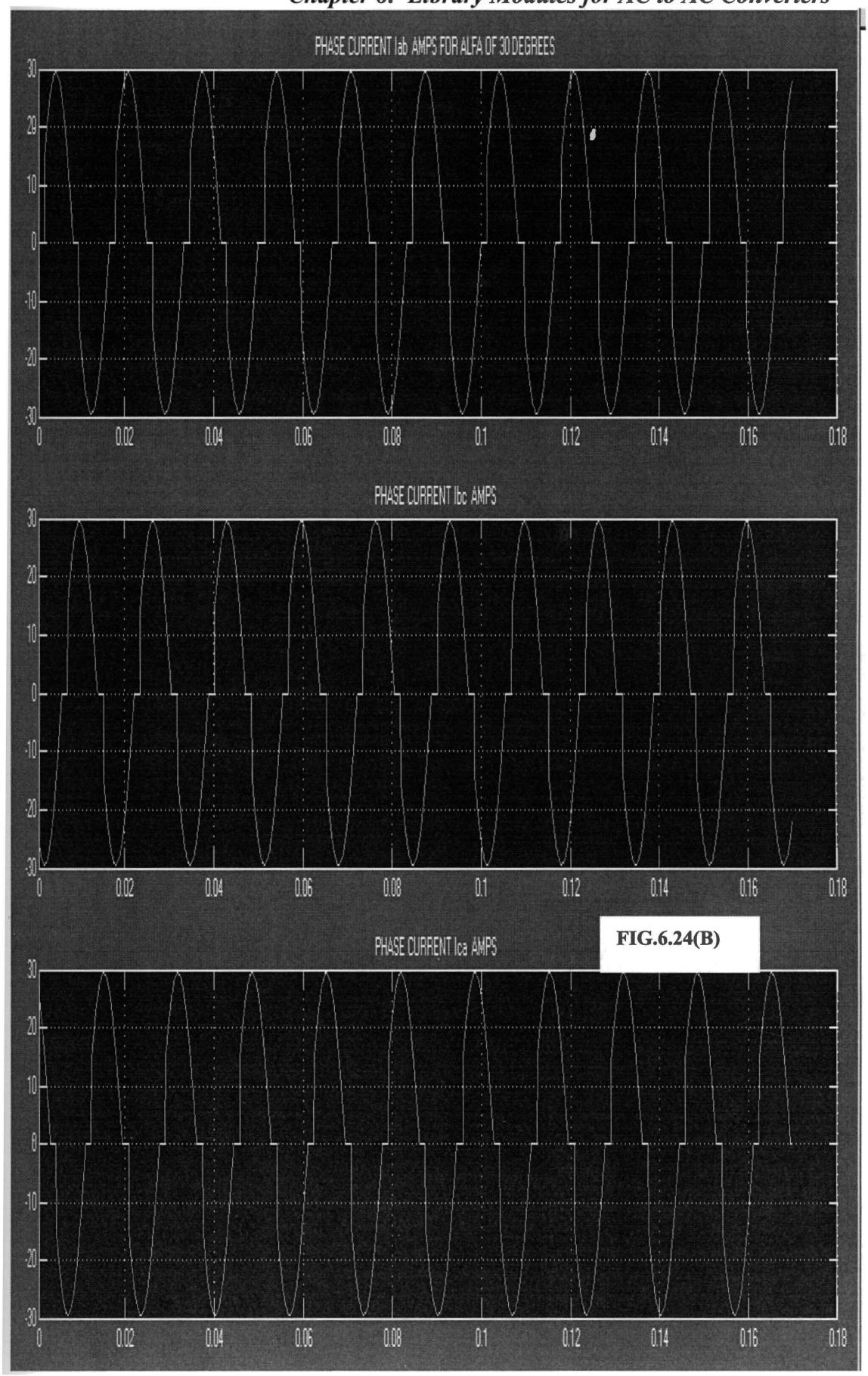
PHASE CURRENT Iab AMPS FOR ALFA OF 30 DEGREES
30
20
10
0
-10
-20
-30
0
0.02
0.04
0.06
0.08
0.1
0.12
0.14
0.16
0.18
PHASE CURRENT Ibc AMPS
30
20
10
0
-10
-20
-30
0
0.02
0.04
0.06
0.08
0.1
0.12
0.14
0.16
0.18
PHASE CURRENT Ica AMPS
30
20
10
0
-10
-20
-30
0
0.02
0.04
0.06
0.08
0.1
0.12
0.14
0.16
0.18

FIG.6.24(B)

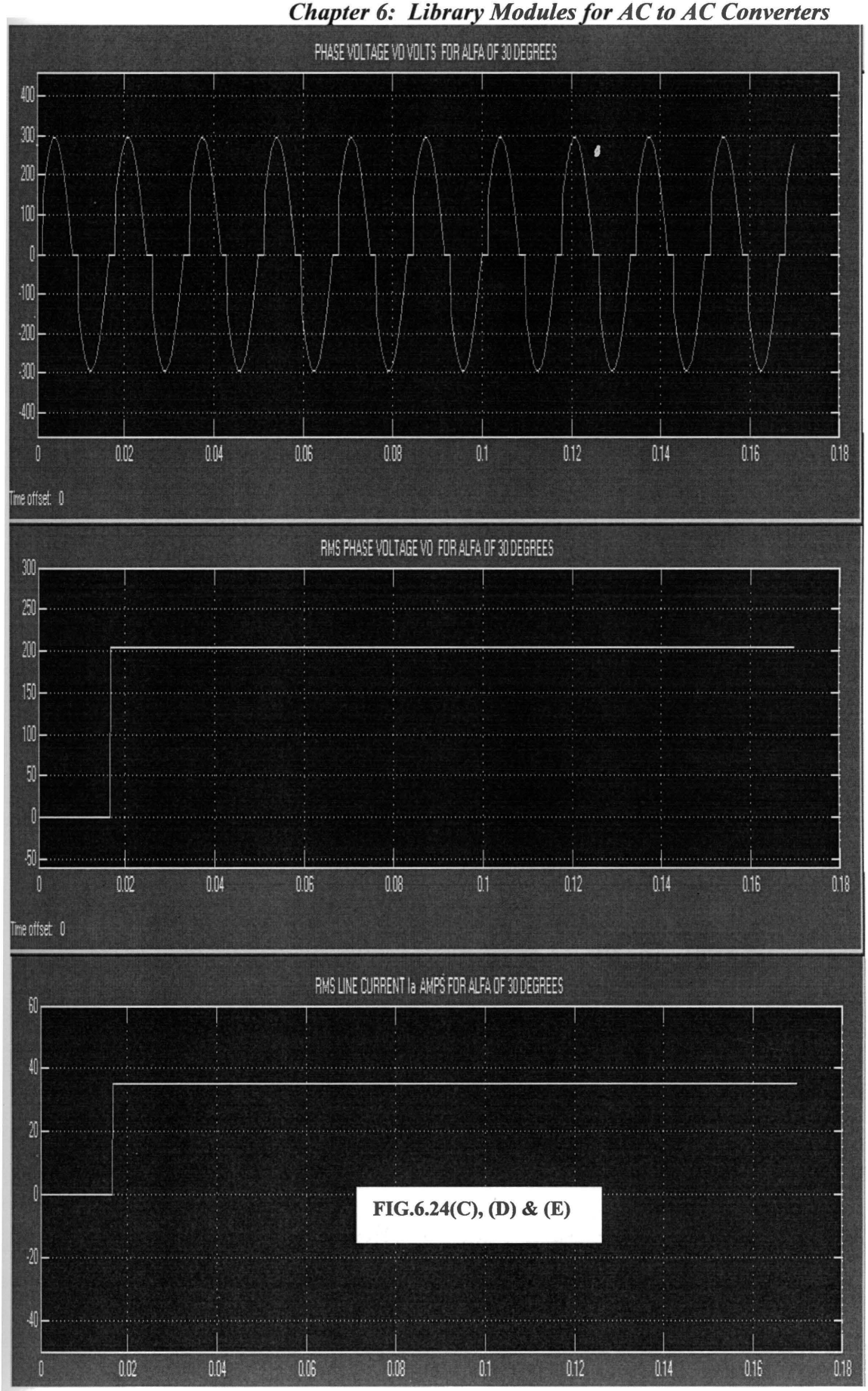
PHASE VOLTAGE VO VOLTS FOR ALFA OF 30 DEGREES
400
300
200
100
0
-100
-200
-300
-400
0
0.02
0.04
0.06
0.08
0.1
0.12
0.14
0.16
0.18
Time offset: 0
RMS PHASE VOLTAGE VO FOR ALFA OF 30 DEGREES
300
250
200
150
100
50
0
-50
0
0.02
0.04
0.06
0.08
0.1
0.12
0.14
0.16
0.18
Time offset: 0
RMS LINE CURRENT Ia AMPS FOR ALFA OF 30 DEGREES
60
40
20
0
-20
-40
0
0.02
0.04
0.06
0.08
0.1
0.12
0.14
0.16
0.18

FIG.6.24(C), (D) & (E)

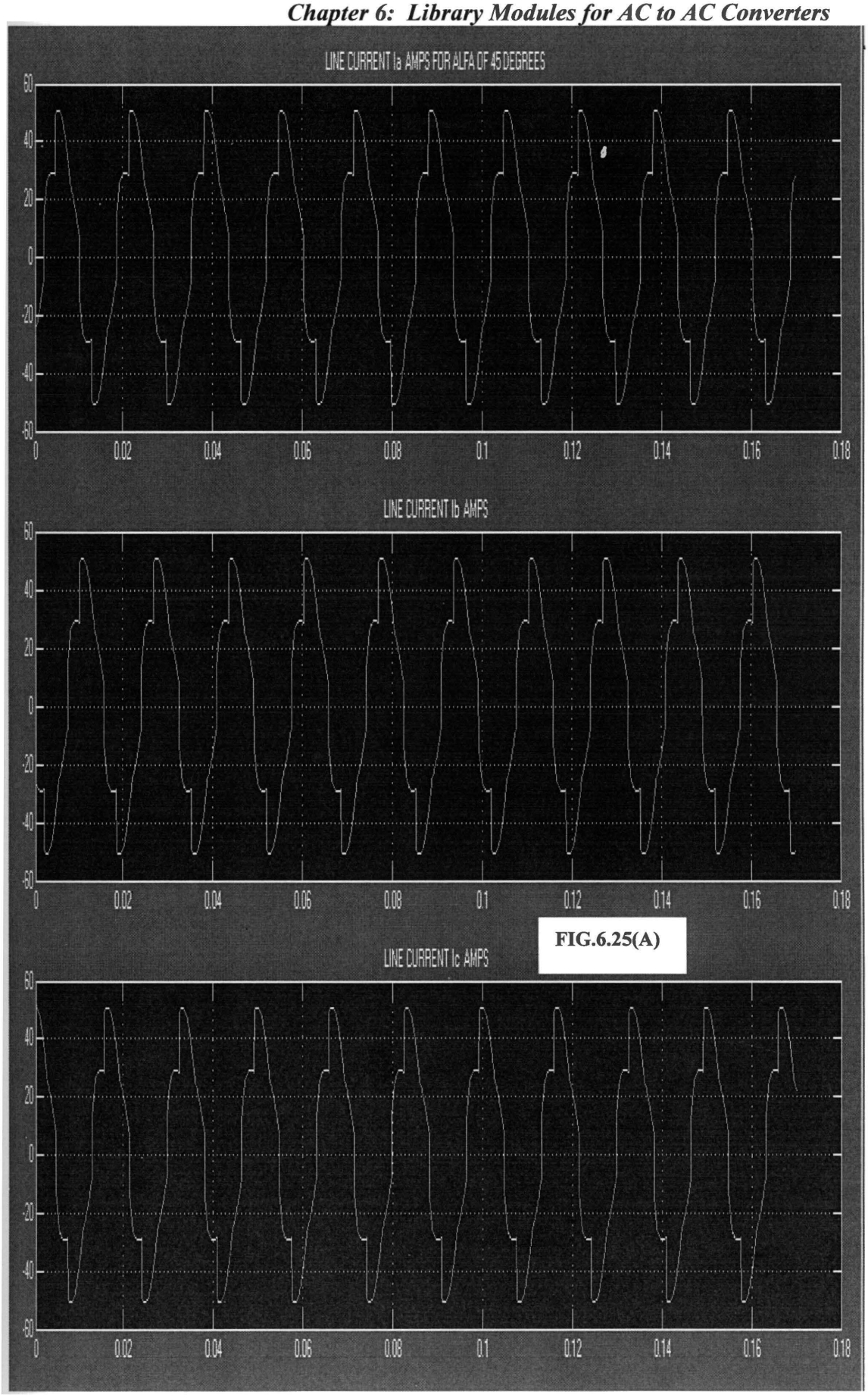
LINE CURRENT Ia AMPS FOR ALFA OF 45 DEGREES
60
40
20
0
-20
-40
-60
0
0.02
0.04
0.06
0.08
0.1
0.12
0.14
0.16
0.18
LINE CURRENT Ib AMPS
60
40
20
0
-20
-40
-60
0
0.02
0.04
0.06
0.08
0.1
0.12
0.14
0.16
0.18
LINE CURRENT Ic AMPS
60
40
20
0
-20
-40
-60
0
0.02
0.04
0.06
0.08
0.1
0.12
0.14
0.16
0.18

FIG.6.25(A)

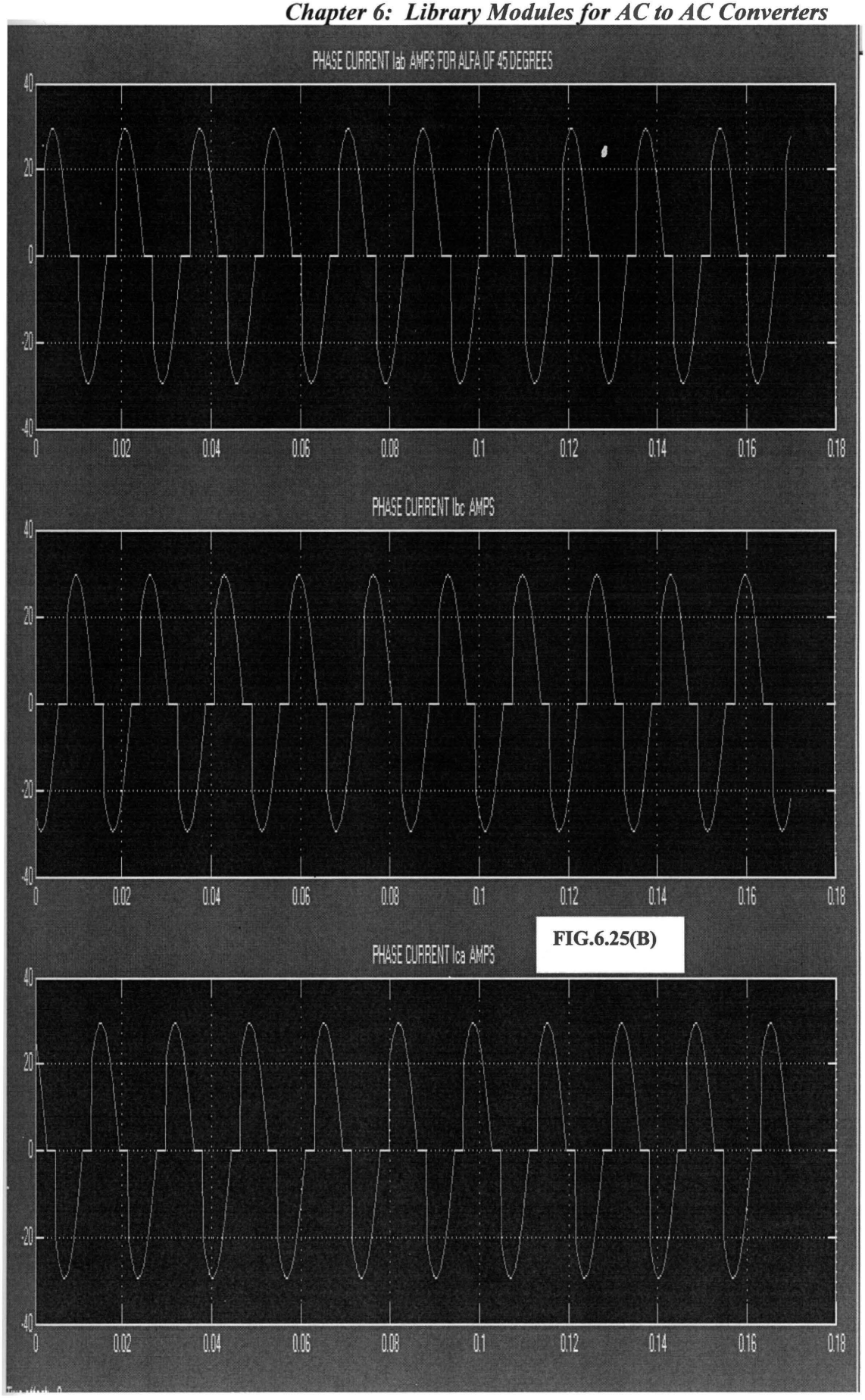
PHASE CURRENT Iab AMPS FOR ALFA OF 45 DEGREES
40
20
0
-20
-40
0
0.02
0.04
0.06
0.08
0.1
0.12
0.14
0.16
0.18
PHASE CURRENT Ibc AMPS
40
20
0
-20
-40
0
0.02
0.04
0.06
0.08
0.1
0.12
0.14
0.16
0.18
PHASE CURRENT Ica AMPS
40
20
0
-20
-40
0
0.02
0.04
0.06
0.08
0.1
0.12
0.14
0.16
0.18

FIG.6.25(B)

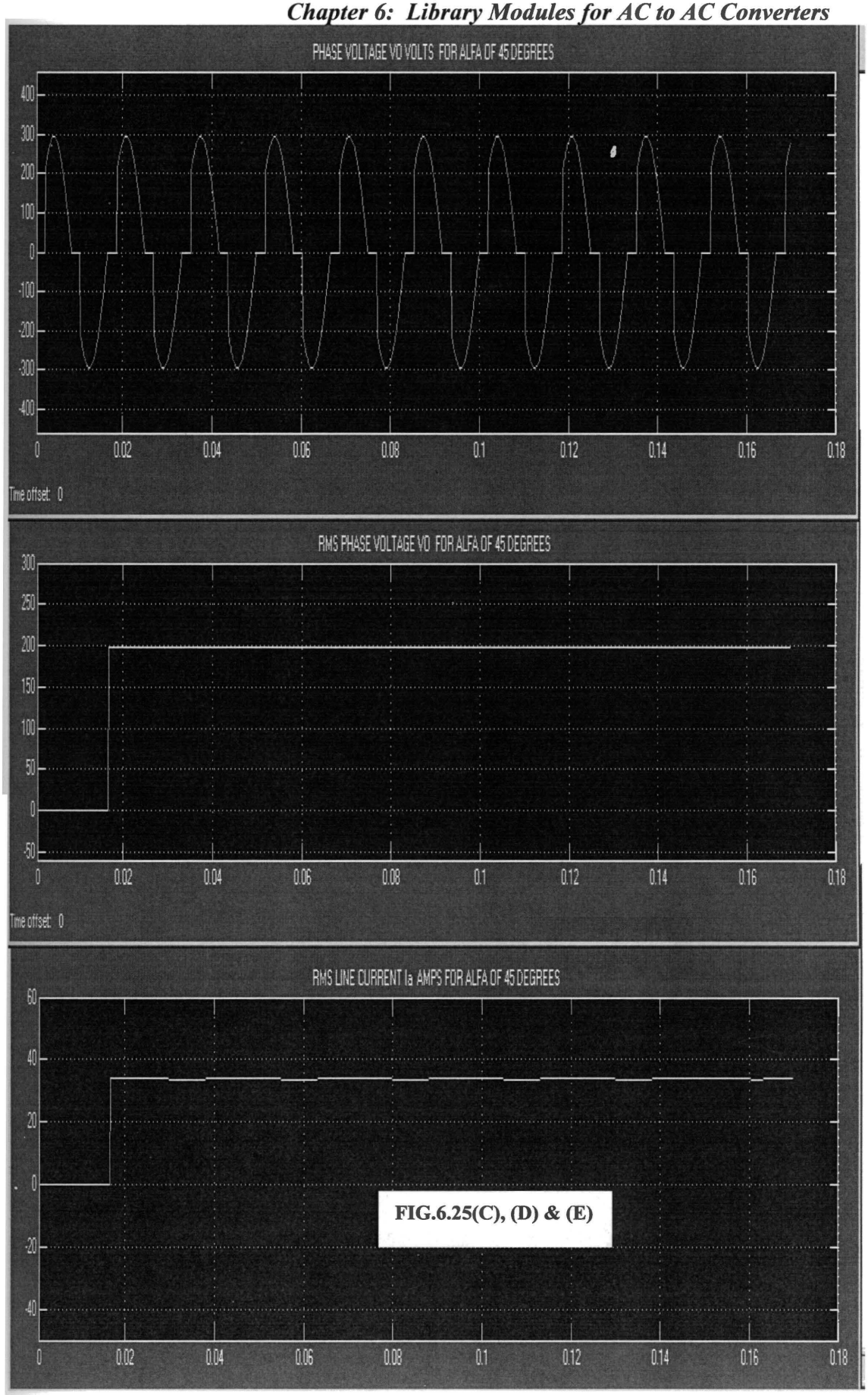
PHASE VOLTAGE VO VOLTS FOR ALFA OF 45 DEGREES
400
300
200
100
0
-100
-200
-300
-400
0
0.02
0.04
0.06
0.08
0.1
0.12
0.14
0.16
0.18
Time offset: 0
RMS PHASE VOLTAGE VO FOR ALFA OF 45 DEGREES
300
250
200
150
100
50
0
-50
0
0.02
0.04
0.06
0.08
0.1
0.12
0.14
0.16
0.18
Time offset: 0
RMS LINE CURRENT Ia AMPS FOR ALFA OF 45 DEGREES
60
40
20
0
-20
-40
0
0.02
0.04
0.06
0.08
0.1
0.12
0.14
0.16
0.18

FIG.6.25(C), (D) & (E)

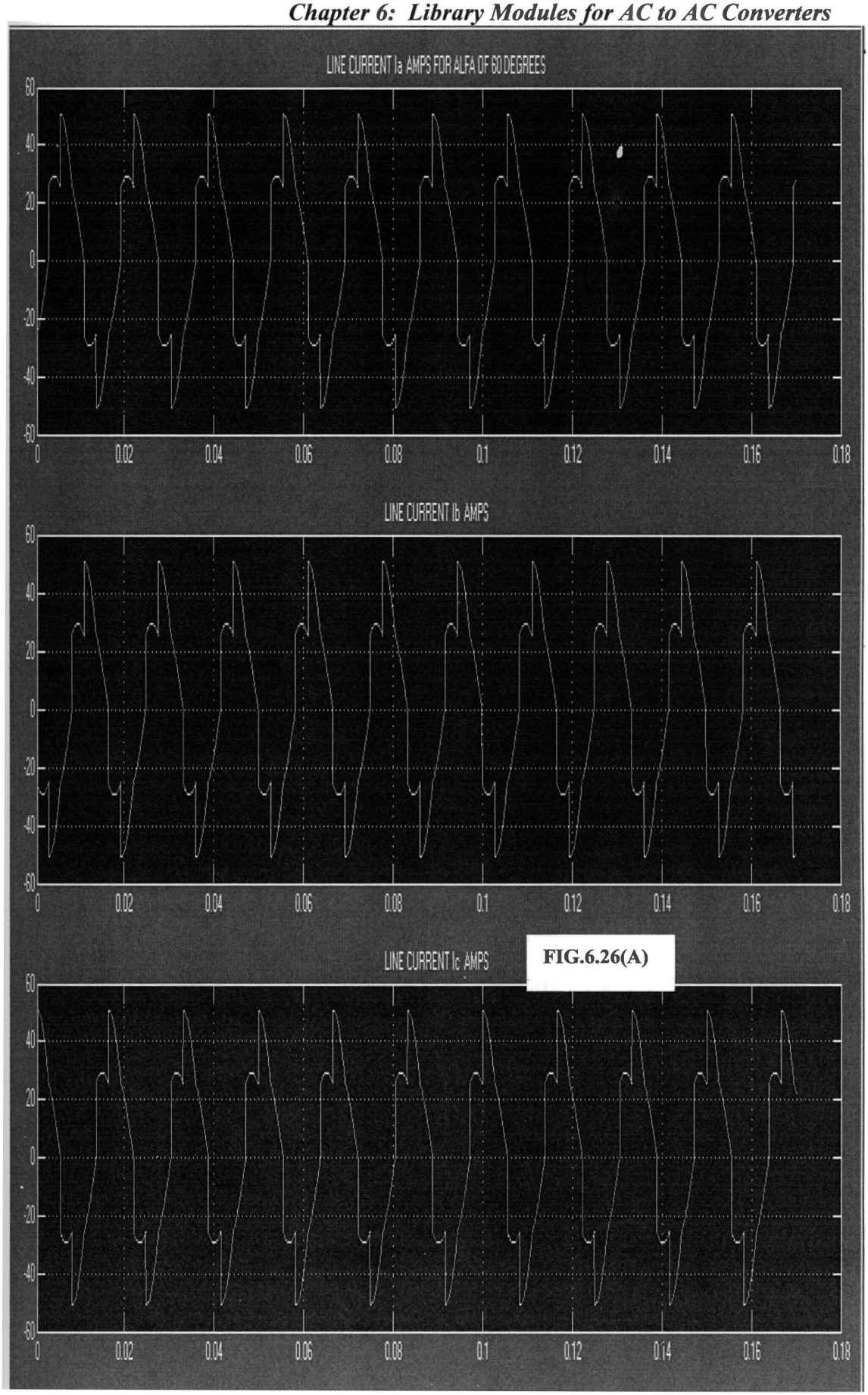
LINE CURRENT Ia AMPS FOR ALFA OF 60 DEGREES
60
40
20
0
-20
-40
-60
0
0.02
0.04
0.06
0.08
0.1
0.12
0.14
0.16
0.18
LINE CURRENT Ib AMPS
60
40
20
0
-20
-40
-60
0
0.02
0.04
0.06
0.08
0.1
0.12
0.14
0.16
0.18
LINE CURRENT Ic AMPS
60
40
20
0
-20
-40
-60
0
0.02
0.04
0.06
0.08
0.1
0.12
0.14
0.16
0.18

FIG.6.26(A)

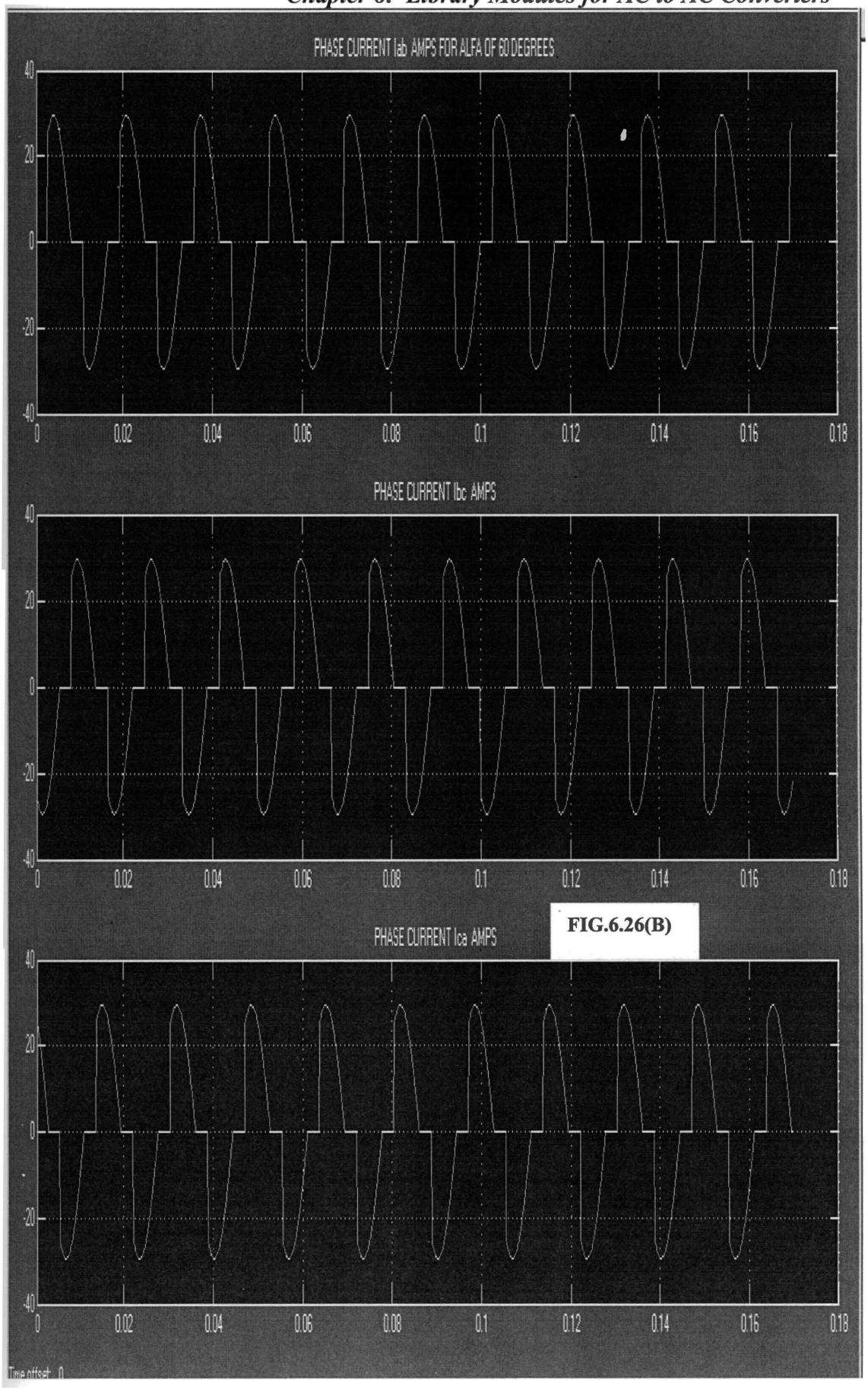
PHASE CURRENT Iab AMPS FOR ALFA OF 60 DEGREES
40
20
0
-20
-40
0
0.02
0.04
0.06
0.08
0.1
0.12
0.14
0.16
0.18
PHASE CURRENT Ibc AMPS
40
20
0
-20
-40
0
0.02
0.04
0.06
0.08
0.1
0.12
0.14
0.16
0.18
PHASE CURRENT Ica AMPS
40
20
0
-20
-40
0
0.02
0.04
0.06
0.08
0.1
0.12
0.14
0.16
0.18
Time offset: 0

FIG.6.26(B)

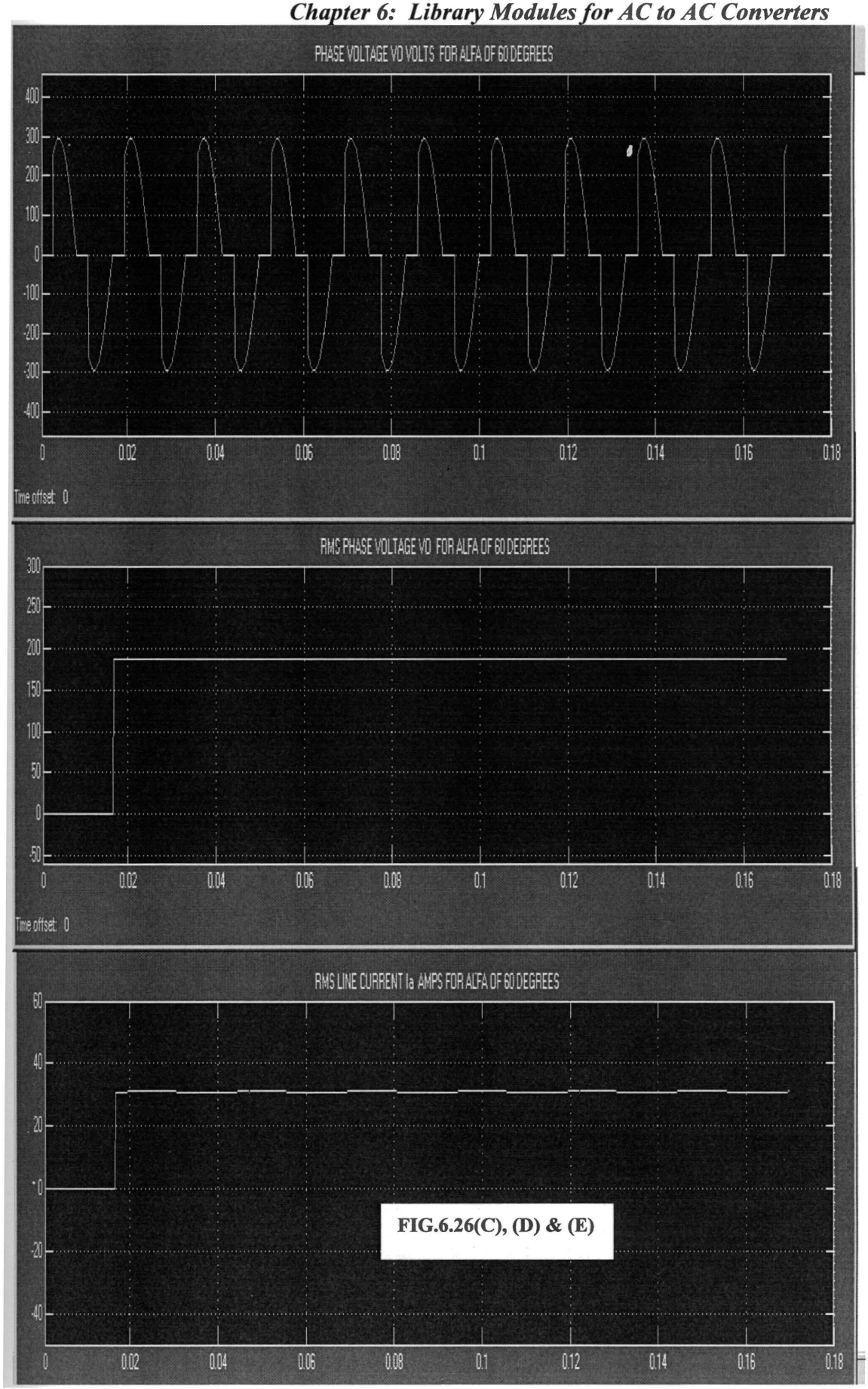
PHASE VOLTAGE VO VOLTS FOR ALFA OF 60 DEGREES
400
300
200
100
0
-100
-200
-300
-400
0
0.02
0.04
0.06
0.08
0.1
0.12
0.14
0.16
0.18
Time offset: 0
RMS PHASE VOLTAGE VO FOR ALFA OF 60 DEGREES
300
250
200
150
100
50
0
-50
0
0.02
0.04
0.06
0.08
0.1
0.12
0.14
0.16
0.18
Time offset: 0
RMS LINE CURRENT Ia AMPS FOR ALFA OF 60 DEGREES
60
40
20
0
-20
-40
0
0.02
0.04
0.06
0.08
0.1
0.12
0.14
0.16
0.18

FIG.6.26(C), (D) & (E)

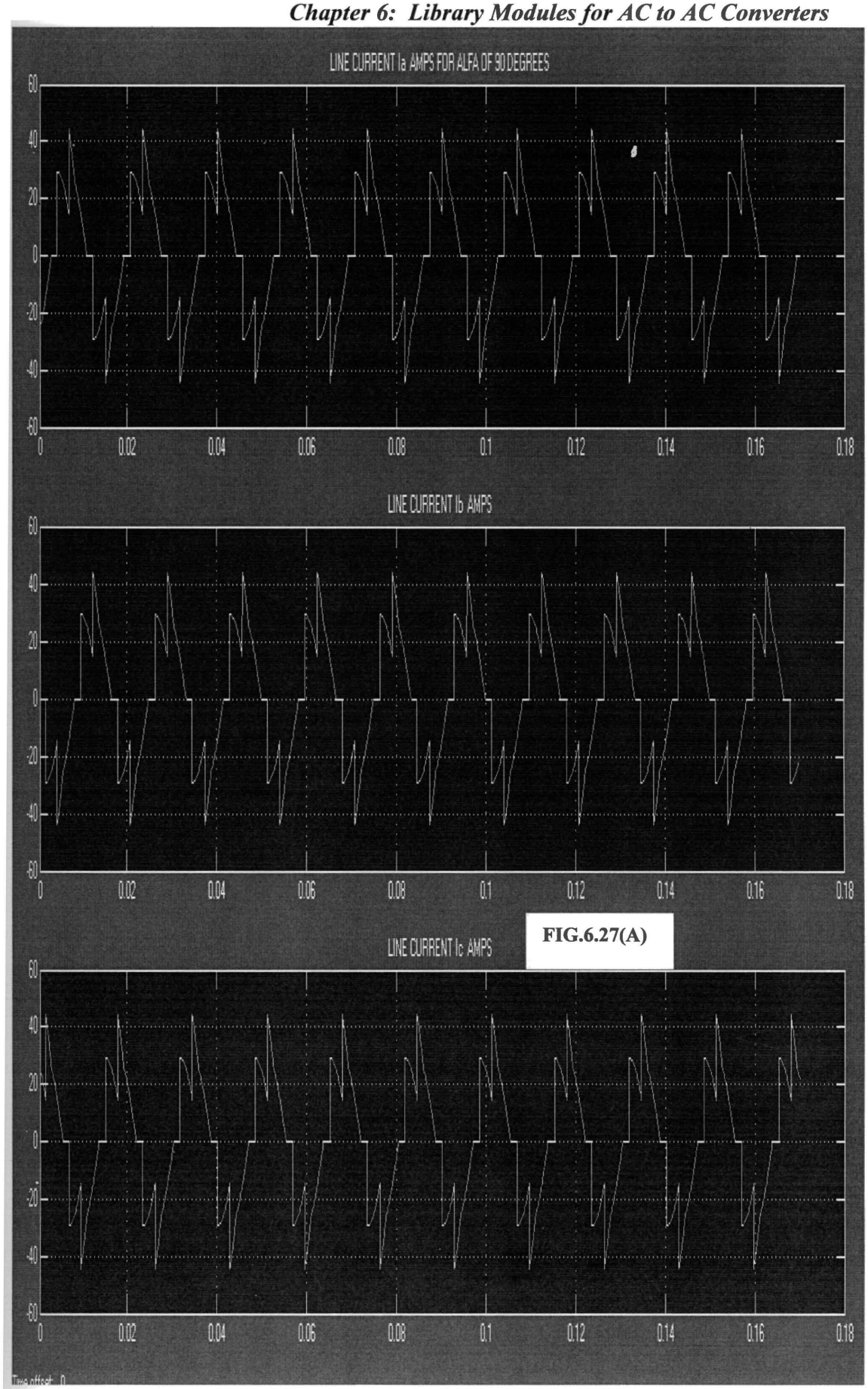
LINE CURRENT Ia AMPS FOR ALFA OF 90 DEGREES
60
40
20
0
-20
-40
-60
0
0.02
0.04
0.06
0.08
0.1
0.12
0.14
0.16
0.18
LINE CURRENT Ib AMPS
LINE CURRENT Ic AMPS

FIG.6.27(A)

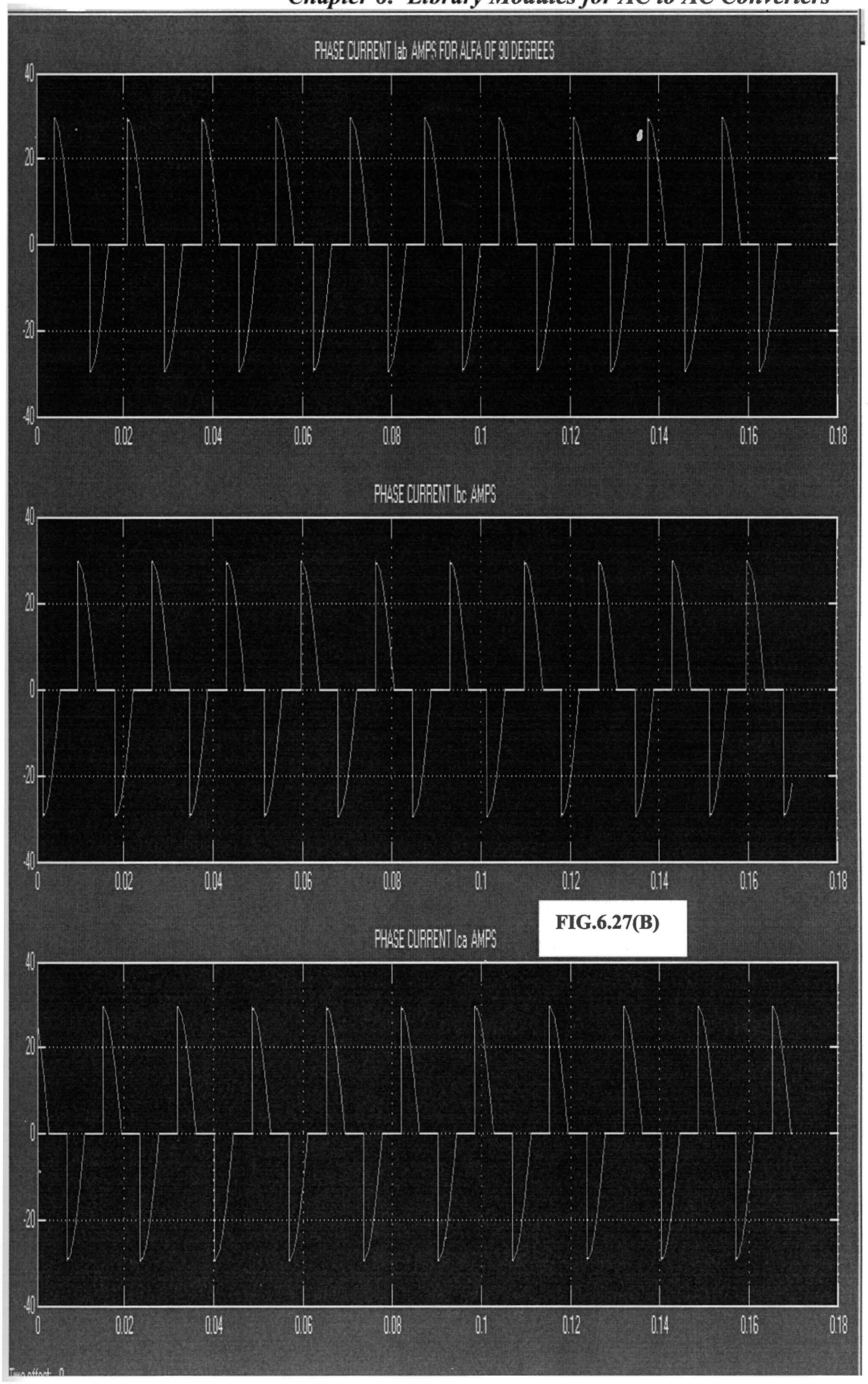
PHASE CURRENT Iab AMPS FOR ALFA OF 90 DEGREES
40
20
0
-20
-40
0
0.02
0.04
0.06
0.08
0.1
0.12
0.14
0.16
0.18
PHASE CURRENT Ibc AMPS
40
20
0
-20
-40
0
0.02
0.04
0.06
0.08
0.1
0.12
0.14
0.16
0.18
PHASE CURRENT Ica AMPS
40
20
0
-20
-40
0
0.02
0.04
0.06
0.08
0.1
0.12
0.14
0.16
0.18

FIG.6.27(B)

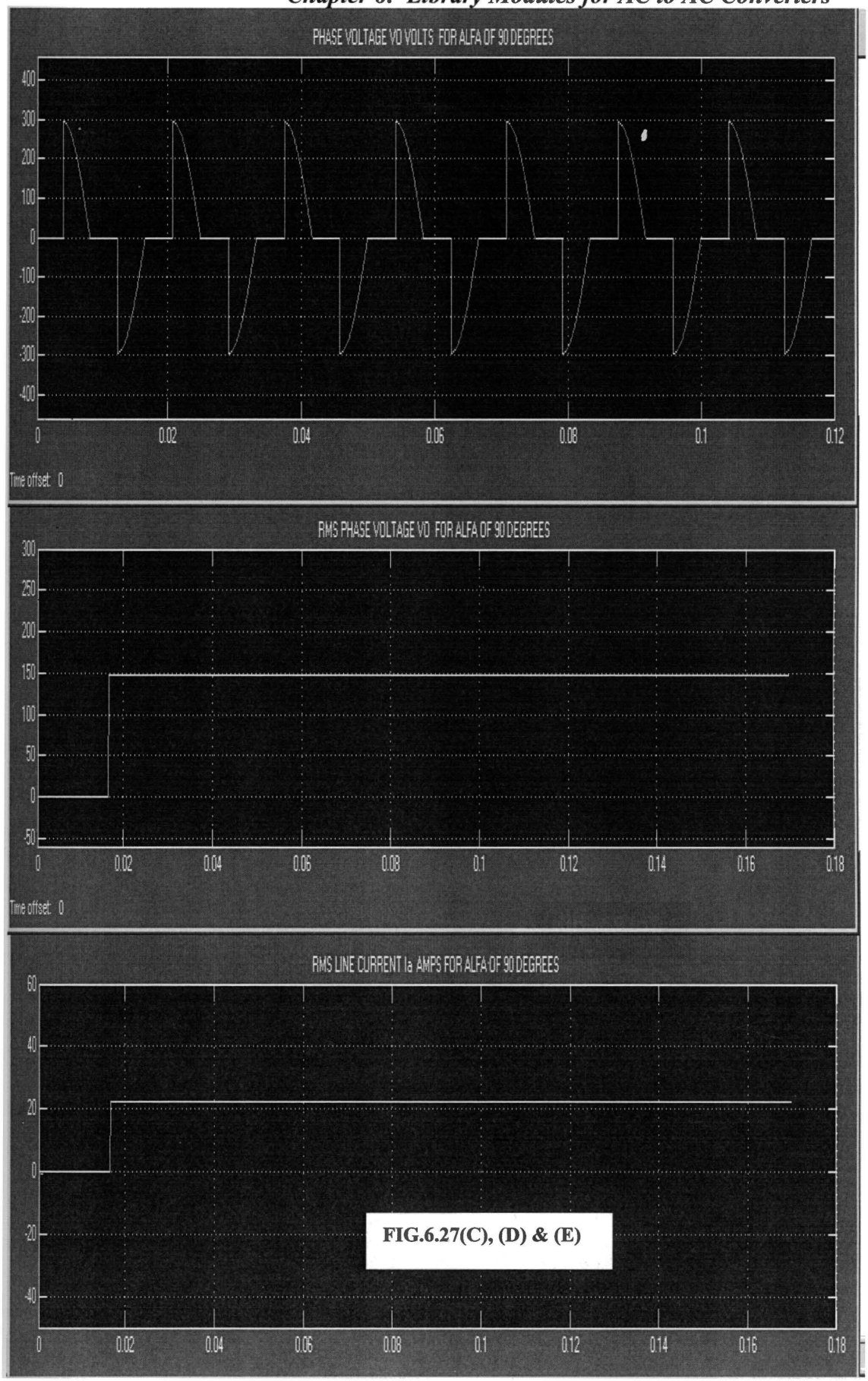
PHASE VOLTAGE VO VOLTS FOR ALFA OF 90 DEGREES
400
300
200
100
0
-100
-200
-300
-400
0
0.02
0.04
0.06
0.08
0.1
0.12
Time offset: 0
RMS PHASE VOLTAGE VO FOR ALFA OF 90 DEGREES
300
250
200
150
100
50
0
-50
0
0.02
0.04
0.06
0.08
0.1
0.12
0.14
0.16
0.18
Time offset: 0
RMS LINE CURRENT Ia AMPS FOR ALFA OF 90 DEGREES
60
40
20
0
-20
-40
0
0.02
0.04
0.06
0.08
0.1
0.12
0.14
0.16
0.18

FIG.6.27(C), (D) & (E)

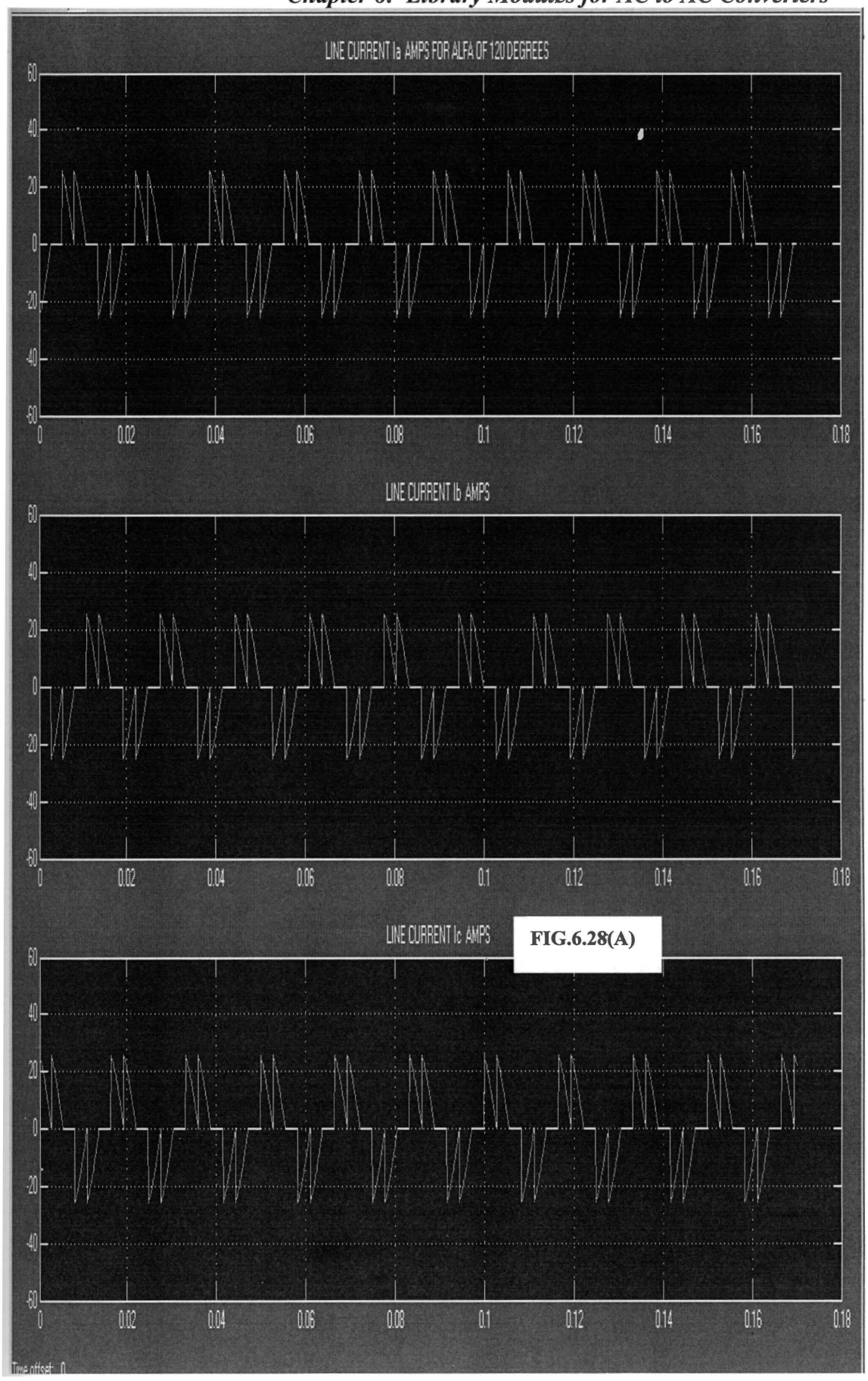
LINE CURRENT Ia AMPS FOR ALFA OF 120 DEGREES
60
40
20
0
-20
-40
-60
0
0.02
0.04
0.06
0.08
0.1
0.12
0.14
0.16
0.18
LINE CURRENT Ib AMPS
LINE CURRENT Ic AMPS
Time offset: 0

FIG.6.28(A)

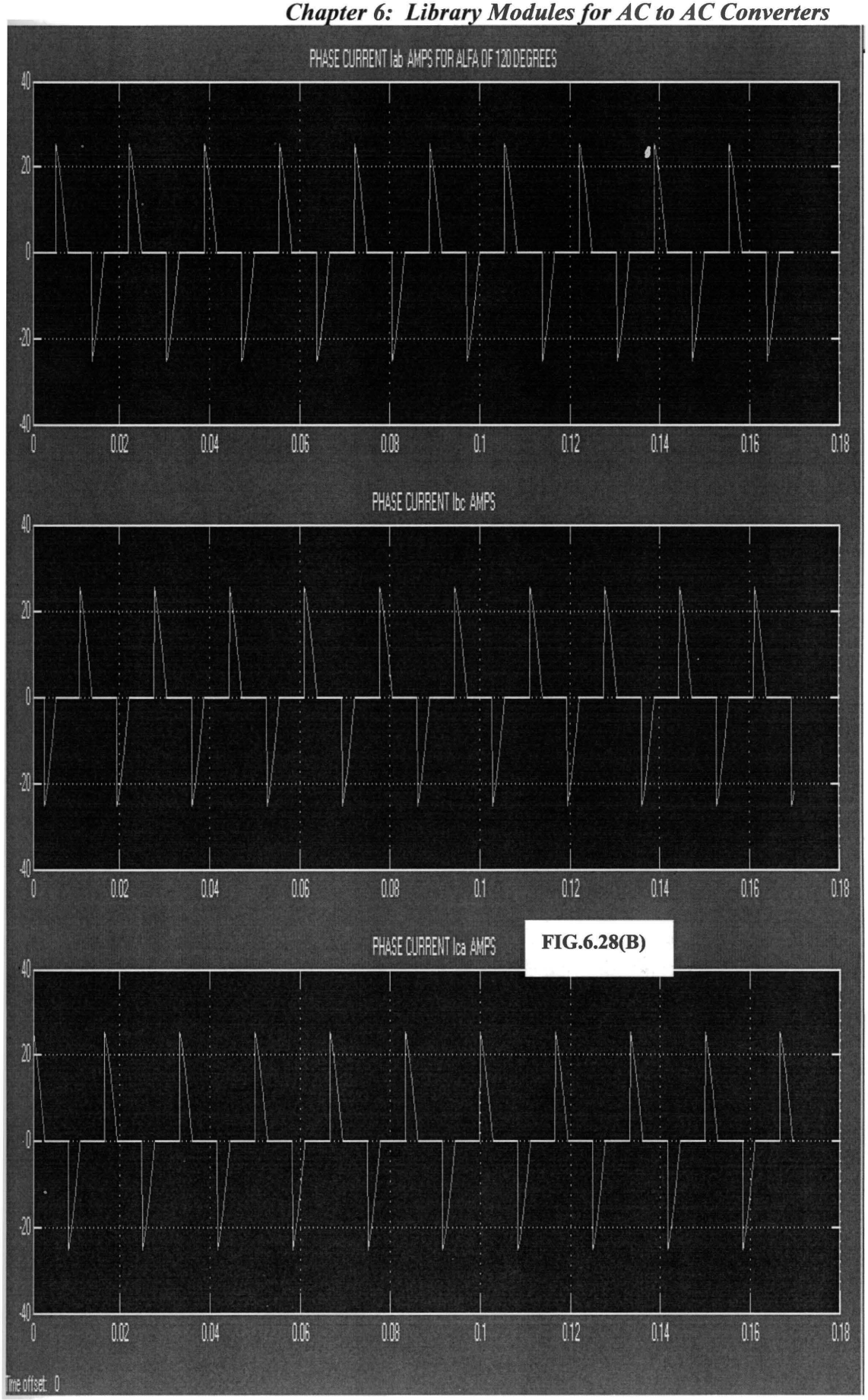
PHASE CURRENT Iab AMPS FOR ALFA OF 120 DEGREES
40
20
0
-20
-40
0
0.02
0.04
0.06
0.08
0.1
0.12
0.14
0.16
0.18
PHASE CURRENT Ibc AMPS
40
20
0
-20
-40
0
0.02
0.04
0.06
0.08
0.1
0.12
0.14
0.16
0.18
PHASE CURRENT Ica AMPS
40
20
0
-20
-40
0
0.02
0.04
0.06
0.08
0.1
0.12
0.14
0.16
0.18
Time offset: 0

FIG.6.28(B)

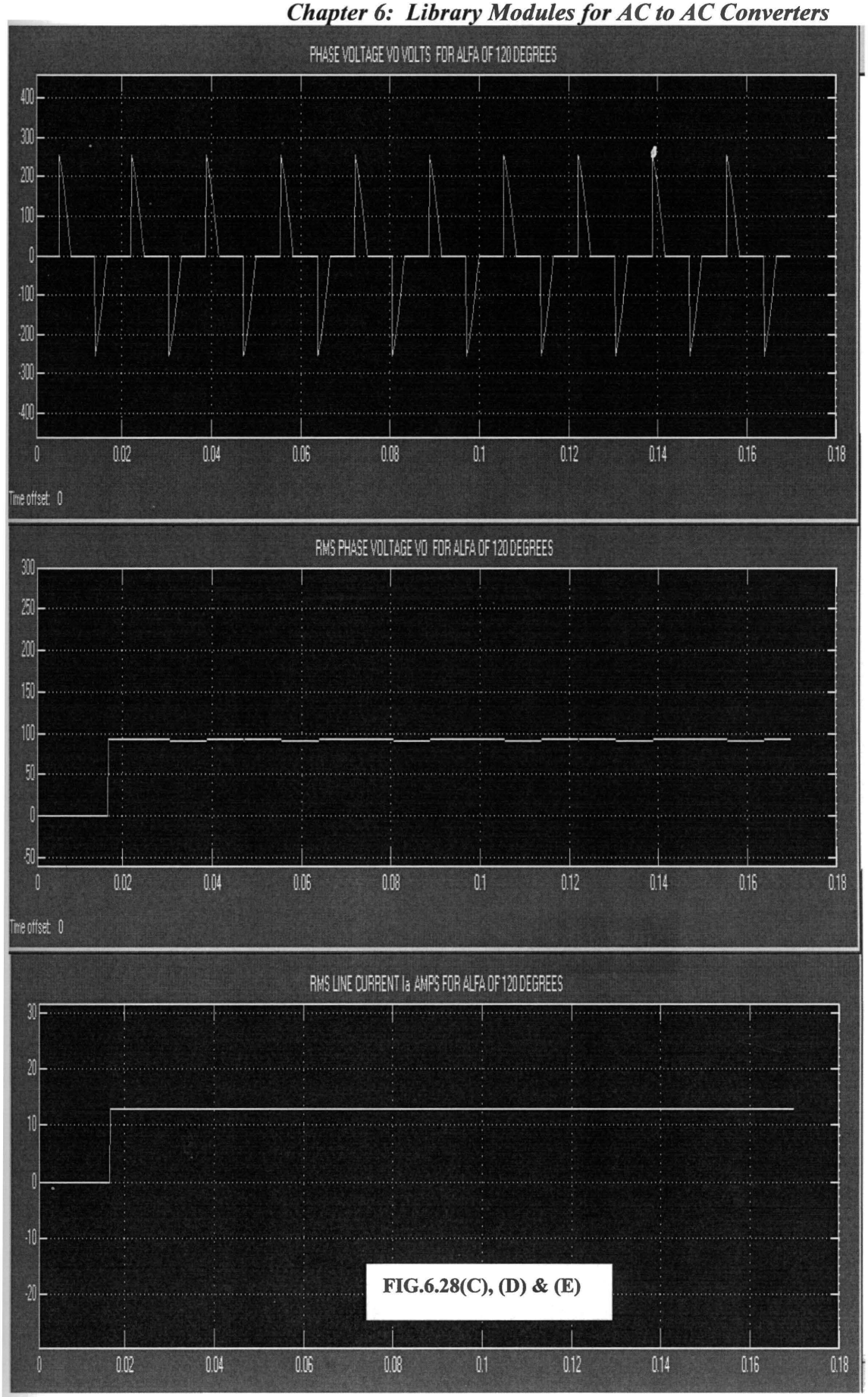
PHASE VOLTAGE VO VOLTS FOR ALFA OF 120 DEGREES
400
300
200
100
0
-100
-200
-300
-400
0
0.02
0.04
0.06
0.08
0.1
0.12
0.14
0.16
0.18
Time offset: 0
RMS PHASE VOLTAGE VO FOR ALFA OF 120 DEGREES
300
250
200
150
100
50
0
-50
0
0.02
0.04
0.06
0.08
0.1
0.12
0.14
0.16
0.18
Time offset: 0
RMS LINE CURRENT Ia AMPS FOR ALFA OF 120 DEGREES
30
20
10
0
-10
-20
0
0.02
0.04
0.06
0.08
0.1
0.12
0.14
0.16
0.18

FIG.6.28(C), (D) & (E)

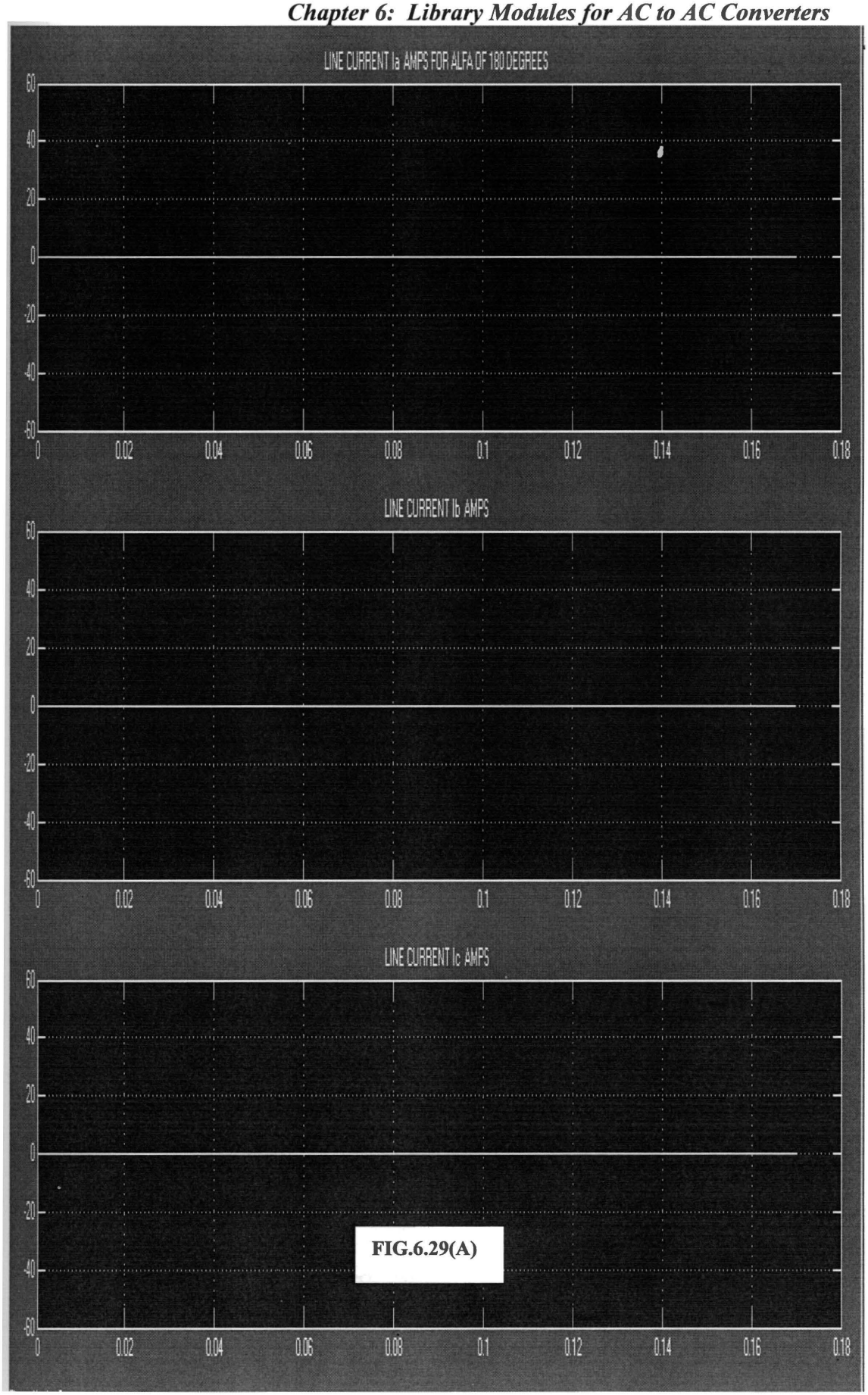
LINE CURRENT Ia AMPS FOR ALFA OF 180 DEGREES
60
40
20
0
-20
-40
-60
0
0.02
0.04
0.06
0.08
0.1
0.12
0.14
0.16
0.18
LINE CURRENT Ib AMPS
60
40
20
0
-20
-40
-60
0
0.02
0.04
0.06
0.08
0.1
0.12
0.14
0.16
0.18
LINE CURRENT Ic AMPS
60
40
20
0
-20
-40
-60
0
0.02
0.04
0.06
0.08
0.1
0.12
0.14
0.16
0.18

FIG.6.29(A)

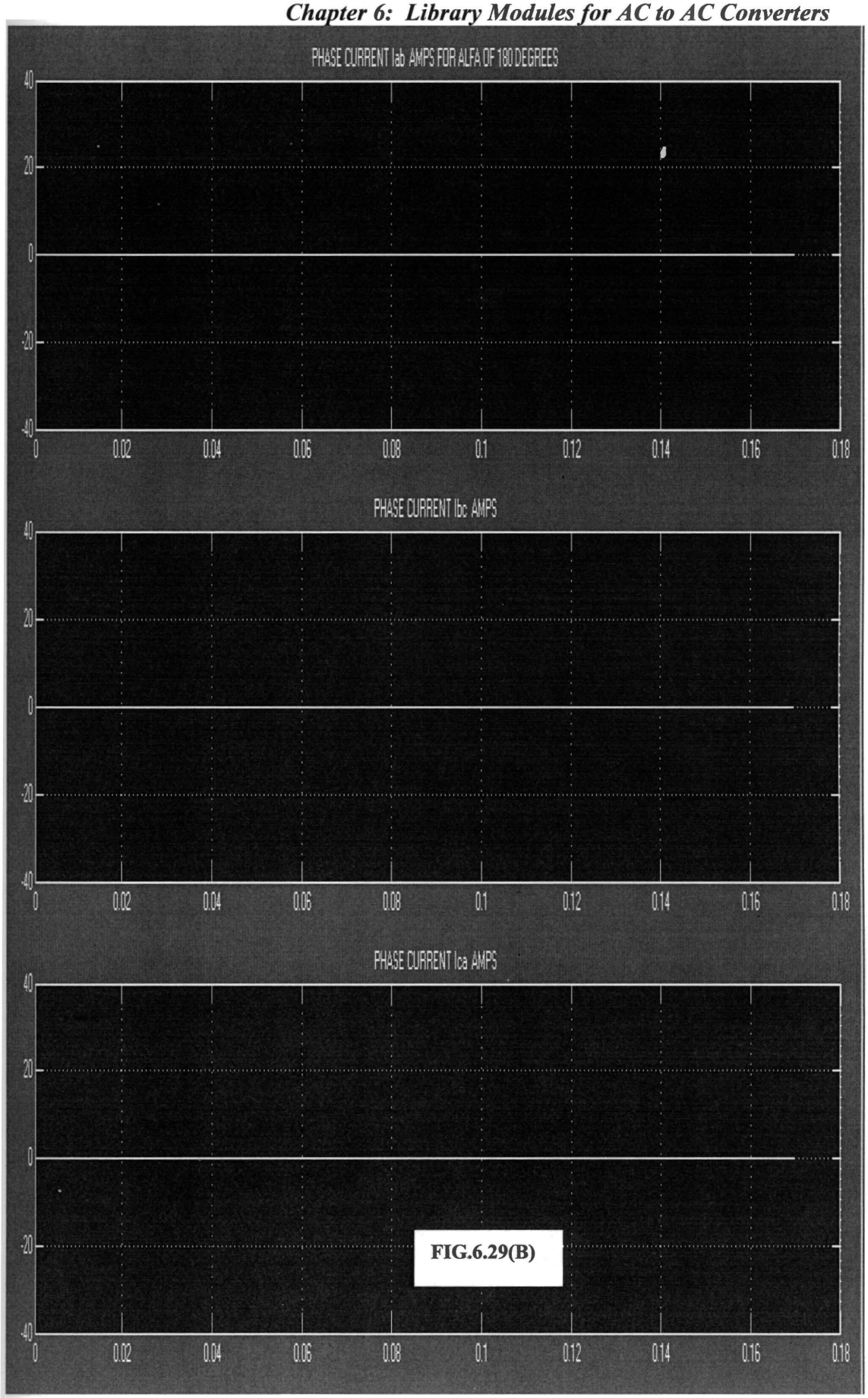
PHASE CURRENT Iab AMPS FOR ALFA OF 180 DEGREES
40
20
0
-20
-40
0
0.02
0.04
0.06
0.08
0.1
0.12
0.14
0.16
0.18
PHASE CURRENT Ibc AMPS
40
20
0
-20
-40
0
0.02
0.04
0.06
0.08
0.1
0.12
0.14
0.16
0.18
PHASE CURRENT Ica AMPS
40
20
0
-20
-40
0
0.02
0.04
0.06
0.08
0.1
0.12
0.14
0.16
0.18

FIG.6.29(B)

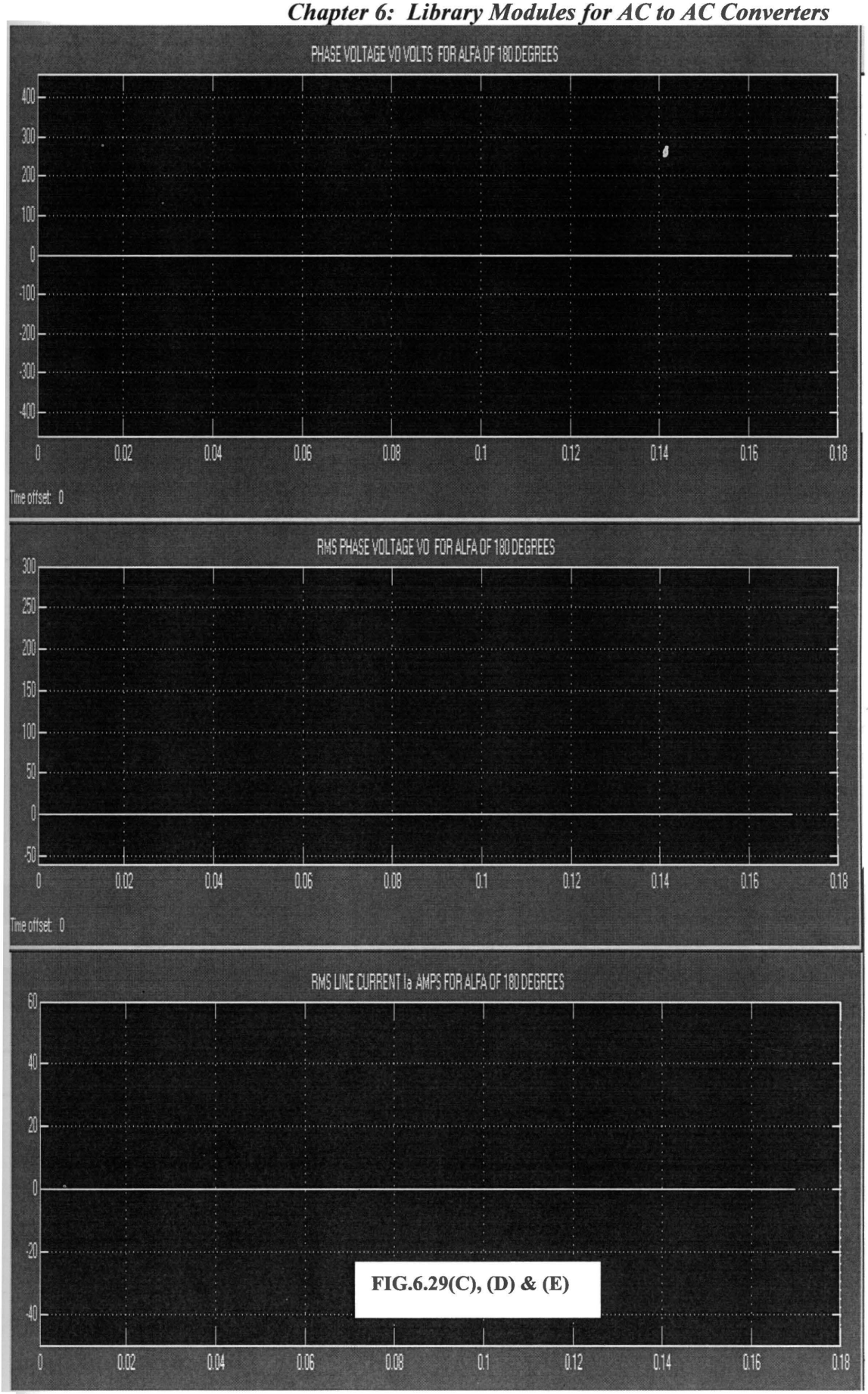
PHASE VOLTAGE VO VOLTS FOR ALFA OF 180 DEGREES
400
300
200
100
0
-100
-200
-300
-400
0
0.02
0.04
0.06
0.08
0.1
0.12
0.14
0.16
0.18
Time offset: 0
RMS PHASE VOLTAGE VO FOR ALFA OF 180 DEGREES
300
250
200
150
100
50
0
-50
0
0.02
0.04
0.06
0.08
0.1
0.12
0.14
0.16
0.18
Time offset: 0
RMS LINE CURRENT Ia AMPS FOR ALFA OF 180 DEGREES
60
40
20
0
-20
-40
0
0.02
0.04
0.06
0.08
0.1
0.12
0.14
0.16
0.18

FIG.6.29(C), (D) & (E)

TABLE 6.5 – Simulation Results for Three Phase AC Controller in Series with Delta Connected Resistive Load

Sl.No.	RMS Line to Line Supply Voltage in Volts	Frequency Hertz	Firing Angle α radians	Per Phase Load Resistance in Ohms	RMS Load Voltage Vo in Volts	RMS Load Current Iab in Amps
1	208	60	π / 6	10	204.9	20.49
2	208	60	π / 4	10	198.1	19.81
3	208	60	π / 3	10	186.6	18.66
4	208	60	π / 2	10	146.5	14.65
5	208	60	2 π / 3	10	91.84	9.184
6	208	60	π	10	0	0

TABLE 6.6 – Calculated Values for Three Phase AC Controller in Series with Delta Connected Resistive Load

Sl.No.	RMS Line to Line Supply Voltage in Volts	Frequency Hertz	Firing Angle α radians	Per Phase Load Resistance in Ohms	RMS Load Voltage Vo in Volts	RMS Load Current Iab in Amps
1	208	60	π / 6	10	173.45	17.345
2	208	60	π / 4	10	160	16.0
3	208	60	π / 3	10	151.25	15.125
4	208	60	π / 2	10	147	14.7
5	208	60	2 π / 3	10	91.944	9.1944
6	208	60	π	10	0	0

The simulation results for various firing angle α are tabulated in Table 6.5. **The RMS load voltage Vo** obtained by using equation 6.15 for various firing angle α and the calculated load current per phase are tabulated in Table 6.6.

6.4 Conclusions

System models for Three Phase AC Controller in series with lines connected to star connected resistive load with isolated neutral and also for Three Phase AC Controller in series with delta connected resistive load are developed and their simulation and theoretical results are presented. Switching Function concept is used in these model development. It is seen from Table 6.2 and 6.3 that as the firing angle α increases the percentage error between the theoretical and simulated results for line to neutral voltage across the load resistor increases. It is also seen from Table 6.5 and 6.6 that as the firing angle α increases, the percentage error between the theoretical and simulated values for Phase Voltage across the load decreases. Also Appendix E provides the comparison of the simulation results of the above three phase ac controllers using the demo version of electronic circuit simulation software PSIM 7.0.

CHAPTER 7

MODELLING OF THREE PHASE INDUCTION MOTOR DRIVES

7.1 Introduction

The steady state models such as equivalent circuits are useful to study the steady state performance of three phase induction motors (IM). This analysis neglects transients due to load and stator frequency variations. Such variations in load and stator frequency occur for variable speed drives which are converter fed from finite sources. The dynamic models of three phase IM consider the effect of variation of supply frequency, load torque, voltages and currents. The dynamics of converter fed three phase IM is to be evaluated to determine the adequacy of the converter switches and converter for a given motor and their interactions to determine the excursions of current and torque in the converter and motor. The dynamic model of three phase IM is derived in the dq0 axis. The abc to dq0 transformation is performed using the well known Park's transformation [1-2, 13]. The reference frame can be any one of arbitrary, stationary, rotor or synchronous. The voltage, current and flux linkage transformations are carried out in a generalised way to any of the above reference frames. The performance obtained in dq0 axis can be transformed back to abc axis by inverse park's transformation.

This chapter deals with the dynamic modelling of three phase IM using dq0 voltage-current equations in all reference frames. The stationary, synchronous and arbitrary reference frames are provided in one model. The desired reference frame can be selected and the performance of three phase IM in this reference frame can be observed.

7.2 Dynamic Model of Three Phase Induction Motor

The model of three phase IM is developed in two axis known as dq axis [13]. A two axis model of a three phase IM is shown in Fig.7.1. The stator windings are displaced

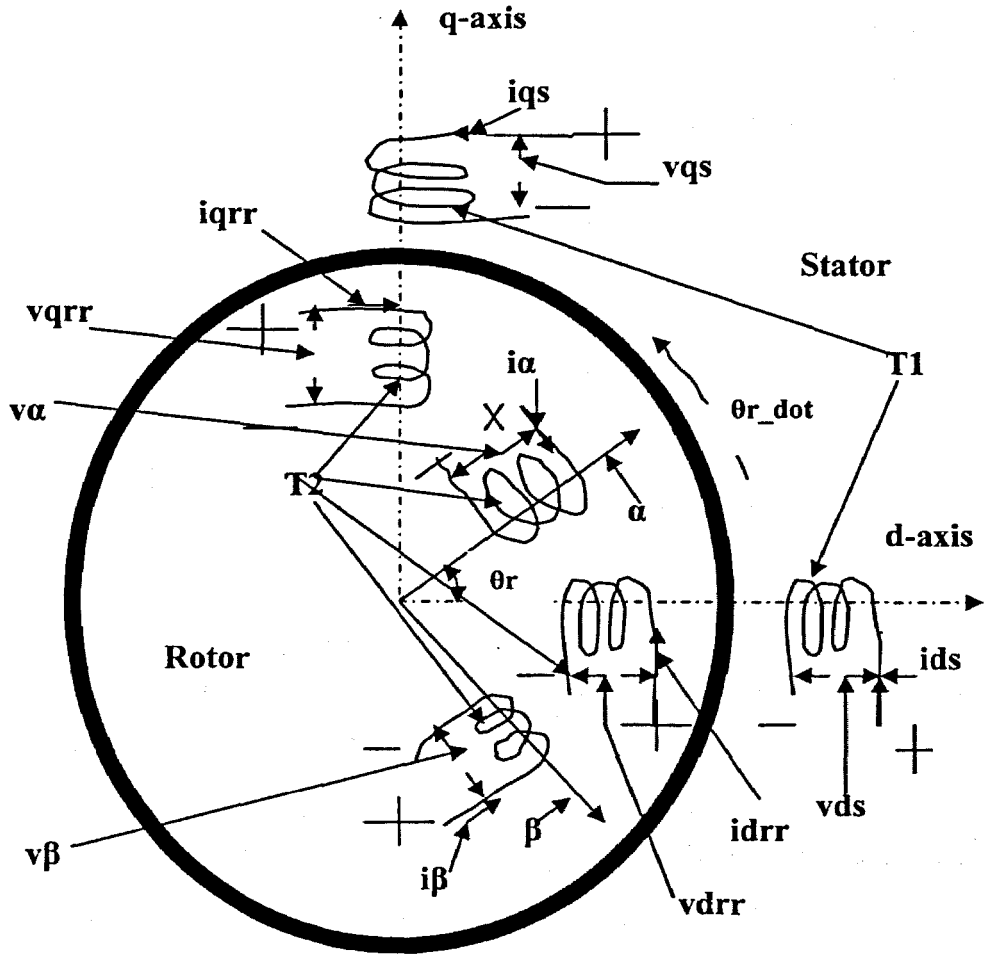

Fig.7.1: Two axis representation of three phase IM

in space by 90 degrees. The rotor winding α is at an angle θr from the stator d-axis winding. The voltages and currents are marked in Fig.7.1. The angle θr is the rotor position in electrical radians at any instant of time. With this arrangement, the mutual inductances between stator and rotor are functions of cos θr and sin θr and thus are time varying. To obtain constant mutual inductance between stator and rotor, the rotor windings are aligned along the d-axis and q-axis, as shown in Fig.7.1. The induction machine equation referred to stator side is given by equation 7.1. In equation 7.1, the following symbols are used:

v_{qs}, v_{qr} - q-axis stator and rotor terminal voltages.

v_{ds}, v_{dr} - d-axis stator and rotor terminal voltages.

$$\begin{bmatrix} v_{qs} \\ v_{ds} \\ v_{qr} \\ v_{dr} \end{bmatrix} = \begin{bmatrix} R_S + sL_S & 0 & sL_m & 0 \\ 0 & R_S + sL_S & 0 & sL_m \\ sL_m & -L_m.\theta_{r\_dot} & R_r + sL_r & -L_r.\theta_{r\_dot} \\ L_m.\theta_{r\_dot} & sL_m & L_r.\theta_{r\_dot} & R_r + sL_r \end{bmatrix} * \begin{bmatrix} i_{qs} \\ i_{ds} \\ i_{qr} \\ i_{dr} \end{bmatrix} \qquad (7.1)$$

i_{qs}, i_{qr} - q-axis stator and rotor winding currents.

Ls, Lr - Stator and Rotor self inductances in Henries per phase.

Lm - Mutual Inductance between stator and rotor in Henries per phase.

Rs, Rr - Stator and equivalent rotor resistance in Ohms per phase.

θr_dot - Rotor angular speed in electrical radians per second $\left(\frac{d\theta_r}{dt}\right)$.

s - Transform operator d/dt.

7.3 Analysis of Three Phase Induction Motor Using DQ-Axis Voltage – Current Equations in Arbitrary Reference Frames

Reference frames are like observer platforms which simplifies the system equations. It is advantageous to derive the system model in any arbitrary reference frame rotating at any arbitrary angular speed ω_c radians per second and then transfer this model to any desired reference frame. The relationship between the stationary reference frame marked by dq-axis and arbitrary reference frame marked by d^cq^c-axis is shown in Fig.7.2 [13]. The relationship between the electrical quantities in the stationary dq reference frame and the arbitrary d^cq^c reference frame is given by equation 7.2 below:

$$\begin{bmatrix} f_{qs} \\ f_{ds} \end{bmatrix} = \begin{bmatrix} \cos\theta_C & \sin\theta_C \\ -\sin\theta_C & \cos\theta_C \end{bmatrix} * \begin{bmatrix} f_{qs}^C \\ f_{ds}^C \end{bmatrix} \qquad (7.2)$$

In equation 7.2, f can be a voltage, current or flux linkage.

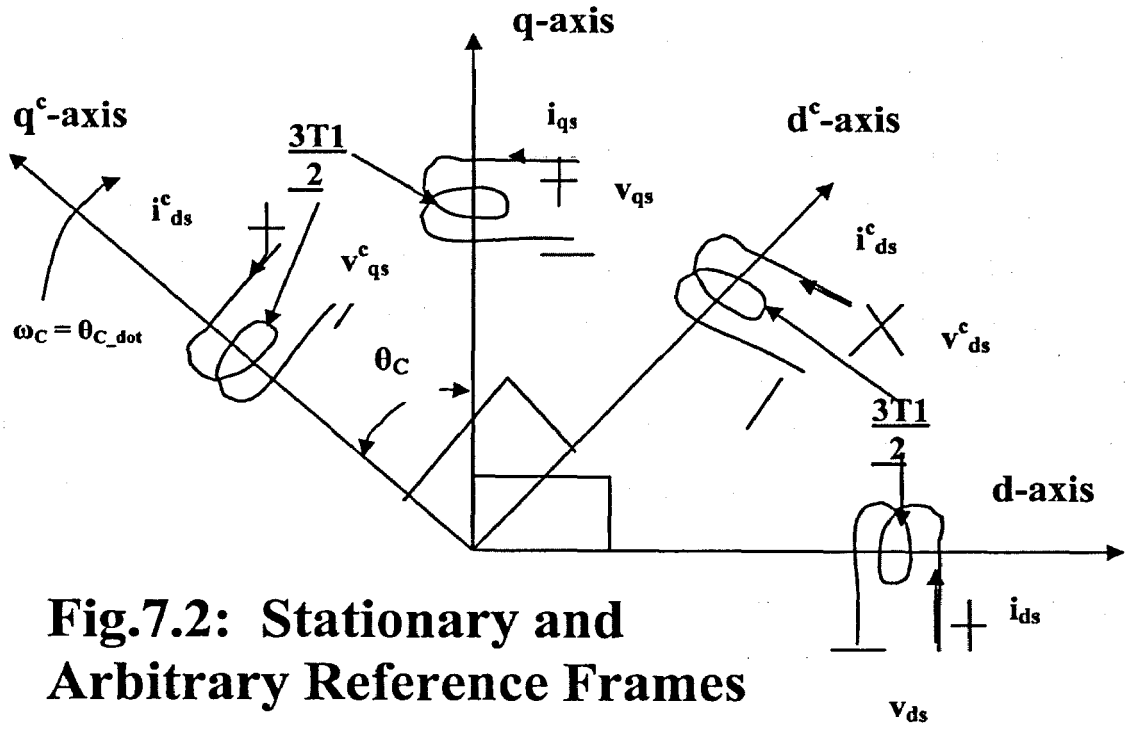

Fig.7.2: Stationary and Arbitrary Reference Frames

Equation 7.1 can be written in arbitrary reference frame as in equation 7.3 below:

$$\begin{bmatrix} v_{qs}^{C} \\ v_{ds}^{C} \\ v_{qr}^{C} \\ v_{dr}^{C} \end{bmatrix} = \begin{bmatrix} R_S+sL_S & \omega_C L_S & sL_m & \omega_C L_m \\ -\omega_C L_S & R_S+sL_S & -\omega_C L_m & sL_m \\ sL_m & (\omega_C-\omega_r)L_m & R_r+sL_r & (\omega_C-\omega_r)L_r \\ -(\omega_C-\omega_r)L_m & sL_m & -(\omega_C-\omega_r)L_r & R_r+sL_r \end{bmatrix} * \begin{bmatrix} i_{qs}^{C} \\ i_{ds}^{C} \\ i_{qr}^{C} \\ i_{dr}^{C} \end{bmatrix} \quad (7.3)$$

The electromagnetic torque Tem of the induction machine is given in equation 7.4 below:

$$T_{em} = \frac{3}{2}.\frac{P}{2}.L_m.\left(i_{qs}^{C}.i_{dr}^{C} - i_{ds}^{C}.i_{qr}^{C}\right) Nw.m \quad (7.4)$$

The transformation of voltages, currents and flux linkages from abc to qd0 and from qd0 to abc axis are done using the matrix in equation 1.1 and 1.2, with θ is replaced by θ_C..

7.3.1 Analysis of Three Phase Induction Motor Using DQ-Axis Voltage – Current Equations in Stationary, Synchronous and Rotor Reference Frames

The model of three phase IM in any other given reference frame can be derived by referring to Fig.7.2 and equation 7.3 and 7.4. For stationary or stator reference frame the angular frequency ω_C is set to zero in equation 7.3. Similarly in the transformation matrix given by equation 1.1 and 1.2, θ is set to zero. Similarly for the synchronous and rotor reference frames, this value of ω_C is set to ω_S and ω_r respectively in equation 7.3. Also in the transformation matrix in equation 1.1 and 1.2, θ is replaced by θ_S and θ_r respectively for the synchronous and rotor reference frames.

The speed of the stator frame is zero and letting $\omega_C = 0$ in equation 7.3, the resulting model in stator reference frame is given in equation 7.5 below:

$$\begin{bmatrix} v_{qs} \\ v_{ds} \\ v_{qr} \\ v_{dr} \end{bmatrix} = \begin{bmatrix} R_S + sL_S & 0 & sL_m & 0 \\ 0 & R_S + sL_S & 0 & sL_m \\ sL_m & -\omega_r.L_m & R_r + sL_r & -\omega_r.L_r \\ \omega_r.L_m & sL_m & \omega_r.L_r & R_r + sL_r \end{bmatrix} * \begin{bmatrix} i_{qs} \\ i_{ds} \\ i_{qr} \\ i_{dr} \end{bmatrix} \quad (7.5)$$

The electromagnetic torque Tem of the induction machine is given in equation 7.6 below:

$$T_{em} = \frac{3}{2}.\frac{P}{2}.L_m.\left(i_{qs}.i_{dr} - i_{ds}.i_{qr}\right) Nw.m \quad (7.6)$$

The speed of the synchronous frame is ω_S and letting $\omega_C = \omega_S$ in equation 7.3, the resulting model in synchronous reference frame is given in equation 7.7 below:

$$\begin{bmatrix} v_{qs}^e \\ v_{ds}^e \\ v_{qr}^e \\ v_{dr}^e \end{bmatrix} = \begin{bmatrix} R_S + sL_S & \omega_S.L_S & sL_m & \omega_S.L_m \\ -\omega_S.L_S & R_S + sL_S & -\omega_S.L_m & sL_m \\ sL_m & (\omega_S - \omega_r)L_m & R_r + sL_r & (\omega_S - \omega_r)L_r \\ -(\omega_S - \omega_r)L_m & sL_m & -(\omega_S - \omega_r)L_r & R_r + sL_r \end{bmatrix} * \begin{bmatrix} i_{qs}^e \\ i_{ds}^e \\ i_{qr}^e \\ i_{dr}^e \end{bmatrix} \quad (7.7)$$

The electromagnetic torque Tem of the induction machine is given in equation 7.8 below:

$$T_{em} = \frac{3}{2}.\frac{P}{2}.L_m.\left(i^e_{qs}.i^e_{dr} - i^e_{ds}.i^e_{qr}\right) Nw.m \quad (7.8)$$

The speed of the rotor frame is ω_r and letting $\omega_C = \omega_r$ in equation 7.3, the resulting model in rotor reference frame is given in equation 7.9 below:

$$\begin{bmatrix} v^r_{qs} \\ v^r_{ds} \\ v^r_{qr} \\ v^r_{dr} \end{bmatrix} = \begin{bmatrix} R_S+sL_S & \omega_r.L_S & sL_m & \omega_r.L_m \\ -\omega_r.L_S & R_S+sL_S & -\omega_r.L_m & sL_m \\ sL_m & 0 & R_r+sL_r & 0 \\ 0 & sL_m & 0 & R_r+sL_r \end{bmatrix} * \begin{bmatrix} i^r_{qs} \\ i^r_{ds} \\ i^r_{qr} \\ i^r_{dr} \end{bmatrix} \quad (7.9)$$

The electromagnetic torque Tem of the induction machine is given in equation 7.10 below:

$$T_{em} = \frac{3}{2}.\frac{P}{2}.L_m.\left(i^r_{qs}.i^r_{dr} - i^r_{ds}.i^r_{qr}\right) Nw.m \quad (7.10)$$

7.4 Model for Three Phase Induction Motor in ALL Reference Frames Using DQ Axis Voltage – Current Equations

The three phase induction motor model in all reference frame using dq-axis voltage current equation can be developed from equation 7.3 [10, 13, 28]. Rearranging equation 7.3, equation 7.11 is obtained as shown below for the arbitrary reference frame ω_C.

The model of the Three Phase IM in ALL reference frames using dq-axis voltage – current equations is shown in Fig.7.3. The model is based on equation 7.11. The various dialog boxes used in this model are shown in Fig.7.4. The various subsystems are shown in Fig.7.5(A) to (E). The various subsystems are detailed below:

Fig.7.5(A) corresponds to the dialog box Three Phase AC Input Data in Fig.7.4. In this the Line to Neutral voltage maximum value and supply angular frequency in radians per

$$\begin{bmatrix} i_{qs} \\ i_{ds} \\ i_{qr} \\ i_{dr} \end{bmatrix} = \int_0^t \left(\begin{bmatrix} L_S & 0 & L_m & 0 \\ 0 & L_S & 0 & L_m \\ L_m & 0 & L_r & 0 \\ 0 & L_m & 0 & L_r \end{bmatrix}^{-1} \mathbf{K} * \mathbf{A} \right) \left\{ \begin{bmatrix} v_{qs} \\ v_{ds} \\ v_{qr} \\ v_{dr} \end{bmatrix} - \begin{bmatrix} R_S & \omega_c L_S & 0 & \omega_c L_m \\ -\omega_c L_S & R_S & -\omega_c L_m & 0 \\ 0 & (\omega_c - \omega_r) L_m & R_r & (\omega_c - \omega_r) L_r \\ -(\omega_c - \omega_r) L_m & 0 & -(\omega_c - \omega_r) L_r & R_r \end{bmatrix} * \begin{bmatrix} i_{qs} \\ i_{ds} \\ i_{qr} \\ i_{dr} \end{bmatrix} \right\} \quad (7.11)$$

second are entered. The outputs of Fig.7.5(A) are given to Fig.7.5(B). The three Fcn blocks performing sin(u(1)) generates three phase AC displaced by 2.09 radians (120 degree). The peak value and angular frequency of this three phase ac corresponds to the peak value of line to neutral voltage and angular frequency entered in the dialog box Three Phase AC Input data in Fig.7.4. In addition Fig.7.5(B) generates θ_C which is obtained by multiplying (ω_{r_elec}*time) and also line to line voltage Vab by subtracting Van and Vbn. The outputs Van, Vbn, Vcn and θ_C are given to the four input mux in Fig.7.5(C). The Fcn7 and Fcn9 blocks connected to this mux solves for Vds and Vqs as given by the matrix equation 1.1 in chapter 1, where θ is replaced by θ_C. Vqr and Vdr referred to stator are zero as the rotor is short circuited. The dialog box Three Phase IM Inductance matrix in Fig.7.4 corresponds to Fig.7.5(C). The stator inductance in henries per phase, rotor inductance referred to stator in henries per phase and mutual inductance between stator and rotor in henries per phase are ented in this dialog box. The DSP Constnat2 block and the general Inverse (LU) blocks in fig.7.5(C) solves the inductance inverse matrix given by K in equation 7.11, which is given to the A input of Matrix multiply block. The six input mux in Fig.7.5(C) with inputs iqs, ids, iqr, idr, ω_C and ω_{re} along with the Fcn3, Fcn4, Fcn5 and Fcn6 block solves the matrix product A shown equation 7.11. The four input mux in Fig.7.5(C) with inputs Vqs, Vds, Vqr and Vdr, the connected subtract block, Matrix multiply block and integrator block solves the complete equation 7.11. Fig.7.5(D) corresponds to the dialog box Three Phase IM Rotor and Load Inertia Data in Fig.7.4. The rotor inertia, load inertia, damping constant, mutual inductance between stator and rotor and the number of poles are entered in the relevant boxes in the appropriate units. The two multiplier blocks

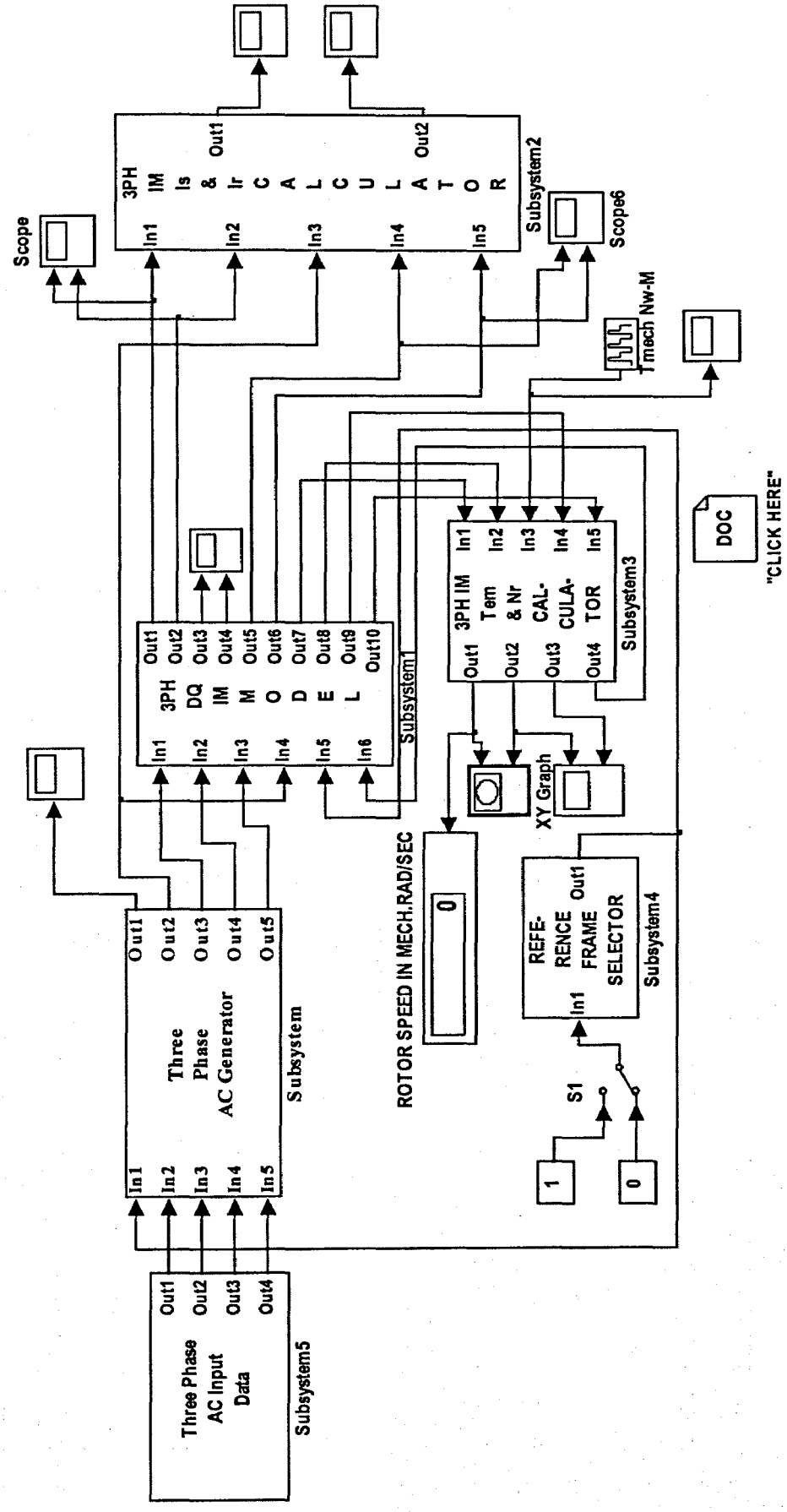

FIG.7.3 DQ-AXIS VOLTAGE - CURRENT MODEL OF THREE PHASE IM IN ALL REFERENCE FRAMES

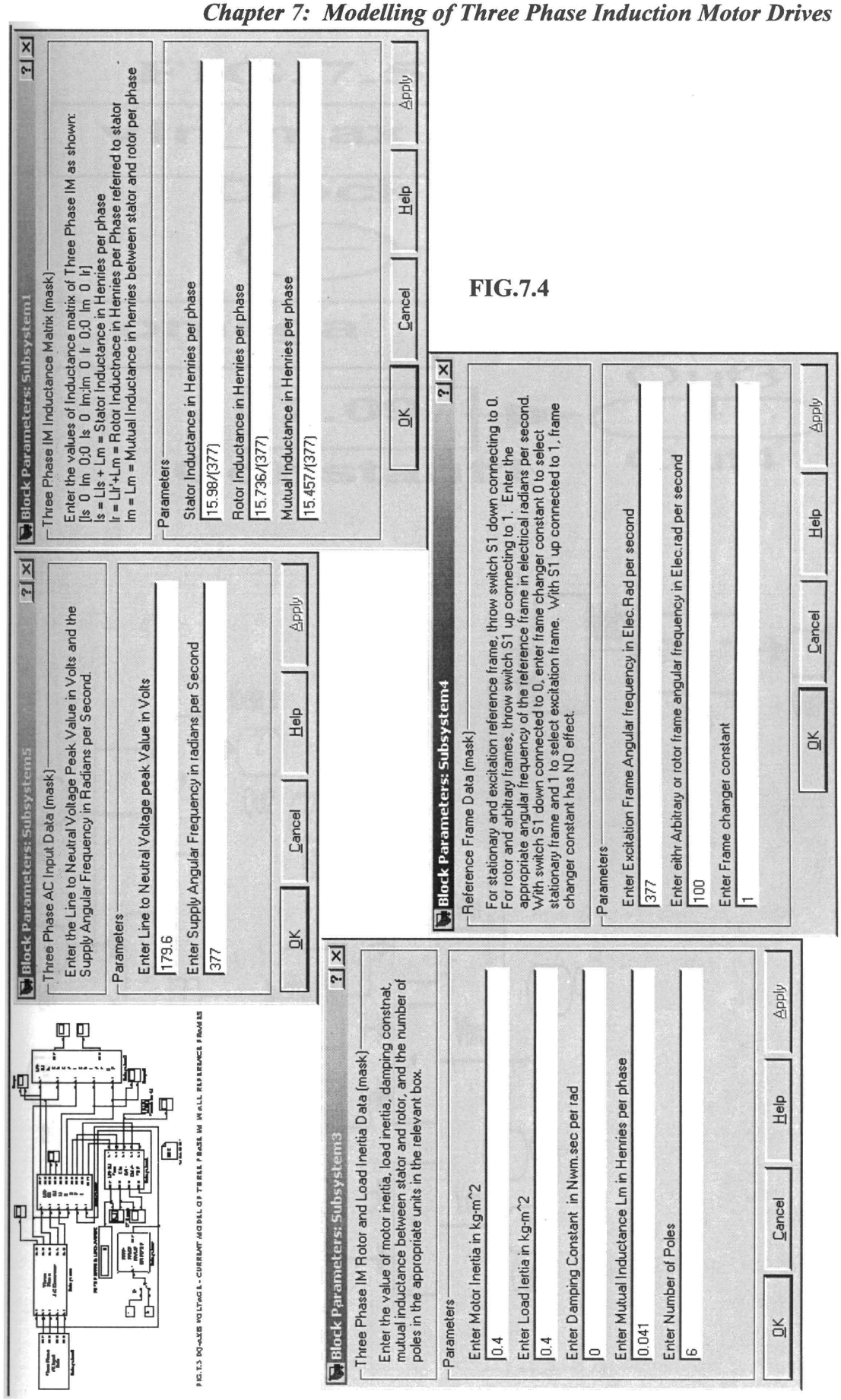
Block Parameters: Subsystem5
Three Phase AC Input Data (mask)
Enter the Line to Neutral Voltage Peak Value in Volts and the Supply Angular Frequency in Radians per Second.
Parameters
Enter Line to Neutral Voltage peak Value in Volts
179.6
Enter Supply Angular Frequency in radians per Second
377
OK
Cancel
Help
Apply
Block Parameters: Subsystem1
Three Phase IM Inductance Maltrix (mask)
Enter the values of Inductance matrix of Three Phase IM as shown:
[ls 0 lm 0;0 ls 0 lm;lm 0 lr 0;0 lm 0 lr]
ls = Lls + Lm = Stator Inductance in Henries per phase
lr = Llr+Lm = Rotor Inductnace in Henries per Phase referred to stator
lm = Lm = Mutual Inductance in henries between stator and rotor per phase
Parameters
Stator Inductance in Henries per phase
15.98/(377)
Rotor Inductance in Henries per phase
15.736/(377)
Mutual Inductance in Henries per phase
15.457/(377)
OK
Cancel
Help
Apply
Block Parameters: Subsystem3
Three Phase IM Rotor and Load Inertia Data (mask)
Enter the value of motor inertia, load inertia, damping constnat, mutual inductance between stator and rotor, and the number of poles in the appropriate units in the relevant box.
Parameters
Enter Motor Inertia in kg-m^2
0.4
Enter Load Ieitia in kg-m^2
0.4
Enter Damping Constant in Nwm.sec per rad
0
Enter Mutual Inductance Lm in Henries per phase
0.041
Enter Number of Poles
6
OK
Cancel
Help
Apply
Block Parameters: Subsystem4
Reference Frame Data (mask)
For stationary and excitation reference frame, throw switch S1 down connecting to 0. For rotor and arbitrary frames, throw switch S1 up connecting to 1. Enter the appropriate angular frequency of the reference frame in electrical radians per second. With switch S1 down connected to 0, enter frame changer constant 0 to select stationary frame and 1 to select excitation frame. With S1 up connected to 1, frame changer constant has NO effect.
Parameters
Enter Excitation Frame Angular frequency in Elec.Rad per second
377
Enter eithr Arbitrary or rotor frame angular frequency in Elec.rad per second
100
Enter Frame changer constant
1
OK
Cancel
Help
Apply

FIG.7.4

FIG.7.5(A)

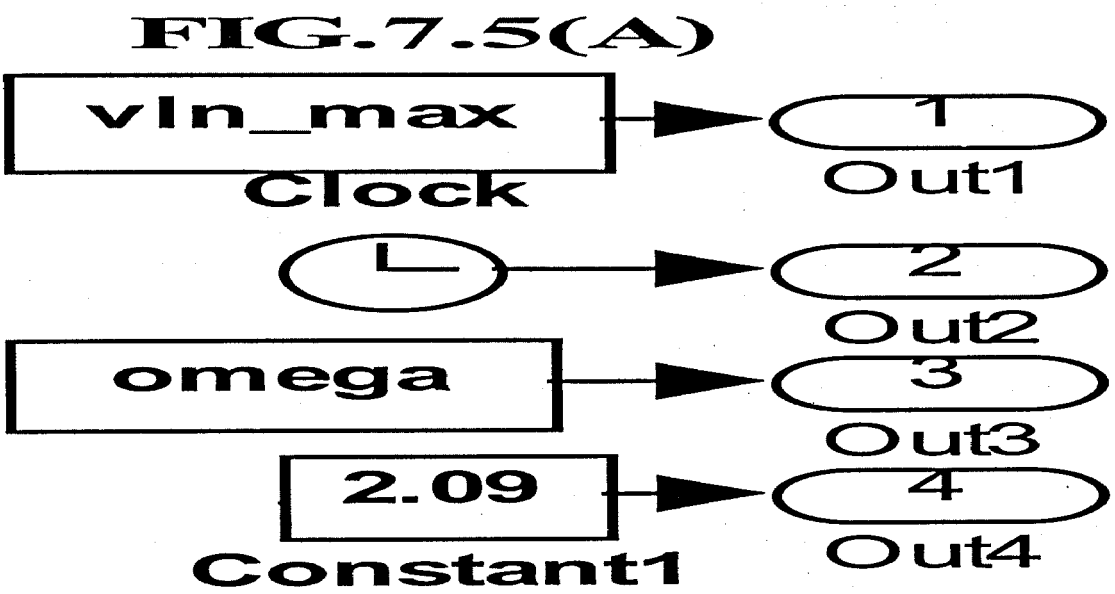

FIG.7.5(B)

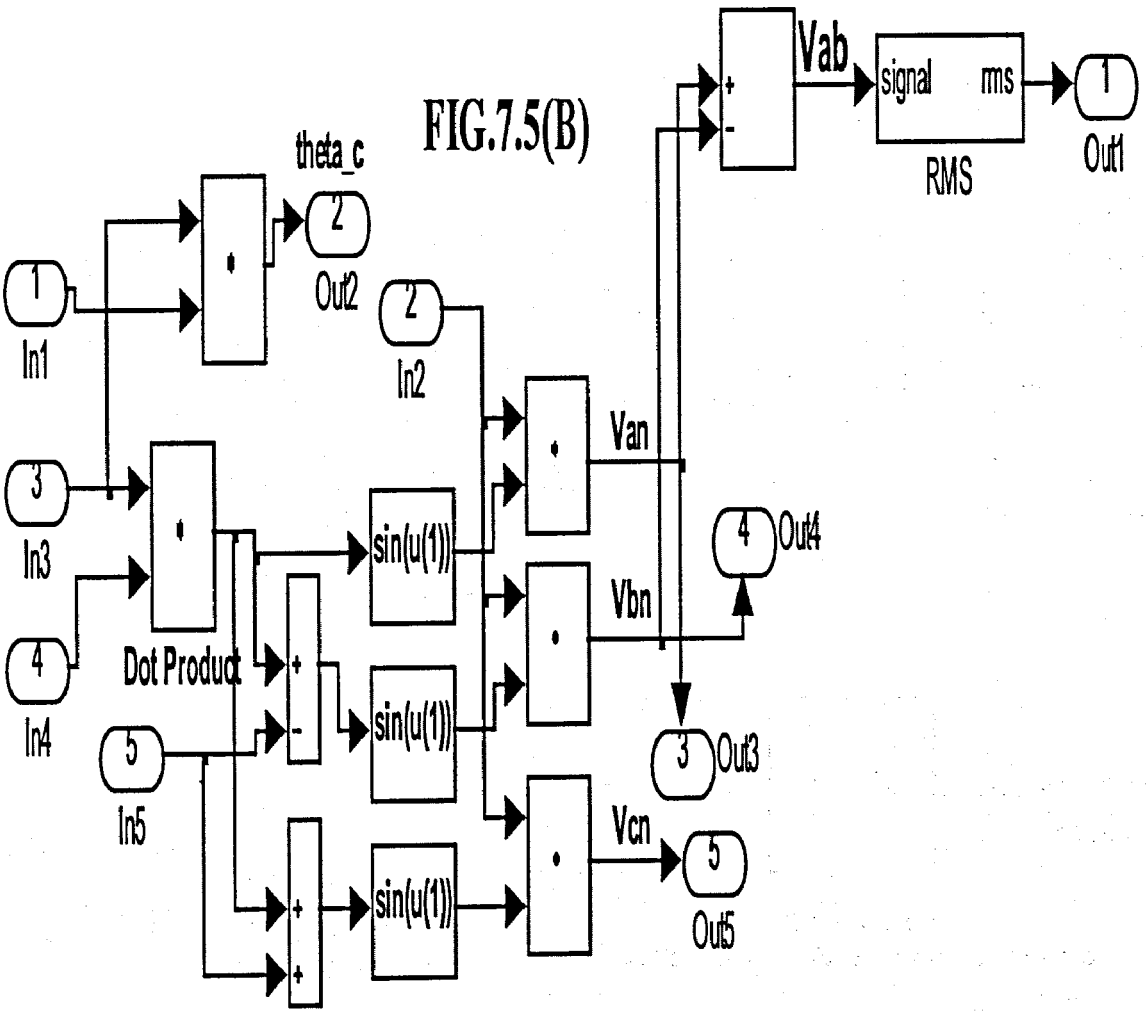

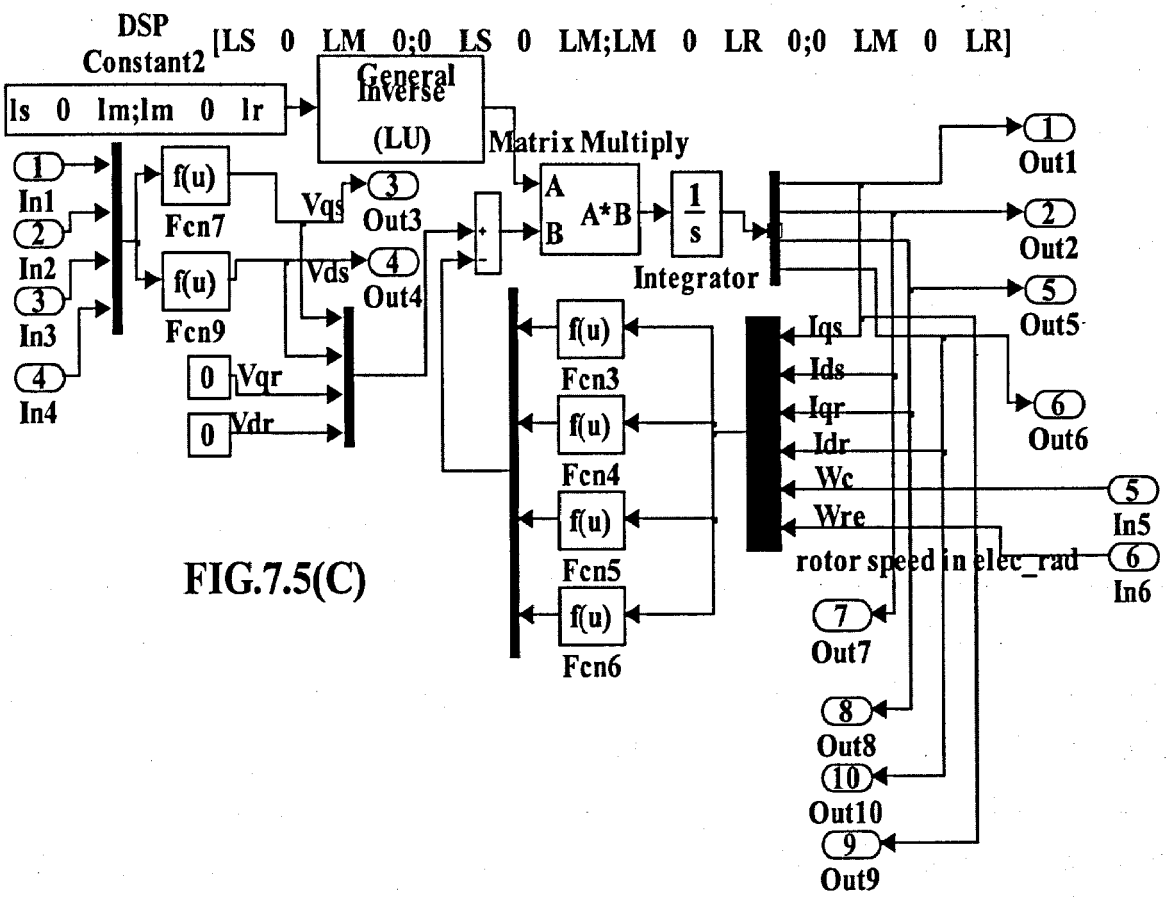

FIG.7.5(C)

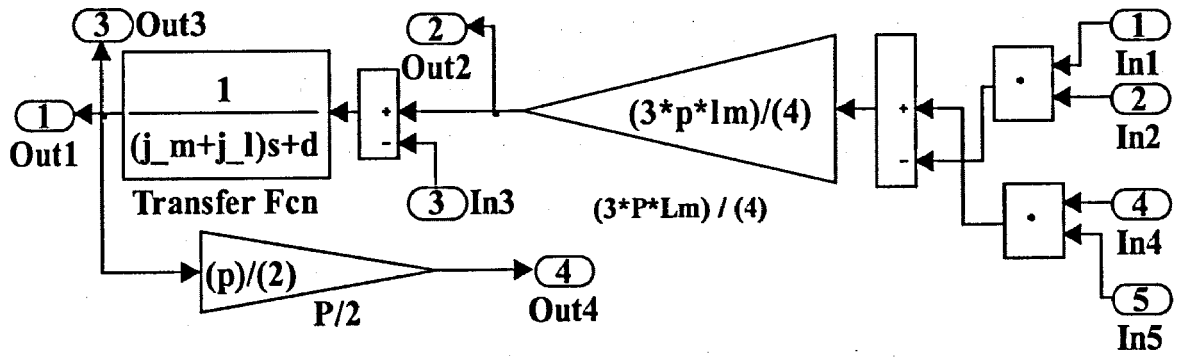

FIG.7.5(D)

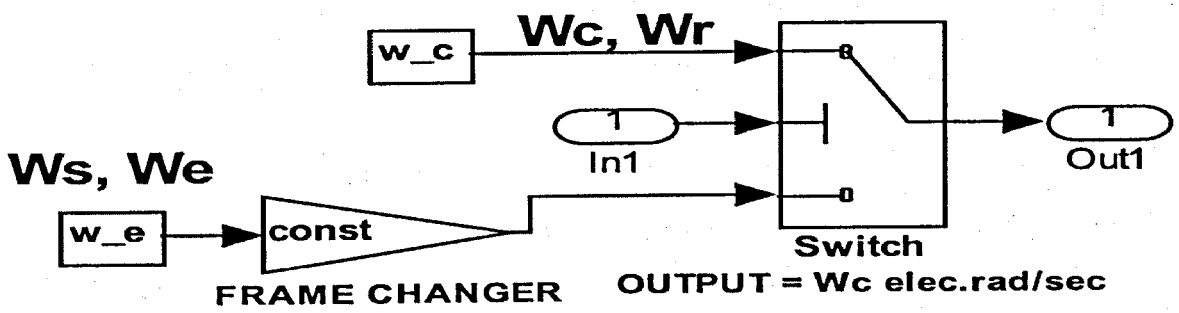

FIG.7.5(E)

along with the gain block with multiplier [(3.P.Lm) / 4] in Fig.7.5(D) solves rotor electromagnetic torque Tem given by equation 7.4. The value of Tem is subtracted from external mechanical load torque Tmech using a subtract block. Tmech is generated using repeating sequence as shown in Fig.7.3. The output (Tem – Tmech) is given to the Transfer Fcn block. The transfer function of the Transfer Fcn block given by [1 / ((j_l + j_m).s + d)] gives rotor angular mechanical speed $\omega_{mech.}$ This value of $\omega_{mech.}$ is multiplied by [P / 2] using gain multiplier block to obtain the rotor angular speed ω_{elec} in electrical radians per second. Also j_l, j_m, d and P are the rotor inertia, load inertia, damping constant and the number of poles respectively. Fig.7.5(E) corresponds to the dialog box Reference Frame data in Fig.7.4. The excitation frame angular frequency, arbitrary/rotor frame angular frequency, Frame changer constant either 0 or 1 (0 for stationary frame and 1 for excitation frame/synchronous frame with switch S1 in Fig.7.3 down connected to zero. This frame changer constant has NO effect if this switch S! is thrown up connected to 1. The switch S1 is up connected to 1 for rotor/arbitrary reference frame frequency) are entered in the relevant box. Referring to Fig.7.5(E), the constant block w_c is connected to u(1) input, switch S1 is connected to u(2) and the constant block w_e is connected u(3) input of the threshold switch marked switch. The threshold value is 0.5. The output of this switch corresponds to u(1), if u(2) is greater than or equal to this threshold value, else this output corresponds to u(3) input. Thus the required frame can be selected.

7.4.1 Simulation Results

The simulation of the three phase IM was carried out in all reference frames using SIMULINK6.0 with ode15s(stiff/NDF) solver. The parameters of the three phase star connected squirrel cage IM used for simulation are given in Table 7.1 [10]. The simulation was carried out in the following reference frames:

1. Stationary(Stator) reference frame $\omega_C = \omega_S = 0$
2. Synchronous(excitation) reference frame $\omega_C = \omega_e = 377$ elec.rad per sec.
3. Rotor reference frame $\omega_C = \omega_r = 210$ elec.rad per sec.
4. Arbitrary reference frame $\omega_C = 100$ elec.rad per sec.

TABLE 7.1

Sl.No.	Three Phase IM Parameters	Value	Unit
1	Rated Power	7.46	kW
2	Rated Stator Voltage Vs	220	Volts
3	Rated supply frequency f	60	Hertz
4	Rated speed Nr	1164	rpm
5	Number of Poles P	6	
6	Stator Resistance Rs	0.294	Ω/ph
7	Stator Leakage Reactance Xls	0.524	Ω/ph
8	Rotor Resistance referred to stator Rr'	0.156	Ω/ph
9	Rotor Leakage reactance referred to stator Xlr'	0.279	Ω/ph
10	Magnetising reactance or Mutual reactance between stator and rotor Xm	15.457	Ω/ph
11	Rated EM Torque of Motor Tem	61.2	Nw.m
12	Moment of Inertia of rotor Jm	0.4	$Kg.m^2$
13	Moment of Inertia of Load Jl	0.4	$Kg.m^2$

In the simulation on all the above reference frames, the load torque Tmech changes as follows:

$$\begin{aligned} T_{mech} &= 30.6 \quad for \quad 0 \le t \le 1sec \\ &= 91.8 \quad for \quad 1 \le t \le 2sec \\ &= 61.2 \quad for \quad 2 \le t \le 3sec \end{aligned} \qquad (7.12)$$

The simulation results for the rotor electromagnetic torque Tem, rotor speed, stator current, rotor current referred to stator and torque-speed curves are shown for each of the above reference frames. Fig.7.6(A) to (E) corresponds to stationary reference frame for $\omega_C = 0$, Fig.7.7(A) to (E) for synchronous (excitation) reference frame for $\omega_C = 377$ elec.rad per second, Fig.7.8(A) to (E) correspond to rotor reference frame for $\omega_C = 210$ elec.rad per second and Fig.7.9(A) to (E) corresponds to arbitrary reference frame for $\omega_C = 100$ elec.rad per second.

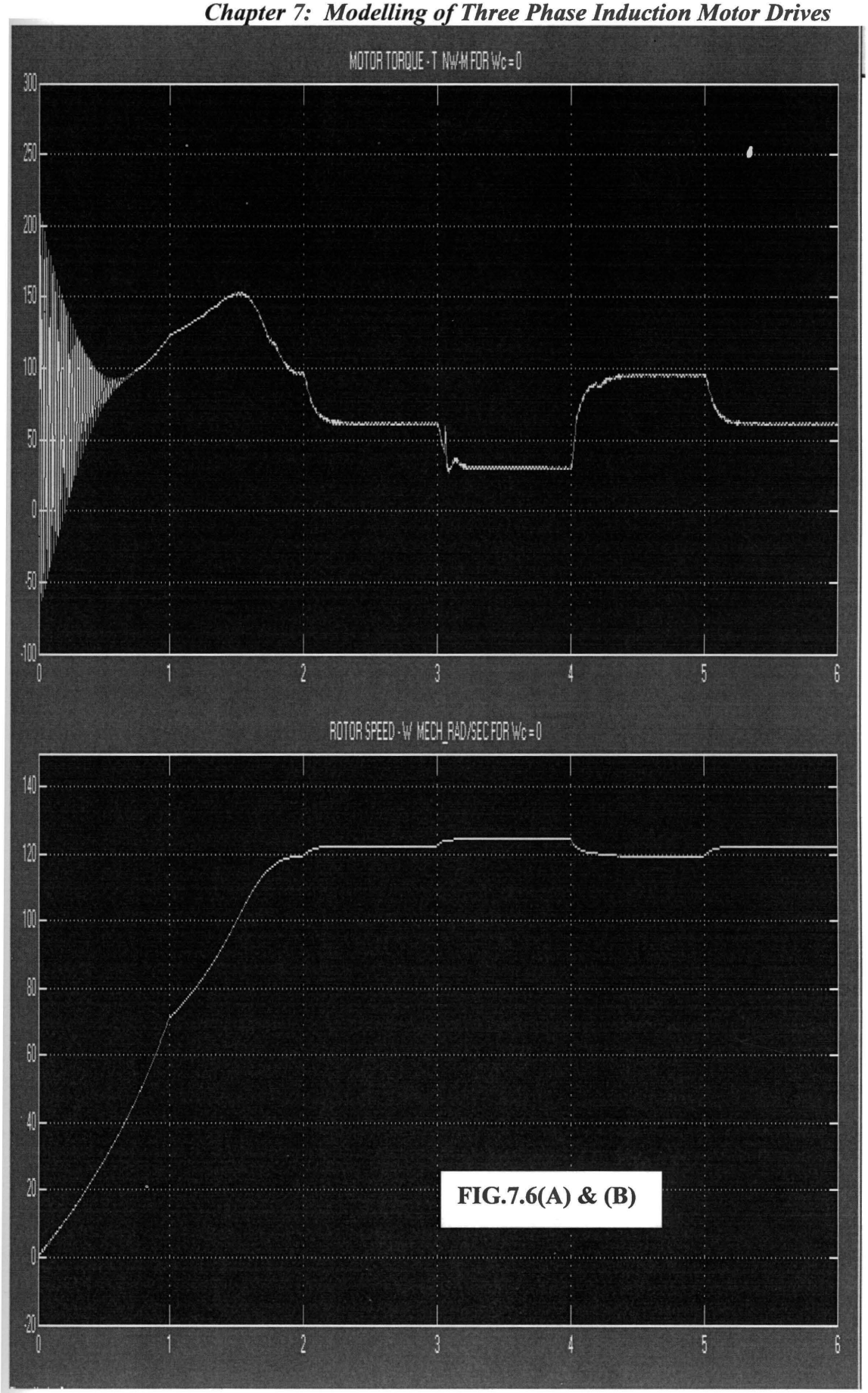
MOTOR TORQUE - T NWM FOR Wc = 0
300
250
200
150
100
50
0
-50
-100
0
1
2
3
4
5
6
ROTOR SPEED - W MECH_RAD/SEC FOR Wc = 0
140
120
100
80
60
40
20
0
-20
0
1
2
3
4
5
6

FIG.7.6(A) & (B)

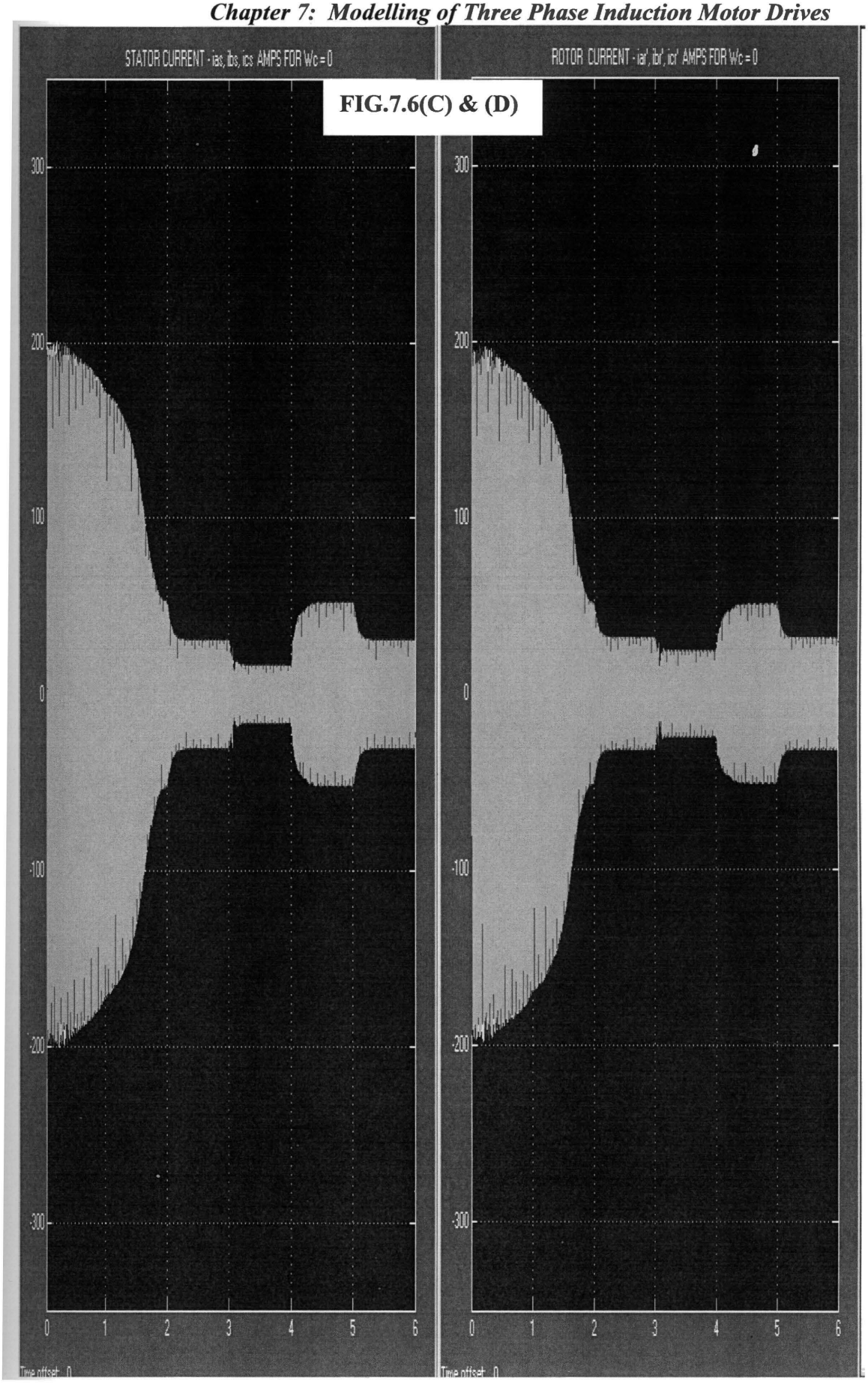
STATOR CURRENT - ias, ibs, ics AMPS FOR Wc = 0
ROTOR CURRENT - ias', ibs', ics' AMPS FOR Wc = 0
300
200
100
0
-100
-200
-300
0
1
2
3
4
5
6
Time offset: 0

FIG.7.6(C) & (D)

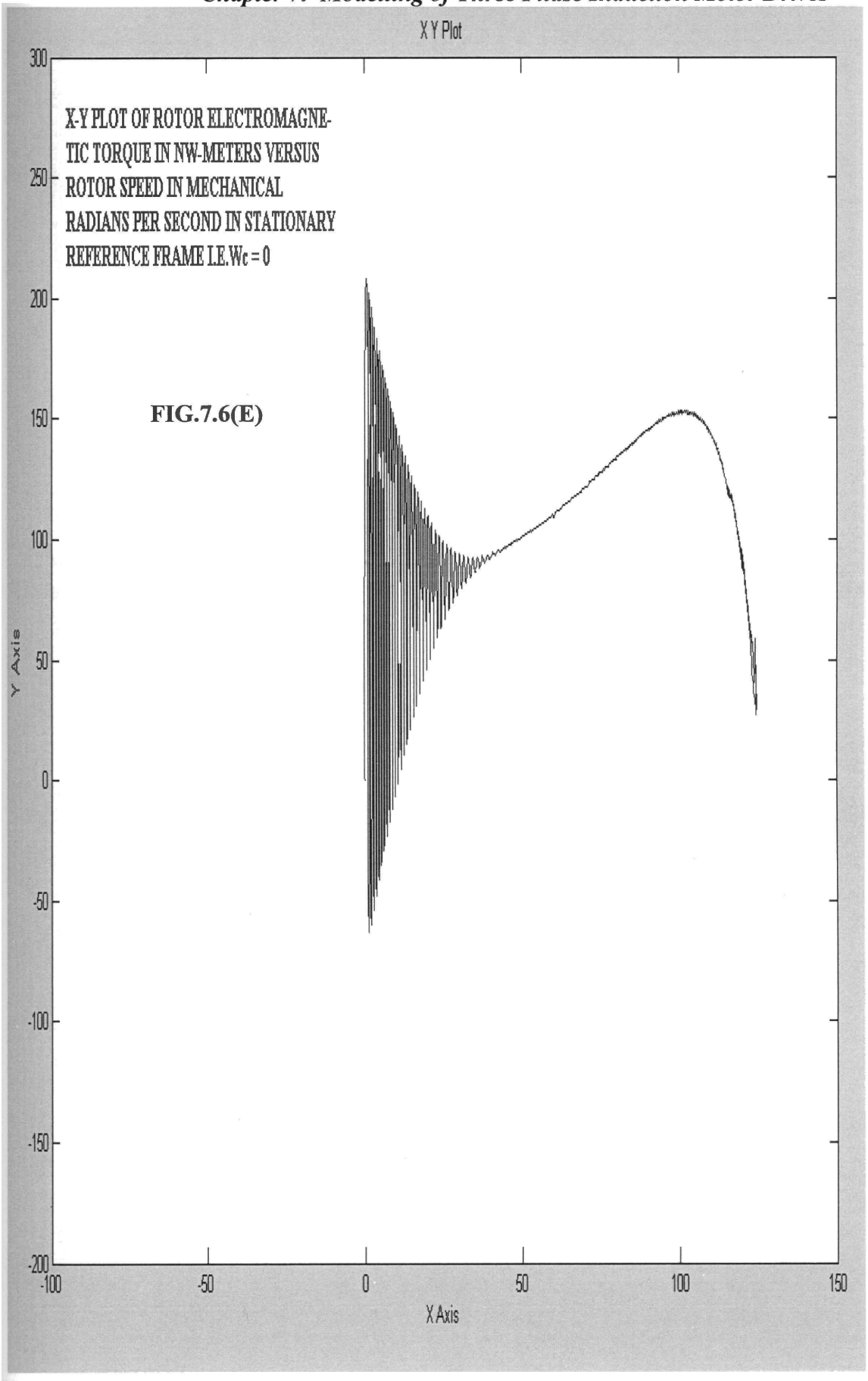
X Y Plot
X-Y PLOT OF ROTOR ELECTROMAGNE-
TIC TORQUE IN NW-METERS VERSUS
ROTOR SPEED IN MECHANICAL
RADIANS PER SECOND IN STATIONARY
REFERENCE FRAME I.E.Wc = 0
Y Axis
X Axis
300
250
200
150
100
50
0
-50
-100
-150
-200
-100
-50
0
50
100
150

FIG.7.6(E)

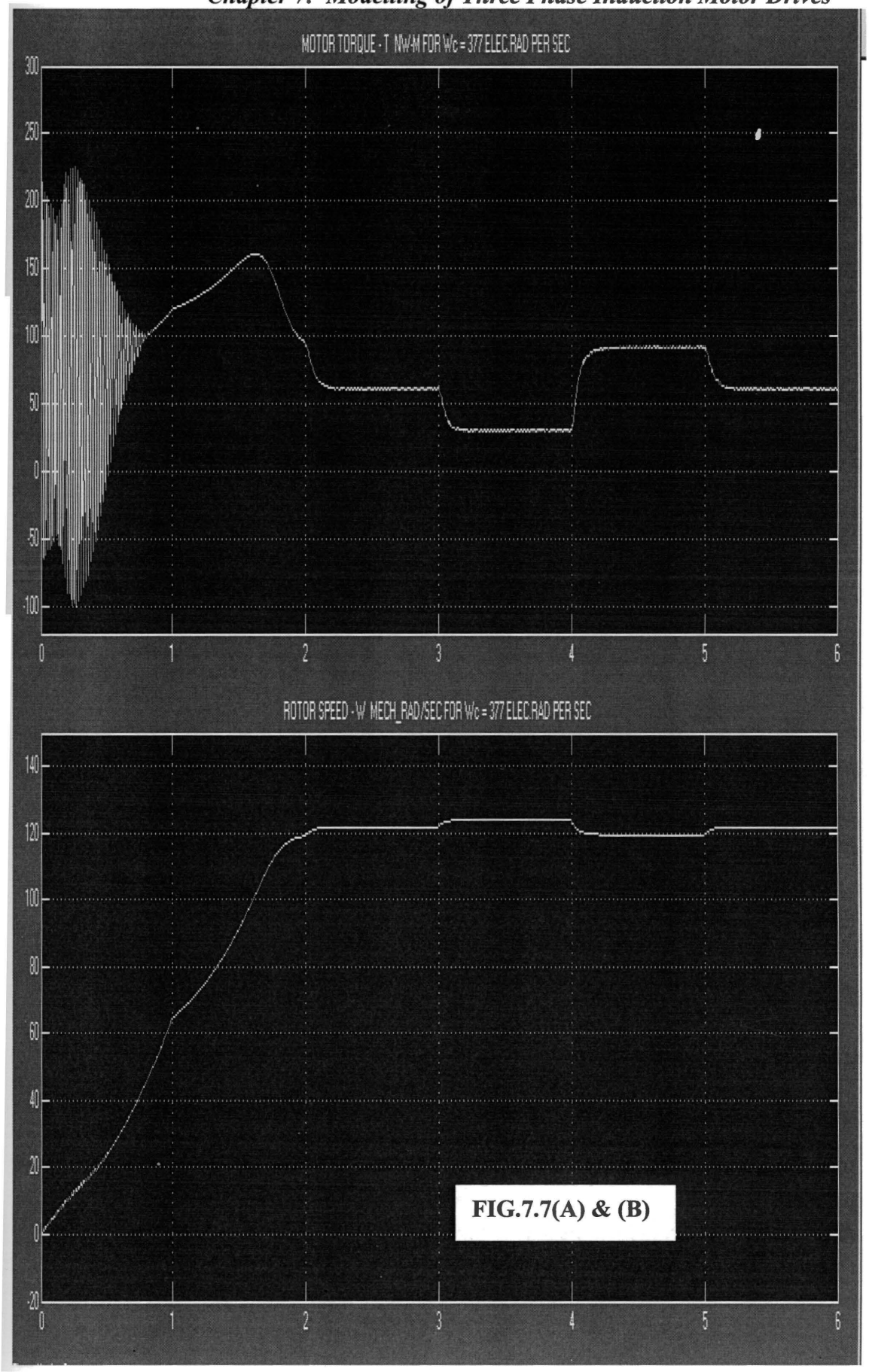
MOTOR TORQUE - T NWM FOR Wc = 377 ELEC.RAD PER SEC
300
250
200
150
100
50
0
-50
-100
0
1
2
3
4
5
6
ROTOR SPEED - W MECH_RAD/SEC FOR Wc = 377 ELEC.RAD PER SEC
140
120
100
80
60
40
20
0
-20
0
1
2
3
4
5
6

FIG.7.7(A) & (B)

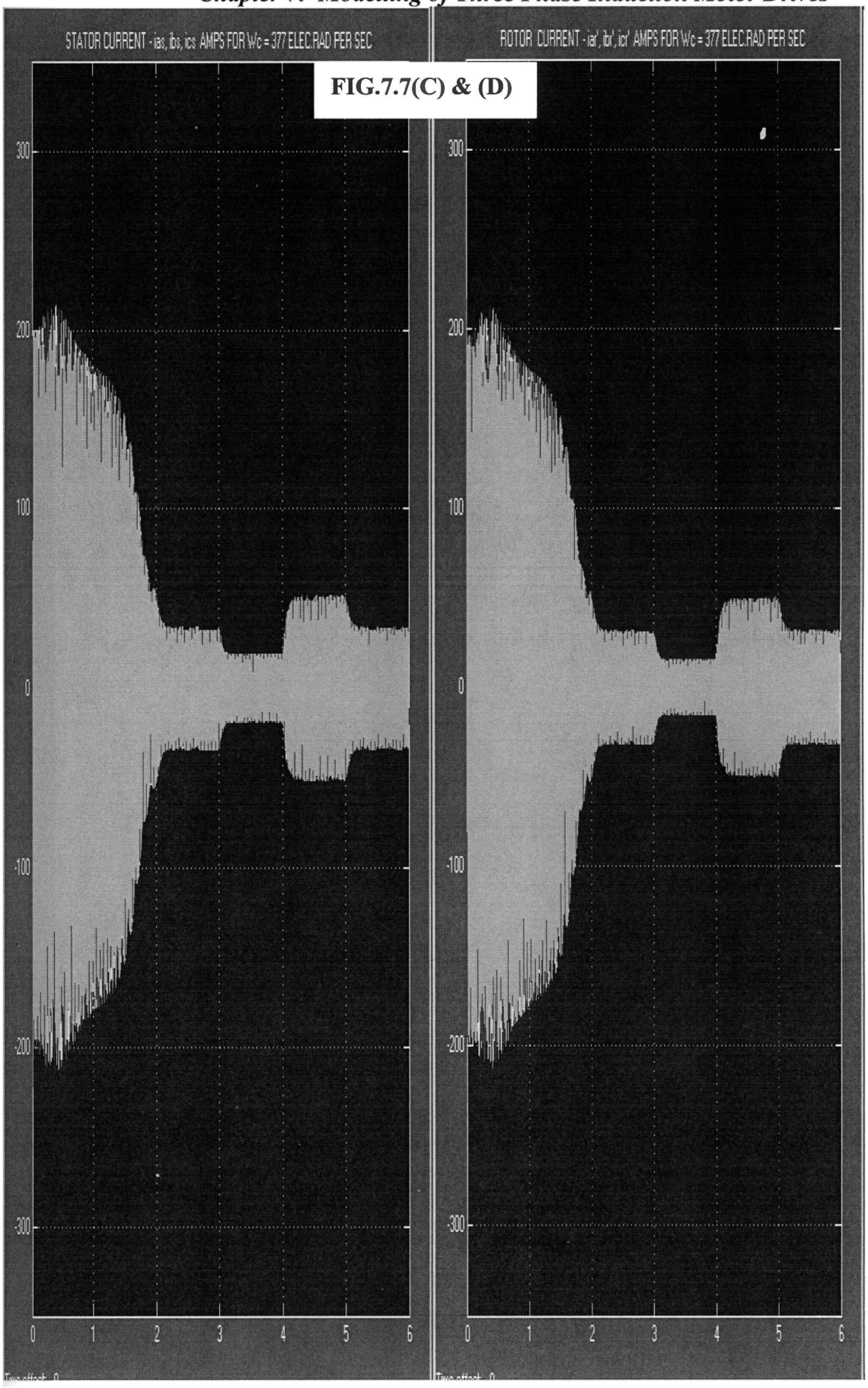
STATOR CURRENT - ias, ibs, ics AMPS FOR Wc = 377 ELEC.RAD PER SEC
ROTOR CURRENT - ia', ib', ic' AMPS FOR Wc = 377 ELEC.RAD PER SEC
300
200
100
0
-100
-200
-300
0
1
2
3
4
5
6

FIG.7.7(C) & (D)

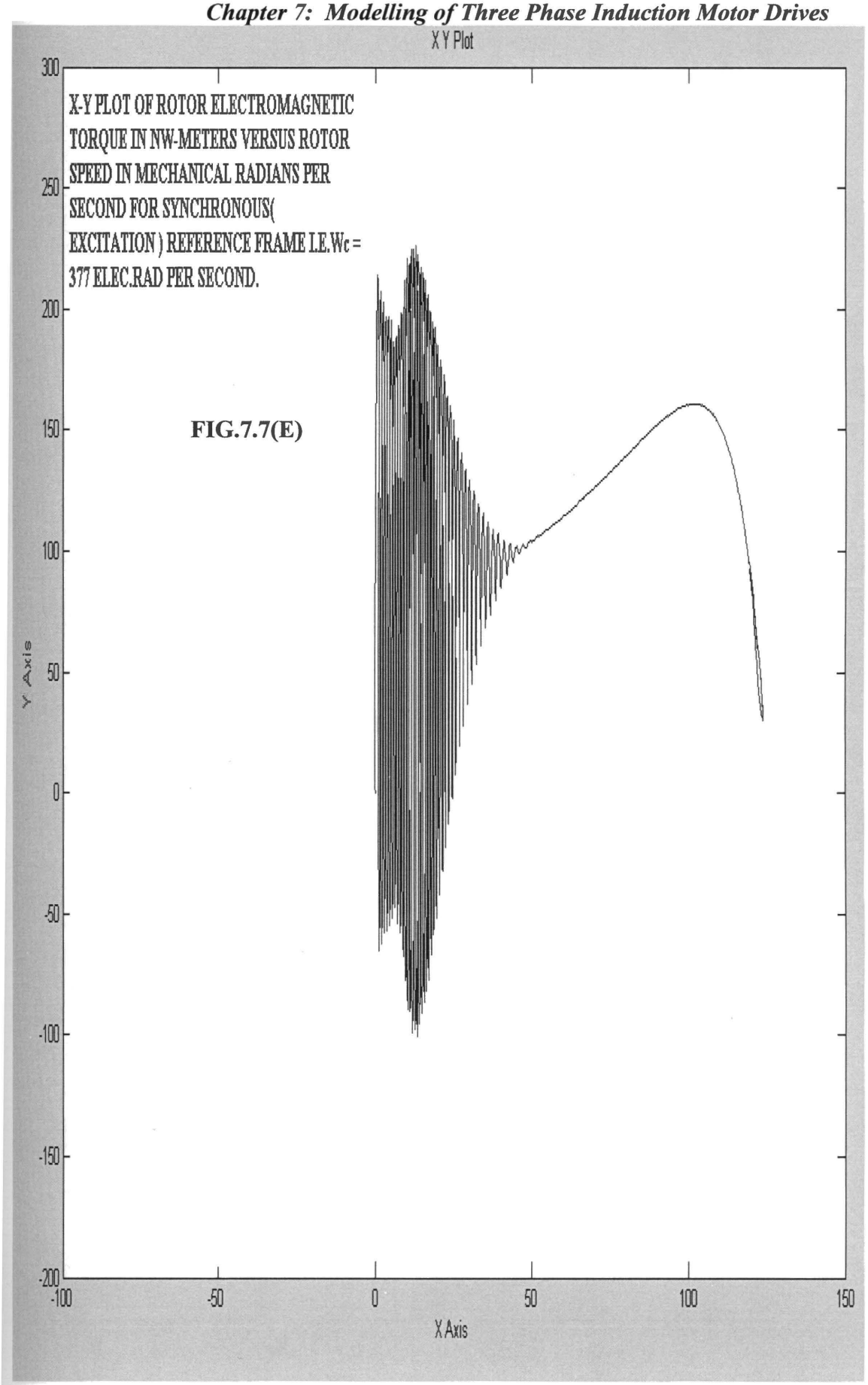
X Y Plot
X-Y PLOT OF ROTOR ELECTROMAGNETIC TORQUE IN NW-METERS VERSUS ROTOR SPEED IN MECHANICAL RADIANS PER SECOND FOR SYNCHRONOUS(EXCITATION) REFERENCE FRAME I.E.Wc = 377 ELEC.RAD PER SECOND.
Y Axis
X Axis
300
250
200
150
100
50
0
-50
-100
-150
-200
-100
-50
0
50
100
150

FIG.7.7(E)

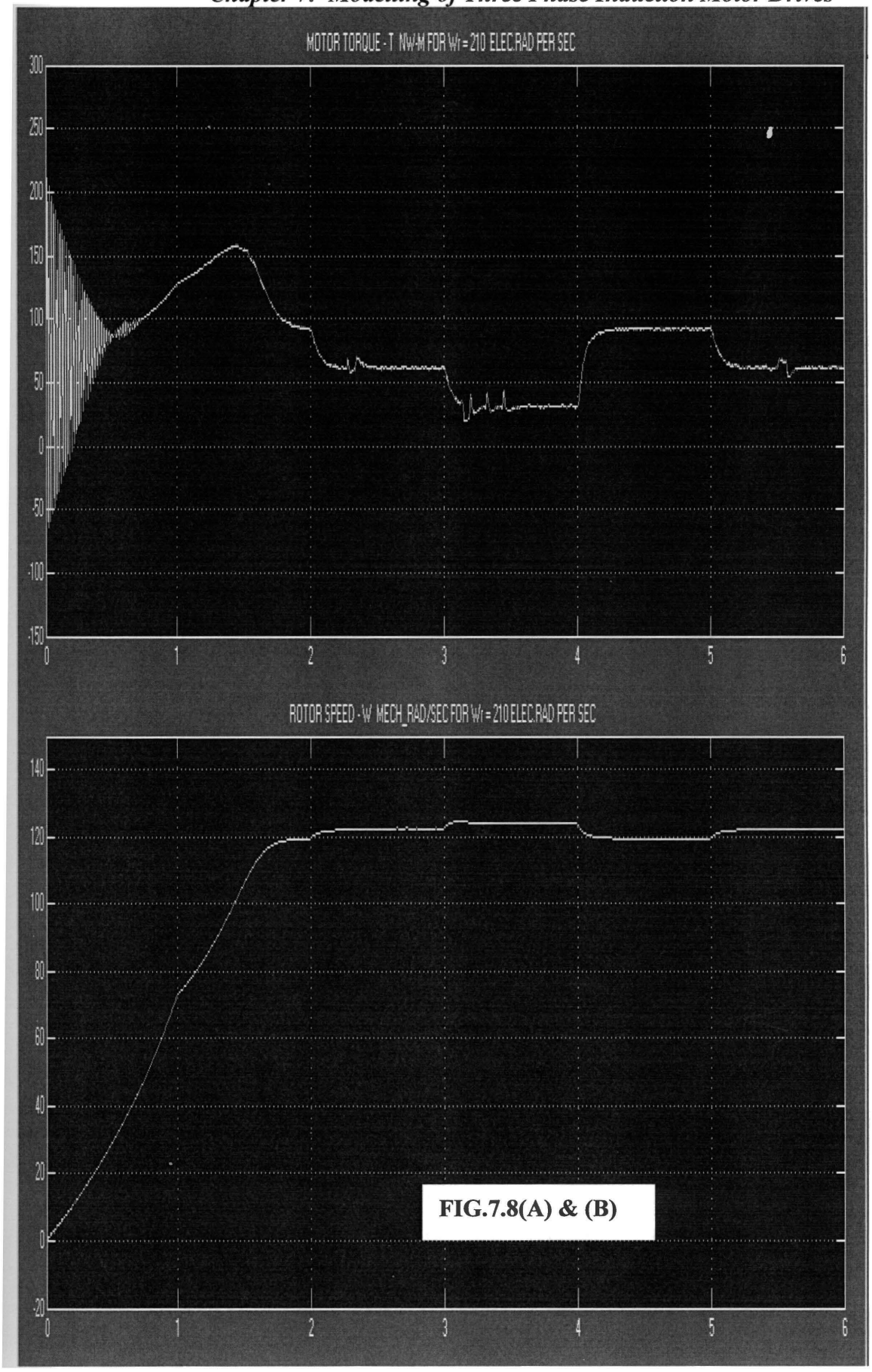
MOTOR TORQUE - T NW-M FOR Wr = 210 ELEC.RAD PER SEC
300
250
200
150
100
50
0
-50
-100
-150
0
1
2
3
4
5
6
ROTOR SPEED - W MECH_RAD/SEC FOR Wr = 210 ELEC.RAD PER SEC
140
120
100
80
60
40
20
0
-20
0
1
2
3
4
5
6

FIG.7.8(A) & (B)

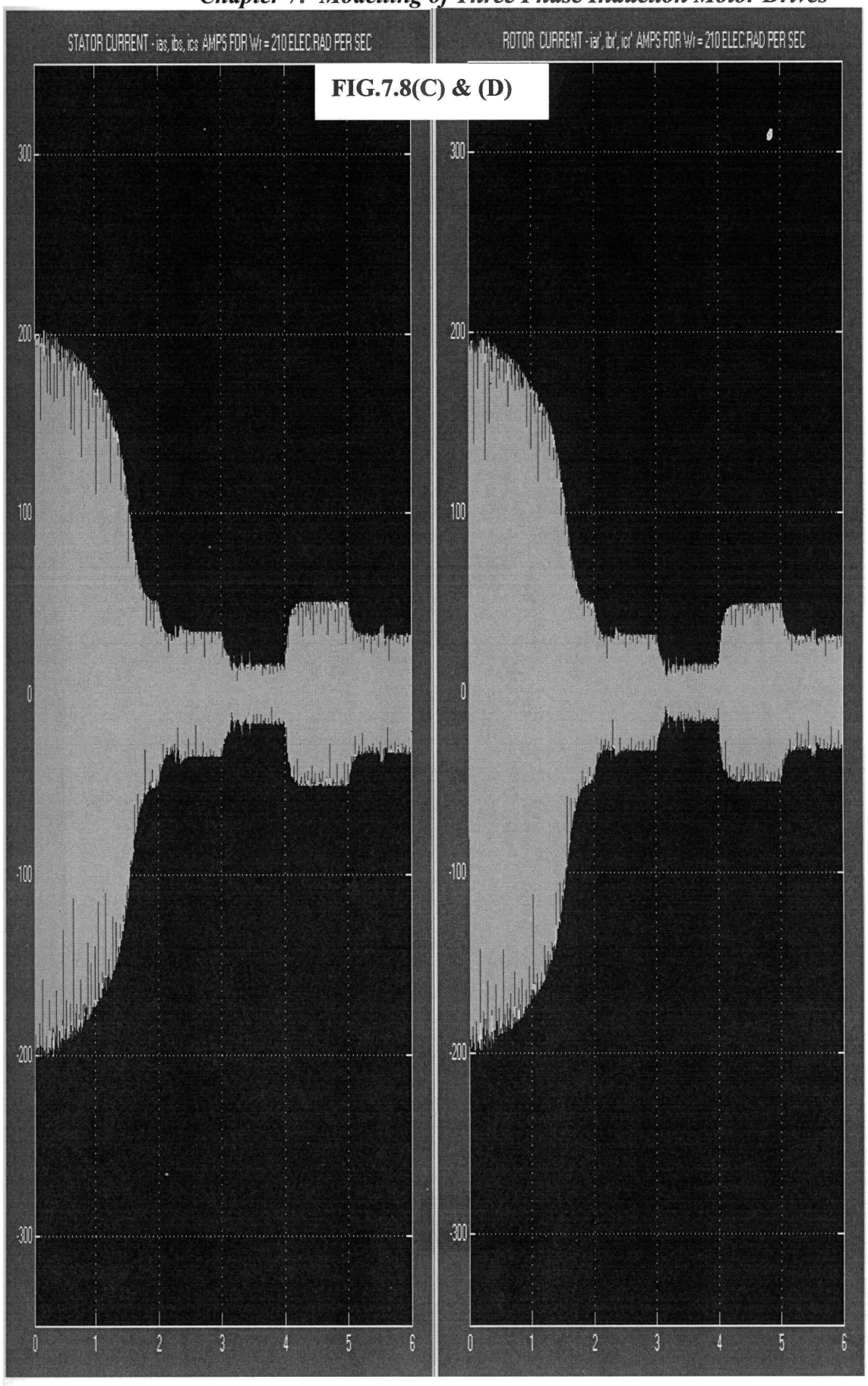
STATOR CURRENT - ias, ibs, ics AMPS FOR Wr = 210 ELEC.RAD PER SEC
ROTOR CURRENT - ia', ib', ic' AMPS FOR Wr = 210 ELEC.RAD PER SEC
300
200
100
0
-100
-200
-300
0
1
2
3
4
5
6

FIG.7.8(C) & (D)

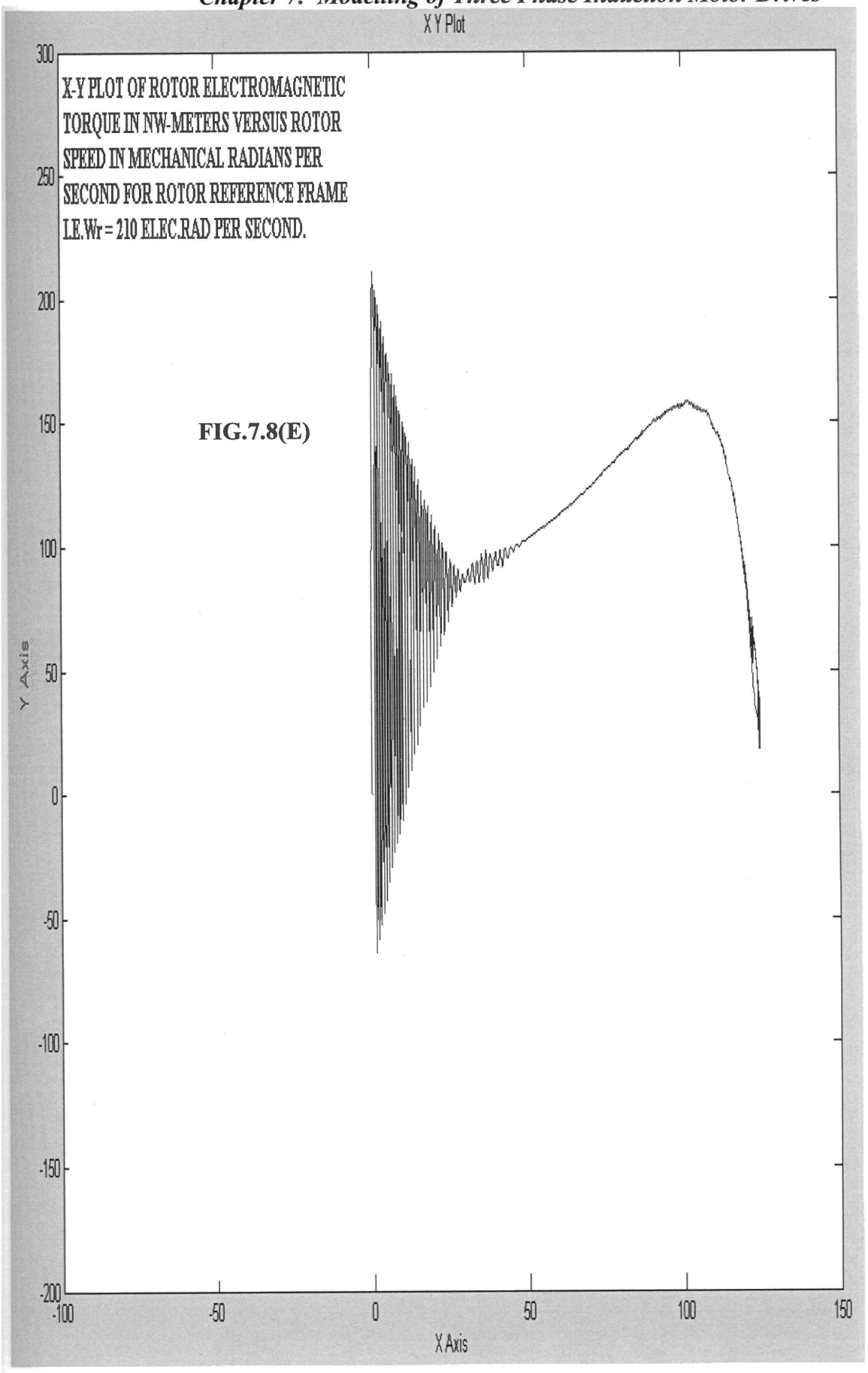
X Y Plot
X-Y PLOT OF ROTOR ELECTROMAGNETIC TORQUE IN NW-METERS VERSUS ROTOR SPEED IN MECHANICAL RADIANS PER SECOND FOR ROTOR REFERENCE FRAME I.E.Wr = 210 ELEC.RAD PER SECOND.
300
250
200
150
100
50
0
-50
-100
-150
-200
Y Axis
-100
-50
0
50
100
150
X Axis

FIG.7.8(E)

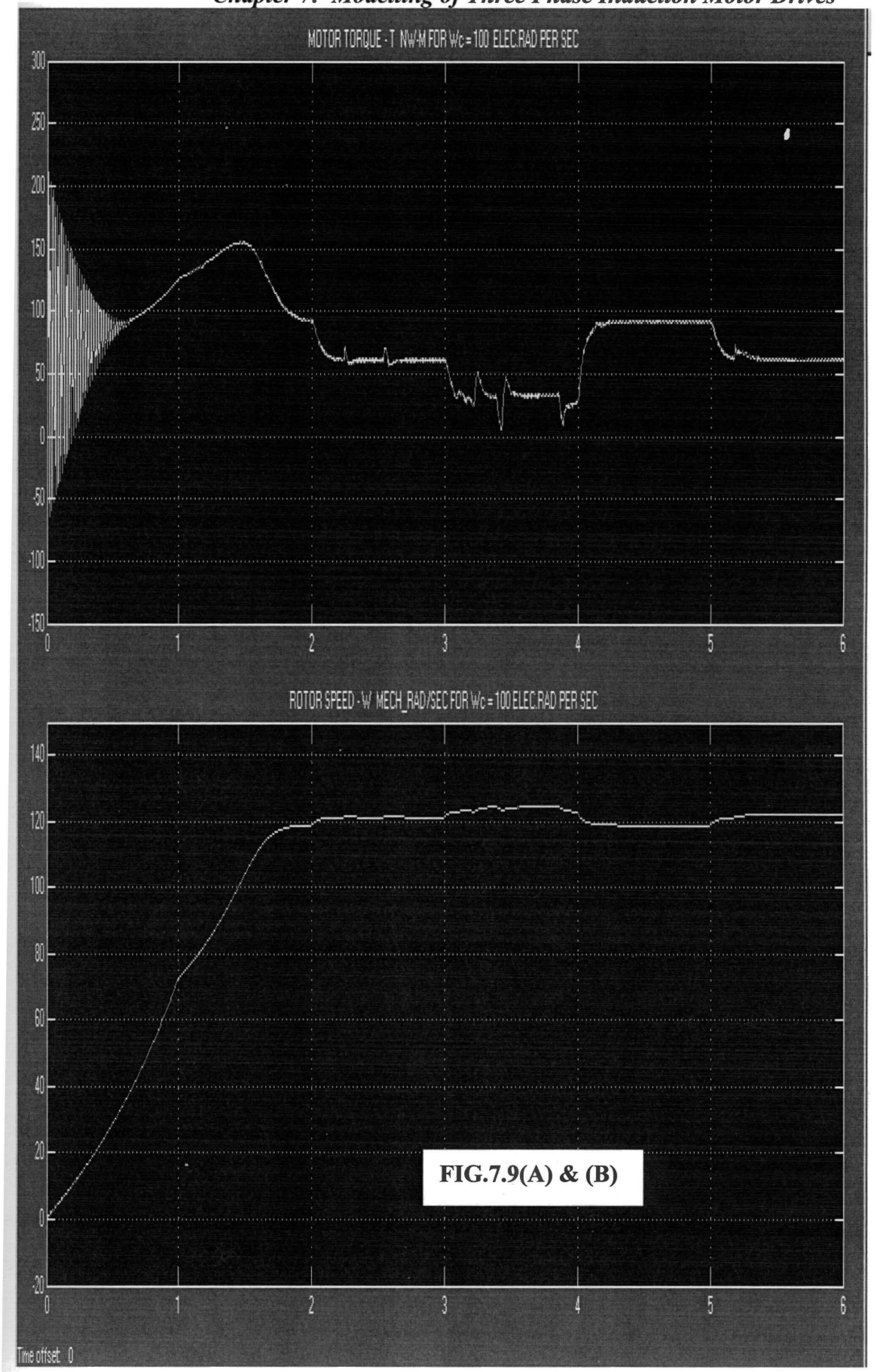
MOTOR TORQUE - T NW-M FOR Wc = 100 ELEC.RAD PER SEC
300
250
200
150
100
50
0
-50
-100
-150
0
1
2
3
4
5
6
ROTOR SPEED - W MECH_RAD/SEC FOR Wc = 100 ELEC.RAD PER SEC
140
120
100
80
60
40
20
0
-20
0
1
2
3
4
5
6
Time offset: 0

FIG.7.9(A) & (B)

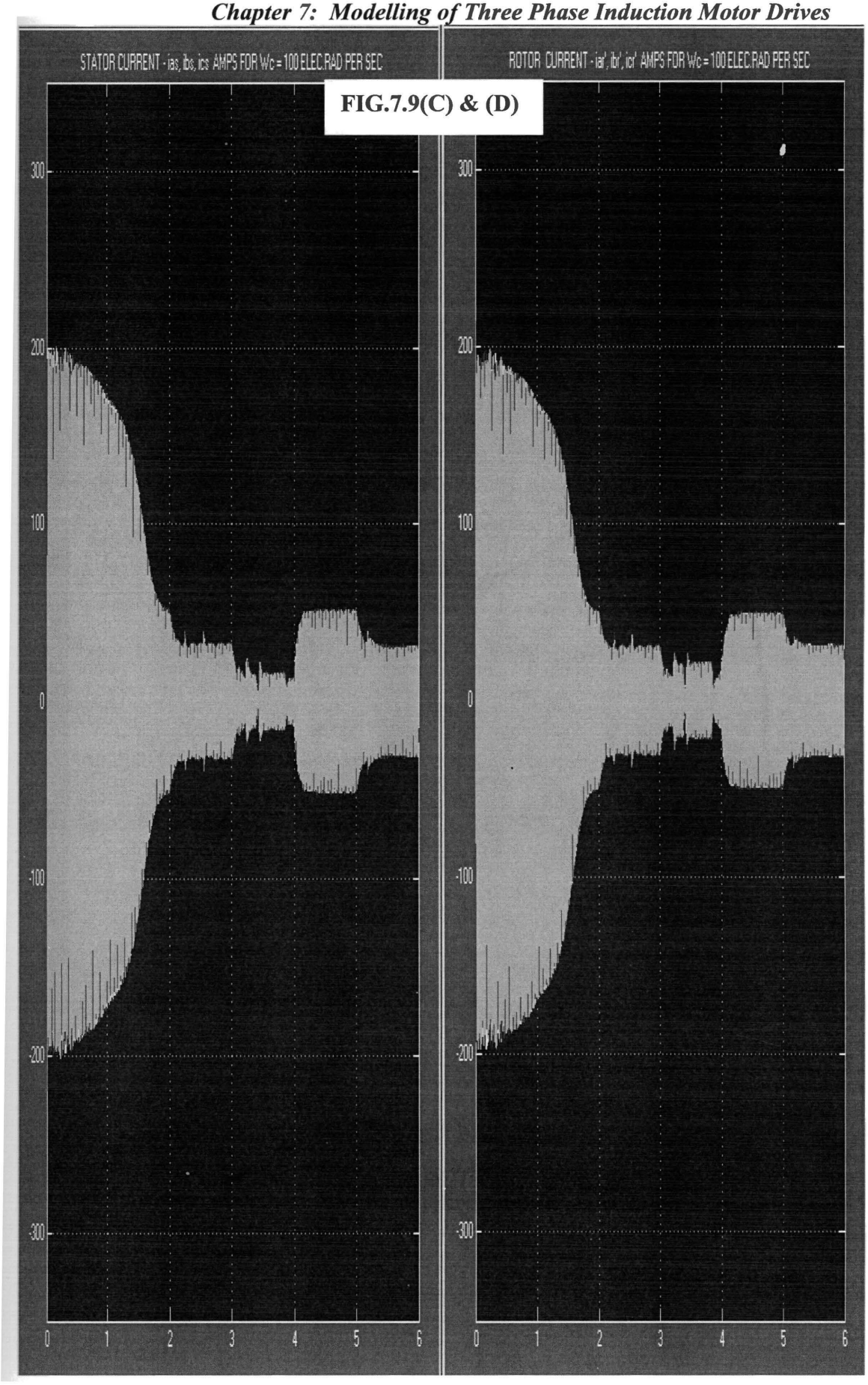
STATOR CURRENT - ias, ibs, ics AMPS FOR Wc = 100 ELEC.RAD PER SEC
ROTOR CURRENT - iar', ibr', icr' AMPS FOR Wc = 100 ELEC.RAD PER SEC
300
200
100
0
-100
-200
-300
0
1
2
3
4
5
6

FIG.7.9(C) & (D)

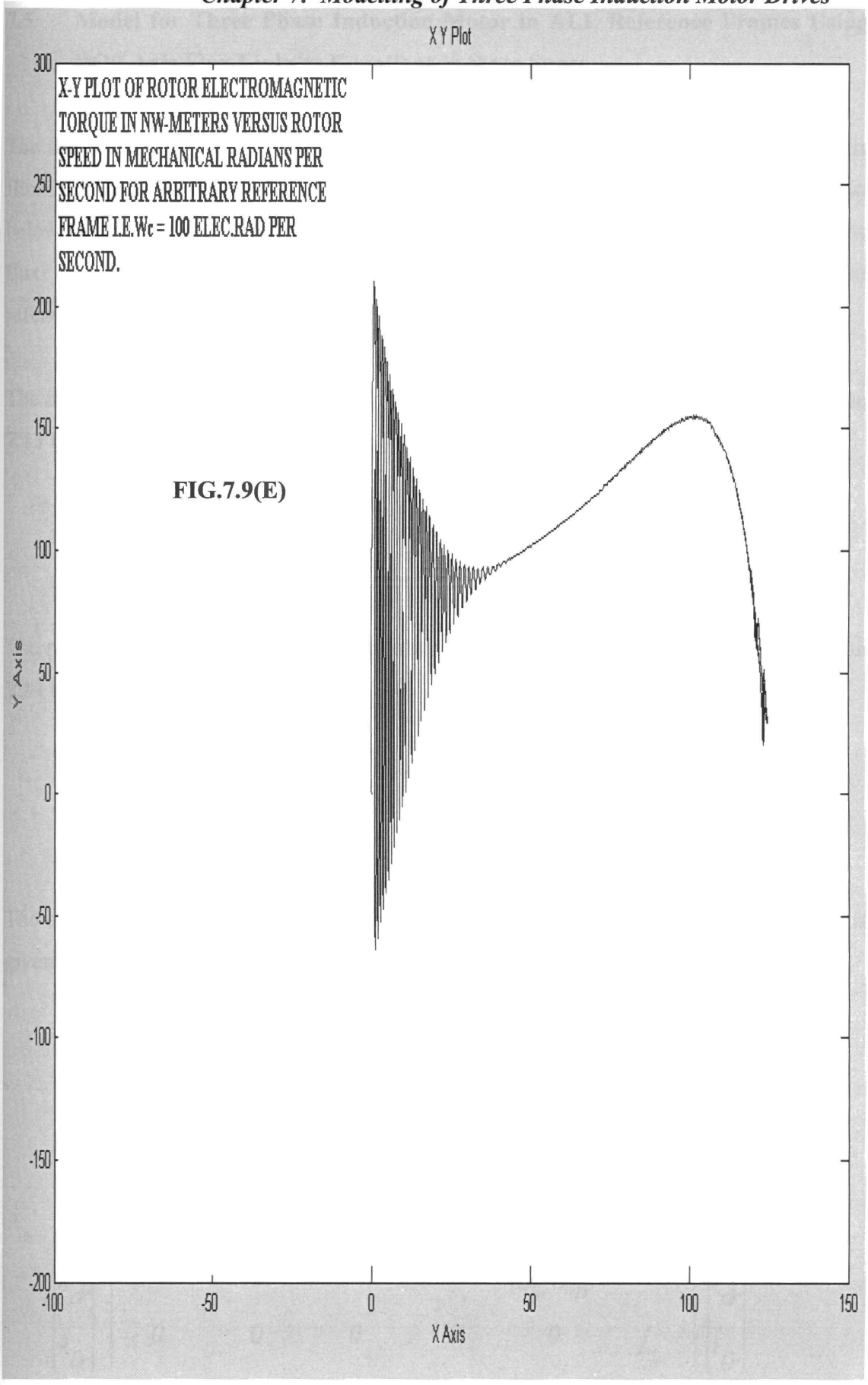
X Y Plot
X-Y PLOT OF ROTOR ELECTROMAGNETIC TORQUE IN NW-METERS VERSUS ROTOR SPEED IN MECHANICAL RADIANS PER SECOND FOR ARBITRARY REFERENCE FRAME I.E.Wc = 100 ELEC.RAD PER SECOND.
Y Axis
X Axis
300
250
200
150
100
50
0
-50
-100
-150
-200
-100
-50
0
50
100
150

FIG.7.9(E)

7.5 Model for Three Phase Induction Motor in ALL Reference Frames Using DQ0-Axis Flux Linkage Equations in State Space

The three phase induction motor model in arbitrary reference frame ω_C, using dq0-axis flux linkage equations in state space are developed as shown in equations 7.13 to below [2, 11, 13]. By letting ω_C the values of 0, ω_e and ω_{re}, in equation 7.13 to , the flux linkage equations in stationary(stator), synchronous(excitation) and rotor reference frames can be obtained.

The stator qd0-axis voltage equation in arbitrary reference frame ω_C is given in equation 7.13 below:

$$\begin{bmatrix} v_{qs} \\ v_{ds} \\ v_{0s} \end{bmatrix} = \begin{bmatrix} s & \omega_c & 0 \\ -\omega_c & s & 0 \\ 0 & 0 & s \end{bmatrix} * \begin{bmatrix} \lambda_{qs} \\ \lambda_{ds} \\ \lambda_{0s} \end{bmatrix} + \begin{bmatrix} r_S \end{bmatrix} * \begin{bmatrix} i_{qs} \\ i_{ds} \\ i_{0s} \end{bmatrix} \qquad (7.13)$$

The rotor qd0-axis voltage equation in arbitrary reference frame ω_C is given in equation 7.14 below:

$$\begin{bmatrix} v'_{qr} \\ v'_{dr} \\ v'_{0r} \end{bmatrix} = \begin{bmatrix} s & (\omega_c - \omega_{re}) & 0 \\ -(\omega_c - \omega_{re}) & s & 0 \\ 0 & 0 & s \end{bmatrix} * \begin{bmatrix} \lambda'_{qr} \\ \lambda'_{dr} \\ \lambda'_{0r} \end{bmatrix} + \begin{bmatrix} r'_r \end{bmatrix} * \begin{bmatrix} i'_{qr} \\ i'_{dr} \\ i'_{0r} \end{bmatrix} \qquad (7.14)$$

The stator and rotor qd0-axis flux linkage equation in arbitrary reference frame ω_C is given in equation 7.15 below:

$$\begin{bmatrix} \lambda_{qs} \\ \lambda_{ds} \\ \lambda_{0s} \\ \lambda'_{qr} \\ \lambda'_{dr} \\ \lambda'_{0r} \end{bmatrix} = \begin{bmatrix} (L_{ls}+L_m) & 0 & 0 & L_m & 0 & 0 \\ 0 & (L_{ls}+L_m) & 0 & 0 & L_m & 0 \\ 0 & 0 & L_{ls} & 0 & 0 & 0 \\ L_m & 0 & 0 & (L'_{lr}+L_m) & 0 & 0 \\ 0 & L_m & 0 & 0 & (L'_{lr}+L_m) & 0 \\ 0 & 0 & 0 & 0 & 0 & L'_{lr} \end{bmatrix} * \begin{bmatrix} i_{qs} \\ i_{ds} \\ i_{0s} \\ i'_{qr} \\ i'_{dr} \\ i'_{0r} \end{bmatrix} \qquad (7.15)$$

The e.m. torue equation for Tem is given in equation 7.16 below:

$$\left.\begin{aligned} T_{em} &= \frac{3}{2}\cdot\frac{P}{2}\cdot(\lambda'_{qr} i'_{dr} - \lambda'_{dr} i'_{qr}) \\ &= \frac{3}{2}\cdot\frac{P}{2}\cdot(\lambda_{ds} i_{qs} - \lambda_{qs} i_{ds}) \\ &= \frac{3}{2}\cdot\frac{P}{2}\cdot L_m\cdot(i'_{dr} i_{qs} - i'_{qr} i_{ds}) \end{aligned}\right| \qquad (7.16)$$

Rearranging equations 7.13 and 7.14, the state space representation of qd0-axis flux linkage equations for the stator and rotor in the arbitrary reference frame ω_C is given below:

$$\begin{bmatrix} \lambda_{qs\_dt} \\ \lambda_{ds\_dt} \\ \lambda_{0s\_dt} \\ \lambda'_{qr\_dt} \\ \lambda'_{dr\_dt} \\ \lambda'_{0r\_dt} \end{bmatrix} = \begin{bmatrix} 0 & -\omega_C & 0 & 0 & 0 & 0 \\ \omega_C & 0 & 0 & 0 & 0 & 0 \\ 0 & 0 & 0 & 0 & 0 & 0 \\ 0 & 0 & 0 & 0 & -(\omega_C-\omega_r) & 0 \\ 0 & 0 & 0 & (\omega_C-\omega_r) & 0 & 0 \\ 0 & 0 & 0 & 0 & 0 & 0 \end{bmatrix} * \begin{bmatrix} \lambda_{qs} \\ \lambda_{ds} \\ \lambda_{0s} \\ \lambda'_{qr} \\ \lambda'_{dr} \\ \lambda'_{0r} \end{bmatrix}$$

$$- \begin{bmatrix} r_S & 0 & 0 & 0 & 0 & 0 \\ 0 & r_S & 0 & 0 & 0 & 0 \\ 0 & 0 & r_S & 0 & 0 & 0 \\ 0 & 0 & 0 & r'_r & 0 & 0 \\ 0 & 0 & 0 & 0 & r'_r & 0 \\ 0 & 0 & 0 & 0 & 0 & r'_r \end{bmatrix} * \begin{bmatrix} i_{qs} \\ i_{ds} \\ i_{0s} \\ i'_{qr} \\ i'_{dr} \\ i'_{0r} \end{bmatrix} + \begin{bmatrix} v_{qs} \\ v_{ds} \\ v_{0s} \\ v'_{qr} \\ v'_{dr} \\ v'_{0r} \end{bmatrix} \qquad (7.17)$$

where λ_{qs_dot} is $\frac{d\lambda_{qs}}{dt}$ and so on. Now calling the 6X1 flux linkage matrix in equation 7.15 as **Γ**, the 6X6 inductance matrix in equation 7.15 as **L**, the 6X1 current matrix as **I**, the 6X6 matrix containing ω_C and ω_r in equation 7.17 as **Ω**, the 6X6 stator and rotor resistance matrix in equation 7.17 as **R** and the 6X1 voltage matrix in equation 7.17 as **V**, equation 7.15 and 7.17 can be combined as in equation 7.18 below:

$$[\Gamma\_dot] = [\Omega]*[\Gamma] - [R]*[L^{-1}]*[\Gamma] + [V] \qquad (7.18)$$

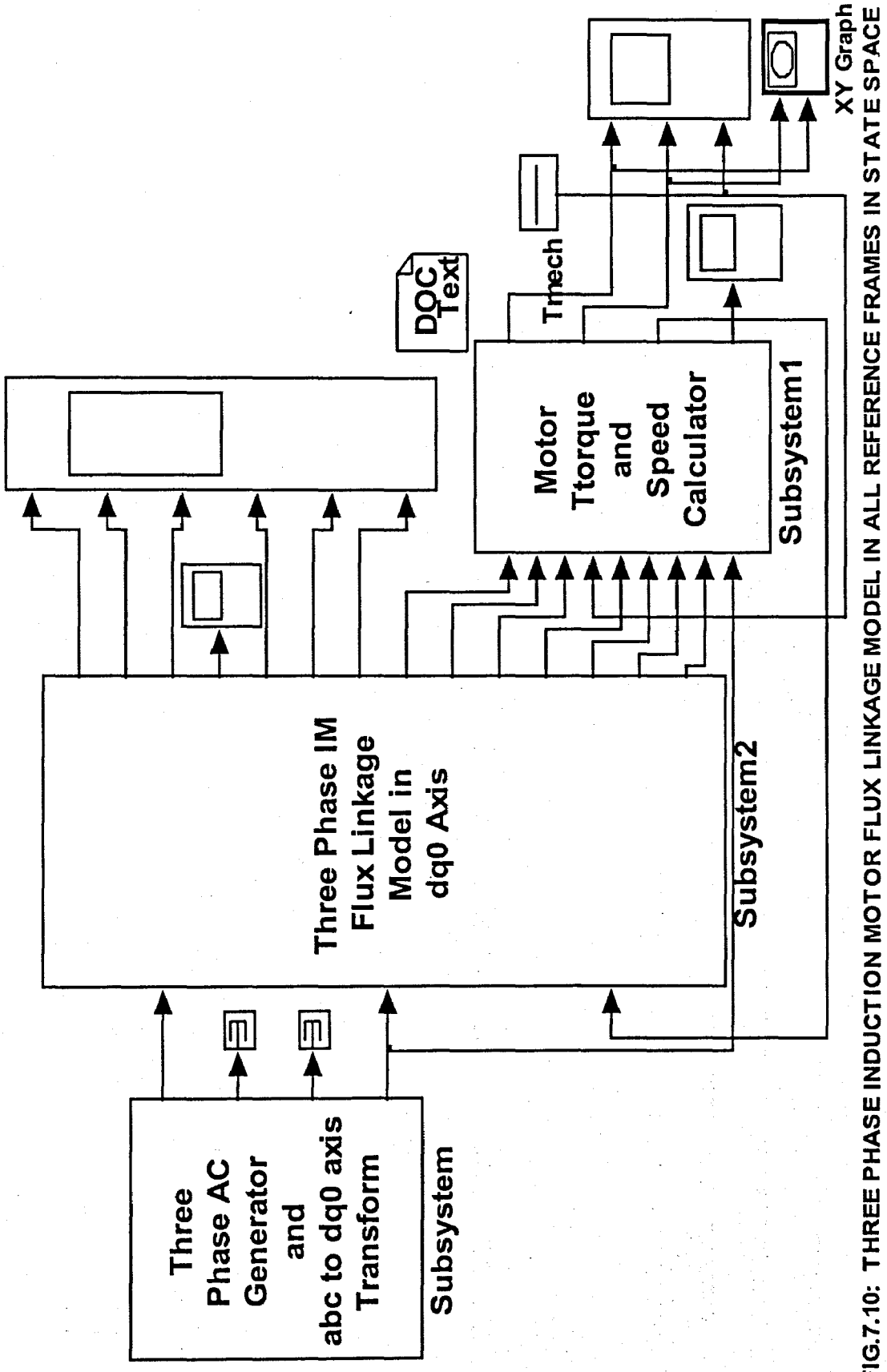

FIG.7.10: THREE PHASE INDUCTION MOTOR FLUX LINKAGE MODEL IN ALL REFERENCE FRAMES IN STATE SPACE

FIG.7.11

Block Parameters: Subsystem
Three Phase AC Generator and abc to dq0 Axis Transform (mask)
Enter the PEAK Value of the line to neutral voltage in volts. Supply frequency in Hertz and the angular frequency of the reference frame in Electrical radians per second.
Parameters
Enter the PEAK value of Line to Neutral Voltage in Volts
179.6
Enter the SUPPLY frequency in Hertz
60
Enter the ANGULAR FREQUENCY OF THE REFERENCE FRAME in Electrical radians per second
d
OK
Cancel
Help
Apply
Block Parameters: Subsystem2
Three Phase IM Model Data (mask)
Enter the Stator Leakage Inductance Lls, Rotor Leakage Inductance referred to Stator Llr', Mutual Inductance between stator and Rotor Lm all in Henries per phase. Enter Stator Resistance Rs, Rotor resistance referred to stator Rr' all in Ohms per phase. Enter Angular Frequency of the reference frame in Electrical radians per second.
Parameters
Enter Stator Leakage Inductance Lls in Henries
0.524/(377)
Enter rotor leakage inductance referred to Stator in Henries
0.279/(377)
Enter Mutual Inductance between Stator and Rotor in Henries
15.457/(377)
Enter Stator resistance in Ohms
0.294
Enter Rotor resistance referred to Stator in Ohms
0.156
Enter Angular Frequency of the Reference Frame in Electrical radians per second
0
OK
Cancel
Help
Apply
Three Phase AC Generator and abc to dq0 axis Transform
Subsystem
Three Phase IM Flux Linkage Model in dq0 Axis
Subsystem2
Motor Torque and Speed Calculator
Subsystem1
dq0 C Text
Tmtech
XY Graph
FIG.7.11 : THREE PHASE INDUCTION MOTOR FLUX LINKAGE MODEL IN ALL REFERENCE FRAMES IN STATE SPACE
Block Parameters: Subsystem1
Rotor Torque and Speed Calculator (mask)
Enter the Mutual Inductance Lm between Stator and Rotor in Henries, the Number of Poles P, the combined Moment of Inertia of the Motor and Load in Kg.m^2 and the Damping Constant in Nw.m.Sec per elec.rad.
Parameters
Enter the Mutual Inductance between Stator and Rotor in Henries
15.457/(377)
Enter the Number of Poles
6
Enter the combined M.I. of motor and Load in kgm^2
0.8
Enter the Damping Constant Nw.m.sec per elec.rad
0
OK
Cancel
Help
Apply

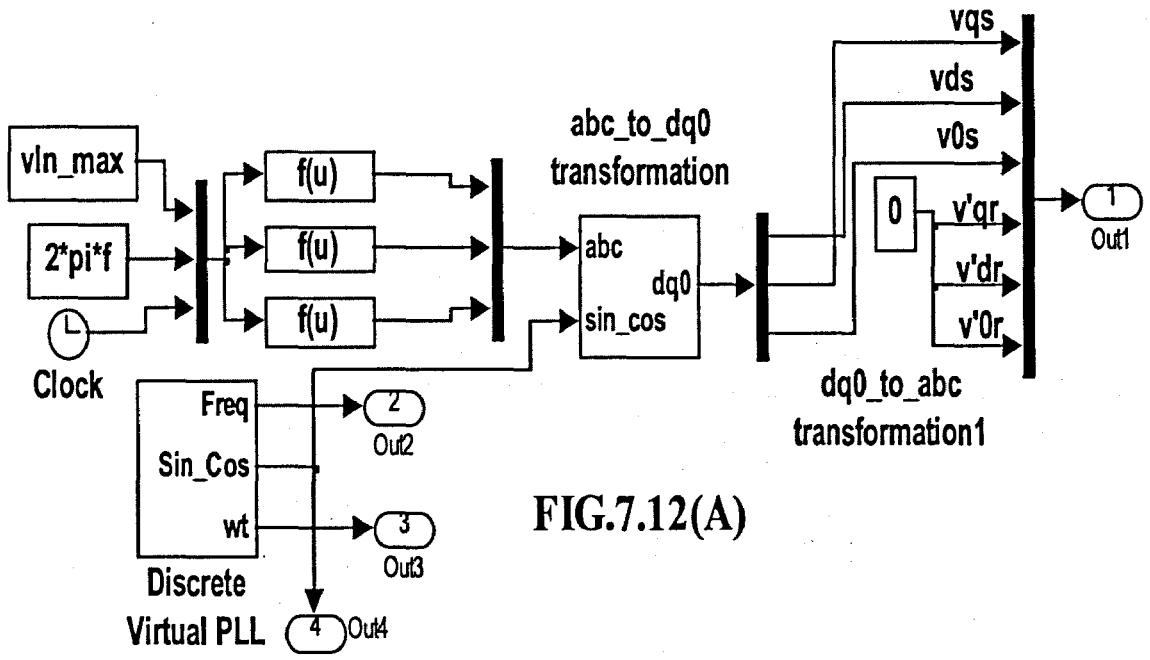

FIG.7.12(A)

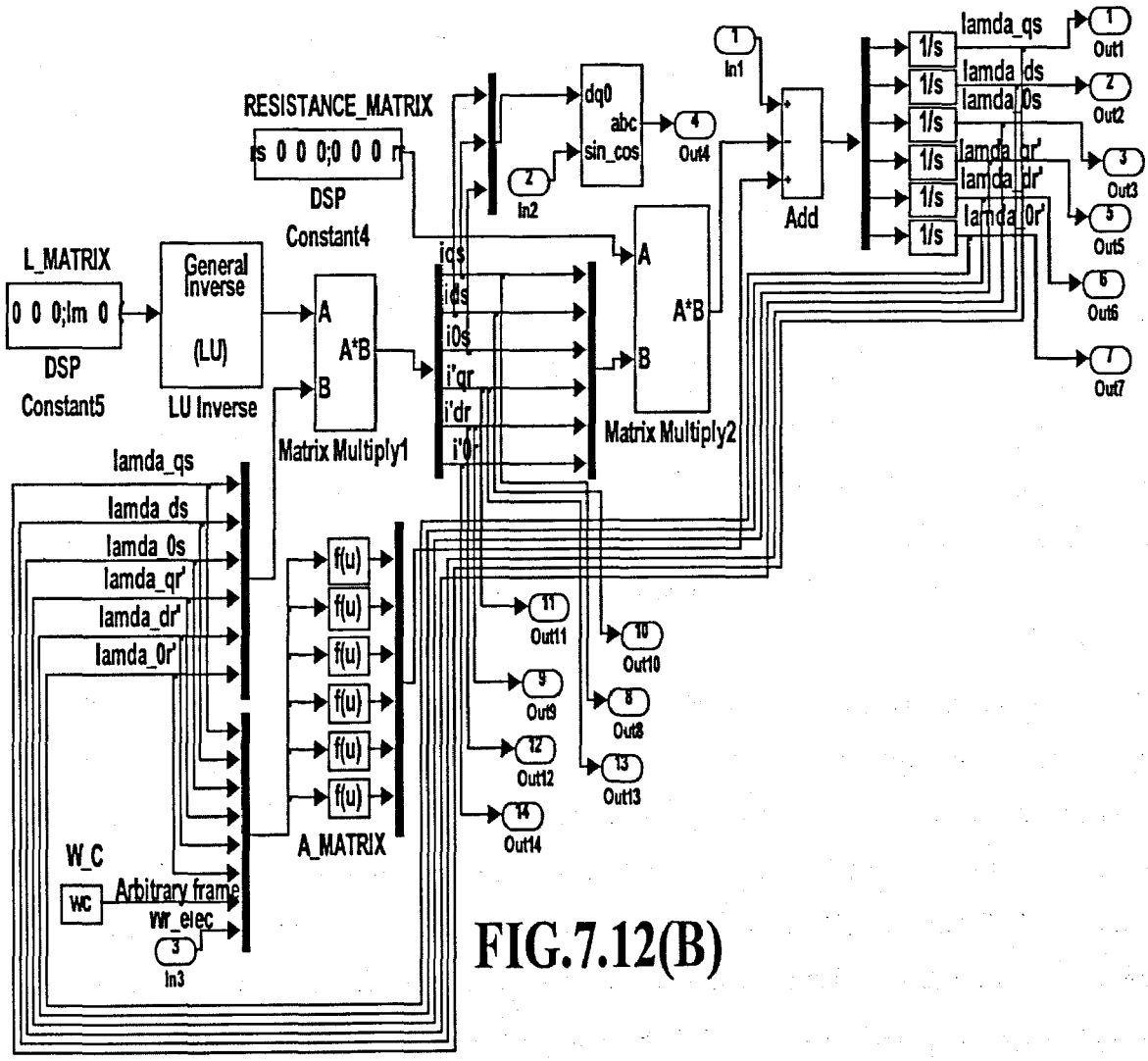

FIG.7.12(B)

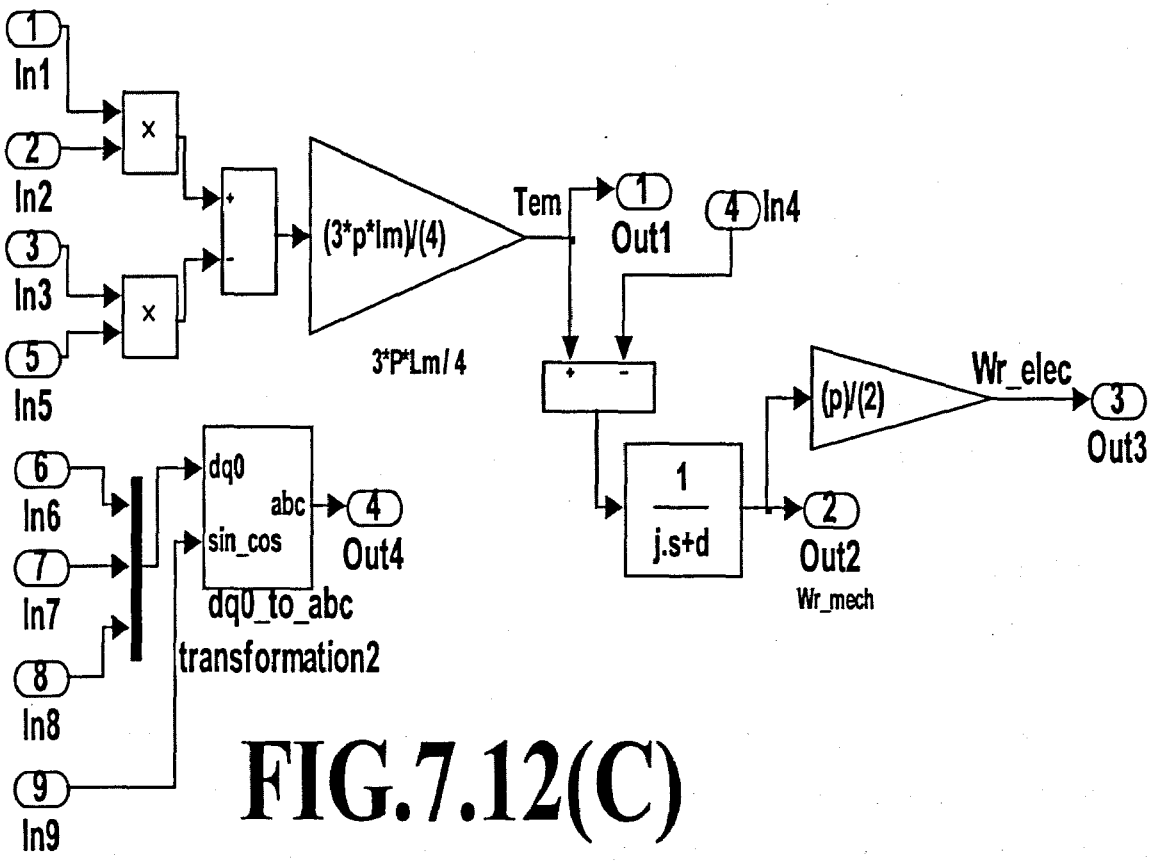

FIG.7.12(C)

Equation 7.18 is in the state space form

$$\vec{x}\_dot = \vec{A}.\vec{x} + \vec{B}.\vec{u}. \qquad (7.18)$$

The model for the three phase IM using the qd0-axis flux linkage equations in state space in ALL reference frames is shown in Fig.7.10. The various dialog boxes are shown in Fig.7.11. The various subsystems used are shown in Fig.7.12(A) to (C). The function of the various subsystems are detailed below:

Fig.7.12(A) corresponds to the dialog box Three Phase AC Generator and abc to dq0 axis transform in Fig.7.11. The line to neutral voltage maximum value, supply frequency in Hertz and the angular frequency of the reference frame in electrical radians per second are entered in these relevant box. The abc to dq0 transform block and the discrete virtual PLL are from SimPowerSystems block set. The virtual PLL generates cos θ_C and sin θ_C and the abc to dq0 axis transform block performs the abc to dq0 axis voltage transformation as per the matrix equation 1.1 in Chapter 1. The dq0 axis rotor voltages are zero as the rotor is short circuited. Fig.7.12(B) corresponds to the dialog

box Three Phase IM Model Data in Fig.7.11. In this dialog box, the values of Lls, Llr', Lm, Rs, Rr' and ω_C relating to stator, rotor and arbitrary frame are entered in the appropriate units. In Fig.7.12(B), the eight input mux with dq0-axis stator and rotor flux linkages Γ, reference frame frequency ω_C and rotor speed ω_{r_elec} in electrical radians per second along with the six Fcn block solves the first term on the R.H.S. of equation 7.18. The DSP constant block marked L_MATRIX and the general inverse (LU) block computes inverse of L matrix. This L^{-1} Matrix is then multiplied by Γ matrix using Matrix Multiply1 block to obtain the dq0 stator and rotor current I matrix. The DSP constant block marked RESISTANCE_MATRIX in Fig.7.12(B) generates the R matrix containing diagonal elements of stator and rotor resistance referred to stator defined in equation 7.17. This R matrix is then multiplied by the I matrix using the Matrix Multiply2 block to obtain the second term in equation 7.18. The dq0-axis voltage V matrix is available from Fig.7.12(A). These three terms are the summed with appropriate signs in the Add block to obtain the derivative of the stator and rotor flux linkage vector Γ_dot matrix. This is then integrated using individual integrator block to obtain the dq0-axis stator and rotor flux linkage vector Γ matrix. Fig.7.12(C) corresponds to the dialog box Rotor Torque and Speed calculator in Fig.7.11. In this the mutual inductance Lm, number of poles P, Moment of Inertia of motor and load and the Damping constant are entered in the appropriate units. In Fig.7.12(C), the two multiplier blocks, the subtract block and the gain multiplier block with the multiplier constant [3*P*Lm / 4] calculates the rotor e.m. torque Tem given by equation 7.16. The mechanical load torque Tmech is generated using the repeating sequence block as shown in Fig.7.10. The value of Tem and Tmech are subtracted using the Subtract block and given to the Transfer Fcn block with the transfer function [1 / ((Jm + Jl).s + D)] to obtain the rotor speed in mechanical radians per second, which is then multiplied by gain block with the multiplier [P / 2] to obtain the rotor speed in ω_{r_elec} electrical radians per second. The dq0 to abc transform block in Fig.7.12(C) transforms the dq0-axis stator and rotor current back to abc axis as per the transformation matrix defined by equation 1.2 in Chapter 1.

7.5.1 Simulation Results

The simulation of the flux linkage model of three phase IM in all reference frame was

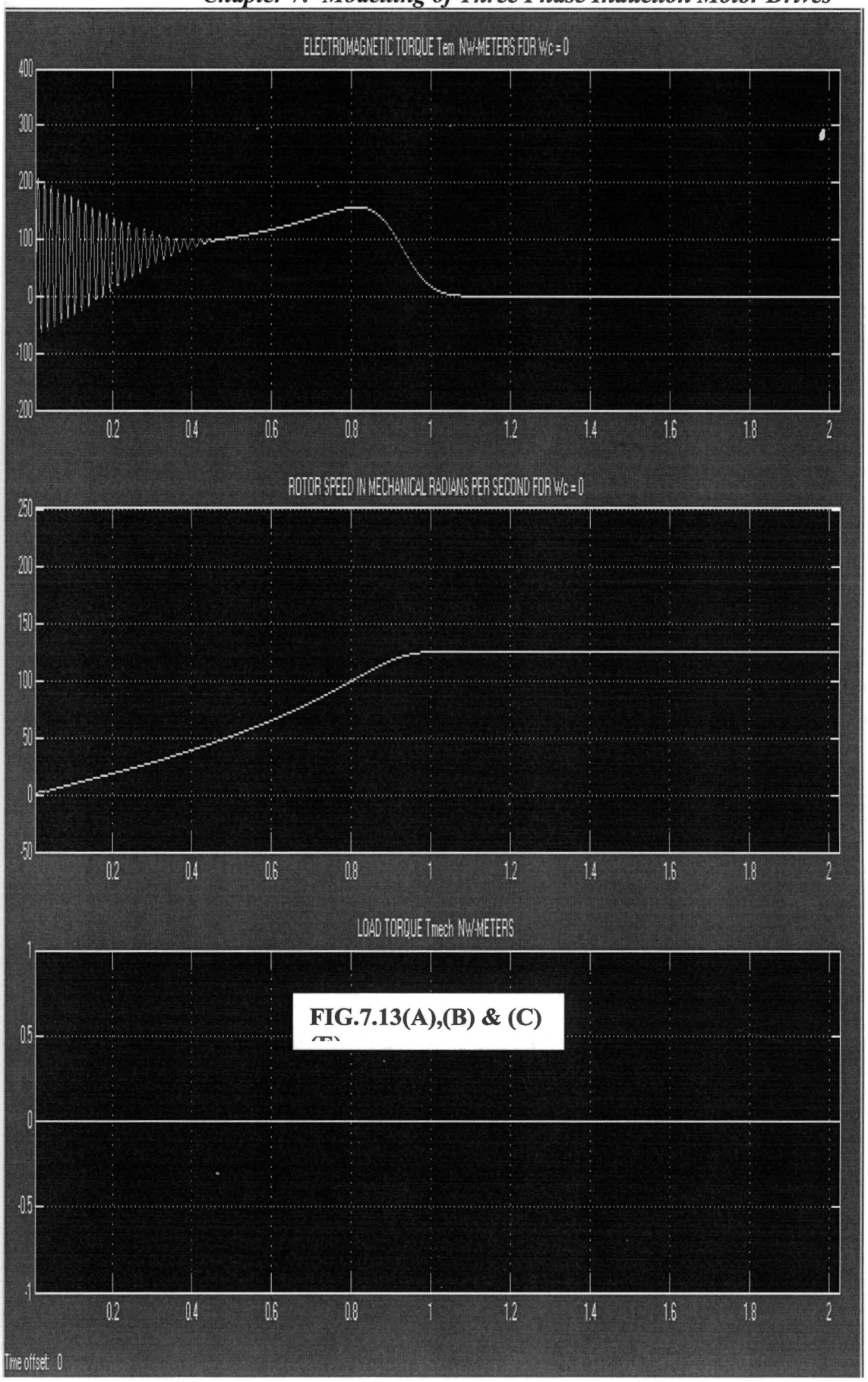
ELECTROMAGNETIC TORQUE Tem NW-METERS FOR Wc = 0
400
300
200
100
0
-100
-200
0.2
0.4
0.6
0.8
1
1.2
1.4
1.6
1.8
2
ROTOR SPEED IN MECHANICAL RADIANS PER SECOND FOR Wc = 0
250
200
150
100
50
0
-50
0.2
0.4
0.6
0.8
1
1.2
1.4
1.6
1.8
2
LOAD TORQUE Tmech NW-METERS
1
0.5
0
-0.5
-1
0.2
0.4
0.6
0.8
1
1.2
1.4
1.6
1.8
2
Time offset: 0

FIG.7.13(A),(B) & (C)

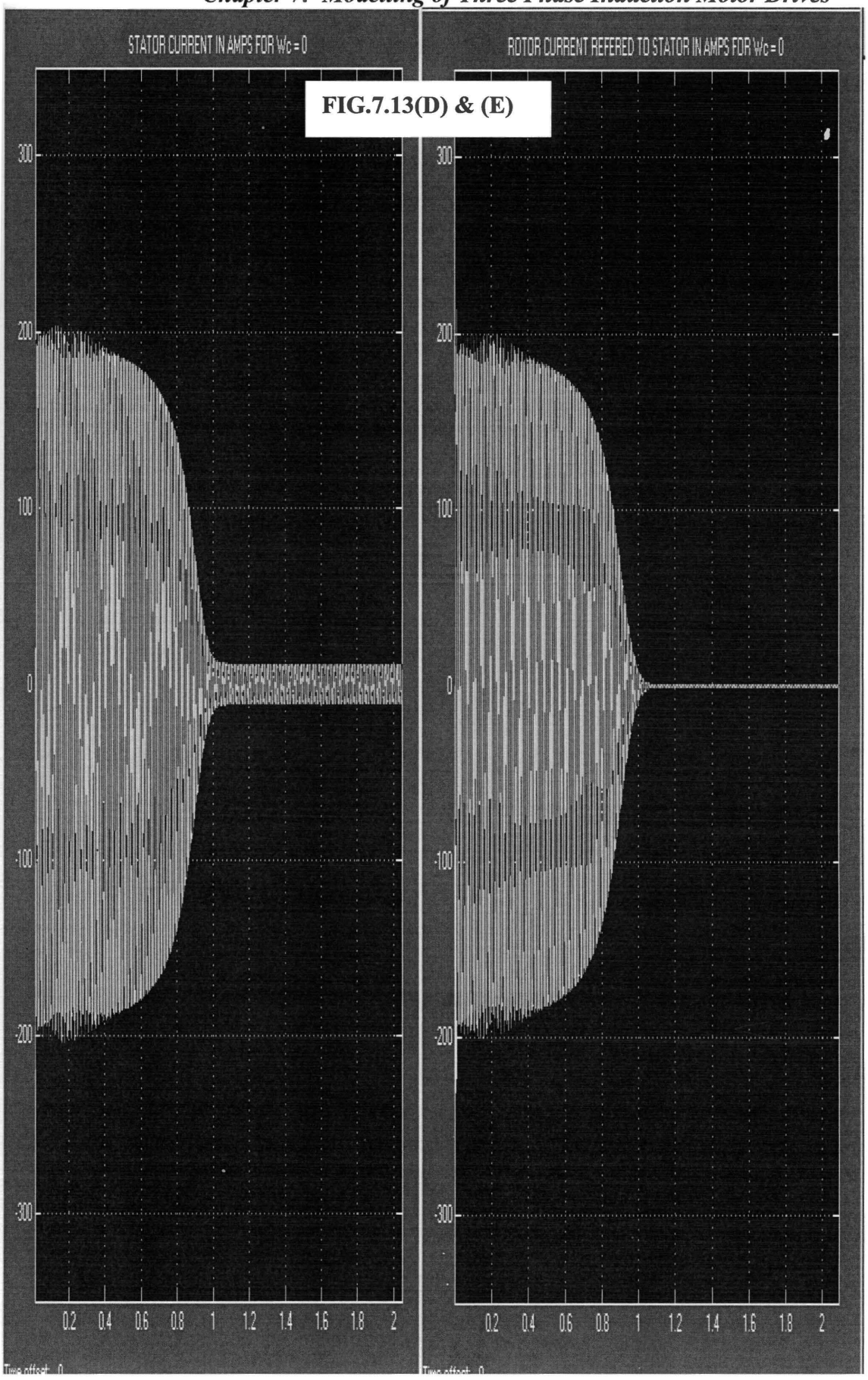
STATOR CURRENT IN AMPS FOR Wc = 0
300
200
100
0
-100
-200
-300
0.2 0.4 0.6 0.8 1 1.2 1.4 1.6 1.8 2
ROTOR CURRENT REFERED TO STATOR IN AMPS FOR Wc = 0
300
200
100
0
-100
-200
-300
0.2 0.4 0.6 0.8 1 1.2 1.4 1.6 1.8 2

FIG.7.13(D) & (E)

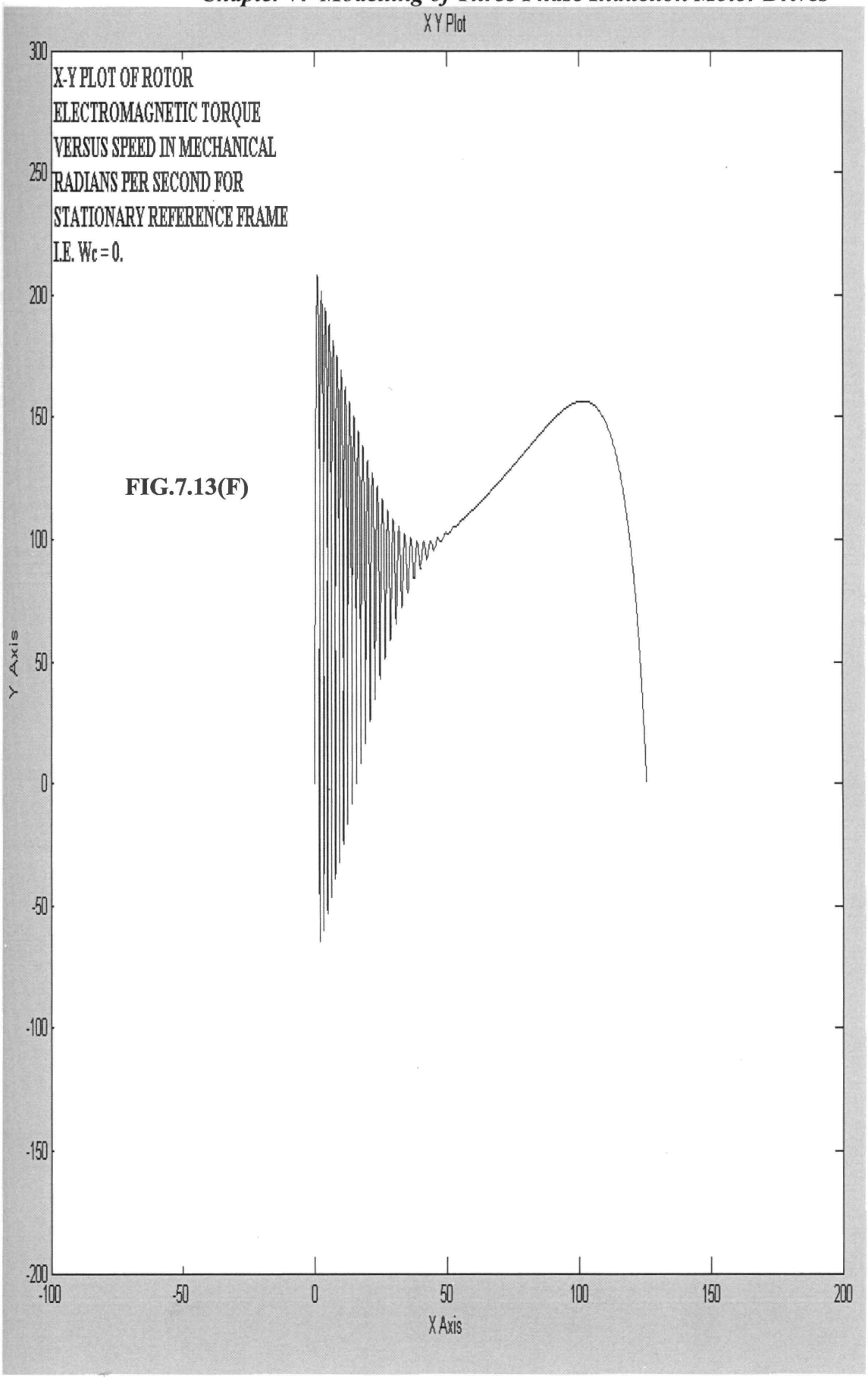
X Y Plot
X-Y PLOT OF ROTOR
ELECTROMAGNETIC TORQUE
VERSUS SPEED IN MECHANICAL
RADIANS PER SECOND FOR
STATIONARY REFERENCE FRAME
I.E. Wc = 0.
300
250
200
150
100
50
0
-50
-100
-150
-200
Y Axis
-100
-50
0
50
100
150
200
X Axis

FIG.7.13(F)

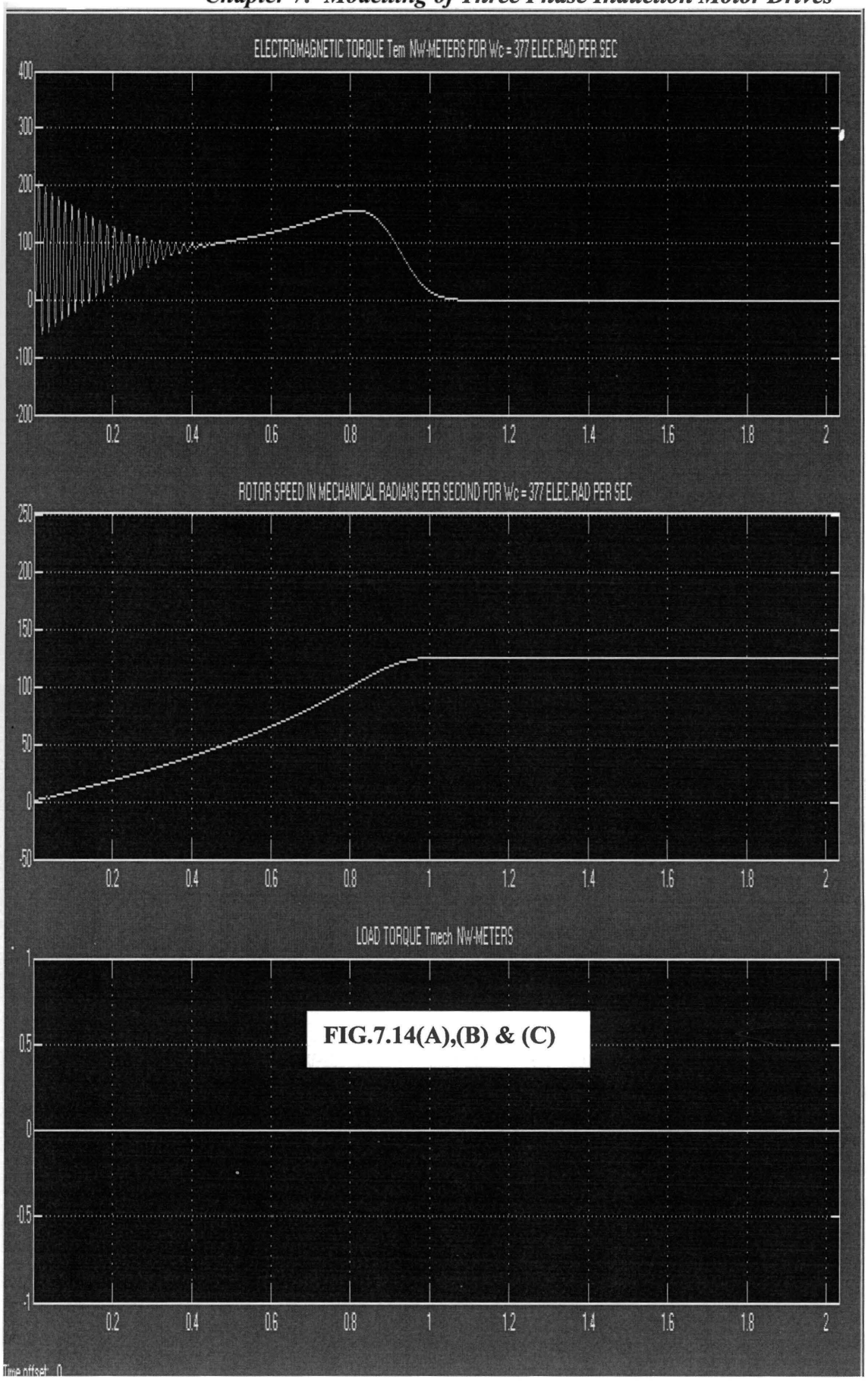
ELECTROMAGNETIC TORQUE Tem NW-METERS FOR Wc = 377 ELEC.RAD PER SEC
400
300
200
100
0
-100
-200
0.2
0.4
0.6
0.8
1
1.2
1.4
1.6
1.8
2
ROTOR SPEED IN MECHANICAL RADIANS PER SECOND FOR Wc = 377 ELEC.RAD PER SEC
250
200
150
100
50
0
-50
0.2
0.4
0.6
0.8
1
1.2
1.4
1.6
1.8
2
LOAD TORQUE Tmech NW-METERS
1
0.5
0
-0.5
-1
0.2
0.4
0.6
0.8
1
1.2
1.4
1.6
1.8
2
Time offset: 0

FIG.7.14(A),(B) & (C)

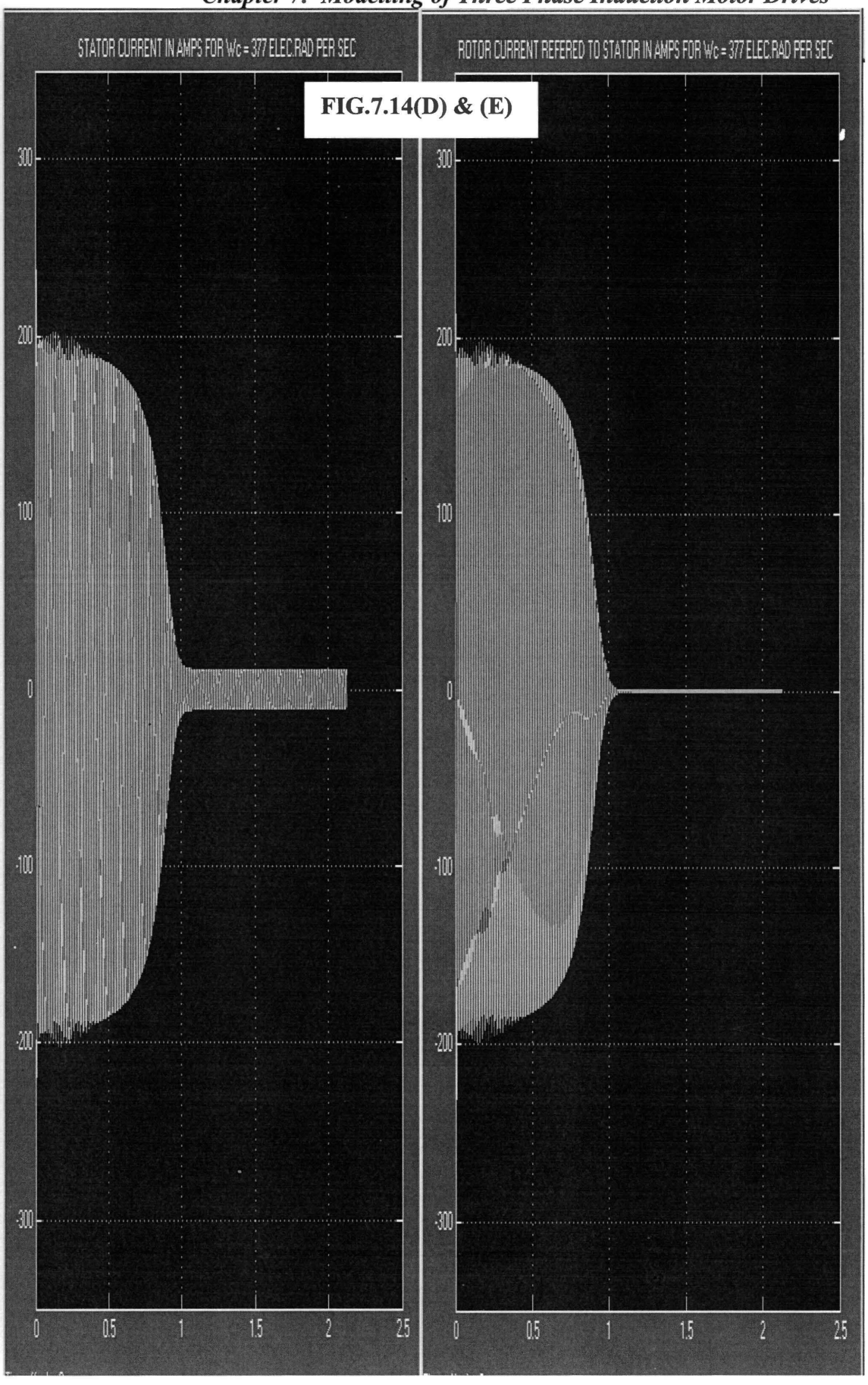
STATOR CURRENT IN AMPS FOR Wc = 377 ELEC.RAD PER SEC
300
200
100
0
-100
-200
-300
0
0.5
1
1.5
2
2.5
ROTOR CURRENT REFERED TO STATOR IN AMPS FOR Wc = 377 ELEC.RAD PER SEC
300
200
100
0
-100
-200
-300
0
0.5
1
1.5
2
2.5

FIG.7.14(D) & (E)

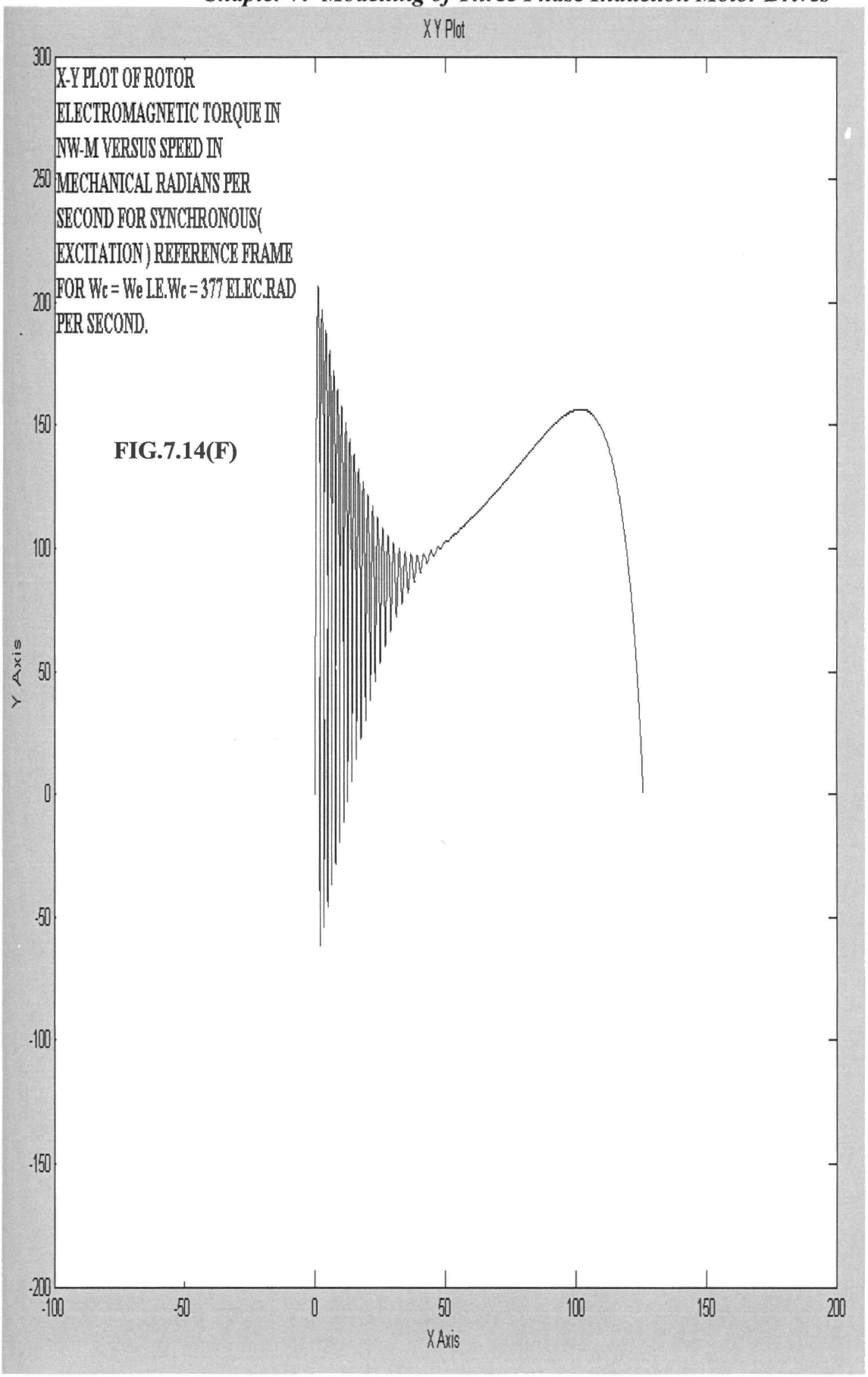
X Y Plot
X-Y PLOT OF ROTOR ELECTROMAGNETIC TORQUE IN NW-M VERSUS SPEED IN MECHANICAL RADIANS PER SECOND FOR SYNCHRONOUS(EXCITATION) REFERENCE FRAME FOR Wc = We I.E.Wc = 377 ELEC.RAD PER SECOND.
Y Axis
X Axis
300
250
200
150
100
50
0
-50
-100
-150
-200
-100
-50
0
50
100
150
200

FIG.7.14(F)

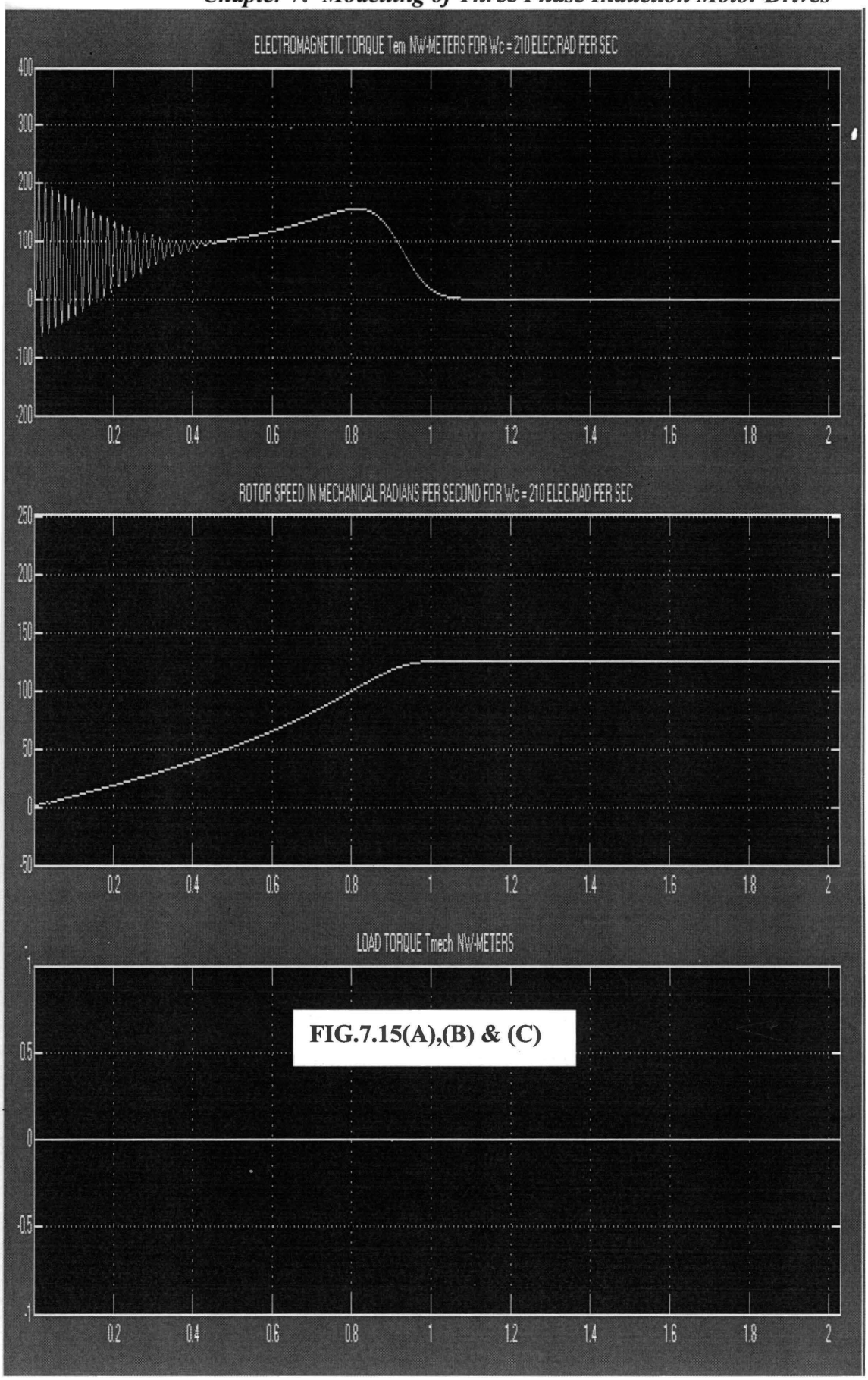
ELECTROMAGNETIC TORQUE Tem NW-METERS FOR Wc = 210 ELEC.RAD PER SEC
400
300
200
100
0
-100
-200
0.2
0.4
0.6
0.8
1
1.2
1.4
1.6
1.8
2
ROTOR SPEED IN MECHANICAL RADIANS PER SECOND FOR Wc = 210 ELEC.RAD PER SEC
250
200
150
100
50
0
-50
0.2
0.4
0.6
0.8
1
1.2
1.4
1.6
1.8
2
LOAD TORQUE Tmech NW-METERS
1
0.5
0
-0.5
-1
0.2
0.4
0.6
0.8
1
1.2
1.4
1.6
1.8
2

FIG.7.15(A),(B) & (C)

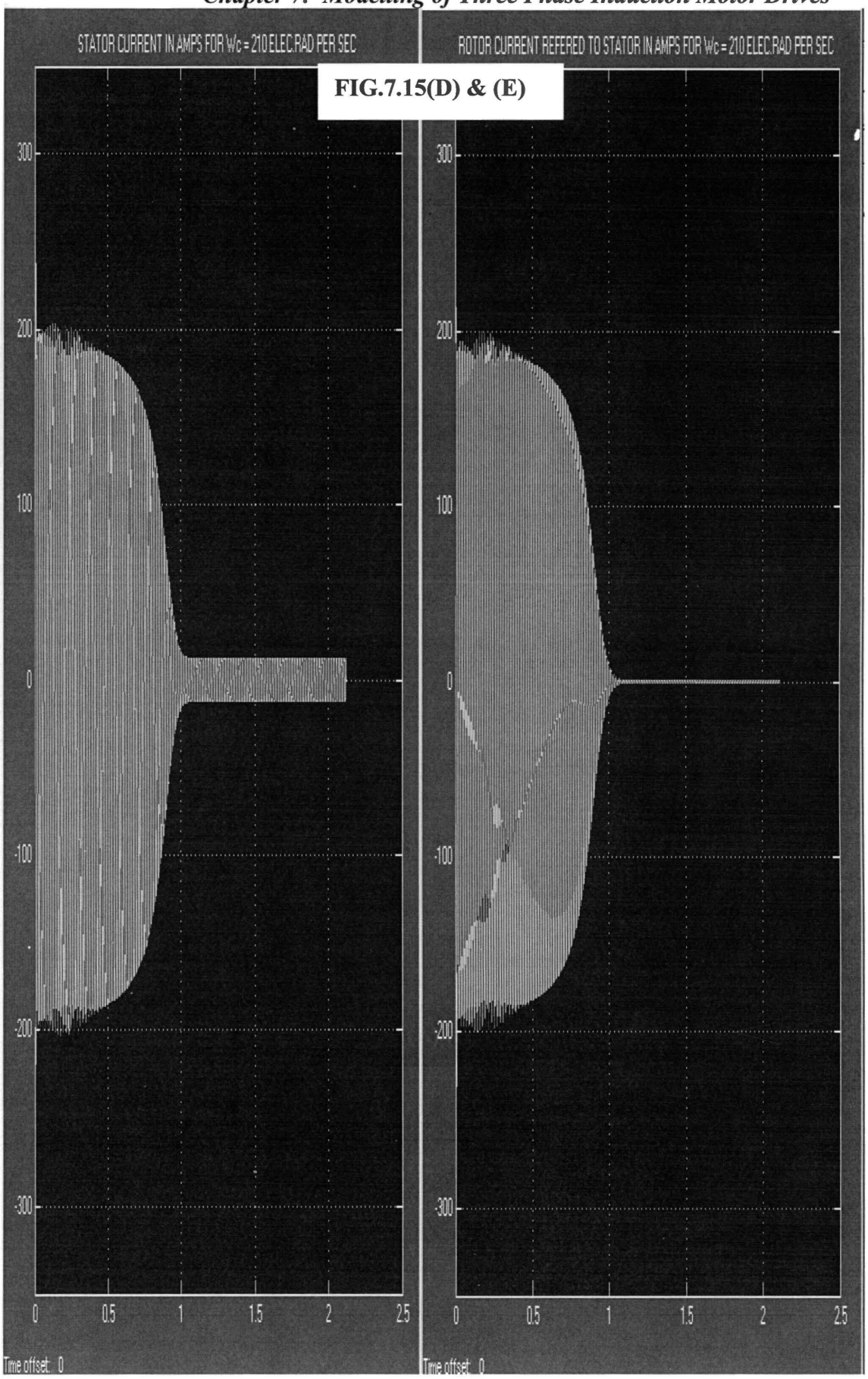
STATOR CURRENT IN AMPS FOR Wc = 210 ELEC.RAD PER SEC
ROTOR CURRENT REFERED TO STATOR IN AMPS FOR Wc = 210 ELEC.RAD PER SEC
300
200
100
0
-100
-200
-300
0
0.5
1
1.5
2
2.5
Time offset: 0

FIG.7.15(D) & (E)

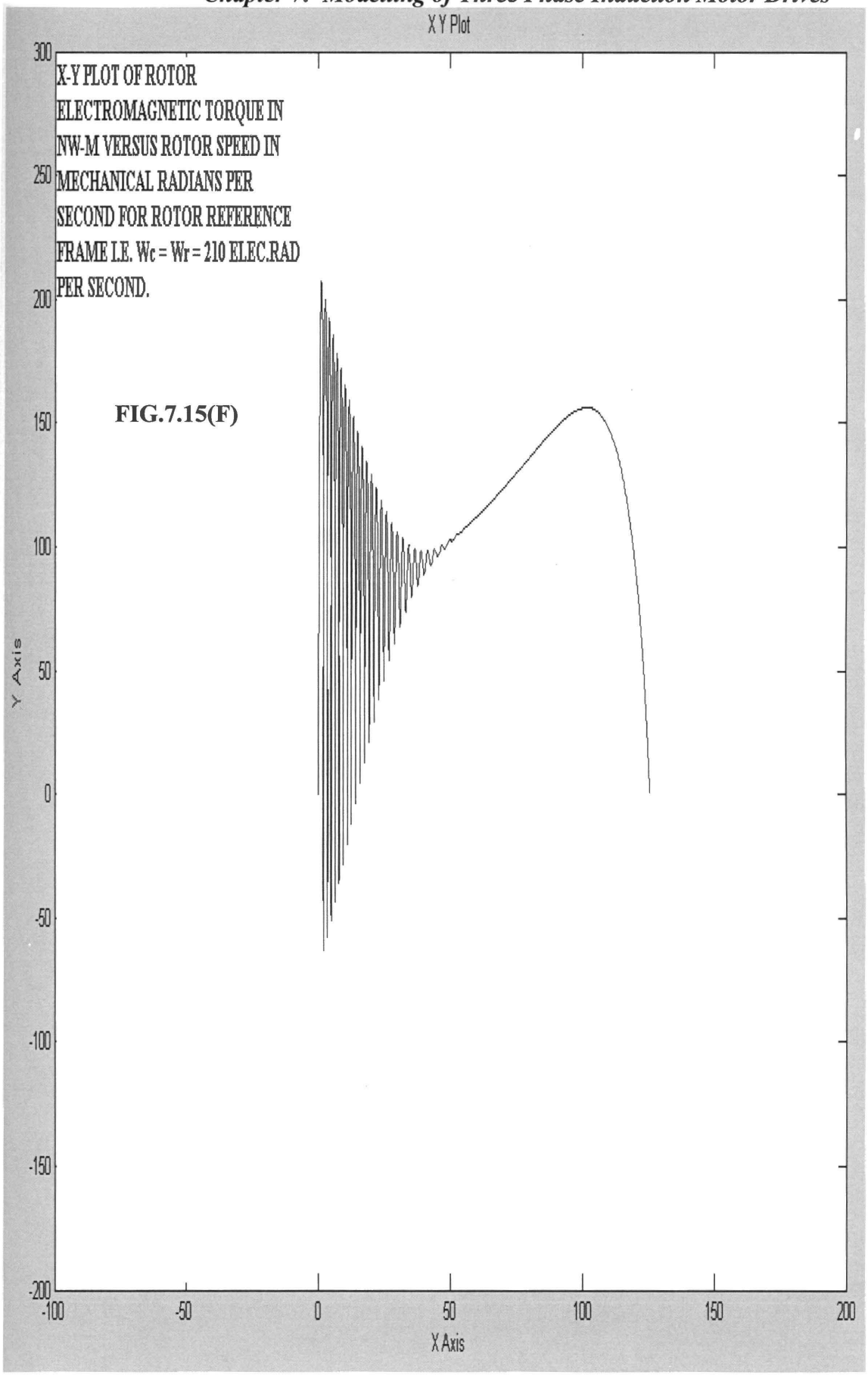
X Y Plot
X-Y PLOT OF ROTOR ELECTROMAGNETIC TORQUE IN NW-M VERSUS ROTOR SPEED IN MECHANICAL RADIANS PER SECOND FOR ROTOR REFERENCE FRAME I.E. Wc = Wr = 210 ELEC.RAD PER SECOND.
Y Axis
X Axis
300
250
200
150
100
50
0
-50
-100
-150
-200
-100
-50
0
50
100
150
200

FIG.7.15(F)

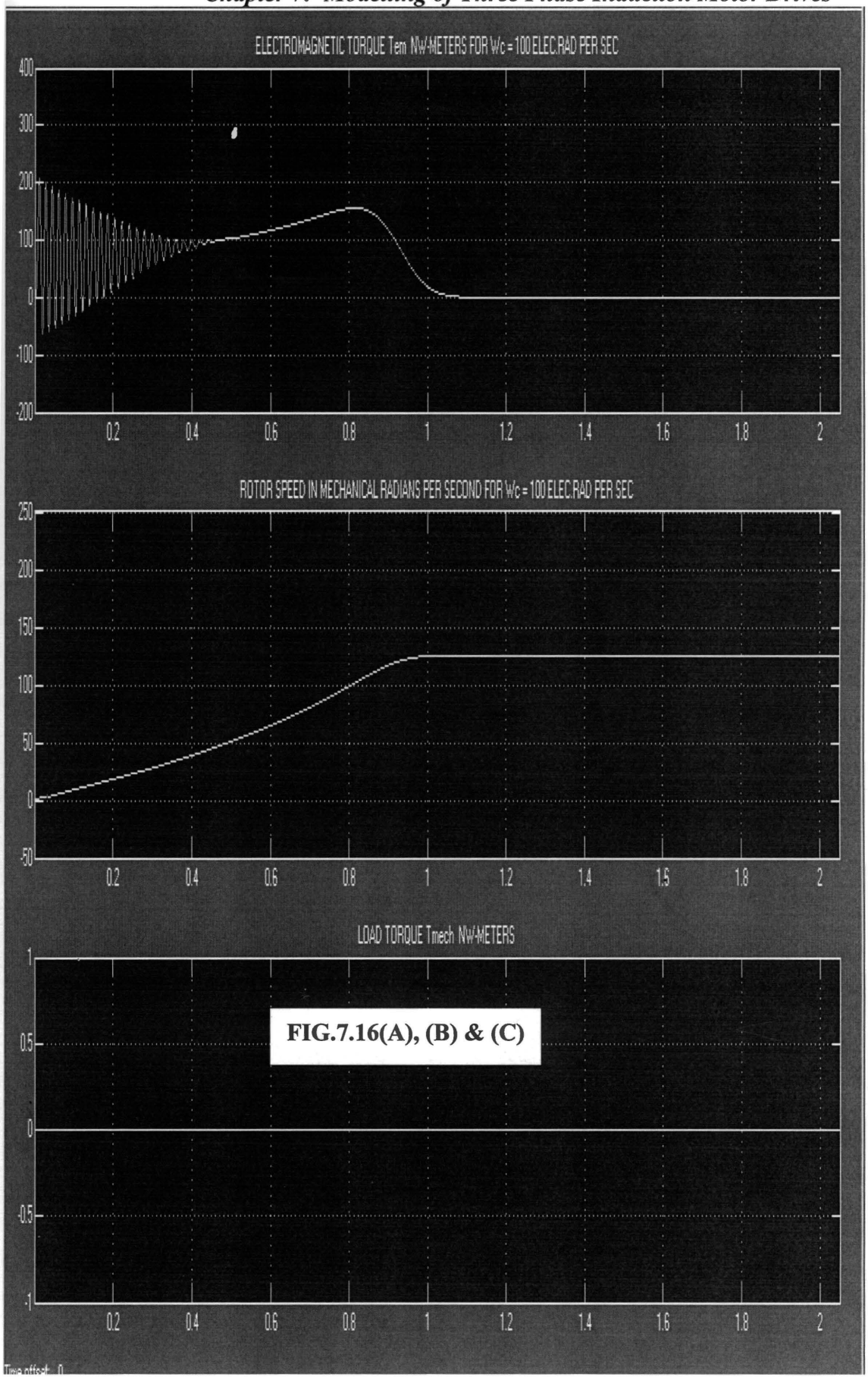
ELECTROMAGNETIC TORQUE Tem NW-METERS FOR Wc = 100 ELEC.RAD PER SEC
400
300
200
100
0
-100
-200
0.2
0.4
0.6
0.8
1
1.2
1.4
1.6
1.8
2
ROTOR SPEED IN MECHANICAL RADIANS PER SECOND FOR Wc = 100 ELEC.RAD PER SEC
250
200
150
100
50
0
-50
0.2
0.4
0.6
0.8
1
1.2
1.4
1.5
1.8
2
LOAD TORQUE Tmech NW-METERS
1
0.5
0
-0.5
-1
0.2
0.4
0.6
0.8
1
1.2
1.4
1.6
1.8
2

FIG.7.16(A), (B) & (C)

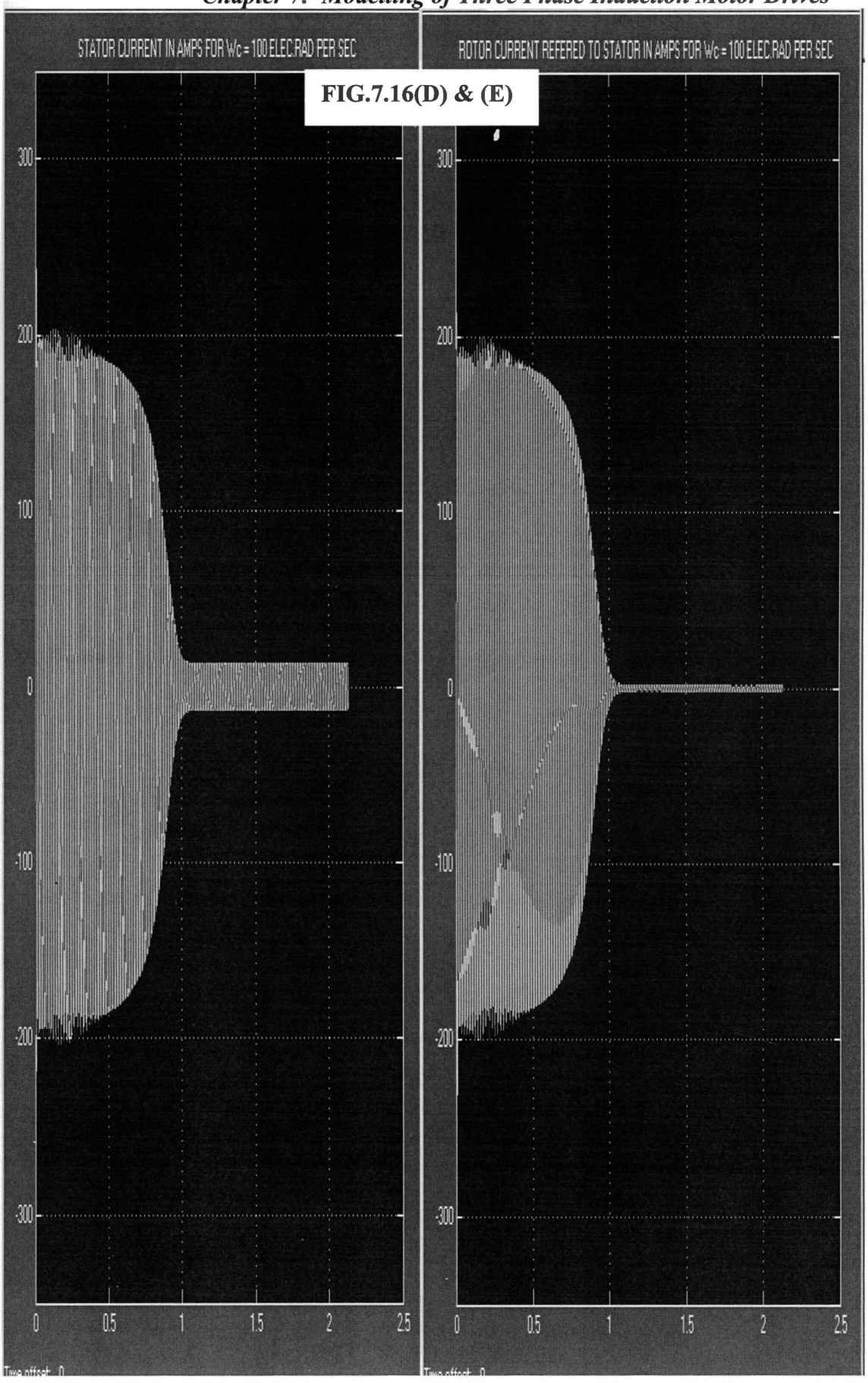
STATOR CURRENT IN AMPS FOR Wc = 100 ELEC.RAD PER SEC
ROTOR CURRENT REFERED TO STATOR IN AMPS FOR Wc = 100 ELEC.RAD PER SEC
300
200
100
0
-100
-200
-300
0
0.5
1
1.5
2
2.5

FIG.7.16(D) & (E)

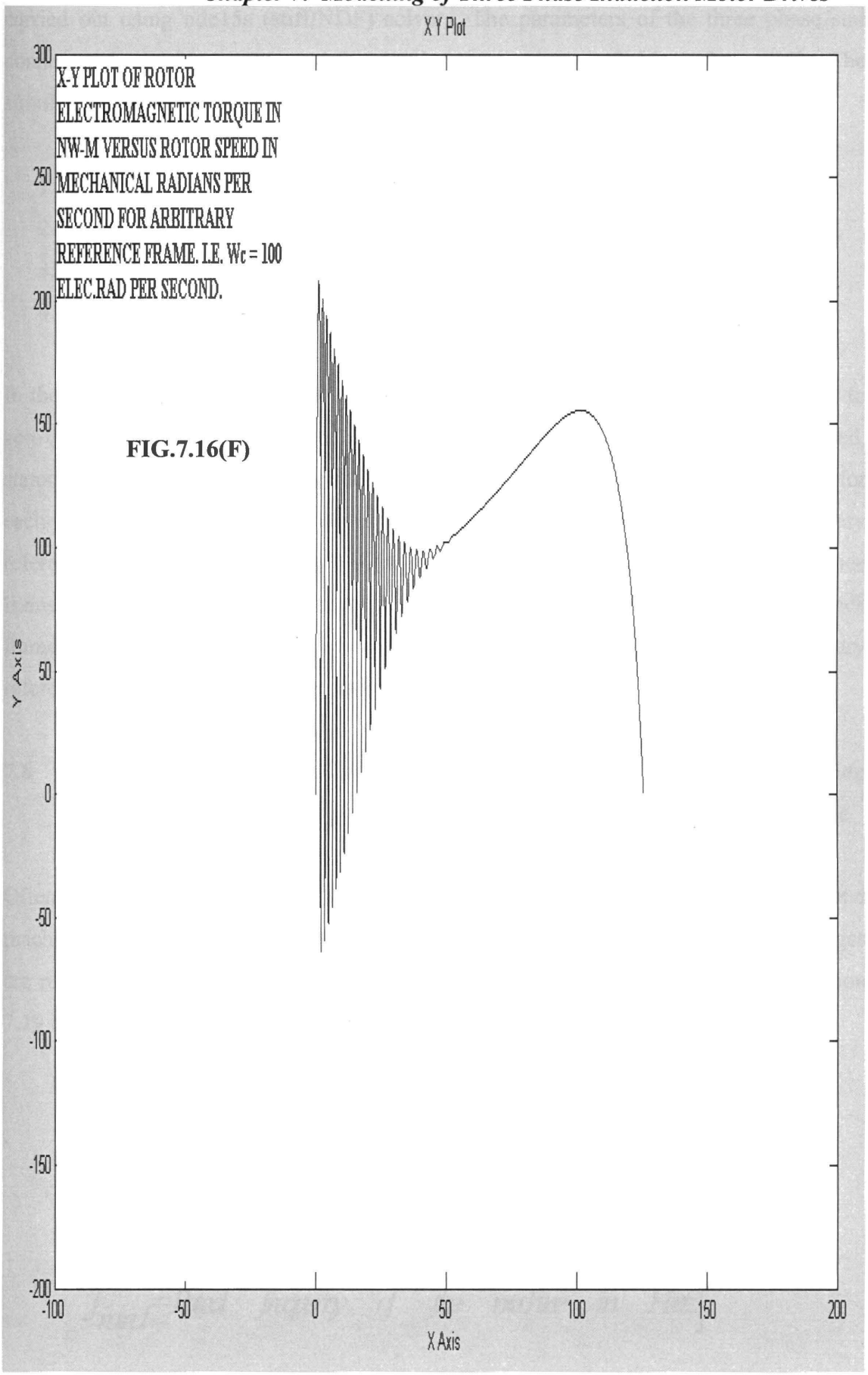
X Y Plot
X-Y PLOT OF ROTOR ELECTROMAGNETIC TORQUE IN NW-M VERSUS ROTOR SPEED IN MECHANICAL RADIANS PER SECOND FOR ARBITRARY REFERENCE FRAME. I.E. Wc = 100 ELEC.RAD PER SECOND.
Y Axis
X Axis
300
250
200
150
100
50
0
-50
-100
-150
-200
-100
-50
0
50
100
150
200

FIG.7.16(F)

carried out using ode15s (stiff/NDF) solver. The parameters of the three phase star connected squirrel cage IM used for simulation are given in Table 1 above [10]. The simulation was carried out in the following reference frames:

1. Stationary(stator) reference frame $\omega_C = \omega_S = 0$
2. Synchronous(excitation) reference frame $\omega_C = \omega_e = 377$ elec.rad per sec.
3. Rotor reference frame $\omega_C = \omega_{re} = 210$ elec.rad per sec.
4. Arbitrary reference frame $\omega_C = 100$ elec.rad per sec.

In the simulation on all the above reference frames, the load torque Tmech was set to zero. The simulation results for the rotor electromagnetic torque Tem, rotor speed, stator current, rotor current referred to stator and torque-speed curves are shown for each of the above reference frames. Fig.7.13(A) to (F) corresponds to stationary reference frame for $\omega_C = 0$, Fig.7.14(A) to (F) for synchronous (excitation) reference frame for $\omega_C = 377$ elec.rad per second, Fig.7.15(A) to (F) correspond to rotor reference frame for $\omega_C = 210$ elec.rad per second and Fig.7.16(A) to (F) corresponds to arbitrary reference frame for $\omega_C = 100$ elec.rad per second.

7.6 Model for Three Phase Induction Motor in ALL Reference Frames Using DQ0-Axis Flux Linkage per second and Machine Reactance in State Space

Often three phase IM equations are expressed in terms of flux linkages per second and machine reactance instead of flux linkages and machine inductances. The flux linkages are related to the base value or rated value of the angular frequency ω_b as in equation 7.19 below:

$$\left.\begin{aligned} \psi &= \omega_b \lambda \quad V \text{ or per unit} \\ x &= \omega_b L \quad H \text{ or per unit} \\ \omega_b &= 2\pi f_{rated} \\ f_{rated} &= \text{Rated frequency of the machine in Hertz} \end{aligned}\right\} \quad (7.19)$$

The three phase IM equations in arbitrary reference frame ω_C can be written as shown below.

The stator qd0-axis voltage equation in arbitrary reference frame ω_C is given in equation 7.20 below:

$$\begin{bmatrix} v_{qs} \\ v_{ds} \\ v_{0s} \end{bmatrix} = \begin{bmatrix} (s/\omega_b) & (\omega_c/\omega_b) & 0 \\ -(\omega_c/\omega_b) & (s/\omega_b) & 0 \\ 0 & 0 & (s/\omega_b) \end{bmatrix} * \begin{bmatrix} \psi_{qs} \\ \psi_{ds} \\ \psi_{0s} \end{bmatrix} + [r_S] * \begin{bmatrix} i_{qs} \\ i_{ds} \\ i_{0s} \end{bmatrix} \qquad (7.20)$$

The rotor qd0-axis voltage equation in arbitrary reference frame ω_C is given in equation 7.21 below:

$$\begin{bmatrix} v'_{qr} \\ v'_{dr} \\ v'_{0r} \end{bmatrix} = \begin{bmatrix} s/(\omega_b) & (\omega_c-\omega_{re})/(\omega_b) & 0 \\ -(\omega_c-\omega_{re})/(\omega_b) & s/(\omega_b) & 0 \\ 0 & 0 & s/(\omega_b) \end{bmatrix} * \begin{bmatrix} \psi'_{qr} \\ \psi'_{dr} \\ \psi'_{0r} \end{bmatrix} + [r'_r] * \begin{bmatrix} i'_{qr} \\ i'_{dr} \\ i'_{0r} \end{bmatrix} \qquad (7.21)$$

The stator and rotor qd0-axis flux linkage per second equation in arbitrary reference frame ω_C is given in equation 7.22 below:

$$\begin{bmatrix} \psi_{qs} \\ \psi_{ds} \\ \psi_{0s} \\ \psi'_{qr} \\ \psi'_{dr} \\ \psi'_{0r} \end{bmatrix} = \begin{bmatrix} (x_{ls}+x_m) & 0 & 0 & x_m & 0 & 0 \\ 0 & (x_{ls}+x_m) & 0 & 0 & x_m & 0 \\ 0 & 0 & x_{ls} & 0 & 0 & 0 \\ x_m & 0 & 0 & (x'_{lr}+x_m) & 0 & 0 \\ 0 & x_m & 0 & 0 & (x'_{lr}+x_m) & 0 \\ 0 & 0 & 0 & 0 & 0 & x'_{lr} \end{bmatrix} * \begin{bmatrix} i_{qs} \\ i_{ds} \\ i_{0s} \\ i'_{qr} \\ i'_{dr} \\ i'_{0r} \end{bmatrix} \qquad (7.22)$$

The e.m. torue equation for Tem is given in equation 7.23 below:

$$\left.\begin{aligned} T_{em} &= \frac{3}{2}\cdot\frac{P}{2.\omega_b}\cdot(\psi'_{qr} i'_{dr} - \psi'_{dr} i'_{qr}) \\ &= \frac{3}{2}\cdot\frac{P}{2.\omega_b}\cdot(\psi_{ds} i_{qs} - \psi_{qs} i_{ds}) \\ &= \frac{3}{2}\cdot\frac{P}{2.\omega_b}\cdot x_m\cdot(i'_{dr} i_{qs} - i'_{qr} i_{ds}) \end{aligned}\right| \qquad (7.23)$$

The machine equations from 7.20 to 7.22 can be expressed in the state space form similar to equation 7.17, where all λ are replaced by ψ and all ω_c and $(\omega_c - \omega_{re})$ terms are multiplied by $(1/\omega_b)$. This flux linkage per second and reactance equation in state space is given below in equation 7.24.

$$\begin{bmatrix} \psi_{qs\_dot} \\ \psi_{ds\_dot} \\ \psi_{0s\_dot} \\ \psi'_{qr\_dot} \\ \psi'_{dr\_dot} \\ \psi'_{0r\_dot} \end{bmatrix} = \begin{bmatrix} 0 & -\omega_C & 0 & 0 & 0 & 0 \\ \omega_C & 0 & 0 & 0 & 0 & 0 \\ 0 & 0 & 0 & 0 & 0 & 0 \\ 0 & 0 & 0 & 0 & -(\omega_C-\omega_{re}) & 0 \\ 0 & 0 & 0 & (\omega_C-\omega_{re}) & 0 & 0 \\ 0 & 0 & 0 & 0 & 0 & 0 \end{bmatrix} * \begin{bmatrix} \psi_{qs} \\ \psi_{ds} \\ \psi_{0s} \\ \psi'_{qr} \\ \psi'_{dr} \\ \psi'_{0r} \end{bmatrix}$$

$$- \omega_b * \begin{bmatrix} r_S & 0 & 0 & 0 & 0 & 0 \\ 0 & r_S & 0 & 0 & 0 & 0 \\ 0 & 0 & r_S & 0 & 0 & 0 \\ 0 & 0 & 0 & r'_r & 0 & 0 \\ 0 & 0 & 0 & 0 & r'_r & 0 \\ 0 & 0 & 0 & 0 & 0 & r'_r \end{bmatrix} * \begin{bmatrix} i_{qs} \\ i_{ds} \\ i_{0s} \\ i'_{qr} \\ i'_{dr} \\ i'_{0r} \end{bmatrix} + \omega_b * \begin{bmatrix} v_{qs} \\ v_{ds} \\ v_{0s} \\ v'_{qr} \\ v'_{dr} \\ v'_{0r} \end{bmatrix} \qquad (7.24)$$

where ψ_{qs_dot} is $\frac{d\psi_{qs}}{dt}$ and so on. Now calling the 6X1 flux linkage per second matrix in equation 7.22 as **Ψ**, the 6X6 inductive reactance matrix in equation 7.22 as **X**, the 6X1 current matrix as **I**, the 6X6 matrix containing ω_C, ω_{re} and ω_b in equation 7.24 as **N**, the 6X6 stator and rotor resistance matrix as **R** and the 6X1 voltage matrix in equation 7.24 as **V**, equation 7.22 and 7.24 can be combined as in equation 7.25 below:

$$[\Psi\_dot] = [N]*[\Psi] - \omega_b*[R]*[X^{-1}]*[\Psi] + \omega_b*[V] \qquad (7.25)$$

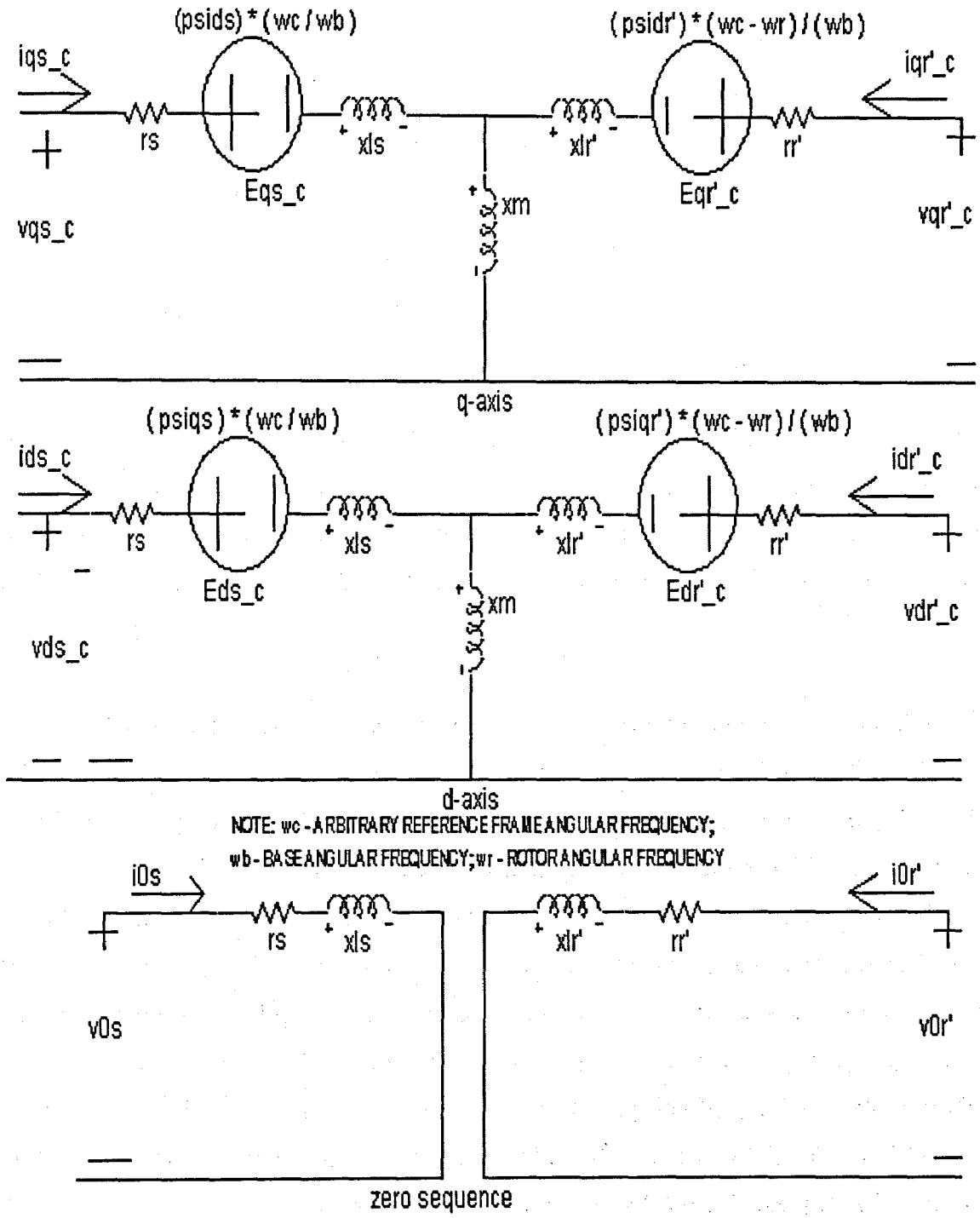

FIG.7.17 EQUIVALENT CIRCUIT OF THREE PHASE I.M. IN ARBITRARY REFERENCE FRAME

The equivalent circuit of the three phase IM in the arbitrary reference frame ω_c using the flux linkage (or the Flux linkage per second) model is shown in Fig.7.17. In Fig.7.17, the following symbols shown in equation 7.26 are used:

$$\left.\begin{aligned} psids &= \psi_{ds} \\ psiqs &= \psi_{qs} \\ psidr' &= \psi'_{dr} \\ psiqr' &= \psi'_{qr} \end{aligned}\right| \qquad (7.26)$$

Equation 7.25 is in the state space form

$$\vec{x}\_dot = \vec{A}.\vec{x} + \vec{B}.\vec{u}. \qquad (7.27)$$

The model for the three phase IM using the qd0-axis flux linkage per second and machine reactance equations in state space in ALL reference frames is shown in Fig.7.18. The various dialog boxes are shown in Fig.7.19. The various subsystems used are shown in Fig.7.20(A) to (C). The function of the various subsystems are detailed below:

Fig.7.20(A) corresponds to the dialog box Three Phase AC Generator and abc to dq0 axis Transform shown in Fig.7.19. Fig.7.20(A) is the same as Fig.7.12(A) which has already been explained in Section 7.5. Fig.7.20(B) corresponds to the dialog box Three Phase IM Model Data in Fig.7.19.. In this dialog box, the values of xls, xlr', xm, Rs, Rr' relating to stator and rotor, rated angular frequency of the machine (or rated supply angular frequency) ω_b, arbitrary frame angular frequency ω_C are entered in the appropriate units. In Fig.7.20(B), the eight input mux with dq0-axis stator and rotor flux linkages per second Ψ multiplied by ω_b , reference frame frequency ω_C and rotor speed ω_{r_elec} in electrical radians per second both multiplied by (1 / ω_b) along with the six Fcn block solves the first term on the R.H.S. of equation 7.25. The DSP constant block marked XL_MATRIX and the general inverse (LU) block computes inverse of X matrix. This X^{-1} Matrix is then multiplied by Ψ matrix using Matrix Multiply1 block to obtain the dq0 stator and rotor current I matrix. The DSP constant block marked RESISTANCE_MATRIX in Fig.7.12(B) generates the R matrix containing diagonal elements of stator and rotor resistance referred to stator defined in equation 7.24. This R matrix is then multiplied by the I matrix using the Matrix Multiply2 block to obtain the second term in equation 7.25. The dq0-axis voltage V matrix is available from

Fig.7.20(A). These three terms are the summed with appropriate signs in the Add block to obtain the derivative of the stator and rotor flux linkage per second vector Ψ_dot matrix. This is then integrated using individual integrator block and then multiplied by ω_b to obtain the dq0-axis stator and rotor flux linkages per second Ψ matrix. Fig.7.20(C) corresponds to the dialog box for Rotor Torque and Speed calculator in Fig.7.19. In this the mutual reactance Xm, number of poles P, Moment of Inertia of motor and load, the Damping constant and the rated angular frequency of the machine ω_b in electrical radians per second are entered in the appropriate units. In Fig.7.20(C), the two multiplier blocks, the subtract block and the gain multiplier block with the multiplier constant [3*P*Xm / (4.ω_b)] calculates the rotor e.m. torque Tem given by equation 7.23. The mechanical load torque Tmech is generated using the repeating sequence block as shown in Fig.7.10. The value of Tem and Tmech are subtracted using the Subtract block and given to the Transfer Fcn block with the transfer function [1 / ((Jm + Jl).s + D)] to obtain the rotor speed in mechanical radians per second, which is then multiplied by gain block with the multiplier [P / 2] to obtain the rotor speed in ω_{r_elec} electrical radians per second. The dq0 to abc transform block in Fig.7.12(C) transforms the dq0-axis stator and rotor current back to abc axis as per the transformation matrix defined by equation 1.2 in Chapter 1.

7.6.1 Simulation Results.

The simulation of the flux linkage per second and machine reactance model of three phase IM in all reference frame was carried out using ode23tb(stiff/TR-BDF2) solver. The parameters of the three phase star connected squirrel cage IM used for simulation are given in Table 1 above [10]. The simulation was carried out in the following reference frames:

1. Stationary(stator) reference frame $\omega_C = \omega_S = 0$
2. Synchronous(excitation) reference frame $\omega_C = \omega_e = 377$ elec.rad per sec.
3. Rotor reference frame $\omega_C = \omega_{re} = 210$ elec.rad per sec.
4. Arbitrary reference frame $\omega_C = 100$ elec.rad per sec.

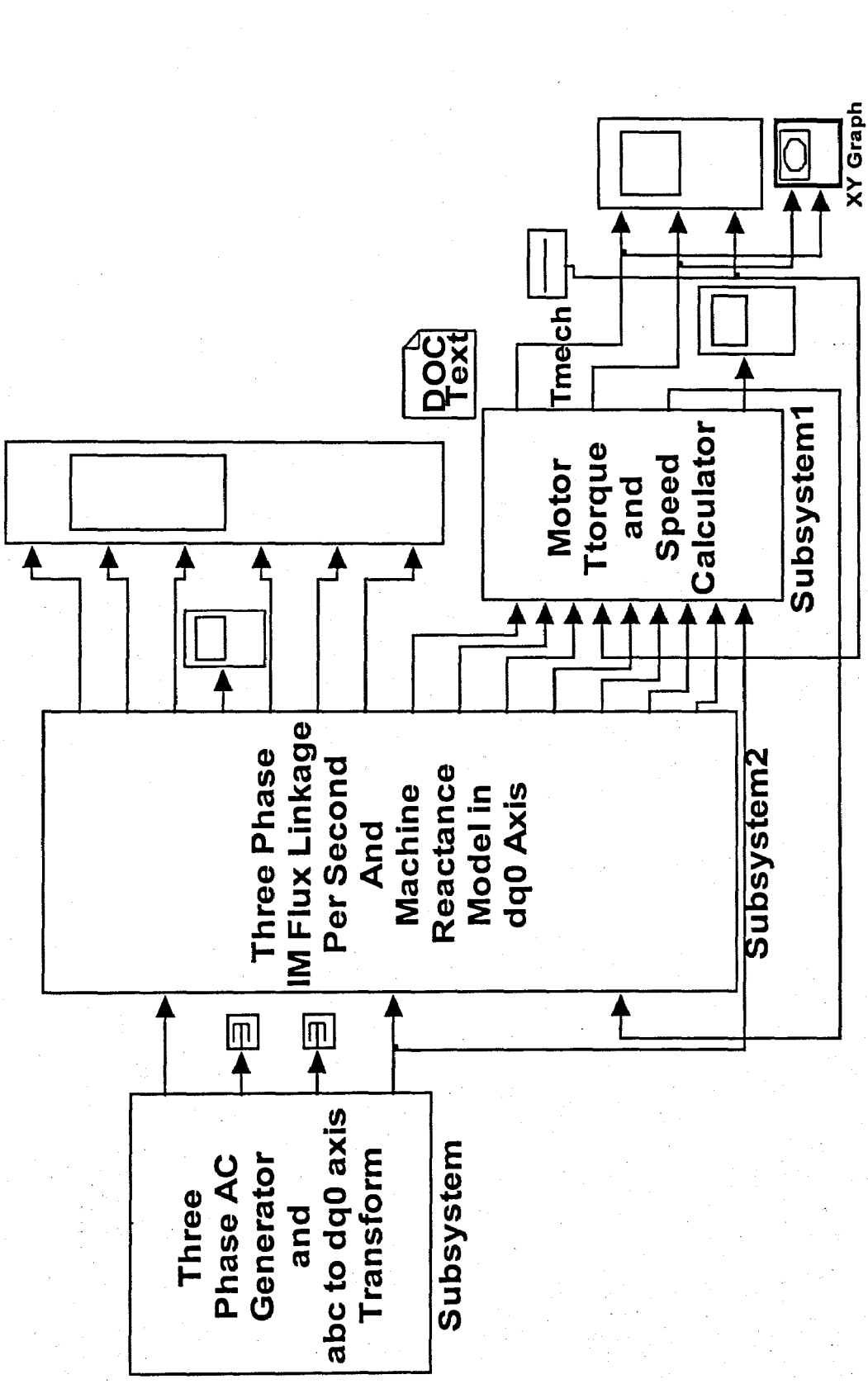

FIG.7.18: THREE PHASE INDUCTION MOTOR FLUX LINKAGE PER SECOND AND MACHINE REACTANCE MODEL IN ALL REFERENCE FRAMES IN STATE SPACE

Block Parameters: Subsystem
Three Phase AC Generator and abc to dq0 Axis Transform (mask)
Enter the PEAK Value of the line to neutral voltage in volts, Supply frequency in Hertz and the angular frequency of the reference frame in Electrical radians per second..
Parameters
Enter the PEAK value of Line to Neutral Voltage in Volts
179.6
Enter the SUPPLY frequency in Hertz
60
Enter the ANGULAR FREQUENCY OF THE REFERENCE FRAME in Electrical radians per second
0
OK
Cancel
Help
Apply
Block Parameters: Subsystem1
Rotor Torque and Speed Calculator (mask)
Enter the Mutual reactance xm between Stator and Rotor in Ohms, the Number of Poles P, the combined Moment of Inertia of the Motor and Load in Kg.m^2, the Damping Constant in Nw.m.Sec per elec.rad and the rated angular frequency of the machine (supply angular frequency) in electrical radians per second.
Parameters
Enter the Mutual Reactance between Stator and Rotor in Ohms
15.457
Enter the Number of Poles
6
Enter the combined M.I. of motor and Load in kgm^2
0.8
Enter the Damping Constant Nw.m.sec per elec.rad
0
Enter the rated angular frequency wb of the machine in electrical radians per second.
2*pi*60
OK
Cancel
Help
Apply
Three Phase AC Generator and abc to dq0 axis Transform
Subsystem
Three Phase IM Flux Linkage Per Second And Machine Reactance Model in dq0 Axis
Subsystem2
Motor Torque and Speed Calculator
Subsystem1
Block Parameters: Subsystem2
Three Phase IM Model Data (mask)
Enter the Stator Leakage reactance xls, Rotor Leakage reactance referred to Stator xlr', Mutual reactance between stator and Rotor xm all in Henries per phase. Enter Stator Resistance Rs, Rotor resistance referred to stator Rr' all in Ohms per phase. Enter Angular Frequency of the reference frame in Electrical radians per second. Also enter the rated angular frequency wb of the machine (supply angular frequency) in electrical radians per second.
Parameters
Enter Stator Leakage reactance xls in Ohms
0.524
Enter rotor leakage reactance xlr' referred to Stator in Ohms
0.279
Enter Mutual reactance between Stator and Rotor in Ohms
15.457
Enter Stator resistance in Ohms
0.294
Enter Rotor resistance referred to Stator in Ohms
0.156
Enter the base or rated angular frequency of the machine wb in electrical radians per second
2*pi*60
Enter Angular Frequency wc of the Reference Frame in Electrical radians per second
0
OK
Cancel
Help
Apply
Ready
51%

FIG. 7.19

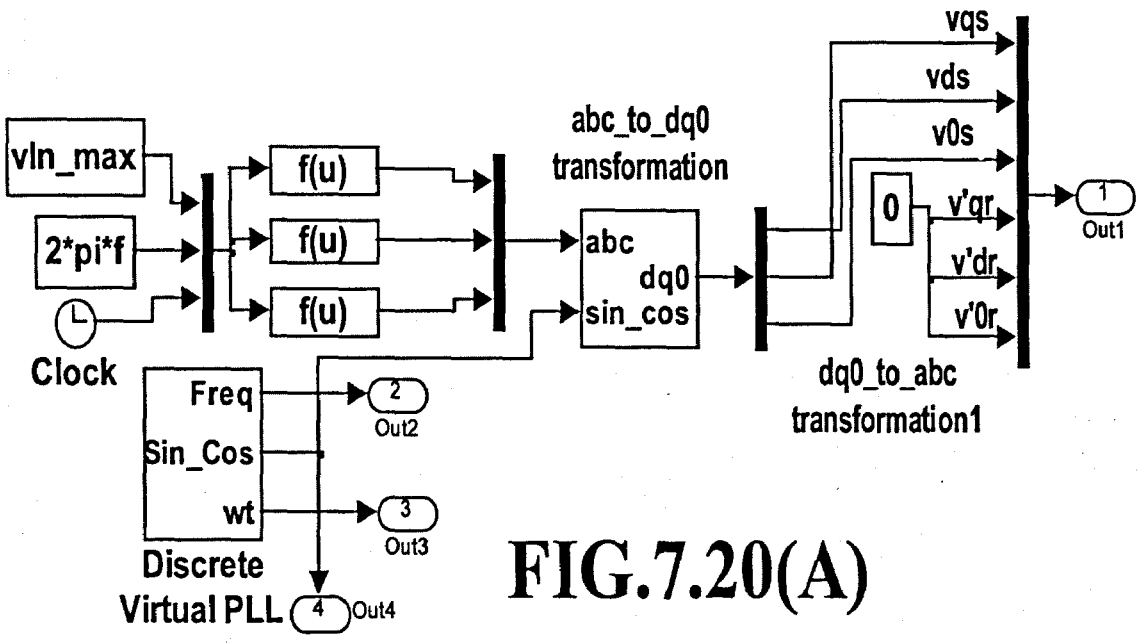

FIG.7.20(A)

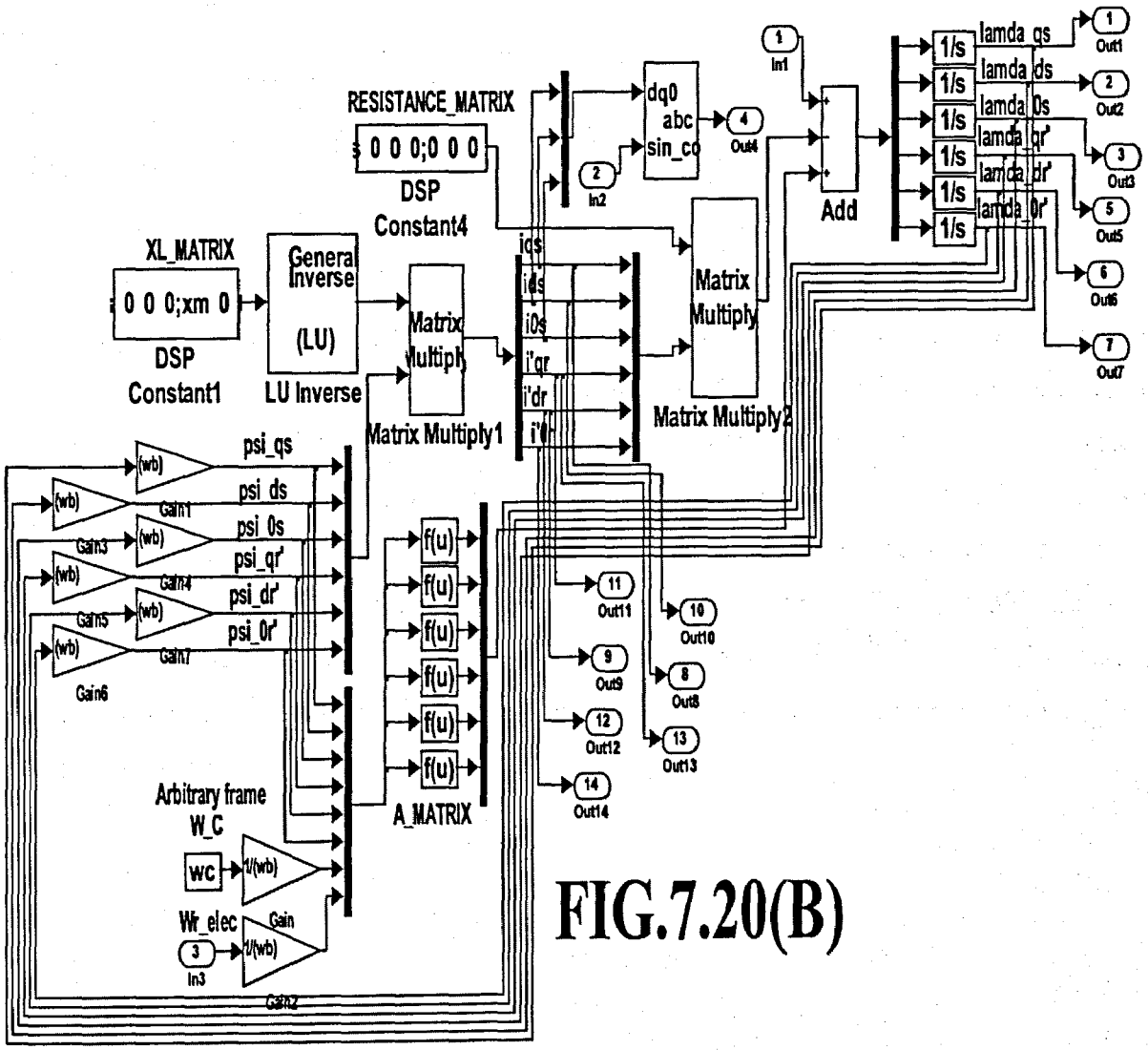

FIG.7.20(B)

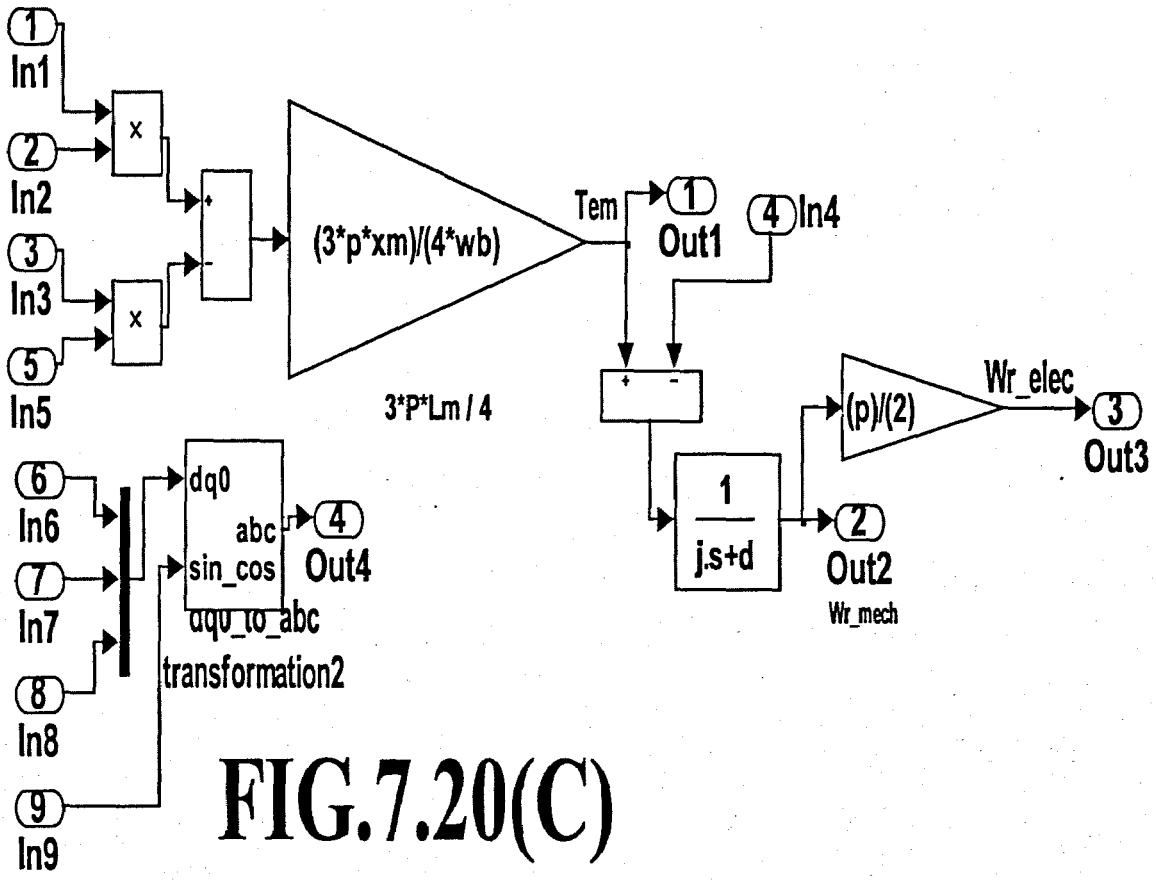

FIG.7.20(C)

In the simulation on all the above reference frames, the load torque Tmech was set to half the rated e.m. torque of the machine which is 30.6 Nw-meters. The simulation results for the rotor electromagnetic torque Tem, rotor speed, stator current, rotor current referred to stator and torque-speed curves are shown for each of the above reference frames. Fig.7.21(A) to (F) corresponds to stationary reference frame for ω_C = 0, Fig.7.22(A) to (F) for synchronous (excitation) reference frame for ω_C = 377 elec.rad per second, Fig.7.23(A) to (F) correspond to rotor reference frame for ω_C = 210 elec.rad per second and Fig.724(A) to (F) corresponds to arbitrary reference frame for ω_C = 100 elec.rad per second.

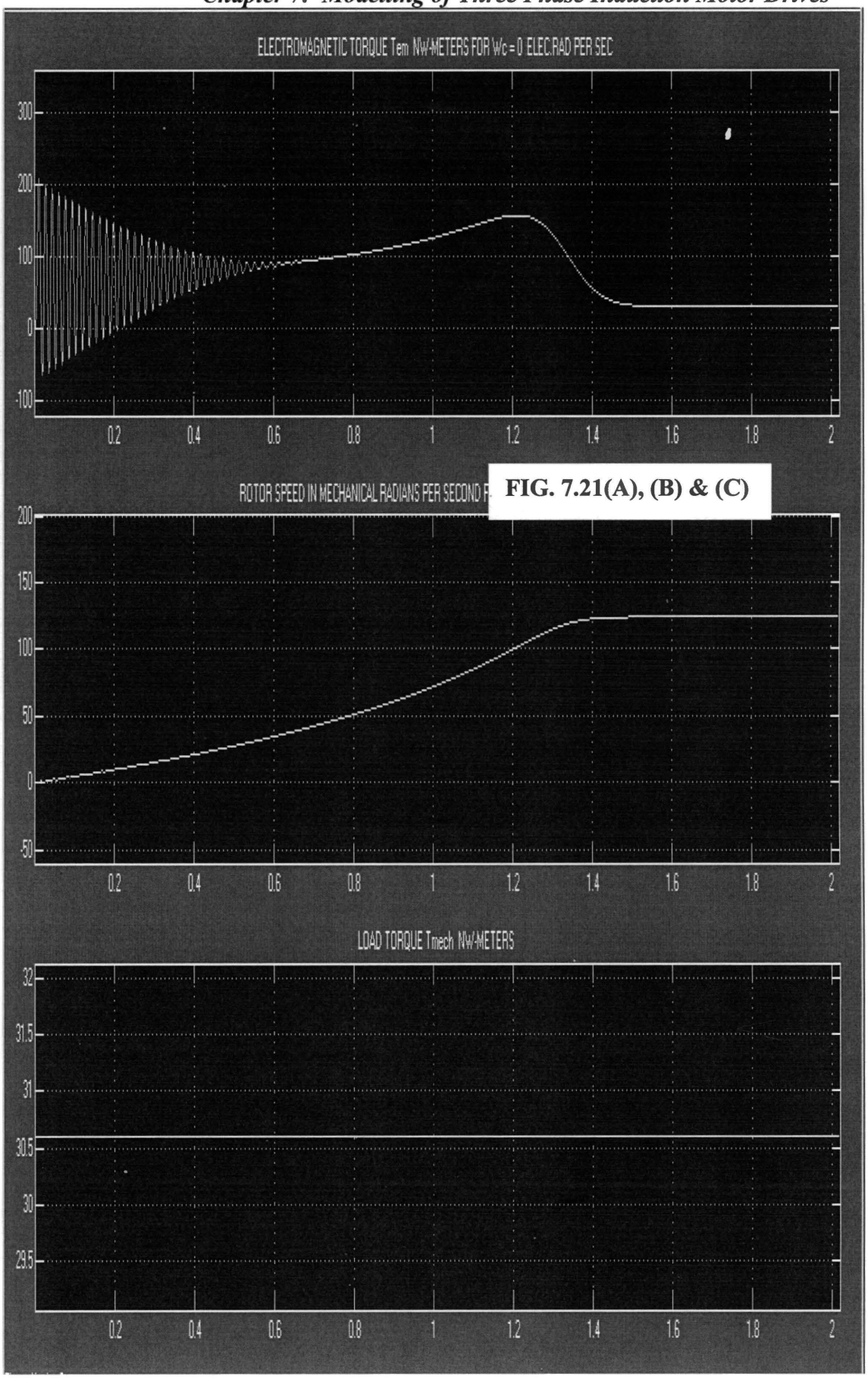
ELECTROMAGNETIC TORQUE Tem NW-METERS FOR Wc = 0 ELEC.RAD PER SEC
300
200
100
0
-100
0.2
0.4
0.6
0.8
1
1.2
1.4
1.6
1.8
2
ROTOR SPEED IN MECHANICAL RADIANS PER SECOND
200
150
100
50
0
-50
0.2
0.4
0.6
0.8
1
1.2
1.4
1.6
1.8
2
LOAD TORQUE Tmech NW-METERS
32
31.5
31
30.5
30
29.5
0.2
0.4
0.6
0.8
1
1.2
1.4
1.6
1.8
2

FIG. 7.21(A), (B) & (C)

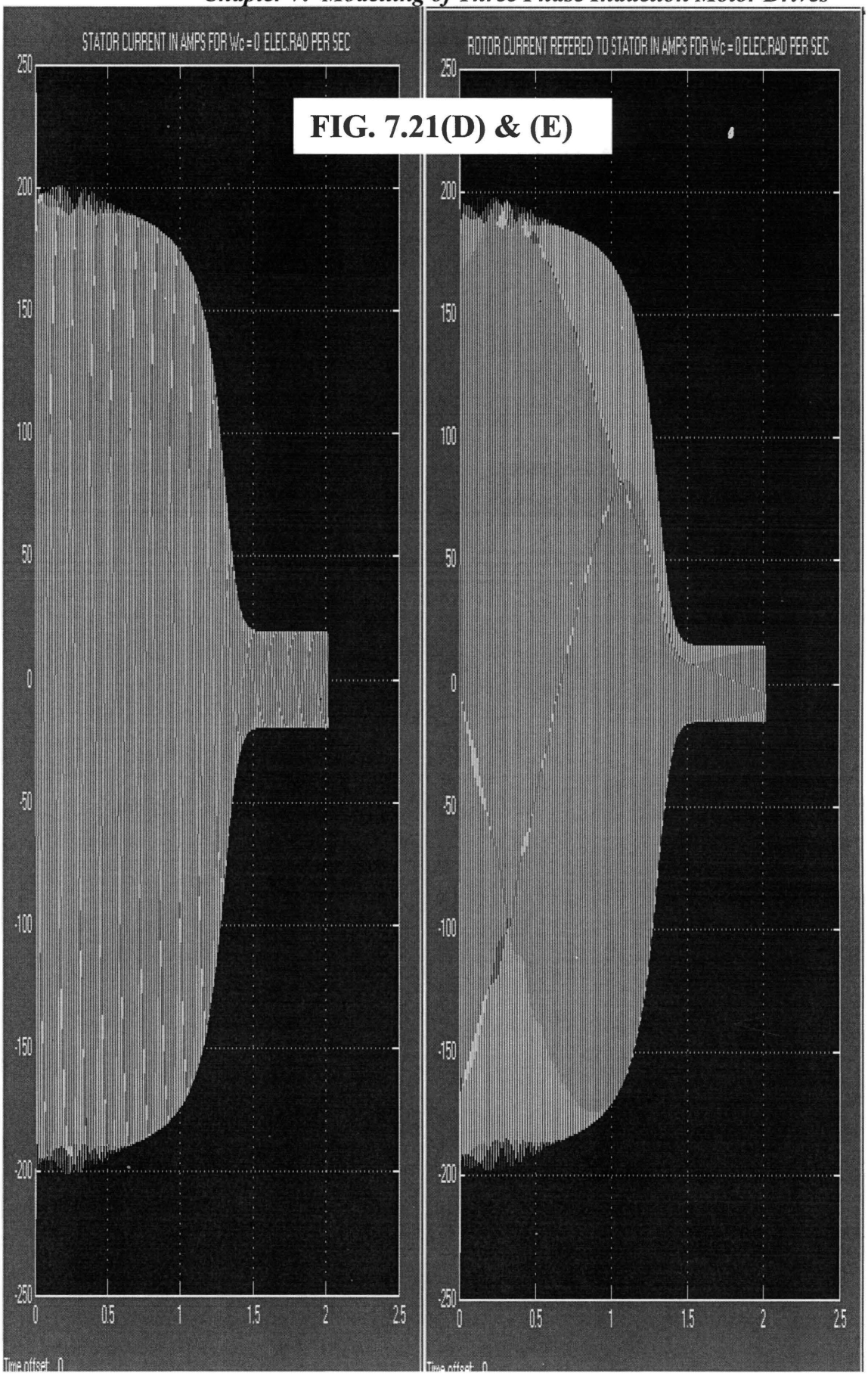
STATOR CURRENT IN AMPS FOR Wc = 0 ELEC.RAD PER SEC
250
200
150
100
50
0
-50
-100
-150
-200
-250
0
0.5
1
1.5
2
2.5
Time offset: 0
ROTOR CURRENT REFERED TO STATOR IN AMPS FOR Wc = 0 ELEC.RAD PER SEC
250
200
150
100
50
0
-50
-100
-150
-200
-250
0
0.5
1
1.5
2
2.5
Time offset: 0

FIG. 7.21(D) & (E)

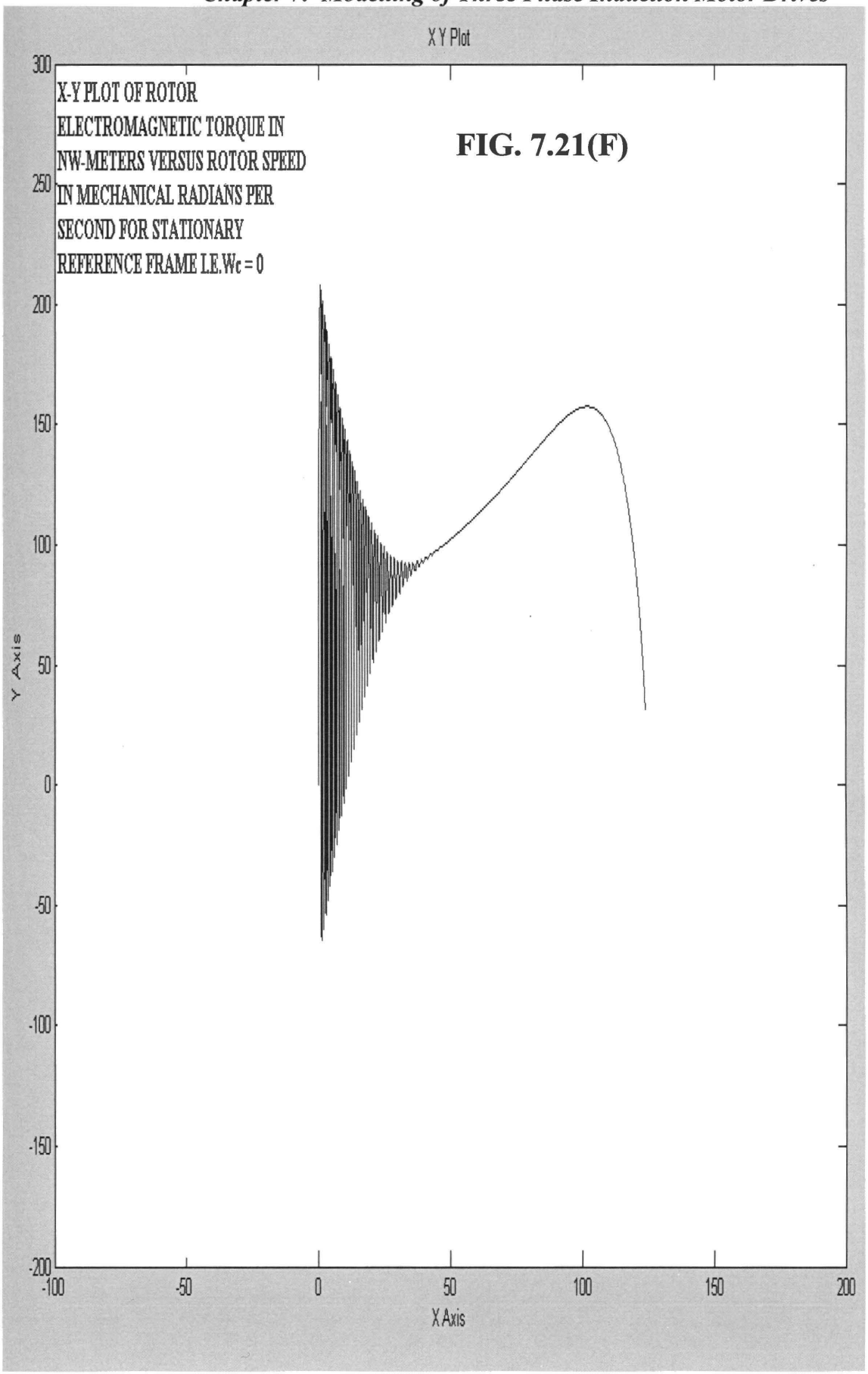
X Y Plot
X-Y PLOT OF ROTOR ELECTROMAGNETIC TORQUE IN NW-METERS VERSUS ROTOR SPEED IN MECHANICAL RADIANS PER SECOND FOR STATIONARY REFERENCE FRAME I.E.Wc = 0
Y Axis
X Axis
300
250
200
150
100
50
0
-50
-100
-150
-200
-100
-50
0
50
100
150
200

FIG. 7.21(F)

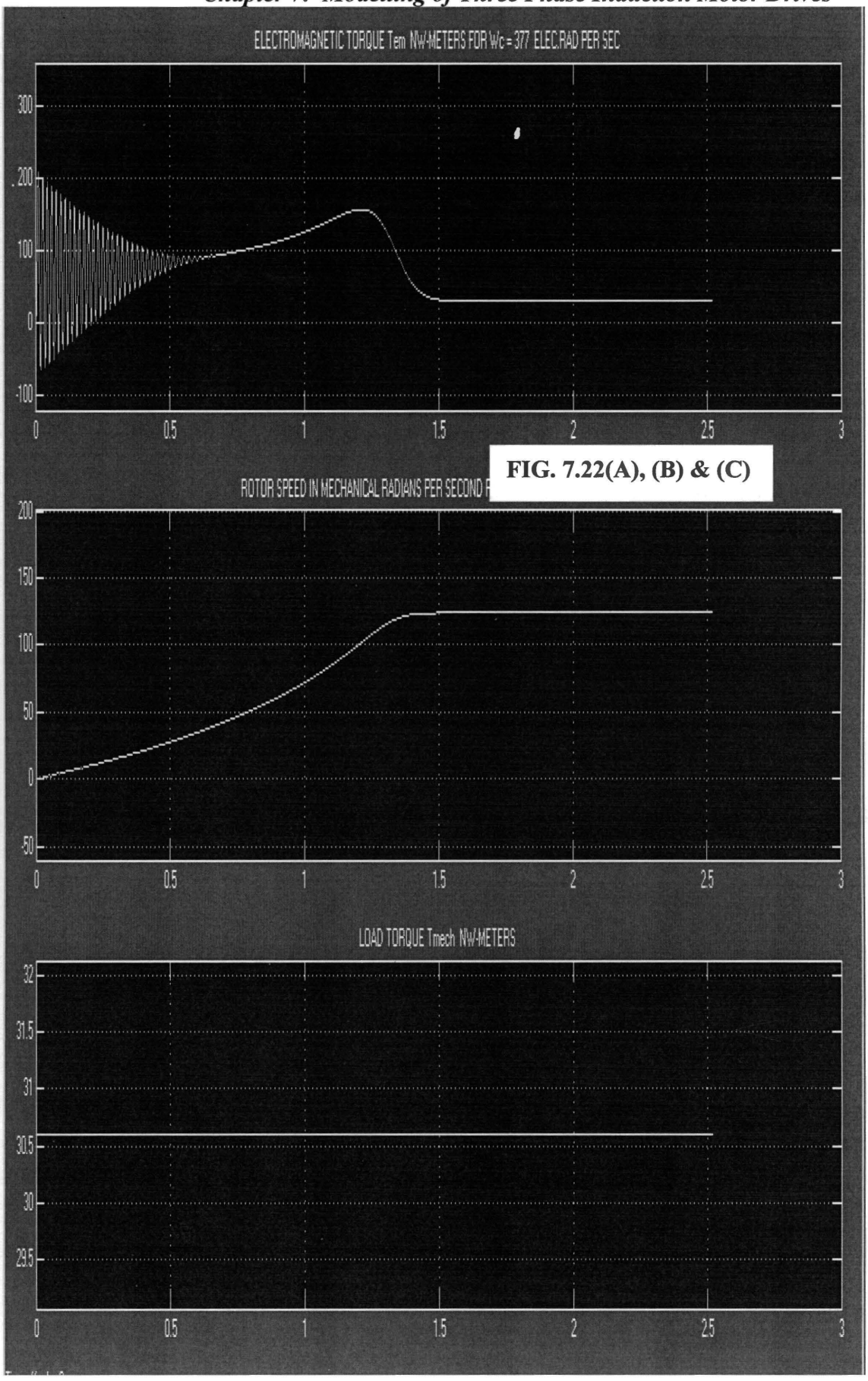
ELECTROMAGNETIC TORQUE Tem NW-METERS FOR Wc = 377 ELEC.RAD PER SEC
300
200
100
0
-100
0
0.5
1
1.5
2
2.5
3
ROTOR SPEED IN MECHANICAL RADIANS PER SECOND
200
150
100
50
0
-50
0
0.5
1
1.5
2
2.5
3
LOAD TORQUE Tmech NW-METERS
32
31.5
31
30.5
30
29.5
0
0.5
1
1.5
2
2.5
3

FIG. 7.22(A), (B) & (C)

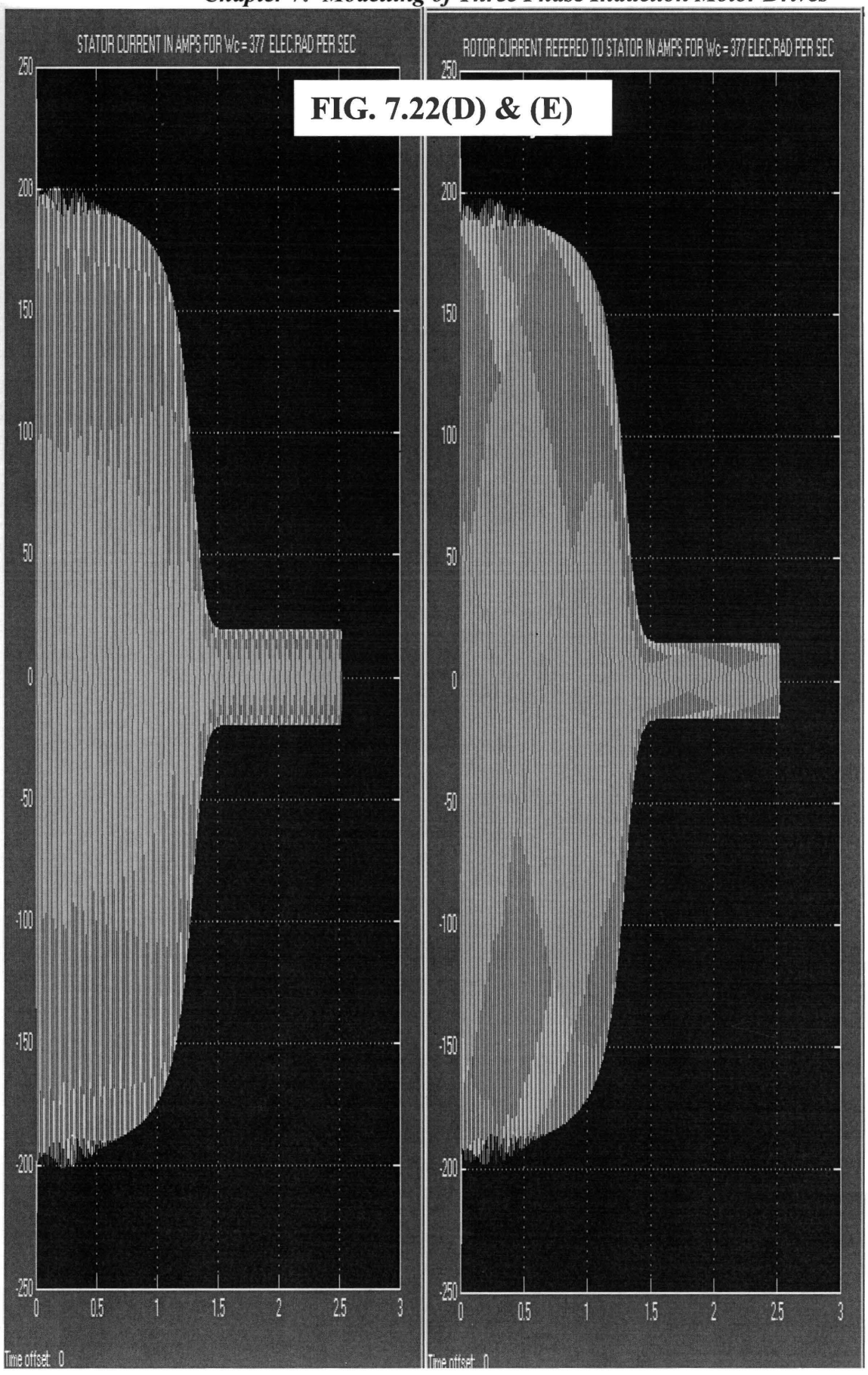
STATOR CURRENT IN AMPS FOR Wc = 377 ELEC.RAD PER SEC
250
200
150
100
50
0
-50
-100
-150
-200
-250
0
0.5
1
1.5
2
2.5
3
Time offset: 0
ROTOR CURRENT REFERED TO STATOR IN AMPS FOR Wc = 377 ELEC.RAD PER SEC
250
200
150
100
50
0
-50
-100
-150
-200
-250
0
0.5
1
1.5
2
2.5
3
Time offset: 0

FIG. 7.22(D) & (E)

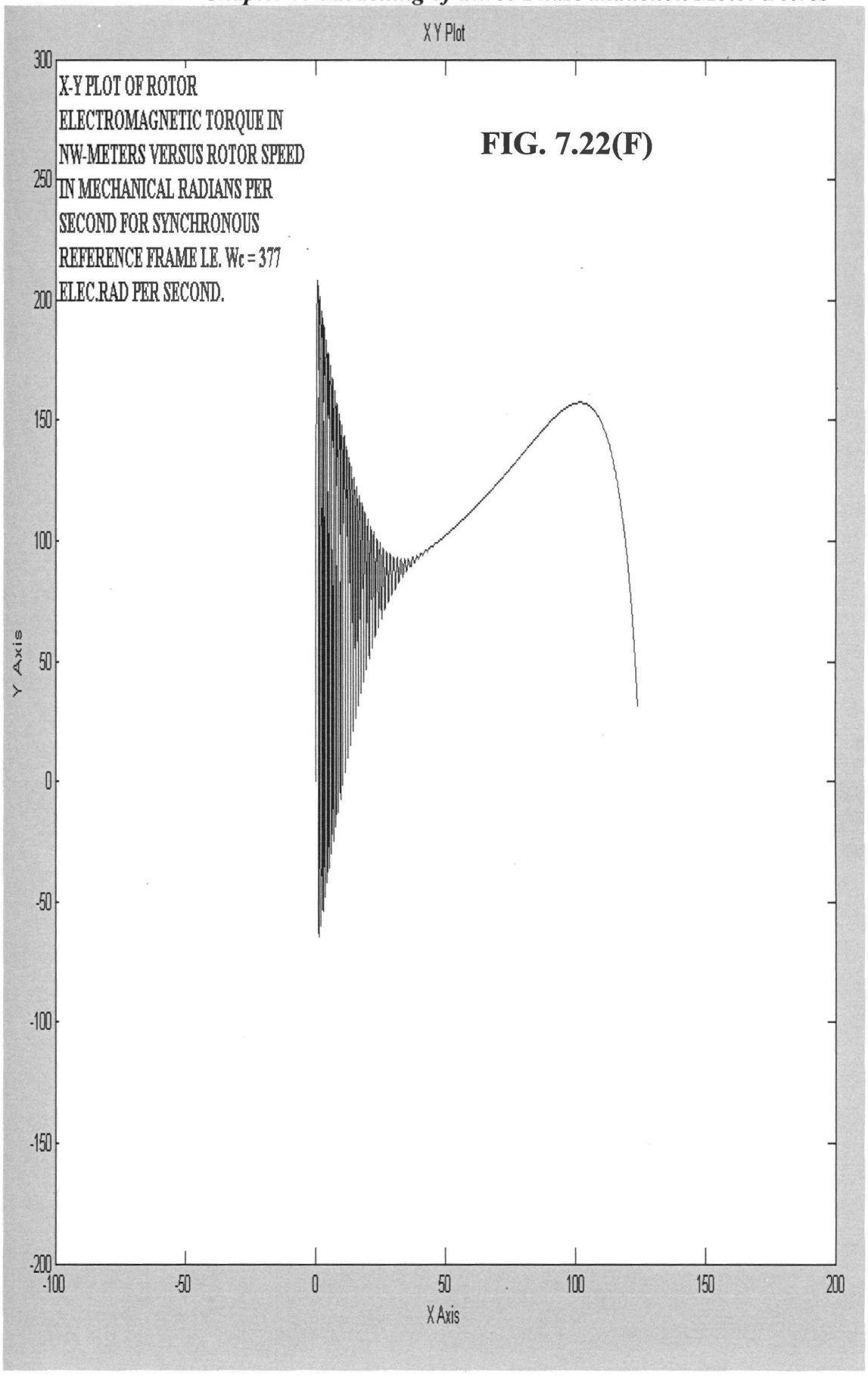
X Y Plot
X-Y PLOT OF ROTOR ELECTROMAGNETIC TORQUE IN NW-METERS VERSUS ROTOR SPEED IN MECHANICAL RADIANS PER SECOND FOR SYNCHRONOUS REFERENCE FRAME I.E. Wc = 377 ELEC.RAD PER SECOND.
Y Axis
X Axis
300
250
200
150
100
50
0
-50
-100
-150
-200
-100
-50
0
50
100
150
200

FIG. 7.22(F)

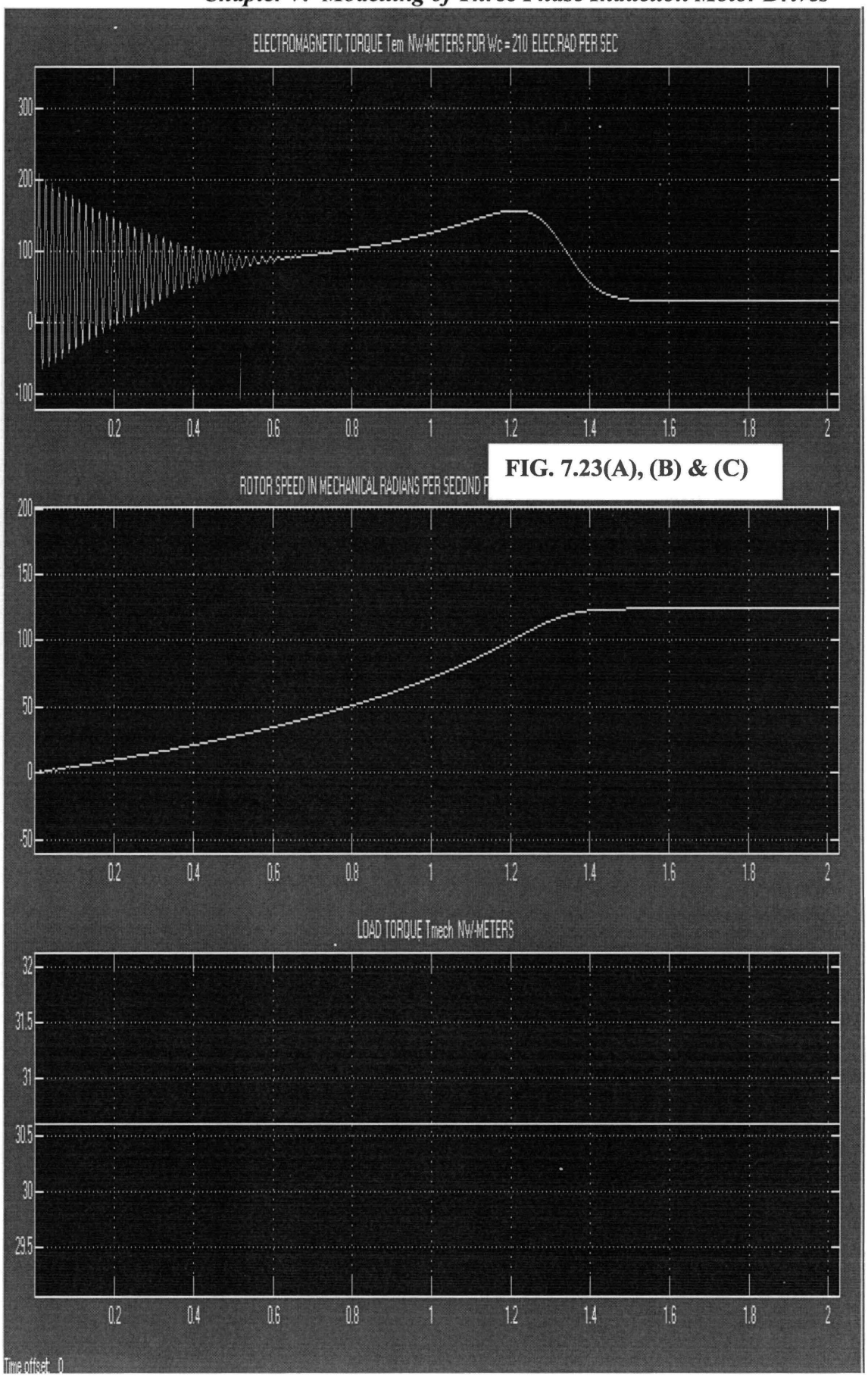
ELECTROMAGNETIC TORQUE Tem NW-METERS FOR Wc = 210 ELEC.RAD PER SEC
300
200
100
0
-100
0.2
0.4
0.6
0.8
1
1.2
1.4
1.6
1.8
2
ROTOR SPEED IN MECHANICAL RADIANS PER SECOND
200
150
100
50
0
-50
0.2
0.4
0.6
0.8
1
1.2
1.4
1.6
1.8
2
LOAD TORQUE Tmech NW-METERS
32
31.5
31
30.5
30
29.5
0.2
0.4
0.6
0.8
1
1.2
1.4
1.6
1.8
2
Time offset: 0

FIG. 7.23(A), (B) & (C)

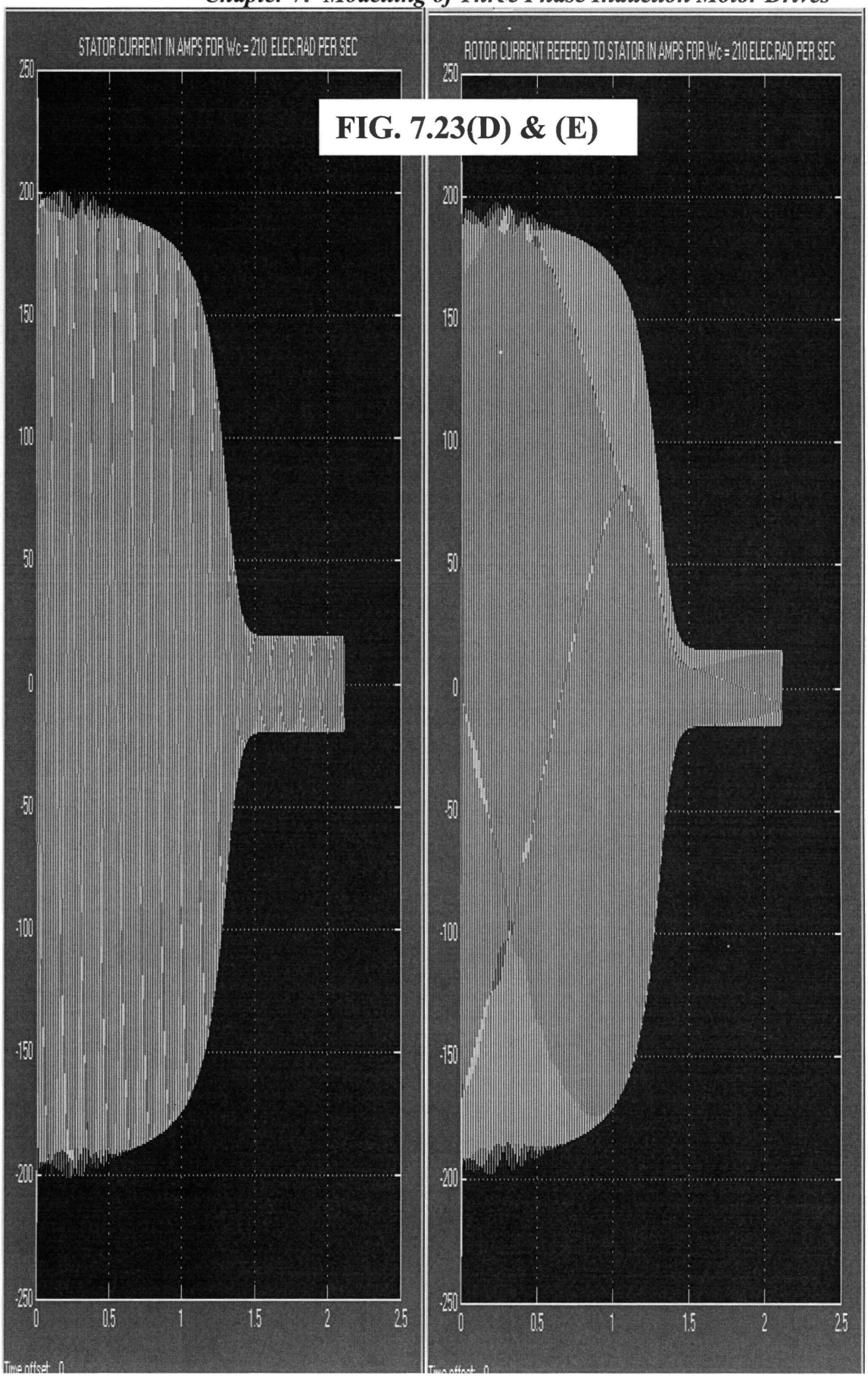
STATOR CURRENT IN AMPS FOR Wc = 210 ELEC.RAD PER SEC
250
200
150
100
50
0
-50
-100
-150
-200
-250
0
0.5
1
1.5
2
2.5
Time offset: 0
ROTOR CURRENT REFERED TO STATOR IN AMPS FOR Wc = 210 ELEC.RAD PER SEC
250
200
150
100
50
0
-50
-100
-150
-200
-250
0
0.5
1
1.5
2
2.5
Time offset: 0

FIG. 7.23(D) & (E)

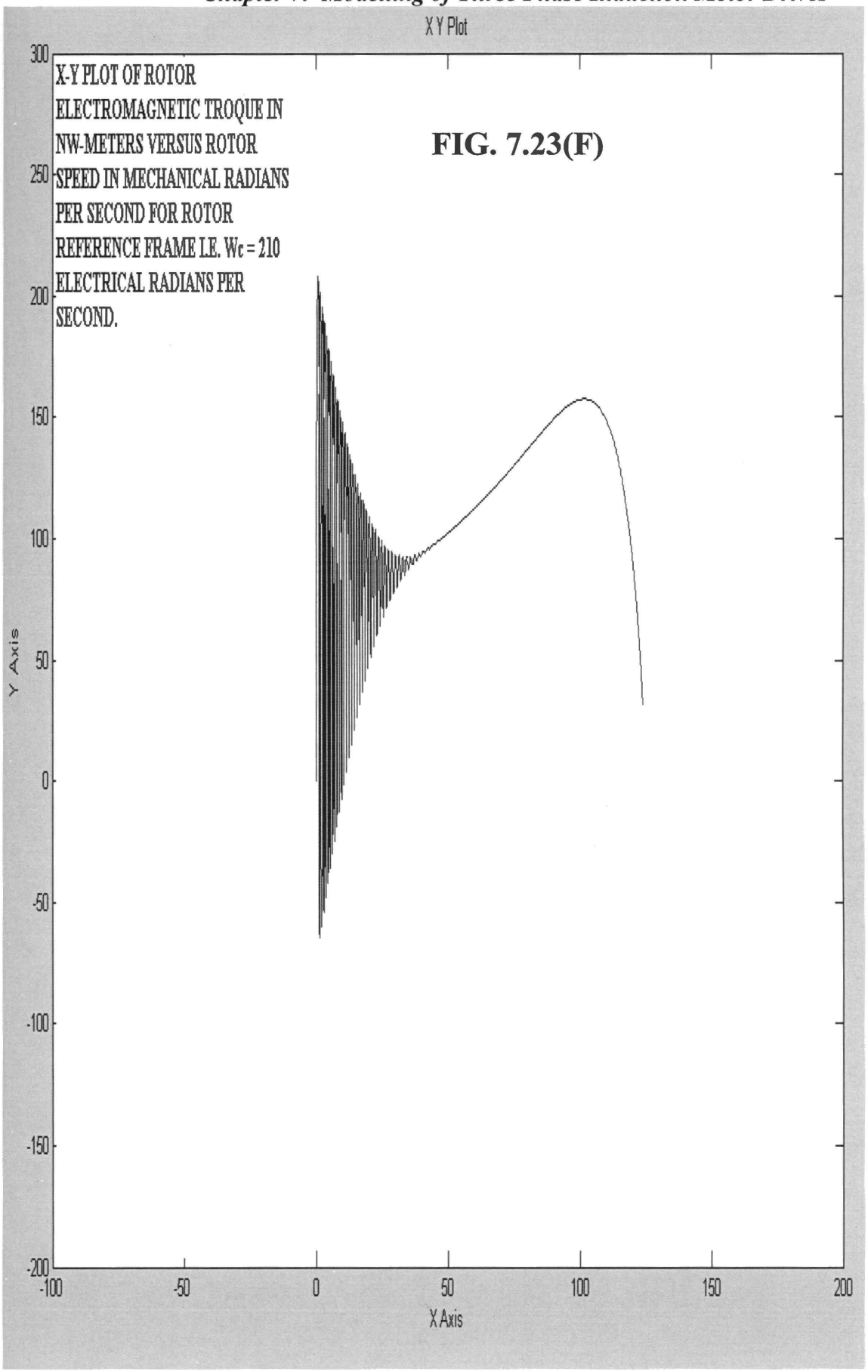
X Y Plot
X-Y PLOT OF ROTOR ELECTROMAGNETIC TROQUE IN NW-METERS VERSUS ROTOR SPEED IN MECHANICAL RADIANS PER SECOND FOR ROTOR REFERENCE FRAME I.E. Wc = 210 ELECTRICAL RADIANS PER SECOND.
300
250
200
150
100
50
0
-50
-100
-150
-200
Y Axis
-100
-50
0
50
100
150
200
X Axis

FIG. 7.23(F)

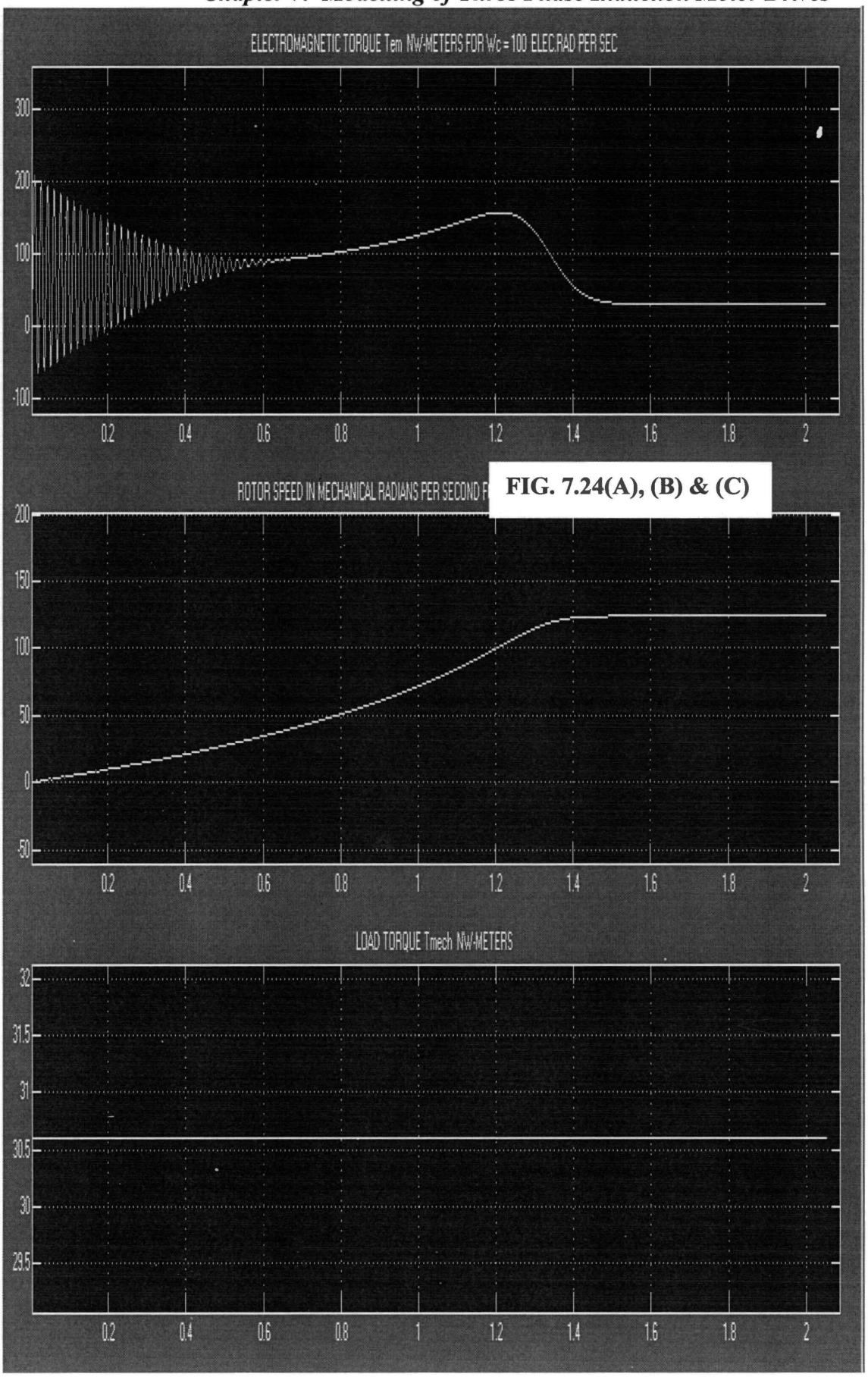
ELECTROMAGNETIC TORQUE Tem NW-METERS FOR Wc = 100 ELEC.RAD PER SEC
300
200
100
0
-100
0.2
0.4
0.6
0.8
1
1.2
1.4
1.6
1.8
2
ROTOR SPEED IN MECHANICAL RADIANS PER SECOND F
200
150
100
50
0
-50
0.2
0.4
0.6
0.8
1
1.2
1.4
1.6
1.8
2
LOAD TORQUE Tmech NW-METERS
32
31.5
31
30.5
30
29.5
0.2
0.4
0.6
0.8
1
1.2
1.4
1.6
1.8
2

FIG. 7.24(A), (B) & (C)

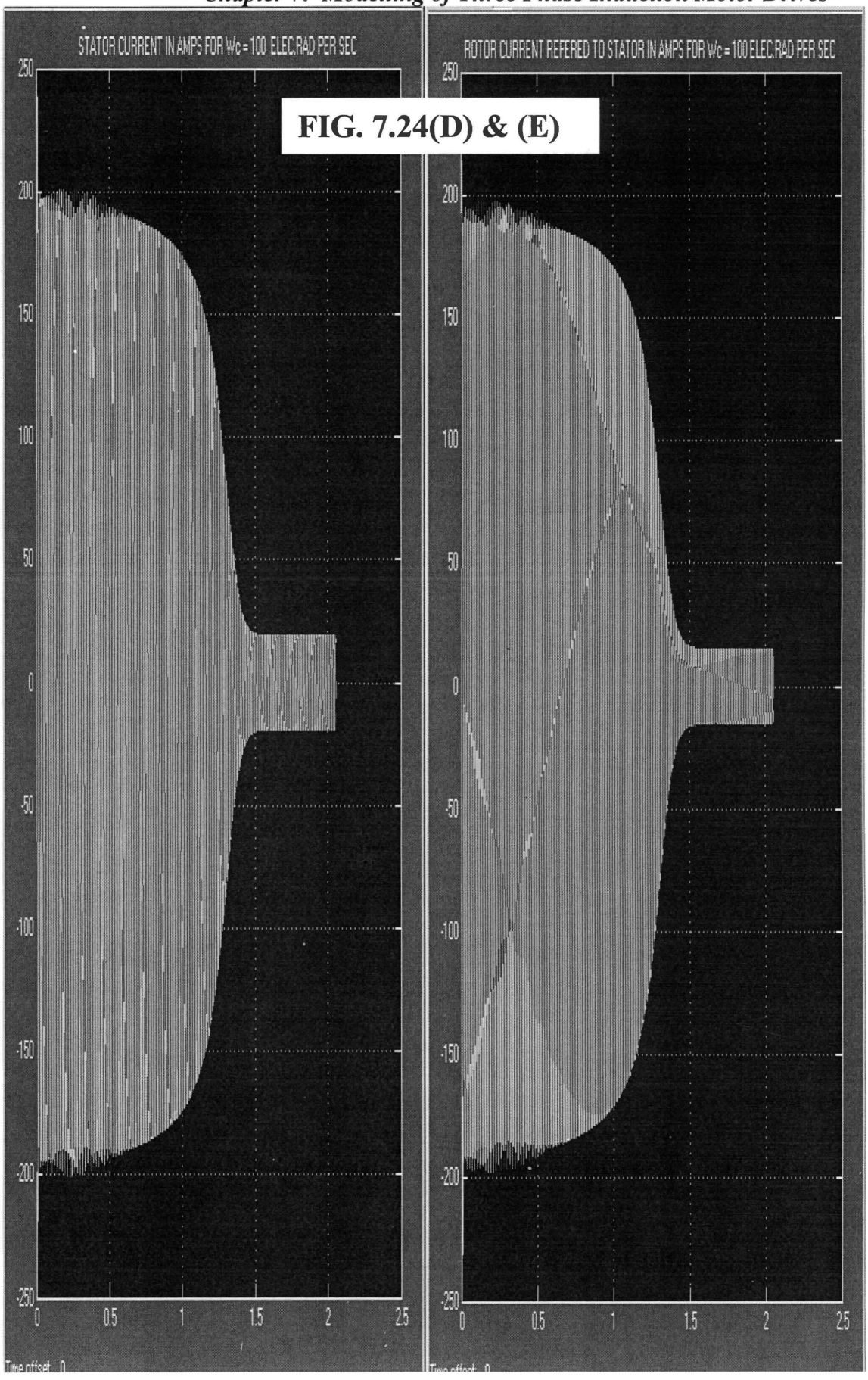
STATOR CURRENT IN AMPS FOR Wc = 100 ELEC.RAD PER SEC
250
200
150
100
50
0
-50
-100
-150
-200
-250
0
0.5
1
1.5
2
2.5
Time offset: 0
ROTOR CURRENT REFERED TO STATOR IN AMPS FOR Wc = 100 ELEC.RAD PER SEC
250
200
150
100
50
0
-50
-100
-150
-200
-250
0
0.5
1
1.5
2
2.5

FIG. 7.24(D) & (E)

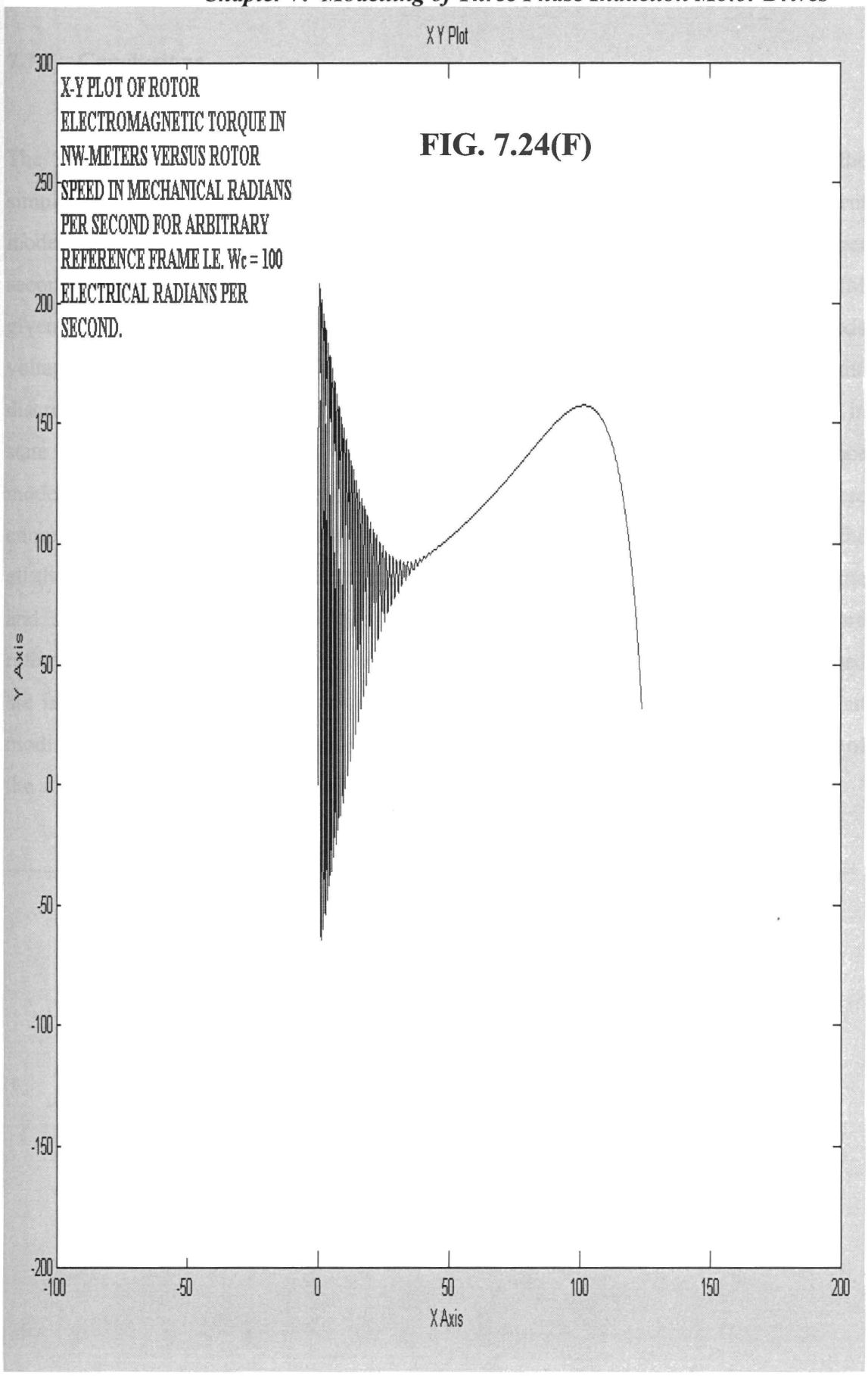
X Y Plot
X-Y PLOT OF ROTOR ELECTROMAGNETIC TORQUE IN NW-METERS VERSUS ROTOR SPEED IN MECHANICAL RADIANS PER SECOND FOR ARBITRARY REFERENCE FRAME I.E. Wc = 100 ELECTRICAL RADIANS PER SECOND.
Y Axis
X Axis
300
250
200
150
100
50
0
-50
-100
-150
-200
-100
-50
0
50
100
150
200

FIG. 7.24(F)

7.7 Conclusions

The SIMULINK model for the three phase IM was successfully developed and the simulation was carried out on all reference frames, using dq0-axis voltage – current model, dq0-axis flux linkage model in state space and the dq0-axis flux linkage per second and machine reactance in state space. The parameters of the three phase IM given in Reference 10 was used all the cases. The simulation results for the dq0-axis voltage – current model in all reference frame closely well agree each other and the discrepancies are minor. The simulation results for the dq0-axis flux linkage model in state space and also for the dq0-axis flux linkage per second and machine reactance model in state space in all reference frames well agree. These simulation results were compared with the results available in the literature reference 10. It was found that the all the simulation results for stator current, rotor current referred to stator, torque-time and speed-time curves and the torque-speed curves well agree with the literature reference and the discrepancies involved are negligibly small. The models developed are interactive in the sense the user can enter any given data of the machine without modifying the internal schematics of the model. Appendix E provides the simulation of the above three phase IM using the demo version of software PSIM 7.0

CHAPTER 8

MODELLING OF SIX STEP INVERTER FED PERMANENT MAGNET SYNCHRONOUS MOTOR DRIVES

8.1 Introduction

Permanent magnet synchronous motors find wide applications in the industry. In PMSM the rotor is made of permanent magnets such as NdFeB and thus avoids rotor field winding. The interior permanent magnet synchronous motor supplied by a six step inverter with electronic commutation is used as variable speed drive in pumps and fans [19]. Permanent magnet brushless DC motors are used in laser printers and hard disk drives [20]. Electronic switching of the six step inverter is controlled by the rotor position which is sensed by using either the optical or the Hall effect sensors [20, 21]. Many sensorless techniques for inverter switching such as the back e.m.f. detection, indirect flux detection by online reactance measurement (INFORM), Kalman Filtering, Phase Current measurement and conduction state of free wheeling diodes have been reported in the literature. There are two types of Permanent Magnet Motors viz. the Permanent Magnet Synchronous Motor (PMSM) and Permanent Magnet Brushless DC Motor (BLDCM). The PMSMs have sinusoidal back e.m.f. The six step inverter switching used for PMSM drives can be either the continuous current (180 degree) mode or the discontinuous current (120 degree) mode.

Modelling of PMSM drives fed by six step continuous current and discontinuous current mode inverter using various computer programming methods are reported in the literature [29 - 42]. Detailed SIMULINK model for PMSM drive fed by six step inverter with fixed switching angle is available in the literature reference [11]. SIMULINK models for PMSM drive fed by six step inverter with a PID controller under transient load torque disturbance is reported in the literature, but lacks schematic details of PMSM and inverter models [44]. The aim of this chapter is to develop

SIMULINK models for PMSM drives supplied by six step continuous and discontinuous current mode inverter with switching angle advancing facility and to study the performance by simulation and experiment.

8.2 Modelling of PMSM Drives

A simple form of the conventional three phase brushless dc motor circuit is shown in Fig.8.1 [20]. Here optical method of sensing the rotor position is used. The rotor shaft is coupled to a revolving shutter and the photo transistors are exposed to light from a lamp in sequence. The logic sequencer is arranged in such a way that when the photo transistor of certain number is exposed to light, the same transistor number is turned ON. The rotor is aligned in such a way that the rotor magnetic field flux makes 90 degree angle with respect to the magnetic field produced by the stator. A clockwise rotor torque is thus produced [20].

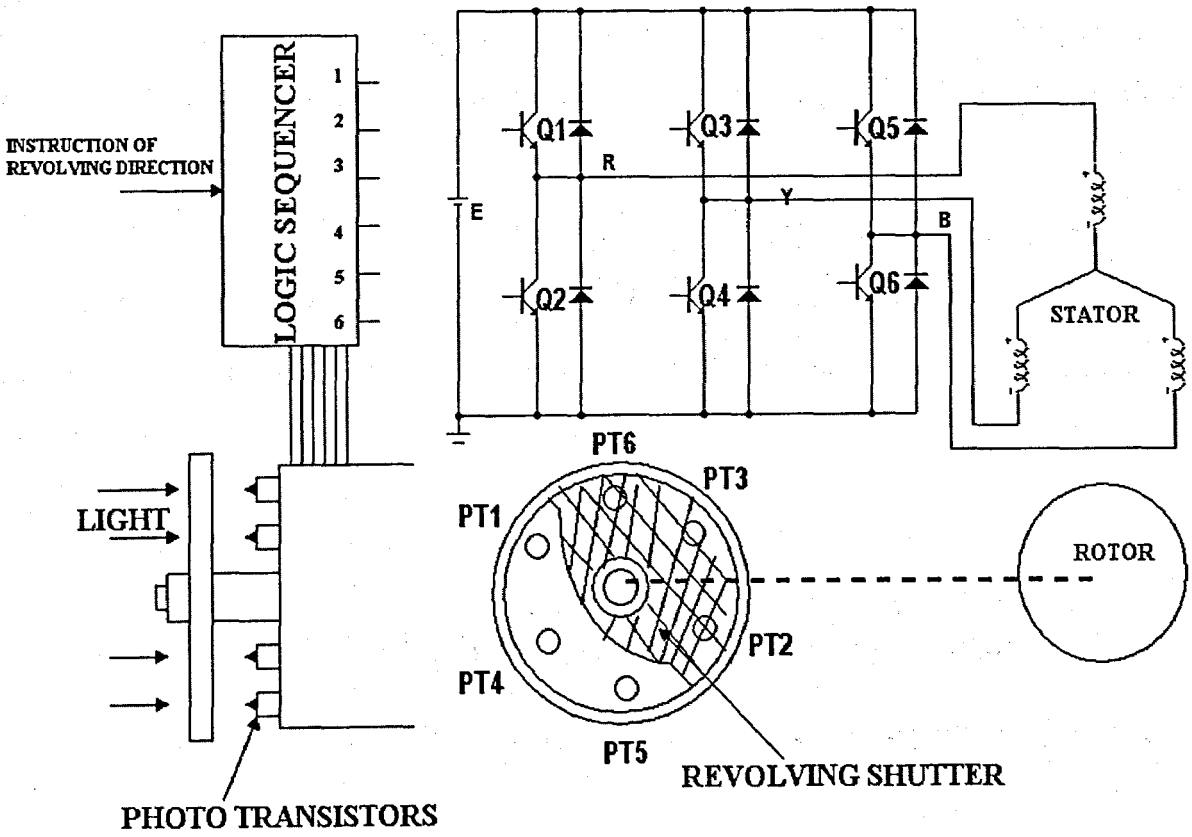

FIG.8.1: THREE PHASE BRUSHLESS DC MOTOR

In deriving the dq-axis model of PMSM drives, the following assumptions are made:

1) Back e.m.f. is sinusoidal 2) Equal turns per phase 3) Rotor flux is concentrated along d-axis 4) NO flux along the q-axis 5) Core loss is negligible 6) Constant rotor flux 7) Rotor reference frame is used to express stator voltage equations and 8) The d-q axis stator windings have fixed phase relationship with rotor magnet axis or d-axis. The modelling equations of PMSM all in **rotor frame** are given below [2, 13, 29 - 30]:

$$v_{qs} = R_s . i_{qs} + s\lambda_{qs} + \omega_{re} . \lambda_{ds} \quad ...(8.1)$$

$$v_{ds} = R_s . i_{ds} + s\lambda_{ds} - \omega_{re} . \lambda_{qs} \quad ...(8.2)$$

where v_{ds} and v_{qs} are the dq-axis stator voltages and ω_{re} is the angular speed of the rotor in electrical radians per second. The dq axis flux linkages are expressed as follows:

$$\lambda_{qs} = L_q . i_{qs} \quad ...(8.3)$$

$$\lambda_{ds} = L_d . i_{ds} + \lambda_m \quad ...(8.4)$$

where λ_m is the amplitude of the stator flux linkages established by the permanent magnet, which is a constant. Using equations 3 and 4 in equations 1 and 2, equation 5 follows:

$$\begin{bmatrix} v_{qs} \\ v_{ds} \end{bmatrix} = \begin{bmatrix} R_s + sL_q & \omega_{re} L_d \\ -\omega_{re} L_q & R_s + sL_d \end{bmatrix} * \begin{bmatrix} i_{qs} \\ i_{ds} \end{bmatrix} + \begin{bmatrix} \omega_{re} \lambda_m \\ 0 \end{bmatrix} \quad ...(8.5)$$

in equation 5, Rs, Ld, Lq are the resistance and inductance of the stator in dq axis respectively.

The electromagnetic torque is given by equation 6 below:

$$T_{em} = \left(\frac{3}{2}\right) . \left(\frac{P}{2}\right) . \left(\lambda_{ds} . i_{qs} - \lambda_{qs} . i_{ds}\right) \quad ...(8.6)$$

where P is the number of poles. Using equation 3 and 4 in equation 6, equation 7 follows:

$$T_{em} = \left(\frac{3}{2}\right) . \left(\frac{P}{2}\right) . \left[\lambda_m . i_{qs} + \left(L_d - L_q\right) . i_{qs} . i_{ds}\right] \quad ...(8.7)$$

The rotor e.m. torque Tem and speed are related as follows:

$$T_{em} = J\frac{d\omega_{rm}}{dt} + D.\omega_{rm} + T_{mech} \quad \ldots(8.8)$$

where ω_{rm} is the rotor speed in mechanical radians per second, J is rotor inertia, D is damping and T_{mech} is the mechanical load torque.

8.2.1 Analysis of Six Step Inverter Fed PMSM Drive

The essential modelling equations of the PMSM with sinusoidal back e.m.f. are given in equations 8.1 to 8.8. The phasor diagram of the PMSM is shown in Fig.8.2 [13]. The vector

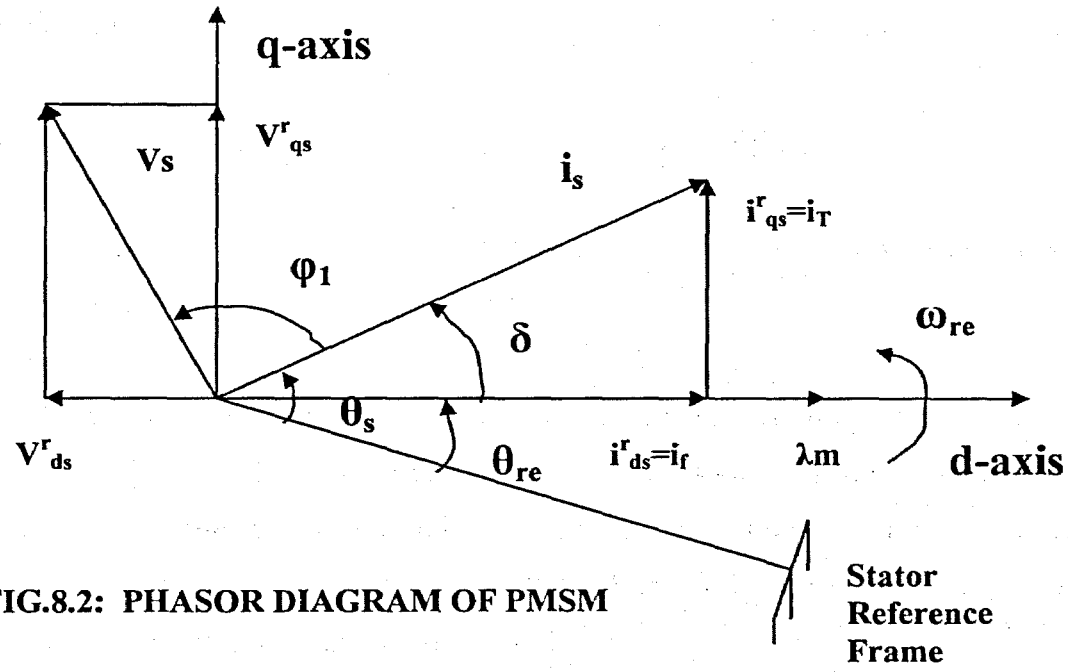

FIG.8.2: PHASOR DIAGRAM OF PMSM

control of PMSM is derived from its dynamic model. Considering the currents as inputs, the three phase currents are given below in equation 8.9.

$$i_{as} = i_S.\sin\left(\omega_{re}t + \delta\right)$$

$$i_{bs} = i_S.\sin\left(\omega_{re}t + \delta - \frac{2\pi}{3}\right)$$

$$i_{cs} = i_S.\sin\left(\omega_{re}t + \delta + \frac{2\pi}{3}\right) \qquad (8.9)$$

Using equation 8.9 in equation 1.1 of chapter 1, with angle θ replaced by $\theta_{re} = \omega_{re}.t$, the stator currents in **rotor reference frame** are obtained as shown in equation 8.10 below.

$$\begin{bmatrix} i_{qs} \\ i_{ds} \end{bmatrix} = i_S \cdot \begin{bmatrix} \sin(\delta) \\ \cos(\delta) \end{bmatrix} \qquad (8.10)$$

Using equation 8.10 in equation 8.7, the electromagnetic torque equation is obtained as shown in equation 8.11 below.

$$T_{em} = \frac{3}{2}.\frac{P}{2}.\left[\frac{1}{2}.\left(L_d - L_q\right).i_S^2.\sin 2\delta + \lambda_m.i_S.\sin\delta\right] \qquad (8.11)$$

For $\delta = \pi/2$, the equation for Tem is modified as in equation 8.12 below.

$$T_{em} = \frac{3}{2}.\frac{P}{2}.\lambda_m.i_S \; Nw.m \qquad (8.12)$$

Thus by maintaining δ, a value of $\pi / 2$, the e.m. torque Tem can be controlled by varying the stator current, as λm is a constant.

The PMSM drives are inverter driven and the sensors provide information on the position of he poles and the dq-axis. By appropriately switching the six step inverter it is possible to change v_{qs} and v_{ds} and the rotor position. Referring to equation 4.16 in Chapter 4, the line to neutral voltage of a PMSM driven by six step 180 degree mode inverter can be expressed as in equation 8.13 below.

$$V_{as} = \frac{2V_{dc}}{\pi} * \left[\sin(\theta_{ev}) + \frac{1}{5}.\sin(\theta_{ev}) + \frac{1}{7}.\sin(\theta_{ev}) + ...\right] ...(8.13)$$

in equation 13, $\omega_e.t = \theta_{ev}$ is the switching angle or the phase angle of the applied voltage. If switching angle is advanced by $\pi/2$ radians by appropriately switching the inverter switches, then θ_{ev} in equation 8.13 can be replaced by $\left(\theta_{ev} + \pi/2\right)$. The equation 8.13 can be written as in equation 8.14 below [29].

$$V_{as} = \frac{2V_{dc}}{\pi} * \left[\cos(\theta_{ev}) + \frac{1}{5}.\cos(5\theta_{ev}) + \frac{1}{7}.\cos(7\theta_{ev}) + ...\right] ...(8.14)$$

In equation 8.13 and 8.14, ω_e is the angular frequency of switching of the inverter in electrical radians per second and is equal to ω_{re}, the angular frequency of the rotor in electrical radians per second. The dq-axis stator voltages in rotor frame can be expressed as in equation 8.15 below.

$$\left.\begin{aligned} V_{qs} &= \sqrt{2}.V_S.\cos(\varphi) \\ V_{ds} &= -\sqrt{2}.V_S.\sin(\varphi) \\ \sqrt{2}.V_S &= \frac{2.V_{dc}}{\pi} \\ \varphi &= \theta_{ev}(0) - \theta_{re}(0) \end{aligned}\right| \qquad (8.15)$$

The steady state voltage equations neglecting harmonics can be written as in equation 8.16 below, by letting s = d/dt = 0 in equation 8.5

$$\begin{bmatrix} V_{qs} \\ V_{ds} \end{bmatrix} = \begin{bmatrix} R_S & \omega_{re}.L_d \\ -\omega_{re}.L_q & R_S \end{bmatrix} * \begin{bmatrix} I_{qs} \\ I_{ds} \end{bmatrix} + \begin{bmatrix} \omega_{re}.\lambda_m \\ 0 \end{bmatrix} \quad ...(8.16)$$

Now letting **Ld = Lq = Ls** and solving equation 8.16, the equation for Iqs can be written as in equation 8.17 below.

$$I_{qs} = \frac{R_S}{\left(R_S^2 + \omega_{re}^2.L_S^2\right)} \cdot \left[V_{qs} - \omega_{re}.\lambda_m - \frac{\omega_{re}.L_S.V_{ds}}{R_S} \right] \qquad (8.17)$$

The e.m. torque Tem in equation 8.7 can be written as in equation 8.18 below.

$$T_{em} = \left(\frac{3P}{4}\right) \cdot \frac{R_S.\lambda_m}{\left(R_S^2 + \omega_{re}^2.L_S^2\right)} \cdot \left[V_{qs} - \omega_{re}.\lambda_m - \frac{\omega_{re}.L_S.V_{ds}}{R_S} \right] \qquad (8.18)$$

Using equation 8.15 in equation 8.18, the torque expression simplifies as in equation 8.19 below.

$$T_{em} = \left(\frac{3P}{4}\right) \cdot \frac{R_S.\lambda_m}{\left(R_S^2 + \omega_{re}^2.L_S^2\right)} \cdot \left[\sqrt{2}.V_S.\cos(\varphi) - \omega_{re}.\lambda_m + \frac{\omega_{re}.L_S.\sqrt{2}.V_S.\sin(\varphi)}{R_S} \right] \qquad (8.19)$$

For maximum e.m. torque Tem differentiating equation 8.19 with respect to φ and equating to zero, the equation 8.20 given below is obtained.

$$\varphi = \varphi_{MT} = \tan^{-1}\left(\frac{\omega_{re}.L_S}{R_S}\right) \qquad (8.20)$$

where φ_{MT} is the value of φ for maximum e.m. torque.

In the case of PMSM driven by six step 120 degree mode inverter, the value of $\sqrt{2}.Vs$ in equation 8.15 becomes [$\sqrt{3}Vdc / \pi$] (equation 4.33 in Chapter 4) and the value of φ for maximum torque given by equation 8.20 holds good. The derivation of φ_{MT} for maximum e.m. torque given by equation 8.20 is based on the literature reference [29].

8.3 Modelling of Six Step Continuous Current Mode Inverter Fed PMSM Drive

The gate drive pattern for six step 180 degree mode inverter also known as continuous conduction mode inverter is shown in Fig.2.6(A) in Chapter 2. The model of the six step continuous current mode inverter fed PMSM drive is shown in Fig.8.3. The various dialog boxes are shown in Fig.8.4. The various subsystems are shown in Fig.8.5(A) to (I). The various subsystems are explained below:

Fig.8.5(A) gives phase advancer and gate drive block. The detailed schematic of these two blocks are shown in Fig.8.5.1(A) and 8.5.1(B) respectively. The dialog boxes Three Phase 180 Degree Mode Inverter Gate Drive data and Three Phase 180 Degree Mode Inverter data in Fig.8.4 corresponds to Fig.8.5.1(A) and 8.5.1(B) respectively. In Fig.8.5.1(A), an arbitrary constant K, rotor speed ω_{re}, time and Phase Advancer are given as input to the mux. This mux output is given to Fig.8.5.1(B). In Fig.8.5.1(B), the outputs R, G and B of Fcn blocks are three phase sine wave with peak value of 10 and angular frequency of ω_{re} elec.rad / sec, with phase advance entered in the phase shifter block of Fig.8.5.1(A) added. The output a, b and c of Fcn blocks are logic 1, when each of the three phase inputs just cross zero and goes positive and zero when the respective input crosses zero and goes negative. The gate drive a, b and c are given to three phase continuous current mode inverter block shown in Fig.8.5(B). Gate drives a, b and c are given to the second input of respective threshold switch blocks, while the

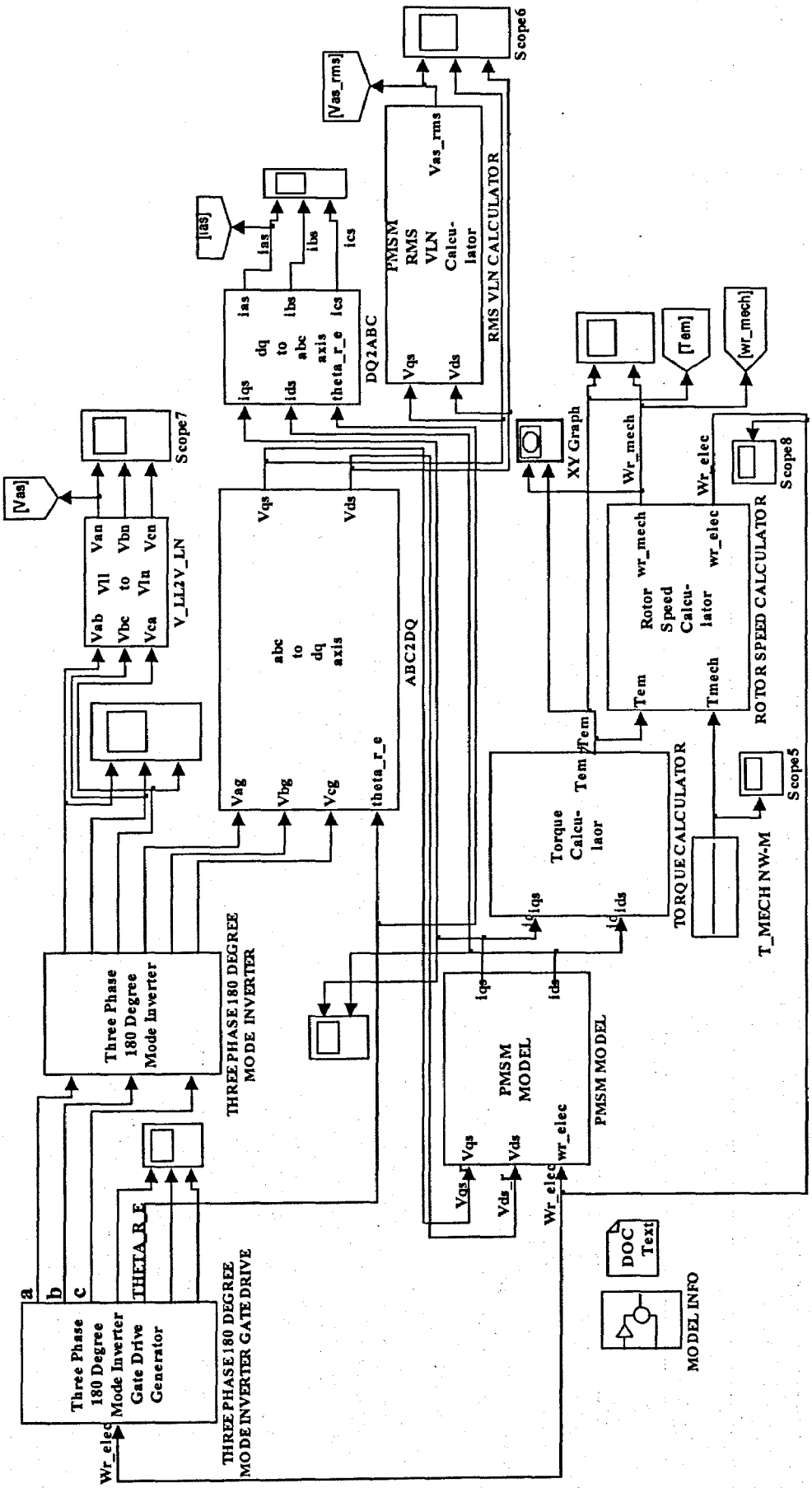

FIG.8.3: THREE PHASE SIX STEP CONTINUOUS CURRENT INVERTER FED PMSM DRIVE MODEL

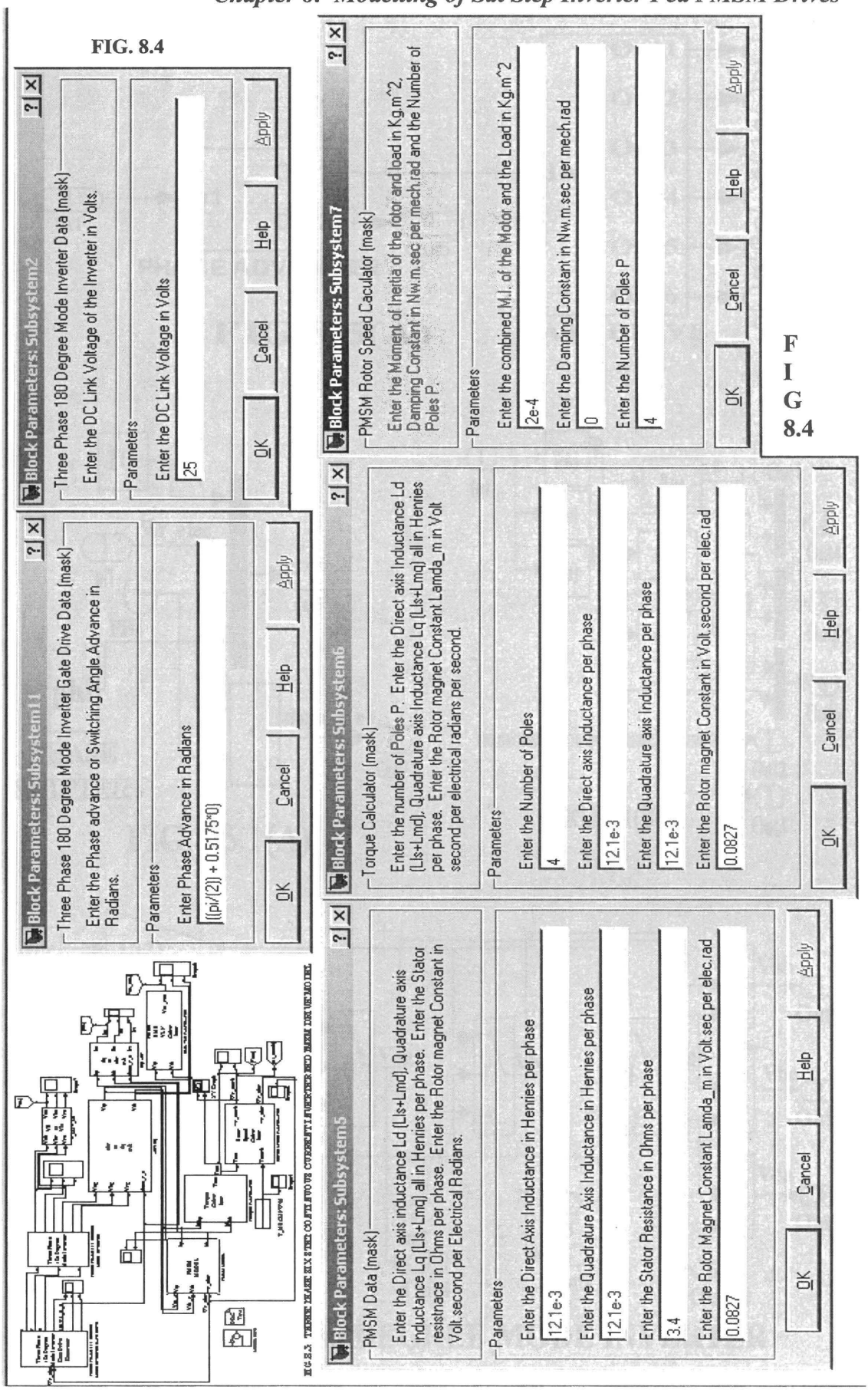
Block Parameters: Subsystem11
Three Phase 180 Degree Mode Inverter Gate Drive Data (mask)
Enter the Phase advance or Switching Angle Advance in Radians.
Parameters
Enter Phase Advance in Radians
[(pi/(2)) + 0.5175*0]
OK
Cancel
Help
Apply
Block Parameters: Subsystem2
Three Phase 180 Degree Mode Inverter Data (mask)
Enter the DC Link Voltage of the Inverter in Volts.
Parameters
Enter the DC Link Voltage in Volts
25
OK
Cancel
Help
Apply
Block Parameters: Subsystem5
PMSM Data (mask)
Enter the Direct axis inductance Ld (Lls+Lmd), Quadrature axis inductance Lq (Lls+Lmq) all in Henries per phase. Enter the Stator resistnace in Ohms per phase. Enter the Rotor magnet Constant in Volt.second per Electrical Radians.
Parameters
Enter the Direct Axis Inductance in Henries per phase
12.1e-3
Enter the Quadrature Axis Inductance in Henries per phase
12.1e-3
Enter the Stator Resistance in Ohms per phase
3.4
Enter the Rotor Magnet Constant Lamda_m in Volt.sec per elec.rad
0.0827
OK
Cancel
Help
Apply
Block Parameters: Subsystem6
Torque Calculator (mask)
Enter the number of Poles P. Enter the Direct axis Inductance Ld (Lls+Lmd), Quadrature axis Inductance Lq (Lls+Lmq) all in Henries per phase. Enter the Rotor magnet Constant Lamda_m in Volt second per electrical radians per second.
Parameters
Enter the Number of Poles
4
Enter the Direct axis Inductance per phase
12.1e-3
Enter the Quadrature axis Inductance per phase
12.1e-3
Enter the Rotor magnet Constant in Volt.second per elec.rad
0.0827
OK
Cancel
Help
Apply
Block Parameters: Subsystem7
PMSM Rotor Speed Caculator (mask)
Enter the Moment of Inertia of the rotor and load in Kg.m^2, Damping Constant in Nw.m.sec per mech.rad and the Number of Poles P.
Parameters
Enter the combined M.I. of the Motor and the Load in Kg.m^2
2e-4
Enter the Damping Constant in Nw.m.sec per mech.rad
0
Enter the Number of Poles P
4
OK
Cancel
Help
Apply

FIG. 8.4

FIG 8.4

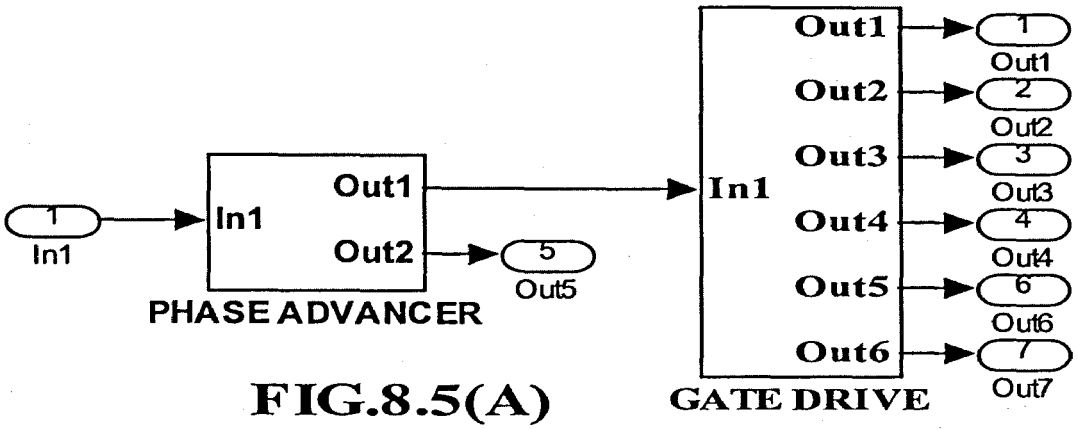

FIG.8.5(A)

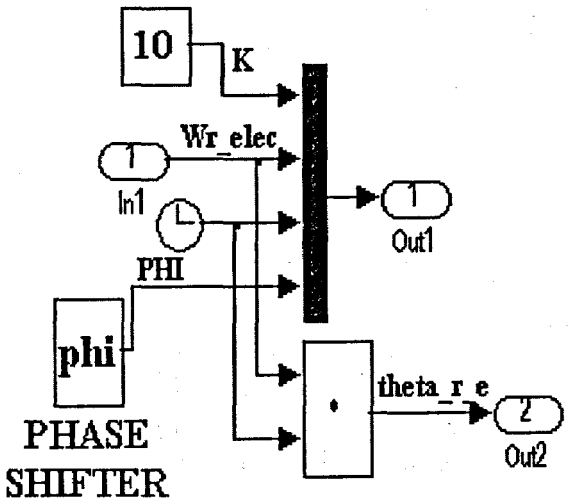

FIG.8.5.1(A)

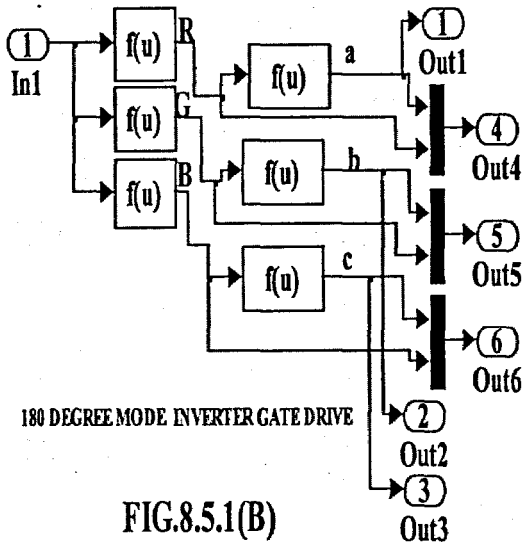

FIG.8.5.1(B)

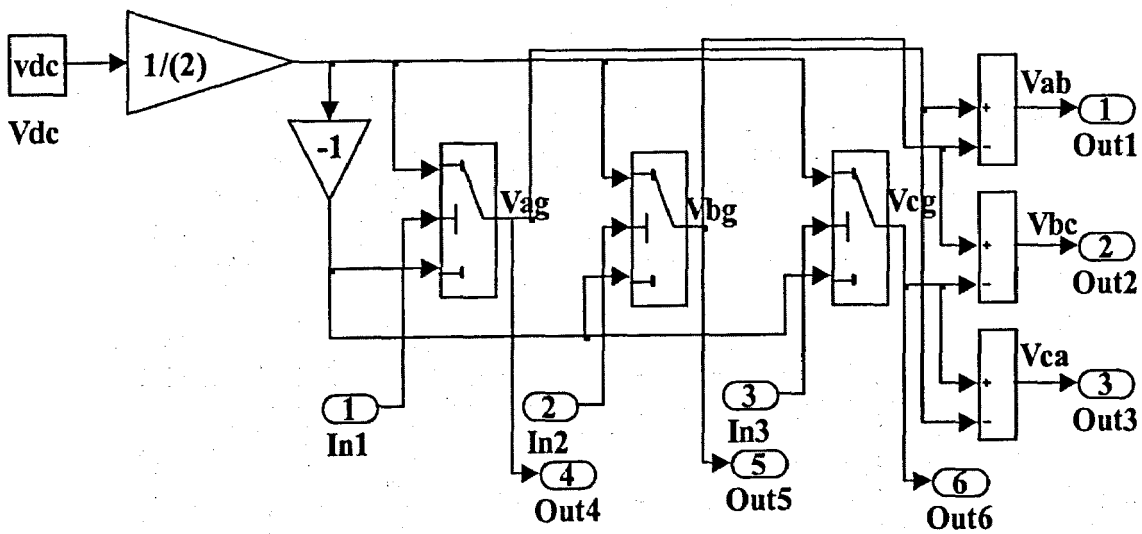

FIG.8.5(B): 180 DEGREE MODE INVERTER

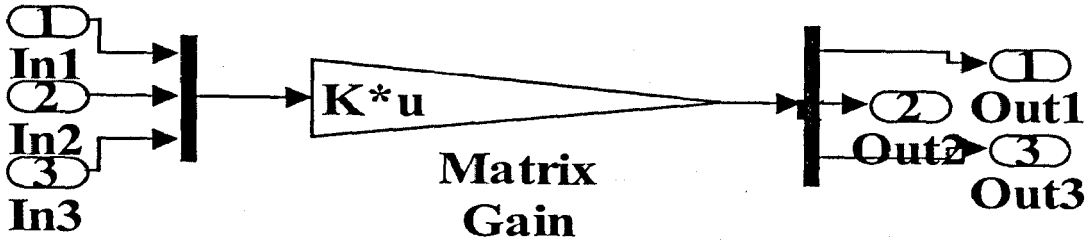

FIG.8.5(C): LL TO LN VOLTAGE TRANSFORM BLOCK

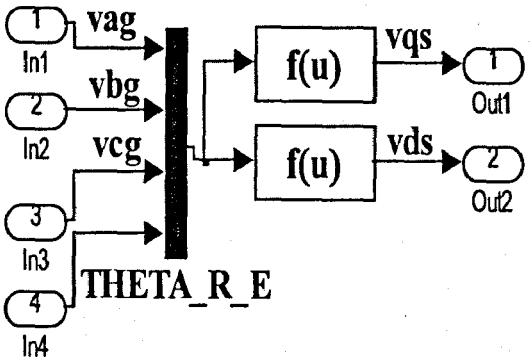

FIG.8.5(D): ABC TO DQ TRANSFORMATION

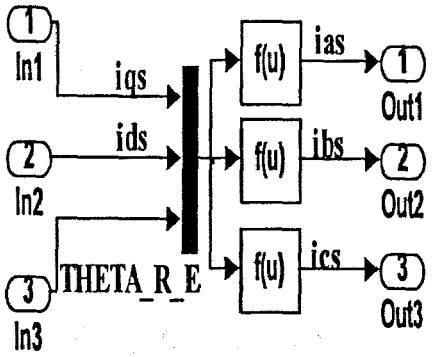

FIG.8.5(E): DQ TO ABC TRANSFORMATION

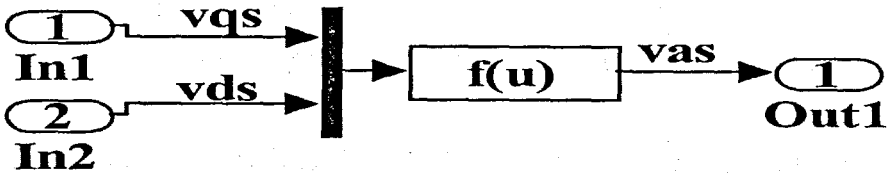

FIG.8.5(F): PMSM PHASE TO NEUTRAL VOLTAGE CALCULATOR BLOCK

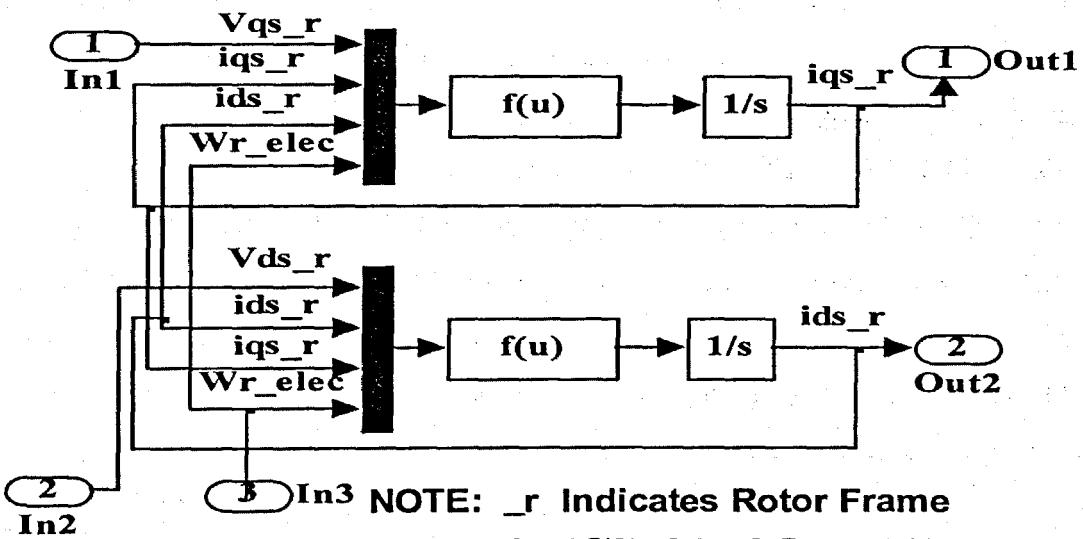

FIG.8.5(G): PMSM MODEL

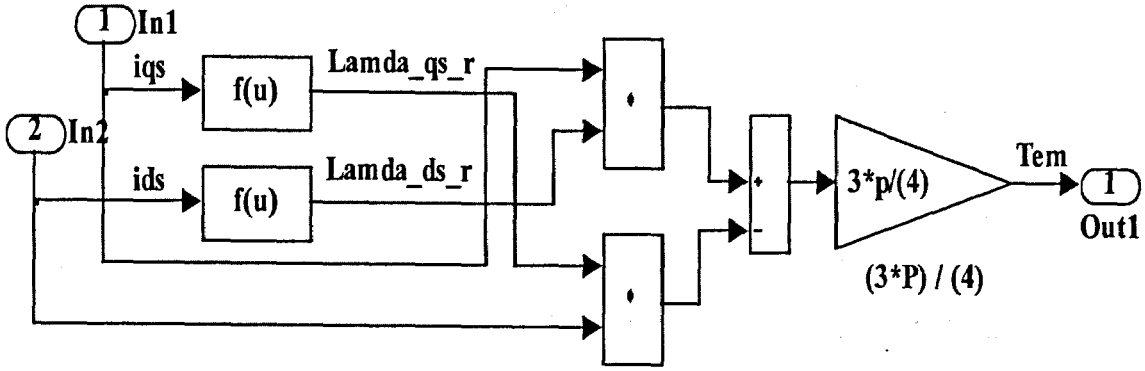

FIG.8.5(H): TORQUE CALCULATOR

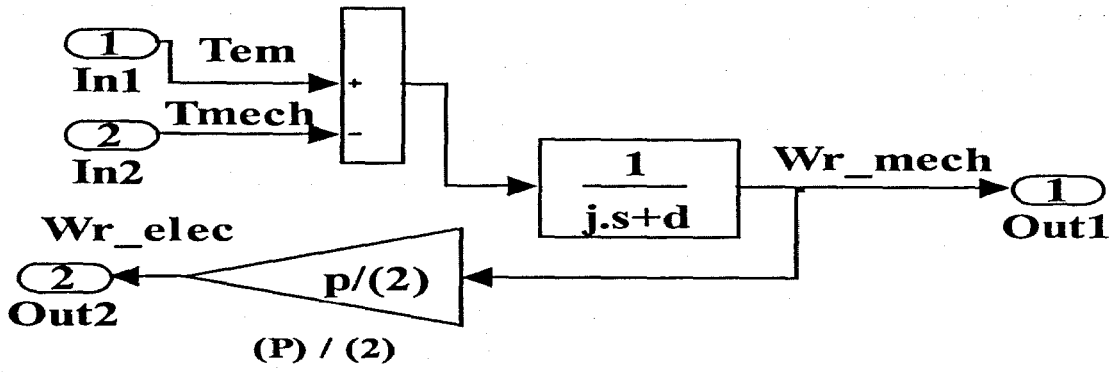

FIG.8.5(I): ROTOR SPEED CALCULATOR

first and third inputs are at +Vdc/2 and –Vdc/2 volts respectively, where Vdc is the dc link voltage. The outputs of the switches are +Vdc/2 when the respective u(2) input is greater than or equal to the threshold value of 0.5, else the outputs are –Vdc/2. The output of the three switches are three phase Line to Ground voltages, where ground is the midpoint of the two series connected sources +Vdc/2 and –Vdc/2 respectively. Using the SUBTRACT blocks the respective three phase line to line voltages are derived. The three Line to line voltages are given to VLL to VLN block shown in Fig.8.5(C) and the three Line to Ground voltages are given to ABC to DQ block shown in Fig.8.5(D). The VLL to VLN transform block is shown in fig.8.5(C). This block transforms Line to Line voltage to Line to Neutral voltage. The matrix gain block essentially transforms the three phase line to line voltage input to the mux block to corresponding Line to neutral voltages output at the demux block. The transformation matrix K in Fig.8.5(C) is defined below in equation 8.21.

$$\frac{1}{3} \cdot \begin{bmatrix} 1 & 0 & -1 \\ -1 & 1 & 0 \\ 0 & -1 & 1 \end{bmatrix} \quad \ldots(8.21)$$

The ABC to DQ transform block is shown in Fig.8.5(D). The four inputs to the mux are the three phase line to ground voltages from inverter block and the rotor position θ_{re} in electrical radians. The two Fcn blocks generate Vqs and Vds as per the transformation matrix given in equation 1.1 in Chapter 1, where θ is replaced by θ_{re}. Fig.8.5(E) performs the dq-axis to abc-axis transformation of the stator currents. The three inputs to the mux are iqs, ids and θ_{re} and the three Fcn blocks perform dq to abc axis transformation of the stator currents as per the transformation matrix defined in equation 1.2 in Chapter 1, where θ is replaced by θ_{re}. The Phase to Neutral voltage calculator block is shown in Fig.8.5(F). Vqs and Vds are the two inputs to the mux and the Fcn block calculates the phase to neutral voltage as given in equation 8.22 below:

$$v_{as} = \sqrt{\frac{v_{qs}^2 + v_{ds}^2}{2}} \qquad (8.22)$$

This is the r.m.s. voltage available across the phase and neutral of PMSM. The PMSM block is shown in Fig.8.5(G). The top mux along with Fcn block and integrator solves for iqs while the bottom part of mux, Fcn block and integrator solves for ids, both defined by equation 8.5 above. The torque calculator block is shown in fig.8.5(H). With iqs and ids as inputs to two Fcn blocks, equations 8.3 and 8.4 are solved to obtain qd axis flux linkages. Equation 8.6 is solved using two multipliers, summer and a gain block to obtain electromagnetic torque T_{em}. The rotor speed calculator block is shown in Fig.8.5(I). The load torque Tmech is applied externally using the repeating sequence block shown in Fig.8.3. Equation 8.8 is solved using the sum block and transfer function block to obtain rotor speed in mechanical radians per second. This is then multiplied by P/2 using gain block to obtain rotor speed ω_{re} in electrical radians per second.

8.3.1 Simulation Results

The simulation was carried out to verify the phase advance algorithm given by equation 8.20. The ode23tb(stiff/TR-BDF2) solver was used for simulation. The data relating to the six step inverter fed PMSM is shown in TABLE 8.1 [2, 29]. To verify the equation 8.20, a speed of 80 mechanical radians per second was selected. The simulation of the

TABLE 8.1

Sl.No.	Parameter	Value	Unit
1	Number of Phases	3	
2	Rated Voltage Vs per Phase	11.25	Volts
3	DC Link Voltage	25	Volts
4	Stator Resistance per Phase Rs	3.4	Ohms
5	Stator Inductnace per Phase Ls (Ld = Lq)	12.1	milli Henries
6	Number of Poles P	4	
7	Moment of Inertia J	2 X 10e-4	Kg.m^2
8	Rotor Magnet Constant λm	0. 0827	Volt.sec per elec.rad

six step continuous current mode inverter fed PMSM was carried out at NO LOAD with a Phase advance of π /2 radians. The plots of torque-time, speed-time and stator currents Fig.8.6(A), (B) and (C). The value of φ_{MT} for maximum torque for a rotor speed of 80 mech.rad per second was found to be 0.5175 electrical radians, using equation 8.20. This phase advance of 0.5175 was added to π /2 in the phase shifter block Fig.8.5.1(A) and the plot of torque-time, speed-time and stator currents at NO LOAD are shown in Fig.8.7(A), (B) and (C). From Fig.8.6(A), (B) and 8.7(A), (B) it was found that the e.m.torque of rotor was 0.19 NW-M and 0.29 NW-M respectively. The mechanical load was set to 0.19 Nw-m with a phase advance of π /2 electrical radians and the plot of stator current, e.m. torque, speed, and torque-speed curve are shown in Fig.Fig.8.8(A), (B), (C) and (D) respectively. The mechanical load was then set to 0.29 Nw-m with a phase advance of [π /2+0.5175] electrical radians and the plot of e.m. torque, speed, stator current and torque-speed curve are shown in Fig.Fig.8.9(A), (B), (C) and (D) respectively. It is seen that by advancing the phase by 0.5175 electrical radians corresponding to φ_{MT}, the e.m. torque of motor has increased by 53 % as compared to NO Phase advance i.e. by maintaining the phase advance by π /2 electrical radians [29].

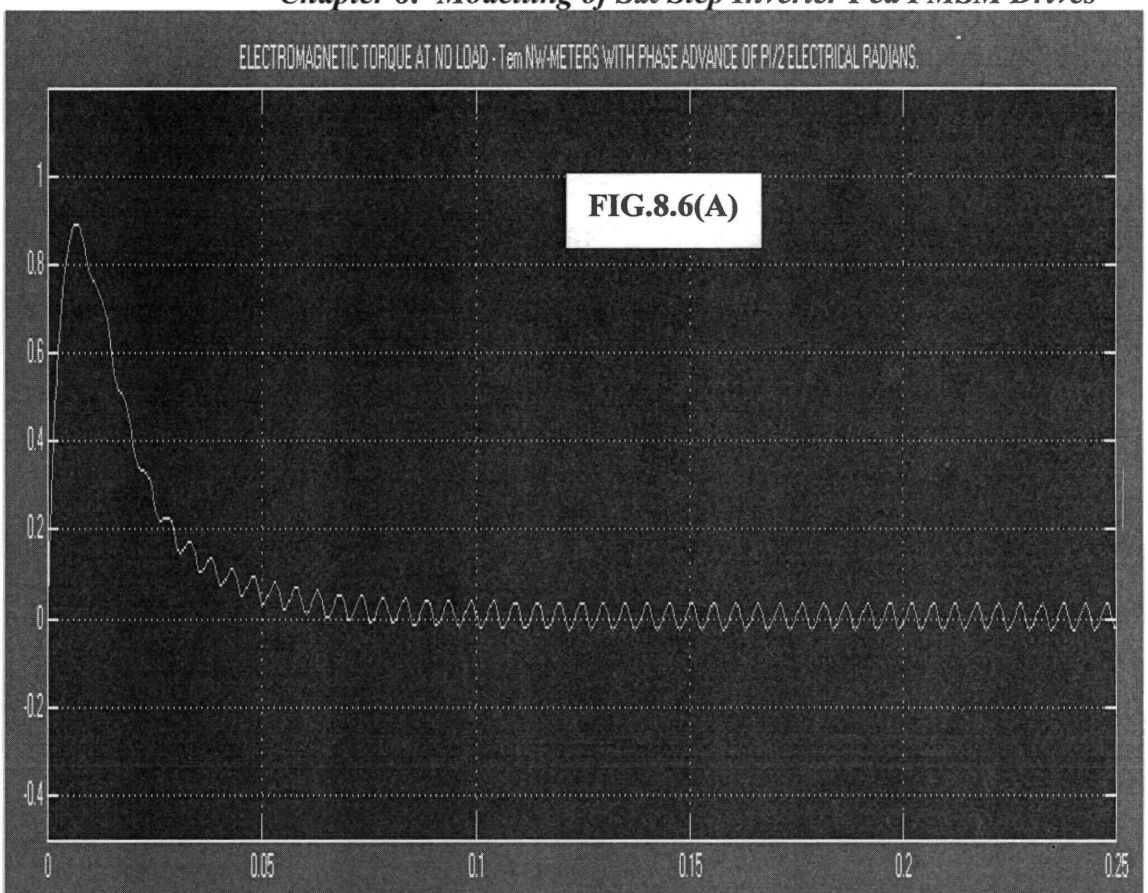

FIG.8.6(A)

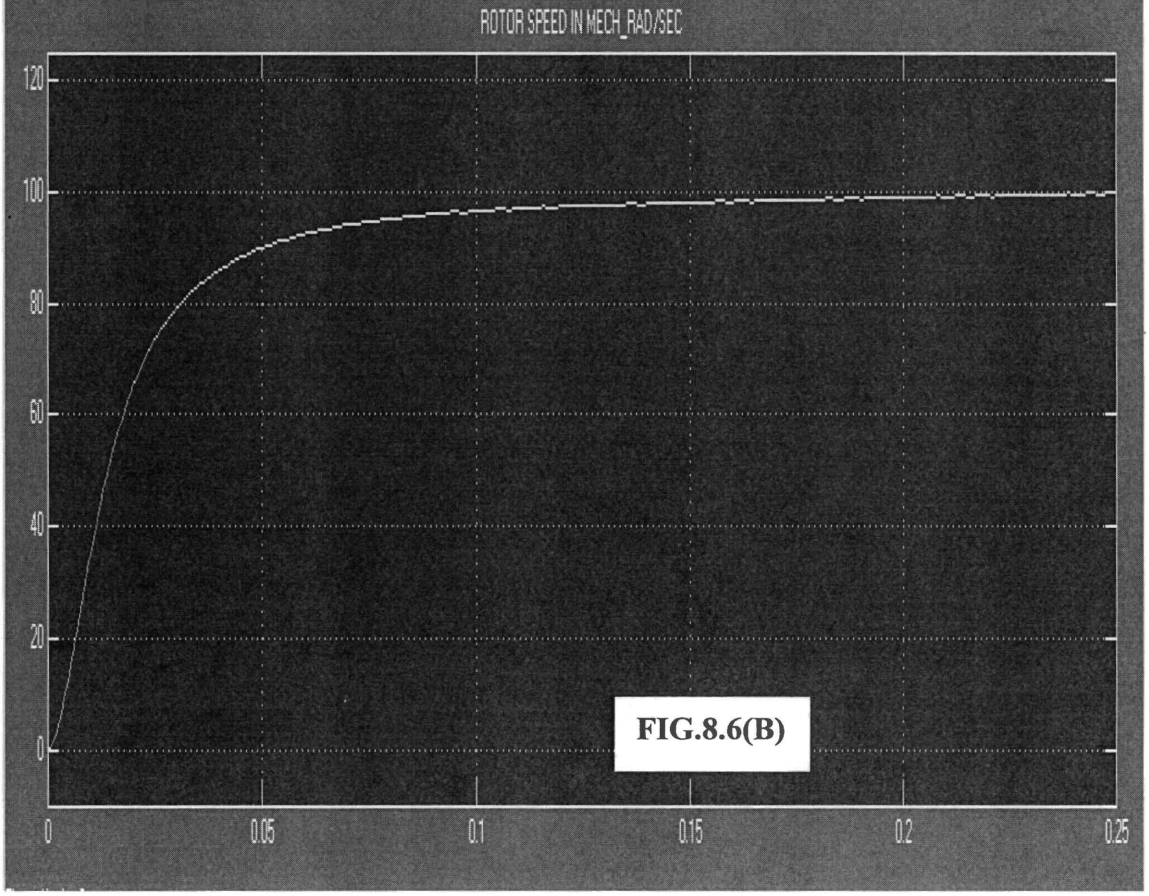

FIG.8.6(B)

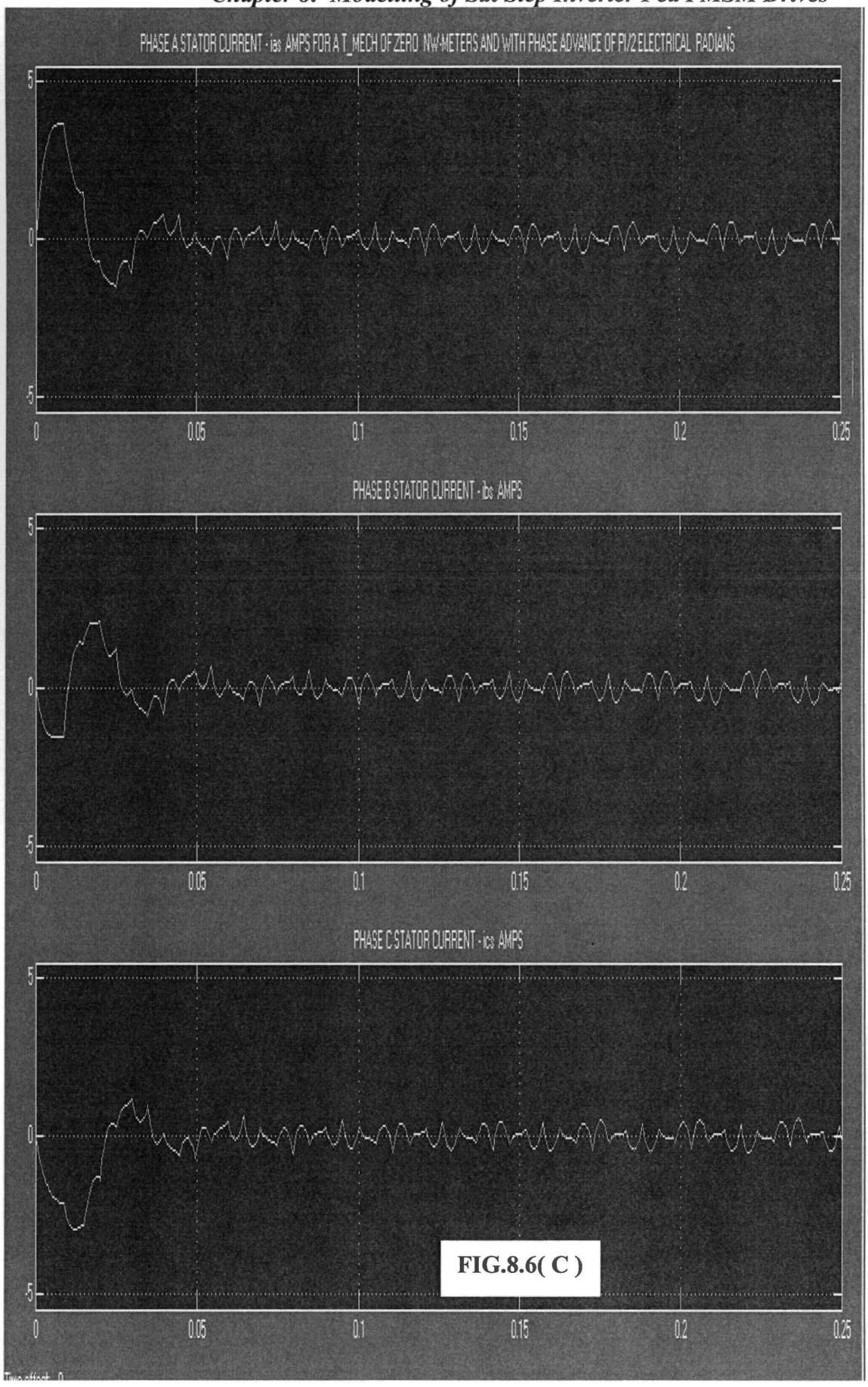
PHASE A STATOR CURRENT - ias AMPS FOR A T_MECH OF ZERO NW-METERS AND WITH PHASE ADVANCE OF PI/2 ELECTRICAL RADIANS
5
0
-5
0
0.05
0.1
0.15
0.2
0.25
PHASE B STATOR CURRENT - ibs AMPS
5
0
-5
0
0.05
0.1
0.15
0.2
0.25
PHASE C STATOR CURRENT - ics AMPS
5
0
-5
0
0.05
0.1
0.15
0.2
0.25

FIG.8.6(C)

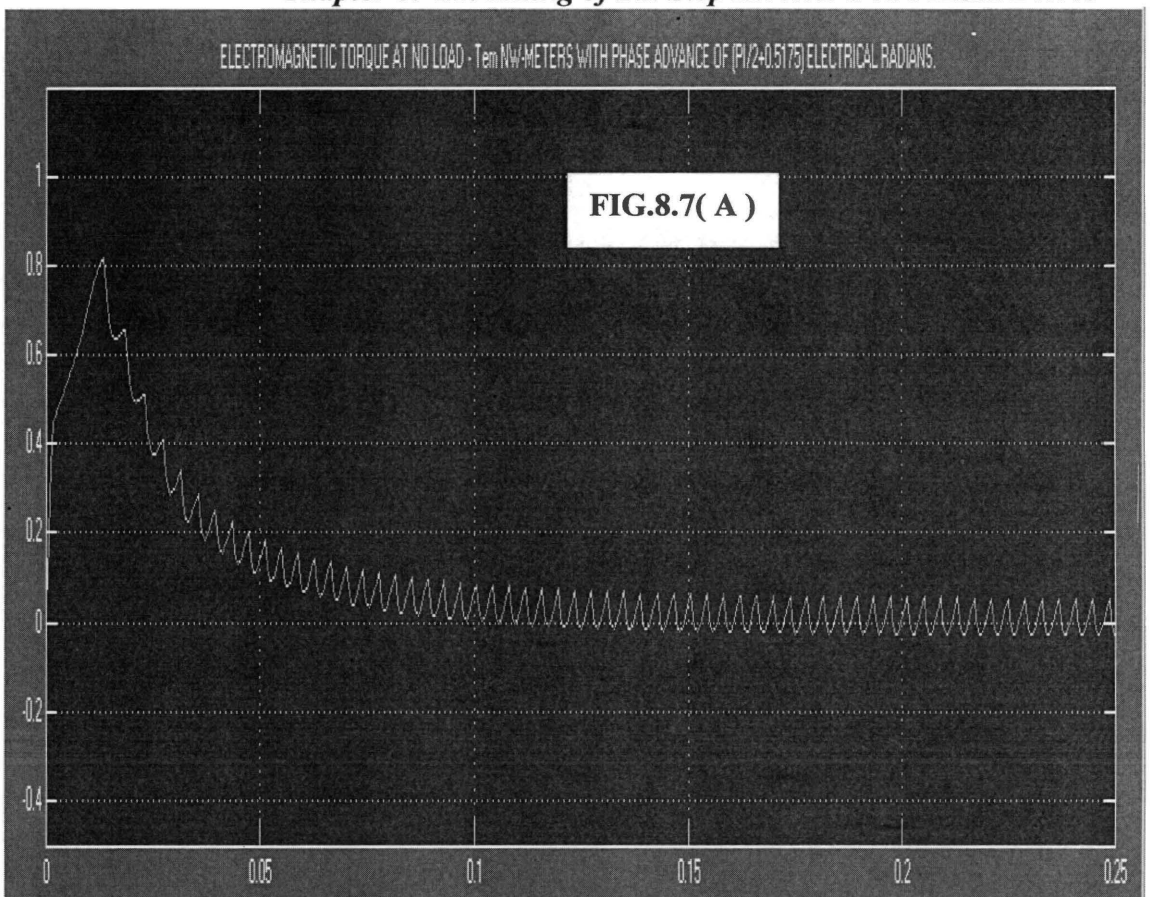

FIG.8.7(A)

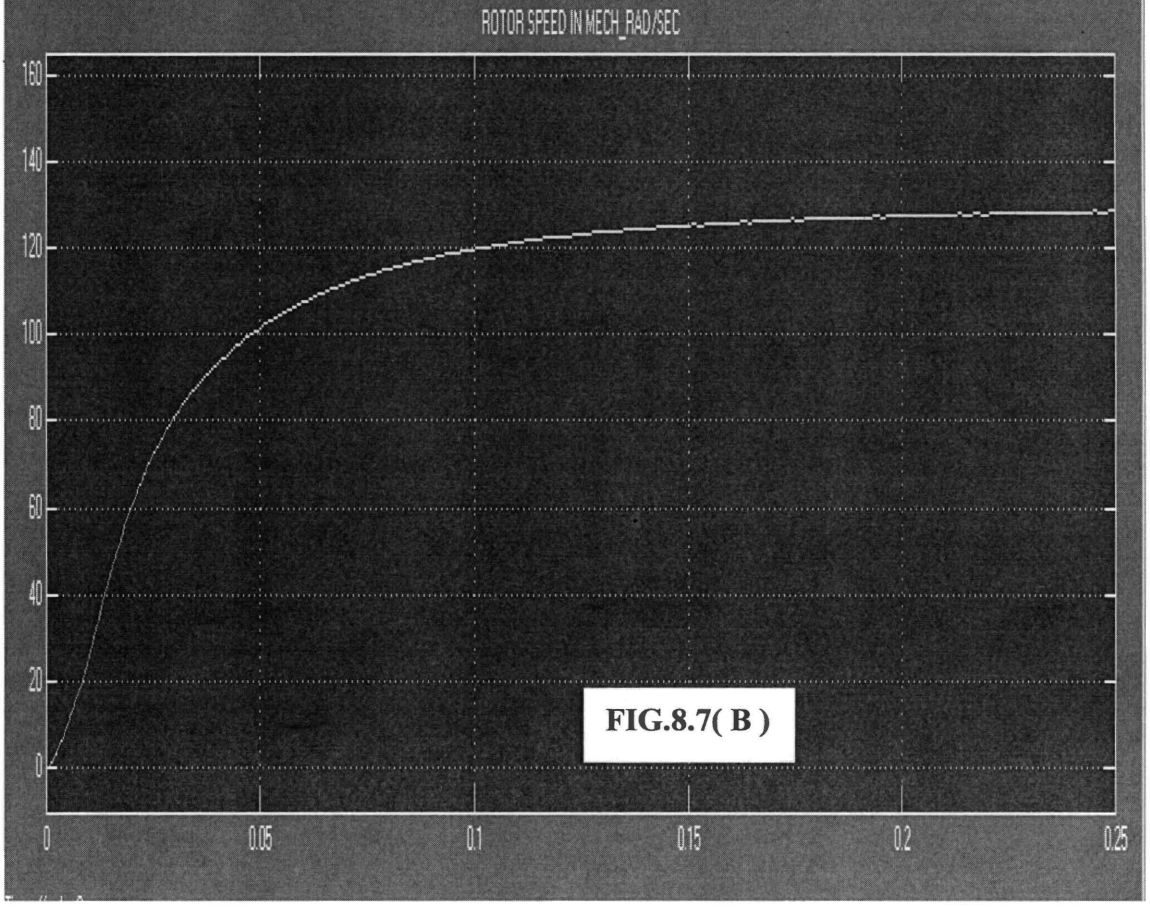

FIG.8.7(B)

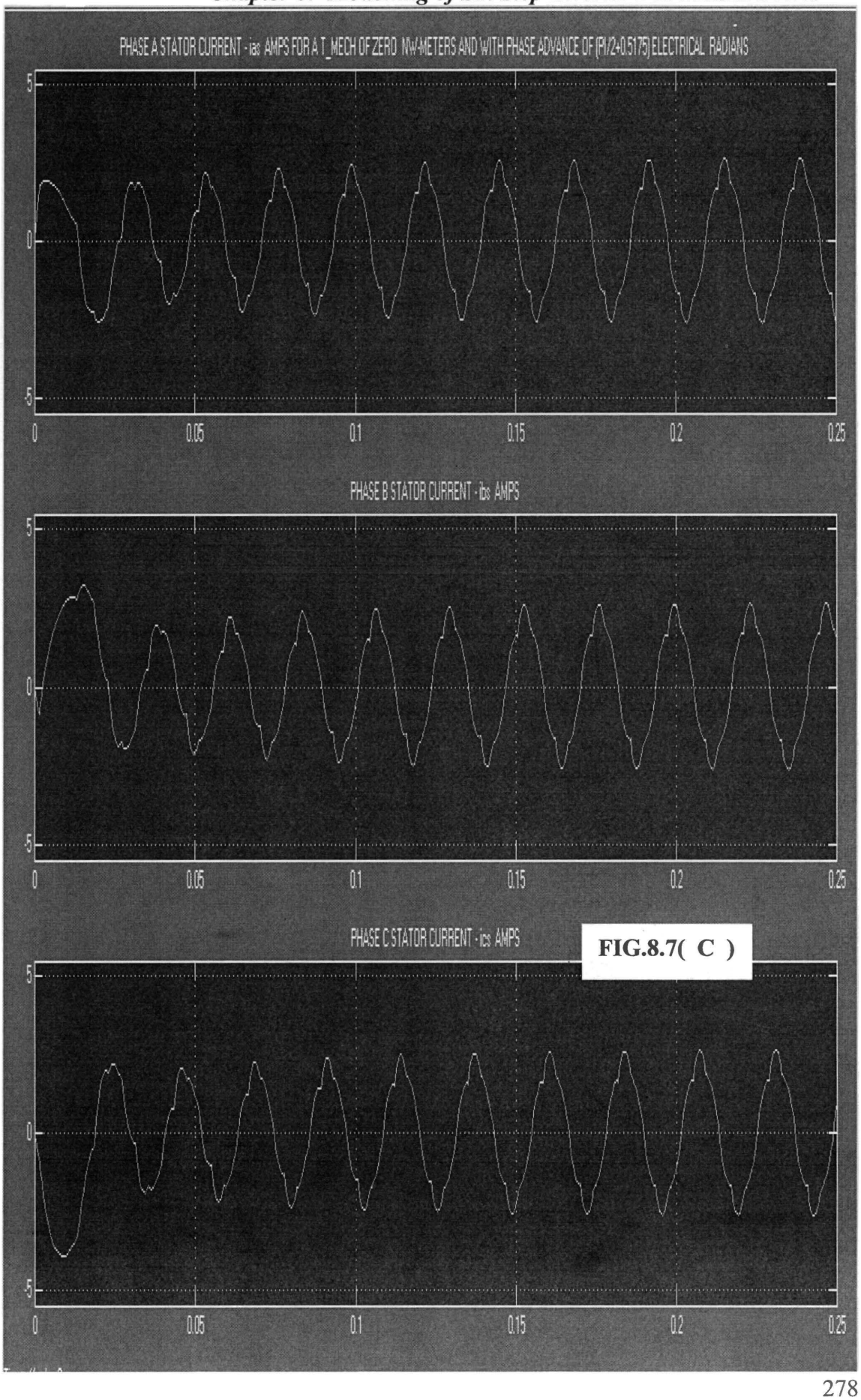
PHASE A STATOR CURRENT - ias AMPS FOR A T_MECH OF ZERO NW-METERS AND WITH PHASE ADVANCE OF (PI/2+0.5175) ELECTRICAL RADIANS
5
0
-5
0
0.05
0.1
0.15
0.2
0.25
PHASE B STATOR CURRENT - ibs AMPS
5
0
-5
0
0.05
0.1
0.15
0.2
0.25
PHASE C STATOR CURRENT - ics AMPS
5
0
-5
0
0.05
0.1
0.15
0.2
0.25

FIG.8.7(C)

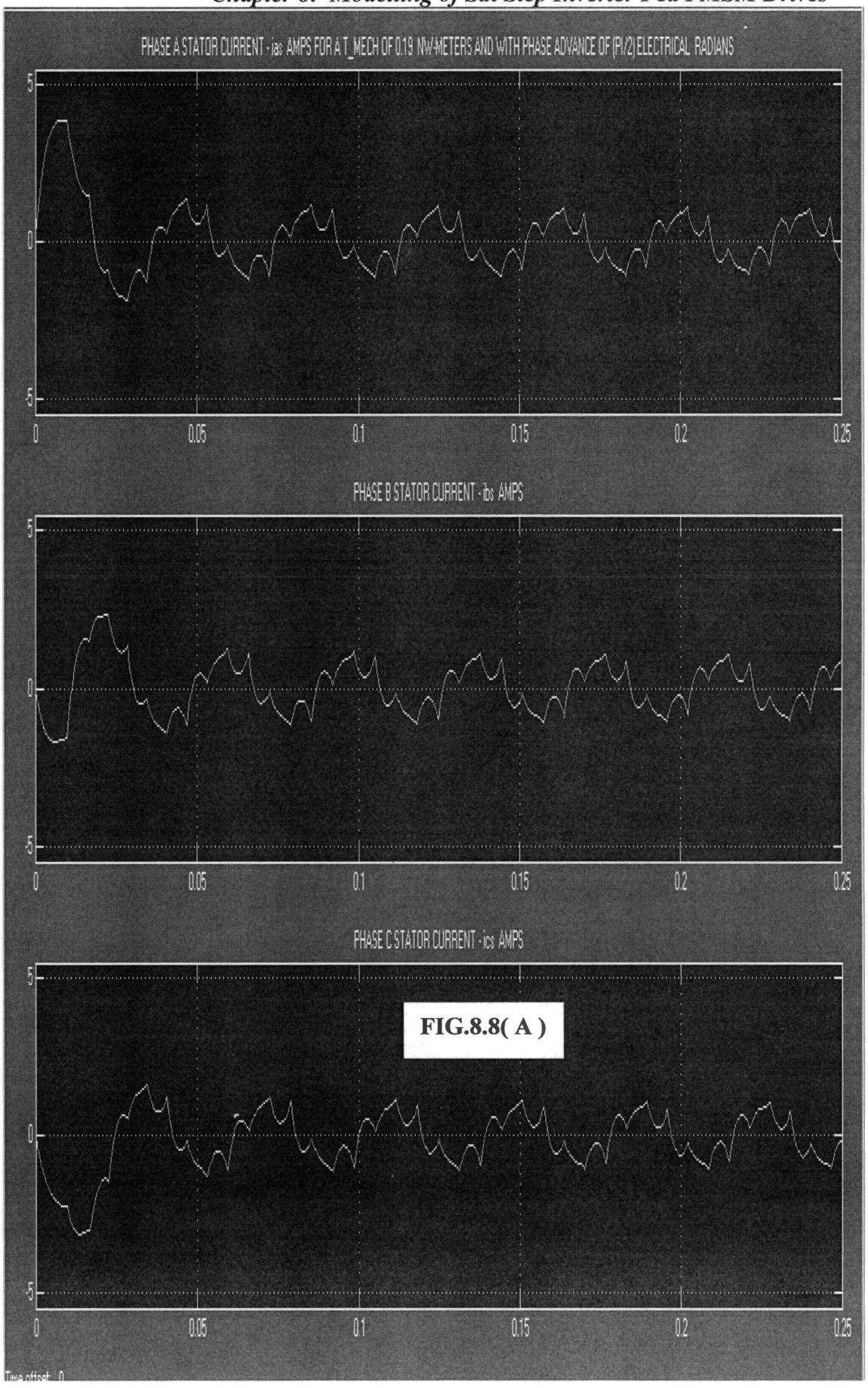
PHASE A STATOR CURRENT - ias AMPS FOR A T_MECH OF 0.19 NW-METERS AND WITH PHASE ADVANCE OF (PI/2) ELECTRICAL RADIANS
5
0
-5
0
0.05
0.1
0.15
0.2
0.25
PHASE B STATOR CURRENT - ibs AMPS
5
0
-5
0
0.05
0.1
0.15
0.2
0.25
PHASE C STATOR CURRENT - ics AMPS
5
0
-5
0
0.05
0.1
0.15
0.2
0.25

FIG.8.8(A)

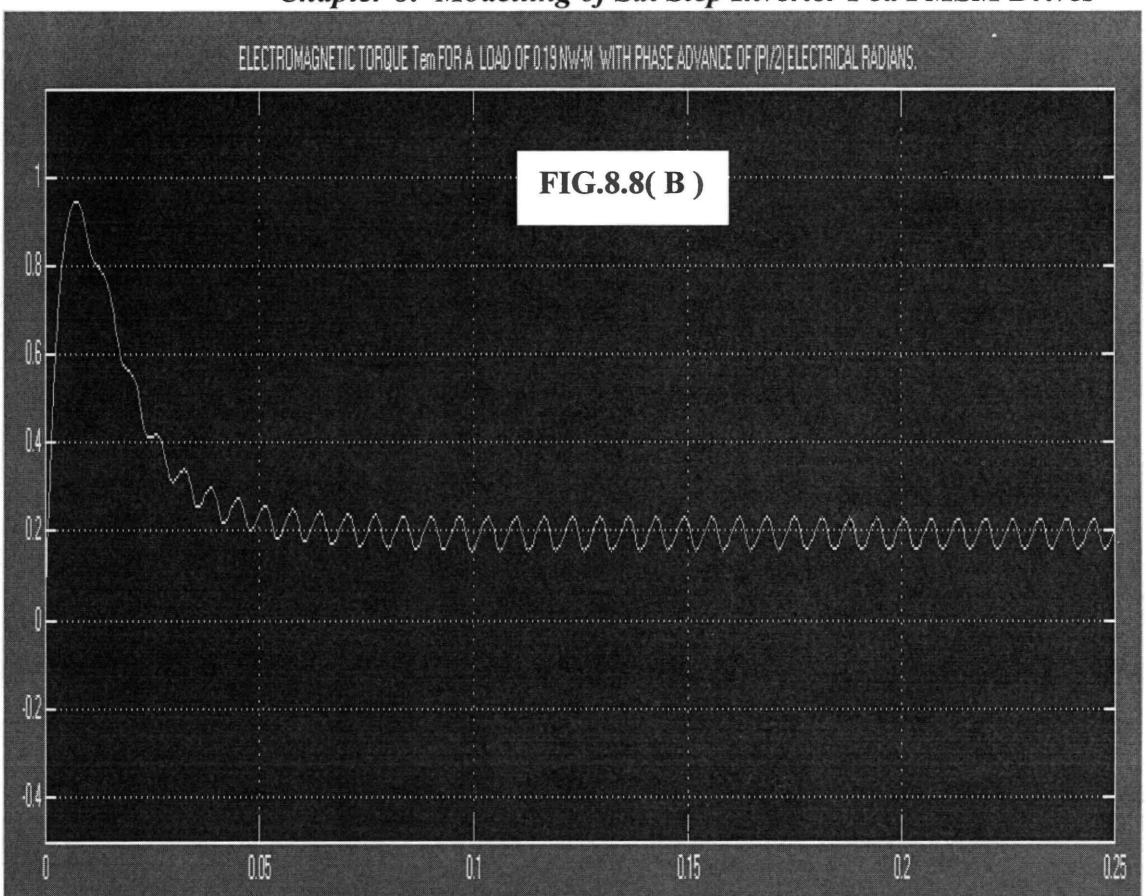

FIG.8.8(B)

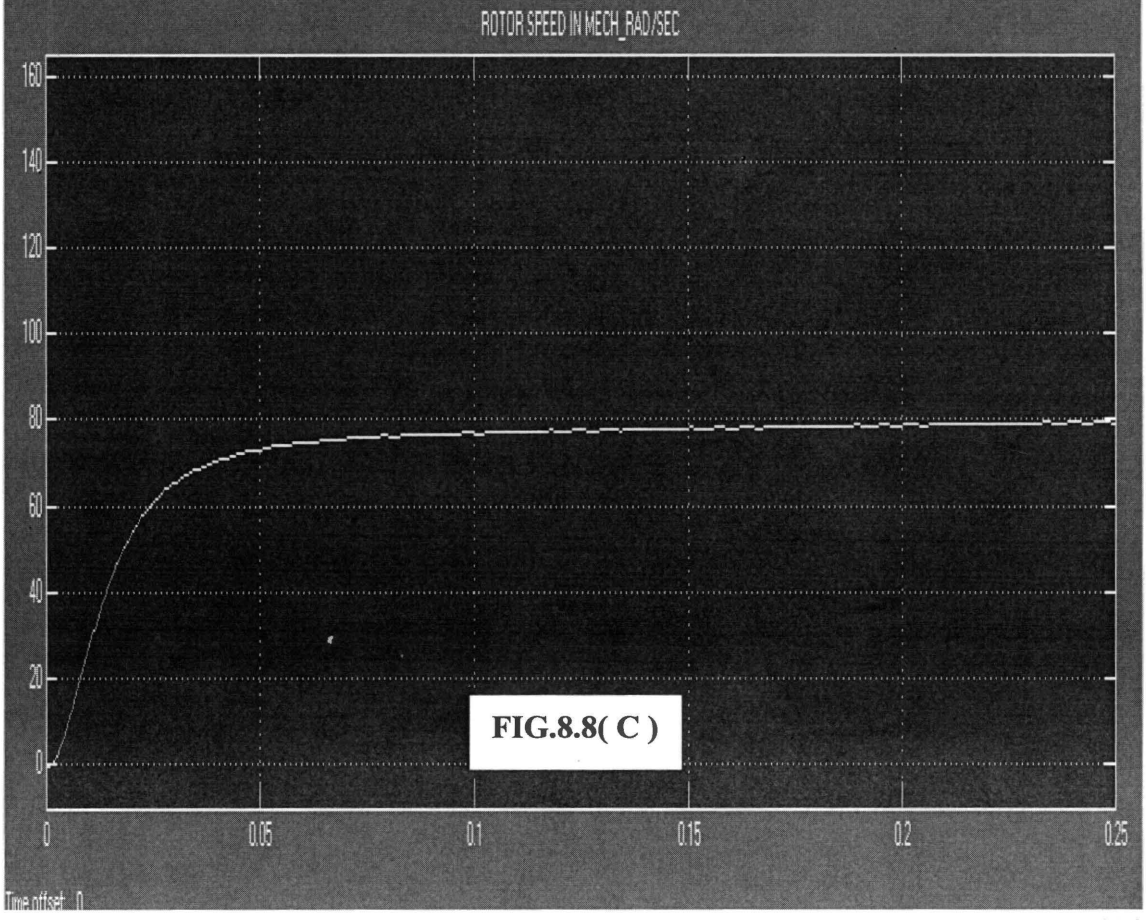

FIG.8.8(C)

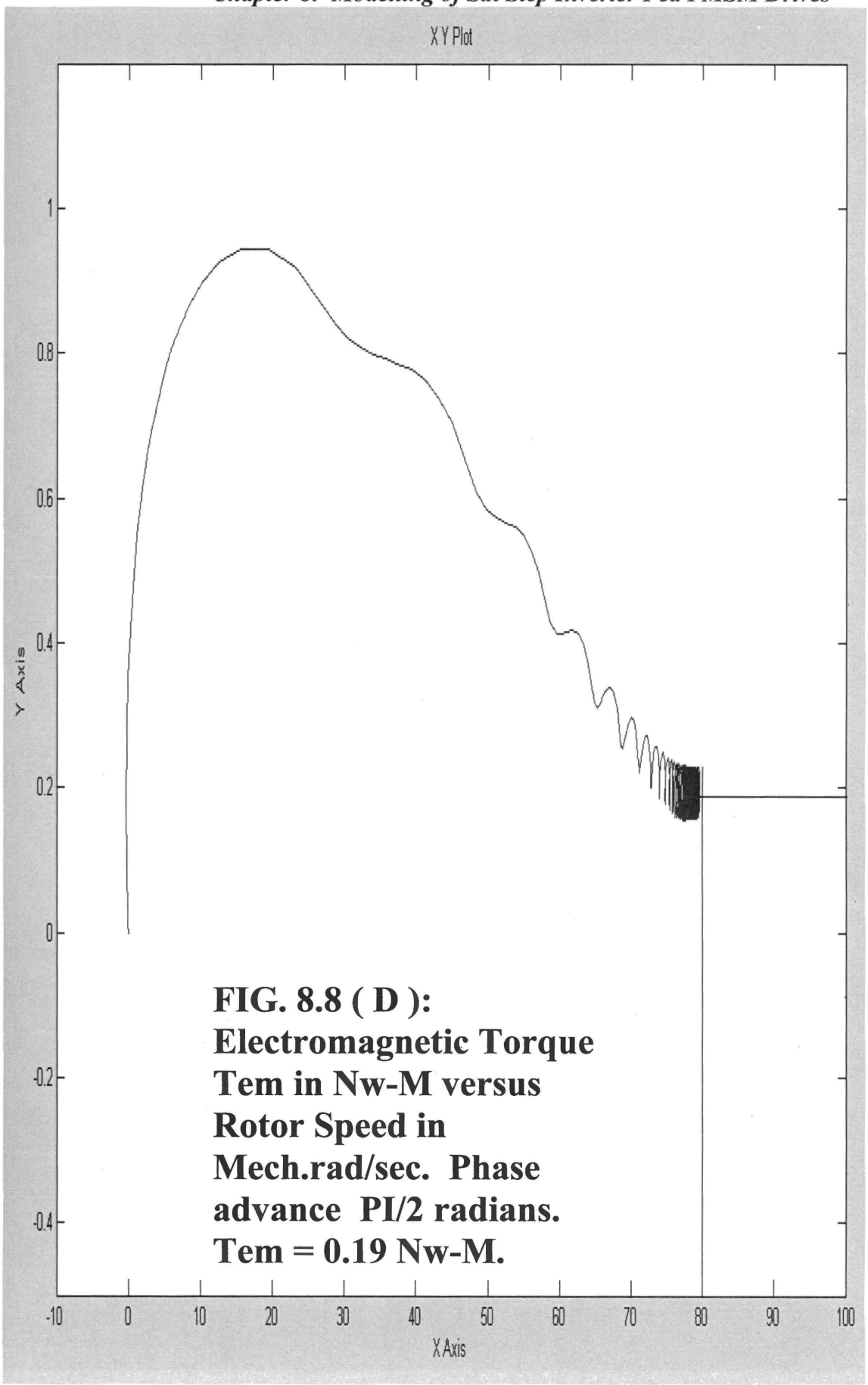

FIG. 8.8 (D): Electromagnetic Torque Tem in Nw-M versus Rotor Speed in Mech.rad/sec. Phase advance PI/2 radians. Tem = 0.19 Nw-M.

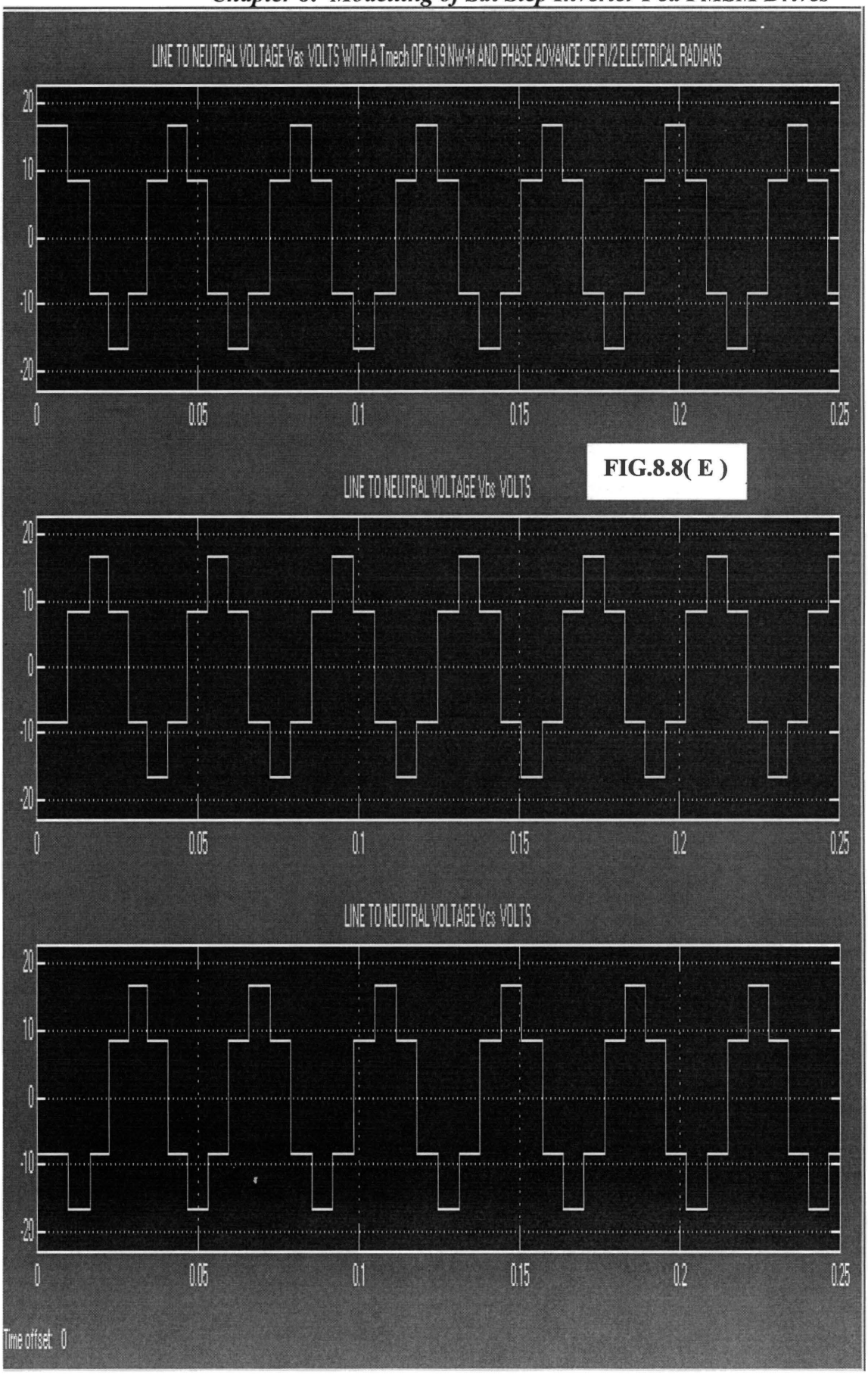
LINE TO NEUTRAL VOLTAGE Vas VOLTS WITH A Tmech OF 0.19 NW-M AND PHASE ADVANCE OF PI/2 ELECTRICAL RADIANS
20
10
0
-10
-20
0
0.05
0.1
0.15
0.2
0.25
LINE TO NEUTRAL VOLTAGE Vbs VOLTS
20
10
0
-10
-20
0
0.05
0.1
0.15
0.2
0.25
LINE TO NEUTRAL VOLTAGE Vcs VOLTS
20
10
0
-10
-20
0
0.05
0.1
0.15
0.2
0.25
Time offset: 0

FIG.8.8(E)

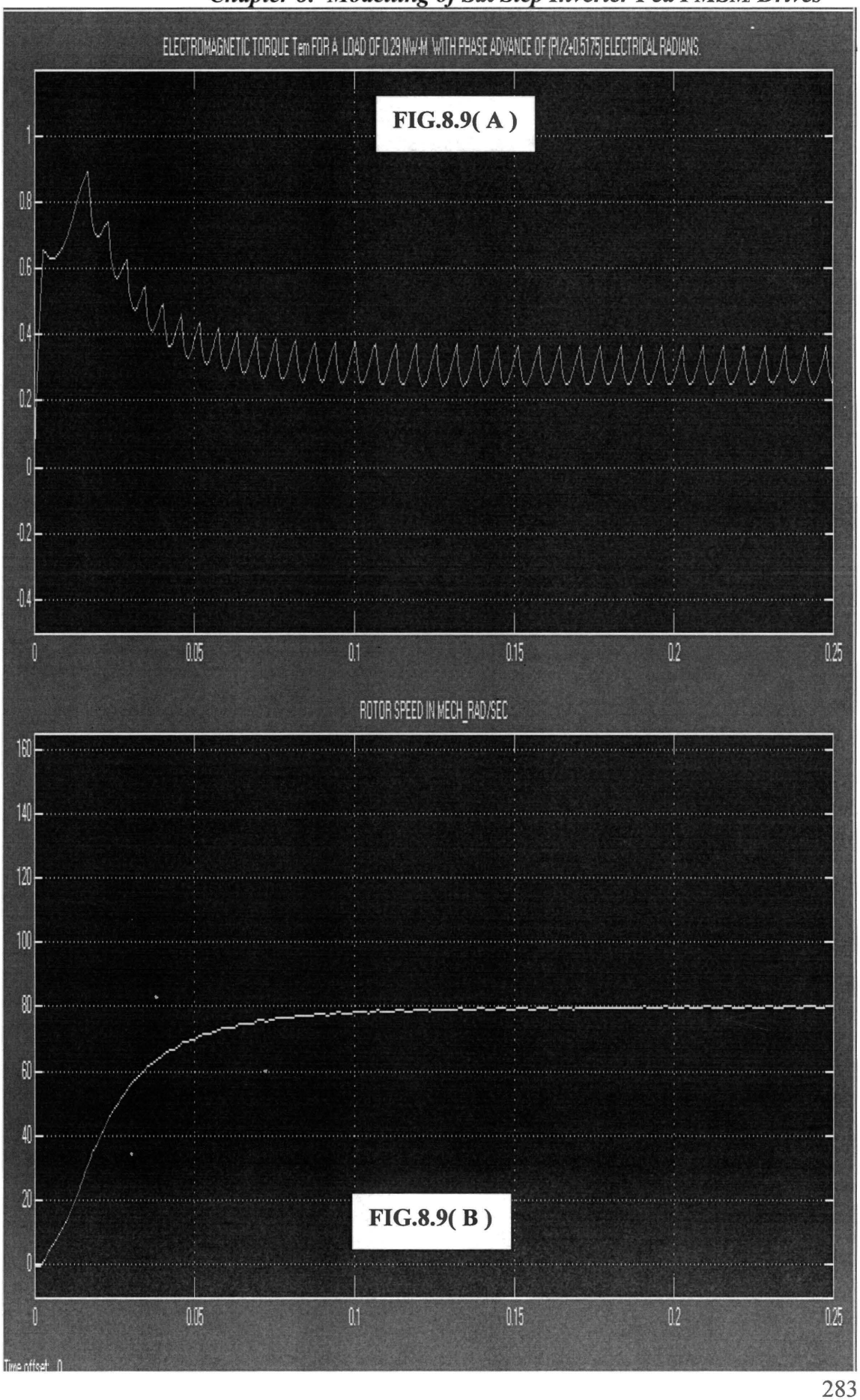

FIG.8.9(A)

FIG.8.9(B)

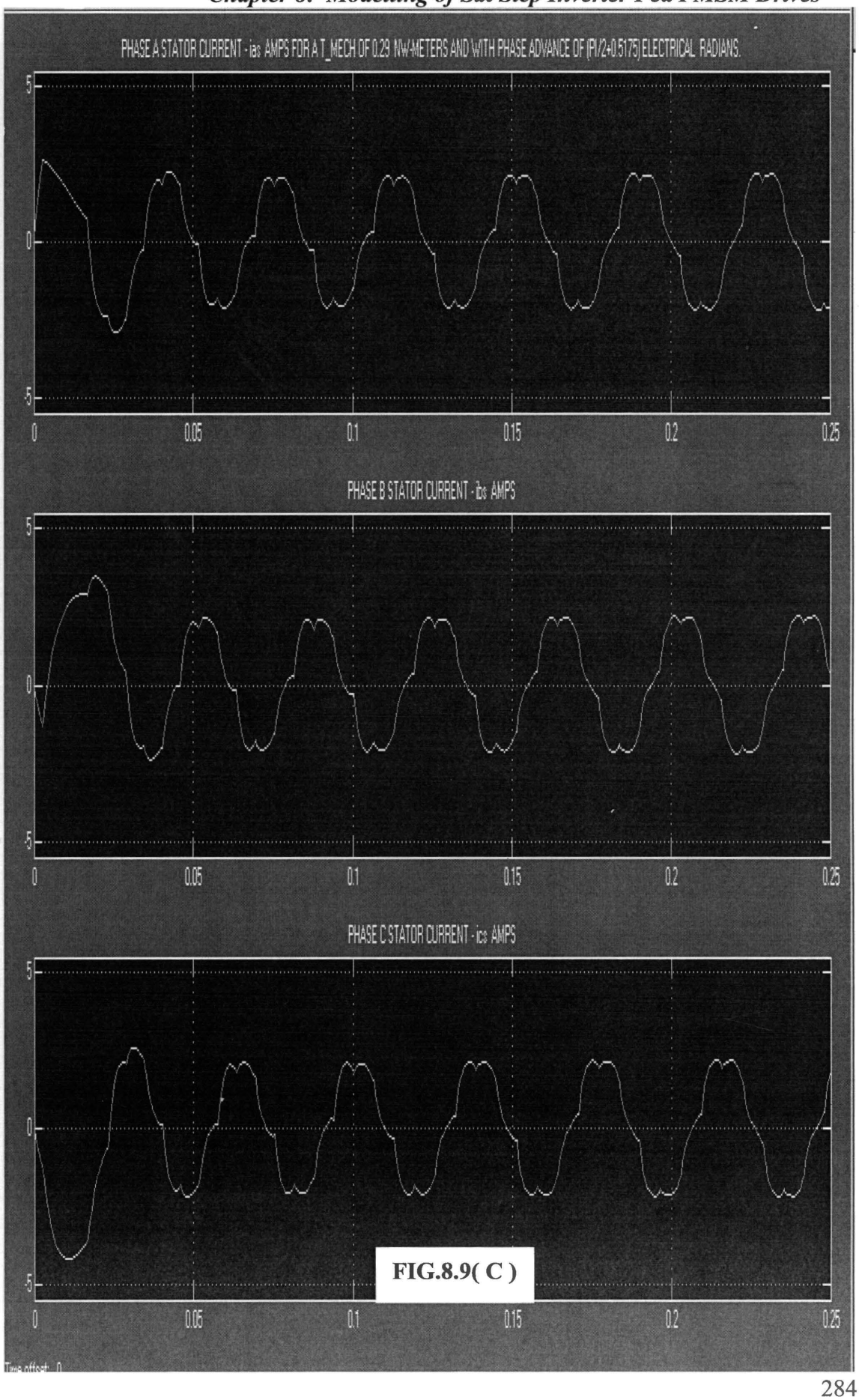
PHASE A STATOR CURRENT - ias AMPS FOR A T_MECH OF 0.23 NW-METERS AND WITH PHASE ADVANCE OF (PI/2+0.5175) ELECTRICAL RADIANS.
5
0
-5
0
0.05
0.1
0.15
0.2
0.25
PHASE B STATOR CURRENT - ibs AMPS
5
0
-5
0
0.05
0.1
0.15
0.2
0.25
PHASE C STATOR CURRENT - ics AMPS
5
0
-5
0
0.05
0.1
0.15
0.2
0.25

FIG.8.9(C)

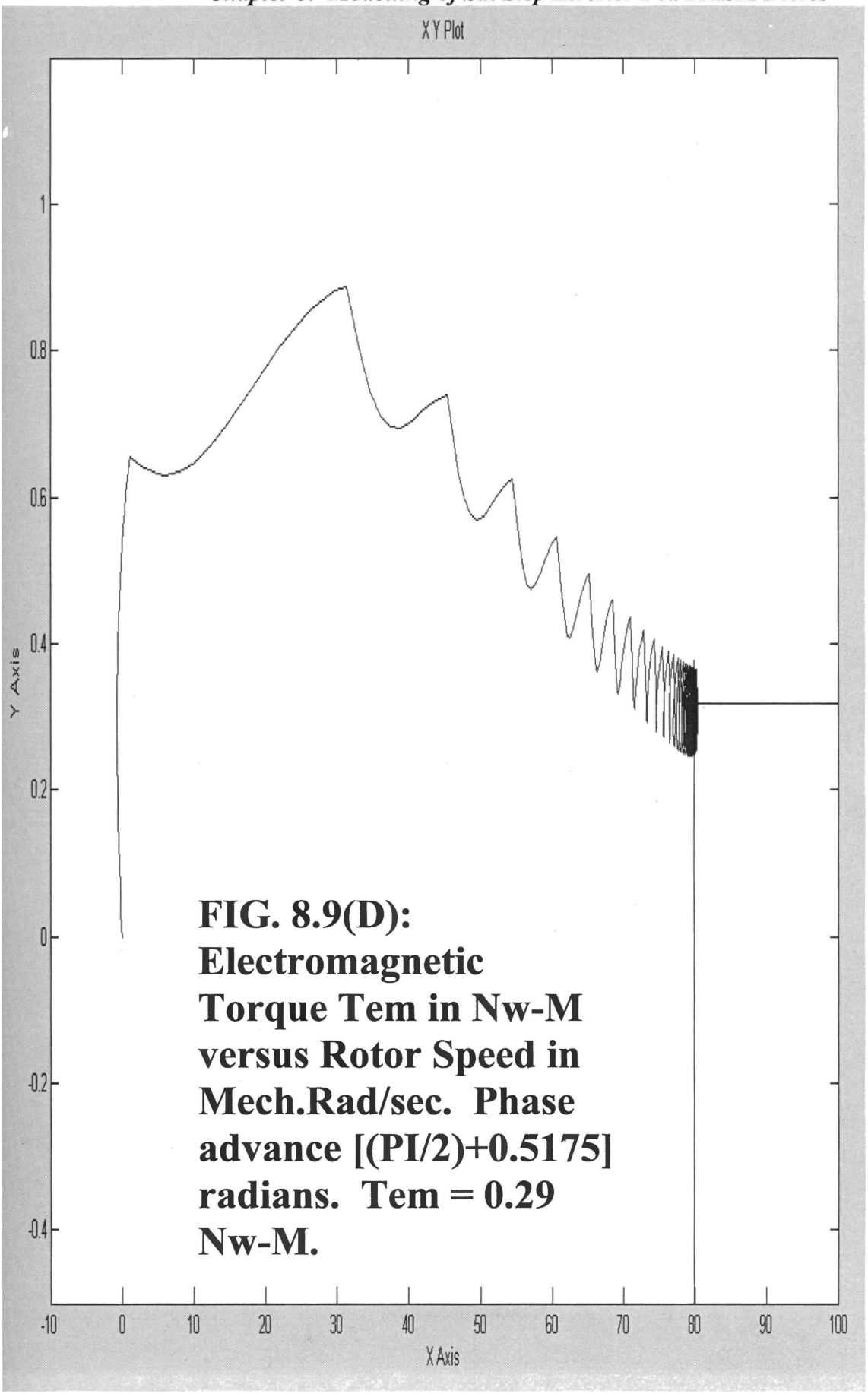

FIG. 8.9(D): Electromagnetic Torque Tem in Nw-M versus Rotor Speed in Mech.Rad/sec. Phase advance [(PI/2)+0.5175] radians. Tem = 0.29 Nw-M.

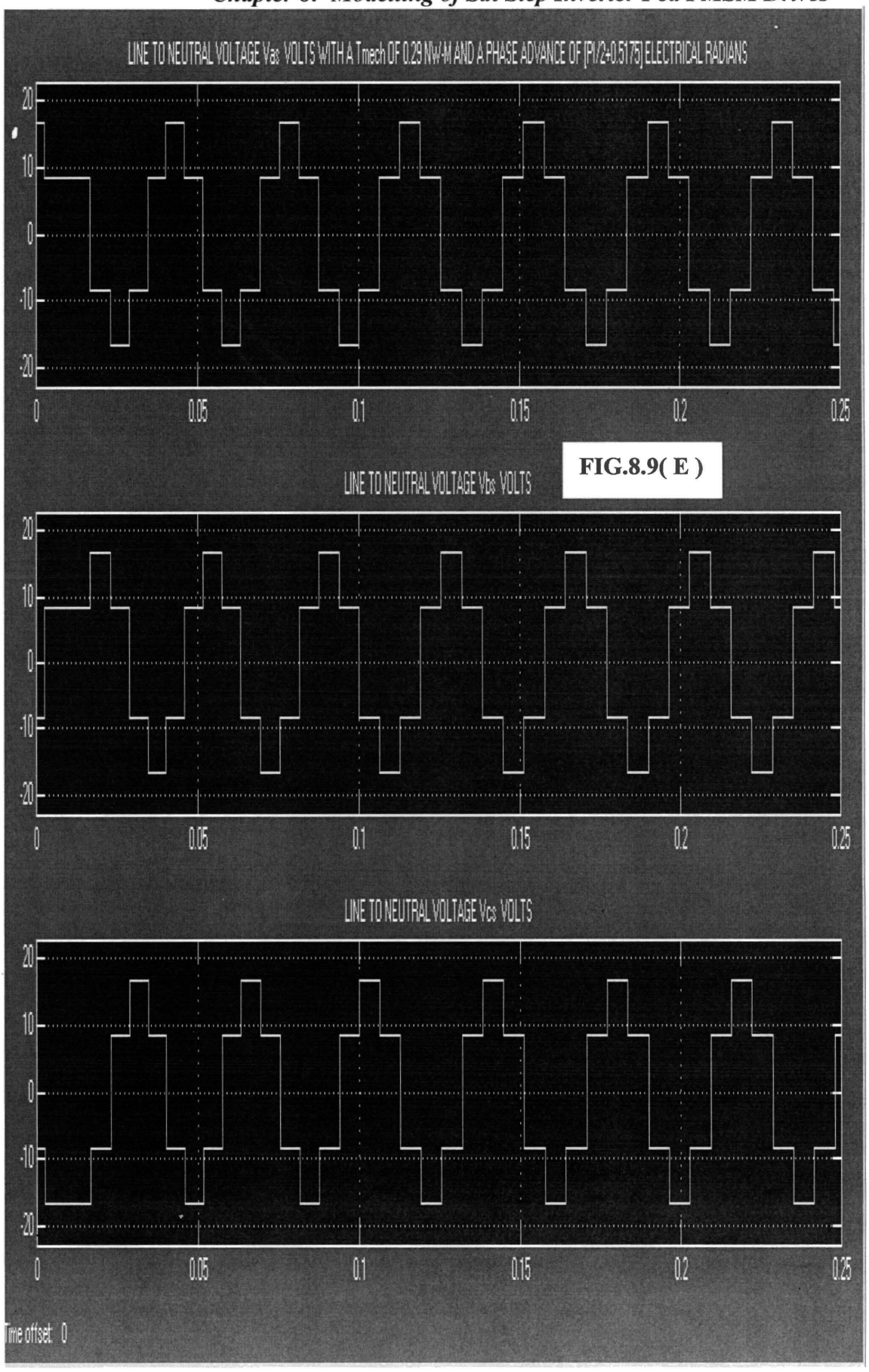
LINE TO NEUTRAL VOLTAGE Vas VOLTS WITH A Tmech OF 0.29 Nw-M AND A PHASE ADVANCE OF [PI/2+0.5175] ELECTRICAL RADIANS
20
10
0
-10
-20
0
0.05
0.1
0.15
0.2
0.25
LINE TO NEUTRAL VOLTAGE Vbs VOLTS
20
10
0
-10
-20
0
0.05
0.1
0.15
0.2
0.25
LINE TO NEUTRAL VOLTAGE Vcs VOLTS
20
10
0
-10
-20
0
0.05
0.1
0.15
0.2
0.25
Time offset: 0

FIG.8.9(E)

8.4 Modelling of Six Step Discontinuous Current Mode Inverter Fed PMSM Drive

The model of the six step discontinuous current mode inverter fed PMSM drive is done by two methods. The gate drive pattern for six step 120 degree mode also known as discontinuous current mode inverter is shown in Fig.2.6(B) in Chapter 2. The two methods of modelling six step discontinuous current mode inverter are explained below:

8.4.1 First Model for Six Step Discontinuous Current Mode Inverter Fed PMSM Drive

The first model of the discontinuous current mode inverter fed PMSM drive is shown in Fi.g.8.10. The various dialog boxes are shown in Fig.8.11. The subsystem relating to Six Step 120 Degree Mode Inverter and Gate Drive is shown in Fig.8.12(A) and Fig.8.12.1(A). The dialog box Three Phase 120 Degree Mode Inverter and Gate Drive in Fig.8.11 corresponds to this subsystem. All other subsystems are the same as for Six Step 180 Degree Mode Inverter shown in Fig.8.5 (C) to (I). The subsystem shown in Fig.8.12(A) and Fig.8.12.1(A) are explained below.

The four input to the mux are the arbitrary constant, ω_{re}, time and switching angle advance. The three phase sine wave AC with angular frequency ω_{re} with phase advance phi added is generated using three Fcn blocks, Fcn, Fcn1 and Fcn2. Each of the three phase AC output are then compared in a Schmitt trigger relay comparator used as zero crossing comparators, with output logic 1 and 0 respectively during the positive and negative half cycle of the input sine wave. The a, b, c output of the three relays are Relay, Relay1 and Relay2 are given to three Fcn blocks, Fcn6, Fcn7 and Fcn8. The three Fcn blocks Fcn6, Fcn7 and Fcn8 subtract the two inputs to their respective mux. The resulting output of these three Fcn blocks are then multiplied by Vdc/2 using multiplier blocks to generate line to ground voltages Vag, Vbg and Vcg of the three phase 120 degree mode inverter, where Vdc is the DC link voltage. The three subtract blocks are used to generate the three phase line to line voltages.

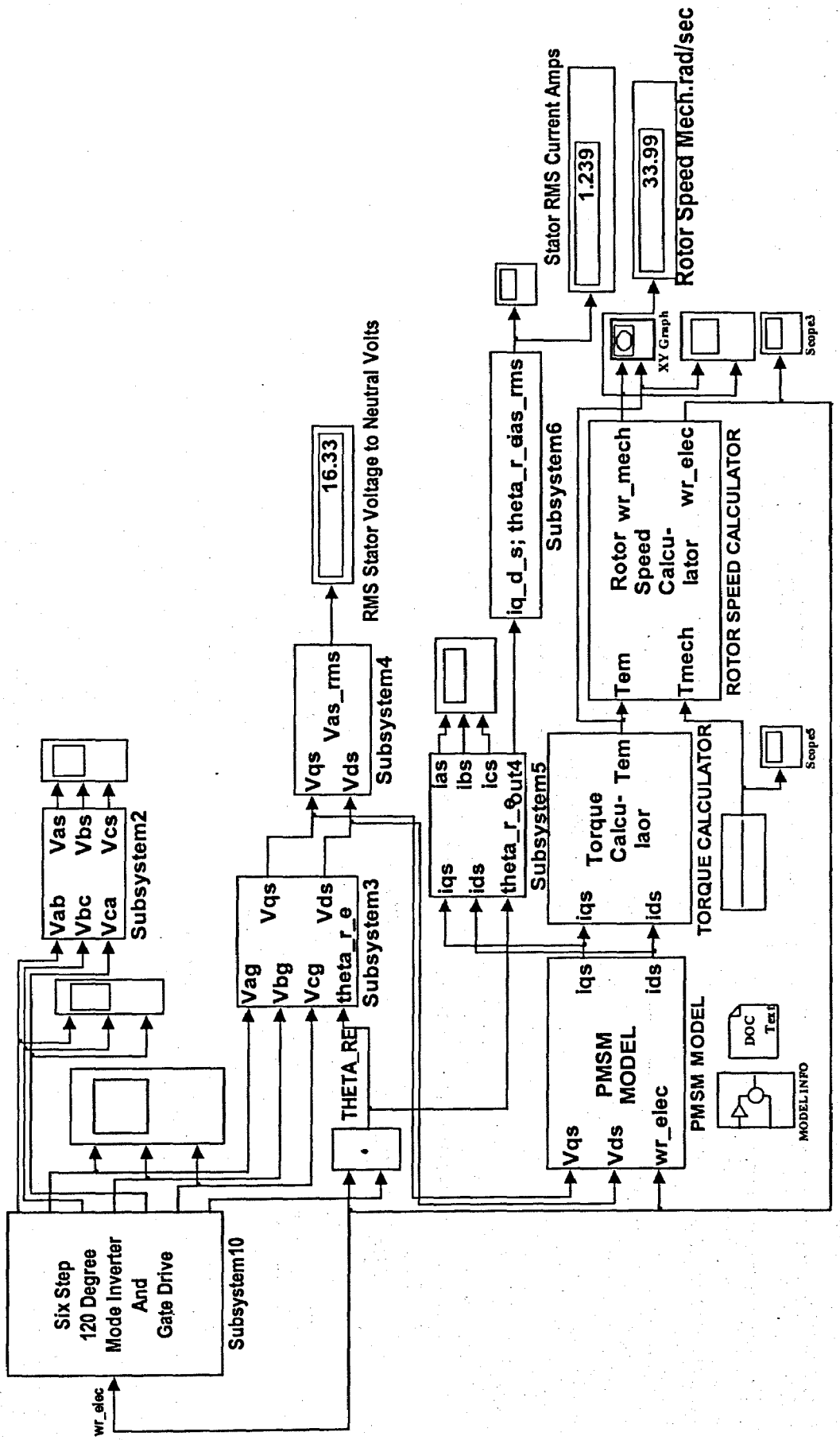

FIG.8.10: LYBOTEC SIX STEP 120 DEGREE MODE INVERTER FED PMSM DRIVE

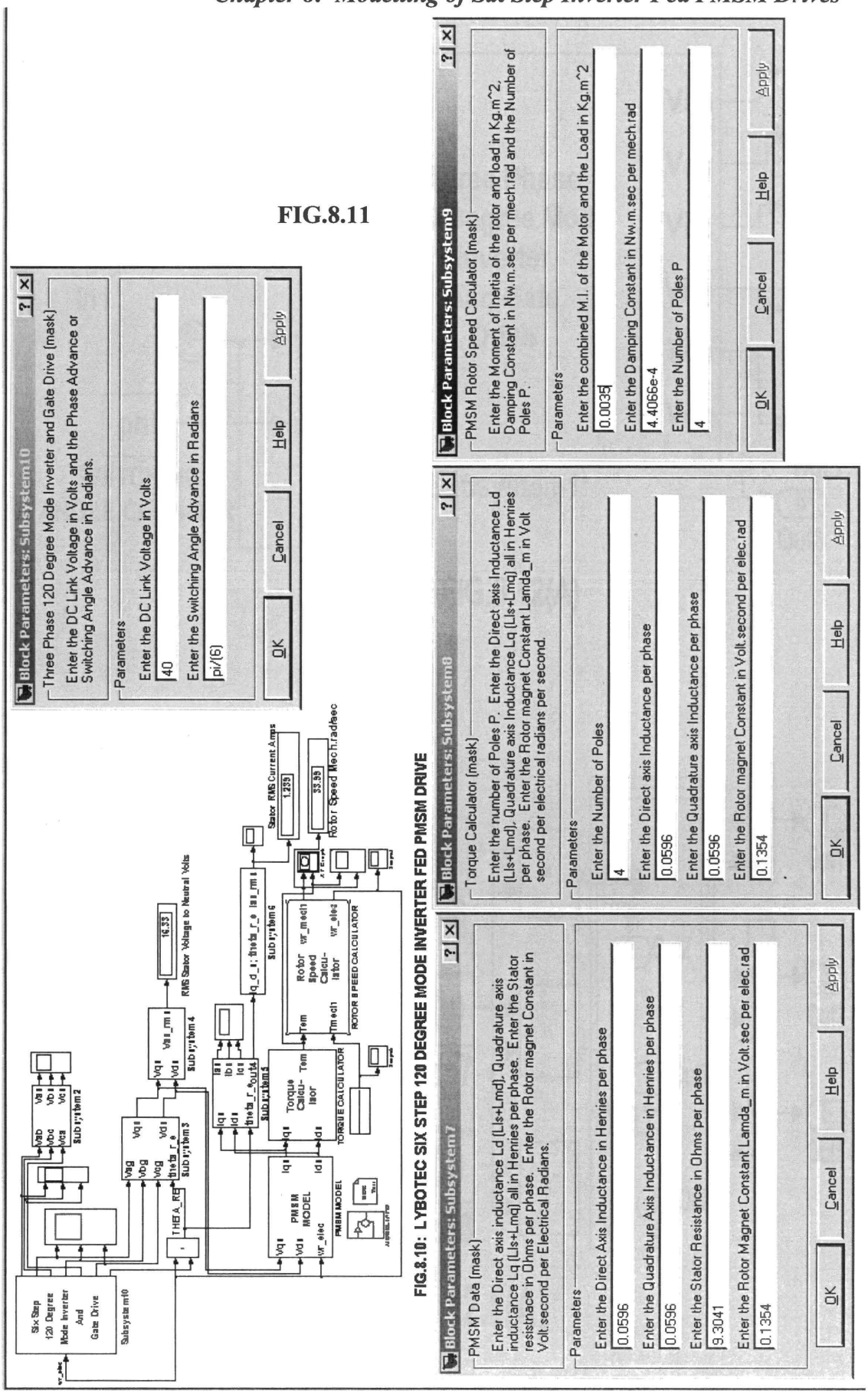

FIG.8.10: LYBOTEC SIX STEP 120 DEGREE MODE INVERTER FED PMSM DRIVE

FIG.8.11

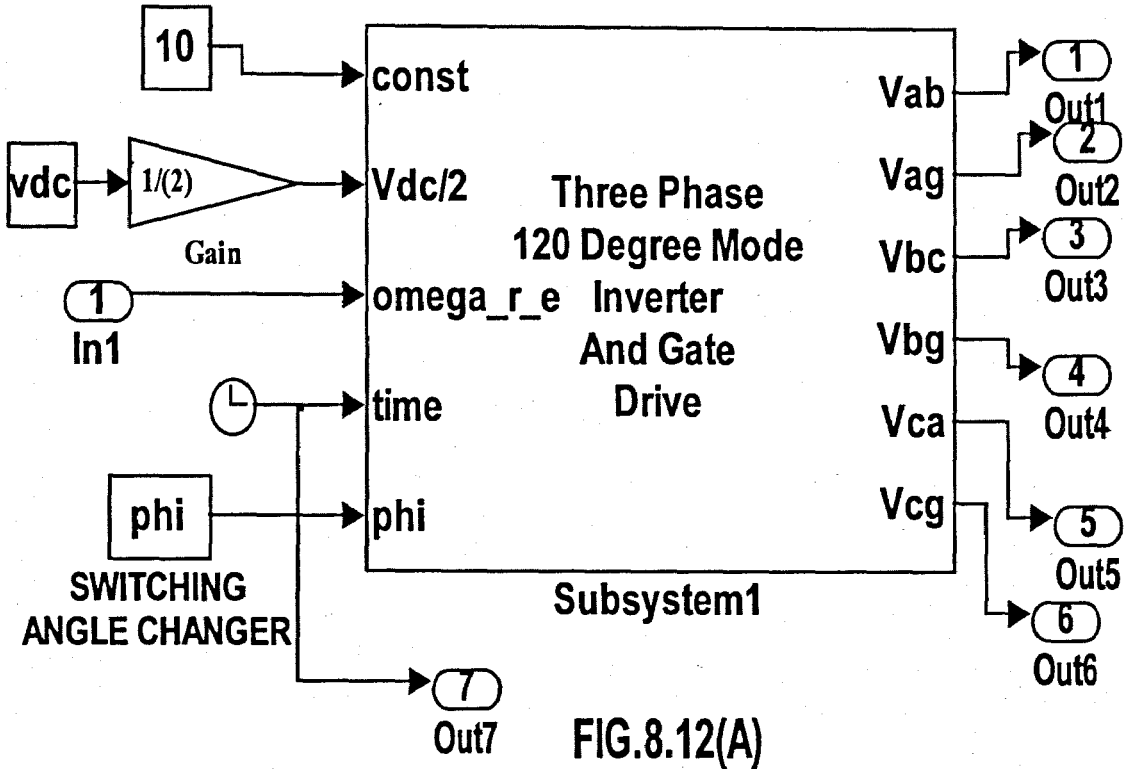

FIG.8.12(A)

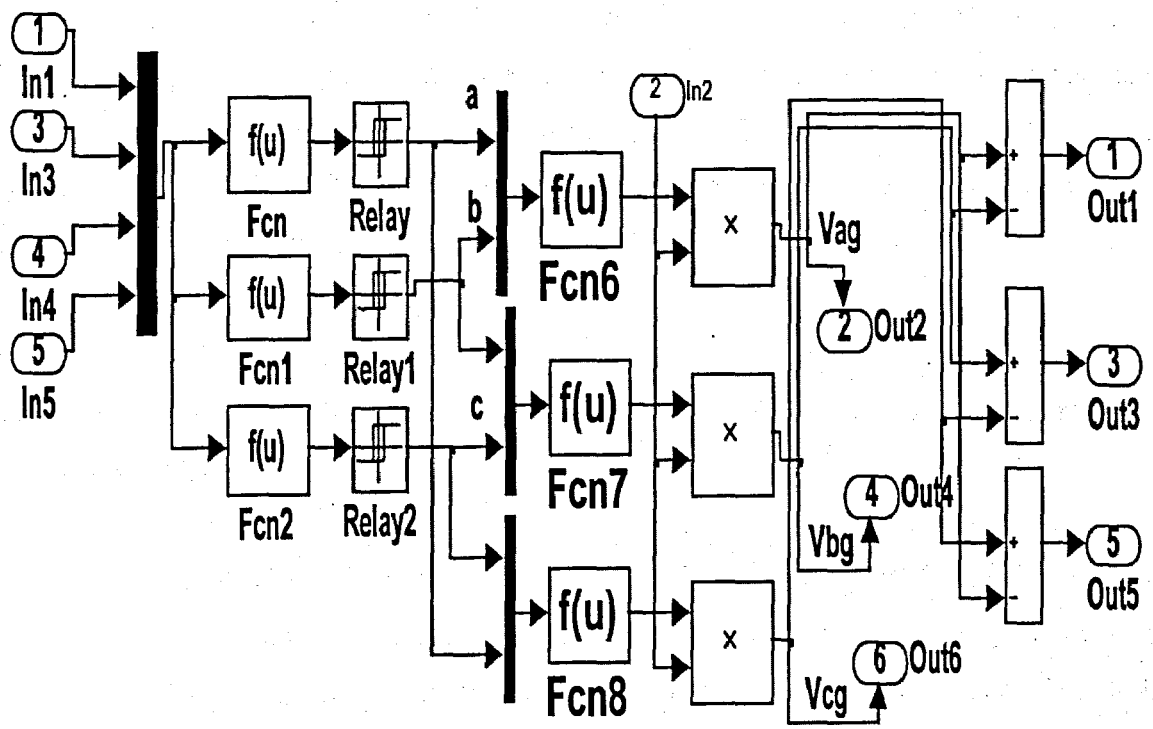

FIG.8.12.1(A)

8.4.2 Simulation Results:

The simulation was carried out using ode15s(stiff/NDF) solver. The data relating to the six step discontinuous current mode Lybotec Inverter fed PMSM drive is shown in Table 8.2. The simulation of this Lybotec inverter fed PMSM was carried out for phase

TABLE 8.2

SL.NO.	PARAMETERS	VALUE	UNIT
1	Number of Phases	3	
2	No. of Poles P	4	
3	Stator Resistance Rs	9.3041	Ohms/Ph
4	Stator Inductance Ls	0.0596	H/Ph
5	Rotor Magnet Constant λm	0.1354	V.Sec/elec.rad
6	Damping Constant D	0.00044066	Nw.M.sec/mech.rad
7	Rotor Inertia J	0.0035	Kg.m^2
8	DC Link Voltage Vdc	40	Volts

advance of π /6 and π /4 electrical radians. These simulation results are compared with the experimentally observed results in the CEMPE laboratory. The simulation of torque, speed, torque-speed and line to neutral voltage of PMSM are shown in Fig.8.13(A) to (E) for a phase advance of π /6 radians. The same simulation results for a phase advance of π /4 radians is shown in Fig.8.14(A) to (E). Also in both cases the recorded value of the R.M.S. Line to Neutral voltage of the PMSM was found to be 16.33 volts, which corresponds to Vdc /$\sqrt{6}$ volts. This derivation is given in equation 4.32 in Chapter 4. Vdc is the DC Link voltage.

8.4.3 Second Model for Six Step Discontinuous Current Mode Inverter Fed PMSM Drive

The second model of the discontinuous current mode inverter fed PMSM drive is shown in Fi.g.8.15. The various dialog boxes are shown in Fig.8.16. The subsystem relating to Six Step 120 Degree Mode Inverter and Gate Drive is shown in Fig.8.17. The dialog box Three Phase 120 Degree Mode Gate Drive and Inverter in Fig.8.16 corresponds to this subsystem. All other subsystems are the same as for Six Step 180 Degree Mode Inverter shown in Fig.8.5 (C) to (I). The subsystem shown in Fig.8.17 is explained below.

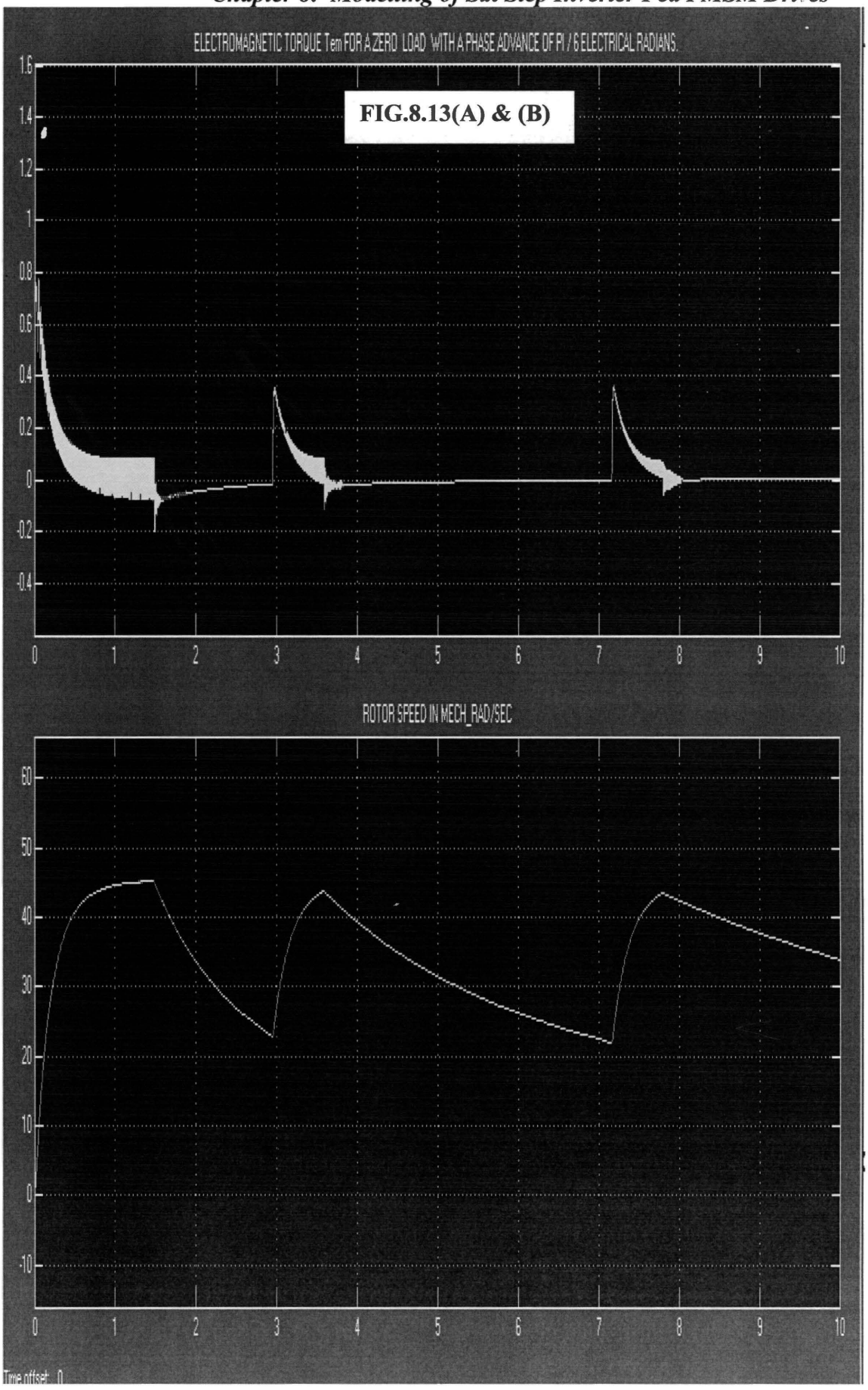
ELECTROMAGNETIC TORQUE Tem FOR A ZERO LOAD WITH A PHASE ADVANCE OF PI / 6 ELECTRICAL RADIANS.
1.6
1.4
1.2
1
0.8
0.6
0.4
0.2
0
-0.2
-0.4
0 1 2 3 4 5 6 7 8 9 10
ROTOR SPEED IN MECH_RAD/SEC
60
50
40
30
20
10
0
-10
0 1 2 3 4 5 6 7 8 9 10
Time offset: 0

FIG.8.13(A) & (B)

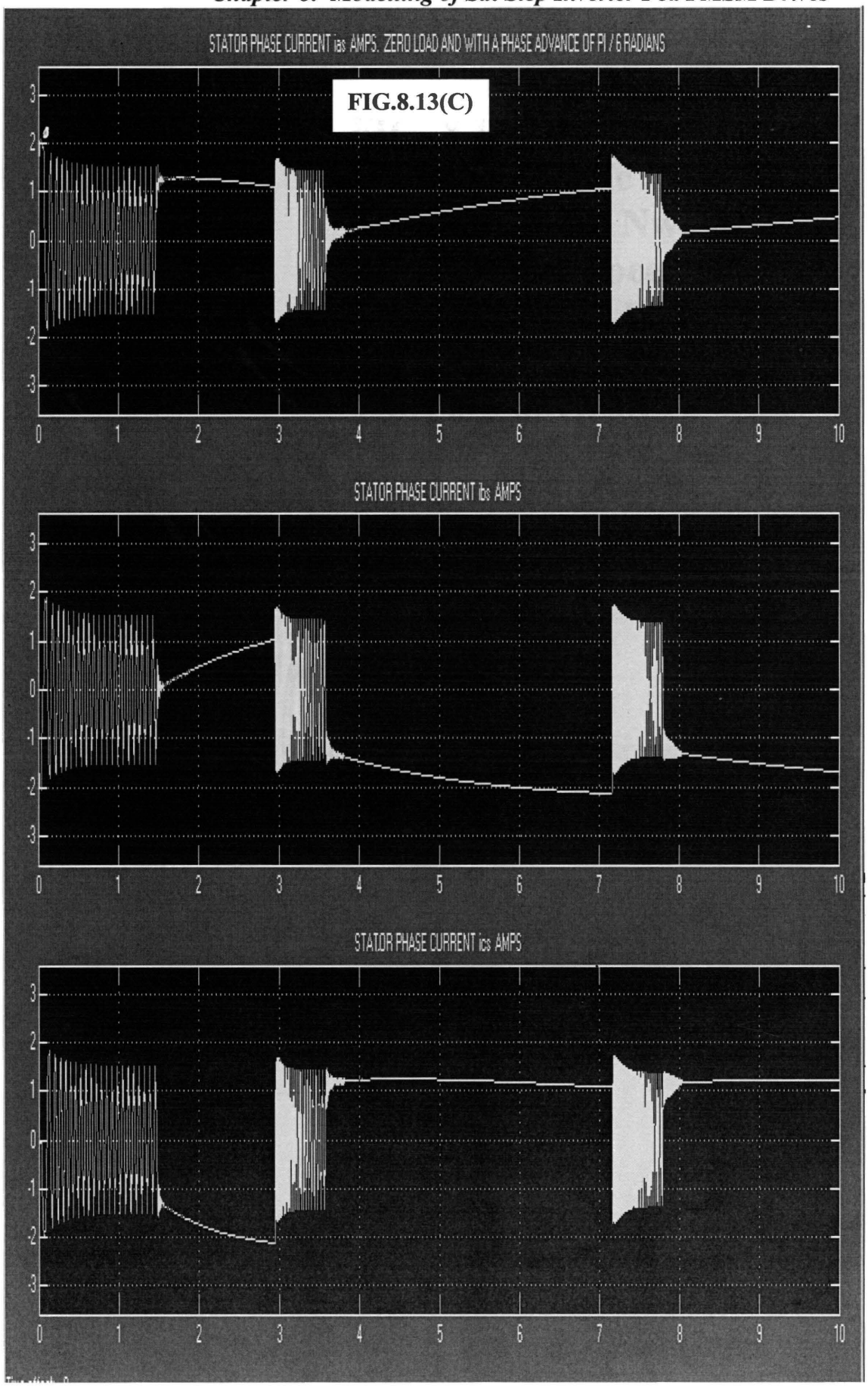
STATOR PHASE CURRENT ias AMPS. ZERO LOAD AND WITH A PHASE ADVANCE OF PI / 6 RADIANS
FIG.8.13(C)
STATOR PHASE CURRENT ibs AMPS
STATOR PHASE CURRENT ics AMPS

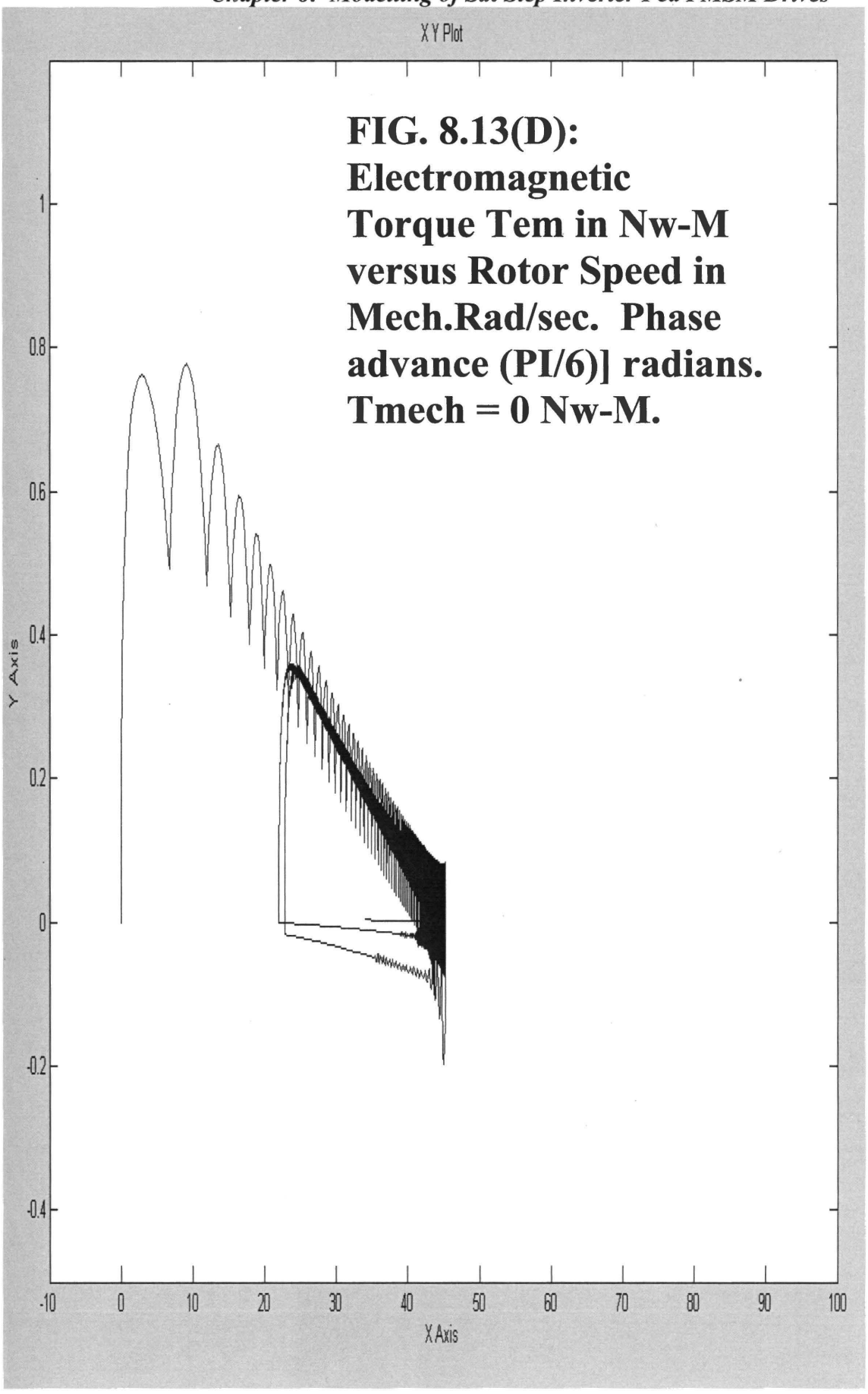

FIG. 8.13(D): Electromagnetic Torque Tem in Nw-M versus Rotor Speed in Mech.Rad/sec. Phase advance (PI/6)] radians. Tmech = 0 Nw-M.

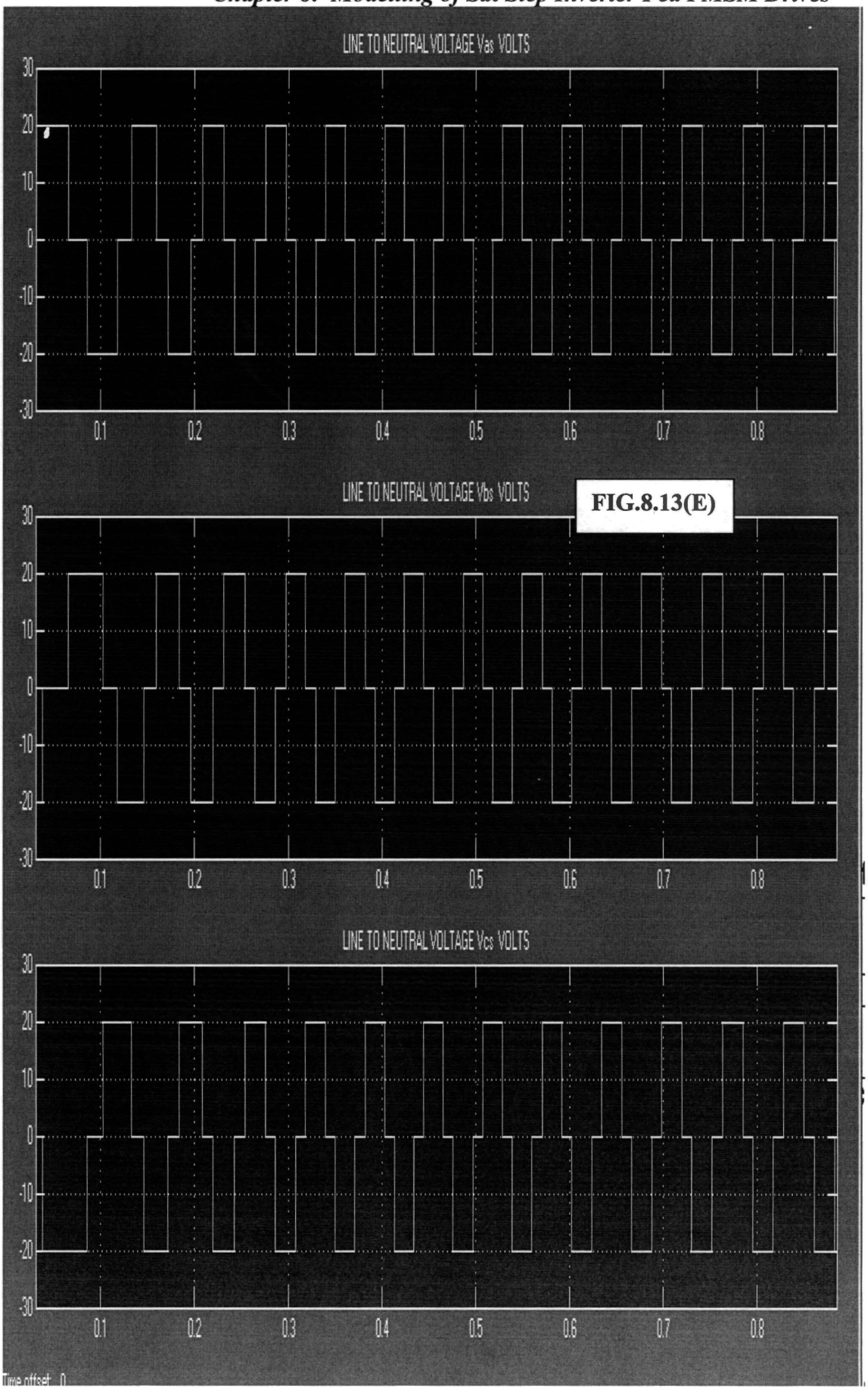
LINE TO NEUTRAL VOLTAGE Vas VOLTS
30
20
10
0
-10
-20
-30
0.1
0.2
0.3
0.4
0.5
0.6
0.7
0.8
LINE TO NEUTRAL VOLTAGE Vbs VOLTS
30
20
10
0
-10
-20
-30
0.1
0.2
0.3
0.4
0.5
0.6
0.7
0.8
LINE TO NEUTRAL VOLTAGE Vcs VOLTS
30
20
10
0
-10
-20
-30
0.1
0.2
0.3
0.4
0.5
0.6
0.7
0.8
Time offset: 0

FIG.8.13(E)

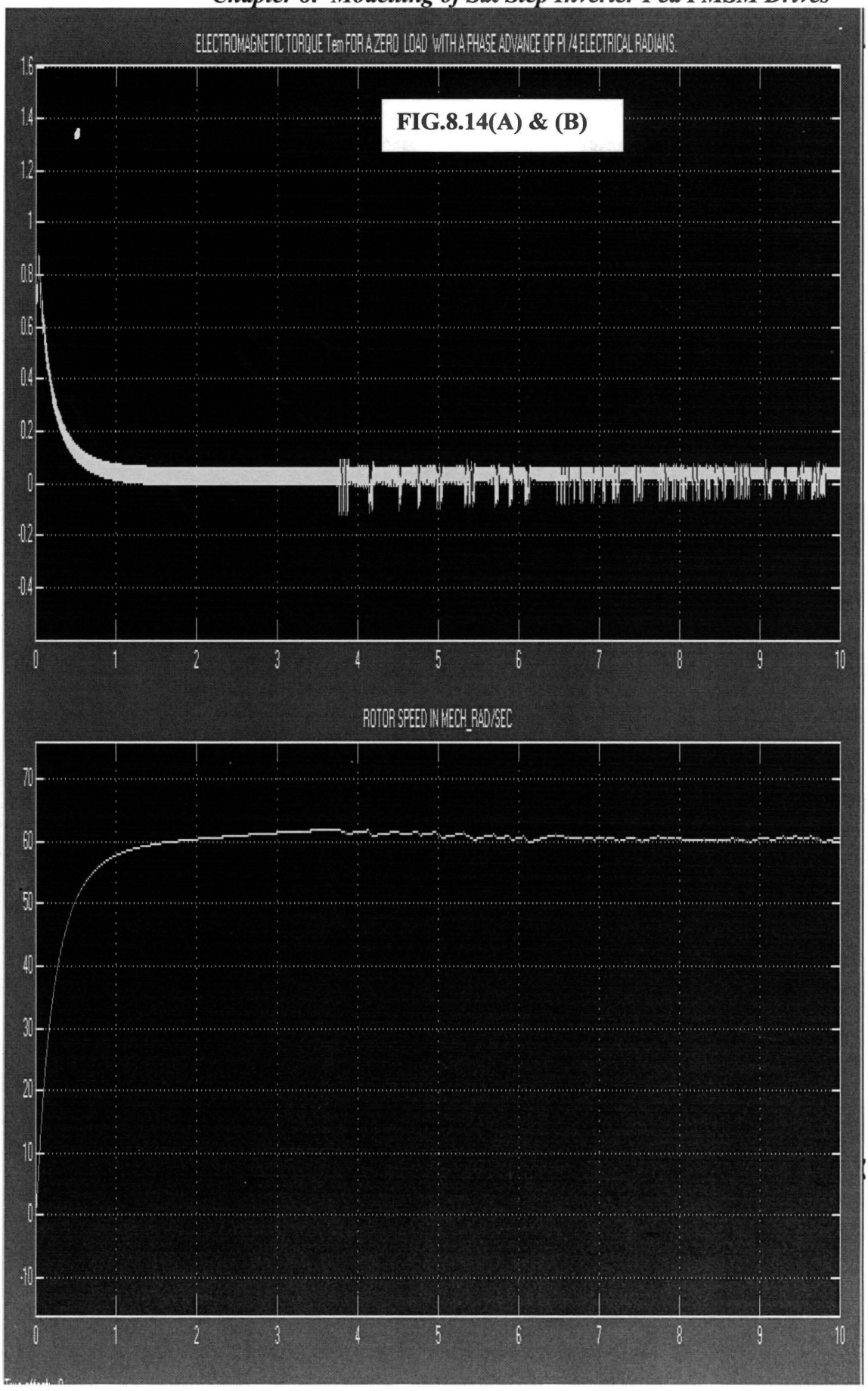
ELECTROMAGNETIC TORQUE Tem FOR A ZERO LOAD WITH A PHASE ADVANCE OF PI /4 ELECTRICAL RADIANS.
1.6
1.4
1.2
1
0.8
0.6
0.4
0.2
0
-0.2
-0.4
0 1 2 3 4 5 6 7 8 9 10
ROTOR SPEED IN MECH_RAD/SEC
70
60
50
40
30
20
10
0
-10
0 1 2 3 4 5 6 7 8 9 10

FIG.8.14(A) & (B)

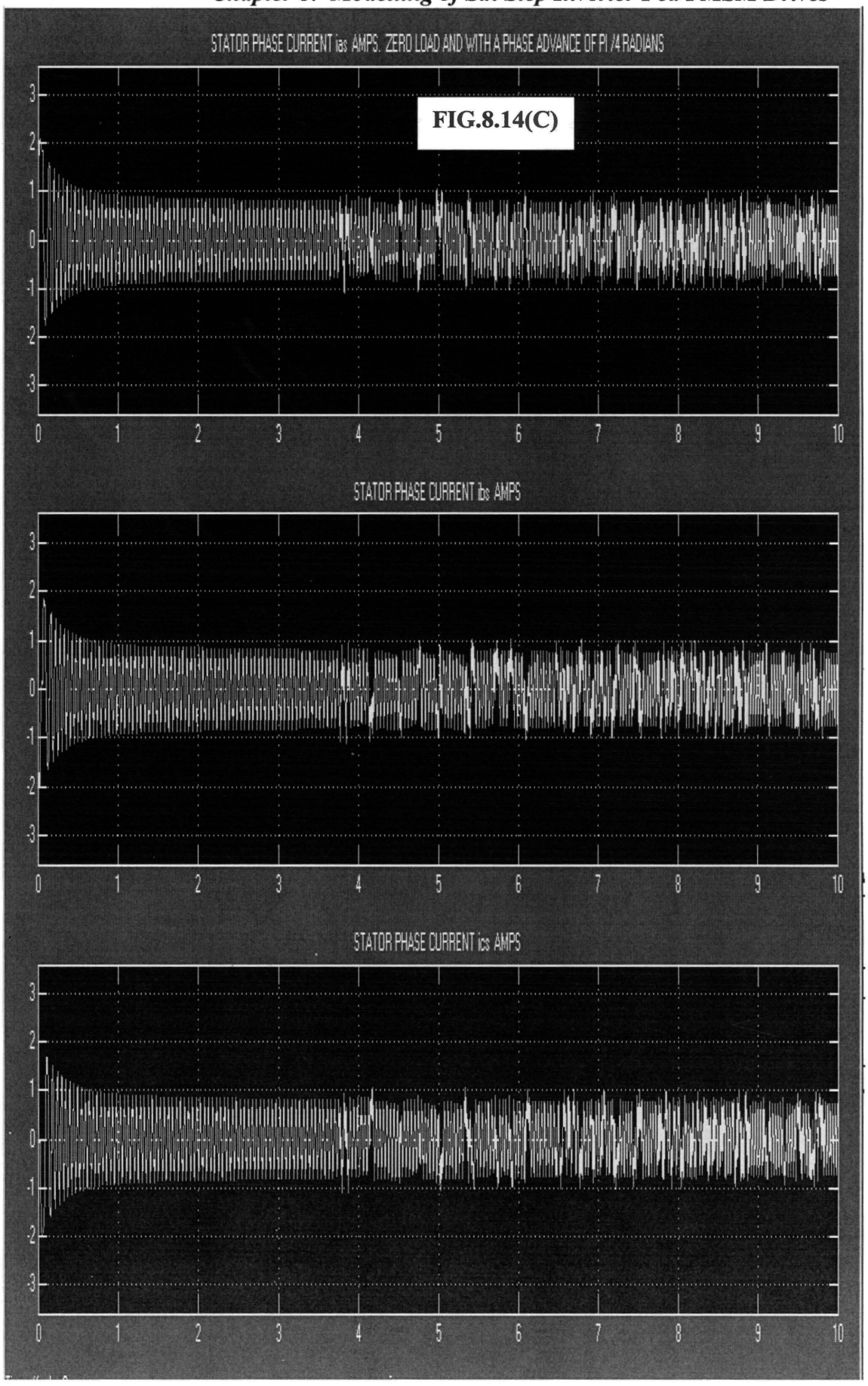
STATOR PHASE CURRENT ias AMPS. ZERO LOAD AND WITH A PHASE ADVANCE OF PI /4 RADIANS
FIG.8.14(C)
STATOR PHASE CURRENT ibs AMPS
STATOR PHASE CURRENT ics AMPS

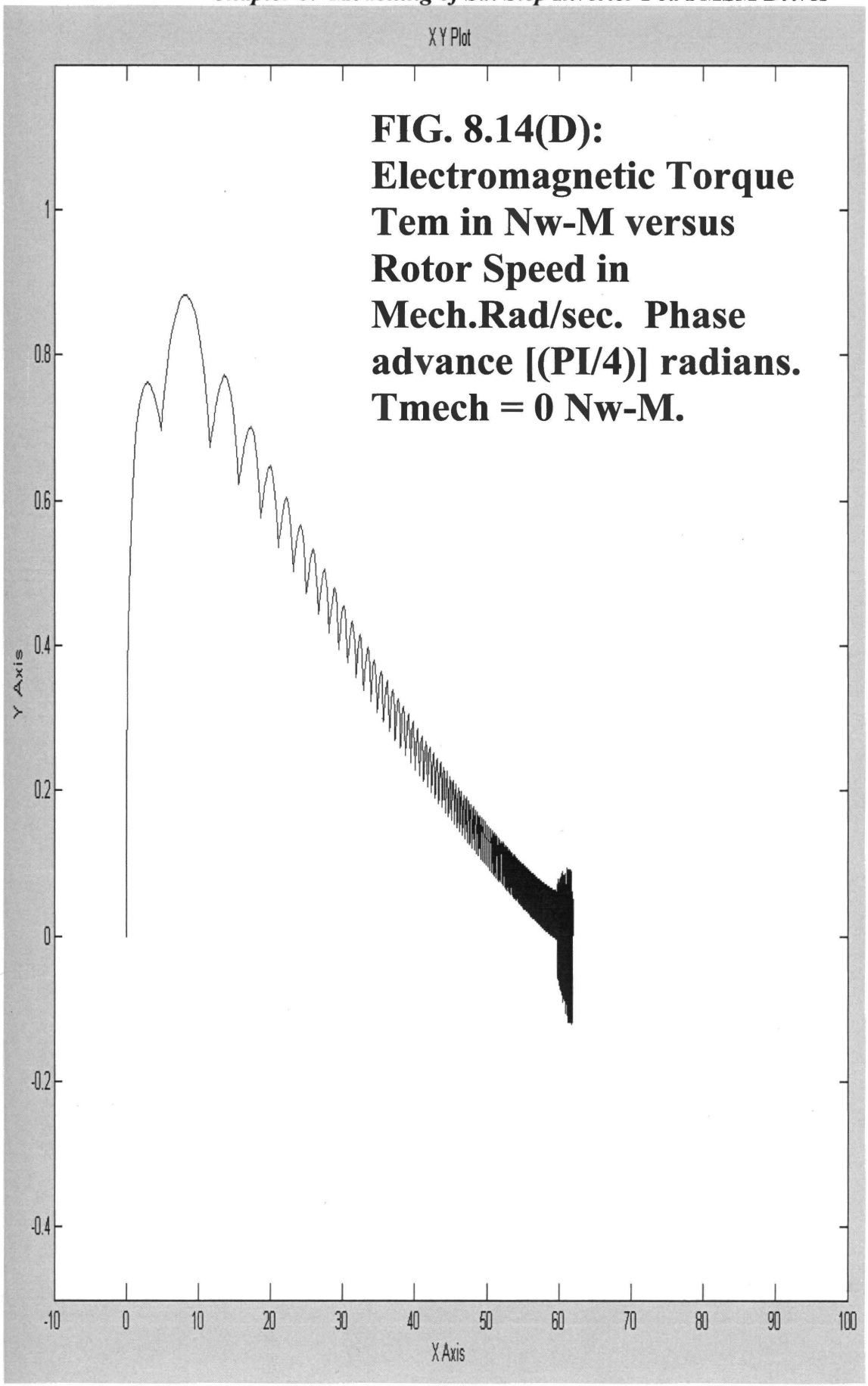

FIG. 8.14(D): Electromagnetic Torque Tem in Nw-M versus Rotor Speed in Mech.Rad/sec. Phase advance [(PI/4)] radians. Tmech = 0 Nw-M.

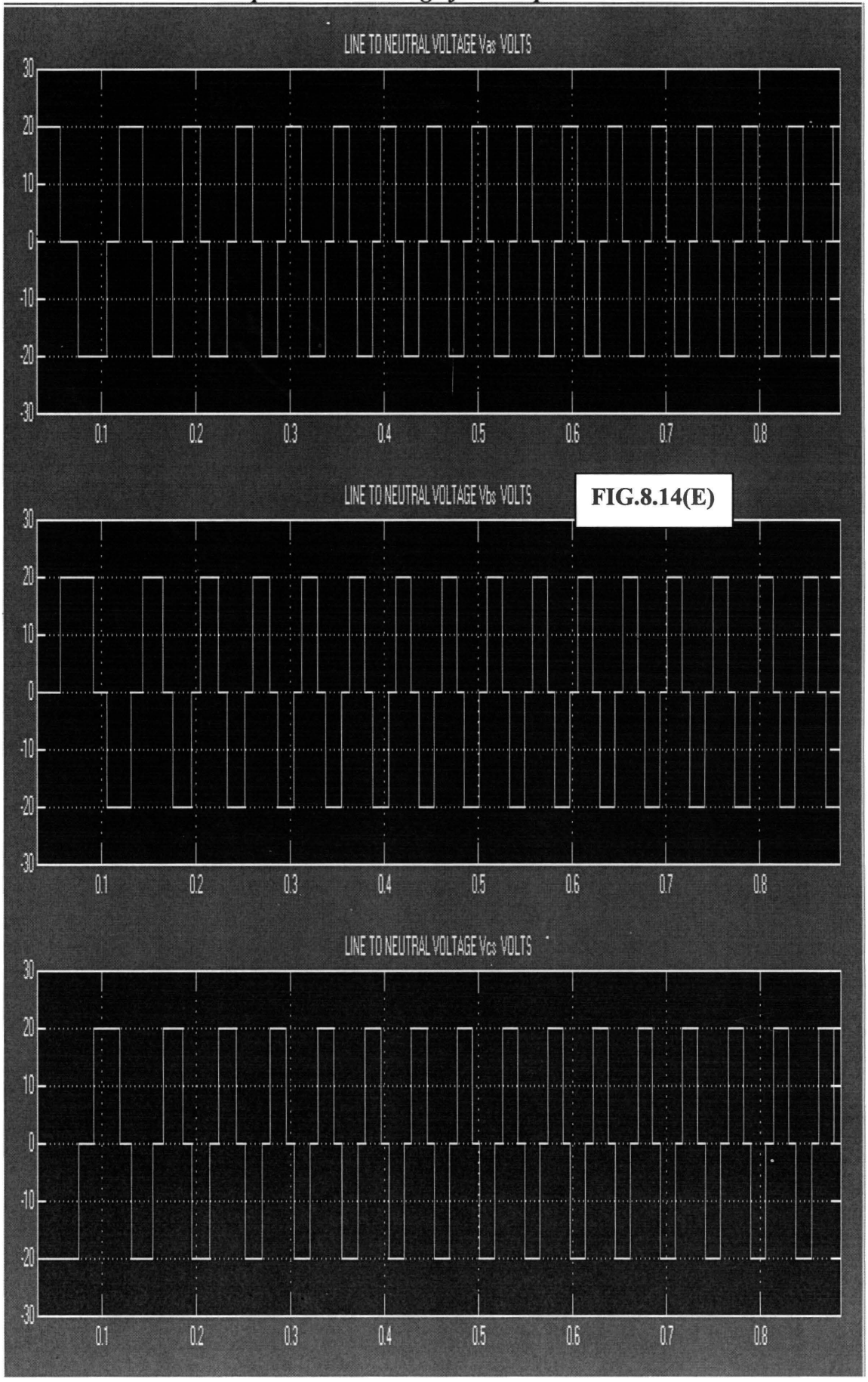
LINE TO NEUTRAL VOLTAGE Vas VOLTS
30
20
10
0
-10
-20
-30
0.1
0.2
0.3
0.4
0.5
0.6
0.7
0.8
LINE TO NEUTRAL VOLTAGE Vbs VOLTS
30
20
10
0
-10
-20
-30
0.1
0.2
0.3
0.4
0.5
0.6
0.7
0.8
LINE TO NEUTRAL VOLTAGE Vcs VOLTS
30
20
10
0
-10
-20
-30
0.1
0.2
0.3
0.4
0.5
0.6
0.7
0.8

FIG.8.14(E)

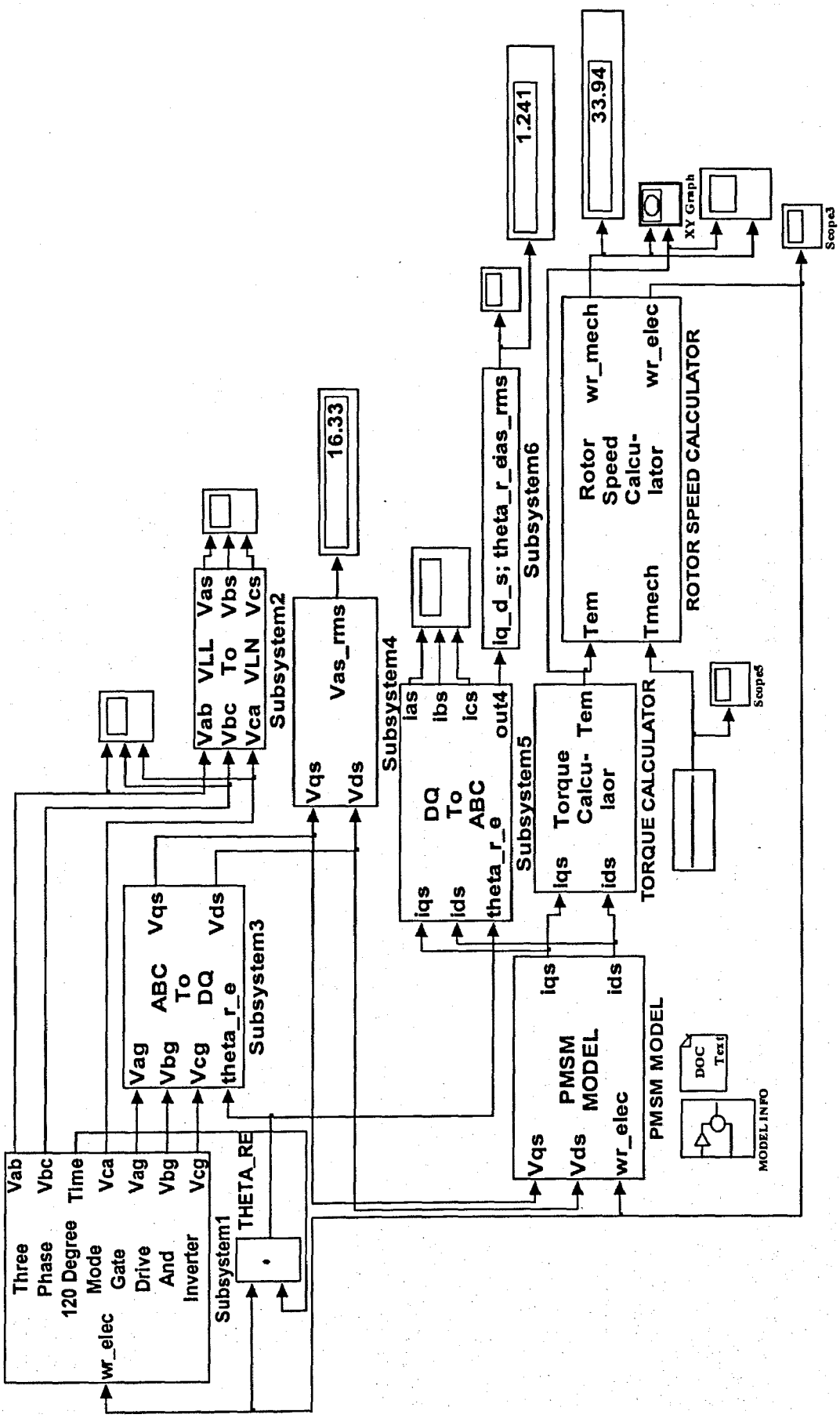

FIG.8.15: LYBOTEC SIX STEP INVERTER FED PMSM DRIVE - SECOND MODEL

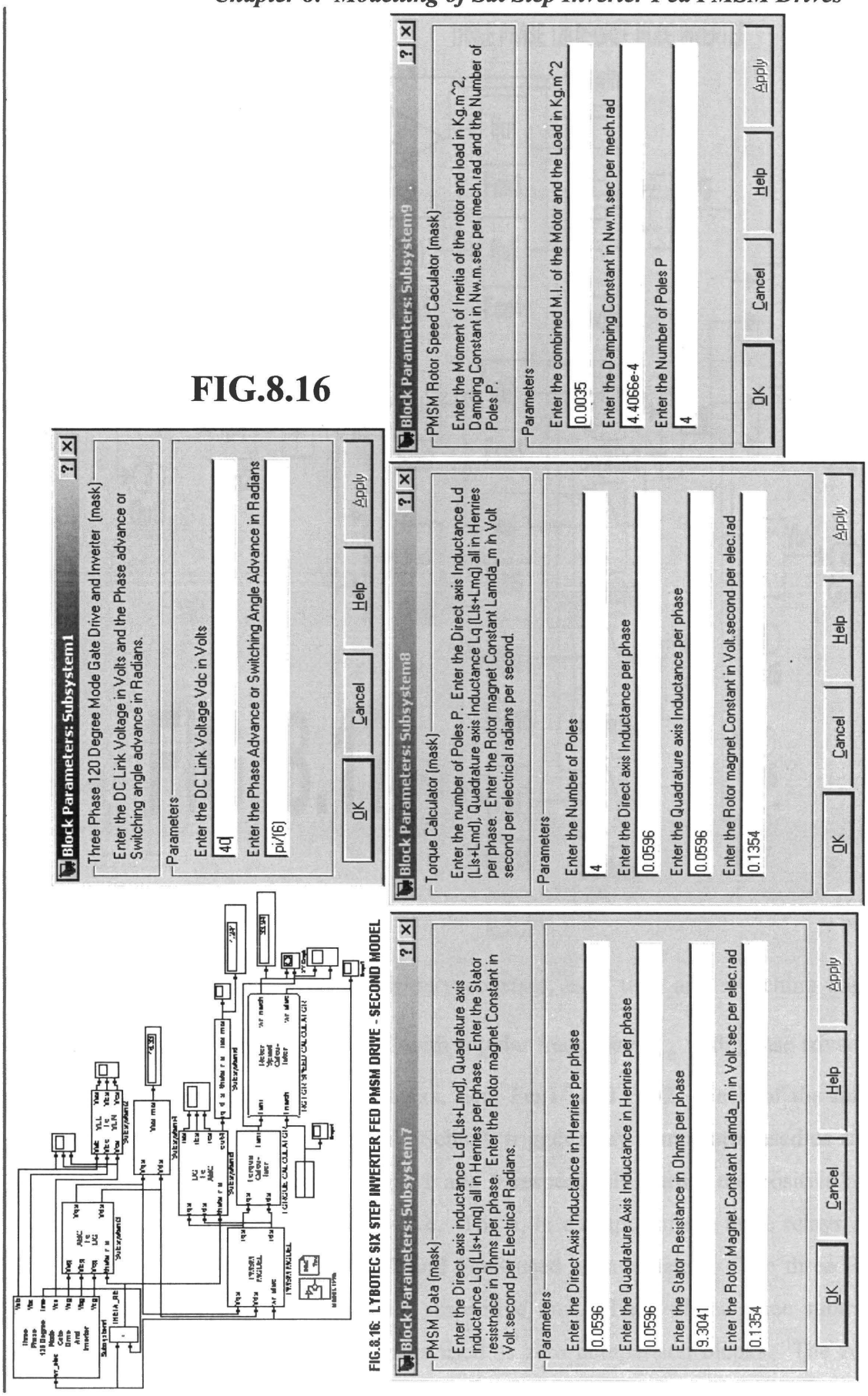

FIG.8.16: LYBOTEC SIX STEP INVERTER FED PMSM DRIVE - SECOND MODEL

FIG.8.16

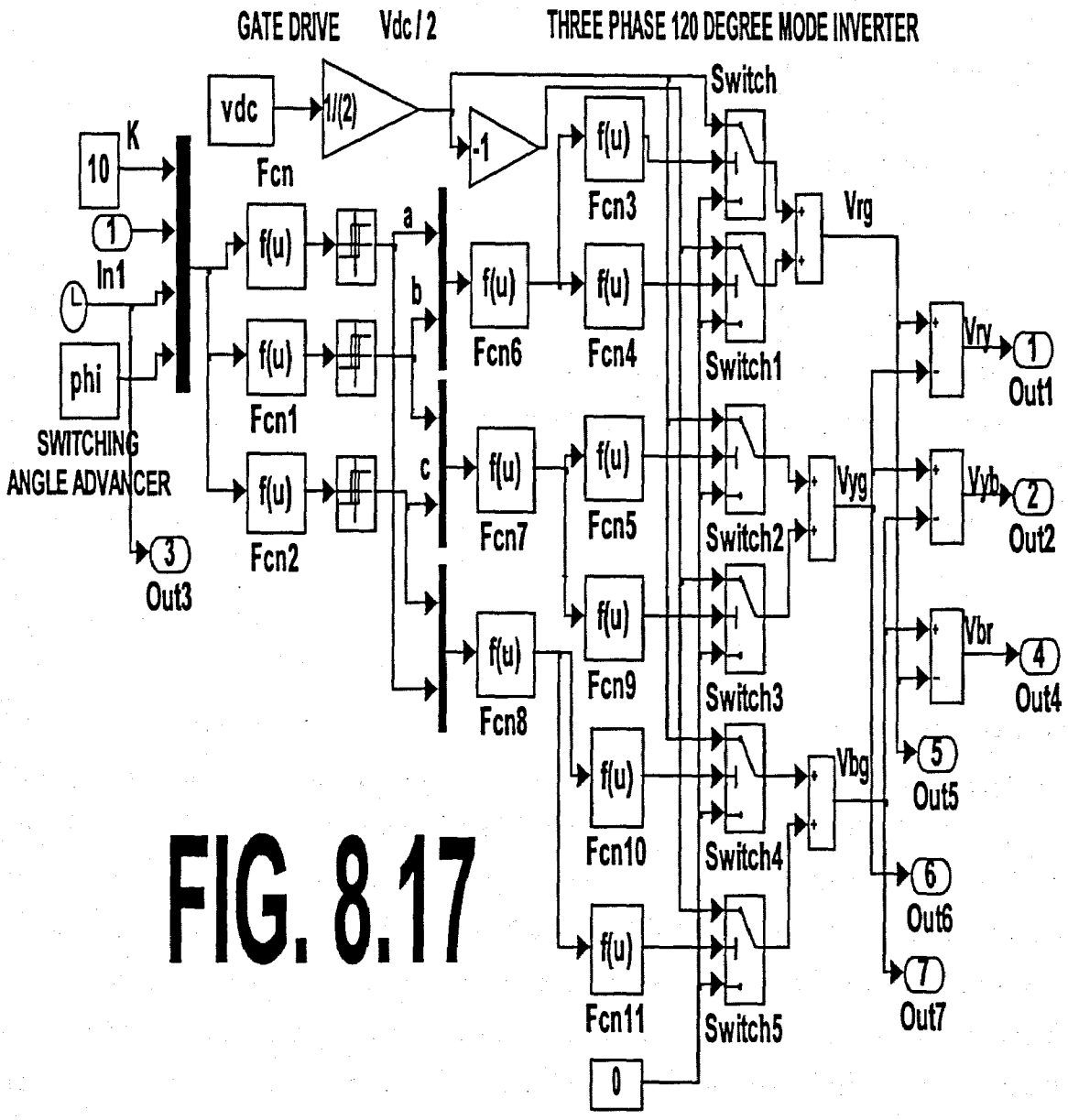

FIG. 8.17

The four input to the mux are the arbitrary constant, ω_{re}, time and switching angle advance. The three phase sine wave AC with angular frequency ω_{re} with phase advance added is generated using three Fcn blocks, Fcn, Fcn1 and Fcn2. Each of the three phase AC output are then compared in a Schmitt trigger relay comparator used as zero crossing comparators, with output logic 1 and 0 respectively during the positive and negative half cycle of the input sine wave. The a, b, c output of the three relays are given to three Fcn blocks, Fcn6, Fcn7 and Fcn8 used as subtractors. The three Fcn blocks subtracts the two inputs to their respective mux. Each of the three subtract blocks are given to a pair of Fcn blocks used as zero comparison blocks. The zero comparison block Fcn3 output logic 1 when the input u(1) is greater than zero, else

output logic 0. Similarly the Fcn4 block output logic 1 when u(1) is less than zero, else output logic 0. The same logic holds good for zero comparison block pairs Fcn5 – Fcn9 and Fcn10 – Fcn11. The output of Fcn3 and Fcn4 blocks are given to the u(2) input of two threshold switches marked Switch and Switch1. The u(1) input to Switch and Switch1 are +Vdc /2 and the u(3) input to Switch and Switch1 are zero. Both Switch and Switch1 output logic 1, when u(2) is greater than or equal to threshold value of 0.5, else the output of both these switches are the u(3) inputs. The same principle holds good for switch pairs Switch2 – Switch3 and Switch4 – Switch5. The output of respective switch pairs are given to SUM block to obtain the three phase line to ground voltages Vrg, Vyg and Vbg. These three line to ground voltages are given in pairs to SUBTRACT blocks to obtain the three phase line to line voltages Vry, Vyb and Vbr.

8.4.4 Simulation Results

The simulation was carried out using ode15s(stiff/NDF) solver. The data relating to the six step discontinuous current mode Lybotec Inverter fed PMSM drive is shown in Table 8.2. The simulation of this Lybotec inverter fed PMSM was carried out for phase advance of π /6 and π /4 electrical radians. These simulation results are compared with the experimentally observed results in the CEMPE laboratory. The simulation of torque, speed, torque-speed and line to neutral voltage of PMSM are shown in Fig.8.18(A) to (E) for a phase advance of π /6 radians. The same simulation results for a phase advance of π /4 radians is shown in Fig.8.19(A) to (E). Also in both cases the recorded value of the R.M.S. Line to Neutral voltage of the PMSM was found to be 16.33 volts, which corresponds to Vdc /$\sqrt{6}$ volts. This derivation is given in equation 4.32 in Chapter 4. Vdc is the DC Link voltage.

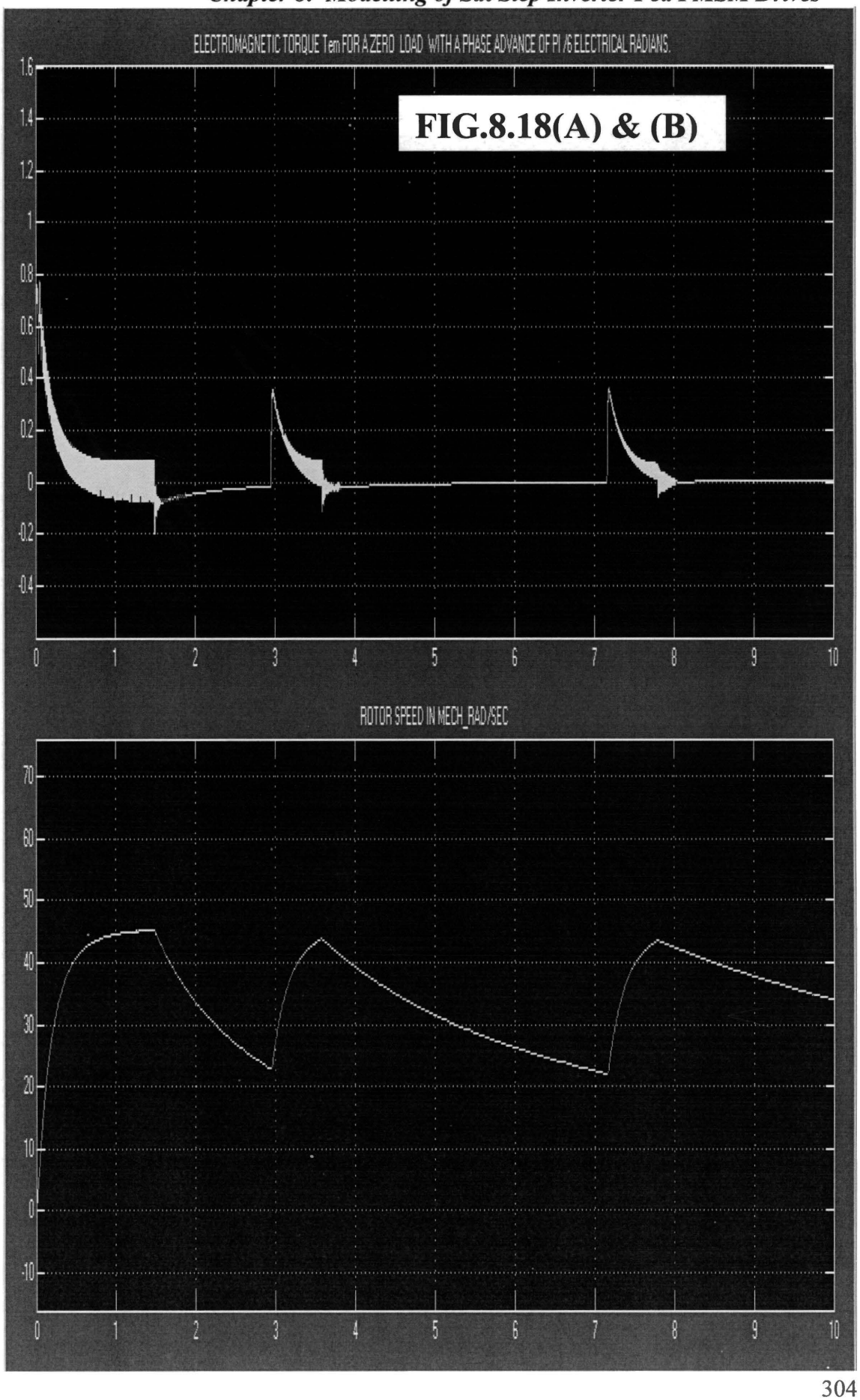
ELECTROMAGNETIC TORQUE Tem FOR A ZERO LOAD WITH A PHASE ADVANCE OF PI /6 ELECTRICAL RADIANS.
1.6
1.4
1.2
1
0.8
0.6
0.4
0.2
0
-0.2
-0.4
0 1 2 3 4 5 6 7 8 9 10
ROTOR SPEED IN MECH_RAD/SEC
70
60
50
40
30
20
10
0
-10
0 1 2 3 4 5 6 7 8 9 10

FIG.8.18(A) & (B)

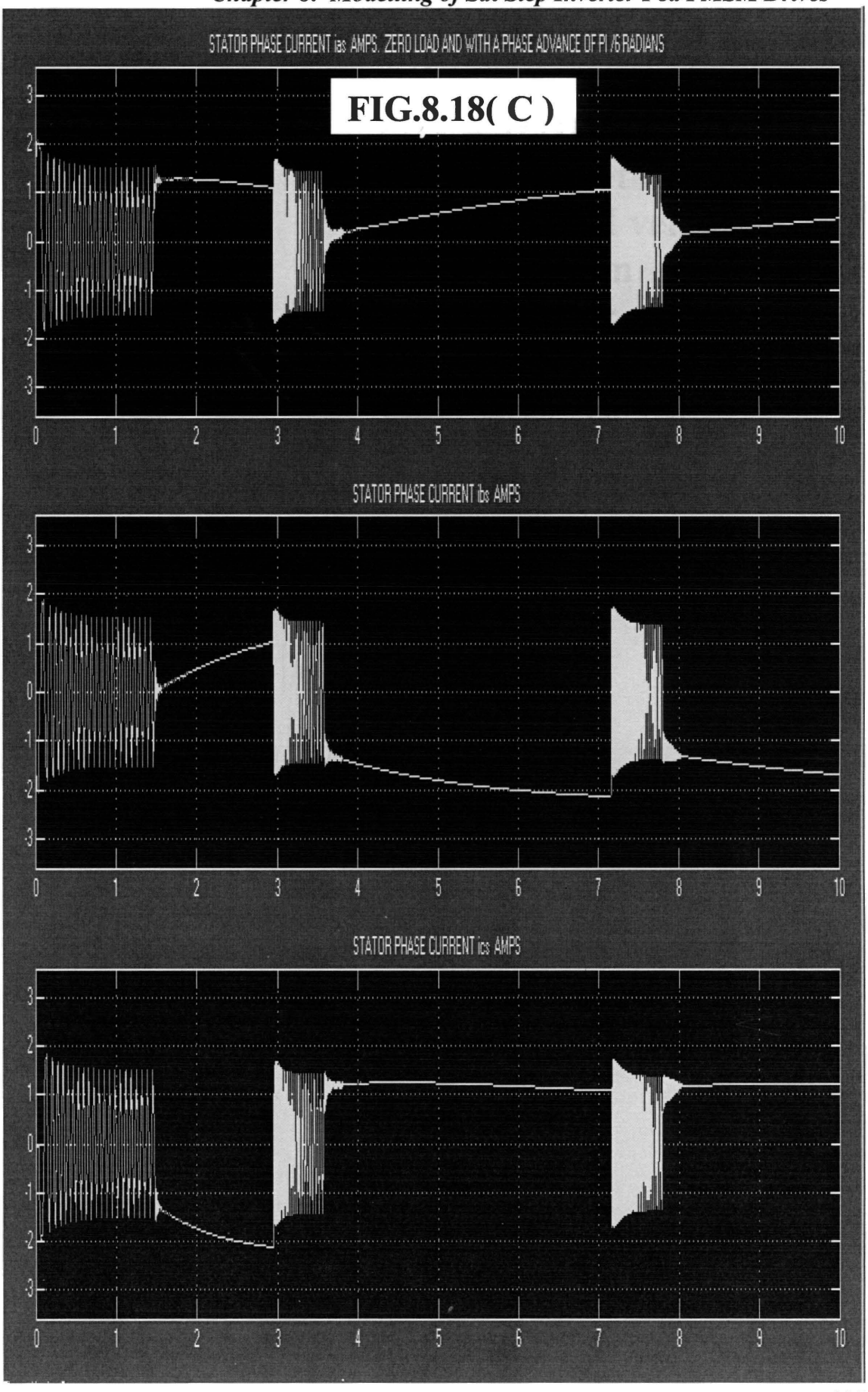
STATOR PHASE CURRENT ias AMPS. ZERO LOAD AND WITH A PHASE ADVANCE OF PI /6 RADIANS
FIG.8.18(C)
STATOR PHASE CURRENT ibs AMPS
STATOR PHASE CURRENT ics AMPS

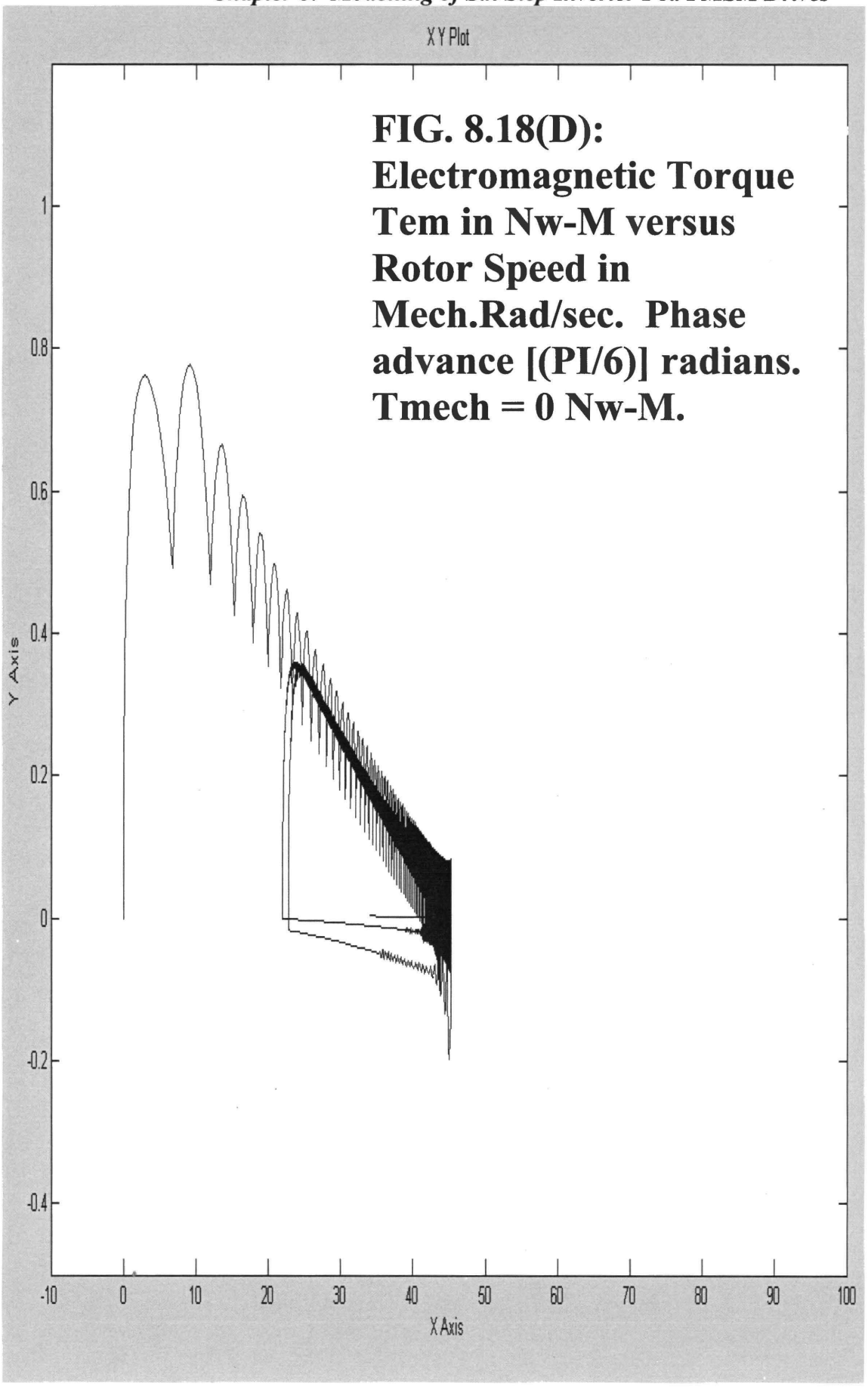

FIG. 8.18(D): Electromagnetic Torque Tem in Nw-M versus Rotor Speed in Mech.Rad/sec. Phase advance [(PI/6)] radians. Tmech = 0 Nw-M.

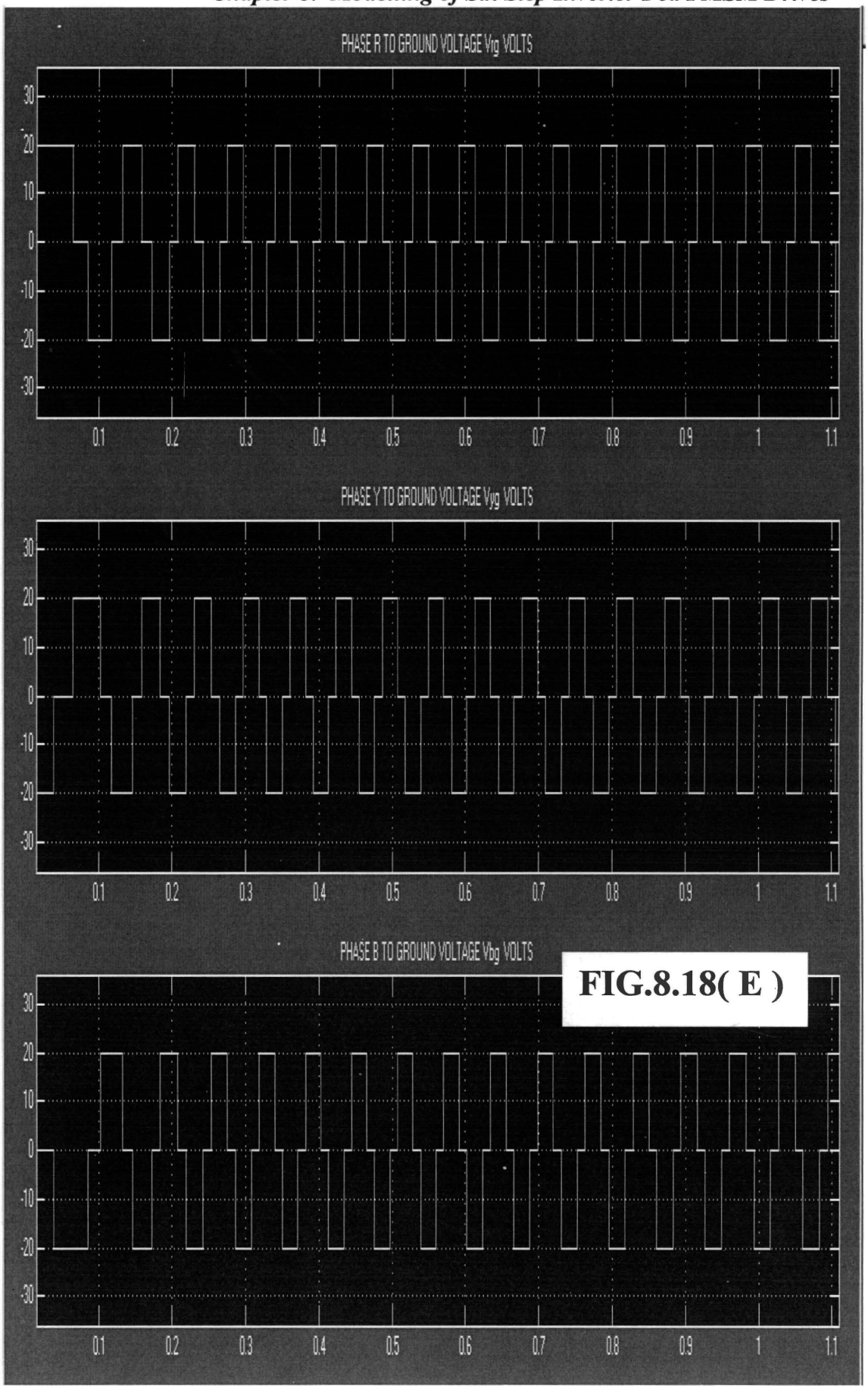
PHASE R TO GROUND VOLTAGE Vrg VOLTS
30
20
10
0
-10
-20
-30
0.1
0.2
0.3
0.4
0.5
0.6
0.7
0.8
0.9
1
1.1
PHASE Y TO GROUND VOLTAGE Vyg VOLTS
30
20
10
0
-10
-20
-30
0.1
0.2
0.3
0.4
0.5
0.6
0.7
0.8
0.9
1
1.1
PHASE B TO GROUND VOLTAGE Vbg VOLTS
30
20
10
0
-10
-20
-30
0.1
0.2
0.3
0.4
0.5
0.6
0.7
0.8
0.9
1
1.1

FIG.8.18(E)

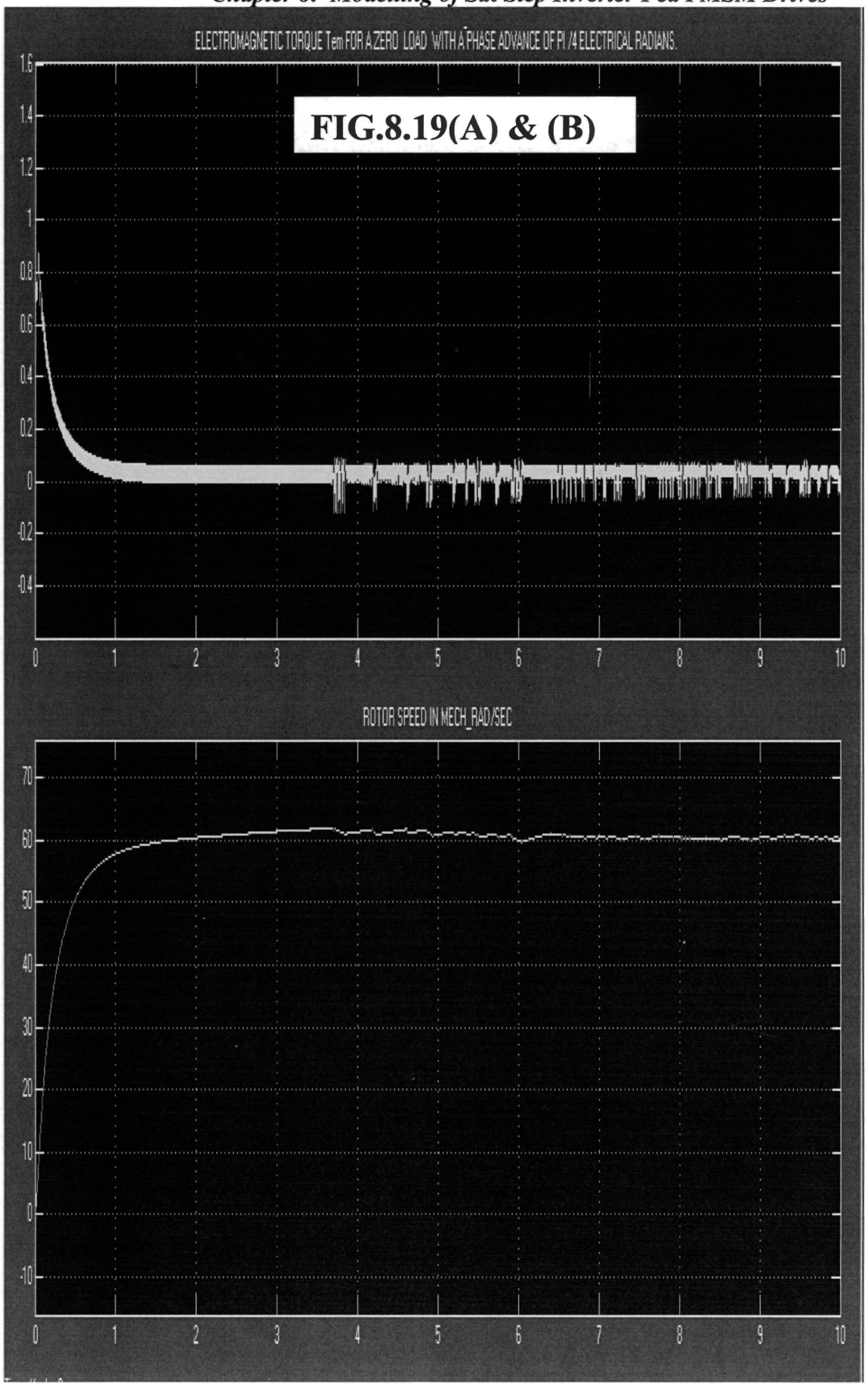
ELECTROMAGNETIC TORQUE Tem FOR A ZERO LOAD WITH A PHASE ADVANCE OF PI /4 ELECTRICAL RADIANS.
1.6
1.4
1.2
1
0.8
0.6
0.4
0.2
0
-0.2
-0.4
0 1 2 3 4 5 6 7 8 9 10
ROTOR SPEED IN MECH_RAD/SEC
70
60
50
40
30
20
10
0
-10
0 1 2 3 4 5 6 7 8 9 10

FIG.8.19(A) & (B)

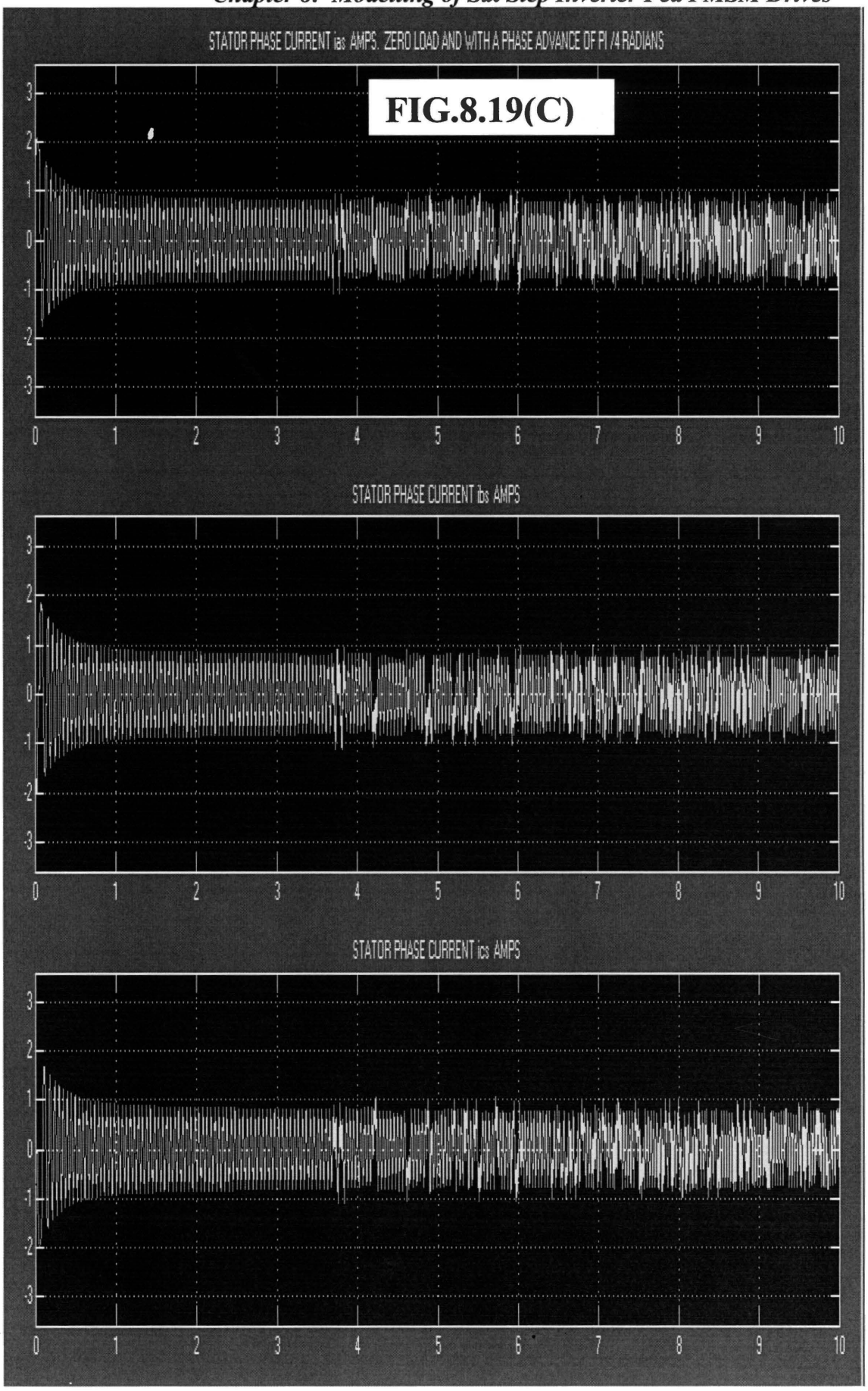
STATOR PHASE CURRENT ias AMPS. ZERO LOAD AND WITH A PHASE ADVANCE OF PI /4 RADIANS
FIG.8.19(C)
STATOR PHASE CURRENT ibs AMPS
STATOR PHASE CURRENT ics AMPS

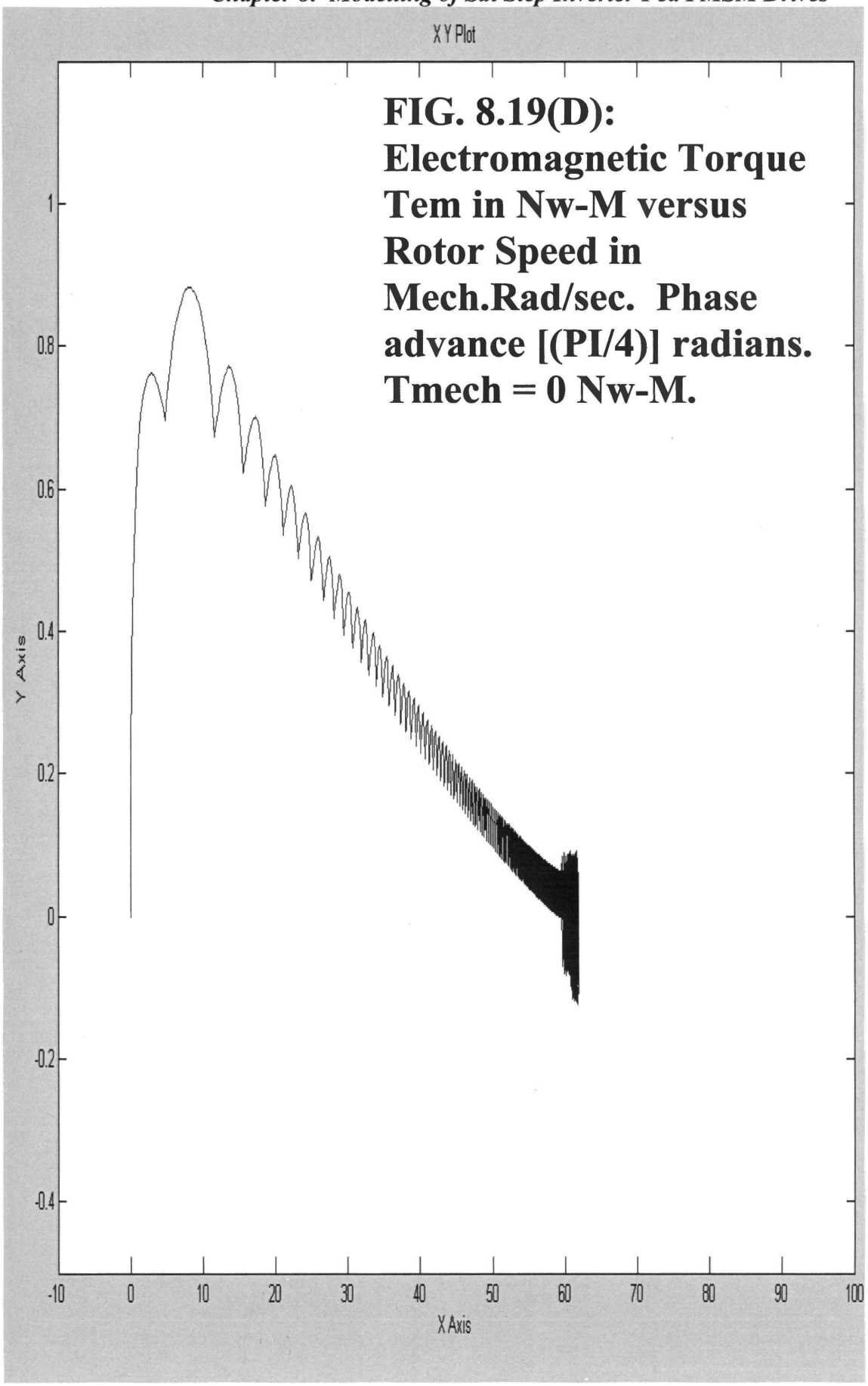

FIG. 8.19(D): Electromagnetic Torque Tem in Nw-M versus Rotor Speed in Mech.Rad/sec. Phase advance [(PI/4)] radians. Tmech = 0 Nw-M.

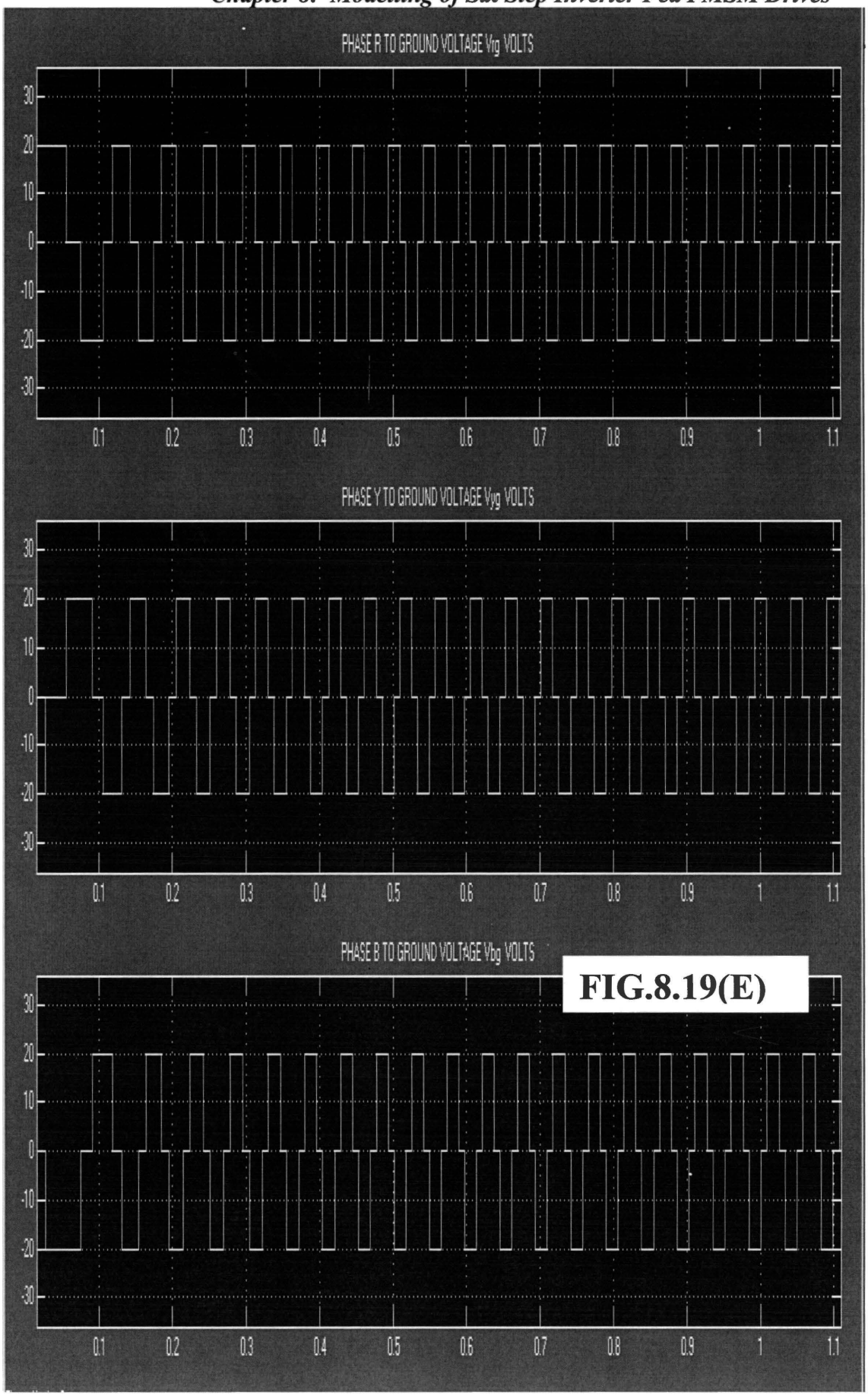
PHASE R TO GROUND VOLTAGE Vrg VOLTS
30
20
10
0
-10
-20
-30
0.1
0.2
0.3
0.4
0.5
0.6
0.7
0.8
0.9
1
1.1
PHASE Y TO GROUND VOLTAGE Vyg VOLTS
30
20
10
0
-10
-20
-30
0.1
0.2
0.3
0.4
0.5
0.6
0.7
0.8
0.9
1
1.1
PHASE B TO GROUND VOLTAGE Vbg VOLTS
30
20
10
0
-10
-20
-30
0.1
0.2
0.3
0.4
0.5
0.6
0.7
0.8
0.9
1
1.1

FIG.8.19(E)

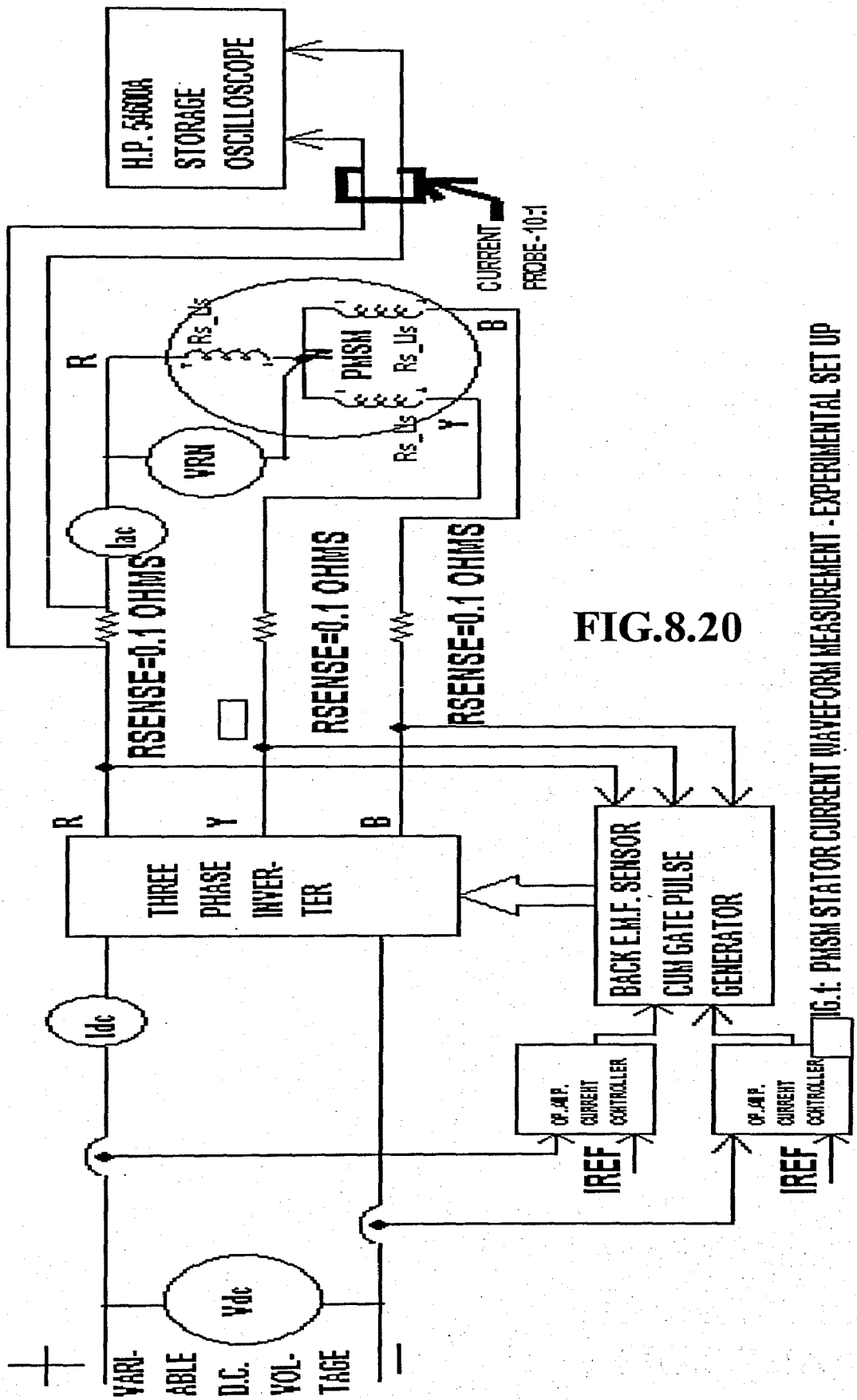

FIG.8.20

IG.1: PMSM STATOR CURRENT WAVEFORM MEASUREMENT - EXPERIMENTAL SET UP

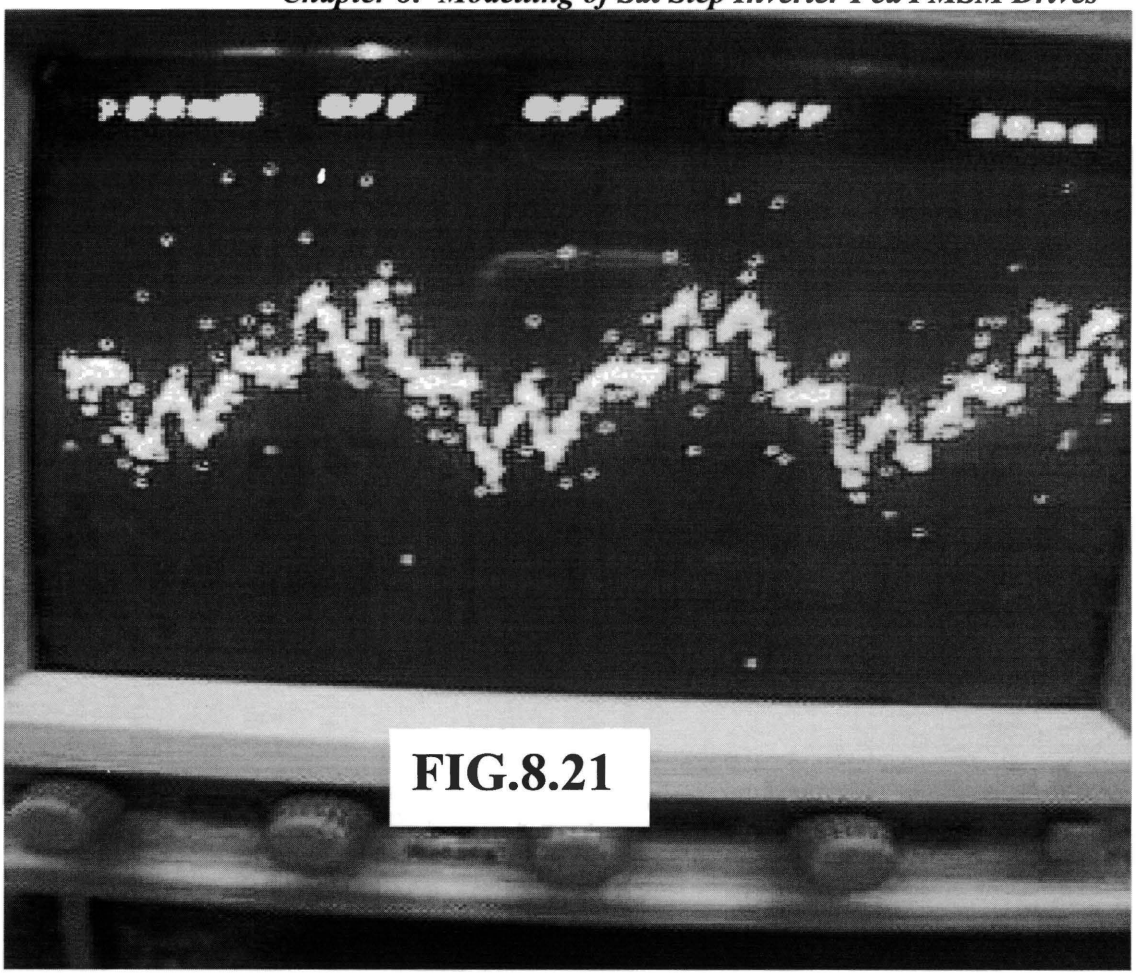

FIG.8.21

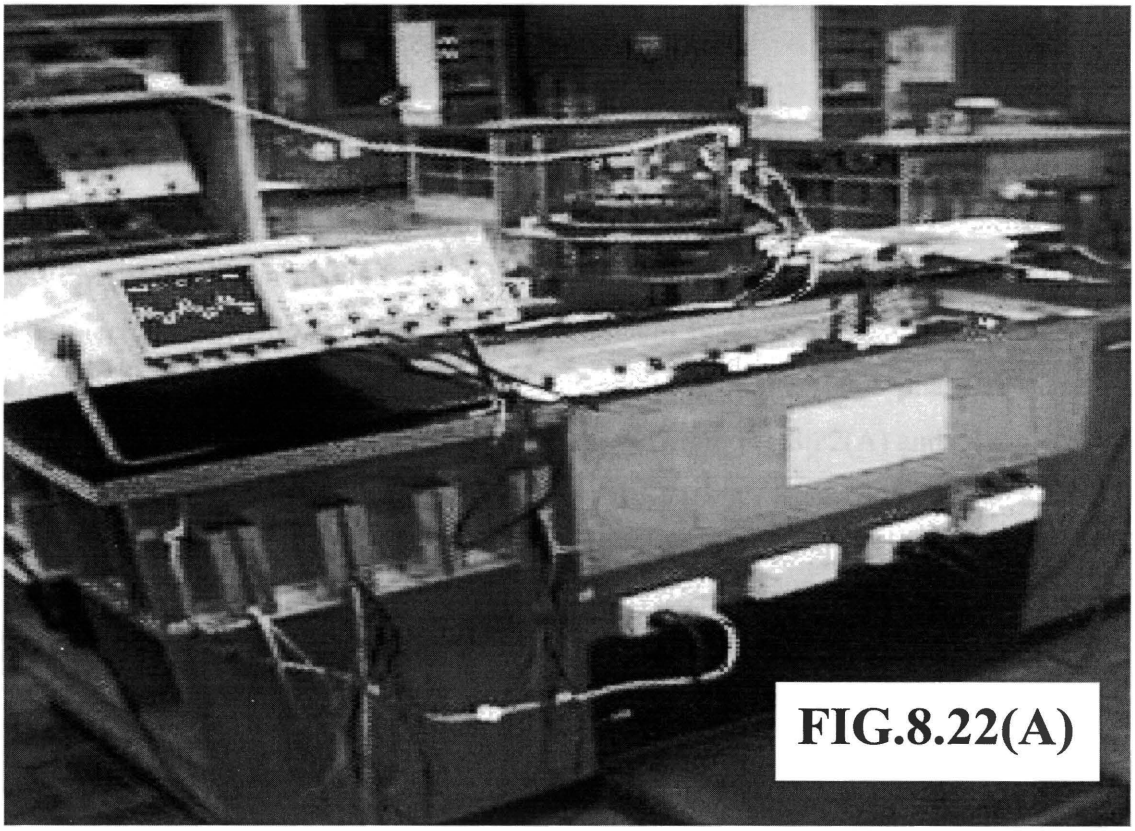

FIG.8.22(A)

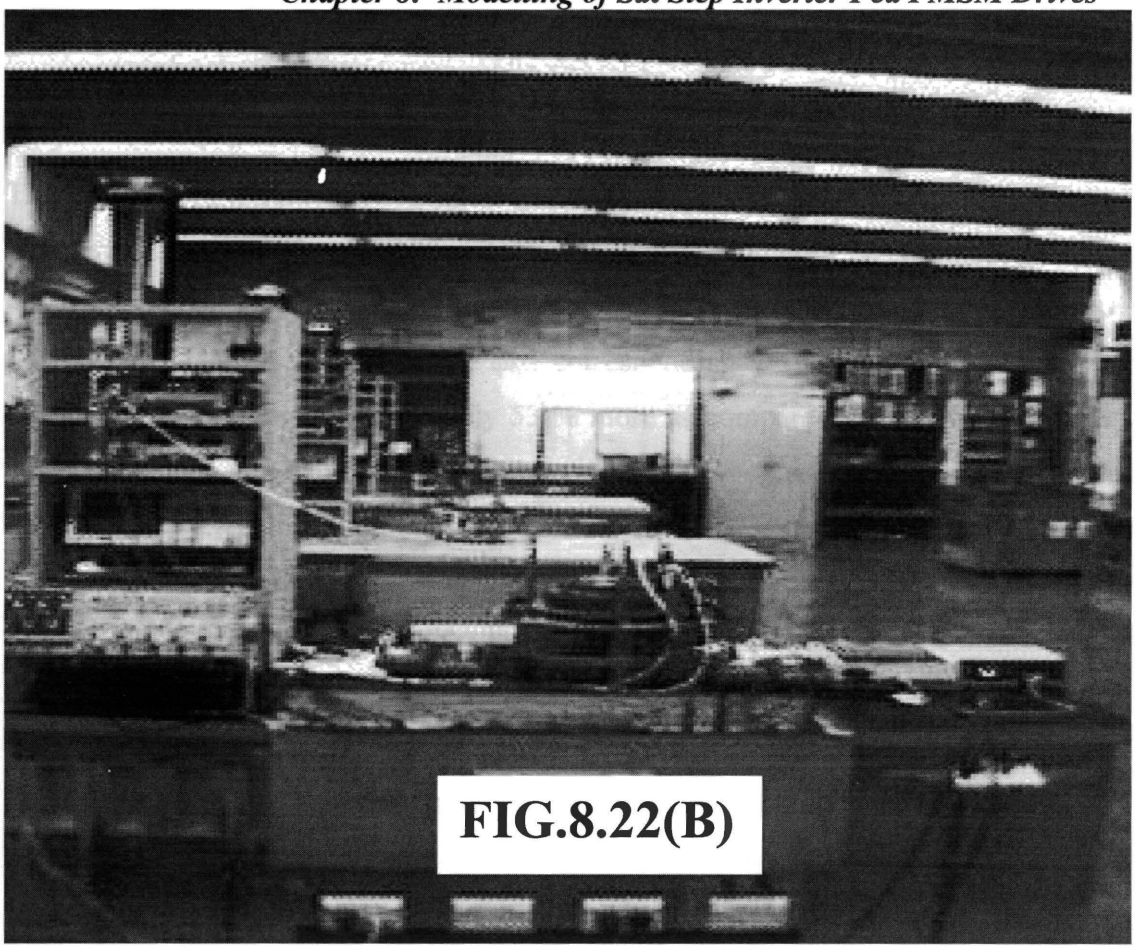

8.5 Experimental Results

The performance of the Lybotec Six Step Inverter was experimentally verified in the CEMPE Laboratories. The experimental connection of the Six step Lybotec Inverter fed PMSM is shown in Fig.8.20. The DC Link Voltage was maintained at 40 Volts. The mechanical load was zero. The experimental readings observed are tabulated as shown in TABLE 8.3. The oscilloscope waveform of the stator phase A current is shown in Fig.8.21. The experimental set up is shown in Fig.8.22(A) and (B).

TABLE 8.3: EXPERIMENTAL OBSERVATION

Sl.No.	Vdc Volts	Idc Amps	Vrn or Vs Volts	Iac Amps	Speed rpm	Speed mech. rad per sec.	Tmech Nw.m
1	40	0.044	17.09	0.042	517	54	0

8.6 Conclusions

The well known unique relationship connecting phase advance to be given to this three phase 180 degree mode inverter switching to obtain maximum electromagnetic torque given by equation 8.20 for a given rotor speed was successfully verified using SIMULINK.. With phase advance φ_{MT} corresponding to maximum torque, it is seen that the rotor torque is approximately 53 % more as compared to NO additional phase advance i.e. phase advance maintained at $\pi/2$ radians. This agree with the literature reference [29]. The simulation of the six step 180 degree mode inverter fed PMSM is also compared by simulation using the built in three phase MOSFET inverter and the PMSM blocks in the SimPowerSystems block set of SIMULINK and the results are given in Appendix E.

For the three phase 120 degree mode inverter, two models were developed. The performance of both the models are identically the same as can be seen from the waveforms in Fig.8.13(A) to Fig.8.14(E) and in Fig.8.18(A) to Fig.8.18(E). The simulated speed with (pi /4) phase advance closely agree with the experimental speed shown in Table 8.3. The peak value of the current in Fig.8.21 is 280 milliamps, while that by simulation for a phase advance of pi /4 radians is different from this value. The current comparison is difficult as the Lybotec inverter uses op.amp current comparators and current limit switches which are NOT incorporated in the above model. More over the hysteresis bandwidth, the exact transfer function of the current controller and also the exact phase advance given to Lybotec Six Step Inverter are unknown. These factors prevent comparison of the stator current waveform by simulation and by experiment. The experimentally observed line to neutral voltage of PMSM is almost close to Vdc /$\sqrt{6}$ Volts. Hence the Lybotec six step inverter must be operating the 120 degree mode.

CHAPTER 9
MODELLING OF A DIGITAL SWITCHING FUNCTION GENERATOR FOR A THREE PHASE VOLTAGE SOURCE INVERTER

9.1 Introduction

The 180 degree mode gate drive pattern for three phase voltage source inverter was shown in Fig.2.6(A) and discussed in detail in Chapter 2. Referring to this figure and the three phase VSI shown in Fig.2.2, the switch functions a, b and c are the 180 degree mode gate drive pattern for switches S1, S3 and S5. This switch function concept was used to model the three phase 180 degree mode voltage source inverter (VSI), discussed in section 4.2 in Chapter 4. The gate drive for three phase VSI is developed using op.amps, Microprocessors/Microcontrollers, EPROM and so on. In this Chapter, the development of a digital switching function generator for a three phase 180 degree mode inverter using the Four Line to One Line Multiplexer (SN74LS153) is presented. Experimental verification of this switching function generator and the pattern of the waveforms obtained are also given. Electronic circuit model for this switching function generator is developed both by using PSPICE and SIMULINK. The results of this switching function pattern obtained by simulation and experiment are compared.

9.2 Digital Switching Function generator Design

The design of this switching function generator using four line to one line multiplexer (SN74LS153) is presented in this section. The block diagram schematic of this digital switching function generator is shown in Fig.2.7(B) in Chapter 2. Referring to Fig.2.7(B), the various units are 1) Clock 2) Modulo six counter 3) Four Line to one line multiplexer and 4) NOT gates. These are explained below:

9.2.1 Clock

The clock is a square pulse generator compatible with TTL I.Cs, with a peak value of +5 volts. This is usually built with crystals along with binary counters to reduce the frequency to the required value. For the purpose of experimental verification in the laboratory, an IC 555 timer wired as an astable multivibrator was used. The clock frequency f_C is selected six times the inverter switching frequency. In this experiment f_C was set to 360 Hertz. A 360 Hertz clock using IC 555 timer is shown in Fig.2.

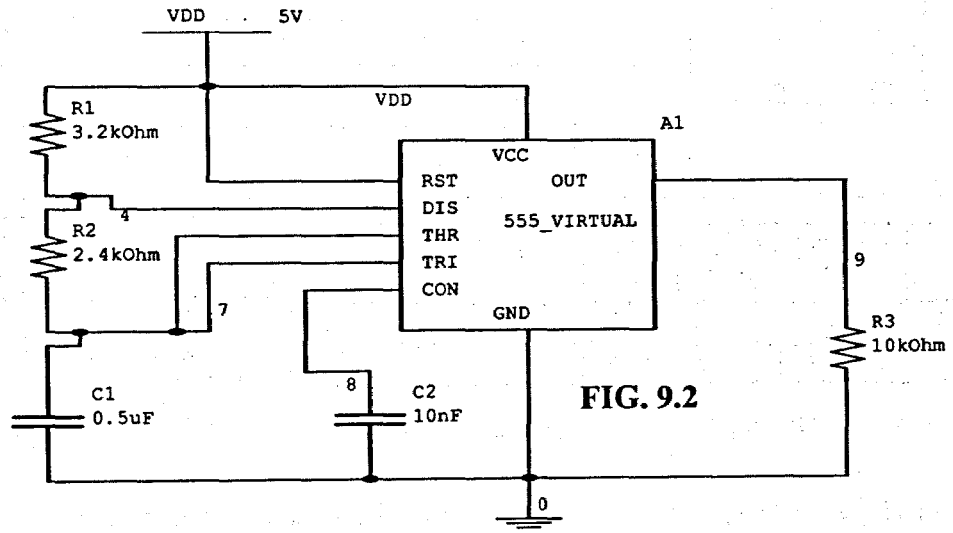

FIG. 9.2

Referring to Fig.9.2, the clock frequency f_C is given by the formula given in equation 9.1 below:

$$f_C = \frac{1.44}{(R_1 + 2R_2)C_1} \qquad (9.1)$$

The Values of R1, R2 and C1 chosen are respectively 3.2 Kilohms, 2.4 Kilohms and 0.5 microfarads.

9.2.2 Modulo Six Counter

The modulo six counter counts up from 0 to 5 in continuous sequence. This is developed using D type flip-flops. The truth table for the design of the modulo six counter to count up from 0 to 5 continuously is shown in Table 1. The C digit is the MSB and A is the LSB. The control inputs Dc, Db and Da to the three D flip-flops are shown

in Table 9.1. The control inputs to the three D flip-flops are derived using Karnaugh maps, shown in Fig.9.2(A), (B) and (C).

TABLE 9.1: MODULO SIX COUNTER DESIGN USING D FLIP-FLOP

PRESENT STATE			NEXT STATE			Dc	Db	Da
C	B	A	C	B	A			
0	0	0	0	0	1	Σm(3,4) + d(6,7) Dc = A.B + C./A	Σm(1,2) + d(6,7) Db = /C.B.A + /A.B	Σm(0,2,4) + d(6,7) Da = /A
0	0	1	0	1	0			
0	1	0	0	1	1			
0	1	1	1	0	0			
1	0	0	1	0	1			
1	0	1	0	0	0			

C \ BA	00	01	11	10
0	0	0	1	0
1	1	0	X	X

Fig.9.2(A): D_C Map

C \ BA	00	01	11	10
0	0	1	0	1
1	0	0	X	X

Fig.9.2(B): D_B Map

C \ BA	00	01	11	10
0	1	0	0	1
1	1	0	X	X

Fig.9.2(C): D_A Map

The control inputs to the D flip- control inputs to the D flops C, B and A are given below:

$$D_C = A.B + C.\overline{A}$$

$$D_B = A.\overline{B}.\overline{C} + B.\overline{A} \qquad (9.2)$$

$$D_A = \overline{A}$$

9.2.3 Four Line to One Line Multiplexer

The four line to one line mux (SN74153) is used to design the switching function generator. The K-maps for developing the switching functions a, b and c are shown in Fig.9.3(A), (B) and (C) respectively. Referring to Fig.9.3(A), (B) and (C), letting B A as the select inputs to the mux, an expression for the external input C can be derived

C \ BA	00	01	11	10
0	1	1	0	1
1	0	0	X	X

Fig.9.3(A): S1 Map

C \ BA	00	01	11	10
0	0	0	1	1
1	1	0	X	X

Fig.9.3(B): S3 Map

C \ BA	00	01	11	10
0	1	0	0	0
1	1	1	X	X

Fig.9.3(C): S5 Map

Gate Drive TABLE 9.2	Minterms	External function input For select inputs B A			
		00	01	10	11
VG1	Σm(0, 1, 2)	/C	/C	/C	C
VG2	Σm(2, 3, 4)	C	0	/C	/C
VG3	Σm(4, 5, 0)	1	C	C	C

as shown in Table 2 to realize the switching functions a, b and c. In Table 9.2, VG1, VG2 and VG3 are the gate drive to switches S1, S3 and S5 in Fig.2.2 of Chapter 2, which are also the switching functions a, b and c.

9.3 Various Models for the Digital Switching Function Generator

The circuit models for the digital switching function generator using the four line to one line multiplexer was developed using both PSPICE and SIMULINK. The inverted switching functions /a, /b and /c are the respective gate drive for the bottom row of switches S4, S6 and S2 in Fig.2.2 of Chapter 2. In the PSPICE model, all these six switching functions were observed by simulation. The line to line and the line to neutral voltages of the three phase inverter could NOT be observed due to node limitations for the demo version of software PSPICE. In SIMULINK, the line to line and line to neutral voltages were observed for a three phase voltage source inverter developed using the MOSFETs in the SimPowerSystems block set. These are discussed in the following sections.

9.3.1 PSPICE Model of the Digital Switching Function Generator

The PSPICE circuit model of the digital switching function generator along with the three phase voltage source inverter is shown in Fig.9.4. The clock to generate 360 Hz is derived using DigClock in PSPICE. The parameters for the DigClock are set to DELAY = 0m, ONTIME = 1.385m and OFFTIME = 1.385m respectively. The modulo six counter to count from 0 to 5 in continuous up sequence is developed using positive edge triggered D flip-flops SN7474. The two four line to one line mux are using SN74153. The control inputs to the three D flip-flops given by equation 9.2 are derived using two input AND (7408) gates, three input AND (7411) gates and the two input OR (7432) gates. The control input to the A flip-flop is derived from its inverted output. The switching functions a, b and c are derived using two dual four line to one line multiplexer SN74153, as per the truth table shown in Fig.9.3(A), (B) and (C) respectively. The outputs B and A of modulo six counter are used as select inputs to these two multiplexers. The output C and /C of flip-flop C of modulo six counter along with 0 and 1 are given as external inputs to these two multiplexers to realize the minterms (switching functions) shown in TABLE 2.

9.3.2 Simulation Results

The simulation results for the clock output CLK, Modulo six counter output C, B, A, switching functions a, b, c with outputs marked SWFCN_A, SWFCN_B, SWFCN_C and the inverted switching functions /a, /b and /c with outputs marked FCN_ABAR, FCN_BBAR and FCN_CBAR, using the circuit model of PSPICE is shown in Fig.9.5.

9.3.3 Model of the Digital Switching Function Generator

The interactive circuit model of the digital switching function generator and its dialog box are shown in Fig.9.6(A) and (B) respectively. The subsystem clock, modulo six counter and four line to one line multiplexer are shown in Fig.9.7(A). The subsystem is explained below:

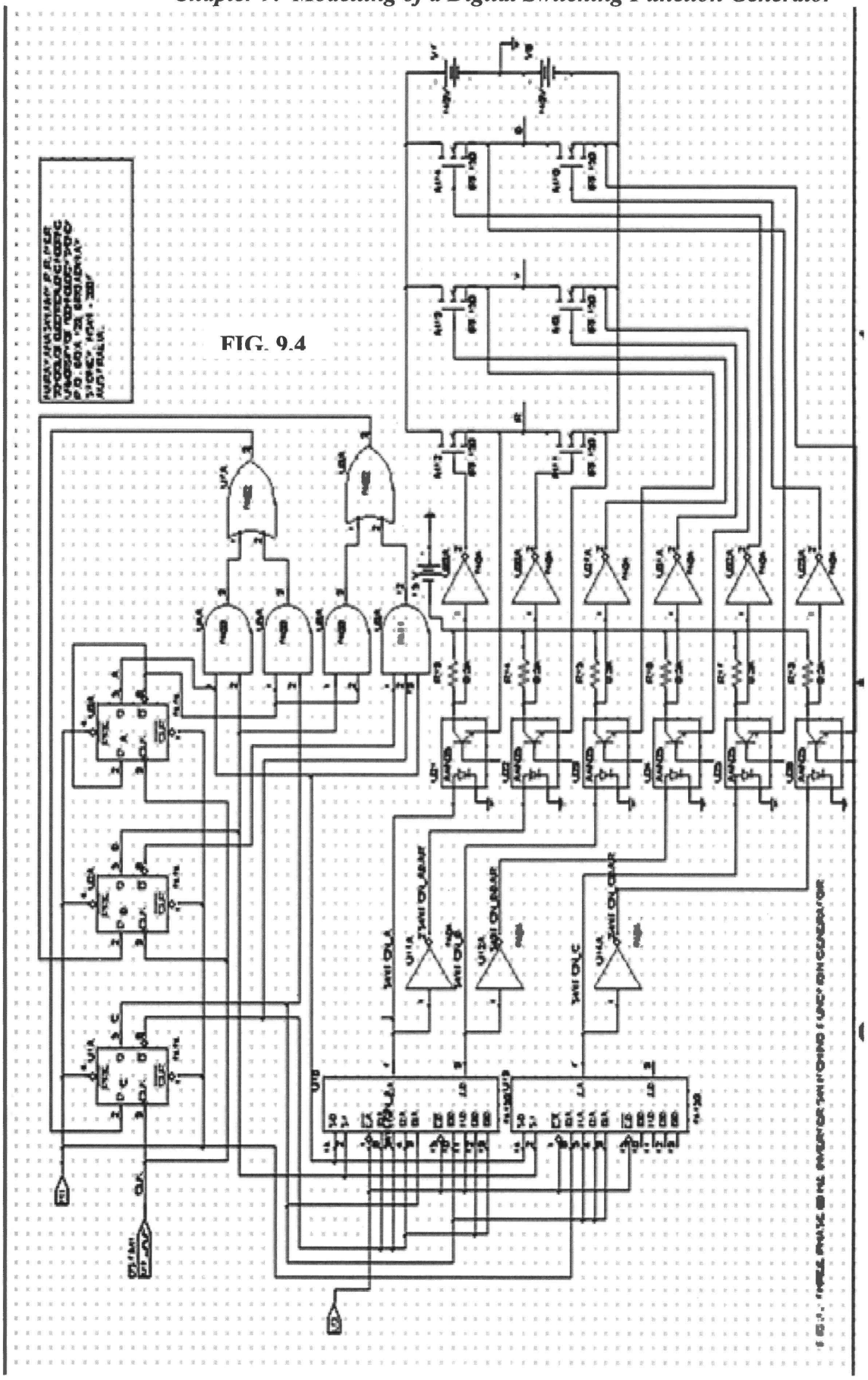

FIG. 9.4

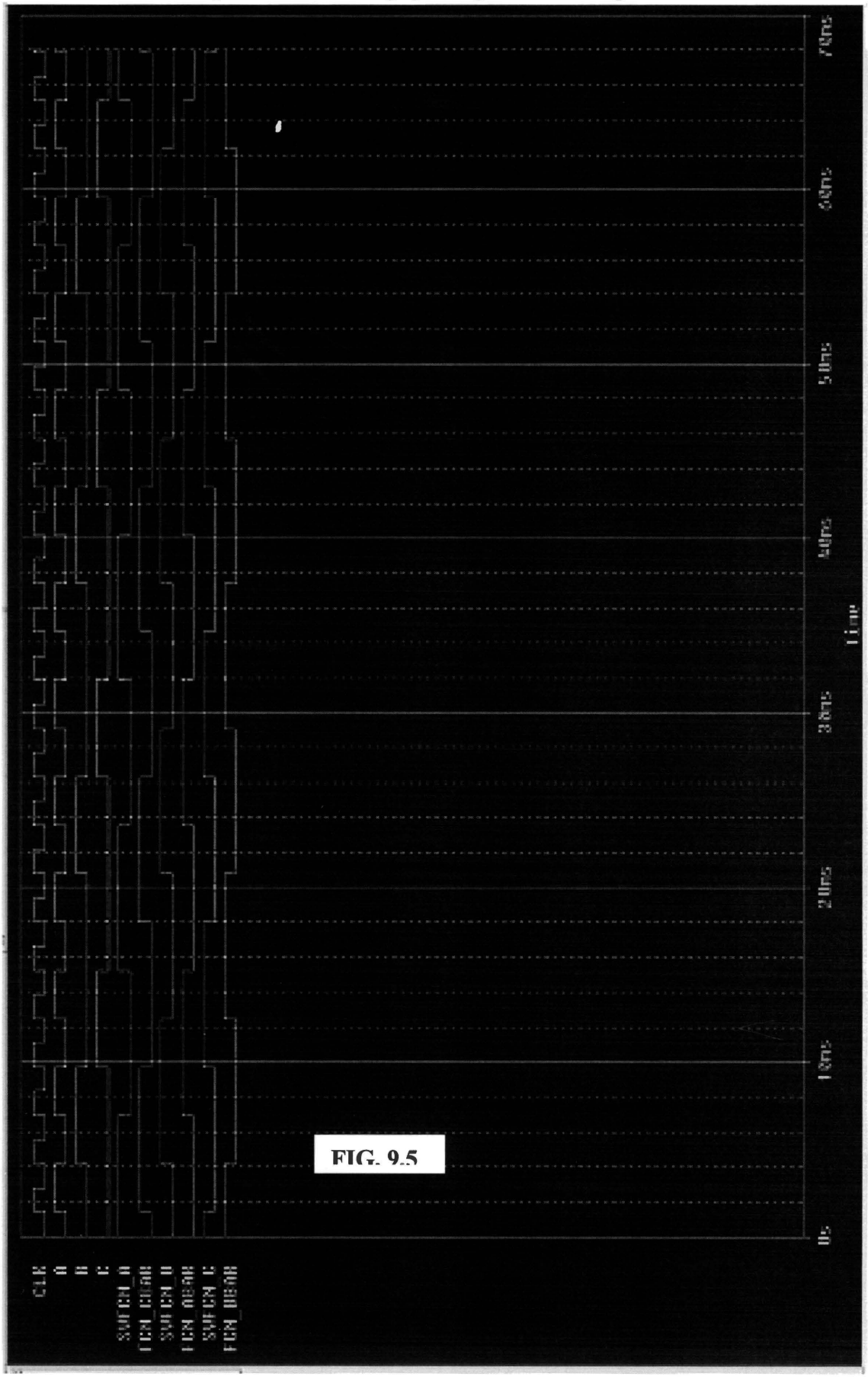
CLK
A
B
C
SWITCH_A
SWITCH_AB
SWITCH_B
SWITCH_BC
SWITCH_C
SWITCH_CA
0s
100ns
200ns
300ns
400ns
500ns
600ns
700ns
1 ms

FIG. 9.5

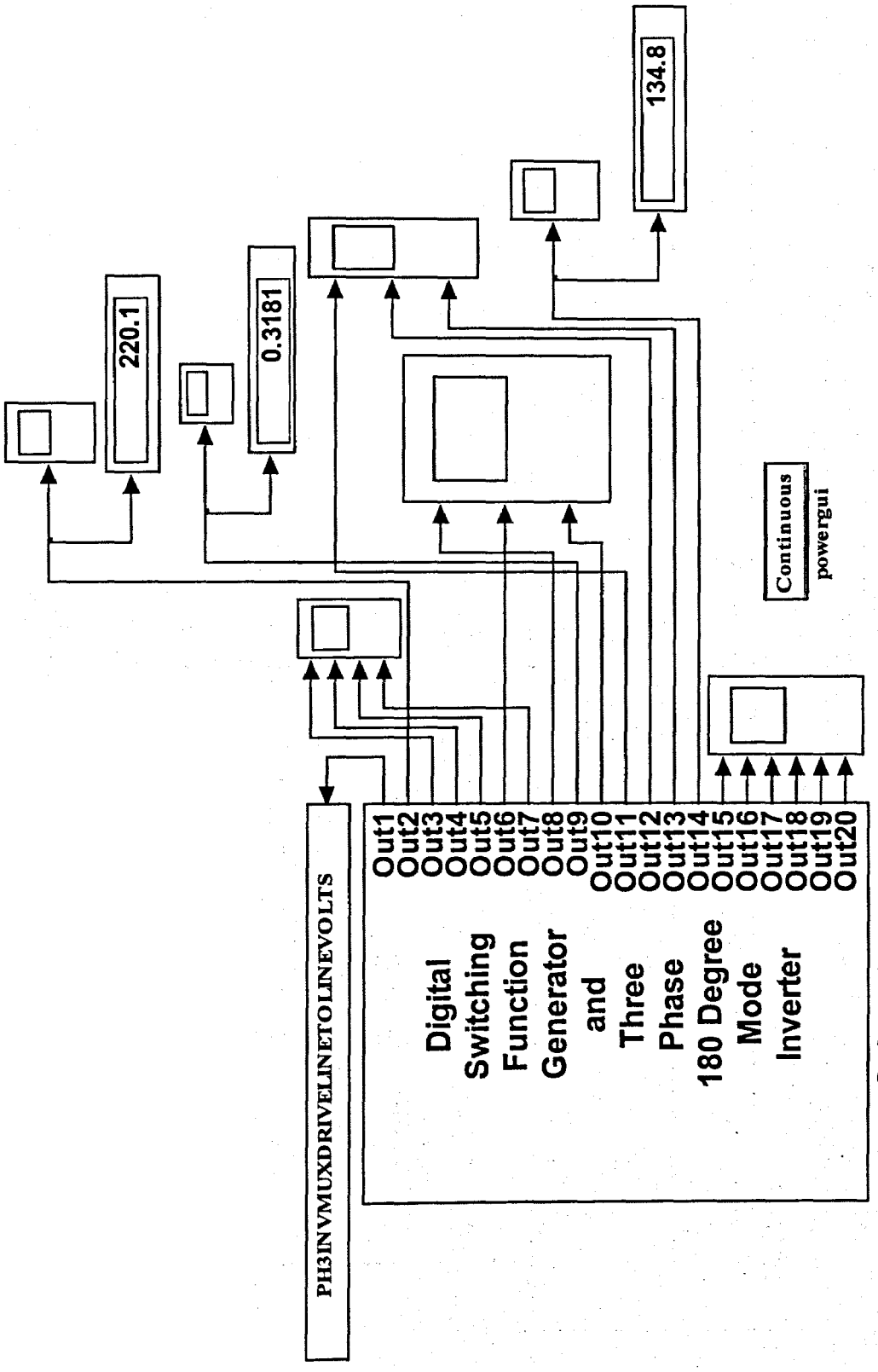

FIG.9.6(A): DIGITAL GATE DRIVE FOR A THREE PHASE VOLTAGE SOURCE INVERTER

Digital Switching Function Generator and Three Phase Inverter
180 Degree Mode Inverter
Subsystem
Block Parameters: Subsystem
Digital Switching Function Generator and Three Phase Inverter (mask)
Enter the Switching Frequency of the Three Phase Inverter in Hertz and the DC Link Voltage in Volts.
Parameters
Enter the Switching Frequency of the Three Phase Inverter in Hertz
60
Enter the DC Link Voltage in Volts
269.6
OK
Cancel
Help
Apply

FIG.9.6(B)

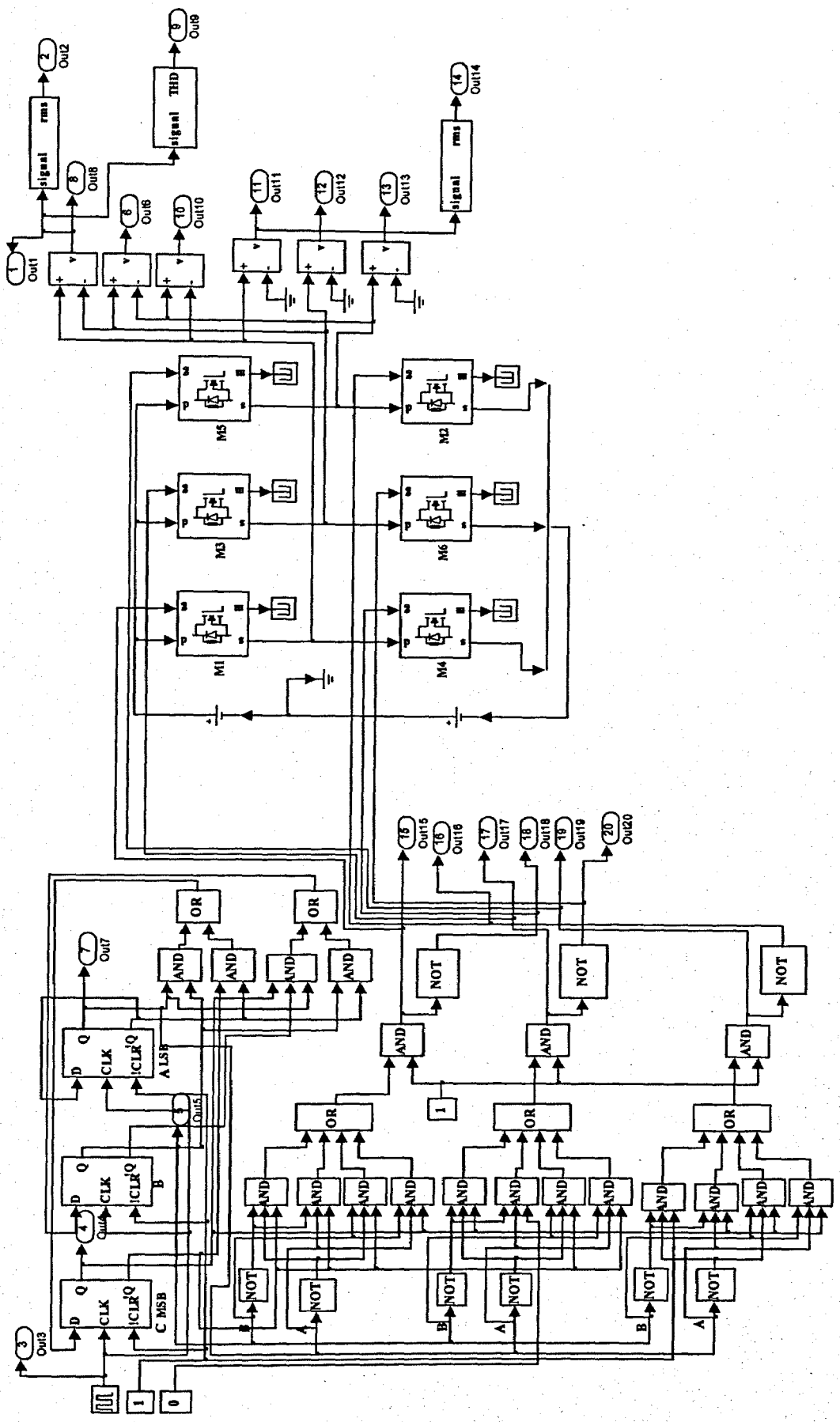

FIG 9.7(A): DIGITAL SWITCHING FUNCTION GENERATOR AND THREE PHASE 180 DEGREE MODE INVERTER

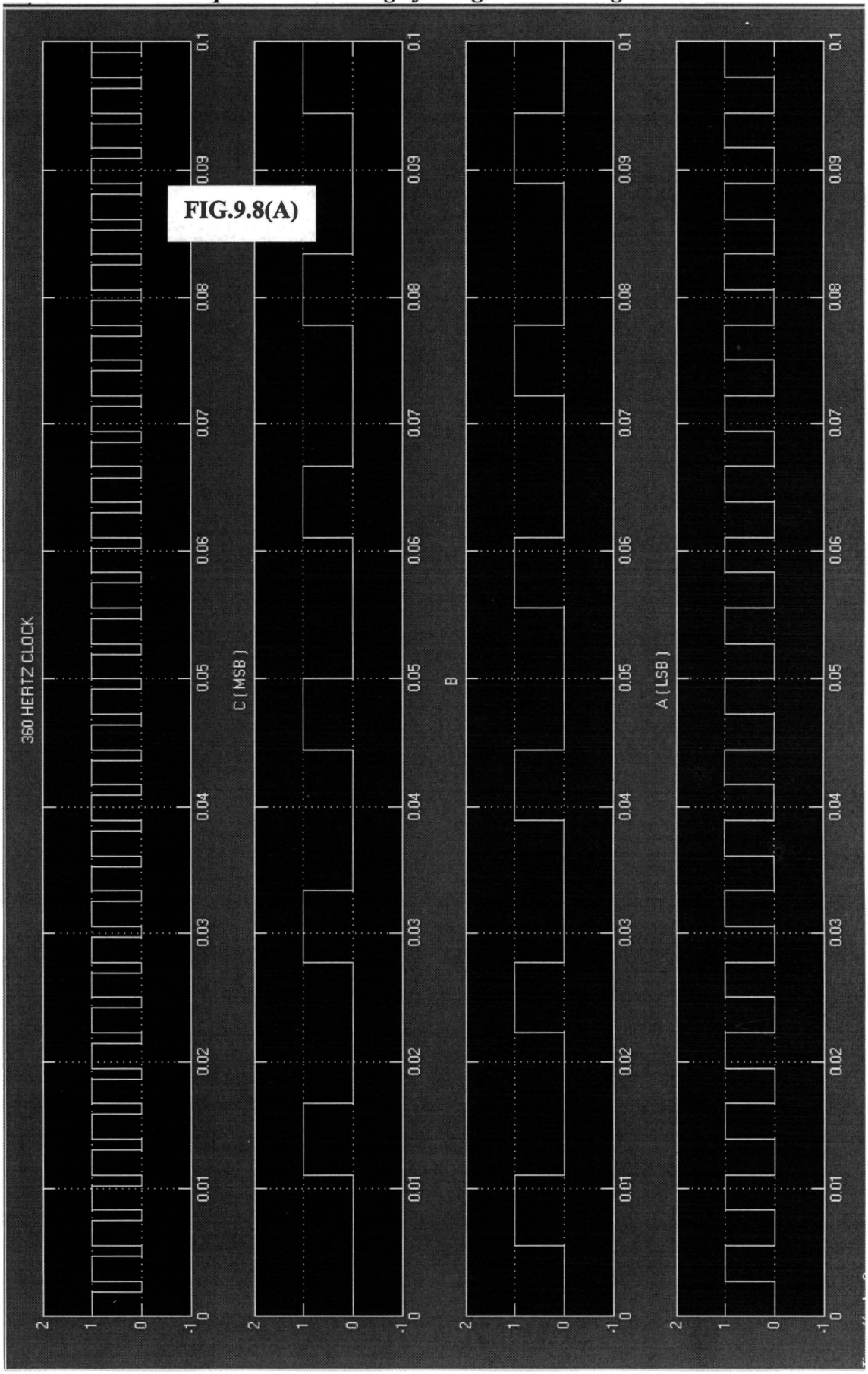
360 HERTZ CLOCK
C (MSB)
B
A (LSB)
0
0.01
0.02
0.03
0.04
0.05
0.06
0.07
0.08
0.09
0.1
2
1
0
-1

FIG.9.8(A)

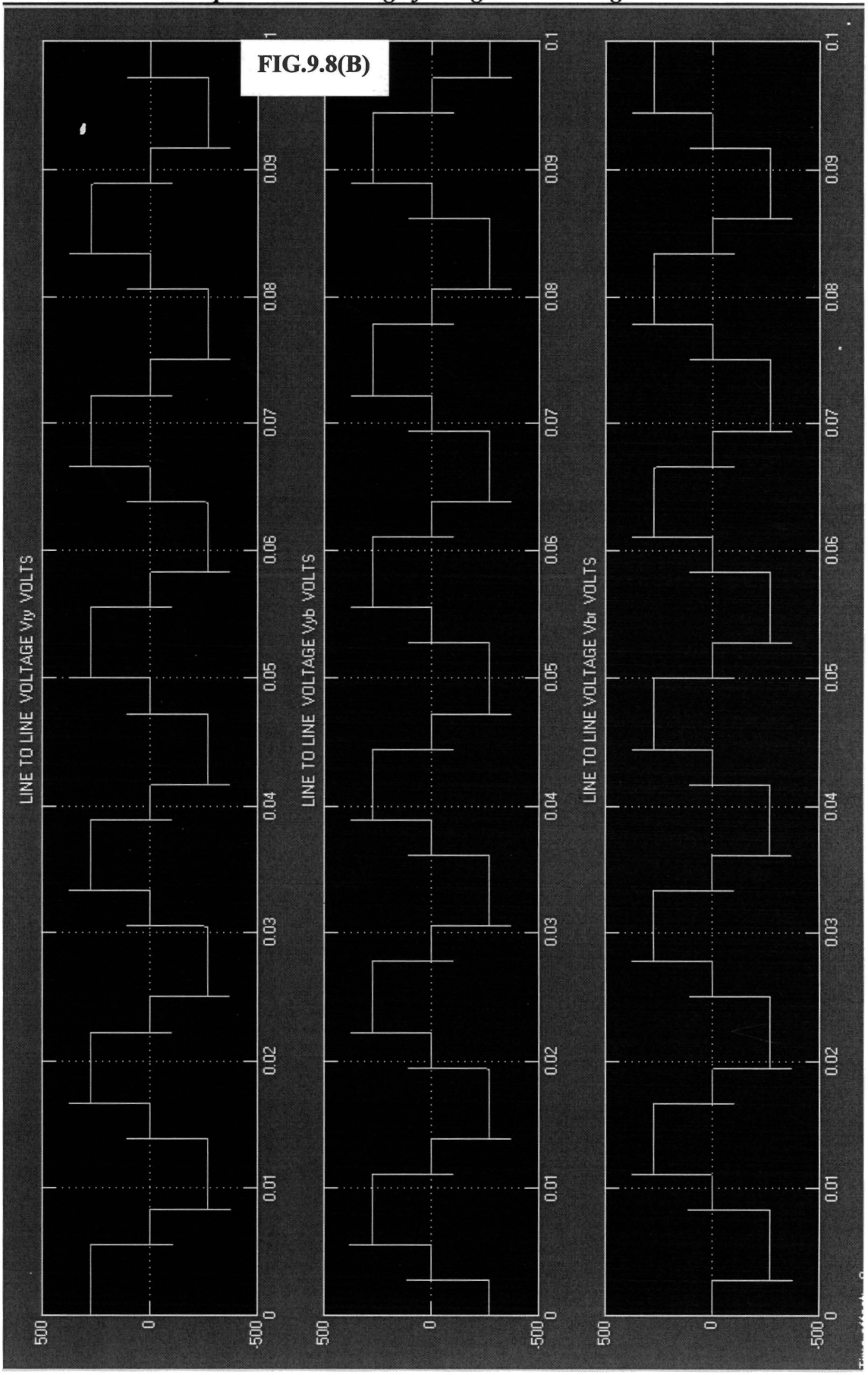
LINE TO LINE VOLTAGE Vry VOLTS
LINE TO LINE VOLTAGE Vyb VOLTS
LINE TO LINE VOLTAGE Vbr VOLTS
500
0
-500
0
0.01
0.02
0.03
0.04
0.05
0.06
0.07
0.08
0.09
0.1

FIG.9.8(B)

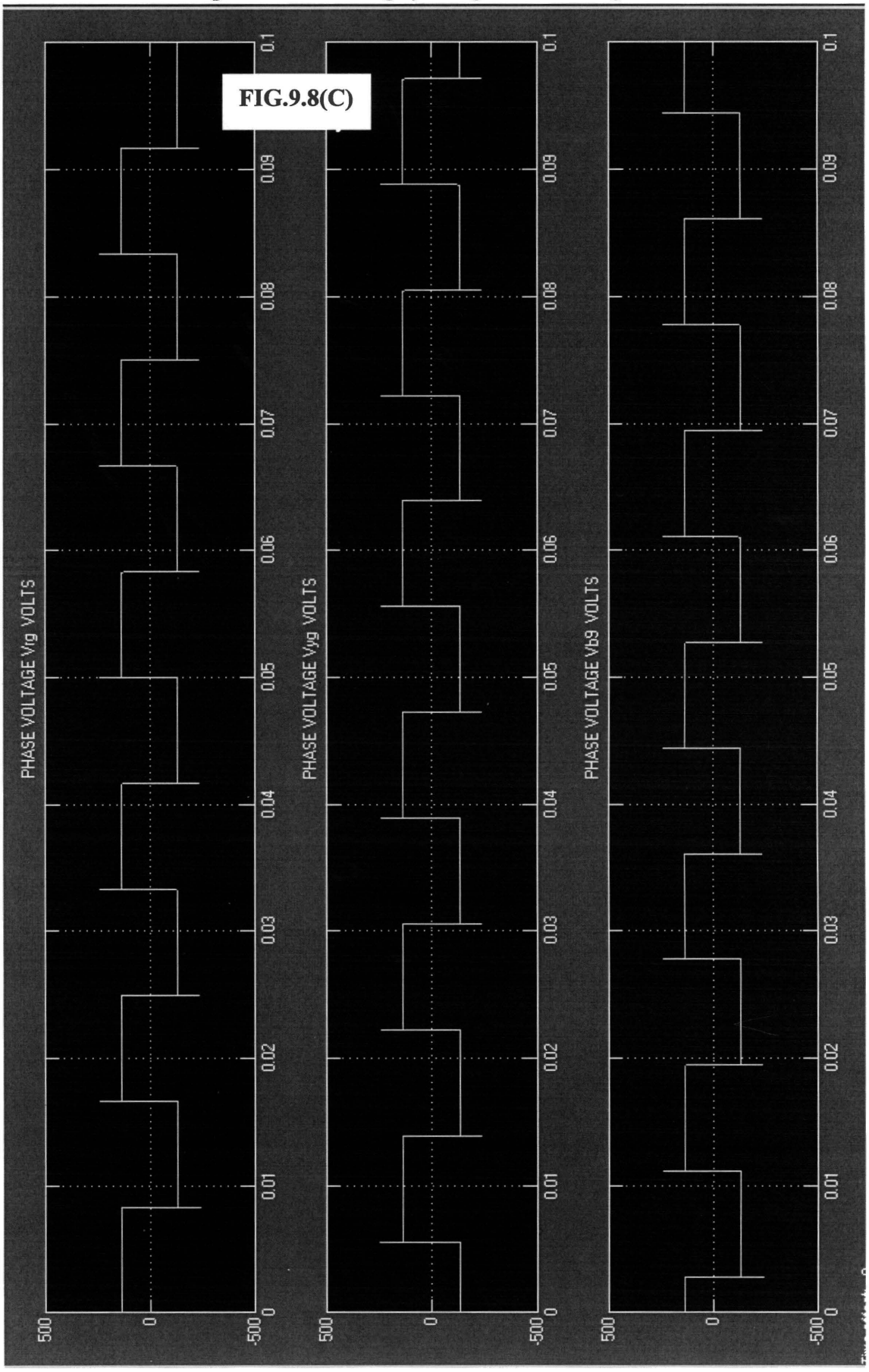
PHASE VOLTAGE Vg VOLTS
PHASE VOLTAGE Vyg VOLTS
PHASE VOLTAGE Vb9 VOLTS
500
0
-500
0
0.01
0.02
0.03
0.04
0.05
0.06
0.07
0.08
0.09
0.1

FIG.9.8(C)

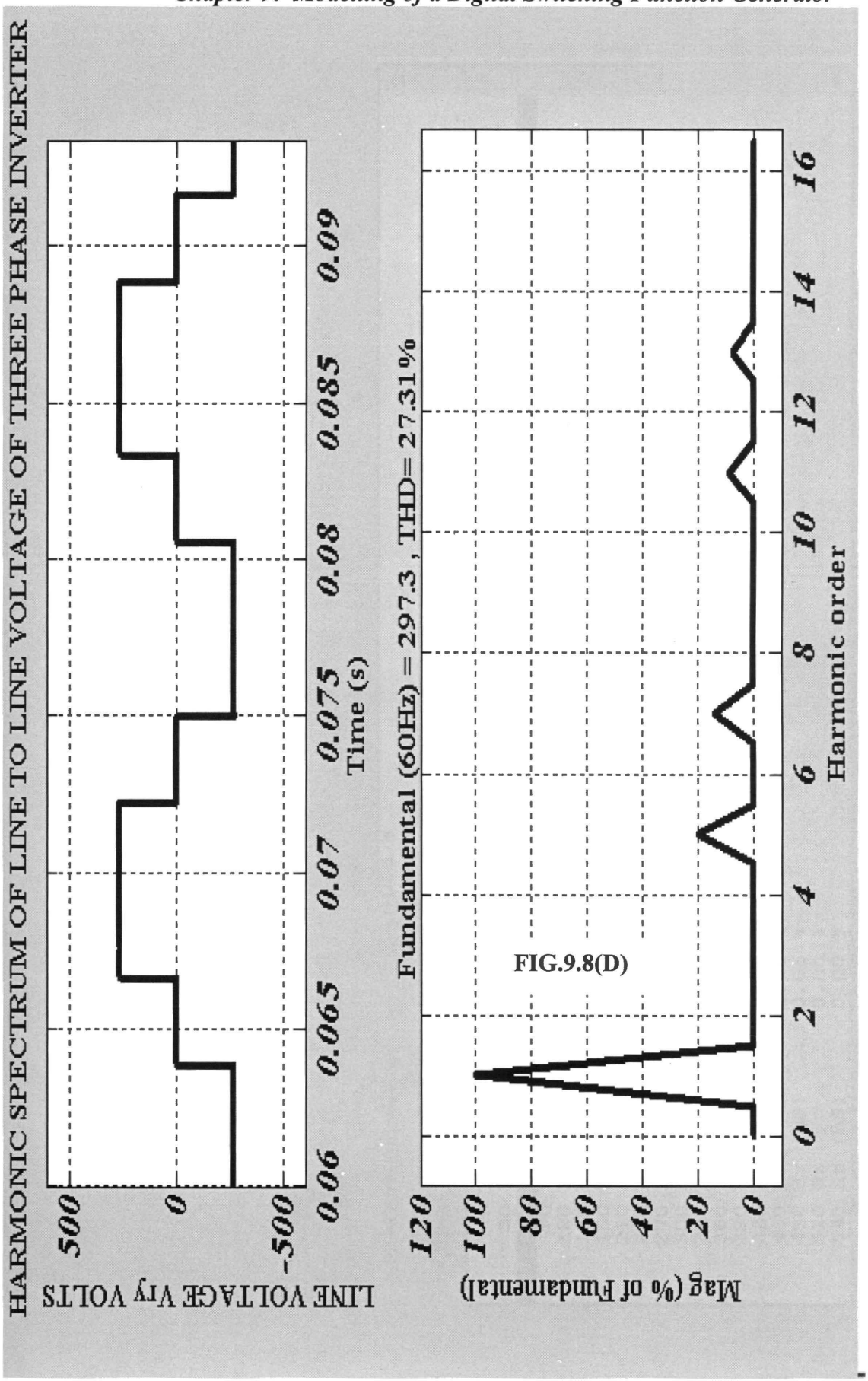
HARMONIC SPECTRUM OF LINE TO LINE VOLTAGE OF THREE PHASE INVERTER
LINE VOLTAGE Vry VOLTS
500
0
-500
0.06
0.065
0.07
0.075
0.08
0.085
0.09
Time (s)
Fundamental (60Hz) = 297.3 , THD= 27.31%
Mag (% of Fundamental)
120
100
80
60
40
20
0
0
2
4
6
8
10
12
14
16
Harmonic order

FIG.9.8(D)

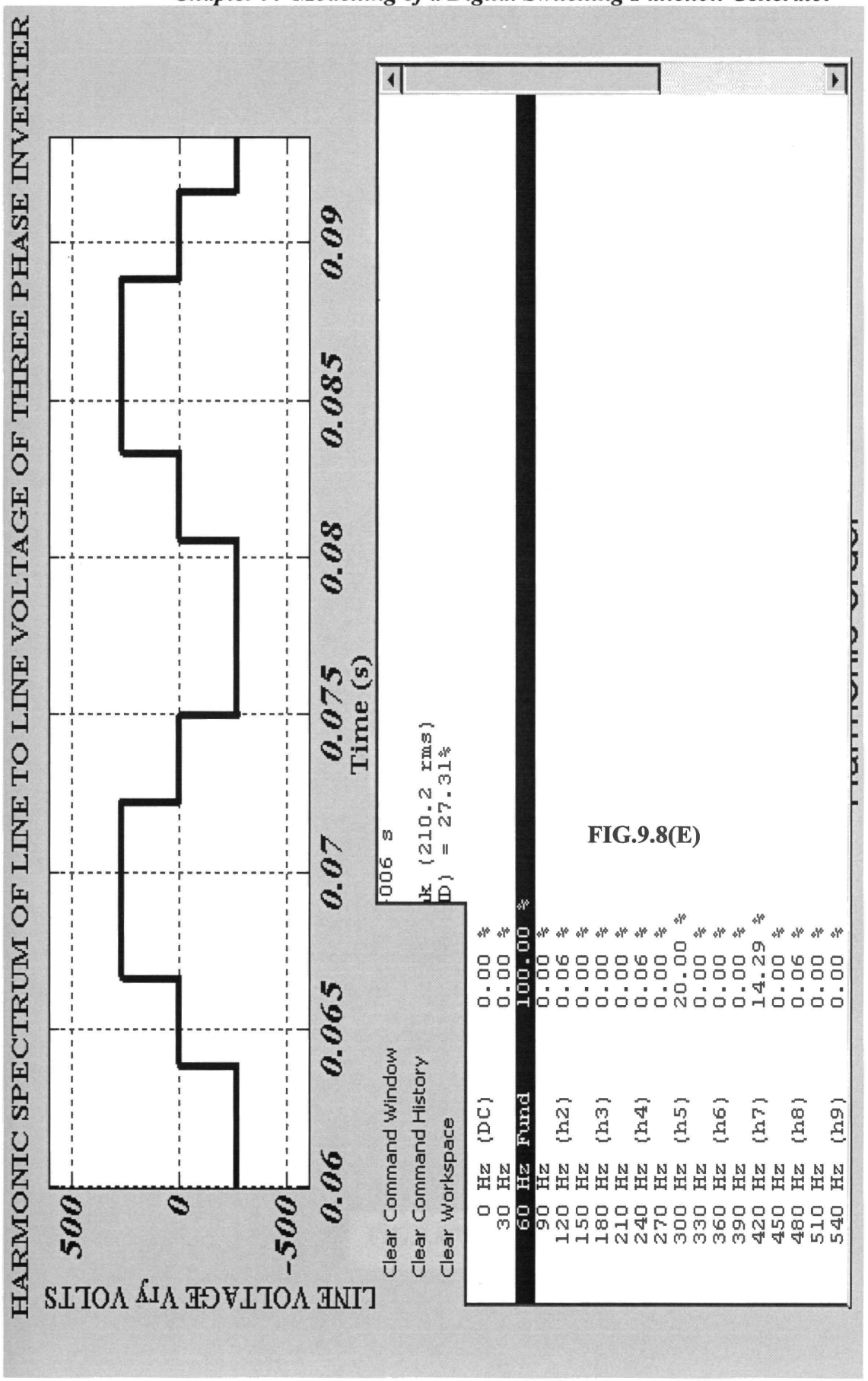
HARMONIC SPECTRUM OF LINE TO LINE VOLTAGE OF THREE PHASE INVERTER
LINE VOLTAGE Vry VOLTS
500
0
-500
0.06
0.065
0.07
0.075
0.08
0.085
0.09
Time (s)
Clear Command Window
Clear Command History
Clear Workspace
006 s
k (210.2 rms)
D) = 27.31%
0 Hz (DC) 0.00 %
30 Hz 0.00 %
60 Hz Fund 100.00 %
90 Hz 0.00 %
120 Hz (h2) 0.06 %
150 Hz 0.00 %
180 Hz (h3) 0.00 %
210 Hz 0.00 %
240 Hz (h4) 0.06 %
270 Hz 0.00 %
300 Hz (h5) 20.00 %
330 Hz 0.00 %
360 Hz (h6) 0.00 %
390 Hz 0.00 %
420 Hz (h7) 14.29 %
450 Hz 0.00 %
480 Hz (h8) 0.06 %
510 Hz 0.00 %
540 Hz (h9) 0.00 %

FIG.9.8(E)

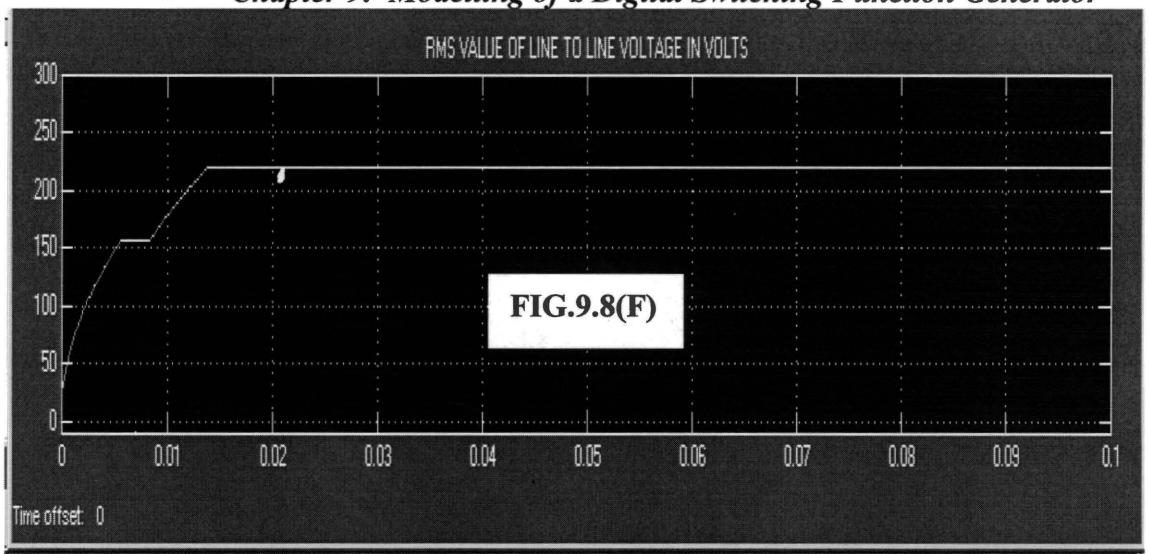

FIG.9.8(F)

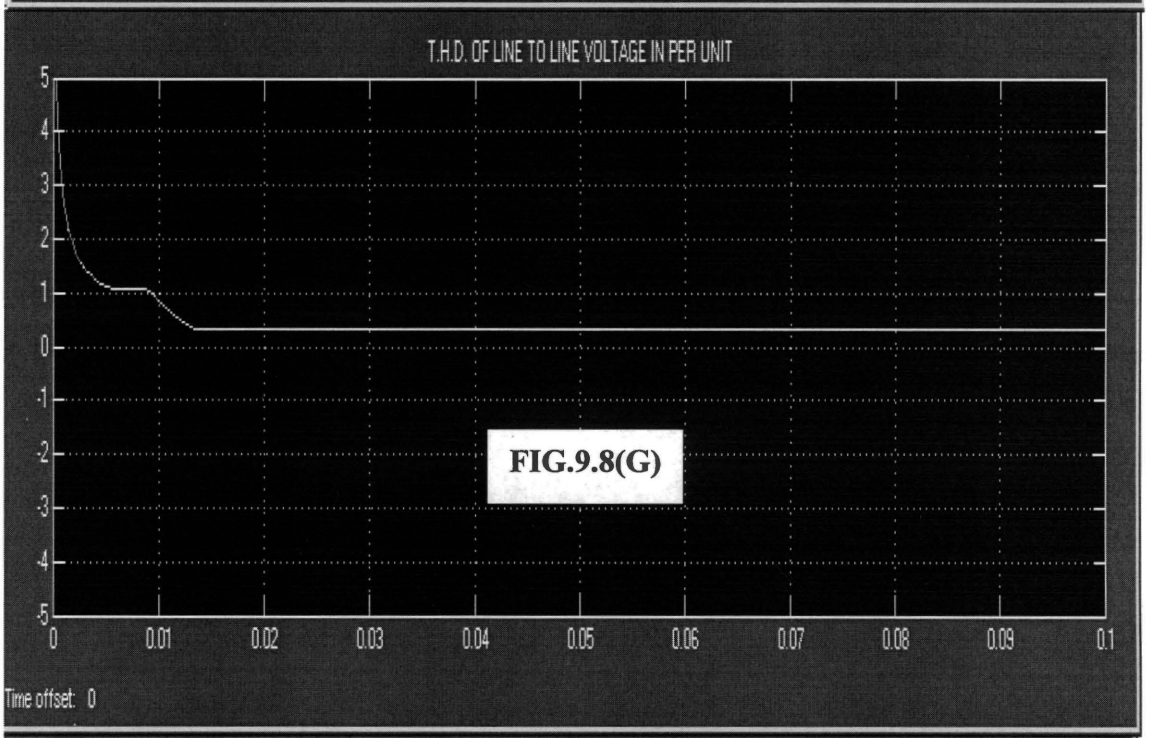

FIG.9.8(G)

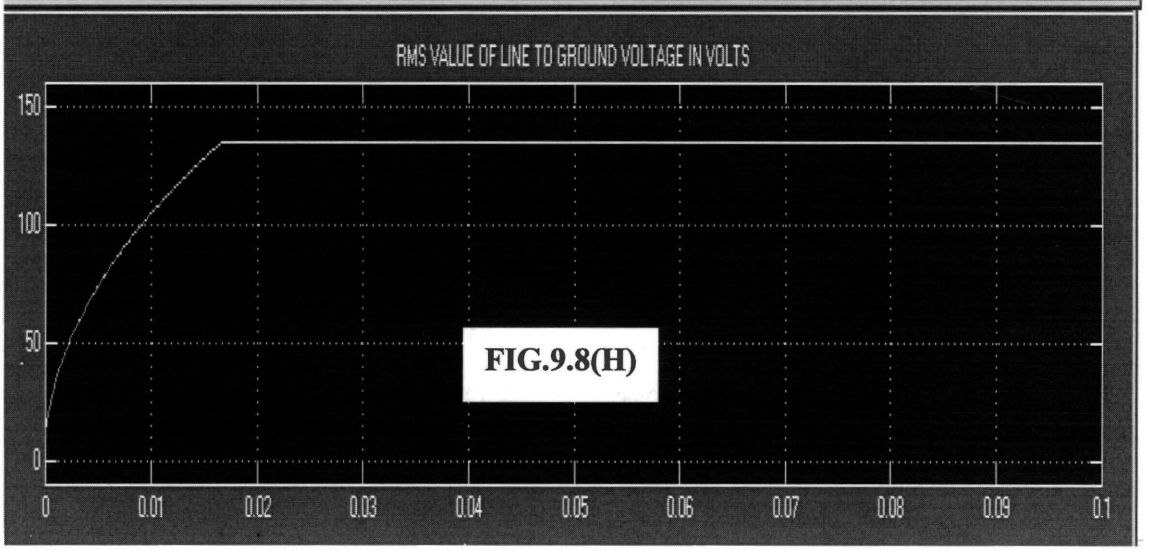

FIG.9.8(H)

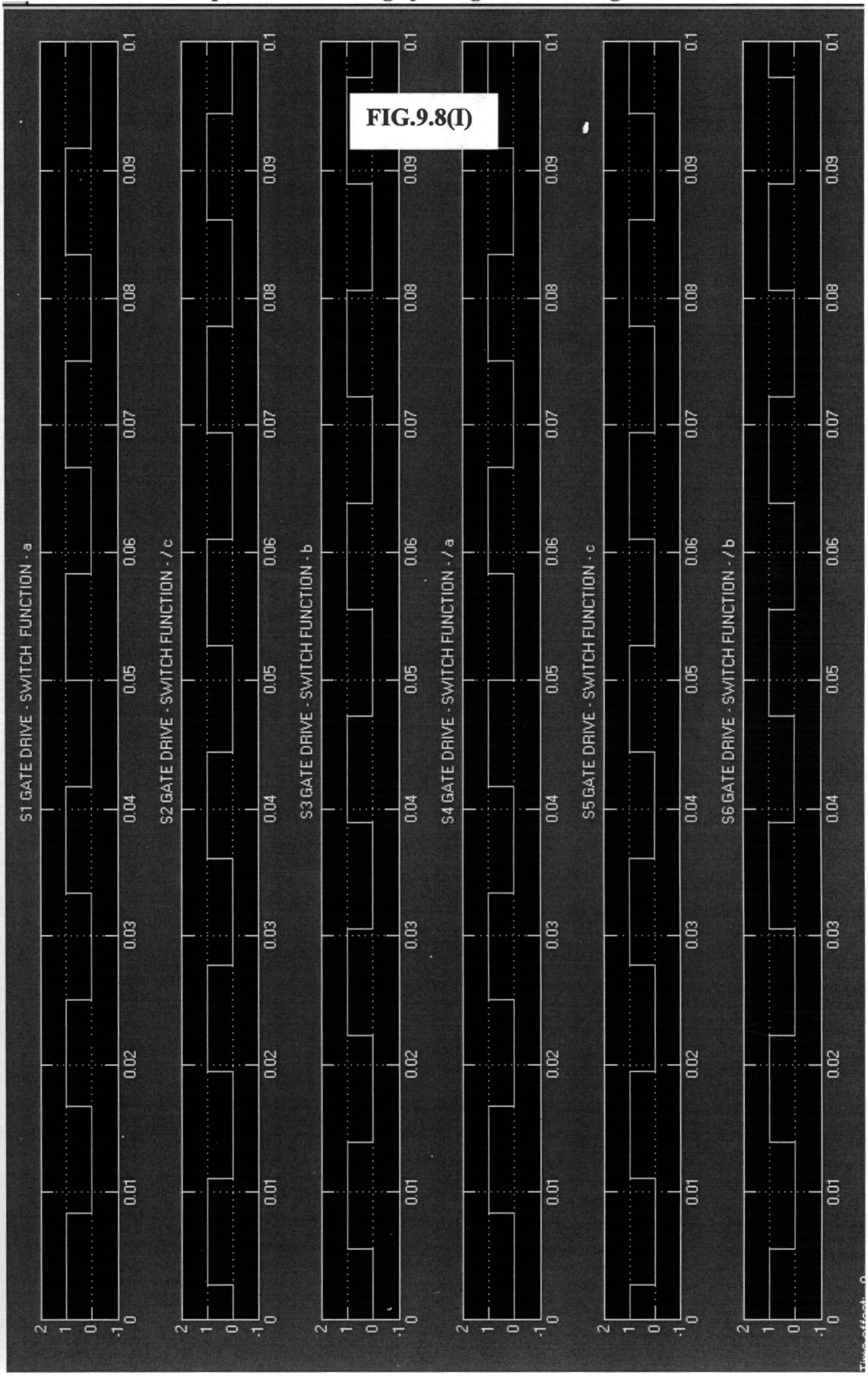
S1 GATE DRIVE - SWITCH FUNCTION - a
S2 GATE DRIVE - SWITCH FUNCTION - / c
S3 GATE DRIVE - SWITCH FUNCTION - b
S4 GATE DRIVE - SWITCH FUNCTION - / a
S5 GATE DRIVE - SWITCH FUNCTION - c
S6 GATE DRIVE - SWITCH FUNCTION - / b

FIG.9.8(I)

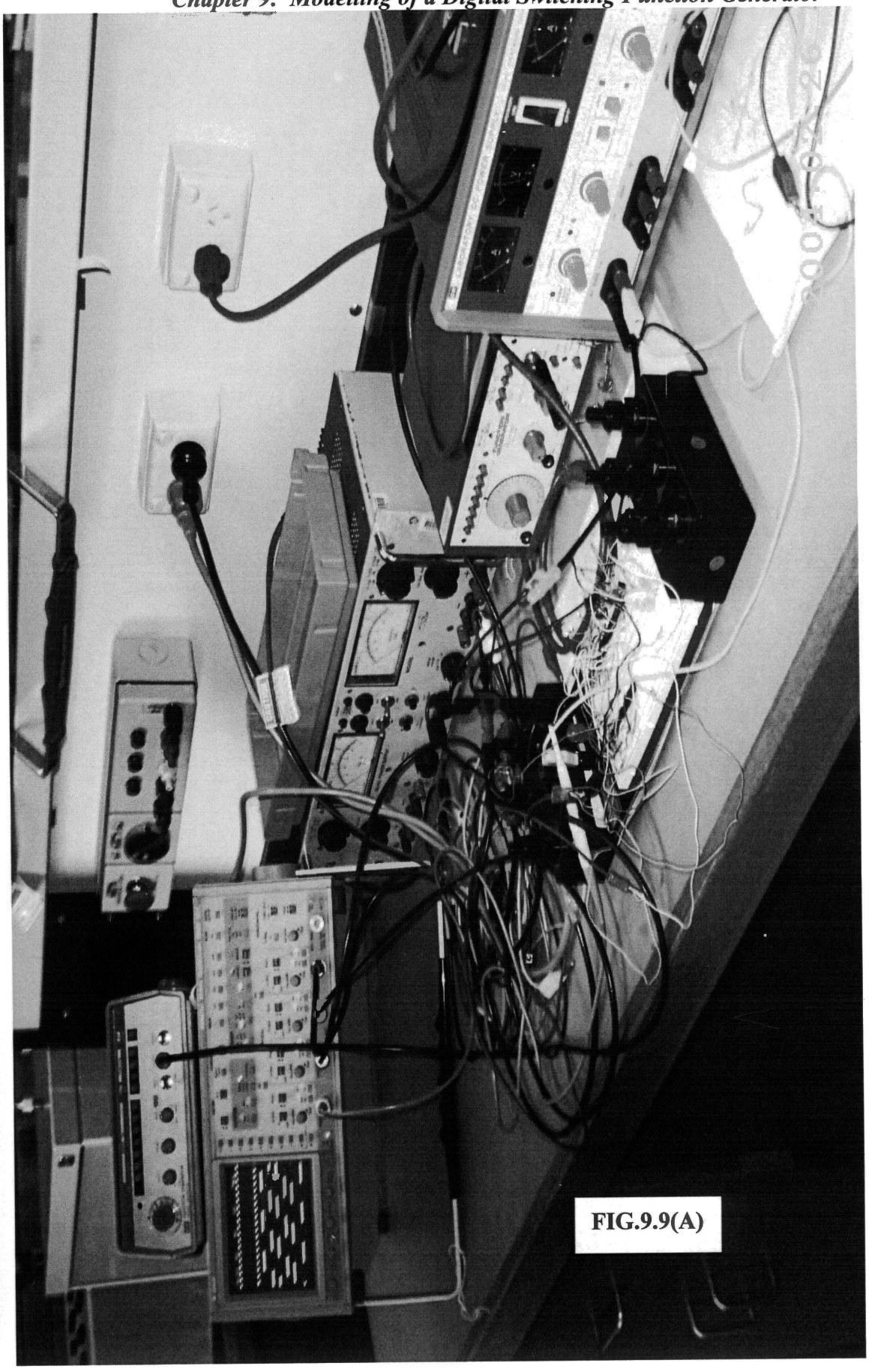

FIG.9.9(A)

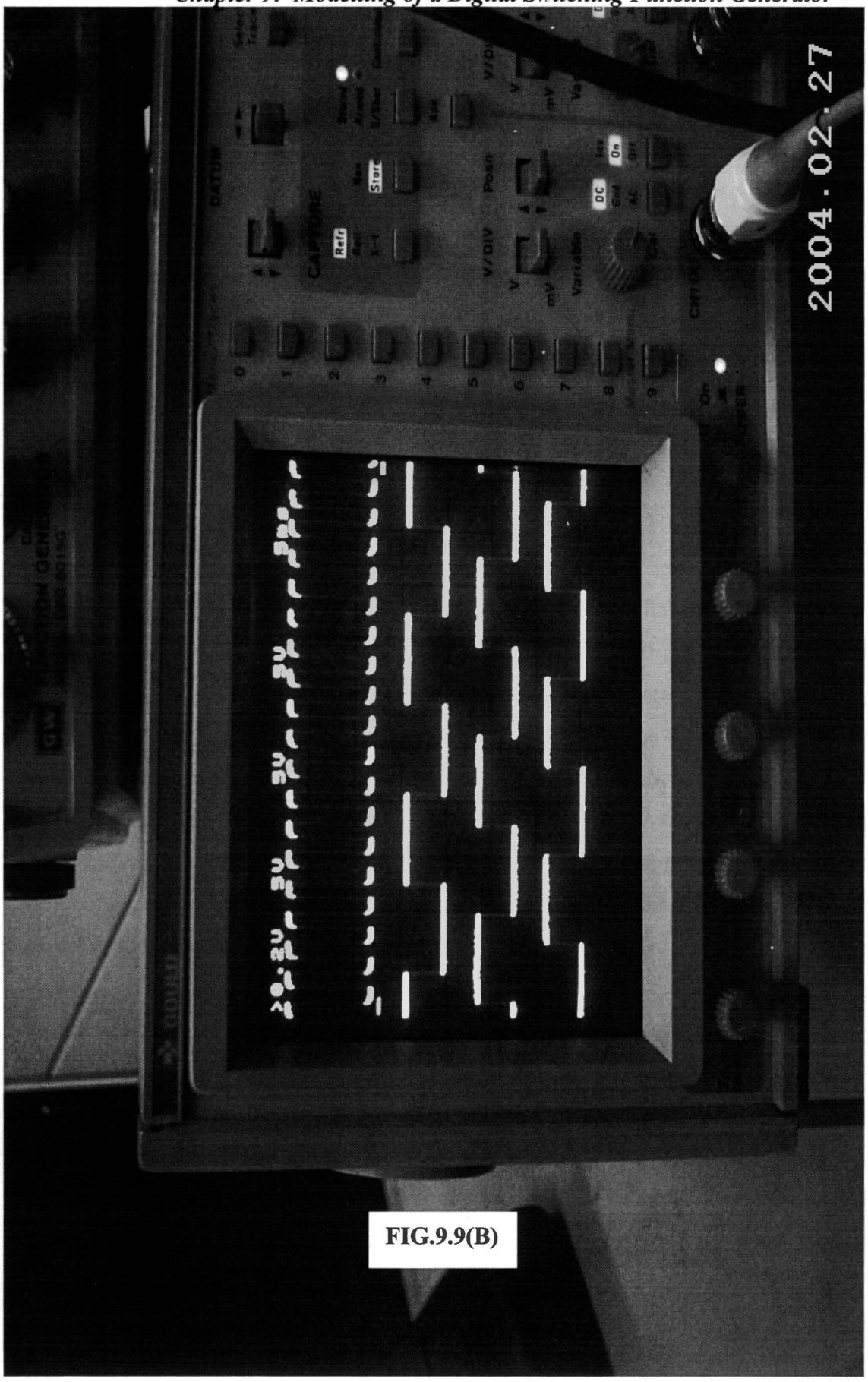

FIG.9.9(B)

In the dialog box marked Digital Switching Function Generator and Three Phase Inverter in Fig.9.6(B), the switching frequency of the inverter is entered as 60 Hz and the DC Link voltage is entered as 269.6 volts respectively. The clock and D flip-flops for modulo six counter are from Sources and Simulink Extras block set. The logic gates, AND, OR and NOT are from Logic and Bit Operations block set. The modulo six conter and its control logic are derived as per equation 9.2. The four line to one line mux is developed using AND, OR and NOT gates as shown in Fig.9.7(A). The output B A of the modulo six counter is used as select inputs and the external inputs to mux are C, /C, 0 and 1 connected as per Table 9.2 to realize the switching functions. The dc source, Three Phase MOSFET inverter, signal rms and THD are from SimPowerSystems block set.

9.3.4 Simulation Results

The simulation results of SIMULINK circuit model of the digital switching function generator are shown in Fig.9.8(A) to (I). The ode15s(stiff/NDF) solver was used for the simulation. Fig.9.8(A) shows the clock and modulo six counter output. Fig.9.8(B) and (C) shows the line to line and line to ground voltages of the three phase inverter. Fig.9.8(D) and (E) shows the harmonic spectrum of the line to line voltage of the three phase inverter. Fig.9.8(F), (G) and (H) respectively shows the RMS value, THD of line to line voltage and the RMS value of the line to ground voltage of the three phase inverter. Fig.9.8(I) shows the gate drive pattern or the switching functions and the inverted switching functions of the three phase 180 degree mode inverter.

9.4 Experimental Observation

The digital switching function generator shown in Fig.2.7(B) in Chapter 2 was fabricated in the CEMPE laboratories using the astable multivibrator used as a 360 Hz clock generator, modulo six counter, four line to one line multiplexer. The experimental set up is shown in Fig.9.9(A). The clock output and the three switching functions a, b and c observed experimentally are shown in the oscilloscope photograph in Fig.9.9(B).

9.5 Conclusions

The complete design of the digital switching function generator using modulo six counter and four line to one multiplexer, for a three phase 180 degree mode inverter is presented in this Chapter. The design was verified for a three phase 60 Hz 180 degree mode inverter by simulation using PSPICE and SIMULINK and also experimentally by wiring the components in the breadboard. The PSPICE and SIMULINK simulation results show the waveforms for the switching functions a, b and c, the inverted switching functions /a, /b and /c and also the waveforms for a, b and c obtained experimentally in the CEMPE laboratory confirms the standard gate drive waveforms given in the literature references [14-17]. Similarly the line to line, line to ground voltage and Harmonic spectrum of line to line voltage obtained by simulation using SIMULINK well confirms the literature references [14-17], the Fig.4.2(A) to (D) and the equations 4.1 and 4.2 in Chapter 4. From equations 4.1 and 4.2 in Chapter 4, it is seen that the third harmonic of line to line voltage of three phase 180 degree mode inverter is zero, the fifth and seventh harmonics are respectively 20 % and 14.28 % respectively. By observation of the harmonic spectrum of the line to line voltage of the above inverter shown in Fig.9.8(D) and (E), it is seen that the third, fifth and seventh harmonics confirms the above values obtained by derivation.

CHAPTER 10
MODELLING OF A SWITCHED MODE POWER SUPPLY USING BUCK CONVERTER

10.1 Introduction

Switched Mode Power Supplies are used for obtaining a regulated dc output voltage from an unregulated dc input voltage. Fig.2.8 in Chapter 2 gives the general block diagram of the SMPS using Buck converter. Referring to Fig.2.8, the buck converter output Vo is attenuated using a potential divider and the resulting output VPOT is subtracted from the reference input VREF using a difference amplifier to get the error output VERR. This VERR output is compared with triangle carrier Vc in a comparator to get the PWM switching pulses to drive the buck converter switch. The PI controller in Fig.2.8 is used to reduce the peak value and the number of cycles of oscillations in the output voltage Vo. Depending on the value of Vo, the duty cycle of the PWM switching pulses so adjusts to maintain the output voltage Vo almost nearly constant irrespective of variations in the input dc voltage Vs. In this type of SMPS, the buck converter is always operated in the CCM. The Switching Function concept is used to model the Buck Converter. CUK and SEPIC converters operated in DCM are also used for SMPS.

10.2 Simulation of A Switched Mode Power Supply using PSIM

The simulation of the SMPS using Buck Converter was carried out using PSIM [5]. The parameters of the SMPS used for simulation is shown in Table 10.1. The Buck converter circuit simulation schematics using PSIM 6.1, without and with PI controller are shown in Fig.10.1(A) and (B) respectively. The gain block K with the value -1 shown in Fig.10.1(A) and (B) is the inverting op amp (a 1K resistor between inverting pin and PI controller, another 1 K resistor between output and inverting pin and the non-inverting pin is grounded as shown in Fig.10.1(C)). This inverting op amp configuration is not shown in Fig.10.1(A) and (B) due to node limitation in the demo

TABLE 10.1 Parameters of the SMPS

Sl.No.	Parameter	Value	Unit
1	Normal Input Voltage Vs	15	Volts
2	Normal Output Voltage Vo	9	Volts
3	Variation of Input Voltage	12 to 18	Volts
4	Load Resistance RL	10	Ohms
5	Inductance L1	300E-6	H
6	Filter capacitance CF	200E-6	F
7	Switching Frequency Fsw	100	kHZ
8	PI Controller – Kp - Ki	0.1 6	

version of PSIM 6.1. The potential divider output VPOT is (8 / 9) of the output voltage Vo. The reference voltage VREF is 9 volts. The error amplifier generates VERR which is (VREF – VPOT). The PI controller generates the transfer function [0.1 + (6/s)]. The triangle carrier generator generates triangle carrier signal V_CARRIER with a frequency of 100 kHZ. The V_CARRIER output and VERR output are compared in an op amp comparator. The output V_DRIVE is the switching pulse drive to the buck converter.

10.2.1 Simulation Results

The simulation of this buck converter SMPS without and with PI controller was carried out using the demo version of PSIM 6.1. The simulation results without PI controller and with PI controller are shown in Fig.10.2(A) and (B) respectively.

10.3 Modelling of the Switched Mode Power Supply

The interactive model of the Switched Mode Power Supply is shown in Fig.10.3. The various dialog boxes and help file are shown in Fig.10.4(A) and (B). The various

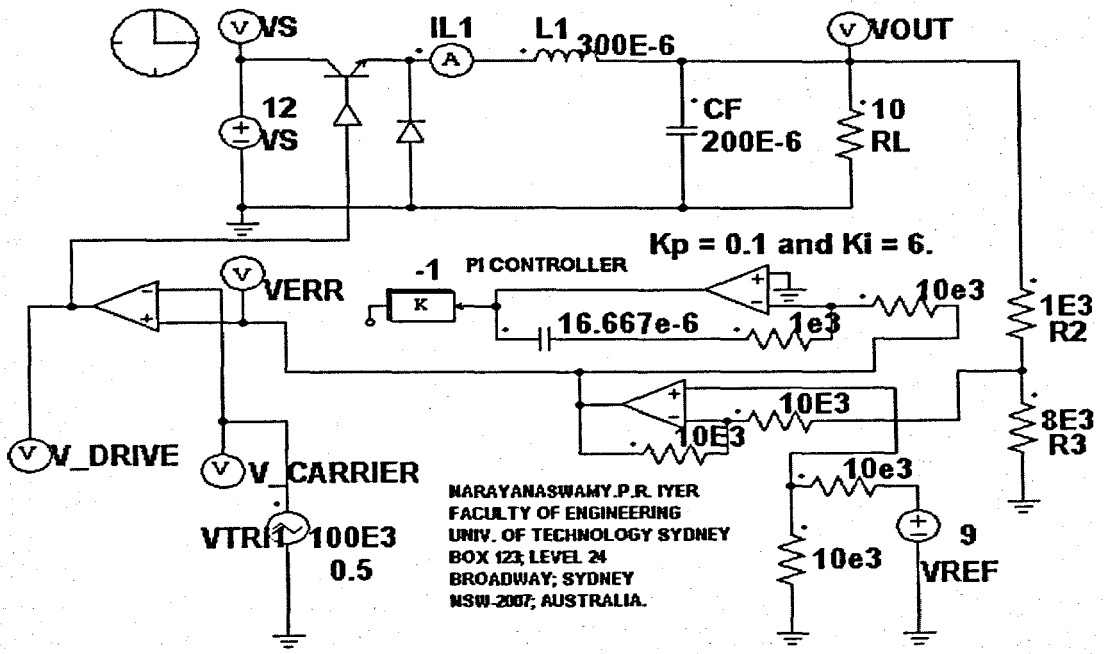

Fig.10.1(A) BUCK CONVERTER SMPS WITHOUT PI CONTROLLER

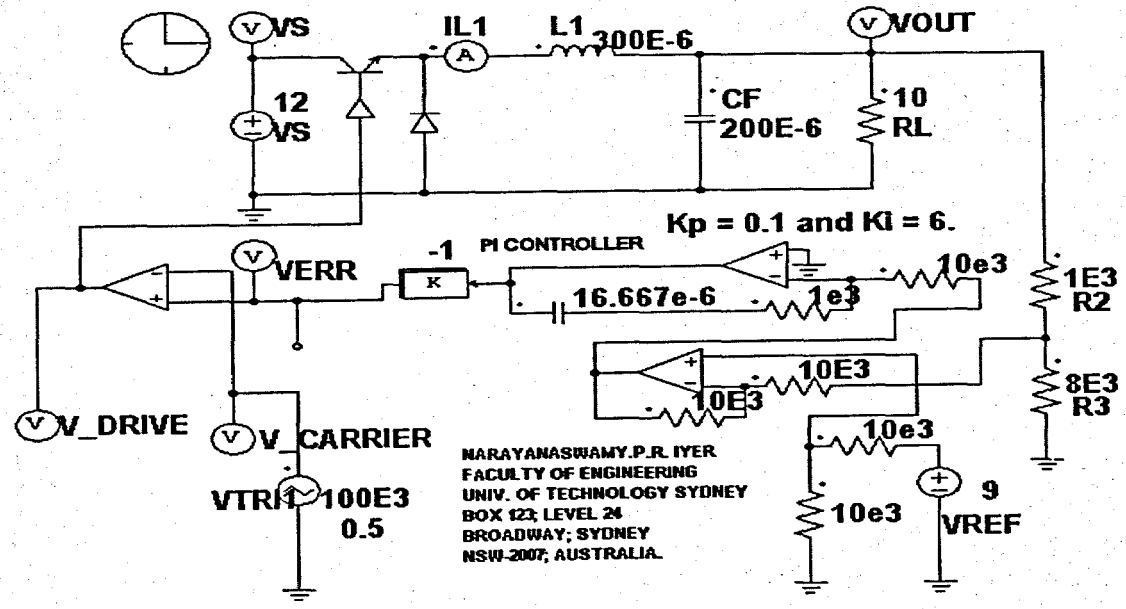

Fig.10.1(B) BUCK CONVERTER SMPS WITH PI CONTROLLER

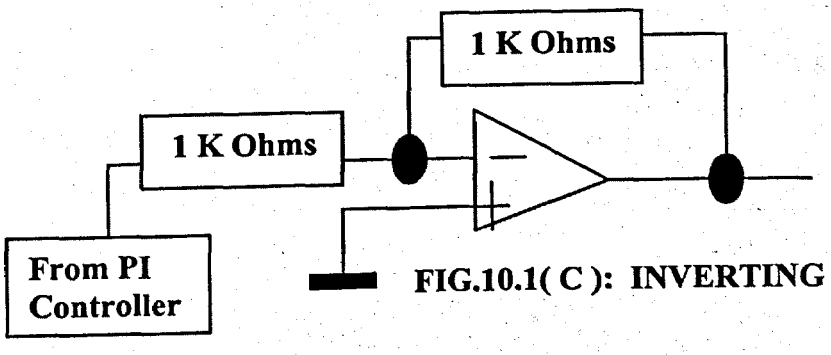

FIG.10.1(C): INVERTING OP. AMP.

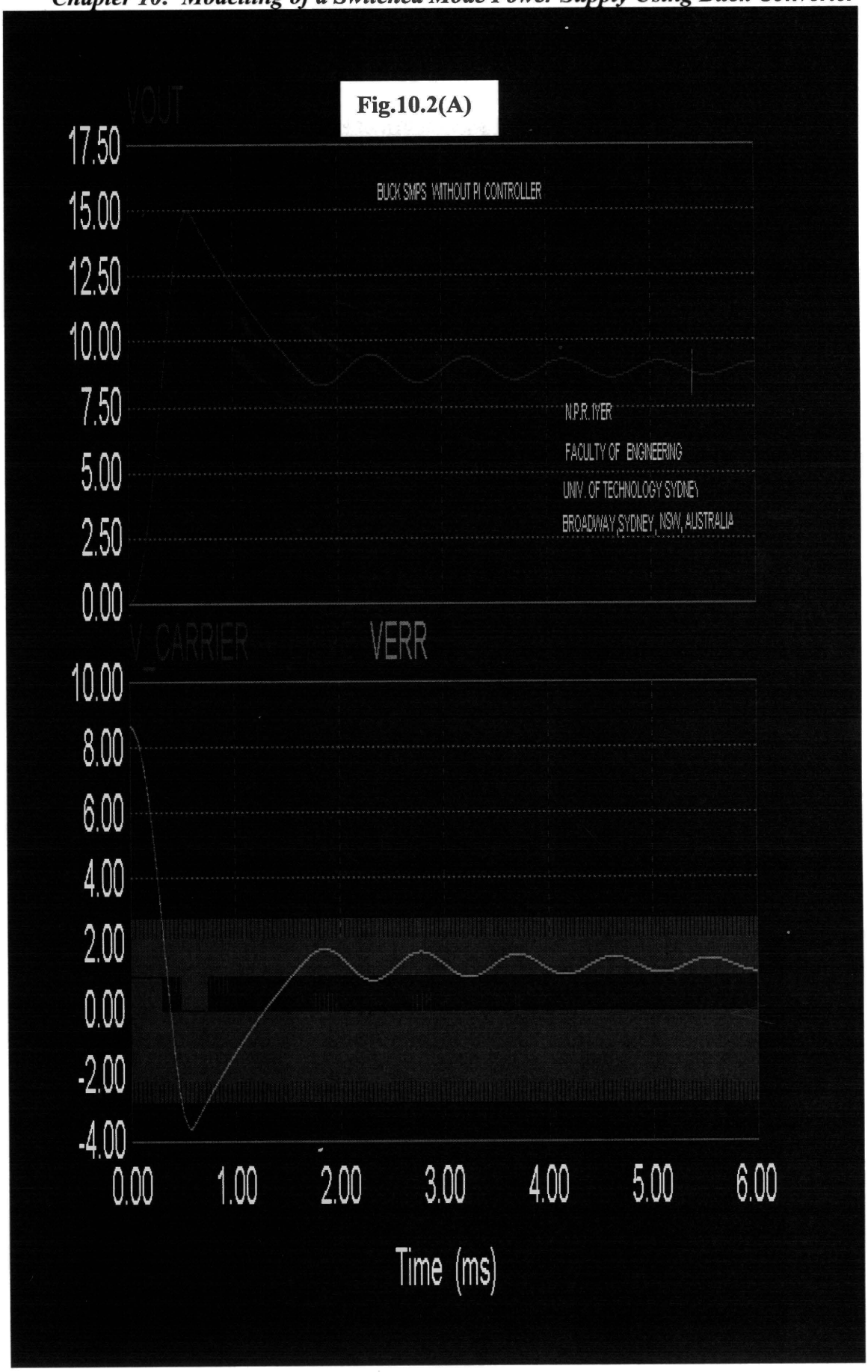
Fig.10.2(A)
VOUT
17.50
15.00
12.50
10.00
7.50
5.00
2.50
0.00
BUCK SMPS WITHOUT PI CONTROLLER
N.P.R.IYER
FACULTY OF ENGINEERING
UNIV. OF TECHNOLOGY SYDNEY
BROADWAY,SYDNEY, NSW, AUSTRALIA
V_CARRIER
VERR
10.00
8.00
6.00
4.00
2.00
0.00
-2.00
-4.00
0.00
1.00
2.00
3.00
4.00
5.00
6.00
Time (ms)

Fig.10.2(B)

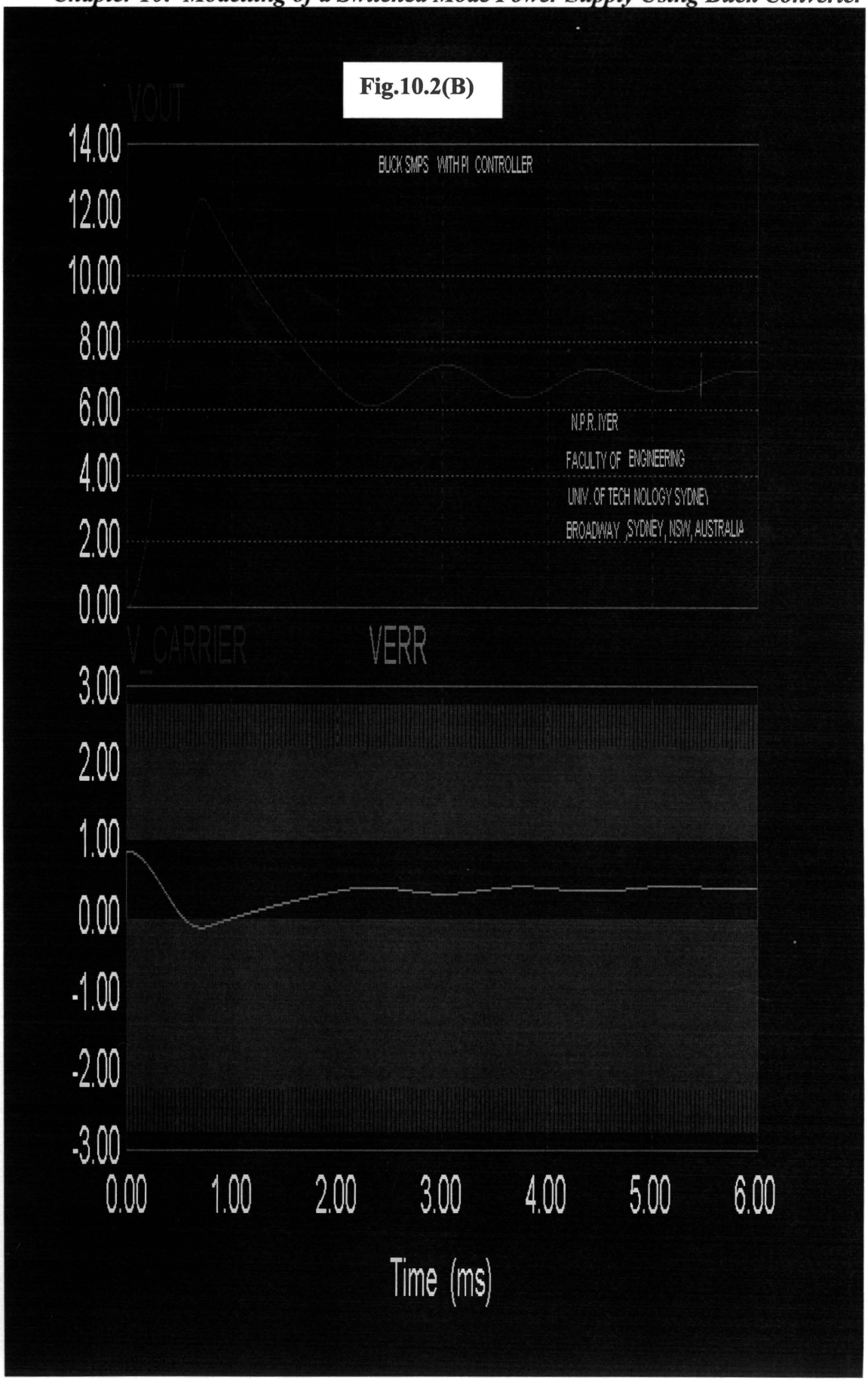
VOUT
BUCK SMPS WITH PI CONTROLLER
14.00
12.00
10.00
8.00
6.00
4.00
2.00
0.00
N.P.R. IYER
FACULTY OF ENGINEERING
UNIV. OF TECH NOLOGY SYDNEY
BROADWAY ,SYDNEY, NSW, AUSTRALIA
V_CARRIER
VERR
3.00
2.00
1.00
0.00
-1.00
-2.00
-3.00
0.00
1.00
2.00
3.00
4.00
5.00
6.00
Time (ms)

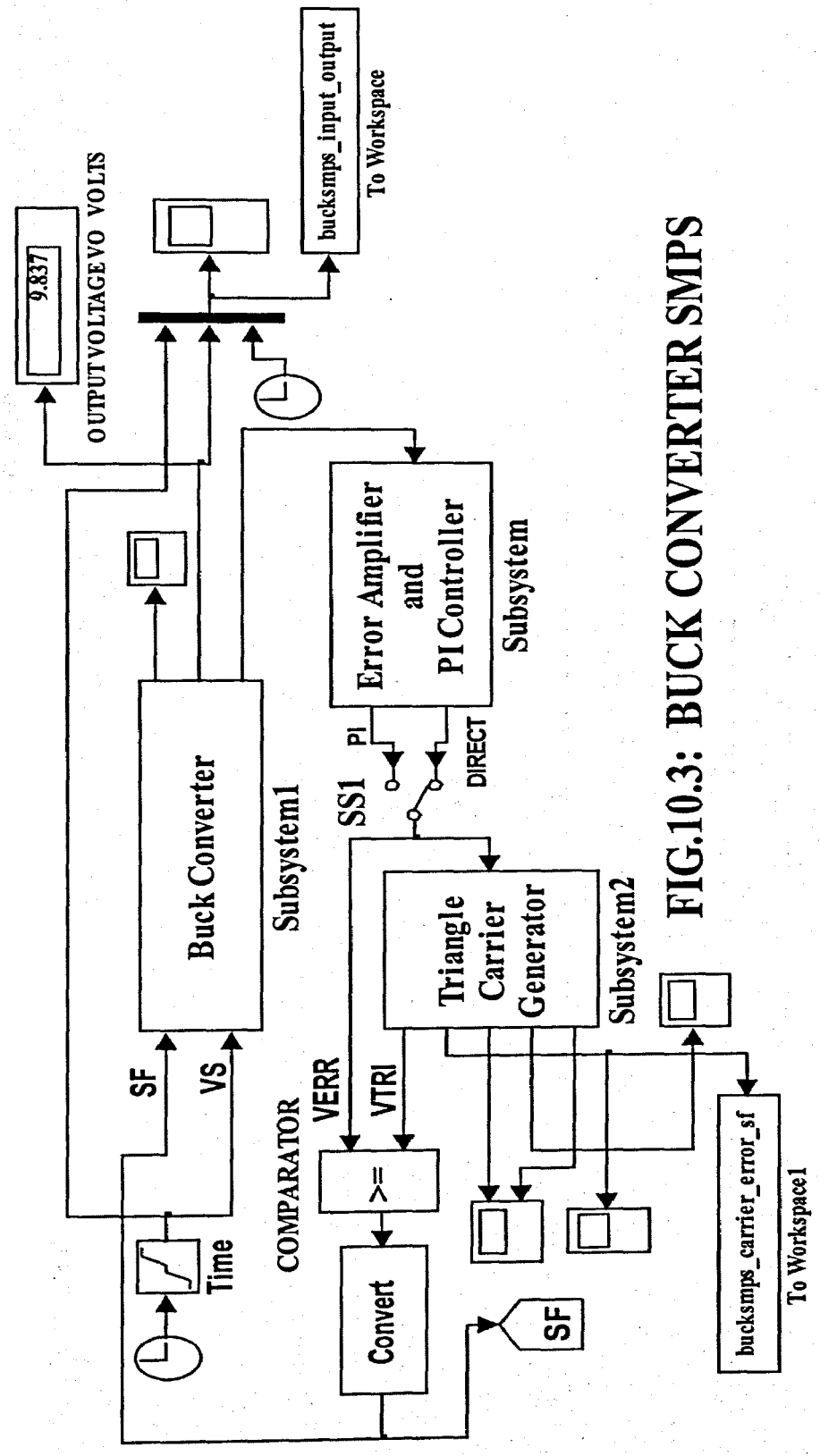

FIG.10.3: BUCK CONVERTER SMPS

Block Parameters: Subsystem2
Triangle Carrier Generator Unit (mask)
This is a Traingle Carrier Generator by integration of Square Pulse. The values for this is determined by the Switching Frequency of the SMPS. The values shown here are for a 100 kHZ switching frequency. The values for other switching frequencies are therefor obtained by trial and error only. Enter the value of amplitude of square pulse generator in Volts.
Switching Period in Seconds, k1, k2 and c in the appropriate box provided. The following function is used to genrate the triangle pulse:
k1*(k2*(u(1) - c). A general method for other switching frequencies of the SMPS is given below:
Let amplitude entered be Vsqm. Let Tsw be the switching period of the SMPS. Let Ton = Toff = Tsw /2. Let k1 = 1e5 be the gain constant entered.
Then during ON time of square pulse, triangle wave reaches the maximum value Vm(triangle) as given below:
Vm(triangle) = (Vsqm /2)*Ton*k1 = (Vsqm /2)*Ton*1e5.
During the OFF time of square pulse, traingle wave reaches the minimum value Vo(triangle) given below:
Vo(triangle) = (-Vsqm /2)*Toff *k1 +Vm(triangle)) = (-Vsqm /2)*Toff *1e5 +Vm(triangle)).
Using the above formula, triangle wave for other switching frequencies of the SMPS can be generated.
SELECTION OF CONSTANTS k1, k2 AND c:
The value of k1 is selcted consistant with the entered values of Vsqm and Tsw. If Tsw is an integer in microseconds then k1 will be a constant multiple of 1e5.
The value of function constant c will be [Vm(triangle) /2].
The value of k2 is suitably adjusted to get normal output voltage for normal input voltage without any type of PI or other controllers.
NOTE:
This triangle carrier generator is connected to the comparator block. If Vsn and Voutn are the normal input and normal output voltage respectively, then the normal duty cycle Dn of the buck converter is
Dn = Voutn / Vsn. Then slect the comparator operator as follows:
If Dn is equal to or greater than 0.5, then comparator operator selected must be greater than or equal to (>=).
If Dn is less than 0.5, then the comparator operator selected must be less than or equal to (<=).
Press Help for further details.
Parameters
Enter the amplitude in Volts
20
Enter the Switching Period in Seconds
10e-6
Enter the Gain Constant k1
1e5
Enter the Function Constants k2
1.1
Enter the Function Constant c
2.5
OK
Cancel
Help
Apply
Block Parameters: Subsystem1
Buck Converter Unit (mask)
Enter the Series Inductor L1 in Henries, Load Resistance RL in Ohms and the Filter Capacitance CF in Farads.
Parameters
Enter the Inductor in Henries
300e-6
Enter the Load Resistance in Ohms
10
Enter the Filter Capacitor in Farads
200e-6
OK
Cancel
Help
Apply
Block Parameters: Subsystem
Error Amplifier and PI Controller Unit (mask)
Enter the Potential Divider Constant, Reference Voltage in Volts, Proportionality Constant Kp and the Integran Constant Ki of PI controller in the appropriate Boxes provided.
Parameters
Enter the Potential Divider Constant
8/(9)
Enter the Reference Voltage in Volts
9
Enter Proportional Constant Kp of PI controller
0.1
Enter the Integral Constant Ki of PI Controller
6
OK
Cancel
Help
Apply
25%
lode15s

FIG.10.4(A)

FIG.10.4(B)

FIG.10.4(B)

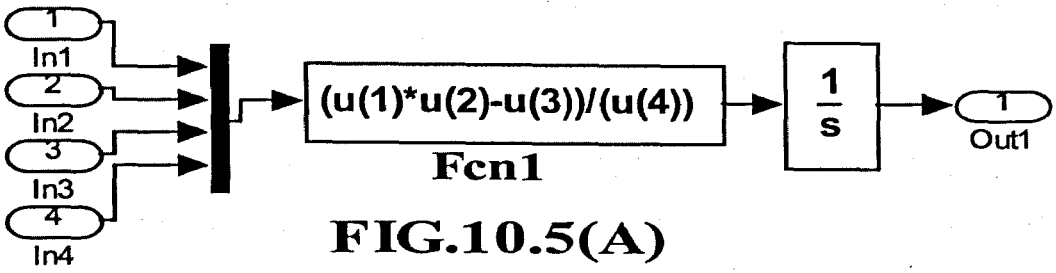

FIG.10.5(A)

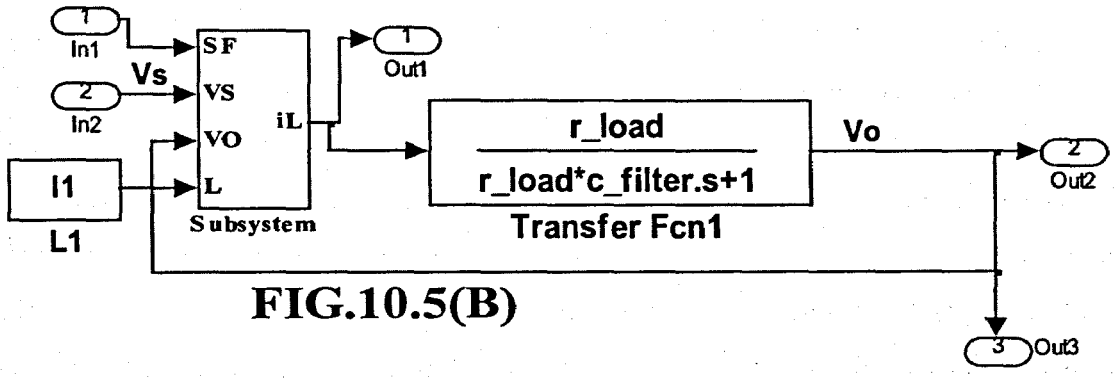

FIG.10.5(B)

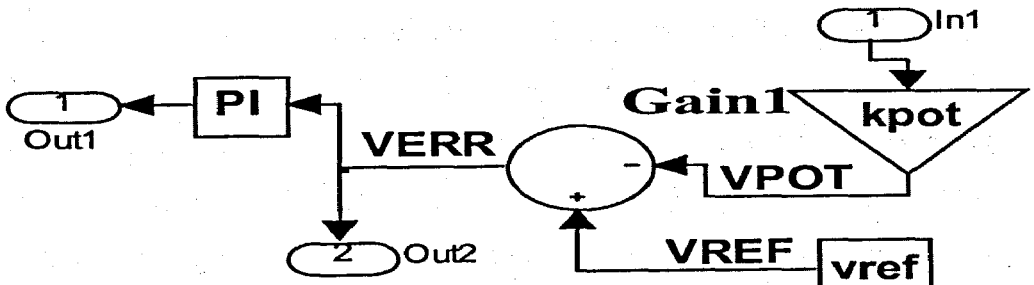

FIG.10.5(C)

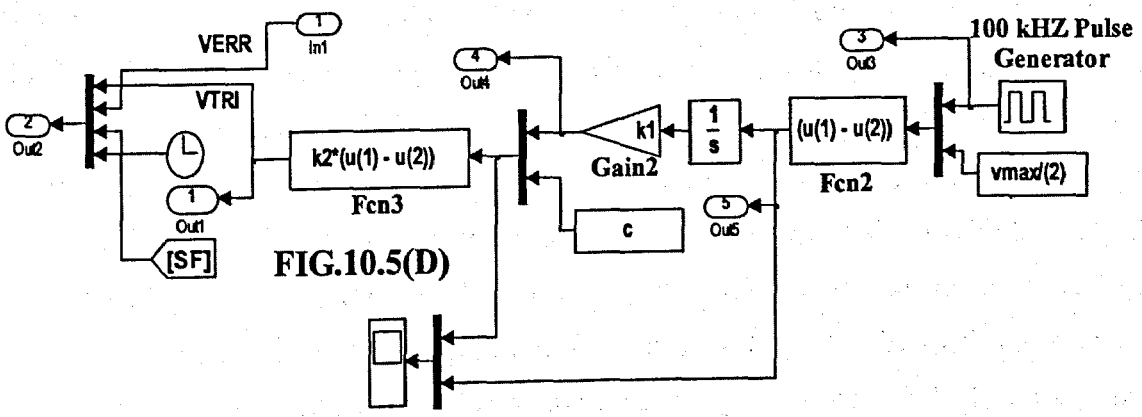

FIG.10.5(D)

subsystems are shown in Fig.10.5(A) to (D). A brief description of the various subsystems is given below:

Fig.10.5(A) and (B) shows the model of the Buck converter used in the SMPS. This corresponds to the dialog box "Buck Converter Unit" shown in Fig.10.4(A). The parameters relating to inductance, load resistance and filter capacitance are entered in the dialog box. The Buck converter circuit is shown in Fig.5.1 in Chapter 5. The modelling of Buck converter using the switching function concept is already discussed in section 5.2.1 of Chapter 5. The same modelling equations from 5.6 to 5.10 of Chapter 5 are used for modelling the Buck Converter used in this SMPS. Fig.10.5(C) corresponds to the dialog box "Error Amplifier and PI Controller" in Fig.10.4(A). The potential divider constant, reference voltage, Proportional constant Kp and Integral constant Ki are entered in the appropriate places in this dialog box. The output voltage Vo is multiplied by this potential divider constant kpot and compared in the error detector with the reference voltage VREF which produces the error output voltage VERR. A selector switch SS1 which directly selects VERR or this VERR through the PI Controller. This output from SS1 is given to comparator block in Fig.10.5(D). Fig.10.5(D) corresponds to the dialog box "Triangle Carrier Generator Unit" in Fig.10.4(A) and the help file shown in Fig.10.4(B). Here triangle carrier pulse is generated by integration of the square pulse. The amplitude of this square pulse, the switching period of SMPS, the gain constant k1, the two function constants k2 and c are entered in the appropriate places in the dialog box. In Fig.10.5(D), the Fcn2 block subtract the amplitude Vmax of the square pulse from half its value there by generating a square pulse with positive and negative peak of +Vmax /2 and –Vmax /2 respectively with a switching period Tsw of the SMPS. This is multiplied by k1 using gain2 block, then this value is subtracted from a constant c and the result is multiplied by another constant k2 using Fcn3 block to get the triangle carrier wave with the switching period of the SMPS. The dialog box "Triangle Carrier Generator Unit" along with the help file in Fig.10.4(B) provide the method to find constants k1, k2, c and the peak value of triangle carrier wave should the switching frequency of the SMPS be different from that of the given value of 100 kHZ.. The triangle carrier pulse output VTRI and the error output VERR either directly or through the PI controller are compared in the relational operator block which is the comparator unit. The convert block converts the logical or

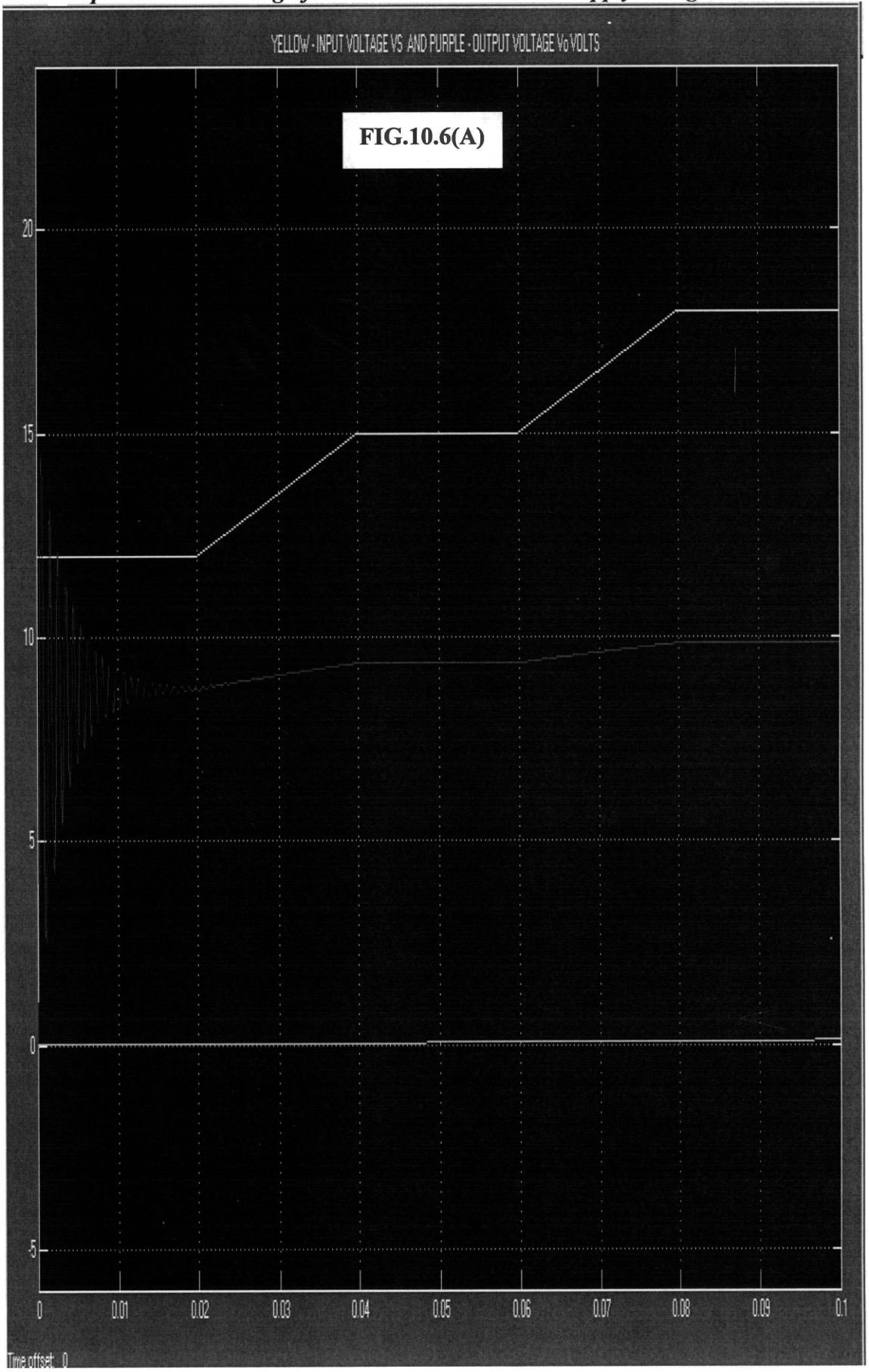
YELLOW - INPUT VOLTAGE VS AND PURPLE - OUTPUT VOLTAGE Vo VOLTS
FIG.10.6(A)
20
15
10
5
0
-5
0
0.01
0.02
0.03
0.04
0.05
0.06
0.07
0.08
0.09
0.1
Time offset: 0

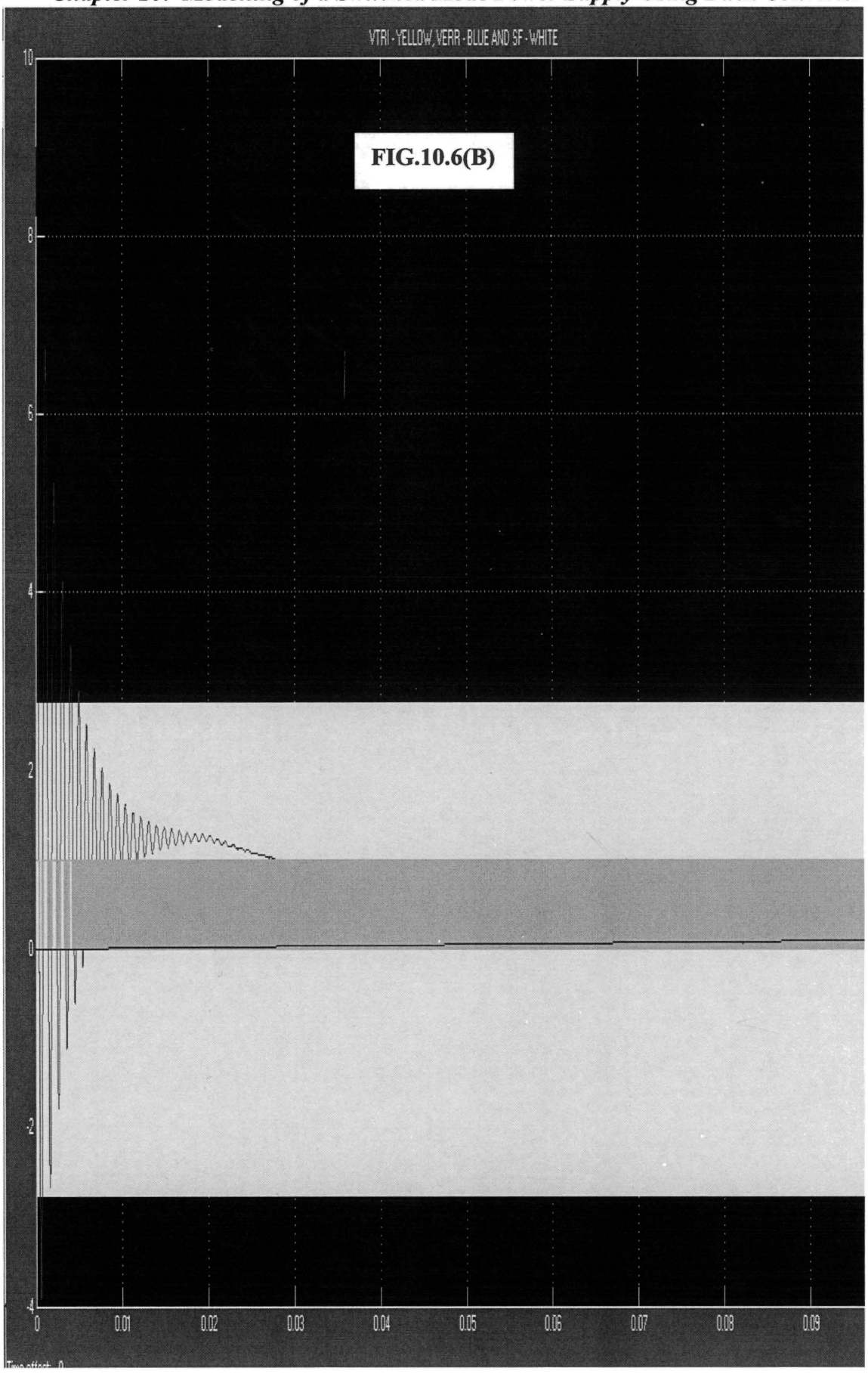
VTRI - YELLOW, VERR - BLUE AND SF - WHITE
10
8
6
4
2
0
-2
-4
0
0.01
0.02
0.03
0.04
0.05
0.06
0.07
0.08
0.09

FIG.10.6(B)

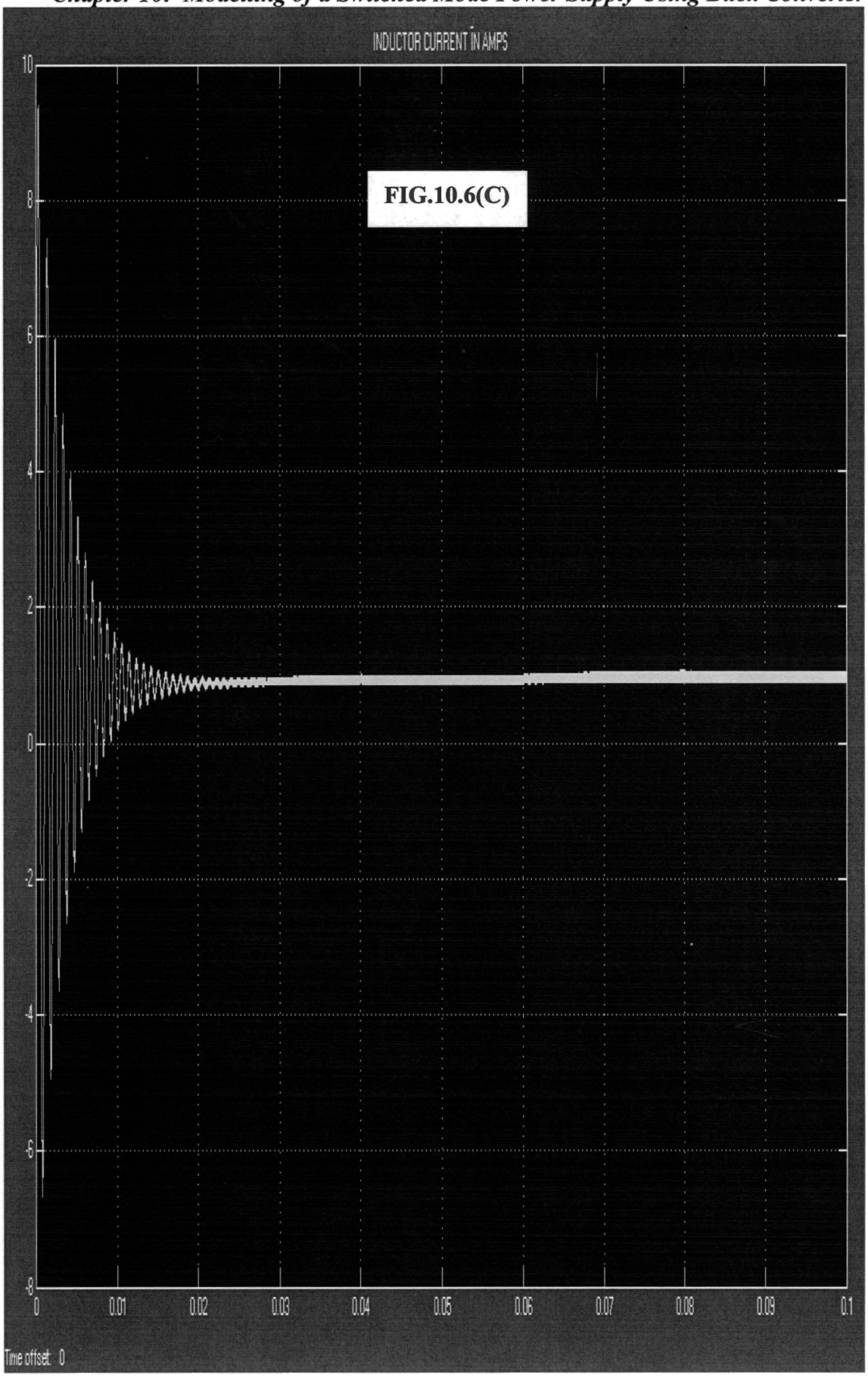
INDUCTOR CURRENT IN AMPS
10
8
6
4
2
0
-2
-4
-6
-8
0
0.01
0.02
0.03
0.04
0.05
0.06
0.07
0.08
0.09
0.1
Time offset: 0

FIG.10.6(C)

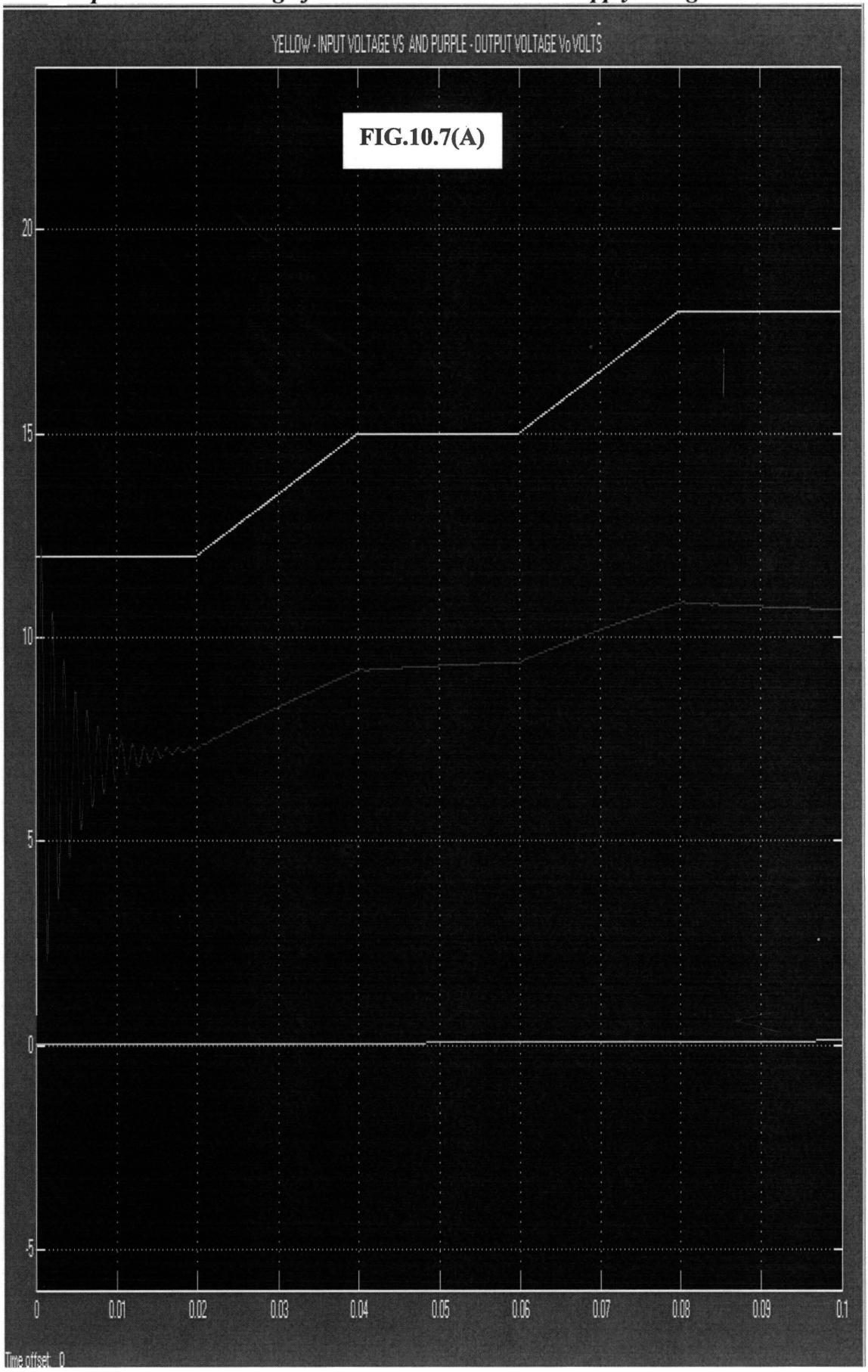
YELLOW - INPUT VOLTAGE VS AND PURPLE - OUTPUT VOLTAGE Vo VOLTS
FIG.10.7(A)
20
15
10
5
0
-5
0
0.01
0.02
0.03
0.04
0.05
0.06
0.07
0.08
0.09
0.1
Time offset: 0

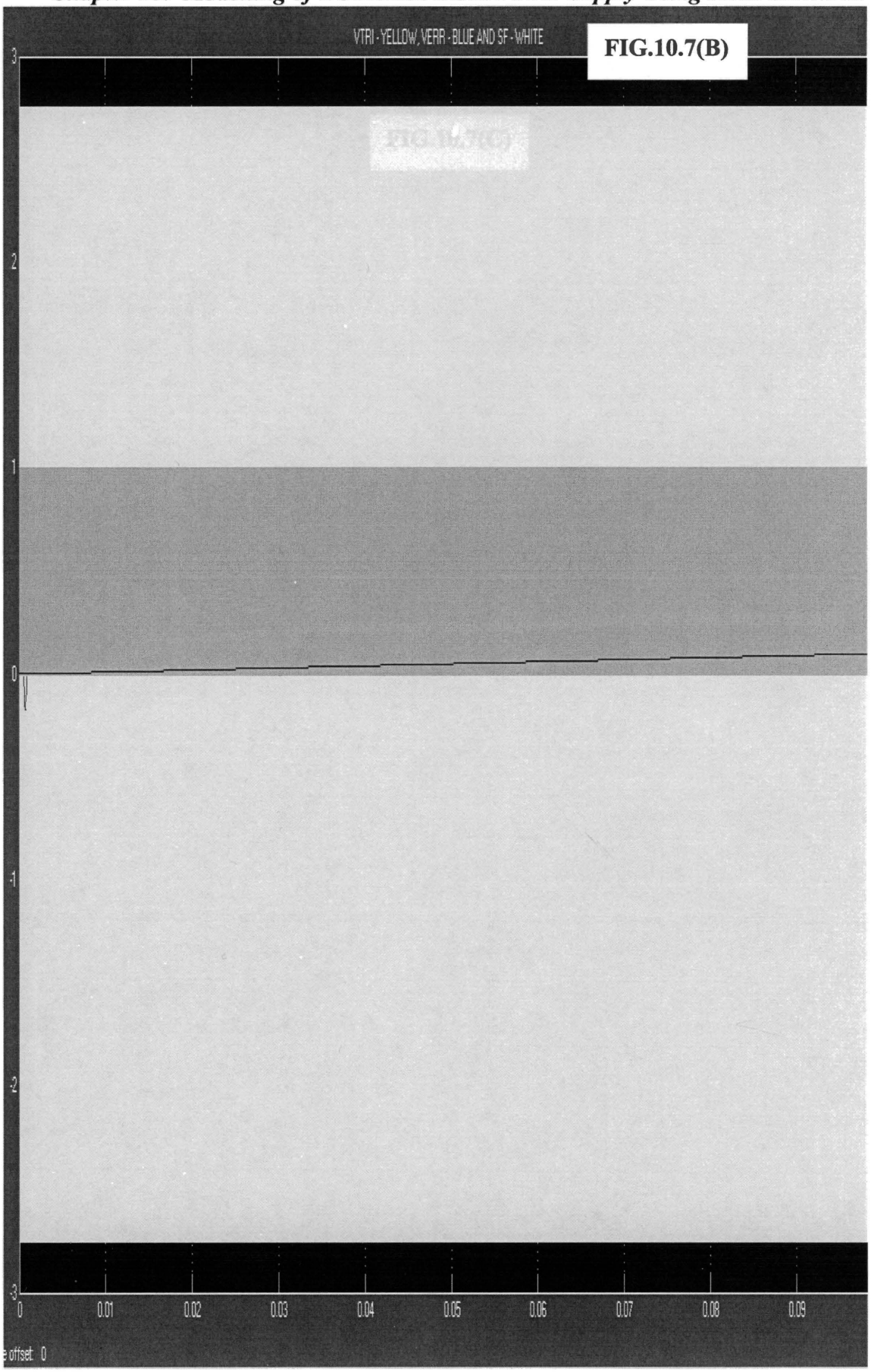
VTRI - YELLOW, VERR - BLUE AND SF - WHITE
3
2
1
0
-1
-2
-3
0
0.01
0.02
0.03
0.04
0.05
0.06
0.07
0.08
0.09
offset: 0

FIG.10.7(B)

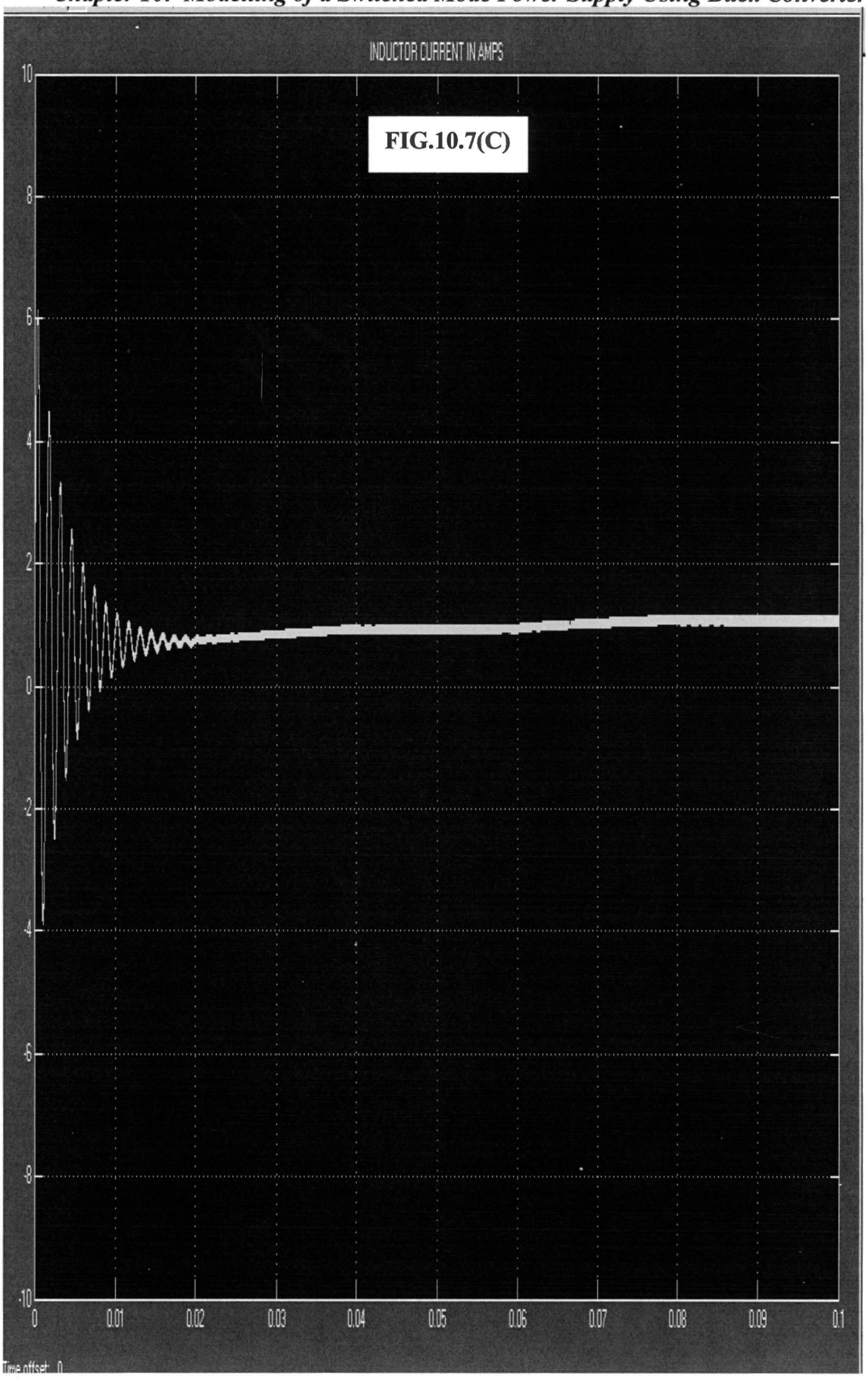
INDUCTOR CURRENT IN AMPS
10
8
6
4
2
0
-2
-4
-6
-8
-10
0
0.01
0.02
0.03
0.04
0.05
0.06
0.07
0.08
0.09
0.1
Time offset: 0

FIG.10.7(C)

Boolean output of the comparator to unsigned integer output. The comparator and convert blocks are shown in Fig.10.3. The selection of the relational operator for the comparator is also explained in the dialog box "Triangle Carrier Generator Unit" in Fig.10.4(A) and also in the help file in Fig.10.4(B). The output of the comparator is the switch function SF which drives the buck converter semiconductor switch.

10.3.1 Simulation Results

The simulation of the buck converter SMPS was conducted without and with PI controller using the ode15s (stiff/NDF) solver with a relative tolerance of 1e-3. The parameters of the SMPS are as shown in Table 10.1. A time varying input DC voltage source using look-up table was used in both cases. The simulation results of the input voltage, output voltage, triangular carrier, error voltage output VERR, switch function SF and the inductor current IL without the PI controller are shown in Fig.10.6(A), (B) and (C). The same results with PI controller are shown in Fig.10.7(A), (B) and (C) respectively.

10.4 Conclusions

The PSIM simulation results shown in Fig.10.2(A) and (B) indicate that the number of oscillation cycles and its peak to peak magnitude is reduced with PI controller as compared to without the PI controller. Examination of the simulation results of the model in Fig.10.6(A) and in Fig.10.7(A) indicates the following points:

- Without PI controller the number of initial switching cycles is as high as 11 for the first 0.01 seconds.
- With PI controller, the number of initial switching cycles is reduced from 11 to 7 for the first 0.01 seconds.
- The peak to peak voltage output during the initial switching cycle is reduced by around 2.4 volts with PI controller as compared to without the PI controller.
- The duty cycle of SF adjusts to a suitable value to maintain the output voltage Vo close to 9 Volts.

- The change in output voltage for a given change in input voltage or regulation of the SMPS is more with PI controller as compared to without the PI controller.
- The normal output voltage is close to 9 volts for a normal input voltage of 15 volts in both cases.

Depending on the chosen values of the parameters for the buck converter, the number of oscillation cycles and their peak values will change in both cases, with and without the PI controller.

CHAPTER 11
MODELLING OF A THREE PHASE PULSE WIDTH MODULATED INVERTER FED INDUCTION MOTOR DRIVE

11.1 Introduction

Many industrial applications require voltage control of inverters to maintain constant output voltage irrespective of variations in the input dc voltage and for constant voltage and frequency control requirements. This is achieved by Pulse Width Modulation commonly known as PWM technique. For three phase inverters, the commonly used PWM techniques are: 1) Sine PWM 2) Third Harmonic Injection PWM 3) Harmonic Injection PWM 4) Trapezoidal PWM 5) Delta Modulation and so on. This Chapter provides the modeling of the first three types of the above PWM techniques and in addition discusses the model of a newly discovered PWM technique known as Clipped Sinusoid PWM.

11.2 Three Phase Sine PWM Technique

The sine PWM is the most fundamental and widely used technique for voltage control of inverters. The principle of generation of the gating pulse for a three phase SINE PWM inverter using op.amps is shown in Fig.11.1(A), using MICROCAP 8. Three phase ac modulating signals at the switching frequency fm Hertz of the inverter is generated. This three phase modulating signal is compared with triangular carrier wave of frequency fc Hertz in a comparator and the resulting pulse width modulated output pulse and their respective inverted pulse in each phase is used to drive the semiconductor switches in each phase of the three phase inverter. The three phase 50 Hz ac sine modulating signal, triangular carrier signal of frequency 2 kHZ and the resulting gate pulse drive for the three phase inverter are shown in Fig.11.1(B) by simulation using MICROCAP 8.. The three phase inverter frequency output will be 50 Hz. If Am and Ac are the peak values of the sine modulating signal and that for the

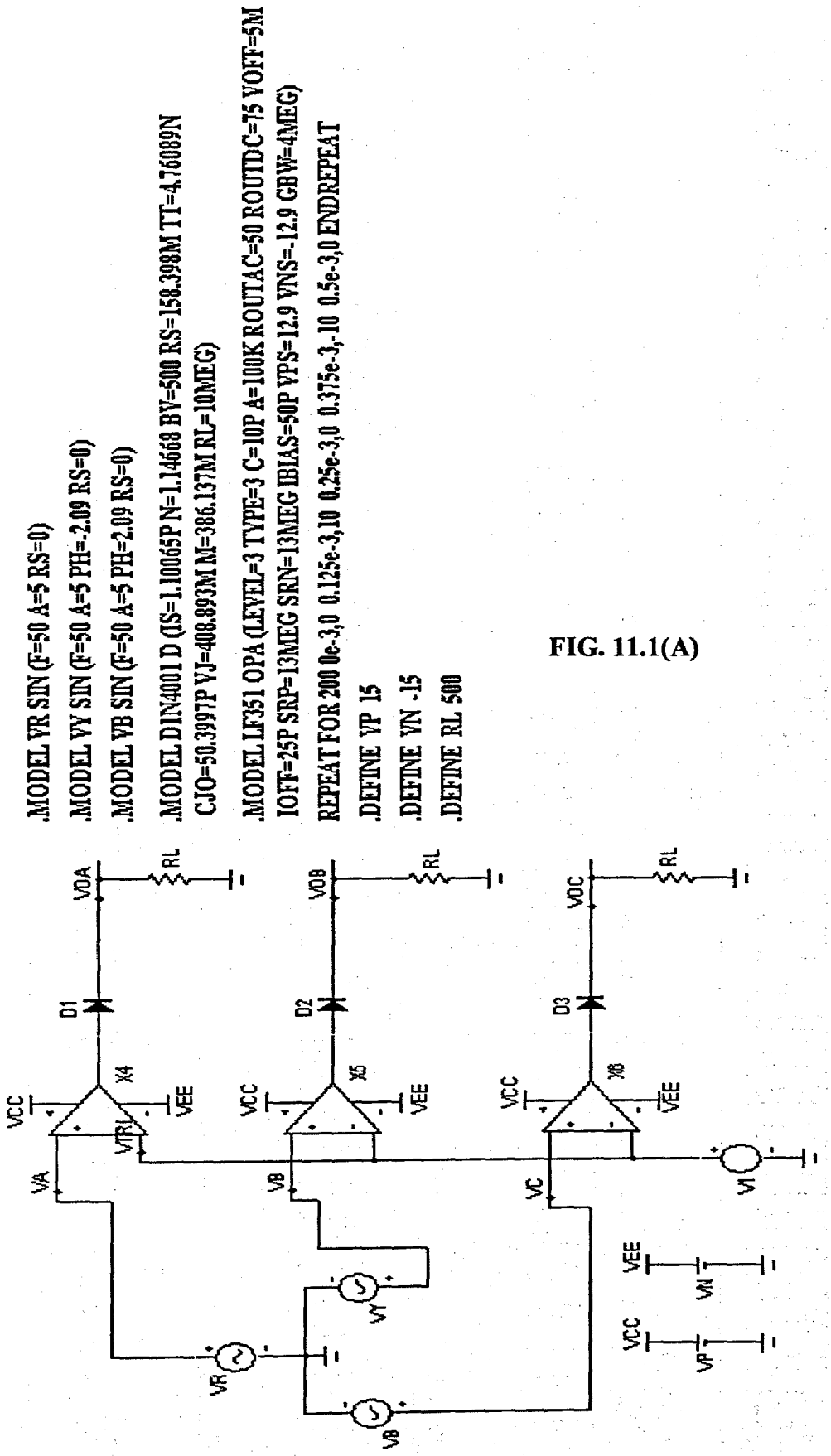
.MODEL VR SIN (F=50 A=5 RS=0)
.MODEL VY SIN (F=50 A=5 PH=-2.09 RS=0)
.MODEL VB SIN (F=50 A=5 PH=2.09 RS=0)
.MODEL D1N4001 D (IS=1.10065P N=1.14668 BV=500 RS=158.398M TT=4.76089N
CJO=50.3997P VJ=408.893M M=386.137M RL=10MEG)
.MODEL LF351 OPA (LEVEL=3 TYPE=3 C=10P A=100K ROUTAC=50 ROUTDC=75 VOFF=5M
IOFF=25P SRP=13MEG SRN=13MEG IBIAS=50P VPS=12.9 VNS=-12.9 GBW=4MEG)
REPEAT FOR 200 0e-3,0 0.125e-3,10 0.25e-3,0 0.375e-3,-10 0.5e-3,0 ENDREPEAT
.DEFINE VP 15
.DEFINE VN -15
.DEFINE RL 500
VDA
VDB
VDC
RL
D1
D2
D3
X4
X5
X6
VCC
VEE
VTRI
VA
VB
VC
VR
VY
VB
VN
VP
VI
THREE PHASE SINE PULSE WIDTH MODULATION

FIG. 11.1(A)

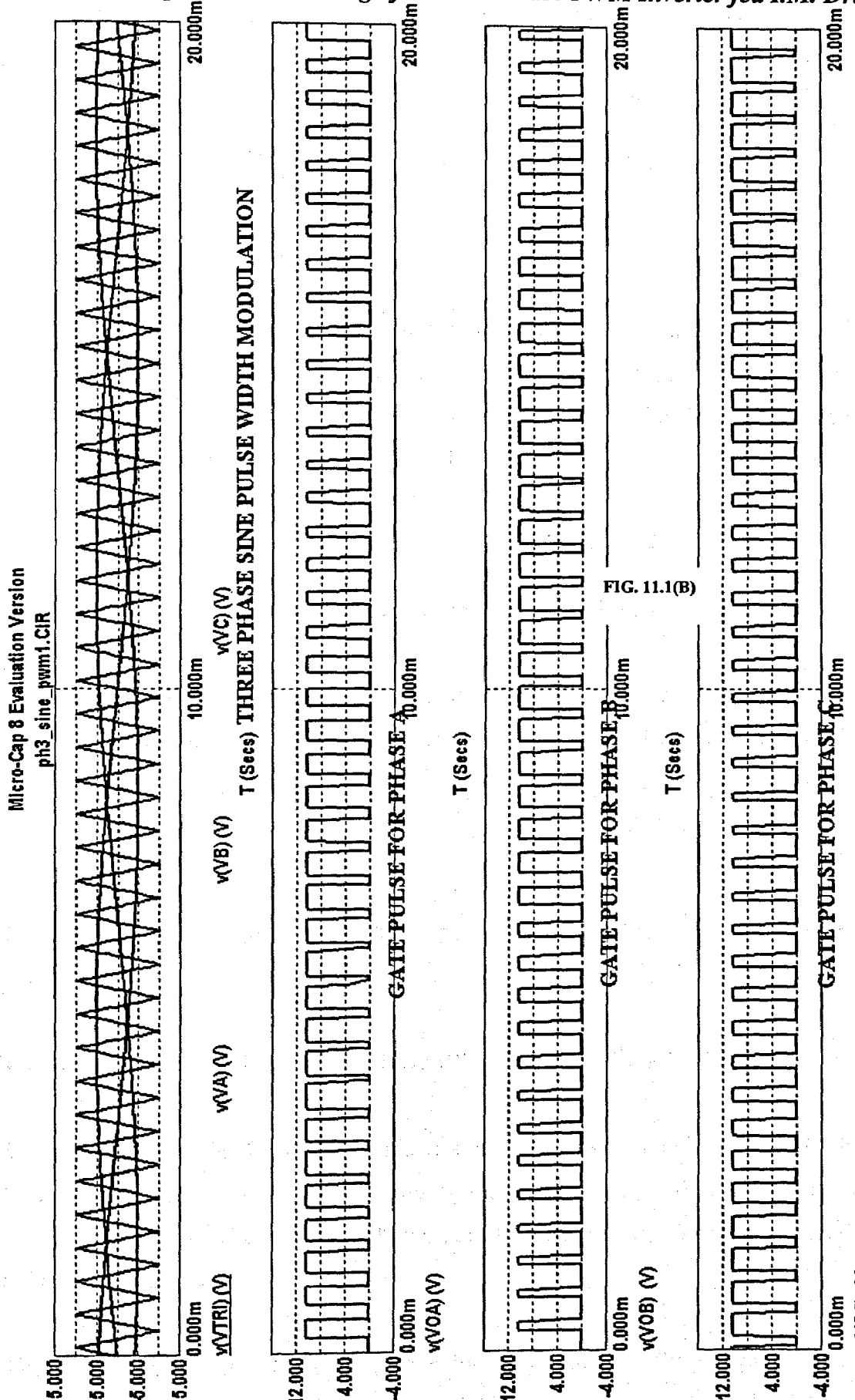
Micro-Cap 8 Evaluation Version
ph3_sine_pwm1.CIR
THREE PHASE SINE PULSE WIDTH MODULATION
v(VTRI) (V)
v(VA) (V)
v(VB) (V)
v(VC) (V)
T (Secs)
15.000
5.000
-5.000
-15.000
0.000m
10.000m
20.000m
GATE PULSE FOR PHASE A
GATE PULSE FOR PHASE B
GATE PULSE FOR PHASE C
v(VOA) (V)
v(VOB) (V)
v(VOC) (V)
12.000
4.000
-4.000

FIG. 11.1(B)

triangular carrier wave, then the Amplitude Modulation Index M and Frequency Modulation index FM are defined as follows:

$$M = \frac{A_m}{A_C} \qquad (11.1)$$

$$FM = \frac{f_C}{f_m} \qquad (11.2)$$

The region where $0 < M <= 1$ is called the linear region or under modulation region and the region where $M > 1$ is called the overmodulation region. In the linear region the maximum value of the fundamental component of the output line to line voltage v_{ab1} can be expressed as given below in equation 11.3:

$$v_{ab1} = \frac{M\sqrt{3}.V_{dc}}{2} \quad for \quad M \leq 1 \quad (11.3)$$

where Vdc is the dc link input voltage of the three phase inverter.

In the overmodulation region the maximum value of the n^{th} harmonic component of the line to line voltage output of the three phase inverter is given by equation 11.4 below:

$$v_{abn} = \frac{4.\sqrt{3}.V_{dc}}{2.n.\pi} \quad for \quad M > 1 \quad (11.4)$$

Thus by varying the value of M, the output voltage of the three phase inverter can be controlled.

11.2.1 Modelling of Three Phase Sine PWM Inverter fed I.M. Drive

The interactive model for the three phase sine PWM inverter fed IM drive is shown in Fig.11.2 [45-46]. The various dialog boxes are shown in Fig.11.3. The various subsystem detailed schematics are shown in Fig.11.4(A) to (E). The various subsystems are explained below:

The three subsystems "Switching Function Generator", "Three Phase Sine PWM Generator" and "Three Phase VSI" in Fig.11.4(A) correspond to the dialog box

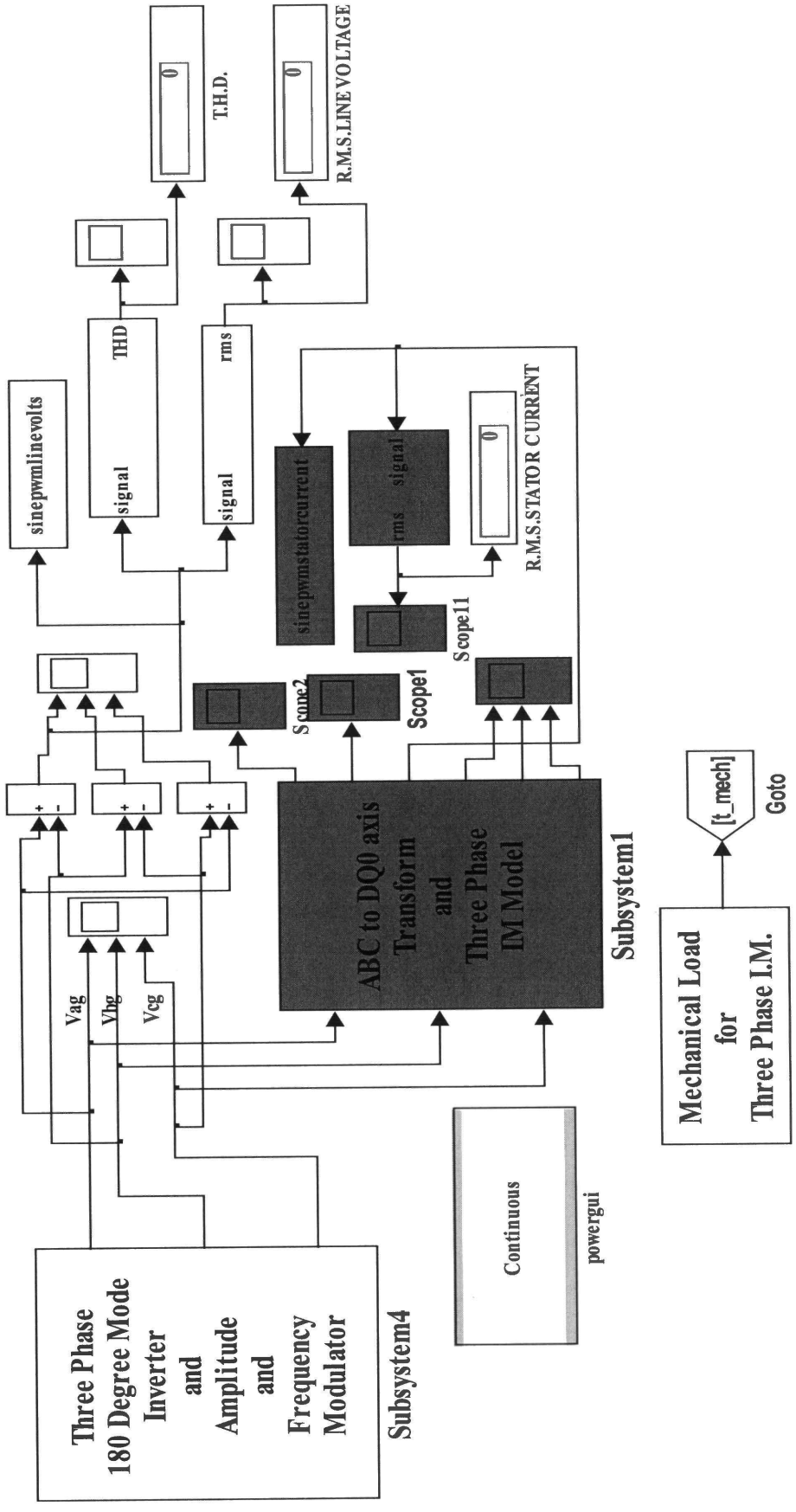

FIG.11.2: THREE PHASE SINE PWM INVERTER FED I.M. DRIVE

Block Parameters: Subsystem1
Three Phase IM Model in Stationary Reference Frame (mask)
Enter the Stator Resistance and Leakage Reactance, Rotor Resistance and Leakage Reactance referred to Stator, Mutual reactance between Stator and Rotor all per phase value, Number of Poles and combined Moment of Inertia of Rotor and Load in the appropriate unit in the box provided.
Parameters
Enter the Stator Resistance in Ohms per Phase
0.1062
Enter the Rotor Resistance referred to Stator in Ohms per Phase
0.0764
Enter the Stator Leakage Reactance in Ohms per Phase
0.2145
Enter the Rotor Leakage Reactance referred to Stator in Ohms per Phase
0.2145
Enter the Mutual Reactance between Stator and Rotor in Ohms per Phase
5.834
Enter the Number of Poles
4
Enter the Rated Angular Frequency of the Machine Radians per second
2*pi*60
Enter the combined M.I. of Rotor and Load in Kg-m^2
2.5
OK
Cancel
Help
Apply
Block Parameters: Subsystem
Three Phase Inverter and Amplitude and Frequency Modulator Unit (mask)
Enter the DC Link Voltage in Volts, peak value of the modulating sine wave vpeak, the frequency of the modulating signal fm in Hertz, carrier signal frequency fc in Hertz. The triangle carrier wave with a peak of +-10 Volts [20 volts p-p] is geniated with a carrier frequency fc by integration of the square pulse. Enter the amplitude of the square pulse vsqm, integration constant c, function constant k1 and multiplication constant k2 as positive integers. These constants vsqm, c, k1 and k2 generate carrier wave with frequency fc Heitz and amplitude 20 Volts(peak to peak). Press help for details.
NOTE: THE ACTUAL A.M. INDEX WILL BE THE ENTERED PEAK VALUE OF MDOULATING SINE WAVE DIVIDED BY TEN [vpeak /10]. THE F.M. INDEX WILL BE [fc / fm].
Parameters
Enter the DC Link Voltage of Inverter in Volts
286
Enter the Frequency of the Modulating Signal i.e. Inverter Frequency in Hertz
60
Enter the peak value of the modulating sine wave
1
Enter the Amplitude of the Square Pulse in Volts
30.4
Enter the Frequency of the Triangular Carrier Wave in Heitz
2e3
Enter the Integrator constant c
0.0001
Enter the Function Constant k1
19
Enter the Multiplication Constant k2
0.5263
OK
Cancel
Help
Block Parameters: Subsystem
Mechanical Load for Three Phase I.M. (mask)
Enter the initial value and final value of time in seconds and the corresponding initial and final values of mechanical load in Nw-meters in the appropriate box provided.
Parameters
Enter the initial time in seconds
0
Enter the Fianl time in seconds
2
Enter the initial value of load in Nw-meters
-0
Enter the final value of load in Nw-meters
-0
OK
Cancel
Help
Apply

FIG. 11.3

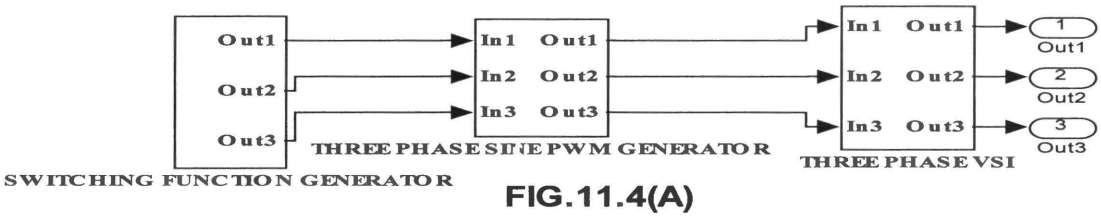

FIG.11.4(A)

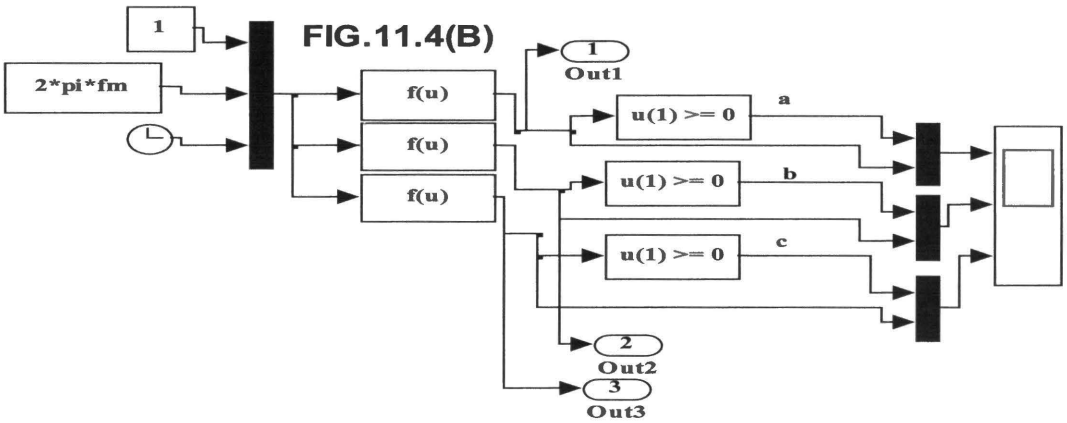

FIG.11.4(B)

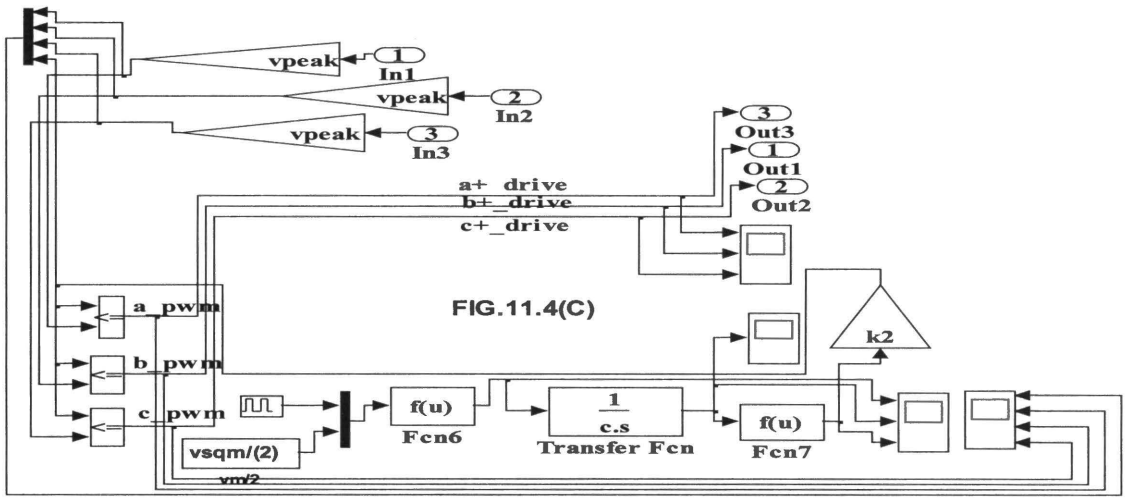

FIG.11.4(C)

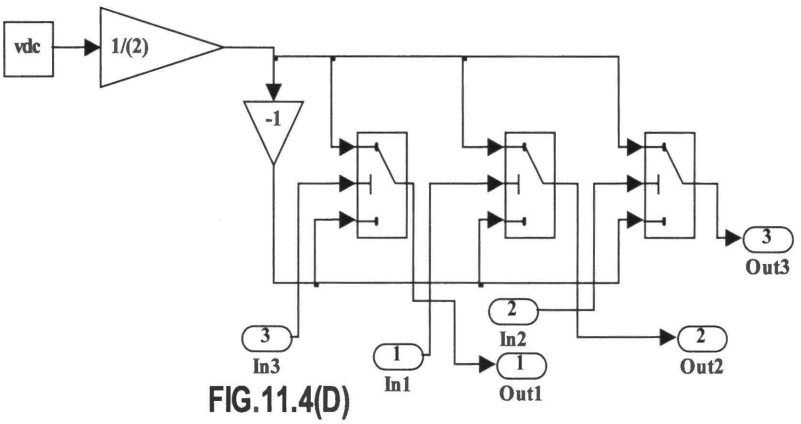

FIG.11.4(D)

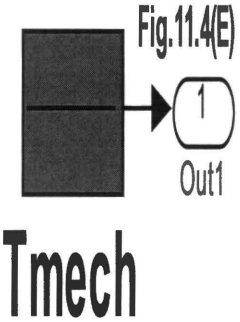

Fig.11.4(E)

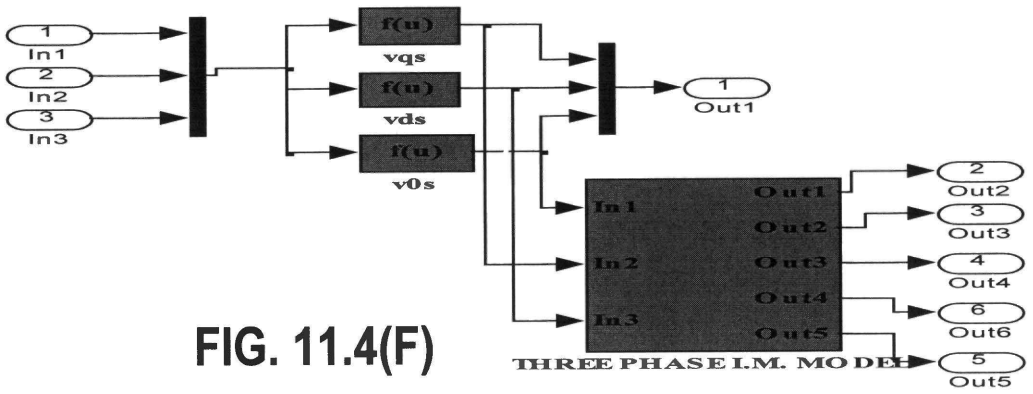

FIG. 11.4(F)

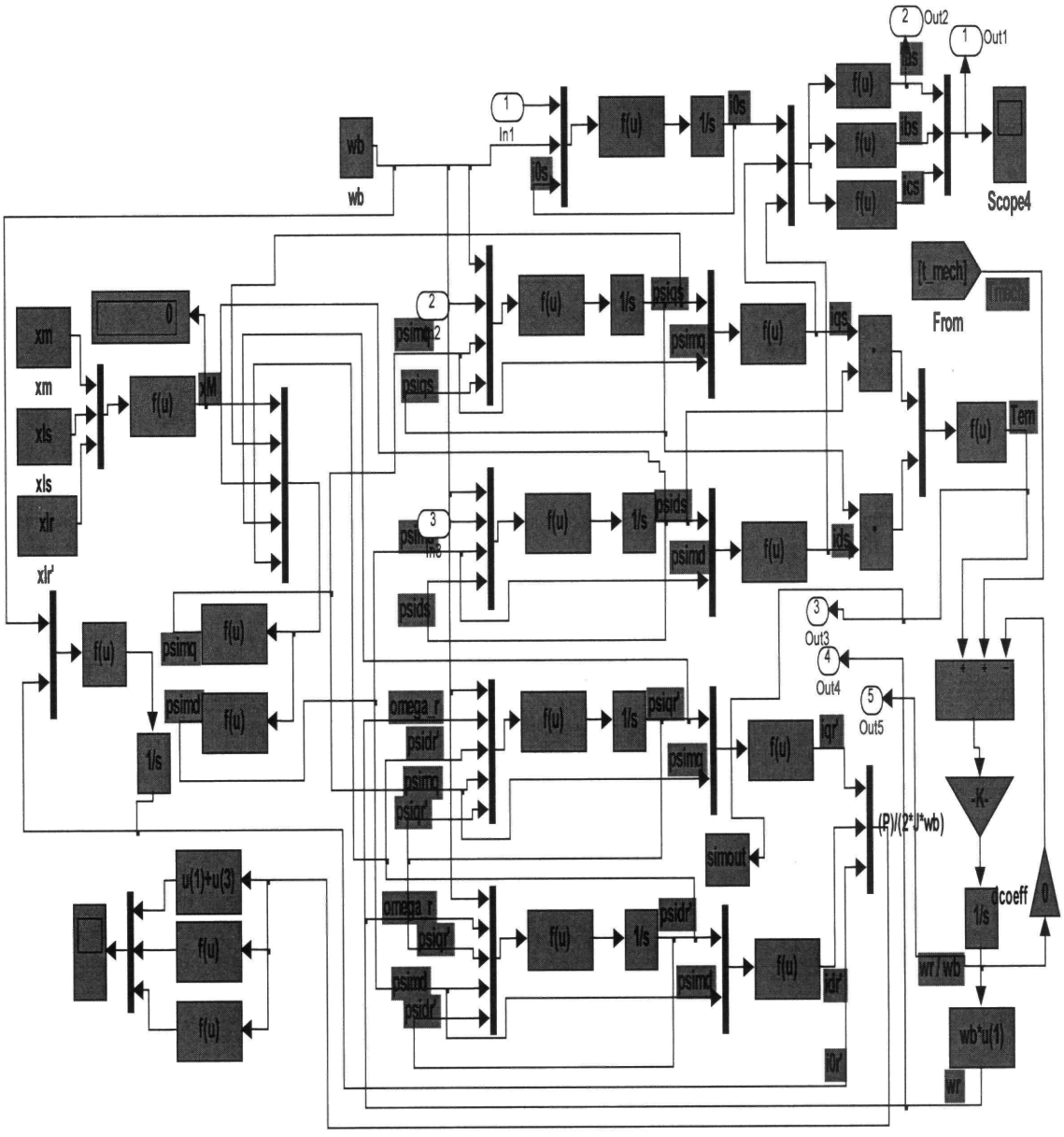

FIG. 11.4(G)


Help
File Edit View Go Favorites Desktop Window Help
Title: Simulink Masked Block: Three Phase Inverter and Amplitude and Frequency Modulator Unit
Using Simulink
Block Reference
Three Phase Inverter and Amplitude and Frequency Modulator Unit
The triangle carrier wave with frequency fc Hertz and amplitude +-10 Volts(20 V p-p) is obtained by integration of the square pulse and multiplying the result by appropriate constants. The values shown in this model are for a carrier frequency of 2 kHZ. For any other carrier frequency fc1, the following procedure may be used: Let vsqm be the amplitude of the square wave and fc1 the frequency entered. Then ON time Ton = OFF time Toff = Tc1 /2, where Tc1 = 1/ fc1. Let c be the integrator constant entered. Then the triangle wave at the output of integrator ramps up during the ON time to a peak value Vm(triangle) given by the following relation: Vm(triangle) = (+vsqm /2)*Ton*(1 /c) = (+vsqm /2)*(Tc1 /2)*(1 /c) ....(1) During the OFF time of the square pulse, the triangle wave ramps down to a value Vo(triangle) given by the following relation: Vo(triangle) = (-vsqm /2)*Toff * (1 /c) + Vm(triangle) = (-vsqm /2)*(Tc1 /2)*(1 /c) + Vm(triangle)...(2). Calculate this Vm(triangle). Then Function Constant k1 = [Vm(triangle) /2]. To get 20 Volts peak to peak, calculate k2 using the formula k2 = (10 / k1) . NOTE: THE ACTUAL A.M. INDEX WILL BE THE ENTERED PEAK VALUE OF MDOULATING SINE WAVE DIVIDED BY TEN (vpeak /10). THE F.M. INDEX WILL BE (fc / fm).
Start
Desktop
My Documents
My Documents
3:01 PM

FIG. 11.4(H)

"Three Phase Inverter and Amplitude and Frequency Modulator Unit" in Fig.11.3 and their models are shown in Fig.11.4(B) to (D).

In Fig.11.4(B) three phase ac with amplitude 1 volt and frequency fm (60Hz) Hertz of the sine wave modulating signal is generated using three Fcn blocks connected to the mux. The three phase ac output of this sine modulating signal is given to three gain blocks with gain vpeak in Fig.11.4(C). The output of these three gain blocks are three phase sine wave modulating signal with a peak value of vpeak. The triangle carrier wave of frequency fc Hz (2 kHz) is generated by integration of the square pulse whose amplitude is Vsqm and frequency fc Hz. The Fcn6 block subtracts this square pulse from Vsqm /2 generating square wave with positive and negative peaks of +Vsqm /2 and –Vsqm /2 respectively. This is then integrated multiplied with a constant of integration 1 /c to get a triangle carrier wave with a maximum value of +Vm(triangle) /2 and minimum value of zero. This triangle carrier wave is then subtracted from the constant k1 to get a triangle carrier wave with a positive and negative peaks of +Vm(triangle) /2 and –Vm(triangle) /2 respectively using Fcn7 block. The value of k1 is +Vm(triangle) /2. The output of Fcn7 block is then multiplied by k2 to get a triangle carrier wave with a positive and negative peak of +10 Volts and -10 Volts respectively. The value of k2 is 10 / k1. The values shown in the dialog box are for generating a carrier wave of 2 kHZ frequency. For any other frequency of the carrier wave the method shown in Fig.11.4(H) can be used. The values relating to dc link voltage of the three phase inverter, modulating signal frequency i.e. inverter frequency, amplitude of the modulating signal vpeak, Vsqm, fc, c, k1 and k2 are entered in the appropriate box. The amplitude modulation index M is the entered value of vpeak /10. This triangle carrier wave and the three phase modulating sine wave ac are compared in the three relational operator blocks used as comparators. The three comparators output the three phase gating pulse a_pwm, b_pwm and c_pwm for the three phase inverter. Fig.11.4(D) shows the model of the three phase inverter. The gating pulse a_pwm, b_pwm and c_pwm are given to the u(2) input of three threshold switches. The u(1) and u(3) inputs to these three switches are the +Vdc /2 and –Vdc /2 inputs. The threshold value for these three switches are 0.5 respectively. When the respective u(2) input of these three switches goes to logic 1, the output is +Vdc /2 and when u(2) is logic 0, the output is –Vdc /2. Thus three phase line to ground voltage is generated.

Fig.11.4(E) correspond to the dialog box "Mechanical Load for Three Phase IM" in Fig.11.3. This block is developed using the Repeating Sequence Block. Fig.11.4(F) and (G) corresponds to the dialog box "Three Phase IM Model in Stationary Reference Frame" in Fig.11.3. Fig.11.4(F) is the model for generating abc to dq0 axis transformation. The three inputs to the mux are the three phase line to ground voltages from the three phase inverter shown in Fig.11.4(D). The abc to dq0 axis transformation of these three phase voltages are performed using three Fcn blocks as per the transformation matrix given by equation 1.1 in Chapter 1, where the value of θ is set to zero. Fig.11.4(G) corresponds to the model of three phase IM in the stationary reference frame using the dq0-axis flux linkage per second equations and machine reactances. The modeling equations used for developing the three phase IM model in the stationary reference frame are given below:

$$\psi^{s}_{qs} = \omega_b \cdot \int \left\{ v^{s}_{qs} + \frac{r_s \cdot (\psi^{s}_{mq} - \psi^{s}_{qs})}{x_{ls}} \right\} . dt$$

$$\psi^{s}_{ds} = \omega_b \cdot \int \left\{ v^{s}_{ds} + \frac{r_s \cdot (\psi^{s}_{md} - \psi^{s}_{ds})}{x_{ls}} \right\} . dt$$

$$i^{s}_{0s} = \frac{\omega_b}{x_{ls}} \cdot \int \left\{ v_{0s} - i_{0s} \cdot r_s \right\} . dt \quad \text{.....(11.5)}$$

$$\psi'^{s}_{qr} = \omega_b \cdot \int \left\{ v'^{s}_{qr} + \frac{\omega_r \cdot \psi'^{s}_{dr}}{\omega_b} + \frac{r'_r \cdot (\psi^{s}_{mq} - \psi'^{s}_{qr})}{x'_{lr}} \right\} . dt$$

$$\psi'^{s}_{dr} = \omega_b \cdot \int \left\{ v'^{s}_{dr} - \frac{\omega_r \cdot \psi'^{s}_{qr}}{\omega_b} + \frac{r'_r \cdot (\psi^{s}_{md} - \psi'^{s}_{dr})}{x'_{lr}} \right\} . dt$$

$$i'_{0r} = \frac{\omega_b}{x'_{lr}} \cdot \int \left\{ v'_{0r} - i'_{0r} \cdot r'_r \right\} . dt \quad \text{.....(11.6)}$$

$$\psi^{s}_{mq} = x_m \cdot (i^{s}_{qs} + i'^{s}_{qr})$$

$$\psi^{s}_{md} = x_m \cdot (i^{s}_{ds} + i'^{s}_{dr}) \quad \text{.....(11.7)}$$

$$\psi^s_{qs} = x_{ls}.i^s_{qs} + \psi^s_{mq} \quad \ldots\ldots\ldots\ldots i^s_{qs} = \frac{\psi^s_{qs} - \psi^s_{mq}}{x_{ls}}$$

$$\psi^s_{ds} = x_{ls}.i^s_{ds} + \psi^s_{md} \quad \ldots\ldots\ldots\ldots i^s_{ds} = \frac{\psi^s_{ds} - \psi^s_{md}}{x_{ls}} \qquad (11.8)$$

$$\psi^{rs}_{qr} = x'_{lr}.i^{rs}_{qr} + \psi^s_{mq} \quad \ldots\ldots\ldots\ldots i^{rs}_{qr} = \frac{\psi^{rs}_{qr} - \psi^s_{mq}}{x'_{lr}}$$

$$\psi^{rs}_{dr} = x'_{lr}.i^{rs}_{dr} + \psi^s_{md} \quad \ldots\ldots\ldots\ldots i^{rs}_{dr} = \frac{\psi^{rs}_{dr} - \psi^s_{md}}{x'_{lr}} \quad \ldots\ldots(11.9)$$

$$\frac{1}{x_M} = \frac{1}{x_m} + \frac{1}{x_{ls}} + \frac{1}{x'_{lr}} \quad \ldots\ldots\ldots\ldots\ldots\ldots(11.10)$$

$$\psi^s_{mq} = x_M \cdot \left(\frac{\psi^s_{qs}}{x_{ls}} + \frac{\psi'^s_{qr}}{x'_{lr}} \right)$$

$$\psi^s_{md} = x_M \cdot \left(\frac{\psi^s_{ds}}{x_{ls}} + \frac{\psi'^s_{dr}}{x'_{lr}} \right) \quad \ldots\ldots\ldots\ldots\ldots\ldots(11.11)$$

The e.m. torque equation of the three phase IM is given below:

$$T_{em} = \frac{3}{2} \cdot \frac{P}{2.\omega_b} \cdot \left(\psi^s_{ds}.i^s_{qs} - \psi^s_{qs}.i^s_{ds} \right) \ldots Nm \ldots\ldots\ldots(11.12)$$

$$J.\frac{d\omega_{rm}}{dt} = T_{em} + T_{mech} - T_{damp} \ldots\ldots Nm \ldots\ldots\ldots(11.13)$$

The flux linkage per second equations for qd-axis corresponding to stator and rotor given by equations 11.5 and 11.6 are solved using Fcn blocks and integrator with appropriate inputs connected to MUX. The qd-axis currents for the stator and rotor given by equations 11.8 and 11.9 are solved using Fcn blocks and the appropriate inputs connected to the two input MUX. The zero axis stator and rotor currents given by equations 11.5 and 11.6 are solved using the Fcn blocks and integrator with appropriate inputs connected to the mux. The constant blocks marked xm, xls and xlr with the three

input mux and FCn block solves for x_M given by equation 11.10. The e.m. torque equation given by 11.12 is solved using the appropriate inputs to the multiplier blocks, Fcn block and the two input mux. Finally the dq0 to abc axis transformation of the stator and rotor currents are performed using three input mux and three Fcn blocks as per the transformation matrix given by equation 1.2 in Chapter with the value of θ set to zero.

11.2.2 Simulation Results

The simulation results of the Three Phase 60 Hz Sine PWM Inverter fed IM drive using ode15s(stiff/NDF) solver are shown in Fig.11.5(A) to (E) and in Fig.11.6(A) to (E) for a.m. indices M of 0.9 and 1.1 respectively, with f.m. index maintained at 33.33.. The simulation results for all the a.m. indices less than and greater than one are tabulated in Table 11.1. The DC Link Voltage of the three phase inverter is 286 volts. The value of fm and fc are 60 Hz and 2 kHZ respectively. The data for the 20 hp, 220 volts three phase, 60 Hz, 4 pole star connected cage IM used for simulation are given below [11].:

rs = 0.1062 ohms/ph, rr' = 0.0764 ohms/ph, xm = 5.834, ohms/ph, xls = 0.2145 ohms/ph, xlr' = 0.2145 ohms/ph, M.I. of rotor = 2.5 kg-m^2., rated current is 49.68 amps, rated speed 1748.3 rev/min and rated slip 0.0287. The rated torque is 81.49 nw-m and the slip at which maximum torque occurs is 0.1758 [11]. These data are shown in the dialog boxes in Fig.11.3.

11.3 Three Phase Third Harmonic Injection PWM Technique

To increase the output line to line voltage and to reduce its third harmonic components in a three phase inverter, in comparison with sine PWM inverter, THIPWM technique was proposed [49-50]. In THIPWM a 17 % third harmonic component is added to the original sine reference waveform. The reference waveform is given below [49-50]:

$$y = 1.15*[\sin(\omega.t) + (1/6)*\sin(3.\omega.t)] \ldots \qquad (11.14)$$

Using the above PWM techniques it is possible to achieve up to 15 % increase in the line to line voltage of the inverter without over modulation, pulse dropping and without

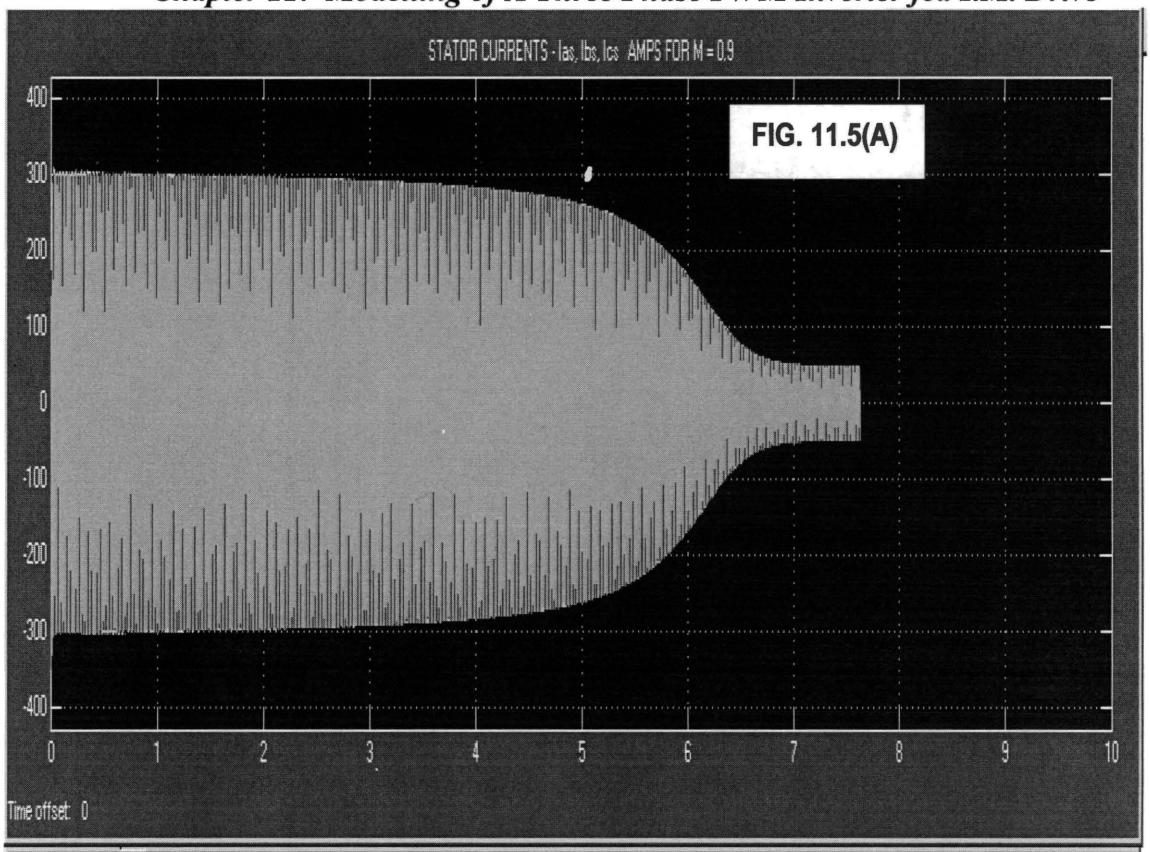

FIG. 11.5(A)

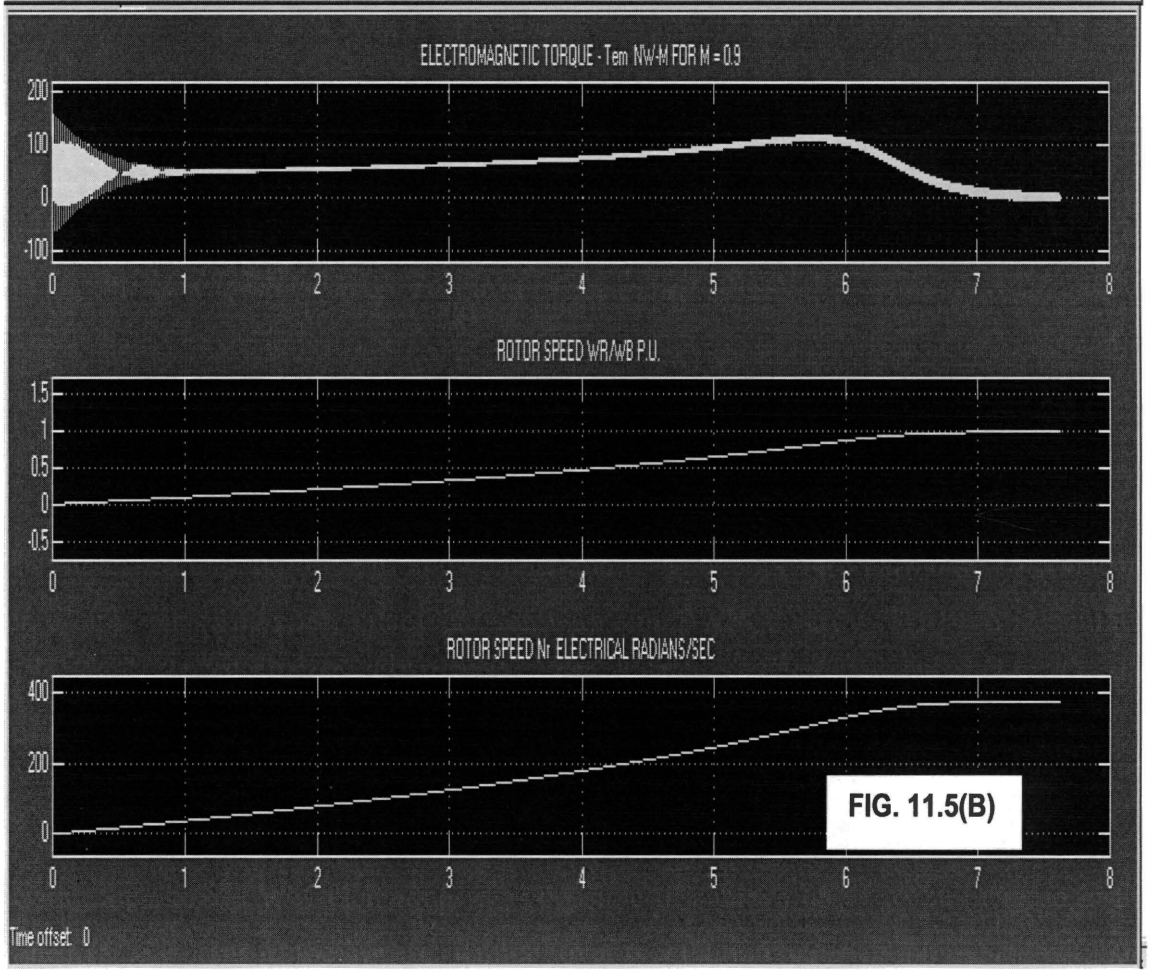

FIG. 11.5(B)

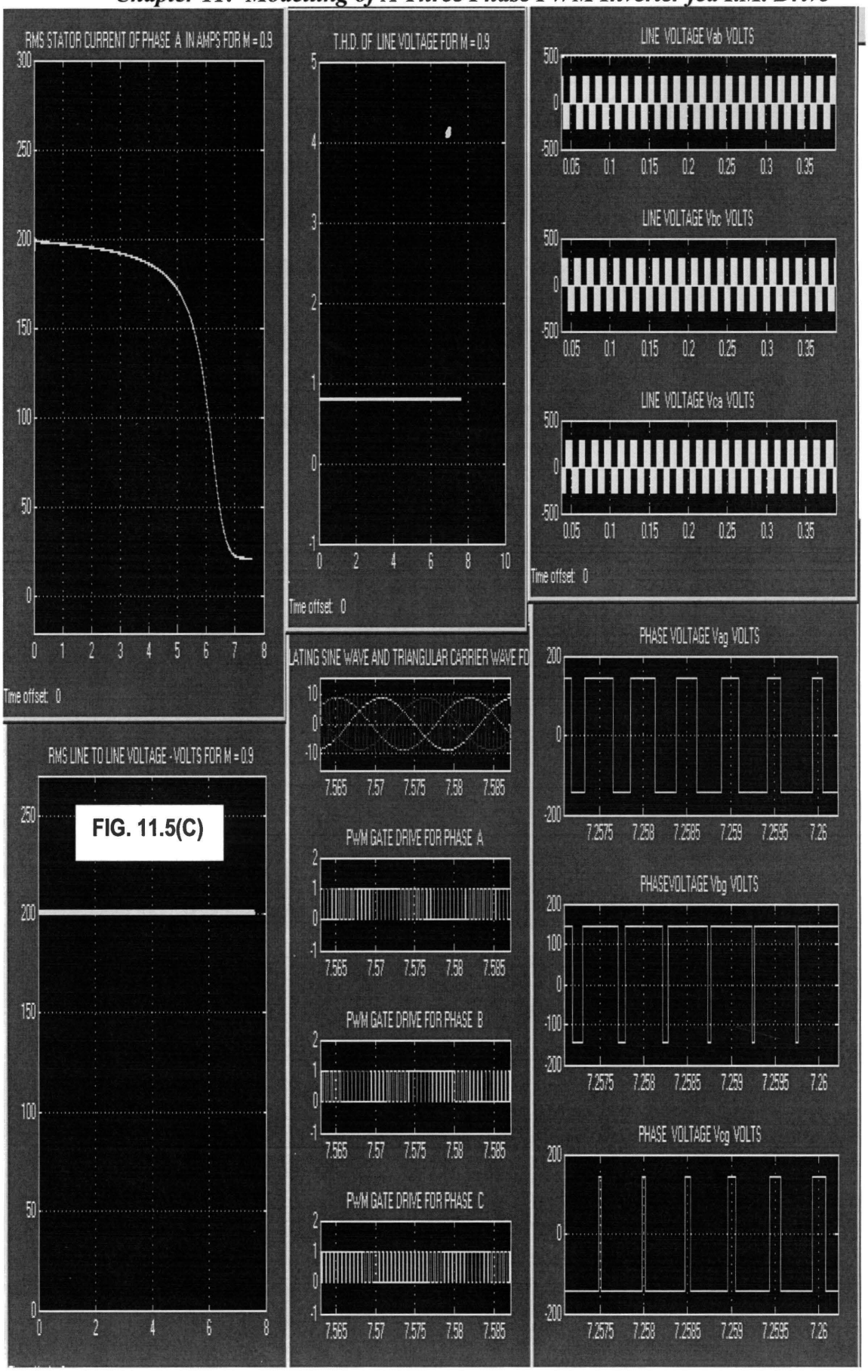
RMS STATOR CURRENT OF PHASE A IN AMPS FOR M = 0.9
Time offset: 0
T.H.D. OF LINE VOLTAGE FOR M = 0.9
Time offset: 0
LINE VOLTAGE Vab VOLTS
LINE VOLTAGE Vbc VOLTS
LINE VOLTAGE Vca VOLTS
Time offset: 0
LATING SINE WAVE AND TRIANGULAR CARRIER WAVE FO
PWM GATE DRIVE FOR PHASE A
PWM GATE DRIVE FOR PHASE B
PWM GATE DRIVE FOR PHASE C
PHASE VOLTAGE Vag VOLTS
PHASEVOLTAGE Vbg VOLTS
PHASE VOLTAGE Vcg VOLTS
RMS LINE TO LINE VOLTAGE - VOLTS FOR M = 0.9
FIG. 11.5(C)

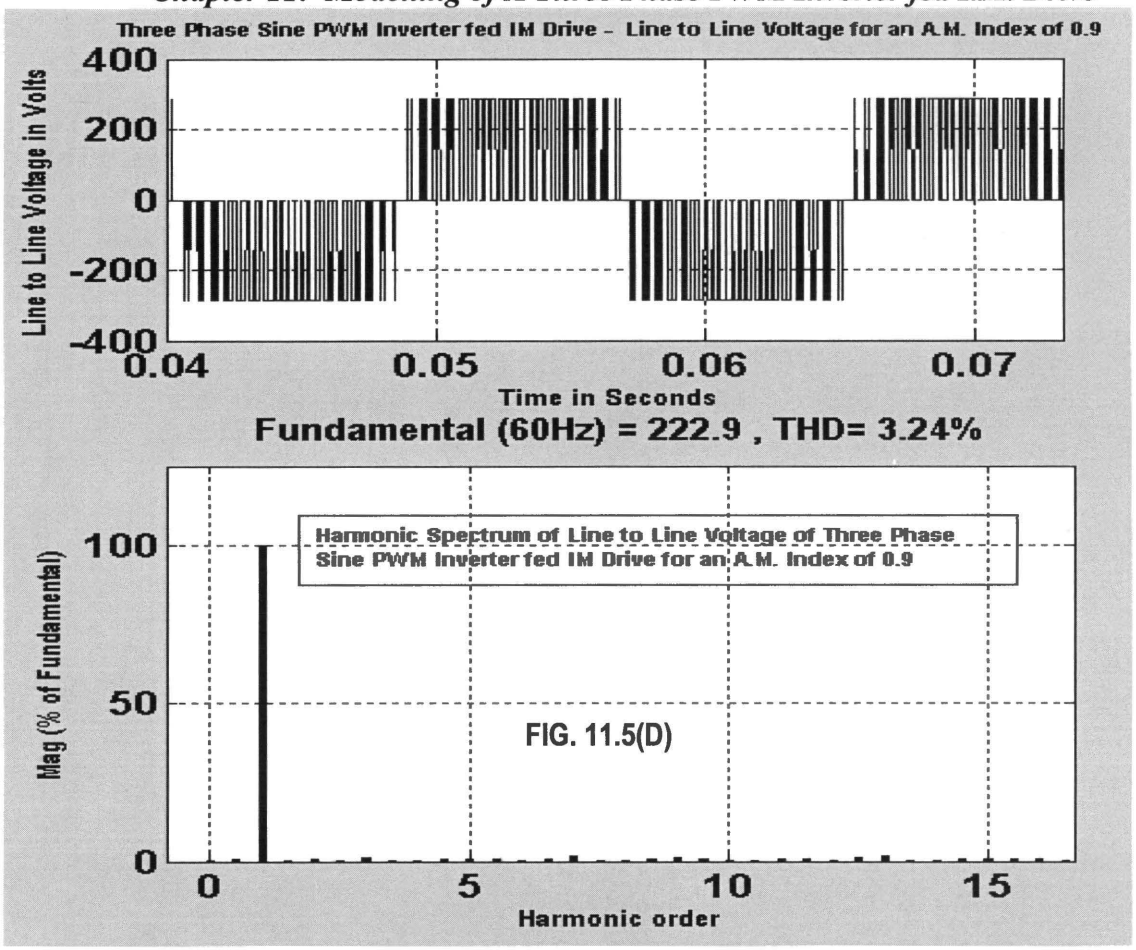

FIG. 11.5(D)

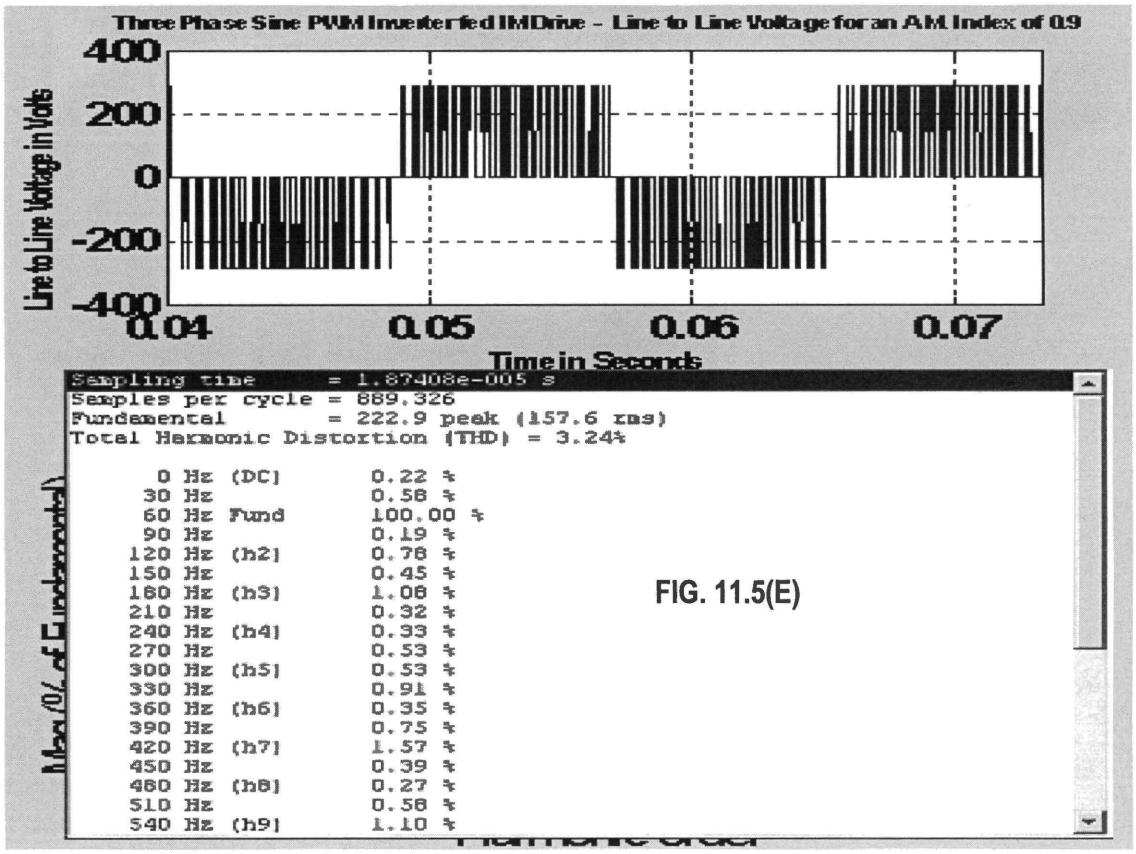

FIG. 11.5(E)

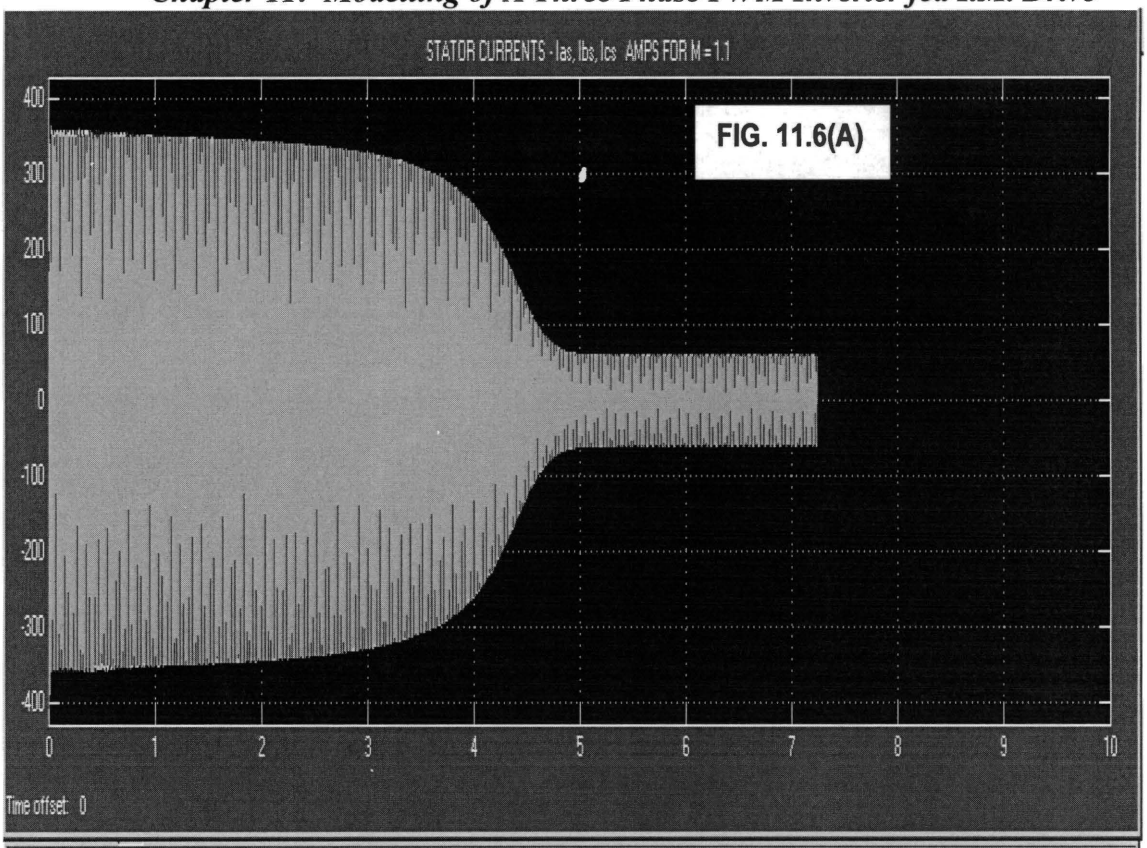

FIG. 11.6(A)

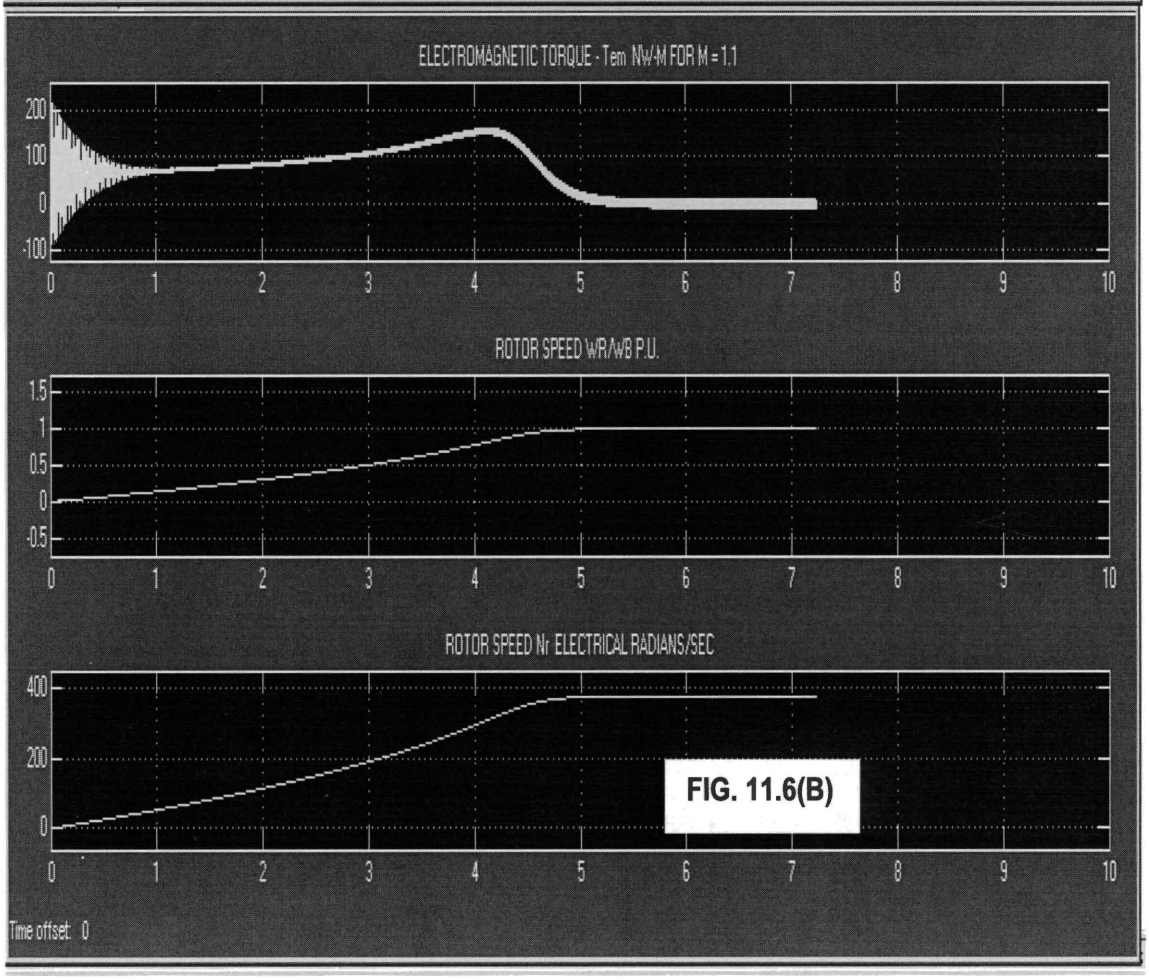

FIG. 11.6(B)

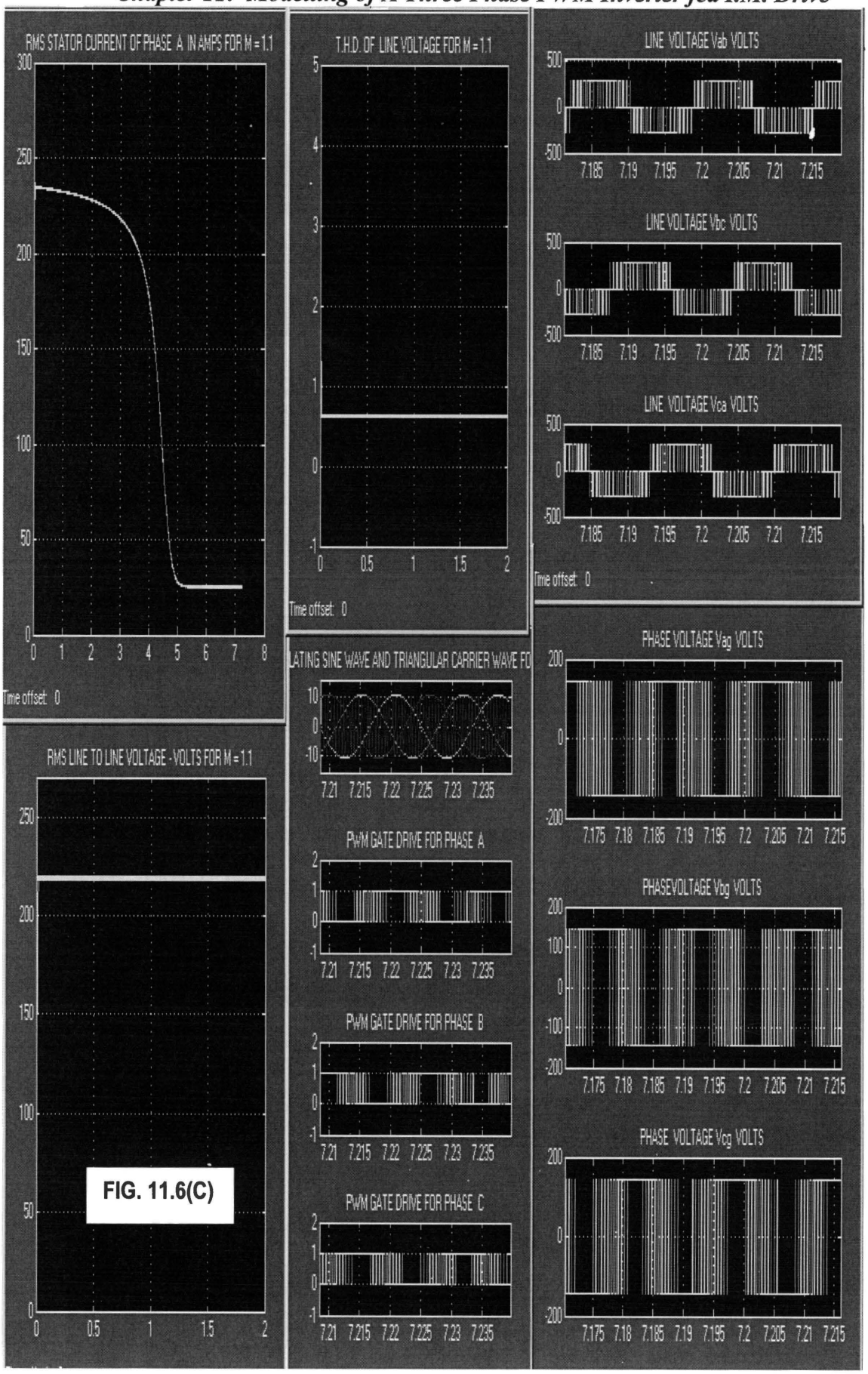
RMS STATOR CURRENT OF PHASE A IN AMPS FOR M = 1.1
Time offset: 0
T.H.D. OF LINE VOLTAGE FOR M = 1.1
Time offset: 0
LINE VOLTAGE Vab VOLTS
LINE VOLTAGE Vbc VOLTS
LINE VOLTAGE Vca VOLTS
Time offset: 0
RMS LINE TO LINE VOLTAGE - VOLTS FOR M = 1.1
LATING SINE WAVE AND TRIANGULAR CARRIER WAVE FO
PWM GATE DRIVE FOR PHASE A
PWM GATE DRIVE FOR PHASE B
PWM GATE DRIVE FOR PHASE C
PHASE VOLTAGE Van VOLTS
PHASEVOLTAGE Vbn VOLTS
PHASE VOLTAGE Vcn VOLTS

FIG. 11.6(C)

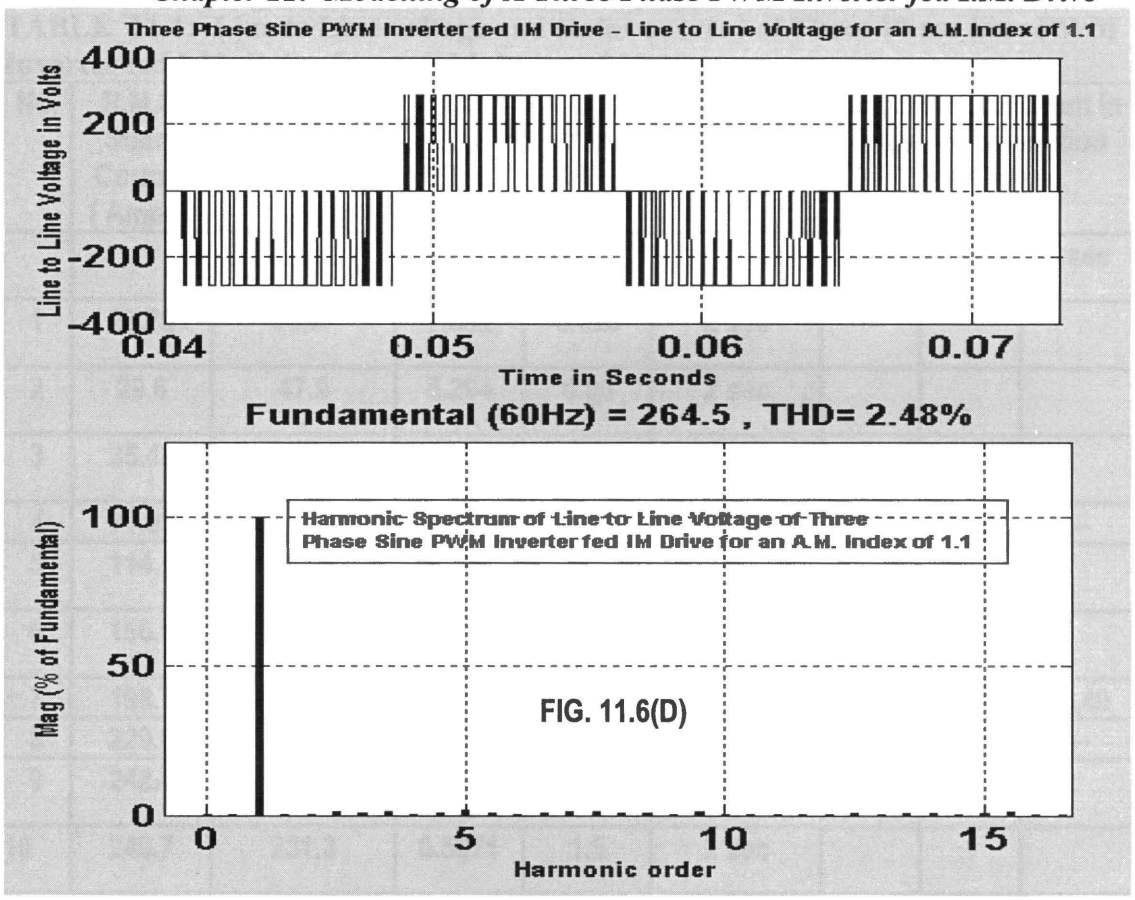

FIG. 11.6(D)

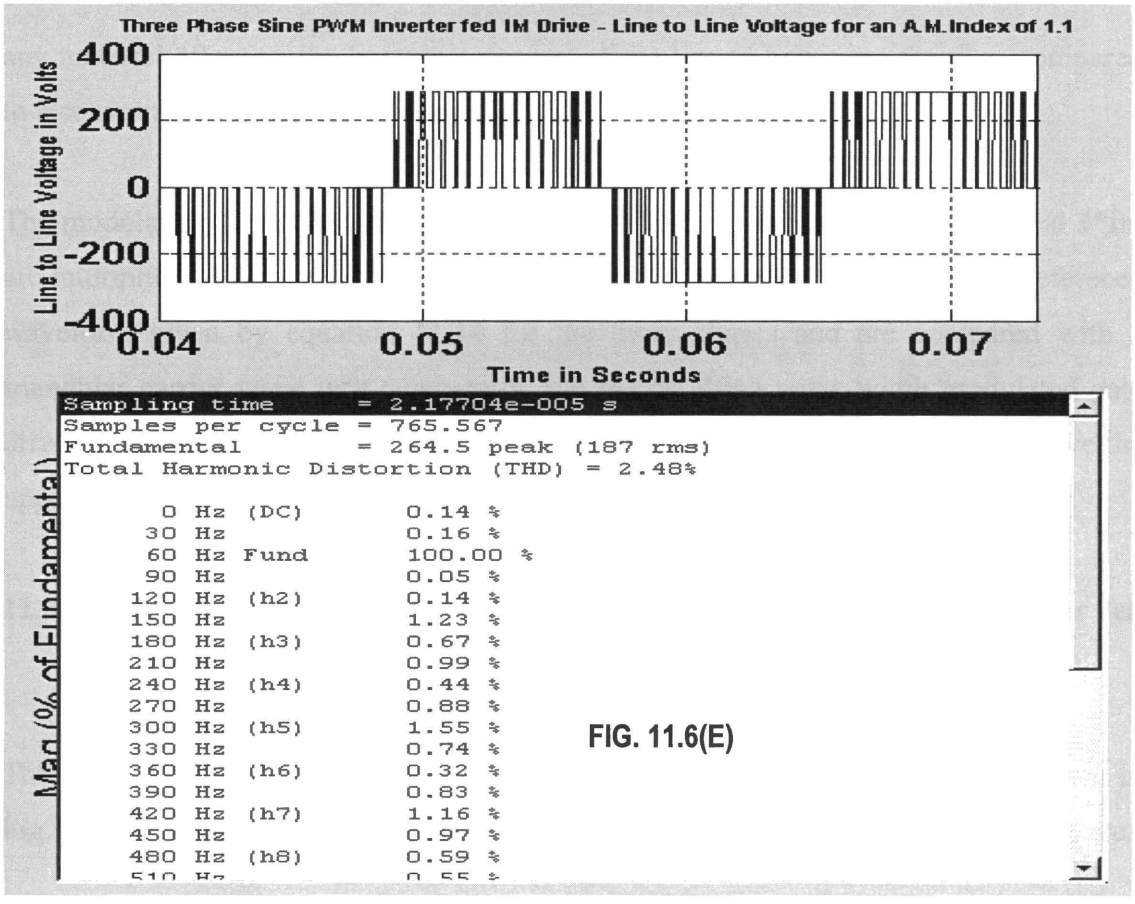

FIG. 11.6(E)

TABLE 11.1: Line to Line voltage and stator current of Three Phase Sine PWM Inverter fed I.M. Drive for an F.M. Index of 33.33.

No.	R.M.S. Stator Current (Amps)	R.M.S. LineVoltage Vab (Volts)	T.H.D.** Of Line to Line Voltage	A.M.In-dex M	Simulation Time in seconds	R.M.S.Stator current in Amps for simulation time shown		
						5 sec	6 sec	7 sec
1	27.78	33.87	7.552	0.025	2 sec			
2	29.6	47.9	5.294	0.05	2 sec			
3	35.42	67.74	3.679	0.1	2 sec			
4	71.95	117.3	1.957	0.3	2 sec	71.6	71.6	---
5	114.1	151.4	1.378	0.5	2 sec			
6	156.6	179.2	1.033	0.7	2 sec			
7	198.7	203.1	0.7793	0.9	2 sec	171.5	87.1	28.49
8	229.8	220.5	0.6103	1.1	2 sec	---	29.91	---
9	242.4	227.6	0.5462	1.3	2 sec			
10	249.7	231.3	0.5071	1.5	2 sec			

any material effect on the harmonic content of the line to line wave form, as compared to a conventional sine PWM inverter [49-50].

The modulating three phase sine wave signals with frequency component fm and 3*fm are multiplied by appropriate constants and added to generate the modulating reference waveform given by equation 11.14 for the three phases and are compared with a triangular carrier wave in a comparator and the resulting pulse width modulated gate drive for each phase and their respective inverted gate drive pulse are used to drive the upper and lower arms of semiconductor switches in the three phases of the inverter.

11.3.1 Modelling of Three Phase Third Harmonic Injection PWM Inverter fed I.M. Drive

The interactive model of the three phase THIPWM inverter fed IM drive is shown in Fig.11.7. The various dialog boxes are shown in Fig.11.8. The various subsystems are

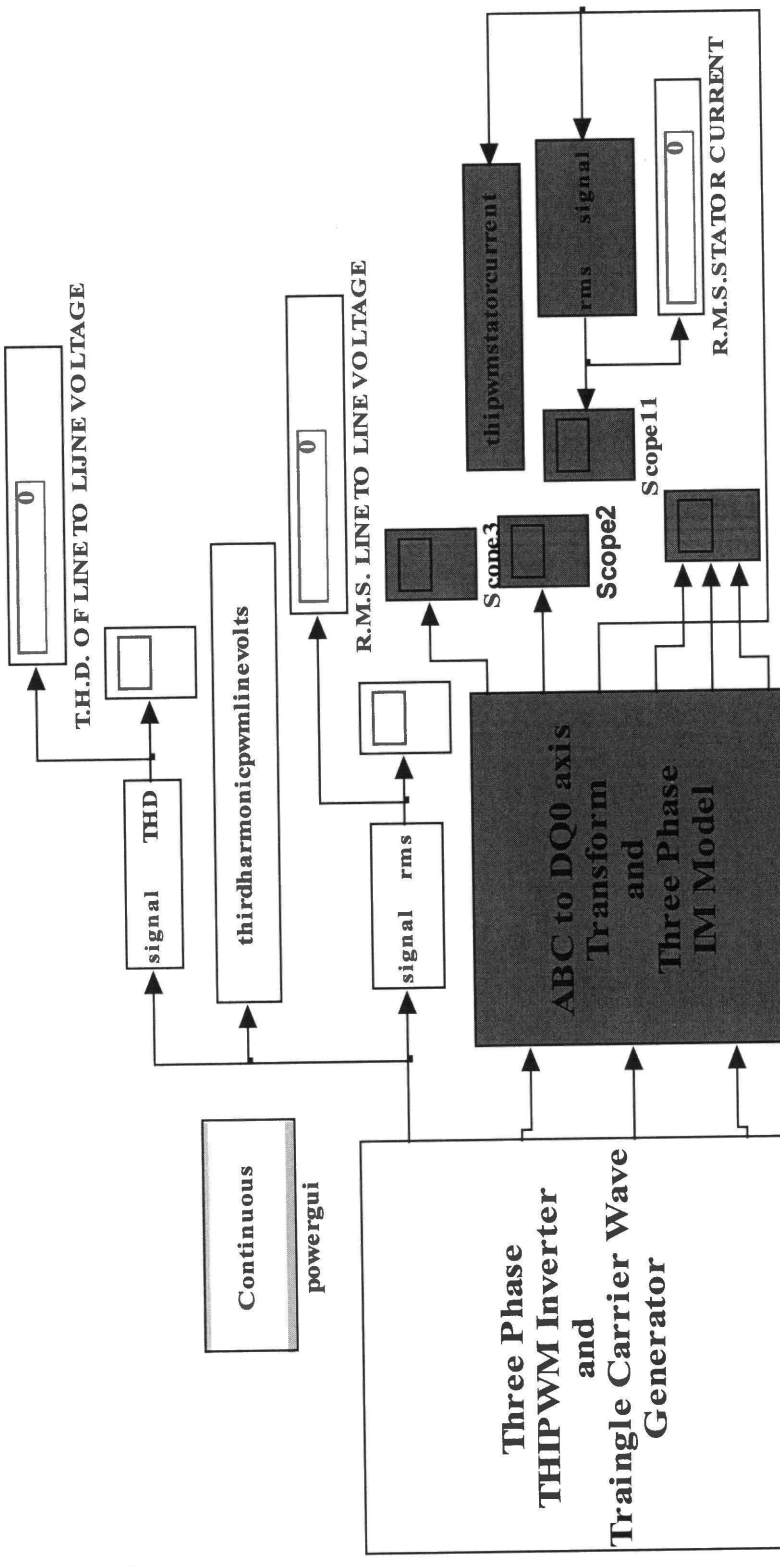

FIG.11.7: THREE PHASE 60 HZ THIRD HARMONIC INJECTION PWM INVERTER FED I.M. DRIVE

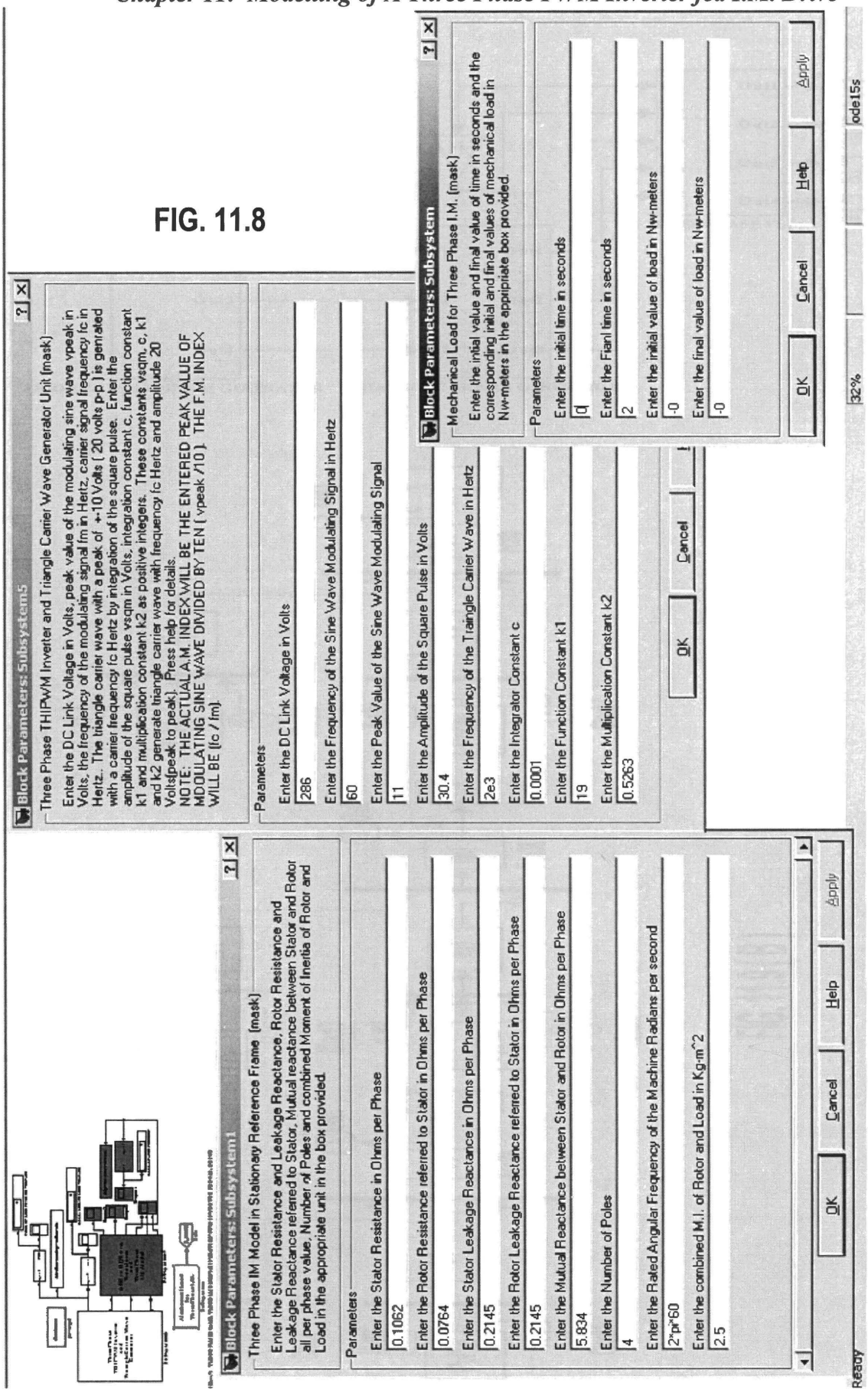
Block Parameters: Subsystem1
Three Phase IM Model in Stationary Reference Frame (mask)
Enter the Stator Resistance and Leakage Reactance, Rotor Resistance and Leakage Reactance referred to Stator, Mutual reactance between Stator and Rotor all per phase value, Number of Poles and combined Moment of Inertia of Rotor and Load in the appropriate unit in the box provided.
Parameters
Enter the Stator Resistance in Ohms per Phase
0.1062
Enter the Rotor Resistance referred to Stator in Ohms per Phase
0.0764
Enter the Stator Leakage Reactance in Ohms per Phase
0.2145
Enter the Rotor Leakage Reactance referred to Stator in Ohms per Phase
0.2145
Enter the Mutual Reactance between Stator and Rotor in Ohms per Phase
5.834
Enter the Number of Poles
4
Enter the Rated Angular Frequency of the Machine Radians per second
2*pi*60
Enter the combined M.I. of Rotor and Load in Kg-m^2
2.5
OK
Cancel
Help
Apply
Block Parameters: Subsystem5
Three Phase THIPWM Inverter and Triangle Carrier Wave Generator Unit (mask)
Enter the DC Link Voltage in Volts, peak value of the modulating sine wave vpeak in Volts, the frequency of the modulating signal fm in Hertz, carrier signal frequency fc in Hertz. The triangle carrier wave with a peak of +-10 Volts (20 volts p-p) is generated with a carrier frequency fc Hertz by integration of the square pulse. Enter the amplitude of the square pulse vsqm in Volts, integration constant c, function constant k1 and multiplication constant k2 as positive integers. These constants vsqm, c, k1 and k2 generate triangle carrier wave with frequency fc Hertz and amplitude 20 Volts(peak to peak). Press help for details.
NOTE: THE ACTUAL A.M. INDEX WILL BE THE ENTERED PEAK VALUE OF MODULATING SINE WAVE DIVIDED BY TEN (vpeak /10). THE F.M. INDEX WILL BE (fc / fm).
Parameters
Enter the DC Link Voltage in Volts
286
Enter the Frequency of the Sine Wave Modulating Signal in Hertz
60
Enter the Peak Value of the Sine Wave Modulating Signal
11
Enter the Amplitude of the Square Pulse in Volts
30.4
Enter the Frequency of the Traingle Carrier Wave in Hertz
2e3
Enter the Integrator Constant c
0.0001
Enter the Function Constant k1
19
Enter the Multiplication Constant k2
0.5263
OK
Cancel
Block Parameters: Subsystem
Mechanical Load for Three Phase I.M. (mask)
Enter the initial value and final value of time in seconds and the corresponding initial and final values of mechanical load in Nw-meters in the appipriate box provided.
Parameters
Enter the initial time in seconds
0
Enter the Fianl time in seconds
2
Enter the initial value of load in Nw-meters
-0
Enter the final value of load in Nw-meters
-0
OK
Cancel
Help
Apply
Ready
32%
ode15s

FIG. 11.8

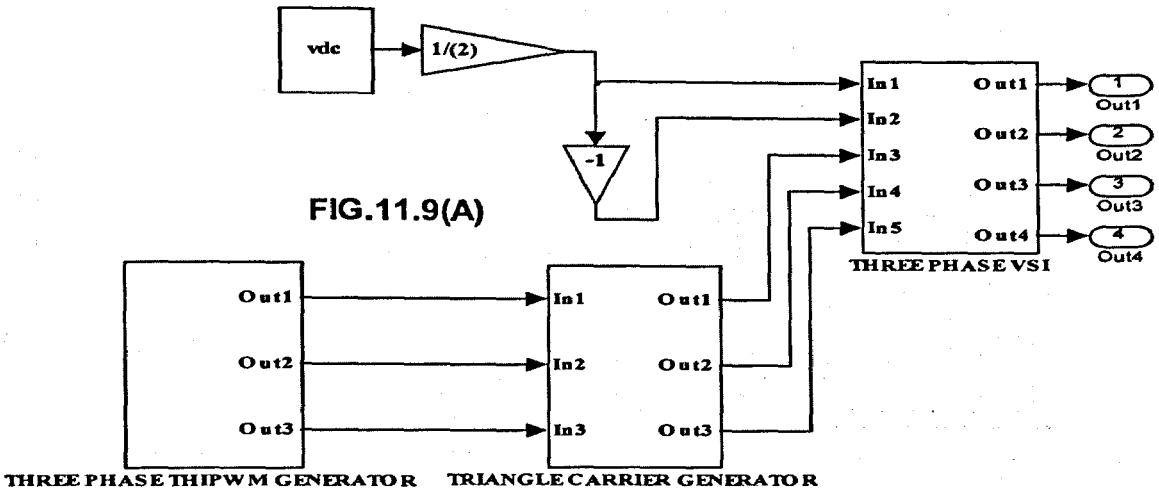

FIG.11.9(A)

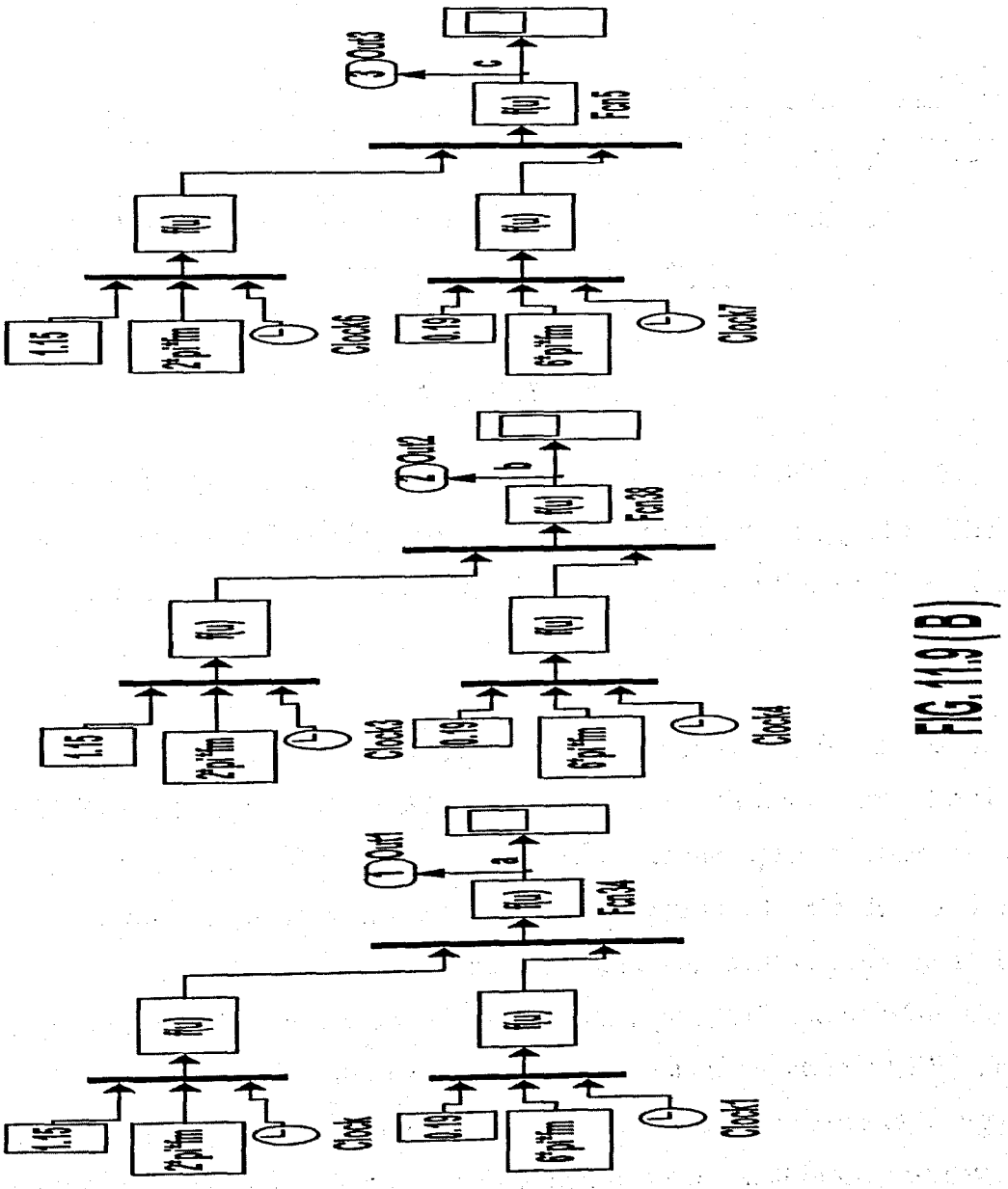

FIG.11.9(B)

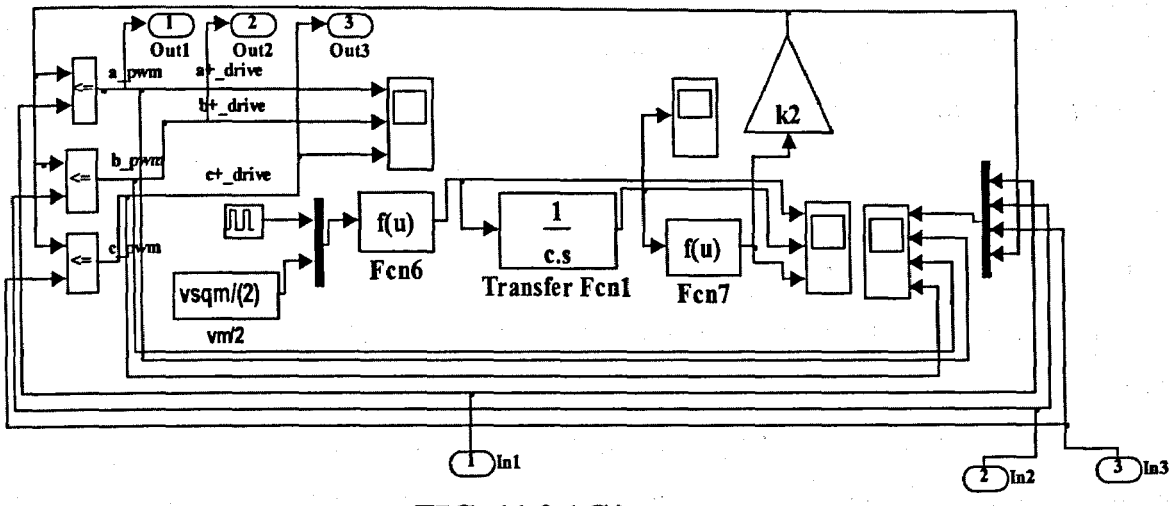

FIG. 11.9 (C)

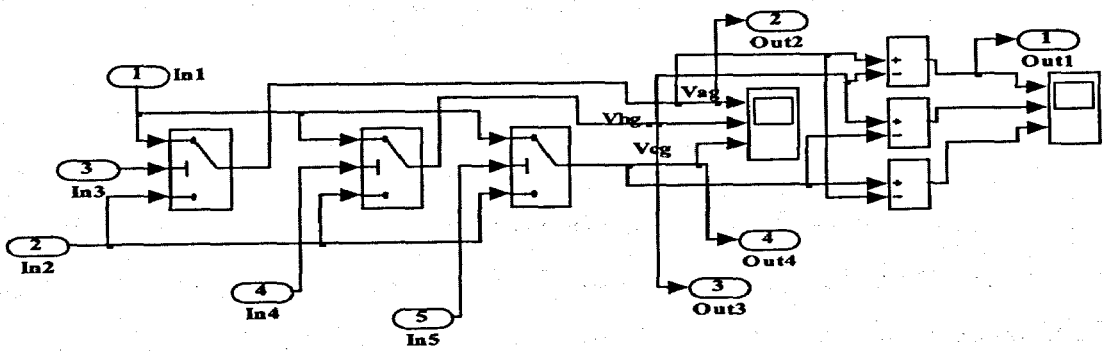

FIG.11.9(D)

shown in Fig.11.9(A) to (E). Fig.11.9(A) correspond to the dialog box "Three Phase THIPWM Inverter and Triangle Carrier Wave Generator Unit" in Fig.11.8. The various subsystems are: Three Phase THIPWM Generator, Triangle Carrier Wave Generator and Three Phase VSI.

The subsystem corresponding to Three Phase THIPWM generator is shown in Fig.11.9(B). In Fig.11.9(B), the modulating sine wave with fundamental fm Hertz and third harmonics are added for the three phases as per the equation given by equation 11.14. The three input mux at the top with input constant blocks 1.15 and 2*pi*fm along with the Fcn block generate the fundamental component in equation 11.14. The three input mux at the bottom with constant block inputs 0.19 and 6*pi*fm along with the Fcn block generate the third harmonic component of equation 11.14. The Fcn3 block sums the two values and multiplies by vpeak to generate the modulating signal a for the Phase R. For Phase Y modulating signal b is generated in the same way as for

Phase R, except that the fundamental component and third harmonic components lags by 2*pi/3 and 2*pi radians respectively. For Phase B, the modulating signal c is generated as for Phase Y, except that the fundamental and third harmonic component leads by 2*pi/3 and 2*pi radians respectively.

The triangle carrier generator model is shown in Fig.11.9(C). The method of development is the same as for three phase sine PWM inverter fed IM drive discussed under section 11.2.1. The same help file shown in Fig.11.4(H) is applicable to generate triangle carrier wave other than 2 kHZ frequency. The Models for Three Phase Inverter, abc to dq0 axis transform, Three phase IM and the Mechanical Load for Three Phase IM are the same as shown in Fig.11.4(D), E, F and G. The modeling equations of the three phase IM are already explained under section 11.2.1.

11.3.2 Simulation Results

The simulation results of the Three Phase 60 Hz THIPWM Inverter fed IM drive using ode15s(stiff/NDF) solver are shown in Fig.11.10(A) to (E) and in Fig.11.11(A) to (E) for a.m. indices M of 0.9 and 1.1 respectively, with f.m. index maintained at 33.33.. The simulation results for all the a.m. indices less than and greater than one are tabulated in Table 11.2. The data for the 20 hp, 220 volts, three phase, 60 Hz, 4 pole star connected cage IM used for simulation are the same as given in section 11.2.2.

11.4 Three Phase Harmonic Injection PWM Technique

The HIPWM is a variation of the THIPWM technique discussed in section 11.3. In HIPWM additional harmonics apart from third harmonics are added to the sine reference waveform. The modulating reference waveform is given below [5 - 6]:

$$y = 1.15 * \sin(\omega.t) + 0.27 * \sin(3.\omega.t) - 0.029 * \sin(9.\omega.t) \quad \ldots\ldots\ldots\ldots\ldots\ldots\ldots\ldots\ldots\ldots (11.15)$$

The resulting flat-topped waveform allows over modulation while improving the frequency spectra of ac terms and dc terms waveforms [50]. The modulating three phase sine wave signals with frequency component fm, 3*fm and 9*fm are multiplied by appropriate constants and added with proper signs to generate the modulating

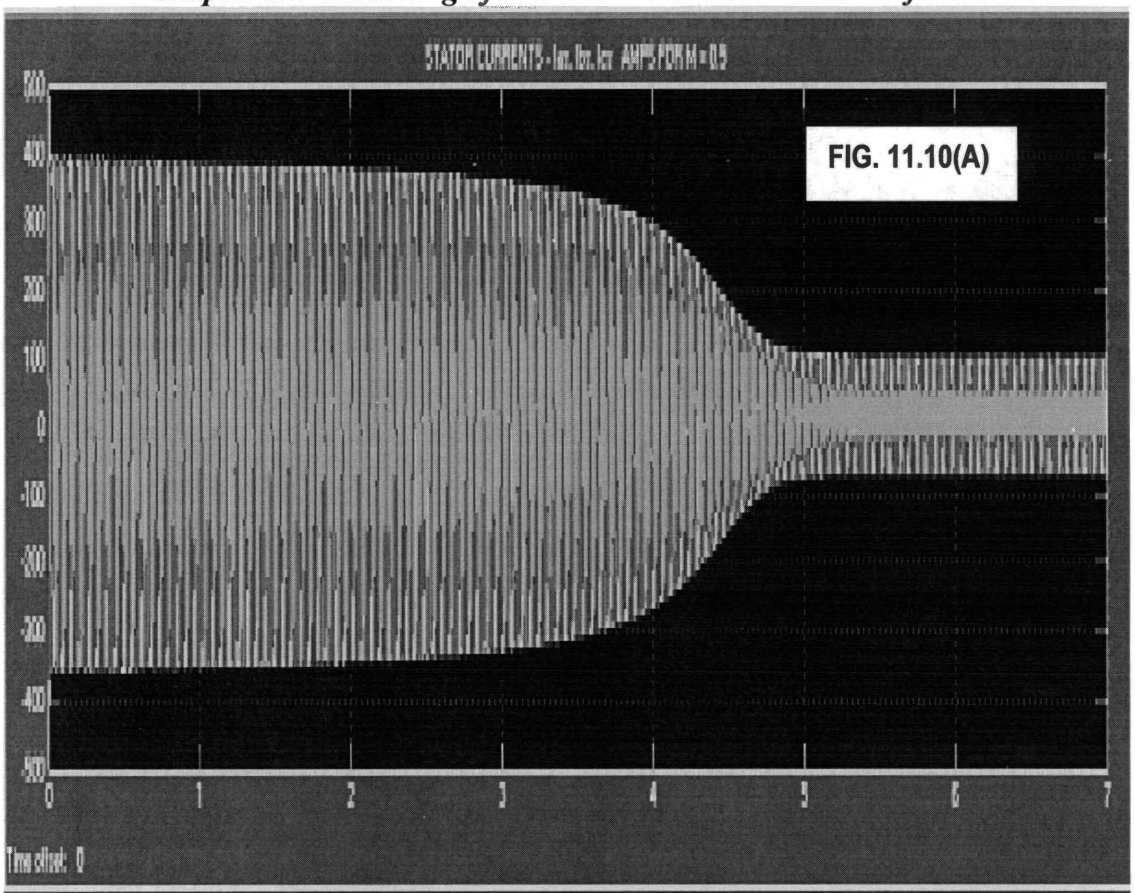
STATOR CURRENTS - Ias, Ibs, Ics AMPS FORM = 0.5
FIG. 11.10(A)
Time offset: 0

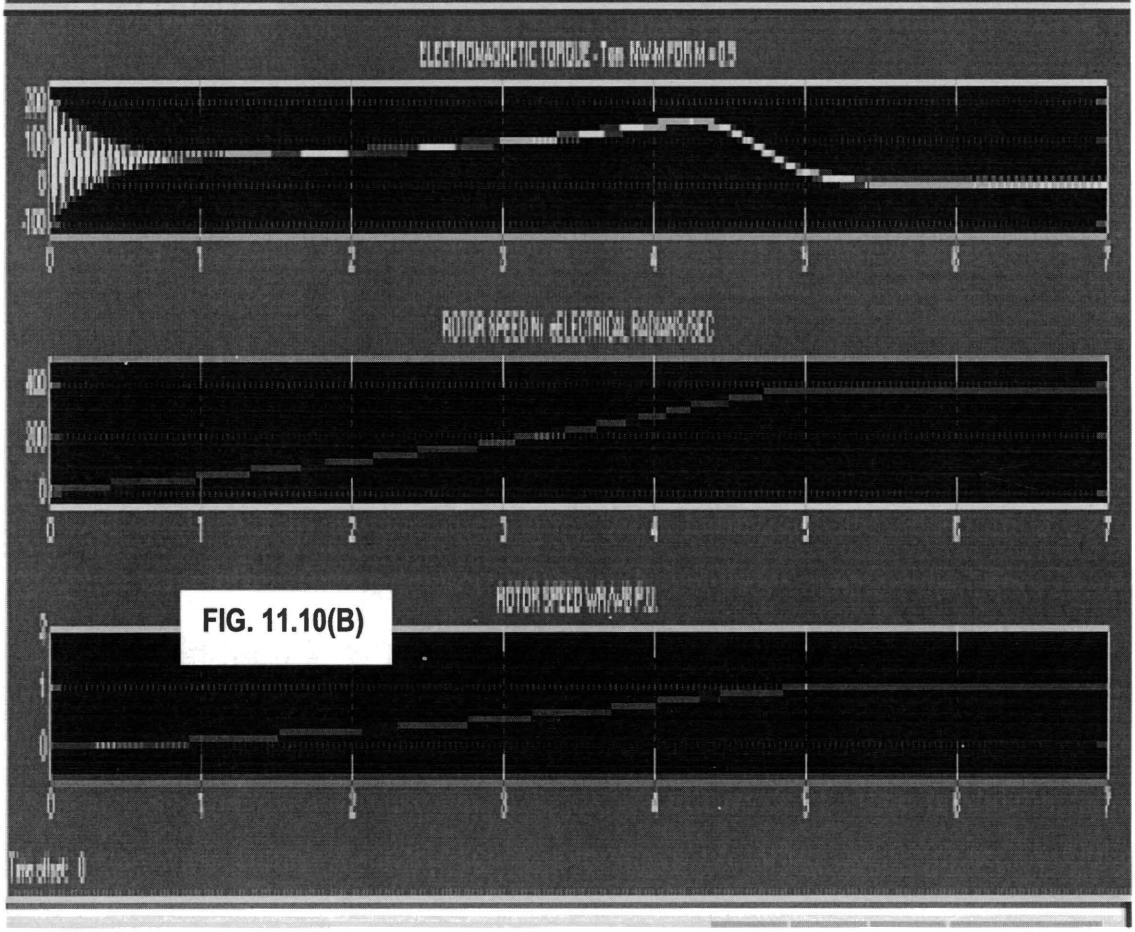
ELECTROMAGNETIC TORQUE - Tem NWM FORM = 0.5
ROTOR SPEED IN ELECTRICAL RADIANS/SEC
ROTOR SPEED WM IN P.U.
FIG. 11.10(B)
Time offset: 0

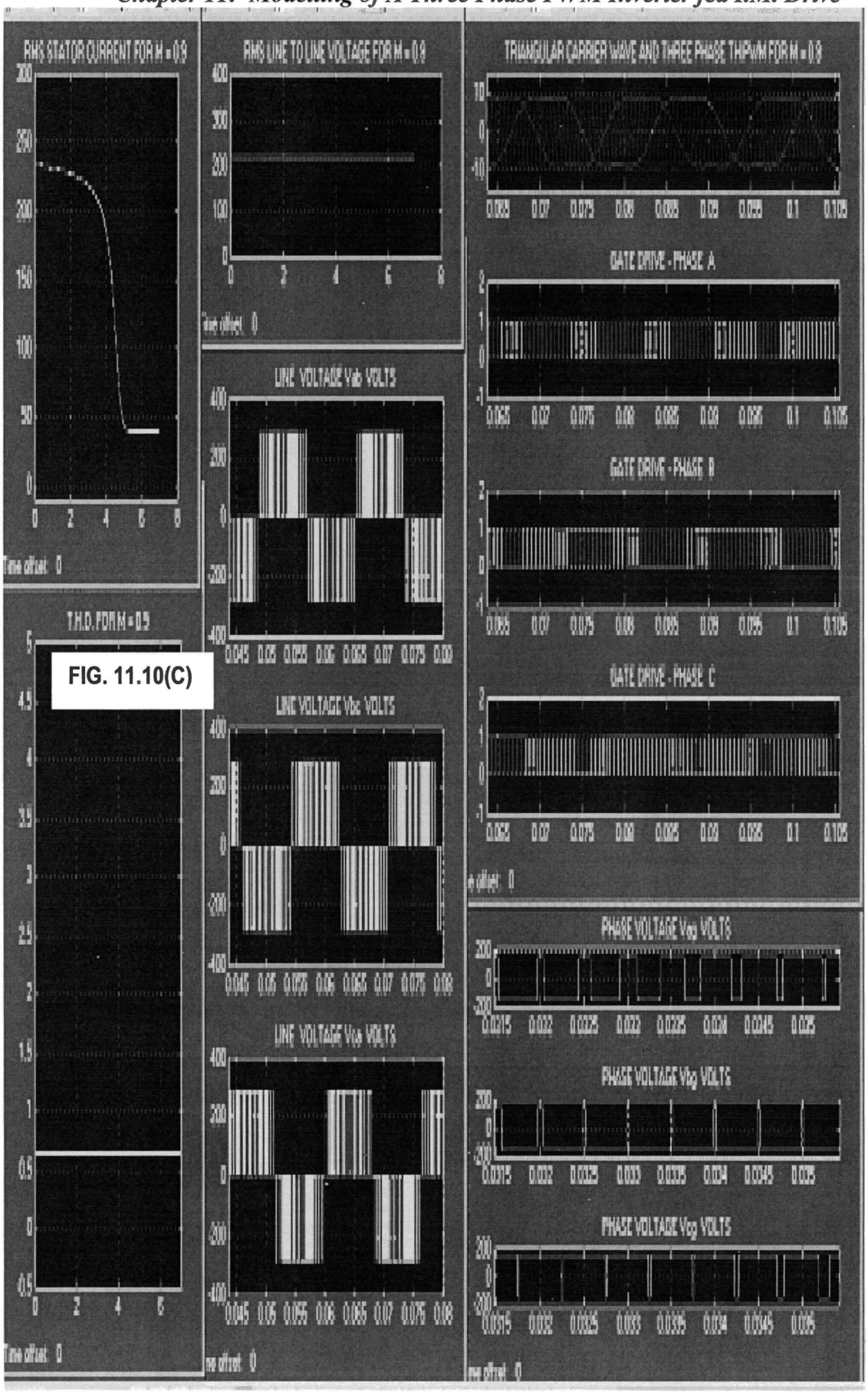
RMS STATOR CURRENT FOR M = 0.9
RMS LINE TO LINE VOLTAGE FOR M = 0.9
TRIANGULAR CARRIER WAVE AND THREE PHASE THPWM FOR M = 0.9
GATE DRIVE - PHASE A
GATE DRIVE - PHASE B
GATE DRIVE - PHASE C
LINE VOLTAGE Vab VOLTS
LINE VOLTAGE Vbc VOLTS
LINE VOLTAGE Vca VOLTS
PHASE VOLTAGE Van VOLTS
PHASE VOLTAGE Vbn VOLTS
PHASE VOLTAGE Vcn VOLTS
T.H.D. FOR M = 0.9

FIG. 11.10(C)

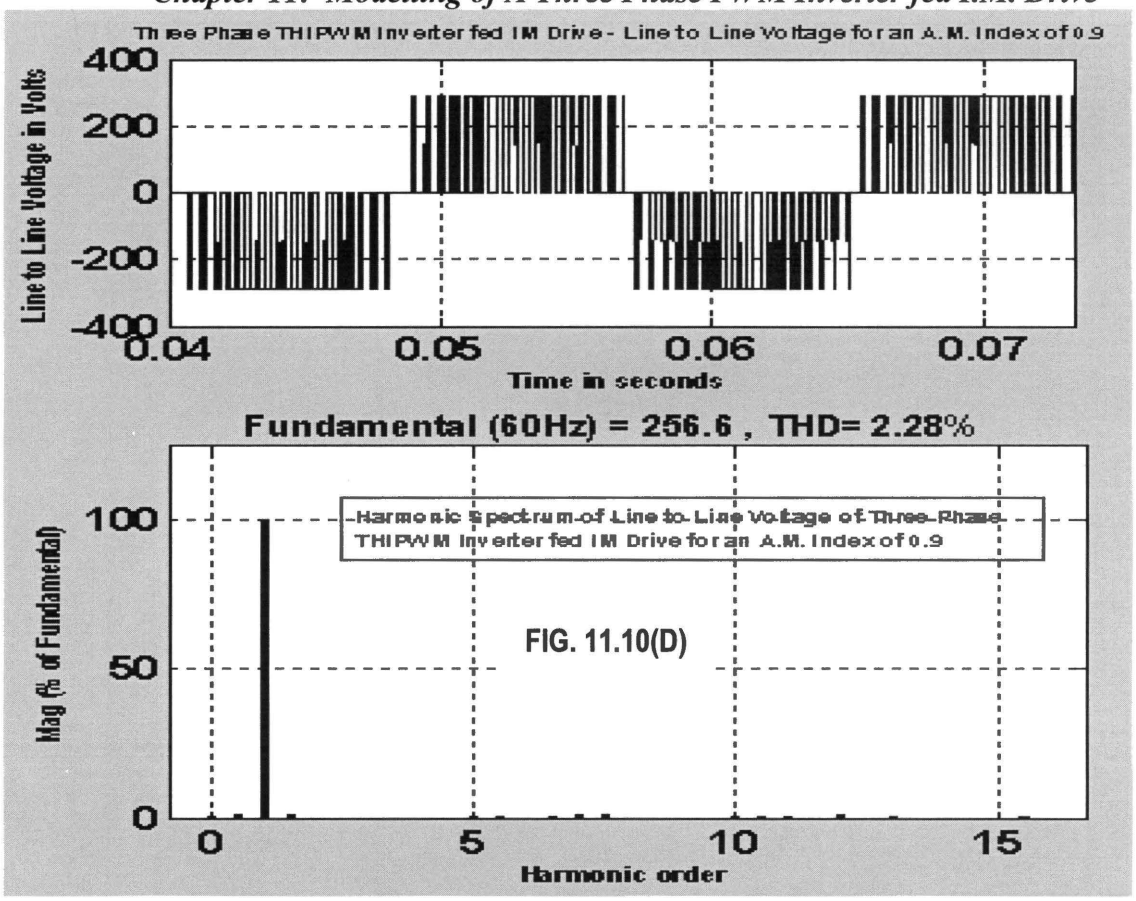

FIG. 11.10(D)

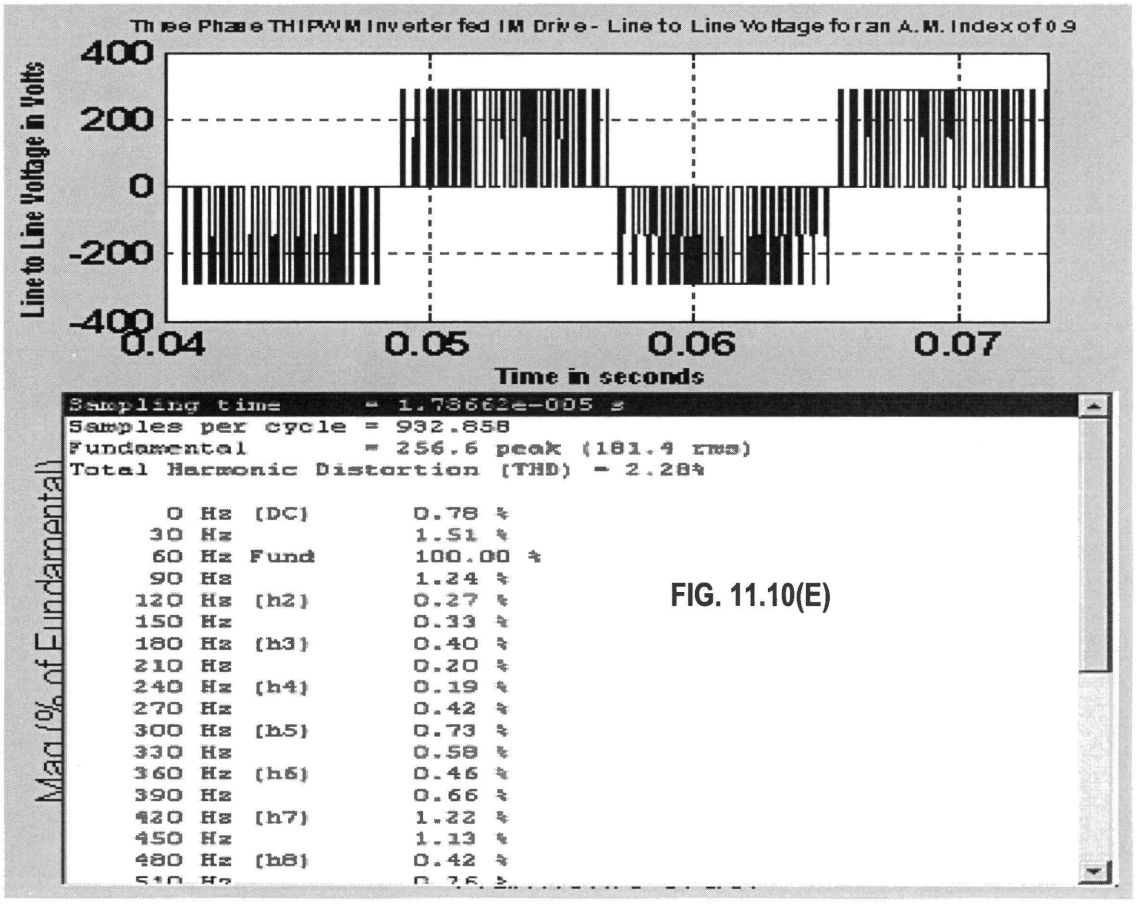

FIG. 11.10(E)

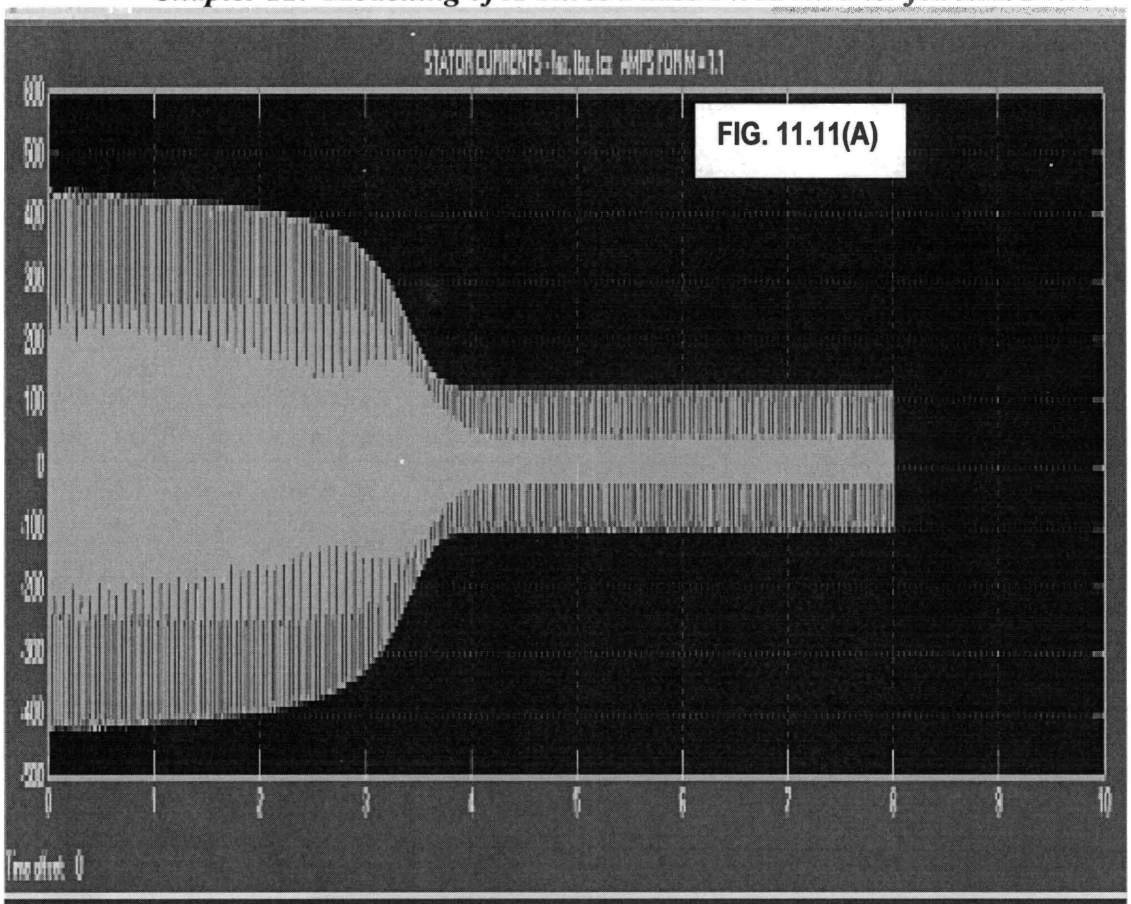
STATOR CURRENTS - Ias, Ibs, Ics AMPS FOR M = 1.1
FIG. 11.11(A)

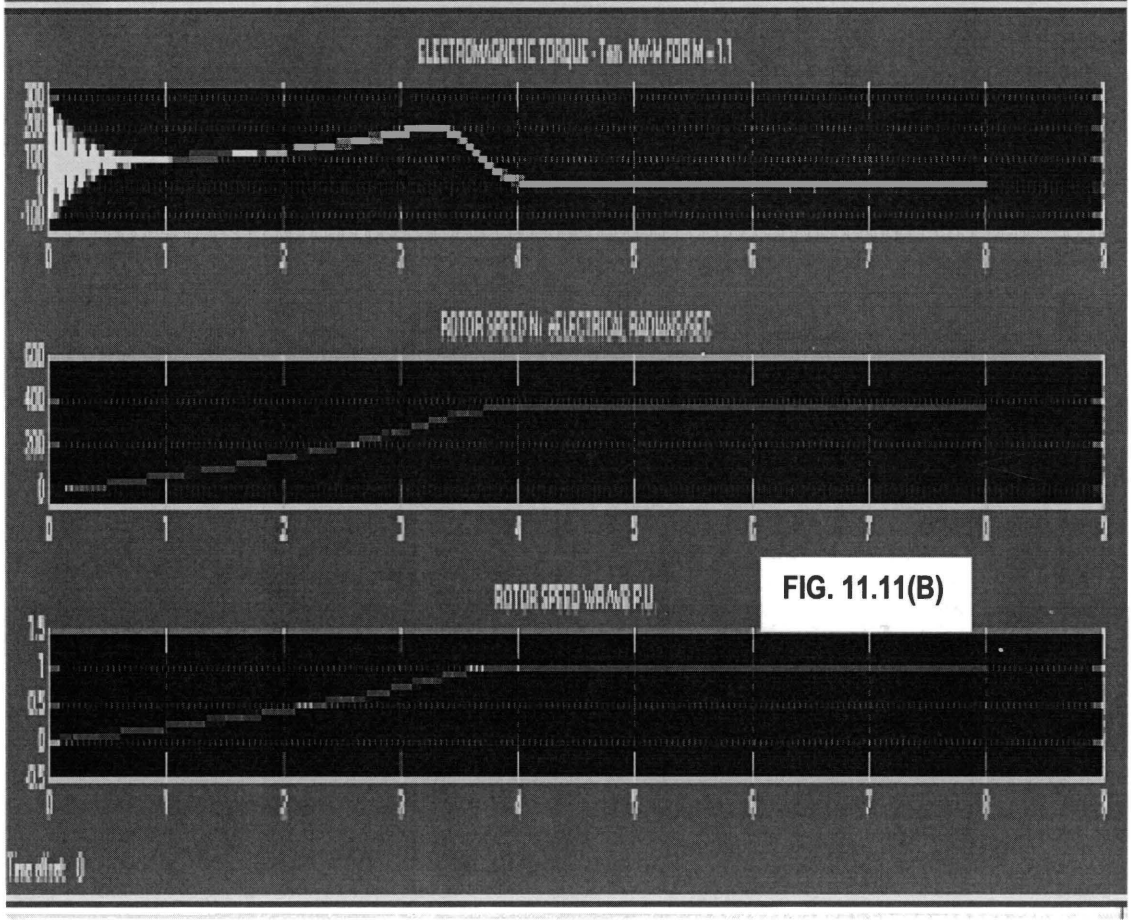
ELECTROMAGNETIC TORQUE - Tem NM-M FOR M = 1.1
ROTOR SPEED Wr -ELECTRICAL RADIANS/SEC
ROTOR SPEED WR/WB P.U
FIG. 11.11(B)

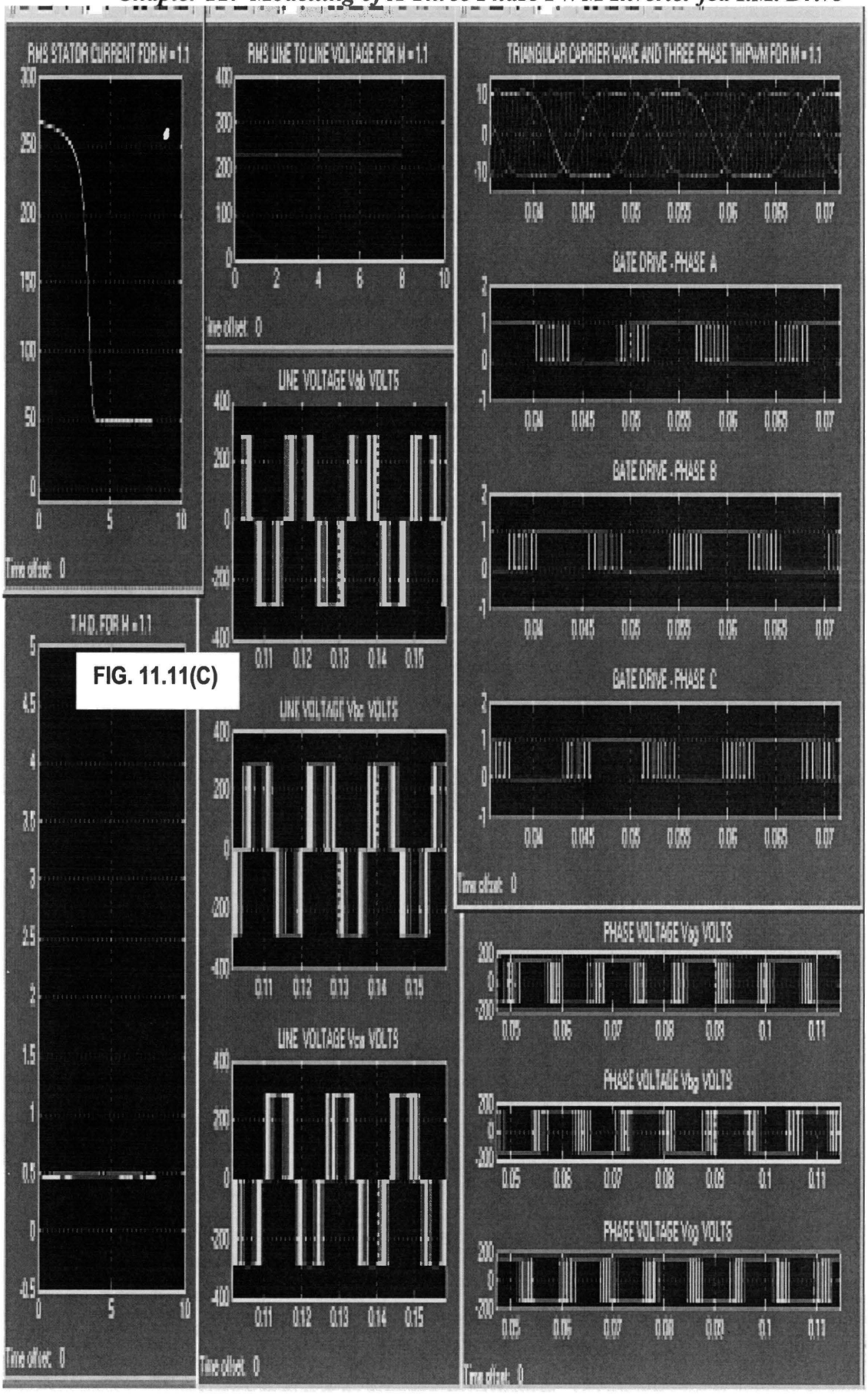
RMS STATOR CURRENT FOR M = 1.1
RMS LINE TO LINE VOLTAGE FOR M = 1.1
TRIANGULAR CARRIER WAVE AND THREE PHASE THIPWM FOR M = 1.1
GATE DRIVE - PHASE A
GATE DRIVE - PHASE B
GATE DRIVE - PHASE C
LINE VOLTAGE Vab VOLTS
LINE VOLTAGE Vbc VOLTS
LINE VOLTAGE Vca VOLTS
PHASE VOLTAGE Van VOLTS
PHASE VOLTAGE Vbn VOLTS
PHASE VOLTAGE Vcn VOLTS
T.H.D. FOR M = 1.1
Time offset: 0

FIG. 11.11(C)

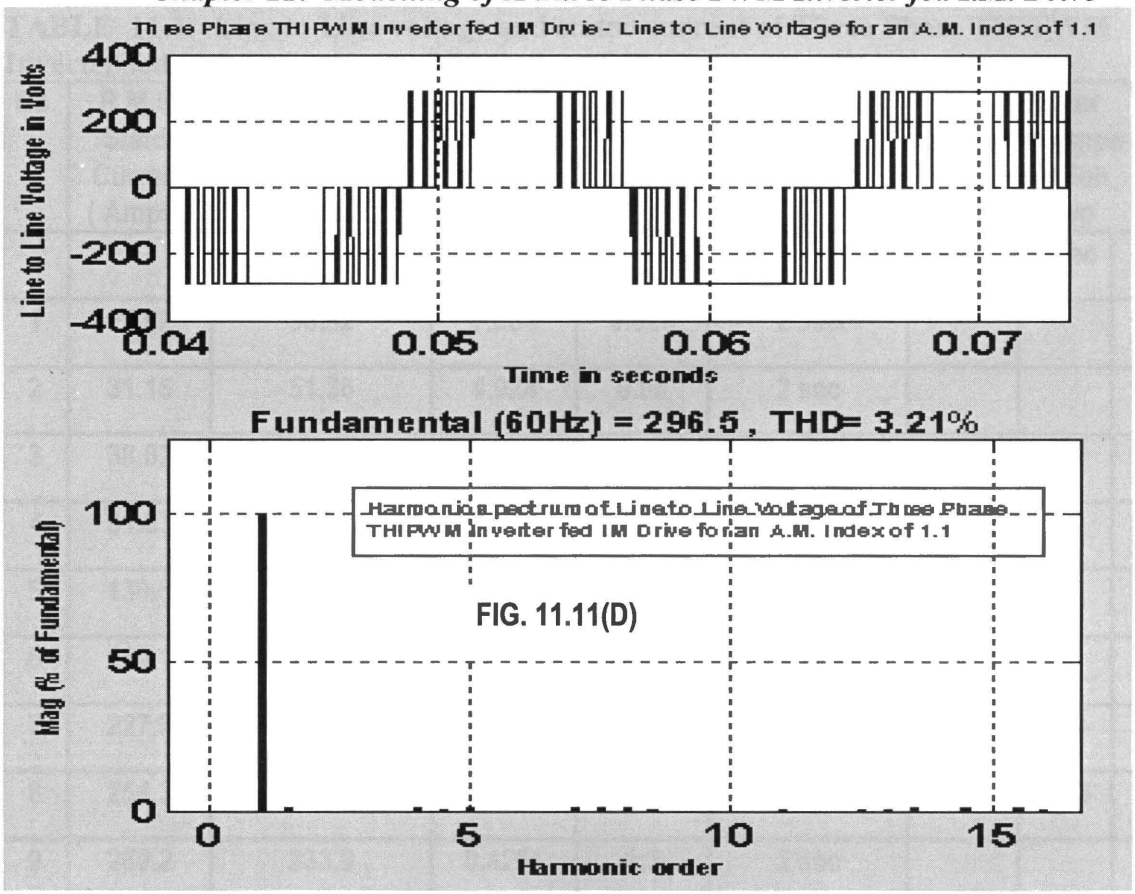

FIG. 11.11(D)

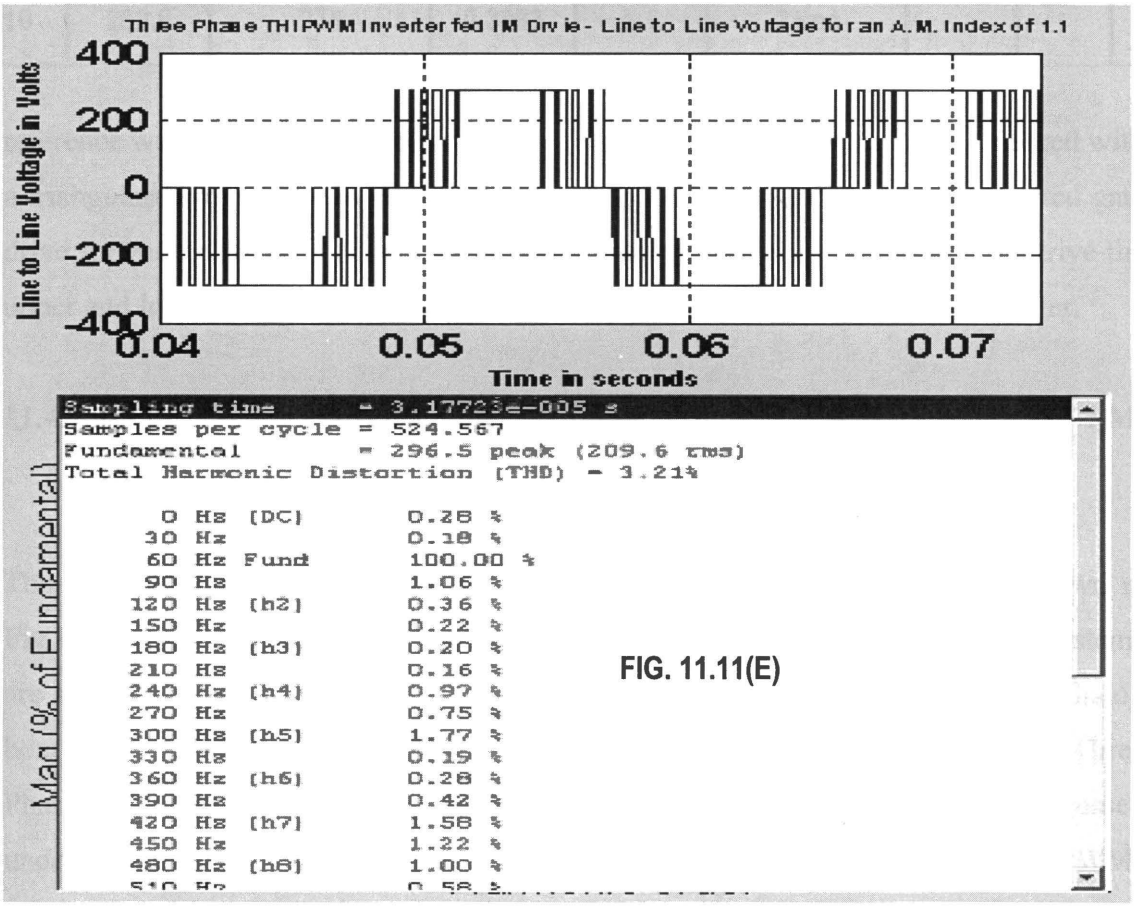

FIG. 11.11(E)

TABLE 11.2: Line to Line voltage and stator current of Three Phase THIPWM Inverter fed I.M. Drive for an F.M. Index of 33.33.

No.	R.M.S. Stator Current (Amps)	R.M.S. LineVoltage Vab (Volts)	T.H.D.** Of Line to Line Voltage	A.M.In-dex M	Simulation Time in seconds	R.M.S.Stator current in Amps for simulation time shown	
						7 sec	8 sec
1	27.82	36.32	7.034	0.025	2 sec		
2	31.15	51.36	4.924	0.05	2 sec		
3	38.02	72.64	3.411	0.1	2 sec		
4	81.83	125.8	1.788	0.3	2 sec		
5	130.8	162.4	1.232	0.5	2 sec		
6	180.1	192.1	0.8929	0.7	2 sec		
7	227.6	217.8	0.6306	0.9	2 sec	39.55	-----
8	254.3	232.5	0.4695	1.1	2 sec	---	47.6
9	260.2	233.9	0.4261	1.3	2 sec		
10	262.6	234	0.3993	1.5	2 sec		

reference waveform given by equation 11.15 for the three phases and are compared with a triangular carrier wave in a comparator and the resulting pulse width modulated gate drive for each phase and their respective inverted gate drive pulse are used to drive the upper and lower arms of semiconductor switches in the three phases of the inverter.

11.4.1 Modelling of Three Phase Harmonic Injection PWM Inverter fed I.M. Drive

The interactive model of the three phase HIPWM inverter fed IM drive is shown in Fig.11.12. The various dialog boxes are shown in Fig.11.13. The various subsystems are shown in Fig.11.14(A) and (B). The other subsystems corresponding to the dialog box "Three Phase IM in Stationary Reference Frame" and Mechanical Load for Three Phase IM" are the same as for three phase sine PWM inverter fed IM drive discussed under section 11.2.1. Fig.11.14(A) correspond to the dialog box "Three Phase HIPWM

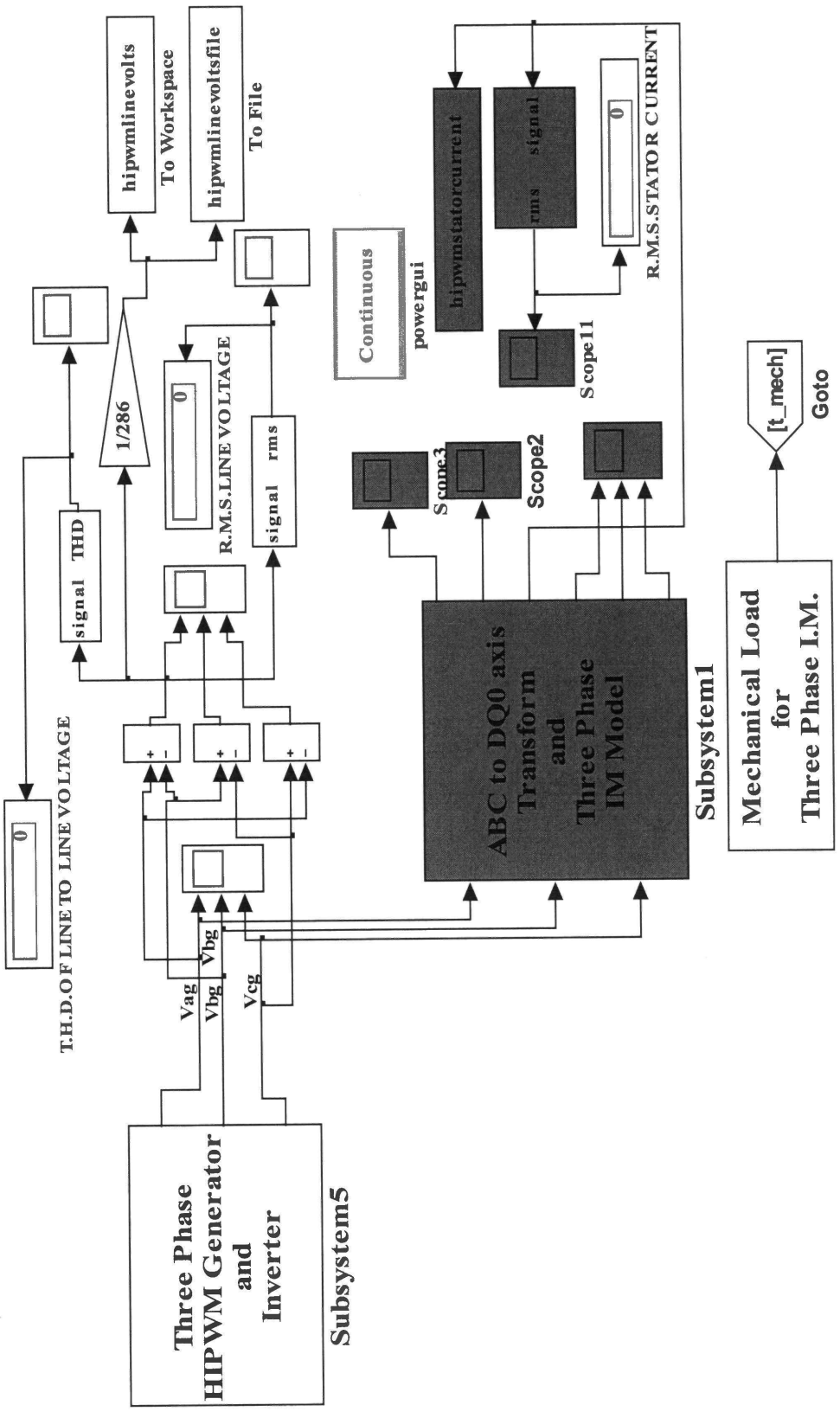

FIG. 11.12: THREE PHASE HIPWM INVERTER FED I.M. DRIVE

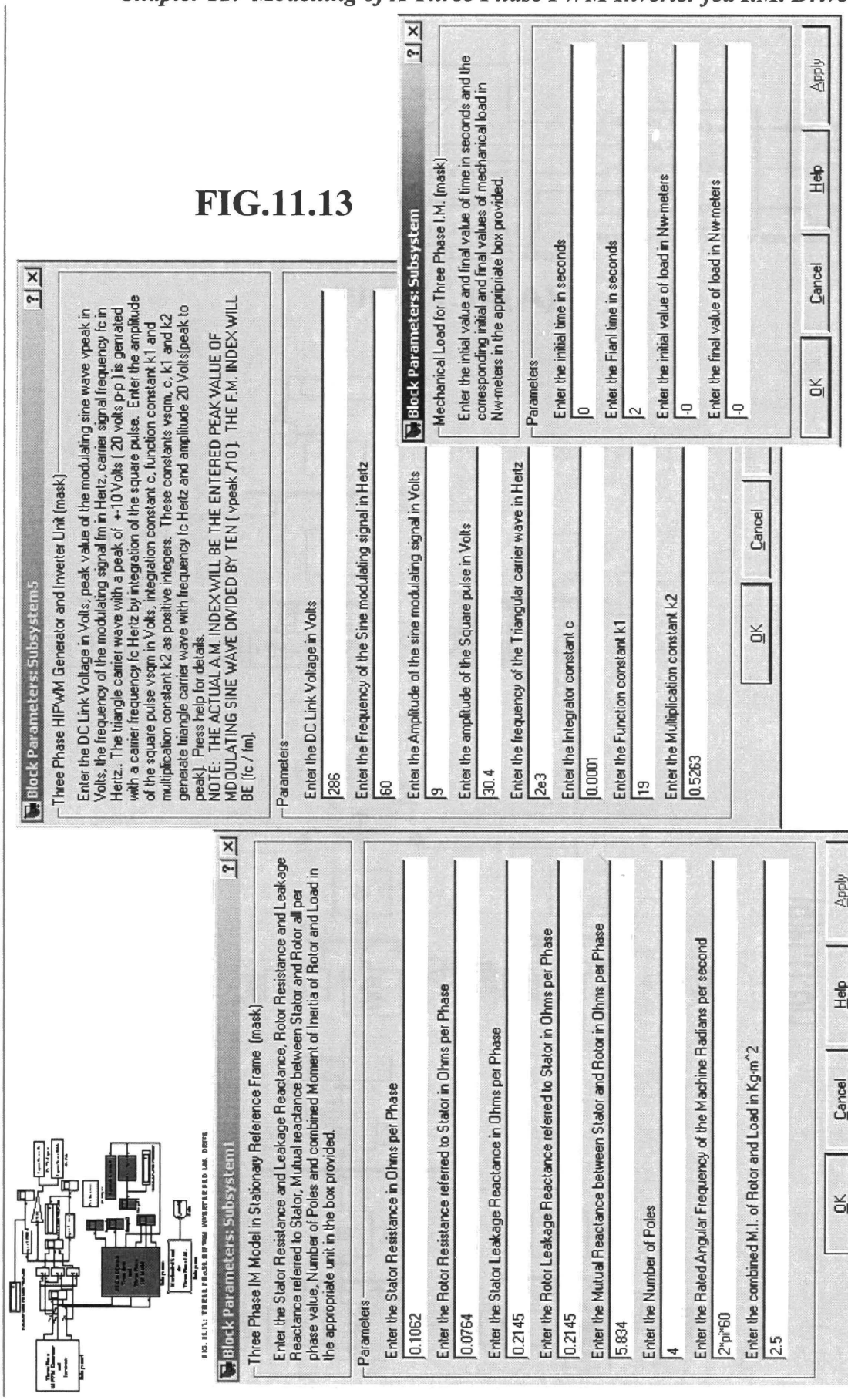
Block Parameters: Subsystem5
Three Phase HIPWM Generator and Inverter Unit (mask)
Enter the DC Link Voltage in Volts, peak value of the modulating sine wave vpeak in Volts, the frequency of the modulating signal fm in Hertz, carrier signal frequency fc in Hertz.. The triangle carrier wave with a peak of +-10 Volts (20 volts p-p) is generated with a carrier frequency fc Hertz by integration of the square pulse. Enter the amplitude of the square pulse vsqm in Volts, integration constant c, function constant k1 and multiplication constant k2 as positive integers. These constants vsqm, c, k1 and k2 generate triangle carrier wave with frequency fc Hertz and amplitude 20 Volts(peak to peak). Press help for details.
NOTE: THE ACTUAL A.M. INDEX WILL BE THE ENTERED PEAK VALUE OF MODULATING SINE WAVE DIVIDED BY TEN (vpeak /10). THE F.M. INDEX WILL BE (fc / fm).
Parameters
Enter the DC Link Voltage in Volts
286
Enter the Frequency of the Sine modulating signal in Hertz
60
Enter the Amplitude of the sine modulating signal in Volts
9
Enter the amplitude of the Square pulse in Volts
30.4
Enter the frequency of the Triangular carrier wave in Hertz
2e3
Enter the Integrator constant c
0.0001
Enter the Function constant k1
19
Enter the Multiplication constant k2
0.5263
OK
Cancel
Block Parameters: Subsystem
Mechanical Load for Three Phase I.M. (mask)
Enter the initial value and final value of time in seconds and the corresponding initial and final values of mechanical load in Nw-meters in the appipriate box provided.
Parameters
Enter the initial time in seconds
0
Enter the Final time in seconds
2
Enter the initial value of load in Nw-meters
-0
Enter the final value of load in Nw-meters
-0
OK
Cancel
Help
Apply
Block Parameters: Subsystem1
Three Phase IM Model in Stationay Reference Frame (mask)
Enter the Stator Resistance and Leakage Reactance, Rotor Resistance and Leakage Reactance referred to Stator, Mutual reactance between Stator and Rotor all per phase value, Number of Poles and combined Moment of Inertia of Rotor and Load in the appropriate unit in the box provided.
Parameters
Enter the Stator Resistance in Ohms per Phase
0.1062
Enter the Rotor Resistance referred to Stator in Ohms per Phase
0.0764
Enter the Stator Leakage Reactance in Ohms per Phase
0.2145
Enter the Rotor Leakage Reactance referred to Stator in Ohms per Phase
0.2145
Enter the Mutual Reactance between Stator and Rotor in Ohms per Phase
5.834
Enter the Number of Poles
4
Enter the Rated Angular Frequency of the Machine Radians per second
2*pi*60
Enter the combined M.I. of Rotor and Load in Kg-m^2
2.5
OK
Cancel
Help
Apply

FIG.11.13

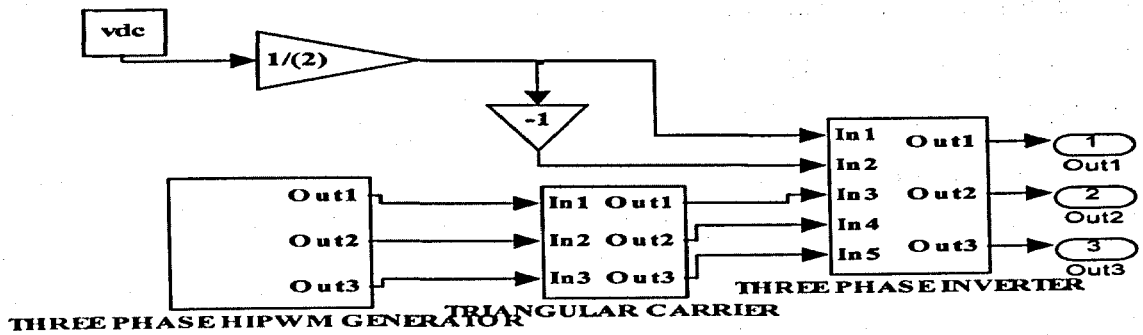

FIG.11.14(A)

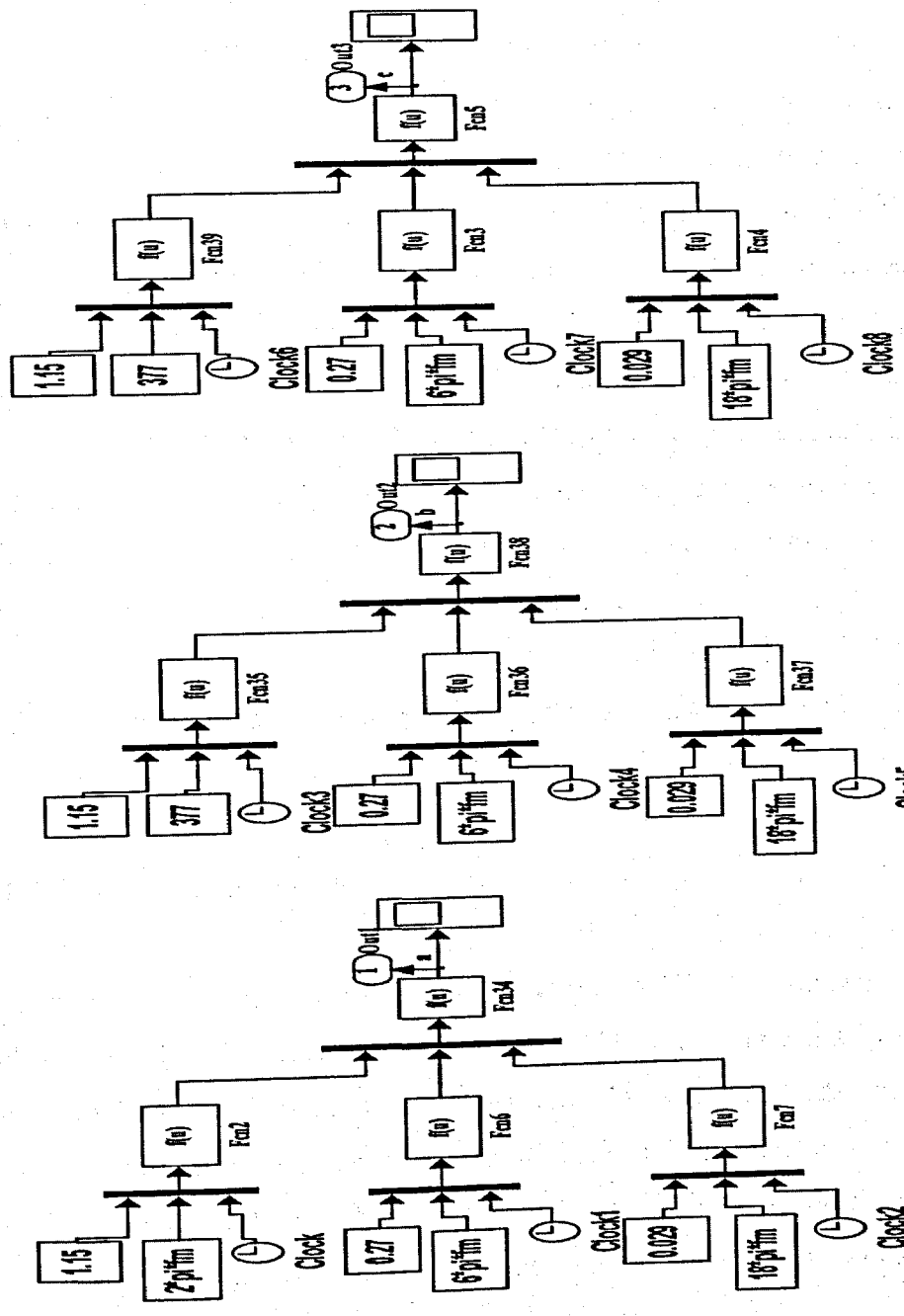

FIG.11.14(B)

Generator and Inverter Unit" in Fig.11.13. The various subsystems are: Three Phase HIPWM Generator, Triangle Carrier and Three Phase Inverter. The models for Triangular carrier and three phase inverter are the same as for three phase THIPWM inverter fed IM Drive discussed under section 11.3.1. The model for the Three Phase HIPWM Generator is explained below: In Fig.11.14(B), the modulating sine wave with fundamental fm Hertz, third harmonics and ninth harmonics are multiplied by appropriate constants and are added with appropriate signs for the three phases as per the equation given by equation 11.15. The three input mux at the top with input constant blocks 1.15 and 2*pi*fm along with the Fcn block generate the fundamental component in equation 11.15. The three input mux at the middle with constant block inputs 0.27 and 6*pi*fm along with the Fcn block generate the third harmonic component of equation 11.15. The three input mux at the bottom with constant block inputs 0.029 and 18*pi*fm along with the Fcn block generate the ninth harmonic component of equation 11.15. The Fcn34 block sums the three values and multiplies by vpeak to generate the modulating signal a for the Phase R. For Phase Y modulating signal b is generated in the same way as for Phase R, except that the fundamental component, third harmonic and the ninth harmonic component lags by 2*pi/3, 2*pi and 6*pi radians respectively. For Phase B, the modulating signal c is generated as for Phase Y, except that the fundamental, third harmonic and ninth harmonic component leads by 2*pi/3, 2*pi and 6*pi radians respectively.

All other models are as explained for three phase sine PWM and three Phase THIPWM inverter fed IM drive in sections 11.2.1 and 11.3.1 respectively.

11.4.2 Simulation Results

The simulation results of the Three Phase 60 Hz HIPWM Inverter fed IM drive using ode15s(stiff/NDF) solver are shown in Fig.11.15(A) to (E) and in Fig.11.16(A) to (E) for a.m. indices M of 0.9 and 1.1 respectively, with f.m. index maintained at 33.33.. The simulation results for all the a.m. indices less than and greater than one are tabulated in Table 11.3. The data for the 20 hp, 220 volts, three phase, 60 Hz, 4 pole star connected cage IM used for simulation are the same as given in section 11.2.2.

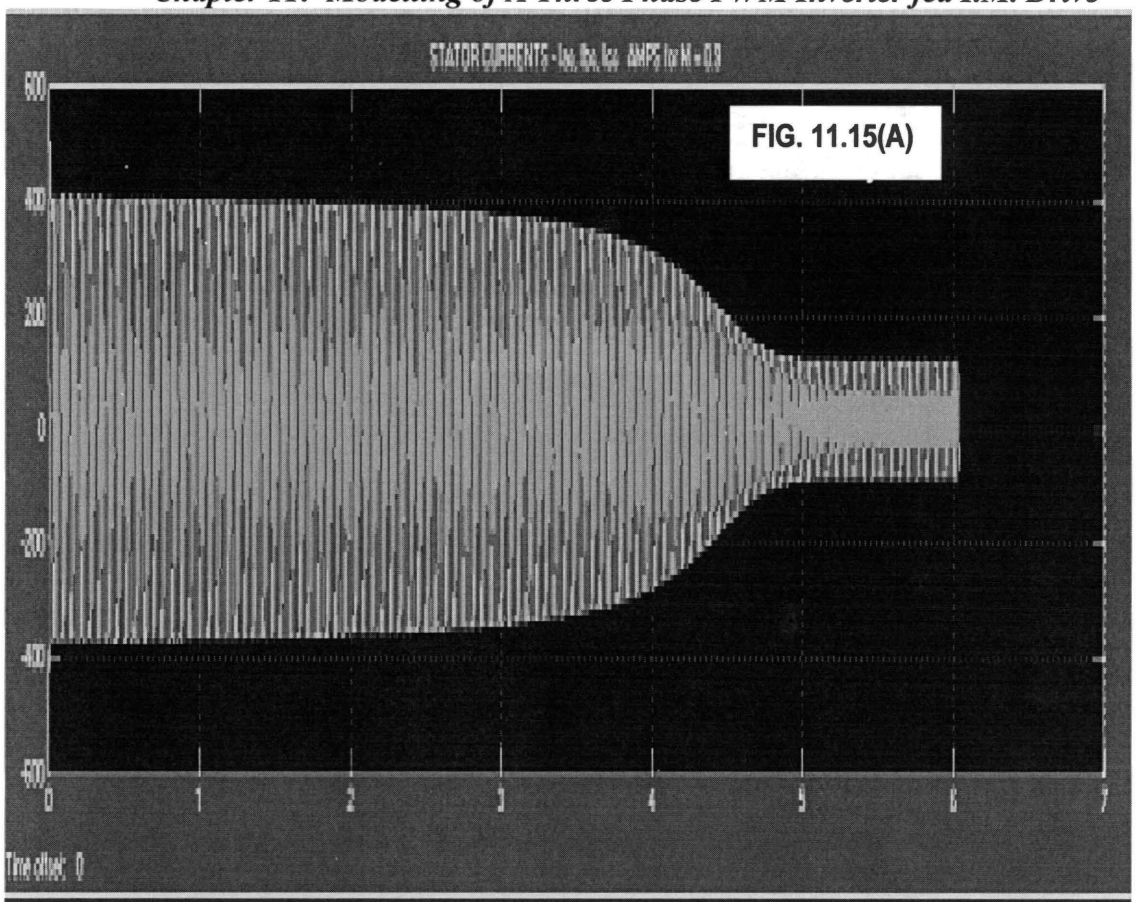

FIG. 11.15(A)

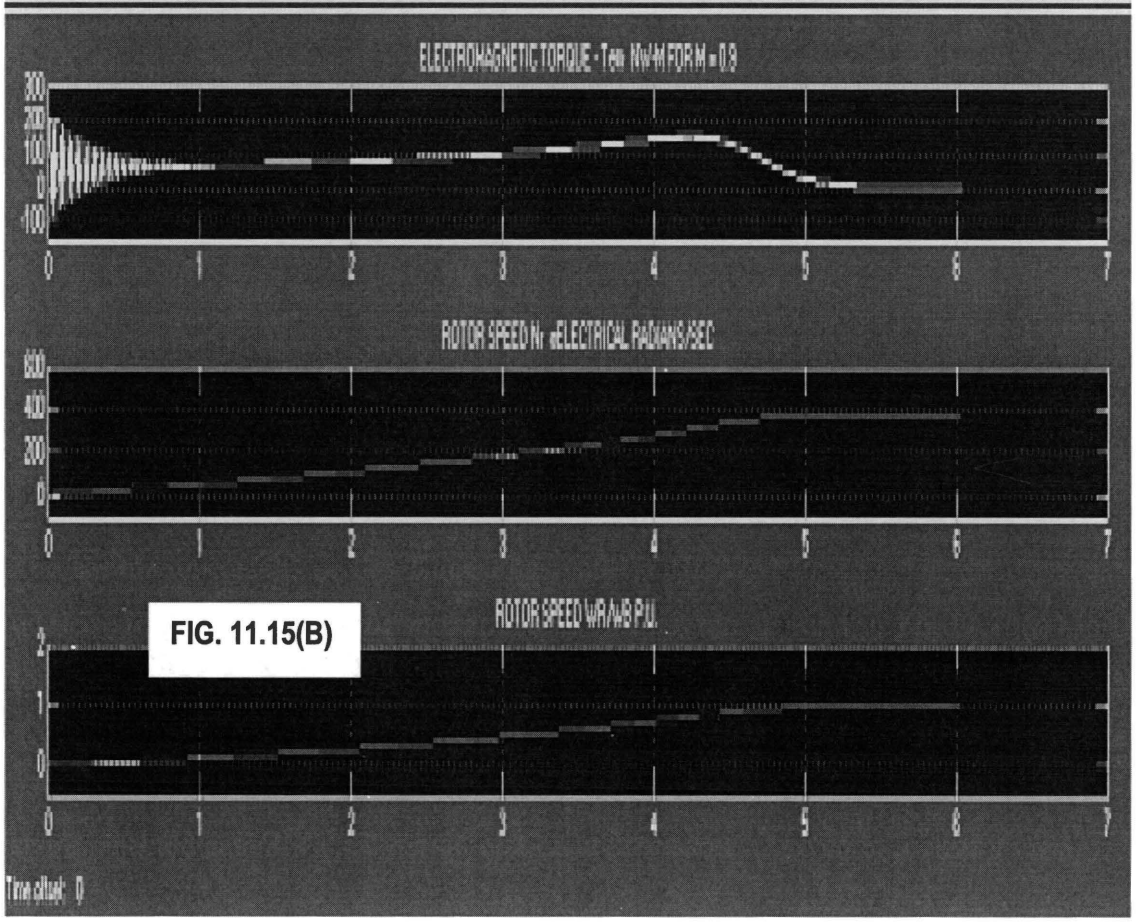

FIG. 11.15(B)

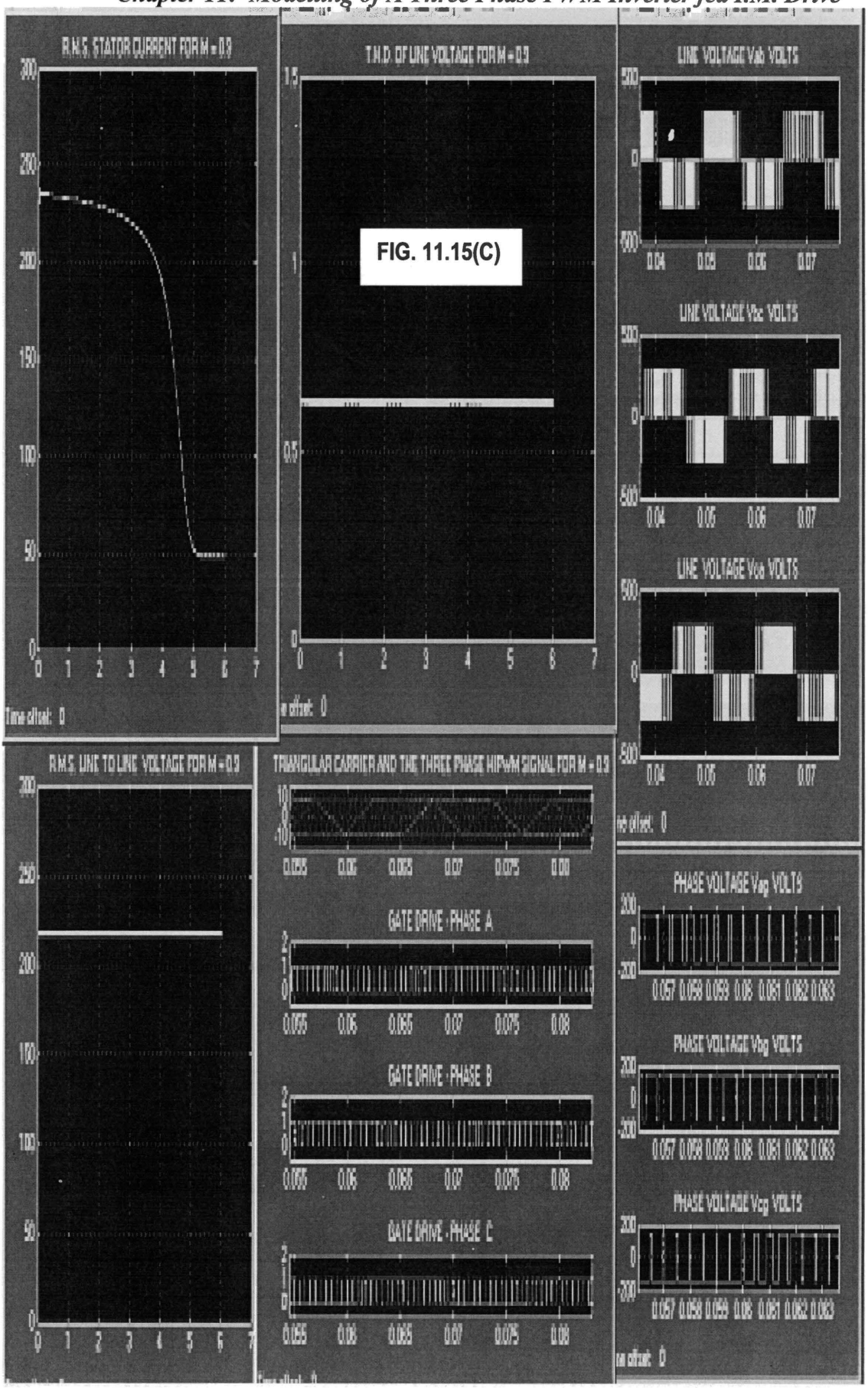
R.M.S. STATOR CURRENT FOR M = 0.9
T.H.D. OF LINE VOLTAGE FOR M = 0.9
FIG. 11.15(C)
LINE VOLTAGE Vab VOLTS
LINE VOLTAGE Vbc VOLTS
LINE VOLTAGE Vca VOLTS
R.M.S. LINE TO LINE VOLTAGE FOR M = 0.9
TRIANGULAR CARRIER AND THE THREE PHASE HIPWM SIGNAL FOR M = 0.9
GATE DRIVE - PHASE A
GATE DRIVE - PHASE B
GATE DRIVE - PHASE C
PHASE VOLTAGE Van VOLTS
PHASE VOLTAGE Vbn VOLTS
PHASE VOLTAGE Vcn VOLTS

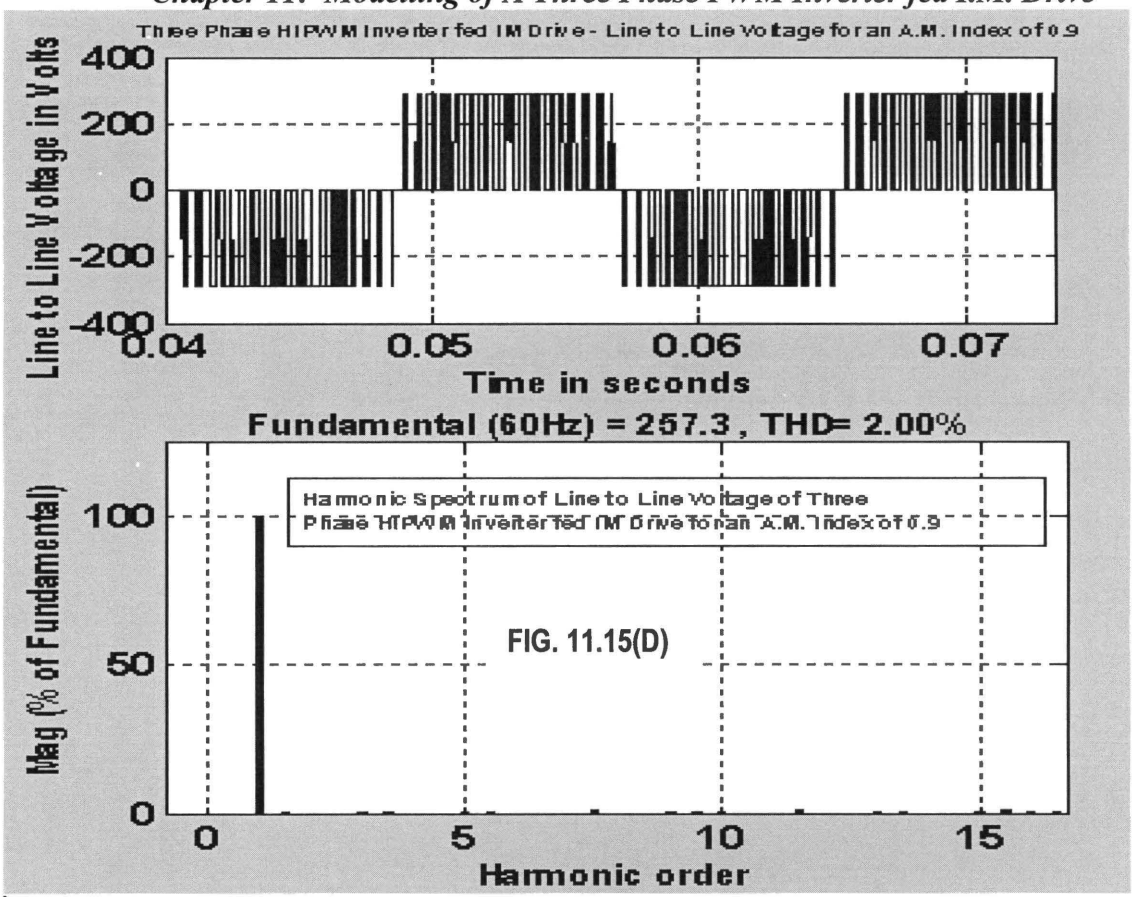

FIG. 11.15(D)

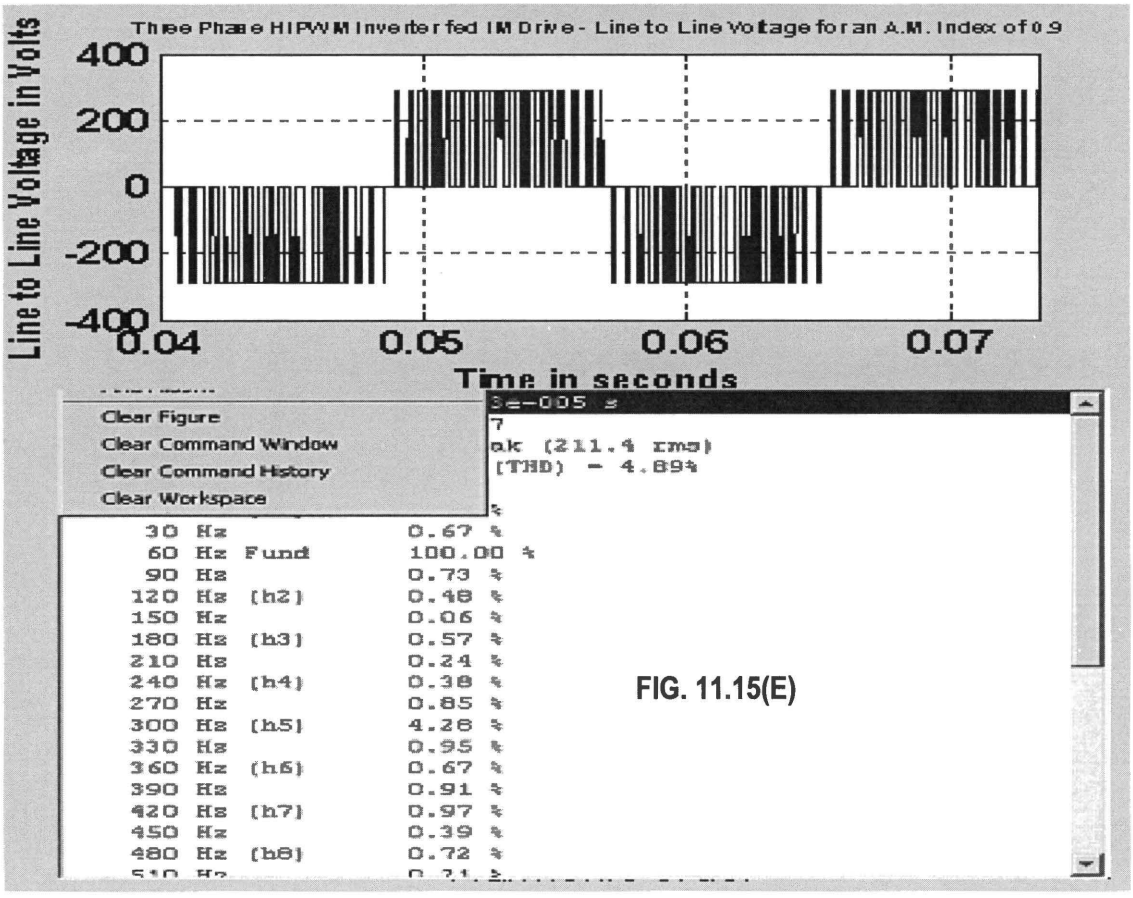

FIG. 11.15(E)

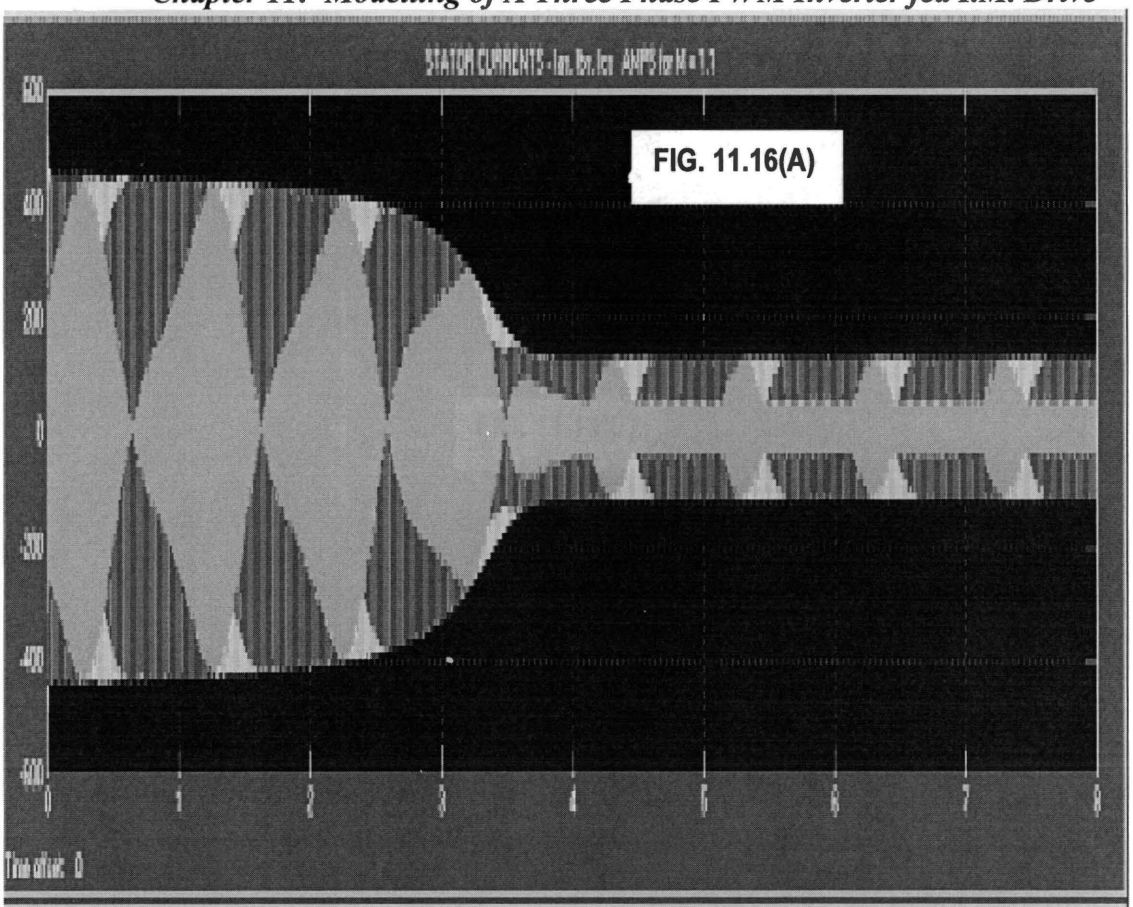
STATOR CURRENTS - Ian, Ibn, Icn AMPS for M = 1.1
FIG. 11.16(A)
Time offset: 0

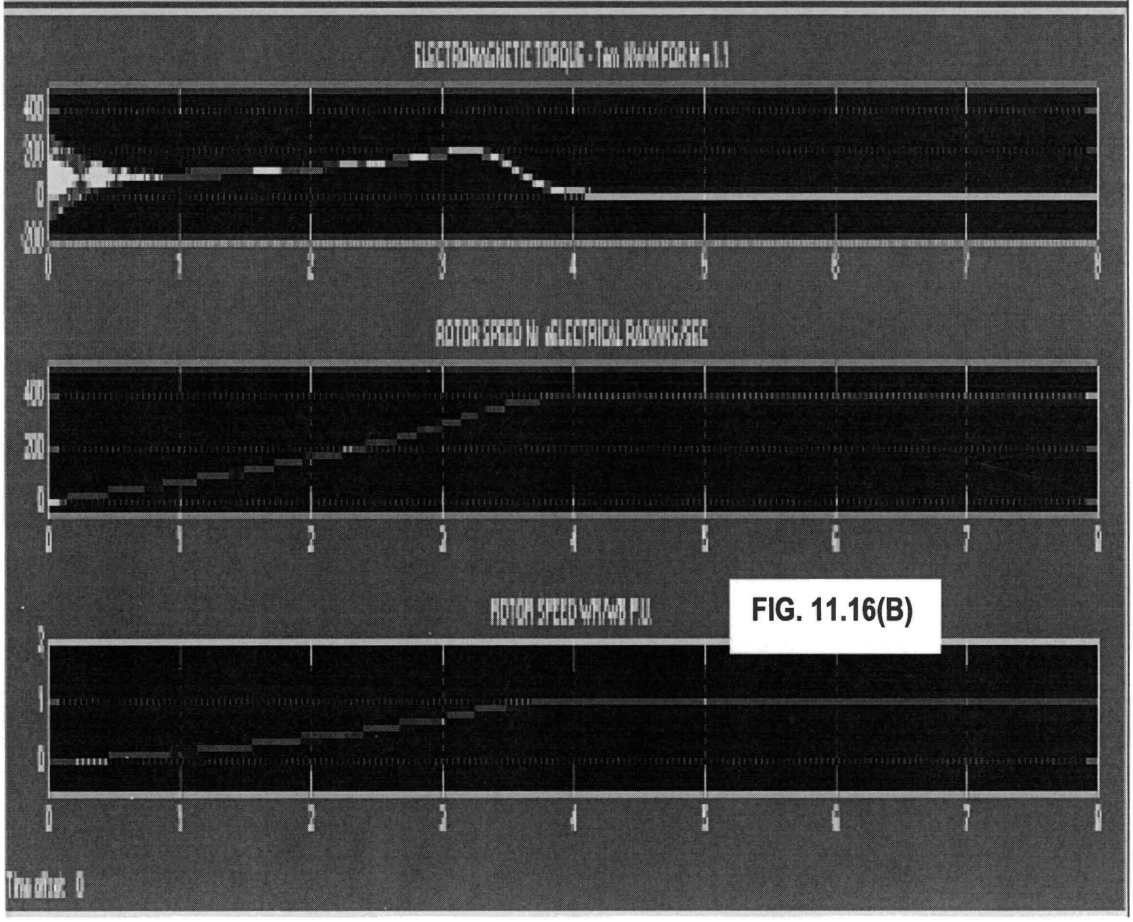
ELECTROMAGNETIC TORQUE - Tem NEWM FOR M = 1.1
ROTOR SPEED W eELECTRICAL RADIANS/SEC
ROTOR SPEED W/Ws PU
FIG. 11.16(B)
Time offset: 0

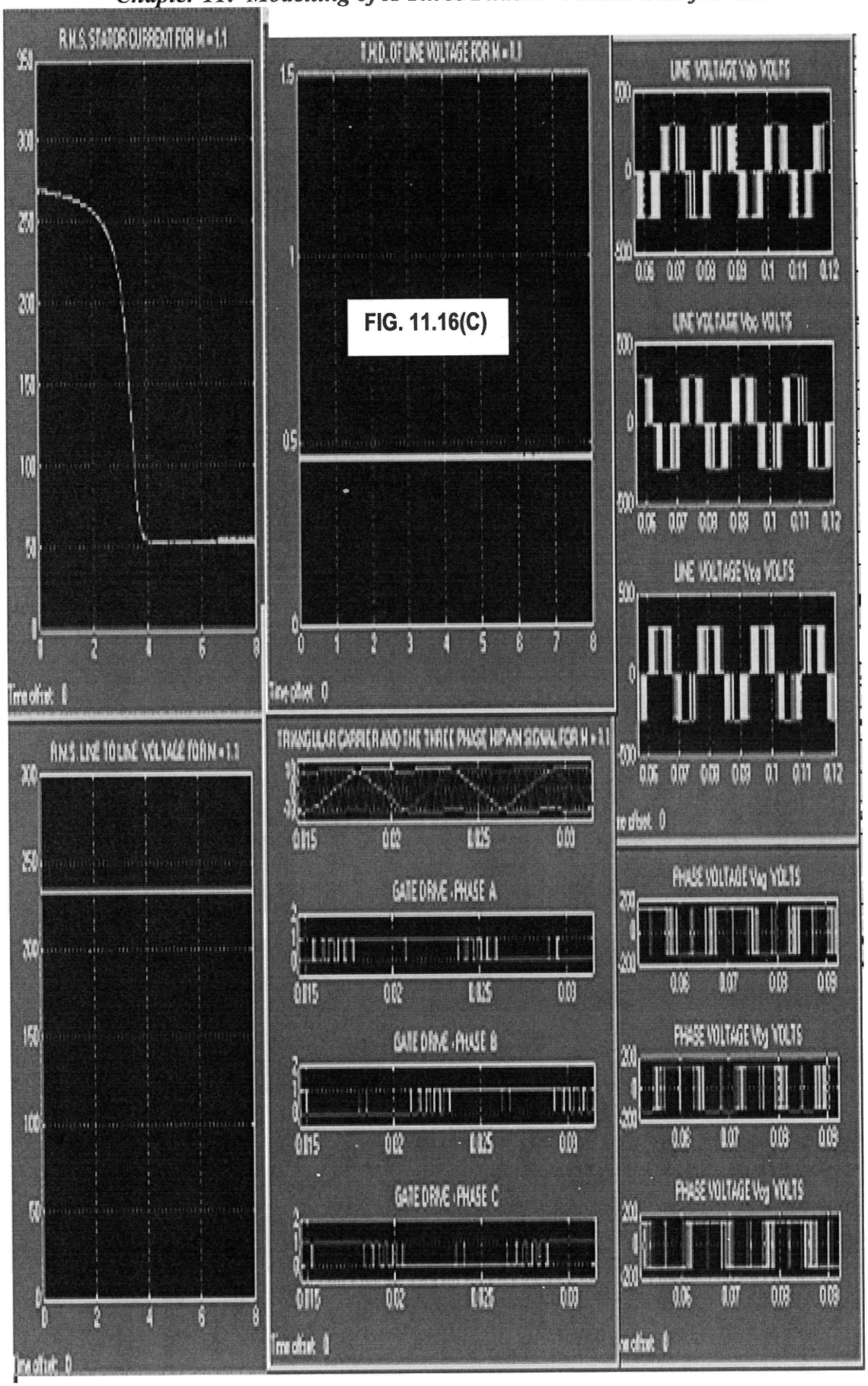
R.M.S. STATOR CURRENT FOR M = 1.1
T.H.D. OF LINE VOLTAGE FOR M = 1.1
LINE VOLTAGE Vab VOLTS
LINE VOLTAGE Vbc VOLTS
LINE VOLTAGE Vca VOLTS
R.M.S. LINE TO LINE VOLTAGE FOR M = 1.1
TRIANGULAR CARRIER AND THE THREE PHASE MPWM SIGNAL FOR M = 1.1
GATE DRIVE : PHASE A
GATE DRIVE : PHASE B
GATE DRIVE : PHASE C
PHASE VOLTAGE Vag VOLTS
PHASE VOLTAGE Vbg VOLTS
PHASE VOLTAGE Vcg VOLTS
FIG. 11.16(C)

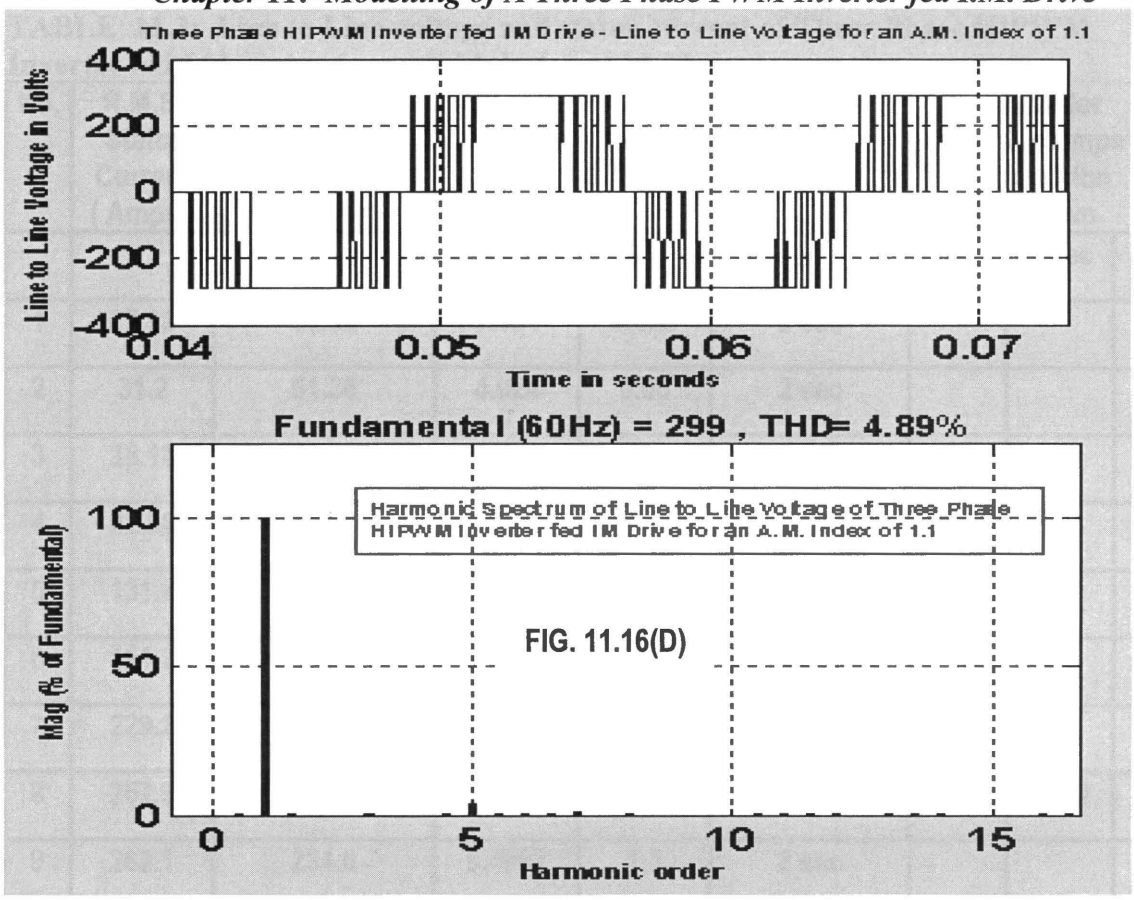

FIG. 11.16(D)

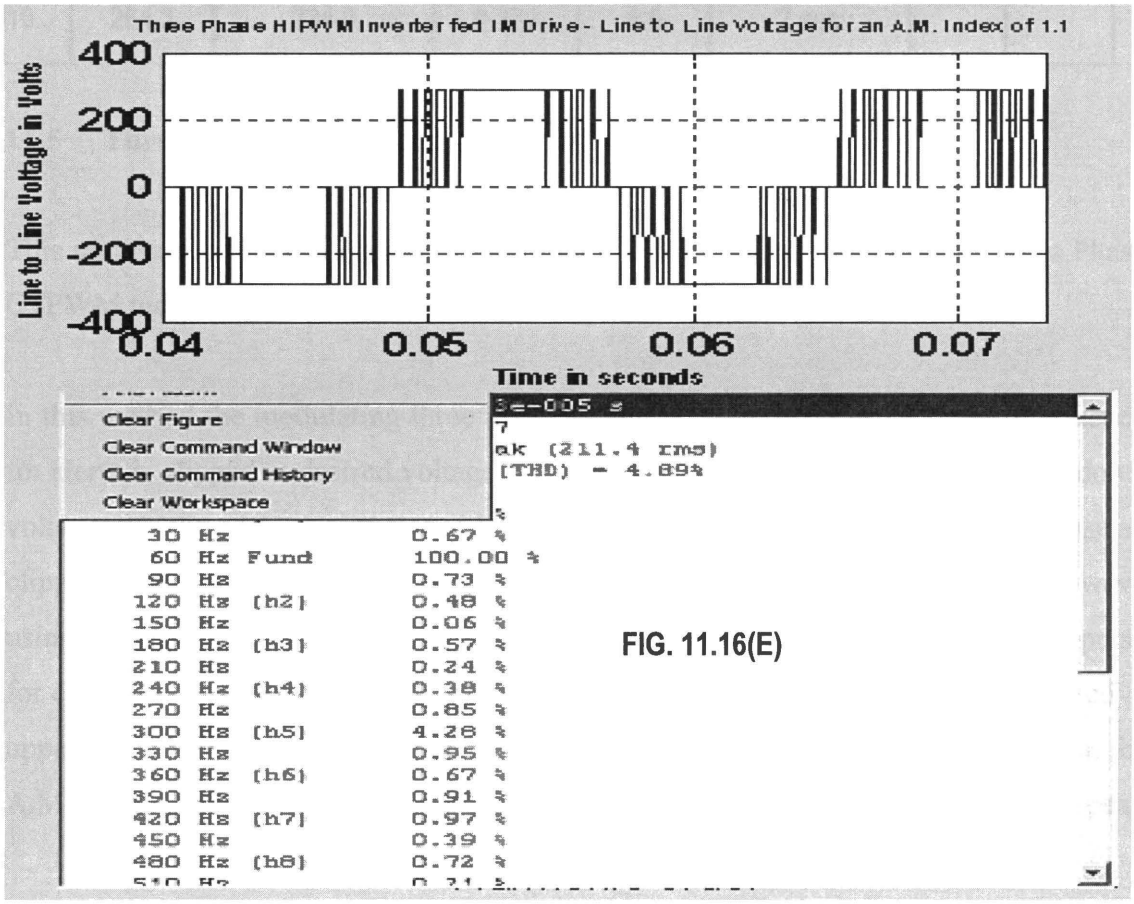

FIG. 11.16(E)

TABLE 11.3: Line to Line voltage and stator current of Three Phase HIPWM Inverter fed I.M. Drive for an F.M. Index of 33.33.

No.	R.M.S. Stator Current (Amps)	R.M.S. LineVoltage Vab (Volts)	T.H.D.** Of Line to Line Voltage	A.M.In-dex M	Simulation Time in seconds	R.M.S.Stator current in Amps for simulation time shown	
						6 sec	8 sec
1	27.83	36.32	7.034	0.025	2 sec		
2	31.2	51.36	4.924	0.05	2 sec		
3	38.18	72.64	3.411	0.1	2 sec		
4	82.38	125.8	1.788	0.3	2 sec		
5	131.8	162.3	1.232	0.5	2 sec		
6	181.3	192.0	0.8932	0.7	2 sec		
7	229.2	217.7	0.6307	0.9	2 sec	47.8	---
8	257.9	233.1	0.4517	1.1	2 sec	---	53.87
9	262.1	234.0	0.4087	1.3	2 sec		
10	264.3	234.0	0.379	1.5	2 sec		

11.5 Three Phase Clipped Sinusoid PWM Technique

This section describes the discovery of the new PWM technique known as Three Phase CSPWM technique. This is explained below:

In this method the modulating three phase ac signal at the inverter switching frequency fm Hertz is clipped at desired voltage levels using zener diode clippers with breakdown voltages +Vclip and –Vclip placed back to back in series. The resulting three phase ac clipped sine wave at the frequency fm Hertz is compared with triangular carrier wave using op.amp. comparators in each of the three phases. The resulting PWM gate pulse for each of the three phases and their respective inverted gate pulse drives the respective upper and lower semiconductor switches in each of the three phases. The definition for A.M. Index and F.M. index are the same as given by equations 11.1 and 11.2. The peak

value of the clipped sine wave Am is measured at the center of the half cycle i.e. at the interval Tm /4 where Tm is the period 1 /fm seconds.

11.5.1 Modelling of Three Phase Clipped Sinusoid PWM Inverter fed IM Drive

The interactive model of the three phase CSPWM inverter fed IM drive is shown in Fig.11.17. The various dialog boxes are shown in Fig.11.18. The subsystem for the dialog box "Three phase sine wave clipper" is shown in Fig.11.19. The other subsystems corresponding to the dialog boxes "Triangle Carrier Generator", "Three Phase Voltage Source Inverter", "Three Phase IM in Stationary Reference Frame" and "Mechanical Load for Three Phase IM" are the same as for three phase sine PWM inverter fed IM drive discussed under section 11.2.1. Fig.11.19 corresponds to the dialog box "Three Phase Sine Wave Clipper" in Fig.11.18. The model for the Three Phase Sine Wave Clipper is explained below:

Referring to Fig.11.19, the three input mux with Function blocks Fcn2, Fcn3 and Fcn4 generate the modulating three phase ac with a peak value of 20 volts and frequency fm Hertz corresponding to the switching frequency of the inverter. Referring to Fcn2 block corresponding to Phase R, Fcn2 output is given to the u(2) and u(3) inputs of Switch3 and also to u(1) and u(2) inputs of switch4. The constant block with the clip voltage value +Vclip is given to the u(1) input of Switch3 and the inverted –Vclip is given to the u(3) input of Switch4. The output of Switch3 and Switch4 are given to u(1) and u(3) input of switch5. The Fcn2 output is given to the u(2) input of Switch5. Switch3 and Switch4 have a threshold value of +Vclip and –Vclip respectively. The threshold value for switch5 is zero. All these threshold switches output u(1) when the u(2) input is greater than or equal to the threshold value, else the output is the u(3) input. Similar connections and threshold values apply for switches 6, 7 and 8 in Phase Y and Switches 9, 10 and 11 in Phase B.

The triangle carrier generator model generate a carrier frequency fc of 2 kHZ. For any other carrier frequency fc Hz, the help file shown in Fig.11.4(H) can be used.

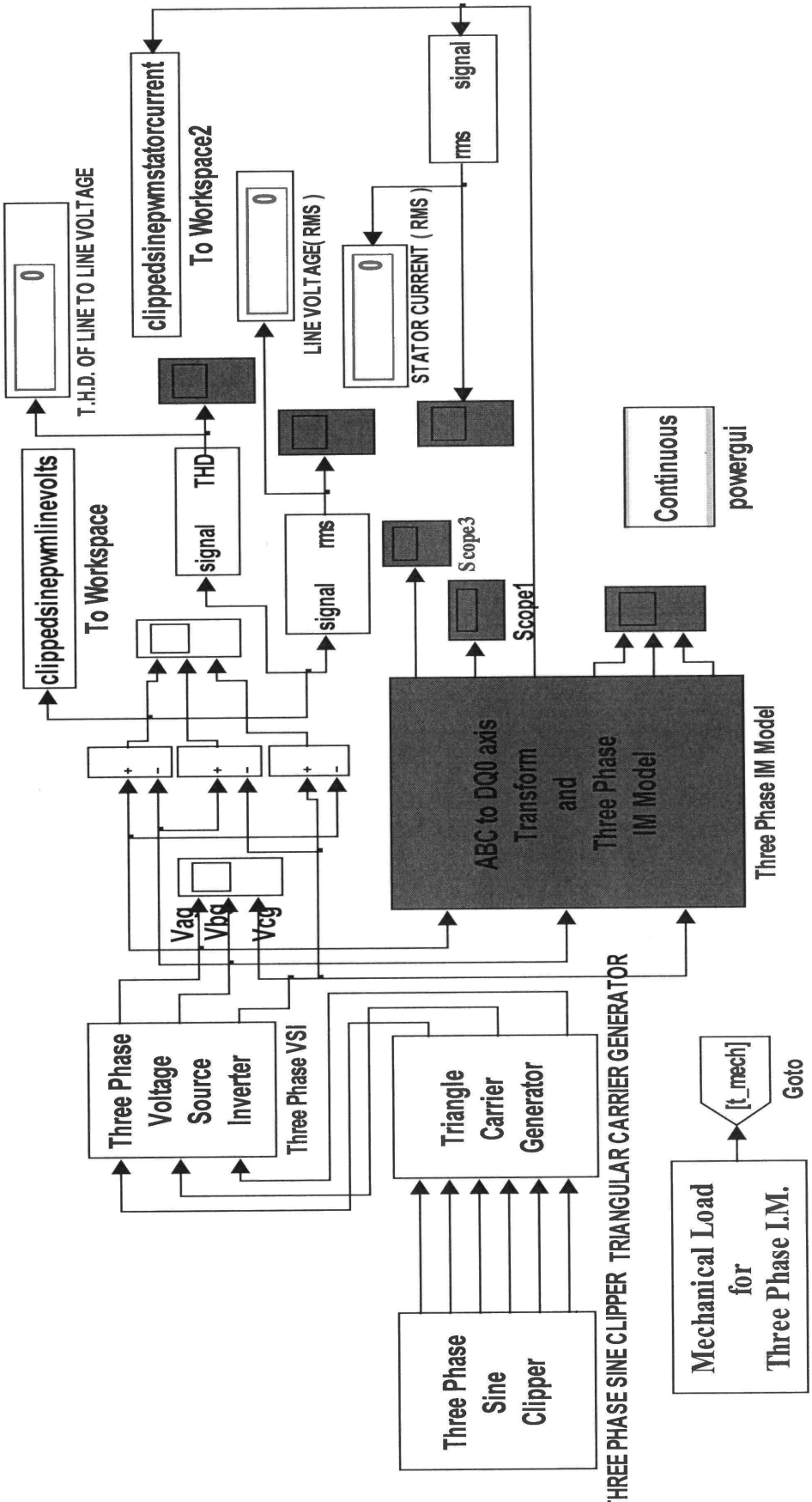

FIG.11.17: THREE PHASE 60 HZ CLIPPED SINUSOID PWM INVERTER FED I.M. DRIVE

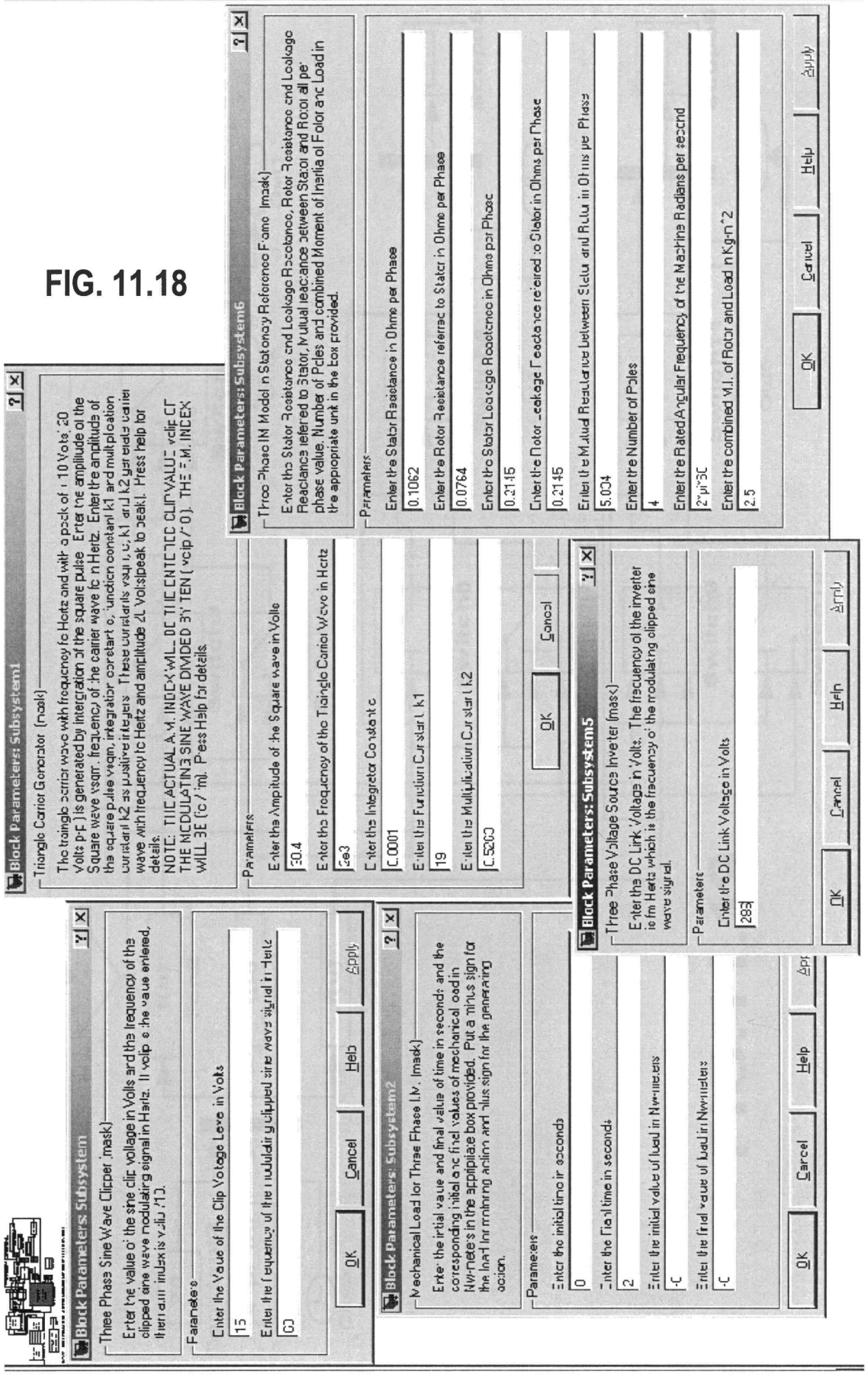
Block Parameters: Subsystem1
Triangle Carrier Generator (mask)
Parameters
Enter the Amplitude of the Square wave in Volts
30.4
Enter the Frequency of the Triangle Carrier Wave in Hertz
5e3
Enter the Integrator Constant c
0.0001
Enter the Function Constant k1
19
Enter the Multiplication Constant k2
0.5000
OK
Cancel
Block Parameters: Subsystem6
Three Phase IM Model in Stationary Reference Frame (mask)
Parameters
Enter the Stator Resistance in Ohms per Phase
0.1062
Enter the Rotor Resistance referred to Stator in Ohms per Phase
0.0764
Enter the Stator Leakage Reactance in Ohms per Phase
0.2145
Enter the Rotor Leakage Reactance referred to Stator in Ohms per Phase
0.2145
Enter the Mutual Reactance between Stator and Rotor in Ohms per Phase
5.034
Enter the Number of Poles
4
Enter the Rated Angular Frequency of the Machine Radians per second
2*pi*50
Enter the combined M.I. of Rotor and Load in Kg-m^2
2.5
OK
Cancel
Help
Apply
Block Parameters: Subsystem5
Three Phase Voltage Source Inverter (mask)
Enter the DC Link Voltage in Volts. The frequency of the inverter is in Hertz which is the frequency of the modulating clipped sine wave signal.
Parameters
Enter the DC Link Voltage in Volts
283
OK
Cancel
Help
Apply
Block Parameters: Subsystem
Three Phase Sine Wave Clipper (mask)
Parameters
Enter the Value of the Clip Voltage Level in Volts
15
Enter the frequency of the modulating clipped sine wave signal in Hertz
60
OK
Cancel
Help
Apply
Block Parameters: Subsystem2
Mechanical Load for Three Phase I.M. (mask)
Parameters
Enter the initial time in seconds
0
Enter the final time in seconds
2
Enter the initial value of load in Newtons
-C
Enter the final value of load in Newtons
-C
OK
Cancel
Help
Apply

FIG. 11.18

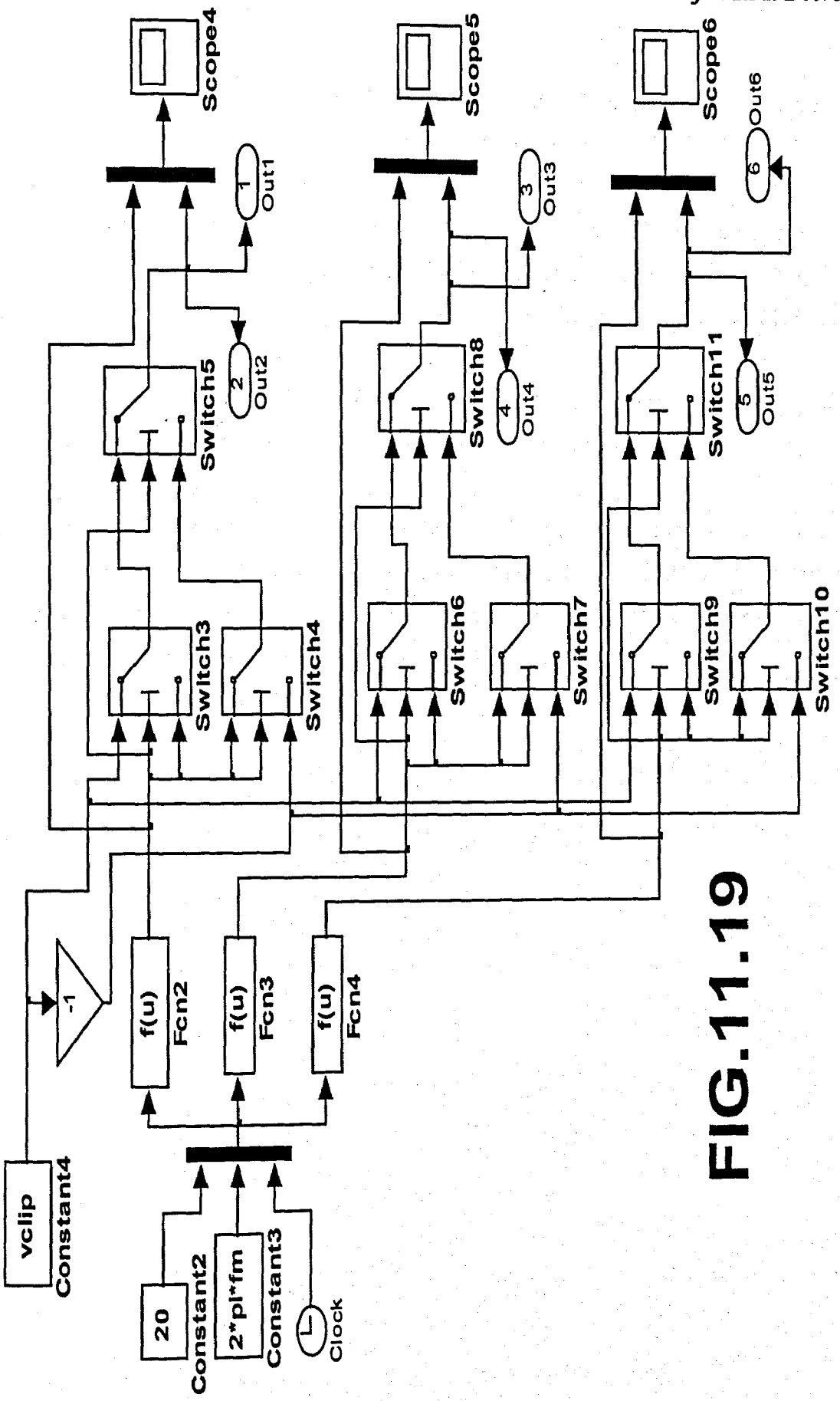
Scope4
Scope5
Scope6
Out1
Out2
Out3
Out4
Out5
Out6
Switch3
Switch4
Switch5
Switch6
Switch7
Switch8
Switch9
Switch10
Switch11
f(u)
Fcn2
f(u)
Fcn3
f(u)
Fcn4
-1
vclip
Constant4
20
Constant2
2*pi*fm
Constant3
Clock

FIG.11.19

11.5.2 Simulation Results

The simulation results of the Three Phase 60 Hz CSPWM Inverter fed IM drive using ode15s(stiff/NDF) solver are shown in Fig.11.20(A) to (E) and in Fig.11.21(A) to (E) for a.m. indices M of 0.9 and 1.1 respectively, with F.M. index maintained at 33.33.. The simulation results for all the a.m. indices less than and greater than one are tabulated in Table 11.4. The data for the 20 hp, 220 volts, three phase, 60 Hz, 4 pole star connected cage IM used for simulation are the same as given in section 11.2.2.

11.6 Comparison of the Total Harmonic Distortion of Line to Line Voltage of Three Phase Inverter by Various PWM Techniques

Tables 11.1 to 11.4 gives the magnitude of line to line voltage and the T.H.D. of Line to Line Voltage of Three Phase Inverter by SINE, THI, HI and CS PWM techniques. A Graph of the plots of Line to Line Voltage magnitude and its T.H.D. by the above PWM techniques are shown in Fig.11.22 and Fig.11.23 respectively.

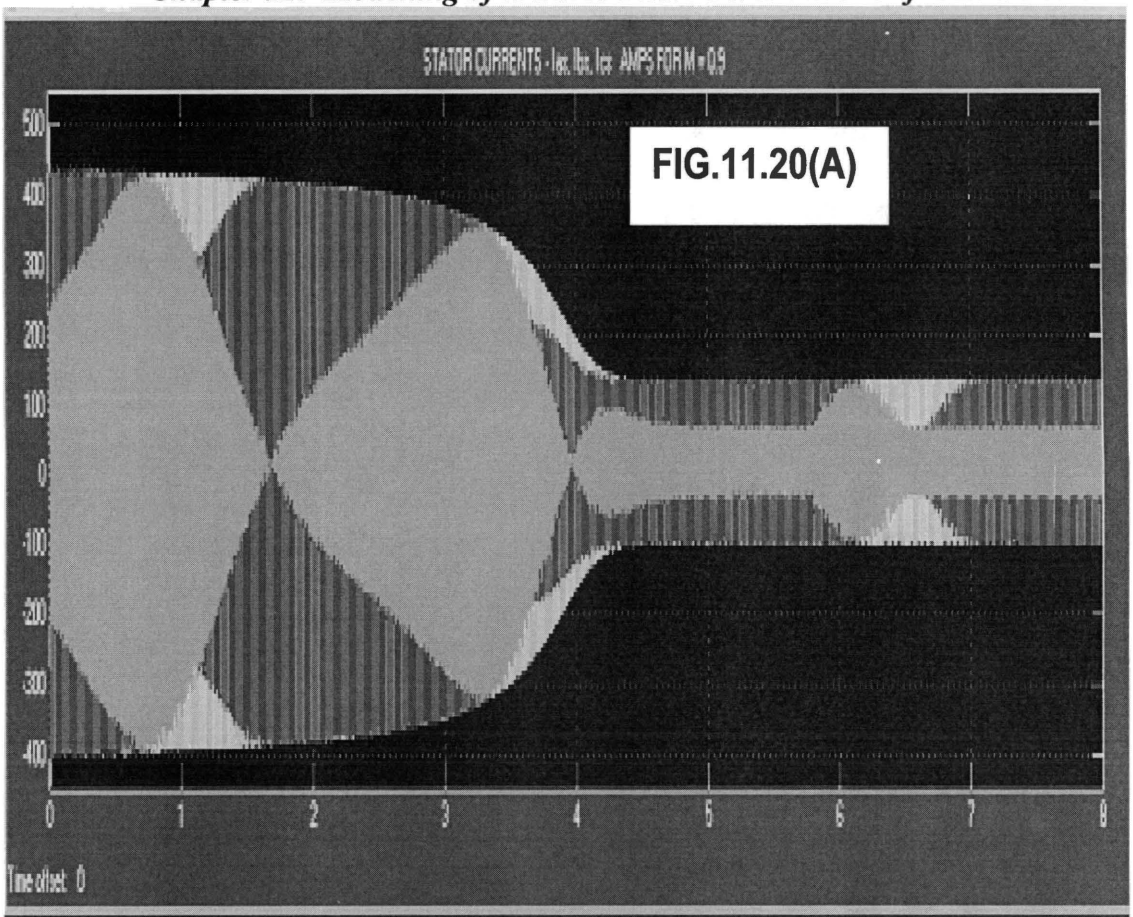

FIG.11.20(A)

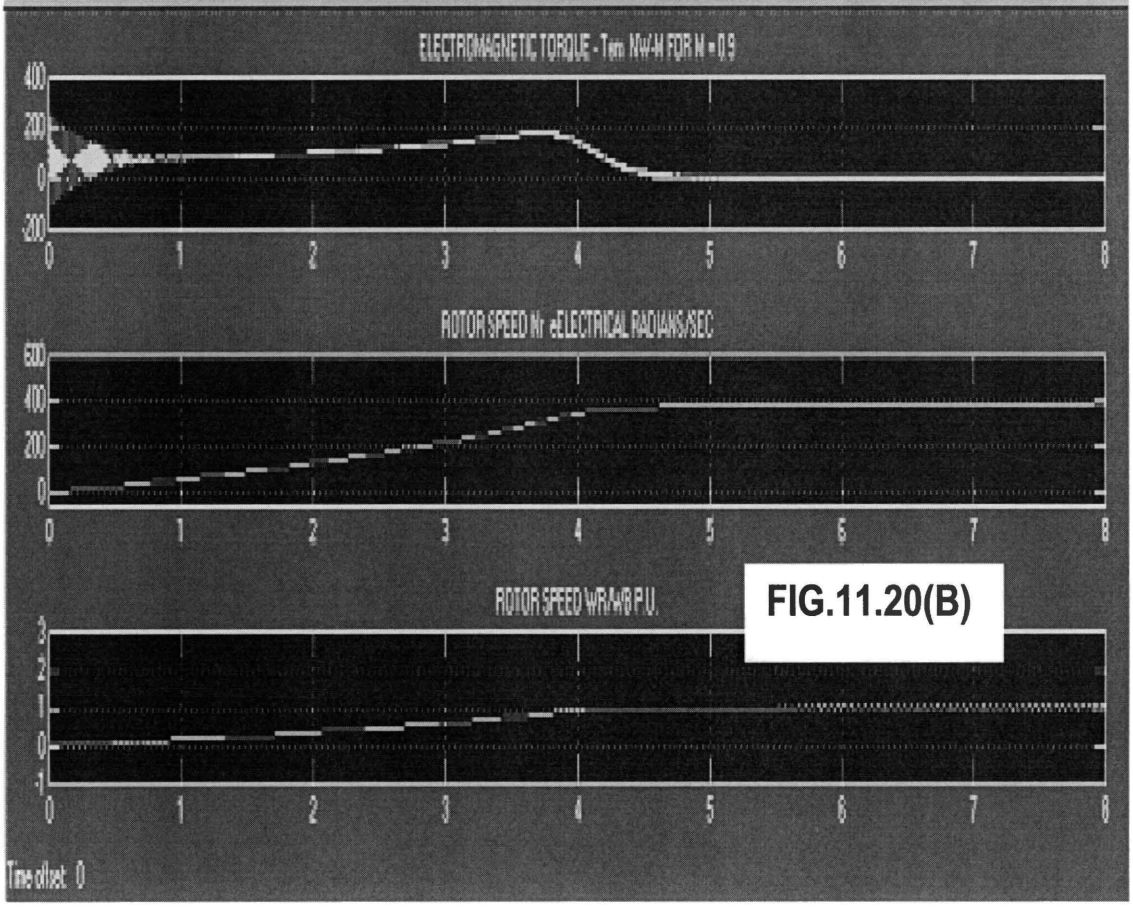

FIG.11.20(B)

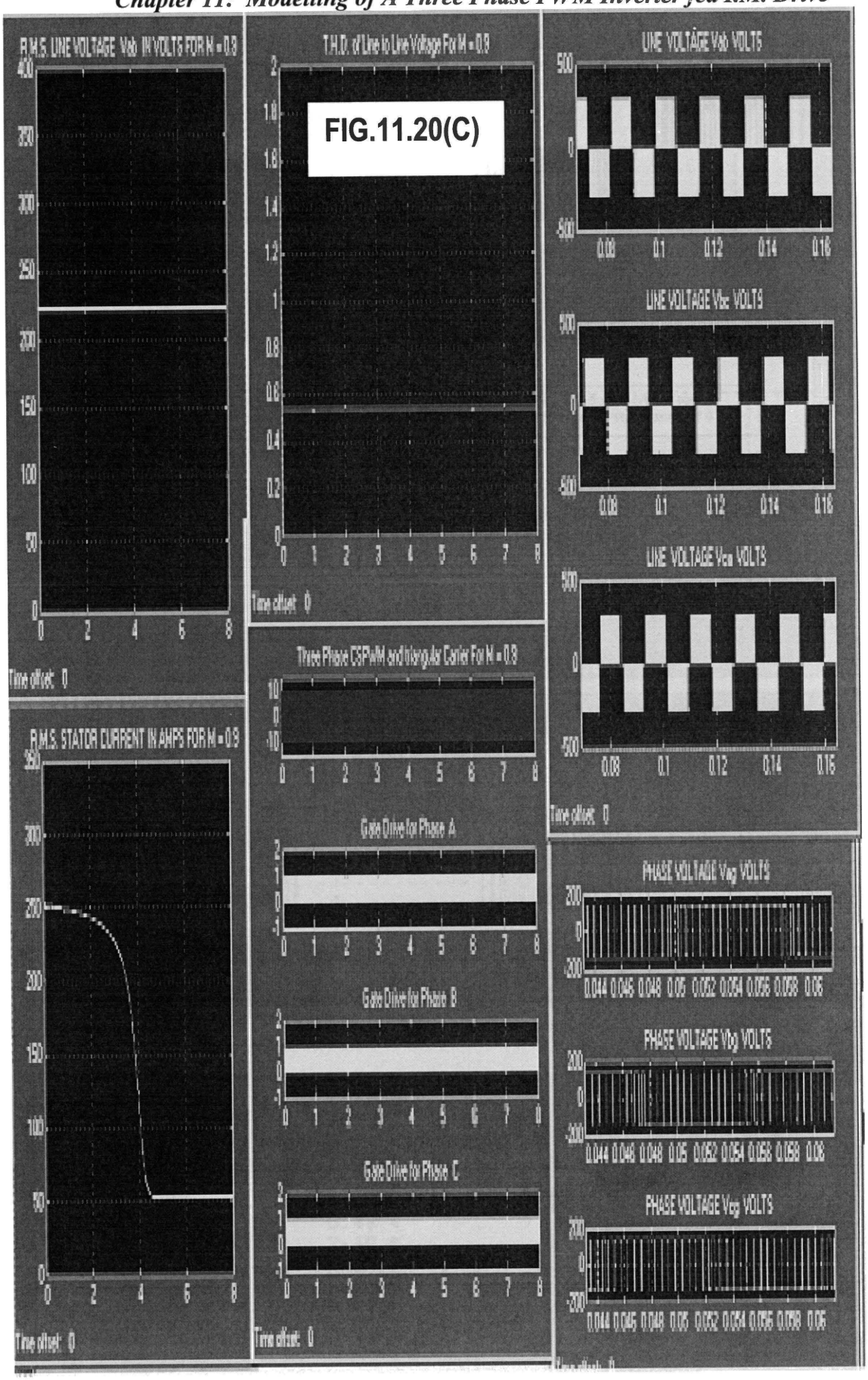
R.M.S. LINE VOLTAGE Vab IN VOLTS FOR M = 0.9
T.H.D. of Line to Line Voltage For M = 0.9
FIG.11.20(C)
LINE VOLTAGE Vab VOLTS
LINE VOLTAGE Vbc VOLTS
LINE VOLTAGE Vca VOLTS
Three Phase CSPWM and triangular Carrier For M = 0.9
R.M.S. STATOR CURRENT IN AMPS FOR M = 0.9
Gate Drive for Phase A
Gate Drive for Phase B
Gate Drive for Phase C
PHASE VOLTAGE Vag VOLTS
PHASE VOLTAGE Vbg VOLTS
PHASE VOLTAGE Vcg VOLTS
Time offset: 0

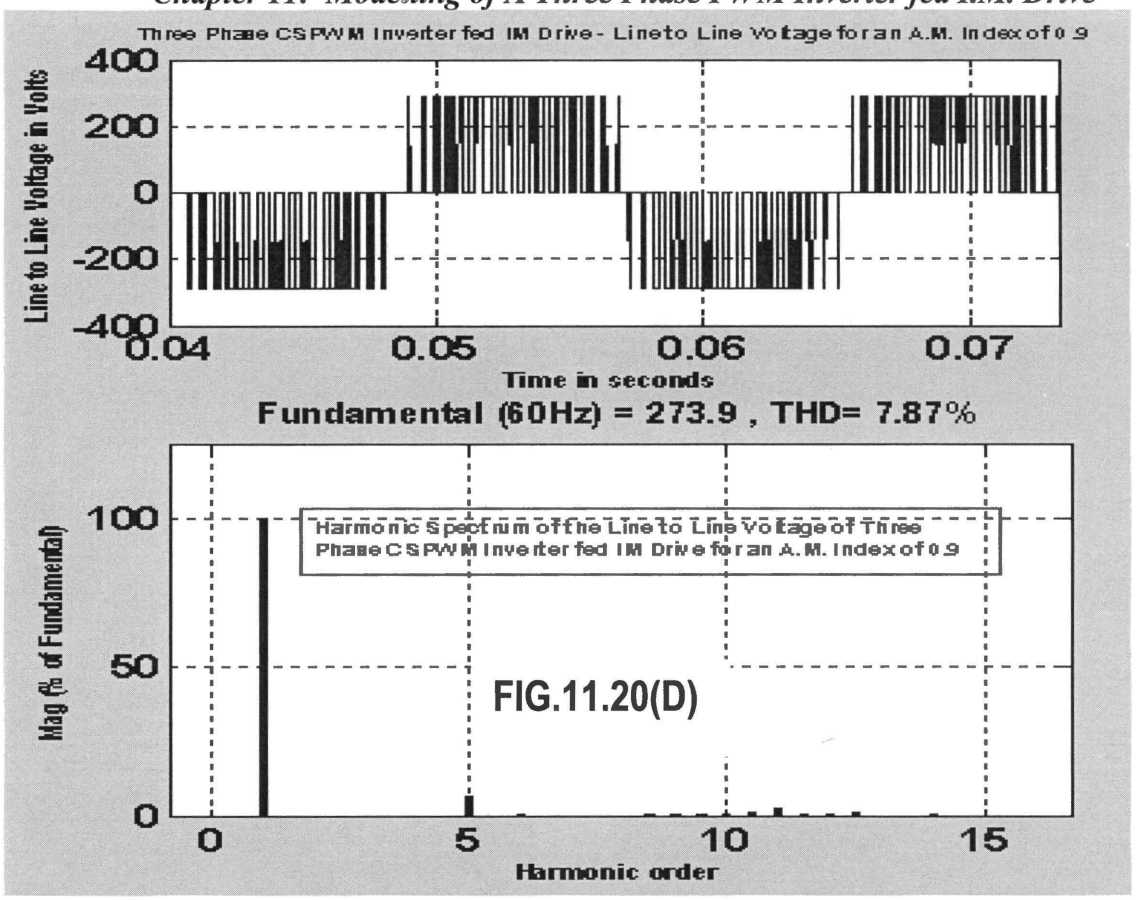

FIG.11.20(D)

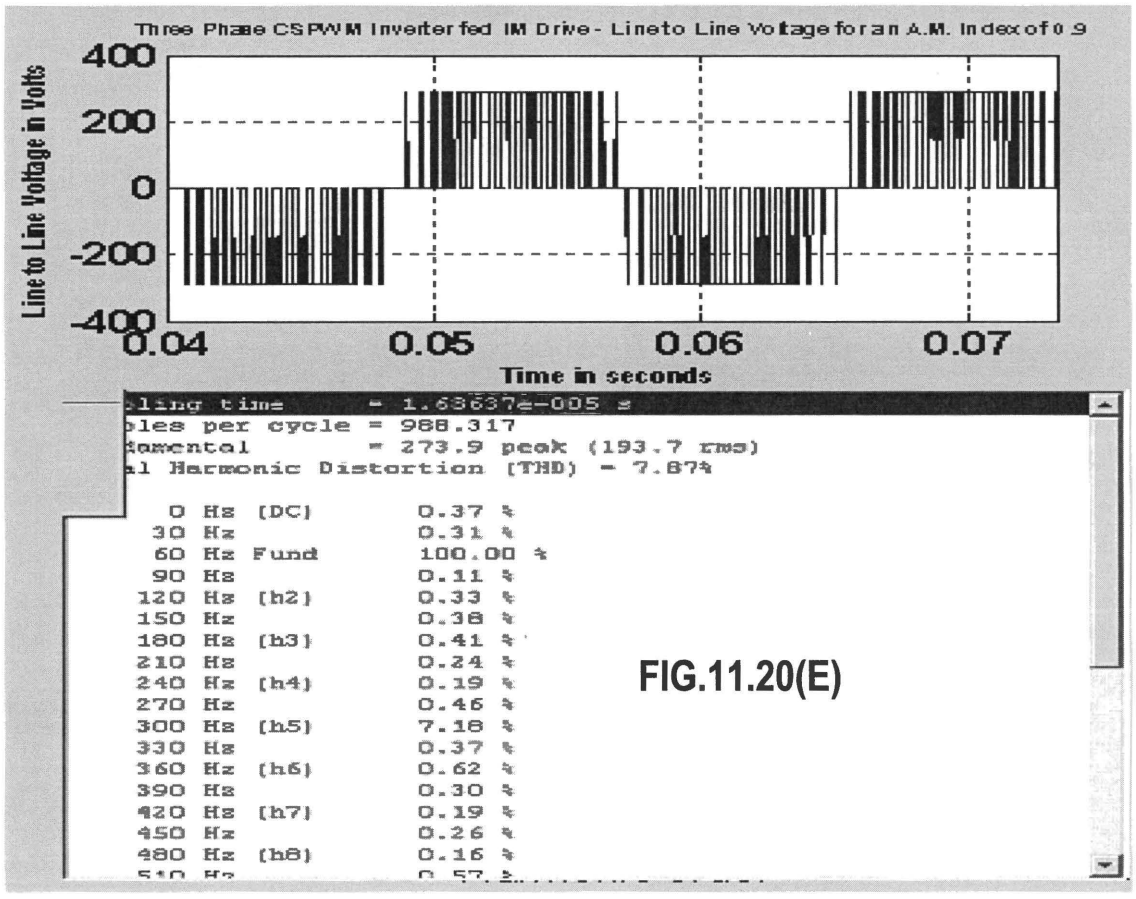

FIG.11.20(E)

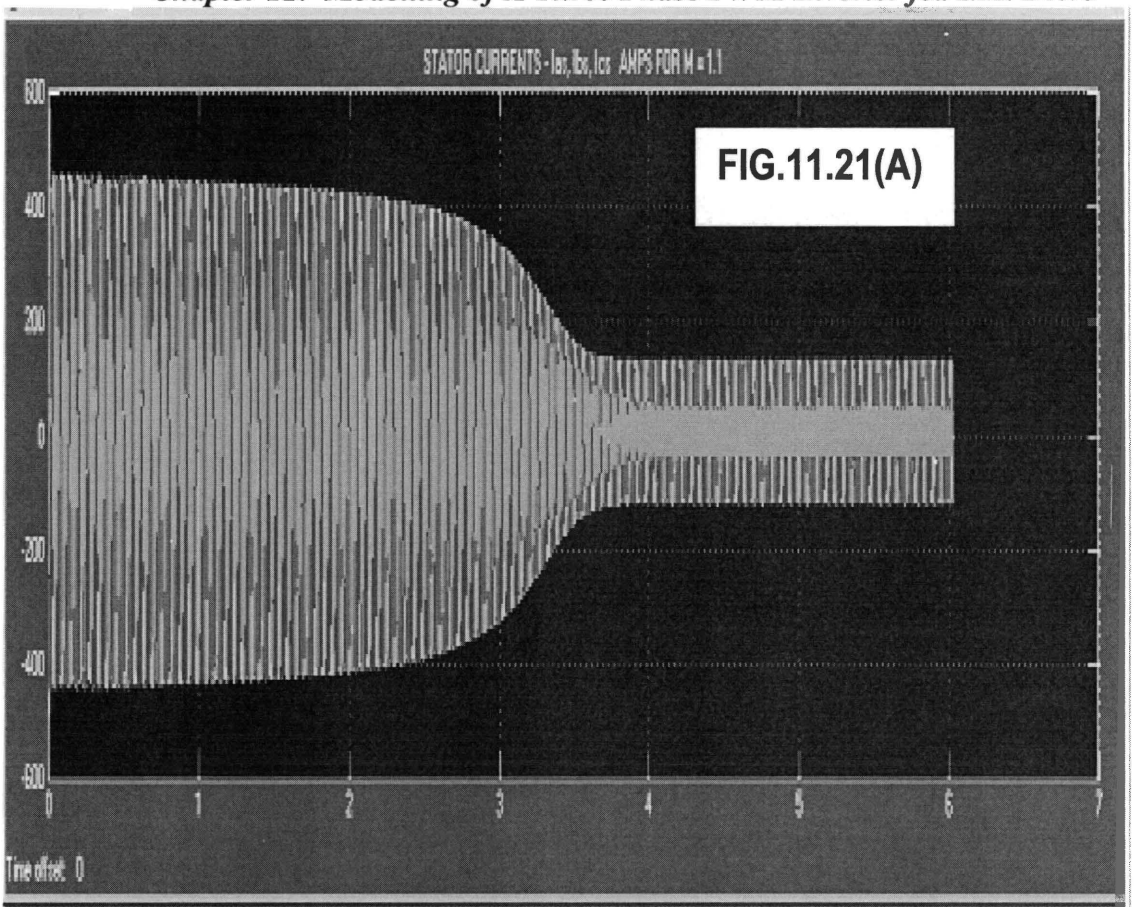

FIG.11.21(A)

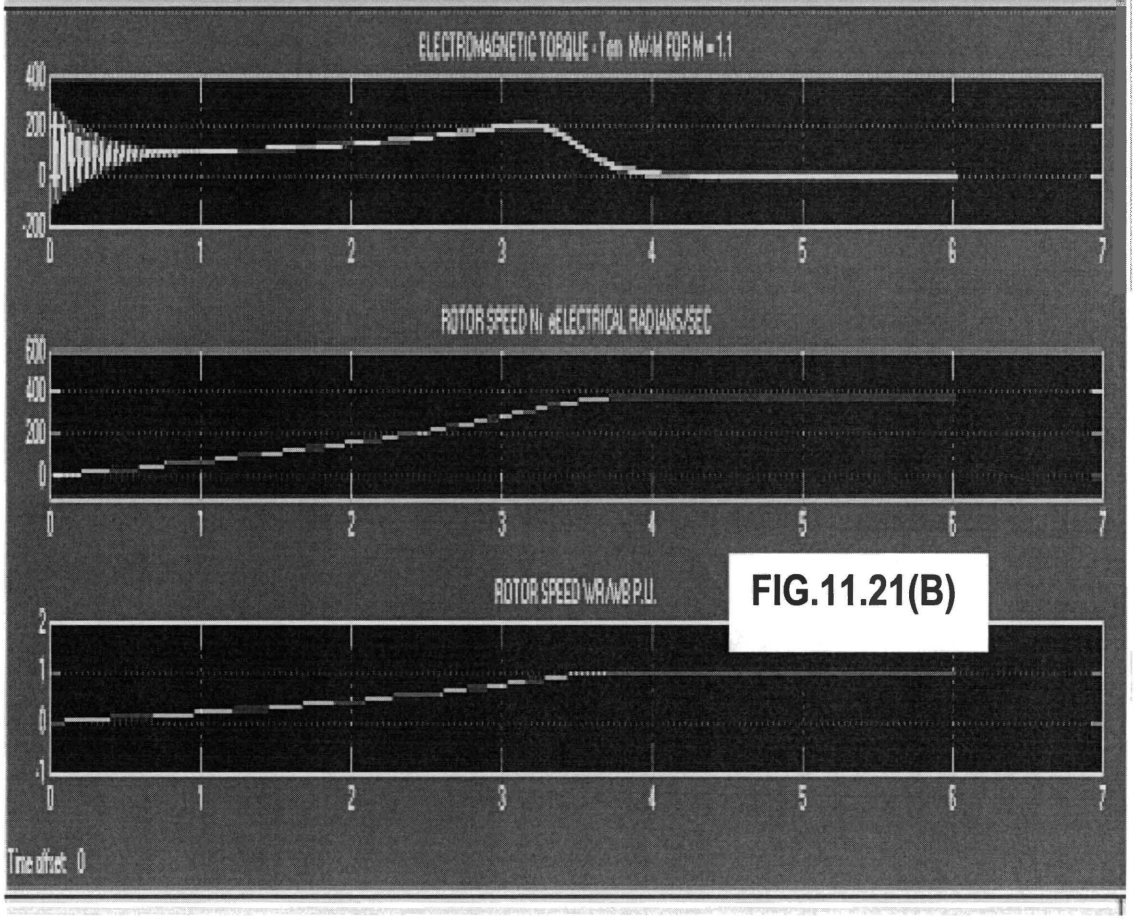

FIG.11.21(B)

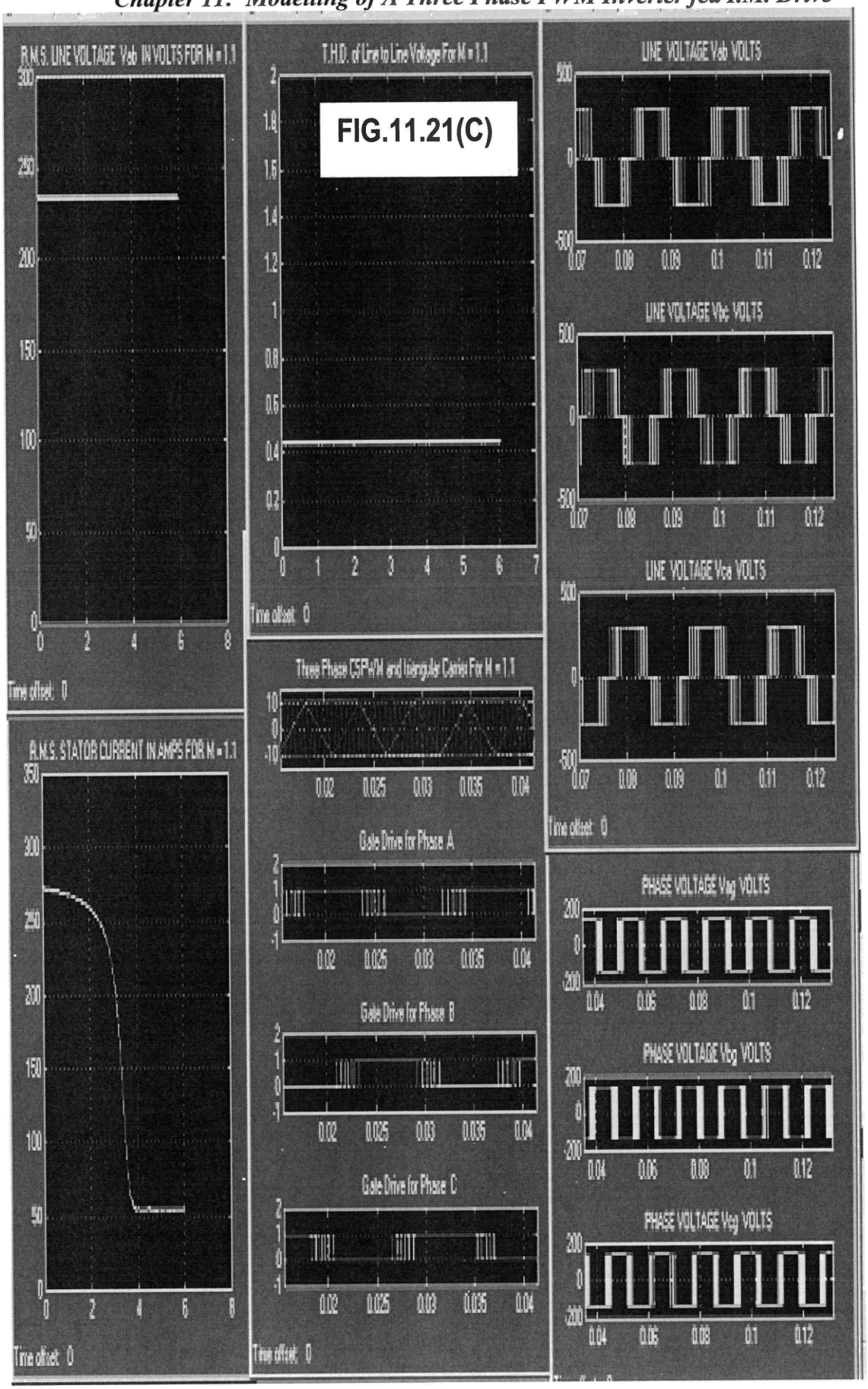
R.M.S. LINE VOLTAGE Vab IN VOLTS FOR M = 1.1
T.H.D. of Line to Line Voltage For M = 1.1
LINE VOLTAGE Vab VOLTS
LINE VOLTAGE Vbc VOLTS
LINE VOLTAGE Vca VOLTS
Three Phase CSPWM and triangular Carrier For M = 1.1
Gate Drive for Phase A
Gate Drive for Phase B
Gate Drive for Phase C
PHASE VOLTAGE Van VOLTS
PHASE VOLTAGE Vbn VOLTS
PHASE VOLTAGE Vcn VOLTS
R.M.S. STATOR CURRENT IN AMPS FOR M = 1.1
Time offset: 0

FIG.11.21(C)

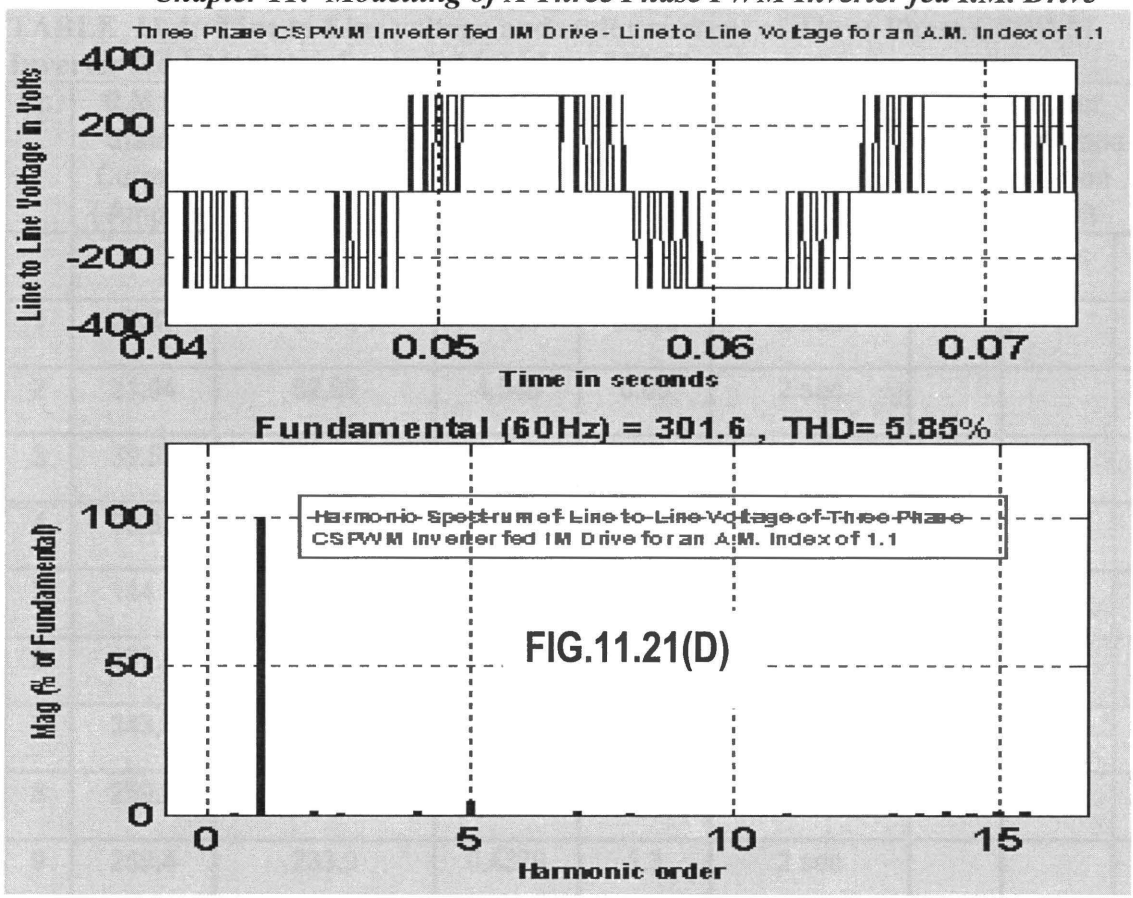

FIG.11.21(D)

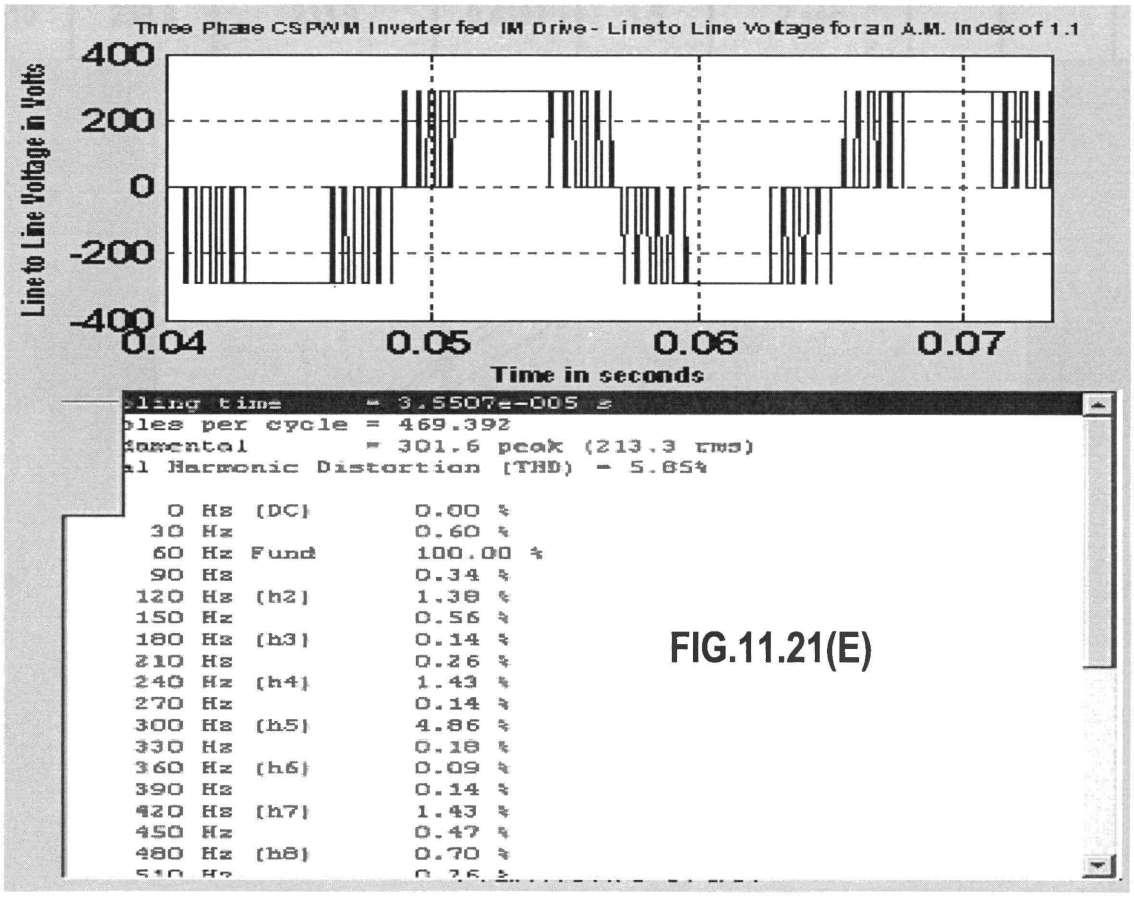

FIG.11.21(E)

TABLE 11.4: Line to Line voltage and stator current of Three Phase CSPWM Inverter fed I.M. Drive for an F.M. Index of 33.33.

No.	R.M.S. Stator Current (Amps)	R.M.S. LineVoltage Vab (Volts)	T.H.D.** Of Line to Line Voltage	A.M.In-dex M	Simulation Time in seconds	R.M.S.Stator current in Amps for simulation time shown	
						6 sec	8 sec
1	27.71	37.26	6.509	0.025	2 sec		
2	31.04	52.69	4.549	0.05	2 sec		
3	39.57	74.47	3.143	0.1	2 sec		
4	90.85	129.0	1.621	0.3	2 sec		
5	144.9	166.5	1.102	0.5	2 sec		
6	197.3	197.1	0.7801	0.7	2 sec		
7	243.0	223.4	0.539	0.9	2 sec	---	52.67
8	259.2	233.9	0.4392	1.1	2 sec	53.1	----
9	259.4	233.9	0.4379	1.3	2 sec		
10	259.3	233.9	0.4397	1.5	2 sec		

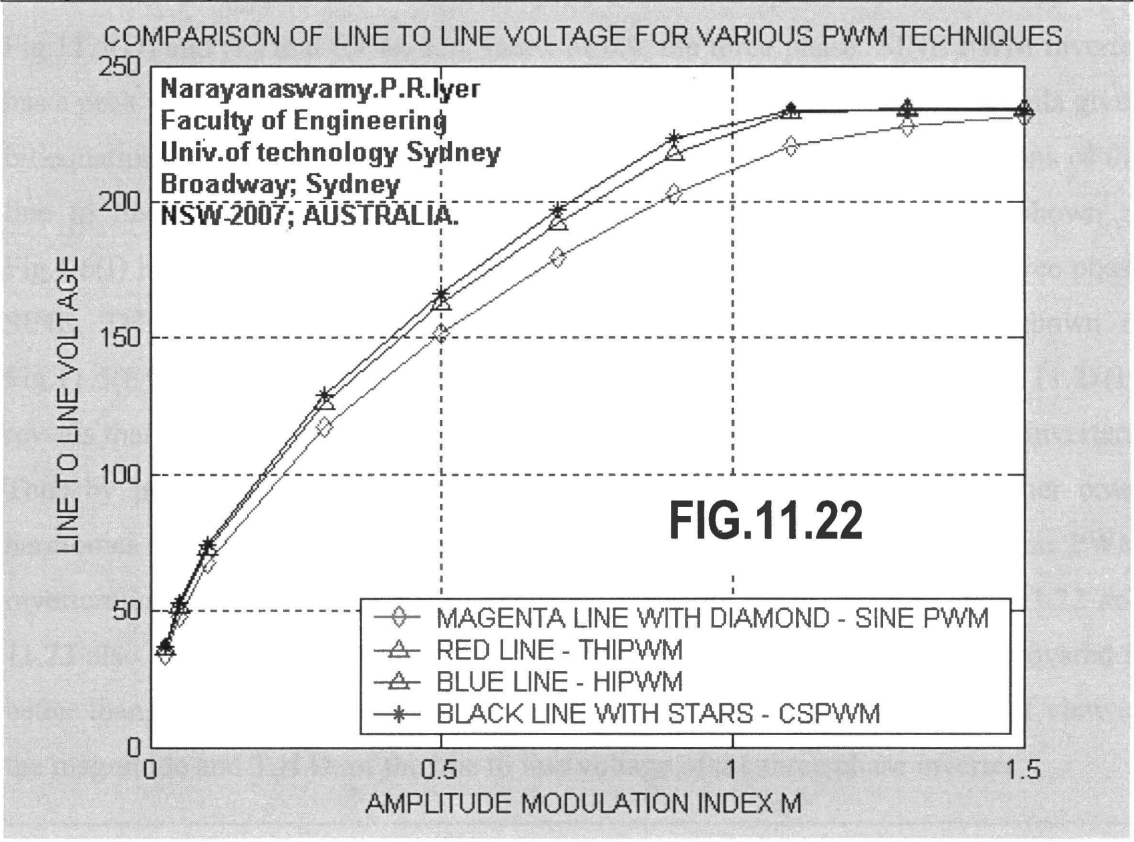

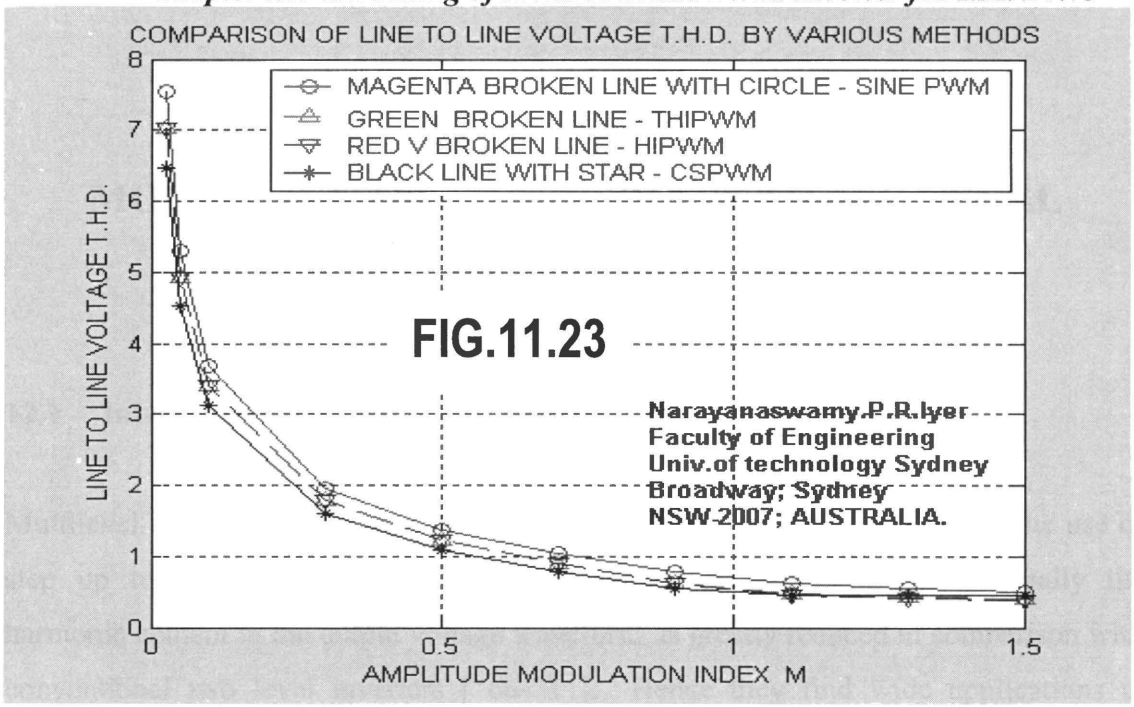

11.7 Conclusions

The models for three phase SINE, THI, HI and CS PWM techniques have been successfully developed and the simulations results are presented. It is seen from Fig.11.5(D) and (E) that for an a.m. index of 0.9, the three phase SINE PWM inverter has a peak value of 222.9 volts for the fundamental which agrees with the formula given by equation 11.3. Also comparing the fifth and seventh harmonic contributions of the line to line voltage of the plain three phase 180 degree mode inverter shown in Fig.4.6(I) in Chapter 4, with that of the same harmonic contributions of the three phase SINE, THI, HI and CS PWM Inverter for a.m. index of 0.9 and 1.1 shown in Fig.11.5(E), 11.6(E), 11.10(E), 11.11(E), 11.15(E), 11.16(E), 11.20(E) and 11.21(E) reveals that these harmonics are well suppressed in the later category of PWM inverters. Thus by modelling and simulation technique, it is confirmed that the higher order harmonics in the line to line voltage are well suppressed in the three phase PWM inverters as compared to three phase 180 degree mode plain inverter. Fig.11.22 and 11.23 also shows that the three phase CSPWM technique which is newly discovered is better than three phase SINE, HI and THI PWM techniques from the point of view of the magnitude and T.H.D. of the line to line voltage of the three phase inverter.

CHAPTER 12
MODELLING OF THREE PHASE THREE LEVEL INVERTERS

12.1 Introduction

Multilevel inverters were proposed to obtain higher output voltages without the use of step up transformer closely following a sinusoidal waveform. Additionally the harmonic content in the output voltage waveform is greatly reduced in comparison with conventional two level inverters [66-71]. Hence they find wide applications in STATCOMs, ASDs etc. This chapter describes the modelling of three phase Diode Clamped Three Level Inverter (DCTLI) and the three phase Flying Capacitor Three Level Inverter (FCTLI). The highest number of levels obtainable with Diode Clamped and Flying Capacitor Multi Level Inverters are limited by factors such as the number and voltage ratings of the clamping diodes and that of capacitors respectively. In general if m is the number of voltage levels in the phase to ground voltage of the three phase multilevel inverter, then the number of voltage levels in the line to line voltage will be (2.m – 1) and the number of switching pulses will be 6*(m – 1) [67 - 69]. Thus for a three phase three level inverter, the number of voltage levels for the line to line voltage will be five and the number of gate pulses required (i.e. semiconductor switches) will be twelve.

12.2 Three Phase Diode Clamped Three Level Inverter

The circuit schematic of the three phase 50 Hz DCTLI is shown in Fig.12.1(A) using MICROCAP7 software. There are four switches per phase, two at the top leg and two at the bottom leg. Two diodes in series are connected in between the top and bottom switches. The two capacitors at the input act as potential divider. The DC input voltage is Vdc volts. The simulation results for the three phase line to ground and line to line voltages are shown in Fig.12.1(B). As can be seen from Fig.12.1(B), the line to ground voltage has three voltage levels and line to line voltage has five voltage levels. .

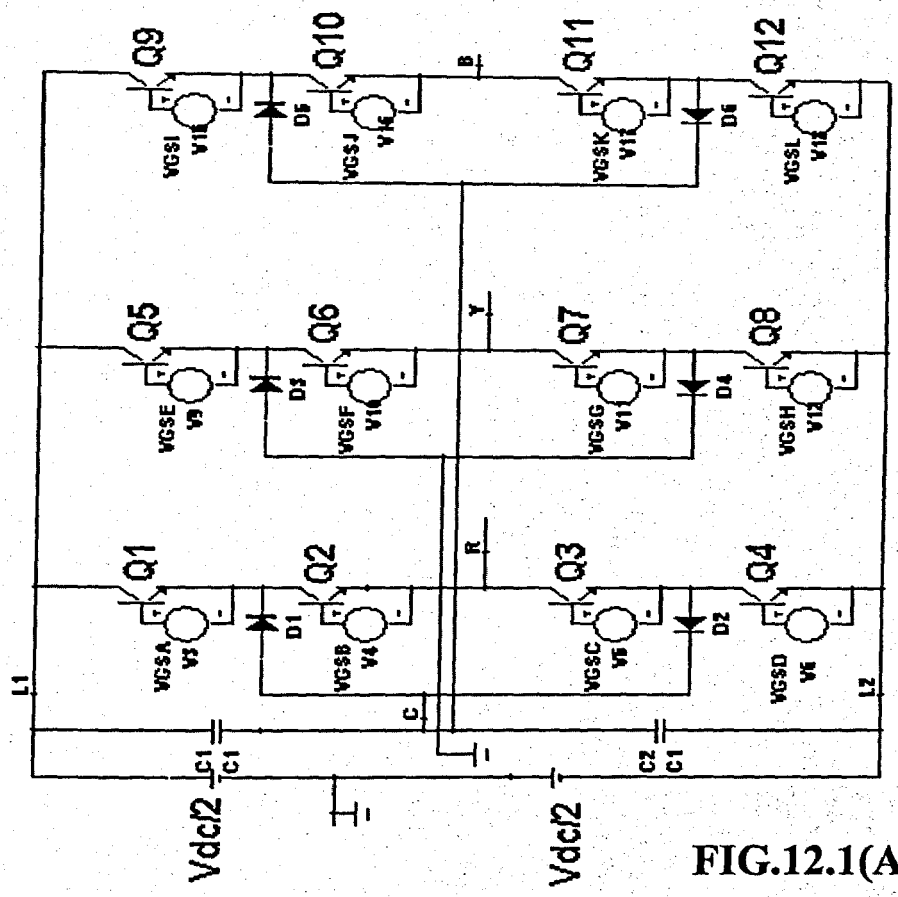

FIG.12.1(A)

```
.DEFINE VDC 100
.DEFINE C1 0.1
.DEFINE VGSA PULSE(0 5 0N 0N 5N 20N)
.DEFINE VGSB PULSE(0 5 15N 0N 15N 20N)
.DEFINE VGSC PULSE(0 5 5N 0N 15N 20N)
.DEFINE VGSD PULSE(0 5 10N 0N 5N 20N)
.DEFINE VGSE PULSE(0 5 6.667N 0N 5N 20N)
.DEFINE VGSF PULSE(0 5 1.667N 0N 15N 20N)
.DEFINE VGSG PULSE(0 5 11.667N 0N 15N 20N)
.DEFINE VGSH PULSE(0 5 16.667N 0N 5N 20N)
.DEFINE VGSI PULSE(0 5 13.333N 0N 5N 20N)
.DEFINE VGSJ PULSE(0 5 8.333N 0N 15N 20N)
.DEFINE VGSK PULSE(0 5 18.333N 0N 15N 20N)
.DEFINE VGSL PULSE(0 5 3.333N 0N 5N 20N)
.MODEL D1N4148 D (IS=5.95862N N=1.91266 BV=500 RS=589.498M TT=1.12599N
CJO=1.33941P VJ=8.66264 M=300M RL=3.14968G)
.MODEL 2N2222 NPN (IS=10.017F BF=506.842 NF=979.99M VAF=100 IKF=696.241M
ISE=0.241303F NE=1.05779 BR=154.978M IKR=999.407 ISC=6.94996P RE=668.817M
CJE=42.4239P VJE=700M MJE=642.887M CJC=36.6437P VJC=700M MJC=558.066M
TF=484.687P XTF=500.001M VTF=10 ITF=9.88166M TR=2.26629U)
```

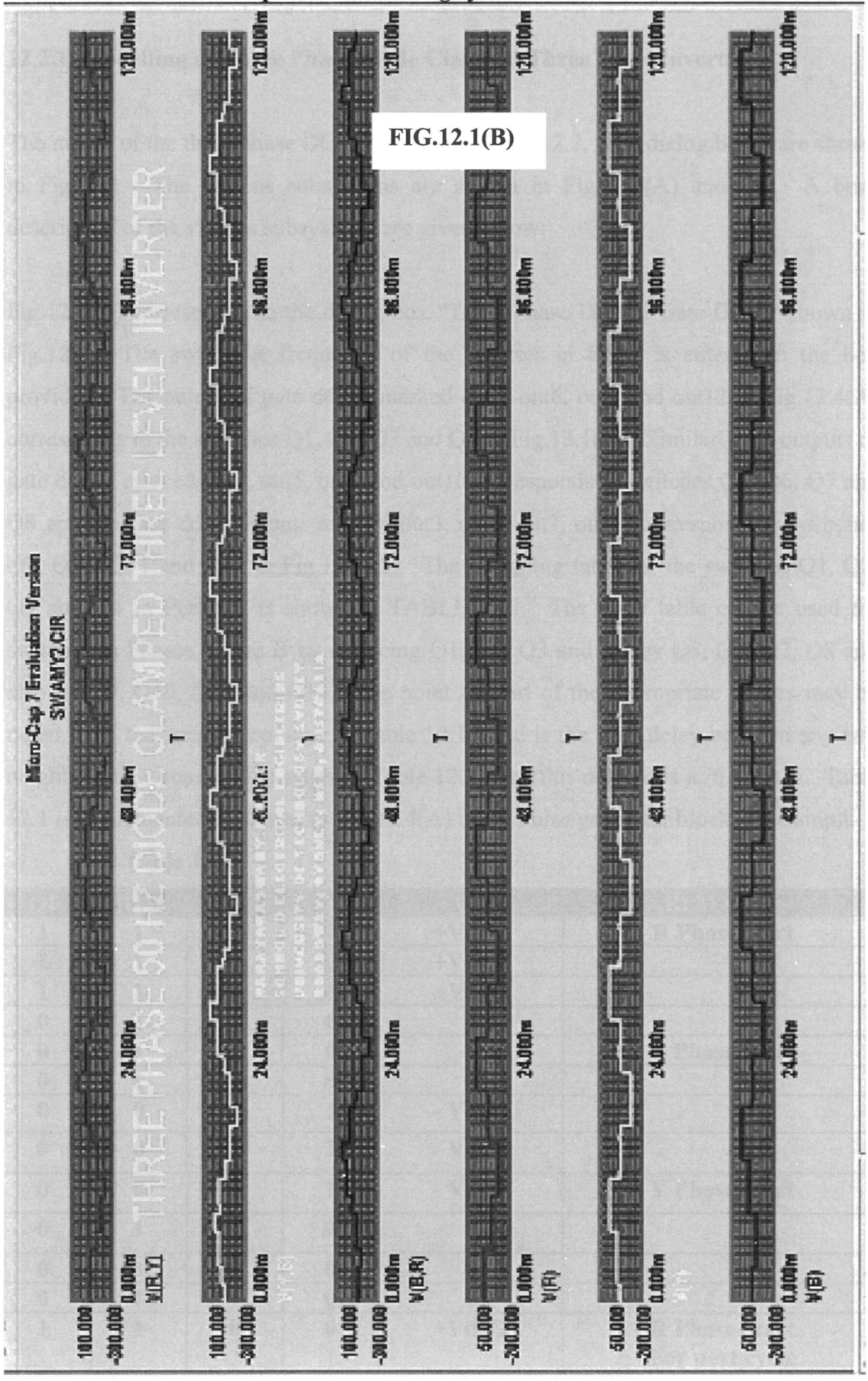
Micro-Cap 7 Evaluation Version
SWAMY2.CIR
THREE PHASE 50 HZ DIODE CLAMPED THREE LEVEL INVERTER
V(R,Y)
V(B,R)
V(R)
V(B)
100.000
-300.000
0.000m
24.000m
48.400m
72.000m
96.400m
120.000m
T

FIG.12.1(B)

12.2.1 Modelling of Three Phase Diode Clamped Three Level Inverter

The model of the three phase DCTLI is shown in Fig.12.2. The dialog boxes are shown in Fig.12.3. The various subsystems are shown in Fig.12.4(A) and (B). A brief description of the various subsystems are given below:

Fig.12.4(A) corresponds to the dialog box "Three Phase DCTLI Gate Drive" shown in Fig.12.3. The switching frequency of the inverter in Hertz is entered in the box provided. The output of gate drives marked out2, out6, out9 and out12 in Fig.12.4(A) corresponds to the switches Q1, Q2, Q3 and Q4 in Fig.12.1(A). Similarly the outputs of gate drives marked out1, out5, out8 and out10 corresponds to switches Q5, Q6, Q7 and Q8 and the gate drive outputs marked out3, out4, out7, out11 corresponds to switches Q9, Q10, Q11 and Q12 in Fig.12.1(A). The switching table for the switches Q1, Q2, Q3 and Q4 in Phase R is shown in TABLE 12.1. The same table can be used for switches in Phases Y and B by replacing Q1, Q2, Q3 and Q4 by Q5, Q6, Q7, Q8 and also by Q9, Q10, Q11 and Q12. The point of start of the appropriate phases may be noted from the remarks column of Table 12.1. If d is the time delay between any two neighbouring consecutive states in Table 12.1, then this delay d is π /6 radians. Table 12.1 is implemented as shown in Fig.12.4(A) using Pulse generator block. The ampli-

Table 12.1

Q1	Q2	Q3	Q4	Vrg	REMARKS
1	1	0	0	+Vdc/2	R Phase start
1	1	0	0	+Vdc/2	
1	1	0	0	+Vdc/2	
0	1	1	0	0	
0	1	1	0	0	B Phase Start
0	1	1	0	0	
0	0	1	1	- Vdc/2	
0	0	1	1	- Vdc/2	
0	0	1	1	- Vdc/2	Y Phase Start
0	1	1	0	0	
0	1	1	0	0	
0	1	1	0	0	
1	1	0	0	+Vdc/2	R Phase Start For next cycle

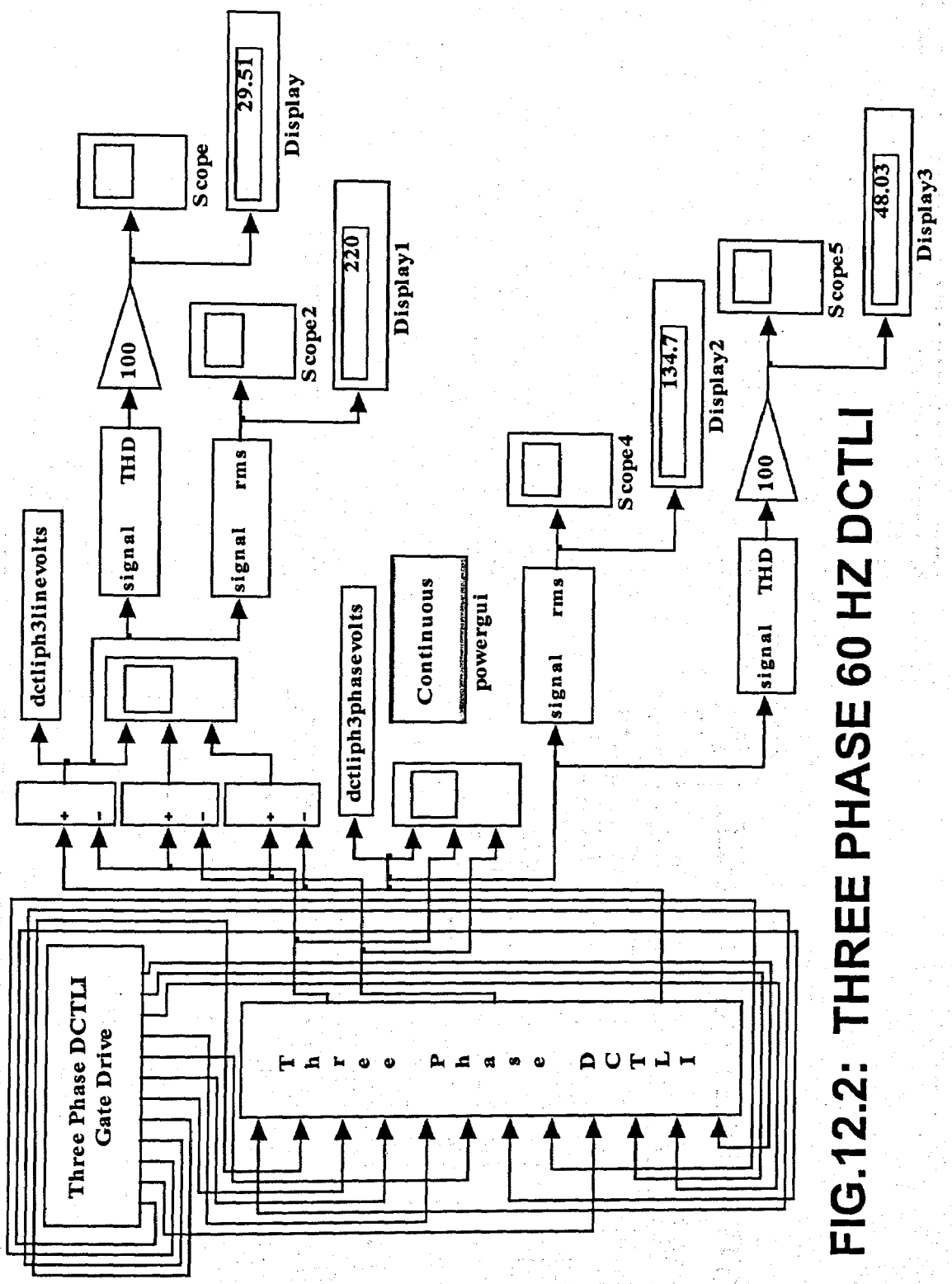

FIG.12.2: THREE PHASE 60 HZ DCTLI

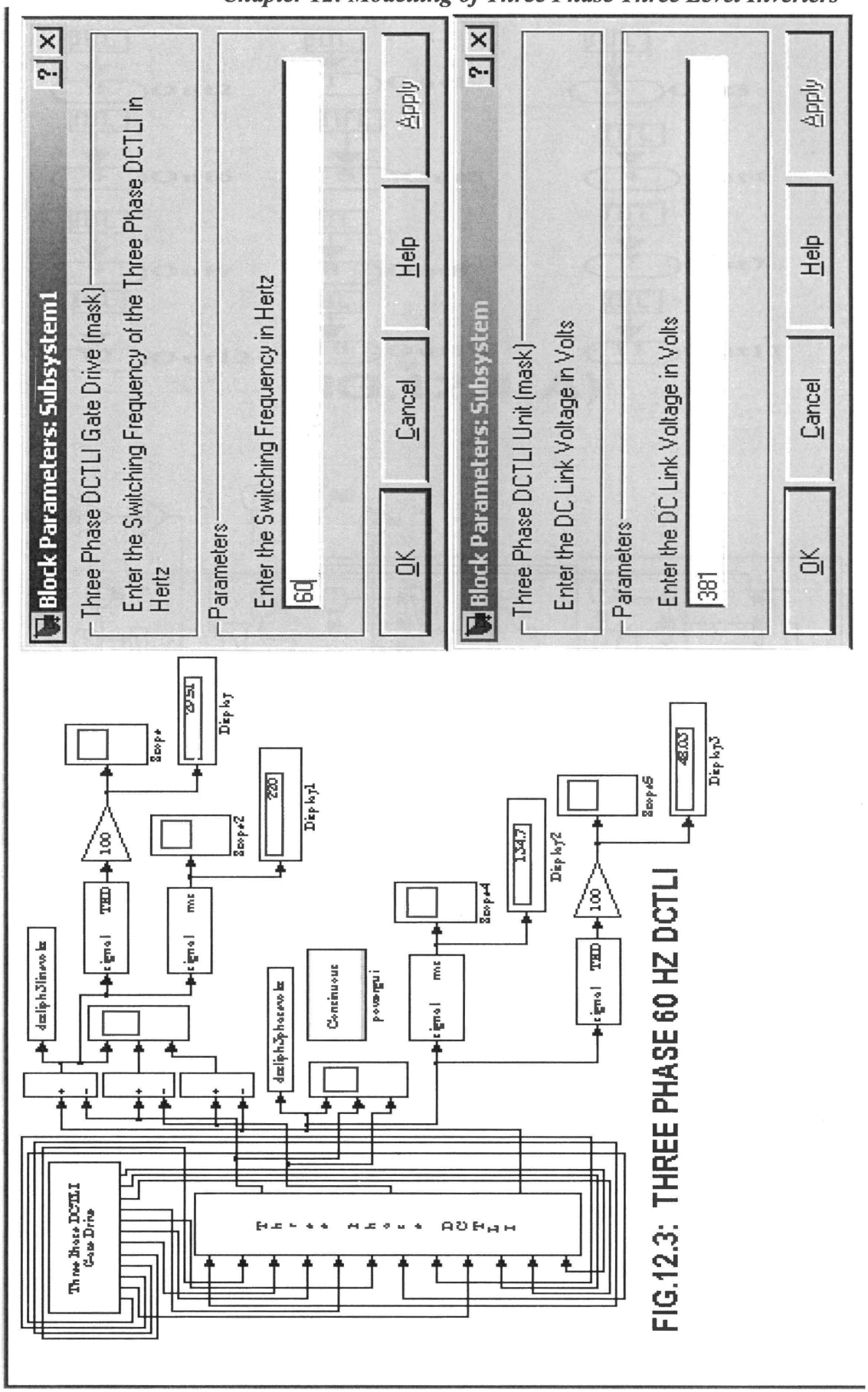

FIG.12.3: THREE PHASE 60 HZ DCTLI

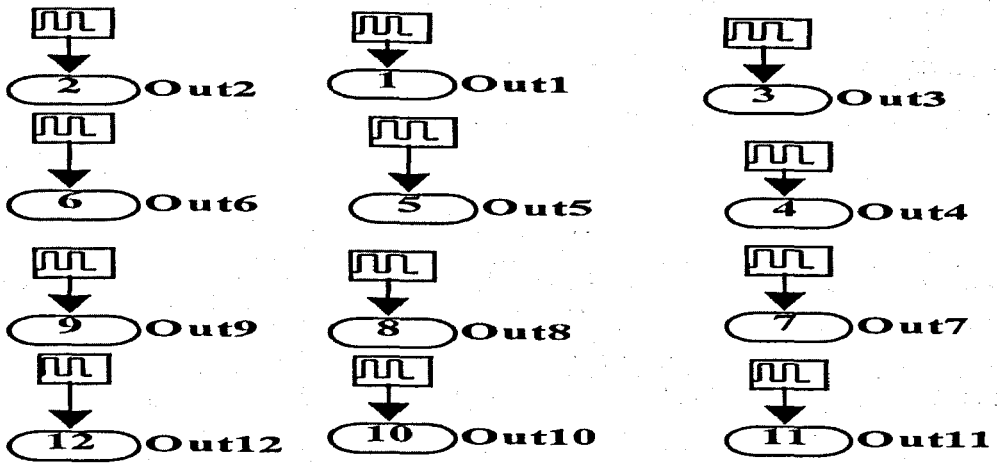

FIG.12.4(A)

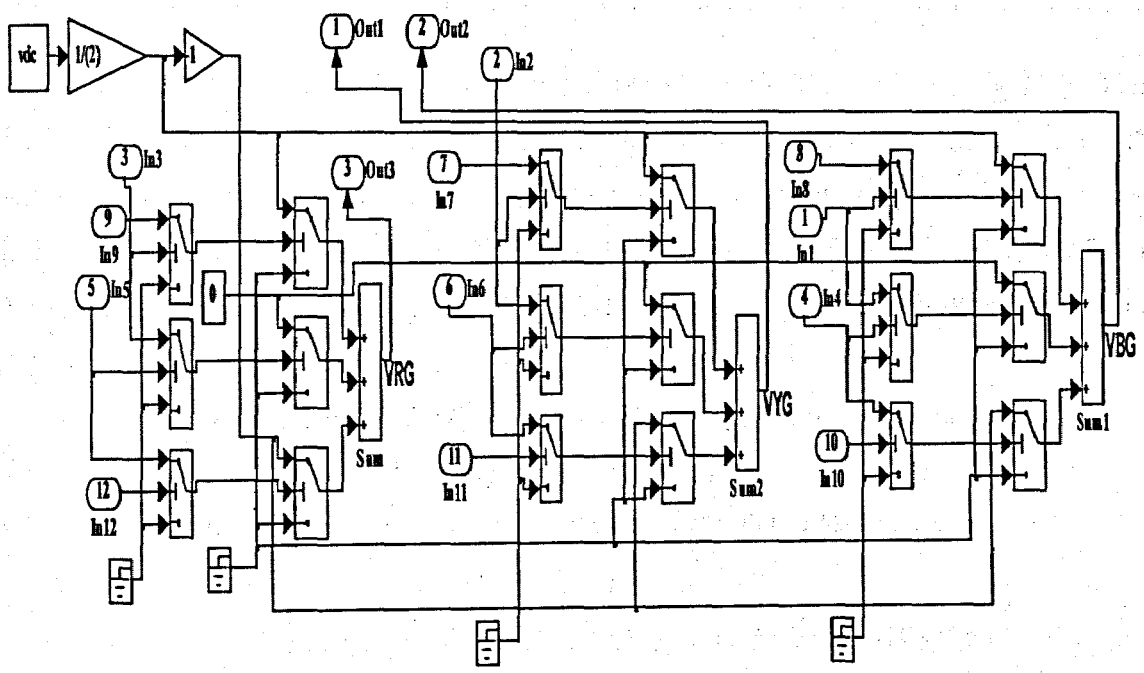

FIG. 12.4 (B)

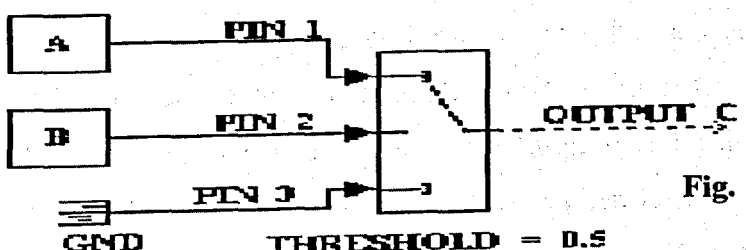

Fig. 12.4(C)

THRESHOLD = 0.5

CRITERIA FOR PASSING FIRST INPUT: U2 >= THRESHOLD

AND GATE

tude of all the pulses in the pulse generator block is set to 1 and the period is set to [1 / fsw], where fsw is the switching frequency of the inverter. The phase delay for each of the switches in Phase R, Y and B are tabulated in Table 12.2. Switch names are in Fig.12.1(A).

TABLE 12.2

Sl.No.	Switch Phase R	Phase Delay Seconds	Switch Phase Y	Phase Delay Seconds	Switch Phase B	Phase Delay Seconds
1	Q1	0	Q5	4/(12.fsw)	Q9	8/(12.fsw)
2	Q2	9/(12.fsw)	Q6	1/(12.fsw)	Q10	5/(12.fsw)
3	Q3	3/(12.fsw)	Q7	7/(12.fsw)	Q11	11/(12.fsw)
4	Q4	6/(12.fsw)	Q8	10/(12.fsw)	Q12	2/(12.fsw)

Fig.12.4(B) corresponds to the dialog box "Three Phase DCTLI Unit" in Fig.12.3. Here the dc link voltage is entered in volts in the box provided. The model of the semiconductor switches shown in Fig.12.1(A) is implemented using threshold switches and summing blocks as shown in Fig.12.4(B). The switches Q1, Q2, Q3 and Q4 in Phase R is implemented as per Table 12.1, according to the following modelling statement:

If (gate pulse for Q1 is HIGH AND Q2 is HIGH) then

Output Vrg = +Vdc/2

Else if (gate pulse for Q2 is HIGH AND Q3 is HIGH) then

Output Vrg = 0

Else if (gate pulse for Q3 is HIGH AND Q4 is HIGH) then

Output Vrg = -Vdc/2

End if

Similar modelling statements holds good for switches in Phase Y and B. The AND gate is implemented using threshold switch as shown in Fig.12.4(C). In Fig.12.4(C), the u(1) and u(2) are the inputs A and B with either Logic 0 or 1 value. The u(3) input is the ground or logic 0. The threshold value of the switch is 0.5. When u(2) is greater than or equal to threshold value, the out put correspond to u(1) input, else the output is the u(3) input. Thus Fig.12.4(C) implements the AND gate. This AND gate principle

is used in Fig.12.4(B). Referring to threshold switches from top to bottom on the extreme left of Fig.12.4(B), The top switch performs AND operation of the gate pulse for Q1 and Q2, the middle switch performs AND operation of the gate pulse for Q2 and Q3 and the bottom switch performs AND operation of the gate pulse for Q3 and Q4. The top, middle and bottom switch outputs on the extreme left are given to u(2) inputs of the second column of the top, middle and bottom switches. The u(1) inputs of the top, middle and bottom switches in the second column are +Vdc/2, zero and –Vdc/2 respectively, while their u(3) inputs are all zeros. All these switches have a threshold value of 0.5 and output u(1) when u(2) input is greater than or equal to threshold value, else the output is the u(3) input and performs the modelling statement given above. The switches for Phase Y and B are developed in the same way. .

12.2.2 Simulation Results

The simulation results of the line to line voltage, line to ground voltage, RMS value of line to line and line to ground voltage and their T.H.D. are shown in Fig.12.5(A) for a three phase 60 Hz DCTLI using ode15s(stiff/NDF) solver. The DC link voltage is 381 volts. The harmonic spectrum of line to line voltage is shown in Fig.12.5(B) and (C) respectively.

12.3 Three Phase Flying Capacitor Three Level Inverter

The circuit schematic of the three phase 50 Hz FCTLI is shown in Fig.12.6(A) using MICROCAP7 software. There are four switches per phase, two at the top leg and two at the bottom leg. The capacitor connecting the switches in each of the three phases is called the flying capacitor. The two capacitors at the input act as potential divider. The DC input voltage is Vdc volts. The simulation results for the three phase line to ground and line to line voltages are shown in Fig.12.6(B). As can be seen from Fig.12.6(B), the line to ground voltage has three voltage levels and line to line voltage has five voltage levels and there are twelve gate pulses i.e. semiconductor switches.

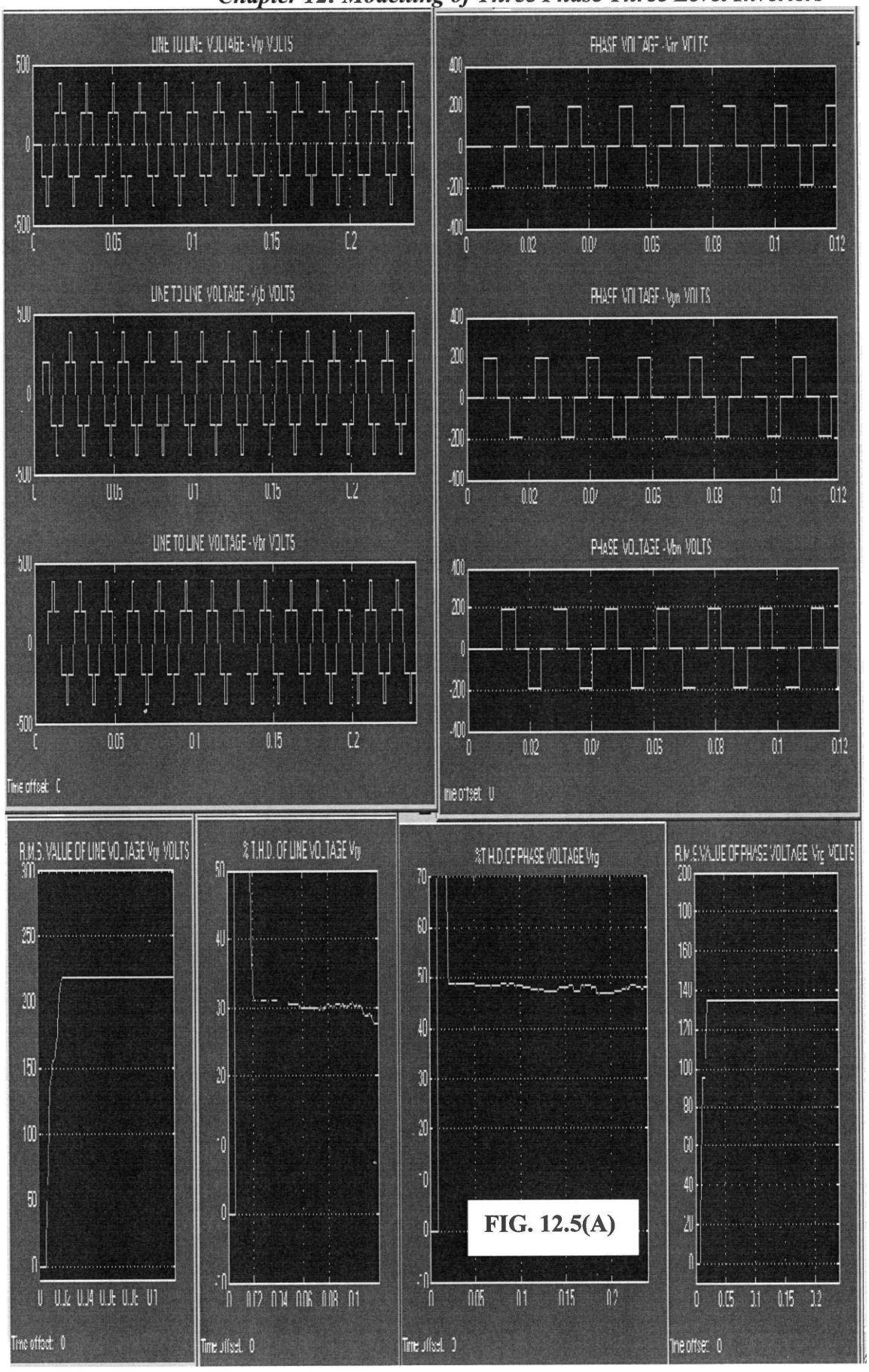
LINE TO LINE VOLTAGE -Vry VOLTS
LINE TO LINE VOLTAGE -Vyb VOLTS
LINE TO LINE VOLTAGE -Vbr VOLTS
Time offset: 0
PHASE VOLTAGE -Vrn VOLTS
PHASE VOLTAGE -Vyn VOLTS
PHASE VOLTAGE -Vbn VOLTS
Time offset: 0
R.M.S. VALUE OF LINE VOLTAGE Vry VOLTS
Time offset: 0
% T.H.D. OF LINE VOLTAGE Vry
Time offset: 0
%T.H.D. OF PHASE VOLTAGE Vrg
Time offset: 0
R.M.S. VALUE OF PHASE VOLTAGE Vrg VOLTS
Time offset: 0

FIG. 12.5(A)

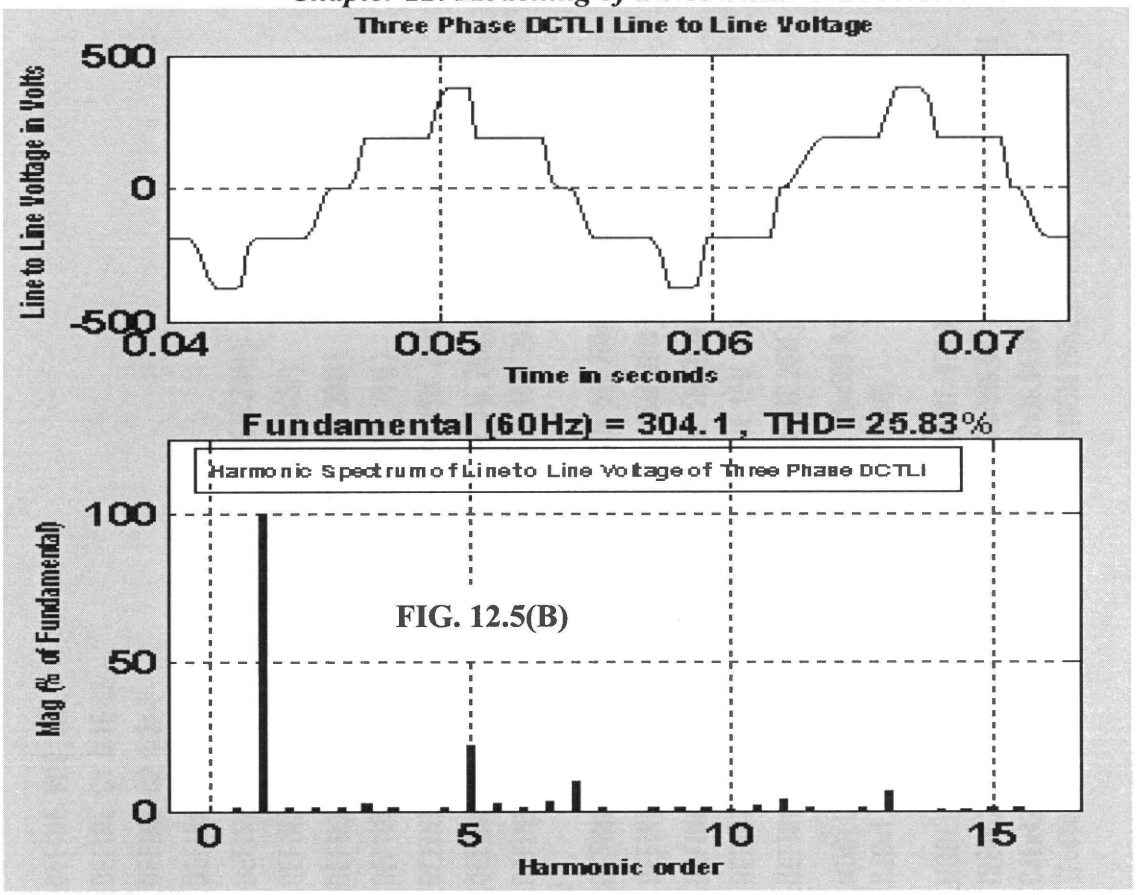

FIG. 12.5(B)

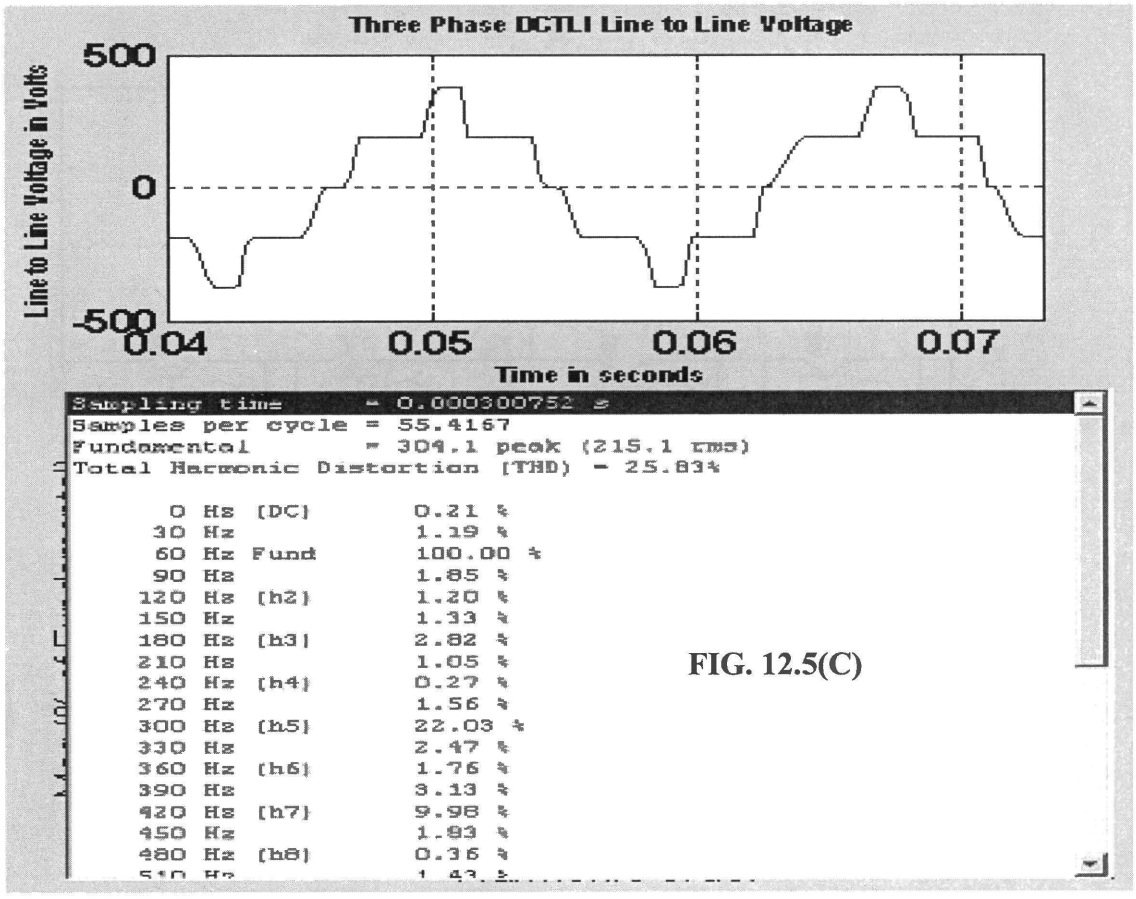

FIG. 12.5(C)

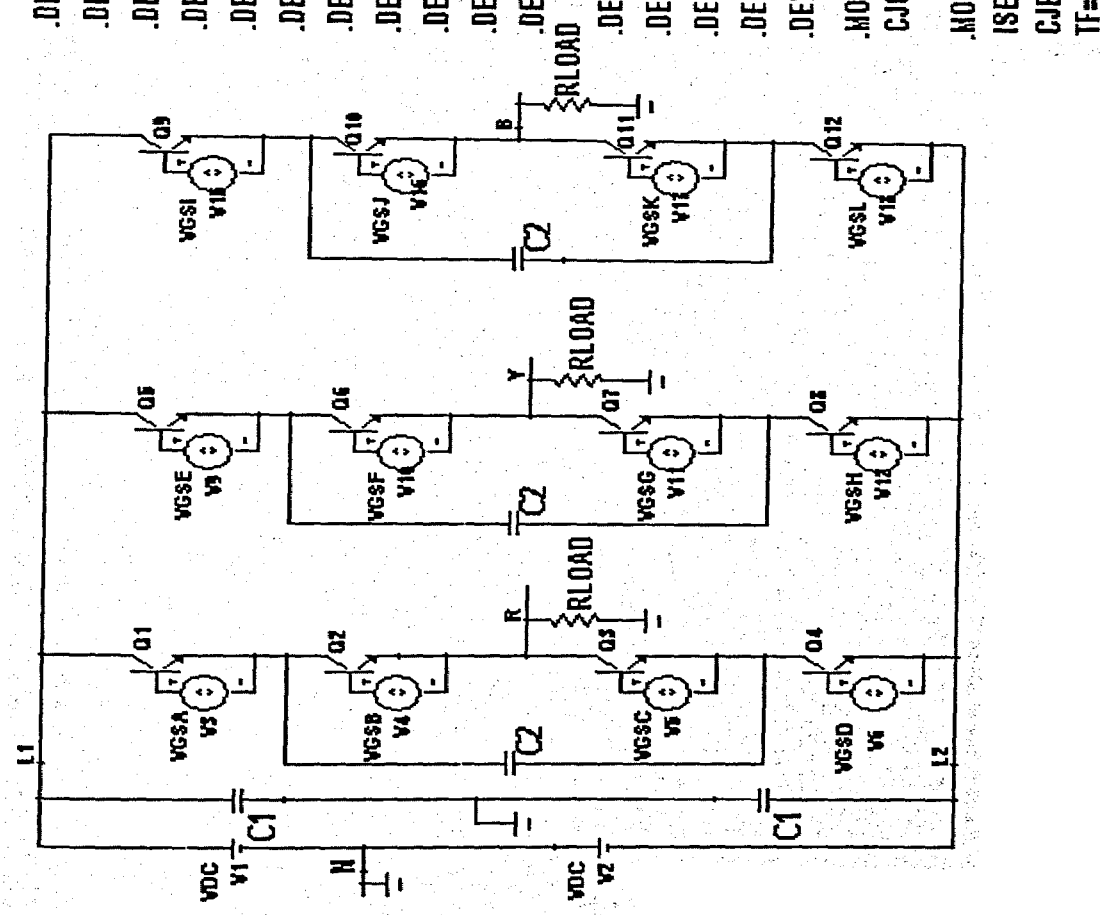
.DEFINE VDC 100
.DEFINE C1 0.1E-12
.DEFINE C2 1.2e-7
.DEFINE RLOAD 500
.DEFINE VGSA PULSE(0 5 15N 0N 0N 15N 20N)
.DEFINE VGSB PULSE(0 5 0N 0N 0N 5N 20N)
.DEFINE VGSC PULSE(0 5 5N 0N 0N 15N 20N)
.DEFINE VGSD PULSE(0 5 10N 0N 0N 5N 20N)
.DEFINE VGSE PULSE(0 5 1.667N 0N 0N 15N 20N)
.DEFINE VGSF PULSE(0 5 6.667N 0N 0N 5N 20N)
.DEFINE VGSG PULSE(0 5 11.667N 0N 0N 15N 20N)
.DEFINE VGSH PULSE(0 5 16.667N 0N 0N 5N 20N)
.DEFINE VGSI PULSE(0 5 8.333N 0N 0N 15N 20N)
.DEFINE VGSJ PULSE(0 5 13.333N 0N 0N 5N 20N)
.DEFINE VGSK PULSE(0 5 18.333N 0N 0N 15N 20N)
.DEFINE VGSL PULSE(0 5 3.333N 0N 0N 5N 20N)
.MODEL D1N4148 D (IS=5.95862N N=1.91266 BV=500 RS=589.498M TT=1.12599N
CJO=1.33941P VJ=8.66264 M=300M RL=3.14968G)
.MODEL 2N2222 NPN (IS=10.017F BF=506.842 NF=979.99M VAF=100 IKF=696.241M
ISE=0.241303F NE=1.05779 BR=154.978M IKR=999.407 ISC=6.94996P RE=668.817M
CJE=42.4239P VJE=700M MJE=642.887M CJC=36.6437P VJC=700M MJC=558.066M
TF=484.887P XTF=500.001M VTF=10 ITF=9.83166M TR=2.26629U)
L1
L2
C1
C2
VDC
V1
N
VDC
V2
R
Y
B
RLOAD
Q1
Q2
Q3
Q4
Q5
Q6
Q7
Q8
Q9
Q10
Q11
Q12
VGSA
V3
VGSB
V4
VGSC
V5
VGSD
V6
VGSE
V9
VGSF
V10
VGSG
V11
VGSH
V12
VGSI
V13
VGSJ
V14
VGSK
V15
VGSL
V16

FIG. 12.6(A)

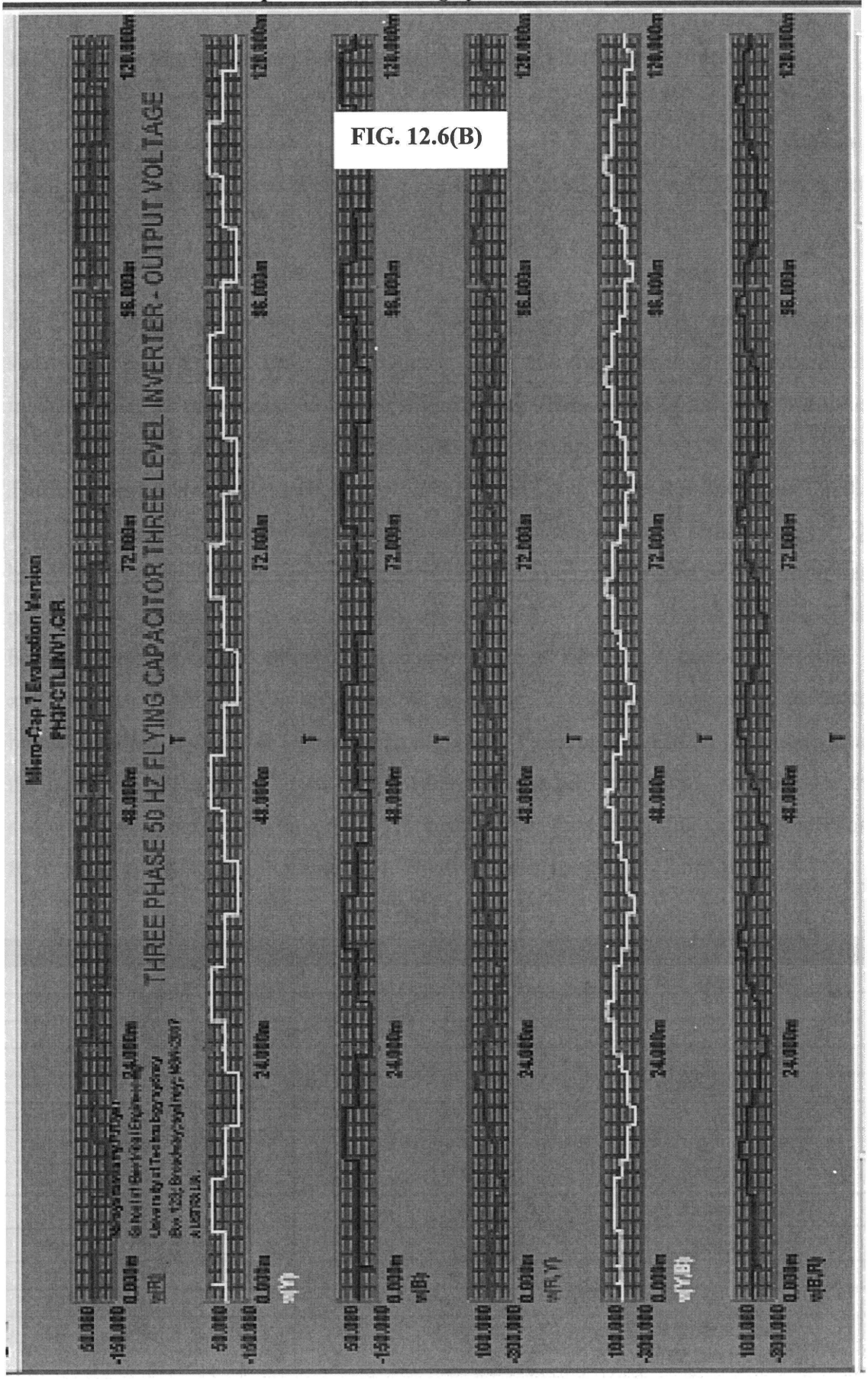
Micro-Cap 7 Evaluation Version
THREE PHASE 50 HZ FLYING CAPACITOR THREE LEVEL INVERTER - OUTPUT VOLTAGE

FIG. 12.6(B)

12.3.1 Modelling of Three Phase Flying Capacitor Three Level Inverter

The model of the three phase FCTLI is shown in Fig.12.7. The dialog boxes are shown in Fig.12.8. The subsystem is shown in Fig.12.9. A brief description of the subsystem is given below:

Fig.12.9 corresponds to the dialog box "Three Phase FCTLI and Gate Drive Unit" shown in Fig.12.8. The DC Link voltage in volts and the switching frequency of the inverter in Hertz are entered in the boxes provided. The output of gate drives marked from Q1 to Q12 in Fig.12.9 corresponds to the switches Q1 to Q12 in Fig.12.6(A). The switching table for the switches Q1, Q2, Q3 and Q4 in Phase R is shown in TABLE 12.3. The same table can be used for switches in Phase Y and B by replacing Q1 to Q4 by Q5 to Q8 and Q9 to Q12 in the respective order. The point of start of the appropriate phases may be noted from the remarks column of Table 12.3. If d is the time delay between any two neighbouring consecutive states in Table 12.3, then this delay d is π /6 radians. Table 12.3 is implemented as shown in Fig.12.9 using Pulse generator blocks, marked Gate Pulse Generator in Fig.12.9. The amplitude of all the pulses in all the pulse generator blocks is set to 1 and the period is set to [1 / fsw], where fsw is the switching frequency of the inverter. The phase delay for each of the switches in Phase R, Y and B are tabulated in Table 12.4. Switch names are in Fig.12.6(A).

TABLE 12.3

Q1	Q2	Q3	Q4	Vrg	REMARKS
1	1	0	0	+Vdc/2	R Phase start
1	1	0	0	+Vdc/2	
1	1	0	0	+Vdc/2	
1	0	1	0	0	
1	0	1	0	0	B Phase Start
1	0	1	0	0	
0	0	1	1	- Vdc/2	
0	0	1	1	- Vdc/2	
0	0	1	1	- Vdc/2	Y Phase Start
1	0	1	0	0	
1	0	1	0	0	
1	0	1	0	0	
1	1	0	0	+Vdc/2	R Phase Start For next cycle

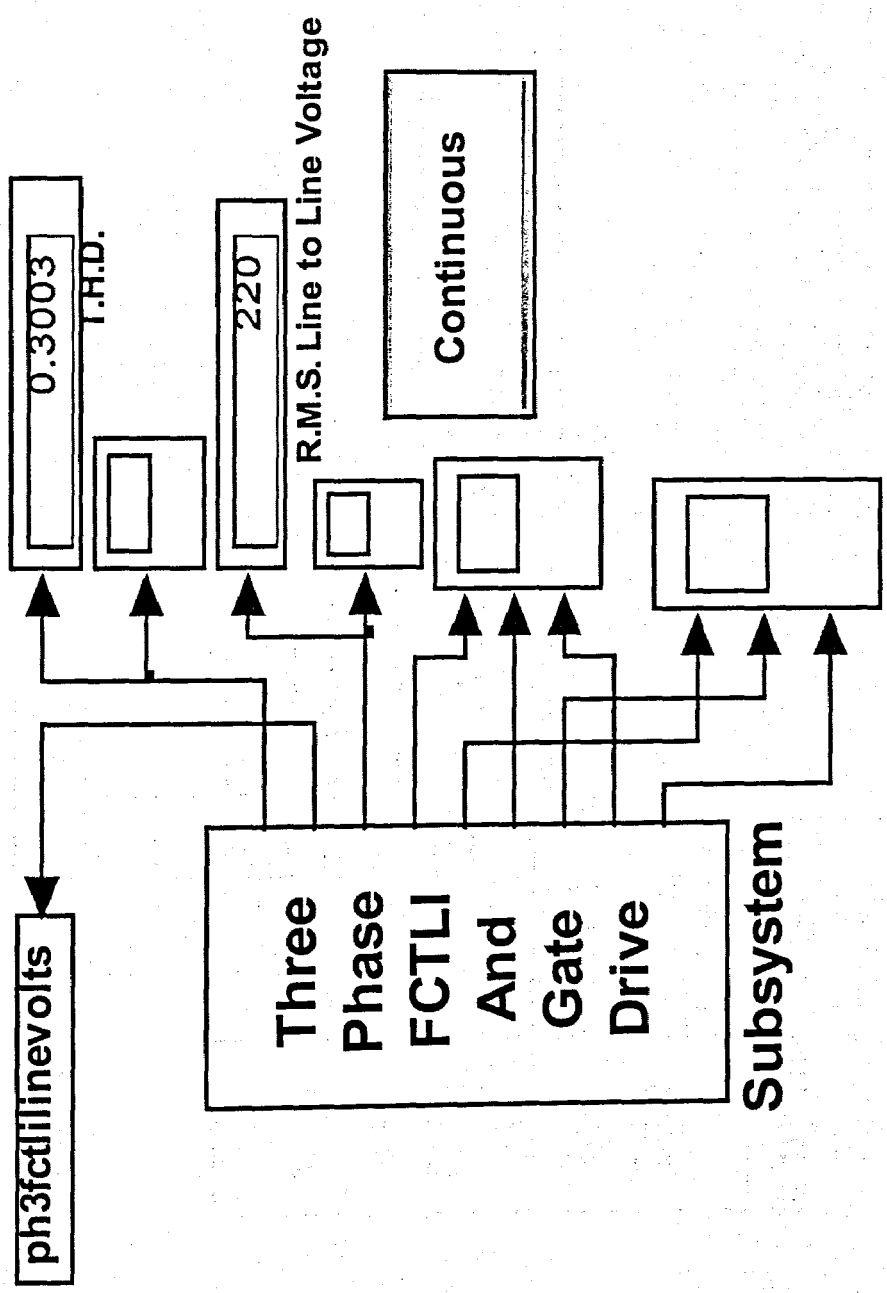

FIG.12.7: THREE PHASE FCTLI

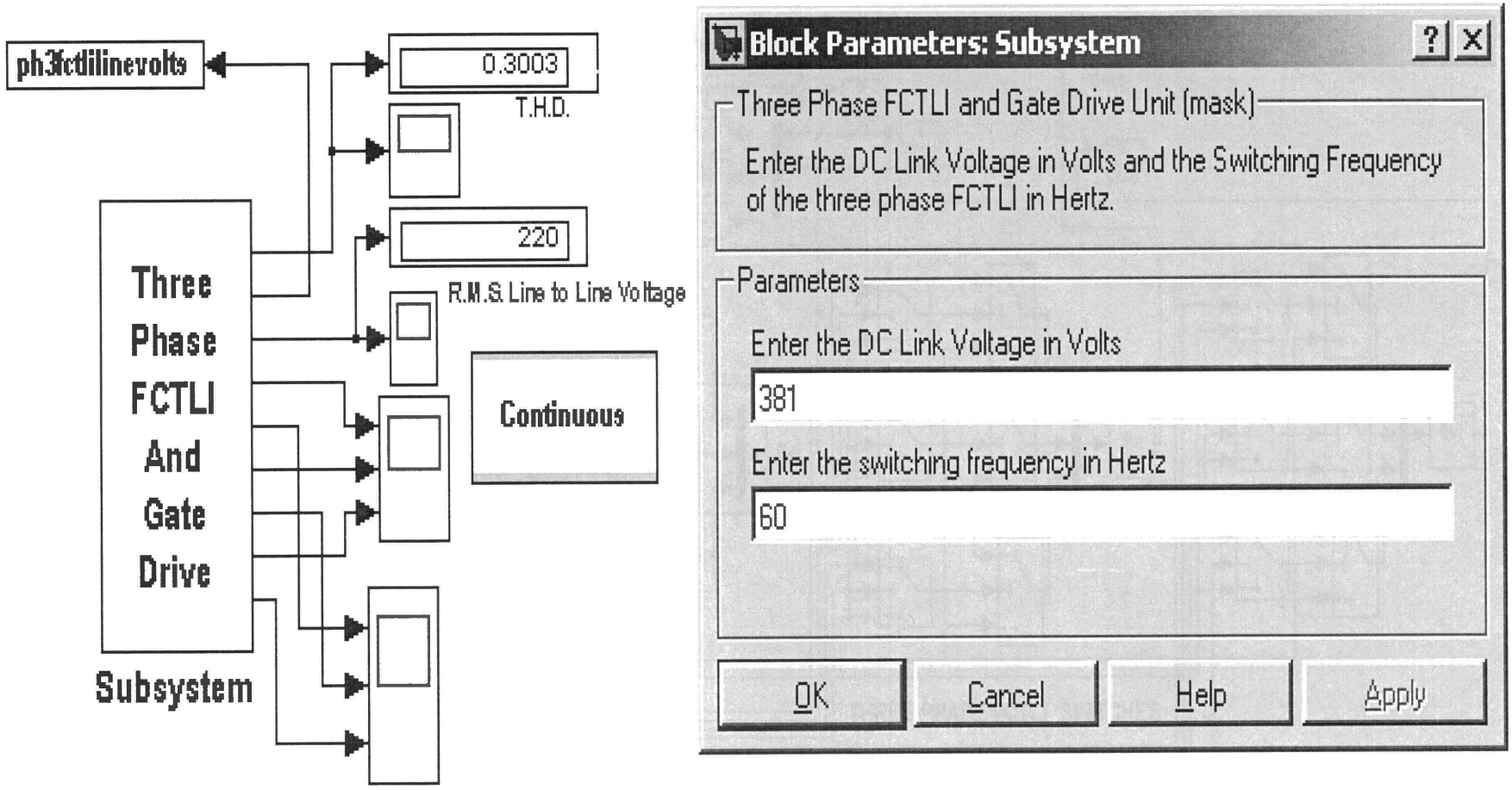

FIG.12.8: THREE PHASE FCTLI DIALOG BOX

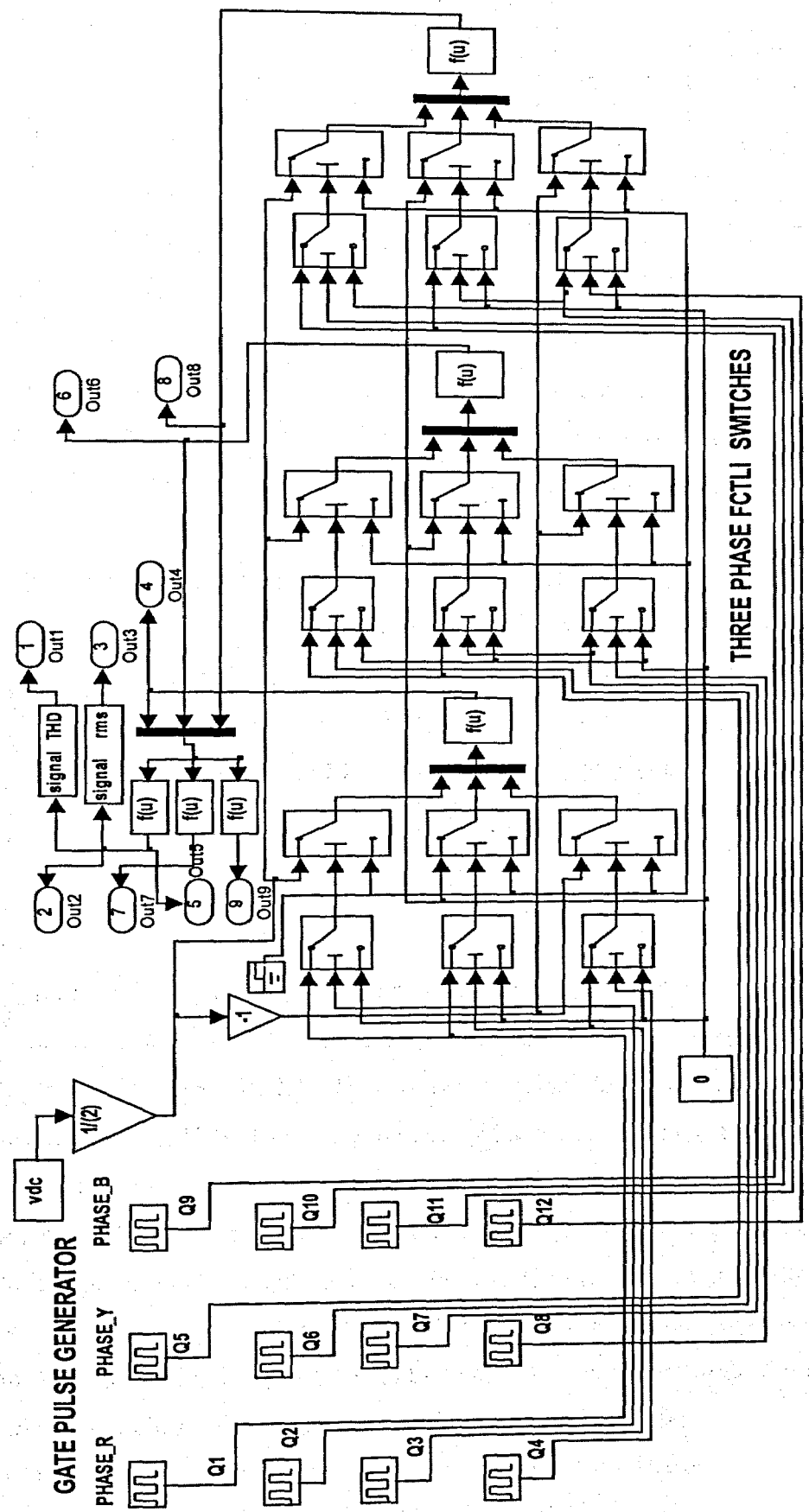
GATE PULSE GENERATOR
PHASE_R
PHASE_Y
PHASE_B
vdc
1/(2)
-1
f(u)
signal THD
signal rms
Out1
Out2
Out3
Out4
Out5
Out6
Out7
Out8
Out9
Q1
Q2
Q3
Q4
Q5
Q6
Q7
Q8
Q9
Q10
Q11
Q12
THREE PHASE FCTLI SWITCHES
0

FIG.12.9

TABLE 12.4

Sl.No.	Switch Phase R	Phase Delay Seconds	Switch Phase Y	Phase Delay Seconds	Switch Phase B	Phase Delay Seconds
1	Q1	9/(12.fsw)	Q5	1/(12.fsw)	Q9	5/(12.fsw)
2	Q2	0	Q6	4/(12.fsw)	Q10	8/(12.fsw)
3	Q3	3/(12.fsw)	Q7	7/(12.fsw)	Q11	11/(12.fsw)
4	Q4	6/(12.fsw)	Q8	10/(12.fsw)	Q12	2/(12.fsw)

Three phase FCTLI switches are implemented using threshold switches and summing Fcn blocks, as shown in Fig.12.9. The switches Q1 to Q4 in Phase R is implemented as per Table 12.3, according to the following modelling statement:

If (gate pulse for Q1 is HIGH AND Q2 is HIGH) then

Output Vrg = +Vdc/2

Else if (gate pulse for Q1 is HIGH AND Q3 is HIGH) then

Output Vrg = 0

Else if (gate pulse for Q3 is HIGH AND Q4 is HIGH) then

Output Vrg = -Vdc/2

End if

Similar modelling statements holds good for switches in Phase Y and B. The AND gate is implemented using threshold switch as shown in Fig.12.4(C), which is already explained in section 12.2.1. This AND gate principle is used for the three phase FCTLI switches in Fig.12.9. Referring to threshold switches from top to bottom on the extreme left of the position marked "Three Phase FCTLI Switches" in Fig.12.9, the top switch performs AND operation of the gate pulse for Q1 and Q2, the middle switch performs AND operation of the gate pulse for Q1 and Q3 and the bottom switch performs AND operation of the gate pulse for Q3 and Q4. The top, middle and bottom switch outputs on the extreme left are given to u(2) inputs of the second column of the top, middle and bottom switches. The u(1) inputs of the top, middle and bottom switches in the second column are +Vdc/2, zero and –Vdc/2 respectively, while their u(3) inputs are all zeros. All these switches have a threshold value of 0.5 and output u(1) when u(2) input is

greater than or equal to the threshold value, else the output is the u(3) input and performs the modelling statement given above. The switches for Phase Y and B are developed in the same way. .

12.3.2 Simulation Results

The simulation results of the line to line voltage, line to ground voltage, RMS value of line to line and line to ground voltage and their T.H.D. are shown in Fig.12.10(A) for a three phase 60 Hz FCTLI using ode15s(stiff/NDF) solver. The DC link voltage is 381 volts. The harmonic spectrum of line to line voltage is shown in Fig.12.10(B) and (C) respectively.

12.4 R.M.S. Value and Harmonic Analysis of the Line to Line Voltage of Three Phase Three Level Inverter

The line to ground voltage of the three phase three level inverter is defined below:

$$
\begin{aligned}
Vrg &= +\frac{Vdc}{2} \quad for \quad 0 \le \omega t \le \pi/2 \\
&= 0 \quad for \quad \pi/2 \le \omega t \le \pi \\
&\quad and \quad for \quad 3\pi/2 \le \omega t \le 2\pi \\
&= -\frac{Vdc}{2} \quad for \quad \pi \le \omega t \le 3\pi/2 \qquad (12.1)
\end{aligned}
$$

$$
\begin{aligned}
Vyg &= +\frac{Vdc}{2} \quad for \quad 2\pi/3 \le \omega t \le 7\pi/6 \\
&= 0 \quad for \quad \pi/6 \le \omega t \le 2\pi/3 \\
&\quad and \quad for \quad 7\pi/6 \le \omega t \le 10\pi/6 \\
&= -\frac{Vdc}{2} \quad for \quad 10\pi/6 \le \omega t \le 13\pi/6 \qquad (12.2)
\end{aligned}
$$

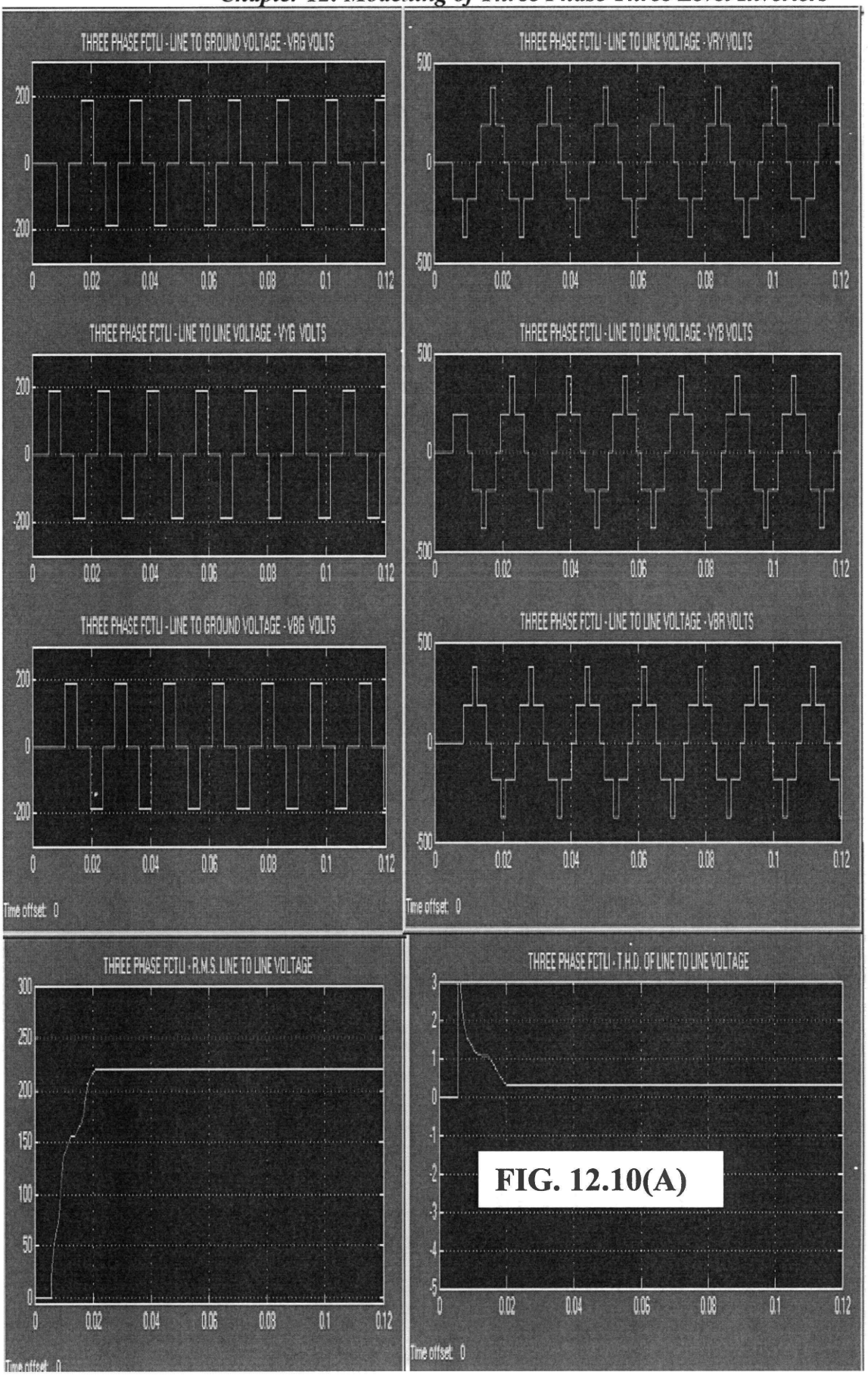
THREE PHASE FCTLI - LINE TO GROUND VOLTAGE - VRG VOLTS
THREE PHASE FCTLI - LINE TO LINE VOLTAGE - VRY VOLTS
THREE PHASE FCTLI - LINE TO LINE VOLTAGE - VYG VOLTS
THREE PHASE FCTLI - LINE TO LINE VOLTAGE - VYB VOLTS
THREE PHASE FCTLI - LINE TO GROUND VOLTAGE - VBG VOLTS
THREE PHASE FCTLI - LINE TO LINE VOLTAGE - VBR VOLTS
Time offset: 0
Time offset: 0
THREE PHASE FCTLI - R.M.S. LINE TO LINE VOLTAGE
THREE PHASE FCTLI - T.H.D. OF LINE TO LINE VOLTAGE
Time offset: 0

FIG. 12.10(A)

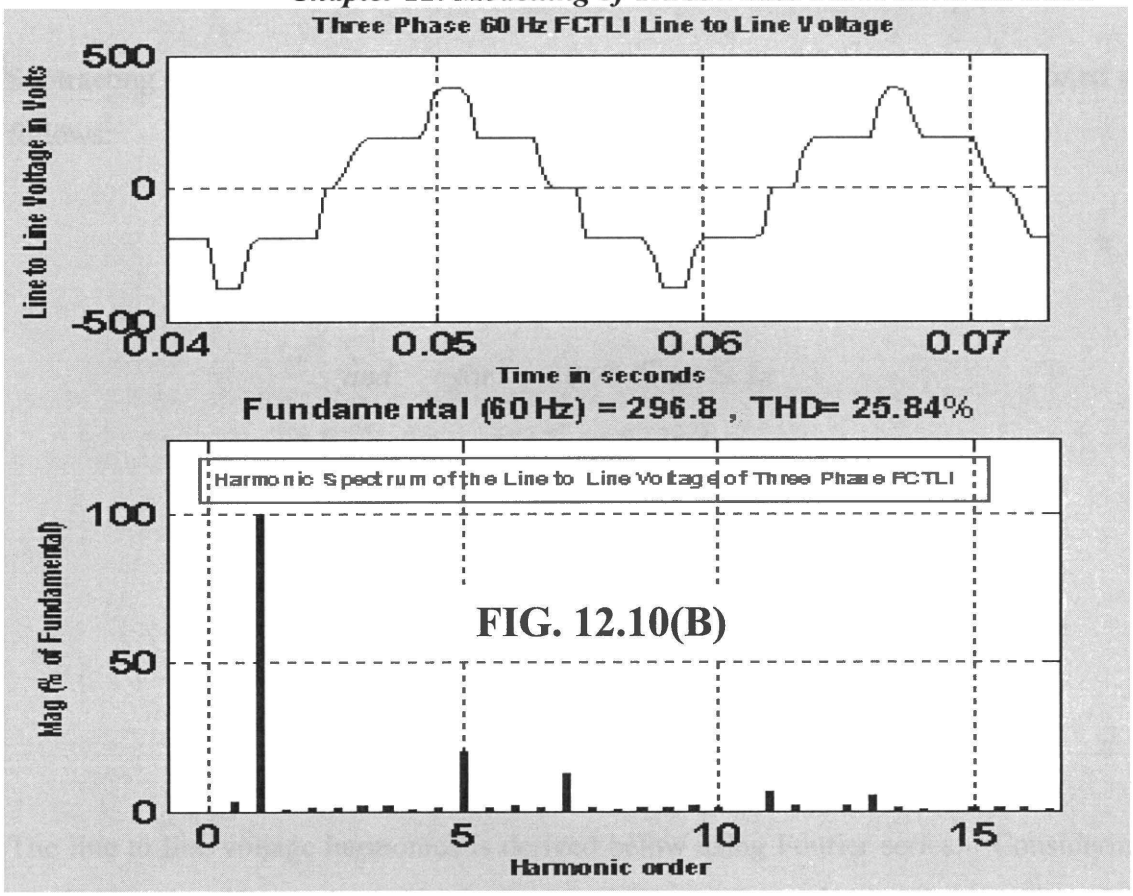

FIG. 12.10(B)

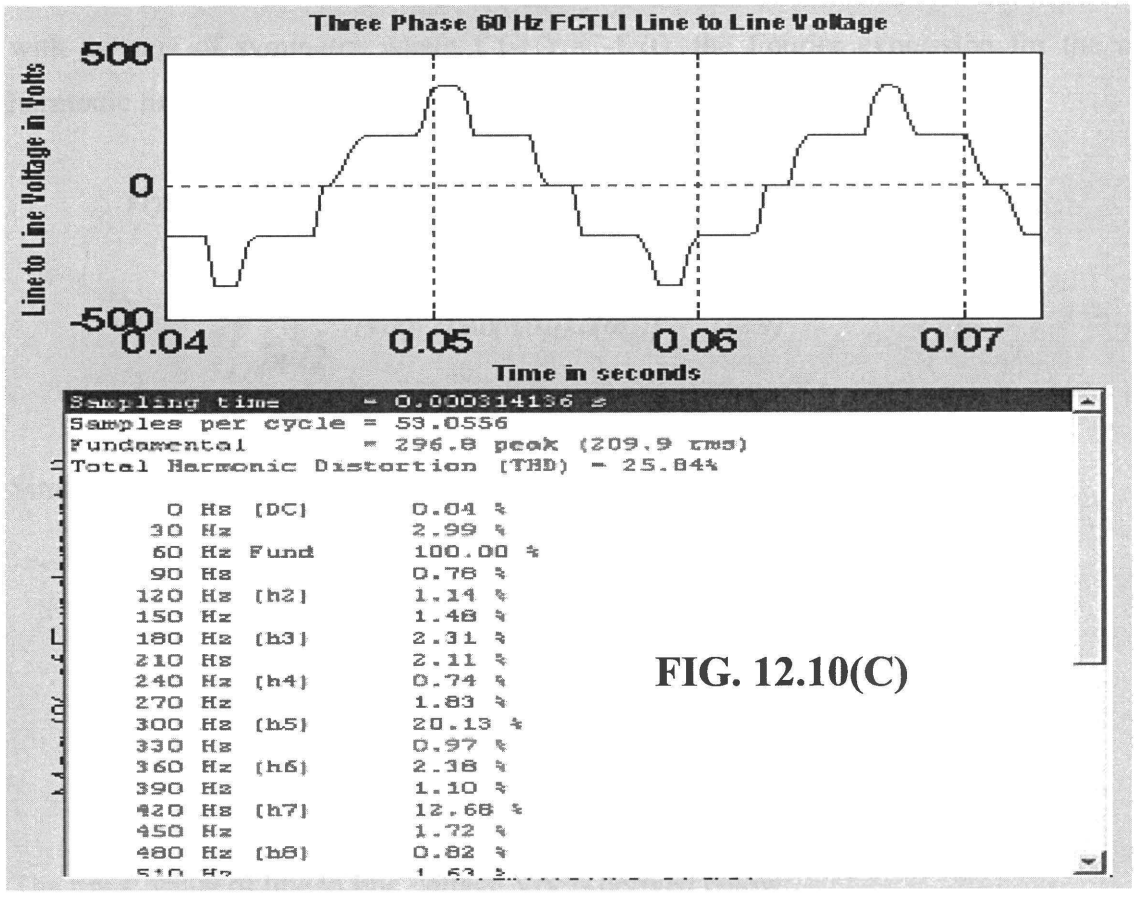

FIG. 12.10(C)

Subtracting equation 12.1 from equation 12.2, the equation for Vry can be defined as follows:

$$
\begin{aligned}
Vry \quad &= +Vdc \quad for \quad 0 \le \omega t \le \pi/6 \\
&= +\frac{Vdc}{2} \quad for \quad \pi/6 \le \omega t \le \pi/2 \\
&\quad and \quad for \quad 10\pi/6 \le \omega t \le 2\pi \\
&= 0 \quad for \quad \pi/2 \le \omega t \le 2\pi/3 \\
&\quad and \quad for \quad 3\pi/2 \le \omega t \le 10\pi/6 \\
&= -\frac{Vdc.}{2} \quad for \quad 2\pi/3 \le \omega t \le \pi \\
&\quad and \quad for \quad 7\pi/6 \le \omega t \le 3\pi/2 \\
&= -Vdc \quad for \quad \pi \le \omega t \le 7\pi/6 \qquad (12.3)
\end{aligned}
$$

The line to line voltage harmonics is derived below using Fourier series. Considering one half cycle of line voltage Vry in Fig.12.10(B) or (C) and using the equation 12.3, with an axis of symmetry where f (-t) = -f (t), the Fourier expression for the n^{th} harmonic line to line voltage Vryn is derived below:

$$
Vryn = \frac{2}{\pi} * \left[\int_{\pi/12}^{5\pi/12} (Vdc/2).\sin(n\omega t).d(\omega t) + \int_{5\pi/12}^{7\pi/12} Vdc.\sin(n\omega t).d(\omega t) + \int_{7\pi/12}^{11\pi/12} (Vdc/2).\sin(n\omega t).d(\omega t) \right] \qquad (12.4)
$$

Simplifying equation 12.4, the following:

$$
Vryn = \frac{2.Vdc.\cos(\pi.n/6)}{\pi.n} * [\cos(\pi n/4) - \cos(3\pi n/4)] \qquad (12.5)
$$

The r.m.s. value of line to line voltage Vry is derived below:

$$[Vry\,(rms)] = \left[\frac{1}{\pi} * \left[\int_{0}^{\Pi/3} (Vdc^2/4).d(\omega.t) + \int_{\pi/3}^{\pi/2} (Vdc^2).d(\omega.t) + \int_{\pi/2}^{5.\pi/6} (Vdc^2/4).d(\omega.t) \right] \right]^{1/2} \quad ...(12.6)$$

$$\mathbf{Vry\,(rms)} = \frac{\mathbf{Vdc}}{\sqrt{3}} \ \mathbf{Volts} \quad .....(12.7).$$

Similarly referring to the line to ground voltage in Fig.12.10(A) and using equation 12.1 and noting that each transitions from one level to next are equally spaced at intervals of Π / 2 radians, the r.m.s value of Line to Ground voltage Vrg, is given by the equation:

$$Vrg\,(rms) = \left[\frac{1}{2.\Pi} * \left[\int_{\pi/2}^{\pi} (Vdc^2/4).d(\omega.t) + \int_{3.\pi/2}^{2.\pi} (Vdc^2/4).d(\omega.t) \right] \right]^{1/2}$$

$$\mathbf{Vrg\,(rms)} = \frac{\mathbf{Vdc}}{2.\sqrt{2}} \ \mathbf{Volts} \quad .....(12.8)$$

Thus for a dc link voltage of 381 volts, the values of Vry(rms) and Vrg(rms) works out to 220 volts and 134.7 volts respectively.

Using the equation 4.18 in section 4.2.3 of chapter 4, the T.H.D. of line to line voltage of three phase three level inverter can be expressed as follows:

$$T.H.D. \quad of \quad Vry = \sqrt{\frac{(Vdc/\sqrt{3})^2}{(\sqrt{3}.Vdc/\pi)^2} - 1}$$

$$= 30.9\% \qquad (12.9)$$

12.5 Conclusions

The models for three phase DCTLI and FCTLI have been successfully developed. In these two models the time intervals for the three voltage levels are equal. By reducing the time duration for the zero voltage level to a lower value compared to the other two

voltage levels, it is possible to reduce the T.H.D. of line to line voltage and improve its harmonic spectrum still further [70]. The T.H.D. of line to line voltage for the above conventional three phase three level inverter with equal time duration for all the three voltage levels is 31.08 % [70]. The T.H.D. of line to line voltage by simulation for the above DCTLI is found to be around 29.5% and that for the FCTLI is found to be 30% respectively, whereas the calculated value is 30.9%. However there is a reduction in the individual harmonic contributions to the line to line voltage for the various higher order such as seventh, as compared to the plain three phase 180 degree mode inverter shown in Fig.4.6(I) in Chapter 4. The R.M.S. line to line voltage displayed in Fig.12.3, Fig.12.5(A) for the DCTLI and in Fig.12.8, Fig.12.10(A) for the FCTLI well agree with the formula given by equation 12.7. It is also seen from Fig.12.1(A) and Fig.12.6(A) that the voltage stress across individual semiconductor switch is reduced for a given DC link voltage, as compared to the plain three phase two level inverter. Appendix E provides the comparison of the simulation of the above three phase DCTLI and FCTLI using the demo version of the electronic circuit simulation software MICROCAP 8.

CHAPTER 13
CONCLUSIONS

This thesis presents interactive models for power electronic converters and electric drives. Major fundamental topology for power electronic converters are covered. Similarly predominant AC drives such as three phase I.M. and PMSM models in the open loop are covered. The concept of switching function is used to develop the models for power electronic converters. These models for power electronic converter systems, solve the differential equations describing the behaviour of the system. The power electronic converter models developed by softwares such as PSIM, MICROCAP and the SimpowerSystems block set of SIMULINK solve the equivalent circuit of the converter model using the sub-circuit parameters of the semiconductor component or the device used in this model. For three phase I.M. and PMSM their dq0-axis voltage-current relationship is used to develop the model. In addition, for the three phase I.M. the dq0-axis flux linkage equations and also the flux linkage per second equations are also used for developing the model.

The user can enter the data relating to the particular power electronic converter or electric drive in the boxes provided for the purpose. The user can follow the instructions given in the dialog boxes for entering the data in the appropriate units in the relevant boxes provided. The user need not go into each block of the model to enter the data. Thus the user saves much time in testing the given power electronic or electric drive system. Additionally help files are also provided for SMPS and three phase PWM inverter fed I.M. drive models with which the user can modify the model for any given switching frequency of the SMPS and for any given triangle carrier frequency for the three phase PWM inverter. Thus only one model is sufficient to test any given power electronic and electric drive system. Thus this type of interactive models find applications in virtual power electronics and drives laboratories.

Additionally harmonic analysis of the three phase two level and three level inverters are made with MATLAB and presented in APPENDIX A. The experimental data and calculations using MATLAB for the Lybotec six step inverter fed PMSM is presented in APPENDIX B. The Lybotec six step inverter block diagram layout is presented in APPENDIX C. APPENDIX D provides the pin layout of Digital Integrated Circuits used for the digital switching function generator discussed in Chapter 9. The model performance of selected power electronic converters, three phase IM and six step inverter fed PMSM drive discussed in this thesis are compared by simulation with electronic circuit simulation softwares. These are presented in APPENDIX E. APPENDIX F provides the literature references cited.

13.1 Work Presented in this Thesis:

The work presented in this thesis is summarized below:

1. Provides interactive models for single phase full wave diode bridge rectifier, single phase full wave SCR bridge rectifier, three phase full wave diode bridge rectifier.
2. Interactive models for three phase 180 degree mode and 120 degree mode inverters are presented. The model performance is supplemented by simulation using software PSPICE.
3. Interactive models for the basic topology of the dc to dc converters such as the Buck, Boost and Buck-Boost converters in the continuous conduction mode are presented.
4. Totally new and original interactive models for three phase ac to ac converters such as the three phase back to back connected thyristors in series with the lines and connected to star connected resistive load, three phase back to back connected thyristors in series with resistive load connected in delta to the lines are presented.
5. Interactive models for three phase I.M. to study the stator and rotor currents and torque transients by direct online starting using dq0-axis voltage-current equations, dq0-axis flux linkage equations in state space, dq0-axis flux linkage per second equations in state space are provided.

6. New and Original interactive models for PMSM drives fed by six step continuous current mode and discontinuous current mode inverter are presented. The model performance for the later type is also supplemented by actual experiments in the laboratory.
7. A novel interactive circuit model for the digital switching function generator suitable for the three phase 180 degree mode two level inverter is presented. The model performance is supplemented by actual experimental investigation in the laboratory and also by using the software PSPICE.
8. Interactive model for SMPS is provided. The model performance is supplemented by simulation using the software PSIM.
9. Interactive models for three phase SINE, THI and HI PWM inverter fed I.M. drive is presented. A newly discovered interactive model for the three phase CS PWM inverter fed I.M. drive is also given. The superiority of the three phase CS PWM inverter from the point of view of T.H.D. of line to line voltage compared to three phase SINE, THI and HI PWM inverters is established.
10. Interactive models for three phase DCTLI and FCTLI are presented. The model performance is supplemented by simulation using the software MICROCAP.
11. The model performance of selected power electronic converters such as single phase FWDBR, FWCBR, three phase FWDBR, six step continuous and discontinuous current mode inverters, buck, boost, buck-boost converters, three phase ac controllers in series with the lines with star connected resistive load and in series with resistive load connected in delta to the lines, three phase IM directly connected to the ac lines presented in this thesis are compared by simulation using the demo version of PSIM 7.0. The model performance of six step continuous current mode inverter fed PMSM drive presented in this thesis is also compared by simulation using the built in three phase MOSFET inverter and PMSM block in the SimPowerSystems block set of SIMULINK. The three phase DCTLI and FCTLI model performance presented in this thesis are compared by simulation using the demo version of MICROCAP 8 software..

13.2 Scope for Further Future Work:

The further future work possible in the area of modelling of power electronic converters and electric drives is discussed below:

1. Modelling of three phase Diode Clamped and Flying Capacitor Three Level and Higher Level Inverters with improved harmonic spectrum and lower T.H.D. for line to line voltage as compared to conventional three phase two level inverters.
2. Modelling of second order and fourth order DC to DC converters such as CUK, SEPIC and ZETA, ULTRA LIFT LUO, QUADRATIC BOOST etc. in the Discontinuous Conduction Mode and their applications for load Power Factor Correction in Power Systems.
3. Modelling of Vector controlled three phase I.M. drives.
4. Modelling of Vector, Direct Torque and Hysteresis Current controlled Six Step Inverter fed PMSM and BLDCM Drives.

Modelling studies on the above four categories supplemented either or both by hardware experiments in the laboratory and also by using electronic and electric drive circuit simulation software packages can be made.

APPENDIX A

HARMONIC SPECTRUM OF THE LINE TO LINE VOLTAGE OF THREE PHASE INVERTERS USING MATLAB

The harmonic spectrum of the line to line voltage of three phase 180 degree mode two level inverter is analysed below using MATLAB.

The equation 4.1 in Chapter 4 is modified as follows to develop the MATLAB program:

$$b_n = \frac{2}{\pi} * \left[\int_{\pi/6}^{5\pi/6} -V_{dc} . \sin\left(n\omega t\right) . d\omega t \right]$$

$$= \frac{2.V_{dc}}{\pi n} * \left[\cos\left(\frac{5n\pi}{6}\right) - \cos\left(\frac{n\pi}{6}\right) \right] \quad for \quad all \quad n \geq 1 \quad (A.1)$$

The MATLAB source code for the harmonic spectrum of line to line voltage of three phase 180 degree mode two level inverter is given below:

```
%Harmonic spectrum of line to line voltage of three phase two level
%180 degree mode inverter
%v_dc is the dc link voltage in per unit
%%Narayanaswamy.P.R.Iyer, Faculty of Engineering, UTS, NSW
v_dc = 1;
%VN1 is the Fourier spectrum of line to line voltage
for N = 1:36;
   m = N;
   x(m) = m;
   VN1(m) = (2*v_dc/(pi*m))*(cos(5*pi*m/6) - cos(pi*m/6));
```

```
end;
bar(abs(VN1),0.125),grid;;
xlabel('Harmonic order  n');
ylabel('Harmonic Spectrum of line to line voltage Vn');
title('Harmonic Spectrum of Line to Line Voltage of Three Phase Two Level Inverter');
%calculation of T.H.D. of line to line voltage
%VN1_1peak is the peak value of fundamental component of VN1.
VN1_1peak = (-2*v_dc/(pi))*(cos(5*pi/6) - cos(pi/6));
VN1_1rms = VN1_1peak/(sqrt(2));
%VLL_rms is the rms value of the line to line voltage
VLL_rms = ((sqrt(2))*v_dc)/(sqrt(3));
thd_percent = abs(sqrt((VLL_rms)^2 - (VN1_1rms)^2)*100/VN1_1rms);
```

The results are given below:

```
>> fftofph3twolevelinv
>> VN1_1peak

VN1_1peak =

   1.1027

>> VN1_1rms

VN1_1rms =

   0.7797

>> VLL_rms

VLL_rms =

   0.8165
```

Appendix A:Harmonic Spectrum of Line to Line Voltage of Three Phase Inverters

```
>> thd_percent

thd_percent =

   31.0842
```

The plot of the harmonic spectrum of the Line to Line voltage of three phase 180 degree mode inverter is shown in Fig.A.1.

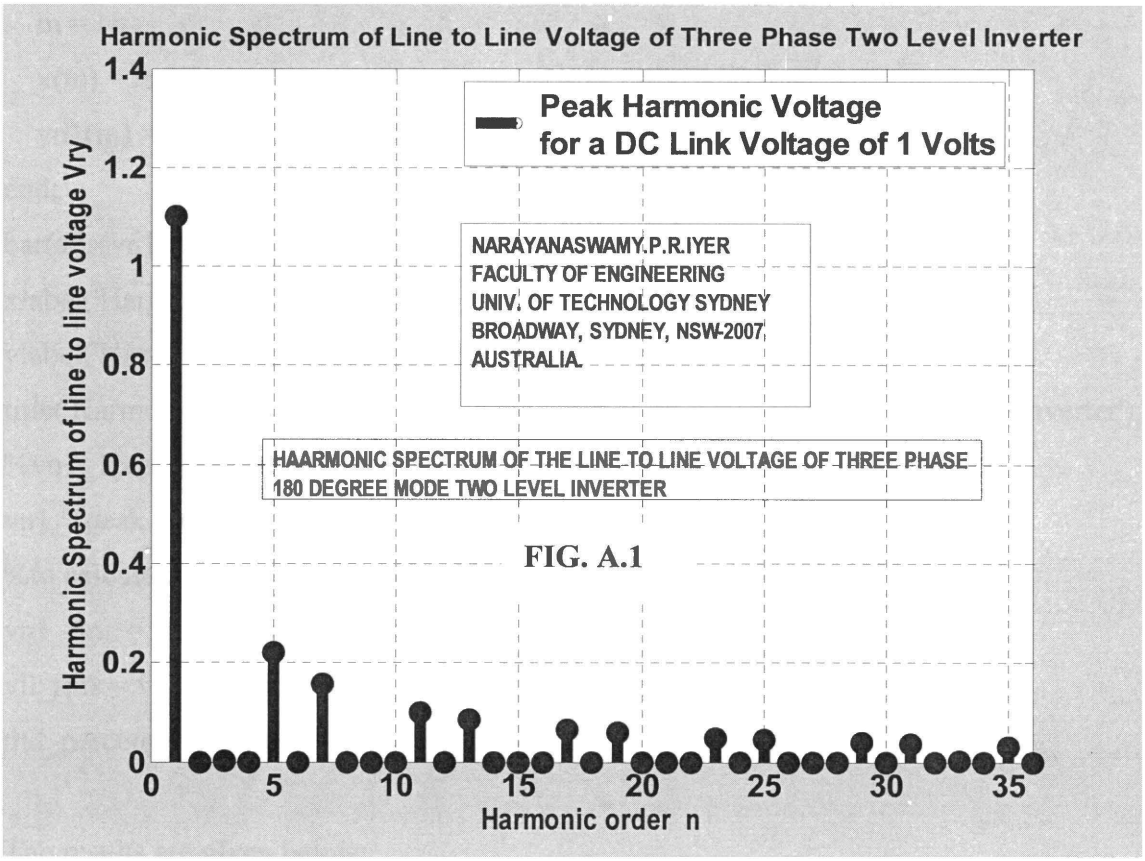

FIG. A.1

The harmonic spectrum of the line to line voltage of three phase three level inverter is analysed below using MATLAB.

The equation 12,5 and 12.7 in Chapter 12 are used to develop the MATLAB program. The MATLAB source code for the harmonic spectrum of line to line voltage of three phase three level inverter is given below:

Appendix A:Harmonic Spectrum of Line to Line Voltage of Three Phase Inverters

```
%Fourier spectrum of line to line voltage of three phase three level
%inverter
%v_dc is Dc link voltage in per unit.
%vn1 is the Harmonic Spectrum of Line to Line voltage.
%%Narayanaswamy.P.R.Iyer, Faculty of Engineering, UTS, NSW.
v_dc = 1;
k = 2/pi;
for N = 1:36;
   m = N;
   x(m) = m;
   vn1(m) = ((k*v_dc*cos(pi*m/6))/(m))*(cos(pi*m/4) - cos(3*pi*m/4));
end;
bar(abs(vn1),0.125),grid;
xlabel('Harmonic Order  n');
ylabel('Harmonic Line to Line Voltage Vn1 per unit');
title('Harmonic Spectrum of Line to Line Voltage of Three Phase Three Level Inverter');
%vn1_1peak is the fundamental component of vn1
vn1_1peak = ((k*v_dc*cos(pi/6)))*(cos(pi/4) - cos(3*pi/4));
%to calculate t.h.d. of line to line voltage
vn1_rms = vn1_1peak/(sqrt(2));
vll_rms = v_dc/(sqrt(3));
thd_percent = sqrt((vll_rms^2) - (vn1_rms^2))*100/vn1_rms;
```

The results are given below:

```
>> fftofph3threelevelinv
>> vn1_1peak

vn1_1peak =

   0.7797

>> vn1_rms
```

Appendix A:Harmonic Spectrum of Line to Line Voltage of Three Phase Inverters

```
vn1_rms =

    0.5513

>> vll_rms

vll_rms =

    0.5774

>> thd_percent

thd_percent =

   31.0842
```

The plot of the harmonic spectrum of the Line to Line voltage of three phase three level inverter is shown in Fig.A.2.

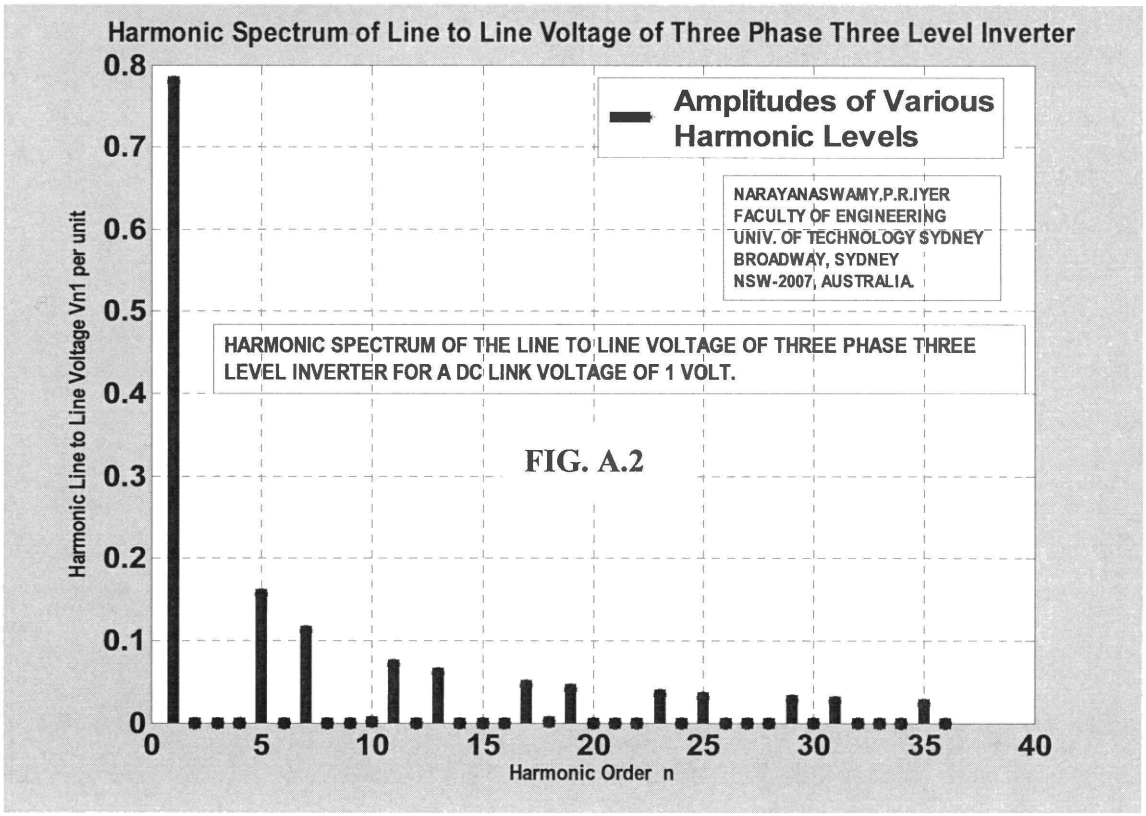

FIG. A.2

Appendix A:Harmonic Spectrum of Line to Line Voltage of Three Phase Inverters

From Fig.A.1 and A.2 it is clear that the amplitude of the fundamental component of the three phase three level inverter is reduced as compared to three phase 180 degree mode two level inverter, for a given dc link voltage. The amplitudes of the seventh and eleventh harmonics are reduced for the three phase three level inverter as compared to the three phase 180 degree mode inverter.

APPENDIX B

PARAMETER MEASUREMENT OF LYBOTEC SIX STEP INVERTER FED PMSM DRIVE

The parameters such as stator resistance Rs, stator leakage inductance Lls, mutual inductance between stator and rotor Lm, rotor magnet constant λm, Moment of Inertia and damping constant of the rotor were measured for the 18 volts, 4 poles, surface magnet PMSM in the laboratory. These are given below:

ACCURATE ROTOR INERTIA AND DAMPING CONSTANT MEASUREMENT FOR PMSM DRIVE

The experimental set up for accurate measurement of rotor inertia and damping constant is shown in Fig.B.1. Here instead of tachometer for rotor speed measurement, storage oscilloscope is used which displays the period of the back e.m.f. of the PMSM, from which the speed of the rotor in electrical and mechanical radians per second is calculated.

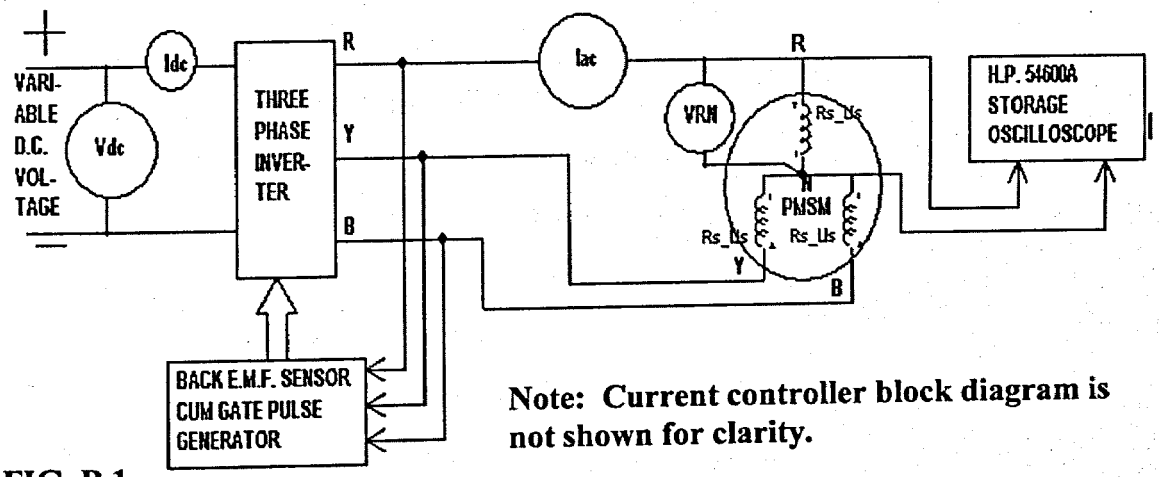

Note: Current controller block diagram is not shown for clarity.

FIG. B.1 PMSM ROTOR DAMPING AND INERTIA MEASUREMENT - EXPERIMENTAL SET UP

The dc link voltage is initially set to 40 volts. The machine is run on NO LOAD. The initial reading of Vdc, Idc, C.R.O. back e.m.f. period(i.e. initial rotor speed) are noted. The dc input to inverter is switched OFF. The time to fall to various rotor speeds are

noted using a stop watch and by observing the corresponding period of back e.m.f. The time to fall to JUST ZERO speed is also noted. These are shown in the MATLAB program which is used to calculate the results displayed as shown below.

The experimental set up for damping constant measurement is the same as shown in Fig.B.1. The PMSM is run on NO LOAD. With dc link voltage of 40 volts, the readings of Vdc, Idc C.R.O. back e.m.f. period are all shown in the MATLAB program below. A graph of Power input to inverter versus square of rotor speed in mech.radians per second is drawn using the MATLAB program given below. This graph is shown in Fig.B.2. The X and Y coordinates are taken from this graph at various intervals and slopes are calculated and the average is found out which gives the damping constant D. The results are displayed at the end of the MATLAB program.

```
%%Lybotech PMSM Experiment for refined measurement of mechanical data.
%%Rotor speed measuremnt using tachometer eliminated by using C.R.O.
%%back e.m.f. period measurement.
%%Program Author: Narayanaswamy. P.R. Iyer; Faculty of Engg.; U.T.S.; NSW
%%NO LOAD test data is used.
%%Number of poles P for PMSM is four.
P = 4;
Vdc = [15 20 25 30 35 40];
Idc = [0.042 0.039 0.039 0.039 0.040 0.044];
Vrn = [6.2 8.5 10.66 12.7 14.95 17.09];
Iac = [0.040 0.042 0.042 0.041 0.040 0.042];
CRO_bemf_period = [160e-3 116e-3 93e-3 77e-3 66e-3 58e-3];
%%tacho_speed_rpm = [189 258 325 389 451 517];
%%measurement of damping constant D
%%wr_mech is rotor angular speed in mech.radians per second
%%N_rpm is the rotor speed in r.p.m.
%%P_in is power input to inverter.
for I = 1:6
  wr_mech(I) = (1/(CRO_bemf_period(I)))*2*pi*2*1/(P);
  N_rpm(I) = (60*wr_mech(I))/(2*pi);
```

```
   wr_mech_square(I) = (wr_mech(I)*wr_mech(I));
   P_in(I) = (Vdc(I)*Idc(I));
end
plot(wr_mech_square,P_in,'k-');
%%damping constant D is measured from slope.
%%coordinates measured from plot of P_in versus wr_mech_square
%%the coordinates of the above plots are x_val and y_val
x_val = [2934  2266  1665  1141  733.5  385.5];
y_val = [1.76  1.4  1.17  0.975  0.78  0.63];
for J = 1:6
   damping_constant1(J) = (y_val(1) - y_val(2))/(x_val(1) - x_val(2));
   damping_constant2(J) = (y_val(2) - y_val(3))/(x_val(2) - x_val(3));
   damping_constant3(J) = (y_val(3) - y_val(4))/(x_val(3) - x_val(4));
   damping_constant4(J) = (y_val(4) - y_val(5))/(x_val(4) - x_val(5));
   damping_constant5(J) = (y_val(5) - y_val(6))/(x_val(5) - x_val(6));
end
damping_D = [damping_constant1(1)  damping_constant2(1)  damping_constant3(1)
damping_constant4(1)  damping_constant5(1)];
damping_constant_D = mean(damping_D);
%%Rotor inertia J_approx neglecting damping constant D
dc_input_volts = [40  40  40  40];
dc_input_amps = [0.043  0.041  0.042  0.043];
bemf_period_init = [58e-3  58e-3  58e-3  58e-3];
%%final rotor speed in all cases are zero.
wr_mech_final = [0  0  0  0];
time = [13.62  13.60  13.91  13.53];
for I = 1:4
   wr_mech_init(I) = (1/(bemf_period_init(I)))*2*pi*2/(P);
   wr_mech_ratechange(I) = (wr_mech_init(I) - wr_mech_final(I))/(time(I));
   t_em(I) = (dc_input_volts(I)*dc_input_amps(I))/(wr_mech_init(I));
   J_approx(I) = (t_em(I))/(wr_mech_ratechange(I));
end
MI_rotor_approx = [J_approx(1)  J_approx(2)  J_approx(3)  J_approx(4)];
```

```
J_approx_avg = mean(MI_rotor_approx);
%%Rotor inertia considering damping constant D
for J = 1:4
   wr_mech_init(J) = (1/(bemf_period_init(J)))*2*pi*2/(P);
   wr_mech_ratechange(J) = (wr_mech_init(J) - wr_mech_final(J))/(time(J));
   t_em(J) = (dc_input_volts(J)*dc_input_amps(J))/(wr_mech_init(J));
   J_true(J) = (t_em(J))/(wr_mech_ratechange(J)) -
(damping_constant_D*wr_mech_init(J))/(wr_mech_ratechange(J));
end
MI_rotor_true = [J_true(1)  J_true(2)  J_true(3)  J_true(4)];
J_true_avg = mean(MI_rotor_true);
%%another set of readings are tabulated below to calculate rotor inertia
%%considering damping constant D
cro_bemf_period_init = [58e-3  58e-3  58e-3  58e-3];
cro_bemf_period_final = [75e-3  77.5e-3  91e-3  100e-3];
delta_time = [5.36  5.59  7.78  8.56];
power_in = [40*0.044  40*0.044  40*0.044  40*0.044];
for K = 1:4
   speed_mech_rad_init(K) = (1/(cro_bemf_period_init(K)))*2*pi*2/(P);
   speed_mech_rad_final(K) = (1/(cro_bemf_period_final(K)))*2*pi*2/(P);
   speed_ratechnage(K) = (speed_mech_rad_init(K) -
speed_mech_rad_final(K))/(delta_time(K));
   J_actual_val1(K) = (power_in(K)/(speed_mech_rad_init(K)* speed_ratechnage(K)))
- (damping_constant_D*speed_mech_rad_init(K))/(speed_ratechnage(K));
   J_actual_val2(K) =
((damping_constant_D)*(speed_mech_rad_init(K)))/(speed_ratechnage(K));
end
rotor_inertia_J1 = [J_actual_val1(1)  J_actual_val1(2)  J_actual_val1(3)
J_actual_val1(4)];
rotor_inertia_J2 = [J_actual_val2(1)  J_actual_val2(2)  J_actual_val2(3)
J_actual_val2(4)];
J_actual1_avg = mean(rotor_inertia_J1);
J_actual2_avg = mean(rotor_inertia_J2);
```

The results are printed below:

```
>> pmsm_mechdata_revised1
>> damping_constant_D

damping_constant_D =

  4.4066e-004

>> J_actual1_avg

J_actual1_avg =

    0.0035

>> J_actual2_avg

J_actual2_avg =

    0.0097
```

The values used are D = 4.4066e-4 Nw.m.sec. per mech.rad and M.I. of rotor J = 0.0035 kg.m^2. The plot of Power input versus square of rotor mechanical angular speed used for calculating damping constant D of rotor is shown in Fig.B.2.

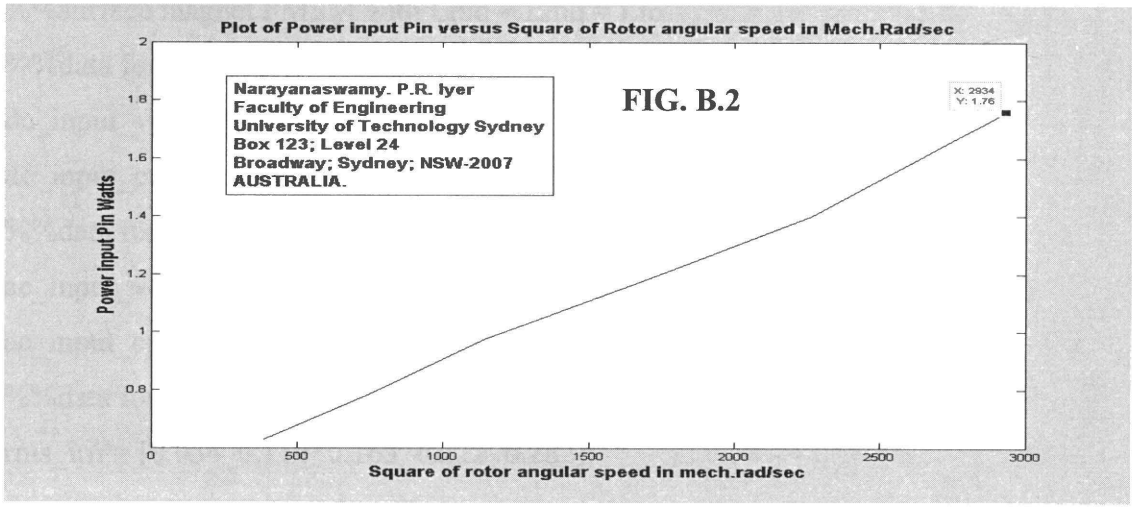

FIG. B.2

MEASUREMENT OF ELECTRICAL PARAMETERS OF PMSM DRIVE

The connection diagram for the measurement of stator resistance, stator leakage inductance and stator mutual inductance between phases are shown below in Fig.B.3(a),

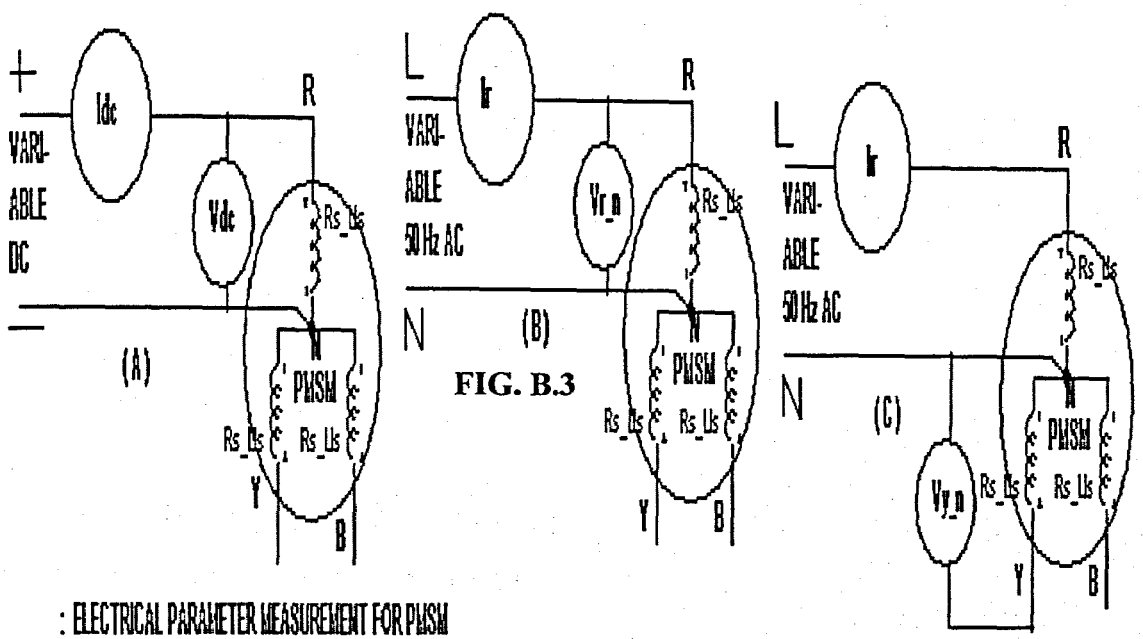

(b) and (c) respectively. The experimental set up for rotor magnet constant is shown in Fig.B.1 above. The data is given in the MATLAB program below. The results are shown at the end of the MATLAB program below:

```
%%measurement of electrical parameters of Lybotech PMSM
%%Narayanaswamy.P.R.Iyer, Faculty of Engineering, UTS, NSW.
%%surface magnet PMSM with Lmd = Lmq = Lm
%%data for stator resistance measurement.
dc_input_volts = [1  2  3  4  5];
dc_input_current = [0.107  0.214  0.326  0.431  0.535];
%%data for stator leakage inductance measurement.Supply frequency 50 Hz
ac_input_volts = [1  2  3  4  5];
ac_input_current = [0.051  0.105  0.160  0.214  0.269];
%%data for mutual inductance measurement.  Supply frequency 50 Hz
rms_irn = [0.054  0.114  0.163  0.222  0.282];
```

```
rms_mutual_voltage_vyn = [0.122  0.253  0.36  0.49  0.625];
%%stator resistance is rs per phase in Ohms.
%%let Lls be the self or leakage inductance in Henries per phase
%%let Lm be mutaul inductance between phases.
%%let Ls =  Lls + Lm be total self inductance
for I = 1:5
   rs(I) = (dc_input_volts(I))/(dc_input_current(I));
   zs(I) = (ac_input_volts(I))/(ac_input_current(I));
   xls(I) = sqrt(zs(I)*zs(I) - rs(I)*rs(I));
   Lls(I) = (xls(I))/(314);
   xm(I) = (rms_mutual_voltage_vyn(I))/(rms_irn(I));
   Lm(I) = (xm(I))/(314);
   Ls(I) = (Lls(I) + Lm(I));
end
res_stator = [rs(1)  rs(2)  rs(3)  rs(4)  rs(5)];
ind_stator = [Ls(1)  Ls(2)  Ls(3)  Ls(4)  Ls(5)];
Rs_stator = mean(res_stator);
Ls_stator = mean(ind_stator);
%%measurement of rotor magnet constant lamda_m volt.sec/elec.rad
%%period is measured from c.r.o. and r.m.s.line to neutral voltage of PMSM
%%from D.M.M.
period = [70.5e-3  79.5e-3  82e-3  92e-3  105.5e-3  119e-3  125.5e-3  131.5e-3];
pmsm_rms_phase_voltage = [12.58  11.16  10.38  9.74  7.86  7.34  6.23  6.07];
for N = 1:8
   omega_r_elec_rad(N) = (2*pi)/(period(N));
   lamda_m(N) = (pmsm_rms_phase_voltage(N))/(omega_r_elec_rad(N));
end
rotor_magnet_constant  =  [lamda_m(1)   lamda_m(2)   lamda_m(3)   lamda_m(4)
lamda_m(5)  lamda_m(6)  lamda_m(7)  lamda_m(8)];
lamda_m_avg = mean(rotor_magnet_constant);
```

The results are printed below:

```
>> pmsm_elec_data2
>> lamda_m_avg

lamda_m_avg =

   0.1354

>> Rs_stator

Rs_stator =

   9.3041

>> Ls_stator

Ls_stator =

   0.0596
```

The Stator Resistance Rs and self inductance Ls per phase are 9.3041 Ohms and 59.6 milli Henries respectively. Rotor magnet constant λm is 0.1354 Volt.sec per elec.rad. The actual values for the electrical and mechanical parameters used for simulation are also tabulated in TABLE 8.2 in Chapter 8.

APPENDIX C
BLOCK DIAGRAM OF SIX STEP LYBOTEC INVERTER

The block diagram of the Lybotec Six Step Inverter used for the PMSM Drive in Chapter 8 is given in Fig.C.1 below:

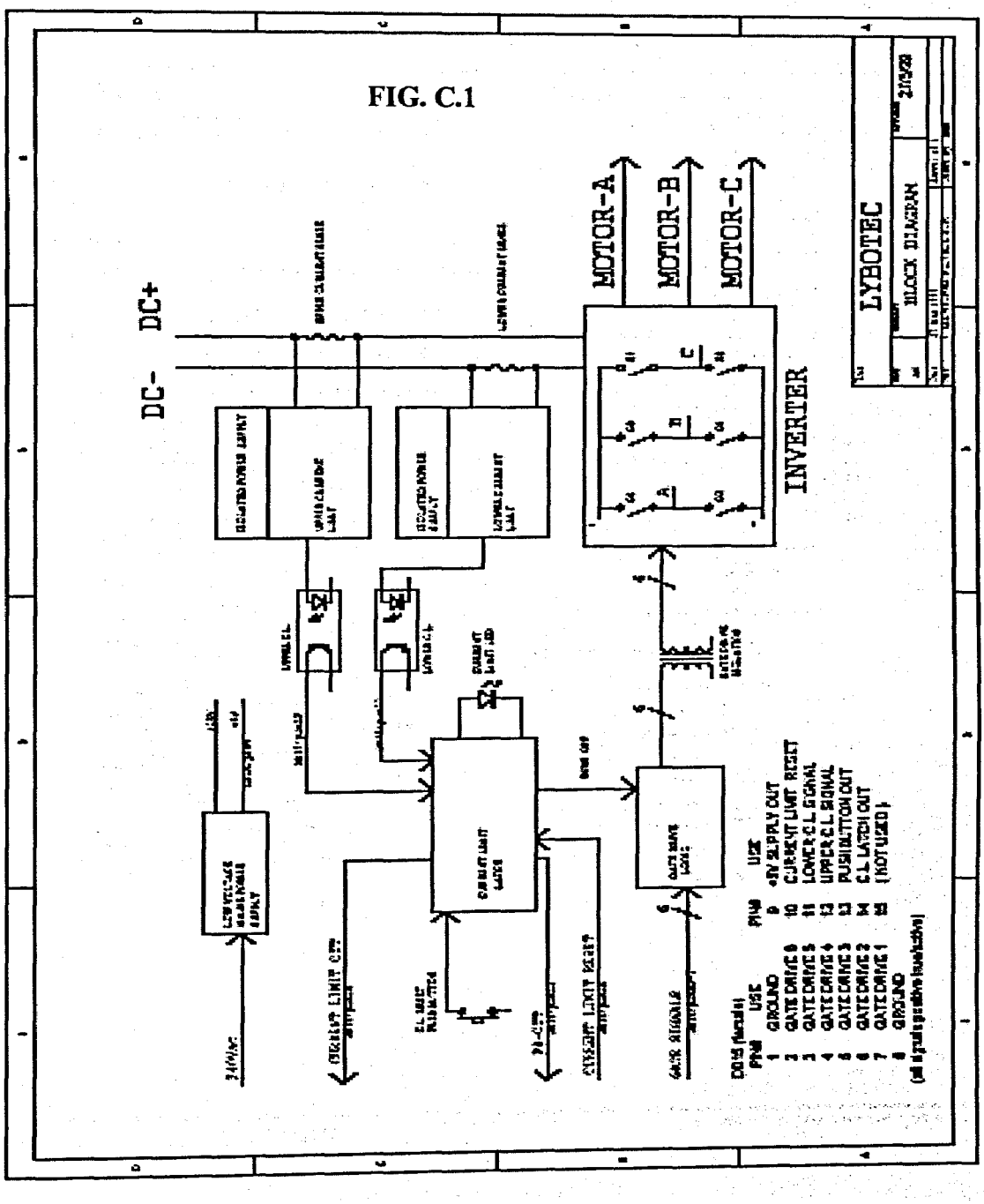

FIG. C.1

APPENDIX D

DATA SHEET FOR DIGITAL INTEGRATED CIRCUITS

The data sheets for the digital ICs used in fabricating the digital switching function generator discussed in Chapter 9 are given below:

SN5408, SN54LS08, SN54S08
SN7408, SN74LS08, SN74S08
QUADRUPLE 2-INPUT POSITIVE-AND GATES
SDLS033 – DECEMBER 1983 – REVISED MARCH 1988

- **Package Options Include Plastic "Small Outline" Packages, Ceramic Chip Carriers and Flat Packages, and Plastic and Ceramic DIPs**
- **Dependable Texas Instruments Quality and Reliability**

description

These devices contain four independent 2-input AND gates.

The SN5408, SN54LS08, and SN54S08 are characterized for operation over the full military temperature range of −55°C to 125°C. The SN7408, SN74LS08 and SN74S08 are characterized for operation from 0° to 70°C.

FUNCTION TABLE (each gate)

INPUTS		OUTPUT
A	B	Y
H	H	H
L	X	L
X	L	L

logic symbol†

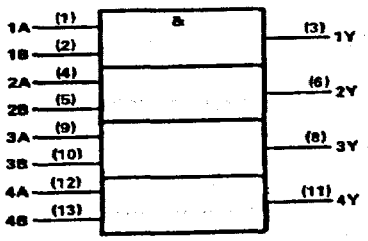

†This symbol is in accordance with ANSI/IEEE Std 91-1984 and IEC Publication 617-12.
Pin numbers shown are for D, J, N, and W packages.

SN5408, SN54LS08, SN54S08 . . . J OR W PACKAGE
SN7408 . . . J OR N PACKAGE
SN74LS08, SN74S08 . . . D, J OR N PACKAGE
(TOP VIEW)

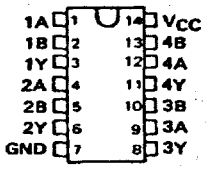

SN54LS08, SN54S08 . . . FK PACKAGE
(TOP VIEW)

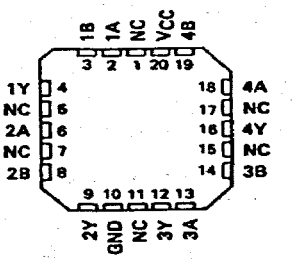

NC—No internal connection

logic diagram (positive logic)

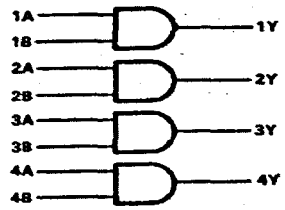

$Y = A \cdot B$ or $Y = \overline{\overline{A} + \overline{B}}$

TEXAS INSTRUMENTS
POST OFFICE BOX 655303 • DALLAS, TEXAS 75265

SN54LS11, SN54S11, SN74LS11, SN74S11
TRIPLE 3-INPUT POSITIVE-AND GATES

SDLS131 – APRIL 1985 – REVISED MARCH 1988

- Package Options Include Plastic "Small Outline" Packages, Ceramic Chip Carriers and Flat Packages, and Plastic and Ceramic DIPs
- Dependable Texas Instruments Quality and Reliability

description

These devices contain three independent 3-input AND gates.

The SN54LS11 and SN54S11 are characterized for operation over the full military temperature range of −55°C to 125°C. The SN74LS11 and SN74S11 are characterized for operation from 0°C to 70°C.

FUNCTION TABLE (each gate)

INPUTS			OUTPUT
A	B	C	Y
H	H	H	H
L	X	X	L
X	L	X	L
X	X	L	L

logic symbol†

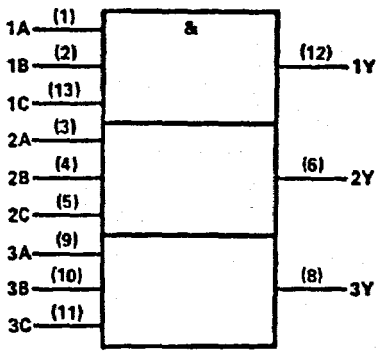

†This symbol is in accordance with ANSI/IEEE Std. 91-1984 and IEC Publication 617-12.
Pin numbers shown are for D, J, N, and W packages.

SN54LS11, SN74S11 . . . J OR W PACKAGE
SN74LS11, SN74S11 . . . D OR N PACKAGE
(TOP VIEW)

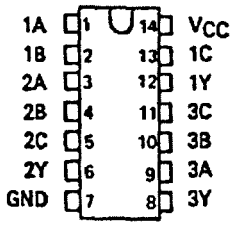

SN54LS11, SN54S11 . . . FK PACKAGE
(TOP VIEW)

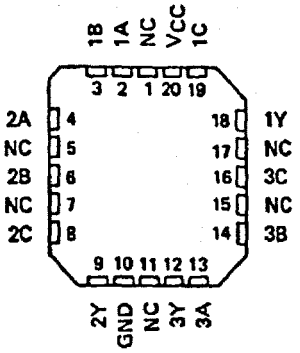

NC—No internal connection

logic diagram (positive logic)

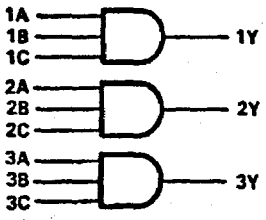

$Y = A \cdot B \cdot C$ or

$Y = \overline{\overline{A} + \overline{B} + \overline{C}}$

TEXAS INSTRUMENTS
POST OFFICE BOX 655303 • DALLAS, TEXAS 75265

SDLS100

SN5432, SN54LS32, SN54S32, SN7432, SN74LS32, SN74S32
QUADRUPLE 2-INPUT POSITIVE-OR GATES

DECEMBER 1983 – REVISED MARCH 1988

- **Package Options Include Plastic "Small Outline" Packages, Ceramic Chip Carriers and Flat Packages, and Plastic and Ceramic DIPs**
- **Dependable Texas Instruments Quality and Reliability**

description

These devices contain four independent 2-input OR gates.

The SN5432, SN54LS32 and SN54S32 are characterized for operation over the full military range of −55°C to 125°C. The SN7432, SN74LS32 and SN74S32 are characterized for operation from 0°C to 70°C.

FUNCTION TABLE (each gate)

INPUTS		OUTPUT
A	B	Y
H	X	H
X	H	H
L	L	L

logic symbol†

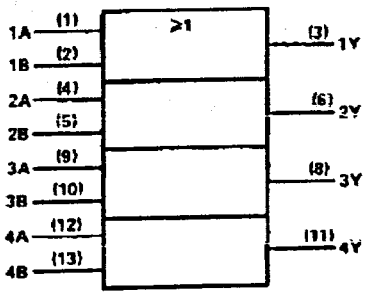

† This symbol is in accordance with ANSI/IEEE Std 91-1984 and IEC Publication 617-12.
Pin numbers shown are for D, J, N, or W packages.

SN5432, SN54LS32, SN54S32 . . . J OR W PACKAGE
SN7432 . . . N PACKAGE
SN74LS32, SN74S32 . . . D OR N PACKAGE
(TOP VIEW)

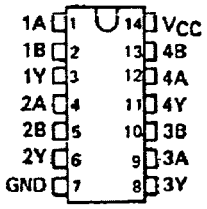

SN54LS32, SN54S32 . . . FK PACKAGE
(TOP VIEW)

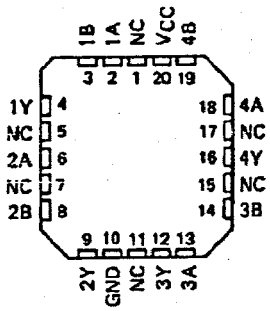

NC – No internal connection

logic diagram

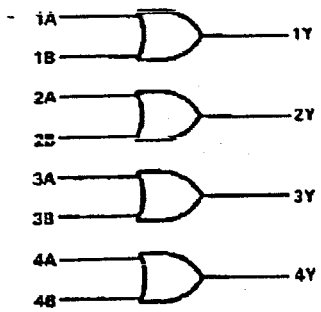

positive logic

$Y = A + B$ or $Y = \overline{\overline{A} \cdot \overline{B}}$

TEXAS INSTRUMENTS
POST OFFICE BOX 655012 • DALLAS, TEXAS 75265

NE555, SA555, SE555
PRECISION TIMERS

SLFS022E – SEPTEMBER 1973 – REVISED MARCH 2004

- Timing From Microseconds to Hours
- Astable or Monostable Operation
- Adjustable Duty Cycle
- TTL-Compatible Output Can Sink or Source Up To 200 mA

NE555 . . . D, P, PS, OR PW PACKAGE
SA555 . . . D OR P PACKAGE
SE555 . . . D, JG, OR P PACKAGE
(TOP VIEW)

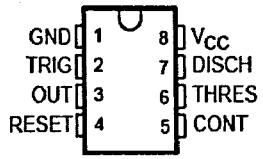

SE555 . . . FK PACKAGE
(TOP VIEW)

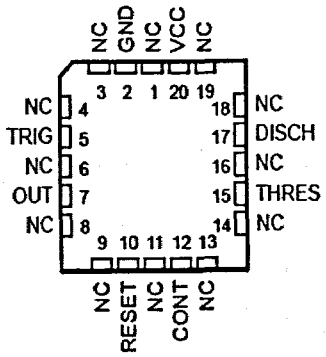

NC – No internal connection

description/ordering information

These devices are precision timing circuits capable of producing accurate time delays or oscillation. In the time-delay or monostable mode of operation, the timed interval is controlled by a single external resistor and capacitor network. In the astable mode of operation, the frequency and duty cycle can be controlled independently with two external resistors and a single external capacitor.

The threshold and trigger levels normally are two-thirds and one-third, respectively, of V_{CC}. These levels can be altered by use of the control-voltage terminal. When the trigger input falls below the trigger level, the flip-flop is set and the output goes high. If the trigger input is above the trigger level and the threshold input is above the threshold level, the flip-flop is reset and the output is low. The reset (RESET) input can override all other inputs and can be used to initiate a new timing cycle. When RESET goes low, the flip-flop is reset and the output goes low. When the output is low, a low-impedance path is provided between discharge (DISCH) and ground.

The output circuit is capable of sinking or sourcing current up to 200 mA. Operation is specified for supplies of 5 V to 15 V. With a 5-V supply, output levels are compatible with TTL inputs.

TEXAS INSTRUMENTS
POST OFFICE BOX 655303 • DALLAS, TEXAS 75265

SN5474, SN54LS74A, SN54S74
SN7474, SN74LS74A, SN74S74
DUAL D-TYPE POSITIVE-EDGE-TRIGGERED FLIP-FLOPS WITH PRESET AND CLEAR

SDLS119 – DECEMBER 1983 – REVISED MARCH 1988

- **Package Options Include Plastic "Small Outline" Packages, Ceramic Chip Carriers and Flat Packages, and Plastic and Ceramic DIPs**
- **Dependable Texas Instruments Quality and Reliability**

description

These devices contain two independent D-type positive-edge-triggered flip-flops. A low level at the preset or clear inputs sets or resets the outputs regardless of the levels of the other inputs. When preset and clear are inactive (high), data at the D input meeting the setup time requirements are transferred to the outputs on the positive-going edge of the clock pulse. Clock triggering occurs at a voltage level and is not directly related to the rise time of the clock pulse. Following the hold time interval, data at the D input may be changed without affecting the levels at the outputs.

The SN54' family is characterized for operation over the full military temperature range of −55°C to 125°C. The SN74' family is characterized for operation from 0°C to 70°C.

FUNCTION TABLE

INPUTS				OUTPUTS	
$\overline{PRE}$	$\overline{CLR}$	CLK	D	Q	$\overline{Q}$
L	H	X	X	H	L
H	L	X	X	L	H
L	L	X	X	H†	H†
H	H	↑	H	H	L
H	H	↑	L	L	H
H	H	L	X	Q_0	$\overline{Q}_0$

† The output levels in this configuration are not guaranteed to meet the minimum levels in V_{OH} if the lows at preset and clear are near V_{IL} maximum. Furthermore, this configuration is nonstable; that is, it will not persist when either preset or clear returns to its inactive (high) level.

SN5474 . . . J PACKAGE
SN54LS74A, SN54S74 . . . J OR W PACKAGE
SN7474 . . . N PACKAGE
SN74LS74A, SN74S74 . . . D OR N PACKAGE
(TOP VIEW)

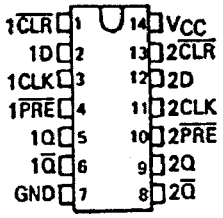

SN5474 . . . W PACKAGE
(TOP VIEW)

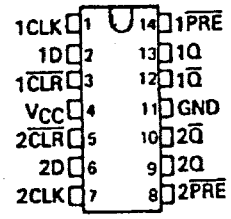

SN54LS74A, SN54S74 . . . FK PACKAGE
(TOP VIEW)

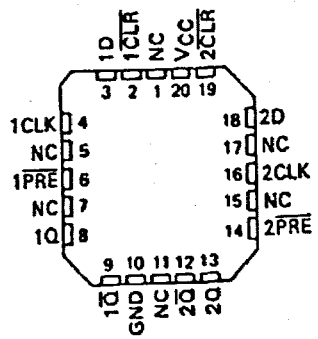

NC - No internal connection

logic symbol‡

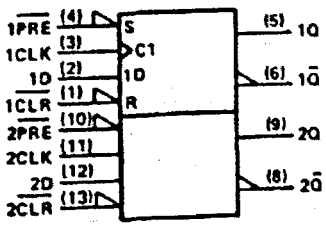

‡This symbol is in accordance with ANSI/IEEE Std 91-1984 and IEC Publication 617-12.
Pin numbers shown are for D, J, N, and W packages.

logic diagram (positive logic)

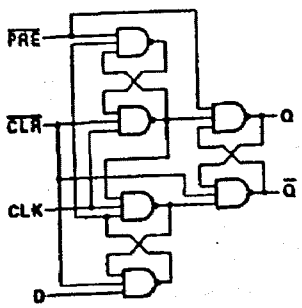

TEXAS INSTRUMENTS
POST OFFICE BOX 655303 • DALLAS, TEXAS 75265

SDLS055

SN54153, SN54LS153, SN54S153
SN74153, SN74LS153, SN74S153
DUAL 4-LINE TO 1-LINE DATA SELECTORS/MULTIPLEXERS

DECEMBER 1972 – REVISED MARCH 1988

- Permits Multiplexing from N lines to 1 line
- Performs Parallel-to-Serial Conversion
- Strobe (Enable) Line Provided for Cascading (N lines to n lines)
- High-Fan-Out, Low-Impedance, Totem-Pole Outputs
- Fully Compatible with most TTL Circuits

TYPE	TYPICAL AVERAGE PROPAGATION DELAY TIMES FROM DATA	FROM STROBE	FROM SELECT	TYPICAL POWER DISSIPATION
'153	14 ns	17 ns	22 ns	180 mW
'LS153	14 ns	19 ns	22 ns	31 mW
'S153	6 ns	9.5 ns	12 ns	225 mW

SN54153, SN54LS153, SN54S153 . . . J OR W PACKAGE
SN74153 . . . N PACKAGE
SN74LS153, SN74S153 . . . D OR N PACKAGE
(TOP VIEW)

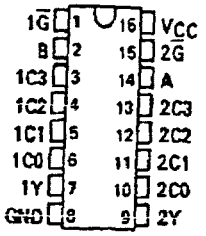

SN54LS153, SN54S153 . . . FK PACKAGE
(TOP VIEW)

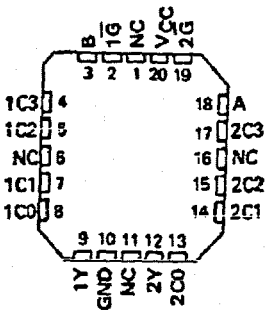

NC – No internal connection

description

Each of these monolithic, data selectors/multiplexers contains inverters and drivers to supply fully complementary, on-chip, binary decoding data selection to the AND-OR gates. Separate strobe inputs are provided for each of the two four-line sections.

FUNCTION TABLE

SELECT INPUTS		DATA INPUTS				STROBE	OUTPUT
B	A	C0	C1	C2	C3	$\overline{G}$	Y
X	X	X	X	X	X	H	L
L	L	L	X	X	X	L	L
L	L	H	X	X	X	L	H
L	H	X	L	X	X	L	L
L	H	X	H	X	X	L	H
H	L	X	X	L	X	L	L
H	L	X	X	H	X	L	H
H	H	X	X	X	L	L	L
H	H	X	X	X	H	L	H

Select inputs A and B are common to both sections.
H = high level, L = low level, X = irrelevant

absolute maximum ratings over operating free-air temperature range (unless otherwise noted)

Supply voltage, V_{CC} (See Note 1) . . . . . 7 V
Input voltage: '153, 'S153 . . . . . 5.5 V
'LS153 . . . . . 7 V
Operating free-air temperature range: SN54' . . . . . −55°C to 125°C
SN74' . . . . . 0°C to 70°C
Storage temperature range . . . . . −65°C to 150°C

NOTE 1: Voltage values are with respect to network ground terminal.

TEXAS INSTRUMENTS
POST OFFICE BOX 655012 • DALLAS, TEXAS 75265

APPENDIX E
COMPARISON OF MODEL PERFORMANCE WITH ELECTRONIC CIRCUIT SIMULATION SOFTWARES

The comparison of the model performance of the power electronic converters and electric drives presented in this thesis is made here with an Electronic and Electric Drive Circuit Simulation software PSIM [5]. The PSIM 7.0 demo version is used for this comparison. The model comparison is made for selected ac to dc, dc to ac, dc to dc, ac to ac and three phase IM using PSIM 7.0 demo version. For Six Step Inverter fed PMSM only, model comparison is made using the three phase MOSFET inverter and PMSM module in the SimPowerSystem Block set of SIMULINK. Similarly for three phase three level inverters, model comparison is made with MICROCAP 8 software. These are due to node and component limitations in the demo version of PSIM 7.0

AC to DC Converters:

The single phase FWDBR discussed in Section 3.2 of Chapter 3 is verified using PSIM 7.0 demo version. The RLE load with parameters shown in Table 3.1 section 3.2.1 is used for simulation. The PSIM simulation diagram is shown in Fig.E.1. The simulation results are shown in Fig.E.2.

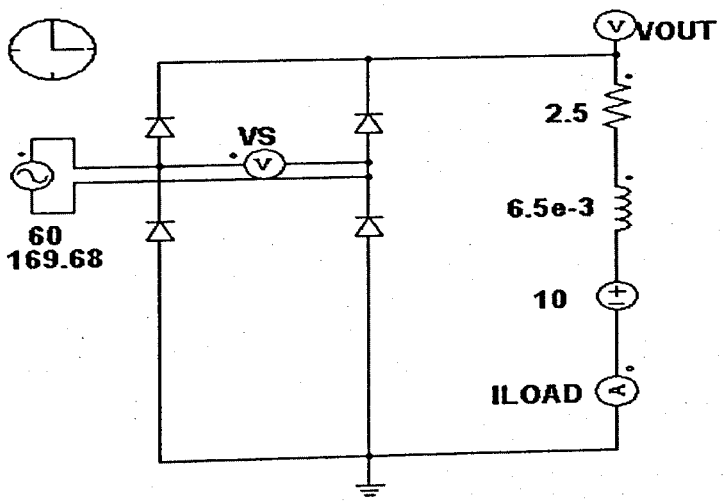

FIG.E.1: SINGLE PHASE FULL WAVE DIODE BRIDGE RECTIFIER

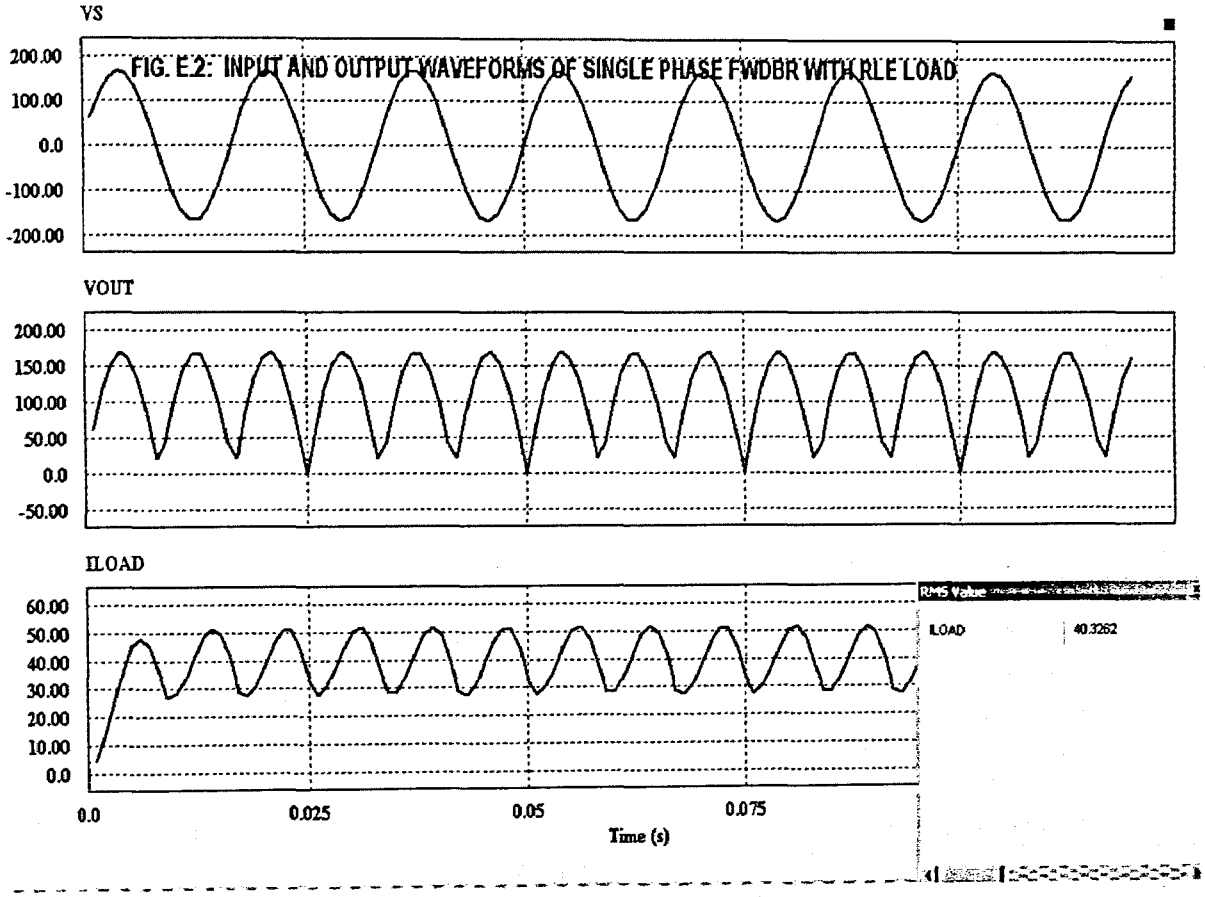

FIG. E.2: INPUT AND OUTPUT WAVEFORMS OF SINGLE PHASE FWDBR WITH RLE LOAD

As can be seen from the display of Fig.E.2, it is seen that the rms value of load current is 40.3262 amperes. The results agree with Table 3.2 and Fig.3.6 (A), (B) and (C) of section 3.2.2.

The single phase Full wave SCR Bridge using PSIM 7.0 is shown in Fig.E.3 for an RLE load, as given in Table 3.3 of section 3.3.1. The simulation results are shown in

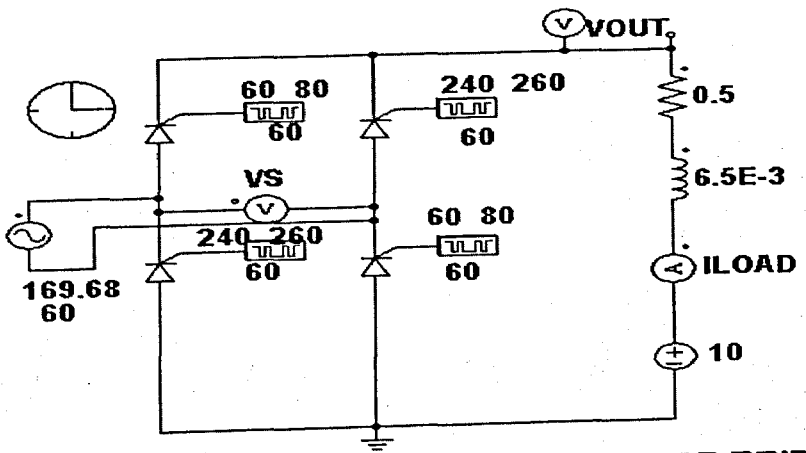

FIG.E.3: SINGLE PHASE FULL WAVE SCR BRIDGE

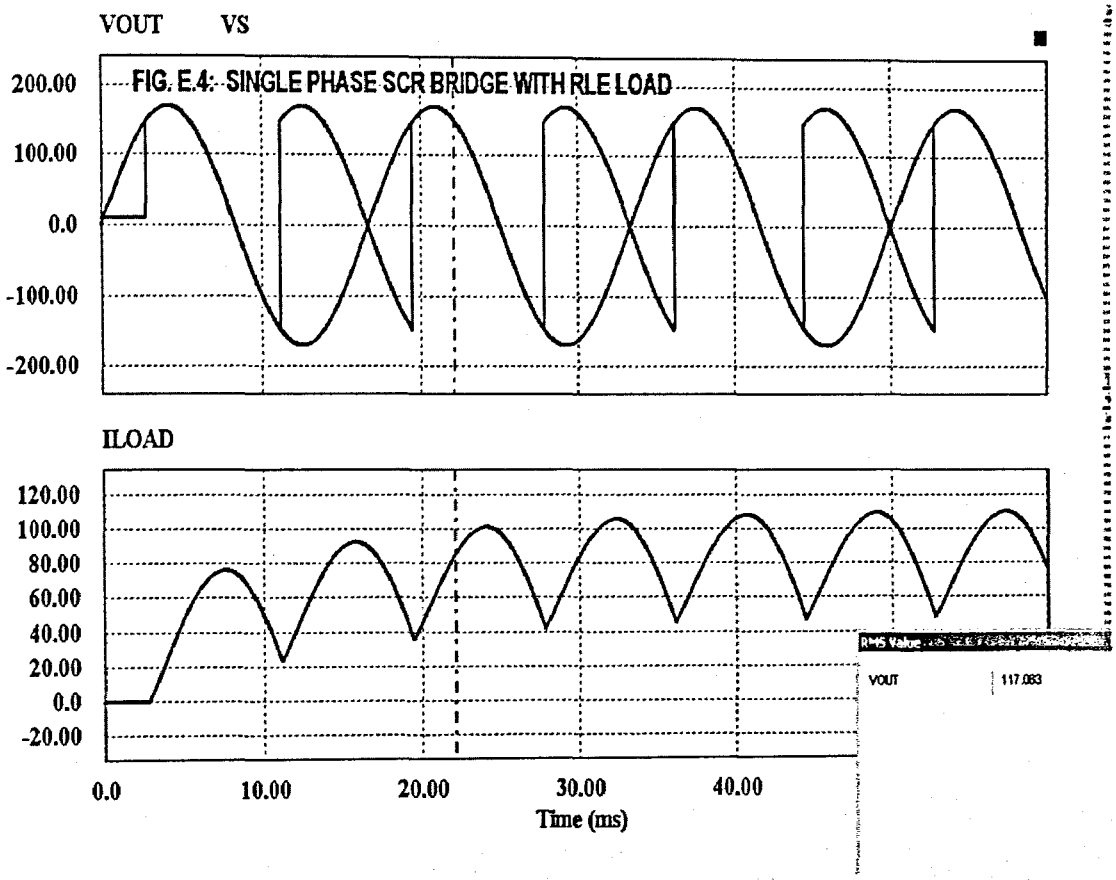

Fig.E.4.for a firing angle α of π /3 radians. The displayed value of r.m.s. dc output voltage is 117.083 volts, which closely agree with the value in Table 3.4 of Section 3.3.2. The wave forms in Fig.E.4 agree with the Fig.3.12(A), (B) and (C) of Section 3.3.2.

The three phase FWDBR simulation using PSIM 7.0 demo version is shown in Fig.E.5. The data for a purely resistive load, shown in Table 3.4 of section 3.4.2 are used. The simulation results are shown in Fig.E.6. The average load current displayed is 23.4782.

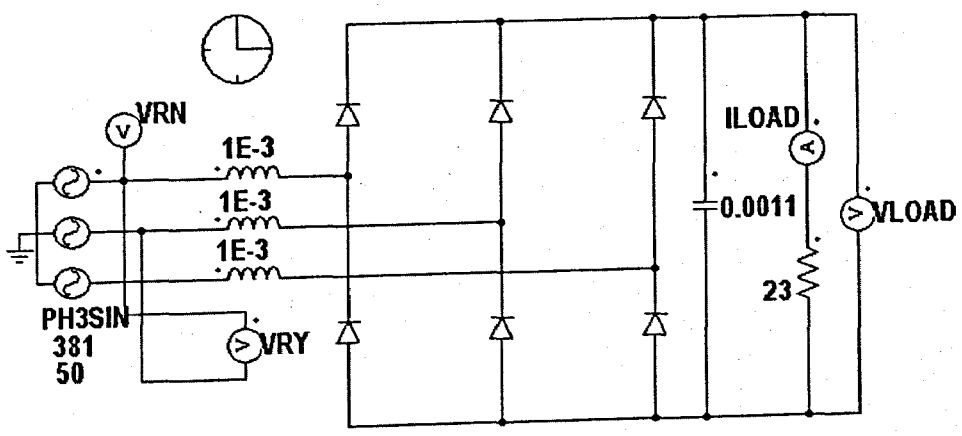

FIG. E.5: THREE PHASE FULL WAVE DIODE BRIDGE RECTIFIER

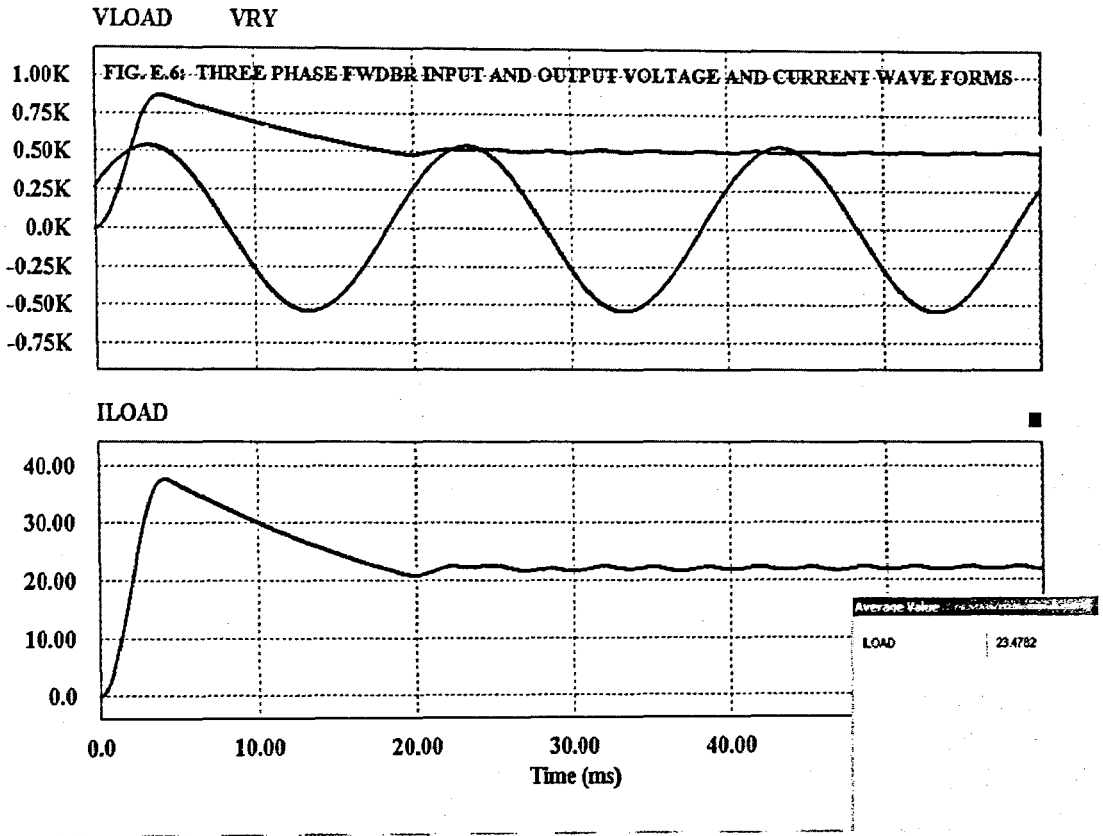

amperes, which closely agree with the corresponding value shown in Table 3.5 of Section 3.4.2. The simulation results in Fig.E.6 also agree with one shown in Fig.3.19 (A), (B) and (C) of Section 3.4.2.

DC to AC Converters:

The models of Six Step 180 Degree Mode and 120 degree Mode inverters shown in Section 4.2.4, Section 4.3.4 and section 4.3.6 of Chapter 4 are compared by simulation using PSIM 7.0 demo version.

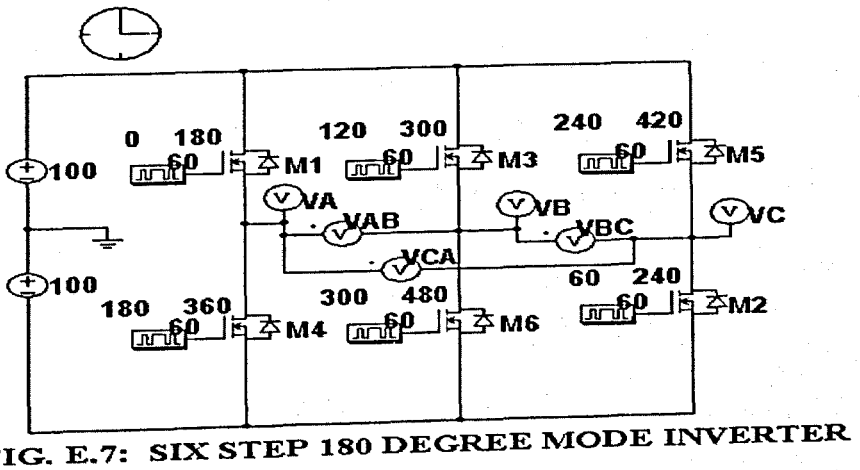

FIG. E.7: SIX STEP 180 DEGREE MODE INVERTER

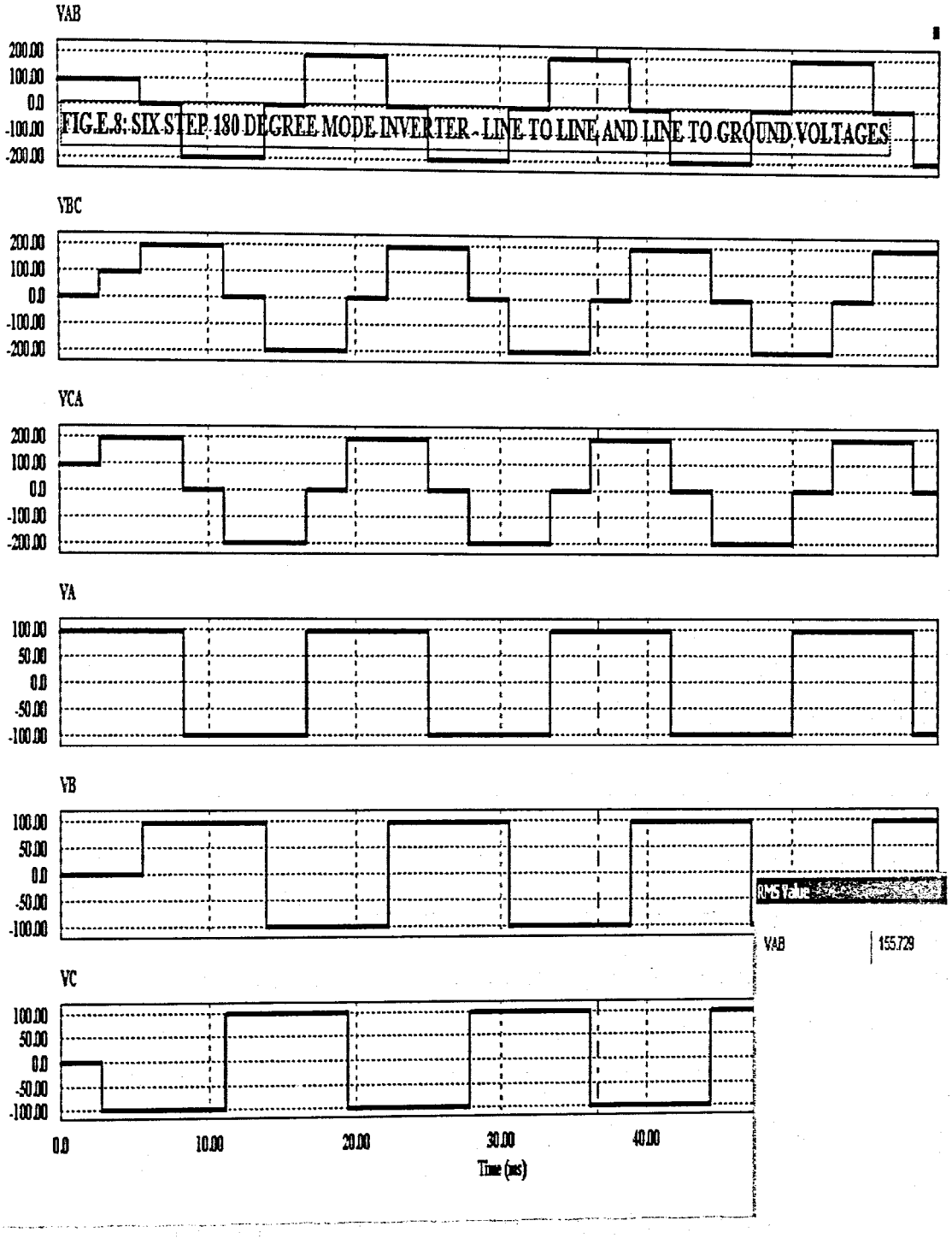

FIG.E.8: SIX STEP 180 DEGREE MODE INVERTER - LINE TO LINE AND LINE TO GROUND VOLTAGES

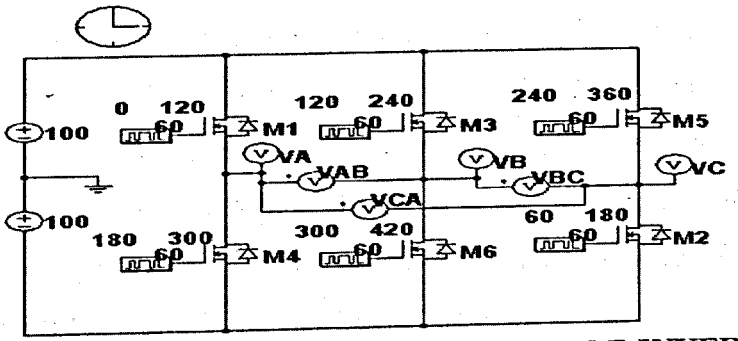

FIG.E.9: SIX STEP 120 DEGREE MODE INVERTER

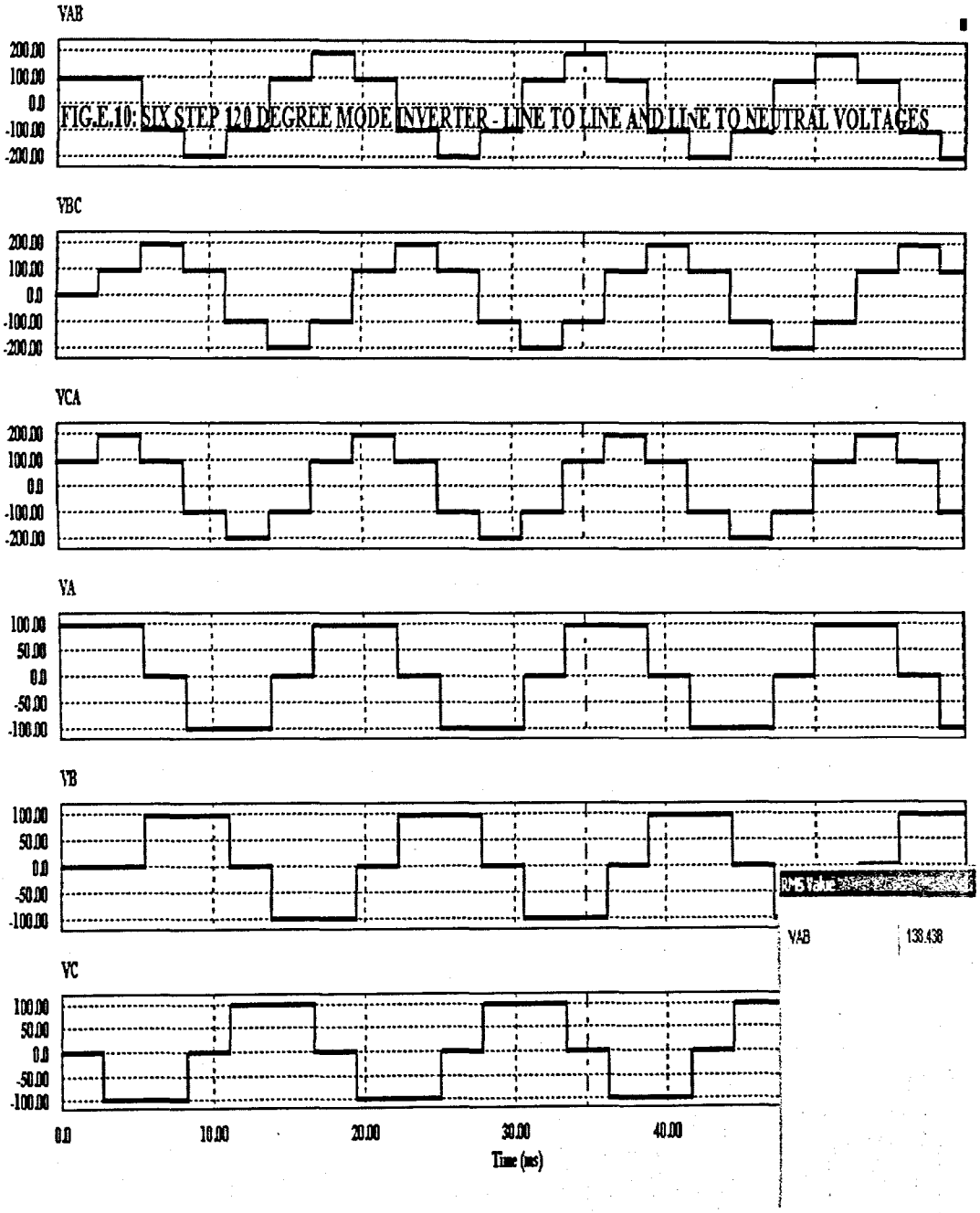

Fig.E.7 and E.9 shows the PSIM schematics for the Six Step 180 degree mode and the 120 degree mode inverter. The simulation results for the six step 180 degree mode inverter is shown in Fig.E.8 and that for the 120 degree mode inverter is shown in Fig.E.10. The r.m.s. value of the line to line voltage for the former is 155.729 Volts and that for the later is 138.438 Volts. The results agree with Table 4.1 of section 4.2.5 for the former and Table 4.3 of section 4.3.5.for the later. The simulation results in Fig.E.8 well agree with Fig.4.6(A) and (B) for three phase 180 degree mode inverter the results in Fig.E.10 agree with Fig.4.11(A) and (B) of Chapter 4.

DC to DC Converters:

The model for the Buck converter shown in Section 5.2.1 of Chapter 5 is compared with that by using PSIM7.0 demo version as shown in Fig.E.11.

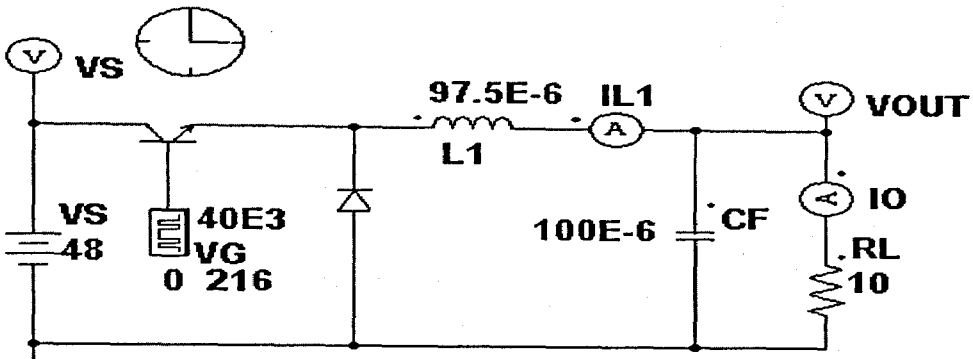

FIG.E.11: BUCK CONVERTER

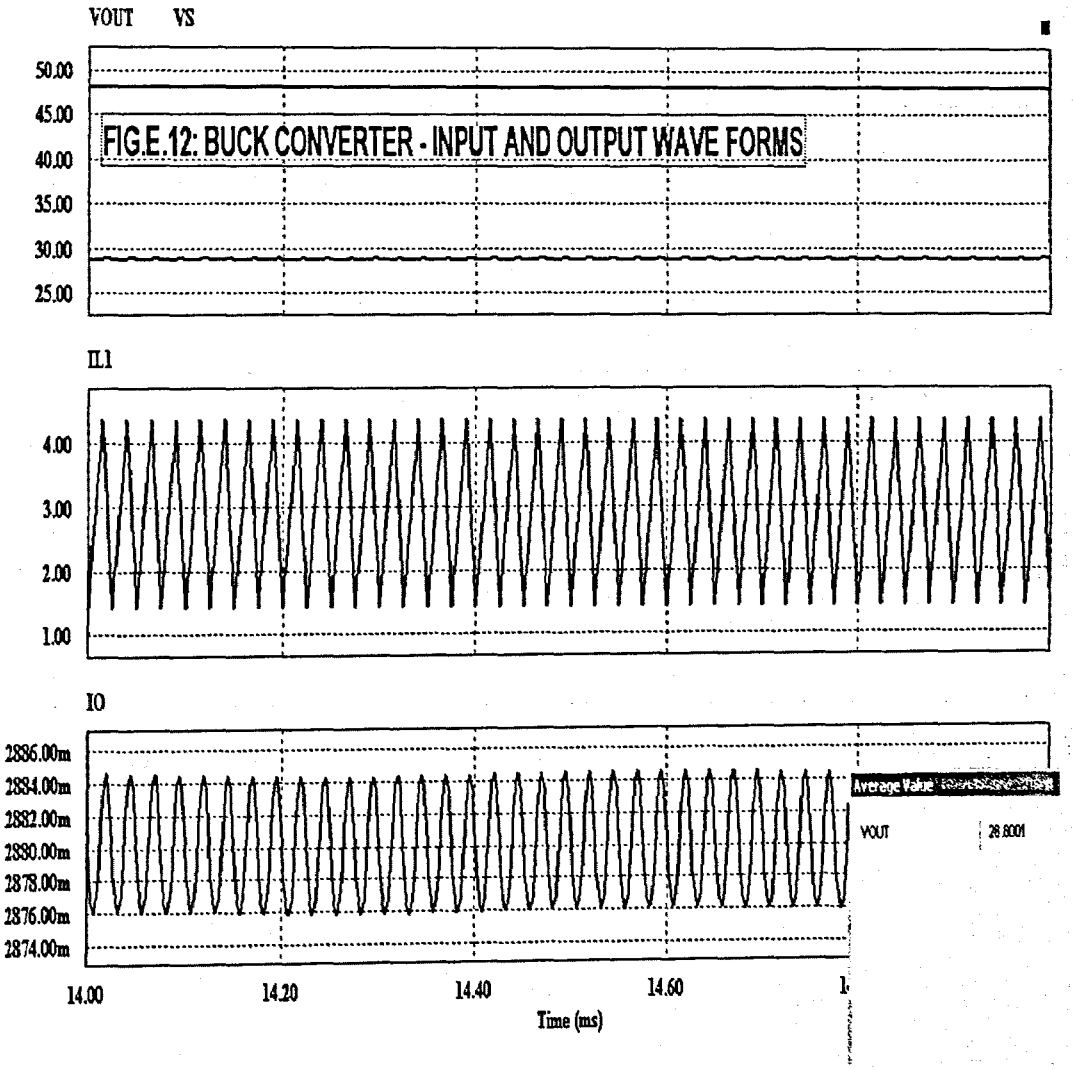

FIG.E.12: BUCK CONVERTER - INPUT AND OUTPUT WAVE FORMS

The data is from Table 5.1 of Section 5.2.2. The simulation results for Vout, IL1, Io and the displayed output voltage of 28.8001 Volts in Fig.E.12 well agree with the Table 5.2 and Fig.5.6(A) to (D) in Section 5.2.2.

The model for the Boost converter shown in Section 5.3.1 of Chapter 5 is compared with that by using PSIM7.0 demo version as shown in Fig.E.13. The data are from

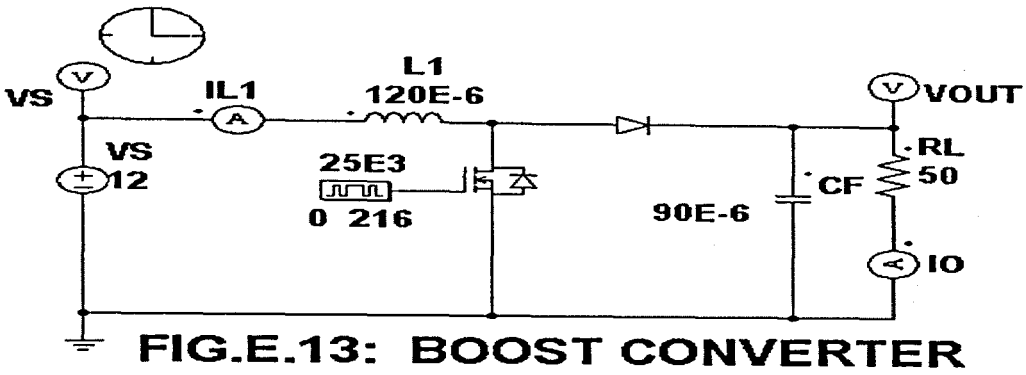

FIG.E.13: BOOST CONVERTER

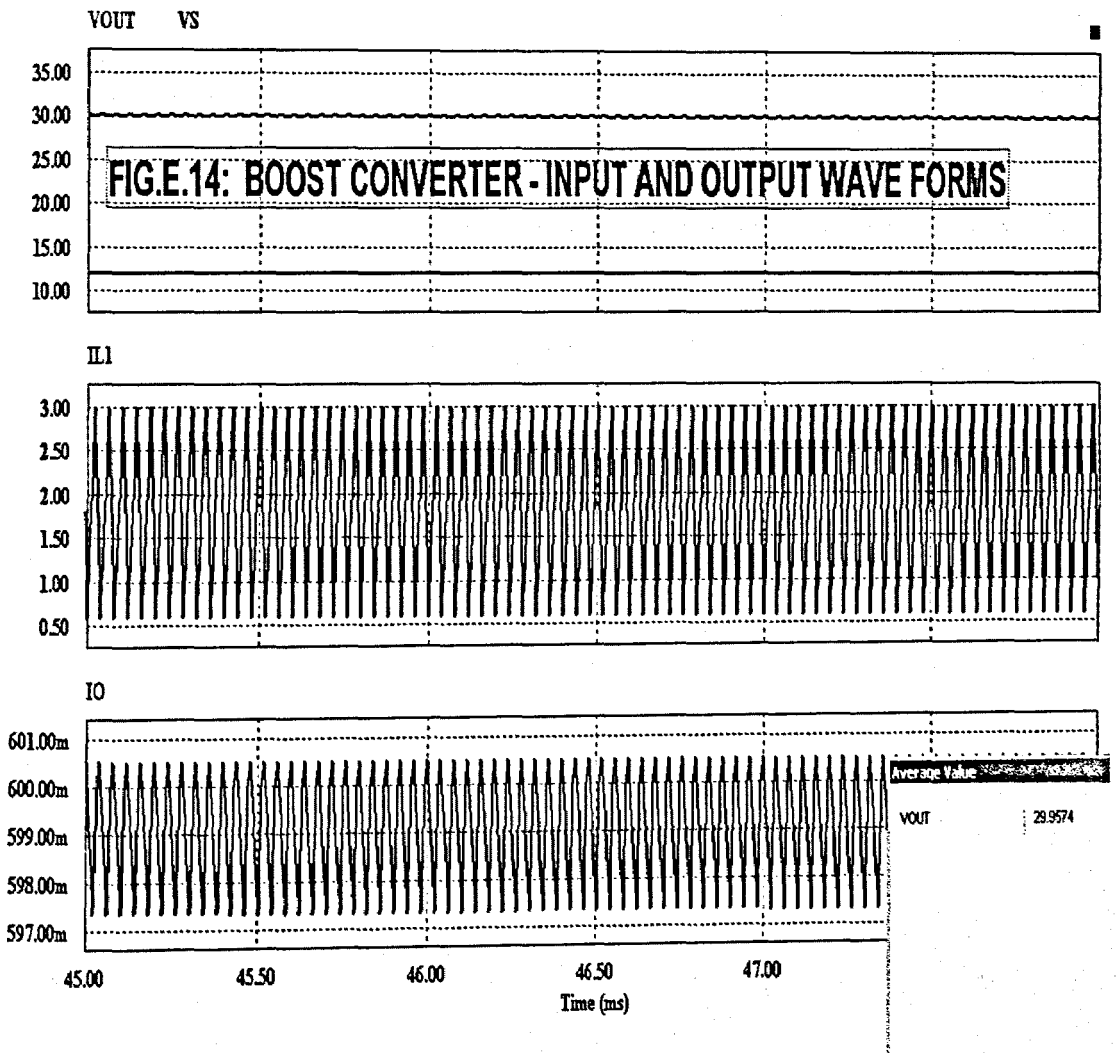

FIG.E.14: BOOST CONVERTER - INPUT AND OUTPUT WAVE FORMS

Table 5.4 of Section 5.3.2. The simulation results for Vout, IL1, Io and the displayed output voltage of 29.9574 Volts in Fig.E.14 well agree with the Table 5.5 and Fig.5.12(A) to (D) in Section 5.3.2.

The model for the Buck-Boost converter shown in Section 5.4.1 of Chapter 5 is compared with that by using PSIM7.0 demo version as shown in Fig.E.15 and Fig.E.17.

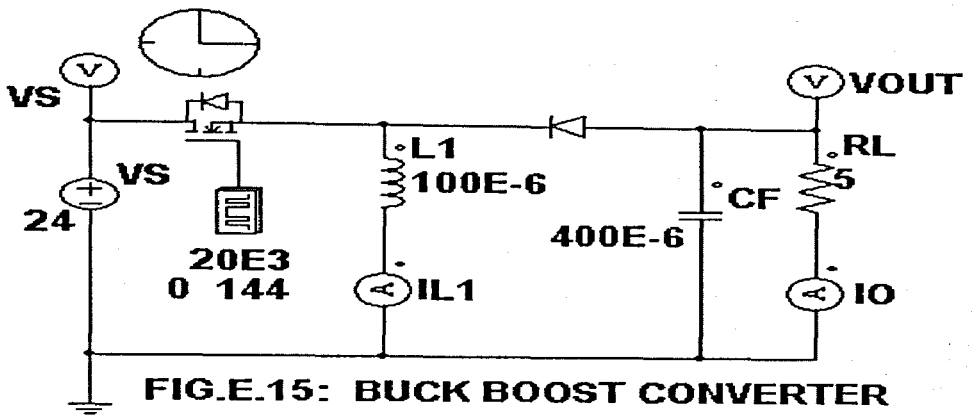

FIG.E.15: BUCK BOOST CONVERTER

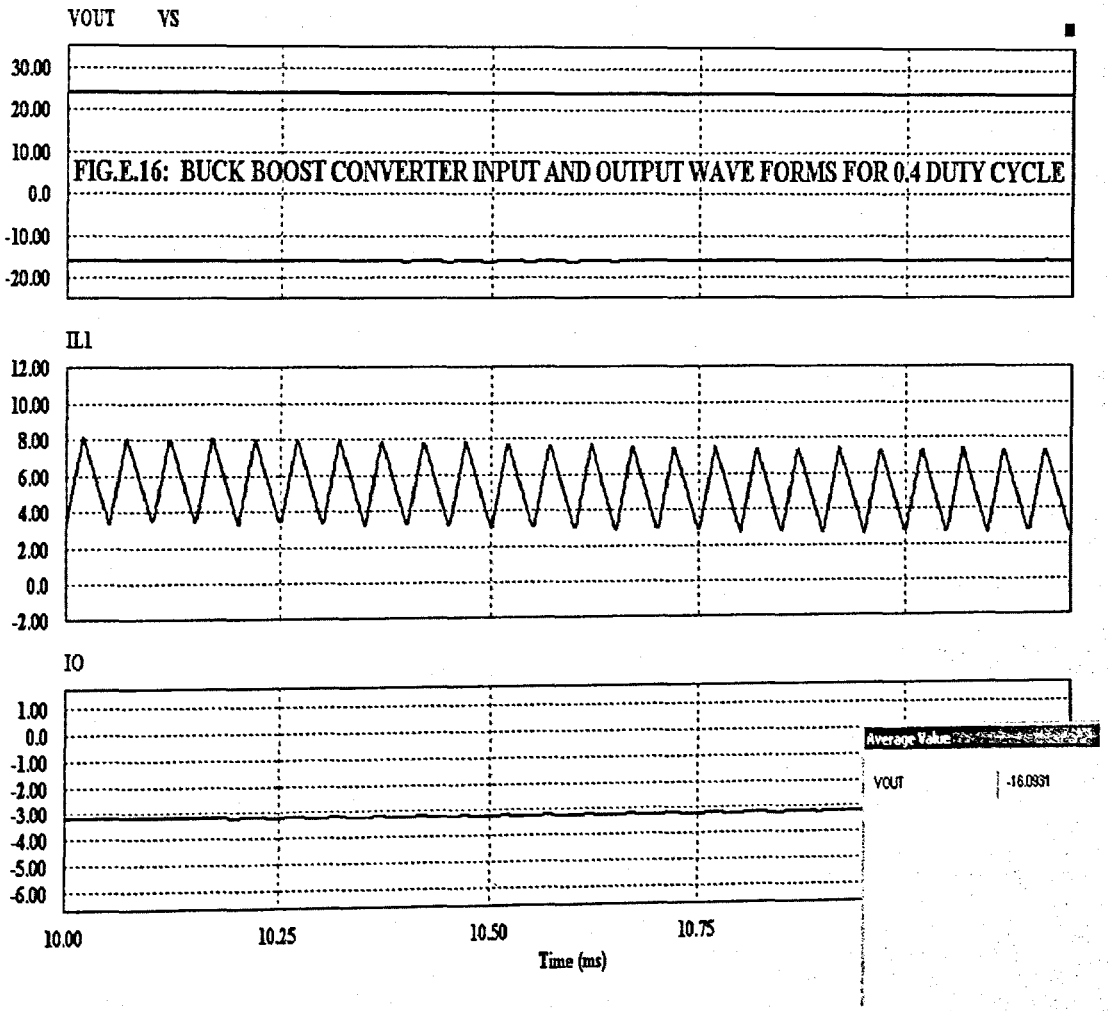

FIG.E.16: BUCK BOOST CONVERTER INPUT AND OUTPUT WAVE FORMS FOR 0.4 DUTY CYCLE

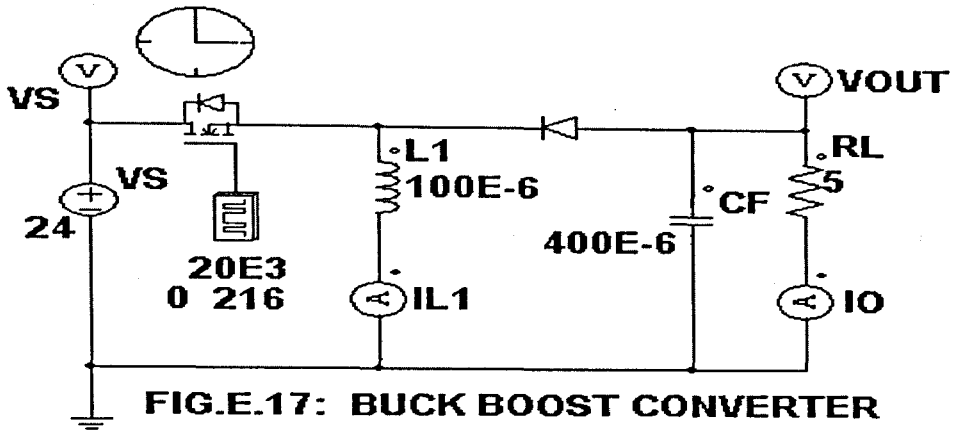

FIG.E.17: BUCK BOOST CONVERTER

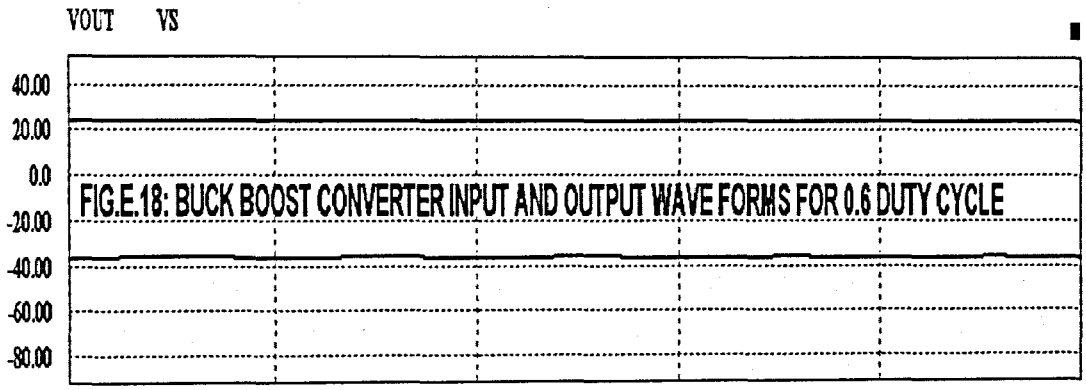

FIG.E.18: BUCK BOOST CONVERTER INPUT AND OUTPUT WAVE FORMS FOR 0.6 DUTY CYCLE

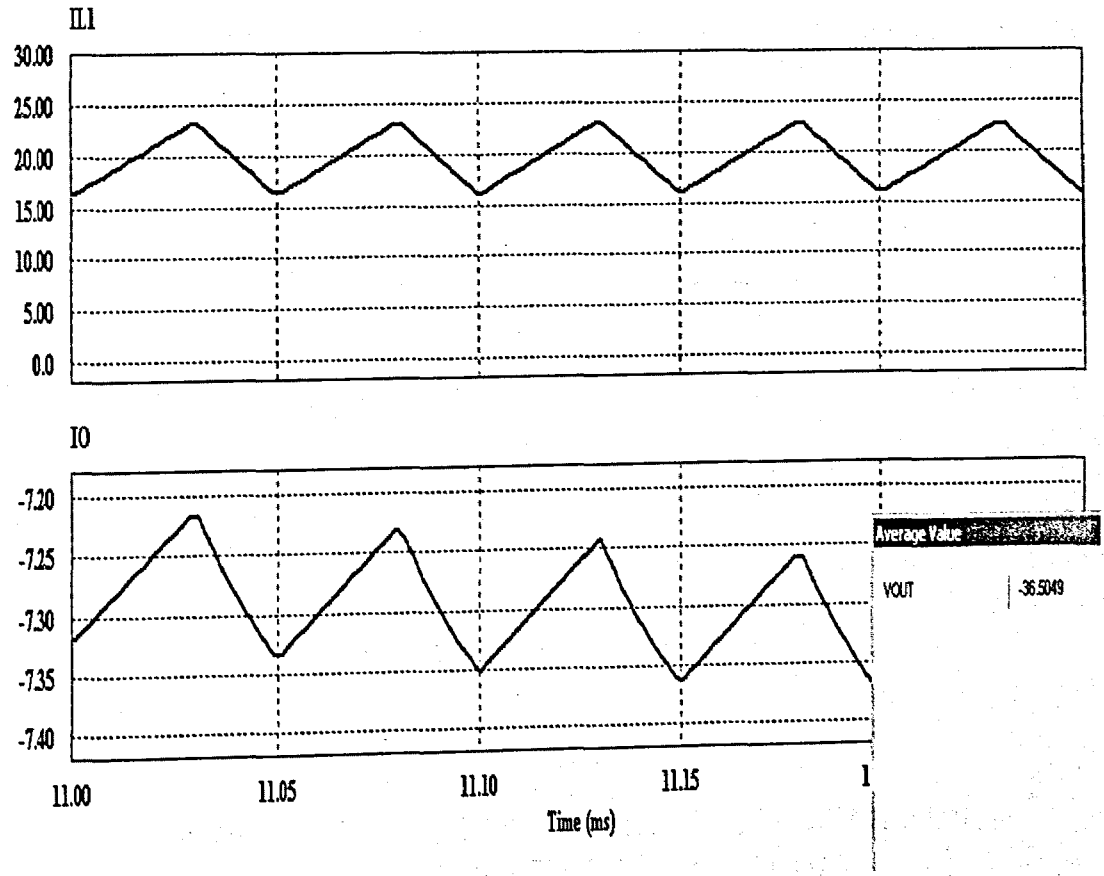

for a duty cycle of 0.4 and 0.6 respectively.

The data is from Table 5.7 of Section 5.4.2. The simulation results for Vout, IL1, Io and the displayed output voltage of -16.0931 Volts for a duty cycle of 0.4 and -36.5049 Volts for a duty cycle of 0.6 in Fig.E.16 and Fig.E.18 well agree with the Table 5.8, Fig.5.18(A) to (D) and Fig.5.19(A) to (D) in Section 5.4.2.

AC to AC Converters:

The three phase ac controller with back to back thyristors in series with the ac lines connected to star connected resistive load with isolated neutral is verified using PSIM 7.0 demo version. The PSIM schematic is shown in Fig.E.19 for a firing angle of 30 degrees.

The data for this three phase ac controller shown in Fig.E.19 are taken from Table 6.1 in Section 6.2.2 of Chapter 6. The simulation results of Fig.E.19 for a firing angle of 30 degrees is shown in Fig.E.20, which agrees with Fig.6.5 in Section 6.2.2.. The r.m.s. line to neutral voltage displayed in Fig.E.20 is 113.399 Volts which closely agrees with the value in Table 6.2 of Section 6.2.2.

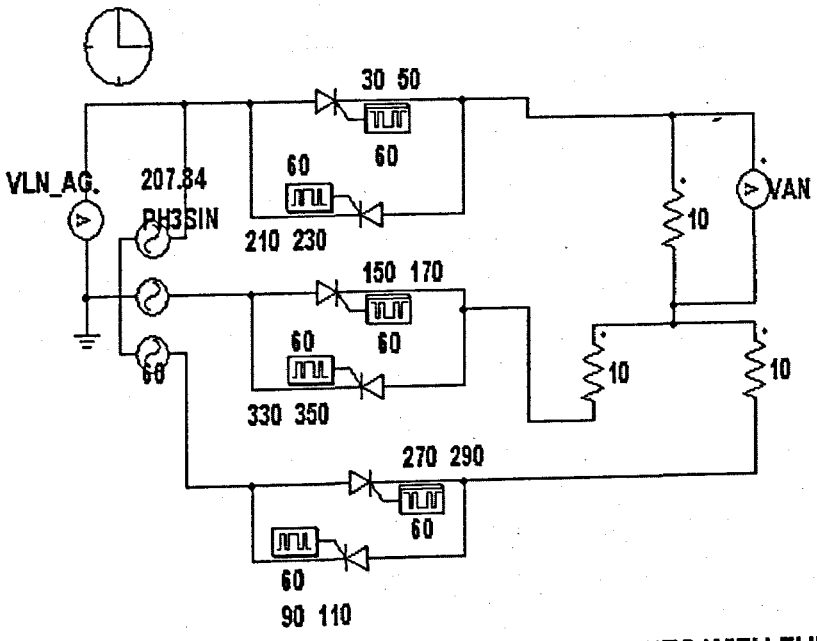

FIG.E.19: THREE PHASE AC CONTROLLER IN SERIES WITH THE LINES WITH STAR CONNECTED RESISTIVE LOAD

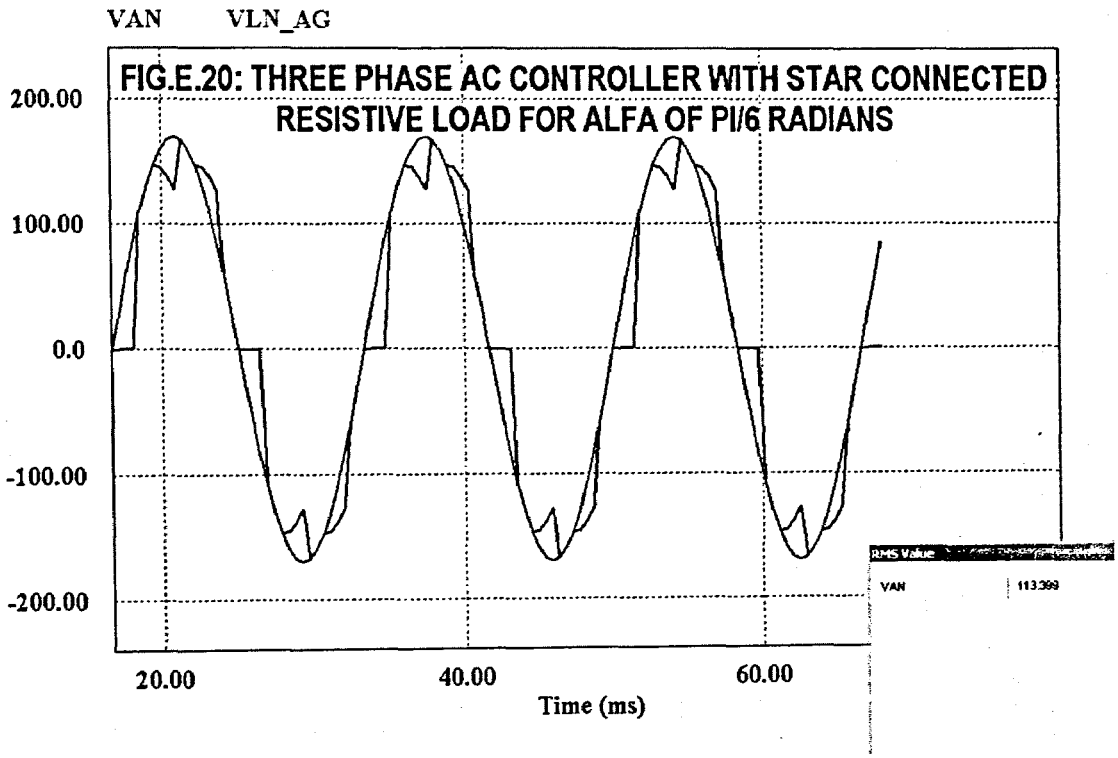

The three phase ac controller with back to back thyristors in series with resistors in delta connected to the ac lines is verified using PSIM 7.0 demo version. The PSIM schematic is shown in Fig.E.21 for a firing angle of 30 degrees.

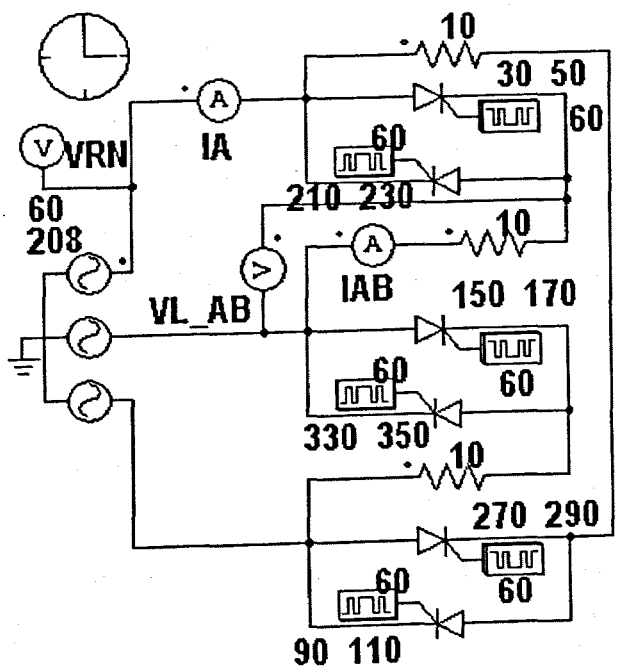

FIG.E.21: THREE PHASE AC CONTROLLER IN SERIES WITH RESISTIVE LOAD IN DELTA

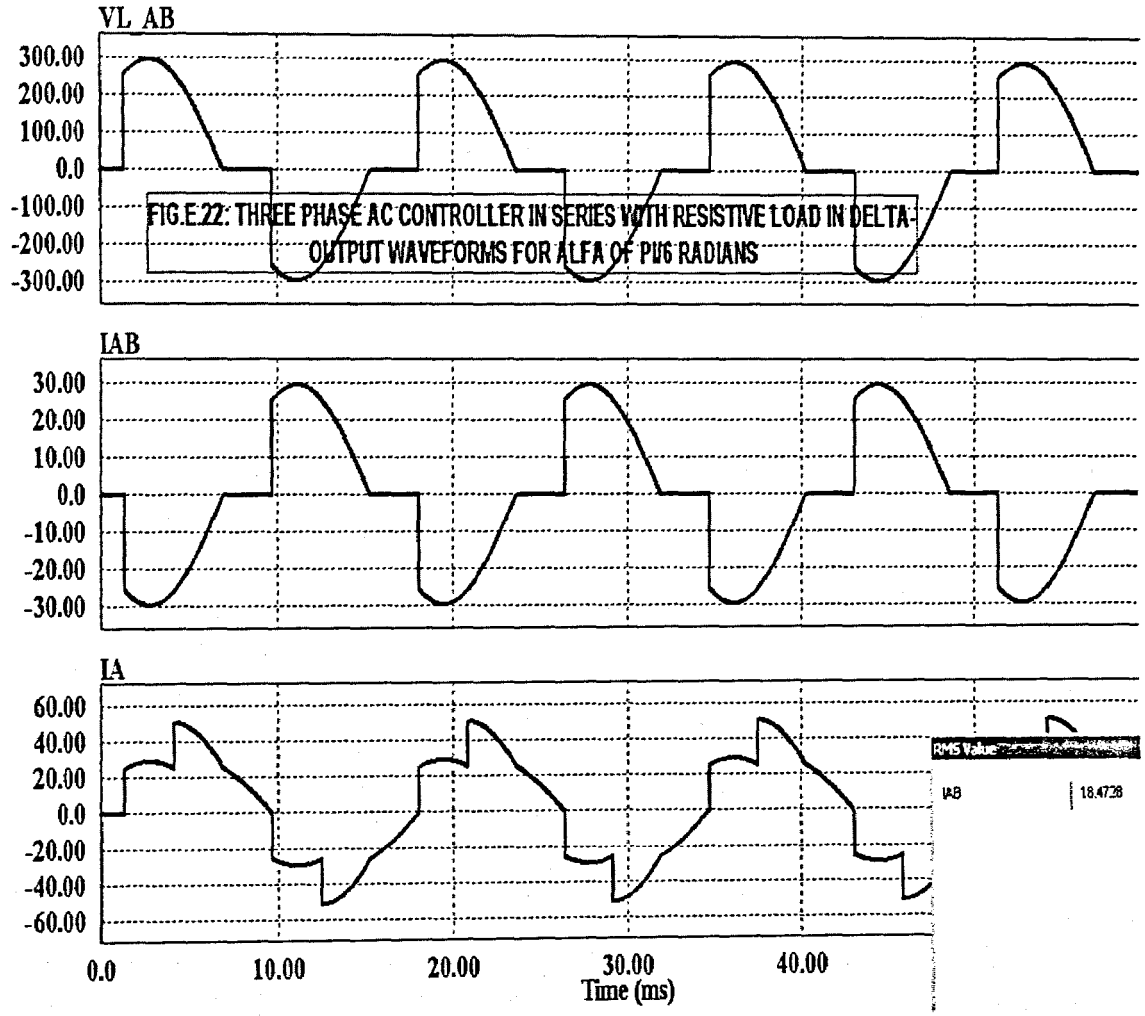

FIG.E.22: THREE PHASE AC CONTROLLER IN SERIES WITH RESISTIVE LOAD IN DELTA-OUTPUT WAVEFORMS FOR ALFA OF PI/6 RADIANS

The data for this three phase ac controller shown in Fig.E.21 are taken from Table 6.4 in Section 6.3.2 of Chapter 6. The simulation results of Fig.E.21 for a firing angle of 30 degrees is shown in Fig.E.22, which agrees with the corresponding waveforms shown in Fig.6.24(A), (B) and (C) in Section 6.3.2. The r.m.s. phase current displayed in Fig.E.22 is 18.4728 Amperes which almost agrees with the value in Table 6.5 of Section 6.3.2.

Three Phase I.M.:

The starting current and torque transients of the three phase IM when directly connected to three phase AC lines are studied using PSIM7.0 demo version. The reference frame is internal to PSIM7.0. The data used for the three phase cage IM is from Table 7.1 in Section 7.4.1 of Chapter 7. The PSIM schematics with the three

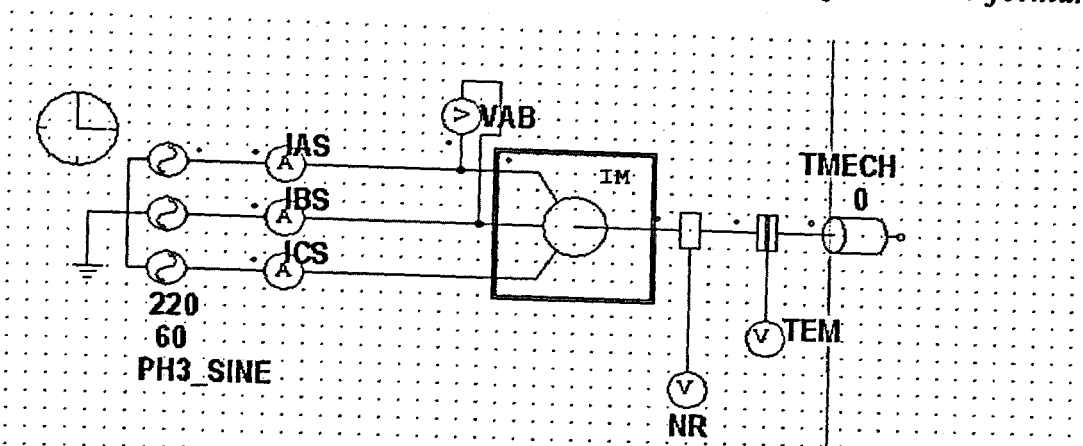

FIG.E.23: THREE PHASE SINE WAVE AC LINE FED INDUCTION MOTOR

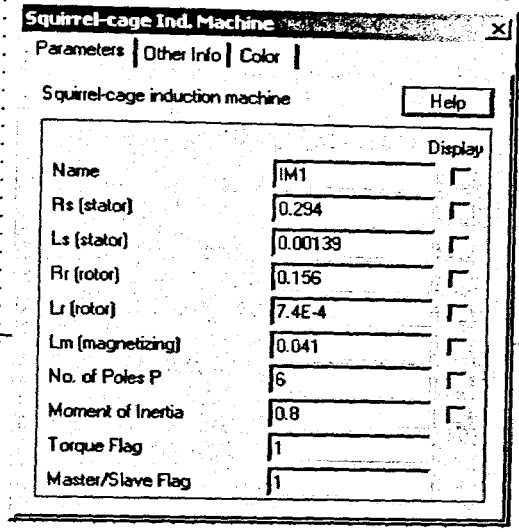

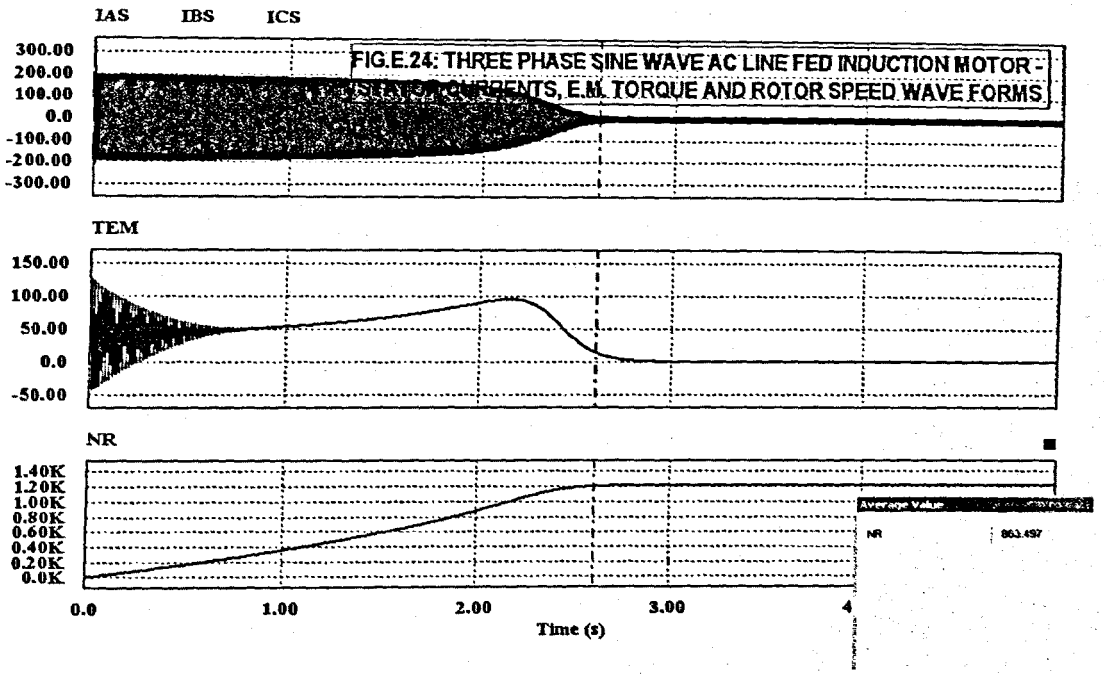

FIG.E.24: THREE PHASE SINE WAVE AC LINE FED INDUCTION MOTOR - STATOR CURRENTS, E.M. TORQUE AND ROTOR SPEED WAVE FORMS

phase IM parameter values entered is shown in Fig.E.23. The starting stator current and e.m.torque transients when directly connected to the three phase ac lines are shown in Fig.E.24, for zero external mechanical load. The peak starting stator current of 200 Amps in Fig.E.24 agrees with the simulation results shown in Fig.7.13(D), 7.14(D), 7.15(D) and 7.16(D) in Section 7.5.1. The speed almost reaches close to 1200 r.p.m. in Fig.E.24 which agrees with Fig.7.13(B), 7.14(B), 7.15(B) and 7.16(B) in Section 7.5.1. The e.m. torque curve in Fig.E.24 agrees only approximately with the simulation results shown in Fig.7.13(A), 7.14(A), 7.15(A) and 7.16(A). in section 7.5.1.

Six Step Inverter fed PMSM Drive:

The six step inverter fed PMSM drive was studied by using the built in model of three phase MOSFET inverter and PMSM in the SimPowerSystems block set of SIMULINK. The is because of the node and component limitations in the demo version of PSIM7.0. The six step 180 degree mode inverter fed PMSM drive discussed in Section 8.3 of Chapter 8 is used for simulation study using SimPowerSystems block set of SIMULINK. The data for the three phase PMSM is given in Table 8.1 of Section 8.3.1.

The simulation diagram using the SimPowerSystems block set of SIMULINK is shown in Fig.E.25(A). The PMSM parameters used are shown in Fig.E.25(B). The three

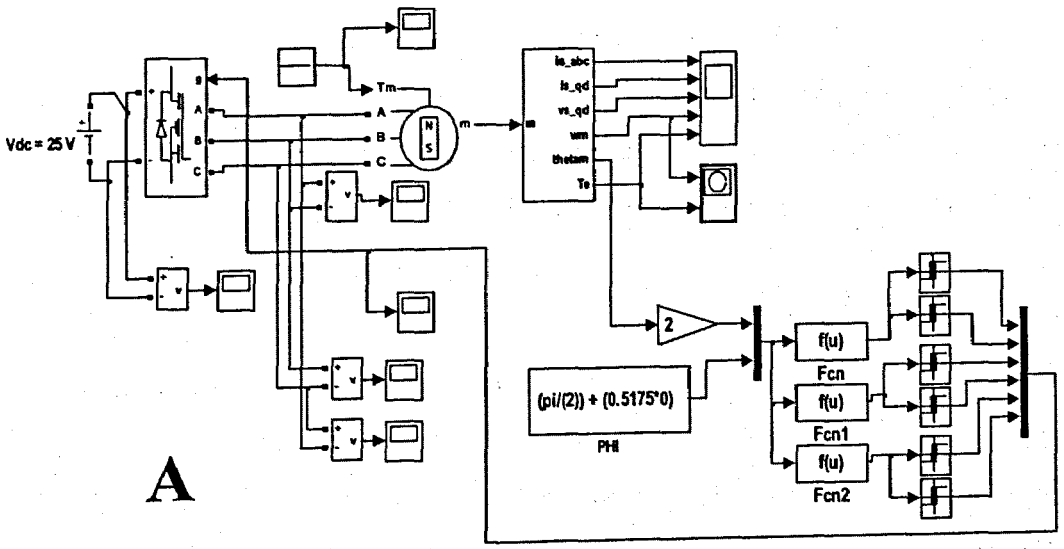

FIG.E.25: SIX STEP 180 DEGREE MODE INVERTER FED PMSM DRIVE

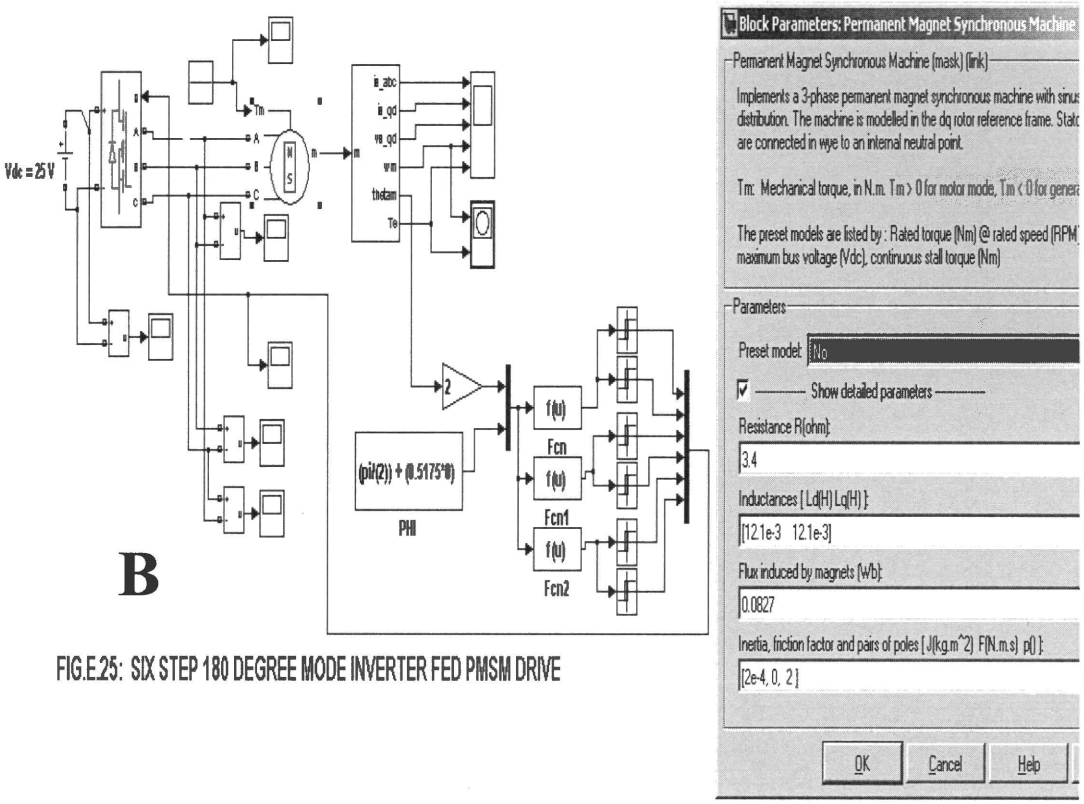

FIG.E.25: SIX STEP 180 DEGREE MODE INVERTER FED PMSM DRIVE

phase 180 degree mode inverter is developed in the same way discussed in Section 8.3 of Chapter 8. In Fig.E.25(B), the Fcn, Fcn1 and Fc2 block generates three phase with a peak value of 10, angular frequency ωre of the rotor with the phase advance phi entered in the block marked PHI, added. Two Relays are connected to each Fcn block. The relay connected to Fcn block at the top output logic 1 during the positive half cycle of the input sine wave and logic 0 during the negative half cycle. Similarly the bottom relay output logic 1 during the negative half cycle of the input sine wave and logic 0 during the positive half cycle. The same principle holds good for the pair of relays connected to Fcn blocks marked Fcn1 and Fcn2. The six gate pulses are given to the gate input of three phase MOSFET inverter through a six input MUX block. The three phase MOSFET block, PMSM block, Measurement block are from the SimPowerSystems block set of SIMULINK.

The simulation was carried out using the ode23tb(stiff/TR-BDF2) solver. The phase advance was made pi/2 radians. The mechanical load was set to 0.19 NW-METERS. The simulation results are shown in Fig.E.26(A), (B), (C) and (D) respectively. Fig.E.26 (A) indicates a maximum rotor speed of around 65 mech.rad per second. Fig.E.26(B) is the e.m.torque-speed curve. Fig.E.26(C) indicates a mechanical load

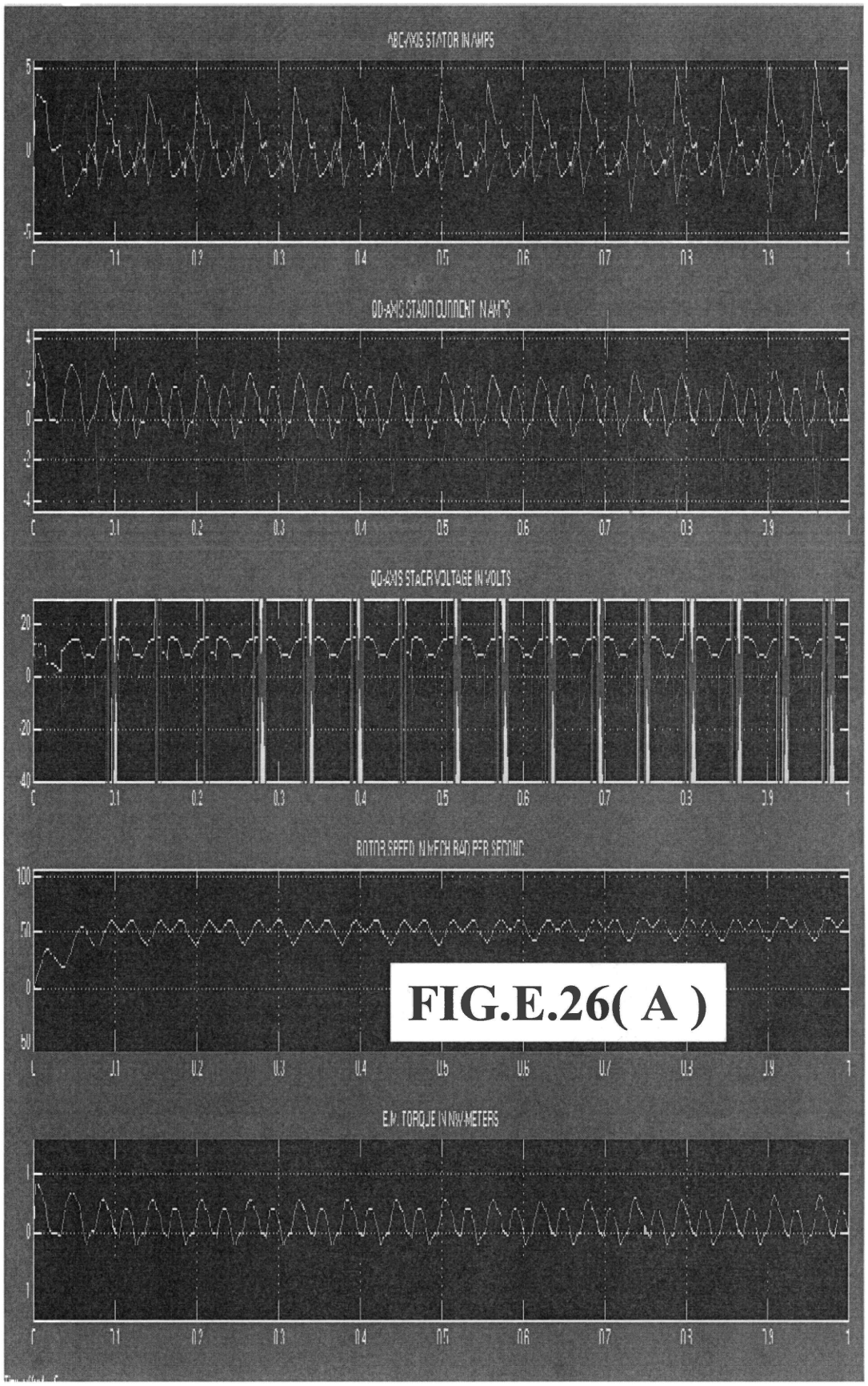
ABC-AXIS STATOR IN AMPS
QD-AXIS STATOR CURRENT IN AMPS
QD-AXIS STATOR VOLTAGE IN VOLTS
ROTOR SPEED IN RADIANS PER SECOND
E.M. TORQUE IN NEWTON METERS

FIG.E.26(A)

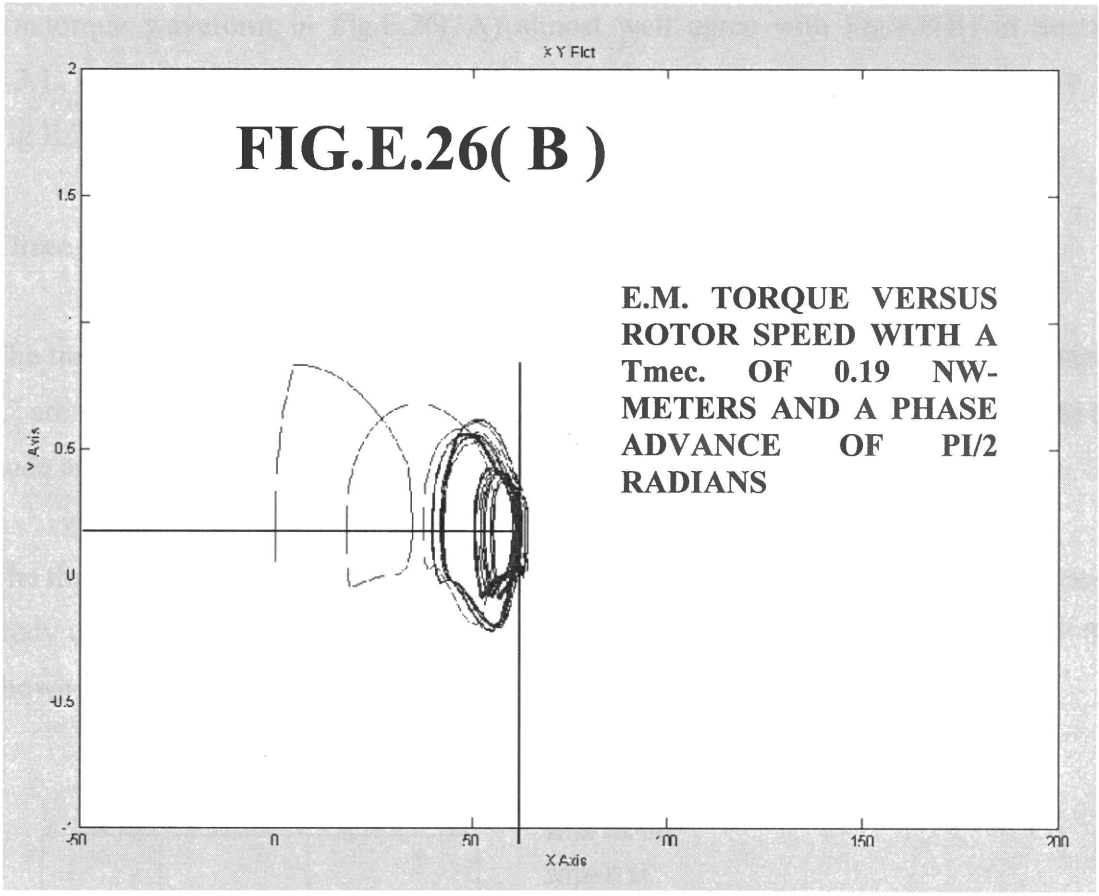

FIG.E.26(B)

E.M. TORQUE VERSUS ROTOR SPEED WITH A Tmec. OF 0.19 NW-METERS AND A PHASE ADVANCE OF PI/2 RADIANS

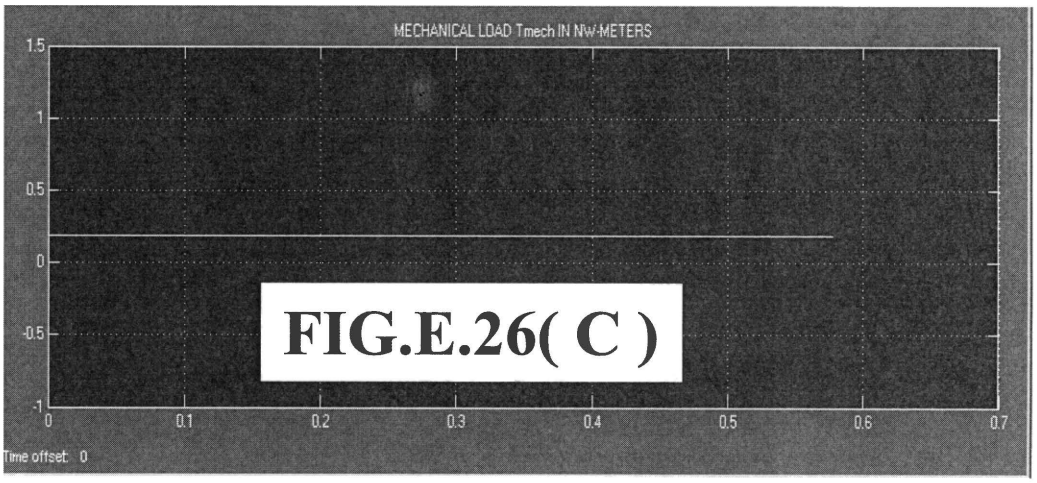

FIG.E.26(C)

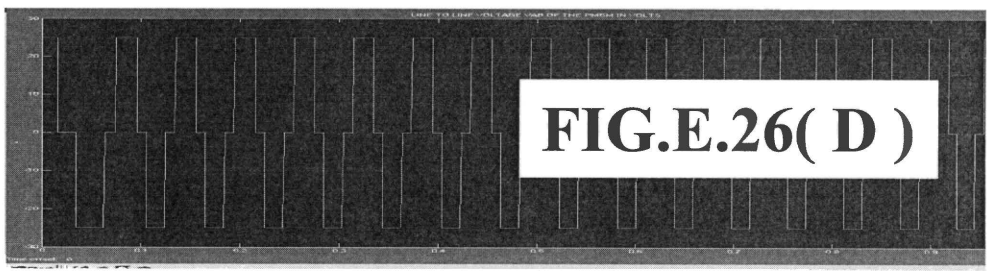

FIG.E.26(D)

of 0.19 Nw-meters. Fig.E.26(D) is the Line to line voltage Vab in Volts. The e.m.torque waveform in Fig.E.26(A) almost well agree with Fig.8.8(B) in Section 8.3.1. Rotor speed-time curve in Fig.E.26(A) and e.m.torque-speed curve in Fig.E.26(B) don't agree well with Fig.8.8(C) and (D) of Section 8.3.1.

Three Phase Three Level Inverters:

The three phase DCTLI and FCTLI discussed in Sections 12.2.1 and 12.3.1 of Chapter 12 are used to study by simulation using MICROCAP 8, instead of PSIM7.0, due to the node and component limitations in the demo version of PSIM 7.0.

The three phase DCTLI discussed in Section 12.2.1 of Chapter 12 is used for simulation study using MICROCAP 8. The three phase DCTLI schematic using MICROCAP 8 is shown in Fig.E.27. The DC Link voltage is 381 Volts.

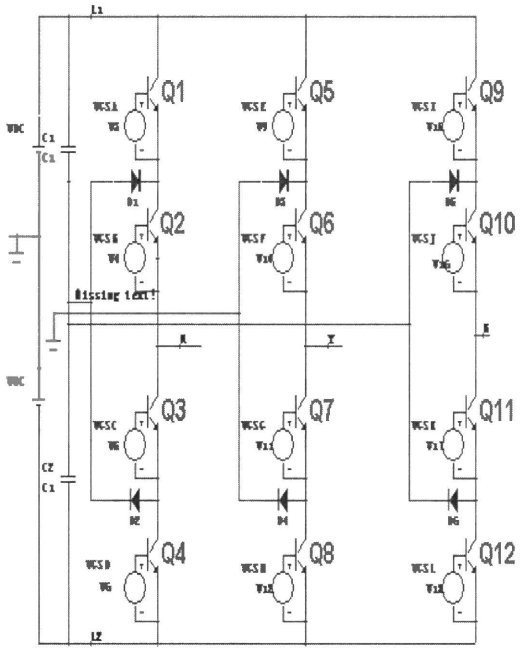


```
.DEFINE VDC 190.5
.DEFINE C1 0.1
.DEFINE VGSA PULSE(0 5 0M 0M 0M 5M 20M)
.DEFINE VGSB PULSE(0 5 15M 0M 0M 15M 20M)
.DEFINE VGSC PULSE(0 5 5M 0M 0M 15M 20M)
.DEFINE VGSD PULSE(0 5 10M 0M 0M 5M 20M)
.DEFINE VGSE PULSE(0 5 6.667M 0M 0M 5M 20M)
.DEFINE VGSF PULSE(0 5 1.667M 0M 0M 15M 20M)
.DEFINE VGSG PULSE(0 5 11.667M 0M 0M 15M 20M)
.DEFINE VGSH PULSE(0 5 16.667M 0M 0M 5M 20M)
.DEFINE VGSI PULSE(0 5 13.333M 0M 0M 5M 20M)
.DEFINE VGSJ PULSE(0 5 8.333M 0M 0M 15M 20M)
.DEFINE VGSK PULSE(0 5 18.333M 0M 0M 15M 20M)
.DEFINE VGSL PULSE(0 5 3.333M 0M 0M 5M 20M)

.MODEL D1N4148 D (IS=5.95862N N=1.91266 BV=500 RS=589.498M TT=1.12599N
CJO=1.33941P VJ=8.66264 M=300M RL=3.14968G)

.MODEL 2N2222 NPN (IS=10.017F BF=506.842 NF=979.99M VAF=100 IKF=696.241M
ISE=0.241303F NE=1.05779 BR=154.978M IKR=999.407 ISC=6.94996P RE=668.817M
CJE=42.4239P VJE=700M MJE=642.887M CJC=36.6437P VJC=700M MJC=558.066M
TF=484.887P XTF=500.001M VTF=10 ITF=9.88166M TR=2.26629U)
```

FIG.E.27: THREE PHASE DCTLI

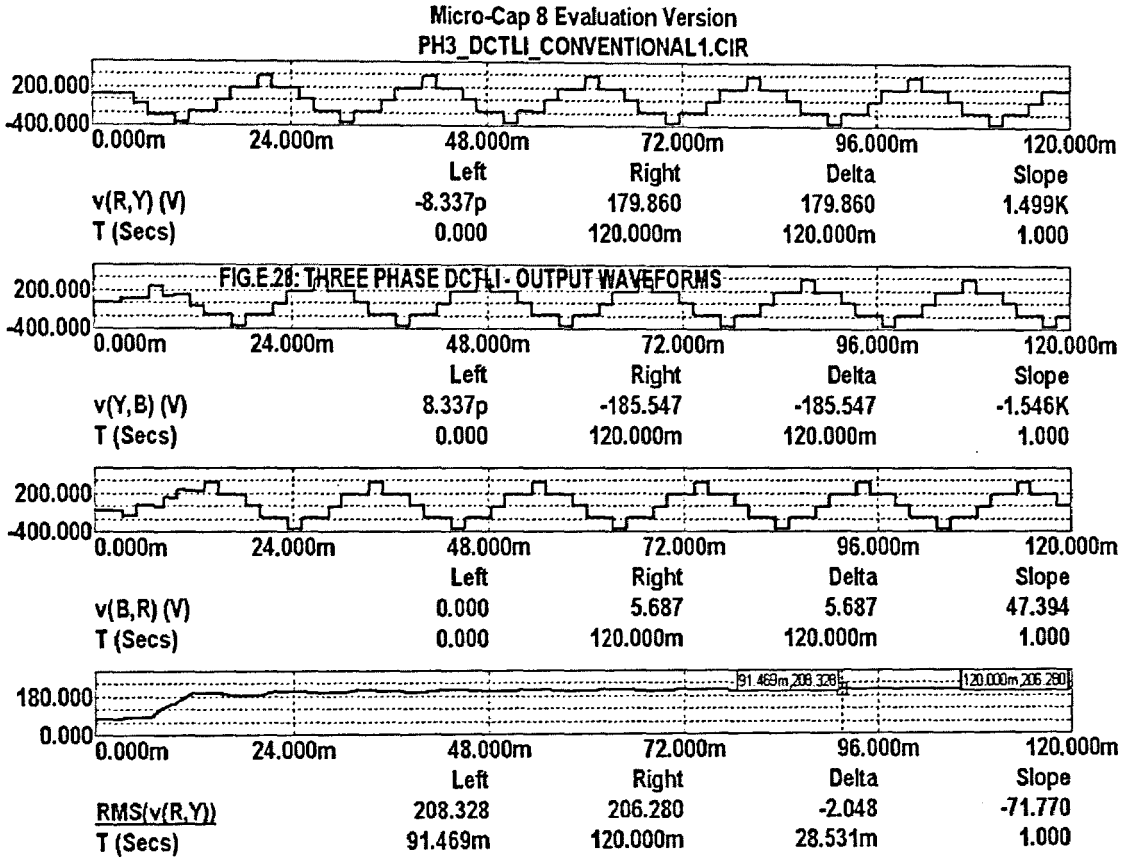

The simulation results are shown in Fig.E.28 for the three phase DCTLI. The r.m.s. value of the line to line voltage Vry indicated in Fig.E.28 is 208 Volts, where as the corresponding value indicated by simulation of the model in Fig.12.5(A) in Section 12.2.2, is 220 Volts..

The three phase FCTLI discussed in Section 12.3.1 of Chapter 12 is used for simulation study using MICROCAP 8. The three phase FCTLI schematic using MICROCAP 8 is shown in Fig.E.29. The DC Link voltage is 381 Volts.

The simulation results are shown in Fig.E.30 for the three phase FCTLI. The r.m.s. value of the line to line voltage Vry indicated in Fig.E.30 is 205.57 Volts, where as the corresponding value indicated by simulation of the model in Fig.12.10(A) in Section 12.3.2, is 220 Volts..

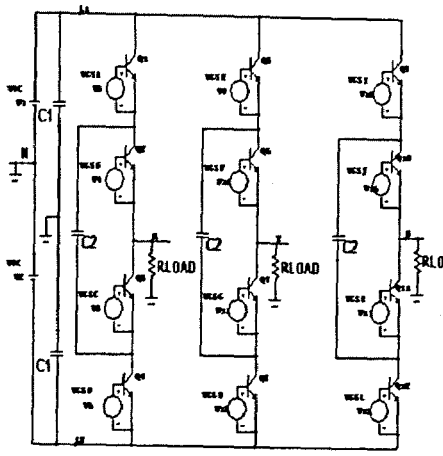


```
.DEFINE VDC 100.5
.DEFINE C1 0.1E-12
.DEFINE C2 1.2e-7
.DEFINE RLOAD 500
.DEFINE VGSA PULSE(0 5 15M 0M 0M 15M 20M)
.DEFINE VGSB PULSE(0 5 0M 0M 0M 5M 20M)
.DEFINE VGSC PULSE(0 5 5M 0M 0M 15M 20M)
.DEFINE VGSD PULSE(0 5 10M 0M 0M 5M 20M)
.DEFINE VGSE PULSE(0 5 1.667M 0M 0M 15M 20M)
.DEFINE VGSF PULSE(0 5 6.667M 0M 0M 5M 20M)
.DEFINE VGSG PULSE(0 5 11.667M 0M 0M 15M 20M)
.DEFINE VGSH PULSE(0 5 16.667M 0M 0M 5M 20M)
.DEFINE VGSI PULSE(0 5 8.333M 0M 0M 15M 20M)
.DEFINE VGSJ PULSE(0 5 13.333M 0M 0M 5M 20M)
.DEFINE VGSK PULSE(0 5 18.333M 0M 0M 15M 20M)
.DEFINE VGSL PULSE(0 5 3.333M 0M 0M 5M 20M)
.MODEL D1N4148 D (IS=5.95862N N=1.91266 BV=500 RS=589.498M TT=1.12599N
CJO=1.33941P VJ=8.66264 M=300M FC=3.14963E)
.MODEL 2N2222 NPN (IS=18.017F BF=506.842 NF=979.99M VAF=100 IKF=696.241M
ISE=8.241383F NE=1.85779 BR=154.978M IKR=999.487 ISC=6.94996P RE=668.817M
CJE=42.4239P VJE=700M MJE=642.887M CJC=36.8437P VJC=700M MJC=558.866M
TF=494.887P XTF=500.001M VTF=10 ITF=9.88166M TR=2.26629U)
```

FIG.E.29: THREE PHASE FCTLI

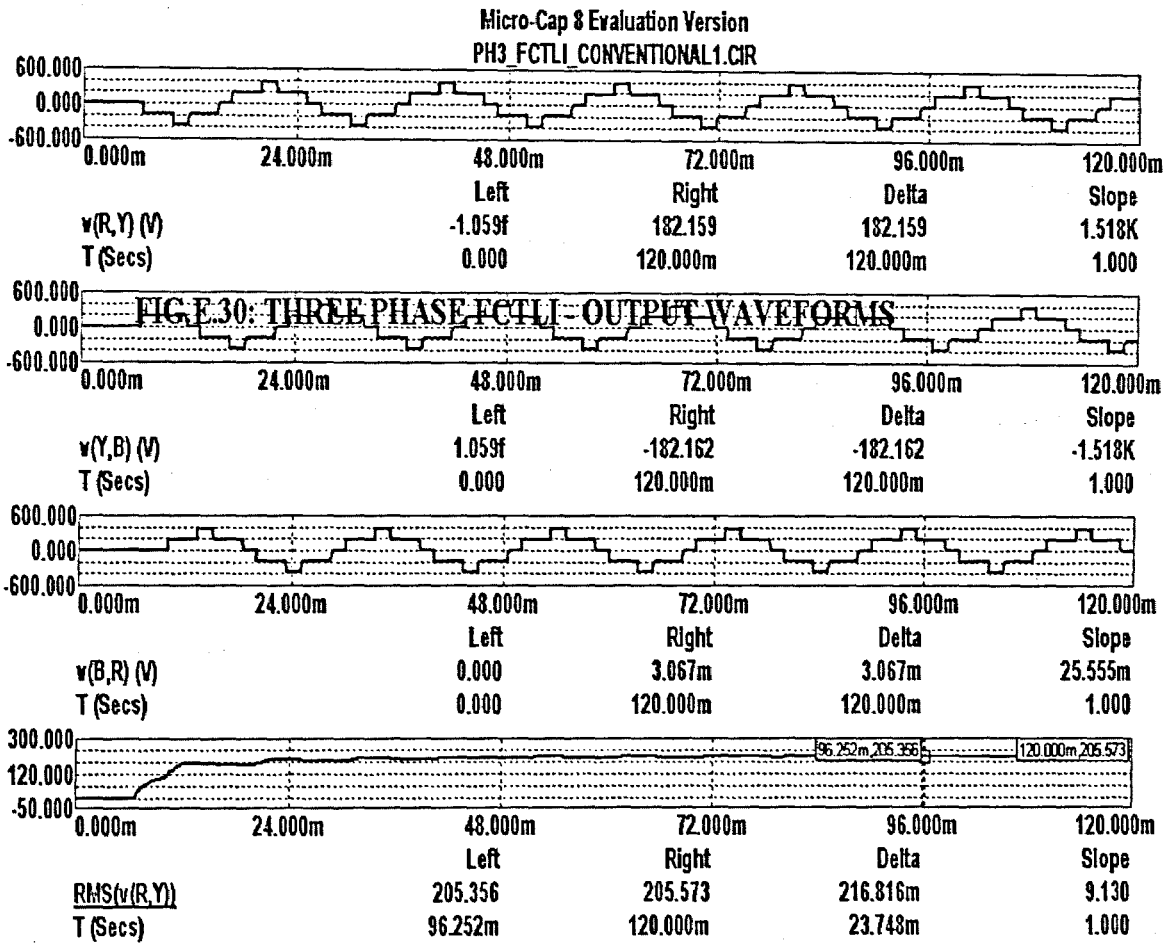

FIG.E.30: THREE PHASE FCTLI - OUTPUT WAVEFORMS

Conclusions:

The simulation results for single phase FWDBR, FWCBR, three phase FWDBR, three phase 180 degree and 120 degree mode inverters, Buck, Boost and Buck-Boost converters, three phase ac controllers, with star connected resistive load and series connected resistive load in delta, using PSIM 7.0 demo version well agree with the corresponding system model simulation using SIMULINK. In the case of three phase IM simulation using PSIM 7.0 demo version, the torque-time curve only approximately agree with that of the model simulation using SIMULINK. Six step inverter fed PMSM simulation was done using the SimPowerSystems block set of SIMULINK. Compared to the corresponding model simulation using SIMULINK, errors are observed for speed-time and e.m. torque-speed curve simulation results. **This may be due to errors or bugs in the PMSM built in model in the SimPowerSystems block set of SIMULINK.** Three phase DCTLI and FCTLI simulation using MICROCAP 8 shows errors of 5.45 % and 6.8% for the r.m.s. line to line voltage, compared to the corresponding value by model simulation using SIMULINK.

By observing the induction motor model simulation using PSIM 7.0 demo version, it is seen that the model simulation was carried out with fixed mechanical load only using the equivalent circuit of the induction motor. No provision for time varying load is available in PSIM 7.0 demo version. More over reference frame is fixed by default and can't be varied. Also for all the above power electronic converters the default sub-circuit parameters of the semiconductor component and the circuit configuration are used for obtaining the simulation results. No mathematical equations describing the system are solved by PSIM or by MICROCAP softwares.

APPENDIX F
LIST OF PUBLICATIONS FROM THIS THESIS

The list of publications from this thesis are given below:

1) Narayanaswamy.P.R.Iyer, Venkat Ramaswamy and Jianguo Zhu: "SIMULINK Model for Three Phase Sine PWM Inverter fed I.M. Drive", 40th International Universities Power Engineering Conference (UPEC 2005), Cork, Ireland, September 2005, pp. 1180 – 1184.

2) Narayanaswamy.P.R.Iyer, Venkat Ramaswamy and Jianguo Zhu: "Three Phase Clipped Sinusoid PWM Inverter – A New technique for Pulse Width Modulation", 40th International Universities Power Engineering Conference (UPEC 2005), Cork, Ireland September 2005, pp. 1185 – 1189..

3) Narayanaswamy.P.R.Iyer and Venkat Ramaswamy: "Modeling and Simulation of A Switched Mode Power Supply Using SIMULINK", Australasian Universities Power engineering Conference (AUPEC 2005), Hobart, Tasmania, September 2005; pp. 562 – 567, ISBN: 1 86295 277 9.

4) Narayanaswamy.P.R.Iyer and Jianguo Zhu: "Modeling and Simulation of A Six Step Discontinuous Current Mode Inverter Fed Permanent Magnet Synchronous Motor Drive Using SIMULINK", Sixth IEEE International Conference on Power Electronics and Drive Systems (PEDS 2005), Kualalumpur, Malaysia, Nov.-Dec. 2005, pp. 1056 – 1061.

5) Narayanaswamy.P.R.Iyer and Jianguo Zhu: "Interactive Modelling of a Six Step Discontinuous Current Mode Inverter fed Permanent Magnet Synchronous Motor Drive"; Paper presented at the 37th IEEE Power Electronics Specialists Conference, Jeju, Korea, June 18 – 22, 2006, PS 1-94, ISBN: 1-4244-9717-7.

6) Narayanaswamy. P.R. Iyer and Jianguo Zhu: "Interactive Modeling and Simulation of a Six Step Continuous Current Mode Inverter fed PMSM Drive using SIMULINK"; Paper presented at the 17th International Conference on Electrical Machines; Chania; Greece; OTM2_4, September 2 – 5, 2006.

7) Narayanaswamy.P.R.Iyer, Venkat Ramaswamy and Jianguo Zhu: "Interactive Modeling of A Three Phase Induction Motor in All Reference Frames Using dq0-Axis Flux Linkage Equations in State Space", Australasian Universities Power Engineering Conference (AUPEC 2006), Melbourne, December 10 – 13, 2006, ISBN: 978 1 86272 669 7.

8) Narayanaswamy P.R. Iyer and Jianguo Zhu: "Modelling and Simulation of A Six Step Discontinuous Conduction Mode MOSFET Inverter fed Permanent Magnet Synchronous Motor Drive", Australasian Universities Power Engineering Conference (AUPEC 2006), Melbourne, December 10 – 13, 2006, ISBN: 978 1 86272 669 7.

REFERENCES

TEXT BOOKS, USER GUIDES AND WEBSITES:

[1] Adkins, B: "The General Theory of Electrical Machines"; Chapman & Hall Ltd., London; 1957.

[2] Paul C. Krause: "Analysis of Electric Machinery";Mc.Graw Hill Inc.;1986;p.p.178-197.

[3] www.mathworks.com: "MATLAB/SIMULINK Release14 Notes; Mathworks Inc.; 2004.

[4] The Mathworks Inc.: "SIMULINK Dynamic System Simulation Software", User's Guide, 1994.

[5] www.powersimtech.com: "PSIM User's guide"; Powersim Inc.; 2003.

[6] www.caspoc.com: CASPOC Release Notes; Integrated Engineering software; 2003.

[7] www.simplorer.com: "SIMPLORER 6.0 Release Notes"; Ansoft corporation; 2003.

[8] www.cadence.com: "PSPICE Schematics Version 9.1", Cadence Design Systems, 2004.

[9] www.spectrum-soft.com: "MICROCAP 8", Spectrum software Inc., 2004.

[10] A.M. Trzynadlowski: "The Field Orientation Principle in Control of Induction Motors"; Kluwer Academis Publishers; 1994.

[11] Chee-Mun-Ong: "Dynamic Simulation of Electric machinery Using MATLAB/SIMULINK"; Prentice Hall Inc.; 1998.

[12] Nasar, S.A. and I. Boldea: "Electric Drives"; CRC Press; 1999.

[13] R. Krishnan: "Electric Motor Drives Modeling Analysis and Control"; Prentice Hall Inc.; 2001.

[14] M.H. Rashid: "Power Electronics Circuits, Devices and Applications", Pearson Education Inc., Pearson prentice Hall, 2004.

[15] Issa batarseh: "Power Electronic Circuits", John Wiley and Sons Inc., 2004.

[16] D.W. Hart: "Introduction to Power Electronics", Prentice Hall Inc., 1997.

[17] Ned Mohan, T.M. Undeland and W.P. Robbins: "Power Electronics: Converters, Applications and Design", John Wiley and Sons; 1995; Ch.4, pp. 61 – 76.

[18] Venkat Ramaswamy: "Power Electronics", Lecture Notes, Faculty of Engineering, University of Technology Sydney, 2003, pp. 8-57.

[19] J.F. Gieras and M. Wing: "Permanent Magnet Motor Technology"; Marcell Dekker Inc.; Newyork; 2002; pp.211 – 212.

[20] T. Kenjo and S. Nagamori: "Permanent-Magnet and Brushless DC Motors"; Oxford Press; 1985; pp.58 – 64.

[21] T.J.E. Miller: "Brushless Permanent and Reluctance Motor Drives"; 1993; pp.80 – 83.

[22] J.G. Zhu: "Electromechanical Systems", PM Brushless DC Motor – Laboratory 6, Faculty of Engineering, UTS, NSW, 2005.

[23] W.M. Holliday: "User Guide for the Lybotec Inverter"; Electrical Engineering; University of Technology Sydney; NSW; Australia; March 2005; pp. 1 – 11.

CONFERENCE AND JOURNAL PAPERS:

[24] B. Ospineci and Leon M. Tolbert: "SIMULINK Implementation of Induction Motor Model – A Modular Approach"; IEMDC '03; Vol. 2; June 2003; p.p. 728 – 734.

[25] M.L. Doumbia, G. Roy and V. Rajagopalan: "An integrated Solution for Simulating Electrical Drive Systems with MATLAB/SIMULINK"; IEEE ISIE '97 ; July 1997; Vol. 3; p.p. 952 – 955.

[26] M.L. Doumbia, G. Roy and V. Rajagopalan: "Modular Approach for Simulating Electrical Drive Systems With MATLAB/SIMULINK"; IEEE Electrical Machines and Drives conference Record; May 1997; TC3-3.1 to TC3-3.3..

[27] K.L. Shi, T.F. Chan and Y.K. Wong: "Modelling of three phase Induction Motor using SIMULINK"; IEEE EMDC Conference Record; May 1997; WB3-6.1 to WB3-6.3.

[28] K.L. Shi, T.F. Chan, Y.K. Wong and S.L Ho: "Modelling and Simulation of the three phase Induction Motor using SIMULINK"; International Journal of Electrical Engineering Education; Vol.36; 1999; p.p. 163 – 172.

[29] P.C. Krause, R.R. Nucera R.J. Krefta and O. Wasynczuk: "Analysis of a Permanent magnet Synchronous Machine Supplied From A 180o Inverter With Phase Control"; IEEE Transactions on Energy Conversion; Vol.EC-2; No.3; September 1987; p.p. 423 – 431.

[30] P. Pillay and R. Krishnan: "Modeling, Simulation and Analysis of Permanent – Magnet Motor Drives, Part I: The Permanent magnet Synchronous Motor Drive"; IEEE Transactions on Industry Applications, Vol.25, No.2, March/April 1989; p.p. 265 - 273.

[31] P. Pillay and R. Krishnan: "Control Charactersitics and Speed Controller Design for a High Performance Permanent magnet Synchronous Motor Drives"; IEEE Transactions on Power Electronics; Vol.5; No.2; April 1990; p.p. 151 – 159.

[32] Cui Bowen, Zhou Jihua and Ren Zhang: "Modeling and Simulation of Permanent Magnet Synchronous Motor Drives"; Proceedings of the Fifth International Conference on Electrical Machines and Systems; 2001; p.p. 905 – 908.

[33] R.R. Nucera, S.D. Sudhoff and P.C. Krause: "Computation of Steady-State Performance of an Electronically Commutated Motor", IEEE Transactions on Industry Appliocations, Vol.25, No.6, Nov./Dec. 1989, pp. 1110 – 1117.

[34] S.D. Sudhoff and P.C. Krause: "Operating modes of the Brushless DC Motor with a 120o Inverter"; IEEE Transactions on Energy Conversion; Vol.5; No.3; September 1990; p.p. 558 – 564.

[35] S.D. Sudhoff and P.C. Krause: "Average-Value Model of The Brushless DC 120o Inverter System" IEEE Transactions on Energy Conversion; Vol.5; No.3; September 1990; p.p. 553 – 557.

[36] Nobuyuki Matsui: "Sensorless Operation of Brushless DC Motor Drives"; IECON '93; November 1993; Vol. 2; p.p. 739 – 744.

[37] Nobuyuki Matsui: "Sensorless PM Brushless DC Motor Drives"; IEEE Transactions on Industrial Electronics; Vol.43; No.2; April 1996; p.p. 300 – 308.

[38] Nobuyuki Matsui and Masakane Shigyo: "Brushless DC Motor Control Without Position and Speed Sensors"; IEEE Transactions on Industry applications; Vol.28; No.1; January/February 1992; p.p. 120 – 127.

[39] Takaharu Takeshita and Nobuyuki Matsui: "Sensorless Brushless DC Motor Drive with EMF Constant Identifier"; IECON '94; September 1994; Vol. 1; p.p. 14 – 19.

[40] P. Pillay and R. Krishnan: "Modeling, Simulation and Analysis of Permanent Magnet Motor Drives, Part II: The Brushless DC Motor Drive"; IEEE Transactions on Industry Applications; Vol.25; No.2; March/April 1989; p.p. 274 – 279.

[41] P. Pillay and R. Krishnan: "Modeling of Permanent magnet Motor Drives"; IEEE Transactions on Industrial Electronics; Vol.35; No.4; November 1988; p.p. 537 – 541.

[42] P. Pillay and R. Krishnan: "An Investigation into the Torque Behaviour of A Brushless DC Motor Drive"; IEEE IAS Conference Record; 1988; Vol. 1; p.p. 201 – 208.

[43] P.C.K. Luk and C.K. Lee: "Efficient Modelling for a Brushless DC Motor Drive"; IEEE IECON '94; September 1994; Vol. 1; p.p. 188 – 191.

[44] S. Ushakumari, P.S. Chandramohanan Nair and R. Sankaran: "Closed Loop Performance of A Permanent Magnet Brushless dc Motor Incorporating the Nonlinearity in Torque-Balance Equation(Transient Operation)"; Electric Power Components and Systems; 2002; pp.1249 – 1260.

[45] B.K. Lee and M. Ehsani: "A Simplified Functional Model for 3-Phase Voltage Source Inverter Using Switching Function Concept"; IEEE IECON '99; Nov. – Dec. 1999; Vol. 1; p.p.462 – 467.

[46] B.K. Lee and M. Ehsani: "A Simplified Functional Simulation Model for Three-Phase Voltage Source Inverter Using Switching Function Concept"; IEEE Transactions on Industrial Electronics; Vol.48; No.2; April 2001; p.p. 309 – 321.

[47] J. Holtz: "Pulse width Modulation – A Survey"; IEEE conference redord; p.p.11 – 18; 1992;

[48] J. Holtz: "Pulse width Modulation for Electronic Power conversion"; Proceedings of the IEEE; Vol.82; No.8; p.p.1194 – 1214; 1994.

[49] J.A. Houldsworth and D.A. Grant: "The Use of harmonic Distortion to Increase the Output Voltage of a Three Phase PWM Inverter"; IEEE Transactions on Industry Applications; Vol.IA-20; NO.5; p.p.1224 – 1227;

[50] M.A. Boost and P.D. Ziogas: "State of the Art Carrier PWM Techniques: A Critical Evaluation"; IEEE Transactions on Industry Applications; Vol.24; No.2; p.p.271 – 280; March / April 1988;

[51] K. Taniguchi and H. Irie: "Trapezoidal modulating signal for three phase PWM Inverter"; IEEE Transactions on Industrial Electronics; Vol.IE3; No.2; p.p.193 – 200; 1986.

[52] Bin Wu, S.B. Dewan, G.R. Slemon: "PWM – CSI Inverter for Induction Motor Drives"; IEEE Transactions on Industry Applications; Vol.28; No.1; p.p. 64 – 71; January/February 1992.

[53] Xiarong Xie, Quiang Song, Gangui Yan and Wenhua Liu: "MATLAB-based Simulation of Three Level PWM Inverter-fed Motor Speed Control System"; IEEE APEC '03; February 2003; Vol. 2; p.p. 1105 – 1110.

[54] V.F. Pires and J.F.A. Silva: "Teaching Nonlinear Modelling, Simulation and Control of Electronic Power Converters Using MATLAB/SIMULINK", IEEE Transactions on Education; Vol.45, No.3, August 2002; pp. 253 – 256.

[55] B. Baha: "Modelling of resonant switched-mode converters using SIMULINK", IEE Proceedings, Electric Power Applications, Vol.145, No.3, May 1998, pp. 159 -163.

[56] B. Baha: "Simulation of Switched-Mode Power Electronic Circuits", IEE International Conference on Simulation, 1998, pp. 209 – 214

[57] A.N. Melendez, J.D. Gandoy, C.M. Penalver and A. Lago: "A New Complete Non-Linear Simulation Model of A Buck DC-DC Converter", IEEE-ISIE'99, 1999, pp. 257–261.

[58] Ned Mohan, W.P. Robbins and T.M. Undeland, R. Nilssen and Olive Mo: "Simulation of Power Electronic and Motion Control Systems"; Proceedings of the IEEE, Vol.82, No.8, August 1994, pp. 1287 – 1292

[59] Bimal K. Bose: "Power Electronics – An Emerging Technology", IEEE Transactions on Industrial electronics, Vol.36, No.3, August 1989, pp. 410 – 411.

[60] D.W. Hart: "Circuit Simulation as an Aid in Teaching the Principles of Power Electronics", IEEE Transactions on Education, Vol.36, No.1, February 1993, pp. 10-16.

[61] G.D. Marques: "A Simple and Accurate System Simulation of Three-Phase Diode Rectifiers"; IEEE - IECON; 1998; pp. 416 – 421.

[62] M.P. Kazmierkowski and L. Malesani: "Current Control Technique for Three-Phase Voltage-Source PWM Converters", IEEE Transactions on Industrial electronics, Vol.45, No.5, October 1998, pp. 691 – 698.

[63] M.N. Uddin, T.S. Radwan, G.H. George and M.A. Rahman: "Performance of current Controllers for VSI-Fed IPMSM Drive", IEEE-IAS Annual meeting, 1999, pp.1018 – 1025.

[64] M.N. Uddin, T.S. Radwan, G.H. George and M.A. Rahman: "Performance of Current Controllers for VSI-Fed IPMSM Drive", IEEE Transactions on Industry applications, Vol.36, No.6, November / December 2000, pp. 1531 – 1537.

[65] M. Kadjoudj, M.E.H. Benbouzid, R. Abdessemed and C. Ghennai: "A Robust Hybrid Current Control for Permanent Magnet Synchronous Motor Drive"; IEEE – IECON'01; pp. 2068 – 2069; 2001.

[66] Clark Hochgraf, Robert Lasseter, Deepak Divan and T.A. Lipo: "Comparison of Multilevel Inverters for Static VAR Compensation"; IEEE; 1994; p.p. 921 – 928.

[67] J.S. Lai and F.Z. Peng: "Multilevel convertors – A New Breed of Power Convertors"; IEEE Transactions on Industry Applications; Vol.32; No.3; May/June 1996; p.p.509-517.

[68] F.Z. Peng, J.S. Lai and J.W. Mckeever and J. VanCoevering "A Multilevel Voltage Source Inverter with Separate DC Sources for Static Var Generation"; IEEE Transactions Industry Applications; Vol. 32; No. 5; Sept/Oct. 1996; p.p. 1130 – 1133.

[69] Jose Rodriguez, J.S. Lai and F.Z. Peng: "Multilevel Inverters: A Survey of Topologies Control and Applications", IEEE Transactions on Industrial Electronics Vol.49, No.4, August 2002, pp. 724 – 738.

[70] Pradeep M. Bhagwat and V.R. Stefanovic: "Generalized Structure of a Multilevel PWM Inverter"; IEEE Transactions on Industry Applications; Vol.IA-19; No.6; November/December 1983; p.p.1057 – 1069.

[71] Akira Nabae, Isao takahashi and Hirofumi Akagi: "A Neutral-Point Clamped PWM Inverter", IEEE Transactions on Industry Applications, Vol.IA-17, No.5, September/October 1981, pp. 518 – 523.